FINAL MONITORING REPORT

Defense Coastal/Estuarine Research Program (DCERP1) Final Monitoring Report

SERDP Project RC-1413

JUNE 2013

Dr. Pat Cunningham
RTI International

This document has been cleared for public release

SERDP
DOD ▪ EPA ▪ DOE

This report was prepared under contract to the Department of Defense Strategic Environmental Research and Development Program (SERDP). The publication of this report does not indicate endorsement by the Department of Defense, nor should the contents be construed as reflecting the official policy or position of the Department of Defense. Reference herein to any specific commercial product, process, or service by trade name, trademark, manufacturer, or otherwise, does not necessarily constitute or imply its endorsement, recommendation, or favoring by the Department of Defense.

REPORT DOCUMENTATION PAGE

Form Approved
OMB No. 0704-0188

Public reporting burden for this collection of information is estimated to average 1 hour per response, including the time for reviewing instructions, searching existing data sources, gathering and maintaining the data needed, and completing and reviewing this collection of information. Send comments regarding this burden estimate or any other aspect of this collection of information, including suggestions for reducing this burden to Department of Defense, Washington Headquarters Services, Directorate for Information Operations and Reports (0704-0188), 1215 Jefferson Davis Highway, Suite 1204, Arlington, VA 22202-4302. Respondents should be aware that notwithstanding any other provision of law, no person shall be subject to any penalty for failing to comply with a collection of information if it does not display a currently valid OMB control number. **PLEASE DO NOT RETURN YOUR FORM TO THE ABOVE ADDRESS.**

1. REPORT DATE *(DD-MM-YYYY)*
27-06-2013

2. REPORT TYPE
Final Technical Report

3. DATES COVERED *(From - To)*
November 2007- October 2012

4. TITLE AND SUBTITLE
DCERP1 FinalMonitoring Report

5a. CONTRACT NUMBER
W912HQ-07-C-0002

5b. GRANT NUMBER

5c. PROGRAM ELEMENT NUMBER

6. AUTHOR(S) Drs. P. Cunningham, K. Baumann, N. Christensen, C. Currin, S. Fegley, J. Fleming, S. Karpanty, H. Paerl, M. Piehler, A. Rodriguez, H. Weyers.

5c . PROJECT NUMBER
SERDP RC-1413

5e. TASK NUMBER

5f. WORK UNIT NUMBER

7. PERFORMING ORGANIZATION NAME(S) AND ADDRESS(ES)
RTI International
Building 09
3040 Cornwallis Road
PO Box 12194
Research Triangle Park, NC 27709-2194

8. PERFORMING ORGANIZATION REPORT NUMBER

9. SPONSORING / MONITORING AGENCY NAME(S) AND ADDRESS(ES)
SERDP/ESTCP
4800 Mark Center Drive
Suite 17D08
Alexandria, VA 22350-3605

10. SPONSOR/MONITOR'S ACRONYM(S)

11. SPONSOR/MONITOR'S REPORT NUMBER(S)

12. DISTRIBUTION / AVAILABILITY STATEMENT

Approved for public distribution; distribution is unlimited.

13. SUPPLEMENTARY NOTES

14. ABSTRACT

The Defense Coastal/Estuarine Research Program (DCERP) is a research-based program that was sited at Marine Corps Base Camp Lejeune (MCBCL), NC. The overall objective of DCERP was to help ensure that MCBCL sustains military training and testing activities using adaptive management based on a relevant and applied monitoring and research program. This program provides a unique opportunity to integrate the results of broadly scoped ecological research to understand the structure and function of diverse coastal ecosystems, while directly integrating this research to address the Base's management needs. To facilitate an understanding of the ecosystem state and dynamics of MCBCL, the following five ecosystem modules were established for monitoring, modeling, and research: the Aquatic/Estuarine, Coastal Wetlands, Coastal Barrier, Terrestrial, and Atmospheric modules and a Data Management Module. This report includes the results and conclusions from the monitoring conducted at MCBCL during the first cycle of the DCERP (July 2007 to October 2012).

15. SUBJECT TERMS
Ecosystem-based management, coastal wetlands, coastal barrier, atmospheric, aquatic-estuarine, terrestrial, estuarine hydrodynamics, nutrient cycling, coastal geomorphology, coastal hydrology, marsh accretion, air quality

16. SECURITY CLASSIFICATION OF:			**17. LIMITATION OF ABSTRACT**	**18. NUMBER OF PAGES**	**19a. NAME OF RESPONSIBLE PERSON**
a. REPORT	**b. ABSTRACT**	**c. THIS PAGE**			Pat Cunningham
Unclassified	Unclassified	Unclassified		734	**19b. TELEPHONE NUMBER** *(include area code)* 919-316-3722

Standard Form 298 (Rev. 8-98)
Prescribed by ANSI Std. Z39.18

Table of Contents

Abstract v

Executive Summary ES-1

Chapter 1. Introduction 1-1

Chapter 2. Significant Findings and Management Implications 2-1

Chapter 3. New River Monitoring near Gum Branch and Jacksonville, NC 3-1

Chapter 4. Tributary Creeks 4-1

Chapter 5. New River Estuary—Water Column 5-1

Chapter 6. Land Cover and Shoreline Erosion 6-1

Chapter 7. Marsh Surface Elevation…. 7-1

Chapter 8. Onslow Bay Hydrodynamics…… 8-1

Chapter 9. Onslow Beach Morphology, Sediment Texture and Composition, and Aeolian Sand Transport…… 9-1

Chapter 10. Shorebirds and Seabirds Monitoring Activity 10-1

Chapter 11. Onslow Beach Benthic Invertebrates, Surf Fish, and Sea Turtles…… 11-1

Chapter 12. Onslow Beach Dune, Shrub, and Marsh Plants…… 12-1

Chapter 13. Monitoring Change in Plant Species Composition, Diversity and Distribution at MCBCL 13-1

Chapter 14. Assessment of Land-Use and Land-Cover Change: Multi-temporal Vegetation Change Detection at Marine Corps Base Camp Lejeune……..... 14-1

Chapter 15. Local and Regional Air Quality Monitoring 15-1

[This page intentionally left blank.]

Abstract (DCERP1 Monitoring Report)

Objectives

Critical military training and testing on lands along the nation's coastal and estuarine shorelines are increasingly placed at risk because of development pressures in surrounding areas, impairments due to other anthropogenic disturbances, and increasing requirements for compliance with environmental regulations. The U.S. Department of Defense (DoD) intends to enhance and sustain its training and testing assets and to optimize its stewardship of natural resources through the development and application of an ecosystem-based management approach on DoD installations. To accomplish this goal, particularly for installations in estuarine/coastal environments, the Strategic Environmental Research and Development Program launched the Defense Coastal/Estuarine Research Program (DCERP) as a minimum 10-year effort at Marine Corps Base Camp Lejeune (MCBCL) in North Carolina. The results of the first six years of the program (DCERP1) are presented here.

The overarching objectives of DCERP are to: (1) understand the effects of military training activities, infrastructure development, and other anthropogenic stressors, as well as natural disturbances, on the coastal ecosystems at MCBCL and other coastal military installations; (2) develop models, tools, and indicators to evaluate ecosystem health; and (3) recommend adaptive management strategies to sustain ecosystem natural resources within the context of an active military installation.

Technical Approach

DCERP1 was implemented in two phases. Phase I of the program was a planning period conducted between November 2006 and June 2007 and resulted in the development of the *DCERP Strategic Plan*, the *DCERP Baseline Monitoring Plan*, and the *DCERP Research Plan*. These three plans collectively serve as the foundation for DCERP activities at MCBCL. Implementation of these plans (Phase II) began in July 2007 and resulted in the establishment of more than 350 monitoring and research sites, completion of 13 research projects, and development of the Data Information and Management System (DIMS). DIMS currently archives DCERP1 monitoring and research data and provides a standard data format that optimizes data storage and retrieval for integrated analysis, allowing for exchange of information among the various DCERP1 partners and other interested researchers and stakeholders.

During Phase I, the DCERP1 Team developed the overall approach that was implemented during Phase II and used to meet the program's objectives. This approach started with identifying ecosystem processes and stressors and developing an overarching conceptual model for DCERP1 that included four ecological modules (i.e., Aquatic/Estuarine, Coastal Wetlands, Coastal Barrier, and Terrestrial Modules). Because the atmosphere has an overarching influence on all four ecosystem modules, it was treated as a fifth ecosystem module (i.e., the Atmospheric Module). After developing the overall conceptual model (and conceptual models for individual modules), the DCERP1 Team identified knowledge gaps in the models, worked with installation staff to identify the needs of MCBCL management, and then determined potential research questions to address these basic knowledge gaps and management needs.

Because DCERP1 was designed to be an adaptive program, the *DCERP Baseline Monitoring Plan* was developed to gather environmental data to address MCBCL's management concerns and support the 13 research projects. The monitoring activities established important baseline conditions in each of the modules against which changes in ecosystem processes from military training activities, other non-military stressors, and natural phenomena (i.e., episodic events, including hurricanes and droughts) could be measured. The monitoring activities also provided data at the temporal frequencies and spatial extents needed to assess variability in the environmental parameters of importance and were used to inform and validate the ecosystem models. Results from the research projects fed back into the adaptive monitoring efforts so that changes in sampling frequency, spatial scale of sampling locations, or parameters to be sampled could be adapted as necessary. Results were used to identify ecosystem indicators and develop associated threshold values, tools, or design models that address MCBCL's management needs. This information was communicated to MCBCL staff to assist them in making decisions about what type of management actions could be taken to mitigate the effects of military-related activities on the ecosystems. After implementing these actions, the DCERP1 Team monitored key environmental variables to ensure that the desired management outcomes were achieved, and then revised the conceptual models as appropriate. The adaptive nature of the approach used by DCERP1, therefore, was not shaped solely by the monitoring and research programs, but by researchers working in concert with MCBCL staff.

Results

Key Scientific Findings

The first objective of DCERP1 was to provide basic scientific information needed to help understand the physical, chemical, and biological processes associated with the coastal ecosystems of MCBCL. The main findings associated with these processes included the hydrodynamics of the New River Estuary (NRE) and the adjacent coastal system, sediment transport among all four MCBCL ecosystems (i.e., terrestrial lands, streams and estuary, coastal wetlands, and coastal barrier island), and nutrient cycling (particularly nitrogen) within the aquatic/estuarine and marsh ecosystems, as well as the role of atmospheric deposition of nitrogen to the ecosystems.

The NRE is a semi-lagoonal estuary with a long history of water quality degradation from loadings of nutrients, particularly nitrogen, resulting in phytoplankton blooms, extended periods of hypoxia or anoxia, and resultant fish kills. Results of DCERP1 indicated that anthropogenic nutrient-driven eutrophication and resulting algal bloom dynamics were controlled by climatically driven hydrologic variability in the NRE. When the water residence time within the estuary was too short to allow for nutrient assimilation by the phytoplankton, then bloom development was constrained. Freshwater discharge is of critical importance from both ecological function and ecosystem "health" perspectives because it controls nitrogen inputs and rates of nitrogen cycling.

In contrast to the NRE, which receives inputs of nutrients (particularly nitrogen from the New River watershed), the marshes of the lower NRE and Intracoastal Waterway (ICW) are, by comparison, nitrogen starved. Nitrate concentrations in shallow groundwater from the uplands contain almost no nitrates, and much of the source inputs from the upper estuary are completely

assimilated by phytoplankton in the upper estuary. The intertidal salt marshes of MCBCL were found to be overwhelmingly large sinks for nitrogen, and nitrogen sink strength was dominated by nitrogen burial during sediment accretion (80–90%) and by denitrification (10–20%).

Wind- and wave-driven hydrodynamic movements were responsible for both NRE shoreline erosion and sediment resuspension in this shallow estuary. Transport of sediments from erosion of sediment banks were found to provide at least half of the sediment required by the lower NRE and ICW marshes to keep pace with sea level rise (SLR) through accretion. Although wind and wave energy were most important as erosional forces in the estuary, within the confined channel of the ICW, boat wake energy became a more important factor affecting shoreline erosion processes. Wave energy from wind and boat wakes, compounded by the effects of routine dredging of the ICW, are the main erosional processes responsible for doubling the width of the ICW channel over the past 70 years. In addition, the very presence of the ICW traps the landward transport of sand from overwash events and aeolian transport across the barrier island, depriving marshes to the west of the ICW of this sand subsidy. As a result, salt marshes on the eastern side of the ICW were found to have a higher elevation above mean sea level than the marshes on the western (landward) side of the ICW. This finding has implications for the sustainability of the marshes landward of the ICW at MCBCL and also in other coastal areas along the ICW's extent.

A comparison of washover extent across the barrier island suggests that the primary forcing mechanism generating overwash processes has been tropical storm activity. Transgressive barriers exemplified by the southwestern portion of Onslow Island may be overwashed more frequently as sea level rises in the future, producing further erosion of dunes and creating more washover fans. Studies of the two most substantial washover deposits generated by Hurricane Irene (in 2011) found that these areas had not been overwashed in the past 70 years, and thus were not just reoccurrences of overwash of previously breached dunes as occurred at several other sites towards the middle of Onslow Island. This suggests that overwash occurs along the barrier both in new areas and those that have previously overwashed.

Longleaf pine (*Pinus palustris*) forest habitat at many southeastern installations are managed to promote habitat quality for the endangered red-cockaded woodpeckers (RCWs; *Picoides borealis*). A basic question of concern was whether forest management practices to improve habitat for RCWs were beneficial or detrimental to other avian species. Research findings from MCBCL suggest that these practices in general appear to benefit the avian community as a whole. This is reflected in measures of community composition. Both species richness (the number of species) and species diversity, which takes into account the relative abundance of the species present, increased as RCW habitat quality increased. This was especially true for another open pine habitat species of concern, Bachmann's sparrow (*Peucaea aestivalis*).

The relationship between vegetation and avian communities was assessed on 45 pine plots and was found to be highly correlated. Both vegetative composition and avifaunal communities were compositionally different among longleaf pine, loblolly pine (*Pinus taeda*), and high-pocosin sites. The overlap between the two communities suggests that the composition of avifaunal communities is correlated with differences in understory vegetative composition that can emerge in the different mature pine stands. Future efforts aimed at recovering avifaunal species may depend upon the recovery of the understory plant communities.

Models, Tools, and Indicators to Assess Ecosystem Health

The second objective of DCERP1 was the development of ecosystem models, decision-support tools, and environmental indicators that could be used to evaluate ecosystem health. For example, the Estuarine Simulation Model (ESM) was based on a previously developed two-layer Officer-type box model of the NRE to predict hydrodynamic exchanges among relatively coarse boxes arranged along the estuarine salinity gradient. The ESM was expanded to include total suspended solids (TSS) and another component, eelgrass (*Zostera marina*), which is the most abundant species of submerged aquatic vegetation in the NRE. The ESM was used to examine the changes in point and non-point source inputs on estuarine water quality variables and ecosystem processes. The Marsh Equilibrium Model (MEM) was applied to MCBCL to forecast changes in the relative elevation of the marsh surface and biomass response to different rates of SLR possible in a climate changed future. Model simulations of different SLR scenarios showed that the marsh vegetation survived 100 years only when the SLR was less than 60 cm (24 in); otherwise, the marsh vegetation rapidly declined. The MEM can be transferred to other locations, but it requires local accretion rates, standing biomass, TSS, and water level data. Finally, the Runup and Overwash Model (ROM) was used to predict where overwash would occur on Onslow Beach. The ROM correctly identified the four overwash areas resulting from the passage of Hurricane Irene (in 2011), illustrating its use forecasting vulnerable areas.

As previously discussed, there was a strong relationship discovered between hydrological flow of the New River and phytoplankton biomass production. Freshwater flow of 27 $m^3 s^{-1}$ was identified as a tipping point for the estuary. At freshwater flows above this threshold, the water residence time in the NRE was too short for nutrient assimilation by phytoplankton in the water column, thereby restricting algal bloom development. Benthic chlorophyll *a* concentration was also found to be an excellent indicator of the effectiveness of the benthic microalgae to act as a nutrient filter. When chlorophyll *a* ranged from 70–83 mg m^{-2} or above, benthic microalgal biomass increased, and nitrogen was sequestered from the water column. When conditions restricted photosynthesis (chlorophyll *a* ranged from less than 70–83 mg m^{-2}), the microalgae released nitrogen into the water column. In shallow estuaries such as the NRE, hydrologic changes can modify both phytoplankton primary production and affect benthic microalgal production, which modulates internal nutrient cycling.

Recommended Adaptive Management Strategies to Sustain Ecosystems

The third objective of DCERP1 was to recommend adaptive management strategies to sustain ecosystem natural resources within the context of an active military installation. These strategies are most applicable to the coastal wetlands, coastal barrier, and terrestrial ecosystems. More than 80% of the NRE shoreline is contained within the boundary of MCBCL. Only 19% of this shoreline has been hardened with revetments, sills, and seawalls. This constrained shoreline development has water quality benefits with respect to reduced nutrients and sediment runoff and allows ecosystem services (e.g., storm surge protection, fish and shellfish nursery areas) of the unhardened shorelines to be preserved. Although historic MCBCL practices of hardening NRE shoreline in high-energy areas are appropriate, marshes and sediment banks (which supply sediment vital for marsh accretion) will be needed in the future to help mitigate for rising sea level. MCBCL Managers should consider whether additional shoreline hardening is needed, and if so, new shoreline hardening should be offset with marsh restoration in hardened areas where

wave energy is low and marsh restoration efforts would be successful. These restoration efforts will promote sustainability by allowing the marshes to migrate landward as sea level rises and continue to provide shoreline ecosystem services not provided by hardened structures.

Marshes along the lower NRE and ICW are an integral part of amphibious training and are a conduit for moving amphibious vessels from the mainside training areas to the barrier island. Reinforced splash points within the ICW have a lower shoreline change compared to unmodified splash points. MCBCL Managers should consider strategies to reduce erosion rates and enhance sustainability of splash points for future training, including reinforcing splash points with concrete ramps, implementing marsh restoration, or diverting some military training activities from overused splash points to underused ones. In addition, if the speed of large V-hulled vessels was reduced in the ICW, then vessel wakes would be sufficiently small so as not to create sediment-eroding waves. A reduction in vessel speed could be achieved by establishing a no-wake zone in the ICW. If properly placed, a 2-mile no-wake zone would increase transit time by only 10 minutes and would substantially reduce the creation of erosion-generating boat wakes.

Similar to the ICW and coastal marshes, the barrier island provides essential beach for U.S. Marines to conduct amphibious assault training. At current training levels (frequency and intensity), military training did not have a measurable impact on the landscape (e.g., sediment texture, topography, habitat) of Onslow Beach. Results from studies conducted during DCERP1 found that natural processes (wind and wave actions) overshadow anthropogenic effects. This was primarily due to installation management constraining training to existing egress and ingress areas along the barrier and restricting vehicular and pedestrian traffic on the dunes and backbarrier marshes.

Forest management at MCBCL and other installations in the southeastern United States is directed toward returning hardwood-pine lands to open canopy longleaf pine-wiregrass communities. Installation restoration goals were better achieved by the combined use of understory/midstory thinning in pine-hardwood plots followed by prescribed burning. Used in combination, these practices removed more woody material and consumed more than three times the fuel of prescribed burning alone. Thinning during the growing season was more effective in reducing the understory/midstory woody plants than dormant season thinning or prescribed burning alone. If these differences persist, then they would indicate a possible benefit of growing season thinning that could be implemented at other installations with longleaf pine restoration goals. In either case (with or without thinning), continued suppression of woody growth requires regular prescribed burns. Additionally, the use of understory/midstory thinning appears to have a secondary benefit in reducing $PM_{2.5}$ emissions, thus providing improved smoke management for installations.

The recovery of RCWs at installations in the southeastern United States drives forestry management strategies. Forest management that specifically targets improving habitat conditions for the RCWs was found to result in habitat changes that benefit the biodiversity of terrestrial ecosystems in general and the total avian community specifically; therefore, this management practice should be encouraged. Installation Managers also should maintain the availability of nesting substrate (e.g., live pines, pine snags, hardwood snags) for the wide variety of cavity-nesting avian species because this determines the strength of interactions among these species.

Specifically, a shortage of dead or dying pine snags would likely result in negative impacts on RCWs due to the takeover of their cavities in live pines by other cavity nesting species.

Benefits

The research and monitoring activities conducted as part of DCERP1 have resulted in a greater understanding of MCBCL's biologically diverse ecosystems and their interactions with military training activities. In addition, the research results provide an understanding of what on- and off-installation activities affect these ecosystems and what management actions could be implemented to best sustain MCBCL military training and testing resources. Through the research projects, the DCERP1 Team developed a series of indicators, models, and tools designed to benefit Installation Managers by providing support for environmental decision making. Knowledge gained from DCERP1 research, supported by a long-term baseline monitoring effort, will provide benefits to other military installations in coastal settings and to the scientific community and the general public at large.

DCERP1 Final Monitoring Report

Executive Summary

Critical military training and testing on lands along the nation's coastal and estuarine shorelines are increasingly placed at risk because of development pressures in surrounding areas, impairments due to other man-made disturbances, and increasing requirements for compliance with environmental regulations**.** The U.S. Department of Defense (DoD) intends to enhance and sustain its training assets and to optimize its stewardship of natural resources through the development and application of an ecosystem-based management approach on DoD installations. To accomplish this goal, the Strategic Environmental Research and Development Program launched the Defense Coastal/Estuarine Research Program (DCERP) in 2006 (originally planned as a 10-year program) at Marine Corps Base Camp Lejeune (MCBCL) in North Carolina. The *DCERP1 Final Monitoring Report* covers measurement activities conducted from November 2007 through October 2012. MCBCL provides an ideal platform for DCERP because it integrates a wide variety of coastal ecosystems—aquatic/estuarine, coastal wetlands, coastal barrier, and terrestrial—all within the boundaries of DoD properties (**Figure ES-1**).

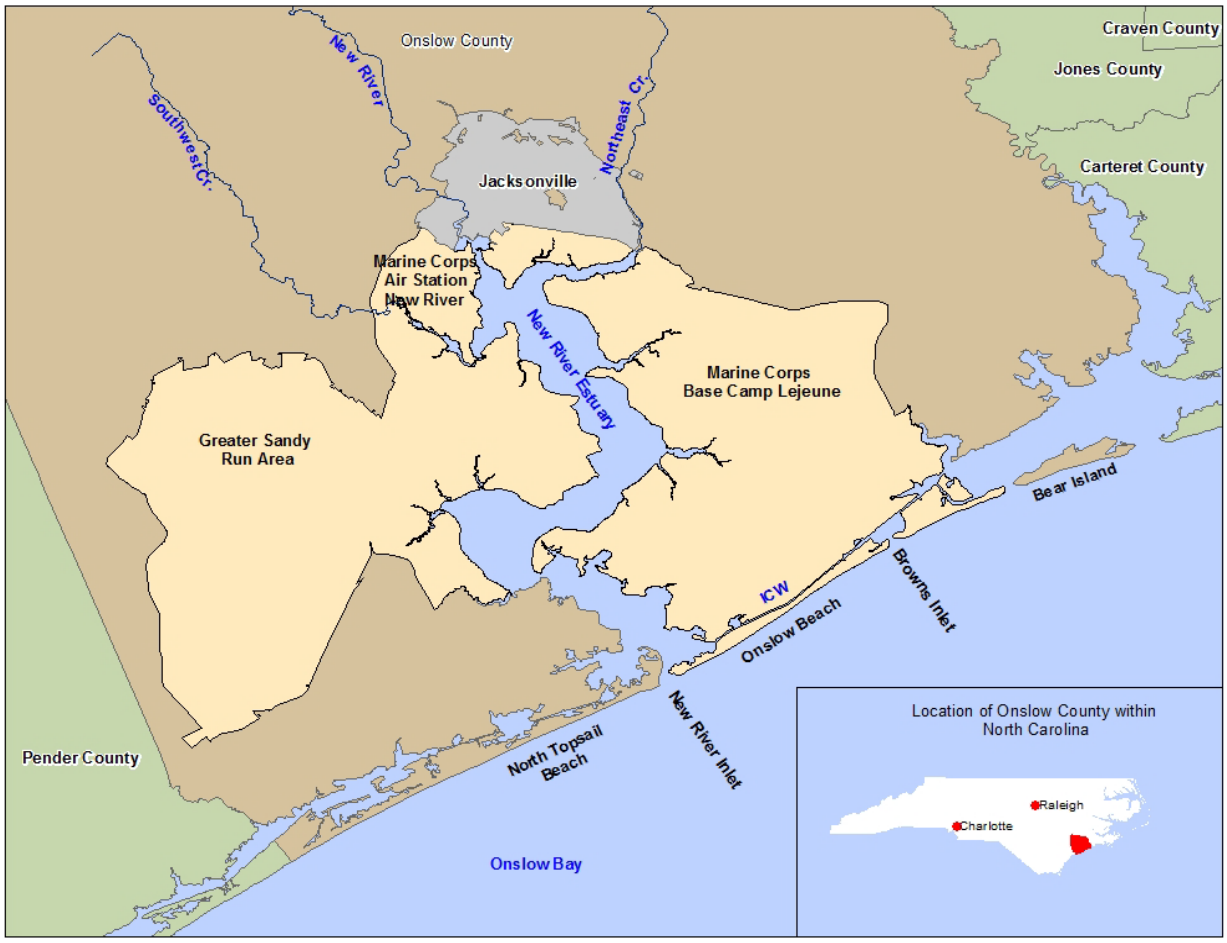

Figure ES-1. DCERP is located at MCBCL in the lower coastal plain of North Carolina.

The overarching objectives of DCERP are to understand the effects of military training activities and infrastructure development, as well as other natural and anthropogenic stressors on these coastal ecosystems; to develop models, tools, and indicators to evaluate ecosystem health; and to recommend adaptive management strategies to sustain ecosystem natural resources within MCBCL's operational goals. The DCERP1 Team consisted of researchers from seven academic institutions, three governmental agencies, and three private companies. The DCERP1 monitoring program collected important information in support of the 13 research projects. This information provided an understanding of the composition, structure, and function of the aquatic/estuarine, coastal wetlands, coastal barrier, and terrestrial ecosystems as they relate to MCBCL's military training mission. These research projects have broader applicability for other DoD installations in similar coastal settings. Although the baseline monitoring program and research projects were closely integrated, the results are presented in separate reports.

As part of our Strategic Plan, the overarching conceptual model for DCERP at MCBCL (**Figure ES-2**) was subdivided into four ecosystem modules (i.e., the Aquatic/Estuarine, Coastal Wetlands, Coastal Barrier, and Terrestrial Modules). Because the atmosphere and its physical–chemical processes influence all four ecosystem modules, it is treated as a fifth module. In addition, a sophisticated Data and Information Management System was developed as part of the Data Management Module. This system, known as the Monitoring and Research Data and Information Management System (MARDIS), was designed to facilitate communication and collaboration among the team researchers and to archive all DCERP research and monitoring data, final DCERP reports, reports to MCBCL, geographic information systems (GIS) data files, and various models and tools developed under DCERP.

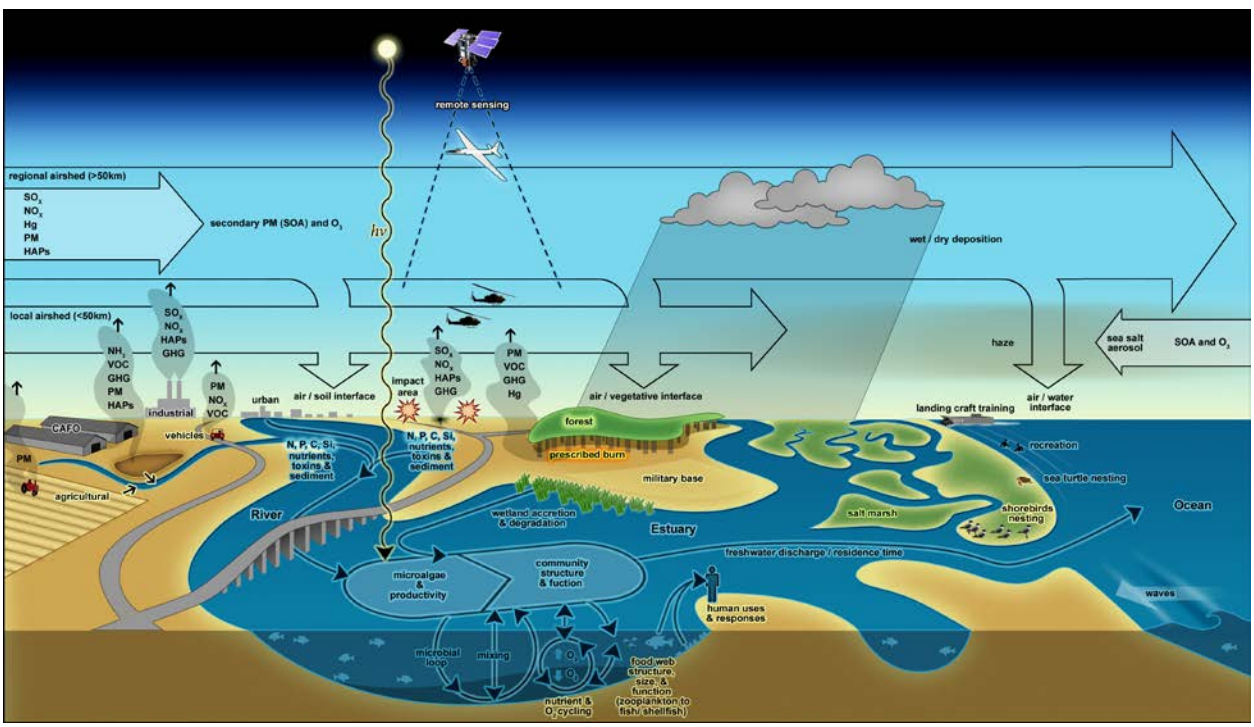

Figure ES-2. Overarching conceptual model for DCERP at MCBCL.

For each of the five ecosystem modules, this Executive Summary delineates the context in which the baseline monitoring was conducted, briefly discusses the environmental processes studied and the methods applied or developed, and the major findings of the monitoring program. In addition, recommendations are provided for MCBCL Managers to use to sustain ecosystem health and at the same time enhance sustainability of the military training mission.

Programmatic Overview

DCERP was established as a highly integrated temporal and spatial monitoring and research program. During this program, monitoring data provided information that validated models, and research data gave feedback on whether the monitoring was adequate to support research hypotheses. Monitoring data were of critical importance to the research effort for several reasons. First, monitoring data established baseline conditions that provided a context against which to compare impacts of major stressors to the various ecosystems. As part of an ecosystem-based management program, there is a need to establish long-term measurement activities that capture basic ecosystem processes. DCERP1 monitoring data were critically important to the team's understanding of the baseline conditions that existed in each ecosystem at the start of DCERP1 and to determining whether anthropogenic and/or natural stressors were changing conditions over time. For example, baseline conditions for pine-dominated vegetative plots across the installation were previously captured by the Carolina Vegetation Survey (CVS) and re-sampled during DCERP1. This effort provided the opportunity for the direct evaluation of change in these stands over an 18-year period when MCBCL Managers implemented a 3-year rotation prescribed burning program in these stands. DCERP1 monitoring efforts also expanded the vegetation monitoring to habitats under-represented in the CVS (e.g., wetlands, hardwood stands). These new data established more comprehensive baseline conditions for a wider spectrum of terrestrial vegetation for the installation that can be used to assess vegetation changes in the future.

Second, for studying the various ecosystem processes, monitoring data provided information to assess the daily, monthly, seasonal, and annual and inter-annual variabilities of key monitoring parameters, thereby providing a better understanding of natural variability, as well as variability resulting from episodic events. These episodic events have great value in understanding ecological processes, but they and their forcing conditions must be properly recorded. An episodic event may be defined differently among different ecosystems because of the scale of the event (i.e., duration, intensity, extent, and frequency) and the various environmental parameters contributing to the resultant stress (e.g., salinity, temperature, wave energy, suspended solids) on the system. In addition to natural variability, the monitoring activities were also designed to capture changes in man-made activities and their impacts on ecosystem processes. Anthropogenic effects such as the accumulated impacts of changes in land use across MCBCL lands are likely to produce a slower rate of change in water quality parameters than those resulting from an extreme episodic event and may be more difficult to capture and distinguish from natural variability. Capturing trends in monitoring results requires appropriate selection of sampling frequency and spatial extent, and different temporal/spatial scales are required for the various ecosystem processes being studied. The frequency required to capture significant trends in the estuary may be quite different in scale from those used in the coastal wetlands or other ecosystems. For example, gradual changes in terrestrial vegetative communities may take 5 or more years before patterns of change become evident, whereas estuarine shoreline erosion or

beach erosion may require decades before a clear trend can be established. As appropriate, an analysis of trends in the monitoring data was conducted to determine whether significant changes in various ecosystem processes had occurred. The same episodic event may also affect ecosystems in different ways. For example, although drought conditions may improve water clarity, which allows benthic microalgae to thrive, drought may result in increasing salinities in upstream areas of the estuary, thereby stressing marsh communities typically exposed to lower salinity conditions or stressing terrestrial vegetative communities. DCERP1 monitoring activities were carefully coordinated and integrated to adequately capture and characterize inter-annual variability and assess the impacts from routine and episodic events on the coastal ecosystem. This coordination and integration are even more important going forward in order to continue collection of comparable monitoring data that will provide a decade of measurement data from some MCBCL systems by the end of DCERP2. This is important because there is an emphasis on studying both the current and future impacts of anthropogenic and natural changes on the various ecosystem processes.

Finally, to aid in effective ecosystem-based management, monitoring data were used to develop and validate predictive models. Some of these models were used during scenario testing to predict the impacts of changes in key parameters to major ecosystem processes under current conditions. One scenario, for example, was how increasing concentrations of nitrogen would impact chlorophyll *a* concentrations in the New River Estuary (NRE). During DCERP2, some of these same predictive models will be used to evaluate key variables controlling ecosystem processes and predict resulting impacts on these ecosystems as key parameters change under future climate conditions.

Aquatic/Estuarine Module

Estuaries integrate inputs from terrestrial habitats, freshwater rivers and streams, the coastal ocean, and atmospheric systems. Accurate estuarine water quality assessment and management necessitates consideration of the interconnections to, and interactions with, these other systems. Many estuaries also exist in regions of rapid population growth and diversifying human activity, which can impact natural ecosystem processes. In the context of the MCBCL region, the Aquatic/Estuarine Module examined the tidal reach of the NRE from the head of the estuary near Jacksonville, NC, to the tidal inlet at Onslow Bay. This tidal reach included freshwater flows from the New River and tributary creeks within Base lands that flow into the NRE or the Intracoastal Waterway (ICW) on the southern boundary of the installation.

The Aquatic/Estuarine Module's monitoring program was designed to achieve multiple goals, including improved understanding of the physical, chemical, and biological processes and interactions that drive water, sediment, and habitat quality within the New River, the MCBCL tributary creeks, and NRE water column; support the research project components; and help to differentiate natural and anthropogenic ecosystem stressors. Additional goals included providing information for designing and implementing a long-term monitoring program that ensures compatibility of MCBCL activities with desirable estuarine water, sediment, and habitat quality and facilitating the conservation of regional natural resources of the NRE for their ecosystem services, recreational, and economic benefits. It should be noted that monitoring of the shallow portions of the NRE were measured as part of the research program, and results are presented in the *DCERP1 Final Research Report*.

Freshwater Inputs

Flow measurements were collected at the headwaters of the New River near Gum Branch and at the point where the New River enters the NRE near Jacksonville, NC. Annual mean river flows were less than the mean annual discharge during all years except 2010 (**Figure ES-3**). Despite the lower than average flows in 4 out of the 5 study years, episodic events (e.g., hurricanes, tropical storms, nor'easters) produced high river flows for brief periods (November 2009–January 2010) and during late spring and summer 2012. Salinity values at the Jacksonville station ranged from 0.04 to 24.8 ppt, depending upon the frequency, magnitude, and timing of rainfall events that regulated freshwater inflow. Salinity was typically lowest during the winter and highest in the summer, decreasing again in fall as storm events increased potential for rainfall. The New River is an important source of nitrogen and phosphorus to the estuary. Although concentrations of phosphorus were typically similar at both gaging stations (Gum Branch and Jacksonville), concentrations of nitrogen were typically higher upstream at Gum Branch than at the Jacksonville gaging station, suggesting that nitrogen was assimilated by phytoplankton through primary production in the river before entering the estuary.

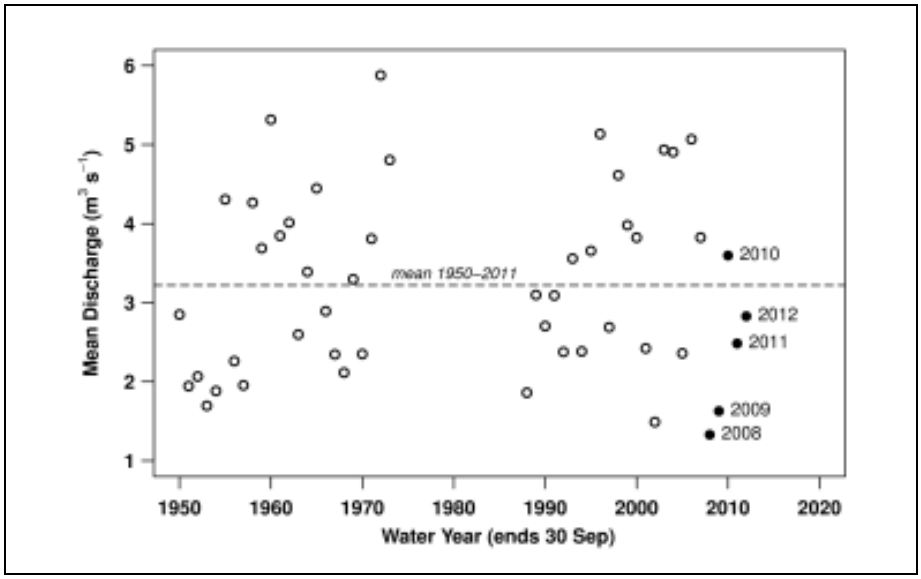

Figure ES-3. Mean annual discharge of the New River at Gum Branch.

Loading rates of nutrients and sediment were generally very low in the MCBCL tributary creeks as compared to the New River and tributaries in other Atlantic coastal plain systems. However, there was a clear cause-and-effect relationship between increased human activity in the watershed (with percent impervious cover as the indicator of land disturbance) and loading of nutrients and sediments to the estuary. Understanding of these inputs is necessary to understand the estuarine dynamics especially in coastal wetlands and shallow embayments.

Estuarine Water Column

The estuarine water quality monitoring effort revealed that the NRE is functionally divided into two estuaries, with dramatically different biological responses noted in each, including contrasting sensitivities to the development and proliferation of harmful algal blooms, hypoxia

potentials, and external inputs versus internal releases of nutrients from the benthic microalgae. Natural processes such as riverine discharge, water temperature, wind stress, water column stratification, and tidal currents exhibited the strongest and most direct linkages with estuarine water quality and habitat condition. Bottom-water hypoxia was closely linked to water temperature and water column stratification, with no apparent relationship to algal blooms, which may have resulted from anthropogenic nutrient loading. Water column turbidity was strongly linked to wind-induced sediment resuspension events (**Figure ES-4**). Periods of high algal biomass were linked to optimal river flow, which provided enough nutrients for phytoplankton biomass development, but also sufficient residence time within the estuary for nutrient assimilation and phytoplankton growth to occur. During periods when flows were too high for phytoplankton biomass development, nutrient concentrations within the estuary were also high. Thus, nutrient concentrations within the NRE were also largely determined by riverine discharge.. The first 5 years of monitoring data provided only a first glimpse of these effects because low mean annual discharge rates predominated in 4 out of the 5 years. A decadal time scale may be needed to fully capture, characterize, and model the impact of climatic extremes.

Recommendations to Installation Managers for Aquatic/Estuarine Ecosystems

1. High levels of nutrient loading from the upper New River watershed (off-Base) are a primary concern for water quality management in the entire NRE basin. Therefore, MCBCL Managers should work in partnership with Onslow County, the City of Jacksonville, and other stakeholders to encourage reduction in upstream sources of nutrient (nitrogen and phosphorus) inputs into the New River within their respective jurisdictions.
2. As development on MCBCL increases, however, MCBCL Managers should be aware that there is increasing potential for enhanced loading of nutrients, sediment, and fecal bacteria to MCBCL tributary creeks and ultimately into the NRE. MCBCL Managers should constrain loadings to tributary creeks through careful selection of sites for future development and application of efficient best management practices as appropriate.
3. Under all but the highest river flow conditions, residence time of the NRE is long enough that phytoplankton have time to fully assimilate nutrient loads. The result is that phytoplankton growth is strongly nutrient limited within most of the NRE, and any increases in nutrient load will result in higher levels of phytoplankton biomass. The poorly flushed region of the estuary from Morgan Bay to Stones Bay is particular susceptible to eutrophication. Therefore, if MCBCL Managers plan to develop the watersheds that drain to more vulnerable areas of the NRE, then mitigation of nutrient and sediment loading should be emphasized because sediment often carries high levels of absorbed nutrients and therefore represents an important non-point nutrient source.

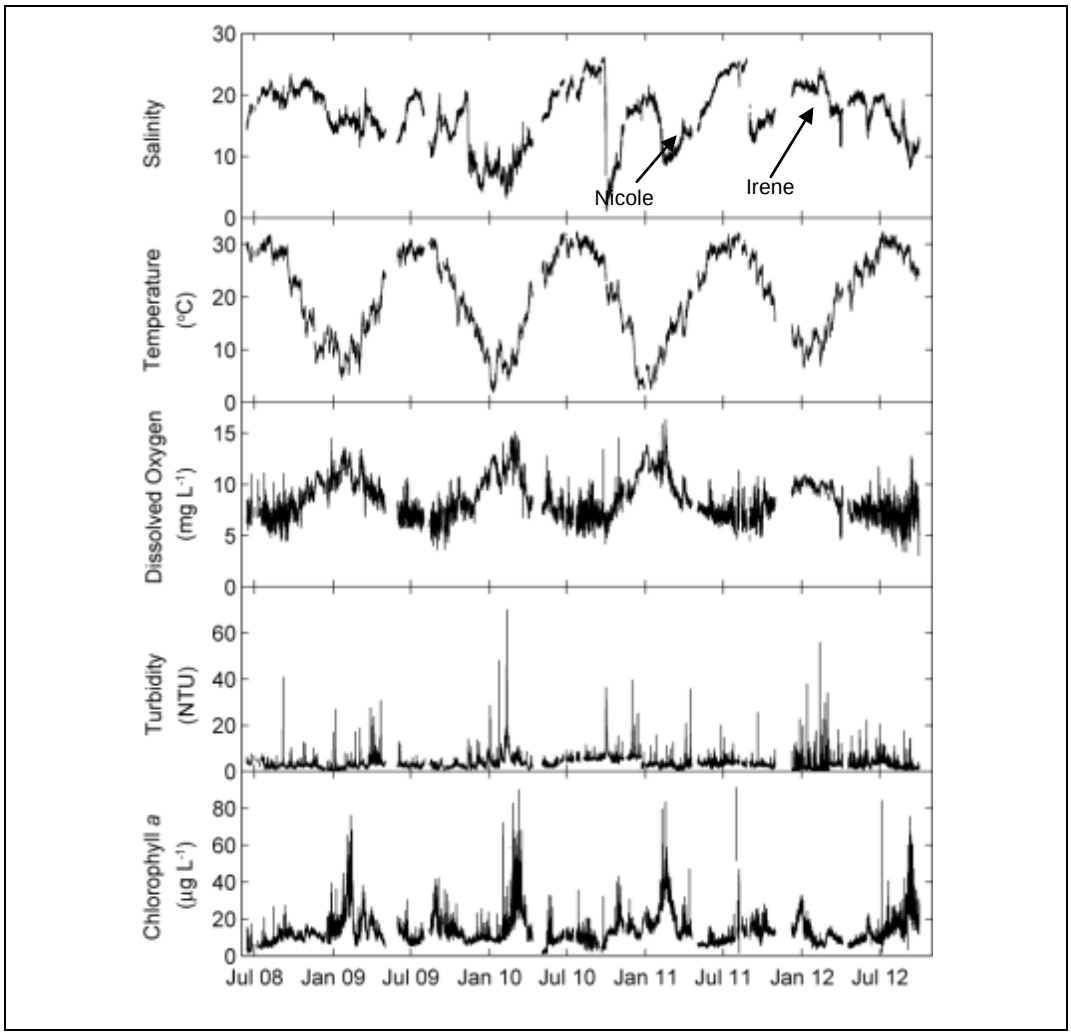

Figure ES-4. Time series of semi-hourly, average water column conditions from the Autonomous Vertical Profile at Morgan Bay from June 14, 2008 through October 1, 2012.

Arrows point to two major tropical storm events that impacted the estuary, the remnants of Tropical Storm Nicole and Hurricane Irene.

4. An effective, comprehensive strategy for mitigating impacts on water quality from future MCBCL activities on MCBCL lands should consider include the following: (1) minimizing sediment and nutrient losses by maintaining natural vegetation and ground cover, particularly within riparian buffer areas; (2) minimizing the percent impervious surfaces (e.g., parking lots, paved lots, roadways) within a watershed; and (3) promoting retention of water within tributary watersheds by preserving and reclaiming wetlands, using retention ponds, minimizing ditching, and controlling stormwater runoff in developed areas with effective best management practices.

Coastal Wetlands Module

Coastal wetlands are a vital component of the estuarine landscape that links terrestrial and freshwater habitats with the sea. Marshes provide a variety of ecosystem services, including improving water quality by transforming nutrients and trapping sediment, attenuating wind wave

and boat wake energy on shorelines, stabilizing the coastal barriers, accreting sediments and building land, and providing recreational opportunities for people. Overall, the Coastal Wetlands Module's monitoring station locations range from the upper portion of the mainstem NRE (Wallace Creek), to mid-estuary (French Creek), to the lower portion of the NRE (Traps Bay and Mile Hammock Bay), and finally to the salt marshes that border either side of the ICW (Freeman Creek and the Onslow Beach Backbarrier). These monitoring stations include sites dominated by black needle rush (*Juncus roemerianus)* in the mid to upper estuary and sites dominated by smooth cordgrass *(Spartina alterniflora)* in the lower estuary and the ICW. This spatial coverage allowed us to demonstrate how changes in marsh geomorphology, tidal amplitude, wave energy exposure, and surface elevation affect the ecological processes (nutrient exchange, sediment accretion, shoreline erosion, marsh primary production) being studied. The analysis of current monitoring data demonstrated significant site variability in the relationship between marsh biomass and surface elevation and in the relationship between tidal inundation and sedimentation rates. Some of this site variability was due to differing tidal amplitude, which was observed in the tide gauge data. Changes in salinity, dominant plant vegetation, and proximity to sediment sources also influenced the measured site-specific responses.

The frequency of sampling ranged from annual measures of primary production to close interval (6–15 minute) sampling of water level. In addition, long-term (more than 50 years) rates of shoreline erosion for the NRE and ICW shorelines were determined using aerial photography. Sampling frequency has proven to be adequate in detecting significant site and annual variabilities. However, several of the ecological processes of interest to the Coastal Wetlands Module's research effort are long-term processes (marsh response to sea level rise [SLR], shoreline erosion) that require 5 to 10 years of monitoring data to distinguish short-term variability from long-term trends and to increase the likelihood of capturing storm events that may be important in exposing the marshes to the maxima and minima of variability in key parameters of interest.

Shoreline Habitat, Location, and Marsh Distribution

The entire NRE and ICW shoreline was classified by habitat types (i.e., Marsh, Swamp Forest, Sediment Banks, Miscellaneous, and Modified [hardened] shorelines). Sediment Banks are the most prevalent habitat type along the NRE shoreline, representing 53% (66 km [41 mi]) of the total shoreline, followed by Marsh (26.5%), Modified (24.3%), and Swamp Forest (7.3%). In contrast, the ICW shoreline was dominated by Marsh (80%), followed by Sediment Banks (19%) and Modified (1%) habitat types.

The distribution of dominant plant species in NRE shoreline habitats illustrates the transition from *Spartina alterniflora*–dominated salt marshes in the ICW and lower NRE to brackish marshes with a mixture of *Juncus roemerianus* and *Spartina cynosuroides*) further up in the estuary. *Phragmites australis*, an invasive marsh species, was documented at several locations along NRE shoreline, mostly between Stones Bay and Wallace Creek. The total area of coastal wetlands on MCBCL is approximately 1,090 ha (2,690 ac). These data provide baseline information to track potential changes in marsh distribution associated with climate change and/or SLR and can be used to guide wetland restoration efforts.

Marsh Vegetation

A total of nine plant species was recorded in the marsh vegetation monitoring plots. The two dominant species are *Spartina alterniflora* and *Juncus roemerianus* however; several other species such as *Distichlis spicata*, *Limonium carolinianum*, *Salicornia virginica*, *Borrichia frutescens*, *Spartina patens*, *Spartina cynosuroides and Typha* sp. were also encountered. The low diversity of marsh plants is consistent with other coastal wetlands in the southeastern United States and also reflects the small change in elevation over the monitoring plots, as marsh diversity typically increases closer to the upland border. The use of permanent plots provides the opportunity to detect changes in plant species over time, particularly in marshes that are near transition zones. The marshes in the lower NRE, including Traps Bay and Pollocks Point, exhibited the highest plant diversity.

Marshes in the ICW were dominated by *Spartina alterniflora*. Mean stem density was significantly different between the three ICW sites, increasing from Freeman Creek (FC), to Onslow Beach Backbarrier (OBB) to Mile Hammock Bay (MHB) **Figure ES-5.** Mean stem height exhibited a different pattern, decreasing from Freeman Creek (68 cm) to Onslow Beach Backbarrier (32 cm) to Mile Hammock Bay (24 cm). Above-ground biomass was calculated using both of these parameters, with the results that mean biomass does not differ significantly (407 and 365 g m^{-2}) for the Freeman Creek and Mile Hammock Bay sites, respectively, and that biomass at both sites is greater than at Onslow Beach Backbarrier (253 g m^{-2}). The difference in biomass between sites was partly due to different marsh surface elevations of the vegetation plots sampled at each site.

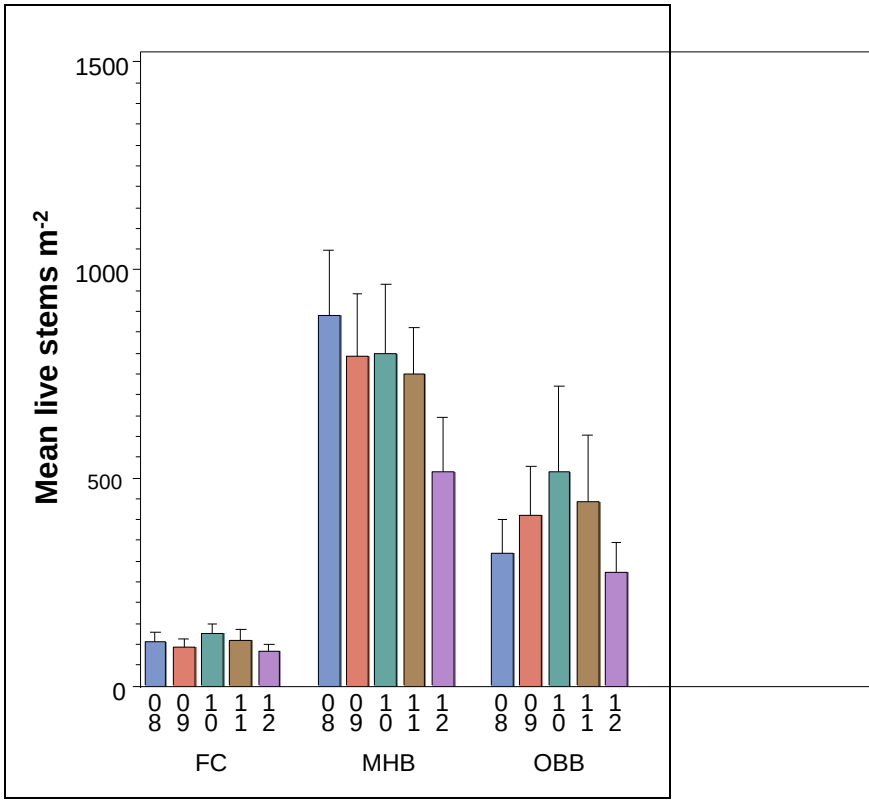

Figure ES-5. *Spartina alterniflora* live stem density in monitoring vegetation plots.

Error bars represent standard error. Sampling dates are 2008 through 2012.

Marsh Surface Elevation and Water Levels

Surface elevation tables and marker horizons were used to measure net marsh surface elevation change and sediment accretion rates at nine salt marsh sites on MCBCL between 2008 and August 2012. Three of the sites were dominated by *Spartina alterniflora* and located adjacent to the ICW, and the remaining sites were located in the NRE. Vegetation ranged from a *Spartina-Juncus* mix to *Juncus* dominated. Seven out of the nine sites showed significant increases in marsh surface elevation during the study period, with significant slopes ranging from 9 mm y^{-1} at a low-elevation *Spartina* site to 2–3 mm y^{-1} at *Spartina* and *Juncus* sites higher in the intertidal zone. Sediment accretion measured with marker horizons at the same sites was two to eight times

greater than net surface elevation change, demonstrating the importance of subsurface processes, particularly compaction, on net marsh elevation change.

Water level, temperature, and salinity were recorded at two stations for the entire 2008–2012 study period. Additional water level data were recorded from three other sites for shorter periods of time and used with the tide gauge data to determine the relationship between water level (inundation), sediment accretion, and surface elevation change. Generally, there was a non-significant relationship between inundation and marsh elevation change and accretion rate over short-term (2–4 months) intervals. Although over the long term, lower elevation sites experienced greater sediment accretion, short-term variability in suspended sediment concentration likely controlled sediment accretion and ultimately marsh elevation change.

Recommendations to Installation Managers for Coastal Wetland Ecosystems

1. MCBCL marshes are at risk both from accelerated SLR and erosion. It is important to recognize, however, that although MCBCL shoreline stabilization efforts to reduce suspended sediments loading and dissolved nitrogen inputs to the NRE result in improved estuarine water quality conditions, these same efforts may be counterproductive for marshes because they deprive marshes of the nutrients and sediments needed to thrive, particularly during a period of accelerated SLR. Given the apparent vulnerability of MCBCL coastal marshes to SLR, MCBCL Managers may want to consider adaptive management practices to conserve salt marsh habitats. Some practices include marsh restoration, particularly along shorelines; thin-layer disposal of dredge material; and possibly fertilizing marshes in the lower NRE and Onslow Beach areas.
2. Results indicate that tidal range and suspended sediment supply are important in controlling the elevation of marshes. This finding suggests that management practices that directly or indirectly affect inlet dynamics and the suspended sediment concentration of tidal waters may affect the health, productivity, and sustainability of MCBCL coastal wetlands. However, it should be noted that most of the relevant management practices are not under MCBCL control, but under the direct authority of other agencies, and may be implemented outside MCBCL boundaries. For example, ongoing dredging to realign the New River Inlet may alter tide range and suspended sediment delivery to marshes in the lower NRE, and maintenance dredging of the ICW and NRE for navigation purposes may also reduce sediment availability to the MCBCL marshes. Therefore, MCBCL Managers need to be aware of these activities and realize their implications for managing MCBCL's coastal wetlands.

Coastal Barrier Module

The Coastal Barrier Module examined the coastal barrier island ecosystem that lies at the interface between the continental shelf and the protected NRE. This barrier island ecosystem encompasses the shallow subtidal and intertidal shore face, tidal inlet, backshore beach, aeolian dune, shrub zone, maritime forest, and washover sand flat habitats. These habitats are defined by intrinsic ecological processes, but are linked by sediment transport, nutrient exchange, and biological uses, each of which undergoes substantial changes over multiple time scales. All habitat areas of the barrier, Onslow Island, were studied during DCERP1, from the New River Inlet to Browns Inlet, which encompasses approximately 12 km (8 mi) of island coastline.

The shoreline of Onslow Beach is sinusoidal, with a central headland separating two shallow, cuspate embayments. The island's morphology also varies along its length. The northern embayment has a wide beach with multiple well-developed dune ridges and is similar to other barrier islands to the northeast such as Bear Island and Bogue Banks. The central headland area has a narrow beach with a single discontinuous dune ridge less than 4 m (13 ft) in height. The beach widens significantly along the southern embayment from 20 m (66 ft) in the northeast to 80 m (262 ft) in the southwest, and the morphology of this portion of the beach is very similar to barrier islands to the south such as Topsail Island. The discontinuous dunes along the southern end are less than 2 m (6.5 ft) in height, and washover fans can be extensive and extend across backbarrier marshes. The highly variable morphology along Onslow Beach is unique; however, this allows DCERP monitoring and research results to be applicable to many other barrier islands worldwide.

The goal of the monitoring activities for the Coastal Barrier Module was to make those necessary measurements and observations that allow isolation and integration of human-derived, including MCBCL training activities, and natural processes to understand the dynamics and health of the coastal barrier ecosystem. The focus was on outputs that served to identify how those components of the ecosystem of greatest concern to MCBCL can be successfully managed and optimized. Fulfilling this goal required not only measurement of conditions and processes from physics to biology, but also analysis, synthesis, integration, and modeling of the information. To achieve these goals, the Coastal Barrier Module's monitoring program included the ocean meteorology, ocean hydrodynamics, geomorphology, sedimentology, and biology of the flora and fauna of the barrier.

Meteorology and Hydrodynamics

Seasonal winds and waves patterns were determined from data collected at offshore buoys and are important to our study because these forces affect barrier island erosion and accretion patterns (**Figure ES-6**). During winter, the strong variable winds from the northeast, northwest, and southwest and high waves from the southeast result in barrier island erosion. Winds become bi-directional during the spring, with the dominant directions of northeast and southwest. During spring, the mid-range sized waves become redistributed as the dominant wave directions are evenly distributed across the island. In summer, the barrier island accretes due to the light southeastern winds and small waves with a large spread in wave direction from the east-northeast, southeast, and southwest. During fall, there is a higher probability of storm events and a higher chance of barrier island erosion due to the return of strong northeast winds and high waves primarily from the southeast. Additionally, higher significant waves heights are recorded annually in the late fall to winter period.

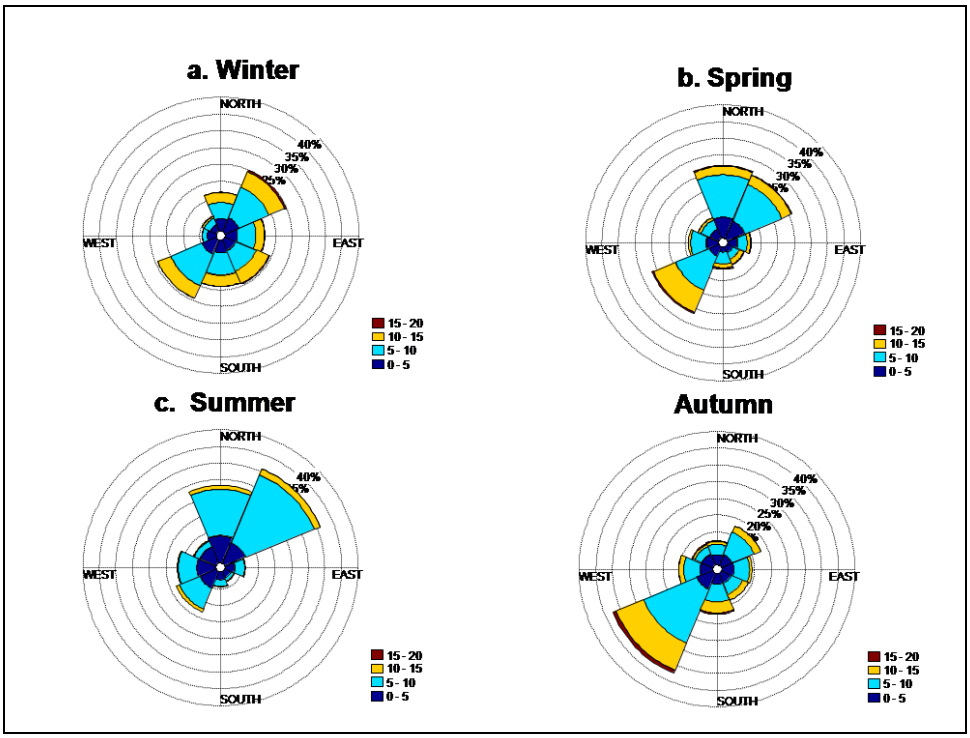

Figure ES-6. Seasonal wind roses (in m s^{-1}) for (A) winter; (B) spring; (C) summer; and (D) autumn from a NOAA buoy 25 km (15 mi) offshore.

Nearshore water velocity and water level were determined from measurements collected 500 m offshore of Onslow Beach. A strong bilateral flow component was identified that followed the along-shore orientation of Onslow Beach and an onshore presence of the flow. On an annual basis, approximately 30–40% of the total along-shore flow is towards Browns Inlet to the northeast, 20% is towards the New River Inlet to the southwest, and 10% is offshore, leaving the remaining 30–40% of flow onshore. Nearshore water levels indicated annual variations. During the summer, water levels were significantly lower in 2008 than in both 2009 and 2010. The difference the between years was approximately 20 cm (7.8 in). Annually, detided and demeaned water levels increased to a maximum during the late summer and early fall period. Part of this may be due to the steric response of the oceans to thermal heating or a combination of this in conjunction with wind directional changes.

Geomorphology

Change in the morphology of the barrier island was determined from detailed laser surveys conducted at 15 sites throughout the study period. Results indicate that Onslow Beach can be divided into three different zones, defined by distinct rates of shoreline movement, including: (1) the accreting area immediately adjacent to the New River Inlet, where the shoreline moved 30.9 to 4.3 m/y (101 to 14 ft/y); (2) the erosional southwestern portion of the island, where the shoreline moved −3.7 to −6.0 m/y (−12 to −20 ft/y); and (3) the relatively stable northeastern portion of the island where the shoreline moved 2.4 to −1.2 m/y (7.9 to −3.9 ft/y; **Figure ES-7**). The spatial distribution of these three zones does not correspond with the various military-use zones, indicating that military activities did not impact erosion rates.

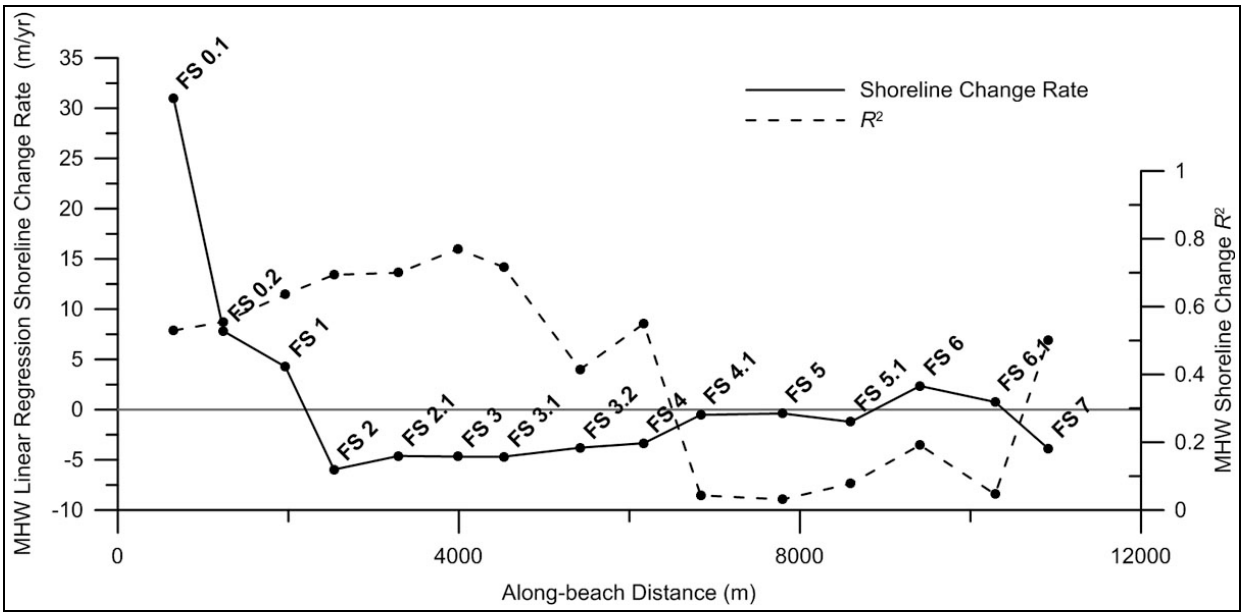

Figure ES-7. Along-beach variations in the rate of shoreline movement at Onslow Beach, NC.

Variations in the underlying geology and associated sediment availability on the inner continental shelf explain why the southwestern (sediment starved) and northeastern (sediment rich) areas of the island are erosional and accretional, respectively. Limestone exposures at the seafloor on the inner continental shelf are not an important source of sand to Onslow Beach. The area adjacent to the New River Inlet is dynamic, and the new area that formed over the past 4 years is expected to erode away during the next 4 years. The northeastern portion of the island is heavily influenced by disposal of dredged material. The irregular shape of the shoreline along the barrier island indicates that island evolution has been characterized by along-beach variations in shoreline movement over the long term (centennial to millennial time scales). The three morphologic change zones are produced by inlet influences in the southwestern portion of the barrier and variable underlying geology, which controls sediment supply to the island. The central headland is produced by a submarine rock ridge that intersects Onslow Beach. This rock ridge is composed of the Oligocene Silverdale Formation, a sandy, molluscan-mold limestone. The Quaternary sediment layer in this area is thin and patchy offshore of the central part of the island, where more than 50% of the inner shelf is exposed limestone, resulting in this portion of Onslow Beach being sediment starved. Offshore from the central and northeastern portions of the barrier, there is a 0.5 to 2.5 m–thick layer of sand, which serves as a local sediment source for the northeastern portion of Onslow Island.

Sediment Transport

Sediment texture and composition are distinct along the length of Onslow Beach. The sediment texture sampled at the erosional southwestern portion of the barrier is distinctly coarser than the sediment sampled at the northeastern end, whereas in the middle portion of the island, sediment is a mixture. These differences were consistent throughout the monitoring period and suggest that there is little exchange of sediment between the southern and northern embayments. Sand

transported along the barrier island by longshore currents is likely not moving across the headland between these two beach zones.

Sand is also transported across the barrier island from the beach to the marshes in the backbarrier and represents a source of sediment to these marshes. Our results found that the percent volume of the marsh composed of wind-driven (aeolian) sand decreases by an order of magnitude approximately 20 m (66 ft) from the marsh edge. Near the edge, the marsh contains greater than 20% aeolian sand (by volume), where it is fronted by a washover fan in the southwestern portion, or less than 10% aeolian sand, where it is fronted by a high-elevation dune ridge in the northeastern portion of the island. Further into the marsh platform, the percent volume of aeolian sand was consistently low at both sites (less than 1%). The height of beach vegetation limited or completely blocked aeolian sediment transport across the island.

Biology

The biological monitoring component of the Coastal Barrier Module measured faunal species including benthic invertebrates, surf fish, ghost crabs, sea turtles, shorebirds as well as the flora of Onslow Island. All of the faunal species monitored exhibited substantial year-to-year variation in abundance, but their life cycles enable them to have substantial resilience to environmental and anthropogenic stressors as long as habitat loss does not occur. One exception to this finding was related to ghost crab populations. Ghost crab abundances were consistently, depressed in the military training area of the island; a pattern that could not be attributed to a spatially explicit distribution of environmental factors (such as lack of habitat or unsuitable sediment type), thereby raising the possibility that some aspect of the military training activities affect ghost crab abundances.

Recommendations to Installation Managers for Coastal Barrier Ecosystems

1. Although military training continues year round on Onslow Island, the extensive training during the summer is best in terms of seasonal wind and wave climates that facilitate sediment accretion and barrier island fortitude. Additionally, MCBCL Managers should consider scheduling military training exercises after a storm to coincide with calmer wind and wave periods because the barrier island equilibrates after such an event.
2. Maintaining the current practice of keeping vehicular and pedestrian traffic off the dunes, especially in the military training zone where the shoreline is rapidly moving landward, will temper shoreline recession (erosion) rates.
3. MCBCL Managers should consider future placement of recreational infrastructure at the northeastern portion of Onslow Beach. This portion of the beach is characterized by low erosion rates, as opposed to placement in the southwestern portion of the barrier where erosion rates are higher. Additional investment in beach infrastructure (permanent structures) should be limited so that losses from future storm impacts are minimized. MCBCL Managers should note that sand placed at the northeastern end of the barrier island through dredge-spoil disposal is not transported naturally along shore past the headland and will not mitigate erosion in the southwestern portion of Onslow Island.
4. The historical MCBCL shorebird data set has both strengths and limitations. Recommendations to improve the Base’s monitoring program include consideration of conducting shorebird surveys on foot and performing targeted surveys each year for those

avian species that are listed as Candidate, Threatened, or Endangered by the federal government, and similarly as Special Concern, Threatened, or Endangered by the State of North Carolina. Targeted surveys should be stratified by key seasons.

5. MCBCL management of the endangered sea turtle populations involves relocation of nests from the military training area to areas of the coastal barrier not impacted by military training activities. Hatching success of these relocated nests are comparable to or exceed hatching success rates achieved on other North Carolina barrier islands (**Figure ES-9**).

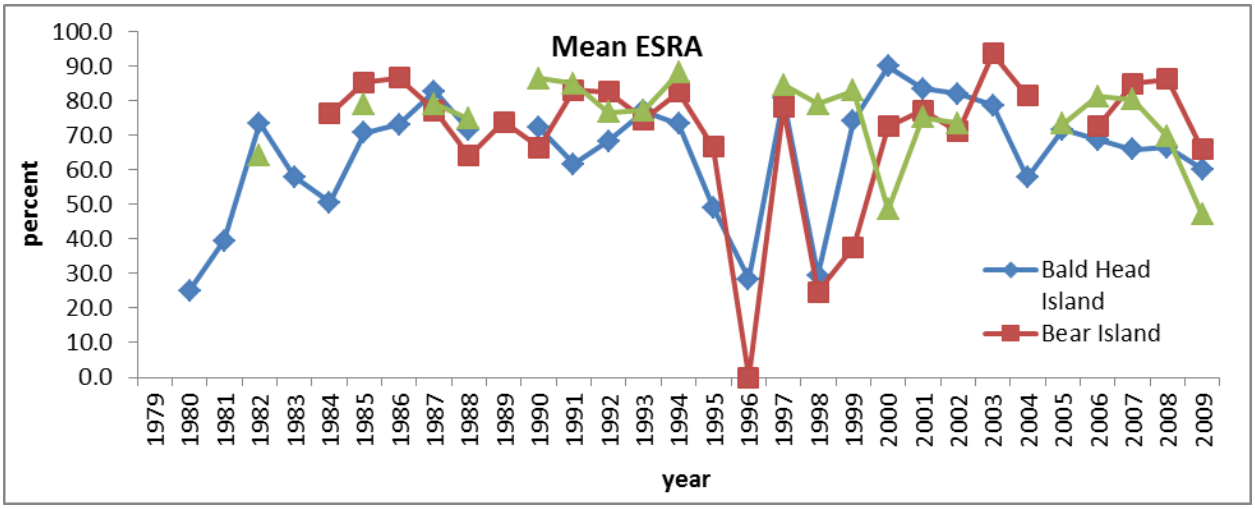

Figure ES-9. Annual mean nest success (ESRA) for Bald Head, Bear, and Onslow Islands.

All available data were used (the years when five or fewer nests were all that hatched are excluded to avoid biasing the percentages with results from very small sample sizes). Statistical analyses were restricted to years in which data were available from all three islands.

6. MCBCL Managers should continue existing practices for finding sea turtle nests, preventing egg depredation, and conducting well-timed inventories to enhance hatchling emergence success rates by freeing trapped, but live, hatchlings. However, MCBCL Managers should expect changes in the near future in nest-site selection by sea turtles because of beach landscape changes such as reduced or absent backbeach areas (leading to inundation of misplaced seaward nests) and scarped dunes, which may slough.
7. Future monitoring of sea turtle nests should record additional variables: (1) precise measurement of nest elevation and location on the beach, (2) proximity of local landscape features (e.g., vegetation, dune or scarp features to the nest, sediment type), and (3) beach width and slope. This information would improve the ability of MCBCL personnel to predict the likely fate of nests in backbeach areas subject to erosion and dune collapse.
8. Existing military training activities and practices are constrained to levels of environmental disturbance that are well within the ecosystem's range of resilience, with the exception of one species: ghost crabs, which had significantly lower populations in the military training zone. Similarly, off-road recreational vehicle (ORRV) activity and pedestrian disturbances are also well constrained. The only significant effects appear to be related to changing the spatial distribution of shorebirds on the island. However,

because several kilometers of beach are still available for bird foraging and resting areas, this displacement does not appear to have any negative effects.

9. The use of the northeastern end of Onslow Beach for disposal of dredge-spoil materials needs to be monitored and constrained. Failure to construct a typical beach profile after the dredge material has been deposited will adversely affect *Donax*, an important shorebird prey resource, and sea turtle nesting in a region of the island that is normally ideal for nesting turtles and their hatchlings. Finally, the sediments deposited by two disposal events were a good match with the existing beach sediments. Disposal of very fine or coarse dredge material on other North Carolina beaches has been shown to have substantial, long-lasting negative effects on the infaunal prey and on surf fish feeding, so MCBCL should continue to encourage disposal of only medium-grained sands to Onslow Beach or request placement of dredge materials elsewhere.
10. Comparing the patterns of distribution of the barrier island vegetation community types to studies conducted within the past two decades indicates very little change except where island transgression is occurring. Current MCBCL management practices of restricting both recreational and military traffic to well-defined corridors overall have prevented habitat loss from vehicular traffic. Recent storms and sea level anomalies have altered the structure of the beach and dunes on the southwestern end of the island, including the area where military training occurs. The absence of the backbeach area in these military training and ORRV zones, however, could lead to greater intensities of pedestrian and vehicular traffic onto and through the dunes and into the habitats behind the dunes. If the frequency and intensity of military training increases, encroachment on the near-beach vegetative communities could increase and negatively impact this community.

Terrestrial Module

The Terrestrial Module's ecosystem-based research was conducted along the gradient of vegetation from the salt marsh at the estuary margin, through brackish and freshwater marsh, to the longleaf pine (*Pinus palustris*) savannas and pocosins (i.e., shrub bogs), which dominate the upland terrestrial environments on MCBCL. Variations in the biota and ecosystem processes along this gradient are driven by variations in hydrology, soils, and fire behavior. Most of the rare species that are characteristic of coastal terrestrial ecosystems, including species of concern on MCBCL, are found in the transitional zones of these gradients. Changing patterns of land use, agriculture, and forest management have greatly altered forest ecosystems across much of the mid-Atlantic lower coastal plain. In particular, vast areas that were once dominated by open longleaf pine savanna now support closed canopy stands of loblolly pine (*Pinus taeda*) with a dense understory and midstory of broad-leaved shrubs and trees. The absence of fire on these landscapes has exacerbated this trend. This situation is typical for large portions of MCBCL. In recent years, longleaf pine restoration at MCBCL has focused on the use of understory and midstory thinning (with HydroAx equipment) to produce savanna-like conditions and allow restoration of historical fire regimes using prescribed burning.

The Terrestrial Module's monitoring program focused on two general objectives: the development of a network of permanent vegetation plots representing the full range of environmental gradients at MCBCL and a geographic information system–based assessment of

changes in land use and land cover on MCBCL lands. The network of permanent vegetation plots provided a detailed understanding of the variation in plant species diversity, composition associated with variations in soil physical and chemical characteristics, and patterns of disturbance. The vegetation monitoring plots were established across a broad range of stand characteristics, particularly those that are of greatest interest to MCBCL management. Forest types include both longleaf and loblolly pine forests across a wide range of age classes, edaphic properties, and disturbance histories. Significant data were also collected on high pocosin systems, which cover much of the installation.

Overall Patterns of Terrestrial Plant Species Composition and Diversity on MCBCL

More than 600 individual plant taxa were found among the 131 vegetation plots distributed across MCBCL. The vegetation plots had an average species richness of 41.6 species per 0.1 ha. The range of species richness among plots was large, with as few as nine species per 0.1 ha in a pocosin stand to as many as 119 species per 0.1 ha in a longleaf pine stand. MCBCL terrestrial vegetation composition and diversity vary in response to two major environmental gradients: near coastal ecosystems, which have a salt spray gradient, and inland terrestrial forests, which have a hydrologic gradient. Near coastal ecosystems (within 1 km [0.62 mi] of the coast) vary from dune to maritime scrub and are heavily influenced by the effects of salt spray. Inland, terrestrial forests vary along a gradient from well-drained soils dominated by longleaf pine to broad-leaved hardwoods and depression wetlands on soils that are not well drained. Loblolly pine (*Pinus taeda*) forests composition and diversity is generally intermediate to longleaf pine forests and broadleaved hardwoods. Species richness was notably lower in pocosin sites than in any other forest type. Soil bulk density was highly correlated with soil organic matter and cation exchange capacity. Thus, soil bulk density is a relatively good proxy for a variety of soil characteristics, and it can be easily measured.

Experimental treatment plots used during Research Project T-1 were included with these 131 sample plots, and analysis of these plots provided a context for understanding the vegetation and environmental gradients across which terrestrial research studies were conducted.

Indicator species analysis identified species that were abundant and concentrated in each forest type. The high number of indicator species in the longleaf pine forest, depression wetlands, coastal dune, and hardwood forest types was a reflection of the unique features of their respective environments and the relative absence of disturbance. The fact that only a single species (i.e., black gum [*Nyssa sylvatica*]) had a significant indicator value for loblolly pine stands was probably indicative of the history of disturbance in these forests and the wide range of conditions over which they occurred.

Patterns of Terrestrial Plant Species Composition and Diversity in Pine-Dominated Ecosystems

In pine-dominated vegetation monitoring plots, a total of 357 taxa were identified. Species richness was highest in longleaf pine stands and lowest in pocosins. Species composition varied in pine-dominated stands in relation to soil and disturbance gradients. Longleaf pine stands occur on soils with high bulk density and low organic matter, and pocosins dominate where bulk density is low and organic matter is high. Loblolly pine stands segregated from longleaf and pocosin stands based on land-use history and the past exclusion of fire. Plant species richness is

markedly lower in disturbed loblolly pine stands than in longleaf pine stands with similar soil conditions.

Changes in Species Composition and Diversity in Longleaf Pine Stands from 1991 to 2010

Twenty-one mature longleaf pine plots were deliberately selected for sampling in DCERP1 because they were previously sampled by the CVS in 1991. This provided the opportunity for the direct evaluation of change in these stands over an 18-year period when MCBCL Managers implemented a 3-year rotation prescribed burning program in these stands. At all spatial scales, from 1 m^2 to 0.1 ha, species richness increased among these 21 longleaf pine plots (**Table ES-1**). The increase in species richness at smaller spatial scales is a favorable indicator of successful restoration in longleaf pine stands and is likely a consequence of regular prescribed burning. The increase in richness was remarkably consistent across the 21 sample plots; the number of species per 0.1 ha increased in 19 plots and remained unchanged in the other two plots. Stands that, based on species composition, appeared to have been disturbed in 1991 had species compositions in 2009 more indicative of undisturbed conditions.

Table ES-1. Mean species richness among 21 permanent plots sampled in 1991 and 2009

Area	Number of Species in 1991	Number of Species in 2009	p Value
0.1 ha	52	58	<0.0001
400 m^2	46	51	<0.0001
100 m^2	31	36	<0.0001
10 m^2	18	21	<0.0001
1 m^2	10	11	<0.04

The p value indicates the probability that differences between sample dates are random.

Greenness Change Analyses

Changes in land-cover types and vegetation greenness gain and loss were also determined using cloud-free Landsat Thematic Mapper images from 1984, 1990, 1998, 2005, 2007, 2009 and 2011. The 1984 image was used as the baseline, and change between subsequent images was determined from this baseline image to determine persistence of change and to reduce variability. Therefore, differences were tracked through all six change periods from 1984 to 2011. Overall, MCBCL experienced a 7.2–10.6% permanent vegetation loss between 1984 and 2009; however, up to 37.8% of the vegetation on MCBCL was reduced or removed at some time during this period. For the most recent change analysis period (2009–2011), 1.7% of the surface area of MCBCL lands experienced significant loss or removal of vegetation in concentrated areas, likely representing new infrastructure construction (**Figure ES-11**). In comparison, based on the 1984–2009 individual change period, between 3.9–10.3% of MCBCL lands have experienced a "persistent" gain in vegetation since 1984. In comparison, during this same period, 3.5% of MCBCL lands have experienced a "persistent" gain in vegetation. Although the Greater Sandy Run Area (GSRA) represents only 33% of the area of MCBCL lands, it accounted for 65–75% of

the permanent greenness gain. The re-growth in the GSRA follows clear-cutting performed by a paper company, which owned this land before it was acquired by MCBCL.

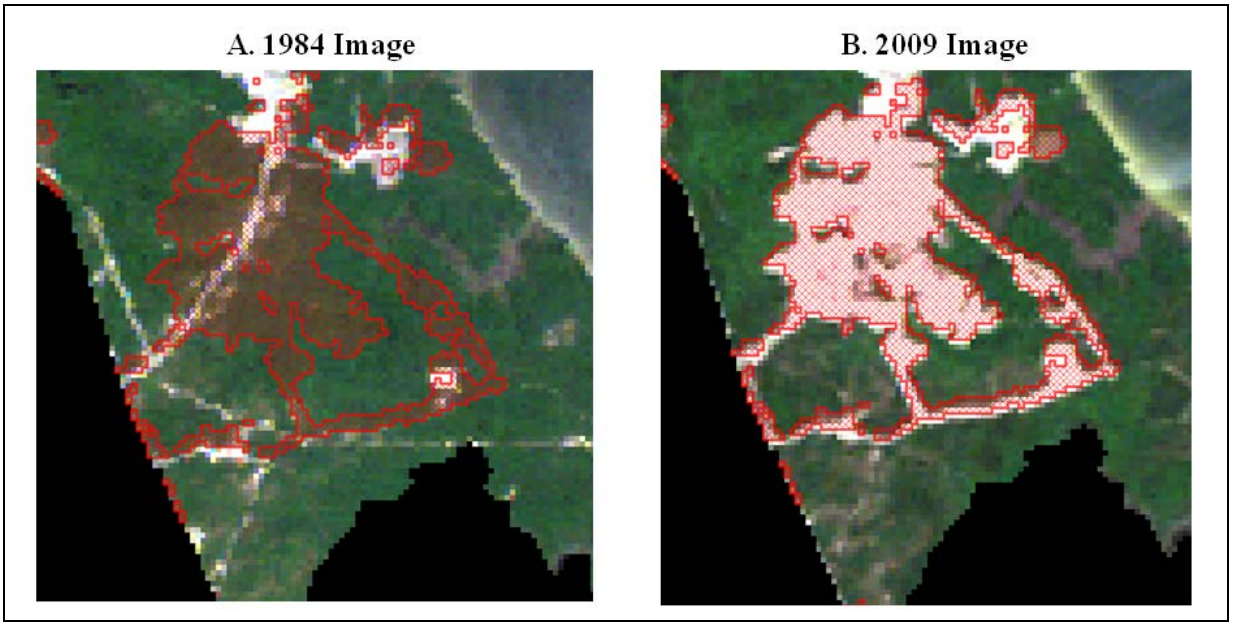

Figure ES-11. New Rifle Range, MCBCL.

Greenness loss patch from 1984–2009 change period depicted over the (A) 1984 and (B) 2009 Landsat Thematic Mapper images.

Recommendations to Installation Managers for Terrestrial Ecosystems

1. Future sampling of the network of permanent vegetation plots across MCBCL will provide important information on vegetation change in response to anthropogenic and natural drivers. Analysis of the 21 longleaf pine plots sampled in both 1991 and 2009 support the value of such longitudinal studies and the assertion that current MCBCL forest management practices (e.g., prescribed burning) are meeting MCBCL restoration objectives.
2. MCBCL Managers can use results of indicator species analysis as a basis for identifying a subset of floral indicator species upon which future vegetation plot sampling can be focused. Use of these floral indicator species should simplify sampling procedures and reduce installation sampling costs.
3. The greenness change analysis could be used by MCBCL Managers to evaluate the distribution of land disturbance across MCBCL. This information could be useful in siting of future development on Base lands or comparing impacts from different building scenarios.

Atmospheric Module

The input of nutrients and potential pollutants via atmospheric deposition interacts with most key terrestrial and aquatic ecological processes occurring at MCBCL. Atmospheric deposition is a direct source of inputs onto the open-water surfaces of the aquatic ecosystem and onto the vegetation surfaces of the terrestrial ecosystem, with the frequency, level, and composition of

these inputs posing an important influence on flora diversity. In addition to direct sources of atmospheric input, the aquatic ecosystem is impacted by atmospheric deposition after it is filtered and altered by passage through the terrestrial ecosystem. Similarly, terrestrial ecosystem impacts might be due to exposure to a complex combination of long-term climatological stress (e.g., temperature, drought) and shorter term air pollutant stress (oxidants and metals).

Fire is a natural part of the terrestrial landscape in the southeastern United States in general and MCBCL in particular. MCBCL Managers use prescribed burning to reduce wildfire risk, maintain training areas, and restore habitat for the federally protected RCW. Despite these benefits, prescribed burning is a major source of $PM_{2.5}$ (fine particulate matter) and other air pollutants because of its incomplete and largely uncontrolled combustion process, which involves flaming and smoldering phases with different effective fuel consumption. Certain fuel and fire meteorological parameters influence the emissions from the different combustion phases of prescribed burning. Coarse particles (PM_c) in the size fraction between 2.5 and 10 µm receive special attention because gravitational settling accelerates their deposition to the surrounding aquatic and terrestrial surfaces. One of the most important PM_c–enhancing factors is the proximity of MCBCL to the Atlantic Ocean, which provides an environment conducive to sulfate formation. Another PM_c–enhancing factor is the reaction of nitric acid with sea-salt aerosol to form coarse-mode sodium nitrate particles, potentially increasing the PM_c mass.

The objective of the Atmospheric Module's monitoring program was to characterize the role of air quality in the natural ecosystem of MCBCL by capturing meteorological and climatological processes and their occurrence in different spatial and temporal scales in support of various DCERP1 research activities. To track and compare meteorological and air pollution trends observed on MCBCL in the context of more regional trends, the network of on-Base monitoring sites was expanded. In addition, procedures were developed for merging data from two major regional networks (i.e., MesoWest and the North Carolina Department of Environment and Natural Resources) into a common and consistent time base (hourly averages) for all acquired parameters. Three on-Base sites began acquiring data in March 2008 that consisted of various meteorological parameters (including photosynthetically active radiation, wind speed and direction, air temperature, and rainfall) and monitoring the concentrations of particulate matter ($PM_{2.5}$ [fine particulate matter], PM_{10} [coarse particulate matter]), and ozone. In October 2010, two additional PM monitoring sites were added on MCBCL to increase spatial resolution in tracking on- and off-Base pollution sources. The reporting of merged quality controlled data from four on-Base sites and a total of nine off-Base sites started in July 2008 and continued until September 2011.

Precipitation

The study domain (four on-Base and nine off-Base monitoring sites) experienced general drought conditions during the study period (2008–2011), except for at a few locations where episodic events added large rainfall amounts during storms. Annual average rainfall amounts consistently decreased along the inland gradient across the larger study domain; however, rainfall amounts did not vary significantly across the local MCBCL landscape.

Ozone

MCBCL lands received the highest average ozone concentration from a southeasterly direction, pointing to effects from photochemical production of ozone in maritime air masses transported by sea breezes. Typically, ozone concentrations were highest near the beach and decreased moving inland toward the City of Jacksonville. Over the past 10 years, ozone levels declined steadily across the region, which was in line with the nationwide trend. The only anomaly in season trends occurred in 2009 when summer ozone formation was slightly higher mainly due to the unusually warm and dry weather conditions in early spring that were favorable to the photochemical production of ozone.

Although the local (on-Base) ozone measurement methodology was not intended to meet regulatory requirements, the metrics employed by the U.S. Environmental Protection Agency (EPA) were applied here as a basis for site comparison of air quality. EPA set two types of air quality standards for ground-level ozone: (1) a primary standard to protect public health, and (2) a secondary standard to protect public welfare, including protection against visibility impairment and damage to building, animals, crops, and vegetation. The secondary standard was used to determine whether vegetation across MCBCL lands was stressed by ozone. Beginning May 27, 2008, the 3-year average ozone design value must not exceed 75 ppb to be considered in attainment. This design value was lowered to 70 ppb in January 2010. Ozone concentrations at the two ground-level MCBCL monitoring sites (NRA and RIP in **Figure ES-12**) were below the 70 ppb standard from 2008–2011. Ozone concentrations at MCBCL during this time, therefore, were not of concern for causing damage to vegetation and no visible signs of vegetation damage were noted on MCBCL lands.

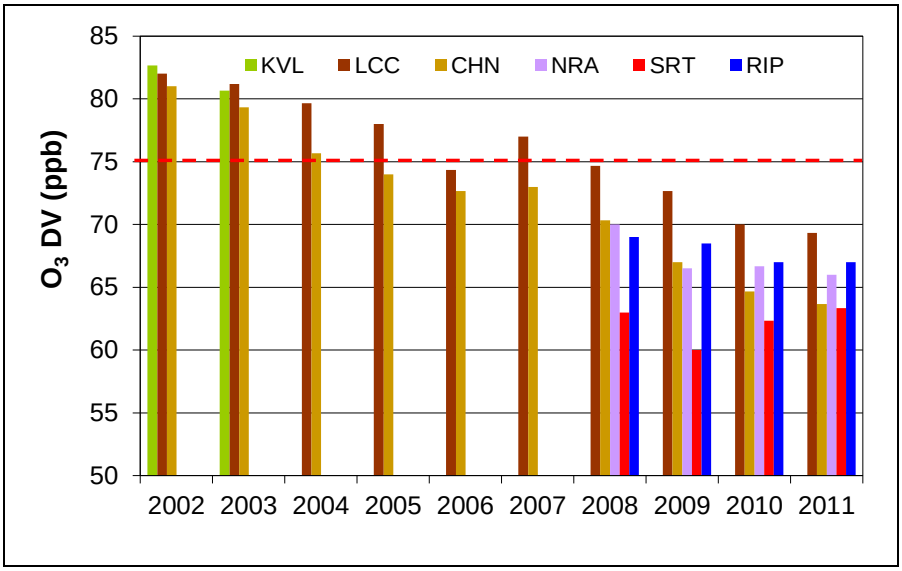

Figure ES-12. Regional comparison of ozone (O_3) design values (DVs) to meet the primary NAAQS from 2002 to 2011.

Particulate Matter

The monitoring approach used allowed the measurement of PM_c from the PM_{10}–$PM_{2.5}$ difference. High-resolution data of simultaneously measured $PM_{2.5}$ and PM_c provide powerful diagnostics into potential sources and source impact processes causing local air pollution. $PM_{2.5}$

levels decreased steadily during the past 10 years (2001–2011). Based on data from off-Base monitoring sites to the southwest and to north of MCBCL, the regional airshed exhibited a trend of increasing $PM_{2.5}$ levels with increasing distance from the coast. This trend correlated with a regional trend of decreasing amounts of rainfall away from the coast because rainfall is the most effective sink for atmospheric $PM_{2.5}$.

Across MCBCL, $PM_{2.5}$ was lowest at the beach and increased farther inland, likely resulting from the addition of $PM_{2.5}$ from residential heating and wood burning in urban areas, especially during winter. The $PM_{2.5}$:PM_c ratio at the New River Air Station (NRA; the on-Base monitoring site farthest away from the coast) was highest in most seasons, especially for air mass transport from northerly and northeasterly directions, which included the major traffic corridor (**Figure ES-13**). For periods when smoke-laden air masses blew into MCBCL from the southwest, both $PM_{2.5}$ and PM_c were elevated. However, results indicated that wildfire smoke emissions contained substantially more $PM_{2.5}$ than PM_c. Smoke plume encounters in winter and early spring yielded an average $PM_{2.5}$:PM_c ratio lower than the maritime background. In contrast, smoke plume encounters in late spring and summer, suggested that these PM_c–enhancing processes from the maritime air were being overwhelmed by fire emissions and new particle formation processes driven by reactive precursor gases and semi-volatile aerosol species emissions. At all sites, but especially the ones on Base, the $PM_{2.5}$ measurements indicated a regional character that was distinctly less homogeneous than that for ozone, pointing to a greater influence of primary emissions sources (for example, military vehicle emissions or prescribed burning) on local MCBCL conditions.

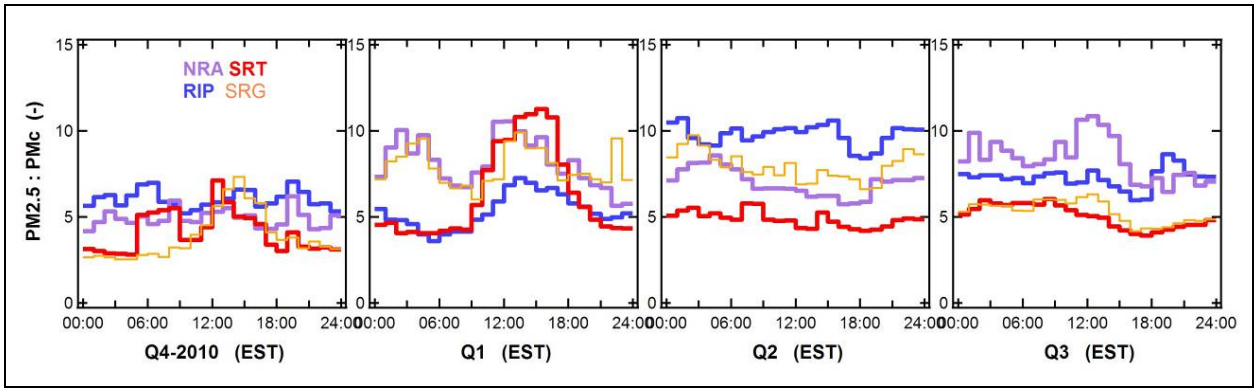

Figure ES-13. Seasonally averaged diurnal profiles of $PM_{2.5}$:PM_c ratio in 2010–2011.

Recommendations to Installation Managers for Atmospheric Systems

1. The bulk of MCBCL–managed forest area receives prescribed burning during the dormant season (from December through March). Based on monitoring results, it appears to be critically important to avoid summer-time wildfires due to their potential for causing significant increases in local and regional ozone and $PM_{2.5}$ levels. Therefore, MCBCL Forest Managers should continue the practice of dormant season prescribed burning to remove unwanted fuel and prevent fuel accumulation in areas prone to wildfires.

Next Steps

DCERP1 concluded in January 2013. The next 5 years of the program (referred to as DCERP2) began in November 2012. Many of the DCERP1 research and monitoring activities will continue into DCERP2 by building on the knowledge gained over the past 5 years. During a 3-month planning period, the DCERP Team will prepare a new Monitoring Plan for the program that focuses on supporting research efforts on several new themes. These themes are evaluating the carbon cycle of the estuary, coastal marshes, and the barrier island; identifying the impacts of climate change on physical, chemical, and biological processes in ecosystems of MCBCL; and providing tools and other products that can be easily transferred to or used by MCBCL, other DoD installations, and other stakeholders. Monitoring will be continued by the Aquatic/Estuarine and Coastal Wetlands Modules as part of DCERP2. Monitoring activities will be conducted by these modules because the monitoring data are needed to measure both the variability associated with large episodic events and the smaller, long-term changes in some ecological processes and to compare these changes to difference with baseline conditions first measured in DCERP1.

The Data and Information Management System developed during DCERP1 will continue to provide support to all modules by capturing and archiving all DCERP1 and DCERP2 final data and products. To turn science into practice, a Web-based Decision-Support System framework (based on a prototype system developed during DCERP1) will be implemented to support tools and models that inform installation management decisions. This framework will be used for hosting all of the DCERP2 decision-support tools and models developed for easy access by researchers, DoD installation personnel, and other interested scientists and stakeholders. These tools and models will provide capabilities to project how changes in key parameters can impact ecosystem processes today and how changes in key parameters can impact ecosystem processes under future climate change conditions using scenarios testing.

[This page intentionally left blank.]

Chapter 1

Introduction

SERDP Project Number: RC-1413

Principal Investigator:
Dr. Patricia Cunningham
RTI International
Research Triangle Park, NC 27709
E-mail: patc@rti.org

June 27, 2013

Final

This report was prepared under contract to the U.S. Department of Defense (DoD) Strategic Environmental Research and Development Program (SERDP). The publication of this report does not indicate endorsement by DoD, nor should the contents be construed as reflecting the official policy or position of DoD. References herein to any specific commercial product, process, or service by trade name, trademark, manufacturer, or otherwise, do not necessarily constitute or imply its endorsement, recommendation, or favoring by DoD.

Table of Contents

List of Acronyms v
Introduction 1
Background 1
Site Selection for DCERP 1
Integration of DCERP with MCBCL's Natural Resources Management 3
Program Organization 4
DCERP Management 4
DCERP Team 5
Overarching DCERP Strategy 6
DCERP Research Strategy 8
Research and Monitoring 11
Research Projects 11
Integration of DCERP Research and Monitoring 13
Report Organization 15
Literature Cited 16
Appendix 1-A: Prioritized List of MCBCL's Conservation and Water Quality Needs 1-A-1

List of Figures

1-1. Site map of MCBCL. 1-2

1-2. Organization of DCERP. 1-5

1-3. Overall DCERP process. 1-8

1-4. Overarching conceptual model for DCERP at MCBCL. 1-10

1-5. Generic roadmap of the integrated DCERP Baseline Monitoring Plan and *DCERP Research Plan* and the development of model tools and indicators. 1-14

List of Tables

1-1. MCBCL–Specific Military Drivers 1-3

1-2. Examples of Military, Non-Military, Legacy, and Natural Stressors to an Ecosystem 1-9

1-3. Summary of the 13 Research Projects of DCERP 1-11

1-4. Summary of Module-Specific DCERP Baseline Monitoring Program Activities 1-13

List of Acronyms

AE	Aquatic/Estuarine Module
Air	Atmospheric Module
CB	Coastal Barrier Module
CW	Coastal Wetlands Module
CWA	Clean Water Act
DCERP	Defense Coastal/Estuarine Research Program
DCERP1	first cycle of the Defense Coastal/Estuarine Research Program
DCERP2	Second cycle of the Defense Coastal/Estuarine Research Program
DIMS	Data and Information Management System
DoD	U.S. Department of Defense
EMD	Environmental Management Division
ESA	Endangered Species Act
INRMP	*Integrated Natural Resources Management Plan*
MCBCL	Marine Corps Base Camp Lejeune
NAVFAC ESC	Naval Facilities Engineering Command/Engineering Service Center
NRE	New River Estuary
OSC	On-site Coordinator
PI	Principal Investigator
PNA	Primary Nursery Area
RCC	Regional Coordinating Committee
RCCC	Resource Conservation and Climate Change (Program)
SERDP	Strategic Environmental Research and Development Program
RCW	red cockaded woodpeckers
T	Terrestrial Module
TAC	Technical Advisory Committee

[This page intentionally left blank.]

Introduction

The overall intent of the Defense Coastal/Estuarine Research Program (DCERP) "is to develop the knowledge required to assess the interaction between military activities and ecological resources in a coastal/estuarine setting, monitor those interactions, and identify adaptive, ecosystem management approaches for sustainment of military lands and adjacent waters," as stated in the initial *DCERP Strategy Report* (SERDP, 2005). The purpose of this *DCERP1 Final Monitoring Report* is to summarize the DCERP monitoring activities and results from July 2007 to October 2012.

Chapter 1 of this *DCERP1 Final Monitoring Report* provides a general introduction to DCERP conducted at Marine Corps Base Camp Lejeune (MCBCL) in North Carolina, briefly highlights the overall program objectives, and describes the activities conducted during Phases I and II of the program. Chapter 1 also describes how the DCERP Team engaged with other team members and MCBCL staff during DCERP1's initial planning period (i.e., Phase I) from November 2006 to June 2007 to develop three key documents to guide implementation of DCERP. These documents are the overarching research strategy (the *DCERP Strategic Plan* [RTI, 2007a]), the design of an ecosystem-based monitoring program (the *DCERP Baseline Monitoring Plan* [RTI, 2007b]), and the identification of detailed research projects (the *DCERP Research Plan* [RTI, 2007c]). This chapter also discusses another Phase I activity, the development of the Data and Information Management System (DIMS) design for the program.

Chapter 1 also highlights the activities slated during the program's subsequent implementation period (i.e., referred to as DCERP1 Phase II from July 2007 to January 2013). For instance, during Phase II, the team members carried out the *DCERP Baseline Monitoring Plan* through the operation of the long-term baseline monitoring program. The Baseline Monitoring Plan was also implemented through the collection, management, analyses, and archiving of data into the DCERP DIMS. Although some of the baseline monitoring activities concluded in November 2011, other baseline monitoring activities continued through 2012 to provide continuity with the second cycle of DCERP (referred to as DCERP2) which is planned for implementation from February 1, 2013, through October 31, 2017.

Background

Site Selection for DCERP

Critical military training and testing on lands along the nation's coastal and estuarine shorelines are increasingly placed at risk because of development pressures in surrounding areas, impairments due to other anthropogenic disturbances, and increasing requirements for compliance with environmental regulations. The U.S. Department of Defense (DoD) intends to enhance and sustain its training and testing assets and to optimize its stewardship of natural resources through the development and application of an ecosystem-based management approach on DoD facilities. DoD's policy has established ecosystem-based management as the preferred approach for military lands (Goodman, 1996). This approach will focus on sustaining and enhancing military training and testing activities by monitoring and managing the interdependent natural resource assets on which the future of these activities depend. To expand its commitment

to improving military readiness while demonstrating the science behind this approach, the Strategic Environmental Research and Development Program (SERDP) has made a commitment of at least 10 years to fund research and monitoring projects that support the sustainability of military training and testing in ecologically and economically important ecosystems. To accomplish this goal, SERDP launched DCERP at MCBCL in North Carolina (**Figure 1-1**).

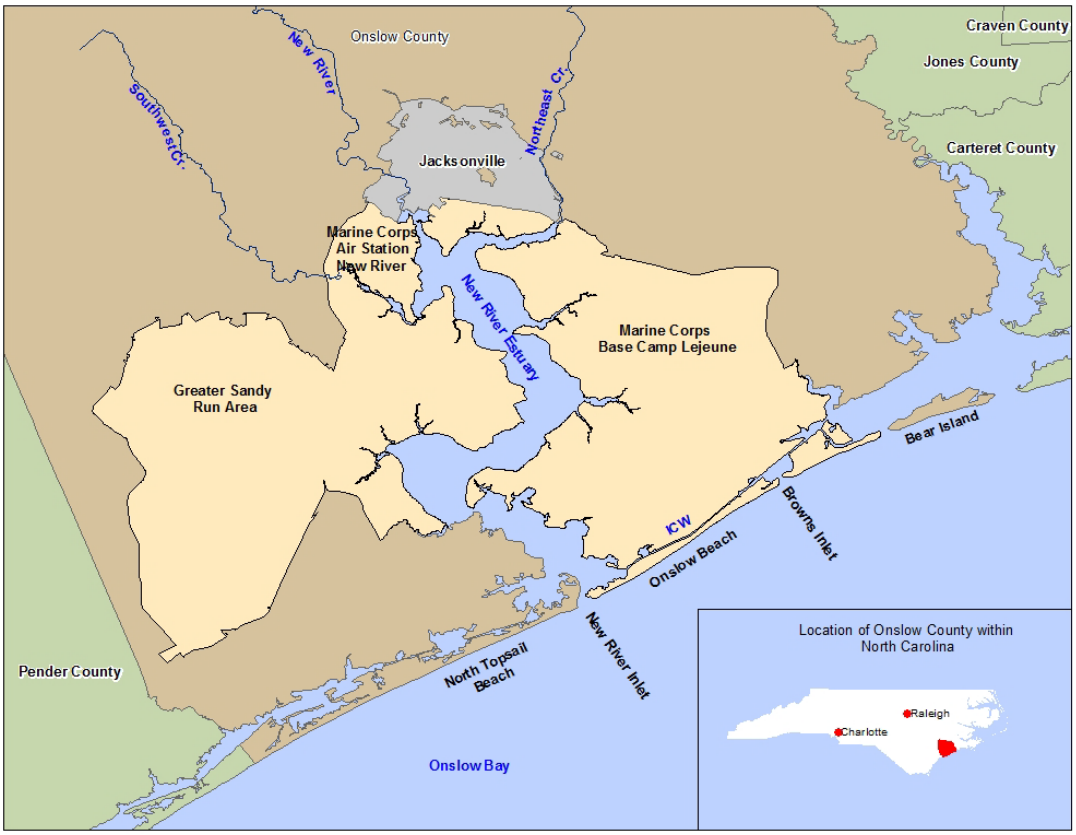

Figure 1-1. Site map of MCBCL.

As a U.S. Marine Corps installation, MCBCL has a single and exclusive mission: military preparedness. MCBCL provides an ideal platform for DCERP because it integrates aquatic/estuarine, coastal wetlands, coastal barrier, and terrestrial ecosystems, all within the boundaries of DoD properties.

MCBCL was chosen as the DCERP site for a variety of reasons, including the following:

- The New River Estuary (NRE) watershed, which borders the site, is relatively small and, therefore, a manageable study site.
- MCBCL occupies a substantial portion (approximately 80%) of the NRE shoreline.
- A barrier island and coastal dune system occurs within MCBCL's boundary that provides a unique amphibious assault training environment.
- The variety of ongoing military operations at MCBCL enables researchers to examine training impacts on a broad range of ecosystems, from upland pine savannas to aquatic and estuarine waters to coastal barriers.

Integration of DCERP with MCBCL's Natural Resources Management

MCBCL's mission is to provide military training that promotes the combat readiness of operating forces, and all MCBCL natural resources management activities on the Base must support this mission. As a military installation, MCBCL has needs, or drivers, that must be satisfied to meet its readiness mission to continue without significant disruption. MCBCL must also comply with related environmental laws and regulations, such as the federal Endangered Species Act (ESA) and the Clean Water Act (CWA), to ensure continuance of its mission. To ensure such compliance, MCBCL developed and adopted an *Integrated Natural Resources Management Plan* (INRMP; MCBCL, 2006a), which outlines the Base's conservation efforts and establishes procedures for fiscal years 2007 through 2011. One goal of the INRMP is to minimize future training restrictions (i.e., no net loss in the ability to train) by increasing the integration between natural resources management planning, training, and operations. One of DCERP's objectives is to assist MCBCL in achieving this goal. As such, MCBCL's natural resource and environmental management personnel were involved throughout the DCERP planning process by participating in all planning workshops and reviewing the *DCERP Strategic, Research, and Baseline Monitoring Plans* that were the final products from Phase I.

Unique to MCBCL are installation-specific drivers that are defined by the Base's mission and geographic location, land uses to support the mission, and natural resources affected by the mission. Identifying the primary military drivers at the MCBCL provided the basis for establishing seven natural resources management objectives for the Base. The objectives are presented in **Table 1-1**.

Table 1-1. MCBCL–Specific Military Drivers

Driver 1	Preserving the integrity of the amphibious maneuver areas, including Onslow Bay, the NRE, and the adjoining training areas and airspace of the MCBCL
Driver 2	Preserving the integrity of MCBCL as a combined-arms training Base by ensuring the continued viability of its impact areas and associated training ranges
Driver 3	Enhancing future training uses of MCBCL ranges, training areas, and airspace by fully integrating the Land Use Master Plan (MCBCL, 2005) and Range Transformation Plan (MCBCL, 2006b)
Driver 4	Ensuring that MCBCL supports all required military training activities, while complying with the ESA and other wildlife requirements
Driver 5	Ensuring that MCBCL supports continued military training use of the NRE and Onslow Bay, while complying with the CWA
Driver 6	Ensuring the viability of the New River Air Station as an aviation facility through the elimination of bird and wildlife strike hazards to aircraft, while complying with the ESA and other wildlife regulatory requirements
Driver 7	Ensuring the viability of MCBCL military training activities, while supporting mission-critical infrastructure development

In addition to these military drivers, MCBCL natural resources management staff identified a prioritized list of conservation and water quality needs that will support implementation of the INRMP (**Appendix 1-A**). Throughout DCERP, every effort was made to include the Base's

areas of concern that were not currently being investigated under existing programs and to inform Base staff of DCERP activities and results.

Program Organization

DCERP is a collaborative effort between SERDP, the Naval Facilities Engineering Command/Engineering Service Center (NAVFAC ESC), MCBCL, and RTI International, which is headquartered in Research Triangle Park, NC. RTI led the DCERP research and monitoring effort at MCBCL and assembled a diverse team of experts from several federal agencies, academia, and the private sector (henceforth referred to as the DCERP Team). The Management Team and the Research Team are discussed in the following two subsections.

DCERP Management

SERDP is an environmental research and development program that is planned and carried out by DoD in full partnership with the U.S. Department of Energy and the U.S. Environmental Protection Agency. The SERDP Resource Conservation and Climate Change (RCCC) Program Manager, Dr. John Hall, ensured that DCERP activities provide for the enhanced knowledge of ecosystem and military interactions within approved scopes of work and budgets. The overarching federal management for DCERP was assigned to the NAVFAC ESC. Dr. Hall served as the Contracting Officer's Representative. In that capacity, he ensured that tasks identified in the Statement of Work were properly performed by the DCERP Principal Investigator (PI), Dr. Patricia Cunningham of RTI. The DCERP PI was responsible for the overall scientific quality, cohesiveness, and relevance of DCERP monitoring and research activities. The DCERP PI was also the primary point of contact for SERDP and MCBCL and coordinated all DCERP activities conducted at MCBCL through the DCERP On-site Coordinator (OSC), Dr. Susan Cohen.

At MCBCL, the DCERP OSC, the Director of the Environmental Management Division (EMD; Mr. John Townson), and the Head of the Environmental Conservation Branch (Mr. Bill Rogers) assisted the DCERP PI with coordinating the environmental monitoring and research activities on the Base. The DCERP OSC was the primary point of contact between MCBCL and the DCERP Team.

Two committees provided guidance and input to the DCERP. The first, the Technical Advisory Committee (TAC), was a group of discipline experts from academia, industry, government, and the military that was assembled by the DCERP OSC to provide scientific and technical review and guidance to ensure the quality and relevance of DCERP. The second committee, the Regional Coordinating Committee (RCC), was a group of local and regional stakeholders that served as one of the recipients of outreach from MCBCL, the DCERP PI, the DCERP OSC, and the SERDP RCCC Program Manager, thereby fostering relationships among the representative organizations and DCERP.

Figure 1-2 illustrates the program's overall organization and lines of communication.

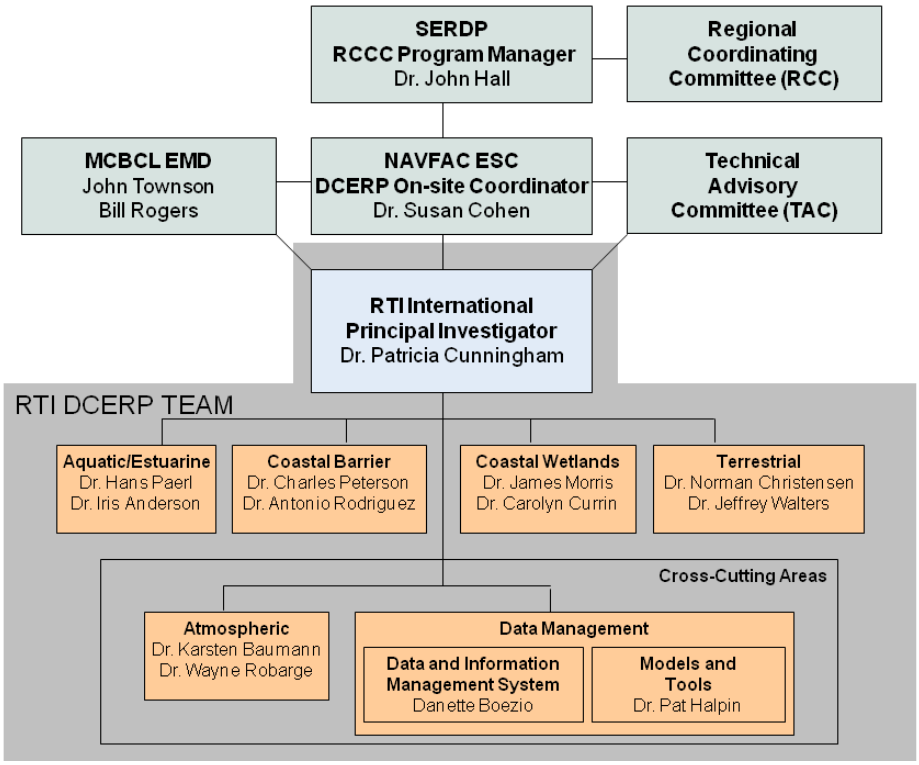

Figure 1-2. Organization of DCERP.

DCERP Team

RTI selected members of the DCERP Team because of their expertise in relevant environmental science disciplines and substantial experience in working together on interdisciplinary aquatic/estuarine, coastal, and terrestrial ecosystem projects. The DCERP Team included the DCERP PI, other environmental scientists from RTI, and researchers from seven academic institutions, three governmental agencies, and two private companies.

DCERP Team

RTI has assembled a diverse team of researchers from the following organizations, collectively referred to as the DCERP Team:

- Atmospheric Research and Analysis, Inc.
- Duke University
- National Oceanic and Atmospheric Administration
- North Carolina State University
- Porter Scientific, Inc.
- RTI International
- University of Connecticut
- University of North Carolina at Chapel Hill
- University of South Carolina
- U.S. Army Corps of Engineers
- U.S. Geological Survey
- Virginia Institute of Marine Science
- Virginia Tech

The DCERP Team was organized into six Module Teams based on the ecosystem-based management objective for the program. Each Module Team was directed by a Module Team Leader and Co-Leader. The DCERP PI and the Module Team Leaders and Co-Leaders composed an Executive Board, which provided input on technical decisions and helped prioritize program needs such as identifying areas of knowledge needing supplemental research and funding support. These Module Teams conducted monitoring and

research activities for DCERP's five ecosystem modules (i.e., Aquatic/Estuarine, Coastal Wetlands, Coastal Barrier, Terrestrial, and Atmospheric) and a Data Management Module.

The DCERP Team addressed the initial DCERP objectives of developing monitoring approaches and identifying key ecological processes through research and modeling studies, all with the goal of supporting the practice of ecosystem-based management for all coastal DoD installations in similar ecological settings.

Overarching DCERP Strategy

DCERP's primary overarching objective was to enhance and sustain MCBCL's military training mission by developing an understanding of estuarine, coastal wetlands, coastal barrier, and terrestrial ecosystem composition, structure, and function within the context of a military training environment. Specific DCERP objectives were to

- Develop the *DCERP Strategic Plan* (overarching strategy) that includes appropriate conceptual and mechanistic ecosystem models to guide monitoring, research, and adaptive management (Phase I)
- Identify significant ecosystem stressors[1] (i.e., military, non-military, legacy, and natural), their sources (on and off Base), and their level of impact on MCBCL's ecological systems through space–time coordinated monitoring and research (Phase II)
- Incorporate information about stressors and other environmental factors into ecosystem models to develop effective indicators of potential changes to ecosystem condition and state, which may require more effective management guidelines to achieve sustainability (Phase II).

During the planning period (Phase I), the DCERP Team designed an integrative monitoring, modeling, and research strategy for MCBCL that is consistent with guidance on ecosystem-based management from the Ecological Society of America (Christensen et al., 1996) and recommendations of the U.S. Commission on Ocean Policy (2004), including principles of adaptive management (Walters, 2001). This strategy transcended air–land–water boundaries to better understand the causes and nature of ecological and environmental changes across the region and locally at MCBCL. Based on interconnectivity, this strategy helped separate the underlying natural (e.g., climatic, biogenic) and anthropogenic–regional processes from locally driven processes, identify stressor-specific indicators of ecosystem status that provide early warnings of ecosystem degradation, and specify the critical thresholds for indicators of potential state shifts that could threaten sustainability. DCERP adapted the following elements of ecosystem-based management described by Christensen et al. (1996):

- ***Sustainability***—The underlying premise is that military usability will persist indefinitely under a well-conceived ecosystem-based management plan.

[1] For DCERP, stressors are defined as activities or events that alter natural ecological processes. Natural ecosystem stressors include natural forces (e.g., hurricanes, sea level rise) whose effects are enhanced by anthropogenic activity (e.g., global warming). The increased frequency and intensity of natural events, in combination with anthropogenic contributions, could cause ecosystem perturbations outside the range of natural variation.

- ***Explicit goals***—Ecosystem-based management identifies specific measurable goals for which management is conducted and which can serve as indicators of success.
- ***Sound science and ecological models***—The success of ecosystem-based management depends upon the quality and completeness of the scientific understanding of the system and models that are required to synthesize information to make sound judgments.
- ***Complexity and connectedness***—Ecosystem-based management recognizes explicitly that important interconnections exist among elements of an ecosystem and that these need to be understood to model the system properly and thereby provide tools to gauge the attainment of sustainability.
- ***Dynamic nature of ecosystems***—Because of both extrinsic drivers and intrinsic interactions, components of ecosystems are not static, and this natural variability must be understood to detect signals from other stressors and to set realistic management goals.
- ***Context and scale***—Ecosystems are driven by processes at multiple spatiotemporal scales, and recognizing the regional setting of these processes is critical for modeling locally driven impacts.
- ***Humans as ecosystem components***—Rather than ignoring humans, ecosystem-based management explicitly places humans in the system as one important element that can play an active role in achieving sustainable management goals.
- ***Adaptability and accountability***—Ecosystem-based management realizes that existing models are always incomplete and predictions are uncertain; therefore, management actions must be treated as hypotheses and tested as a practical means of ensuring success and providing feedback to improve the models.

To successfully meet the objectives previously listed, the DCERP Team

- Ensured relevance of the program to MCBCL's operations
- Ensured that outcomes reflect an adaptive management approach to ecosystem sustainability
- Developed and applied models that incorporate regional and local military drivers to support the sustainability or enhancement of military operations
- Used ecosystem-based models, including mission drivers, to identify methods and tools to support the sustainability or enhancement of ecosystem function and health
- Ensured implementation of essential monitoring, high-quality research, and data management procedures
- Conducted effective outreach and communication of information to the scientific community, MCBCL, other military facilities, other stakeholders, and the general public.

Details about the specific activities performed by the DCERP Team are presented in the following section.

DCERP Research Strategy

During the earliest stages of DCERP, the DCERP Team developed the overall process (**Figure 1-3**) that was used to meet the program's objectives. This process started with identifying ecosystem processes and stressors, developing these into an overarching conceptual model of DCERP, and then creating individual ecological models.

An important part of the DCERP process was to ensure that the ecological models developed for each individual module were designed to integrate the ecological processes and stressors with the Base's military drivers and conservation and water quality needs, as determined by MCBCL for the management of natural resources. The following subsections (Ecosystem Stressors, Overarching Conceptual Model, and Individual Ecological Models) describe each of these activities performed by the DCERP Team.

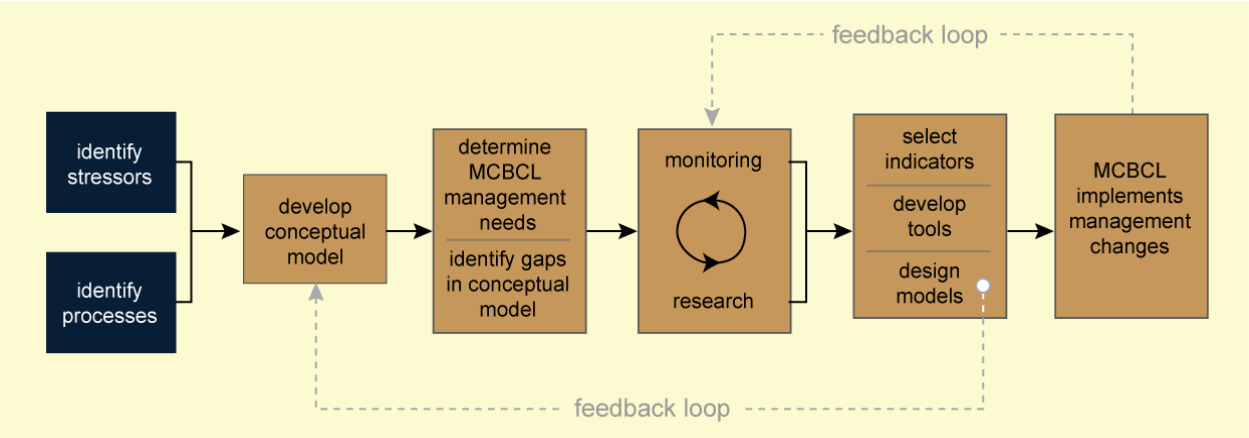

Figure 1-3. Overall DCERP process.

Ecosystem Stressors

Although the main processes are generally understood, the biological, chemical, and physical ecosystem processes at MCBCL had not been researched extensively, especially within the context of outside stressors. The DCERP Team defined stressors as activities or events that alter ecological processes. The DCERP Team grouped stressors into four major categories: military, non-military, legacy, and natural. **Table 1-2** provides a definition for each category and specific examples relevant to DCERP.

Table 1-2. Examples of Military, Non-Military, Legacy, and Natural Stressors to an Ecosystem

Stressors	Examples
Military	Military stressors are unique activities or events that are associated with military training and testing at MCBCL. Some examples of military stressors include the use of military tracked vehicles and amphibious watercraft troop movements on the Base and the use of firing ranges and impact areas.
Non-military	Non-military stressors are any anthropogenic activities that can occur on or off Base. Some examples of non-military stressors include runoff of nutrients from confined animal feeding operations, agricultural practices, or urban lands; industrial and municipal discharges; atmospheric deposition of nutrients and contaminants; local residential or commercial development; groundwater withdrawals; and prescribed burning activities.
Legacy	Legacy stressors are anthropogenic activities that have occurred in the past, but whose effects are continuing today. Some examples of legacy stressors include construction of the Intracoastal Waterway, early ditching activities to drain land, historic use of fire, agricultural activities, and timber harvesting.
Natural	Natural ecosystem stressors include natural forces (e.g., hurricanes, sea level rise) whose effects are enhanced by anthropogenic activity (e.g., global warming). The increased frequency and intensity of natural events, in combination with anthropogenic contributions, could cause ecosystem perturbations outside the range of natural variation.

Overarching Conceptual Model

Once the DCERP Team members defined and grouped the stressors into the four major categories, they developed the overarching conceptual model of DCERP for the MCBCL region. This region includes the terrestrial lands of MCBCL, the NRE, associated coastal wetlands, and the coastal barriers along Onslow Bay, as well as the overarching influence of local and regional atmospheric conditions. **Figure 1-4** presents the overarching conceptual model for DCERP.

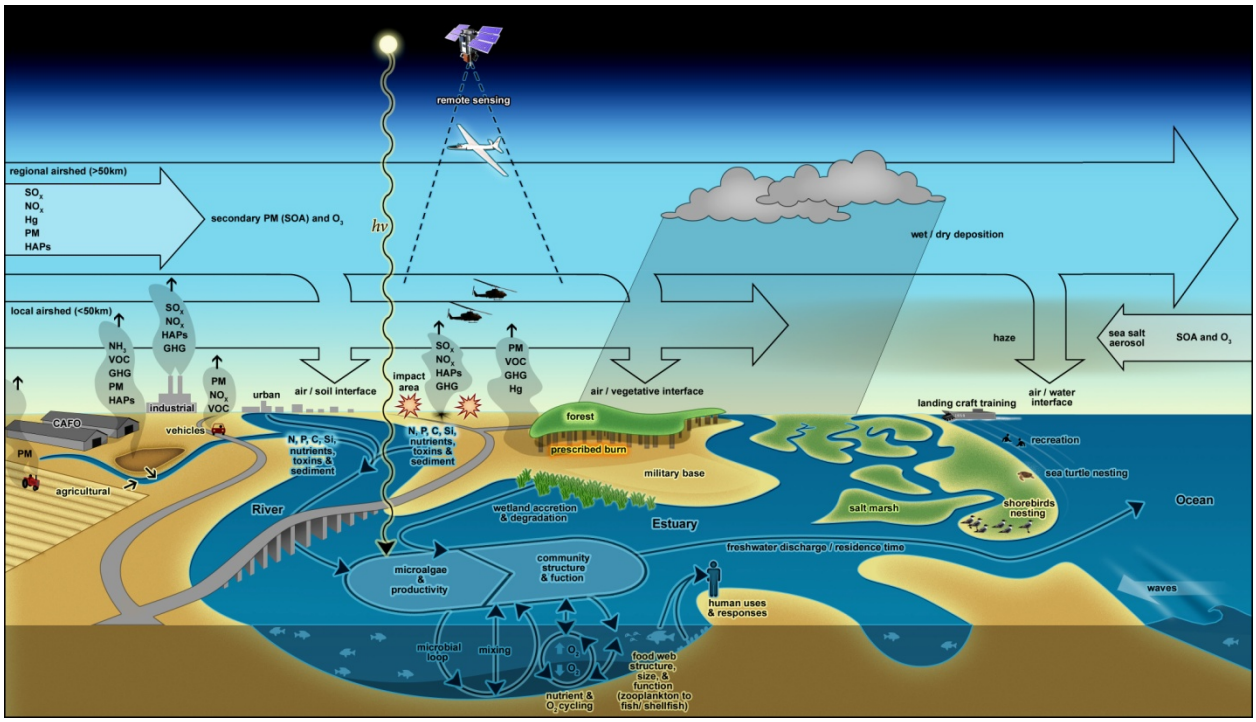

Figure 1-4. Overarching conceptual model for DCERP at MCBCL.

Individual Ecosystem Modules

To facilitate an understanding of the state of the ecosystems and dynamics of the MCBCL region, during the strategic planning process, each of the ecosystem Module Teams then divided the overarching conceptual model of DCERP into four ecosystem modules for monitoring, modeling, and research. These four modules are as follows: Aquatic/Estuarine, Coastal Wetlands (land–estuary margin), Coastal Barrier, and Terrestrial. These modules were linked to each other and to local and regional disturbances and pollutant sources of anthropogenic origin via atmospheric and aquatic transport mechanisms. Because the atmosphere has an overarching influence on all four ecosystem modules, it was treated as a fifth ecosystem module (i.e., the Atmospheric Module). All of the modules developed conceptual models for their respective ecosystems. After developing the overarching conceptual model and the individual ecosystem conceptual models, the DCERP Module Teams identified knowledge gaps in the conceptual models, worked with the Base staff to identify the needs of MCBCL management, and then determined potential research questions to fill these basic knowledge gaps and address these needs. Individual ecological models are presented in Chapter 2 of this *DCERP1 Final Research Report*.

A sixth module, the Data Management Module, involved a diverse group of data management and analysis specialists who have expertise in the development of data management procedures for the DCERP DIMS, including coordination of geospatial data, statistical analysis, and model integration. The Data Management Module involved the following two components: (1) a database and information management system and (2) model and tool development component.

SERDP envisioned the database and information management system component to be a dynamic system to facilitate the collection, integration, and exchange of environmental data

among the DCERP Team and serve as the permanent repository for research and monitoring data and for associated information (e.g., documents, reports, maps, photographs) collected during DCERP's implementation. The model and tool development component provides the ultimate cross-cutting function of incorporating the simple models, which were developed by the individual research projects, into integrated management tools and models. All data and products produced by DCERP were archived in the DCERP DIMS. A summary of this system will be provided in a separate report.

Overall, DCERP has provided basic scientific information needed to develop management plans to modulate the impacts of military training activities and to sustain both the natural resources and use of the Base for military training now and in the future.

Research and Monitoring

The main purpose of DCERP was to gain a better understanding of ecosystem, processes, and impacts of stressors on these processes, which is critical for implementing ecosystem-based management strategies. DCERP was designed to be an adaptive program; therefore, the DCERP Team developed the *DCERP Baseline Monitoring Plan* to gather environmental data to address MCBCL's management concerns and support the research projects identified in the *DCERP Research Plan*. The research projects and baseline monitoring activities of DCERP are described in the following subsections.

Research Projects

To support MCBCL's objectives, the DCERP Team conducted 13 research projects (**Table 1-3**), which focused on understanding knowledge gaps identified through the development of each ecosystem module's conceptual model, including innovative techniques for addressing these knowledge gaps. Specifically, the DCERP Team tested ecosystem response to the previously mentioned four stressors (i.e., military, non-military, legacy, and natural), examined potential indicators of ecosystem change, and evaluated various management practices to help sustain MCBCL ecosystems and their natural resource assets. Final results of all DCERP research projects are summarized in the *DCERP1 Final Research Report*.

Table 1-3. Summary of the 13 Research Projects of DCERP

Research Project Title	Senior Researcher; Project Duration
AE-1: Develop and Deploy Microalgal Indicators as Measures of Water Quality, Harmful Algal Bloom Dynamics, and Ecosystem Condition	Hans Paerl; 7/2007–9/2012
AE-2: Quantifying and Predicting Watershed Inputs of Nutrients, Sediments, and Pathogens to Tributary Creeks on Marine Corps Base Camp Lejeune	Mike Piehler; 7/2007–9/2012
AE-3: Developing Indicators of Ecosystem Function for Shallow Estuaries: Benthic Functional Responses in the New River Estuary	Iris Anderson; 7/2007–9/2012

(continued)

Table 1-3. Summary of the 13 Research Projects of DCERP (continued)

Research Project Title	Senior Researcher; Project Duration
CW-1: Drivers and Forecasts of the Responses of Tidal Salt Marshes to Sea Level Rise	Jim Morris; 7/2007–9/2012
CW-2: Forecasting Influence of Natural and Anthropogenic Factors on Estuarine Shoreline Erosion Rates	Mark Fonseca; 9/2007–9/2012
CW-3: Hydraulic Exchange and Nutrient Reactivity in the New River Estuary Wetlands	Craig Tobias; 7/2008–9/2012
CB-1: Short-Term Barrier Evolution: Overwash at Onslow Beach Through Assessment of Training Activities and Model Predictions	Jesse McNinch; 7/2009–9/2012
CB-2: Long-Term Barrier Evolution Related to Variations in Underlying Geology and Land Use	Tony Rodriguez; 7/2009–9/2012
CB-3: Understanding the Top-Down and Bottom-Up Drivers of Shorebird Nest Success and Habitat Use in Relation to Beach Management Practices on MCBCL	Sarah Karpanty and Jim Fraser; 7/2007–12/2011
T-1: Effects of Different Understory Restoration Management Options on Terrestrial Ecosystem Structure and Function	Norman Christensen; 1/2008–9/2012
T-2: Effects of Habitat Management for Red-Cockaded Woodpeckers on Bird Communities	Jeffrey Walters; 1/2008–9/2012
Air-1: Optimization of Prescribed Burning by Considering Mechanical Thinning as a Viable Land Management Option	Karsten Baumann; 7/2008–9/2012
Air-2: Nitrogen Deposition to Terrestrial and Aquatic Ecosystems	Wayne Robarge; 7/2007–9/2012

Results from research projects feed back into the adaptive *DCERP Baseline Monitoring Plan* so that changes in sampling frequency, spatial extent of sampling locations, or parameters to be sampled could be adapted as necessary. The DCERP Team used results from the research and monitoring efforts to identify ecosystem indicators and develop associated threshold values, tools, or design models that address MCBCL's management needs. Team members then communicated this information to MCBCL personnel to assist them in making decisions about what management actions should be taken. After implementing these changes, the DCERP Team monitored the effects of these management changes (via feedback loops) to ensure that the desired outcomes were achieved and revised the conceptual models as appropriate. The adaptive nature of DCERP, therefore, was not fueled solely by the monitoring and research programs, but by researchers working in concert with the MCBCL staff.

Baseline Monitoring Program

For the purposes of DCERP1, baseline monitoring was defined to include the monitoring of basic (fundamental) parameters that support the broader research agenda, provide data that are useful to more than one ecosystem module, must be monitored for a minimum of 5–10 years; and will likely be transitioned in a scaled-down form to MCBCL to monitor directly at the end of DCERP efforts. The DCERP1 baseline monitoring program included the activities presented in

Table 1-4. Final results of all DCERP baseline monitoring activities are summarized in this document titled the *DCERP1 Final Monitoring Report*.

Table 1-4. Summary of Module-Specific DCERP Baseline Monitoring Program Activities

Modules	Activities
Aquatic/ Estuarine[a]	Hydrodynamics: Stream flow and discharge (New River, tributary creeks) Chemistry: Nutrients, salinity, pH, oxygen, temperature (New River, NRE, tributary creeks) Sedimentology: Total suspended solids (New River, tributary creeks), turbidity (NRE) Biology: Primary productivity, phytoplankton, fluorescence (NRE)
Coastal Wetlands	Land cover and shoreline erosion: Location, elevation Hydrodynamics: Tide gauges (hydroperiod) Chemistry: Nutrients, salinity, hydraulic conductivity (shallow groundwater) Sedimentology: Accretion rates, organic content, particle size
Coastal Barrier	Hydrodynamics: Wave velocity, wave heights/period, currents, shoreline position, morphology Meteorology (ocean): Air temperature, wind velocity, barometric pressure, humidity, solar radiation Sedimentology: Texture, compaction, composition, sediment volume Biology: Benthic invertebrates, fish, shorebirds/seabirds, dune/shrub/marsh vegetation, sea turtles
Terrestrial	Land cover/land use: Determine changes in land cover/land use (vegetation types, buildings, roads) Biology: Vegetative community assessment, fuel load Soil: Soil bulk density, pH, organic matter content
Atmospheric	Meteorology (air): Wind speed, wind direction, relative humidity, temperature, photosynthetically active radiation, precipitation U.S. Environmental Protection Agency criteria pollutants: Ozone, fine and coarse particulate matter (mass)

[a] Sedimentology, chemistry, and biology of the NRE benthic zone were characterized in Research Project AE-3.

Integration of DCERP Research and Monitoring

DCERP's approach closely integrated the *DCERP Baseline Monitoring Plan* and the *DCERP Research Plan* so that the outcomes of research projects were used to modify the adaptive *DCERP Baseline Monitoring Plan*. In turn, the monitoring data were used to develop, refine, and verify the models, tools, and indicators created as part of the research effort; therefore, the models, tools, and indicators were modified and refined as additional research and monitoring data became available.

The research projects also incorporated data from MCBCL's environmental monitoring activities, and other local, state, federal, and private monitoring activities to provide an integrated approach to ecosystem-based management and alleviate redundancy in data collection activities. All research projects did not start simultaneously during DCERP; they were phased in to integrate research linkages among the various modules.

To achieve integration and synthesis of DCERP results within and among the six Module Teams, the DCERP Team initiated a variety of program activities, including monthly reporting of activities, Webinars, and in-person meetings. Team members also worked closely with their respective module researchers, with researchers from other modules, and with Base staff to prepare various publications and presentations for the scientific community, MCBCL, local stakeholders, and the general public.

Figure 1-5 shows how the models, tools, and indicators that are designed, developed, tested, and verified can be transitioned to MCBCL to assist in monitoring and forecasting ecosystem changes. The models, tools, and indicators developed from the research projects should also help to streamline the baseline monitoring to a limited set of key parameters that will easily be transitioned to MCBCL at the end of DCERP. A goal of DCERP is to disseminate monitoring and research results and information from associated models, decision-support tools, and indicators to MCBCL and to other users groups, including other DoD installations in similar ecological settings, the scientific community, other stakeholders (e.g., the New River Roundtable or the Onslow Bight Conservation Forum), and the general public.

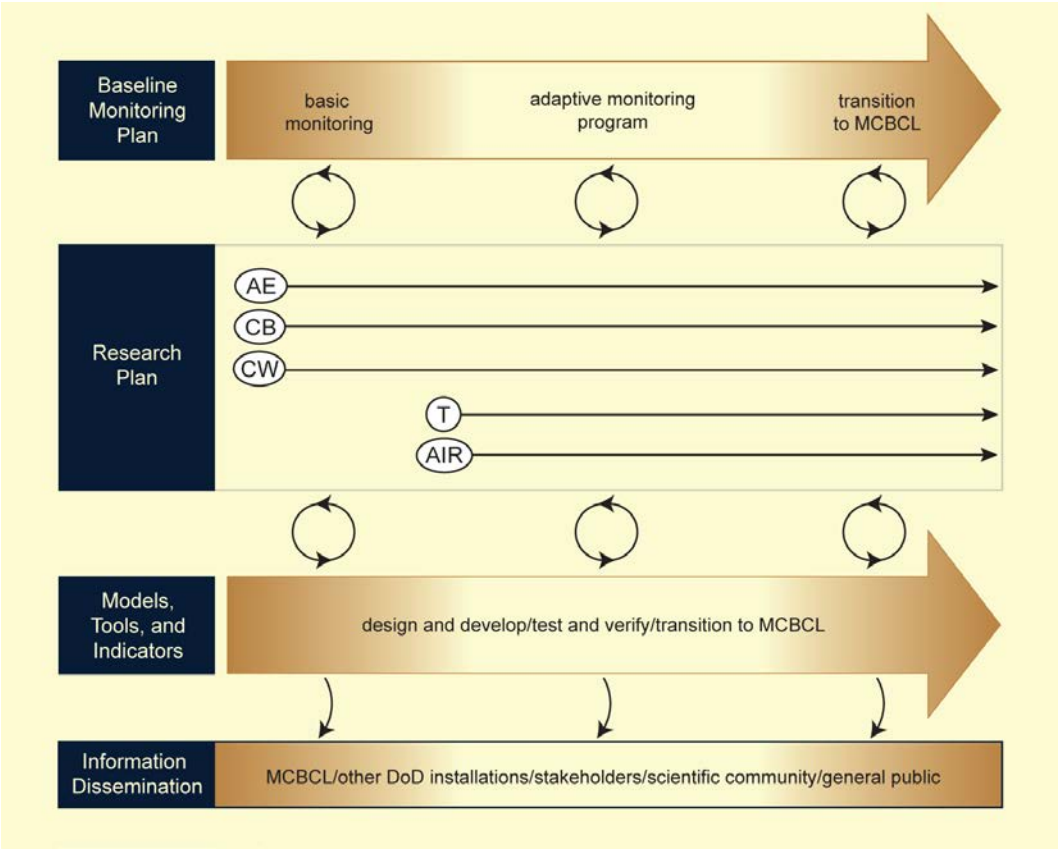

Figure 1-5. Generic roadmap of the integrated DCERP Baseline Monitoring Plan and *DCERP Research Plan* and for development of model tools and indicators.

Note: AE = Aquatic/Estuarine Module; CB = Coastal Barrier Module; CW = Coastal Wetlands Module; T = Terrestrial Module; AIR = Atmospheric Module

In 2009, 2010, and 2011, SERDP provided additional funding for activities not anticipated in the original *DCERP Baseline Monitoring Plan* and the *DCERP Research Plan* if the activity met

specified criteria. The request for additional funding could be made if the activity: (1) needed immediate funding to prevent a negative effect on DCERP, (2) was supported by a TAC recommendation, or (3) supported a new requirement based upon new monitoring or research results or enhanced work that was already funded. This further enabled the program to adapt to new findings and management needs.

Report Organization

This *DCERP1 Final Monitoring Report* summarizes the DCERP monitoring activities and results during the Phase II implementation period (July 2007 to January 2013). Chapter 2 of this *DCERP Monitoring Report* provides a description of each ecosystem, lists the major monitoring activities of each module, and summarizes significant findings, recommendations to MCBCL Managers, and implications for future monitoring at MCBCL. Chapters 3 through 15 provide detailed reports for each module's monitoring activities listed in **Table 1-4** of this chapter. As part of each chapter, the investigators restated the goals of the monitoring activity, provided background to their monitoring activities to set these within the context of the historical monitoring data or the current state of the science at the outset of DCERP, described the methods and materials used, and provided results, discussions, and conclusions, including an assessment of spatial and/or temporal trends in their data.

In addition, an Executive Summary is provided that will serve as a stand-alone summary document prepared as an outreach tool for MCBCL. The Executive Summary covers the same time period described here and specifically highlights significant results and trends applicable to MCBCL's natural resources management staff, the Base's environmental mission drivers, and direct benefits to MCBCL that were derived from DCERP.

Literature Cited

Christensen, N.L., A. Bartuska, J.H. Brown, S. Carpenter, C. D'Antonio, R. Francis, J.F. Franklin, J.A. MacMahon, R.F. Noss, D.J. Parsons, C.H. Peterson, M.G. Turner, and R.G. Woodmansee. 1996. The scientific basis for ecosystem management. *Ecological Applications 6*:665–691.

Goodman, S.W. 1996. Ecosystem management at the Department of Defense. *Ecological Applications 6*:706–707.

MCBCL (Marine Corps Base Camp Lejeune). 2006a. *Integrated Natural Resource Management Plan (INRMP)*. U.S. Marine Corps, Camp Lejeune, NC. Available at http://www.lejeune.usmc.mil/emd/INRMP/INRMP.htm.

MCBCL (Marine Corps Base Camp Lejeune). 2006b. *2020 Range Transformation Plan, Version 4*. Range Development, Training and Operations Department. Integrated Geographic Information Repository. Marine Corps Base Camp Lejeune, NC.

MCBCL (Marine Corps Base Camp Lejeune). 2005. *Land Use Master Plan*. Prepared by Eagan McAllister Associates, Inc. Integrated Geographic Information Repository. Marine Corps Base Camp Lejeune, NC.

RTI (RTI International). 2007a. *Defense Coastal/Estuarine Research Program (DCERP) Strategic Plan*. Prepared for Strategic Environmental Research and Development Program (SERDP), Arlington, VA.

RTI (RTI International). 2007b. *DCERP Baseline Monitoring Plan*. Prepared for Strategic Environmental Research and Development Program (SERDP), Arlington, VA.

RTI (RTI International). 2007c. *DCERP Research Plan*. Prepared for Strategic Environmental Research and Development Program (SERDP), Arlington, VA.

SERDP (Strategic Environmental Research and Development Program). 2005. *DCERP Strategy Report*. U.S. Department of Defense, Defense Coastal/Estuarine Research Program, Marine Corps Base Camp Lejeune, NC.

U.S. Commission on Ocean Policy. 2004. *An Ocean Blueprint for the 21st Century*. Final Report. Washington, DC.

Walters, C. 2001. *Adaptive Management of Renewable Resources*. The Blackburn Press: Caldwell, NJ.

Appendix 1-A

Prioritized List of MCBCL's Conservation and Water Quality Needs

MCBCL Conservation and Water Quality Needs
High-Priority Needs
Primary Nursery Area (PNA) mitigation/delineation
Onslow Beach erosion
Air quality/smoke management
Measuring good quality habitat for red cockaded woodpeckers (RCW)
N1/BT3 monitoring for whales and marine mammals
RCW flexibility for Range Development—Regional RCW credit
Stormwater runoff reduction and water quality studies
Near field water quality studies
Distinguish and quantify effects of point and non-point inputs nutrient, sediment and pathogen inputs
Water quality/primary nursery areas
Physical-chemical-biological interactions and their control on water quality/habitat
Medium-Priority Needs
Wetland (marsh) restoration opportunities in the New River Estuary
Species at risk—beach amaranth
Species at risk—sea turtles
Species at risk—shorebirds
Species at risk—RCW
Fire effects on vegetation and quantifying/qualifying prescribed burns
Species at risk—rough-leaved loosestrife
Habitat restoration and tactical vehicle off-road impacts
Northern pocosin in the Great Sandy Run Area (GSRA)
RCW monitoring
Additional military effects/RCW study
Longleaf /loblolly decline
Benthic organism Index of Biological Integrity
Benthic-water column exchange and hypoxia research
Blue crab studies
Determine nutrient, sediment and pathogens loadings from the watershed; determine transformations of nutrients within the estuary; and the determine interactive role of climatic/hydrologic roles
Identify and quantify nutrients controlling primary production and excess production and algal blooms

MCBCL Conservation and Water Quality Needs
Determine causes and effects of harmful algal blooms; link nutrient-productivity to hypoxia potentials
Low-Priority Needs
Coliform counts—Freeman Creek (and other 303[d] Total Maximum Daily Load–identified tributaries)
Invasive species: alligator weed and *Phragmites*
Habitat restoration and tactical vehicle off-road impacts—maritime forest

[This page intentionally left blank.]

Chapter 2

Significant Findings and Management Implications

SERDP Project Number: RC-1413

Principal Investigator:
Dr. Patricia Cunningham
RTI International
Research Triangle Park, NC 27709
E-mail: patc@rti.org

June 27, 2013

Final

This report was prepared under contract to the U.S. Department of Defense (DoD) Strategic Environmental Research and Development Program (SERDP). The publication of this report does not indicate endorsement by DoD, nor should the contents be construed as reflecting the official policy or position of DoD. References herein to any specific commercial product, process, or service by trade name, trademark, manufacturer, or otherwise, do not necessarily constitute or imply its endorsement, recommendation, or favoring by DoD.

Table of Contents

List of Acronyms 2-v
Introduction 2-1
Programmatic Overview 2-1
    Establishing Baseline Conditions 2-1
    Assessing Variability and Trends in Key Ecosystem Parameters 2-2
    Model Development, Calibration, and Validation 2-5
Aquatic/Estuarine Module 2-6
    Summary of the Ecosystem 2-6
    Aquatic/Estuarine Module's Monitoring Program 2-7
    Conclusions and Implications from the Aquatic/Estuarine Module 2-8
Coastal Wetlands Module 2-11
    Summary of the Ecosystem 2-11
    Coastal Wetlands Module's Monitoring Program 2-12
Coastal Barrier Module 2-16
    Summary of the Ecosystem 2-16
    Coastal Barrier Module's Monitoring Program 2-17
    Conclusions and Implications from the Coastal Barrier Modules 2-19
Terrestrial Module 2-23
    Summary of the Ecosystem 2-23
    Terrestrial Module's Monitoring Program 2-24
    Conclusions and Implications from the Terrestrial Module 2-25
Atmospheric Module 2-27
    Summary of Atmospheric Conditions 2-27
    Atmospheric Module's Monitoring Program 2-28
    Conclusions and Implications from the Atmospheric Module 2-29
Literature Cited 2-32

List of Figures

2-1. Conceptual model for the Aquatic/Estuarine Module. 2-7
2-2. Conceptual model for the Coastal Wetlands Module. 2-12
2-3. Conceptual model for the Coastal Barrier Module. 2-17
2-4. Conceptual model for the Terrestrial Module. 2-23
2-5. Conceptual model for the Atmospheric Module. 2-28

List of Tables

2-1. Models developed and/or applied by the RTI DCERP Team. 2-5
2-2. Aquatic/Estuarine Module monitoring components. 2-8
2-3. Coastal Wetlands Module Monitoring Components 2-12
2-4. Coastal Barrier Module monitoring components 2-18
2-5. Terrestrial Module Monitoring Components 2-24
2-6. Atmospheric Module Monitoring Components 2-29

List of Acronyms

µm	Micrometer
ac	Acre
ADCIRC	Advanced Circulation (Model)
AE	Aquatic/Estuarine Module
AVP	Autonomous Vertical Profiler
BBN	Bayesian Belief Network
BMA	benthic microalgae
BOMO	Boat Wake Model
CAFO	confined animal feeding operation
CB	Coastal Barrier Module
cfs	cubic feet per second
cm	Centimeter
CVS	Carolina Vegetation Survey
CW	Coastal Wetlands Module
DCERP	Defense Coastal/Estuarine Research Program
DCERP1	the first cycle of the Defense Coastal/Estuarine Research Program
DCERP2	the second cycle of the Defense Coastal/Estuarine Research Program
DoD	U.S. Department of Defense
EPA	U.S. Environmental Protection Agency
ESM	Estuarine Simulation Model
ft	feet, foot
ft y^{-1}	feet per year
g m^{-2}	grams per square meter
GSRA	Greater Sandy Run Area
ha	Hectare
in	Inches
km	Kilometer
km^2	square kilometer
m	Meter
m^2	square meter
m y^{-1}	meters per year
ICW	Intracoastal Waterway
MCBCL	Marine Corps Base Camp Lejeune
MEM	Marsh Equilibrium Model
mi	Mile
mi^2	square mile
mm	Millimeter

mm y^{-1}	millimeters per year
NOAA	National Oceanic and Atmospheric Administration
NRE	New River Estuary
ORRV	off-road recreational vehicle
$PM_{2.5}$	fine particulate matter; particulate matter with a diameter of less than or equal to 2.5 micrometers
PM_{10}	coarse particulate matter; particulate matter with a diameter of less than or equal to 10 micrometers
PM_c	coarse particles; the coarse fraction of PM_{10} from the difference between the measured PM_{10} and $PM_{2.5}$
ppb	parts per billion
ppt	parts per thousand
RCW	red-cockaded woodpecker
ROM	Runup and Overwash Model
SERDP	Strategic Environmental Research and Development Program
SWAN	Simulating Waves Nearshore (Model)
T	Terrestrial Module
USGS	U.S. Geological Survey
WEMo	Wave Exposure Model
WSM	Watershed Simulation Model
WWTF	wastewater treatment facility

Introduction

This chapter of the *DCERP1 Final Monitoring Report* provides a brief summary of the significant monitoring findings and their management implications for the Defense Coastal/Estuarine Research Program (DCERP) conducted at Marine Corps Base Camp Lejeune (MCBCL) in North Carolina. DCERP's overarching objective was to enhance and sustain MCBCL's military training mission by conducting installation-relevant basic and applied research and monitoring in support of an ecosystem-based management approach. To meet this objective, the RTI DCERP Team focused on developing an understanding of ecosystem composition, structure, and function within the context of a military training environment. DCERP was established as a temporally and spatially integrated monitoring and research program, whereby monitoring data informed research results, and then provided feedback on whether the monitoring program was adequate to support research hypotheses.

Monitoring data were of critical importance to the research effort for several reasons. First, monitoring data established baseline conditions that provided a context against which to compare impacts of major stressors to the various ecosystems. Second, for studying the various ecosystem processes, monitoring data provided long-term information to assess the daily, monthly, seasonal, annual, and inter-annual variability, as appropriate, in key monitoring parameters, thereby providing a better understanding of natural variability and variability resulting from episodic events. In this coastal system, periods of severe drought and storm events were of major importance in evaluating the range of variability in key parameters that may become more variable under future climate-change conditions. Finally, monitoring data were used to validate many of the models that were used to study current conditions and their impact on the MCBCL ecosystems to aid in effective ecosystem-based management. Some of these models developed during DCERP1 will be used in scenario testing during DCERP2 to evaluate variables controlling current ecosystem processes and also to determine their potential impacts on these key ecosystem processes under future climate-change conditions.

Programmatic Overview

Establishing Baseline Conditions

As part of an ecosystem-based monitoring program, there is a need to establish long-term measurement activities that capture ecosystem processes. The DCERP monitoring activities were critically important to the team's understanding of the baseline conditions that existed in each ecosystem (i.e., aquatic/estuarine, coastal wetlands, coastal barrier, terrestrial, and atmospheric) at the start of the program to determine whether anthropogenic and/or natural stressors were changing conditions over time. For the Aquatic/Estuarine Module, understanding the hydrodynamics in the estuary required flow data on the New River coupled to information on the bathymetry of the New River Estuary (NRE) so that the areal extent of the shallow bottom areas and the surface area and volume of the estuary could all be used to scale up various processes such as nutrient cycling, sediment transport, and primary productivity to the entire estuary. The Coastal Wetlands Module classified the entire NRE and the Intracoastal Waterway (ICW) shoreline by habitat types (Marsh, Swamp Forest, Sediment Banks, Miscellaneous, and Modified [hardened] shorelines) and identified the dominant marsh plants at each location. This information on shoreline classification was coupled with information on wave energy regimes to

assess shoreline erosion and for identifying sources of sediment for the marshes of the lower NRE and ICW. Measurement of marsh elevation was also important for determining changes in accretion or erosion rates in marshes over time. Tide gauges were installed at three locations to provide accurate measurement of tidal amplitude, which is important to determine accretion rates in coastal marshes and to determine response of marshes to sea level rise.

Nowhere was baseline data needed more than on the coastal barrier island. Bathymetry of the immediate offshore (less than 10-m depth [33-ft]) of Onslow Beach and the New River Inlet was required to understand wave and current hydrodynamics. The geomorphology of offshore sediment deposits that might augment beach accretion and rock outcroppings that could modulate wave patterns and influence run-up and overwash processes were also collected to better understand processes affecting the barrier island's morphology and its biological communities. The precise topographic features of the barrier island were tracked through time semi-annually and before and after storm events to evaluate long-term changes in wave-driven overwash, resulting in washover deposits and wind driven sediment (aeolian) transport across the barrier island. Baseline monitoring was also collected to determine the species composition and populations of intertidal invertebrates, ghost crabs, nearshore fish, and dune vegetation. These data were collected in the different use zones of Onslow Beach to determine changes in these populations related to military training, other anthropogenic activities, and storm events though time, as well as study the top-down/bottom up processes affecting predator and prey interactions and habitat quality.

For the Terrestrial Module, baseline conditions for pine-dominated vegetative communities across the installation had been previously captured by the Carolina Vegetation Survey (CVS). However, DCERP1 monitoring documented current conditions at the existing CVS sites and expanded the total number of vegetation monitoring sites in habitats under-represented in the CVS such as wetlands and hardwood stands. These new data established more comprehensive baseline conditions of terrestrial vegetation for the installation that can be resampled in the future. In addition to site-specific monitoring, a Greenness Change Analysis was conducted for the entire installation and surrounding area using Landsat imagery data. Data from 1984 was used as a baseline against which to measure the enhancement or reduction of greenness in various years through 2011. This analyses tracked loss of greenness due to infrastructure development and forestry management practices such as clear-cutting and the gain of greenness where clear cut or thinned forest areas or ranges had undergone vegetation regrowth. These data can be useful in DCERP2 for assessing the implications of various forestry practices on carbon management at MCBCL.

Finally, the Atmospheric Module established four meteorological monitoring sites across MCBCL to obtain additional baseline observations to evaluate gradients of atmospheric conditions (the beach to inland areas). These monitoring results were compared to measurements from the regional airshed at other meteorological stations in surrounding counties. Thus, trends locally on MCBCL and in the regional airshed were determined.

Assessing Variability and Trends in Key Ecosystem Parameters

Monitoring programs need to collect data at appropriate frequencies to capture important details about daily, seasonal, annual, and inter-annual variations in key parameters. Monitoring

programs all need to be designed to capture episodic events such as hurricanes, floods, droughts, and heat waves. These events have great value in understanding ecological processes, but they and their forcing conditions must be properly recorded. An episodic event may be defined differently among different ecosystems because of both the scale of the event (i.e., duration, intensity, extent, and frequency) and the various environmental parameters contributing to the resultant stress (e.g., salinity, temperature, wave energy, and suspended solids) on the system. For example, a hurricane may result in significant rainfall, which can subsequently affect runoff of sediment and nutrients from the terrestrial landscape to the receiving aquatic/estuarine system. In contrast, the coastal barrier may not be significantly affected by extensive rainfall, but instead by the impact of wind-driven waves resulting in wave runup and overwash of the barrier island, causing significant erosion or accretion. The monitoring and modeling of these episodic events become important when considering future climate change, which is likely to alter the means and magnitude of the variability of important climate or weather-related processes that will persist in the future (Diffenbaugh et al., 2005; Emanuel, 2005; Goldenberg et al., 2001; Kunkel et al., 2003; Milly et al., 2008; Webster et al., 2005).

During the first 5 years of DCERP, MCBCL was impacted by several episodic events that produced a wide range of hydrologic conditions. These events included a drought during summer 2008 that produced one of the lowest annual river flows observed in several decades, Tropical Storm Hanna in September 2008, and Tropical Storm Nicole in 2010, which produced a severe rain event (57 cm[22 in] of rainfall over 3 days). In 2011, Hurricane Irene made landfall approximately 45 miles northwest of MCBCL as a Category 1 hurricane, making it the strongest tropical storm to affect the area during DCERP1. The monitoring activities within each of the DCERP ecosystem modules were designed to address both measurement of routine variability in ecosystem processes and unpredictable episodic events.

The Aquatic/Estuarine Module's monitoring program collected data at a variety of frequencies to provide a comprehensive perspective of processes operating in the estuary. At two locations in the NRE, autonomous vertical profilers (AVPs) continuously recorded conditions in the water column 24 hours a day and thus were extremely useful in capturing detailed information on the impacts of an event on surface- and bottom water-quality conditions. These data complimented monthly, more intensive monitoring at eight stations throughout the estuary. Episodic events were evaluated in terms of both inter-annual variability within the estuary and their immediate impact on estuarine dynamics. This was demonstrated by both inter-annual trends in various water quality parameters and shifts in the phytoplankton community response to the event as determined by changes in chlorophyll *a* and in the proportions of diagnostic pigments (indicative of different algal taxonomic groups). The 2010 rainfall event demonstrated that there are water residence time thresholds (i.e., flushing rates) that control phytoplankton production, composition, and bloom dynamics in the NRE. This event impacted both annual phytoplankton production and immediate changes in water quality conditions following the event. The record drought of 2008 was also an episodic event, but the impact was more gradual than that of the severe rainfall event. This longer term event led to an upstream displacement of algal blooms accompanied by significant changes in phytoplankton composition. These changes likely impacted the food web, dissolved oxygen, and biogeochemical cycling dynamics, and, ultimately water quality conditions.

Episodic events are critical for understanding the coastal barrier, where storm-driven wind energy, wave energy, and water dynamics are the most significant stressors potentially impacting biogeochemical cycling and the trophic structure of this ecosystem. The Coastal Barrier Module's monitoring program needed to capture these episodic storm events that were drivers of accretion and erosion processes. Monitoring was conducted twice each year and before and after storm events to capture immediate changes in sediment transport across the barrier and from the adjacent offshore areas. A monitoring site was added to the program to capture the impacts of dredge spoil dumped on the northeastern end of the island to follow dispersal of the sediment over time. Monitoring was also conducted before and after major military training exercises. The accuracy of this data is critical in providing MCBCL with the best information, so MCBCL Managers can plan and prepare to adapt to changes associated with episodic storm events, as well as anthropogenic events that occur at the annual to inter-annual intervals.

Capturing trends in monitoring results requires appropriate selection of sampling frequency and spatial extent. Different time and space scales are required for the various ecosystem processes being studied. The frequency required to capture significant trends in the estuary may be quite different in scale from those used in the coastal wetlands or other ecosystems. For example, gradual changes in terrestrial, vegetative communities may take 5 or more years before patterns of change become evident. Similarly, estuarine shoreline erosion may require decades before a trend can be established. As appropriate, an analysis of trends in the monitoring data was conducted to determine whether significant changes in various ecosystem processes had occurred. The same episodic event may affect ecosystems in different ways. For example, although drought conditions may improve water clarity, allowing benthic microalgae (BMA) to thrive, drought may result in increasing salinities in upstream areas of the estuary, thereby stressing marsh communities typically exposed to lower salinity conditions or stressing terrestrial vegetative communities.

In addition to natural variability, the monitoring activities were also designed to capture changes in man-made activities and their impacts on the ecosystem. Anthropogenic effects such as the accumulated impacts of changes in land use within the New River basin and across MCBCL lands are likely to produce a slower change in water quality conditions that may not be captured within a short 5-year study period. For example, the U.S. Marine Corps's Grow the Force (GTF) campaign in North Carolina was initiated almost simultaneously as when DCERP began at MCBCL. This staffing-up campaign resulted in the need for MCBCL to train and house more than 8,000 additional active-duty and civilian personnel and their families (USMC, 2009). To support this growth, the U.S. Marine Corps planned a combination of new infrastructure (e.g., buildings, roads), upgrades to existing infrastructure, and relocation of existing personnel. Although some additional training and firing ranges were established to meet the increase, the major effect on MCBCL was the rapid expansion of cantonment facilities (e.g., housing, schools, medical buildings) needed to provide services to the additional population. In total, the Environmental Impact Statement projected construction or infrastructure upgrades would disturb 761 ha (1,880 ac) of MCBCL lands to meet the GTF campaign. The impacts of this increased infrastructure development were captured by the RTI DCERP Team's analysis of Landsat monitoring and showed that loss of greenness was occurring much more rapidly from 2009–2011 than it had from 1984–2009. Changes in water quality will take additional years of data collected during DCERP1 to determine the effects on the NRE. In summary, DCERP monitoring activities were carefully coordinated and integrated to adequately capture and characterize inter-annual

variability and assess the impacts from routine and episodic events on the coastal ecosystem. This is even more important going forward into DCERP2 because of the emphasis on studying the impacts of climate changed futures potentially including increased temperature, periods of drought and high precipitation, increased magnitude of storm events, and rising sea level.

Model Development, Calibration, and Validation

Another major objective of DCERP1 was to develop models and tools to help installation staff make more informed ecosystem-based management decisions that would help sustain military training and natural resource assets of MCBCL. Historic monitoring data were utilized to calibrate many of the models, and the DCERP1 monitoring data were used to validate the models. Some of these models were used to conduct scenarios associated with changes in current conditions or assessing potential impacts of future conditions. A listing of models developed as part of DCERP is provided in **Table 2-1**. Additional information about each model is provided in the *DCERP1 Final Research Report*.

Table 2-1. Models developed and/or applied by the RTI DCERP Team.

Model Name	Research Project	Objective
Bayesian Belief Network (BBN)	AE-1	To examine the variables critical to eutrophication and guide monitoring and assessment procedures
Watershed Simulation Models (WSMs)	AE-2	To understand the effects of natural and anthropogenic stressors on watershed loads to the NRE
Estuarine Simulation Model (ESM)	AE-3	To scale up results to the entire NRE system and understand the effects of natural and anthropogenic stressors on the NRE
Bio-optical Model (for the NRE)	AE-3	To guide monitoring and assessment procedures and understand the effects of water quality parameters on light attenuation in the NRE
Marsh Equilibrium Model (MEM)	CW-1	To forecast changes in marsh elevation and assess vulnerability of marshes to sea level rise
Wave Exposure Model (WEMo)	CW-2	To classify shorelines by wind wave energy; predict distribution of storm waves on top of surge under different storm scenarios; determine seafloor shear stress to predict areas of high sediment resuspension in the NRE; and identify vulnerable installation assets
Boat Wake Model (BOMO)	CW-2	To perform boat wake impact forecasting and geographic assessments
Runup and Overwash Model (ROM)	CB-1	To predict changes in the beach in response to short-term storms and/or changes in the physical parameters (e.g., beach slope, removal of dunes) and forecast locations of wave runup and overwash
Advanced Circulation (ADCIRC) Model	Coastal Barrier Monitoring Program	To simulate the velocity flow field and pathways of sediment transport
Simulating Waves Nearshore (SWAN) Model		

The remainder of Chapter 2 is organized according to the five ecosystem modules: Aquatic/Estuarine, Coastal Wetlands, Coastal Barrier, Terrestrial, and Atmospheric Modules. Each module section contains short descriptions of the key biological, chemical, and physical processes and stressors that impact each ecosystem as presented in the conceptual models and the findings of the program. Finally, the major findings and implications of the DCERP1 monitoring

activities within each module are discussed in the context of three categories: Key Scientific Findings, Findings with Implications for MCBCL Management Practices, and Findings with Implications for DCERP2. It should be noted that some findings may fit into more than one of these categories**;** however, we have tried to minimize duplication and, therefore, have put the findings in the most appropriate category.

Aquatic/Estuarine Module

Summary of the Ecosystem

Estuaries integrate inputs from terrestrial habitats, freshwater rivers and streams, the coastal ocean, and atmospheric systems. Accurate assessment and management of estuarine water quality necessitates consideration of the interconnections to, and interactions with, these other systems. Many estuaries also exist in regions of rapid population growth and diversifying human activity that can impact natural ecosystem processes. In the context of the MCBCL region, the Aquatic/Estuarine Module studied the tidal reach of the NRE from the head of the estuary near Jacksonville, NC, to the tidal inlet at Onslow Bay, including 10 tributary creeks within Base lands that flow into the NRE or the ICW.

The NRE is a relatively small (88 km^2 [34 mi^2]), shallow (approximately 3 m [9.8 ft] mean depth) coastal plain estuary. Most of the estuary is located within U.S. Department of Defense property boundaries. The NRE is comprised of a series of lagoons and is confined by barrier islands restricting water exchange with the Atlantic Ocean. Flushing time in the NRE varies seasonally with storm and runoff events, ranging from 8 to 187 days, with an average of 70 days (Ensign et al., 2004). The semi-lagoonal nature of the NRE plays a significant role in its sensitivity to nutrient inputs because long flushing times allow more time for algal nutrient assimilations, growth, and internal nutrient recycling. Principal tributaries discharging into the NRE include the New River and Southwest and Northeast Creeks. In addition, numerous small creeks, whose catchment areas lie within MCBCL boundaries also discharge into the NRE. Land use in both the New River and Southwest Creek watersheds is dominated by agriculture and includes numerous swine confined animal feeding operations (CAFOs). Prior to 1998, discharges from CAFOs, a wastewater treatment facility (WWTF) in the City of Jacksonville, and seven WWTFs on MCBCL resulted in massive phytoplankton blooms, widespread hypoxia, and fish kills. As a result, the estuary was named one of the most eutrophic in the southeastern United States (Bricker et al., 1999; Mallin et al., 2005). In 1998, the Jacksonville WWTF was upgraded to secondary treatment with land spraying of effluent, and the MCBCL facilities were consolidated into one new WWTF with biological nutrient removal located at French Creek. The upgrades to the WWTFs have markedly improved water quality (Mallin et al., 2005). However, the NRE continues to receive high nutrient loads from external sources due to inputs from the New River watershed upstream of Jacksonville, episodic WWTF spills from Jacksonville and the MCBCL WWTF, remineralization of legacy organic matter in the upper reaches of the system, atmospheric deposition, and from tidal exchanges with Onslow Bay. Development on MCBCL, with attendant increases in impervious area, forest clear-cutting, and development of roads, housing and other infrastructure, also has the potential to impact the small tributary creeks that discharge into the NRE.

The Aquatic/Estuarine Module investigated how anthropogenic loadings (nutrients and sediment inputs) from the New River watershed off Base and the 10 MCBCL tributaries affected the BMA and pelagic phytoplankton that together are the predominant primary producers of this estuary. Phytoplankton production and community structure are controlled by nutrient inputs, water residence time, and the degree of stratification in the estuary. In contrast, BMA production is controlled by water clarity that allows the BMA to sequester nutrients under autotrophic conditions, but causes a release of nutrients back into the water column under heterotrophic conditions. Water clarity that controls BMA production is reduced by the presence of suspended sediments, chromophoric (colored) dissolved organic matter, and pelagic phytoplankton biomass—all parameters regulated by climate-driven hydrologic flows from the New River and from forcings from tidal activity and wave energy. Furthermore, the effects of climatic variability, including acute or episodic events (e.g., tropical storms, hurricanes, floods, droughts) and longer term trends (e.g., warming, precipitation patterns), on estuarine structure and function were characterized and quantified to better understand the interactive and potentially confounding impacts of climate (change) on water quality and habitat condition (**Figure 2-1**).

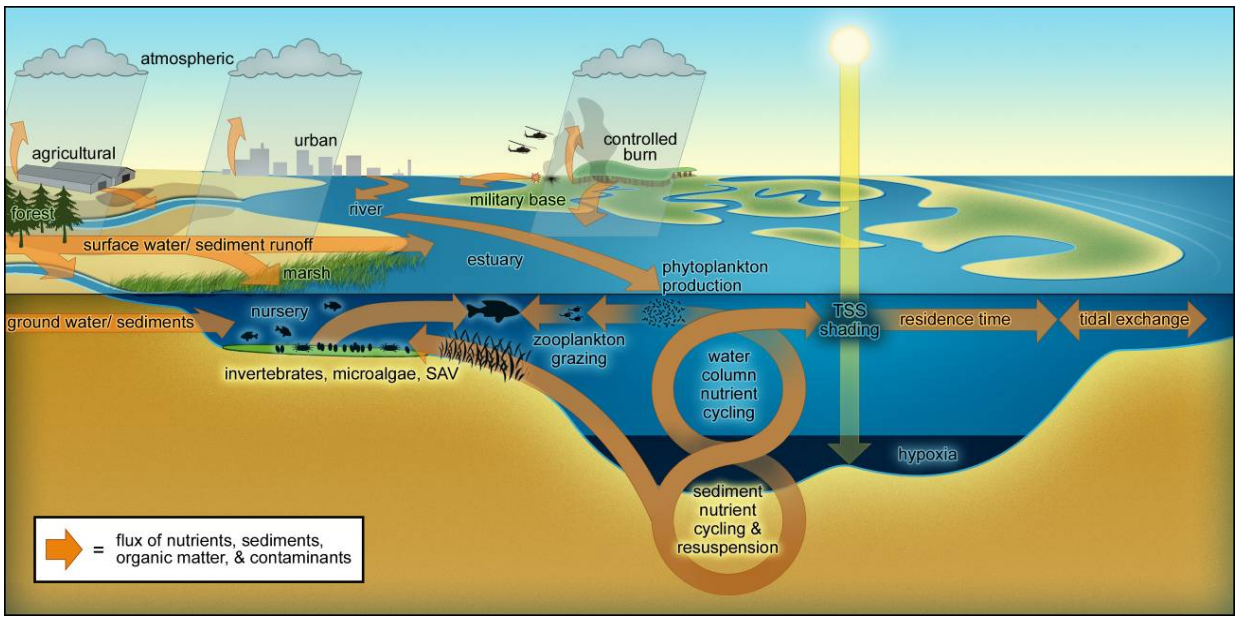

Figure 2-1. Conceptual model for the Aquatic/Estuarine Module.

Aquatic/Estuarine Module's Monitoring Program

The Aquatic/Estuarine Module monitoring program, which is summarized in **Table 2-2**, was designed to achieve multiple goals. These goals include improved understanding of the physical, chemical, and biological processes and interactions that drive water, sediment, and habitat quality within the New River, the MCBCL tributary creeks, and NRE water column; support the research project components; and help to differentiate natural and anthropogenic ecosystem stressors. Differentiating the stressors includes the consideration of episodic weather-related events, such as hurricanes, nor'easters, floods, and droughts, which have thus far been shown to be very important drivers whose impacts vary greatly inter-annually. Additional goals included providing information to assist in designing and implementing a long-term monitoring program that ensures compatibility of MCBCL activities with desirable estuarine water, sediment, and

habitat quality and facilitating the conservation of regional natural resources of the NRE for their ecosystem services, recreational, and economic benefits.

Table 2-2. Aquatic/Estuarine Module monitoring components.

Area	Variable	Spatial Scale	Temporal Scale
New River	Water level and discharge	2 stations: New River near Gum Branch (active U.S. Geological Survey station) and at Jacksonville (added with DCERP funding)	Continuous
	Nutrients and sediment	New River at Jacksonville	Monthly (outgoing tide)
	Water temperature, dissolved oxygen, pH, and salinity	New River at Jacksonville	Continuous
Tributary creeks	Water level (streamflow) and temperatures	10 stations (paired)	Continuous
	Nutrients (nitrogen and phosphorus), total suspended solids, and fecal indicator bacteria	10 stations (paired)	Grab; monthly (baseflow); episodic (stormflow)
NRE—water column	Fluorescence (chlorophyll a), chromophoric (colored) dissolved organic matter, nutrients (nitrogen and phosphorus), and total suspended solids	10 stations (8 vertical profiles and 2 continuous autonomous vertical profilers, one at the same location as one of the profiles)—longitudinal from the New River to the inlet	Monthly for profiles and Dataflow; year-round for autonomous vertical profilers
	Photosynthetically active radiation, salinity, water temperature, dissolved oxygen, pH, turbidity, and flow		
	Primary productivity, chlorophyll *a* by fluorometry and high-performance liquid chromatography, phytoplankton pigments (biomass)		

Conclusions and Implications from the Aquatic/Estuarine Module

Key Scientific Findings—Fundamental Cause-and-Effect Relationships

<u>New River Discharge and Inputs</u>

The New River discharge into the NRE was of primary importance in driving the hydrodynamics of the estuarine system, including the transport of sediment and nutrients. Annual mean river flows ranged from a low of 46.9 cfs (in 2008) to a high of 127 cfs (in 2010). River flow during DCERP1 was less than the mean annual discharge of 114 cfs (over the historic period of record) during all years except 2010. Despite the lower than average flows in 4 out of the 5 years of DCERP1, episodic events (hurricanes, tropical storms, nor'easters) produced high river flows for brief periods (November 2009–January 2010) and during late spring–summer 2012. In October 2010, flows reached a maximum level when Tropical Storm Nicole dumped 57 cm (22 inches) of rain in the Jacksonville, NC, area in a 3-day period. Salinity values were also modulated within

the upper estuary by the hydrologic variations of the New River with salinity values ranging from 0.04 to 24.8 ppt in Jacksonville. Values were typically lowest during the winter and gradually increased from March through September. Salinity then typically declined when rainfall from tropical storms and hurricanes occurred; however, this seasonal pattern was not consistently observed in all years and was modulated by the timing, frequency, and magnitude of precipitation events. The New River provided inputs of both nitrogen and phosphorus to the estuary. Although concentrations of phosphorus were typically similar at both gauges, concentrations of nitrogen were typically higher upstream at Gum Branch than at the Jacksonville gaging station, suggesting that nitrogen was assimilated by phytoplankton through primary production in the river before entering the estuary.

Tributary Creeks Inputs

Although loading rates of nutrients and sediment were generally very low in the MCBCL tributary creeks monitored during this study as compared to other Atlantic coastal plain creeks, there was a clear cause-and-effect relationship between increased human activity in the watershed (with percent impervious cover as the indicator of land disturbance) and loading of nutrients and sediments into the estuary. A significantly higher loading of total suspended solids and nutrients was found in 2009–2010 (wetter year) as compared to 2008–2009 (drier year). In addition, the percent increase in loading between 2008–2009 (dry year) and 2009–2010 (wet year) was compared from the affected sites to the percent increase in loading from the reference sites. Loading of total suspended solids increased (dry year versus wet year) significantly more in the affected streams than in the reference streams. However, nutrient loading increases from the dry year to the wet year were not significantly different between the reference and affected paired sites.

NRE Water Column

A primary goal of this monitoring activity was to determine how natural and anthropogenic stressors impact water quality and habitat condition of the NRE and, when possible, to identify stressors that are readily manageable from those that are not. A common theme emerged from an analysis of this comprehensive 5-year data set: natural processes such as riverine discharge, water temperature, wind stress, water column stratification, and tidal currents exhibited the strongest and most direct linkages with estuarine water quality and habitat condition. Bottom-water hypoxia was closely linked to water temperature and water column stratification with no apparent relationship to algal blooms, which may have resulted from anthropogenic nutrient loading. Water column turbidity was strongly linked to wind-induced sediment resuspension events. Periods of high algal biomass were linked to optimal levels of river flow, which provided enough nutrients for phytoplankton biomass development, and sufficient residence time within the estuary for growth to occur. During periods when flows were too high for phytoplankton biomass development, nutrient concentrations within the estuary were high. Thus, nutrient concentrations within the NRE were also largely determined by riverine discharge.

Findings with Implications for MCBCL Management Practices

- Nutrient and TSS loading from MCBCL tributary creeks were generally quite low compared to other similar coastal plain watersheds on the East Coast. As development on

MCBCL increases, there is the potential for enhanced loading of materials through MCBCL tributary creeks.

- The high level of nutrient loading from the upper New River watershed is a primary concern for water quality and habitat condition in the NRE. Downstream gradients of nutrient concentrations (nitrogen and phosphorus) along the New River to the upper estuary indicate that most of the nutrient loading to the estuary is from riverine sources that lie upstream and outside of MCBCL jurisdictional boundaries.
- Under normal or average flow conditions, residence time of the NRE is long enough that phytoplankton have time to fully assimilate nutrient loads. The result is that phytoplankton growth is strongly nutrient limited within most of the NRE, and any increases in nutrient load will result in higher levels of phytoplankton biomass. The poorly flushed region of the estuary from Morgan Bay to Stones Bay is particular susceptible to eutrophication. Therefore, if MCBCL plans to develop the watersheds that drain to these more vulnerable areas of the NRE, mitigation of nutrient and sediment loading should be emphasized because sediment often carries high levels of absorbed nutrients and therefore represents an important non-point nutrient source.
- An effective, comprehensive strategy for mitigating impacts on water quality from future MCBCL activities should include all of the following: (1) minimizing sediment losses by maintaining natural vegetation and ground cover particularly within riparian buffer areas, (2) minimizing the percent impervious surfaces (e.g., parking lots, paved lots, roadways) within a watershed, and (3) promoting water retention within tributary watersheds by preserving and reclaiming wetlands, using retention ponds, minimizing ditching, and controlling stormwater runoff in developed areas with effective best management practices.

Findings with Implications for DCERP2

- The U.S. Geological Survey (USGS) gaging station at Gum Branch has been measuring river flow in the New River for more than 65 years. This historic period of record provides long-term information on flow that cannot be obtained from the temporary Jacksonville gaging station installed in 2008. The USGS gaging station in Jacksonville also suffered from being positioned at a location where tidal influences caused bi-directional flow, which made it difficult to interpret river flow data. Because of this, during DCERP2, the flow into the NRE will be determined from the Gum Branch gaging station and supplemented with additional water quality monitoring data collected at the head of the estuary.
- During DCERP1, an understanding of the relationships between land activities and nutrient and suspended solids loadings in coastal tributary creeks was improved. In addition, critical climate factors such as storminess and patterns of precipitation were confirmed to have major impacts on coastal creek material transport. During DCERP2, the focus will be on headwater creeks as sentinels and indicators of human impacts in coastal watershed systems, but will shift the emphasis to measuring carbon transport and transformations in these systems. Based on the assessment of DCERP1 data, monitoring will continue on only five tributaries instead of 10.

- Based upon the findings of the biogeochemical significance of the upper estuary, plans for DCERP2 include enhanced sampling of the upper estuary near Jacksonville, which is critical for understanding the effects of nutrient loading, particularly nitrate-nitrogen, on carbon flows within the estuary. Both denitrification and phytoplankton uptake and assimilation are very important processes driving the downstream attenuation of nitrate-nitrogen in the upper estuary. From a carbon budget perspective, these two processes act in opposite manners as sources and sinks of atmospheric carbon dioxide. Understanding the relative magnitudes of these two processes is critical for the development of the estuarine carbon budget and for understanding how future changes in nitrate-nitrogen loadings will impact the ability of the estuary to serve as a net source or sink of carbon.

Coastal Wetlands Module

Summary of the Ecosystem

Coastal wetlands are a vital component of the estuarine landscape that links terrestrial and freshwater habitats with the sea. Marshes provide a variety of ecosystem services, including improving water quality by transforming nutrients and trapping sediment, attenuating wind wave and boat wake energy on shorelines, stabilizing the coastal barriers, accreting sediments and building land, and providing recreational opportunities for people. Marshes provide critical habitat area for a diverse group of estuarine organisms, including commercially important fish and shellfish species (**Figure 2-2**). The Coastal Wetlands Module investigated factors affecting the sustainability of coastal marshes relative to military training impacts, projected sea level rise, and shoreline erosion by wind waves and vessel wakes, as well as the role of salt marshes in cycling nutrients within the MCBCL coastal ecosystem. Salt marshes within the MCBCL region occur in the lower NRE and along both shores of the ICW and are typically dominated by smooth cordgrass (*Spartina alterniflora*) and black needle rush (*Juncus roemerianus*). *Spartina* and *Juncus* are the dominant plant species in salt marshes on the Atlantic and Gulf Coasts, making these research results readily transferrable to other locations. They are also the only wetlands on MCBCL that adjoin and occasionally intercept amphibious military training exercises and that play a role in coastal barrier island stabilization. The ICW bisects the backbarrier island salt marsh system on MCBCL, providing an opportunity to examine the potential impact of boating activity and dredging operations on coastal wetlands.

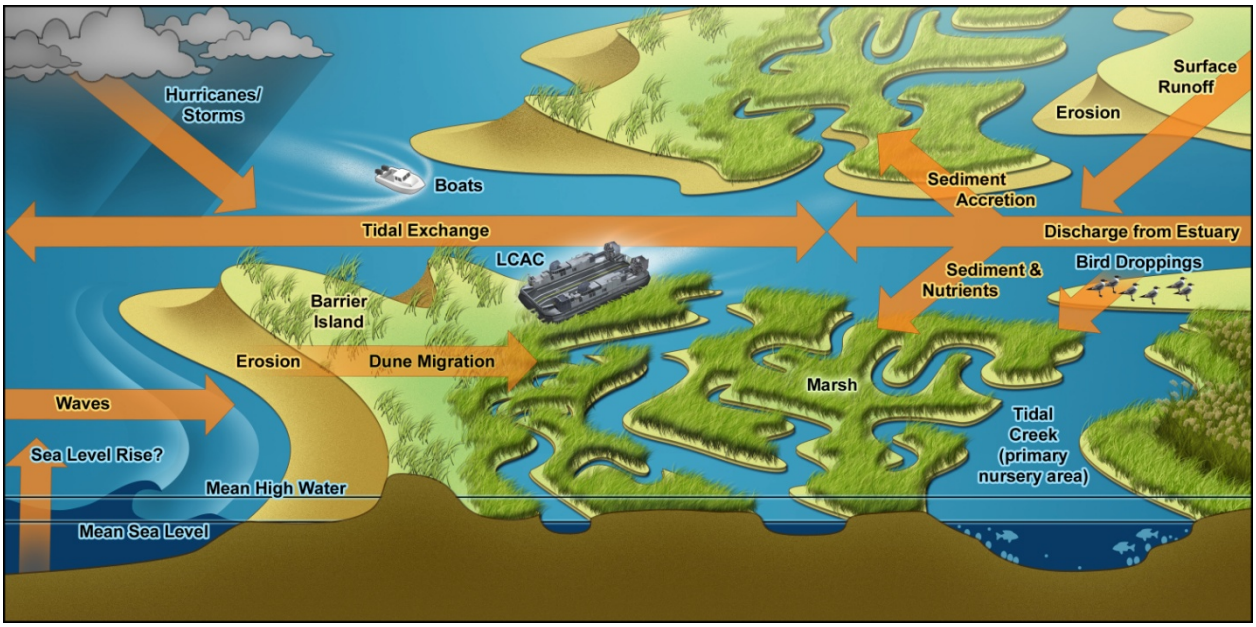

Figure 2-2. Conceptual model for the Coastal Wetlands Module.

Coastal Wetlands Module's Monitoring Program

The Coastal Wetlands Module monitoring effort provided crucial baseline information to support the three research projects of the Coastal Wetlands Module and established and maintained tide gages, which provided the first recognized tidal datums for MCBCL. The Coastal Wetlands Module monitoring effort also measured marsh surface elevation and sediment accretion in *Spartina* and *Juncus* marshes, annually measured marsh above-ground primary production, monitored nutrients in shallow groundwater within the marsh zone, and assessed the quality and accuracy of remote sensing products available to the Base Managers. This monitoring effort has also installed elevation benchmarks to assist future surveys, environmental planning, and infrastructure installation. Components of the Coastal Wetlands Module monitoring effort are presented in **Table 2-3**.

Table 2-3. Coastal Wetlands Module Monitoring Components

Component	Variables	Spatial Scale	Temporal Scale
Land cover and shoreline erosion	Wetland habitat distribution and composition	Entire NRE (2009) and ICW shoreline between Mile Hammock Bay and Browns Inlet (2010)	Aerial photographs and imagery from 1938 to present
	Marsh composition and abundance by species, density, and mean stem height	7 stations (Sites 4–11)	Annually
	Shoreline location and elevation	Entire NRE; 8 stations in detail (Sites 4–11)	Dependent on imagery; biennially and event based (see the Digital Elevation Model)

(continued)

Table 2-3. Coastal Wetlands Module Monitoring Components (continued)

Component	Variables	Spatial Scale	Temporal Scale
Marsh surface elevation	Marsh surface elevation (and sediment accretion)	9 stations (Sites 1–9) 1 m2 horizontal ±2 mm of sediment accretion ±2 cm vertical	Once every 1–3 months
	Water level, temperature, and salinity (for hydroperiod calculations)	2 stations	Continuous 6-minute intervals
	Sediment (percentage of organic content, particle size)	9 stations	Biennially
	Digital Elevation Models—surface elevation	9 stations 100 m of shoreline ±2 cm vertical	Biennially and event based
Nutrient chemistry	Ammonia, nitrate, salinity, sulfate, dissolved organic nitrogen, soluble reactive phosphorus, ferrous, hydrogen sulfide, dissolved organic carbon, hydraulic gradient, and hydraulic conductivity	3 stations	Chemistry—seasonal; hydrology—continuous

Overall, the Coastal Wetlands Module's monitoring station locations range from the brackish marshes of the upper NRE dominated by *Juncus roemerianus* to the salt marshes that border either side of the ICW dominated by *Spartina alterniflora*. This spatial coverage allowed us to demonstrate how changes in marsh geomorphology, tidal amplitude, wave energy exposure, and surface elevation affect the processes (nutrient exchange, sediment accretion, shoreline erosion, marsh primary production) being studied. Our analysis of current monitoring data demonstrated significant site variability in the linkage between marsh biomass and surface elevation and in the relationship between tidal inundation and sedimentation rates. Some of this site variability was due to differing tidal amplitude, which was observed in the tide gauge data, whereas changes in salinity, dominant plant vegetation, and proximity to sediment sources also influenced the measured site-specific responses.

The frequency of sampling ranged from annual measures of primary production to close interval (6- to 15-minute) sampling of water level. In addition, long-term (more than 50 years) rates of shoreline erosion for the NRE and ICW shorelines were determined using aerial photography. Sampling frequency proved to be adequate in detecting significant site and annual variability. However, several of the processes of interest to the Coastal Wetlands Module's research effort are long-term processes (marsh response to sea level rise, shoreline erosion) that require fairly long-term (5 to 10 years) monitoring to distinguish short-term variability from long-term trends and to increase the likelihood of capturing storm events that may be important. Findings presented in this report that are based on less than 5 years of data should be interpreted with caution. These relationships and findings will be re-evaluated based on DCERP2 monitoring data.

Key Scientific Findings—Fundamental Cause-and-Effect Relationships

Shoreline Habitat, Location, and Marsh Distribution

The entire NRE and ICW shoreline was classified by habitat types (Marsh, Swamp Forest, Sediment Banks, Miscellaneous, and Modified [hardened] shorelines). Sediment Banks are the most prevalent habitat type along the NRE shoreline, representing 53%, (66 km [41 mi]), of the total shoreline followed by Marsh (26.5%), Modified (24.3%), and Swamp Forest (7.3%). In contrast, the ICW shoreline was dominated by Marsh (80%), followed by Sediment Bank (19%) and Modified (1%).

The distribution of dominant plant species in NRE shoreline habitats illustrates the transition from *Spartina alterniflora*–dominated salt marshes in the ICW and lower NRE to brackish marshes with a mixture of *Juncus roemerianus* and *Spartina cynosuroides* further up in the estuary. *Phragmites australis*, an invasive marsh species, was documented at several locations along the NRE shoreline. The total area of coastal wetlands on MCBCL is approximately 1,090 ha (2,690 ac). These data provide baseline information to track potential changes in marsh distribution associated with climate change and/or sea level rise and can be used to guide restoration efforts of wetlands.

Marsh Vegetation

A total of nine plant species was recorded in the marsh vegetation monitoring plots between 2008 and 2012. The two dominant species were *Spartina alterniflora* and *Juncus roemerianus*; however, *Distichlis spicata*, *Limonium carolinianum*, *Salicornia virginica*, *Borrichia frutescens*, *Spartina patens*, *Spartina cynosuroides and Typha* sp were also encountered. The low diversity of marsh plants is consistent with other coastal wetlands in the southeastern United States and also reflects the small change in elevation over the monitoring plots, as marsh diversity typically increases closer to the upland border. The use of permanent plots provides the opportunity to detect changes in plant species over time, particularly in marshes that are near transition zones. The marshes in the lower NRE exhibited the highest plant diversity.

Marshes in the ICW are dominated by *Spartina alterniflora*. Mean stem density was significantly different between the three ICW sites, increasing from Freeman Creek (104 stems per square meter), to Onslow Beach Backbarrier (391 stems per square meter) to Mile Hammock Bay (749 stems per square meter). Mean stem height exhibited a different pattern, decreasing from Freeman Creek (68 cm) to Onslow Beach Backbarrier (32 cm) to Mile Hammock Bay (24 cm). Above-ground biomass was calculated using both of these parameters, with the results that mean biomass does not differ significantly (407 and 365 g m^{-2}) for the Freeman Creek and Mile Hammock Bay sites, respectively, and that biomass at both sites are greater than at Onslow Beach Backbarrier (253 g m^{-2}). The difference in biomass between sites was partly due to different marsh surface elevations of the vegetation plots sampled at each site.

Marsh Surface Elevation and Water Levels

Surface elevation tables and marker horizons were used to measure net marsh surface elevation change and sediment accretion rates at nine salt marsh sites on MCBCL between 2008 and August 2012. Three of the sites were dominated by *Spartina alterniflora* and located adjacent to

the ICW, and the remaining sites were located in the NRE. Vegetation ranged from a *Spartina-Juncus* mix to *Juncus* dominated. Seven out of the nine sites showed significant increases in marsh surface elevation during the study period, with significant slopes ranging from 9 mm y^{-1} at a low-elevation *Spartina* site to 2–3 mm y^{-1} at *Spartina* and *Juncus* sites higher in the intertidal zone. Sediment accretion measured with marker horizons at the same sites was two to eight times greater than net surface elevation change, demonstrating the importance of subsurface processes, particularly compaction, on net marsh elevation change.

Water level, temperature, and salinity were recorded at 6-minute intervals, consistent with the National Oceanic and Atmospheric Administration (NOAA) temporary tide gauge requirements, at two stations for the entire 2008–2012 study period. Additional water level data were recorded from three other sites for shorter periods of time and used with the tide gauge data to determine the relationship between water level (inundation), sediment accretion, and surface elevation change. Generally, there was a non-significant relationship between inundation and marsh elevation change and accretion rate over short-term (2–4 months) intervals. Although over the long term, lower elevation sites experienced greater sediment accretion, short-term variability in suspended sediment concentration likely controlled sediment accretion and ultimately marsh elevation change.

Findings with Implications for MCBCL Management Practices

- MCBCL marshes are at risk both from accelerated sea level rise and erosion. It is important to recognize, however, that although MCBCL shoreline stabilization efforts to reduce suspended sediments loading and dissolved nitrogen inputs to the NRE result in improved estuarine water quality conditions, these same efforts may be counterproductive for marshes because they deprive marshes of the nutrients and sediments needed to thrive, particularly during a period of accelerated sea level rise. Given the apparent vulnerability of MCBCL coastal marshes to sea level rise, MCBCL Managers may want to consider adaptive management practices to conserve salt marsh habitats. Some practices include marsh restoration, particularly along shorelines; thin-layer disposal of dredge material; and possibly fertilizing marshes in the lower NRE and Onslow Beach areas.
- Results indicate that tidal range and suspended sediment supply are important in controlling the elevation of marshes. This finding suggests that management practices that directly or indirectly affect inlet dynamics and the suspended sediment concentration of tidal waters may affect the health, productivity, and sustainability of MCBCL coastal wetlands. However, most of the relevant management practices are not under MCBCL control, but under the direct authority of other agencies, and may be implemented outside MCBCL boundaries. For example, ongoing efforts to realign the New River Inlet may alter tide range and suspended sediment delivery to marshes in the lower NRE, and maintenance dredging of the ICW and NRE for navigation purposes may also reduce sediment availability to the MCBCL marshes. Therefore, MCBCL Managers need to be aware of these activities and realize their implications for managing MCBCL's coastal wetlands.

Findings with Implications for DCERP2

- Marshes are known to have, per unit area, one of the highest burial rates for organic carbon of any ecosystem type, and this process is largely driven by the increase in surface elevation needed for the marshes to keep pace with sea level rise. The baseline information on spatial and temporal variability in marsh surface elevation change measured during DCERP1 will be crucial to DCERP2 experimental and modeling efforts to understand the marsh carbon cycle and predict impacts of sea level rise on marsh carbon sequestration.
- Erosion of the marsh shoreline edge represents a potential significant loss of carbon. The documented extent of marsh shoreline in both the mainstem NRE and the ICW and the calculated long- and short-term erosion rates and sediment volume changes when combined with DCERP2 experiments on the lability of marsh carbon liberated via erosion will allow the contribution of marsh edge erosion to the NRE carbon budget to be calculated.
- DCERP1 results also provided insight into important factors affecting the ability of marshes to sustain surface elevation and biomass under sea level rise, including the following: (1) site variability in the relationship between elevation and marsh above-ground biomass, (2) patterns in decadal and short-term marsh shoreline erosion rates along the NRE and the ICW, (3) differences in marsh surface elevation on both sides of the ICW, and (4) significant variability in tidal range between Browns Inlet (1.0 m) and New River Inlet (less than 0.5 m). These results led to DCERP2 research questions on the role of alterations in inlet dynamics and maintenance dredging in controlling the sediment supply sustaining salt marshes along the ICW and highlighted the need for additional information on suspended sediment dynamics and marsh below-ground production and decomposition to support predictive models and recommendations for adaptive management.

Coastal Barrier Module

Summary of the Ecosystem

Onslow Beach is a northeast-southwest trending, wave-dominated barrier island located south from where the Outer Banks barrier-island chain ends. This 12 km (7.5 m)–long barrier fronts salt marsh and is bounded by the New River Inlet to the southwest and Browns Inlet to the northeast. The shoreline of Onslow Beach is sinusoidal, with a central headland separating two shallow, cuspate embayments. The island's morphology also varies along its length. The northern embayment has a wide beach (approximately 80-m [260-ft] wide) with multiple well-developed dune ridges (7–9 m [23–30 ft] in height) and is similar to other barrier islands to the northeast such as Bear Island and Bogue Banks. The central headland area has a narrow beach (approximately 20-m [66-ft] wide) with a single discontinuous dune ridge less than 4 m (13 ft) in height. The beach widens significantly along the southern embayment from 20 m (66 ft) in the northeast to 80 m (262 ft) in the southwest, and the morphology of this portion of the beach is very similar to barrier islands to the south such as Topsail Island. The discontinuous dunes along the southern end are less than 2 m (6.5 ft) in height, and washover fans can be extensive (250-m [820-ft] wide) and extend across backbarrier marshes. The highly variable morphology along

Onslow Beach is unique; however, this allows DCERP research results to be applicable to many other barrier islands worldwide.

The Coastal Barrier Module examined the coastal barrier island ecosystem that lies at the interface between the continental shelf and the protected NRE. This barrier island ecosystem encompasses the shallow subtidal and intertidal shore face, tidal inlet, backshore beach, aeolian dune, shrub zone, maritime forest, and washover sand flat habitats. These habitats are defined by intrinsic ecological processes, but are linked by sediment transport, nutrient exchange, and biological uses, each of which undergoes substantial changes over multiple time scales (**Figure 2-3**). All habitat areas of the barrier, Onslow Island, were studied during DCERP, from the New River Inlet to Browns Inlet, which encompasses approximately 12 km (7.5 m) of island coastline. Research efforts were designed to support the long-term sustainability of the island as an important coastal resource necessary for amphibious military training, for recreation for MCBCL personnel, and for maintaining important habitats for protected species.

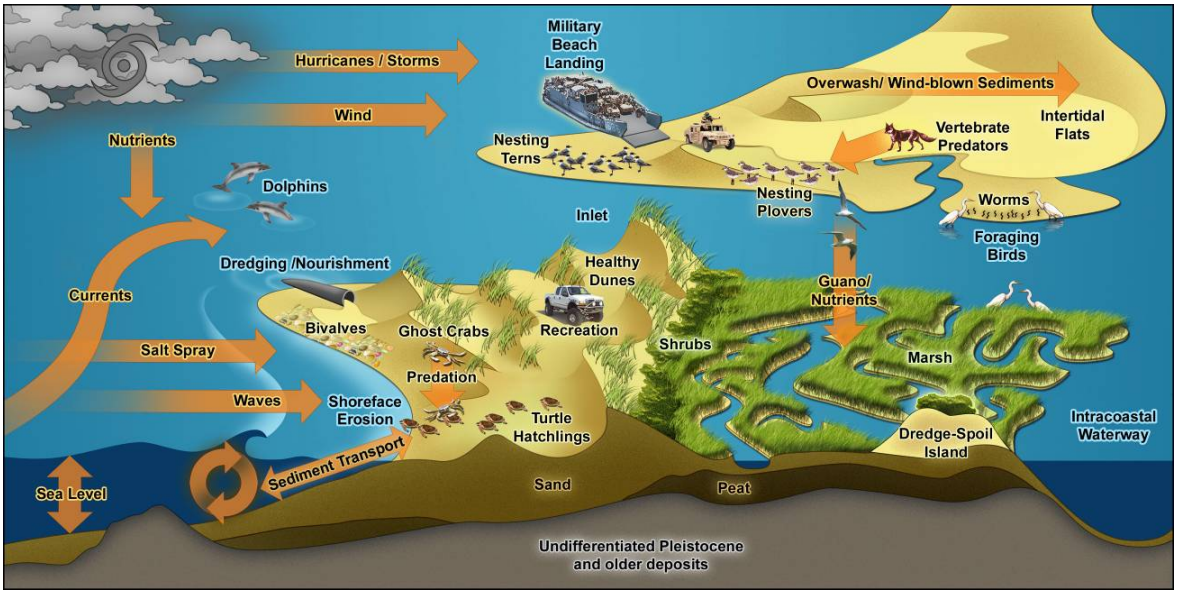

Figure 2-3. Conceptual model for the Coastal Barrier Module.

Coastal Barrier Module's Monitoring Program

The goal of the monitoring activities for the Coastal Barrier Module was to make those necessary measurements and observations that allow isolation and integration of human-derived, including MCBCL training activities, and natural processes to understand the dynamics and health of the coastal barrier ecosystem. The focus was on outputs that served to identify how those components of the ecosystem of greatest concern to MCBCL can be successfully managed and optimized. Fulfilling this goal required not only measurement of conditions and processes from physics to biology, but also analysis, synthesis, integration, and modeling of the information. To achieve these goals, the Coastal Barrier Module's monitoring program included offshore meteorology conditions; hydrodynamics (including wave velocity, wave heights, period, and direction); information on currents, tides, and water temperature; geomorphology (including barrier morphology and shoreface bathymetry); sedimentology; and biology (including vegetation, shorebirds, benthic invertebrates, surf fish, and sea turtles) (**Table 2-4**).

Table 2-4. Coastal Barrier Module monitoring components

Component	Variables	Spatial Scale	Temporal Scale
Meteorology (ocean)	Air temperature, wind speed, air pressure, solar radiation, and wind direction	2 stations: 5 and 25 miles seaward of the New River Inlet	Continuous
Hydrodynamics	Horizontal and vertical wave velocity, wave heights, and period; direction; currents; and water temperature	2 stations: 5 and 25 miles seaward of the New River Inlet	Continuous
	Horizontal and vertical wave velocity, wave heights, period, and direction	2 stations: Located seaward of Focus Site 3 and at Bogue Pier	Continuous
Hydrodynamics (continued)	Tide data	Acquired from NOAA's sites in Charleston, SC; Wilmington, NC; and Norfolk, VA	Continuous
	Shoreline position, sandbar position, and morphology; and nearshore wave period, direction, and height	Entire length of authorized beach and individual sites	Every 3 years (entire); semiannually and before and after storms (site specific)
Geomorphology	Shoreface bathymetry	The nearshore (2-m to 10-m) depths of the coastal barrier island, including the New River Inlet and Onslow Bay	Baseline survey (2007)
	Barrier morphology	15 sites across Onslow Island and 3 sites across Bear Island	Semiannually (May and September) and before and after storms
Sedimentology	Compaction, texture, and composition	20 samples from each of the 10 focus sites (7 on Onslow Island and 3 on Bear Island)	Semiannually (May and September) and before and after storms
	Aeolian transport volume	3 sites on Onslow Island	Weekly
Biology	Benthic invertebrate abundance and biomass by size class and community structure	2 replicate vertical transects from each of the 10 focus sites (7 on Onslow Island and 3 on Bear Island)	Semiannually and before and after storms
	Shorebird and seabird abundance and community structure	Entire length of Onslow Beach, the New River Inlet, and Browns Inlet shorelines	Approximately every 10 days (data collected by MCBCL)
	Dune, shrub, and marsh plants areal cover; vegetation height; and surface elevation	Vertical transects at 7 sites	Once every 5 years
	Surf fish abundance and community composition	2 replicates at each of the 10 focus sites (7 on Onslow Island and 3 on Bear Island)	Annually in the fall
	Site selection for sea turtle nests, false crawls, and success of nesting effort	Nesting and false crawls recorded along the entire length of Onslow Beach, the New River Inlet, and Browns Inlet shorelines	Nesting and false crawls assessed daily in season (data collected by MCBCL)

Sampling was conducted continuously or routinely for some parameters and during unscheduled times to respond to planned human activities (e.g., military training events, pier removal, dredge-spoil disposals) and episodic storm events (e.g., nor'easters, hurricanes). In August 2011, the region was affected by Hurricane Irene, a Category 1 hurricane that caused significant overwash on the island. Changes to island morphology and ecology were finally able to be documented and our hypotheses were able to be tested to predict how the island would respond to a large storm event.

Conclusions and Implications from the Coastal Barrier Modules

Key Scientific Findings—Fundamental Cause-and-Effect Relationships

Seasonal Variability of Winds and Waves

Seasonal winds and waves patterns were determined from data collected at offshore buoys and are important because these forces affect barrier island erosion and accretion patterns. In summer, the barrier island should accrete due to the light southeastern winds and small waves with a large spread in wave directions from the east-northeast, southeast, and southwest. During fall, there is a higher probability of storm events and a higher chance of barrier island erosion due to the return of strong northeast winds and high waves primarily from the southeast. Additionally, higher significant waves heights are recorded annually in the late fall to winter period.

Annual Trends—Currents, Waves, and Water Levels

Nearshore water velocity and water level were determined from measurements collected 500 m offshore of Onslow Beach. A strong bilateral flow component was identified that followed the along-shore orientation of Onslow Beach and an on-shore presence of the flow. On an annual basis, approximately 30–40% of the total along-shore flow is towards Browns Inlet to the northeast, 20% is towards the New River Inlet to the southwest, and 10% is offshore, leaving the remaining 30–40% of flow onshore. Annually, detided and demeaned nearshore water levels increased to a maximum during the late summer and early fall period. Part of this may be due to the steric response of oceans to thermal heating or a combination of this in conjunction with wind directional changes. During the summer, water levels were significantly lower in 2008 than in both 2009 and 2010. The difference between the years was approximately 20 cm (7.8 in).

Barrier Morphology

Change in the morphology of the barrier island was determined from detailed laser surveys conducted at 15 sites throughout the study period. Results indicate that Onslow Beach can be divided into three different zones, defined by distinct rates of shoreline movement. These zones include: (1) the accreting area immediately adjacent to the New River Inlet, where the shoreline moved 30.9 to 4.3 m y^{-1} (101 to 14 ft y^{-1}); (2) the erosional southwestern portion of the island, where the shoreline moved −3.7 to −6.0 m y^{-1} (−12 to −20 ft y^{-1}); and (3) the relatively stable northeastern portion of the island, where the shoreline moved 2.4 to −1.2 m y^{-1} (7.9 to −3.9 ft y^{-1}). The spatial distribution of these three zones does not correspond to the various military-use zones, indicating that military activities did not impact erosion rates.

These zones are influenced by variations in the underlying geology and associated sediment availability on the inner continental shelf, which explain why the southwestern portion of the island is sediment starved and northeastern portion of the island is sediment rich. The irregular shape of the barrier island shoreline indicates that island evolution has also been characterized by long-term (centennial to millennial) along-beach variations in shoreline movement. The three morphologic change zones are also influenced by inlet dynamics, which control sediment supply to the island. Away from the inlet, there is very little sand offshore of the southwestern portion of the island, resulting in this portion of Onslow Beach being sediment starved. In contrast, the northeastern portion of the island has thick (0.5 to 2.5 m) layer of sand offshore, which serves as a local sediment source for this portion of Onslow Beach.

Sediment Transport

Sediment texture and composition are distinct along Onslow Beach. The sediment texture sampled at the erosional southwestern portion of the barrier is distinctly coarser than the sediment sampled at the northeastern end, whereas in the middle portion of the island, sediment is a mixture. These differences were consistent throughout the monitoring period and suggest that there is little exchange of sediment between the southern and northern embayments. Sand transported along the barrier island by longshore currents is likely not moving across the headland between these two beach zones.

Sand is also transported across the barrier island from the beach to the marshes in the backbarrier and represents a source of sediment to these marshes. Our results found that the percent volume of the marsh composed of wind-driven (aeolian) sand decreases by an order of magnitude approximately 20 m (66 ft) from the marsh edge. Near the edge, the marsh contains greater than 20% aeolian sand (by volume), where it is fronted by a washover fan in the southwestern portion, or less than 10% aeolian sand, where it is fronted by a high-elevation dune ridge in the northeastern portion of the island. Further into the marsh platform, the percent volume of aeolian sand was consistently low at both sites (less than 1%). The height of beach vegetation limited or completely blocked aeolian sediment transport across the island.

Biological Barrier Island Monitoring

The biological monitoring component of the Coastal Barrier Module measured faunal species, including benthic invertebrates, surf fish, ghost crabs, sea turtles, and shorebirds, and the flora of Onslow Island. All of the faunal species monitored exhibited substantial year-to-year variations in abundance, and their life cycles enable them to have substantial resilience to environmental and anthropogenic stressors as long as habitat loss does not occur. One exception to this finding was related to ghost crab populations. Ghost crab abundances were consistently depressed in the military training area of the island. This was a pattern that could not be attributed to a spatially explicit distribution of environmental factors (e.g., lack of habitat or unsuitable sediment type), thereby raising the possibility that some aspect of the military training activities have affected ghost crab abundances.

Findings with Implications for MCBCL Management Practices

Military Training Exercises and Other Land Uses

- Although military training continues year round on Onslow Island, the extensive training during the summer is best in terms of seasonal wind and wave climates that facilitate sediment accretion and barrier island fortitude.
- MCBCL Managers should consider future placement of recreational infrastructure at the northeastern portion of Onslow Island, which is characterized by low erosion rates. MCBCL Managers should note that sand placed at the northeastern end of the barrier island through dredge-spoil disposal is not transported naturally along shore past the headland and will not mitigate erosion in the southwestern portion of Onslow Island.
- Currently, military traffic through dune fields is restricted to well-defined corridors, thus constraining impacts. There is no evidence that beach erosion, sediment character, sediment compaction, and intertidal benthos or surf fish abundances are influenced in the long-term (months to years) by military training activities.
- Existing military training activities and practices are constrained to levels of environmental disturbance that are well within the ecosystem's range of resilience, with the exception of one species: ghost crabs, which had significantly lower populations in the military training zone. Similarly, off-road recreational vehicle (ORRV) activity and pedestrian disturbances are also well constrained. The only significant effects appear to be related to changing the spatial distribution of shorebirds on the island. However, because several kilometers of beach are still available for bird foraging and resting areas, this displacement does not appear to have any negative effects.

Protected Species Management

- Based on review of the MCBCL shorebird data, we recommend that the Base consider conducting shorebird surveys on foot and performing targeted surveys each year for those avian species that are listed as Candidate, Threatened, or Endangered by the federal government, and similarly as Special Concern, Threatened, or Endangered by the State of North Carolina. Targeted surveys should be stratified by key seasons (e.g., winter, spring migration, breeding period, and fall migration surveys should be conducted annually), but be repeated at the same frequency and intensity across years.
- MCBCL management of the endangered sea turtle populations involves removing nests from the military training area and relocating these to unimpacted areas of the coastal barrier and should be continued. Hatching success of turtle eggs are comparable to or exceed hatching success rates achieved on other North Carolina barrier islands.
- However, MCBCL Managers should expect changes in the near future in nest-site selection by sea turtles because of beach landscape changes such as reduced or absent backbeach areas (leading to inundation of misplaced seaward nests) and scarped dunes, which may slough. Future monitoring of sea turtle nests should record additional variables: (1) precise measurement of nest elevation and location on the beach; (2) proximity of local landscape features (e.g., vegetation, dune or scarp features to the nest,

sediment type); and (3) beach width and slope. This information would improve the ability of MCBCL personnel to predict the likely fate of nests in backbeach areas subject to erosion and dune collapse.

Management of Dredge-Spoil Disposal on Onslow Beach

- The use of the northeastern end of Onslow Beach for disposal of dredge-spoil materials needs to be monitored and constrained. Failure to construct a typical beach profile after the dredge material has been deposited will adversely affect sea turtle nesting in a region of the island that is normally ideal for nesting turtles and their hatchlings. Also, the relatively small volume disposals that have occurred had short-term, negative effects on *Donax* spp, an important shorebird prey resource. Larger volume disposals can be expected to cause longer lasting, more substantial decreases in shorebird prey abundance.

- Sediments deposited by two disposal events were a good match with the existing beach sediments without large proportions of either very fine or very coarse dredge material. Disposal of very fine or very coarse dredge material on other North Carolina beaches has been shown to have substantial, long-lasting negative effects on the infaunal prey and on surf fish feeding. MCBCL Managers should encourage disposal of only medium-grained sands to Onslow Beach or placement of dredge materials elsewhere.

Management of Dune, Shrub, and Marsh Plant Communities

- Current MCBCL management practices of restricting both recreational and military traffic to well-defined corridors overall have prevented habitat loss from vehicular traffic. Recent storms and sea level anomalies have altered the structure of the beach and dunes on the southwestern end of the island, including the area where military training occurs. The absence of the backbeach area in these military training and ORRV zones, however, could lead to greater intensities of pedestrian and vehicular traffic onto the dunes and into the habitats behind the dunes. If the frequency and intensity of military training increases, encroachment on the near-beach vegetative communities could increase and negatively impact this community.

Findings with Implications for DCERP2

- As a part of DCERP2, the coupled Advanced Circulation (ADCIRC) + Simulating Waves Nearshore (SWAN) Model validated during DCERP1 will be used as input into a morphological model to simulate response of the transgressive barrier. Quality wind, wave, and velocity data near Onslow Beach are essential to understanding fully the dynamics associated with barrier island morphology. During DCERP2, data from the wave buoys can be used for modeling purposes; however, the deployment of wave buoys and Acoustic Wave and Current profilers closer to the shore than those deployed during DCERP1 monitoring is recommended.
- Sea level rise will produce further erosion of dunes and create more washover fans on Onslow Island. Information gained from DCERP1 will enable us to quantify this encroachment on existing habitats and follow the rates of primary or secondary plant community succession in DCERP2.

Terrestrial Module

Summary of the Ecosystem

The Terrestrial Module's ecosystem-based research was conducted along the gradient of vegetation from the salt marsh at the estuary margin, through brackish and freshwater marsh, to the longleaf pine savannas and pocosins (i.e., shrub bogs), which dominate the upland terrestrial environments on MCBCL. Variations in the biota and ecosystem processes along this gradient are driven by variations in hydrology, soils, and fire behavior. Most of the rare species that are characteristic of coastal terrestrial ecosystems, including species of concern on MCBCL, are found in the transitional zones of these gradients. Changing patterns of land use, agriculture, and forest management have greatly altered forest ecosystems across much of the mid-Atlantic lower coastal plain. In particular, vast areas once dominated by open longleaf pine savanna now support closed canopy stands of loblolly pine (*Pinus taeda*) with a dense understory and midstory of broad-leaved shrubs and trees. The absence of fire on these landscapes has exacerbated this trend. This situation is typical for large portions of MCBCL. In recent years, longleaf pine restoration at MCBCL has focused on the use of understory and midstory thinning (with HydroAx equipment) to produce savanna-like conditions and allow restoration of historical fire regimes using prescribed burning. **Figure 2-4** presents the conceptual model for the Terrestrial Module and illustrates the complementary nature of these critical physical, chemical, and biotic processes, disturbances, and interactions.

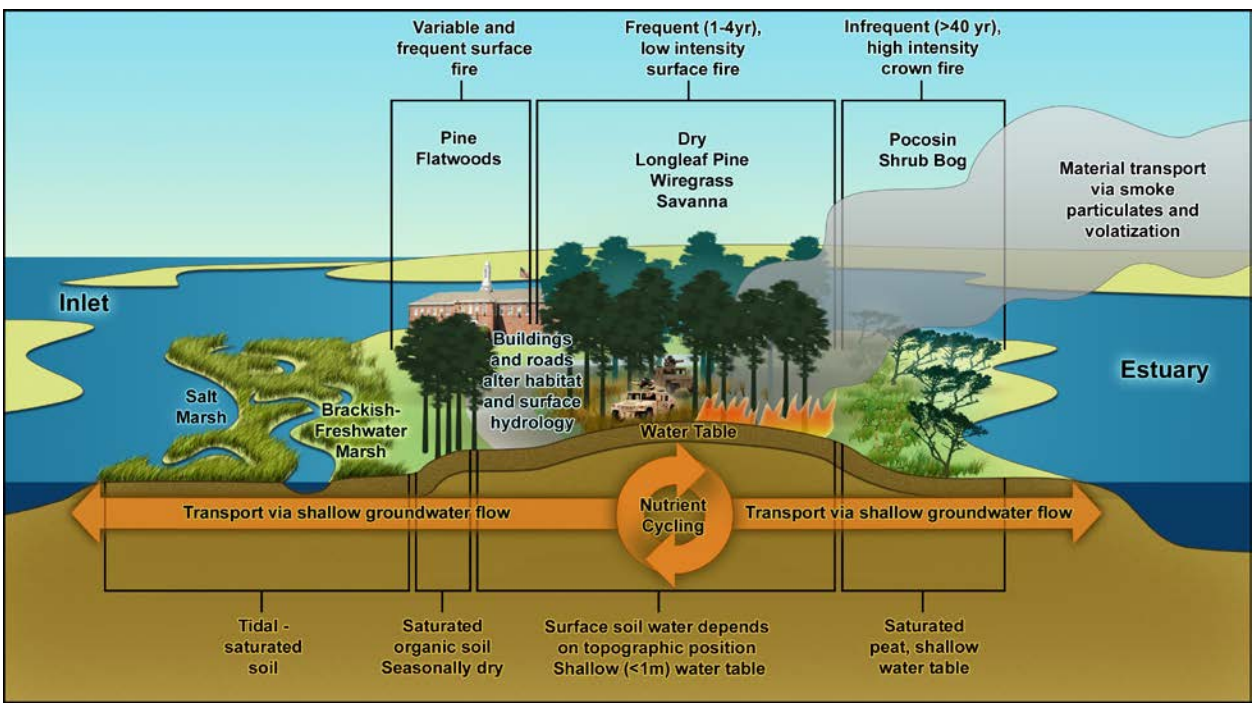

Figure 2-4. Conceptual model for the Terrestrial Module.

The locations of transitions from one ecosystem to another along this gradient are often influenced by disturbance (fire) history (Christensen, 1981; Garren, 1943). Fire is a natural part of this landscape, and natural fire regimes (frequency and intensity) change across this soil–hydrology–vegetation gradient, from frequent surface fires in longleaf pine savannas to relatively

infrequent and intense crown fires in pocosins. The Terrestrial Module's research focused on the critical knowledge gaps related to efforts to restore longleaf pine ecosystems on sites across MCBCL that were modified by past forest management practices. The research examined the effects of alternative midstory restoration strategies (e.g., prescribed burning, mechanical thinning) on understory plant, insect, and avian communities, particularly the federally protected, red-cockaded woodpecker (RCW; *Picoides borealis*). In addition, the research provided information regarding whether management for a single species (i.e., RCW) is beneficial or detrimental to other avian species.

Terrestrial Module's Monitoring Program

The Terrestrial Module's monitoring program focused on two general objectives: the development of a network of permanent vegetation plots representing the full range of environmental gradients at MCBCL and a geographic information system–based assessment of changes in land use and land cover on MCBCL lands (**Table 2-5**). The network of permanent vegetation plots provided a detailed understanding of the variation in plant species diversity, composition associated with variations in soil physical and chemical characteristics, and patterns of disturbance.

Table 2-5. Terrestrial Module Monitoring Components

Components	Variable	Spatial Scale	Temporal Scale
Flora	Species composition, diversity, and distribution	131, 0.1-ha sample sites distributed across MCBCL	Initial sample collected during 2009 and 2010; 5-year intervals thereafter
Forest floor and soil	Fuel load, soil bulk density, pH, and organic matter (soil and fuel moisture)	Associated with each of the 131 sampling sites above	Initial sample collected during 2009 and 2010; 5-year intervals thereafter
Land-cover and land-use change	Land-cover types and vegetation greenness gain and loss	Local and regional (to include lands on Base and within the watershed surrounding MCBCL)	Annual Landsat data from 1984, 1990, 2005, 1998, 2005, 2007, 2009, and 2011

The vegetation monitoring plots were established across a broad range of stand characteristics, particularly those that are of greatest interest to MCBCL management. Forest types include both longleaf and loblolly pine forests across a wide range of age classes, edaphic properties, and disturbance histories. Significant data were also collected on high pocosin systems, which cover much of the installation, compared to other land-cover types on MCBCL. Changes in land-cover types and vegetation greenness gain and loss were also determined using cloud-free Landsat Thematic Mapper images from 1984, 1990, 1998, 2005, 2007, 2009 and 2011. The 1984 image was used as the baseline, and change between subsequent images was determined from this baseline image to determine persistence of change and to reduce variability. Therefore, changes were able to be tracked through all six change periods from 1984 to 2009.

Conclusions and Implications from the Terrestrial Module

Key Scientific Findings—Fundamental Cause-and-Effect Relationships

Overall Patterns of Terrestrial Plant Species Composition and Diversity on MCBCL

More than 600 individual plant taxa were found among the 131 permanent vegetation plots distributed across MCBCL. The vegetation plots had an average species richness of 41.6 species per 0.1 ha. The range of species richness among plots was large, with as few as nine species per 0.1 ha in a pocosin stand to as many as 119 species per 0.1 ha in a longleaf pine stand. MCBCL terrestrial vegetation composition and diversity vary in response to two major environmental gradients: near coastal ecosystems and inland terrestrial forests. Near coastal ecosystems (within 1 km [0.62 mi] of the coast) vary from dune to maritime scrub and are heavily influenced by the effects of salt spray. Inland, terrestrial forests vary along a gradient from well-drained soils dominated by longleaf pine to broad-leaved hardwoods and depression wetlands on soils that are not well drained. Regarding composition and diversity, loblolly pine forests are generally broad-leaved hardwoods and are intermediate to longleaf pine forests. Species richness was notably lower in pocosin sites than in any other forest type. Soil bulk density was highly correlated with soil organic matter and cation exchange capacity. Soil bulk density is thus a relatively good proxy for a variety of soil characteristics, and it can be easily measured.

Indicator species analysis identified species that were abundant and concentrated in each forest type. The high number of indicator species in the longleaf pine forest, depression wetlands, coastal dune, and hardwood forest types was a reflection of the unique features of their respective environments and the relative absence of disturbance. The fact that only a single species (i.e., black gum [*Nyssa sylvatica*]) had a significant indicator value for loblolly pine stands was probably indicative of the history of disturbance in these forests and the wide range of conditions over which they occurred.

Patterns of Terrestrial Plant Species Composition and Diversity in Pine-Dominated Ecosystems

In pine-dominated vegetation monitoring plots, a total of 357 taxa were identified. Species richness was highest in longleaf pine stands (57.9 species per 0.1 ha) and lowest in pocosins (17.6 species per 0.1 ha). Species composition varied in pine-dominated stands in relation to soil and disturbance gradients. Longleaf pine stands occur on soils with high bulk density and low organic matter, and pocosins dominate where bulk density is low and organic matter is high. Loblolly pine stands segregated from longleaf and pocosin stands based on land-use history and the past exclusion of fire. Plant species richness is markedly lower in disturbed loblolly pine stands than in longleaf pine stands with similar soil conditions.

Changes in Species Composition and Diversity in Longleaf Pine Stands from 1991 to 2010

Twenty-one mature longleaf pine plots were deliberately selected for sampling in DCERP1 because they were previously sampled by the CVS in 1991. This provided the opportunity for the direct evaluation of change in these stands over an 18-year period when MCBCL Managers implemented a 3-year rotation prescribed burning program in these stands. At all spatial scales, from 1 m^2 to 0.1 ha, species richness increased among these 21 longleaf pine plots. The increase in species richness at smaller spatial scales is a favorable indicator of successful restoration in

longleaf pine stands and is likely a consequence of regular prescribed burning. The increase in richness was remarkably consistent across the 21 sample plots; the number of species per 0.1 ha increased in 19 plots and remained unchanged in the other two plots. Stands that, based on species composition, appeared to have been disturbed in 1991 had species compositions in 2009 more indicative of undisturbed conditions.

Greenness Change Analyses

Overall, MCBCL experienced a 7.2–10.6% (3,648–5,373 ha [9,014–13,277 ac]) permanent vegetation loss between 1984 and 2009; however, up to 37.8% (19,060 ha [47,098 ac]) of the vegetation on MCBCL was reduced or removed at some time during this period. For the most recent change analysis period (2009–2011), 1.7% of the surface area (840 ha [2,076 ac]) of MCBCL lands experienced significant loss or removal of vegetation in concentrated areas, likely representing new infrastructure construction. In comparison, based on the 1984–2009 individual change period, between 3.9–10.3% (1,993–5,265 ha [4,925–13,010 ac]) of MCBCL lands have experienced a "persistent" gain in vegetation since 1984. Although the Greater Sandy Run Area (GSRA) represents only 33% of the area of MCBCL lands, it accounted for 65–75% of the permanent greenness gain. The re-growth in the GSRA follows clear-cutting performed by a paper company, which owned this land before it was acquired by MCBCL. These areas are large blocks of forest re-growth. The re-growth areas occurring on the mainside of the Base are small areas, much of which is associated with landscaping activities undertaken following construction.

Findings with Implications for MCBCL Management Practices

- Future sampling of the network of permanent vegetation plots across MCBCL will provide important information on vegetation change in response to anthropogenic and natural drivers. Analysis of the 21 longleaf pine plots sampled in both 1991 and 2009 support the value of such longitudinal studies and the assertion that current MCBCL forest management practices (e.g., prescribed burning) are meeting MCBCL restoration objectives.
- Indicator species analysis provides a basis for identifying a subset of floral indicator species upon which future sampling can be focused, which can, in turn, greatly simplify sampling procedures and reduce sampling costs.
- Our analyses found that from 1984–2005, there was a greenness loss on more than 4.66% of MCBCL lands (a rate of 0.22% loss per year). During the 4-year period (2005–2009), greenness loss increased to 0.64% per year; this was a much greater rate of annual loss than the average observed during the previous 21 years. Additional greenness loss occurred after 2009 and before 2011 that covered 1.7% of MCBCL. This is a rate of 0.85% loss per year, which is very similar to the rates found for 2005–2007 (0.84%) and 2007–2009 (1.10%). These change data clearly identified a rapid period of development, resulting in vegetation loss at a rate of at least three to five times the long-term average rate observed prior to the GTF campaign.

Findings with Implications for DCERP2

- Continuation of greenness change analyses will allow analysis for both transient and permanent vegetation changes on MCBCL. These change data will provide information needed to understand and assess the impacts of carbon management associated with various forest management practices across MCBCL.

Atmospheric Module

Summary of Atmospheric Conditions

The input of nutrients and potential pollutants via atmospheric deposition interacts with most key terrestrial and aquatic ecological processes occurring at MCBCL as illustrated in **Figure 2-5**. Atmospheric deposition is a direct source of inputs onto the open-water surfaces of the aquatic ecosystem and onto the vegetation surfaces of the terrestrial ecosystem, with the frequency, level, and composition of these inputs posing an important influence on flora diversity. In addition to direct sources of atmospheric input, the aquatic ecosystem is impacted by atmospheric deposition after it is filtered and altered by passage through the terrestrial ecosystem. This impact occurs during all time scales, ranging from rapid inputs following large rainfall events (runoff) to slow, but critical, changes in baseflow from the superficial aquifer (Hunsaker et al., 1994; Osgood and Zieman, 1998). Similarly, terrestrial ecosystem impacts might be due to exposure to a complex combination of long-term climatological stress (e.g., temperature, drought) and shorter term air pollutant stress (oxidants and metals).

Fire is a natural part of the terrestrial landscape in the southeastern United States in general and MCBCL in particular. In addition, natural fire regimes (e.g., frequency, intensity, season) vary across a soil–hydrology–vegetation gradient, from frequent surface fires in longleaf pine savannas to relatively infrequent and intense crown fires in pocosins. MCBCL Managers use prescribed burning to reduce wildfire risk, maintain training areas, and restore habitat for the federally protected RCW. Despite these benefits, prescribed burning is a major source of $PM_{2.5}$ (fine particulate matter) and other air pollutants because of its incomplete and largely uncontrolled combustion process, which involves flaming and smoldering phases with different effective fuel consumption. Certain fuel and fire meteorological parameters influence the emissions from the different combustion phases of prescribed burning, which, in turn, participate in transport processes within the atmospheric boundary layer, causing air quality impacts on local and regional scales (Friedli et al., 2007; Lee et al., 2005). Coarse particles (PM_c) in the size fraction between 2.5 and 10 µm receive special attention with local impacts because gravitational settling accelerates their deposition to the surrounding aquatic and terrestrial surfaces. One of the more important PM_c–enhancing factors involves the proximity of MCBCL to the Atlantic Ocean, which provides an environment conducive to sulfate formation. Another PM_c–enhancing factor is the reaction of nitric acid with sea-salt aerosol to form coarse mode sodium nitrate particles, potentially increasing the PM_c mass.

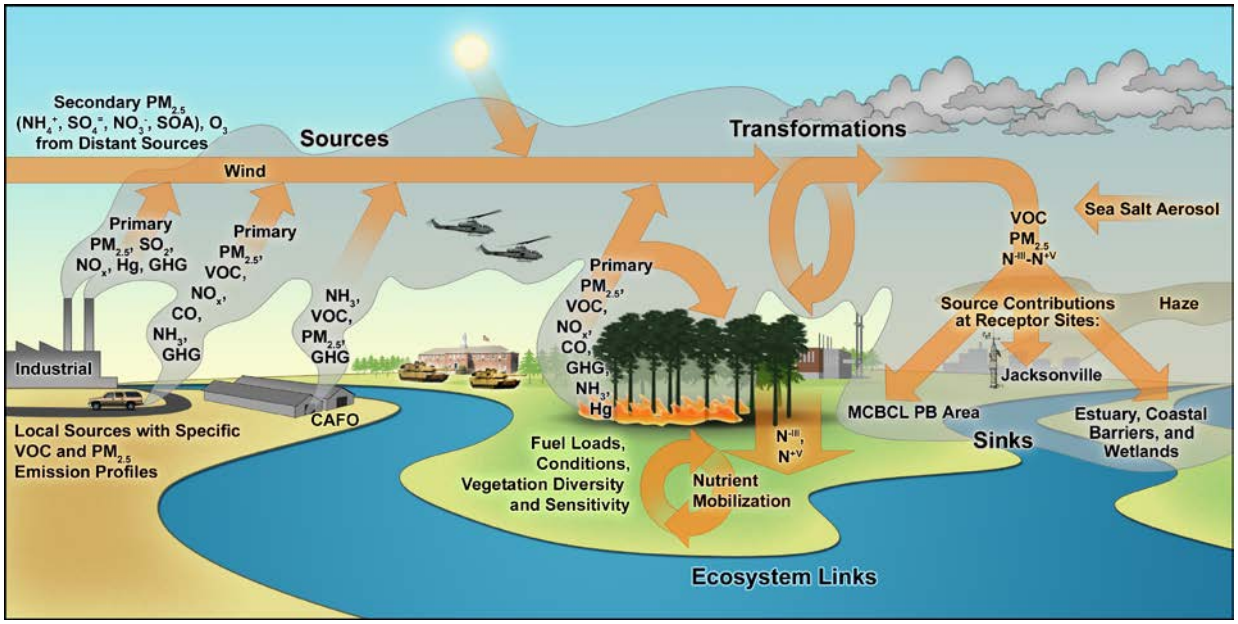

Figure 2-5. Conceptual model for the Atmospheric Module.

Atmospheric Module's Monitoring Program

The objective of Atmospheric Module's monitoring activities was to characterize the role of air quality in the natural ecosystem of MCBCL by capturing meteorological and climatological processes and their occurrence in different spatial and temporal scales in support of various DCERP1 research activities. To track and compare meteorological and air pollution trends observed on MCBCL in the context of more regional trends, a network of on-Base monitoring sites was established. In addition, procedures were developed for merging data from two major regional networks (i.e., MesoWest and the North Carolina Department of Environment and Natural Resources) into a common and consistent time base (hourly averages) for all acquired parameters. Three on-Base sites began acquiring data in March 2008 that consisted of various meteorological parameters (including photosynthetically active radiation, wind speed and direction, air temperature, and rainfall) and monitoring the concentrations of particulate matter ($PM_{2.5}$ [fine particulate matter], PM_{10} [coarse particulate matter]), and ozone (**Table 2-6**). In October 2010, two additional PM monitoring sites were added on MCBCL to increase spatial resolution in tracking on- and off-Base pollution sources. The reporting of merged quality controlled data from four on-Base sites and a total of nine off-Base sites started in July 2008 and continued until September 2011.

Table 2-6. Atmospheric Module Monitoring Components

Component	Parameters	Temporal Scale	Spatial Scale
Meteorology	WS, WD, BP, TEMP, RH, PAR, PCP	Minutes to hourly	4 on-Base stations
	WS, WD, BP, TEMP, RH, PCP, VIS, CIG, FT, FM	Minutes to hourly	9 off-Base stations
EPA criteria pollutants	Ozone	Minutes to hourly	3 on-Base stations
	Sulfur dioxide	Hourly	2 off-Base stations
	PM_{10} and $PM_{2.5}$ mass	Minutes to hourly	4 on-Base stations

BP = barometric pressure; CIG = ceiling; EPA = U.S. Environmental Protection Agency; FT = fuel temperature; FM = 10-hour fuel moisture; PAR = photosynthetically active radiation; PCP = precipitation; $PM_{2.5}$ = particulate matter with a diameter less than or equal to 2.5 micrometers; PM_{10} = particulate matter with a diameter less than or equal to 10 micrometers; RH = relative humidity; TEMP = temperature; VIS = visibility; WD = wind direction; WS = wind speed.

Conclusions and Implications from the Atmospheric Module

Key Scientific Findings—Fundamental Cause-and-Effect Relationships

Precipitation

The study domain (four on-Base and nine off-Base monitoring sites) experienced general drought conditions during the study period (2008–2011), except for at a few locations where episodic events added large rainfall amounts during storms. Annual average rainfall amounts consistently decreased along the inland gradient across the larger study domain; however, rainfall amounts did not vary significantly across the local MCBCL landscape.

Ozone

MCBCL lands received the highest average ozone concentration from a southeasterly direction, pointing to effects from photochemical production of ozone in maritime air masses transported by sea breezes. Typically, ozone concentrations were highest near the beach and decreased moving inland toward the City of Jacksonville. Over the past 10 years, ozone levels declined steadily across the region, which was in line with the nationwide trend. The only anomaly in season trends occurred in 2009 when summer ozone formation was slightly higher, mainly due to the unusually warm and dry weather conditions in early spring that were favorable to the photochemical production of ozone.

Although the local (on-Base) ozone measurement methodology was not intended to meet regulatory requirements, the metrics employed by the U.S. Environmental Protection Agency (EPA) were applied as a basis for site comparisons of air quality. EPA set two types of air quality standards for ground-level ozone: (1) a primary standard to protect public health, and (2) a secondary standard to protect public welfare, including protection against visibility impairment and damage to building, animals, crops, and vegetation. The secondary standard was used to determine whether vegetation across MCBCL lands was stressed by ozone. Beginning May 27, 2008, the 3-year average of the maximum 8-hour average ozone concentration must not exceed 75 ppb to be considered in attainment. This value was lowered to70 ppb in January 2010. Ozone

concentrations at the two ground-level MCBCL monitoring sites were below the 70 ppb standard from 2008–2011, ranging 65 to 70 ppb. Ozone concentrations at MCBCL during this time, therefore, were not of concern for causing damage to vegetation and no visible signs of vegetation damage were noted on MCBCL lands.

Particulate Matter

$PM_{2.5}$ levels decreased steadily during the past 10 years (2001–2011). Based on data from off-Base monitoring sites to the southwest and north of MCBCL, the regional airshed exhibited a trend of increasing $PM_{2.5}$ levels with increasing distance from the coast. This trend correlated with a regional trend of decreasing amounts of rainfall away from the coast because rainfall is the most effective sink for atmospheric $PM_{2.5}$.

The monitoring approach used allowed the measurement of PM_c from the PM_{10}–$PM_{2.5}$ difference. High-resolution data of simultaneously measured $PM_{2.5}$ and PM_c provide powerful diagnostics into potential sources and source impact processes causing local air pollution. For example, a large $PM_{2.5}$:PM_c ratio indicates the depletion of PM_c due to gravitational settling and surface deposition, influence from combustion sources, and formation of new particles from nucleation and heterogeneous gas-particle conversion processes that are typical for secondary organic aerosol. In contrast, a low $PM_{2.5}$:PM_c ratio would point to a potential influence from windblown dust and marine (sea-salt) aerosols. One of the more important conditions enhancing PM_c in our study domain stems from the proximity of MCBCL to the Atlantic Ocean. This proximity provides an environment that is conducive to: (1) sulfate formation via oxidation of sulfur dioxide to sulfate in sea-salt containing cloud droplets and deliquesced sea-salt aerosols and (2) the reaction of nitric acid with sea-salt aerosol to form coarse mode sodium nitrate particles. Under marine conditions, the sea-salt displacement reaction can be expected to yield a complete conversion of nitrate from the fine to the coarse aerosol mode, thereby potentially increasing the PM_c mass.

Across MCBCL, $PM_{2.5}$ was lowest at the beach and increased farther inland, likely resulting from the addition of $PM_{2.5}$ from residential heating and wood burning in urban areas, especially during winter. The $PM_{2.5}$:PM_c ratio at the New River Air Station (the on-Base monitoring site farthest away from the coast) was highest in most seasons, especially for air mass transport from northerly and northeasterly directions, which included the major traffic corridors for thousands of daily commuters to MCBCL. For periods when smoke-laden air masses blew into the Base lands from the southwest, both $PM_{2.5}$ and PM_c levels were elevated. However, the PM_c elevation relative to other directions was smaller than for $PM_{2.5}$, indicating that the wildfire smoke emissions contained substantially more $PM_{2.5}$ than PM_c. Smoke plume encounters at the Greater Sandy Run Tower site in winter and early spring yielded an average $PM_{2.5}$:PM_c ratio noticeably lower than the maritime background, pointing to PM_c enhancing processes in the confluence of smoke plumes and maritime air mass during colder months. In contrast, smoke plume encounters at the Greater Sandy Run Tower site in late spring and summer, however, suggested that these PM_c–enhancing processes were being overwhelmed by large $PM_{2.5}$ fire emissions and new particle formation processes driven by reactive precursor gases and semi-volatile aerosol species emissions. These emissions caused a consistently higher $PM_{2.5}$:PM_c ratio in smoke plumes that were carried by the sea breeze during warmer months. At all sites, but especially the ones on Base, the $PM_{2.5}$ measurements indicated a regional character that was distinctly less

homogeneous than that for ozone, pointing to a greater influence of primary emissions sources (military training involving movement of heavy equipment or prescribed burning) on local MCBCL conditions.

Findings with Implications for Base Management Practices

- The bulk of MCBCL, which is managed forest area, receives prescribed burning during the dormant season (from December through March). Based on monitoring results, it appears to be critically important to avoid summer-time wildfires due to their potential for causing significant increases in local and regional ozone and $PM_{2.5}$ levels. Therefore, MCBCL Forest Managers should continue the practice of dormant season prescribed burning to remove unwanted fuel and prevent fuel accumulation in areas prone to wildfires.

Findings with Implications for DCERP2

- The Atmospheric Module established a network of meteorological stations across MCBCL lands during DCERP1 to determine whether there were gradients in rainfall and air quality parameters. Although gradients were found in ozone and $PM_{2.5}$, the results suggest that meteorological information already being captured at the New River Air Station's monitoring site was adequate for characterizing conditions across MCBCL, and this information could be supplemented by publicly available data collected by regional off-Base stations. Because DCERP2 will focus on climate change and its influence on various biochemical processes, it will be most important for researchers to have access to historic meteorological data available from stations that have operated for at least 50 years so that analysis of means and maxima and minima can be evaluated. During DCERP2, the climatologists will obtain data from the New River Air Station and other regional sites as appropriate to assess past and recent variabilities in meteorological parameters that could inform climate-change scenarios.

Literature Cited

Bricker, S.B., C.G. Clement, D.E. Pihalla, S.P. Orlano, and D.R.G. Farrow. 1999. *National Estuarine Eutrophication Assessment: Effects of Nutrient Enrichment in the Nation's Estuaries*. National Oceanic and Atmospheric Administration, National Ocean Service, Special Projects Office and the National Centers for Coastal Ocean Science, Silver Spring, MD. 71 pages.

Christensen, N.L. 1981. Fire regimes in southeastern ecosystems. Pp. 112–136 in *Fire Regimes and Ecosystem Properties*. Edited by H.A. Mooney, T.M. Bonnicksen, N.L. Christensen, J.E. Lotan, and W.A. Reiners. General Technical Report WO-26. U.S. Department of Agriculture, Forest Service.

Diffenbaugh, N.S., J.S. Pal, R.J. Trapp, and F. Giorgi. 2005. Fine-scale processes regulate the response of extreme events to global climate change. *Proceedings of the National Academy of Sciences 102*:15774–15778.

Emanuel, K. 2005. Increasing destructiveness of tropical cyclones over the past 30 years. *Nature 436*:686–688.

Ensign, S.H., J.N. Halls, and M.A. Mallin. 2004. Application of digital bathymetry data in an analysis of flushing times of two North Carolina Estuaries. *Computers and Geosciences 30*:501–511.

Friedli, H.R., L.F. Radke, N.J. Payne, D.J. McRae, T.J. Lynham, and T.W. Blake. 2007. Mercury in vegetation and organic soil at an upland boreal forest site in Prince Albert National Park, Saskatchewan, Canada. *Journal of Geophysical Research 112*(G1):G01004.

Garren, K.H. 1943. Effects of fire on vegetation of the southeastern United States. *Botanical Review 9*:617–654.

Goldenberg, S.B., C.W. Landsea, A.M. Mestas-Nuñez, and W.M. Gray. 2001. The recent increase in Atlantic hurricane activity: Causes and Implications. *Science 293*:474–478.

Hunsaker, C.T., C.T. Garten, and P.J. Mulholland. 1994. Modeling nitrogen cycling in forested watersheds of Chesapeake Bay. Pp. in *Proceedings of the Water Environment Federation 67th Annual Conference & Exposition 4*:481–491, Chicago, IL. October 15–19.

Kunkel, K.E., D.R. Easterling, K. Redmond and K. Hubbard. 2003. Temporal variations of extreme precipitation events in the United States: 1895–2000. *Geophysical Research Letters 30*:1900.

Lee, S., H. Kim, B. Yan, C. Cobb, C. Hennigan, S. Nichols, M. Chamber, E. Edgerton, J. Jansen, Y. Hu, M. Zheng, R. Weber, and A. Russell. 2008. Diagnosis of aged prescribed burning plumes impacting an urban area. *Environmental Science and Technology 42*:1438–1444.

Mallin, M.A., M.R. McIver, H.A. Wells, D.C. Parsons, and V.L. Johnson. 2005. Reversal of eutrophication following sewage treatment upgrades in the New River Estuary, North Carolina. *Estuaries 28*:750–760.

Milly, P.C.D., J. Betancourt, M. Falkenmark, R.M. Hirsch, Z.W. Kundzewicz, D.P. Lettenmaier, and R.J. Stouffer. 2008. Stationarity is dead: Whiter water management? *Science 319*:573–574.

Osgood, D.T., and J.C. Zieman. 1998. The influence of subsurface hydrology on nutrient supply and smooth cordgrass (*Spartina alterniflora*) production in a developing barrier island marsh. *Estuaries 21*(4B):767–783.

U.S. Marine Corps. 2009. U.S. Marine Corps Grow the Force at Marine Corps Base Camp Lejeune, Marine Corps Air Station New River, and Marine Corps Air Station Cherry Point, NC. Final Environmental Impact Statement.

Webster, P.J., G.J. Holland, J.A. Curry, and H.R. Chang. 2005. Changes in tropical cyclone number, duration, and intensity in a warming environment. *Science 309*:1844–1846.

[This page intentionally left blank.]

Chapter 3

New River Monitoring near Gum Branch and Jacksonville, NC

SERDP Project Number: RC-1413

Aquatic/Estuarine Module

Lead Researchers:
Holly S. Weyers
USGS
Raleigh, NC
E-mail: hsweyers@usgs.gov

June 27, 2013

Final

This report was prepared under contract to the U.S. Department of Defense (DoD) Strategic Environmental Research and Development Program (SERDP). The publication of this report does not indicate endorsement by DoD, nor should the contents be construed as reflecting the official policy or position of DoD. References herein to any specific commercial product, process, or service by trade name, trademark, manufacturer, or otherwise, do not necessarily constitute or imply its endorsement, recommendation, or favoring by DoD.

Table of Contents

List of Acronyms 3-v
Abstract 3-1
Objectives of the Monitoring Activity 3-1
Background 3-2
Materials and Methods 3-2
    Water Level and Discharge 3-2
    Continuous Water Quality 3-4
    Nutrients 3-4
    Additional Transect Sampling 3-4
Results and Discussion 3-4
    Water Level and Discharge 3-4
    Continuous Water Quality 3-9
    Nutrients 3-11
    Additional Transect Sampling 3-13
Assessment of Trends in the Data 3-17
    Assessment of Monitoring Design 3-17
    Assessment Seasonal and Annual Variability in the Data 3-17
    Recommendations for Future Monitoring 3-17
Conclusions and Implications for Future Research 3-17
    Key Scientific Findings—Fundamental Cause-and-Effect Relationships 3-17
    Findings Supportive of Current Base Management Practices 3-17
    Findings with Implications for Future Base Management 3-17
    Findings with Implications for DCERP2 3-18
Literature Cited 3-19

List of Figures

3-1. Map of the two USGS stream gaging stations and other sampling site locations on the New River. 3-3

3-2. Measured daily mean streamflow and long-term average daily mean streamflow for New River at Gum Branch (Stream Gaging Station 02093000), 2006–2012. 3-5

3-3. A duration hydrograph of the observed 28-day average flows during 2008–2012 at New River near Gum Branch (Stream Gaging Station 02093000). 3-6

3-4. Maximum and minimum daily water levels for the New River at Jacksonville (Stream Gaging Station 0209303205), October 2009–November 2012. 3-7

3-5. Instantaneous and daily mean (filtered) discharge for the New River at Jacksonville (Stream Gaging Station 0209303205), October 2009–November 2012. 3-9

3-6. Salinity values in the New River at Jacksonville (Stream Gaging Station 0209303205). 3-10

3-7. DO values for the New River at Jacksonville (Stream Gaging Station 0209303205). 3-11

3-8. Nitrate concentrations at the New River near Gum Branch (Stream Gaging Station 02093000) and at Jacksonville (Stream Gaging Station 0209303205), 2008–2012. 3-12

3-9. Phosphorous concentrations at New River near Gum Branch (Stream Gaging Station 020930000 and at Jacksonville (Stream Gaging Station 0209303205), 2008–2012. 3-13

3-10. Nitrate concentrations for 2011 transect sampling. 3-16

3-11. Total dissolved phosphorus concentrations for 2011 transect sampling. 3-16

List of Tables

3-1. Aquatic/Estuarine Module monitoring components 3-1

3-2. Annual mean and period of record streamflow statistics for the New River near Gum Branch (USGS Stream Gaging Station 02093000). 3-2

3-3. Daily minimum DO values less than or equal to 4 mg/L for 2008–2012 measure in the New River at Jacksonville (Stream Gaging Station 0209303205). 3-11

3-4. Salinity values (in ppt) for 2011 transect sampling locations and USGS stations on the New River. 3-14

3-5. Phosphate values (µg/L) for 2011 transect sampling and USGS stations on the New River. 3-14

3-6. Nitrate values (µg/L) for 2011 transect sampling and USGS stations on the New River. 3-15

3-7. Discharge values (ft^3/s) for 2011 transect sampling and USGS stations on the New River. 3-15

List of Acronyms

µg/L	micrograms per liter
ADVM	acoustic Doppler velocity meter
cfs	cubic feet per second
DCERP	Defense Coastal/Estuarine Research Program
DCERP1	first cycle of the Defense Coastal/Estuarine Research Program
DCERP2	second cycle of the Defense Coastal/Estuarine Research Program
DO	dissolved oxygen
DoD	U.S. Department of Defense
ESM	Estuarine Simulation Model
ft^3/s	cubic feet per second
m	meter
MCBCL	Marine Corps Base Camp Lejeune
mg/L	milligrams per liter
NRE	New River Estuary
NWIS	National Water Information System
ppt	parts per thousand
SERDP	Strategic Environmental Research and Development Program
USGS	U S Geological Survey
WSM	Watershed Simulation Model

[This page intentionally left blank.]

Abstract

The overall objective of the U.S. Geological Survey (USGS) effort was to monitor stream flow on the New River in two locations (i.e., New River near Gum Branch and New River near Jacksonville, NC). Continuous monitoring of flow and water quality data from these gages was used to assist Defense Coastal/Estuarine Research Program researchers in understanding conditions at the upper limit of the New River Estuary. Specifically, the stream gage and continuous water quality monitoring efforts include improving the understanding of the complex interactions of the physical, chemical, and biotic processes that drive water and habitat quality; supporting the research components; and helping to differentiate natural from anthropogenic ecosystem forcing mechanisms, including the consideration of extreme weather-related events, such as hurricanes, nor'easters, floods, and droughts.

Keywords: Dissolved oxygen, Gum Branch, New River Jacksonville, nitrate, phosphate, salinity, streamflow, stream gage

Objectives of the Monitoring Activity

The overall objective of the USGS effort was to monitor stream flow on the New River in two locations (New River near Gum Branch and New River near Jacksonville). Continuous monitoring of flow and water quality data from these gages was used to provide an understanding conditions at the upper limit of the New River Estuary. Specifically, the monitoring activities for the New River were designed to support the goals of the entire Aquatic/Estuarine Module. These goals include improving the understanding of the complex interactions of the physical, chemical, and biotic processes that drive water and habitat quality; supporting the research project of the module; and helping to differentiate natural from anthropogenic ecosystem forcing mechanisms, including the consideration of extreme weather-related events, such as hurricanes, nor'easters, floods, and droughts. The New River monitoring data also support the refinement and validation of the Watershed Simulation Model (WSM) and Estuarine Simulation Model (ESM) that requires information on the river discharge as well as other physical characteristics of the New River system. **Table 3-1** provides a summary of the New River monitoring activity.

Table 3-1. Aquatic/Estuarine Module monitoring components

Variable	Spatial Scale	Temporal Scale
Water level and discharge	2 stations: New River near Gum Branch (active USGS station) and at Jacksonville (added with DCERP funding)	Continuous
Water temperature, dissolved oxygen, pH, and salinity	New River at Jacksonville	Continuous
Nutrients	New River at Jacksonville	Monthly (outgoing tide)
Discharge, salinity, and nutrients	Four stations between Gum Branch and Jacksonville	Quarterly for 2011

Background

U.S. Geological Survey (USGS) Stream Gaging Station 02093000, New River near Gum Branch, NC, was established in August 1949 and operated continuously through September 1973, when it was discontinued for many years. The stream gage was subsequently reactivated in July 1987 and remains operational at this time (December 2012). As a result, approximately 63 years of total streamflow record are available for analysis. Summaries of available data for this site can be obtained from the National Water Information System's (NWIS's) Web Interface at http://waterdata.usgs.gov/nc/nwis/nwisman/?site_no=02093000. Average annual streamflow for the period of record and water years 2006 through 2011 are listed below and are available on the USGS's Web site.[1]

Table 3-2. Annual mean and period of record streamflow statistics for the New River near Gum Branch (USGS Stream Gaging Station 02093000)

Water Year	Annual Mean Streamflow (cfs)
2006	178.9
2007	135.1
2008	46.9
2009	57.5
2010	127.0
2011	87.7
Period of record[a]	114.0

[a] Water years 1950–1973 and 1988–2011

USGS Stream Gaging Station 0209303205, New River, below the U.S. Highway 17 bridge at Jacksonville, NC, was installed during the study period specifically to support the Defense Coastal/Estuarine Research Program (DCERP). Data are available for river stage, elevation, velocity, and discharge from October 2008 to December 2012 when the gage was discontinued. Summaries of available data for this site can be obtained from the NWIS's Web Interface at http://waterdata.usgs.gov/nc/nwis/nwisman/?site_no=0209303205.

Due to the short period of record for the site, annual streamflow statistics cannot be put in context of a longer historical period; however, net downstream flow conditions reported for the upstream gage at Gum Branch can be inferred to be similar to conditions observed at Jacksonville.

Materials and Methods

Water Level and Discharge

Figure 3-1 shows the location of the existing USGS Stream Gaging Station 02093000 on the New River near Gum Branch and the DCERP–funded USGS Stream Gaging Station

[1] http://waterdata.usgs.gov/nc/nwis/annual/?search_site_no=02093000&agency_cd=USGS&referred_module=sw&format=sites_selection_links

0209303205 on the New River near Jacksonville, NC, immediately downstream from the U.S. Highway 17 bridge.

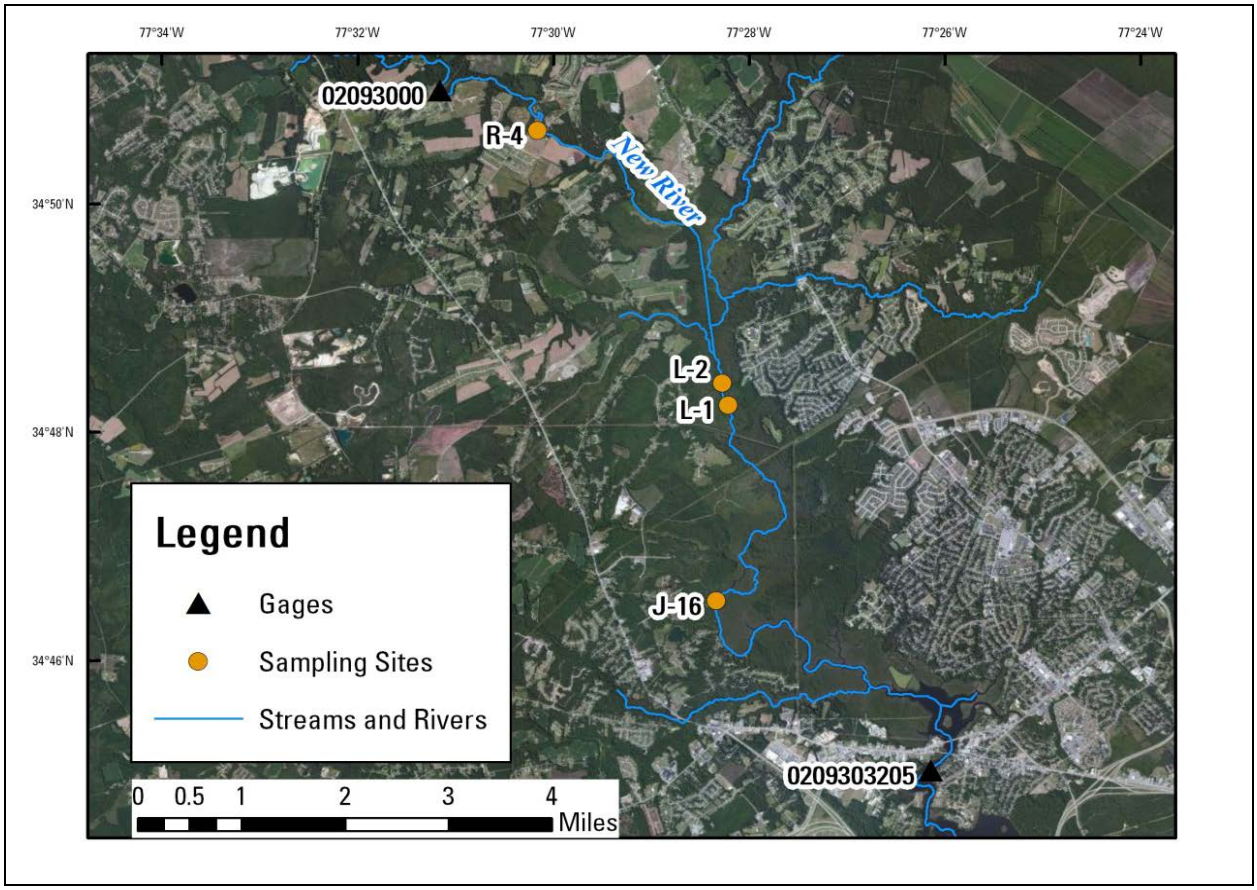

Figure 3-1. Map of the two USGS stream gaging stations and other sampling site locations on the New River.

Stream flow and river stage were continuously monitored during the duration of DCERP at both stations. As a part of USGS gage operation protocols (Buchanan and Somers, 1969), in addition to providing near real-time stream flow information at both stations, periodic independent flow verification measurements of stream and tidal flow were made to calibrate the stream gage and filter the data. To measure stream flow at the Jacksonville Stream Gaging Station 0209303205, an acoustic velocity meter was installed. The original meter was mounted on a bridge piling, but after several months of data collection it was determined that this location was not providing the best results. In 2009, a new meter was mounted on the bottom of the channel, near mid-channel, and measured a representative index velocity throughout the water column. Periodic measurements of total flow in the channel were made to establish a linkage between the cross-sectional mean velocity and the index velocity. Standard USGS methods were used during all data collection, processing, and archiving. Tidal stream flow data collection methods are documented by Morlock et al. (2002), Oberg et al. (2005), Ruhl and Simpson (2005), and Simpson (2002).

Continuous Water Quality

Beginning in October 2009, a real-time continuous water quality monitor was installed in the New River at the Jacksonville Stream Gaging Station 0209303205 to monitor changes in water quality parameters. Data were collected at 15-minute intervals, transmitted hourly, and were publicly available in near real-time on USGS's Web pages. Continuous water quality data were collected in accordance with USGS guidelines as published by Wagner et al. (2006). Standard protocols include collection of cross-sections for site selection and annual verification, independent field meter checks during calibration processes, and daily review of real-time data and deletion of any spurious data and evaluation of site maintenance needs. Parameters monitored included pH, temperature, dissolved oxygen (DO) and DO percent saturation, and specific conductance. The service interval was every 1–4 weeks depending on site conditions, and additional visits were made as needed based upon daily review of real-time data.

Nutrients

Nutrient and sediment samples were collected New River Jacksonville Stream Gaging Station 0209303205 approximately 15 times per year during ebb flow or in conjunction with servicing of the real-time water quality monitor. All samples were analyzed at the University of North Carolina at Chapel Hill's Institute of Marine Sciences for total dissolved nitrogen, ammonium, total nitrogen, particulate nitrogen, nitrate + nitrite, total phosphorus, particulate phosphate, total dissolved phosphorus, and chlorophyll *a*. Vertical profiles of temperature, DO, pH, and salinity were made at least monthly and every time a sample was collected. Water temperature, salinity, pH, and DO concentrations were continuously measured at approximately mid-depth and all sampling efforts followed the described procedures from the USGS (1997–1999) and Horowitz et al. (1994) for collecting water quality samples and measuring field properties.

Additional Transect Sampling

To better define the head of tide and study processes affecting nitrogen concentrations in the New River upstream of Jacksonville, supplemental discharge measurements and nutrient samples were collected in 2011 at four locations between the Gum Branch and the Jacksonville stations. Transect sampling rather than establishment of an additional gauging station was chosen for discharge determination and additional water quality data collection due to the lack of access to the river and inability to find a suitable location for a gauging station. Determination (calculation) of discharge involved measuring water depth and velocity at 1-m increments along a bank-to-bank transect. In addition, depth-integrated water samples were collected simultaneously at these same measurement points and composited for a cross-sectional nutrient sample. Four such bank-to-bank transects were conducted by USGS staff each quarter at locations indicated on **Figure 3-1**.

Results and Discussion

Water Level and Discharge

Streamflow at New River near Gum Branch (USGS Stream Gaging Station 02093000) was generally less than normal for most of the study period (**Figure 3-2)** and was often much lower

than normal from June 2010 through January 2012. In a few instances, flows were above normal (November 2009 through mid-January 2010 and during the late spring and early summer of 2012). Flows reached maximum levels (October 1, 2010) when a powerful weather system (remnants of Tropical Storm Nicole) dumped 22 inches of rain over Marine Corps Base Camp Lejeune (MCBCL) in a 3-day period (see Chapter 16 of the *DCERP1 Final Research Report* for more information on this rainfall event). This rain event severely altered flow at both Gum Branch and Jacksonville stations (**Figure 3-2**) and resulted in the highest recorded stage reading since Hurricane Floyd on October 16, 1999. However, the increased flows resulting from the high rainfall event only lasted 2 weeks and measured flows returned to levels that were well below normal for the remainder of 2010 and much of 2011 with higher flows returning later in 2012. Thus, flows for 2009, 2010, 2011, and early 2012 remained slightly less than normal, and this pattern is somewhat different from that observed in much of the remainder of North Carolina. Although much of North Carolina was in a drought of historic proportions from 2005–2007, the drought abated in late 2007, and streamflows returned to near normal or above for most of the State of North Carolina.

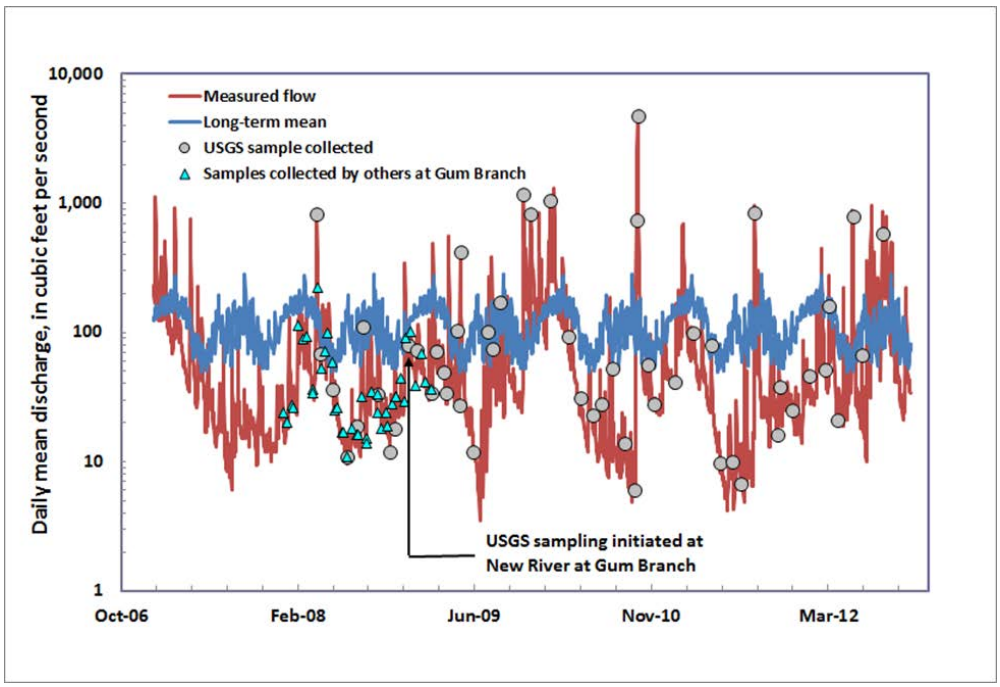

Figure 3-2. Measured daily mean streamflow and long-term average daily mean streamflow for New River at Gum Branch (Stream Gaging Station 02093000), 2006–2012.

Figure 3-3 shows a duration hydrograph of the observed 28-day average flows during 2006–2012 at the New River near Gum Branch (Stream Gaging Station 02093000). The duration hydrograph depicts the recent and observed streamflow conditions against a backdrop of historical statistics computed for each calendar day and presented as percentiles. For a given calendar day, the 28-day average flows ending on this date for each year of record are compiled and ranked to determine the 28-day percentiles for the indicated calendar day. The same analysis could not be performed for New River at Jacksonville due to the lack of historic data.

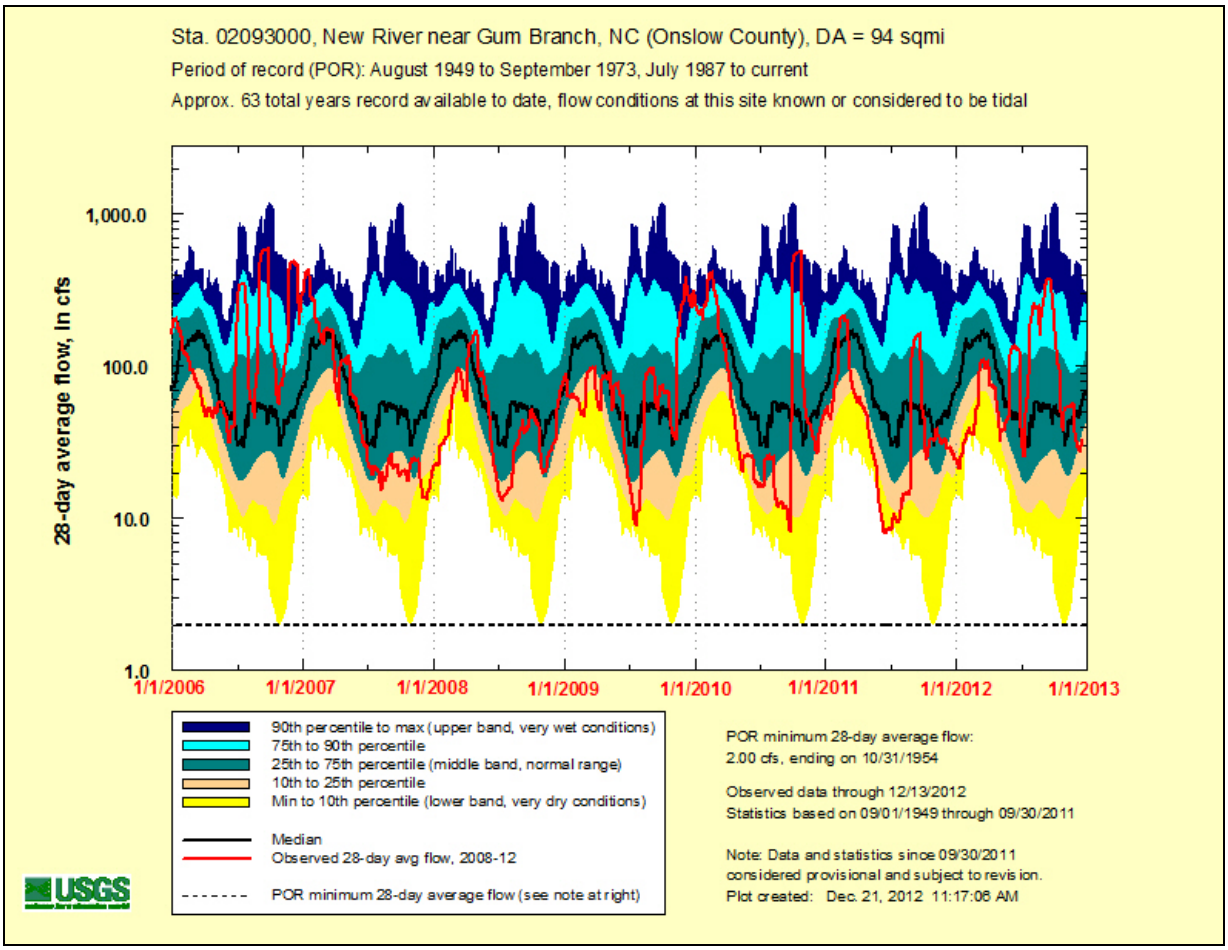

Figure 3-3. A duration hydrograph of the observed 28-day average flows during 2008–2012 at New River near Gum Branch (Stream Gaging Station 02093000).

A percentile is a value on a scale of 100 that indicates the percent of a distribution that is equal to or below it. For example, a river discharge at the 90th percentile is greater than or equal to 90% of the discharge values recorded on this day of the year during the entire period of record. In general, a percentile greater than 75 is considered to be above normal, a percentile between 25 and 75 is considered to be normal, and a percentile less than 25 is considered to be below normal. For the 2006–2012 study period, inspection of the 28-day flows for Gum Branch does indicate several periods of prolonged below-normal conditions. The variations in 28-day flows generally echo the historical annual cycle as depicted by the percentiles. One particular instance of below-normal streamflow conditions occurred from approximately March 2011 through August 2011, during which 28-day average flows reached very close to the record low for the calendar dates during early summer 2011.

Throughout the study period tidal elevations recorded at the New River at Jacksonville (USGS Gaging Station 0209303205) tended to be lowest in the winter months (December to March; **Figure 3-4**) particularly for winter 2010–2011 and 2011–2012. Water levels remained relatively uniform for the majority of the study period, with the exception of the October 1, 2010, event in which levels reached the highest values of the entire period of record as a result of the unusual

rain event (remnants of Tropical Storm Nicole). Following this rain event, water levels reached their lowest values for the year in late October 2010 through early January 2011.

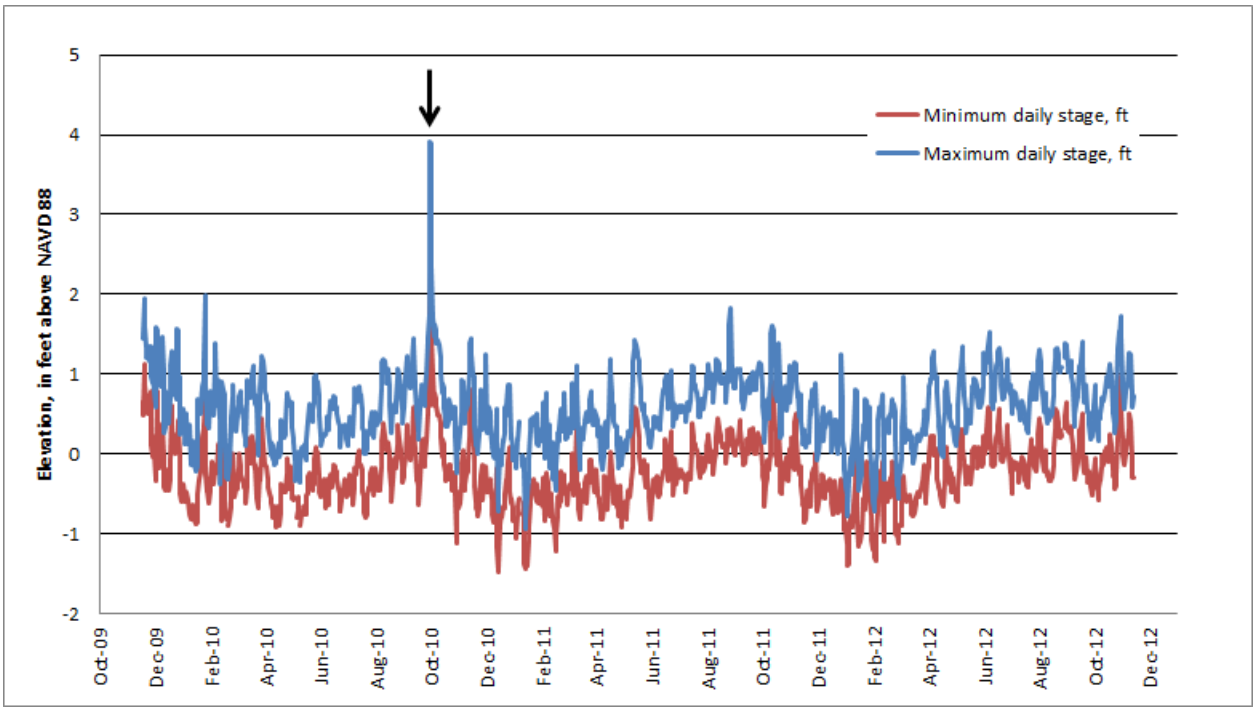

Figure 3-4. Maximum and minimum daily water levels for the New River at Jacksonville (Stream Gaging Station 0209303205), October 2009–November 2012.

Arrow indicates a rain event on October 1, 2012, which was associated with the remnants of Tropical Storm Nicole.

Additionally, a continuous record of discharge was computed for the New River at Jacksonville, NC, (Stream Gaging Station 0209303205)for the period from October 1, 2008 to December 2013, using the index-velocity method (Levesque and Oberg, 2012). A collection of continuous velocity data, using an acoustic Doppler velocity meter (ADVM), and stage data are required to compute continuous records of streamflow using this method. In the index-velocity method, two ratings (or relations) are developed and maintained: a stage-area rating and an index-velocity rating. The stage-area rating is developed by surveying a stable cross-section in the stream near the permanently mounted ADVM. The channel area for a given stage then can be determined from the surveyed cross-section. An index-velocity rating is developed by using the relation between the measured mean cross-sectional velocity, over a range of conditions, at the surveyed cross-section and the simultaneous index velocity measured with the permanently mounted ADVM. Continuous records of stage and index velocity are converted to a channel area and mean velocity using these respective ratings. The channel area then can be multiplied by the mean velocity over time to compute a continuous record of streamflow (Gotvald and Oberg, 2008). The index-velocity rating for the New River at Jacksonville was developed using a suite of USGS scripts written in the R statistical software package (Venables et al., 2012). The R scripts were used to synchronize and synthesize index-velocity data with discharge measurements and develop an index-velocity relation that best represented the complex hydraulic conditions at the site. A total of 118 discrete discharge measurements collected between 2009 and 2012 were used in the development of the index-velocity rating.

At tidally influenced sites, often the quantity of real interest to a user is net (or seaward) freshwater discharge or basin yield. Net discharge cannot be determined from the maximum and minimum statistics and it cannot be inferred or determined from daily (24-hour) averaging due to the strong lunar influence that repeats every 24.8412 hours. Thus, other approaches must be used. One way to obtain net flows is to remove the effects of tidal components through the application of a low-pass filter to the short-interval instantaneous time series data (referred to as unit-value data). A filter is a mathematical process that extracts or emphasizes data residing within a specified range or frequency of a record. Common digital filters apply a system of weights to exclude, include, or emphasize data, often through a process that combines sequential members of a time series within a computational window. A moving average, for example, could be considered a filter, smoothing out extremes and outputting adjusted records more closely representing a mean tendency. Filters are often used in oceanographic applications to remove background sea-level fluctuations from the effects of tsunamis and storm surges. The term, "de-tided" refers to records from which tide components have been removed. Commonly used digital filters include the Lanczos-window, Butterworth, and Godin filters.

The USGS's Office of Surface Water has implemented the Godin filter (Godin, 1972) that interacts with the NWIS's database to facilitate the filtering of tidally-influenced discharge data. The Godin filter results are very predictable and consistent. The Godin filter drops exactly 35 hourly data points from the beginning and end of the input series as well as adjacent to any gap in the unit-value data. Moreover, unlike some other low-pass filters, appending new data points either to the beginning or end of the input series will not cause a change in filtered values calculated previously. It is well suited for use in the computation of daily values, since higher frequency variations are not preserved. The Godin filter is applied to unit-value data sequentially, essentially as a moving window, performing a cascading series of moving averages, each centered on the unit value and extending backward and forward in time. However, the filter always omits the 35 hourly data points from the beginning and end of the input series as well as adjacent to any gap in the unit-value data. Processing will yield the same result for any given point in time regardless of the starting or ending times input for processing.

Figure 3-5 represents the results of the filtering process for New River at Jacksonville. This figure illustrates that there is a wide range in instantaneous discharge values (from approximately 2,000 cfs to −2,000 cfs throughout the study period). Filtering of the data resulted in a daily mean filtered value (represented by the red line), which indicates that generally there is a slight net positive flow at the gaged location that can only be determined through the filtering process.

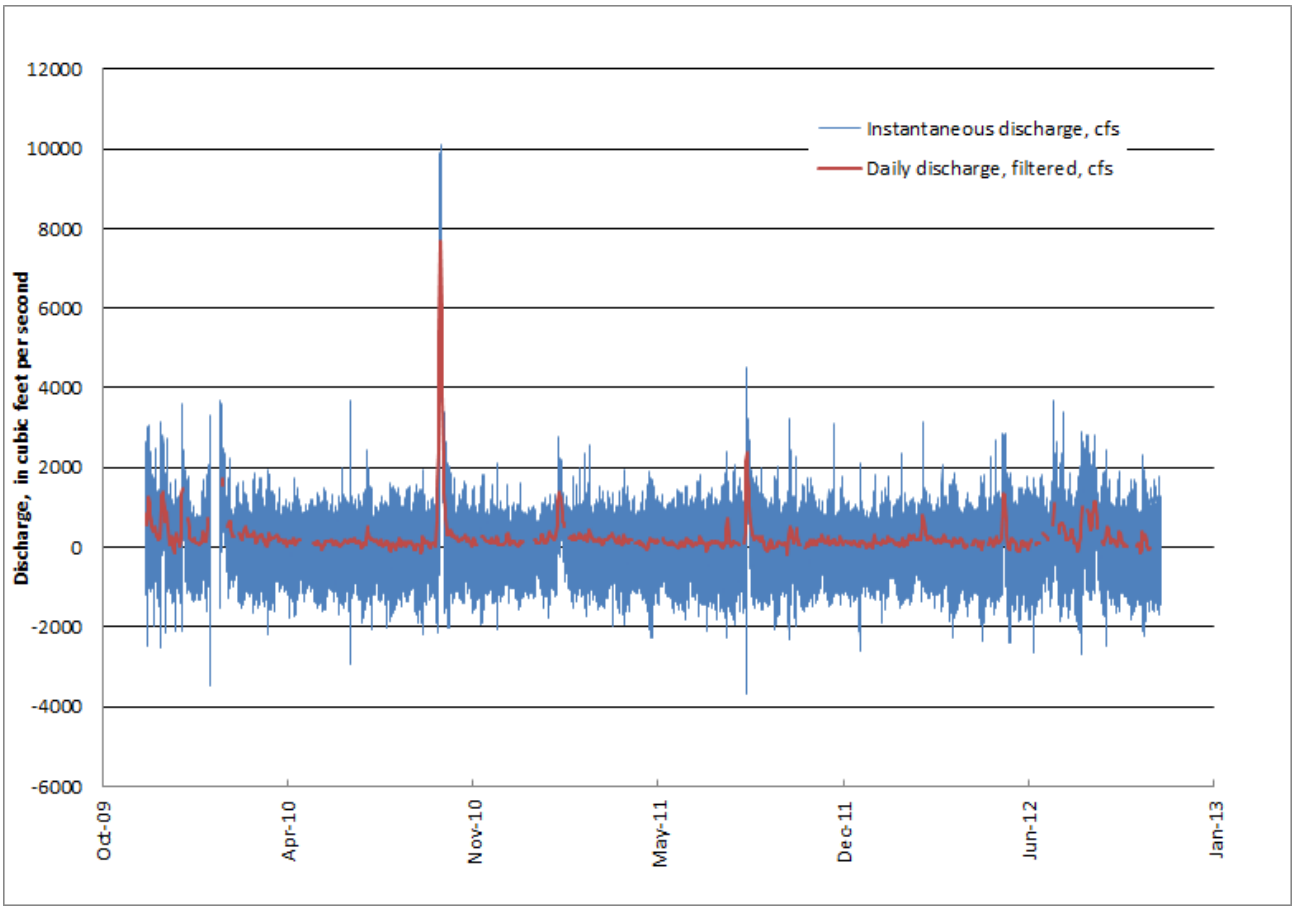

Figure 3-5. Instantaneous and daily mean (filtered) discharge for the New River at Jacksonville (Stream Gaging Station 0209303205), October 2009–November 2012.

Continuous Water Quality

During the 2009–2012 study period, salinity values at Jacksonville ranged from 0.04 ppt to 24.8 ppt. The salinity values are the lowest during the winter months and gradually increase from March through September (**Figure 3-6**), and then typically decline in late summer early fall. During 2010, salinity values sharply declined during the month of September and into early October as the result of the October 1 rain event (remnants of Tropical Storm Nicole) and remained below 10 ppt until after November 1, indicating high freshwater outflow during this period. In 2011, salinity values were lowest in late winter (late February) and gradually increased until August when freshwater flows increased slightly through September causing a drop in salinity values. Salinity then slightly increased during the late fall 2011 through late February 2012 and was generally higher than wintertime values found for 2010 and 2011 as a result of more frequent rain events during this period for 2012.

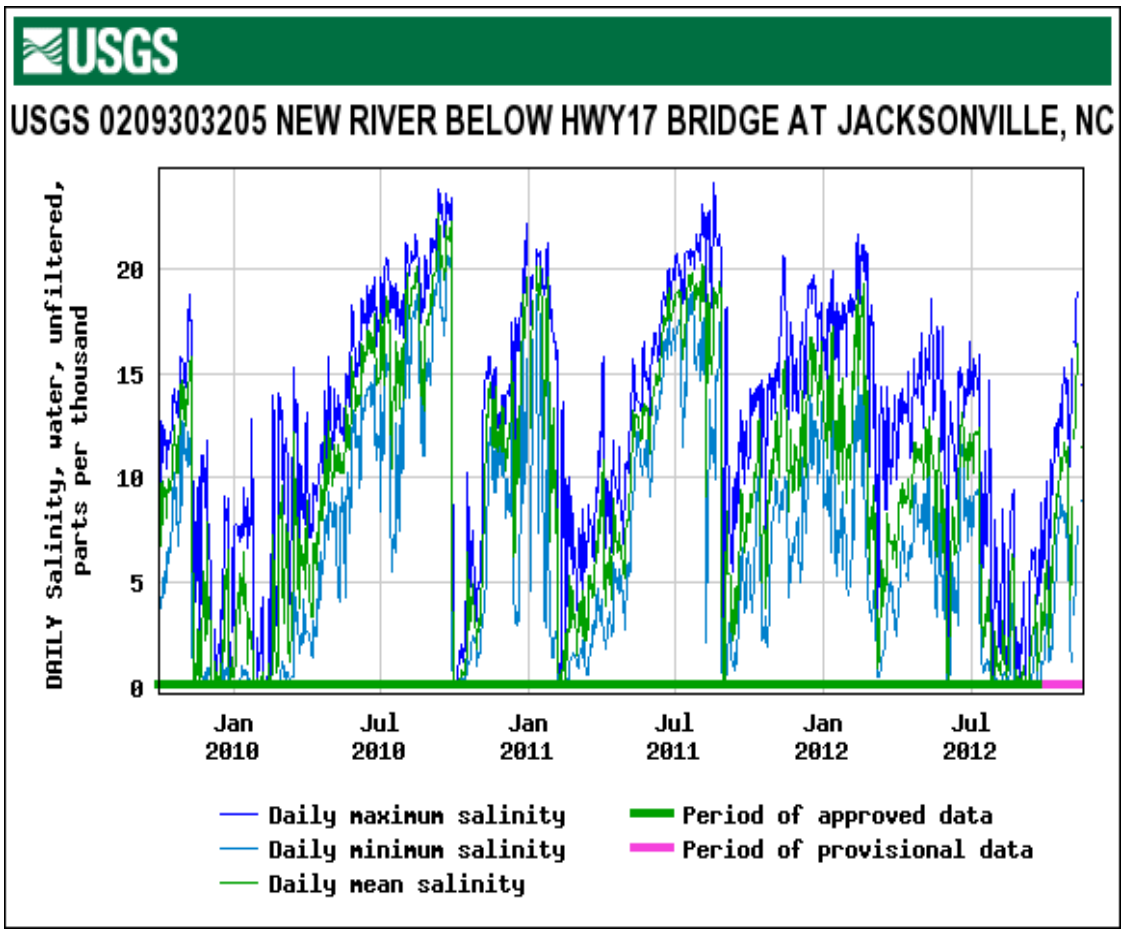

Figure 3-6. Salinity values in the New River at Jacksonville (Stream Gaging Station 0209303205).

DO concentrations at Jacksonville (Stream Gaging Station 0209303205) ranged from 0.0 mg/L to a maximum of 19.8 mg/L during the 2008–2012 study period (**Figure 3-7**). For days containing approved DO data (a total of 1,466 days), DO minimum values of 0.0 mg/L were recorded for a total of 119 days (see **Table 3-3**). In addition, there were 394 days when a recorded DO minimum of less than 1 mg/L was evident, meaning that for the period of record DO values of 1 mg/L or less were recorded 35% of the days. Results from **Table 3-3** also indicate that for 1,002 days or the 1,466 days of record, a daily DO minimum of less than 4 mg/L was recorded. In comparing the DO results from year to year, 2009 had the most days with a recorded daily minimum of less than or equal to 4 mg/L, and 2012 had the fewest number of days with a recorded daily minimum DO of less than or equal to 4 mg/L. This corresponds to the flow conditions at this station with 2008 and 2009 having lower recorded flow than 2010, 2011, and 2012. Sustained periods of DO concentrations of less than 4 mg/L are known to be harmful to aquatic life.

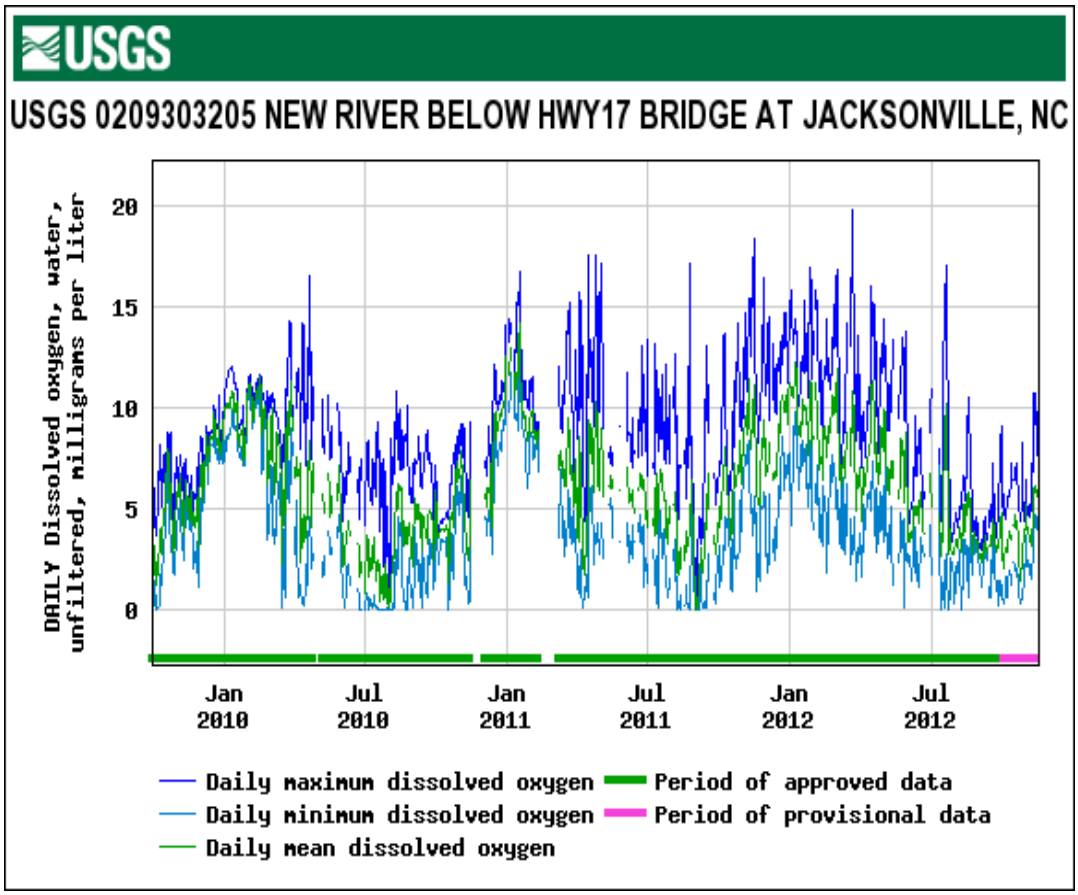

Figure 3-7. Dissolved oxygen values for the New River at Jacksonville (Stream Gaging Station 0209303205).

Table 3-3. Daily minimum dissolved oxygen values less than or equal to 4 mg/L for 2008–2012 measure in the New River at Jacksonville (Stream Gaging Station 0209303205).

Calendar Year	Number of Days of Approved Record	Number of Days with Minimum DO Equal to 0 mg/L	Number of Days with Minimum DO <1 mg/L	Number of Days with minimum DO <4 mg/L, but ≥1 mg/L	Total Number of Days with Minimum DO ≤4 mg/L
2008	293	38	136	102	238
2009	325	38	109	145	259
2010	311	30	83	101	189
2011	288	9	45	110	160
2012	249	4	21	132	156

Nutrients

Nitrate concentrations were noticeably higher at the Gum Branch location than at the Jacksonville sampling location (**Figure 3-8**). The mean nitrate concentration in the New River at Jacksonville was 307 µg/L compared to 1,561 µg/L upstream at Gum Branch. Similarly, total phosphorus concentrations were higher at Gum Branch (mean = 147 µg/L) than at Jacksonville (mean = 89 µg/L; **Figure 3-9**). During the entire study period, both nitrate and phosphorus data

trends were similar for both sites except for the October 1, 2010 samples. Samples collected during this storm event indicated a reduction in nitrate concentrations at both Gum Branch and Jacksonville. For phosphorus values, the storm event reduced phosphorus concentrations at Gum Branch, but indicated an increase in phosphorus concentrations at the Jacksonville station (114 µg/L on September 28, 2010, compared to 173 µg/L on October 1, 2010). Data from 2008 were provided by the Onslow County Cooperative Extension Service and the North Carolina Division of Water Quality. Samples in 2009, 2010, 2011, and 2012 were collected primarily by the USGS. There appears to be one sample that may have been mishandled or misanalyzed in 2008. At the Gum Branch station, a total phosphorus value of 5,200 µg/L was reported, making this the highest reported phosphorus value of the entire study. Examination of all other available data for that date does not indicate any type of event that could explain such a high value. Therefore, this value was not included in this *DCERP1 Final Monitoring Report*.

Water-quality samples collected at the New River at Gum Branch and at Jacksonville are critical to understanding nutrient inputs to the New River Estuary (NRE). The data collected during 2008–2010 suggest that nitrate decreases from the Gum Branch station to the Jacksonville station, but the relation for total phosphorus between the two sites is less clear. Many of the samples collected during this study were collected at relatively low flows (**Figure 3-2**) because of the persistence of low flows in the watershed. Typically, most of the nutrients are transported during higher flows and is indicated in the phosphorus data from the October 1 sample, so it is important to continue to sample high flows in order to obtain a good estimate of nutrient inputs in all flow conditions.

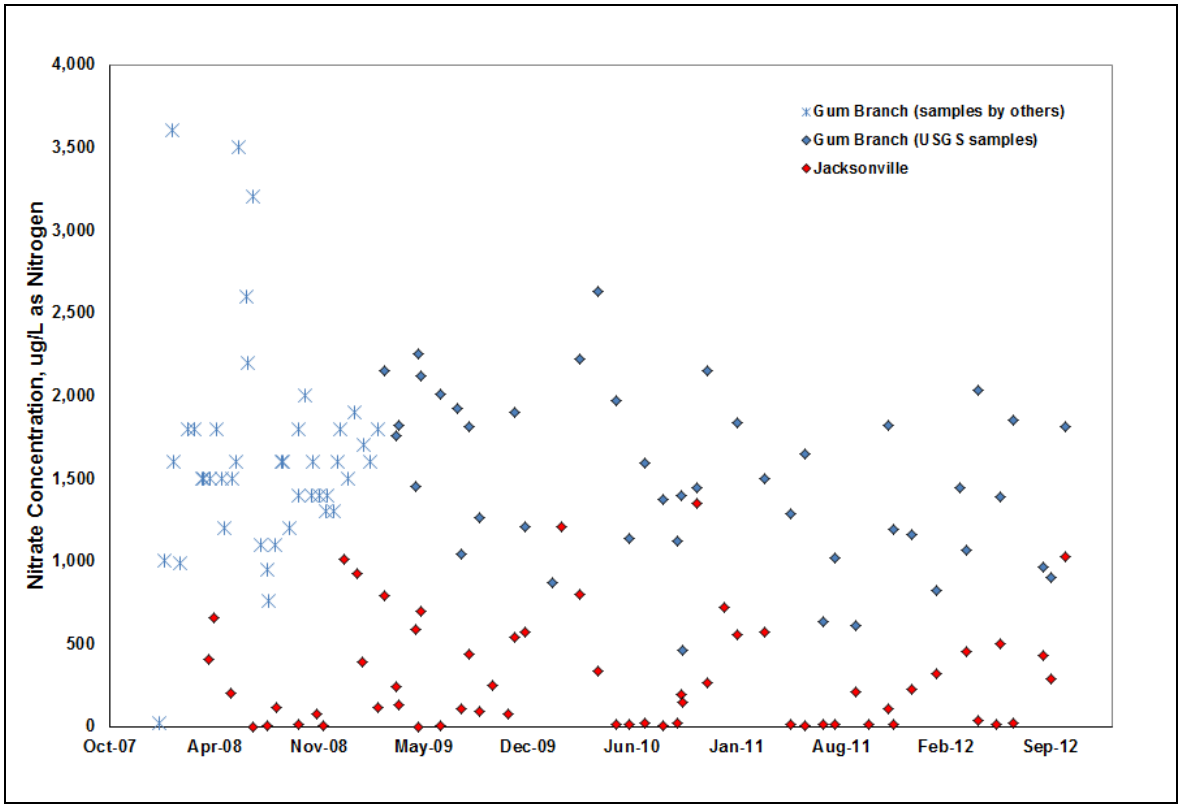

Figure 3-8. Nitrate concentrations at the New River near Gum Branch (Stream Gaging Station 02093000) and at Jacksonville (Stream Gaging Station 0209303205), 2008–2012.

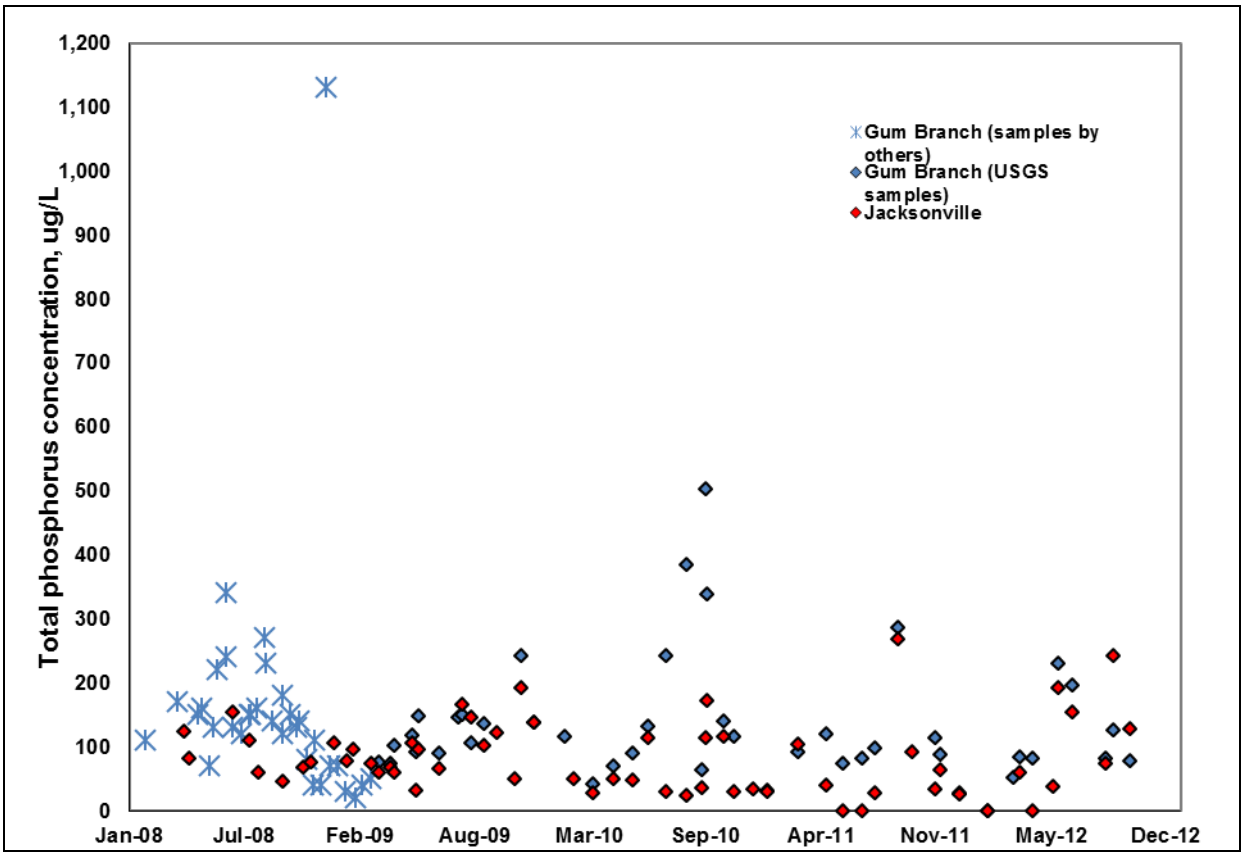

Figure 3-9. Phosphorous concentrations at New River near Gum Branch (Stream Gaging Station 020930000 and at Jacksonville (Stream Gaging Station 0209303205), 2008–2012.

Additional Transect Sampling

To obtain better coverage at higher flows, transect sampling was conducted in 2011 between the Gum Branch and Jacksonville stations, and this should provide more insight into sources of nutrient loads to the estuary. The additional information on the river flow, nutrient and sediment concentrations, and determination of the upper estuary head of tide boundary is required during a high precipitation year to better assess nutrient inputs to the NRE from the New River under both baseflow and stormflow conditions. Additionally, it was hoped that this information would also allow for calculation of more accurate loading estimates important to the both Watershed Simulation Model (WSM) and the Estuarine Simulation Model (ESM), provide information about the biologically active zone between the two existing gauging stations where nitrate concentrations decline, and identify the head of tide for the New River.

Tables 3-4 through 3-6 present the results from the transect sampling. **Table 3-4** lists salinity values (in ppt) for transect samples collected in 2011. Results indicate that the only Site J16 and the New River at Jacksonville station consistently had salinity values greater than 1.0 ppt for the chosen sampling dates. On July 19, 2011, Site L1 was slightly brackish (salinity value of 6.3 ppt), but when you compare this value with the discharge data in **Table 3-6**, it is apparent that the sample was collected on an incoming tide. Site L2 could not be accessed on this date, but results from Site R4 showed no significant salinity (0.24 ppt). Comparison of discharge and

salinity data from all of the transects indicated that the saline conditions most often do not extend above Site J16 (see **Figure 3-1**).

Table 3-4. Salinity values (in ppt) for 2011 transect sampling locations and USGS stations on the New River.

Sites are listed in order from upstream to downstream.

Date	New River at Gum Branch	R4	L2	L1	J16	New River at Jacksonville
3/29/2011	—	0.14	0.12	0.13	4.5	—
7/19/2011	0.25	0.24	—	6.3	—	19.6
11/9/2011	0.16	0.16	—	—	13	14.6
11/10/2011	—	—	—	—	—	—
12/13/2011	0.17	0.18	0.17	0.17	14	15.5

Tables 3-4 and 3-5 provide the results of nutrient analyses from the 2011 transect locations. Trends in nitrate and phosphate concentrations for the transect locations mirror the trends for nutrients discussed previously for the New River at Gum Branch and Jacksonville Stations. Phosphate and nitrate concentrations tended to decrease from upstream to downstream with the exception of the Sites R4 and L1 (**Figures 3-10 and 3-11**). When comparing nutrient data with salinity and discharge information, nothing seems to indicate a reason for these sites to have slightly elevated nutrients. However, as previous data from the estuary indicated, concentrations of elevated nitrate near Richlands, NC (Site R4) may explain the concentrations found during the 2011 collection effort. Furthermore, it is possible that nitrate is making its way to the waterways via agricultural field drains. This water is then able to bypass any field borders or riparian buffers that were installed to prevent erosion, reduce surface runoff, and utilize shallow nutrients. Another possibility is that elevated nutrients are runoff from increased urbanization and residential development near Richlands.

Table 3-5. Phosphate values (µg/L) for 2011 transect sampling and USGS stations on the New River.

Sites are listed in order from upstream to downstream.

Date	New River at Gum Branch	R4	L2	L1	J16	New River at Jacksonville
3/29/2011	—	112	75	109	84	—
7/19/2011	97	0	—	200	—	29
11/9/2011	87	90	—	—	—	63
11/10/2011	—	—	—	—	56	—
12/13/2011	29	69	—	—	—	26
12/14/2011	—	—	65	46	82	—

Table 3-6. Nitrate values (µg/L) for 2011 transect sampling and USGS stations on the New River.

Sites are listed in order from upstream to downstream.

Date	New River at Gum Branch	R4	L2	L1	J16	New River at Jacksonville
3/29/2011	—	1,710	1,320	1,450	1,290	—
7/19/2011	1,020	961	—	509	—	—
11/9/2011	1,190	1,330	—	—	—	16
11/10/2011	—	—	—	—	33	—
12/13/2011	1,160	—	—	—	—	226
12/14/2011	—	—	980	1,130	746	—

Table 3-7. Discharge values (ft^3/s) for 2011 transect sampling and USGS stations on the New River.

Sites are listed in order from upstream to downstream.

Date	New River at Gum Branch	R4	L2	L1	J16	New River at Jacksonville
3/29/2011	—	52.9	117	109	−183	—
7/19/2011	—	12.2	—	−75.6	—	—
11/9/2011	—	44	—	—	−353	—
11/10/2011	—	—	—	—	—	—
12/13/2011	—	12.7	−15	−58.6	−75.3	—

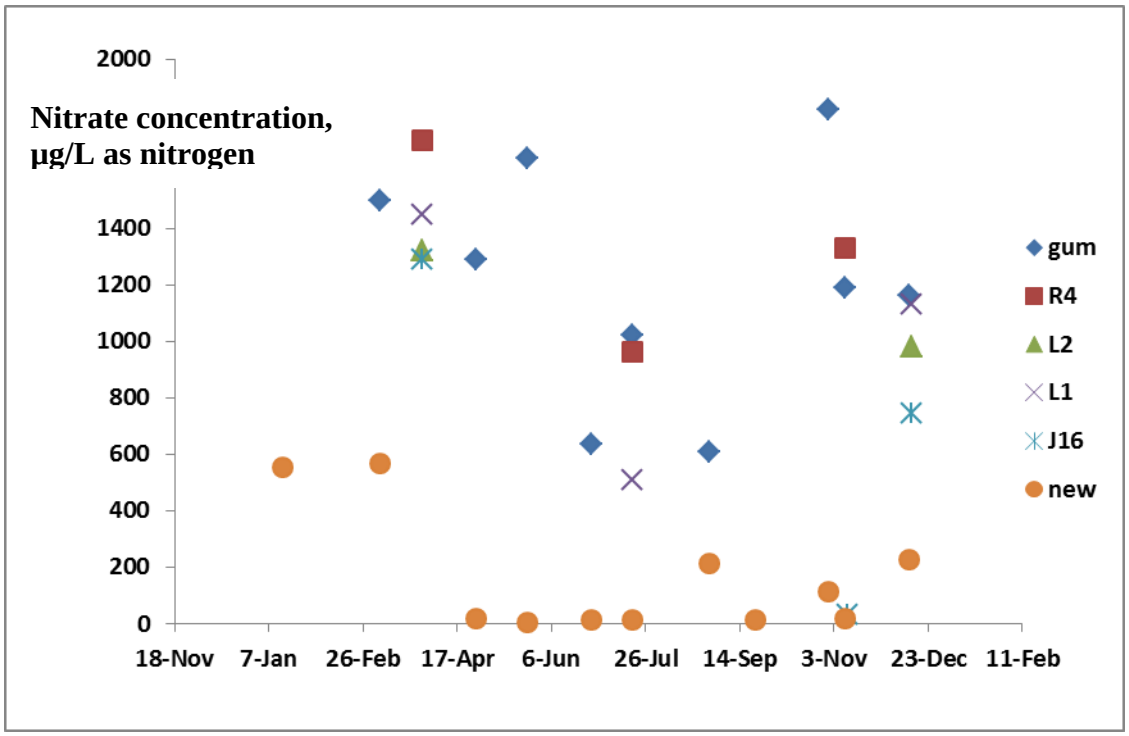

Figure 3-10. Nitrate concentrations for 2011 transect sampling.

Sites in legend are listed in order from upstream to downstream locations.

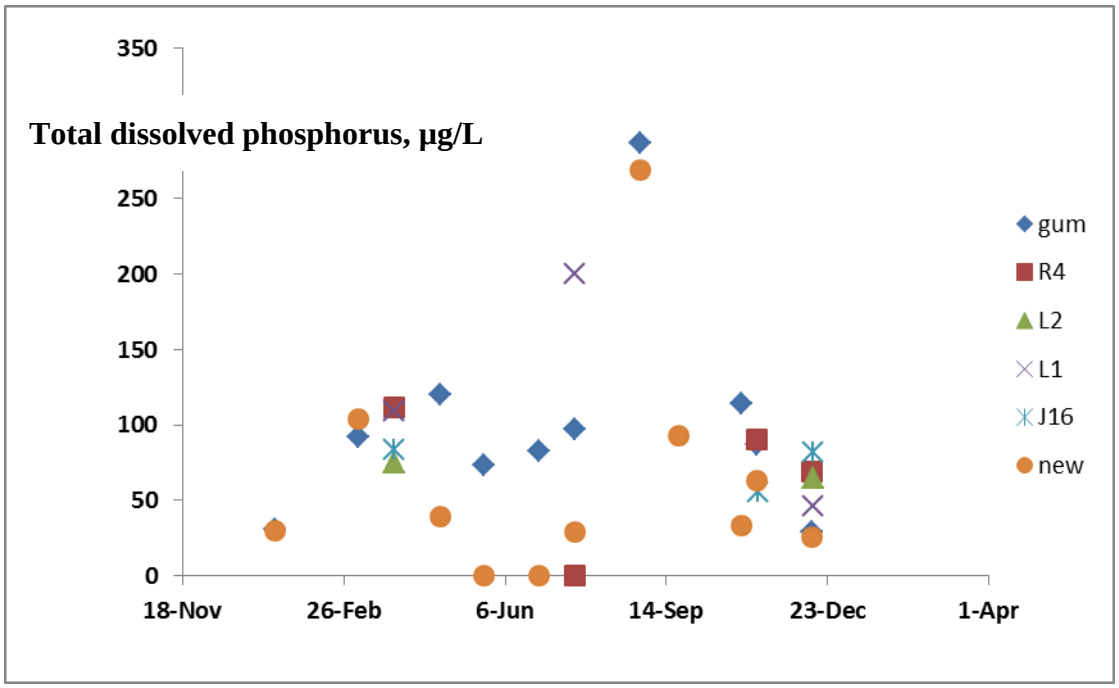

Figure 3-11. Total dissolved phosphorus concentrations for 2011 transect sampling.

Sites in legend listed in order from upstream to downstream locations.

Assessment of Trends in the Data

Assessment of Monitoring Design

The design for this monitoring activity was restricted to the use of the one long-term gage at Gum Branch, and an additional gage was added at the head of the estuary. No other sampling locations for positioning another gauging station were available on the river, and that prompted implementation of the transect surveys to assist in delineating the head of tide location.

Assessment Seasonal and Annual Variability in the Data

This assessment was provided in the Background and Results and Discussion sections.

Recommendations for Future Monitoring

Future monitoring needs to be driven by the needs of the research project and/or management needs.

Conclusions and Implications for Future Research

Key Scientific Findings—Fundamental Cause-and-Effect Relationships

In summary, annual mean river flows from the New River ranged from a low of 46.9 cfs (in 2008) to a high of 127 cfs (in 2010). River flow during DCERP1 was less than the mean annual discharge of 114 cfs during all years except 2010. Episodic events (hurricanes, tropical storms, nor'easters) produced high river flows for brief periods (November 2009–January 2010) and during late spring–summer 2012. In October 2010, flows reached a maximum level with the remnants of Tropical Storm Nicole produce a high rain event. Salinity values were also modulated within the upper estuary by the hydrologic variations of the New River with salinity values ranging from 0.04 to 24.8 ppt at the Jacksonville station. The New River provided inputs of both nitrogen and phosphorus to the estuary. Although concentrations of phosphorus were typically similar at both Gum Branch and Jacksonville stations, concentrations of nitrogen were typically higher upstream at Gum Branch, suggesting that nitrogen was assimilated by phytoplankton through primary production in the river before entering the estuary.

Findings Supportive of Current Base Management Practices

This section is not applicable to this monitoring activity.

Findings with Implications for Future Base Management

The analyses of data for this monitoring activity illustrate the importance of a long-term gage in the New River Watershed. MCBCL should support the continuation of the operation of the USGS stream gage and the Gum Branch Station.

Findings with Implications for DCERP2

Monitoring on the New River should be continued in DCERP2 to provide baseline data on freshwater flow and nutrient loading to the NRE. Flow during DCERP1 was lower than the mean annual flow; therefore the program would benefit from continued monitoring in DCERP2 to capture the future hydrologic conditions. In addition, preliminary transect surveys have shown potential unknown sources of nutrient downstream of the Gum Branch station, which should be further explored.

Literature Cited

Buchanan, T.J. and W.P. Somers. 1969. *Discharge Measurements at Gaging Stations: U.S. Geological Survey Techniques of Water-Resources Investigations*. Book 3, Chapter A8, page 65. Available at http://pubs.usgs.gov/twri/twri3a8.

Godin, G. 1972. *The Analysis of Tides*. University of Toronto Press. 264 pages.

Gotvald, A.J., and K.A. Oberg. 2008 *Acoustic Doppler Current Profiler Applications Used in Rivers and Estuaries by the U.S. Geological Survey*. USGS Fact Sheet 2008-3096. Available at http://pubs.usgs.gov/fs/2008/3096.

Horowitz, A.J., C.R. Demas, K.K. Fitzgerald, K.K., T.L. Miller, and D.A. Rickert. 1994. *U.S. Geological Survey Protocol for the Collection and Processing of Surface-Water Samples for the Subsequent Determination of Inorganic Constituents in Filtered Water*. USGS Open-File Report 94–539. U.S. Department of the Interior, U.S. Geological Survey, Earth Science and Information Center, Reston, VA.

Levesque, V.A., and K.A. Oberg. 2012. Computing discharge using the index velocity method: U.S. Geological Survey Techniques and Methods 3–A23. 148 pages. Available at http://pubs.usgs.gov/tm/3a23/pdf/tm3-a23.pdf.

Morlock, S.E., H.T. Nguyen, and J.H. Ross. 2002. *Feasibility of Acoustic Doppler Velocity Meters for Production of Discharge Records from U.S. Geological Survey Streamflow-Gaging Stations*. USGS Water-Resources Investigations Report 01-4157. U.S. Department of the Interior, U.S. Geological Survey, Reston, VA.

Oberg, K.A., S.E. Morlock, and W.S. Caldwell. 2005. *Quality-Assurance Plan for Discharge Measurements Using Acoustic Doppler Current Profilers*. USGS Scientific Investigations Report 2005–5183. U.S. Department of the Interior, U.S. Geological Survey, Reston, VA.

Ruhl, C.A., and M.R. Simpson. 2005. *Computation of Discharge Using the Index-Velocity Method in Tidally Affected Areas*. USGS Scientific Investigations Report 2005–5004. U.S. Department of the Interior, U.S. Geological Survey, Reston, VA.

Simpson, M. 2002. *Discharge Measurements Using a Broad-Band Acoustic Doppler Current Profiler*. USGS Open-File Report 01-01. U.S. Department of the Interior, U.S. Geological Survey, Reston, VA.

USGS (U.S. Geological Survey). 1997–1999. National Field Manual for the Collection of Water-Quality Data. Book 9, Chapters A1–A9 in *U.S. Geological Survey Techniques of Water-Resources Investigations*. U.S. Department of the Interior, U.S. Geological Survey, Reston, VA. Available at http://pubs.water.usgs.gov/twri9A.

Venables, V.M., D.M. Smith, and the R Development Core Team. 2012. *An Introduction to R, User's Manual*. Version 2.14.2. 109 pages. February 29.

Wagner, R.J., R.W. Boulger, Jr., C.J. Oblinger, and B.A. Smith. 2006. *Guidelines and Standard Procedures for Continuous Water-Quality Monitors: Station Operation, Record Computation, and Data Reporting*. USGS Techniques and Methods Report 1-D3. U.S. Department of the Interior, U.S. Geological Survey, Reston, VA.

Chapter 4

Tributary Creeks

SERDP Project Number: RC-1413

Aquatic/Estuarine Module

Lead Researcher:
Dr. Michael F Piehler
The University of North Carolina at Chapel Hill Institute of Marine Sciences
Morehead City, NC
E-mail: piehler@unc.edu

June 27, 2013

Final

This report was prepared under contract to the U.S. Department of Defense (DoD) Strategic Environmental Research and Development Program (SERDP). The publication of this report does not indicate endorsement by DoD, nor should the contents be construed as reflecting the official policy or position of DoD. References herein to any specific commercial product, process, or service by trade name, trademark, manufacturer, or otherwise, do not necessarily constitute or imply its endorsement, recommendation, or favoring by DoD.

Table of Contents

List of Acronyms 4-vi
Abstract.....4-1
Objectives of the Monitoring Activity.....4-1
Background.....4-2
Materials and Methods.....4-3
Study Sites 4-3
Creek TSS Loading Relationship with Wetland Demand for Sediment 4-6
Results and Discussion.....4-7
Annual Patterns in Loading.....4-7
Monthly and Seasonal Patterns in Loading 4-9
Ratios of Concentrations and Species of Nitrogen 4-20
Creek TSS Loading Relationship with Wetland Demand for Sediment 4-23
Assessment of Trends in the Data 4-24
Assessment of Monitoring Design.....4-24
Assessment Seasonal and Annual Variability in the Data 4-24
Recommendations for Future Monitoring 4-24
Conclusions and Implications for Future Research 4-24
Key Scientific Findings—Fundamental Cause-and-Effect Relationships.....4-24
Findings Supportive of Current and Future Base Management Practices.....4-24
Findings with Implications for DCERP2.....4-25
Literature Cited.....4-26

List of Figures

4-1. Location of study area in Eastern North Carolina. 4-3

4-2. Annual loads of water, total suspended solids (TSS), nitrate (NO_x), ammonium (NH_4), dissolved organic nitrogen (DON), and phosphate (PO_4) at 10 creeks. 4-8

4-3. Monthly loading of water, total suspended solids (TSS), nitrate (NO_x), ammonium (NH_4), dissolved organic nitrogen (DON), and phosphate (PO_4) at Camp Johnson. 4-10

4-4. Monthly loading of water, total suspended solids (TSS), nitrate (NO_x), ammonium (NH_4), dissolved organic nitrogen (DON), and phosphate (PO_4) at French Creek. 4-11

4-5. Monthly loading of water, total suspended solids (TSS), nitrate (NO_x), ammonium (NH_4), dissolved organic nitrogen (DON), and phosphate (PO_4) at Freeman Creek. 4-12

4-6. Monthly loading of water, total suspended solids (TSS), nitrate (NO_x), ammonium (NH_4), dissolved organic nitrogen (DON), and phosphate (PO_4) at Gillets Creek. 4-13

4-7. Monthly loading of water, total suspended solids (TSS), nitrate (NO_x), ammonium (NH_4), dissolved organic nitrogen (DON), and phosphate (PO_4) at Southwest Creek (SWC). 4-14

4-8. Monthly loading of water, total suspended solids (TSS), nitrate (NO_x), ammonium (NH_4), dissolved organic nitrogen (DON), and phosphate (PO_4) at Traps Creek. 4-15

4-9. Monthly loading of water, total suspended solids (TSS), nitrate (NO_x), ammonium (NH_4), dissolved organic nitrogen (DON), and phosphate (PO_4) at Cogdel Creek. 4-16

4-10. Monthly loading of water, total suspended solids (TSS), nitrate (NO_x), ammonium (NH_4), dissolved organic nitrogen (DON), and phosphate (PO_4) at Courthouse Bay. 4-17

4-11. Monthly loading of water, total suspended solids (TSS), nitrate (NO_x), ammonium (NH_4), dissolved organic nitrogen (DON), and phosphate (PO_4) at Tarawa. 4-18

4-12. Monthly loading of water, total suspended solids (TSS), nitrate (NO_x), ammonium (NH_4), dissolved organic nitrogen (DON), and phosphate (PO_4) at New River Air Station. 4-19

4-13. Seasonal DIN:DIP concentrations at sites from lowest watershed imperviousness to highest included Camp Johnson (CJ), French, Freeman, Gilletts, Southwest Creek (SWC), Traps, Cogdel, Courthouse Bay (CHB), Tarawa, and New River Air Station. 4-21

4-14. (Top Panel) DIN:DIP concentrations at 10 sites from lowest watershed imperviousness to highest included Camp Johnson (CJ), French, Freeman, Gillets, Southwest Creek (SWC), Traps, Cogdel, Courthouse Bay (CHB), Tarawa, and New River Air Station (NRAIR). (Middle Panel) Quadratic relationship beteen 10 sties and (bottom panel) eight sites showing mean DIN:DIP and percent watershed imperviousness. 4-22

4-15. Species of nitrogen loaded from each watershed in each year in grams per hectare per year 4-23

List of Tables

4-1. Land cover and watershed area of study sites.....4-4

4-2. Percentages of wetland demand for sediment provided by stream TSS under hypothetical sea level rise scenarios. 4-23

List of Acronyms

µm	micrometer
µM	micromole
°C	degrees Celsius
A	area
CHB	Courthouse Bay
CJ	Camp Johnson
cm	centimeter
DCERP1	first cycle of the Defense Coastal/Estuarine Research Program
DCERP2	second cycle of the Defense Coastal/Estuarine Research Program
DIN:DIP	ratios of dissolved inorganic nitrogen to dissolved inorganic phosphorus
DoD	U.S. Department of Defense
DON	dissolved organic nitrogen
ft	feet, foot
ha	hectare
LiDAR	light detection and ranging
m	neter
m/m	meters per meter
m/s	meters per second
m^2	square meter
m^3	cubic meter
m^3/s	cubic meters per second
MCBCL	Marine Corps Base Camp Lejeune
mm	nillimeter
mm/y	millimeters per year
n	Manning “n” constant
N	nitrogen
NH_4	ammonium
NLCD	National Land Cover Dataset
NO_x	nitrate + nitrite
NR Air	New River Air Station
NRE	New River Estuary
P	phosphorus
PO_4	orthophosphate
Q	discharge
QC	quality control
R	hydraulic radius

S	channel slope, water surface slope
SERDP	Strategic Environmental Research and Development Program
SWC	Southwest Creek
TDN	total dissolved nitrogen
TSS	total suspended solids
V	velocity

[This page intentionally left blank.]

Abstract

Human activities in coastal landscapes are quickly reflected in the transport of freshwater and accompanying material such as nutrients and sediments. Coastal creeks are both a habitat and are transport vectors for landscape-derived materials. Understanding the relationship of land use and precipitation patterns to loads and concentrations of nutrient and suspended solids informs broad areas of coastal decision making. Headwater streams in the New River Estuary (NRE), NC, were investigated for four years, during which water samples were collected during base- and throughout storm-flow. Samples were analyzed for nutrient and total suspended solids concentrations, and flow was measured continuously.

There was a seasonal pattern in creek discharge with peaks in the winter and generally lower discharge during summer. Elevated levels of summer stream discharge corresponded with storm events. Seasonal patterns of discharge were less evident in developed watersheds likely due to the reduced effects of vegetation on the watershed hydrology.

As development in watersheds increased, so did the proportion of loading of nutrients and sediments delivered in storm flow. Increased development reduces stormwater infiltration in the watershed and creates faster flow paths to streams during storms.

The ratio of nitrogen to phosphorus in the creek loading to the estuary increased as level of development in the watershed increased. Because the New River Estuary phytoplankton community has been found to be nitrogen limited, this higher nitrogen to phosphorus ratio in developed creeks increases the potential for stimulation of phytoplankton in the estuary.

Creeks loaded significant amounts of total suspended solids to the estuary. In most creeks, the supply of sediment was less than 1% of the total demand for sediment to keep up with sea level rise. However, Cogdel Creek had both a large supply of total suspended solids and relatively low area of wetlands, resulting in the delivery of more than 100% of the sediment required to keep up with sea level rise.

Monitoring headwater creeks provided both ecological data to support the understanding of the water, nutrient and sediment cycles in the New River Estuary and data to be used as indicators of changes in human activities in small coastal watersheds.

Keywords: flow, loading, nitrogen, phosphorus, total suspended solids, watershed, nitrogen to phosphorus ratio

Objectives of the Monitoring Activity

We measured stream flow and nutrient and sediment concentrations in ten coastal creeks to estimate loading to the NRE. We will relate stream flow to precipitation intensity, duration and frequency data provided from meteorological monitoring. Creek sampling stations were spatially stratified to assess variability within the estuarine salinity zones and to determine the effects of on land activities on stream flow, and sediment and nutrient delivery to the estuary. Flow and loading

of sediment and nutrients were related to land use to link land activities and aquatic and estuarine ecosystem function.

These activities were directly linked to other Aquatic/Estuarine monitoring activities through providing loading rates of sediments and nutrients to the NRE. Delivery of nutrients and sediments from creeks to the estuary is an important materials transport mechanism and is often affected by changes in on-land activities.

This monitoring activity was also linked to the Coastal Wetlands Module. For marshes, suspended solids are beneficial rather than detrimental and provide material for accretion. The ability of many marshes to maintain their elevation is dependent upon a supply of suspended sediments. The tidal creek monitoring sites include creeks in the mesohaline and back-barrier, where the Coastal Wetlands Module measured elevation changes in marshes. Linking these elevation measurements to the creek's sediment supply could be an important step toward understanding mechanistic links between watershed activities and marsh sustainability.

These monitoring activities were also to be linked to the Terrestrial Module. The stream sampling sites represent an integration of the effects of watershed processes on the load of nutrients, and sediments transported from the landscape. Finally, this monitoring was integrated with the data collected by the Atmospheric Module in that precipitation drove stream discharge and deposition of nitrogen may have been an important contributor to stream nitrogen loading.

Background

Human activities in coastal regions can result in result in detrimental watershed alteration. Land use change of coastal systems can have significant impacts on nutrient loading (Schwartz, 2010) and sediment-transport pathways (Corbett et al., 2008). Efforts such as reforestation to reduce erosion and dam building have dramatically reduced sediment yield to many major southeastern watersheds (Stevenson et al., 1988). Sediment starvation of wetland systems of the coastal zone over the past half century may have led to undernourishment (Stevenson et al., 1988). On the other side of the spectrum, land alteration such as deforestation and construction increases sediment loading to coastal streams (Schwartz, 2010). This poses a challenge for land use planning because sediment is required for wetland systems, yet an oversupply can be damaging to water column and benthic communities. Similar issues apply to nutrient loading. Some nutrient is supply is required to support the base of the estuarine food web, but excessive supplies can lead to eutrophication (Paerl, 1997).

Stream nutrient and sediment loading is understudied in coastal regions, likely due to the challenges of measuring flow in very flat landscapes that are often influenced by tides. Here, we studied 10 streams through 4 years to improve our understanding of the connections between land use and stream nutrient and sediment loading in coastal streams and to determine the contribution of the streams to the water, nutrient and sediment cycles of the estuary.

Materials and Methods

Study Sites

The NRE, situated in North Carolina's Coastal Plain (**Figure 4-1**), is composed of shallow (1 to 2 m), broad lagoons, with water flow constrained at the mouth by barrier islands (Mallin et al., 2005). Despite improvements to sewage treatment plants in 1998, the NRE has continued to have some phytoplankton blooms and periods of severe bottom water hypoxia (Mallin et al., 2005).

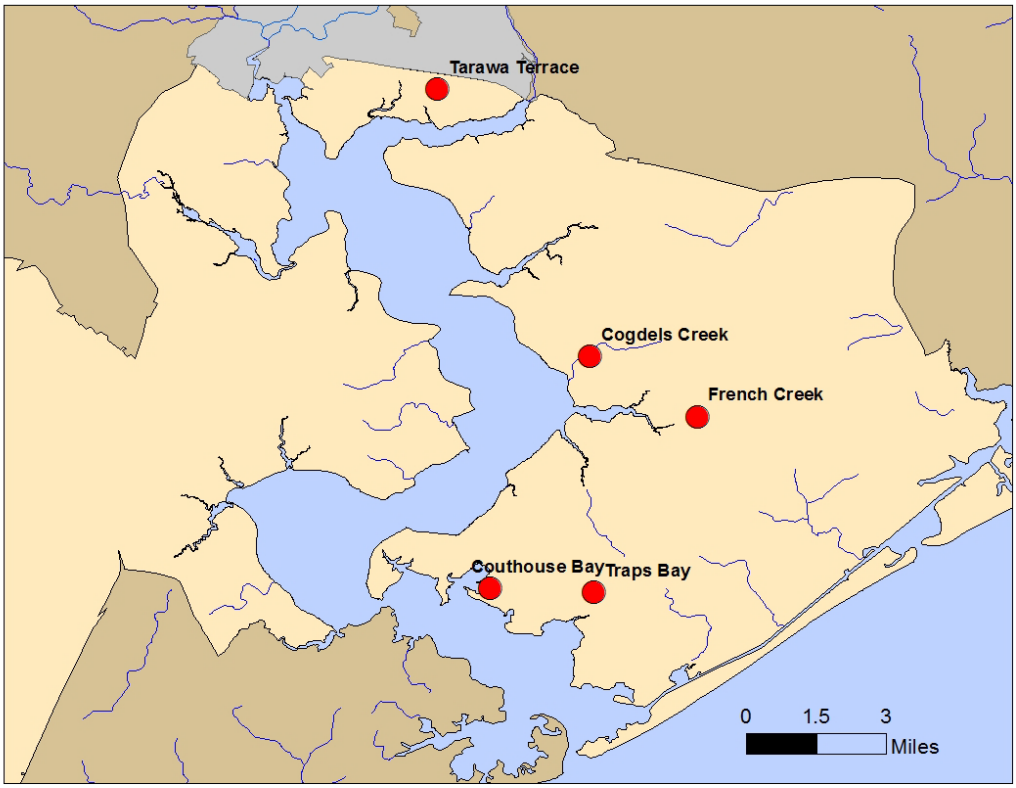

Figure 4-1. Location of study area in Eastern North Carolina.

Sampling locations for this study are represented by circles.

Ten mixed-cover watersheds of the NRE were investigated to assess impacts of various land uses on stream water quality and patterns of material delivery. The watersheds' characteristics are summarized (**Table 4-1**).

The 10 watersheds drained into headwater streams that were monitored for in-stream water quality and discharge from 2008 through 2011. Monitoing was reduced to 5 sites in 2012; however, those results are not discussed in this report. The NRE lies within Marine Corps Base Camp Lejeune (MCBCL), which started expanding in 2008 to accommodate a large influx of U.S. Marines (approximately 5,000) and their families. Land uses on MCBCL are typical of military installations and included residential neighborhoods, barracks, industrial parks, and impact zones for ordnance training. The characteristic low elevation and shallow slopes of the North Carolina Coastal Plain have profound implications for mechanisms that deliver material to streams, altering loading patterns as compared to watersheds of a steeper gradient. Coastal North Carolina has a

humid, subtropical climate, with temperatures ranging from 12.8–13.9°C and average precipitation of 142 cm per year. Rainfall is distributed almost evenly throughout the year, with a slight increase from June through September (MCBCL, 2006), minimizing seasonal patterns of material delivery to streams. Watersheds were delineated using 20-ft (6.1-m) elevation light detection and ranging (LiDAR; M. Brush) with ArcGIS (ESRI, Redland, CA). Resulting watersheds were converted to polygons and combined with the National Land Cover Dataset (NLCD) 2001 data to assign areas for each land-use category.

Table 4-1. Land cover and watershed area of study sites.

Percent impervious is indicated in parentheses (source: Homer et al., 2007).

Site	Forested Land (ha)	Impervious Surface (ha)	Developed Land (ha)	Total Area (ha)
Cogdel	280.53	115.25 (13.8%)	209.16	835.83
French	80.28	8.56 (1.1%)	27.72	807.30
Freeman	151.56	9.32 (1.6%)	21.69	588.24
Gillets	70.74	12.94 (2.86%)	35.28	452.97
Tarawa	24.48	32.28 (23.2%)	63.90	139.14
Camp Johnson	16.47	0.06 (0.27%)	0.00	22.32
Air Station	14.76	20.96 (26.55%)	39.42	78.93
Southwest Creek	35.55	2.33 (3%)	6.66	77.49
Courthouse Bay	3.06	4.85 (15.5 %)	19.62	31.32
Traps	5.76	2.11 (4.13%)	6.39	51.03

Data collection throughout the study period consisted of continuous flow measurements and manual sampling (water grab, water depth measurement, and water velocity using a Sontek Flowtracker acoustic Doppler velocimeter) that occurred every other week to characterize baseflow as well as after rain events (defined as greater than 2.5 cm of rain) to characterize storm flow. More frequent automated sampling was conducted to enhance resolution during storm events at some sites equipped with automated samplers (ISCO models 6700 or 6712). Automated samplers were located at Cogdel, French, Gillets, and Freeman sites from July 2008 to June 2011 and at Camp Johnson, Tarawa, Courthouse Bay, and Traps sites from December 2009 through June 2011. Samplers were programmed to trigger above a threshold stream velocity set for storms and water samples were collected at flow-paced intervals once the samplers were enabled. Automated grab samples were collected as soon as possible after a rain event and brought back to the laboratory for processing. Water samples were selected to encompass a period including before, rising, peak and falling limbs of hydrographs for each storm at each site.

All water samples were analyzed for total suspended solids (TSS) and nutrients [$NO_{2/3}^{-}$−N (referred to as nitrate + nitrite [NO_x]), NH_4^{+}−N (ammonium [NH_4]), PO_4^{3+}−P (phosphate [PO_4]), and total dissolved nitrogen (TDN)]. Water samples were filtered through Whatman glass fiber filters (GFFs; 25mm in diameter, 0.7 µm nominal pore size), and the filtrate was analyzed with a Lachat Quick-Chem 8000 automated ion analyzer for $NO_{2/3}$–N, NH_4^{+}–N, and PO_4^{3+}–P and TDN concentrations using standard protocols (Lachat Instruments, Milwaukee, WI; NO_2^{-} and NO_3^{-} Method 31- 107-04-1-A, NH_4 Method 31-107-06-1-A, and PO_4 Method 31-115-01-3-G). Dissolved organic nitrogen (DON) was calculated as the difference between TDN and the sum of

$NO_{2/3}^{-}$−N and NH_4^{+}−N. Additional water was filtered through pre-cleaned and dried Whatman GFF prefilters (47 mm in diameter, 0.7-µm nominal pore size) and residue was dried and weighed for measurement of TSS using standard protocols (APHA, 1998; Method 2540 D, 2-57).

Nutrient concentrations that were below the detection limit but above zero were reported as the measured value and concentrations measured as negative were reported as zeros. Detection limits were as follows in micromoles (µM): NO_x (0.043), NH_4 (0.182), PO_4 (0.059), and TDN (2.529). This was done instead of replacing values with the minimum detection value to avoid overestimating concentration and load calculations.

Flow Computation

ISCO automated samplers were equipped with ISCO Model 750 area velocity modules with flow sensors that measured velocity (ultrasonic Doppler) and level (pressure transducer) in culvert pipes. Velocity and level were measured continuously and recorded at 30-minute intervals throughout the study period when the ISCO was present at a particular site, and volumetric flow rates were calculated using velocity and cross sectional area of water in the pipe. Rainfall data were recorded at Cogdel and Freeman sites at 30-minute intervals via a tipping gauge connected to the ISCO sampler.

Level gauges (pressure transducers) were placed in sites when ISCO samplers were not available. Water depth was recorded at 30-minute intervals throughout the study period. Discharge was calculated using the Manning equation (as shown below) at all sites except at the Air Station and Southwest Creek sites.

$$Q=VA$$

or

$$Q=\left(\frac{1}{n}\right)AR^{2/3}S^{1/2}\times A$$

where

A = Area (m^2)
n = Manning “n” constant
R = Hydraulic radius (m)
S = Channel slope (m/m)
V = Velocity (m/s)
Q = Discharge (m^3/s)

Field measurements were made of stream slope and other streambed characteristics to apply as parameters in the Manning equation. Cross-sectional profiles were obtained by measuring channel width and height at three representative locations along the stream reach, and used to calculate *A* and *R*. Water surface slope (*S*) was measured at three locations along the stream reach via the hydrostatic leveling technique described by Gordon et al. (2004). Adjustments were made to calibrate the Manning equation calculated values to field measurements of water level and water

velocity (Flowtracker) made during routine monthly sampling and indexed to ISCO flow sensor data at sites where ISCO's were subsequently deployed.

A stage discharge relationship based on water level from pressure transducers and manual velocity measurements was used to calculate discharge at the Air Station site. At the Southwest Creek site, pressure transduced water level was adjusted to downstream of pipe, but channel configurations were from conditions upstream of pipe. Mechanical errors resulting in missing level or velocity data were estimated once discharge had been calculated. Baseflow was interpolated through periods of missing data. To estimate magnitude of missing storms, nearby storms from 2 to 3 months before and after the missing data time period were used as a model. In each storm, the difference in flow was calculated from base to peak, and from base to inflection point of the falling limb. A second-order polynomial curve was fit to a scatter plot of storm precipitation total versus difference to peak discharge, or difference to inflection point on falling limb. These equations were then used to calculate peak and falling inflection point discharges of missing storms based on the total precipitation during that missing storm. Placement of points on the time axis mirrored nearby creeks with similar precipitation patterns, and discharge was interpolated between points.

Load Calculations

A graphical separation technique was utilized to delineate between the baseflow component and total stream flow during storm events (Ward and Robinson, 2000). Groundwater contribution during storms was determined by extending antecedent conditions by interpolating from baseflow before the rain event to the point of greatest inflection on the falling limb of the hydrograph. A mass balance equation was used to determine the resultant storm flow contribution to nutrient and TSS load.

Collection of water samples at sites when ISCOs were deployed was at a fine temporal resolution throughout storms, which enabled development of a continuous record of nutrient and TSS concentrations by interpolating between measured samples. When ISCOs were not present, extrapolating measured data to half hour intervals was accomplished by applying quality control (QC; flow versus concentration) generated polynomials to calculate concentration based on water flow. QC relationships were created using all available data within the study period, but applied only to those times and sites when ISCOs were not present.

Creek TSS Loading Relationship with Wetland Demand for Sediment

The seven watersheds were analyzed using geographic information systems to determine the percentage of wetlands that were downstream of gauged sites. The area of wetlands (based on National Wetlands Inventory data) within the watershed were compared to the amount of total watershed area for each site. The area of freshwater and saltwater brackish wetlands that fell within the watershed area for each site was totaled and converted to hectares (ha), which represent the area of wetlands into which each watershed feeds. To calculate the amount of sediment that each stream contributed to their respective wetland areas, the annual load of TSS in kilograms for each site was multiplied by the inverse of the standard bulk density measurement of 2 g/cm^3 to determine the final volume of sediment in cubic meters (m^3). The area of wetlands (in ha) was multiplied by three possible sea level rise scenarios: 4 mm, 10 mm, and 15 mm per year,

respectively. After conversion, the volume of water added to the wetland area per year was presented in cubic meters. The volume of TSS (in m^3) was divided by the volume of water (in m^3) and multiplied by 100 to determine the percentage of sediment loaded from the stream that contributes to the amount of sediment that the wetland needs for accretion to keep up with each sea level rise scenario.

Results and Discussion

Annual Patterns in Loading

Annual loads of water, TSS, NO_x, NH_4, DON, and PO_4 for each of the 10 creeks are presented in **Figure 4-2, panels a–f**. Creek watersheds have higher proportions of imperviousness moving from left to right. Within the sites, the largest annual load of water was from 2009–2010. The one exception was Courthouse Bay, which had the highest water load from 2011–2012. This departure from the general pattern may have been a result of significant construction activity in the Courthouse Bay watershed that appeared to increase the imperviousness in the area near our sampling station. The prevailing trend in water load was to increase with increased imperviousness. Total suspended solid loading was also generally highest in 2009–2010 at all sites. The pattern of increased TSS loading with increased imperviousness was again generally true. A notable exception was Camp Johnson. At this site a gravel road adjacent to the site provided an augmented source of TSS that increased the measured load beyond the level than would have been predicted by the level of development in the sub-watershed. The road was resurfaced during our study, after which we observed both higher TSS concentrations and water flows. At all sites nitrate loading was generally quite low and the patterns in annual variability were not as consistent. Loads did increase with increasing imperviousness and the largest increases were seen above 15% watershed imperviousness. Loading of NH_4 was generally very low in all watersheds with the exception of Camp Johnson, Courthouse Bay, and the New River Air Station sites. Higher loading in Camp Johnson and Courthouse Bay sites was likely attributable to the fact that these streams were intermittant and had significant plant and algal growth in the stream beds. When these plants and algae senesce, they are significant sources of NH_4 (McMillan et al., 2010). DON loading showed annual variability at most sites and in most cases the highest load was in 2009-2010. There were larger loads of DON than any other form of nitrogen. Interestingly, New River Air Station site had the highest loads of DON, despite being the most developed site. It is likely that the sources of DON varied among watersheds depending upon the land use. Phosphate loading was extremely low at all sites, with highest loading at New River Air Station site. Low loads of phosphorus led to elevated dissolved inorganic nitrogen to dissolved inorganic phosphorus ratios that will be discussed further.

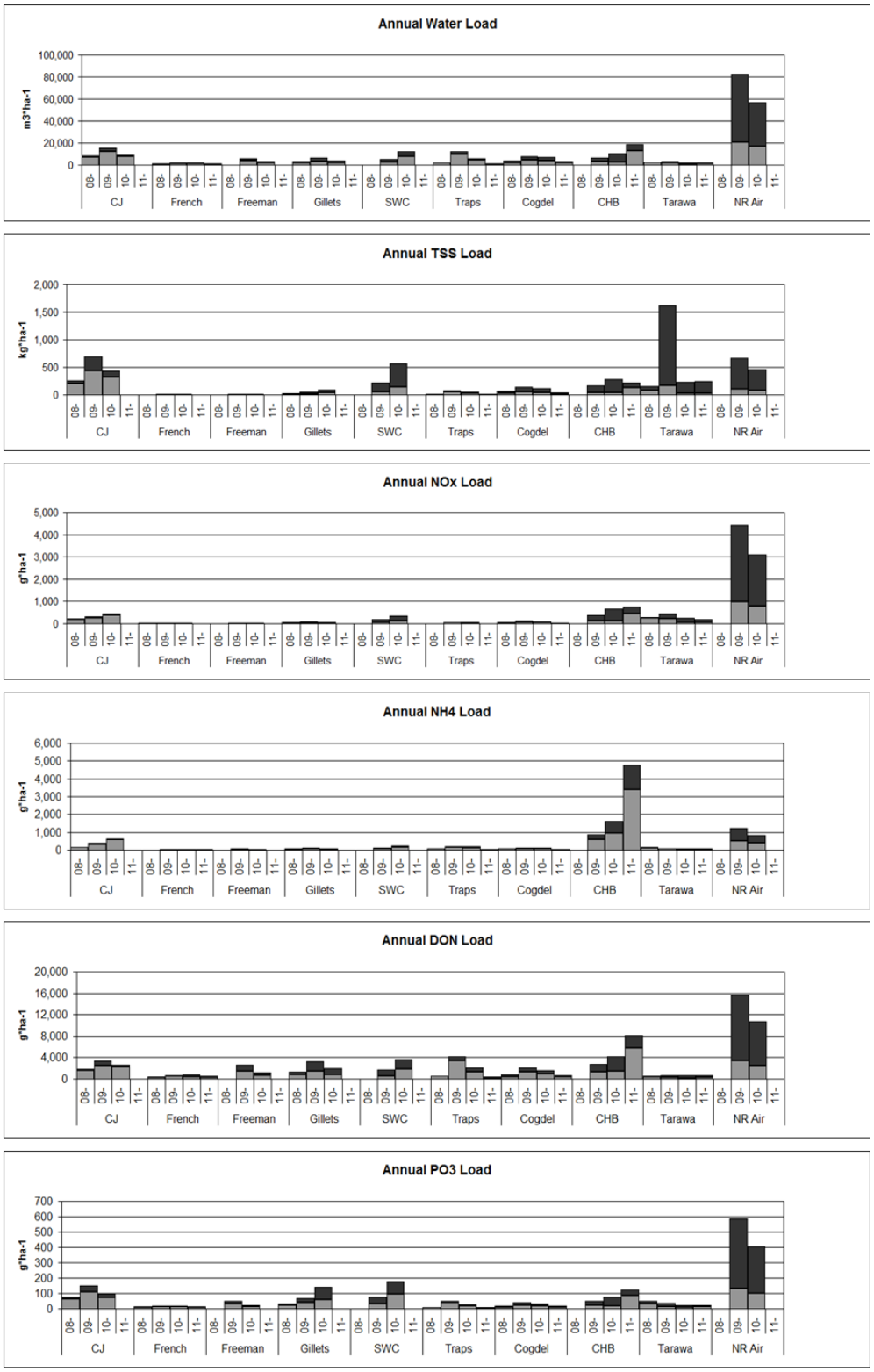

Figure 4-2. Annual loads of water, total suspended solids (TSS), nitrate (NO_x), ammonium (NH_4), dissolved organic nitrogen (DON), and phosphate (PO_4) at 10 creeks.

Sites from lowest watershed imperviousness to highest included Camp Johnson (CJ), French, Freeman, Gilletts, Southwest Creek (SWC), Traps, Cogdel, Courthouse Bay (CHB), Tarawa and New River Air Station (NR Air).

Monthly and Seasonal Patterns in Loading

Monthly loading of all constituents at all sites through 4 years is shown in **Figures 4-3** through **4-12**. The prevailing pattern in water loading (panel "a" in all figures) is higher in winter months and lower in summer months. There were several exceptions to this pattern, however. In some non-winter months there were occasional large loads. This was attributable to large storm events that were almost always tropical in origin. The pattern of winter peaks and summer troughs was most evident in several of the less developed creeks (e.g., French Creek). The seasonal pattern was not present at the Camp Johnson site (**Figure 4-3**) despite its low level of development. This was likely attributable to the ephemeral nature of the stream leading to unconventional water delivery patterns and the generation of NH_4 through the remineralization of plant material that flourished during low-flow conditions. As imperviousness in the sub-watersheds increased (e.g., Courthouse Bay, Tarawa Terrace, and New River Air Station sites) the predictable summer peak winter trough pattern was much less evident (**Figures 4-10**, **4-11** and **4-12**). There was a relationship between increasing watershed imperviousness and the proportion of materials loaded in stormflow. New River Air Station site had the highest level of imperviousness in its watershed and had nearly all of the loading in stormflow (**Figure 4-12**). At nearly all sites, NH_4 loading was predominantly in baseflow, whereas nitrate (NO_3), TSS, DON, and PO_4 loading were delivered during storms. As mentioned previously, the stream loading of NH_4 was likely from senescing algae and plants in the creeks, which elevated NH_4 levels during baseflow.

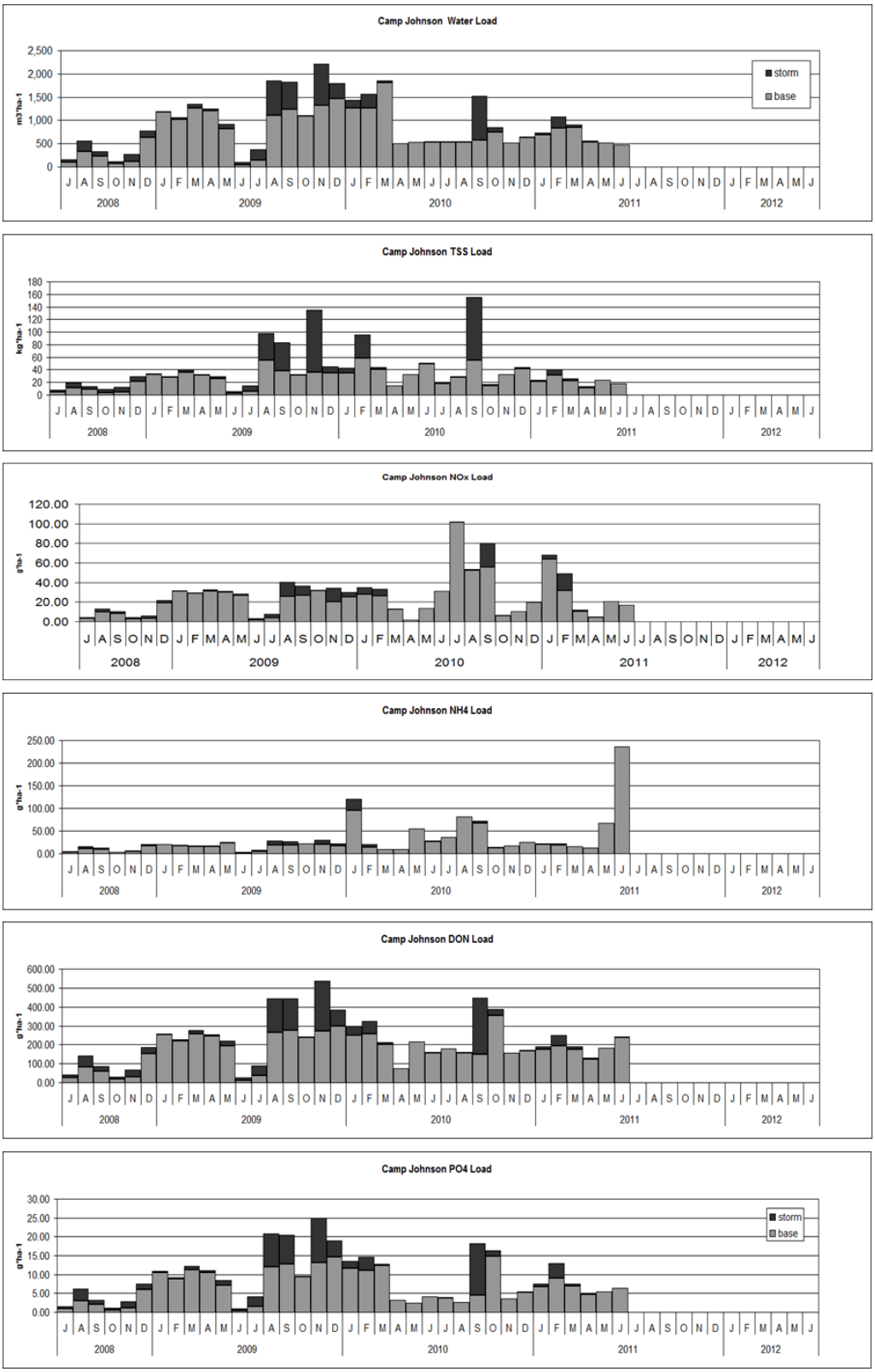

Figure 4-3. Monthly loading of water, total suspended solids (TSS), nitrate (NO_x), ammonium (NH_4), dissolved organic nitrogen (DON), and phosphate (PO_4) at Camp Johnson.

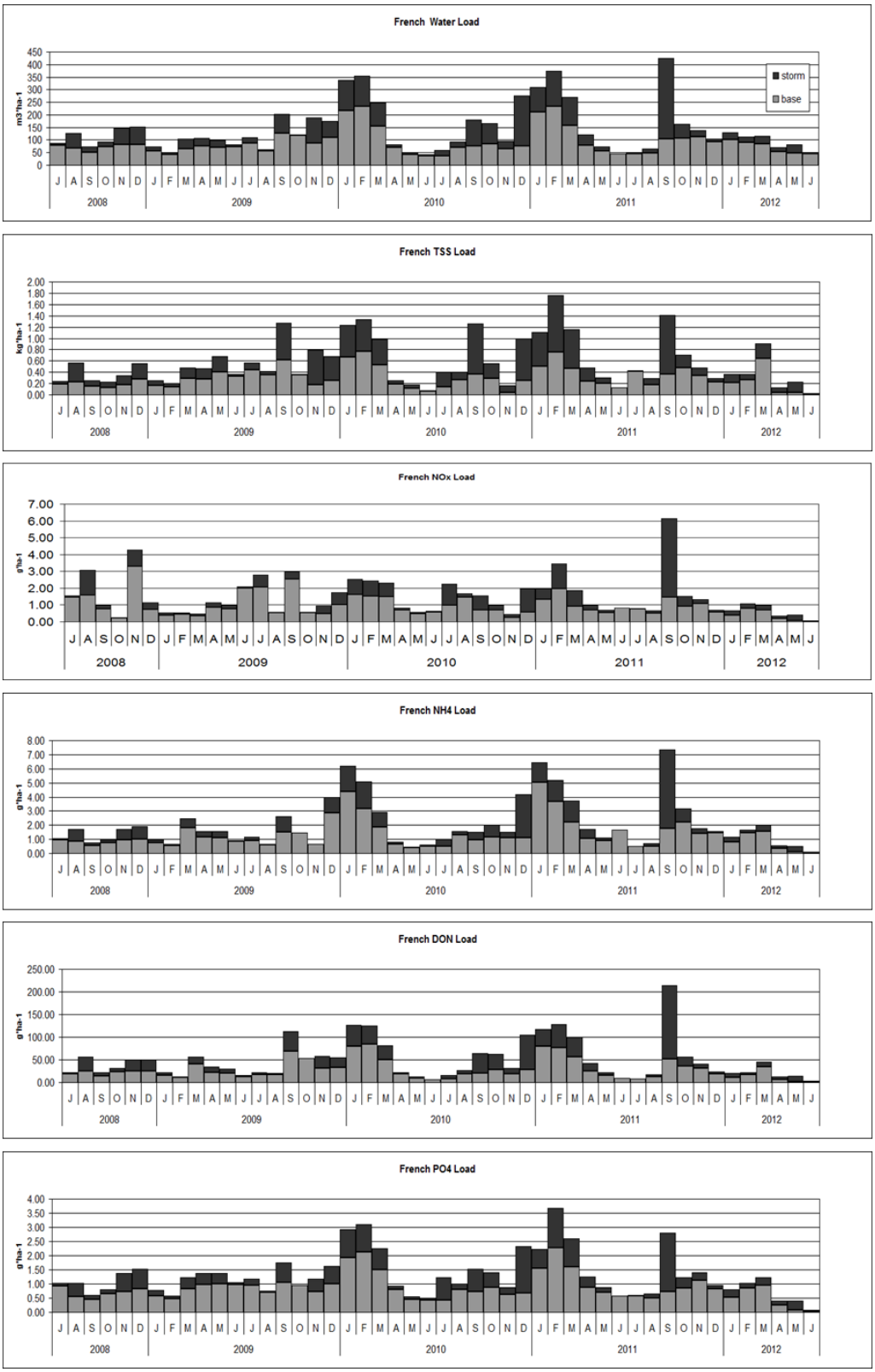

Figure 4-4. Monthly loading of water, total suspended solids (TSS), nitrate (NO_x), ammonium (NH_4), dissolved organic nitrogen (DON), and phosphate (PO_4) at French Creek.

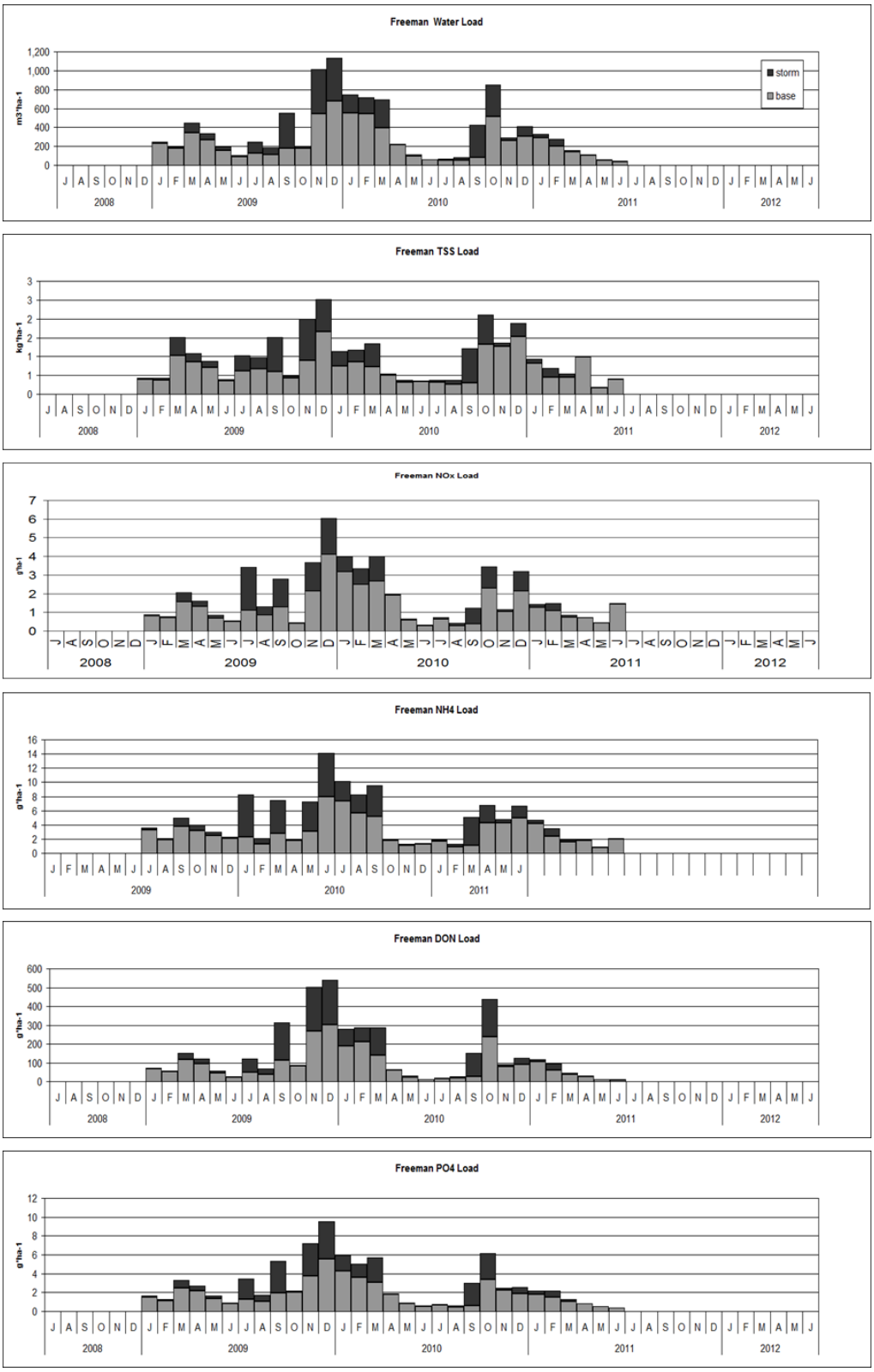

Figure 4-5. Monthly loading of water, total suspended solids (TSS), nitrate (NO_x), ammonium (NH_4), dissolved organic nitrogen (DON), and phosphate (PO_4) at Freeman Creek.

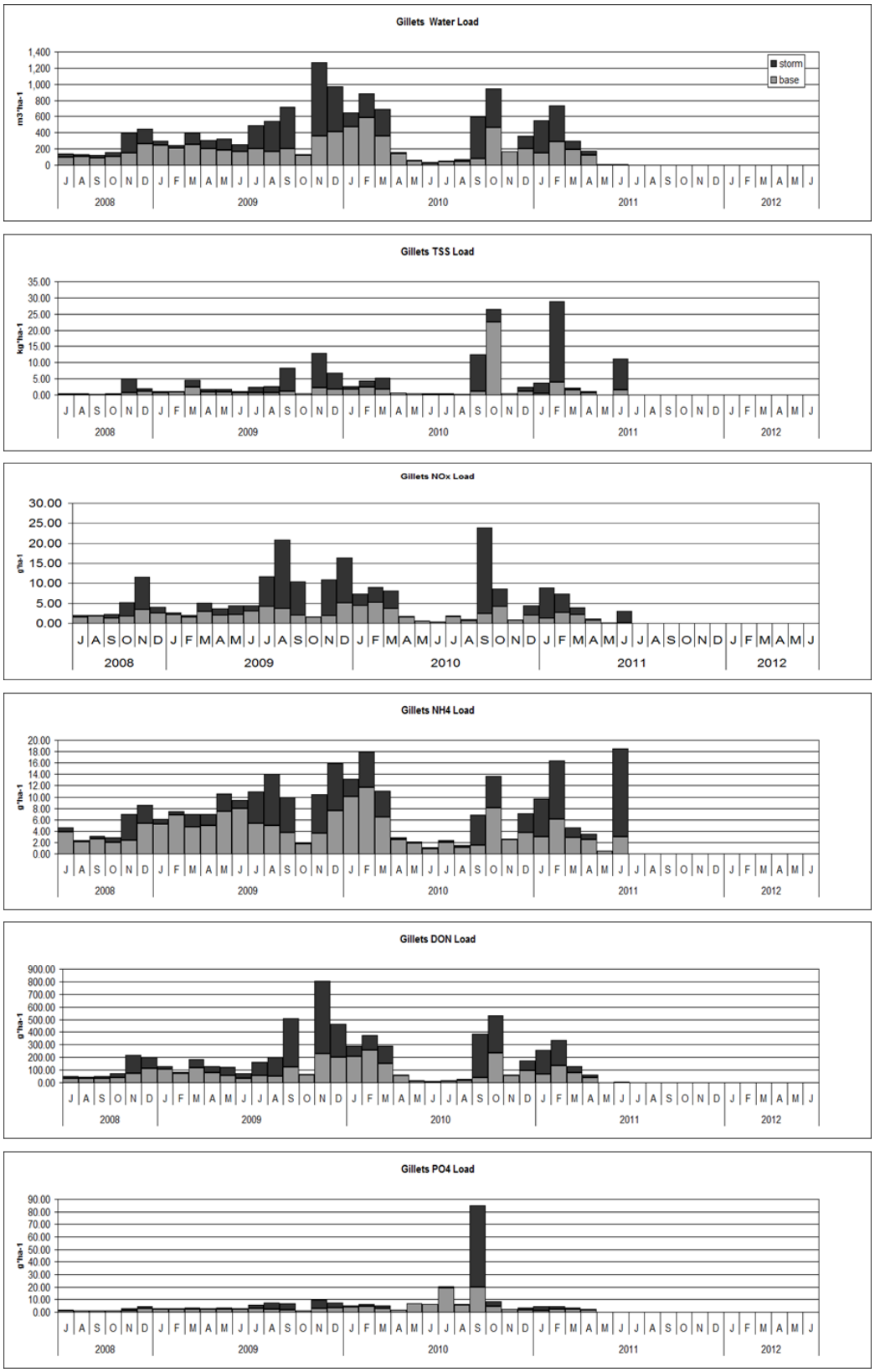

Figure 4-6. Monthly loading of water, total suspended solids (TSS), nitrate (NO_X), ammonium (NH_4), dissolved organic nitrogen (DON), and phosphate (PO_4) at Gillets Creek.

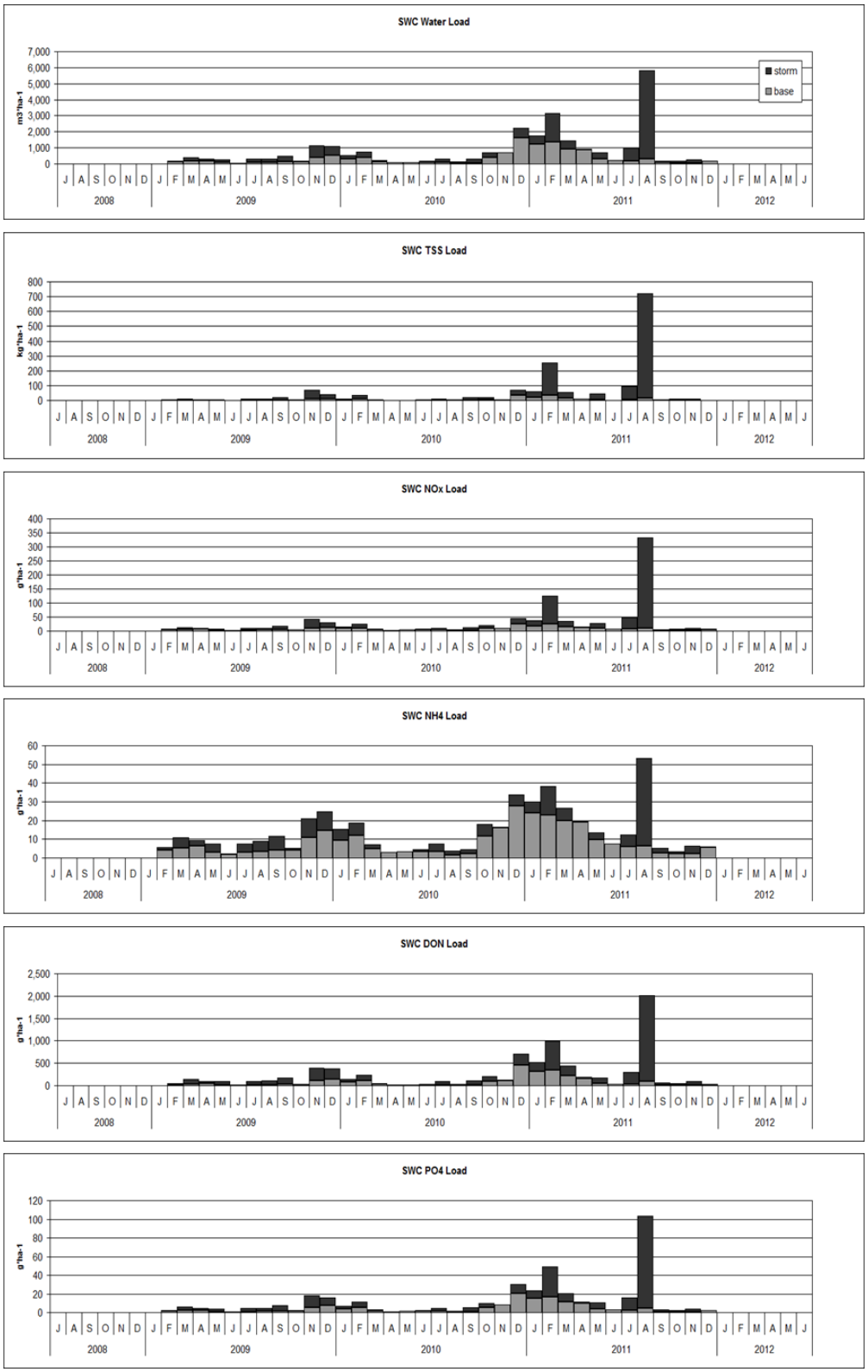

Figure 4-7. Monthly loading of water, total suspended solids (TSS), nitrate (NO_x), ammonium (NH_4), dissolved organic nitrogen (DON), and phosphate (PO_4) at Southwest Creek (SWC).

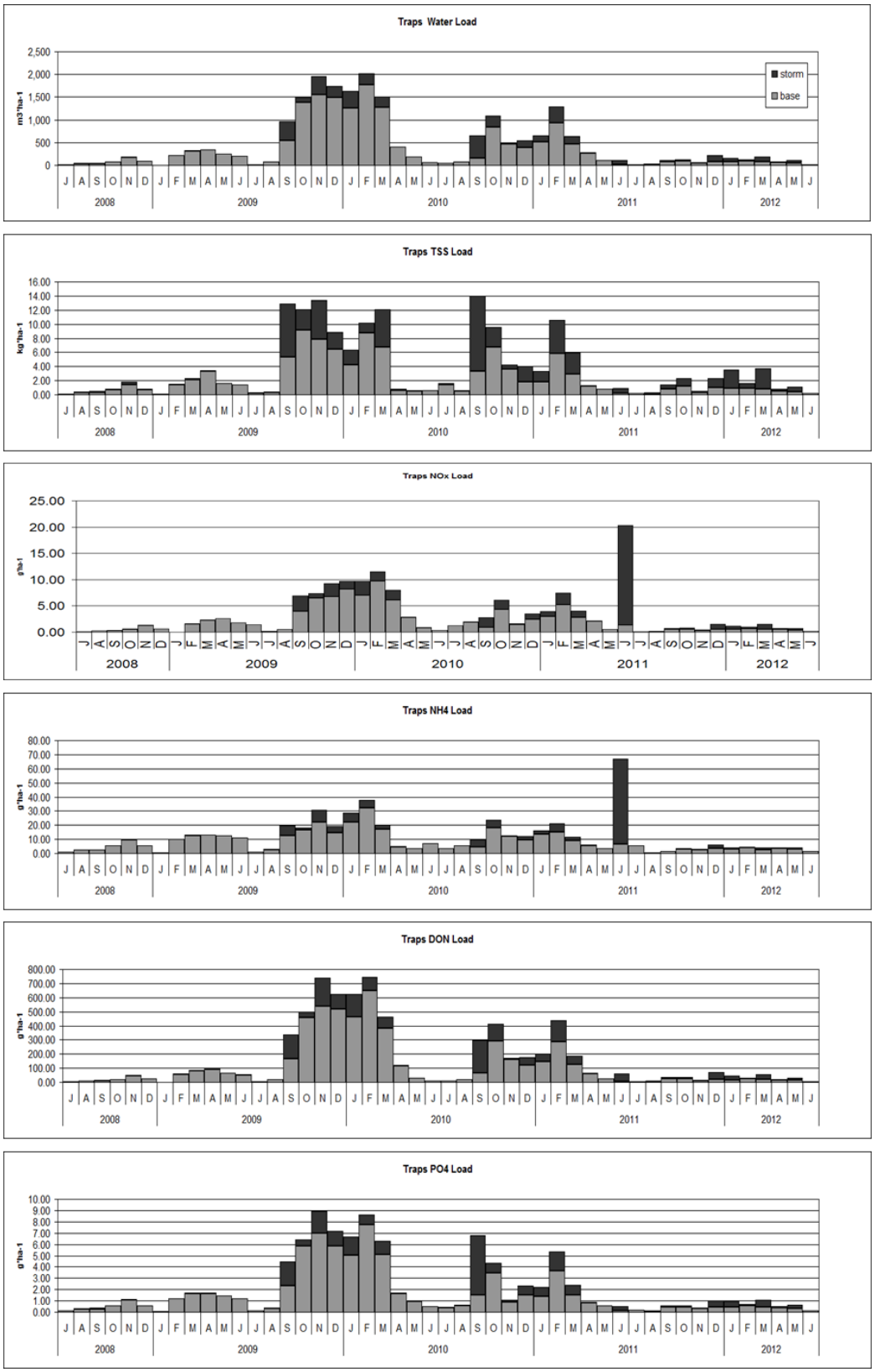

Figure 4-8. Monthly loading of water, total suspended solids (TSS), nitrate (NO_x), ammonium (NH_4), dissolved organic nitrogen (DON), and phosphate (PO_4) at Traps Creek.

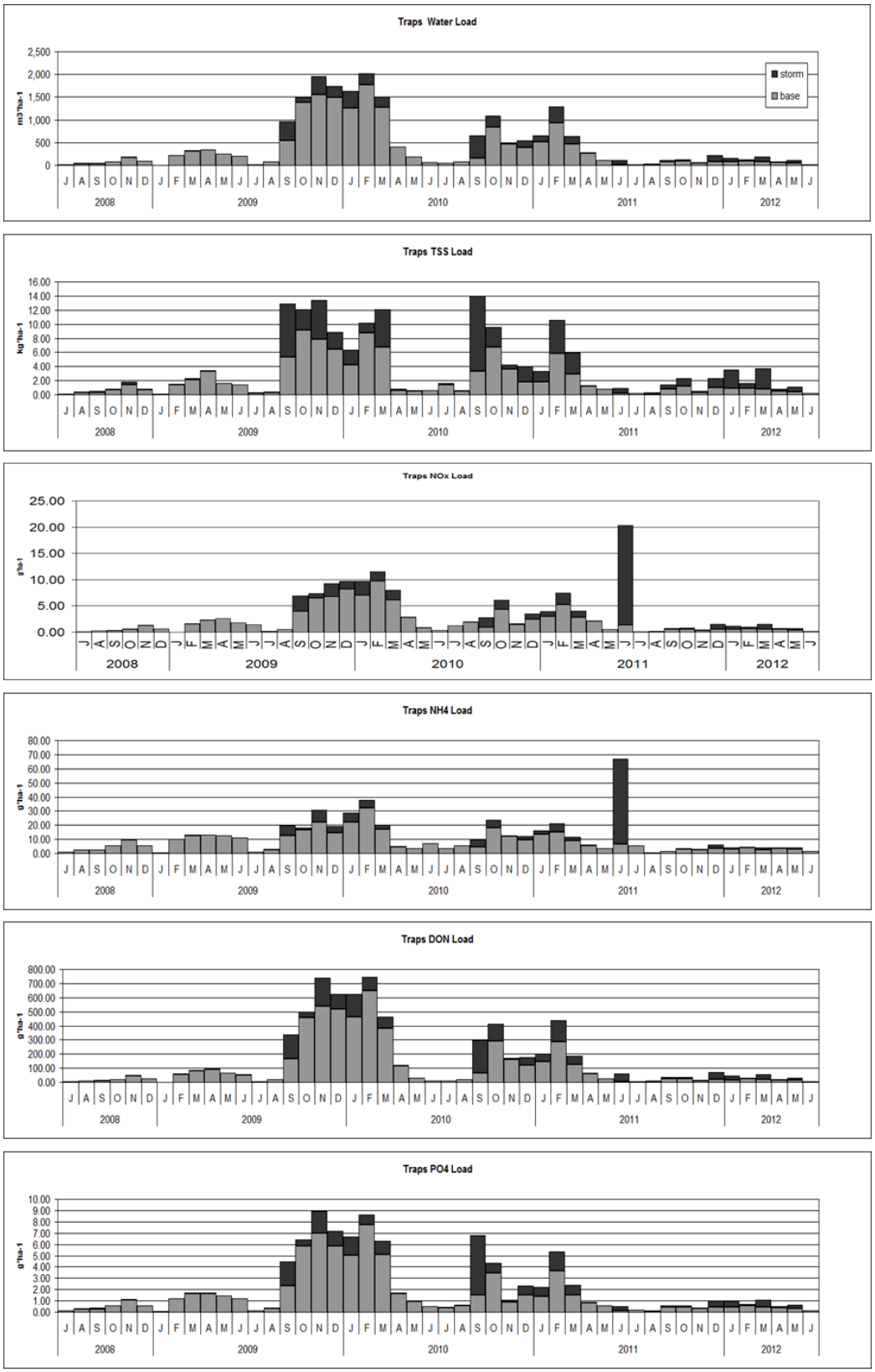

Figure 4-9. Monthly loading of water, total suspended solids (TSS), nitrate (NO_x), ammonium (NH_4), dissolved organic nitrogen (DON), and phosphate (PO_4) at Cogdel Creek.

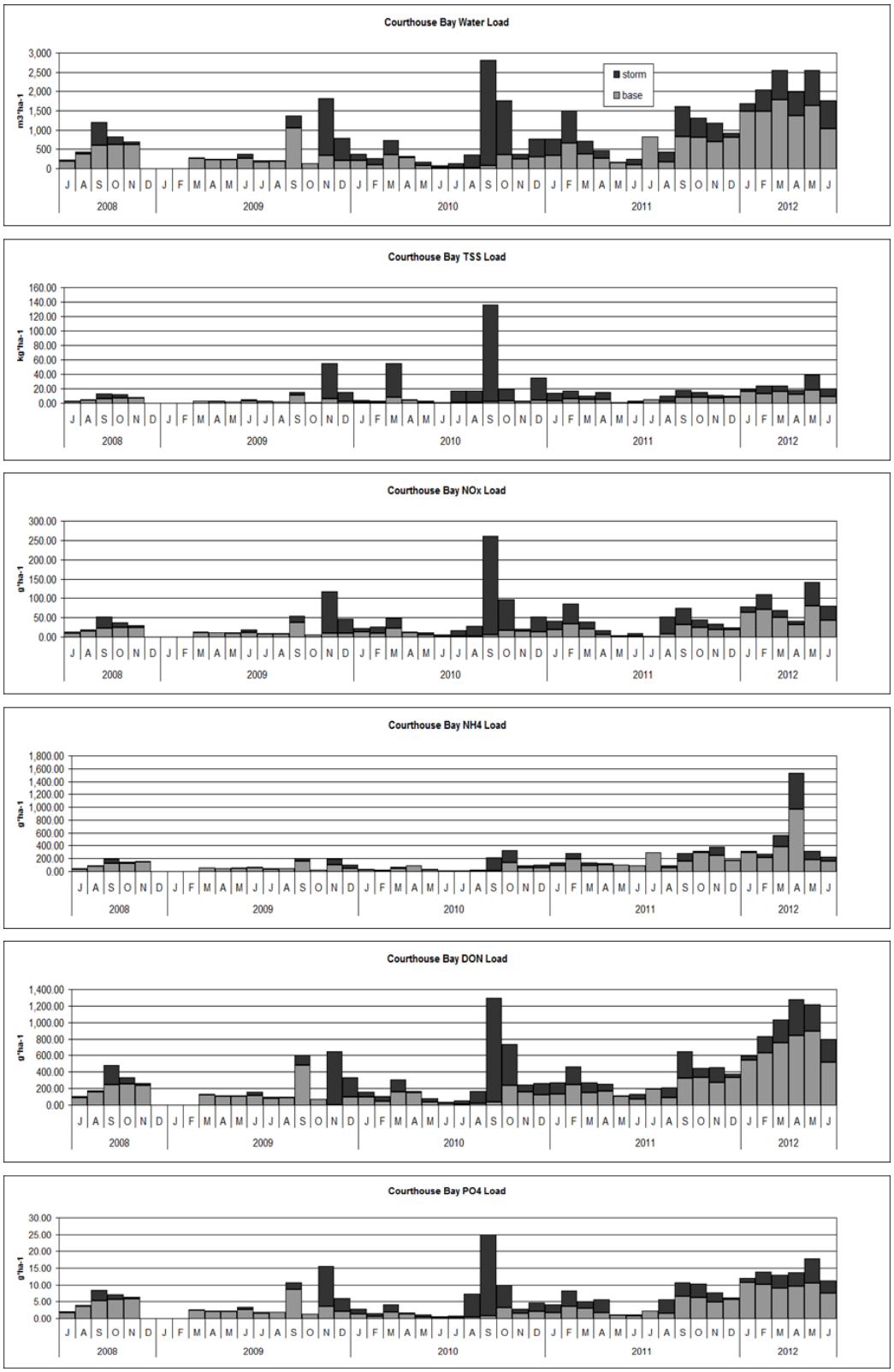

Figure 4-10. Monthly loading of water, total suspended solids (TSS), nitrate (NO_x), ammonium (NH_4), dissolved organic nitrogen (DON), and phosphate (PO_4) at Courthouse Bay.

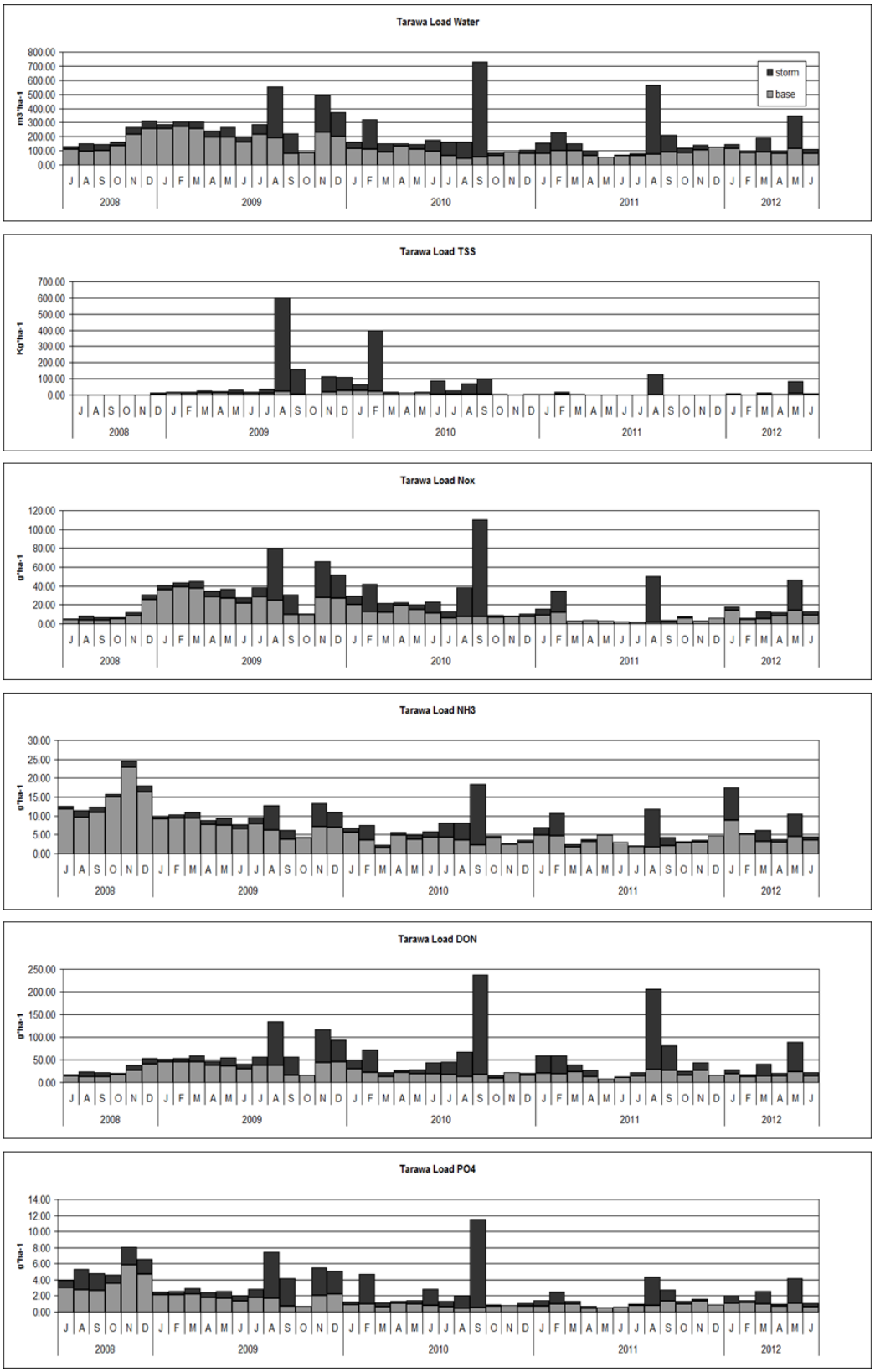

Figure 4-11. Monthly loading of water, total suspended solids (TSS), nitrate (NO_x), ammonium (NH_4), dissolved organic nitrogen (DON), and phosphate (PO_4) at Tarawa.

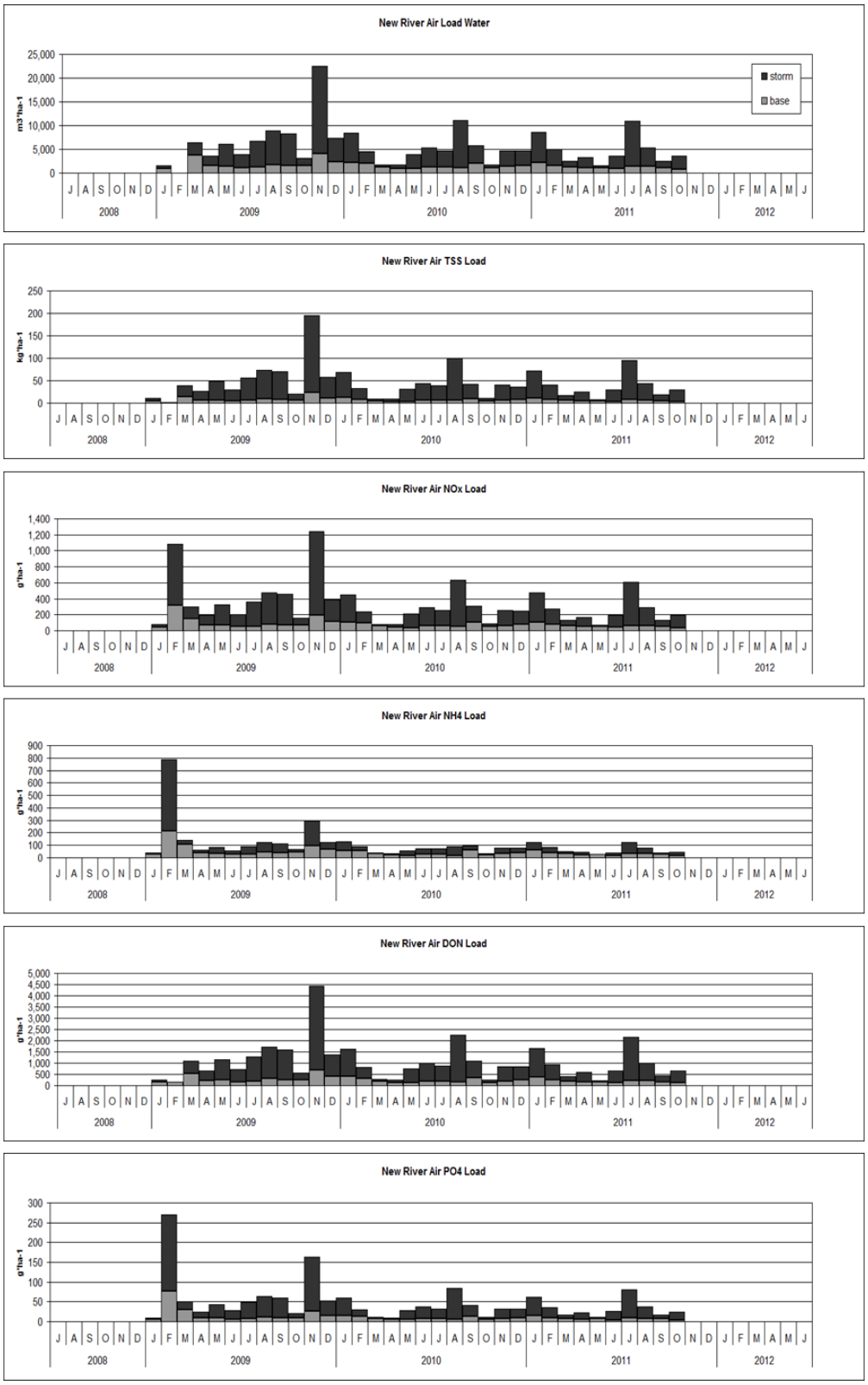

Figure 4-12. Monthly loading of water, total suspended solids (TSS), nitrate (NO_x), ammonium (NH_4), dissolved organic nitrogen (DON), and phosphate (PO_4) at New River Air Station.

Ratios of Concentrations and Species of Nitrogen

The ratios of concentrations of nitrogen to phosphorus, and the type of nutrient loaded (e.g., NO_3 versus NH_4) have implications for the ecological impacts for the receiving waters. Ratios of dissolved inorganic nitrogen to dissolved inorganic phosphorus (DIN:DIP) were generally lower in less developed creeks than more developed creeks (**Figure 4-13, panels a–j**). Camp Johnson was again an outlier with higher DIN:DIP than anticipated. As previously described, local conditions (proximity of a resurfaced gravel road) and the ephemeral nature of Camp Johnson Creek likely contributed to the elevated NH_4 concentrations that elevated the DIN:DIP. Courthouse Bay Creek was the other ephemeral creek and also had higher than anticipated DIN:DIP. Including all 10 creeks there was a significant binomial relationship (r^2=0.4, **Figure 4-14, panel b**) between annual average DIN:DIP and percent watershed imperviousness. When the two ephemeral streams were excluded from the analysis, the relationship was much stronger (r^2=0.92, **Figure 4-14, panel c**). The combined effect of increased DIN:DIP ratio and the previously described increase in nutrient loading with increased imperviousness could result in synergistic stimulation of productivity in this nitrogen-limited system. A final factor that must be considered in gauging the holistic impact of increased watershed imperviousness on ecosystem function is alteration of the forms of nitrogen loaded to receiving waters. **Figure 4-15** demonstrates that as imperviousness increases, both the amount of nitrogen that is highly biologically available (NO_3 and NH_4) and the proportion of highly available nitrogen increase. These results underscore the need to consider factors beyond magnitude of loading when assessing impacts of watershed alteration in coastal ecosystems.

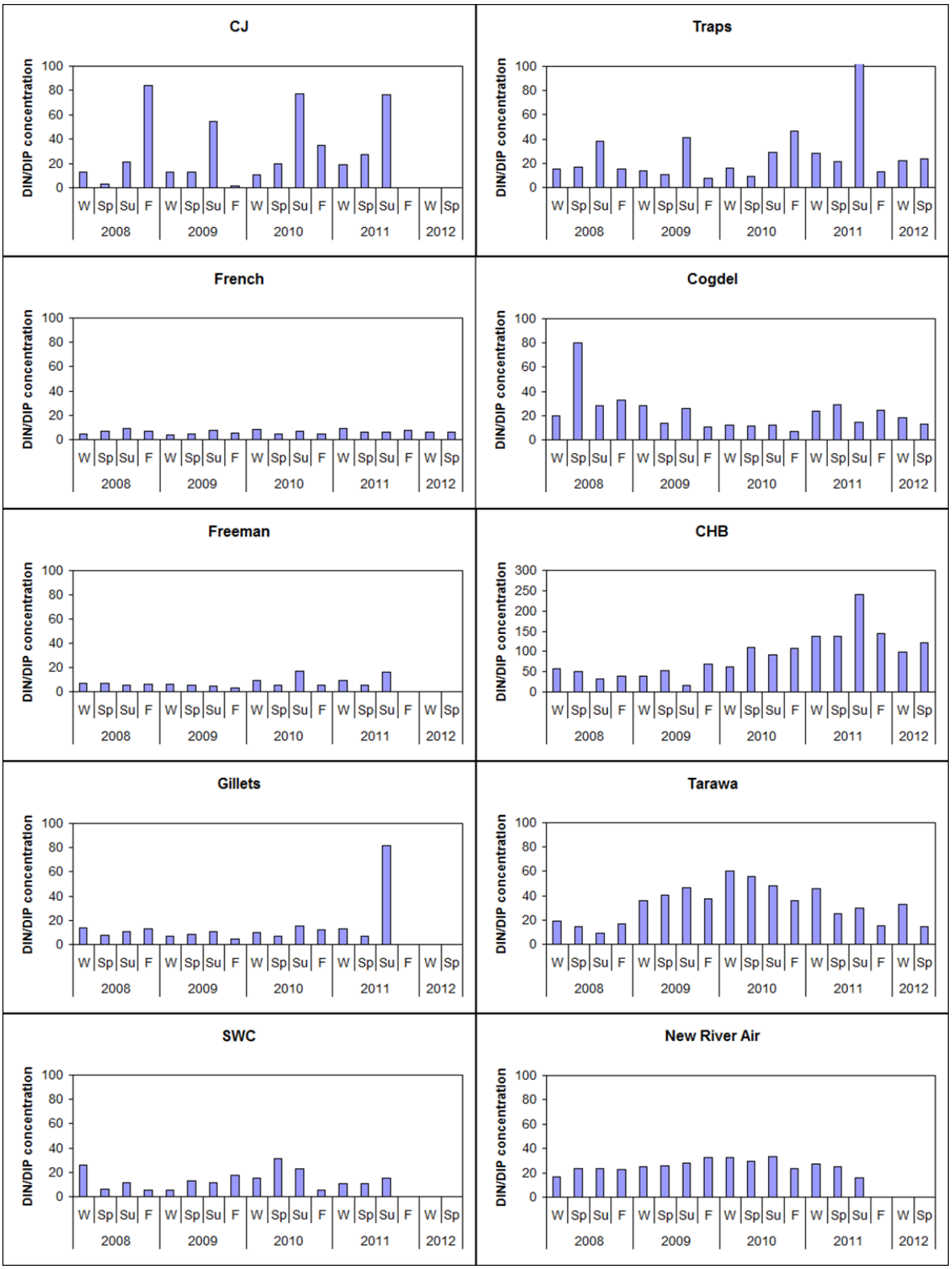

Figure 4-13. Seasonal DIN:DIP concentrations at sites from lowest watershed imperviousness to highest included Camp Johnson (CJ), French, Freeman, Gilletts, Southwest Creek (SWC), Traps, Cogdel, Courthouse Bay (CHB), Tarawa, and New River Air Station.

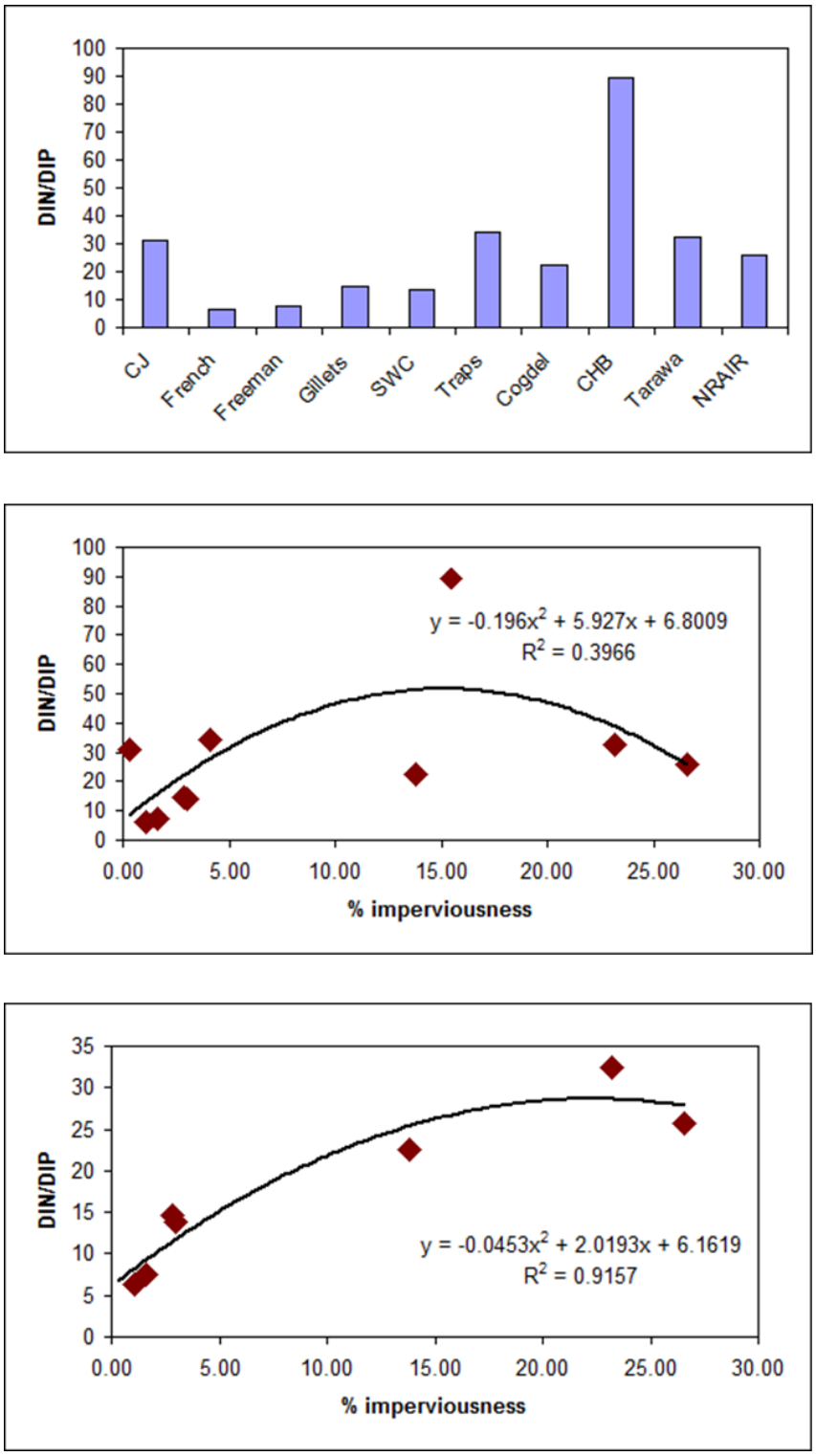

Figure 4-14. (Top Panel) DIN:DIP concentrations at 10 sites from lowest watershed imperviousness to highest included Camp Johnson (CJ), French, Freeman, Gillets, Southwest Creek (SWC), Traps, Cogdel, Courthouse Bay (CHB), Tarawa, and New River Air Station (NRAIR). (Middle Panel) Quadratic relationship beteen 10 sties and (bottom panel) eight sites showing mean DIN:DIP and percent watershed imperviousness.

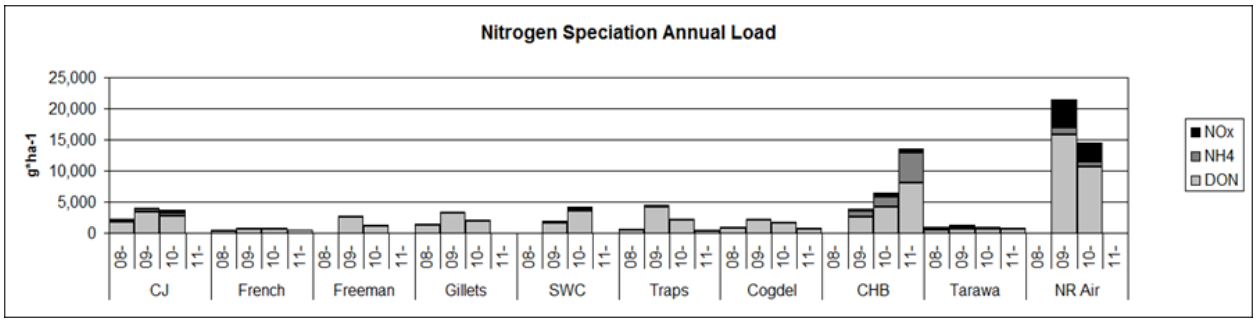

Figure 4-15. Species of nitrogen loaded from each watershed in each year in grams per hectare per year.

Imperviousness increases from left to right.

Creek TSS Loading Relationship with Wetland Demand for Sediment

At Courthouse Bay, Freeman, French, Gillets, and Traps sites, the amount of sediment supplied by creek loading was less than 1% of the annual demand (**Table 4-2**) for all sea level rise scenarios. This indicates that wetlands in these watersheds are receiving their sediment from different sources. There were some scenarios in which the creek was potentially an important source of sediment for wetlands in its watershed. For example, in the4 mm/y sea level rise scenario, Cogdel Creek loading of TSS supplied more sediment than its wetlands required. Note that Tarawa Creek does not have any wetlands in its watershed, and thus all of its sediment input can be considered a surplus of sediment loading. Excessive sediment in an ecosystem could have detrimental effects on water quality and habitat.

Table 4-2. Percentages of wetland demand for sediment provided by stream TSS under hypothetical sea level rise scenarios.

No wetlands were present in the Tarawa Creek watershed.

	4 mm/y	10 mm/y	15 mm/y
Courthouse Bay	0.249	0.100	0.066
Cogdel	106.793	42.717	28.482
Freeman	0.241	0.096	0.064
French	0.784	0.313	0.209
Gillets	0.758	0.303	0.202
Tarawa	Not applicable	Not applicable	Not applicable
Traps	0.274	0.110	0.073

Sea level rise and insufficient sediment supply could result in a drastic loss of wetlands. This situation is seen in many of Louisiana's coastal wetlands where sea level rise, rapid subsidence, and an anthropogenically reduced sediment supply combine to produce a much higher rate of relative sea level rise resulting in a large-scale loss of coastal wetlands (Morris et al., 2002). Each watershed must be assessed individually to create the best management plan, because the sediment dynamics are complex and variable.

Assessment of Trends in the Data

Assessment of Monitoring Design

The placement and number of creek sampling sites was sufficient to accomplish the monitoring objectives stated in this report. Data gathering through this project revealed generally very low loads of nutrients and modest loads of suspended solids. At the time of this work, much of the MCBCL had relatively low levels of imperviousness and most streams had large intact riparian buffers. Data in this report and in the *DCERP1 Final Research Report* (see Chapter 3 for Research Project AE-2) demonstrated a strong relationship between watershed imperviousness and loading of nutrients and suspended solids. The largest increases in loading were present in watersheds with 15% and greater impervious area. Because many of the streams were in watersheds with very low levels of imperviousness, we were able to reduce the number of stream sampling sites from 10 to five and not lose the ability to relate imperviousness to loading. Regression analyses of data sets with only five streams did not reveal reduced significance in the correlation of loading with impervious area in the watershed.

Assessment Seasonal and Annual Variability in the Data

There were general patterns in annual loading, with higher loads of all constituents in years with higher precipitation (shown in **Figures 4-3** through **4-12)**. Seasonal patterns in discharge and loading were generally higher water volumes and loading in winter and lower water volumes and loads in summer. Exceptions to this annual pattern included large events in summer months that elevated loads.

Recommendations for Future Monitoring

As previously described, the findings support refining future creek monitoring to include five rather than 10 sites. The demonstrable relationship between land use and loading of materials in creeks validates the use of stream headwaters as monitoring stations to indicator sites of cumulative impacts of land use on transport of material from land to water in coastal systems.

Conclusions and Implications for Future Research

Key Scientific Findings—Fundamental Cause-and-Effect Relationships

Connecting watershed development to loading and concentrations of nutrients in coastal streams is the key finding of this monitoring effort. Though loading rates were not generally high in the creeks monitored during this study, there was a clear cause and effect relationship between increased human activity in the watershed (with impervious cover as the proxy) and loading of nutrients and sediments to the estuary.

Findings Supportive of Current and Future Base Management Practices

At the time of this study, MCBCL had large areas of undeveloped land and this was reflected in the low levels of impervious cover in many of the study watersheds. Additionally, many of the creeks had large intact, forested buffers. Nutrient and TSS loading in this study was generally quite low in this project. Low loading per area of watershed is reflective of both sound

development practices and land management by MCBCL. As building has increased throughout this study and land use changes, there is the potential for enhanced loading of materials through MCBCL creeks, but data collected in this study indicate that MCBCL management has been very sound.

Findings with Implications for DCERP2

Monitoring results in DCERP1 support future focus on coastal headwater creeks in DCERP2. In DCERP1, we improved our understanding of the links between on land activities and nutrient and suspended solids loading in coastal creeks. In DCERP2, we will again focus on headwater creeks as sentinels and indicators of human impacts in coastal systems, but will shift the emphasis to carbon transport and transformation. DCERP1 also confirmed that critical climate factors such as storminess and patterns of precipitation have large impacts on coastal creek material transport. DCERP2 will further pursue assessments of likely impacts of changes in climate in the future.

Literature Cited

APHA (American Public Health Association). 1998. S*tandard Methods for the Examination of Water and Wastewater*, 20th Edition. American Public Health Association. 1,325 pages.

Corbett, D.R., J.P. Walsh, L. Cowart, S.R. Riggs, D.V. Ames, and S.J. Culver. 2008. Shoreline Change Within the Albemarle-Pamlico Estuarine System, North Carolina: A White Paper. East Carolina University, Greenville, NC. 16 pages. Available at http://www.ecu.edu/icsp/ICSP/Reports_files/EstuarineShorelineChangeDec2008.pdf.

Gordon, N.D., T.A. McMahon, B.L. Finlayson, C.J. Gippel, and R.J. Nathan. 2004. *Stream Hydrology: An Introduction for Ecologists*. Second Edition. John Wiley & Sons, Ltd: West Sussex, England.

Mallin, M.A., M.R. McIver, H.A. Wells, D.C. Parsons, and V.L. Johnson. 2005. Reversal of eutrophication following sewage treatment upgrades in the New River Estuary, North Carolina. *Estuaries 28*(5):750–760.

MCBCL (Marine Corps Base Camp Lejeune). 2006. *Integrated Natural Resources Management Plan (2007–2011)*. Marine Corps Base Camp Lejeune, Onslow County, NC.

Homer, C., J. Dewitz, J. Fry, M. Coan, N. Hossain, C. Larson, N. Herold, A. McKerrow, J.N. VanDriel, and J. Wickham. 2007. Completion of the 2001 National Land Cover Database for the Conterminous United States. *Photogrammetric Engineering and Remote Sensing*. *73*(4):337–341.

McMillan, S.K., M.F. Piehler, S.P. Thompson, and H.W. Paerl. 2010. Denitrification of nitrogen released from senescing algal biomass in coastal agricultural headwater streams. *Journal of Environmental Quality 39*:274–281.

Morris, J.T., P.V. Sundareshwar, C.T. Nietch, B. Kjerfve, and D.R. Cahoon. 2002. Responses of Coastal Wetlands to Rising Sea Level. *Ecology 83*(10):2869–2877.

Paerl, H.W. 1997. Coastal eutrophication and harmful algal blooms: Importance of atmospheric deposition and groundwater as “new” nitrogen and other nutrient sources. *Limnology and Oceanography 42*:1154–1165.

Schwartz, R. 2010. *Land Use Affects the Timing and Magnitude of Material Delivery to Headwater Streams in Coastal North Carolina*. Master’s Thesis, University of North Carolina Chapel Hill, Chapel Hill, NC. 80 pages.

Stevenson, J.C., L.G. Ward, and M.S. Kearney. 1988. Sediment transport and trapping in marsh systems: Implications of tidal flux studies. *Marine Geology 80*: 37–59.

Ward, R.C., and M. Robinson. 2000. *Principles of Hydrology*, 4th Edition. McGraw-Hill Publishing Company: Berkshire, England. 450 pages.

Chapter 5

New River Estuary—Water Column

SERDP Project Number: RC-1413
Aquatic/ Estuarine Module

Lead Researchers:
Dr. Hans Paerl
Dr. Richard Luettich
Dr. Nathan Hall
Dr. Ben Peierls
Anthony Whipple

University of North Carolina at Chapel Hill Institute of Marine Sciences
Morehead City, NC
E-mail: hans_paerl@unc.edu

Supporting Researcher:
Dr. Janelle Reynolds-Fleming
Seahorse Coastal Consulting
Morehead City, NC
E-mail: janelle.fleming@gmail.com

June 27, 2013

Final

This report was prepared under contract to the U.S. Department of Defense (DoD) Strategic Environmental Research and Development Program (SERDP). The publication of this report does not indicate endorsement by DoD, nor should the contents be construed as reflecting the official policy or position of DoD. References herein to any specific commercial product, process, or service by trade name, trademark, manufacturer, or otherwise, do not necessarily constitute or imply its endorsement, recommendation, or favoring by DoD.

Table of Contents

List of Acronyms 5-viii
Abstract 5-1
Objectives of the Monitoring Activity 5-1
Background 5-2
Materials and Methods 5-3
Monthly Discrete Sampling 5-4
Monthly Vertical Profiles 5-5
Autonomous Vertical Profilers 5-6
Autonomous vertical profilers 5-6
Current Measurements 5-6
Dataflow Transects 5-7
Freshwater Inputs and Flushing Time 5-8
Nutrients and Suspended Particulate Matter 5-8
Phytoplankton Biomass and Primary Productivity 5-9
Data Analyses and Statistical Approaches 5-9
Results and Discussion 5-9
Freshwater Inputs to the NRE 5-9
Tidal Flow and Estuarine Circulation 5-10
ADCIRC Model 5-15
Seasonality of Water Quality 5-24
Covariation Between Water Quality Parameters 5-26
Sediment Resuspension at the AVP Sites 5-30
Spatial Gradients of Salinity, Nutrients, Phytoplankton Biomass, and Organic Carbon 5-36
Evaluation of Main Stem Versus Tributary Effects on Water Quality 5-38
Frequency of Bottom Water Hypoxia 5-40
Assessment of Trends in the Data 5-44
Assessment of Monitoring Design 5-44
Assessment of Seasonal and Annual Variabilities in the Data 5-52
Recommendations for DCERP2 Monitoring 5-56
Conclusions and Implications for Future Research 5-57
Key Scientific Findings—Fundamental Cause-and-Effect Relationships 5-57
Findings Supportive of Current Base Management Practices 5-58

Findings with Implications for Future Base Management 5-58
Findings with Implications for DCERP2 5-58
Literature Cited 5-59
Appendix 5-A: Supporting Data 5-A-1
Appendix 5-B: List of Scientific Publications 5-B-1
Appendix 5-C: List of Students 5-C-1

List of Figures

5-1. Conceptual diagram of the linkages between external and internal processes that affect NRE water quality. 5-3

5-2. Map of the NRE study site and location of sampling stations. 5-5

5-3. Schematic diagram and photograph of the AVP at Morgan Bay. 5-6

5-4. Diagram of the Dataflow system used to gather high-resolution downstream transects of key water quality parameters. 5-7

5-5. Daily mean discharge of the New River at Gum Branch. 5-10

5-6. Mean annual discharge of the New River at Gum Branch. 5-10

5-7. Downstream and across channel depth profiles of current velocities at Marker 12 from June 10–14, 2008. 5-11

5-8. Long-term average depth profiles of along channel current velocities at Channel Marker 12, the Highway 172 bridge, Stones and Morgan Bays. 5-12

5-9. Downstream and across channel depth profiles of current velocities (cm/s) at the Highway 172 bridge from February 21–25, 2008. 5-13

5-10. Downstream and across channel depth profiles of current velocities (cm/s) at Stones Bay from September 17–21, 2009. 5-14

5-11. Downstream and across channel depth profiles of current velocities at Stones Bay from September 12–16, 2009. 5-15

5-12. Refined model grid of the NRE and Onslow Beach area showing bathymetry (feet below sea level) and grid nodes. 5-16

5-13. Tidal amplitude comparison between modeled (*x*-axes) and in situ (*y*-axes) water level at three locations: (A) AWAC, (B) Marker 12, and (C) the bridge. 5-17

5-14. Tidal phase comparison between Modeled (*x*-axes) and in situ (*y*-axes) water level at three locations: (A) AWAC, (B) Marker 12, and (C) the bridge. 5-18

5-15. Comparison of observed (DATA) and modeled (ADCIRC) tidal ellipses for six of the major diurnal and semi-diurnal tidal constituents at the Marker 12 location. 5-19

5-16. Comparison of observed (DATA) and modeled (ADCIRC) tidal ellipses for six of the major diurnal and semi-diurnal tidal constituents at the Morgan Bay location. 5-20

5-17. The NRE divisions delineated by red lines, and sample drogues (filled red, yellow, blue, and green, blue-green, and black circles) seeded in each section at the beginning of a model run. 5-21

5-18. The NRE divisions and sample drogues seeded in each section at the end of a model run (approximately 200 d after initial seeding). 5-22

5-19. Box and whisker plots of flushing time along the axis of the NRE calculated using the date-specific freshwater replacement method. 5-24

5-20. Time series of semi-hourly, average water column conditions from the AVP at Morgan Bay from June 14, 2008 through October 1, 2012. 5-25

5-21. Time series of semi-hourly, average water column conditions from the AVP at Stones Bay from June 14, 2008 through October 1, 2012. 5-26

5-22. Variance preserving Fourier power spectra of key water quality parameters from the semi-hourly AVP records from Stones and Morgan Bays. 5-29

5-23. Seasonality in the amplitude of the diel cycle of DO at Stones and Morgan Bays. 5-30

5-24. Wind direction and speed for Morgan and Stones Bays for 2008–2012. 5-32

5-25. Turbidity versus wind speed (A); wave height (B); and sheer stress (C). 5-33

5-26. Data from both the AVP and the ADCP taken from Stones Bay beginning October 16, 2009, extending into October 21, 2009. 5-35

5-27. Box and whisker plots of the along stream distribution of salinity, DIN, PO_4^{3-}, chl *a*, POC, and DOC. 5-37

5-28. Box and whisker plots of water quality indicators from the mid-channel Station 7 and Stations 6 and 8 at the mouths of Southwest and Northeast Creeks, respectively. 5-39

5-29. Histogram of bottom water temperatures from all data from Stations 1–8 and during moderate (less than 4 mg L^{-1} DO) and severe (less than 2 mg L^{-1}) bottom water hypoxia, *x*-axis labels are the centroids of 2°C bins. 5-41

5-30. Observed and modeled bottom water DO at the Morgan Bay AVP from June 2008 through November 2012. 5-43

5-31. Observed and modeled bottom water DO with stratification intensity at the Morgan Bay AVP from July through December 2009. 5-44

5-32. Map showing track lines of 44 Dataflow sampling transects in relation to the eight monthly monitoring stations in the NRE. 5-45

5-33. Influence of spatial sampling interval on the precision of estimates of the transect means for 44 Dataflow transects. 5-46

5-34. Influence of temporal sampling interval on the precision of estimates of the record means for four annual records from the AVPs at Stones and Morgan Bays. 5-48

5-35. Box and whisker plots of the relative standard error of record (Dataflow and AVP) means of key water quality parameters across a range of potential spatial and temporal sampling intervals. 5-50

5-36. Box and whisker plots of the slopes of the exponential decay of the variance of the mean transect evaluated at 4 km spatial resolution for the Dataflow (DF) transects and at 30 d temporal resolution for the Morgan Bay (MB-AVP) and Stones Bay (SB-AVP) AVP annual records. 5-52

5-37. Inter-annual variability of key water quality parameters pertaining to basic water chemistry, light and nutrient availability, phytoplankton biomass, and primary productivity. 5-53

5-38. Seasonality of key water quality parameters pertaining to basic water chemistry, light and nutrient availability, phytoplankton biomass, and primary productivity..... 5-56

List of Tables

5-1. Description of monitoring activities. 5-3

5-2. Percentage of drogues that leave their original seed box and leave the inlet for the seven different ADCIRC Model scenarios. 5-22

5-3. Average transit time in days of drogues that leave their original seed box (Out Box) and leave the inlet (To Inlet) for the seven different model scenarios..... 5-23

5-4. Results of Pearson's correlations for key water quality parameters from the AVPs at Stones and Morgan Bays..... 5-27

5-5. Results from Kruskal-Wallis comparisons of medians from Stations 6, 7, and 8 for basic water quality, nutrients, and phytoplankton indicators..... 5-39

5-6. Frequency of bottom water hypoxia by water year and by station with water depth and stratification intensity..... 5-40

5-7. Results from Kruskal-Wallis comparison of median values of 15 key water quality parameters from the NRE grouped by water-year and by season..... 5-54

List of Acronyms

°C	degrees Celsius
µg L^{-1}	micrograms per liter
µm	micrometer
µmol	micromole
µmol L^{-1}	micromoles per liter
ADCIRC	Advanced Circulation (Model)
ADCP	acoustic Doppler current profiler
AVP	autonomous vertical profiler
AWAC	acoustic wave and current
BMA	benthic microalgae
chl *a*	chlorophyll *a*
chl *b*	chlorophyll *b*
CDOM	chromophoric dissolved organic matter
cm	centimeter
cm s^{-1}	centimeter per second
CO_2	carbon dioxide
CTD	conductivity-temperature-depth (sensor)
d	day
DCERP	Defense Coastal/Estuarine Research Program
DCERP2	second cycle of the Defense Coastal/Estuarine Research Program
DIN	dissolved inorganic nitrogen, sum (NO_3^-, NO_2^-, and NH_4^+)
DO	dissolved oxygen
DOC	dissolved organic carbon
DoD	U.S. Department of Defense
DON	dissolved organic nitrogen
Hz	hertz
ICW	Intracoastal Waterway
K_d	light attenuation coefficient for photosynthetically active radiation
km	kilometer
km hr^{-1}	kilometers per hour
kPa	kilopascal
L	liter
m	meter
m h^{-1}	meters per hour
m^{-2} s^{-1}	square meters per second
m^{-3} s^{-1}	cubic meters per second
MCBCL	Marine Corps Base Camp Lejeune

mg L^{-1}	milligrams per liter
mL	milliliter
mm	millimeter
NH_4^+	ammonium
NO_2^-	nitrite
NO_3^-	nitrate
$NO_3^- + NO_2^-$	nitrate + nitrite
NRE	New River Estuary
PAR	photosynthetically active radiation
PN	particulate nitrogen
PO_4^{-3}	orthophosphate
POC	particulate organic carbon
PP	particulate phosphorus
SD	standard deviation
SERDP	Strategic Environmental Research and Development Program
SiO_3^{-2}	silicate
TDN	total dissolved nitrogen
TDP	total dissolved phosphorus
TSS	total suspended solids
UNC-IMS	University of North Carolina at Chapel Hill's Institute of Marine Sciences
USGS	U.S. Geological Survey
WEMo	Wave Exposure Model
YSI	Yellow Springs Instrument Inc.

[This page intentionally left blank.]

Abstract

Water quality, pelagic habitat condition, and trophic status as well as the natural and anthropogenic drivers of these indicators of ecological condition were monitored in the water column of the New River Estuary (NRE) over the period from fall 2007 through fall 2012. Conditions within the estuary were assessed by monthly transect surveys and continuous autonomous vertical profiling systems. Physical drivers of circulation were assessed by acoustic Doppler current profilers deployed throughout the estuary and by flow meters at the head of the estuary. Additional sampling was performed within the upstream, freshwater reaches of the New River to quantify riverine material fluxes to the estuary. Results were used to evaluate the roles of natural and anthropogenic stressors on water quality and habitat condition within the estuary to assess compatibility of Marine Corps Base Camp Lejeune activities with desirable water, sediment, and habitat quality. Analyses of the monitoring data indicate that physical processes such as riverine discharge, stratification, wind stress, and sediment resuspension are dominant drivers of variability in water quality and habitat condition. Bottom water hypoxia was closely linked to temperature and stratification with no apparent relationship to algal blooms, which may have resulted from anthropogenic nutrient loading. Periods of high algal biomass were linked to optimal levels of river flow, which provided enough nutrients for phytoplankton biomass development, but also sufficient residence time within the estuary for growth to occur. Similarly, water column turbidity was strongly linked to wind-induced sediment resuspension events, which were then advected from initial sites of resuspension by tidal and wind driven flow. Although the short-term variability in these indicators of ecological condition were strongly linked to physical factors that are not under human control, this does not indicate a lack of anthropogenic effects on water quality. Anthropogenic effects such as the accumulated impact of changes in land use within the basin are likely to form a slower moving trend that would not be captured within a short 5-year study period. Data collected from this monitoring program will serve as a comprehensive baseline against which the longer-term anthropogenic trends in water quality and ecological condition may be assessed. Characterization of the temporal and spatial scales of variability has provided guidance for the design and implementation of future research and monitoring efforts for the NRE and similar estuarine systems. Monitoring data were additionally used to parameterize a mechanistic Estuarine Simulation Model and a probabilistic Bayesian Belief Network model for water quality in the NRE and to provide the ecological framework for the other research components of the Aquatic/Estuarine and Coastal Wetlands Modules.

Keywords: Carbon, dissolved oxygen, estuary, nitrogen, phosphorus, residence time, riverine discharge, salinity, tides, turbidity

Objectives of the Monitoring Activity

The main objective of this monitoring activity was to monitor the input, distribution, use, cycling, and fate of nutrients and sediments and other physico-chemical parameters (e.g., dissolved oxygen, pH, salinity) affecting the productivity, trophic state, water quality, and habitat condition of the NRE. Sampling locations were distributed along the downstream axis of the estuary to assess the variability within the estuarine salinity zones, tidal, and mixing regimes. The sampling design allowed us to examine the impacts of terrestrial, atmospheric, coastal

wetlands, and oceanic exchanges of materials (sediment, nutrients, etc.) on the ecosystem and to evaluate the effects of specific military activities (i.e., sedimentation, nutrient releases, and discharge events) versus off-base human and natural (climatic) drivers of ecological condition. This monitoring activity was designed to evaluate the short- and long-term effects of these drivers on the structure, function, and sustainability of the NRE in a regime of climatic variability and served as a critical source of data for supporting the Aquatic/Estuarine Module research projects and modeling activities.

The Aquatic/Estuarine Module's water column monitoring program, which is summarized in **Table 5-1**, is designed to achieve multiple goals. These goals include improving the understanding of the physical, chemical, and biological processes and interactions that drive water, sediment, and habitat quality; supporting the research components; and helping to differentiate the magnitudes and effects of natural and anthropogenic ecosystem stressors. Differentiating the stressors includes the consideration of extreme weather-related events, such as hurricanes, nor'easters, floods, and droughts, which have thus far been shown to be very important drivers whose impacts vary greatly between years. Additional goals include providing information for designing and implementing a long-term monitoring program that ensures compatibility of MCBCL activities with desirable estuarine water, sediment, and habitat quality and facilitating the conservation of regional natural resources for ecosystem, recreational, and economic benefits. The monitoring component is adaptive and will be adjusted in response to climatic and anthropogenically driven changes in the NRE watershed and new information gained from research components and modeling, as well as the availability of more effective and efficient indicators and methods for their deployment.

Background

Estuaries integrate inputs from terrestrial, freshwater, oceanic, and atmospheric systems (Day and Kemp, 1989; Hobbie, 2000; Valiela et al., 1997), and the accurate assessment and management of estuaries necessitates consideration of their connections to, and interactions with, these other systems. Many estuaries also exist in regions of rapidly expanding and diversifying human activity (Boesch et al., 2001; Cloern, 2001; Nixon, 1995). In the context of the Marine Corps Base Camp Lejeune (MCBCL) region, the Aquatic/Estuarine Module examined the tidal reach of the New River Estuary (NRE) from near Jacksonville, NC, to the tidal inlet at Onslow Bay. Understanding and sustaining the function of the NRE cannot occur without quantifying and distinguishing natural processes from human-influenced watershed- and airshed-based impacts, as well as human activities that occur in the estuary (Boesch et al., 2001; Malone et al., 1999; Nixon, 1995; Paerl, 1997; see **Figure 5-1**). Furthermore, the effects of climatic variability, including acute or episodic events (e.g., tropical cyclones, floods, droughts) and longer term trends (e.g., warming, precipitation patterns), on estuarine structure and function must be characterized and quantified to understand and take into consideration the interactive and potentially confounding impacts of climate (change) on water quality and habitat condition (Cloern and Jassby, 2010; Kennish and Paerl, 2010; Paerl et al., 2010). Five years of water quality monitoring on the NRE demonstrated significant, and at times, dominant effects that climate events and change can have on the nutrient inputs, water quality, trophic state, overall ecological condition, resourcefulness, utility (for military training, commercial, and recreational purposes), and sustainability of the NRE. Fortunately, the Aquatic/Estuarine Module monitoring design was able to capture the level of complexity and variability in biogeochemical and trophic

responses needed to assess ecological condition and change of the NRE; only long-term monitoring and modeling will reveal the full extent of anthropogenic and climatically induced perturbations and changes impacting this system. The Aquatic/Estuarine Module's monitoring activities were closely coupled to and provided critical baseline data for the research activities within this module (see **Figure 5-1** and **Table 5-1**). Additionally, coordination and information exchange occurred in conjunction with the monitoring and research activities for the Coastal Wetlands, Atmospheric, Terrestrial, and Coastal Barrier Modules.

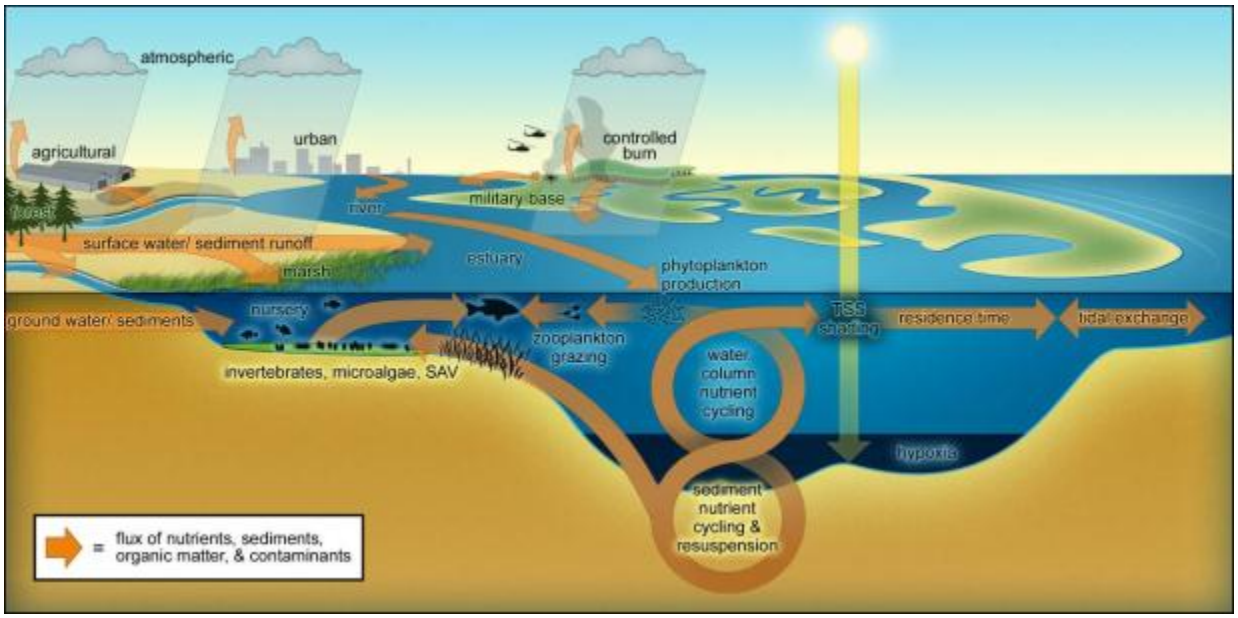

Figure 5-1. Conceptual diagram of the linkages between external and internal processes that affect NRE water quality.

Materials and Methods

A multi-faceted monitoring program provided key information on water quality, biogeochemistry, and ecosystem function within the NRE (**Table 5-1**). The four components of the monitoring effort were designed to capture the full range of temporal and spatial variability inherent to dynamic estuarine systems.

Table 5-1. Description of monitoring activities.

Monitoring Activity	Variable	Spatial Scale	Temporal Scale
Monthly discrete sampling	Nutrients, phytoplankton biomass and primary production, phytoplankton community composition, suspended sediments, particulate carbon, chromophoric dissolved organic matter	Surface (0.2 m) and bottom water (0.5 m above bottom) samples from 8 stations from Highway 17 to the Intracoastal Waterway Additional samples from U.S. Geological Survey gaging stations	Year round, monthly

(continued)

Table 5-1. Description of monitoring activities. (continued)

Monitoring Activity	Variable	Spatial Scale	Temporal Scale
Monthly vertical profiles	Depth profiles of temperature, salinity, dissolved oxygen, pH, turbidity, chlorophyll (via in vivo fluorescence), photosynthetically active radiation	8 stations, profiles conducted with 0.5 m vertical resolution	Year round, monthly, coincident with discrete sampling
Dataflow transects	Surface water transects of temperature, salinity, dissolved oxygen, pH, turbidity, chlorophyll (via in vivo fluorescence)	Near Highway 17 to the Intracoastal Waterway, 10 m spatial resolution	Year round, monthly, coincident with discrete sampling
Autonomous vertical profilers	Depth profiles of temperature, salinity, dissolved oxygen, pH, turbidity, chlorophyll(via in vivo fluorescence) and measurements of wind speed and direction	Profiles from Stones Bay and Morgan Bay sites with 10-cm depth resolution	Year round, 2 profiles per hour

Monthly Discrete Sampling

A transect of eight sampling stations (Stations 1–8 in **Figure 5-2**) were visited monthly using a 25-foot Parker research vessel for collection of water samples from the surface (0.2 m) and bottom (0.5 m above the bottom) using a non-destructive diaphragm pump. Sample collection occurred during the hours of 0800 through 1300. Water samples were dispensed into pre-cleaned 4 L polyethylene bottles and maintained under dark, in situ temperature conditions by placing them in coolers until samples were delivered to the laboratory at the University of North Carolina at Chapel Hill's Institute of Marine Sciences (UNC-IMS) by approximately 1500. Samples were processed immediately upon delivery to the laboratory for measurements of nutrients, phytoplankton biomass, suspended sediments, and particulate organic matter (see the Methods section below).

In addition to the eight monthly sampling stations between Highway 17 and the Intracoastal Waterway (ICW), additional sampling efforts were conducted upstream of Highway 17 by the U.S. Geological Survey (USGS) and by the sampling efforts of DCERP Research Project AE-3. Surface water grab samples were collected with biweekly to monthly frequency into pre-cleaned polyethylene bottles at two USGS gaging stations that continuously monitor water level, temperature, salinity, and flow velocity. Gaging Station Number 0209303205 (**Figure 5-2**) is at the head of the NRE near Jacksonville, NC. Gaging Station Number 02093000 near Gum Branch is the only gaging station along the freshwater reaches of the New River. Discrete sampling at Gum Branch occurred throughout the study period, but sampling at Gaging Station Number 020903205 began April 2008. Starting in November 2010, additional samples were collected near Wilson Bay and upstream of the old Highway 17 bridge. Collectively, these upstream samples collected by staff at USGS and NC Cooperative Extension Service provided data on the loading of nutrients, sediments, and phytoplankton biomass to the estuary and aided in elucidating processes that occurred within the freshwater to brackish water transition zone, a

region of intense chemical and biological activities within many estuaries (Boynton and Kemp 1985; Cloern, 1999; Fisher et al., 1988; Paerl et al., 1995 and 2010).

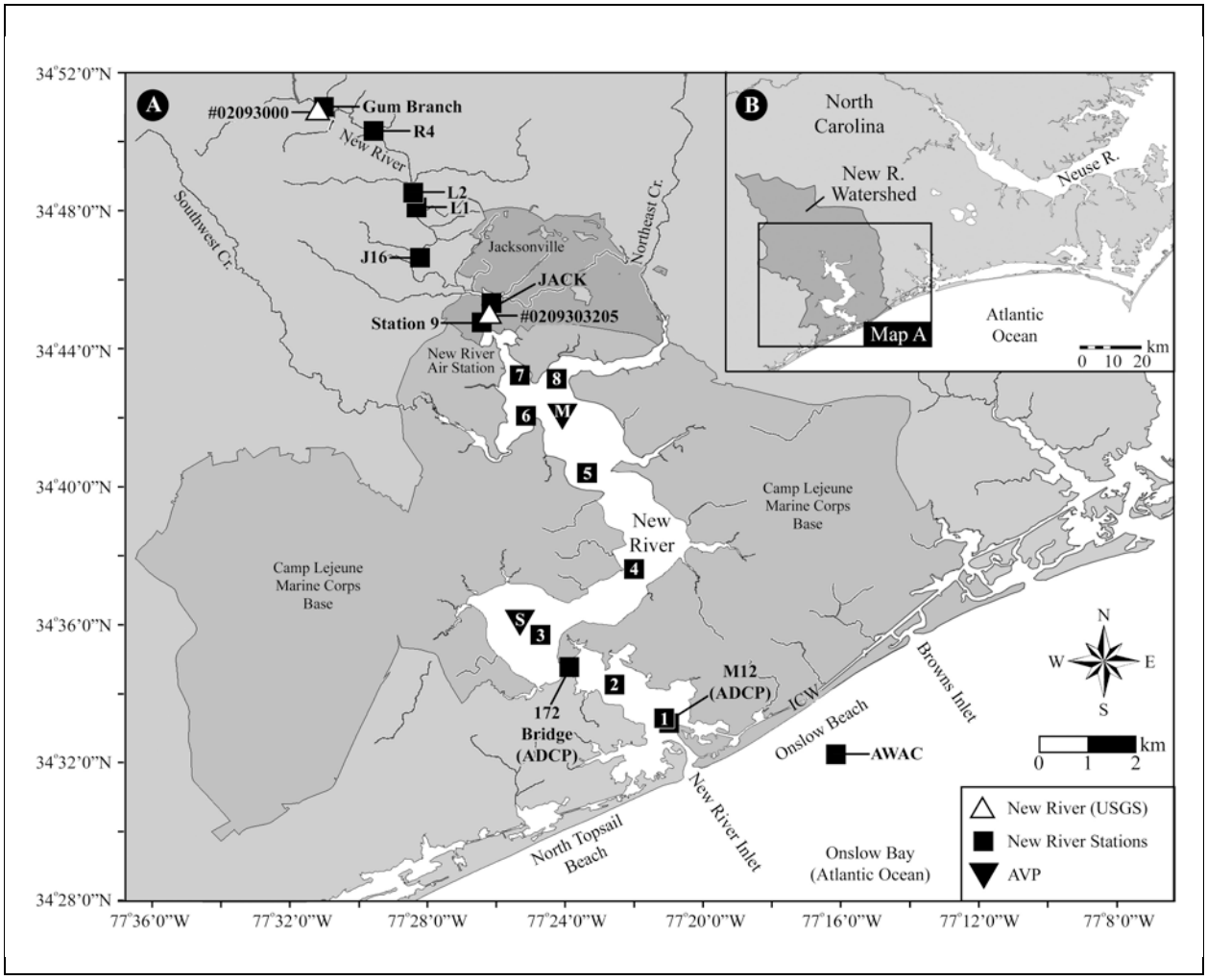

Figure 5-2. Map of the NRE study site and location of sampling stations.

Monthly Vertical Profiles

Coincident with monthly discrete sample collection, vertical profiles of key water quality parameters were collected from each of the eight stations using a Yellow Springs Instrument Inc. (YSI) 6600 multiparameter datasonde coupled to a LI-COR 2π photosynthetically active radiation (PAR) sensor. Temperature, salinity, pH, dissolved oxygen (DO), turbidity, chlorophyll a (chl *a*: by in vivo fluorescence), and PAR were measured at 0.5 m–depth intervals throughout the water column. The *in vivo* fluorometer actually measures the sum of chlorophyll types a, b, c1, c2, and c3. However, chlorophyll a dominates this sum (Hall et al., 2012). Therefore, hereafter in vivo fluorescence measurements are described in terms of chlorophyll *a*. YSI instruments were calibrated prior to each monthly monitoring cruise. PAR attenuation coefficients (K_d) were calculated as the slope of the natural log of PAR versus depth according to Beer's law.

Autonomous Vertical Profilers

Autonomous vertical profilers (AVPs) were deployed from June 2008 through October 2012 in central Stones Bay at Station 3 (see **Figure 5-2**), and in Morgan Bay upstream of Station 5 (**Figure 5-2**) and were used to continuously monitor key water quality parameters. The AVPs consist of a moored floating platform housing a computer controlled winch mechanism that lowers and raises a YSI Model 6600 multiparameter water quality datasonde at programmable time intervals (**Figure 5-2**) (Reynolds-Fleming et al., 2002). Winch speed and sampling frequency of the AVP system and datasonde were configured to produce full water column profiles of temperature, salinity, DO concentration, chl concentration (by fluorescence), and turbidity every 30 minutes and achieve vertical depth resolution of approximately 10 cm. An anemometer (RM Young) affixed to the mast of the AVP measured six minute averages of wind speed and direction every 30 minutes (**Figure 5-3**). Data were stored locally on the AVP computers, and telemetered back to the laboratory each night. Datasondes were exchanged with freshly cleaned and calibrated datasondes as necessary but at least on a monthly basis.

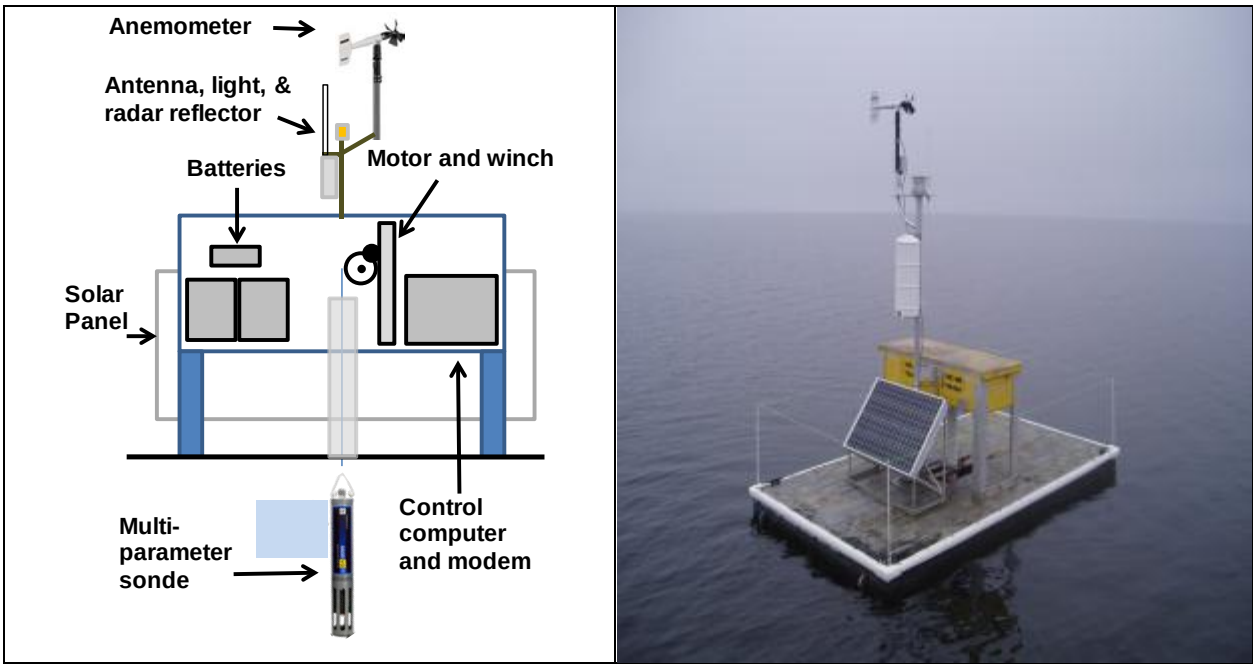

Figure 5-3. Schematic diagram and photograph of the AVP at Morgan Bay.

Current Measurements

Teledyne RD Instrument's acoustic Doppler current profilers (ADCPs) were deployed throughout the NRE to understand current flows and tidal extent. Two ADCPS were deployed by Marker 12 and the Highway 172 bridge from late-February to early-July 2009. These ADCPs were attached to steel frames that rested on the sediment surface with the ADCP looking upward to make full water column profiles of water velocity minus a 1-m blanking between the instrument and sediment surface. Also attached to the steel frames were conductivity-temperature-depth (CTD) sensors, which provided concomitant salinity, temperature, and water depth data with the ADCP current measurements. Two ADCPS were also deployed in close proximity to the AVPs in Stones and Morgan Bays from mid-July to mid-December 2009. These

ADCPs were deployed flush to the estuary floor to maximize the full vertical sampling capability at these shallow stations and the AVPs collected coincidental temperature, salinity, and depth measurements. For all deployments, the ADCPs were programmed in fast ping-rate mode 12 using 20 pings per ensemble and collected profiles in 10-cm bins every 6 minutes yielding a standard deviation in velocity measurements of 1.27 cm s^{-1}.

Current velocity and water level data were analyzed to understand the tidal influence on circulation within the NRE. Harmonic analyses were performed to extract the dominant tidal constituents from the velocity and depth records using T-tide run in MATLAB (Pawlowicz et al., 2002). These measurements of tidal amplitude and phase were then used to validate the high-resolution Advanced Circulation (ADCIRC) Model of the NRE region.

Dataflow Transects

Transects of key water quality parameters were produced for surface waters of the NRE using a Dataflow system (see Madden and Day, 1992) shown in **Figure 5-4**. Use of the Dataflow system commenced in February 2009 and was used coincidentally with monthly sampling efforts to expand the spatial resolution of the downstream transect produced by the eight discrete sampling stations. While the vessel is underway, surface waters enter the Dataflow system through a through-hull fitting in the bottom of a research vessel (Parker 25). Water is then pumped through a debubbler into a flow chamber attached to a YSI 6600 multiparameter water quality datasonde, which measures salinity, temperature, DO, turbidity, pH, and chl *a* (via in vivo fluorescence). With a 0.5-Hz sampling frequency, the spatial resolution is approximately 10 m at a normal forward speed of approximately 20 km hr^{-1}. Dataflow datasondes were calibrated prior to each transect.

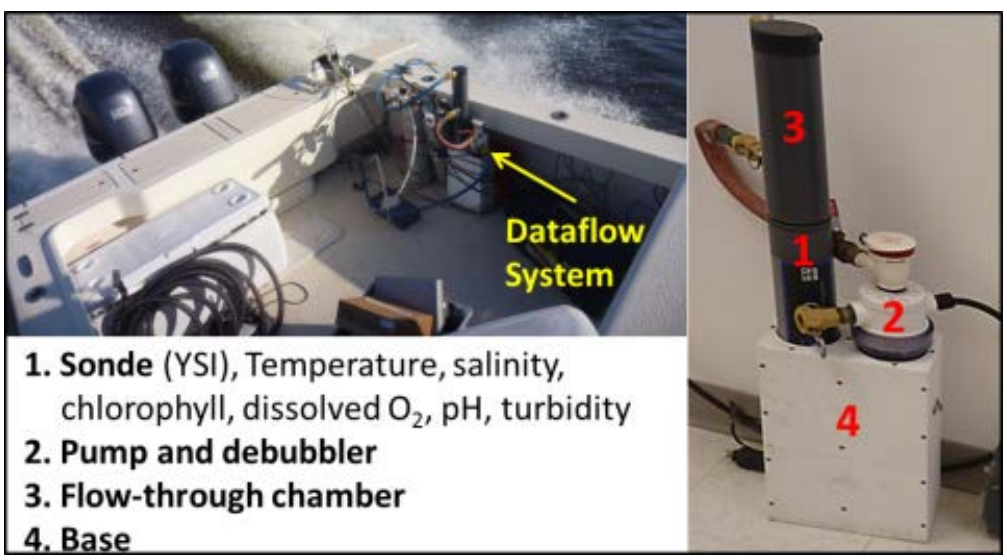

Figure 5-4. Diagram of the Dataflow system used to gather high-resolution downstream transects of key water quality parameters.

Freshwater Inputs and Flushing Time

Freshwater discharge to the NRE was continuously quantified by the USGS near Gum Branch (**Figure 5-2**; USGS Gaging Station Number 02093000). Approximately 78% of the watershed of the NRE is ungaged (Ensign et al., 2004). Ungaged freshwater inputs were estimated by multiplying the gauged freshwater discharge by the ratio of ungaged: gaged watershed area, exclusive of the estuary water surface (Ensign et al., 2004).

Flushing time was calculated using the date-specific freshwater replacement method (Alber and Sheldon, 1999). Flushing time is the amount of time necessary for the combination of riverine discharge and seawater inflows to replace the volume of an estuary or estuarine segment (Sheldon and Alber, 2006). The date-specific version of this traditional measure of transport time scale was chosen because it accounts for changing river flow conditions and the time lags between river gage and downstream locations (Alber and Sheldon, 1999). Flushing time, as calculated here, is also correctly interpreted as the average age of freshwater within an estuary (Sheldon and Alber, 2006). This interpretation is utilized to provide time scales for the biological transformation of riverine nutrient loads into phytoplankton biomass as freshwater is advected and mixed downstream within the NRE.

The estuary was divided into nine segments encompassing sampling Stations 1–8 and the USGS station near Jacksonville (Gaging Station Number 0209303205; **Figure 5-2**). Volumes for each segment were estimated using raster bathymetry data from the National Geophysical Data Center's Coastal Relief Model according to methods detailed by Ensign et al. (2004). Salinity of each segment was taken as the vertically averaged salinity of the monthly profiles at each of the eight monthly sampling stations. For the most upstream segment, encompassing the USGS Gaging Station Number 0209303205, salinity at the approximately 1-m instrument depth was assumed representative of the entire water column. The flushing time for each segment was calculated using the cumulative freshwater volume upstream of the downstream boundary of each segment, and represents the average time freshwater spent upstream of each segment (i.e., average freshwater age within the estuary). Calculating the cumulative flushing times from the head to the exit of the estuary in this manner allows use of the discretely sampled snapshots of phytoplankton biomass and nutrient concentrations to reconstruct the time course of phytoplankton biomass development and nutrient draw down during downstream transport within the estuary.

Nutrients and Suspended Particulate Matter

Nutrient analyses were conducted on water collected from the eight monthly estuarine stations and from the two USGS gaging stations. All water samples were gently filtered (less than 25 kPa) through 25 mm in diameter Whatman GF/F glass fiber filters (0.7 µm nominal pore size). Total dissolved nitrogen (TDN), nitrate (NO_3^- + nitrite [NO_2^-], labeled as NO_3^-), ammonium (NH_4^+), orthophosphate (PO_4^{-3}), and silicate (SiO_3^{-2}) concentrations were determined using colorimetric flow injection analyses (Lachat QuickChem 8000, Lachat Instruments, Milwaukee, WI) and standard protocols (Lachat QuikChem methods 31-107-04-3-B, 31-107-04-1-C, 31-107-06-1-A, and 31-115-01-3-C, respectively). Mean detection limits for TDN, NO_3^-, NH_4^+, PO_4^{-3}, and SiO_3^{-2} were 2.33, 0.03, 0.22, 0.03, and 0.53 µmol L^{-1}, respectively.

Concentrations of chromophoric dissolved organic matter (CDOM), a key determinant of light attenuation, were measured at the eight monthly estuarine stations fluorometrically according to methods detailed in Lunetta et al. (2009) and are expressed as quinine sulfate equivalents (µg L^{-1}). Water samples were vacuum filtered (less than 25 kPa) using pre-combusted Whatman glass fiber filters and the filtrate was stored in scintillation vials in the dark at 4°C until fluorometric analysis using a Turner Designs TD-700 fluorometer. Total suspended solids (TSS) were measured according to Standard Methods 2540 D (APHA, 1998): water samples were filtered on pre-rinsed, pre-dried, tared Whatman glass fiber filters. Filters were dried at 105°C and then weighed using a calibrated Mettler Toledo AB-S analytical balance. Solids concentration is the difference in filter weights before and after filtration divided by volume of water filtered.

Phytoplankton Biomass and Primary Productivity

Chl *a*, a common measure of phytoplankton biomass, was determined from all water samples collected at the routine monthly transect stations and from the two USGS gaging stations. (**Figure 5-2**). Fifty-milliliter aliquots were filtered onto 25 mm diameter Whatman GF/F glass fiber filters. Storage, extraction, and fluorometric analyses follow those described by Wetz et al. (2011).

Primary productivity was measured via the in situ ^{14}C method (Paerl, 2002) for surface waters from the eight monthly sampling stations from the hours of approximately 0900 to 1300 on the day following sample collection. Water samples were maintained overnight and incubations were performed under ambient light and temperature conditions in an outdoor pond at the UNC-IMS with circulating seawater (Mallin and Paerl, 1992). Light conditions associated with vertical mixing were simulated using a field light simulator (Mallin and Paerl, 1992). Light availability was measured throughout each incubation period with a LI-COR 2π PAR meter. The average PAR flux during the incubations was 234 µmol photons m^{-2} s^{-1} (standard deviation [SD]=94). Light-dark ^{14}C assay methods followed those described in Paerl (2002) with the exception that activity of samples was measured on a Beckman Coulter LS 6500 liquid scintillation counter and dissolved inorganic carbon concentration was measured on a Shimadzu total organic carbon analyzer (TOC-5000A).

Data Analyses and Statistical Approaches

A wide variety of data analyses and statistical procedures were used to explore spatial and temporal variability and interrelationships between water quality parameters and their drivers. Analysis and statistical methods are described in detail within each section followed by the results of the analyses.

Results and Discussion

Freshwater Inputs to the NRE

The New River dominates freshwater inputs to the NRE and freshwater contributions from smaller tributaries generally follow similar temporal patterns (Ensign et al., 2004; Peierls et al., 2012). New River discharge at the USGS Gum Branch gaging station varied widely over the

study period, spanning greater than three orders of magnitude from approximately 0.1 to 135 $m^3 s^{-1}$ (**Figure 5-5**). The extreme level of stream flow variability represents nearly the full range of conditions captured in the long-term discharge record that goes back to 1949 (Hall et al., 2012). Despite the occurrence of very high flows associated with tropical storms and nor'easters, overall the 5-year study period was characterized by drought conditions with annual water-year mean discharge below the long-term average (**Figure 5-6**). Water years 2008 and 2009 were the driest and third driest water years on record, respectively (**Figure 5-6**). Only water-year 2010 had above-average discharge (**Figure 5-6**), and this was largely due to the flood conditions that followed passage of the remnants of Tropical Storm Nicole (**Figure 5-5**).

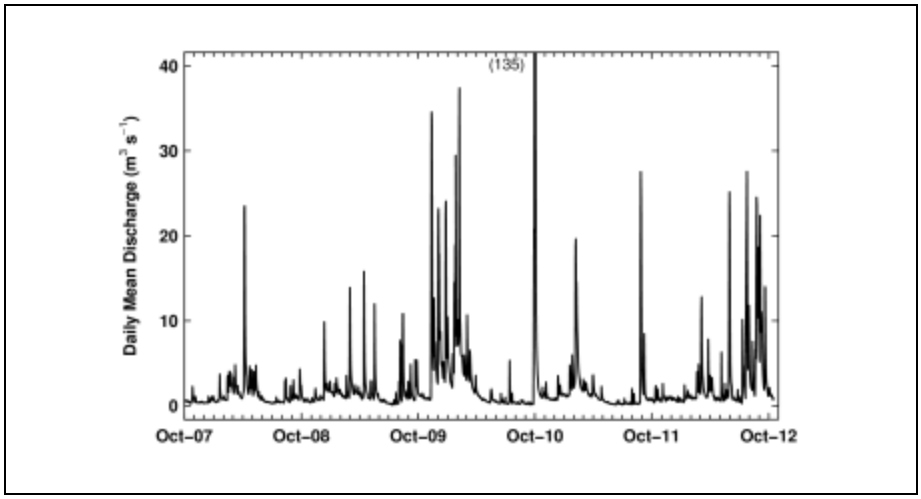

Figure 5-5. Daily mean discharge of the New River at Gum Branch.

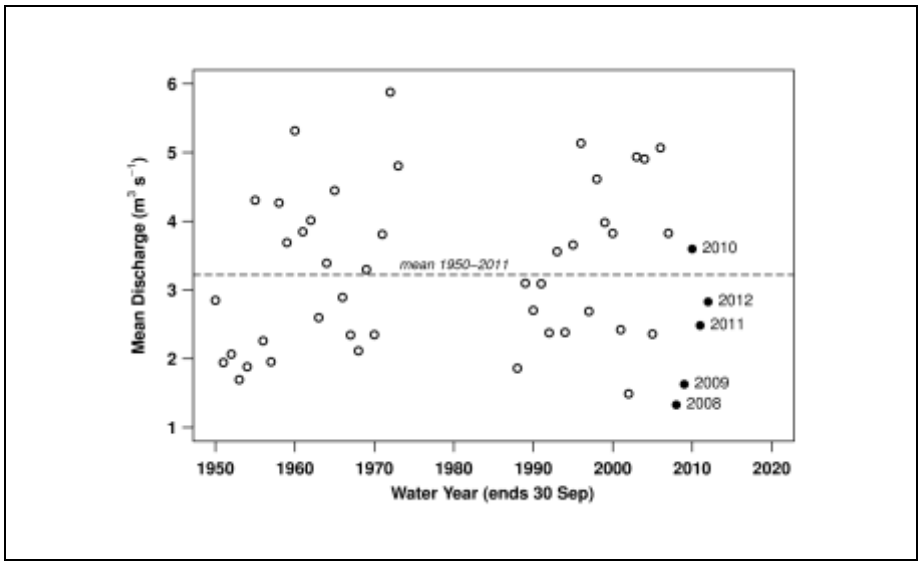

Figure 5-6. Mean annual discharge of the New River at Gum Branch.

Tidal Flow and Estuarine Circulation

The velocity data from the ADCP deployments at four sites along the main axis of the NRE indicated the extent of the influences of tidal and gravitational flows within the NRE. Tidal

variability in flows was greater nearer the inlet, while riverine discharge and wind were greater influences on circulation at upstream locations. Flows at Marker 12 are very tidally driven (**Figure 5-7**) with greater than 90% of the variability in the flow due to the dominant tidal constituents. At Marker 12, flows were vertically uniform upstream during the flood tide with maximum flow speeds of 1.9 m s^{-1} and exhibited vertical structure downstream during the ebb tide with maximum flow speeds of 2.3 m s^{-1} (**Figure 5-7**). The vertical structure seen during the ebb tide may in part have been due to the influence of the ICW and the location of the ADCP. Long-term average flows indicate a downstream preference between 5–10 cm s^{-1} with stronger downstream flows at the surface and reduced upstream flows at the bottom (**Figure 5-8**).

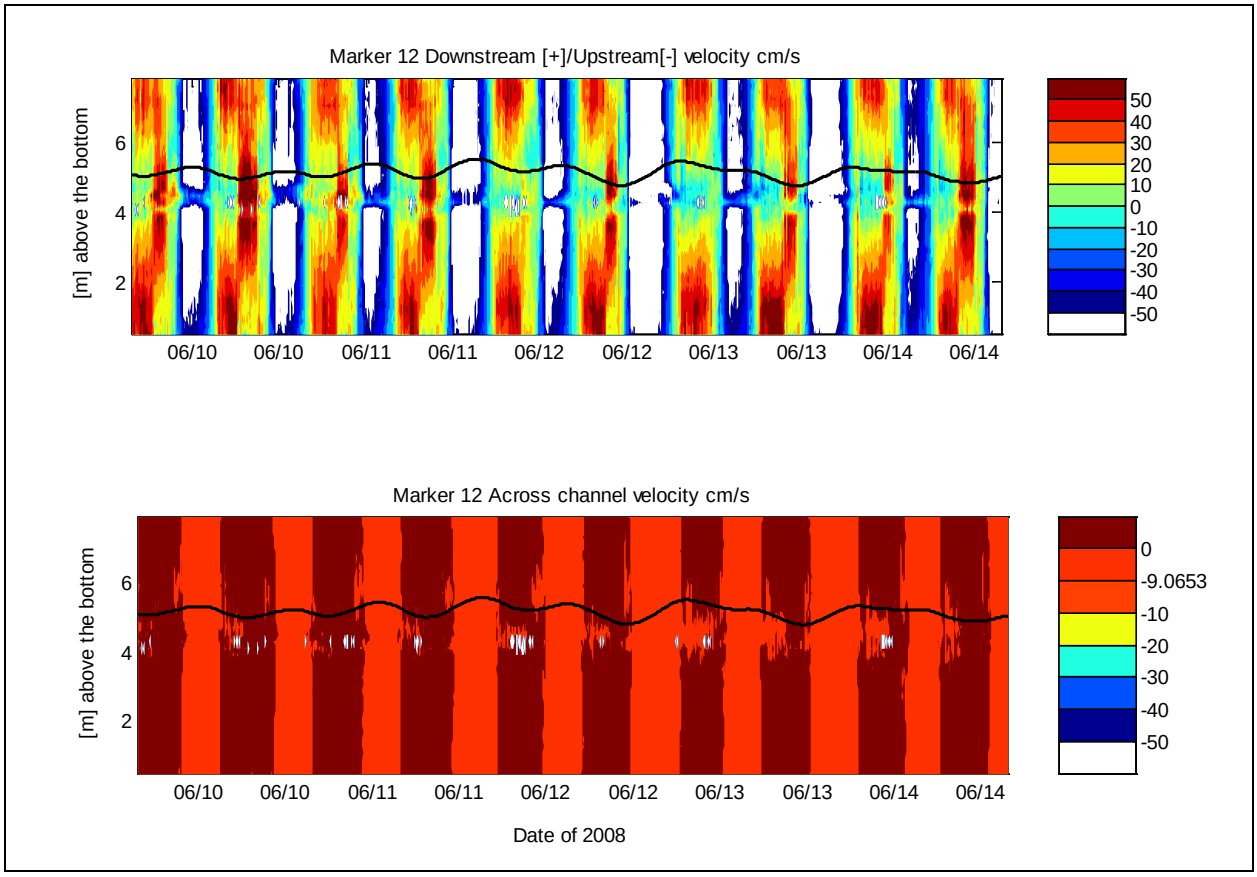

Figure 5-7. Downstream and across channel depth profiles of current velocities at Marker 12 from June 10–14, 2008.

Solid black line indicates the water surface level. Values above the line are reflections of those below and should be disregarded.

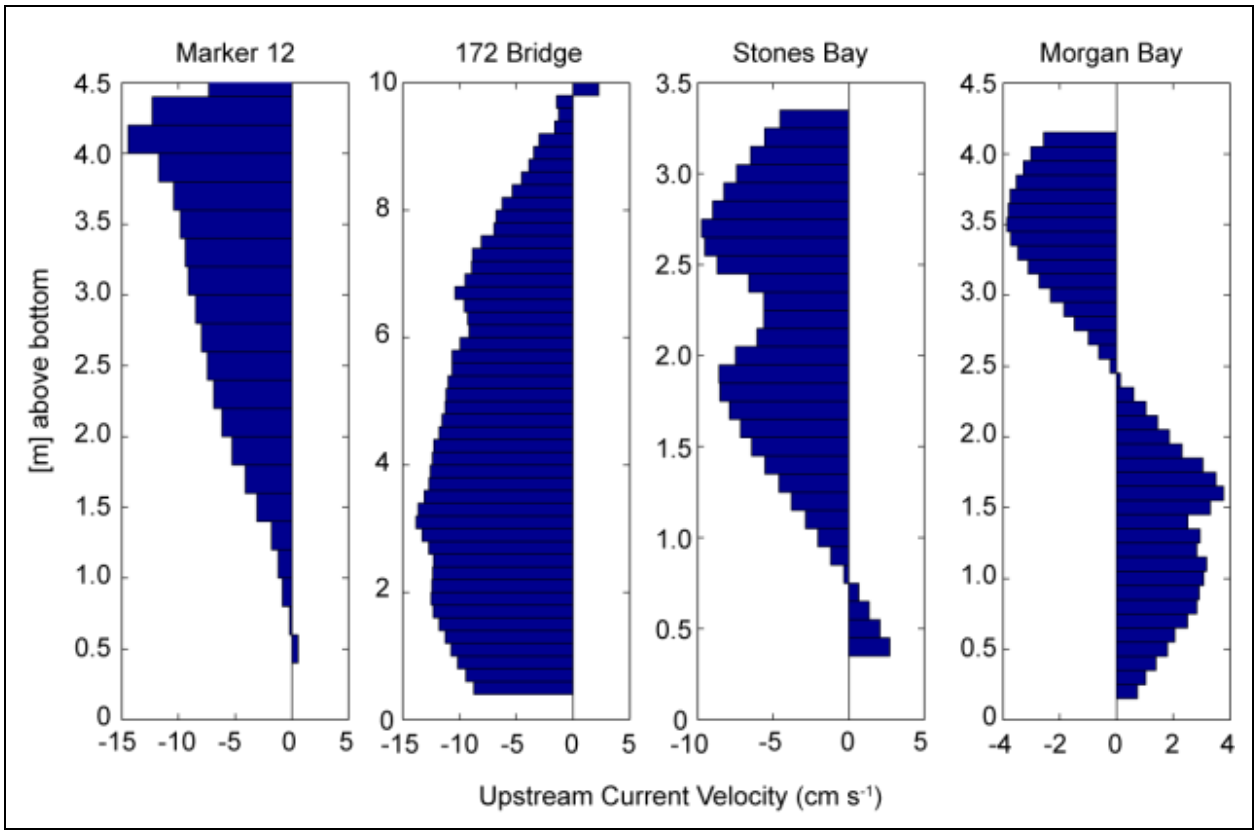

Figure 5-8. Long-term average depth profiles of along channel current velocities at Channel Marker 12, the Highway 172 bridge, Stones and Morgan Bays.

Positive (negative) values indicate upstream (downstream) flow.

The ADCP at the Highway 172 bridge was located near a gate piling at the bottom of a large basin with large shoals. Similar to Marker 12, tidal influence was strong at the Highway 172 bridge, with approximately 80% of the variability in the flow due to tides. Flows are vertically uniform upstream during the flood tide with maximum flow speeds of 1.7 m s^{-1} and have some vertical structure downstream during the ebb tide with maximum flow speeds of 1.68 m s^{-1} (**Figure 5-9**). Long-term average flows indicate a downstream preference at 10 cm s^{-1} with slower downstream flows at the surface and stronger downstream flows at the bottom (**Figure 5-8**).

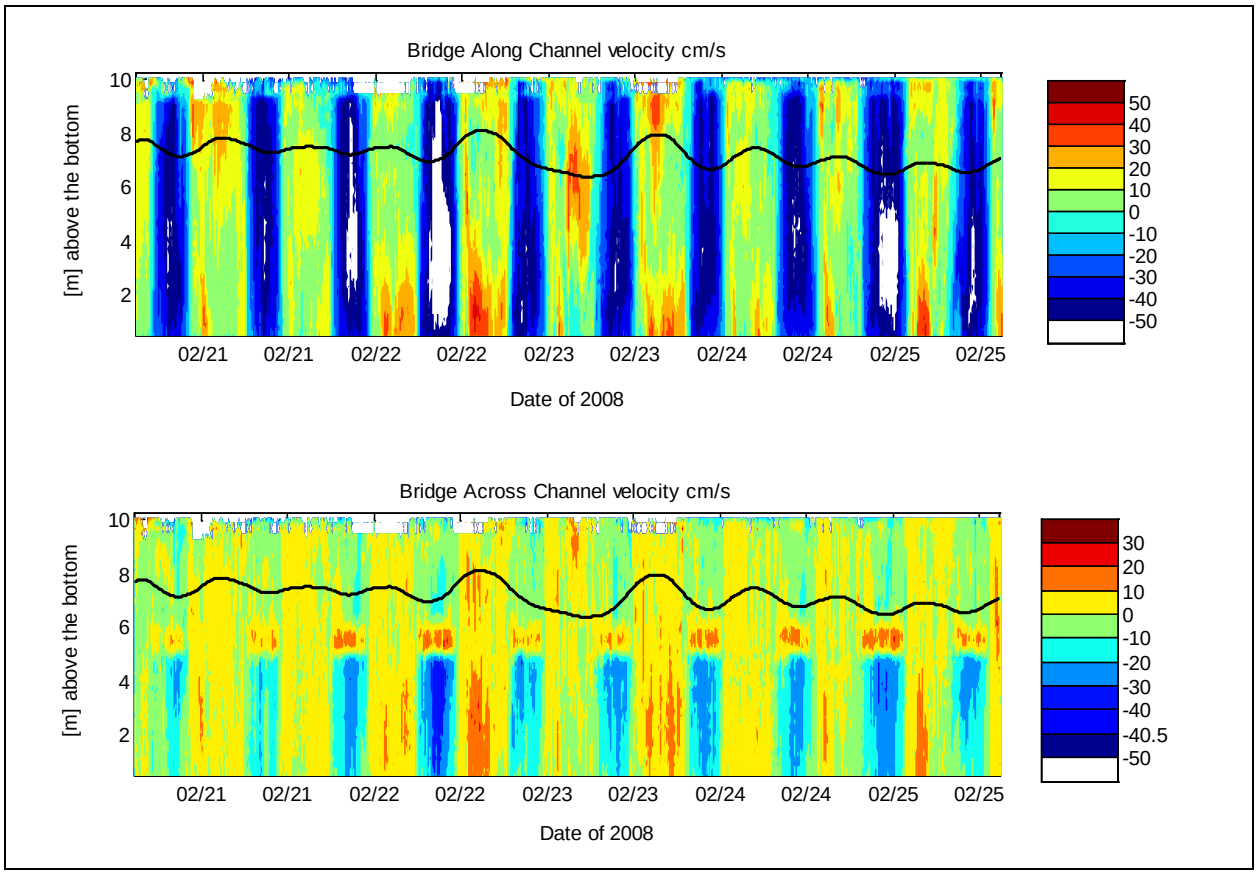

Figure 5-9. Downstream and across channel depth profiles of current velocities (cm/s) at the Highway 172 bridge from February 21–25, 2008.

Solid black line indicates the water surface level. Velocities above the surface are reflections of velocities below and should be disregarded.

Stones Bay is still tidally driven with approximately 50% of the variability in the flow due to tides. Typical estuarine flow was evident at this location with downstream flow in the surface waters and upstream flow in the bottom water. Maximum downstream flows reached 1.1 m s^{-1} and maximum upstream flows reached 0.85 m s^{-1} (**Figure 5-10**). The long-term average is estuarine with an average upstream flow at the bottom of 2 cm s^{-1} and average downstream flow at the surface of 5 cm s^{-1} (**Figure 5-8**).

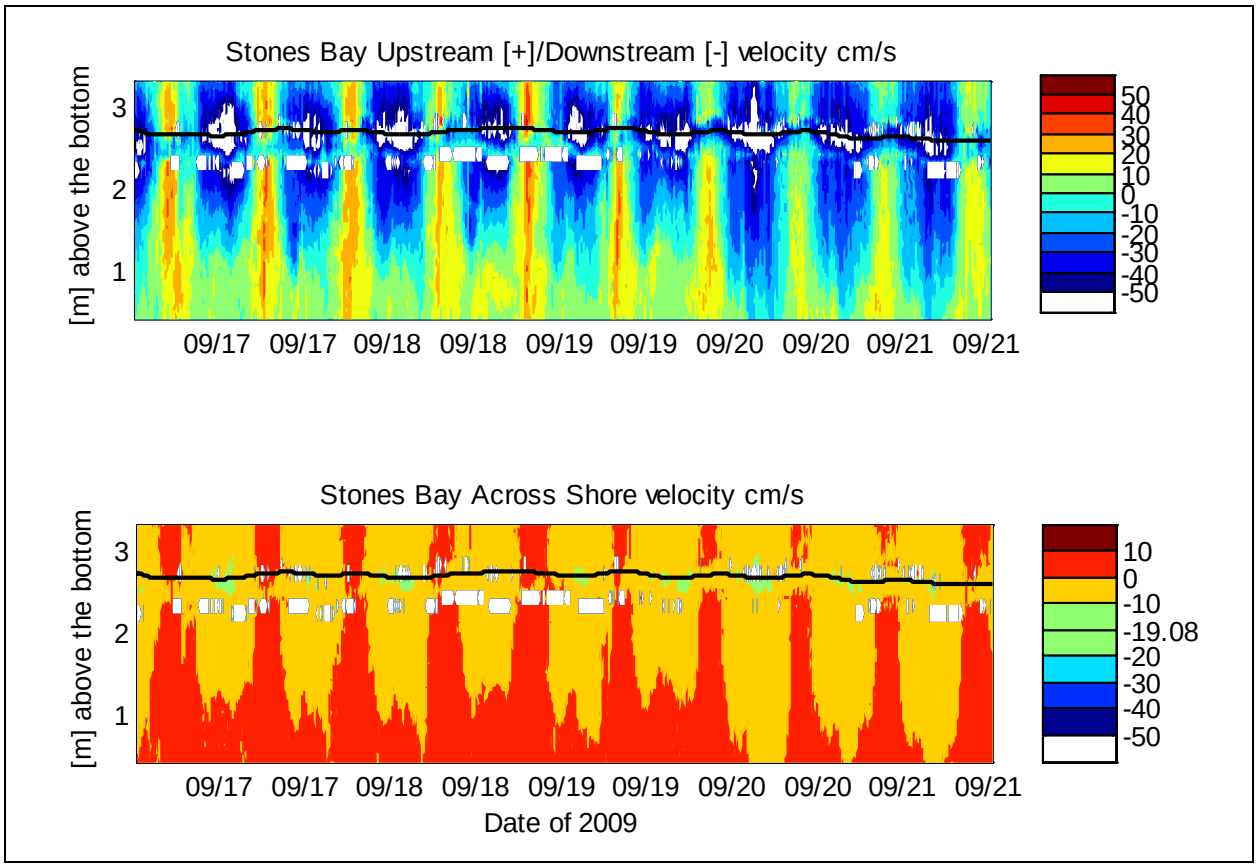

Figure 5-10. Downstream and across channel depth profiles of current velocities (cm/s) at Stones Bay from September 17–21, 2009.

Solid black line indicates the water surface level. Velocities above the surface are reflections of velocities below and should be disregarded.

Morgan Bay is minimally tidal with less than 24% of the variability in the flow due to tides. Flow speeds can range between 1.4 m s^{-1} downstream and 0.88 m s^{-1} upstream (**Figure 5-11**) and are due primarily to freshwater discharge and wind. The longer term average exhibits typical estuarine flow with upstream water near the bottom and downstream surface waters on the order of 2 cm s^{-1} (**Figure 5-8**).

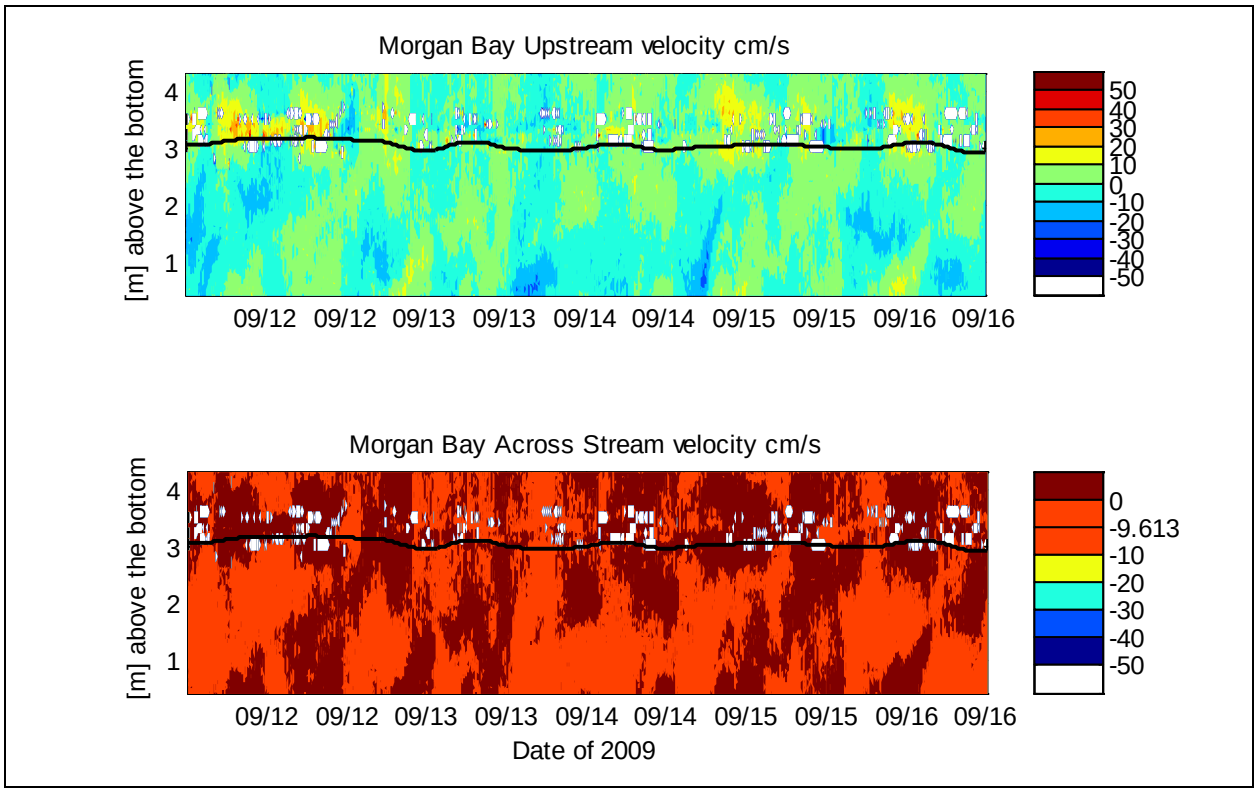

Figure 5-11. Downstream and across channel depth profiles of current velocities at Stones Bay from September 12–16, 2009.

Solid black line indicates the water surface level. Velocities above the surface are reflections of velocities below and should be disregarded.

ADCIRC Model

Validation of the ADCIRC Model

Current velocity and water level data collected by the ADCPs were also used to validate a hydrodynamic model of the NRE. The ADCIRC Model is a hydrodynamic circulation numerical model that simulates water level and current over an unstructured gridded domain. ADCIRC is used for modeling tidal-, wind- and wave-driven circulation in coastal waters; forecasting hurricane storm surge and flooding; and for modeling inlet sediment transport/morphology change and dredging/material disposal studies. For the Defense Coastal/Estuarine Research Program (DCERP), the ADCIRC Model was used to simulate the velocity flow field and pathways of transport for different regions within the NRE under different fresh water flux and standard tidal boundary conditions. These numeric models are constrained by bathymetry (collected by DCERP's Coastal Barrier Module in 2009), constant average flow conditions, and tidal parameters. Initially, the model grid was refined for better flow characterization (**Figure 5-12**).

ADCIRC captured the dominant circulation processes within the NRE. The tidal component of modeled water levels compared favorably to in situ tidally variable water level data collected at three stations: the acoustic wave and current (AWAC) location off Onslow Beach; Marker 12 just inside the New River Inlet; and by the Highway 17 bridge (**Figure 5-2**). Model tidal

amplitude and phase for six of the major diurnal and semi-diurnal tidal constituents were within the 10% of in situ data (**Figure 5-13** and **5-14**). Modeled depth averaged velocity compared well with observed velocities at locations that were strongly tidal (**Figure 5-15**). At Morgan Bay, a location with less tidal influence (modeled velocities were less accurate, but were still within reasonable agreement with observed values; **Figure 5-16**).

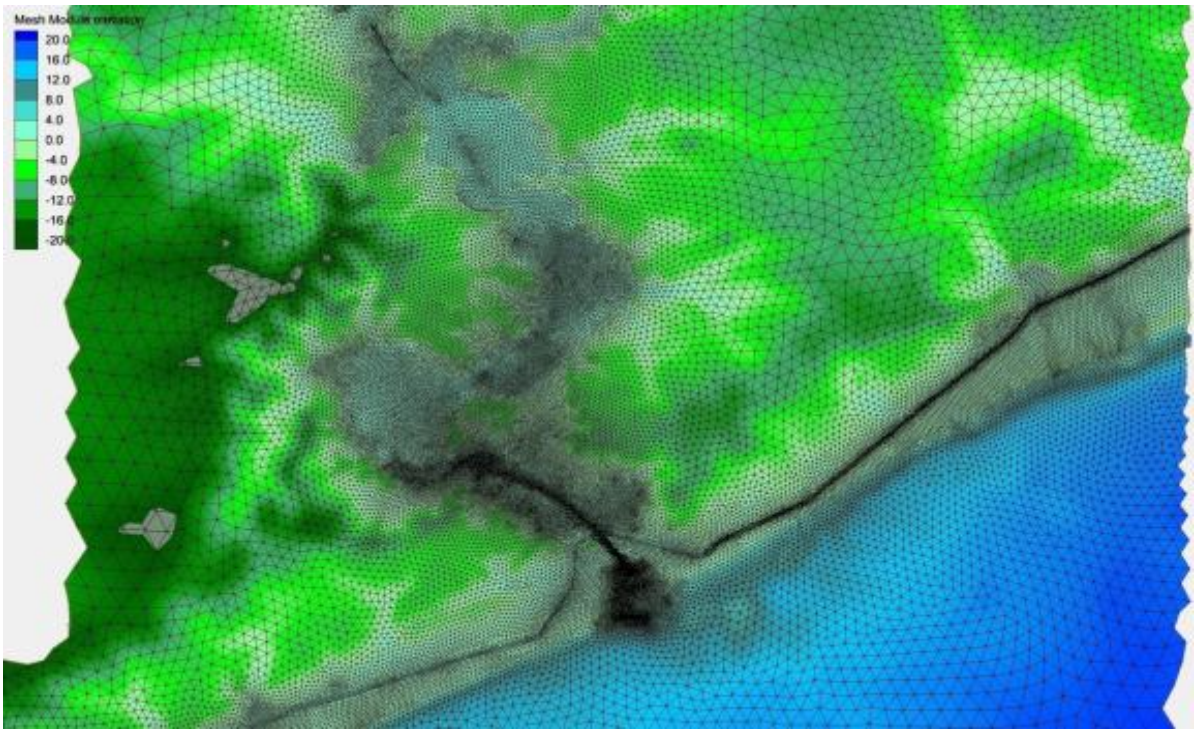

Figure 5-12. Refined model grid of the NRE and Onslow Beach area showing bathymetry (feet below sea level) and grid nodes.

Bathymetry data were produced by DCERP (Coastal Barrier Module) using swath bathymetry and side scan sonar in August 2009.

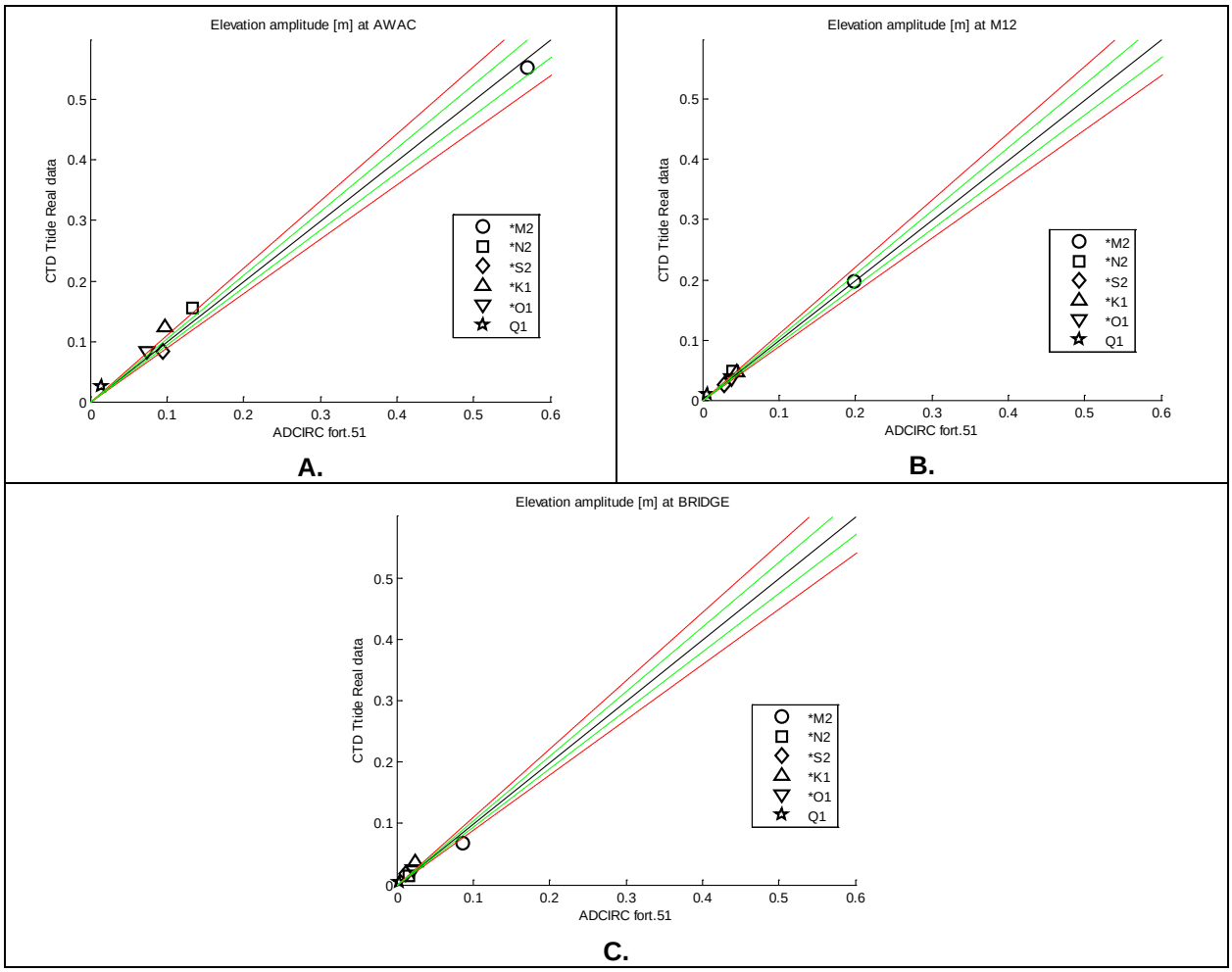

Figure 5-13. Tidal amplitude comparison between modeled (*x*-axes) and in situ (*y*-axes) water level at three locations: (A) AWAC, (B) Marker 12, and (C) the bridge.

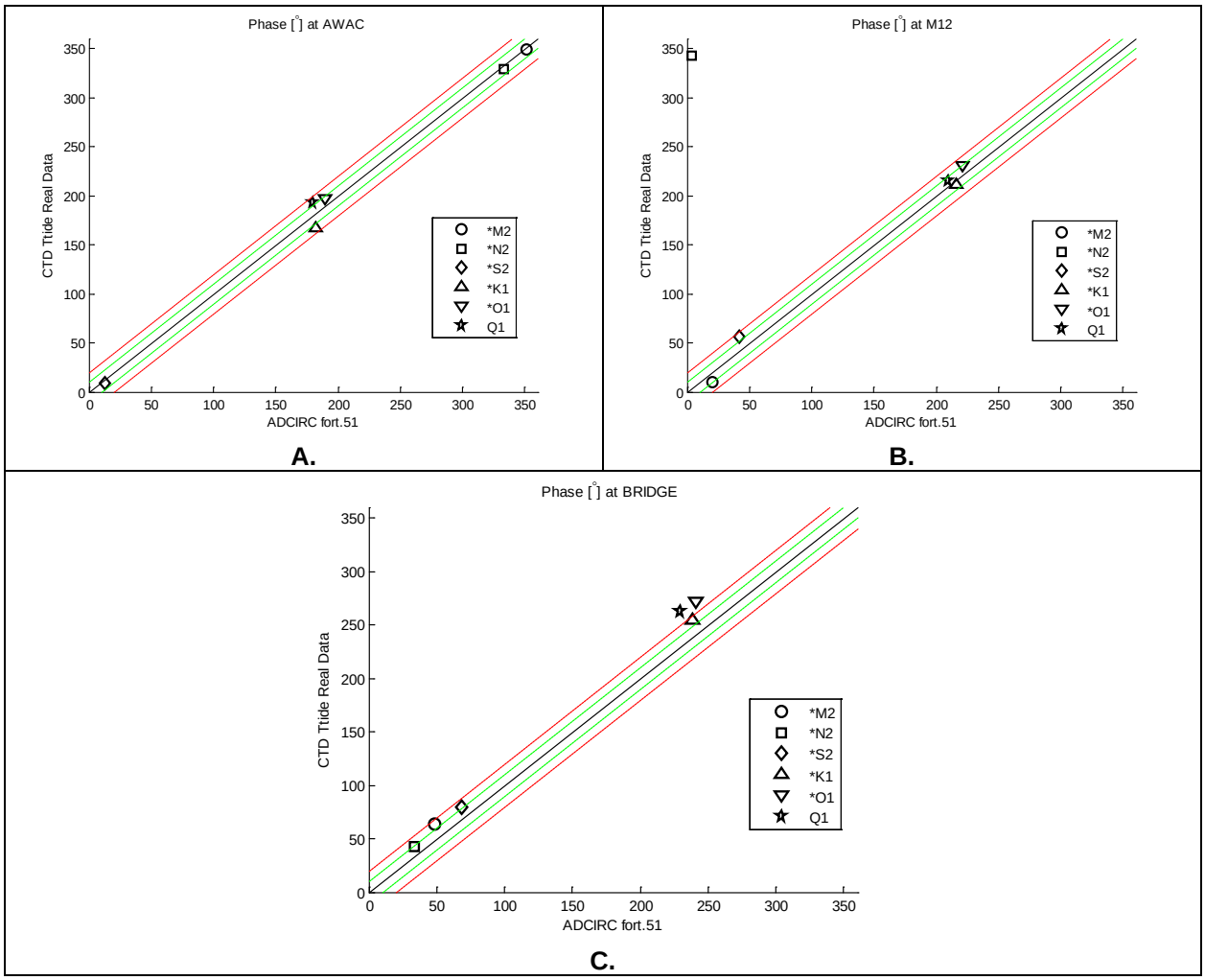

Figure 5-14. Tidal phase comparison between Modeled (*x*-axes) and in situ (*y*-axes) water level at three locations: (A) AWAC, (B) Marker 12, and (C) the bridge.

.

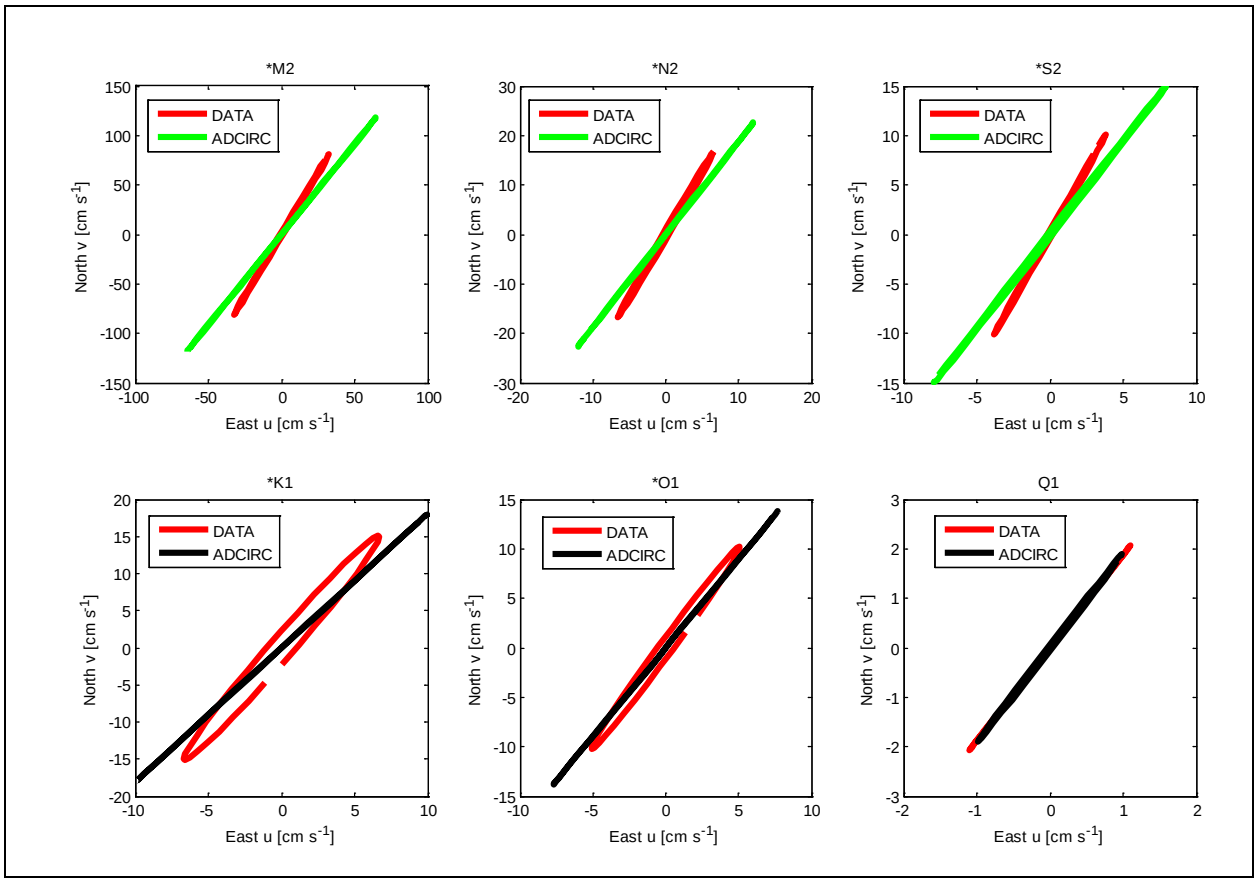

Figure 5-15. Comparison of observed (DATA) and modeled (ADCIRC) tidal ellipses for six of the major diurnal and semi-diurnal tidal constituents at the Marker 12 location.

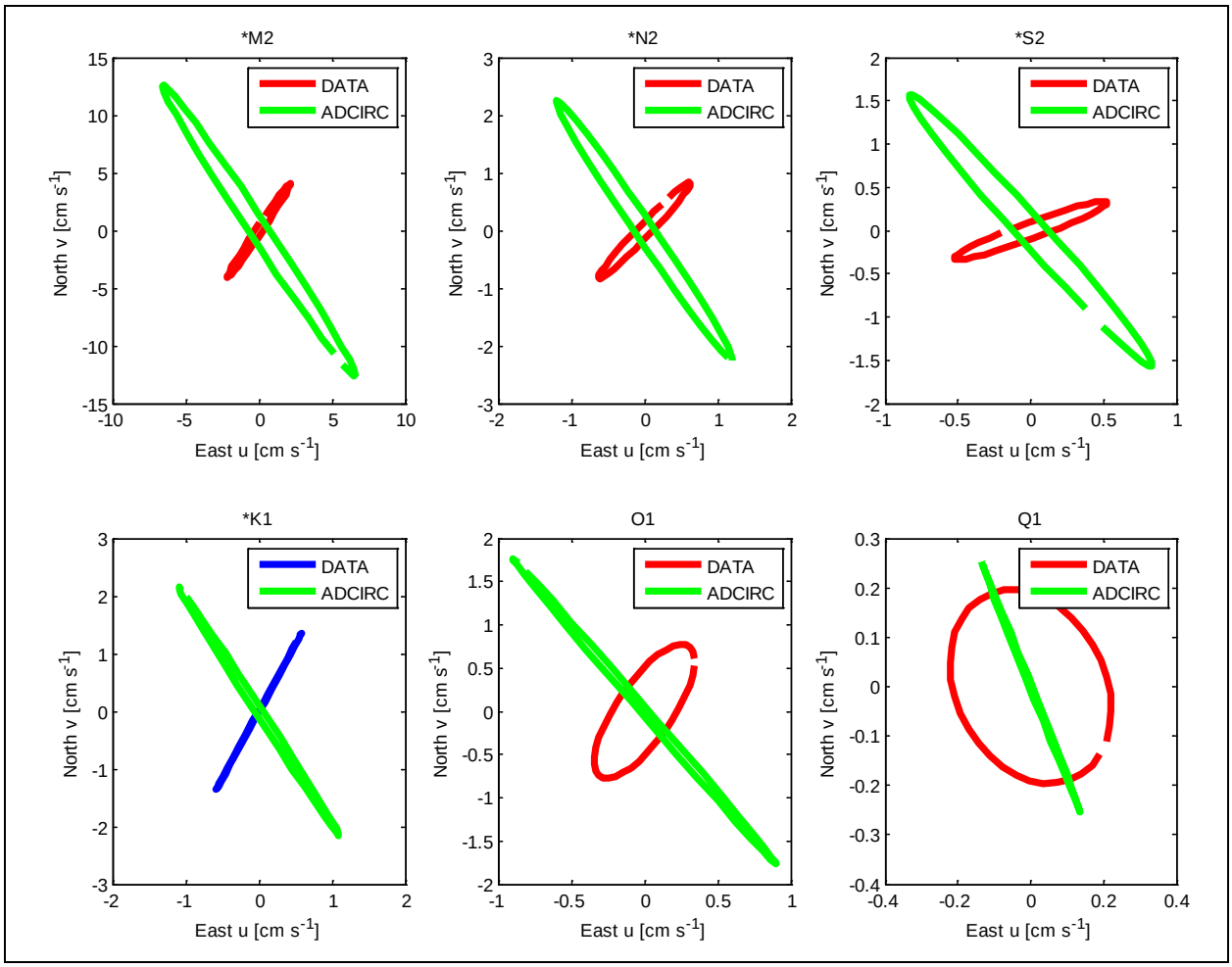

Figure 5-16. Comparison of observed (DATA) and modeled (ADCIRC) tidal ellipses for six of the major diurnal and semi-diurnal tidal constituents at the Morgan Bay location.

Determinations of Residence Time Using ADCIRC and the Flushing Time Method

Modeled flows through the NRE were used to calculate residence times of simulated water parcels and to investigate the relative importance of tidal flows versus river flow in determining retention within the estuary. Six sections along the estuary were delineated and "seeded" with model drogues (**Figure 5-17**). Model drogues are simulated passive tracers that were used to track water parcel movements through the model domain. The model was then run to completion for 200 days and the average time of transit for the particles within each region was computed. This measure of residence time through the estuary was calculated at various locations in the estuary based on tides and constant flow conditions. Three constant flow conditions were included as model input: average of 3 m^3/s; two times the average or 6 m^3/s; and high discharge flow rates of 30 m^3/s. The average flow rate is based on the USGS long-term average at the Gum Branch Road location. High discharge flow rates of 30 m^3/s were comparable to flows observed after Hurricane Irene in 2011. Additionally, the percentage of drogues that moved through the different boxes and out of the estuary was calculated. An example of one of the model solutions is presented in **Figure 5-18**. A summary table of results is presented in **Tables 5-2 and 5-3**.

As discharge increases, the transit time out of the original seed box and through the inlet decreases. In general, transit times decreased by a half when discharge doubled and decreased by a quarter when discharge was increased by an order of magnitude. Additionally, tides within the NRE increase transit time between 2 and 20 days depending on the magnitude of freshwater discharge. Large freshwater flows flush the system quickly, approximately 10–15 days, regardless of the tidal influence. Very low freshwater flows or no freshwater flows, as represented by the tides only runs, would increase residence times within the NRE, except for locations near the New River Inlet. There are quite a few recirculation zones within the NRE based on the percentages of drogues that moved to the inlet from the 200 drogues seeded in each box section. With higher freshwater flows, the percentages of drogues that move out the inlet also increase. Stones Bay, Box 4, and the other sections towards the inlet create interesting opportunities for further inspection. It appears that drogues become trapped in these areas more and may circulate for long periods of time in the region of the inlet and ICW without exiting the inlet to the shelf waters. Although these modeling results are suggestive of the existence of these recirculation zones, further ADCP deployments within these areas would be required to ground truth their existence and fully understand these complicated flow patterns.

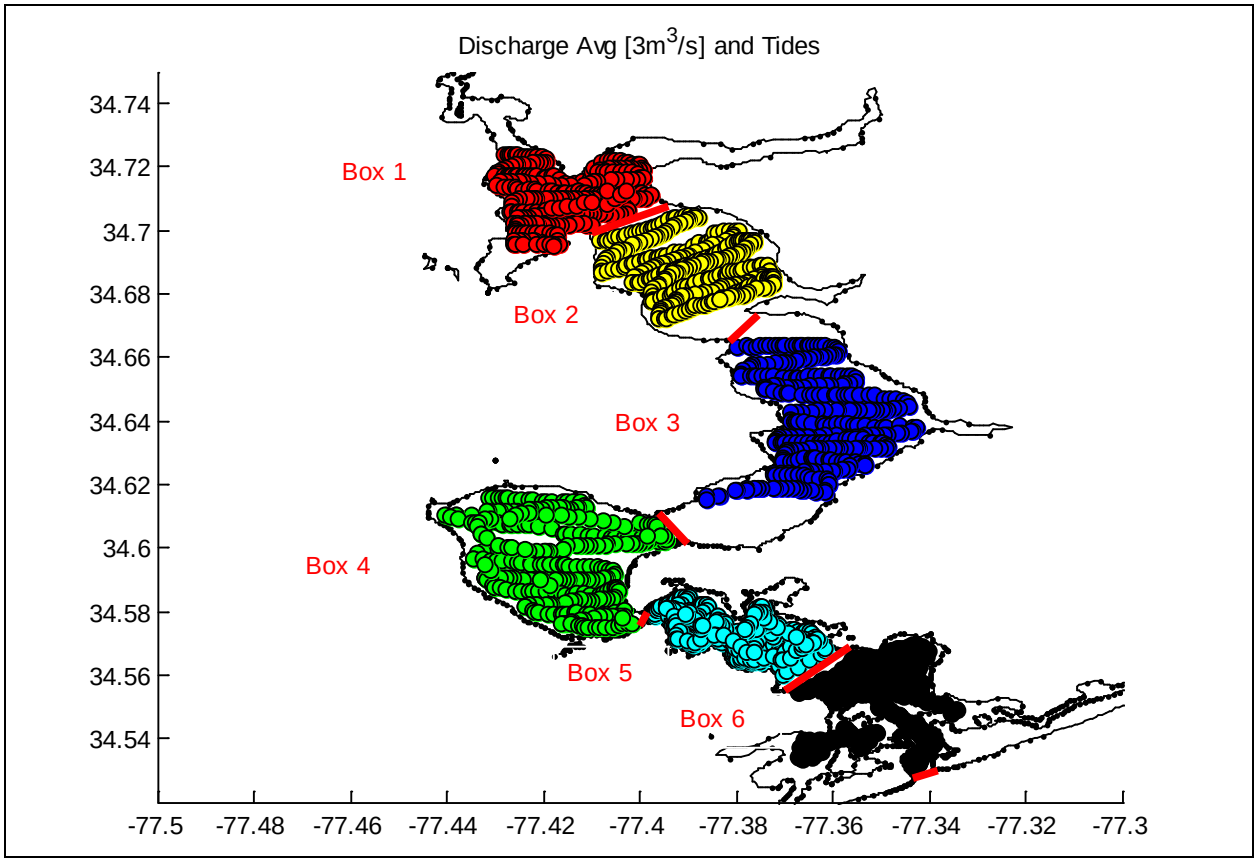

Figure 5-17. The NRE divisions delineated by red lines, and sample drogues (filled red, yellow, blue, and green, blue-green, and black circles) seeded in each section at the beginning of a model run.

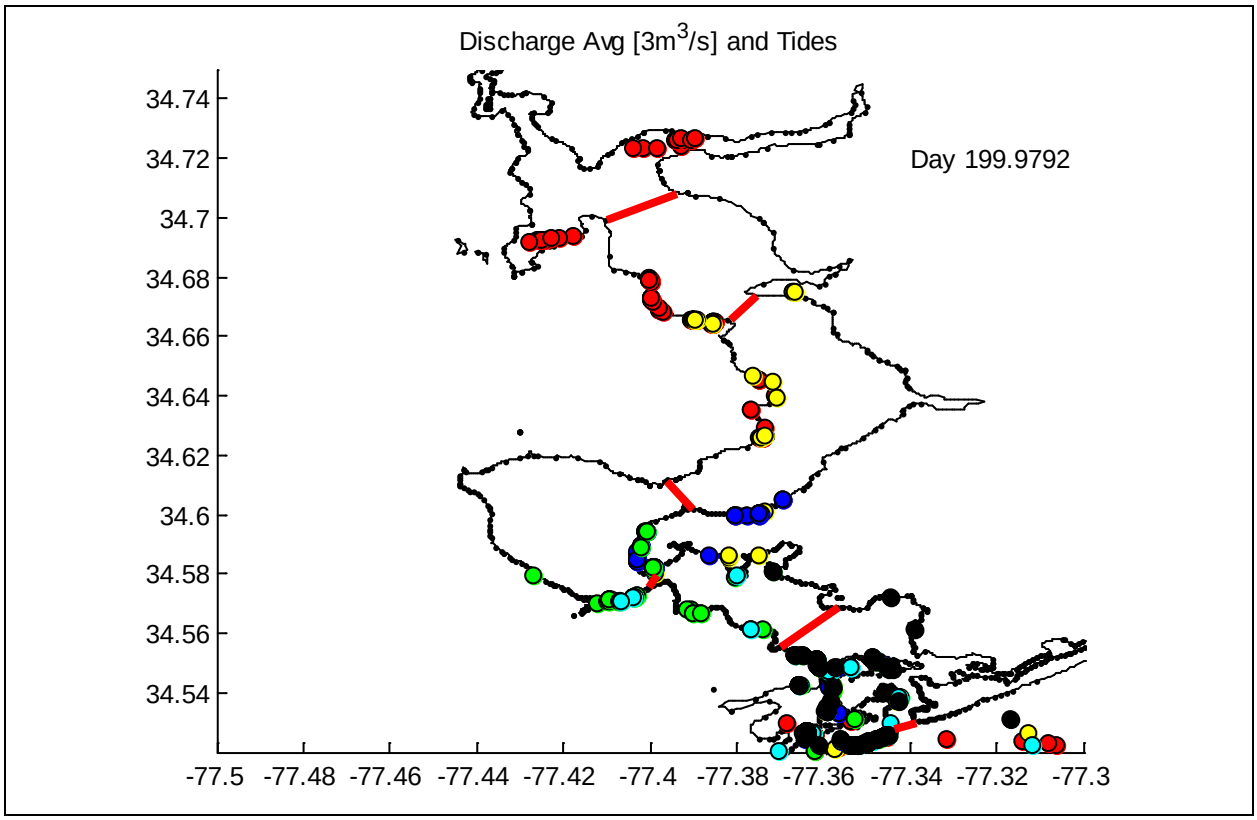

Figure 5-18. The NRE divisions and sample drogues seeded in each section at the end of a model run (approximately 200 d after initial seeding).

Format is identical to Figure 5-17.

Table 5-2. Percentage of drogues that leave their original seed box and leave the inlet for the seven different ADCIRC Model scenarios.

Summary of results from ADCIRC determinations of average transit time and percentage of model drogues that moved through each box and out the inlet for model runs with three discharge levels, with, and without tides.

Percentage of Drogues to Leave an Area		Tides and Discharge Run			Discharge Only			Tides Only
		Average 3 m^3/s	2x Average 6 m^3/s	High 30 m^3/s	Average 3 m^3/s	2x Average 6 m^3/s	High 30 m^3/s	
Box 1	Out Box	93.3	97.3	99	87	91.7	100	14.7
	To Inlet	37.7	31.3	58	25.3	27	30.3	0
Box 2	Out Box	98.3	97.3	97.3	97	97	97.3	31.3
	To Inlet	45.3	44.3	78.7	36	37	45.3	0
Box 3	Out Box	94.7	92.3	92	86.7	87.7	91	9
	To Inlet	48.7	44	67.7	35.7	39	42.3	2.7
Box 4	Out Box	86.7	84.3	87.3	85.3	85	90	66
	To Inlet	33.7	31.7	79.7	15	17.7	20	31.7

(continued)

Table 5-2. Percentage of drogues that leave their original seed box and leave the inlet for the seven different ADCIRC Model scenarios. (continued)

Percentage of Drogues to Leave an Area		Tides and Discharge Run			Discharge Only			Tides Only
		Average 3 m^3/s	2x Average 6 m^3/s	High 30 m^3/s	Average 3 m^3/s	2x Average 6 m^3/s	High 30 m^3/s	
Box 5	Out Box	98	99.7	99.7	96.7	97	98.7	78
	To Inlet	32.3	39.3	90.7	41.7	43.7	49.7	50.3
Box 6	Out Box	59.3	63.2	98	48.7	49.3	51	63.8
	To Inlet	59.3	63.2	98	48.7	49.3	51	63.8

Table 5-3. Average transit time in days of drogues that leave their original seed box (Out Box) and leave the inlet (To Inlet) for the seven different model scenarios.

Average Transit Time (Days)		Tides and Discharge Run			Discharge Only			Tides Only
		Average 3 m^3/s	2x Average 6 m^3/s	High 30 m^3/s	Average 3 m^3/s	2x Average 6 m^3/s	High 30 m^3/s	
Box 1	Out Box	20 ±18.2	17.9 ±19.2	11.3 ±3.1	22 ±26.9	17.5 ±18.2	11.5 ±3.7	79.8 ±39.3
	To Inlet	74 ±36.1	36.8 ±18.8	17.5 ±4.6	54.7 ±15.8	32.4 ±7.8	14.5 ±1.1	—
Box 2	Out Box	16.8 ±3.9	13.2 ±1.6	10.6 ±0.3	15.6 ±3.1	12.8 ±1.5	10.6 ±0.3	49.4 ±38.8
	To Inlet	65.4 ±37.6	31.9 ±18.2	15.8 ±4.8	48 ±15.2	28.7 ±7.1	13.8 ±1.1	—
Box 3	Out Box	25.1 ±7.6	16.5 ±3.5	13.1 ±1.7	19.8 ±6.6	15.1 ±3.4	12.1 ±1.1	75.6 ±43.4
	To Inlet	46.8 ±30.7	27.7 ±21.6	14.4 ±4.9	38.8 ±14.8	23.9 ±6.7	12.8 ±1.1	115.4 ±46.8
Box 4	Out Box	25.4 ±14.8	15.9 ±8.1	10.8 ±1.1	17.9 ±11.2	13.7 ±5.2	10.9 ±1.1	72. ±47.8
	To Inlet	53.7 ±49.9	29.4 ±24.7	14.3 ±11.9	26 ±11.5	17.7 ±5.5	11.8 ±1.5	77.2 ±43.3
Box 5	Out Box	13.4 ±5.1	11.2 ±1.3	10.24 ±0.3	12.4 ±2.3	11.3 ±1.7	10.3 ±0.3	26.7 ±31.8
	To Inlet	51.6 ±51.2	22.8 ±15.6	12.7 ±11.4	15.5 ±2.1	13.1 ±1.5	10.9 ±1.3	49.7 ±44.7
Box 6	Out Box	23.7 ±33.5	15.4 ±10.0	11.2 ±2.2	12.4 ±2.1	11.3 ±1.1	10.4 ±0.8	26.2 ±31.5
	To Inlet	23.7 ±33.5	15.4 ±10.0	11.2 ±2.2	12.4 ±2.1	11.3 ±1.1	10.4 ±0.8	26.2 ±31.5

Values are means (± SD). Cells with dashed lines in the "tides only" model run indicate that no drogues left the inlet.

In the ADCIRC Model, the best estimate of residence time for the whole estuary is the average transit time of drogues from Box 1 to the inlet. Similarly, the residence time calculated as flushing time using the date specific freshwater replacement method at Station 1 represents the average transit time (water age) of freshwater through the estuary. These two methods of estimating the residence time of the estuary were compared for cross-validation purposes. For ADCIRC Model runs that included tides, estimates of residence time varied from approximately 17 d under the highest flow conditions to 74 d under average flow conditions (**Table 5-3**). At Station 1 (the station closest to the inlet), the median calculated freshwater age was approximately 80 d (**Figure 5-19**), which compares well with the 74 d residence time predicted by the ADCIRC Model for average flows. The upper and lower ranges of flushing times (approximately 150 d and approximately 10 d) were somewhat more extreme than the range of

residence times produced by the ADCIRC Model. However, this is easily explained by the fact the river flow conditions used as input for the ADCIRC Model did not include the full range of extreme flow conditions observed during the study period (**Figures 5-5**). In general, these modeled and calculated estimates of residence time agree very well, and this cross validation provides confidence in both methods for estimation of the time scales of transport for materials within the NRE.

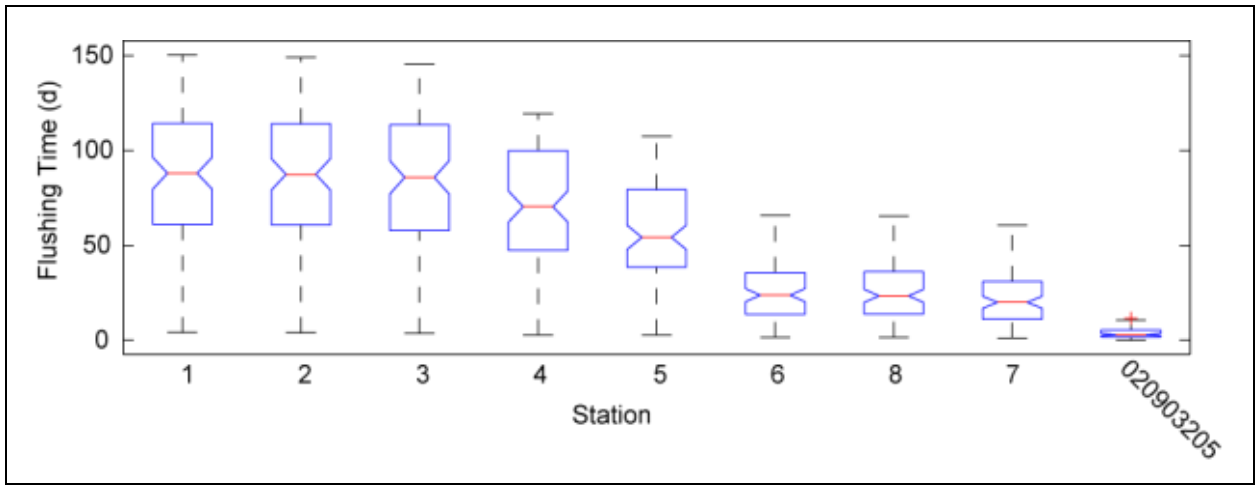

Figure 5-19. Box and whisker plots of flushing time along the axis of the NRE calculated using the date-specific freshwater replacement method.

Seasonality of Water Quality

The multiannual, semi-hourly time series of key water quality parameters produced by the AVPs at Stones and Morgan Bays demonstrate a large degree of seasonality of key water quality parameters (**Figures 5-20** and **5-21**). Temperature oscillated between summer highs of approximately 30 degrees Celsius in late July and early August to winter lows of approximately 2–7 degrees Celsius in late January. The warm 2011–2012 winter is clearly visible as minimum water temperatures were approximately 5 degrees warmer than the previous three winters.

DO was strongly impacted by temperature due to solubility characteristics. Winter maxima averaged approximately 12–14 mg L^{-1} and summer minima were approximately 6–7 mg L^{-1}. Short-term variability of DO is much greater during the warmer months than during the colder months due to the enhanced biological impacts of photosynthesis and respiration on oxygen dynamics during the warm period (shown below). Maximum annual salinities generally occurred during the summer, but winter-time decreases in salinity were highly variable. The most notable depressions in salinity were during the wet fall and winter of 2009 through early 2010, and the dramatic salinity drops following Tropical Storm Nicole in late September 2010, and following Hurricane Irene in late August 2011. Turbidity and chl *a* also showed oscillations at seasonal time scales with both generally showing maxima during the spring and late summer periods. This trend is more evident in the Morgan Bay record (**Figure 5-20**) for chl *a* and for turbidity in the Stones Bay record (**Figure 5-21**). These differences between sites suggest potential differences in drivers of turbidity and chl *a* between the two sites.

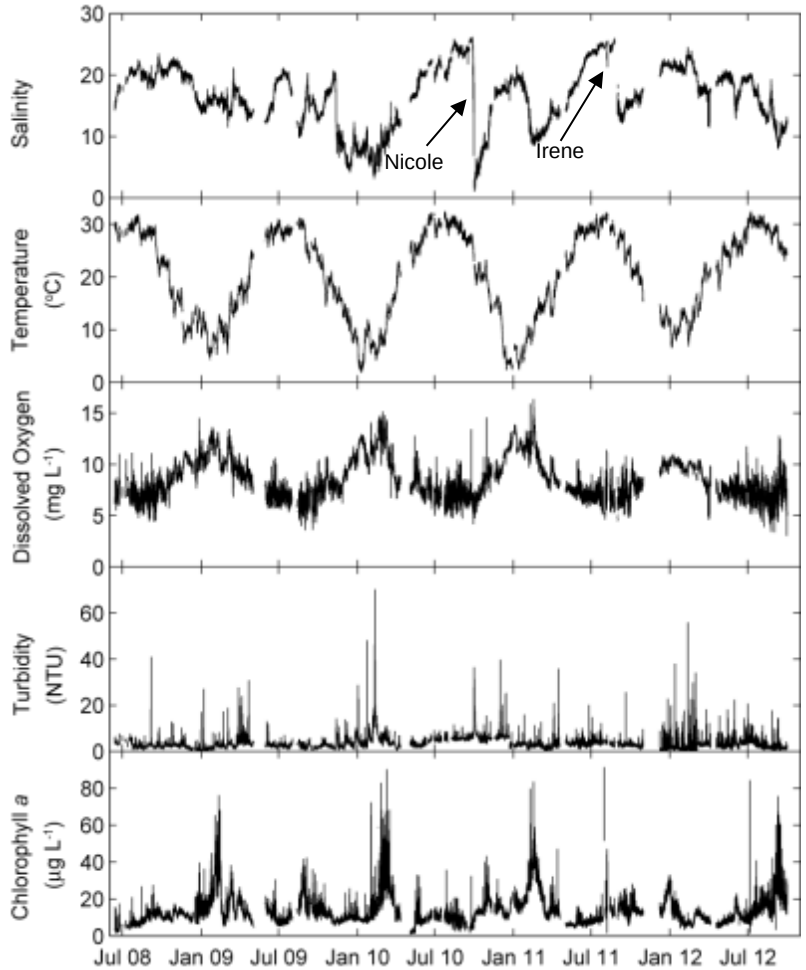

Figure 5-20. Time series of semi-hourly, average water column conditions from the AVP at Morgan Bay from June 14, 2008 through October 1, 2012.

Arrows point to two major tropical storm events that impacted the estuary, the remnants of Tropical Storm Nicole and Hurricane Irene.

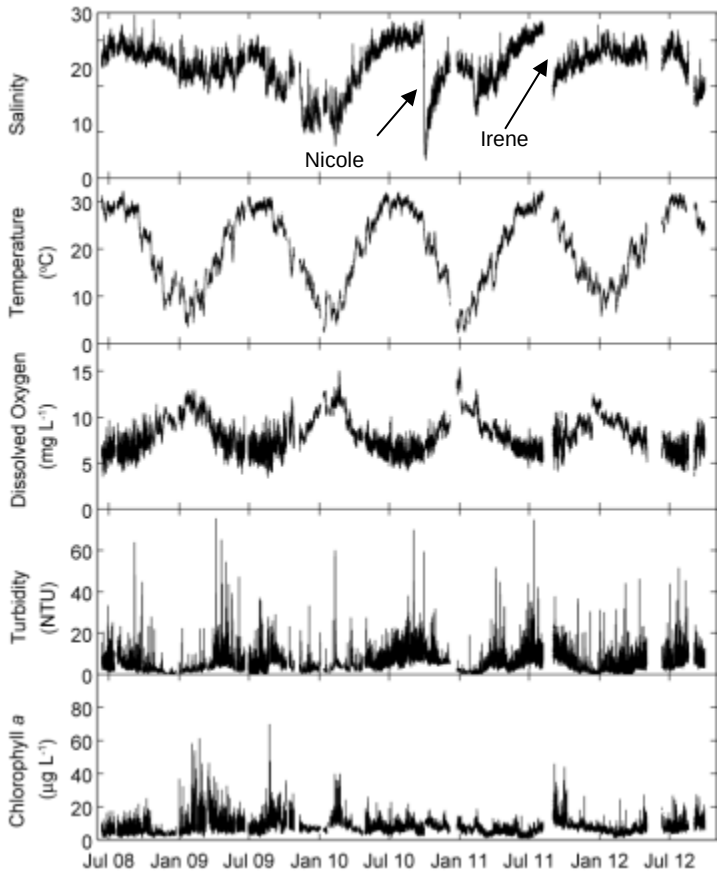

Figure 5-21. Time series of semi-hourly, average water column conditions from the AVP at Stones Bay from June 14, 2008 through October 1, 2012.

Arrows point to two major tropical storm events that impacted the estuary, the remnants of Tropical Storm Nicole and Hurricane Irene.

Covariation Between Water Quality Parameters

Interrelationships between water quality parameters at the two AVP sites were assessed using Pearson's correlations. Results are shown in **Table 5-4**. Due to autocorrelation within each parameter, the number of samples (*N*) in each data record is much greater than the true degrees of freedom. Use of *N* as an estimate of the degrees of freedom would result in unacceptable Type 1 error in testing the null hypothesis that no correlation exists. Estimates of equivalent degrees of freedom which take into account autocorrelation were calculated according to Emery and Thompson (1997) and are used to calculate *p* values for each parameter pair.

Table 5-4. Results of Pearson's correlations for key water quality parameters from the AVPs at Stones and Morgan Bays.

	Temperature	Salinity	DO	Turbidity	Chl *a*
	Stones Bay				
Temperature	{29}	**0.46**	**−0.89**	**0.44**	−0.04
Salinity	0.00	{39}	**−0.40**	0.13	**−0.35**
DO	0.00	0.01	{37}	**−0.41**	0.18
Turbidity	0.01	0.21	0.00	{81}	**0.19**
chl *a*	0.41	0.01	0.13	0.04	{99}
	Morgan Bay				
Temperature	{35}	**0.33**	**−0.85**	−0.05	**−0.31**
Salinity	0.02	{51}	**−0.29**	−0.17	**−0.36**
DO	0.00	0.03	{44}	0.04	**0.45**
Turbidity	0.38	0.11	0.39	{124}	0.00
Chl *a*	0.03	0.00	0.00	0.49	{110}

Pearson's *R* and *p* values lie above and below the diagonal, respectively. Equivalent degrees of freedom for each parameter lie along the diagonal in brackets. Bold *R* values are significant at $\alpha = 0.05$.

Many of the interrelationships between water quality variables were similar between AVP sites. The significant positive relationships between temperature and salinity at both sites reflect the tendency toward higher freshwater inputs during the winter and spring when evapotranspiration within the watershed is at an annual minimum (Litaker et al., 1987). Due to the strong influence of temperature on gas solubility, DO showed a significant negative correlation with temperature (**Table 5-4**). The negative relationship between salinity and DO at both stations is most likely a product of the covariation of these two variables with temperature. The negative relationships between chl *a* and salinity underscore the influence of the riverine nutrient load delivered by freshwater riverine inputs that fuels higher phytoplankton biomass.

Significant differences in interrelationships between water quality parameters did exist between the two AVP stations. At Stones Bay, turbidity was highly correlated with temperature (by covariation with DO as well), but at Morgan Bay, no relationship between turbidity and temperature was observed. It is unclear what drives this seasonal pattern in turbidity at Stones Bay. Sediment resuspension due to wind and wave energy is a dominant source of turbidity within the NRE. However, it seems unlikely that physical processes drive this seasonal pattern because tidal energy is fairly constant throughout the year, and wind energy to the NRE reaches an annual minimum during the summer months (Figure 5-24). It seems likely that the seasonal turbidity signal is of biological or anthropogenic origin, perhaps due to foraging of demersal finfish or perhaps due to the shrimp trawling industry. At Stones Bay, chl *a* was positively related to turbidity and temperature (a covariate of turbidity) while at Morgan Bay chl *a* was unrelated to turbidity and negatively related to temperature (probably due to covariation with salinity/nutrient input). These differences likely reflect the greater importance of resuspension of benthic microalgae (BMA) at downstream regions which receive less direct riverine nutrient load, are shallower and thus have more surface area covered by BMA, and are more easily resuspended. The BMA community in the Stones Bay region is dominated by diatoms and the

relatively higher concentrations of diatom biomass in this region despite low direct nutrient inputs (Hall et al., 2012) provides further evidence for the importance of sediment resuspension as a subsidy to the water column microalgal community in the lower NRE.

Dominant Temporal Scales of Water Quality Variability

Variance preserving, Fourier power spectra were calculated for the AVP records of average water column water quality data. Prior to analyses, data series were demeaned and data gaps were subsequently filled with zeros. Overlapping (50%) Hamming windows of length 35040 were used to increase confidence in spectral estimates. This window length represents a time span of 2 years, (730 d × 48 data points per day = 35,040) and allows estimation of power from a cycle every 2 years to 1 cycle per hour.

At both sites, variability in all water quality parameters was primarily confined to two bands, a seasonal band with periods ranging from annual to monthly, and a tidal band with periods from 0.26 to 1.1 d (**Figure 5-22**). Temperature showed two distinct peaks that correspond to the seasonal cycle with a 365 d period and a diurnal (1 d) cycle of daytime heating and nighttime cooling. DO showed the same two peaks for both AVP records, again underscoring the large degree of control by solubility effects from temperature. However, DO also showed peaks at 0.52 d that corresponds with the semi-diurnal (M2) tidal constituent that dominates tidal variability within the NRE.

Salinity at both sites contained a broad region of high power at seasonal to monthly time scales that is associated with the time scales of variability of freshwater input with broad peaks that were maximum in the semi-annual to annual period. Tidal variability in salinity was also apparent with the lunar semi-diurnal (M2) being the most significant constituent. The solar diurnal tidal constituent (S1, 1 d period) is also apparent for both AVP records. Due to closer proximity to New River Inlet, Stones Bay is much more tidally influenced as revealed by the relative peak heights for the dominant tidal constituents (M2 and S1). At Stones Bay, smaller amplitude tidal constituents such as the lunar diurnal (O1, 1.07 d period), lunar quarter diurnal (M4, 0.26 d period), and the terdiurnal (M3, 0.35 d period) are apparent in the salinity record whereas these smaller peaks are not apparent for salinity at Morgan Bay.

Tidal scale variability is also apparent in turbidity and chl *a* records for both stations. The semidiurnal signal likely represents the impacts of tidal advection of waters containing varying concentrations of turbidity and phytoplankton biomass past the station (Litaker et al., 1987). Over short time scales (evaporation unimportant), salinity behaves as a passive tracer. The fact that the diurnal signal in turbidity and chl *a* is equal to (Stones Bay) or greater than (Morgan Bay) the semidiurnal tidal band suggests that the main factor producing the diel constituent is probably not due to tides but rather is due to a daily rhythm of inputs of turbidity and phytoplankton to the water column. Daily cycles in phytoplankton biomass can arise when growth exceeds grazing during the day and grazing exceeds growth during the nighttime hours (Litaker et al., 1987). Mechanisms for daily cycles in turbidity are likely due to daily sea breeze cycles that produce oscillations in wave energy that drives sediment resuspension. An annual cycle of turbidity at Stones Bay is apparent while at Morgan Bay, no clear peaks other than the diurnal peak were observed. Again, this suggests different controlling mechanisms for turbidity between the two stations. The record for salinity at the Morgan Bay AVP also shows a semi-

annual peak. At both AVP sites, peak power in the seasonal band for chl *a* occurred near the semi-annual period rather than exactly on the annual period; evidence that biomass is more strongly related to variations in freshwater input rather than seasonal changes in light or temperature.

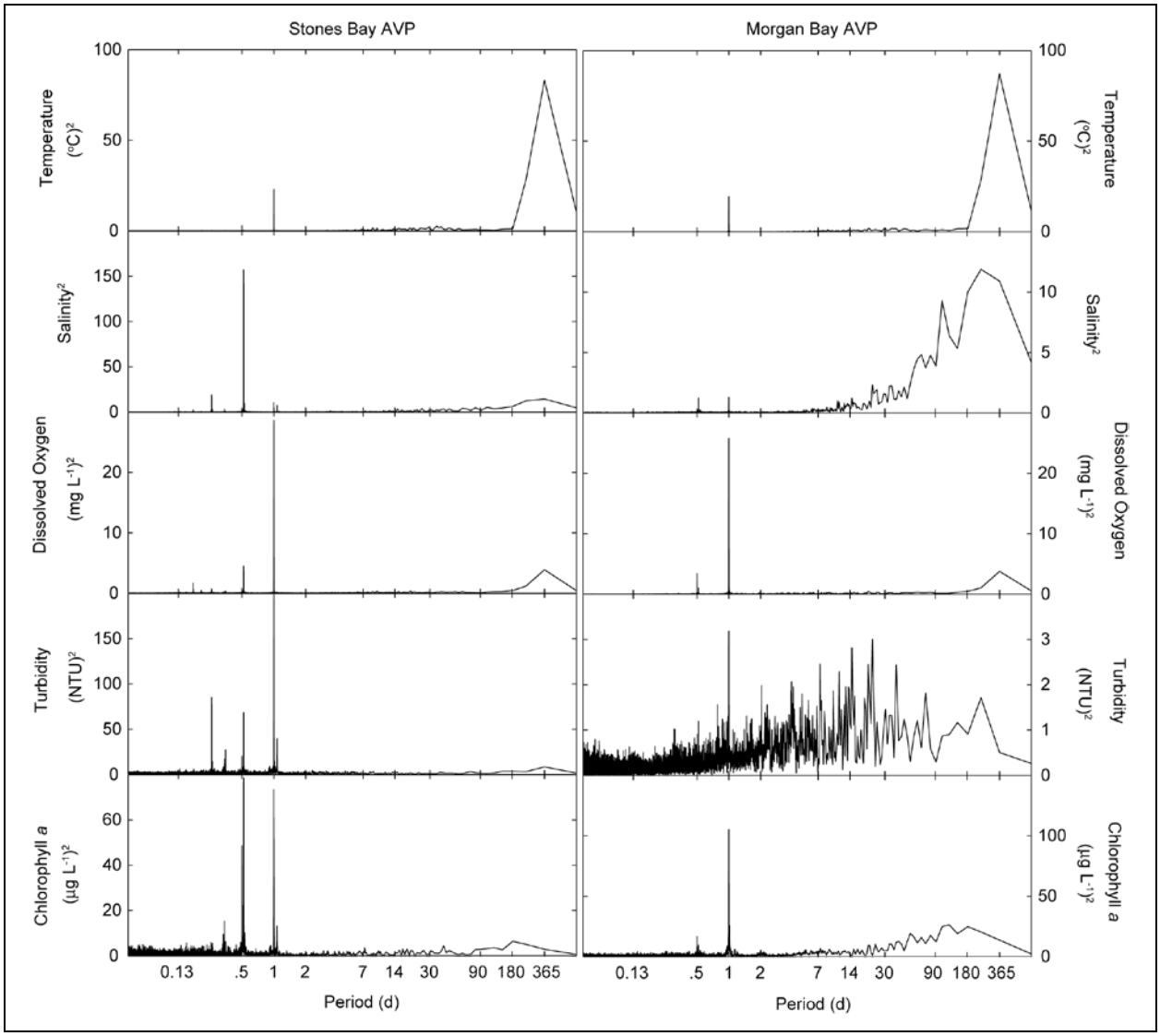

Figure 5-22. Variance preserving Fourier power spectra of key water quality parameters from the semi-hourly AVP records from Stones and Morgan Bays.

Note the different *y*-axes for the two AVP sites.

The diel cycle of DO at both AVP sites was examined in greater detail because the daily balance between respiration and photosynthesis provides key information on the net trophic (autotrophic versus heterotrophic) status of the estuary. Mean water column DO concentrations were averaged by the time of day (Eastern Standard Time) the casts were made (e.g., all casts made at 02:30 hours were averaged). Seasonality of the diel cycle in oxygen is shown by examining the diel cycles from mid-winter (January) and mid-summer (July) months (**Figure 5-23**). For both AVPs and for both winter and summer, the phase of the diel signal results in maximum DO in

the evening, near the end of the photoperiod (approximately 17:00 hours). This is consistent with a daytime buildup of DO in the water column, while photosynthesis exceeds respiration, and nighttime depletion of DO while respiration continues, but oxygen production by photosynthesis is negligible. The diel cycle is much more pronounced during July at both stations due to temperature induced enhancement of both respiration and photosynthesis. The influence of photoperiod length on DO dynamics is also evident with daily minima occurring at approximately 08:00 hours during the winter, but earlier (approximately 06:00 to 07:00 hours) during the summer.

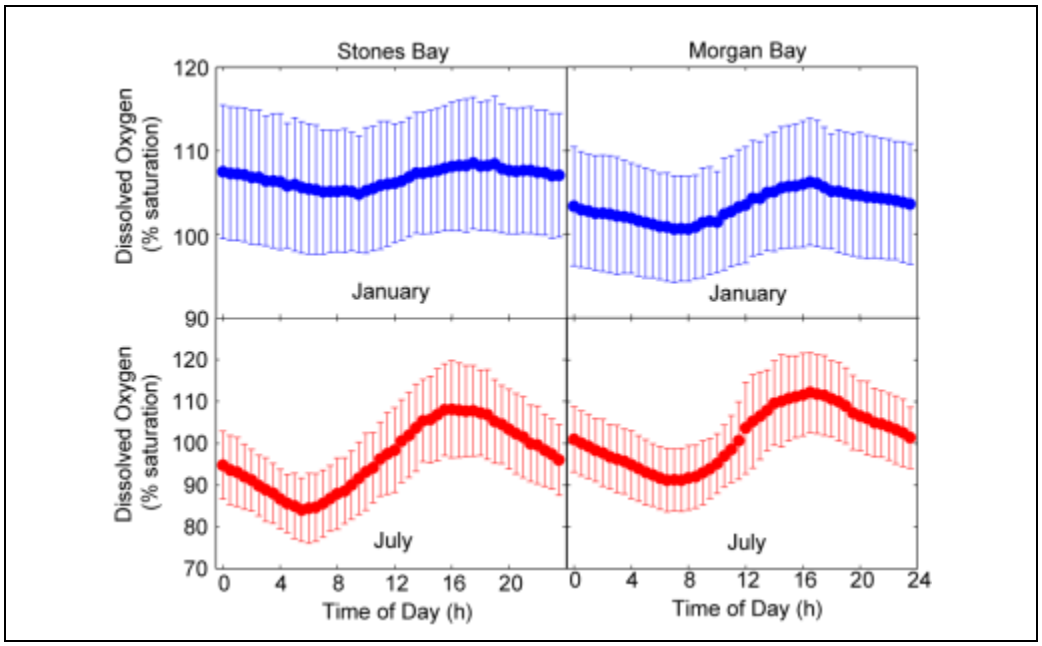

Figure 5-23. Seasonality in the amplitude of the diel cycle of DO at Stones and Morgan Bays.

Data points are mean (error bars SD) values of all data collected at each time of day during the months of January and July.

Sediment Resuspension at the AVP Sites

In addition to wind and water profile data from the AVPs and the ADCP deployments, the Wave Exposure Model (WEMo; Malhotra and Fonseca, 2007) was run for the two AVP sites to estimate wave heights and bottom stress values. WEMo produces a spatially registered GIS grid of wave characteristics (height, period, energy, speed) based on wind data collected by the AVPs, fetch determined by NRE shoreline (determined by NOAA), and bathymetry data (collected by DCERP).

Wind conditions throughout the data collection period from mid-2008 through October 2012 are summarized in **Figure 5-24**. The wind rose plots in panels a and b show that winds were most frequently observed coming from the southwest and northeast which are known to be the seasonally dominant directions in this area for summer and winter respectively. Stones Bay shows both a higher frequency of, and stronger, southwest winds. The hodograph in the center panel shows the diurnal wind pattern that helps to clarify the difference in winds between the two sites. At both sites, winds from Hours 1–10 (representing time-of-day in local standard time)

come from the northwest. After this time, the wind in each bay begins to back toward the southwest. Stones Bay reaches a stable southwest direction by Hour 14 and remains there until Hour 17 after which the speed decreases and then begins to veer back to the northwest. Morgan Bay does not stabilize in the southwest direction, but rather continues to rotate throughout the day reaching the southwest direction around Hour 15 and beginning to veer toward the northwest after Hour 18. The mean wind speed in Stones Bay is approximately a half meter per second faster than in Morgan Bay (4.1 versus 3.6 m s^{-1}), and there is a significant time-of-day effect in both bays as shown in panel *d*. Afternoon wind speeds average 1.5 m s^{-1} faster than night/early morning. Seasonally, (**panel *e***) the increased wind speed in Stones Bay is greatest from approximately Day 90 to Day 225, or roughly March through August (the months of ocean warming). The timing of the diurnal southwest winds and the seasonality of the increased wind speeds are consistent with a sea-breeze effect. Fetch in the predominant northeast-southwest wind directions is larger for Stones Bay being approximately 2 km to the southwest and up to nearly 10 km to the northeast. The Morgan Bay site is much more protected in these directions with approximately 1 km of fetch.

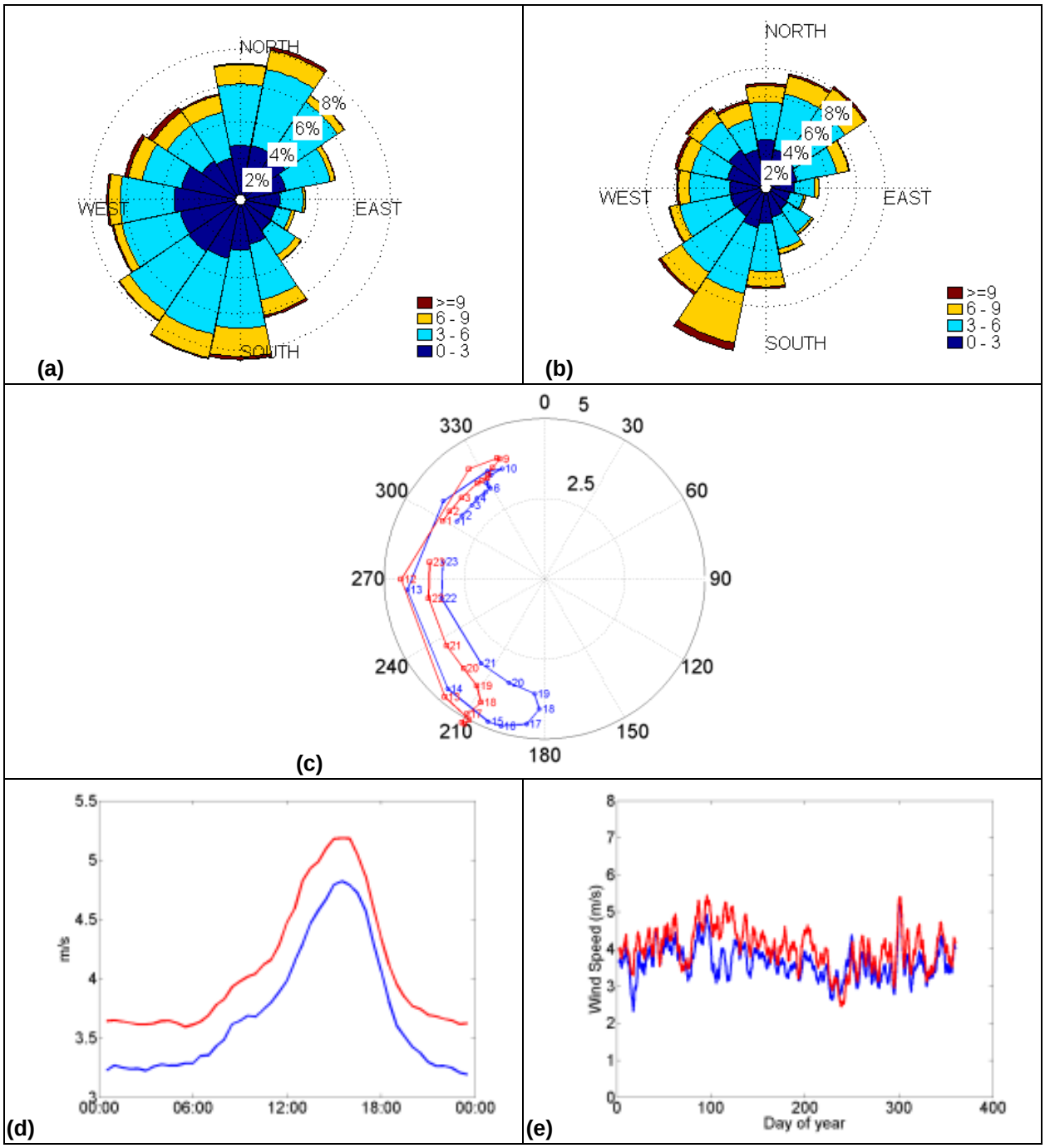

Figure 5-24. Wind direction and speed for Morgan and Stones Bays for 2008–2012.

Wind rose plots for Morgan Bay (panel *a*) and Stones Bay (panel *b*). Directions are given as the direction from which the wind is blowing. Overall segment length represents frequency of occurrence as labeled by the concentric rings. Color patches represent wind speeds in meters per second. Color patch length shows the frequency of occurrence of the wind speed range in that direction, on the same length scale as the concentric rings. Panel *c* shows the mean wind hodograph for each bay. Data labels are hour of day (some labels were omitted for clarity). Panel *d* shows mean wind speeds by time of day. Panel *e* shows wind speed as a function of day of the year. For panels *c*, *d*, and *e*, Morgan Bay is in blue, and Stones Bay is in red.

Figure 5-25 shows turbidity plotted as a function of wind speed. After turbidity observations are sorted by wind speed they are smoothed by a 100-point moving average filter to reduce variability and expose trends. Both bays clearly show an increasing turbidity response with wind speed. Stones Bay responds with higher turbidity values at identical wind speeds.

Because no measurements were taken directly of waves and their associated bottom stress, values were estimated through the use of modeling. WEMo was used to calculate wave heights and bed shear stress for the entire 4-year record of AVP data and plotted against turbidity (**Figure 5-25b and c**, respectively). The plots again show an increasing relationship with turbidity. The response of Stones Bay to wave height is higher than that of Morgan Bay; much higher for the most extreme values of wave height. The response of each bay to bed shear stress shows a cross-over between about 0.1 and 0.17 Newton m^{-2}. Whereas in the data thus far Stones Bay has always shown a larger response to wind and wave height, here the opposite is true. In this region, Morgan Bay is more turbid than Stones Bay for identical bed shear stress values. Again, as shear stress increases, turbidity values in Stones Bay cross over and become much greater for the extreme values of stress.

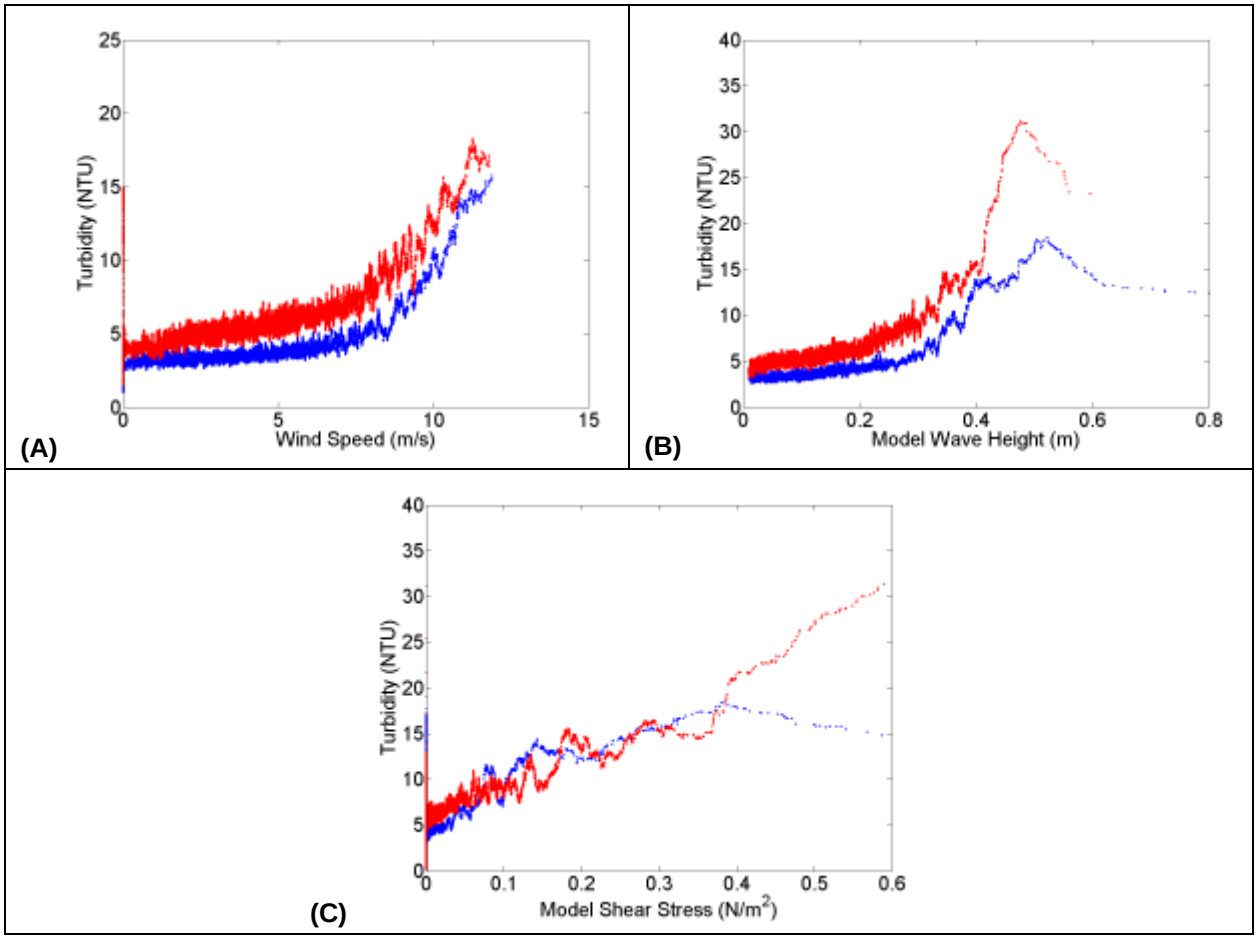

Figure 5-25. Turbidity versus wind speed (A); wave height (B); and sheer stress (C).
Wave height and bed shear stress were model output from WEMo. Morgan Bay is in blue, and Stones Bay is in red.

Figure 5-26 shows an example of data where, after close examination, it is clear that the observed resuspended sediment is being advected to the measurement site. Wind vectors in the top panel show that the period of time from October 16 through most of October 19 was moderately windy, with speeds ranging from 5–8 m s^{-1}. The remaining part of the time was calm. During the windy period, the wind was blowing in a largely down-estuary direction. This encourages the fresher surface water to flow down-estuary, which in the absence of significant vertical mixing allows for estuarine return flow of up-estuary directed bottom water. This can be observed in the brown line of the bottom panel where it is shown that the bottom current direction is pointing upstream for the first two days of the observation period. This can also be seen in the salinity record where there is an approximately half-meter thick salty layer that remains on the bottom as the rest of the water column modulates in salinity with the tide. High turbidity values in the record closely match high salinity during the windy period (r=0.70 with 1 hour lag in turbidity). Because the high turbidity values recur with the same frequency as the flood tide, if the source of the turbidity were local resuspension one might expect that the turbidity would closely correlate with current speed, however it does not (r=0.27), the turbidity correlates with salinity. This is an indication that it is being advected in on the flood tide from somewhere down-estuary. When the wind becomes more calm the turbidity clears up (r=0.27 with 0.5-hour lag in turbidity), which is an indication that wind/wave induced stress is an essential factor creating sediment resuspension from down-estuary.

Sediment resuspension in the NRE is dominated by the effects of wind-driven waves. Of the two bays that we studied, Stones Bay has been shown to have stronger winds largely due to the earlier arrival and higher speeds of the diurnal southwest winds. Stones Bay is overall more turbid than Morgan Bay. Turbidity rises as a smooth function of wind speed; however it begins to rise more rapidly at speeds of approximately 7 m s^{-1}. Limited fetch, deeper water, and slower current speeds protect Morgan Bay from higher bed stresses; consequently the sediments in Morgan Bay are less frequently suspended. The turbidity response to similar wind speeds and wave heights is greater in Stones Bay (the less protected environment). Through the use of wave modeling we show that for Morgan Bay, more sediment is eroded for equivalent stress values when the stresses are low. For larger values of stress, Stones Bay shows a greater response to increasing stress. Current speeds during the observation period were not shown to have an effect on turbidity.

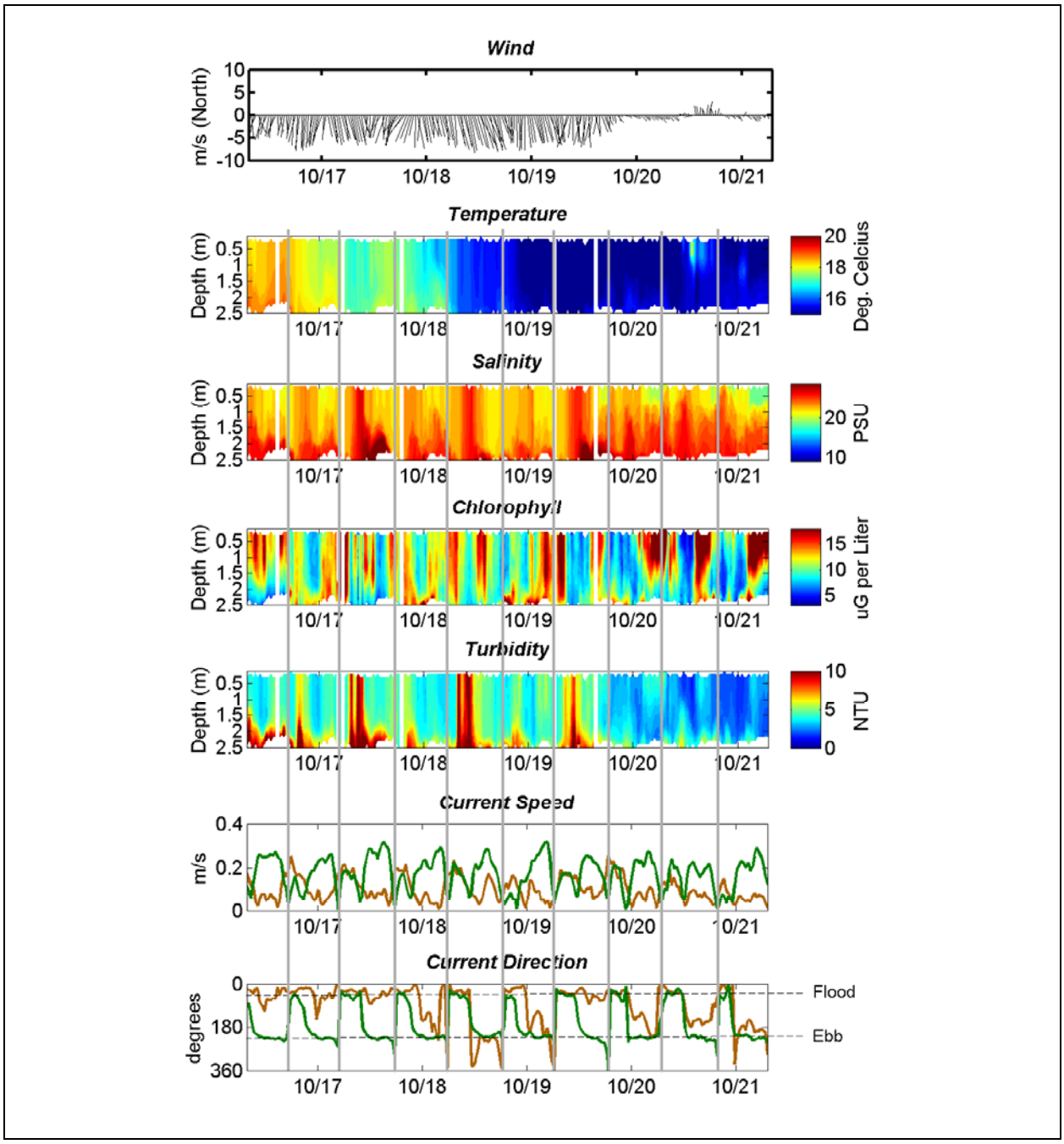

Figure 5-26. Data from both the AVP and the ADCP taken from Stones Bay beginning October 16, 2009, extending into October 21, 2009.

The top panel shows wind with the line segments pointing in the direction toward which the wind was blowing. The following four panels show data taken from the vertical profiler with water depths measured from the surface. The last two panels show data from the ADCP where green represents water near the surface (2.0 m above bottom ≈ 0.5 m below the surface) and brown represents water near the bottom (0.5 m above bottom ≈ 2.0 m below the surface). Vertical lines indicate the onset of flood derived from the surface water current directions.

Spatial Gradients of Salinity, Nutrients, Phytoplankton Biomass, and Organic Carbon

Station J16 (37.6 km upstream from the inlet) was generally the upper limit of salt water intrusion in the NRE (**Figure 5-27**). However, during the low flow period of July 2011 salinity reached approximately 6 at Station L1 (41.9 km upstream). Dissolved inorganic nitrogen (DIN) decreased in a near monotonic fashion from Gum Branch toward the inlet. The exception was a tendency for DIN to increase between Stations L2 and L1. The approximately 0.4 mg L^{-1} increase between these stations located only 400 m apart was statistically significant ($p=0.015$, $N=13$, paired t-test for samples collected on the same days) and is likely due to effluent from the Lauradale waste water treatment plant outflow (National Pollutant Discharge Elimination System permit: NC0036226) located near Station L1 (NCDENR, 2007).

The steep decline in DIN in the upper 10 km of the river was not accompanied by increases in chl *a* (**Figure 5-27**). Also, phosphate (PO_4^{-3}) did not decline in a similar manner to nitrate as would be expected if phytoplankton uptake were the dominant driver of the observed downstream decline in DIN within the freshwater reaches. DIN in the freshwater reaches is dominated by NO_3^- (Hall et al., 2012). Together, the evidence suggests that DIN attenuation in the freshwater reaches of the New River is most likely due to denitrification rather than phytoplankton uptake. Denitrification likely constitutes a large loss term of DIN and large flux of carbon dioxide (CO_2) out of the freshwater reaches.

The downstream gradient of particulate organic carbon (POC) matches the downstream gradient of chl *a* (**Figure 5-27**), which suggests that algal carbon is a dominant source of POC in the NRE. Particulate carbon fluxes to the sediment are the major mechanism for long-term carbon storage within estuaries (Day et al., 1989; Hobbie 2000). Therefore, denitrification within the freshwater reaches may also impact the net carbon budget of the estuary by reducing algal primary production due to the decreased downstream flux of bioavailable nitrogen.

Unlike POC, dissolved organic carbon (DOC) concentrations were higher at upstream stations, which suggests that the major source is terrestrially derived material from within the watershed. On average DOC concentrations were approximately 2 times higher than POC concentrations. The impact of this large flux of organic matter to the NRE on its carbon budget is unclear. Much of the terrestrial DOC within the river is likely to be refractive (Raymond and Bauer, 2001). However, exposure to sunlight during transport through the estuary may help breakdown refractive, high molecular weight DOC into smaller, more bioavailable forms (Osburn et al., 2012). Understanding the biological reactivity of this large pool of carbon is a key unknown within the NRE and estuaries in general (Osburn et al., 2012; Raymond and Bauer, 2001).

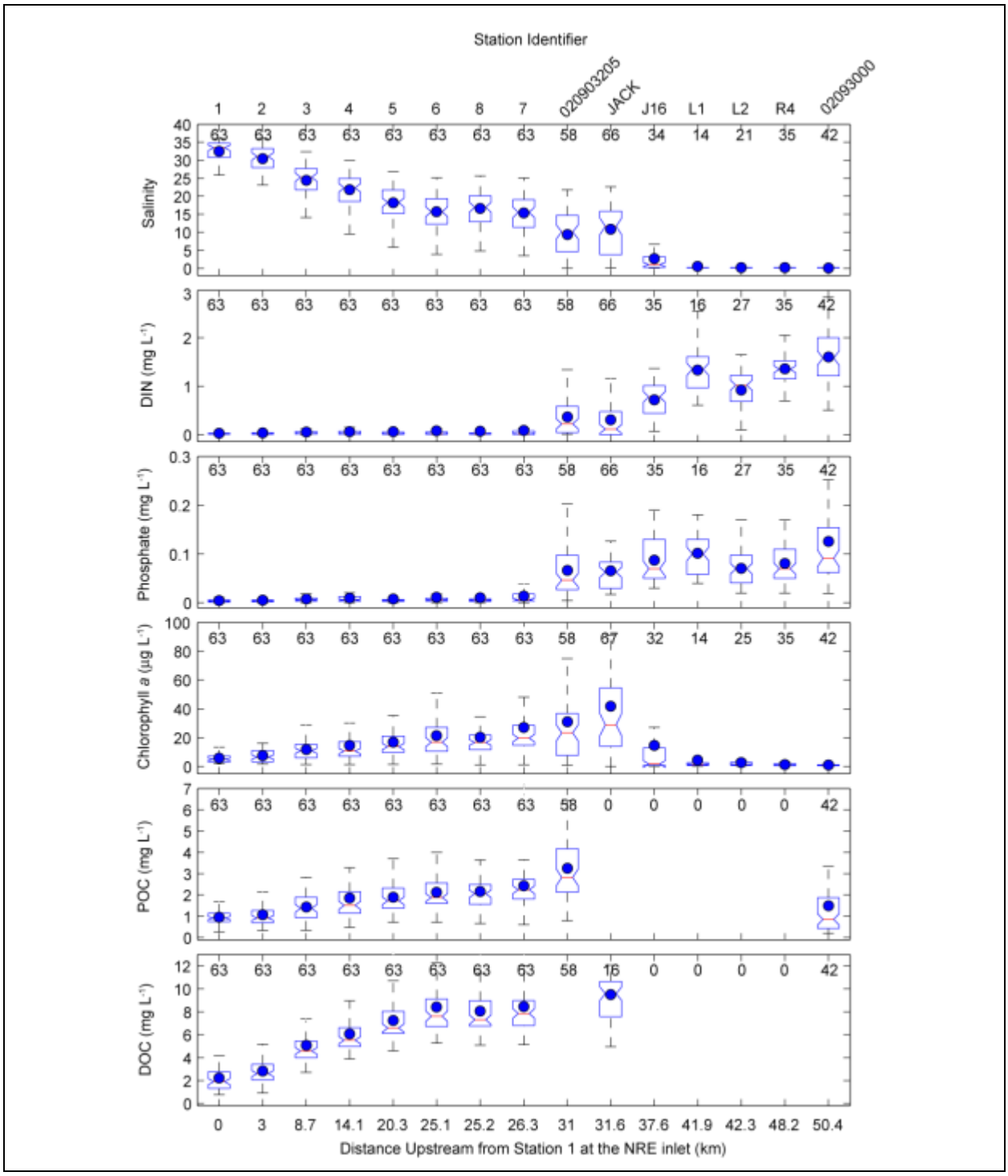

Figure 5-27. Box and whisker plots of the along stream distribution of salinity, DIN, PO_4^{3-}, chl *a*, POC, and DOC.

Numbers at top of each panel represent the number of samples (N). Horizontal red lines represent median values. Notches represent the 95% confidence interval for the median. Blue boxes are interquartile range. Whiskers are 1.5 times the interquartile range. Outliers are not shown. Solid blue circles represent arithmetic mean values.

Phytoplankton biomass rose steeply at Station J16 and reached a maximum at the old Highway 17 bridge where salinity averaged approximately 10. The steep gradients of DIN and chl *a* over this 6 km reach of the estuary indicate that this is a region of high biological significance with regards to nutrient and carbon cycles of the estuary. The phytoplankton biomass maxima occur as the nutrient-laden freshwater ages during downstream transport within the estuary allowing phytoplankton time to assimilate the riverine DIN load and grow (Hall et al., 2012; Peierls et al., 2012). This occurs at a freshwater age of approximately a week (Hall et al., 2012; Peierls et al., 2012), which, during the study period, occurred most often in the upper estuary near Jacksonville (**Figure 5-19**). As a result, DIN drops precipitously within the upper estuary, and is most often at submicromolar levels downstream of Station 7 (**Figure 5-27**). These levels of DIN are low enough to limit phytoplankton growth (Altman and Paerl, 2012; Cloern, 1999) and cause chl *a* to decline steadily with increasing distance downstream. Phosphate also declines as phytoplankton biomass builds. However, for most of the year recycling and diffusion from the sediments maintains PO_4^{-3} at levels that should saturate phytoplankton growth rates (Hall et al., 2012). The exception is during the cooler months when high demand by algal blooms and reduced rates of recycling can lead to growth limiting concentrations (Hall et al., 2012). Because inputs of new nutrients are largely derived from the river, changes in river flow shift the chl *a* maximum and the region of steep decline in nutrients further downstream during higher flows and upstream during lower flows (Hall et al., 2012; Peierls et al., 2012).

Evaluation of Main Stem Versus Tributary Effects on Water Quality

Although it is clear that the New River is a dominant source of nutrients to the estuary, the tributaries are also sources of nutrients and other potential pollutants to the estuary. Two of the primary tributaries of the upper NRE are Northeast and Southwest Creeks. As in the main stem of the estuary, both of these creeks have, at times, exhibited symptoms of eutrophication including harmful algal blooms and bottom water hypoxia. It is difficult, however, to determine whether these symptoms are due to in situ eutrophication from nutrient loading within the tributary watersheds or due to inputs of impacted waters from the main stem. There is some concern about the potential for substantial nutrient loads to the main stem from Northeast Creek due to occasionally high measurements of DIN (Mallin and McIver, 2010). To provide a qualitative understanding of the influences of these tributaries on water quality within the main stem of the NRE, water quality indicators were compared between Stations 6 and 8 (mouths of Southwest and Northeast Creeks, respectively) and Station 7. If nutrient or sediment inputs from these tributaries are substantially degrading water quality within the main stem, then one would expect water quality to be comparatively poor at the creek mouths compared to the main stem. **Table 5-5** shows the p values for Kruskal-Wallis comparisons of median values from surface water quality indicators collected at Stations 6, 7, and 8 from 2007–2011. Only six of the 27 parameters tested showed significant differences (α liberally set at 0.1) between the stations. These six parameters were turbidity, primary productivity, particulate nitrogen, and all measured forms of phosphorus (e.g., particulate phosphorus, PO_4^{-3}, total dissolved phosphorus). For each of these parameters, concentrations were highest within the mainstem compared to the mouths of the creeks (**Figure 5-28**). Mixing of creek water into the main stem waters would, therefore, decrease the mainstem concentrations of these parameters. It is important to note that this does not mean that water quality within these creeks has not been degraded. It just indicates that these tributaries do not appear to be contributing to the degradation of water quality within the main stem of the estuary.

Table 5-5. Results from Kruskal-Wallis comparisons of medians from Stations 6, 7, and 8 for basic water quality, nutrients, and phytoplankton indicators.

Basic Water Quality	P value	Nutrients	P value	Phytoplankton	p value
Salinity	0.43	NO_3^-	0.26	Chl *a*	0.11
DO	0.94	NH_4^+	0.96	1˚ Productivity	**0.06**
Turbidity	**0.021**	DIN	0.82	Peri	0.34
K_{PAR}	0.16	TDN	0.18	Fuco	0.41
CDOM	0.56	DON	0.17	19-hex	0.39
TSS	0.90	PO_4^{-3}	**0.018**	Viol	0.25
POC	0.12	TDP	**0.029**	Allo	0.22
DOC	0.55	SiO_2	0.44	Zea	0.90
		PN	**0.046**	Chl *b*	0.55
		PP	**0.001**		

CDOM = chromophoric dissolved organic matter; Chl *a* = chlorophyll *a*; chl *b* = chlorophyll *b*; DIN = dissolved inorganic nitrogen; DO = dissolved oxygen; DOC = dissolved organic carbon; DON = dissolved organic nitrogen; K_{PAR} = attenuation coefficient for photosynthetically active radiation; NH_4^+ = ammonium; NO_3^- = nitrate; PO_4^{-3} = phosphate; POC = particulate organic carbon; TDN = total dissolved nitrogen; TDP = total dissolved phosphorus; TSS = total suspended solids; SiO_2 = silica; PN = particulate nitrogen; PP = particulate phosphorus; pigment abbreviations are in the List of Acronyms; 1˚ Productivity = primary productivity

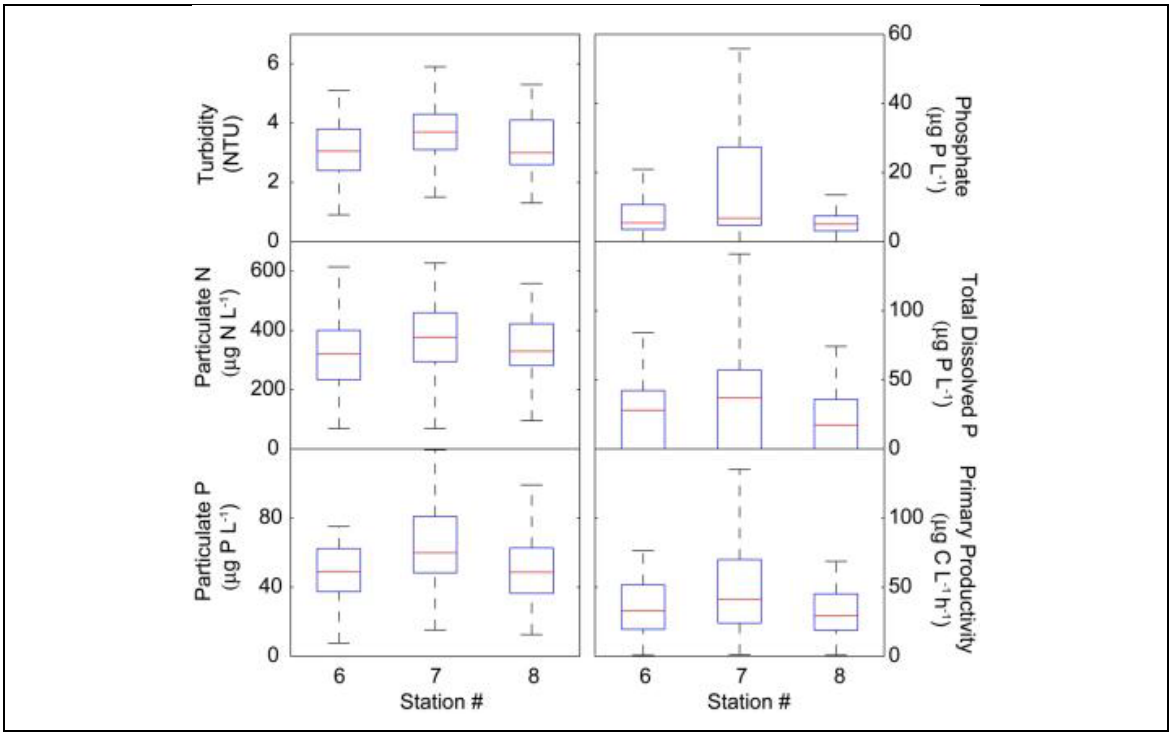

Figure 5-28. Box and whisker plots of water quality indicators from the mid-channel Station 7 and Stations 6 and 8 at the mouths of Southwest and Northeast Creeks, respectively.

Median values in red. Blue boxes are interquartile range. Whiskers are 1.5 times the interquartile range.

Frequency of Bottom Water Hypoxia

We determined the frequency by year and station of hypoxic conditions using near-bottom readings from the vertical profile data (**Table 5-6**). Hypoxia can be defined by a range of DO concentrations. We followed the moderate (less than 4 mg/L) and severe hypoxia (less than 2 mg/L) definitions of Buzzelli et al. (2002). Note that we did not examine the vertical or across-channel spatial extent of these hypoxic conditions. **Figure 5-29** shows a histogram of the frequency of moderate and severe bottom water hypoxia in relation to the temperature of the bottom water. The frequency of all measured bottom water temperatures are shown for comparative purposes. It is clear that both moderate and severe hypoxia were restricted to times of the year when water temperatures were high. No bottom water hypoxia events were detected when bottom water temperatures were below 22°C.

Table 5-6. Frequency of bottom water hypoxia by water year and by station with water depth and stratification intensity.

		Total Sample Number (N)	Number of Hypoxic Samples		Water Depth (m) Mean (SD)	Stratification Intensity Bottom–Surface Salinity
			<4 mg L^{-1}	<2 mg L^{-1}		
By water year	2008	96	6	0	2.8 (0.7)	2.1 (2.3)
	2009	104	13	7	2.8 (0.6)	3.3 (3.1)
	2010	96	0	0	2.8 (0.8)	2.7 (3.7)
	2011	112	11	3	2.8 (0.7)	2.5 (3.4)
	2012	96	9	3	2.7 (0.6)	2.0 (1.7)
By station[a]	CL-1	63	0	0	3.7 (0.7)	0.9 (1.7)
	CL-2	63	0	0	3.0 (0.4)	2.3 (2.8)
	CL-3	63	2	0	2.2 (0.3)	2.1 (1.9)
	CL-4	63	10	3	3.5 (0.3)	4.1 (3.3)
	CL-5	63	9	3	3.0 (0.3)	3.4 (3.3)
	CL-6	63	6	3	2.3 (0.3)	2.4 (3.8)
	CL-7	63	4	1	2.1 (0.2)	2.4 (2.9)
	CL-8	63	8	3	2.5 (0.2)	2.1 (2.7)

[a] Measurement depth was 0.5 m less than the water depth at each station.

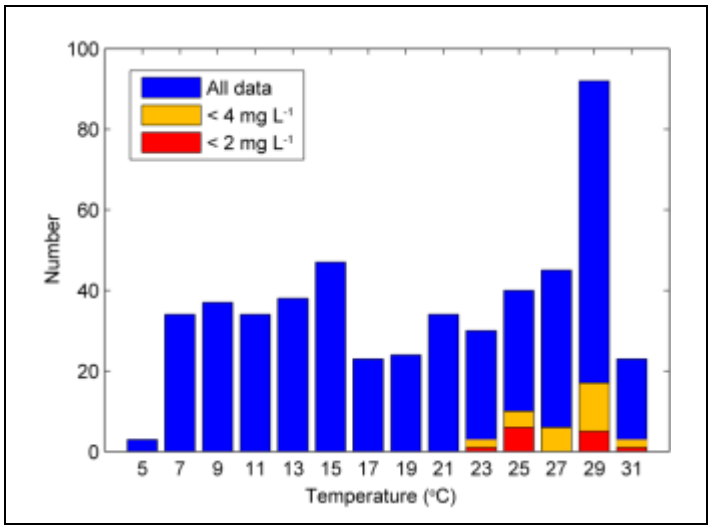

Figure 5-29. Histogram of bottom water temperatures from all data from Stations 1–8 and during moderate (less than 4 mg L^{-1} DO) and severe (less than 2 mg L^{-1}) bottom water hypoxia, *x*-axis labels are the centroids of 2°C bins.

Between water-years, the greatest frequency of hypoxia was seen in water-year 2009, followed by 2011 and 2012 (**Table 5-6**). Water-years 2008 and 2010 were notable for their low frequencies of occurrence of hypoxic events. Spatially, hypoxia was most common at the middle and upper estuarine Stations 4, 5, 6, and 8 (**Table 5-6**). Hypoxia was never observed at the downstream Stations 1 and 2.

Bottom water hypoxia is a complicated phenomenon that results from a combination of biological and physical drivers (Malone et al., 1988; Sanger et al., 2011). As previously mentioned, temperature is both a physical driver through its impact on oxygen solubility but also a strong biological driver by controlling rates of microbial respiration. Availability of organic carbon as a substrate for respiration is another important biological driver of bottom water hypoxia, and consequentially bottom water hypoxia is often intimately related to the production and deposition of organic matter by phytoplankton in the overlying surface waters (Malone et al., 1988). Riverine discharge delivers nutrients that fuel phytoplankton production but also decreases surface water salinity and enhances stratification. Riverine discharge, therefore, also has important impacts on both the biological and physical drivers of hypoxia. Shelf waters of Onslow Bay are generally near saturation with respect to oxygen (Dafner et al., 2007). As high oxygen Onslow Bay water is advected upstream in the bottom layer, oxygen depletion proceeds at a rate that is dependent on the balance between oxygen loss via respiration and oxygen inputs that occur when oxygen is mixed or diffuses into the bottom water from above. Turbulent mixing driven by winds and tides is generally much more important than diffusion in re-aerating the bottom waters. This is likely the reason why hypoxia was not observed at the downstream stations. Bottom waters at these stations were likely too “new” and the vertical mixing due to tides too vigorous for hypoxia to occur.

To gain a greater understanding of the role physical drivers play in the temporal and spatial occurrence of hypoxic events, we compared the frequency of hypoxia to water column depth and stratification intensity. Depth is an important determinant of oxygen penetration because stronger vertical mixing is required to mix oxygen downward into deeper layers and bottom waters of

deeper stations are more like to lie below the pycnocline which acts as a barrier to vertical mixing. Additionally, deeper areas are often low-energy, depositional centers for fine-grained, organic-rich sediments which contributes to high biological oxygen demand. The difference between bottom and surface water salinity is used as a surrogate for density differences between the two layers (Hall et al., 2012), an indicator of the intensity of vertical mixing which ventilates the bottom waters.

The analyses reveal that some of the prominent temporal and spatial patterns can be explained by water depth and stratification intensity. The high frequency of hypoxic events during 2009 coincided with the highest observed average stratification intensity. Spatially, the high frequencies of hypoxia at Stations 4 and 5 are also explained by high degrees of stratification and by the greatest water depths.

A simple regression model was designed to assess the influence of physical factors (temperature and stratification) on bottom water DO at the Morgan Bay AVP site.

$$DO_{bottom} = DO_{saturation} + t * r_{20} Q_{10}^{(T-20)/10} + v\Delta S$$

Daily average vertical profiles of temperature, salinity, and DO were constructed by averaging across the 10 cm depth bins for the 48 semi-hourly profiles. Bottom water DO, temperature, and salinity were then defined as the deepest measured DO concentration, temperature, and salinity of the daily average vertical profiles. Similarly, surface water salinity was defined as the shallowest measured salinity for each daily average vertical profile. Differences between surface and bottom salinity (ΔS) were used as an indicator of stratification intensity (Hall et al., 2012). Under well-mixed conditions, DO should be near saturation ($DO_{saturation}$) throughout the water column and bottom water oxygen should decline with time since the last mixing event as stratification resumes and impedes mixing of surface water oxygen into the bottom waters (Borsuk et al., 2001). The empirical model was designed to represent these vertical processes while horizontal processes were ignored. This simplification of bottom water DO dynamics is appropriate when longitudinal gradients in bottom water DO are minimal compared to vertical gradients and residence times (advective time-scales) are much longer than the frequency of mixing events (Borsuk et al., 2001). The co-occurrence of hypoxia between stations in the mid-estuarine region of the NRE (Stations 4–7) and the long flushing times (months) of the estuary (Ensign et al., 2004; Hall et al., 2012; Peierls et al., 2012), justify these assumptions. Mixing events were defined as times when ΔS of the semi-hourly records were less than 0.5. This value was based on work in the Neuse River Estuary that showed 0.5 to be a threshold ΔS value below which there was no well-defined pycnocline, and vertical physical/chemical gradients were negligible (Hall, 2009). The time since the last mixing event (t, in days) was then determined by subtracting the time of each daily average vertical profile from that of the most recent mixing event. Depletion of bottom water DO was assumed to be exponentially (a Q_{10} relationship) related to temperature due to effects of temperature on biogeochemical oxygen consumption processes (e.g., respiration, sulfide oxidation, nitrification; Borsuk et al., 2001). DO saturation concentration was calculated based on bottom water temperature according to (Borsuk et al., 2001). Model coefficients r_{20}, v, and Q_{10} were estimated by fitting the model to bottom water DO data from the Morgan Bay AVP (June 2008–October 2012) using the non-linear least square curve fitting routine “lsqcurvefit” in MATLAB version 7.11 R2011b (The Mathworks, Natick, MA).

The best fit model was as follows:

$$DO_{bottom} = DO_{saturation} + t*0.084*2.19^{(T-20)/10} - 0.17\ \Delta S;\ R^2 = 0.79$$

This simple empirical model fit the data well (**Figure 5-30**) and captured 79% of the observed variability in bottom water DO at Morgan Bay. Much of the variability is due to the seasonal effect of temperature on DO solubility (**Figure 5-30**). However, the model also captures the shorter term impacts of changes in stratification. **Figure 5-31** provides a more detailed look at the observed and modeled DO dynamics during the period from late summer through early winter 2009. During this period there were several prolonged stratification events (mid-August, late September, and late November) during which DO was low or declining. Mixing events where ΔS declined and DO increased abruptly are also evident (late August, late September, and late November) and the model captures the impacts of these events reasonably well.

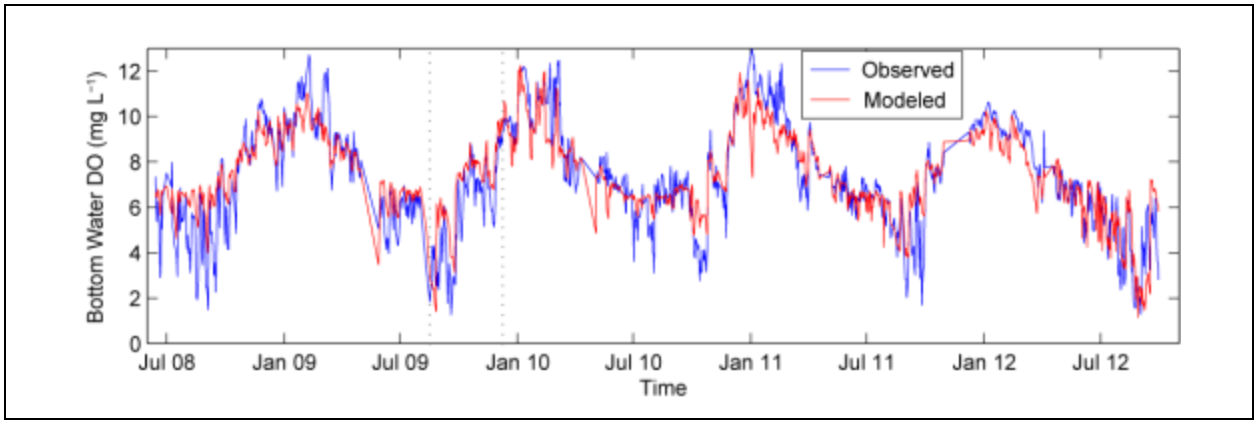

Figure 5-30. Observed and modeled bottom water DO at the Morgan Bay AVP from June 2008 through November 2012.

Vertical dashed lines indicate the time period covered in Figure 5-31.

The model coefficients are also in reasonable agreement with literature values for shallow marine systems. The rate of oxygen consumption at 20°C (r_{20} = 0.084 mg L^{-1} d^{-1}) is close to the value (r_{20} = 0.13 mg L^{-1} d^{-1}) estimated for the Neuse River Estuary using a similar empirical model (Borsuk et al., 2001). The observed Q_{10} of 2.19 is only slightly higher than the average (Q_{10} = 1.75) of sediment oxygen consumption rates for 336 estuaries compiled by Bailey (2005). As expected, the coefficient for the stratification effect was negative which is consistent with the role of stratification in impeding oxygen penetration from the surface layer.

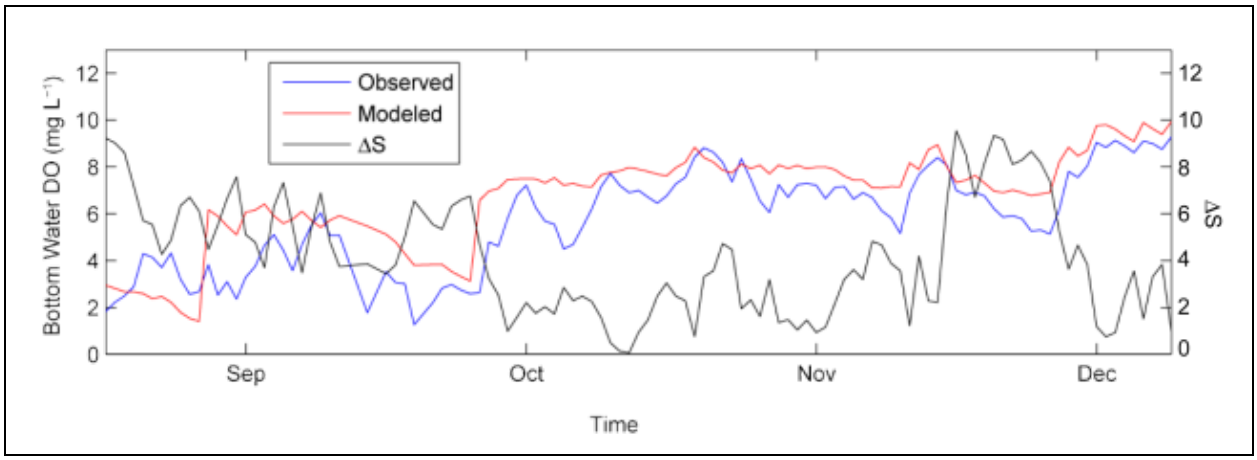

Figure 5-31. Observed and modeled bottom water DO with stratification intensity at the Morgan Bay AVP from July through December 2009.

The success of this simple, physically driven (temperature and salinity were the only inputs), empirical model suggests that hypoxia formation in the NRE is largely regulated by physical processes. The thin bottom water layer of the NRE (approximately 1 m) lies above organic rich muds. This ensures that biochemical oxygen demand is consistently high. All that is necessary for hypoxia formation is the impedance of vertical mixing from the surface layer by stratification. Higher temperatures increase the rate of oxygen depletion once stratification is established.

The tight control of hypoxia by stratification and temperature is consistent with findings in the nearby Neuse River Estuary (Borsuk et al., 2001; Buzzelli et al., 2002) and may be a common characteristic of shallow estuaries that are prone to intermittent periods of stratification and that are underlain by organic rich (high biochemical oxygen demand) sediments. This indicates that short-term (days to months) variability in bottom water DO is weakly coupled to short-term variability in phytoplankton production in the overlying waters. As such, the classic sequence of algal proliferation, sedimentation, and decay that often drives hypoxia of lakes and deeper estuaries (Borsuk et al., 2001; Buzzelli et al., 2002) is not likely to be observed in the NRE. However, over longer-term periods (years), eutrophication (or oligotrophication) related changes in the organic content and biochemical oxygen demand of the sediments are likely to alter bottom water oxygen consumption rates with resultant changes in the frequency and duration of hypoxic events.

Assessment of Trends in the Data

Assessment of Monitoring Design

Spatial Resolution

Data collected from the Dataflow instrumentation provided high spatial resolution (approximately 10 m) data necessary to determine the dominant spatial distribution patterns of five key water quality parameters (temperature, salinity, DO, turbidity, and chl *a*). This information was used to quantitatively assess the degree with which the down-stream spacing of the eight monthly sampling stations was capable of capturing the spatial variability of key water

quality components. From February 2009 through October 2012, 45 monthly Dataflow transects were conducted. Data for one profile were lost due to instrument malfunction reducing the number of transects to 44. Some of the water quality parameters for one transect (June 14, 2010) were also impacted by an instrument malfunction and were eliminated from the subsequent analyses. Prior to analyses of the Dataflow transects, cross-river excursions and loops were removed to produce a single transect line along the main axis of the estuary. The spatial coverage of the 44 transect lines are shown in **Figure 5-32**. All 44 transect profiles of temperature, salinity, DO, turbidity, and chl *a* data are available in **Appendix 5-A**.

Figure 5-32. Map showing track lines of 44 Dataflow sampling transects in relation to the eight monthly monitoring stations in the NRE.

Assuming that the Dataflow sampler captures the vast majority of the variability in water quality along the axis of the estuary, we statistically determined the effect of increasing or decreasing the spatial sampling resolution on the percentage of water quality variability that is captured. The methodology employed is described in detail by Jassby et al. (1997). Latitude and longitude data were converted to distance (km) from the beginning of each transect. Linear interpolation was used to produce an evenly spaced data series with a 0.02 km (20 m) sampling interval. This resulted in only minor adjustments to data values due to the close proximity of the raw sample spacing (mean = 13.7 m; SD =5.1 m) to the extrapolated interval. This transect was considered to represent the "true" variability of water quality within the estuary. Data from the "true" transect were then resampled across a range of potential equidistant spatial sampling intervals from very coarse (10s of km) to very fine intervals (10s of m).

If the original "true" transect contained *N* data points, and the resampled transect contained *n* data points, then there are $m = N/n$ possible resampled transects for each sampling interval. Cases where *m* was not an integer value were handled using circular systematic sampling whereby sampling was wrapped back to the beginning of the record (Jassby et al., 1997). For each transect, the means of the resampled data sets (y_k) were then compared against the "true" transect mean ($\bar{Y}$) to determine the influence of spatial sampling interval on precisely representing the "true" transect mean. This was accomplished by calculating the variance of the estimated transect mean ($\bar{y}_{\text{sys}}$) as shown in Equation 5-1:

$$\text{var}\left(\bar{y}_{\text{sys}}\right) = \frac{1}{m}\sum_{k=1}^{m}(y_k - \bar{Y})^2 \qquad \text{(Eq. 5-1)}$$

In **Figure 5-33**, var($\bar{y}_{sys}$) has been normalized by var($\bar{y}_{sys}$) for the case when n = 1, and the data points represent the mean values and standard deviations for the normalized var($\bar{y}_{sys}$) from the 44 Dataflow transects. As sample spacing decreases (equivalently sample number is increased), the resampled transects approach the "true" full transect ($n = N$) and the error in reproducing the "true" transect mean (variance of the transect mean) approaches zero. This methodology produces a set of exponential decay curves that provide an objective tool for: (1) estimating the number of equally spaced sampling stations necessary to provide a given level of precision in estimation of estuary wide mean water quality conditions, and (2) comparing the spatial autocorrelation structure of water quality parameters, between transects, and between estuarine systems (Jassby et al., 1997). The slope of the decay functions describe the sensitivity of accurately depicting mean water quality conditions within the estuary to changes in sampling interval. As will be shown below, this information is useful for evaluating how changes in either temporal or spatial sampling resolution will impact the ability of monitoring efforts to accurately and precisely represent mean estuarine water quality conditions.

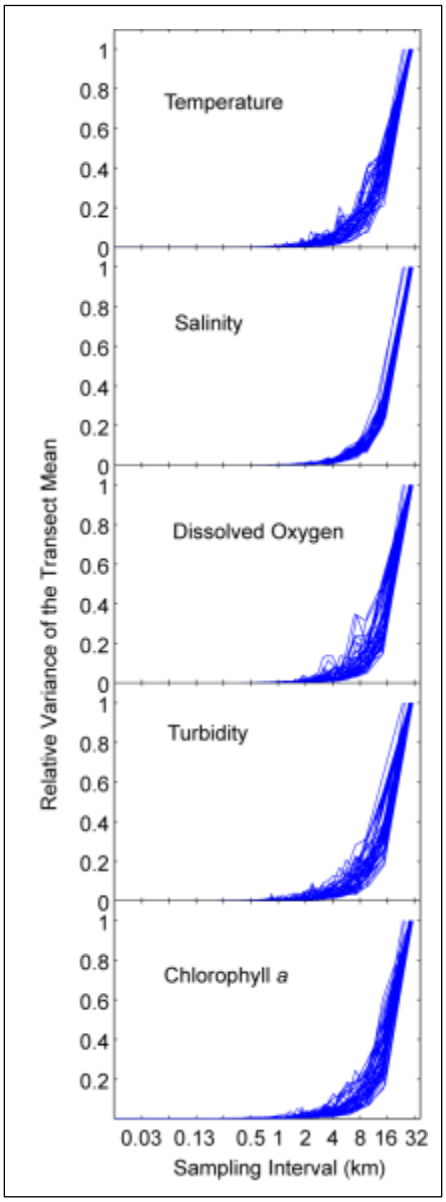

Figure 5-33. Influence of spatial sampling interval on the precision of estimates of the transect means for 44 Dataflow transects.

Curves represent the variance of the transect means normalized by the variance with only one sample per transect (n = 1).

These analyses of the spatial and temporal variability of water quality conditions involve only those values that can be measured rapidly and in situ to produce a very high resolution data set. These basic water quality parameters represent a small subset of the water quality parameters measured during the project period. However, given the strong relationships between these variables and other water quality parameters, it is likely that the underlying spatial and temporal structures of unassessed parameters are similar. For example, the structure of the variability of CDOM is likely to be similar to that of salinity because freshwater inputs are the dominant source of CDOM to the estuary. Similarly, the variance structure of nutrient concentrations is likely similar to those of salinity and chl *a* since freshwater inputs and phytoplankton uptake represent primary sources and sinks, respectively, of nutrients within the NRE.

For each water quality parameter, the number of equidistant samples required to precisely capture the "true" transect mean decreased rapidly from 32 km (1 sample per transect) through

approximately 8-km spacings (**Figure 5-33**). Below spacings of approximately 8 km, the rate of decline in the error started to asymptote toward zero. Differences in dominant modes of variability between water quality parameters determined the rate of decay of error in the mean estimate as sample number increased. Variations in salinity were generally smooth through space and, as a result, estimates of mean transect salinity with a relative variance of less than 10% could be made with a sampling interval of 8 km or about 4 equidistant sampling stations within the estuary. At a 4-km interstation sampling interval, the approximate sampling interval for the monthly discrete sampling stations, the relative variance for salinity was consistently less than 5% for all 44 transects. Temperature, DO, turbidity, and chl *a* contained a higher degree of small-scale variability and greater degree of variability in spatial structure between transects. For these parameters, an 8-km interstation interval resulted in an approximately 5–30% relative variance of the transect mean, and at a 4-km spacing, the relative variance ranged from less than 5% to greater than 10%.

Temporal Resolution

To assess the effectiveness of the temporal resolution of the monthly water quality monitoring program, data from the AVP's were similarly used to produce high temporal resolution time series of these key water quality parameters. For each parameter, data for each bihourly profile were averaged to produce a mean water column concentration. Missing data values were linearly interpolated from nearest neighbors. Each data set from the two AVPs was broken into four, year-long records that ran from June to June from 2008 through 2012. As with the Dataflow records, annual means of these records were considered to represent "true" mean conditions within the NRE against which means produced with increasingly large sampling intervals are compared. Analysis of these annual ensembles, rather than the full 4-year records, was performed to increase the confidence of estimates of how the variance of the record means changes with decreased temporal sampling resolution. Splitting the data into annual periods precludes information on the decay of variance at sampling intervals greater than a year. However, such a crude level of temporal resolution for estuarine monitoring is rarely considered.

The vast majority of variability in temperature lies in the annual cycle. As a result, the decay of temperature variance with increased sampling resolution is consistently very steep when sampling resolution increases from one sample per year to four samples per year (**Figure 5-34**). Bi-monthly sampling (approximately 64 d sampling period) results in a relative variance for temperature of approximately 1%. Because DO is so closely tied to temperature through its solubility characteristics, it exhibited a similar consistent decay and bimonthly sampling resulted in a relative variance of less than 5%. Short-term variability was more important for salinity, turbidity, and chl *a*. However, even for these variables that are highly impacted by short-term effects like precipitation and nutrient loading events, tidal oscillations, and wind events, the relative variance of the annual mean decreased to approximately 5% at a monthly sampling period.

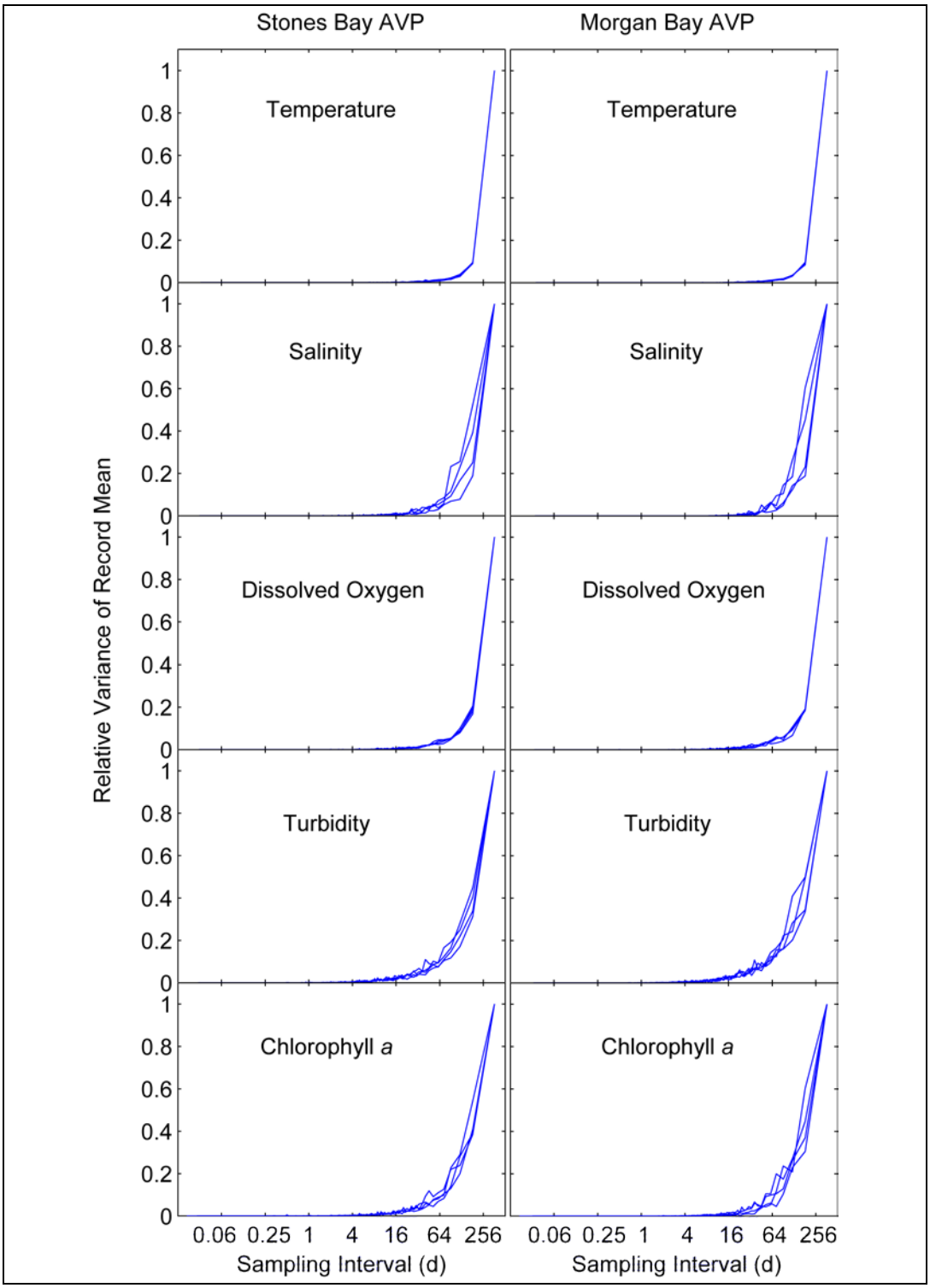

Figure 5-34. Influence of temporal sampling interval on the precision of estimates of the record means for four annual records from the AVPs at Stones and Morgan Bays.

Curves represent the variance of the transect means normalized by the variance with only one sample per annual record (n = 1).

Figure 5-35 shows the standard error of estimated means for both spatial (Dataflow) and temporal (AVP) records across a range of potential spatial and temporal sampling intervals. Within a transect, variability in temperature and DO was relatively minor, and this resulted in a relatively good estimation (less than 10% standard error) of transect means with the approximately 4-km sampling resolution employed by the routine monthly monitoring program. The spatial patchiness of turbidity and chl *a* and the strong downstream salinity gradient resulted in much higher (10–30%) standard errors for these variables at a 4-km sampling resolution. Chl *a*, in particular, had a high degree of small-scale patchiness. As a result, to consistently produce a standard error less than 10% would require a spatial sampling resolution of less than 0.25 km.

Compared to variability in standard errors among transects, variability in standard errors among years was much smaller as indicated by the tight interquartile ranges and lack of outliers within the boxplots for the AVP records. The two AVP records also displayed very similar patterns of decline in standard errors as temporal sampling interval increased. For both AVP records, standard errors for temperature and DO fell to approximately 10% with only quarterly sampling (90 d) as a result of strong seasonal components to their variability. Standard errors for salinity also decreased rapidly with the Morgan Bay record having a standard error below 10% at a 90 d sampling. Standard error for the Stones Bay record did not fall to 10% at a 90 d sampling interval. This difference is likely due to the higher degree of short-term, tidal variability at Stones Bay as indicated by the greater drop in standard error from 1 d to 0.5 d sampling intervals. For both AVP records, chl *a* and turbidity had standard errors of 10–30% at a quarterly sampling interval but fell below 10% with monthly sampling.

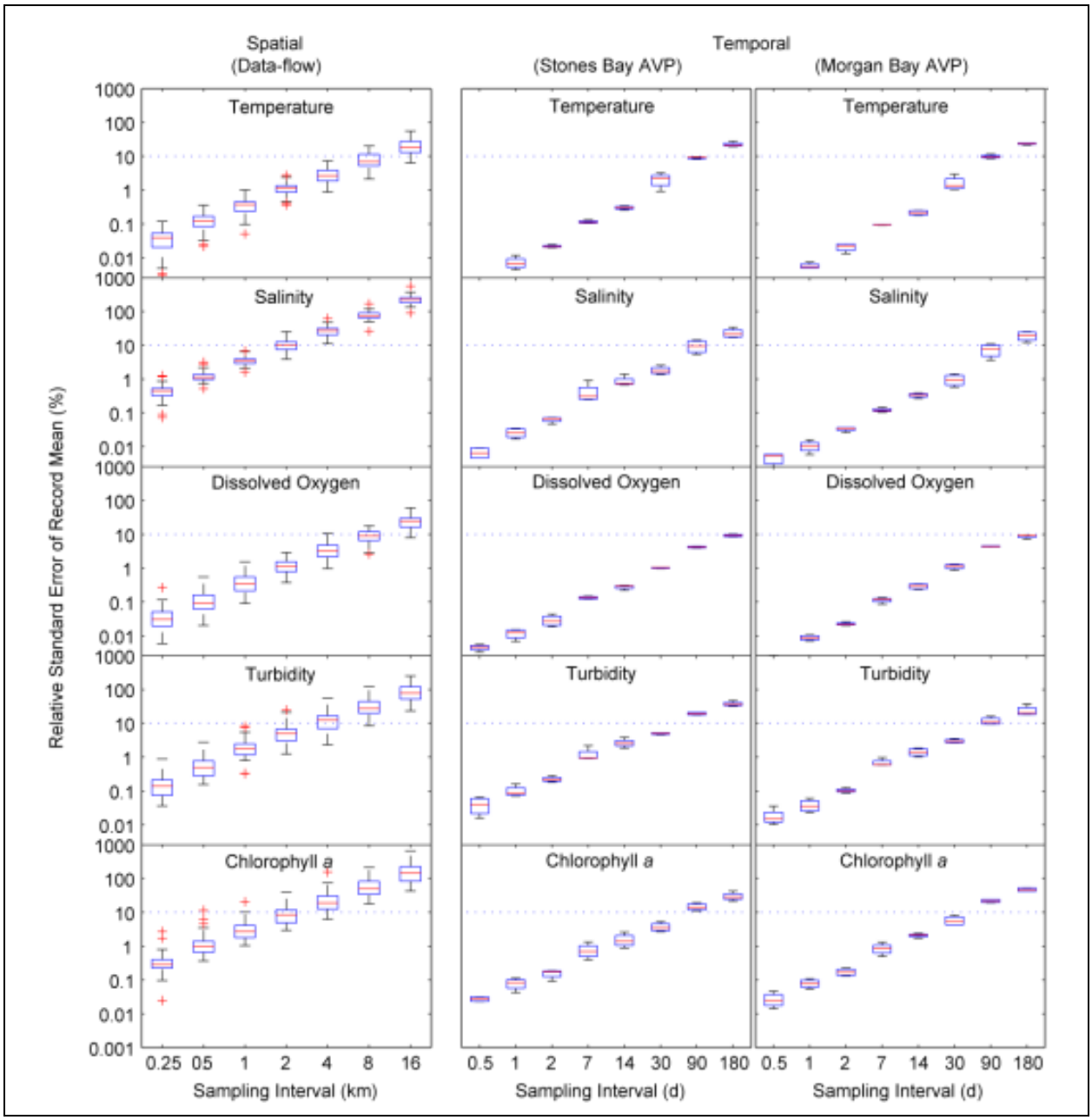

Figure 5-35. Box and whisker plots of the relative standard error of record (Dataflow and AVP) means of key water quality parameters across a range of potential spatial and temporal sampling intervals.

Boxes represent the interquartile range for the standard errors of the 44 Dataflow and four annual AVP records. Red horizontal lines are the median values. Whiskers represent 1.5 times the interquartile range. Values outside the whiskers are represented with red "+" symbols. Dashed lines indicate a standard error of 10%.

To compare how changes in spatial or temporal sampling resolution would affect the monitoring program's ability to reproduce record means, slopes of the exponential decay of the variance of the record means were compared within the region of the decay curves (**Figures 5-33** and **5-34**) that approximated the sampling resolution of the monitoring program.

The exponential decay of variance of the record means as sampling interval decreases can be expressed as shown in Equation 5-2:

$$\mathrm{var}\left(\bar{y}_{\mathrm{sys}}\right) = \beta \frac{1}{n^{\propto}} \qquad \text{(Eq. 5-2)}$$

where α is a coefficient that describes the rate of decay as sample number (*n*) increases and β is a proportionality constant (Jassby et al., 1997). Decay of the variance of the record means as shown in **Figures 5-33** and **5-34** were fit to this function using a least-squares minimization procedure ("lsqcurvefit," MATLAB version R2010b, Natick, MA) to obtain estimates for α and β. The derivative of Equation 2 with respect to *n* is shown in Equation 5-3:

$$\frac{d\mathrm{var}\left(\bar{y}_{\mathrm{sys}}\right)}{dn} = \propto \beta n^{\propto - 1} \qquad \text{(Eq. 5-3)}$$

Using the best-fit parameters for α and β, we evaluated Equation 5-3 with *n* values that corresponded to the sampling intervals (approximately 4 km spatial, and approximately 30 d temporal) of the monthly monitoring program. This provides a quantitative measure of the sensitivity of the variance of the mean to changes in spatial and temporal sampling interval from the current monitoring program design. This allows for an objective means for determining how enhancing or reducing spatial or temporal monitoring efforts will affect the monitoring programs ability to accurately and precisely quantify the average condition of the estuary.

Figure 5-36 shows boxplots of the slopes of the exponential decay of the variance of the mean evaluated at the sample number corresponding to the temporal and spatial resolution of the monthly monitoring program. Higher values indicate a greater sensitivity to change in the number of equidistant samples or equivalently sampling interval. There was no consistent trend across variables in sensitivity to changes in spatial or temporal sampling interval. This indicates that, in general, the spatial and temporal resolutions of the monitoring program were well balanced with respect to its ability to reproduce spatial and temporal averages of estuarine conditions. However, for a unit increase in sampling effort, better approximations for salinity could be gained by increasing spatial resolution while for temperature the opposite is true. For turbidity and chl *a*, the impacts of changes in temporal resolution versus spatial resolution varied depending on which AVP record was examined. For Stones Bay, which is more prone to turbidity events driven by wind induced resuspension and tidal advection of suspended sediments, increased temporal resolution would more effectively reduce error of mean estimates than increased spatial resolution.

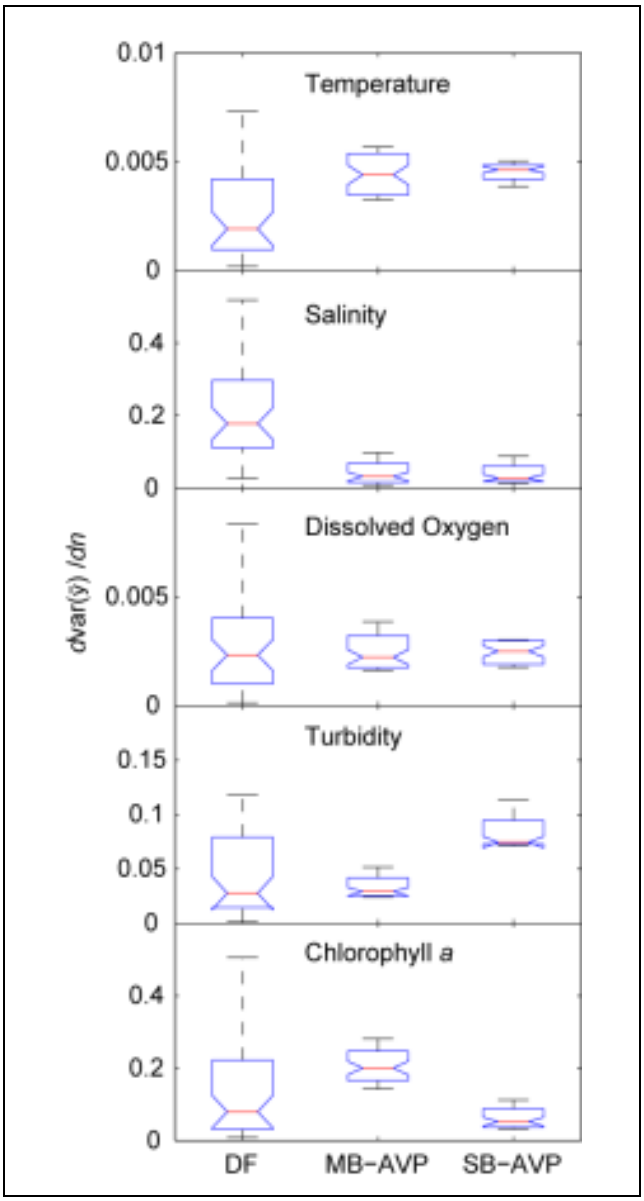

Figure 5-36. Box and whisker plots of the slopes of the exponential decay of the variance of the mean transect evaluated at 4 km spatial resolution for the Dataflow (DF) transects and at 30 d temporal resolution for the Morgan Bay (MB-AVP) and Stones Bay (SB-AVP) AVP annual records.

Boxes represent the interquartile ranges, red lines indicate median values, while whiskers represent 1.5 times the interquartile range. Notches represent the 95% confidence intervals for the median values.

Assessment of Seasonal and Annual Variabilities in the Data

Inter-annual Variability

Median values of 15 key water quality parameters that represent light conditions, nutrient concentrations, sediment concentrations, phytoplankton biomass and production were compared between water years 2008–2012. Values that were below the limits of detection were assigned a

value of zero. **Figure 5-37** shows box plots of the inter-annual variability of the 15 parameters and **Table 5-7** shows results from a Kruskal-Wallis comparison of medians between years. Vertical averages (mean of surface and bottom water samples) from all of the eight monthly sampling stations (Stations 1-8) were used for the analyses.

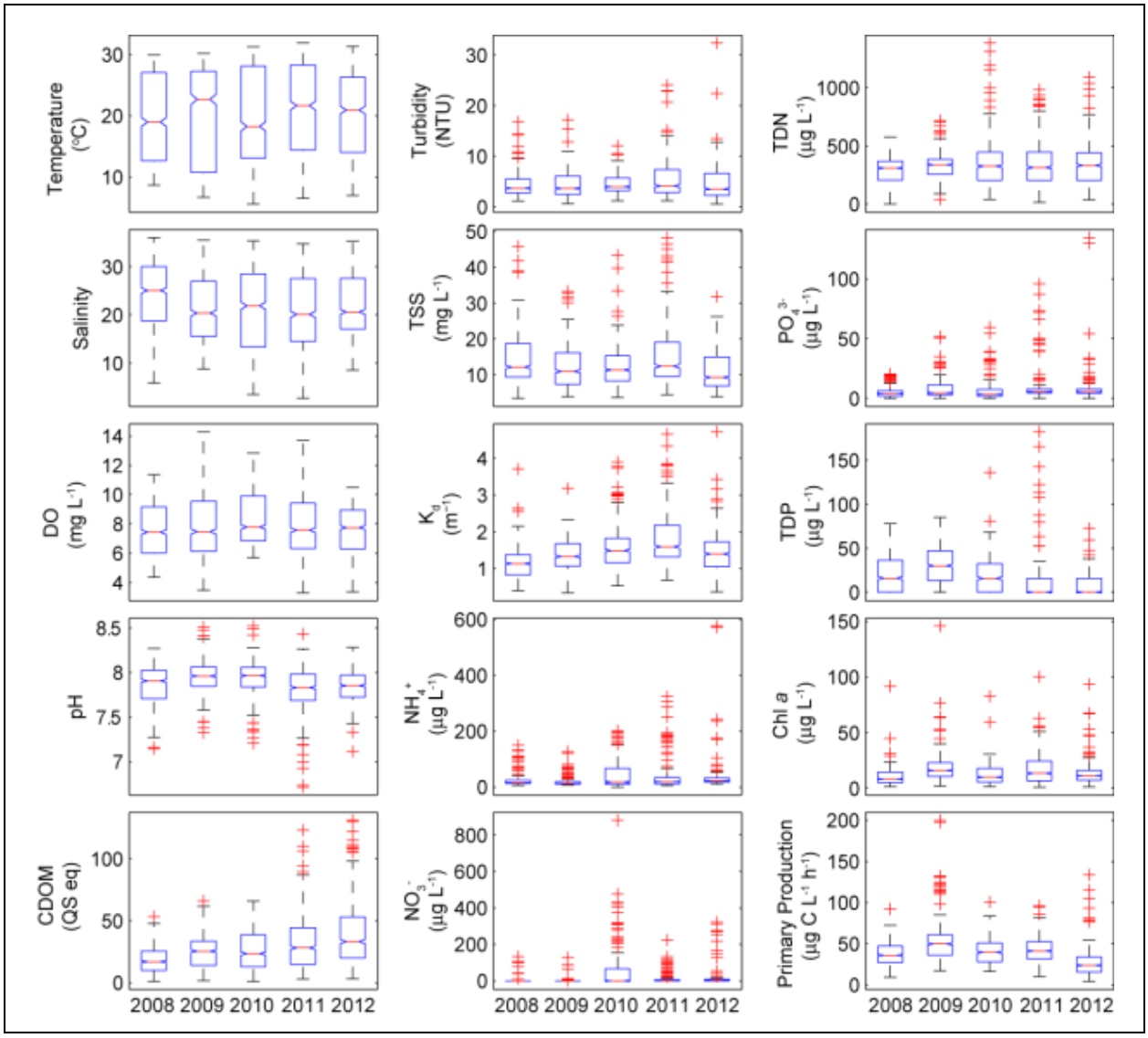

Figure 5-37. Inter-annual variability of key water quality parameters pertaining to basic water chemistry, light and nutrient availability, phytoplankton biomass, and primary productivity.

Boxes represent the interquartile range. Red horizontal lines are the median values. Notches in the boxes represent the 95% confidence interval for the median values. Whiskers represent 1.5 times the interquartile range. Values outside the whiskers are represented with red "+" symbols. Data are grouped by water-year. Abbreviations are provided in the list of abbreviations.

Kruskal-Wallis tests revealed significant inter-annual variability for all but three parameters, temperature, turbidity, and TDN. Even during this period of rapid global warming, similarity of temperature between years was not surprising over such a short 5-year time period. Turbidity

within the NRE is largely driven by sediment resuspension due to tides and wind (Whipple et al., 2012, in preparation) rather than runoff from the watershed. Therefore, the lack of inter-annual variability in turbidity is also understandable because there is no indication that tides or winds have changed over the study period. In contrast, the lack of significant inter-annual variability in TDN was surprising. Variability in nutrient loads to the estuary is largely governed by fluctuations in riverine discharge of the New River (Hall et al., 2012), which varied significantly between water-years (**Figure 5-6**). Thus, one would expect high flow years to be accompanied by higher TDN concentrations within the estuary. The drought year of 2008 showed no outliers while the other years with significant freshwater discharge events and lower salinities (**Figure 5-37**) contained numerous outliers. Therefore, there is some indication of the influence of flow on TDN. The stability of TDN between years suggests that part of the TDN pool is relatively stable through time. This stability is certainly not due to the inorganic pools, which showed significant inter-annual variation (**Figure 5-37** and **Table 5-7**) that followed trends in freshwater input. This suggests that the inter-annual stability of TDN is likely due to the dissolved organic nitrogen (DON) fraction. Impacts of the stability of DON on phytoplankton production and biomass are currently not known because the DON pool is composed of unspecified bioavailable and refractory components (Altman and Paerl, 2012). However, it seems likely that much of the DON is refractory because inter-annual trends in phytoplankton biomass and productivity track inputs of DIN (NO_3^- and NH_4^+) more closely than TDN with peaks during the 2009 and 2010 wet years (**Figure 5-37**). Nutrient limitation bioassays that included amendments of NRE waters with New River DON generally support this conclusion (Altman and Paerl, 2012).

Table 5-7. Results from Kruskal-Wallis comparison of median values of 15 key water quality parameters from the NRE grouped by water-year and by season.

Parameter	p Values for Kruskal-Wallis Comparisons Between	
	Years	Seasons
Temperature	8×10^{-1}	$\mathbf{6 \times 10^{-83}}$
Salinity	$\mathbf{2 \times 10^{-3}}$	$\mathbf{1 \times 10^{-2}}$
Dissolved oxygen	6×10^{-2}	$\mathbf{5 \times 10^{-68}}$
pH	$\mathbf{7 \times 10^{-6}}$	$\mathbf{1 \times 10^{-5}}$
Chromophoric dissolved organic matter	$\mathbf{2 \times 10^{-6}}$	$\mathbf{6 \times 10^{-4}}$
Turbidity	1×10^{-1}	$\mathbf{9 \times 10^{-11}}$
Total suspended solids	$\mathbf{5 \times 10^{-5}}$	$\mathbf{4 \times 10^{-12}}$
Light attenuation coefficient	$\mathbf{4 \times 10^{-12}}$	$\mathbf{6 \times 10^{-4}}$
Ammonium	$\mathbf{4 \times 10^{-9}}$	$\mathbf{4 \times 10^{-11}}$
Nitrate	$\mathbf{7 \times 10^{-23}}$	$\mathbf{4 \times 10^{-12}}$
Total dissolved nitrogen	3×10^{-1}	$\mathbf{9 \times 10^{-19}}$
Phosphate	$\mathbf{4 \times 10^{-6}}$	$\mathbf{2 \times 10^{-20}}$
Total dissolved phosphorus	$\mathbf{2 \times 10^{-13}}$	$\mathbf{2 \times 10^{-10}}$
Chlorophyll *a*	$\mathbf{1 \times 10^{-7}}$	$\mathbf{3 \times 10^{-6}}$
Primary production	$\mathbf{2 \times 10^{-15}}$	$\mathbf{5 \times 10^{-14}}$

Values in bold indicate significance at $\alpha = 0.05$.

Light attenuation within the estuary increased from 2008 through 2011, but decreased slightly in 2012. Suspended sediments scatter light, whereas CDOM and phytoplankton biomass (chl *a*) are the principal light absorbers in estuaries (Biber et al., 2008; Woodruff et al., 1999). Together, these three optically active constituents are the dominant drivers of light attenuation. Despite having significant inter-annual variability, none of these constituents followed the same inter-annual pattern as light attenuation. So, it appears that the observed increase in light attenuation was produced by changes in the relative contributions of these parameters to light attenuation.

Seasonal Variability

Significant variability between seasons was observed for all 15 of the water quality parameters analyzed (**Table 5-7**). As previously shown with the AVP data, the strong seasonal cycle in DO is driven by changes temperature dependent solubility (**Figure 5-38**). Salinity showed the weakest degree of seasonality of the 15 parameters, although a significant trend of higher summer salinities and lower spring salinities was detected. Concentrations of nitrogen species (NH_4^+, NO_3^-, and TDN) were highest during the fall and winter, and phosphorus species were highest during the summer and fall seasons and were much lower during winter and spring. Although the NRE is nitrogen-limited throughout much of the year, the winter season appears to be time when phosphorus limitation is most likely to occur. This conclusion is supported by results from previous nutrient limitation bioassays (Mallin et al., 2005) and observed stoichiometry of nutrient concentrations during winter dinoflagellate blooms (Hall et al., 2012). Light attenuation reaches a minimum during winter when turbidity, suspended sediments, CDOM, and chl *a* are also at their annual minimum. The summer maximum of total suspended sediments is also reflected in turbidity measurements (**Figures 5-38** and **5-21** from the Stones Bay AVP data). It is unclear what produces this trend, but it likely results from seasonal changes in wind direction (Whipple et al., 2012, in preparation). Phytoplankton biomass and productivity are highest during the summer months, probably as a result of more favorable light levels for growth in this somewhat CDOM stained and turbid estuary.

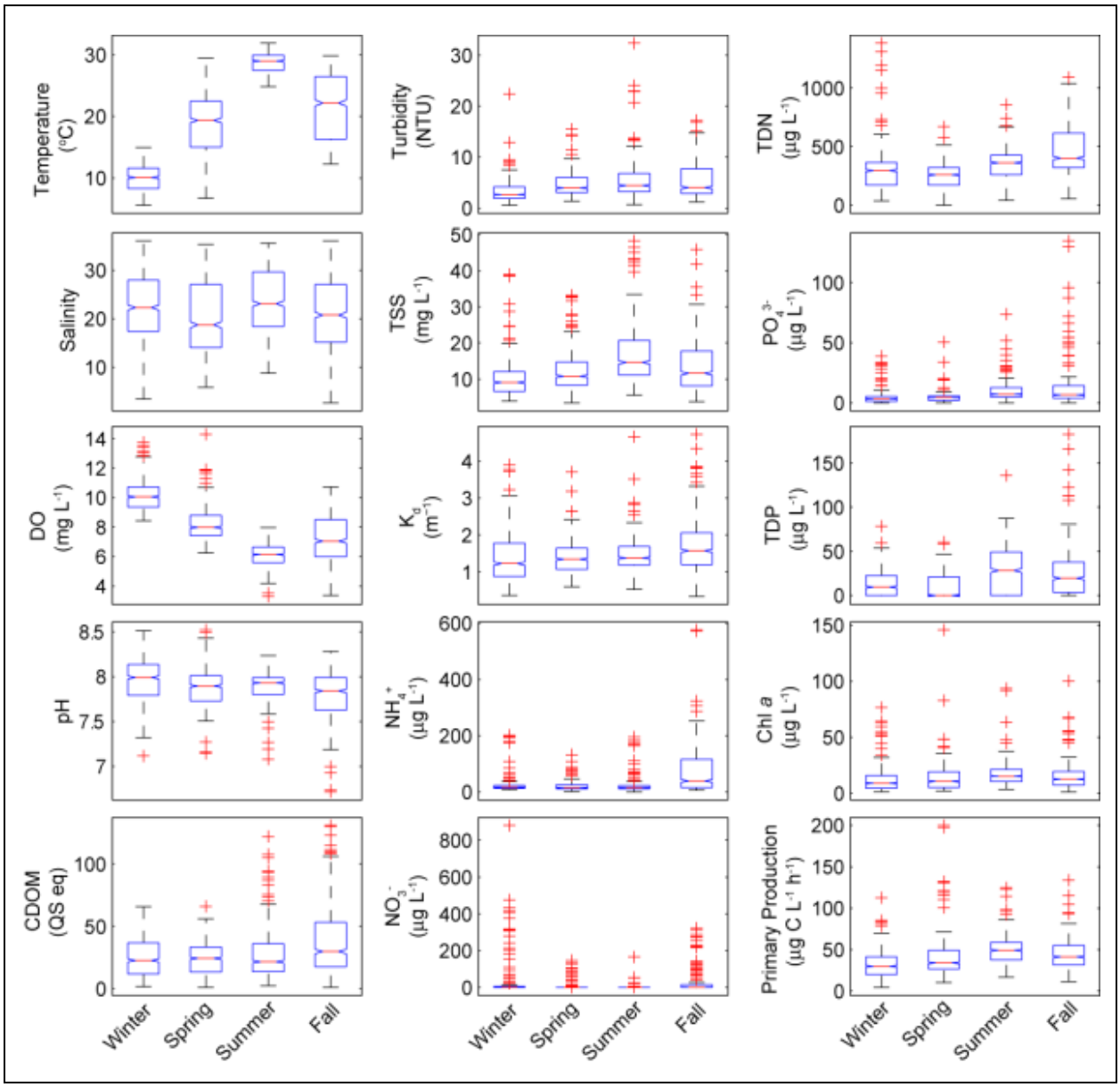

Figure 5-38. Seasonality of key water quality parameters pertaining to basic water chemistry, light and nutrient availability, phytoplankton biomass, and primary productivity.

Box plot configuration is identical to Figure 5-37. Data are grouped by seasons (winter: December–February, spring: March–May, summer: June–August, and fall: September–November). Abbreviations are provided in the list of abbreviations.

Recommendations for DCERP2 Monitoring

The current monitoring approach of monthly sampling along a transect of eight stations spaced roughly 4 km apart captures a large degree of the variability in water quality and habitat condition within the estuary and produces acceptable levels of error (generally less than 10% standard error) in capturing mean estuarine conditions. Sampling error that arises from the temporal and spatial resolution of the monitoring design is nearly equal. Therefore, the temporal

and spatial resolution of the monitoring program are well balanced with respect to its ability to capture mean conditions of the major regions of the estuary including all those regions surrounded by MCBCL.

However, the eight monthly monitoring stations do not capture the entire freshwater to marine continuum of the NRE. Under most of the observed flow regimes during this 5-year study period, saltwater intrusion penetrated upstream of Jacksonville. The low salinity and tidal fresh-water reaches of the NRE have been comparatively under sampled. The limited sampling by the USGS, the North Carolina Division of Water Quality, and Research Project AE-3 that has occurred from Jacksonville upstream shows that the upper estuarine and lower tidal-freshwater reaches of the estuary are highly active zones of chemical and biological transformations. Much of the nutrient attenuation from sources within the watershed occurs within this region and the area around Jacksonville is commonly the site of algal bloom formation which subsequently can be flushed into downstream regions of the estuary. Enhanced monitoring of these upper estuarine and tidal-freshwater regions would provide a greater understanding of the fluxes and composition of materials entering the larger downstream estuarine reaches.

Conclusions and Implications for Future Research

Key Scientific Findings—Fundamental Cause-and-Effect Relationships

A primary goal of this monitoring activity was to determine how natural and anthropogenic stressors impact water quality and habitat condition of the NRE, and when possible, to identify stressors that are readily manageable from those that are not. Nutrient concentrations, chl *a*, turbidity, and DO are common indicators of estuarine water quality used to establish ratings of overall estuarine health and habitat condition (U.S. EPA, 2012). With regards to these indicators, a common theme emerged from analysis of this comprehensive 5-year data set: natural processes such as riverine discharge, temperature, wind stress, stratification, and tidal currents exhibited the strongest and most direct linkages with water quality and habitat condition.

Bottom water hypoxia was closely linked to temperature and stratification with no apparent relationship to algal blooms which may have resulted from anthropogenic nutrient loading. Water column turbidity was strongly linked to wind-induced sediment resuspension events. Periods of high algal biomass were linked to optimal levels of river flow which provided enough nutrients for phytoplankton biomass development but also sufficient residence time within the estuary for growth to occur. During periods when flows were too high for phytoplankton biomass development, nutrient concentrations within the estuary were high. Thus, nutrient concentrations within the estuary were also largely determined by riverine discharge.

Although the short-term variability in these indicators of ecological condition were strongly linked to physical factors that are not under human control, this does not indicate a lack of anthropogenic effects on water quality. Acute anthropogenic events such as sewage spills or upgrades to sewage treatment facilities have had readily observable impacts on water quality within the NRE (Mallin et al., 2005). However, these types of acute anthropogenic events did not occur during the 5-year study period. Anthropogenic effects such as the accumulated impact of changes in land use within the basin are likely to form a slower moving trend that would not be captured within a short 5-year study period. As development within the NRE watershed

continues, this comprehensive data set will serve as an invaluable baseline against which to evaluate future changes in water quality.

Findings Supportive of Current Base Management Practices

The high level of nutrient loads to the estuary is a primary concern for water quality and habitat condition. Downstream gradients of nutrient concentrations along the river to upper estuary indicate that most of the nutrient load to the estuary is from upstream riverine sources that lie upstream of MCBCL. Comparison of nutrient concentrations between the mouths of two major tributaries with main stem nutrient concentrations corroborates this conclusion. The comparatively low load of nutrients, sediments, and other pollutants from the land area comprising MCBCL likely stems from the large areas of undeveloped forest and wetlands within the Base.

Findings with Implications for Future Base Management

Under all but the highest river flow conditions, residence times of the NRE are long enough that phytoplankton have time to fully assimilate nutrient loads. The result is that within much of the estuary, including most of the region surrounded by MCBCL, phytoplankton growth is strongly nutrient limited and any increases in nutrient load would result in higher levels of phytoplankton biomass. The region downstream of the Highway 172 bridge appears less susceptible to eutrophication due to strong tidal flushing. The poorly flushed region from Stones Bay to Morgan Bay is particular susceptible to eutrophication. As MCBCL plans for development of areas that drain to this region of the estuary, mitigation of nutrient loading to this region of the estuary should be emphasized. Sediment inputs should also be mitigated because they often carry high levels of absorbed nutrients and therefore represent an important non-point nutrient source. An effective strategy for mitigating impacts on water quality from future Base activities could include the following: (1) minimizing sediment losses by maintaining natural vegetation and ground cover particularly within riparian areas, (2) minimizing impervious surfaces (e.g., parking lots, pave lots), (3) minimizing the use of chemical fertilizers in residential areas (e.g., lawns, gardens, golf courses), and (4) promoting retention of water within tributary watersheds by preserving and reclaiming wetlands, using retention ponds, minimizing ditching, and controlling stormwater runoff in developed areas.

Findings with Implications for DCERP2

Based upon the finding of the biogeochemical significance of the upper estuary, plans for DCERP2 include enhanced sampling of the upper estuary near Jacksonville. This enhanced sampling will be critical for understanding the effects of nutrient loading, particularly NO_3^-, on carbon flows within the estuary. It is clear that both denitrification and phytoplankton uptake/assimilation are very important processes driving the downstream attenuation of NO_3^- in the upper estuary. From a carbon budget perspective, these two processes act in opposite manners as sources and sinks of atmospheric CO_2. The denitrification process oxidizes organic carbon with a net release of CO_2. Phytoplankton uptake of NO_3^- fuels phytoplankton primary production, the conversion of CO_2 to organic matter and the first step toward permanent carbon burial in the sediments. Understanding the relative magnitudes of these two processes is critical

for the estuarine carbon budget and for understanding how future changes in NO_3^- load will impact the ability of the estuary to serve as a net source or sink of carbon.

Literature Cited

Alber, M., and J.E. Sheldon. 1999. Use of a date-specific method to examine variability in the flushing times of Georgia estuaries. *Estuarine, Coastal and Shelf Science 49*:469–482.

Altman, J.C., and H.W. Paerl. 2012. Composition of inorganic and organic nutrient sources influences phytoplankton community structure in the New River Estuary, North Carolina. *Aquatic Ecology 42*:269–282.

APHA (American Public Health Association). 1998. Standard Methods for the Examination of Water and Wastewater. American Public Health association, Washington, DC.

Bailey, E.M. 2005. *Measurements of Nutrient and Oxygen Fluxes in Estuarine and Coastal Marine Sediments: Literature Review and Data Report*. University of Maryland Center for Environmental Science. Chesapeake Biological Laboratory. Reference Number: 05-091.

Biber, P.D., C.L. Gallegos, and W.J. Kenworth. 2008. Calibration of a bio-optical model in the North River, North Carolina (Albemarle-Pamlico Sound): A tool to evaluate water quality impacts on seagrasses. *Estuaries and Coasts 31*:177–191.

Boesch, D.F., E. Burreson, W. Dennison, E. Houde, M. Kemp, V. Kennedy, R. Newell, K. Paynter, R. Orth, and W. Ulanowicz. 2001. Factors in the decline of coastal ecosystems. *Science 293*:629–638.

Borsuk, M.E., C.A. Stow, R.A. Luettich, Jr., H.W. Paerl, and J.L. Pinckney. 2001. Modelling oxygen dynamics in an intermittently stratified estuary: Estimation of process rates using field data. *Estuarine, Coastal and Shelf Science* 52:33–49.

Boynton, W.R., and W.M. Kemp. 1985. Nutrient regeneration and oxygen-consumption by sediments along an estuarine salinity gradient. *Marine Ecology Progress Series 23*:45–55.

Buzzelli, C.P., R.A. Luettich, S.P. Powers, C.H. Peterson, J.E. McNinch, J.L. Pinckney, and H.W. Paerl. 2002. Estimating the spatial extent of bottom-water hypoxia and habitat degradation in a shallow estuary. *Marine Ecology Progress Series* 230:103–112.

Cloern, J. 1999. The relative importance of light and nutrient limitation of phytoplankton growth: A simple index of coastal ecosystem sensitivity to nutrient enrichment. *Aquatic Ecology 33*:3–15.

Cloern, J.E. 2001. Our evolving conceptual model of the coastal eutrophication problem. *Marine Ecology Progress Series 210*:223–253.

Cloern, J.E., and A.D. Jassby. 2010. Patterns and scales of phytoplankton variability in estuarine-coastal ecosystems. *Estuaries and Coasts 33*:230–241.

Dafner, E.V., M.A. Mallin, J.J. Souza, H.A. Wells, and D.C. Parsons. 2007. Nitrogen and phosphorus species in the coastal and shelf waters of Southeastern North Carolina, Mid-Atlantic U.S. coast. *Marine Chemistry 103*:289–303.

Day, J.W., and W.M. Kemp (Eds.). 1989. *Estuarine Ecology*. Wiley Interscience: New York, NY.

Emery, W.J. and R.E. Thomson. 1997. *Data analysis methods in physical oceanography*. Elsevier Science Inc.: New York, NY.

Ensign, S.H., J.N. Halls, and M.A. Mallin. 2004. Application of digital bathymetry data in an analysis of flushing times of two North Carolina Estuaries. *Computers and Geosciences 30*:501–511.

Fisher, T.R., L.W. Harding, D.W. Stanley, and L.G. Ward. 1988. Phytoplankton, nutrients, and turbidity in the Chesapeake, Delaware, and Hudson estuaries. *Estuarine Coastal and Shelf Science 27*:61–93.

Hall, N.S. 2009. *Effects of the Vertical Structure of the Water Column on the Phytoplankton in a Shallow, Lagoonal Estuary*. Ph.D. dissertation, University of North Carolina at Chapel Hill, Chapel Hill, NC.

Hall, N.S., H.W. Paerl, B.L. Peierls, A.C. Whipple and K.L. Rossignol. 2012. Effects of climatic variability on phytoplankton biomass and community structure in the eutrophic, microtidal, New River Estuary, North Carolina, USA. *Estuarine and Coastal Shelf Science*. doi: http://dx.doi.org/10.1016/j.ecss.2012.10.004.

Hobbie, J.E. (Ed.). 2000. *Estuarine Sciences—A Synthetic Approach to Research and Practice*. Island Press: Washington, DC.

Jassby, A.D., B.E. Cole, and J.E. Cloern. 1997. The design of sampling transects for characterizing water quality in estuaries. *Estuarine Coastal and Shelf Science 45*:285–302.

Kennish, M., and H.W. Paerl. 2010. Coastal Lagoons: Critical Habitats of Environmental Change. *CRC Marine Science Series*. CRC Press: Boca Raton, FL.

Litaker, R.W., C.S. Duke, B.E. Kenney, and J. Ramus. 1987. Short-term variability and phytoplankton abundances in a shallow tidal estuary. I. Winter and summer. *Marine Biology 96*:115–121.

Lunetta, R.S., J.F. Knight, H.W. Paerl, J.J. Streicher, B.L. Peierls, T. Gallo, J.G. Lyon, T.H. Mace, and C.P. Buzzelli. 2009. Measurements of water colour using AVIRIS imagery to

assess the potential for an operational monitoring capability in the Pamlico Sound Estuary, USA. *International Journal of Remote Sensing 30*:3291–3314.

Madden, C.J., and J.W. Day. 1992. An instrument system for high-speed mapping of chlorophyll *a* and physiochemical variables in surface waters. *Estuaries 15*:421–427.

Malhotra, A. and M.S. Fonseca. 2007. *WEMo (Wave Exposure Model): Formulation, Procedures and Validation*. Center for Coastal Fisheries and Habitat Research, NOAA/NOS/NCCOS. Beaufort, NC. NOAA Technical Memorandum NOS NCCOS #65.

Mallin, M.A., and M.R. McIver. 2010. *New River Estuary Water Quality 2008–2009*. University of North Carolina at Wilmington Center for Marine Science Report 10-02. Report to Environmental Management Division, U.S. Marine Corps Base Camp Lejeune, NC.

Mallin, M.A., M.R. McIver, H.A. Wells, D.C. Parsons, and V.L. Johnson. 2005. Reversal of eutrophication following sewage treatment upgrades in the New River Estuary, North Carolina. *Estuaries 28*:750–760.

Mallin, M.A., and H.W. Paerl. 1992. Effects of variable irradiance on phytoplankton productivity in shallow estuaries. *Limnology and Oceanography 37*:54–62.

Malone, T.C., A. Malej, L.W. Harding Jr., N. Smodlaka, and R.E. Turner (Eds.). 1999. Coastal and estuarine studies. *Ecosystems at the Land-Sea Margin: Drainage Basin to Coastal Sea (Volume 55*). American Geophysical Union: Washington, DC.

Malone, T.C., L.H. Crocker, S.E. Pike, and B.W. Wendler. 1988. Influences of river flow on the dynamics of phytoplankton production in a partially stratified estuary. *Marine Ecology Progress Series 48*:235–249.

Nixon, S.W. 1995. Coastal marine eutrophication: A definition, social causes, and future concerns. *Ophelia 41*:199–219.

NCDENR (North Carolina Department of Environment and Natural Resources). 2007. *White Oak River Basin Wide Water Quality Plan*. North Carolina Department of Environment and Natural Resources, Division of Water Quality, Planning Section, Raleigh, NC. May.

Osburn, C.L., L.T. Handsel, M.P. Mikan, H.W. Paerl, and M.T. Montgomery. 2012. Fluorescence tracking of dissolved and particular organic matter in a river-dominated estuary. *Environmental Science & Technology 46*:8628–8636.

Paerl, H.W. 2002. Primary productivity and producers. Pp. 329–341 in *Manual of Environmental Microbiology (2nd edition)*. Edited by C.J. Hurst. ASM Press: Washington, DC.

Paerl, H.W. 1997. Coastal eutrophication and harmful algal blooms: Importance of atmospheric deposition and groundwaters as “new” nitrogen and other nutrient sources. *Limnology and Oceanography 42*:1154–1165.

Paerl, H.W., K.L. Rossignol, N S. Hall, B.L. Peierls, and M.S. Wetz. 2010. Phytoplankton community indicators of short- and long-term ecological change in the anthropogenically and climatically impacted Neuse River Estuary, North Carolina, USA. *Estuaries and Coasts 33*:485–497.

Paerl, H.W., M.A. Mallin, C.A. Donahue, M. Go, and B.L. Peierls. 1995. *Nitrogen Loading Sources and Eutrophication of the Neuse River Estuary, NC: Direct and Indirect Roles of Atmospheric Deposition*. UNC Water Resources Research Institute Report No. 291. 119 pages.

Pawlowicz, R., B. Beardsley, S. Lentz. 2002. Classical tidal harmonic analysis including error estimates in MATLAB using T tide. *Computers & Geosciences 28*:929–937.

Peierls, B.L., N.S. Hall and H.W. Paerl. 2012. Non-monotonic responses of phytoplankton biomass accumulation to hydrologic variability: A comparison of two coastal plain North Carolina estuaries. *Estuaries and Coasts 35*(6)1376–1392.

Raymond, P.E., and J.E. Bauer. 2001. Use of ^{14}C and ^{13}C natural abundances for evaluating riverine, estuarine, and coastal DOC and POC sources and cycling: A review and synthesis. *Organic Geochemistry 42*:469–485.

Reynolds-Fleming, J.V., F.G. Fleming, and R.A. Luettich. 2002. Portable autonomous vertical profiler for estuarine applications. *Estuaries 25*(1):142–147.

Sanger, D.M., E.M. Smith, G. Voulgaris, E.T. Koepfler, S.M. Libes, G.H.M. Riekerk, D.C. Bergquist, D.I. Greenfield, P.A. Wren, C.A. McCoy, R.F. Viso, R.N. Peterson, and J.D. Whitaker. 2011. Constrained enrichment contributes to hypoxia formation in Long Bay, South Carolina (USA), an open water urbanized coastline. *Marine Ecology Progress Series 461*:15–30.

Sheldon, J.E., and M. Alber. 2006. The calculation of estuarine turnover times using freshwater fraction and tidal prism models: A critical evaluation. *Estuaries and Coasts 29*:133–146.

U.S. EPA (U.S. Environmental Protection Agency). 2012. *National Estuary Program Coastal Condition Report IV*. Report number EPA-842-R-10-003. U.S. Environmental Protection Agency, Washington, DC. April.

Valiela, I., G. Collins, J. Kremer, K. Lajtha, M. Geist, B. Seely, J. Brawley, and C.H. Sham. 1997. Nitrogen loading from coastal watersheds to receiving estuaries: New method and application. *Ecological Applications 7*:358–380.

Wetz, M.S., E.A. Hutchinson, R.S. Lunetta, H.W. Paerl, and J.C. Taylor. 2011. Severe droughts reduce estuarine primary productivity with cascading effects on higher trophic levels. *Limnology and Oceanography 56*:627–638.

Whipple, A.C., J.V. Reynolds-Fleming, R. Neve, and R.A. Luettich Jr. 2012, in preparation. Spatial differences in sediment resuspension in the New River Estuary, North Carolina, USA. To be submitted to *Estuarine Coastal and Shelf Science*.

Woodruff, D.L., R.P. Stumpf, J.A. Scope, and H.W. Paerl. 1999. Remote estimation of water clarity in optically complex estuarine waters. *Remote Sensing of Environment 68*:41–52.

[This page intentionally left blank.]

Appendix 5-A

Supporting Data

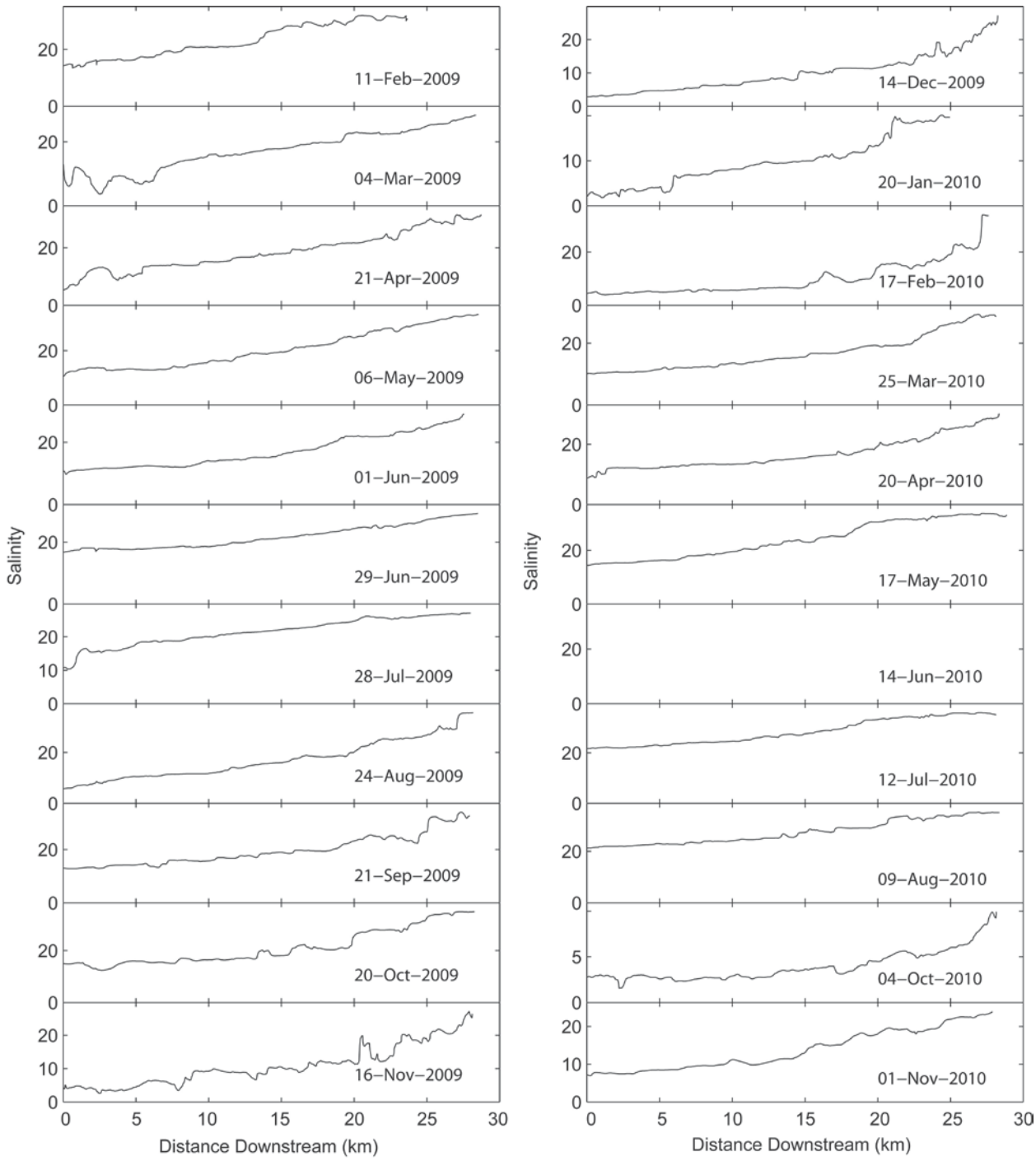

(continued)

Figure 5-A-1. Dataflow traces for salinity.

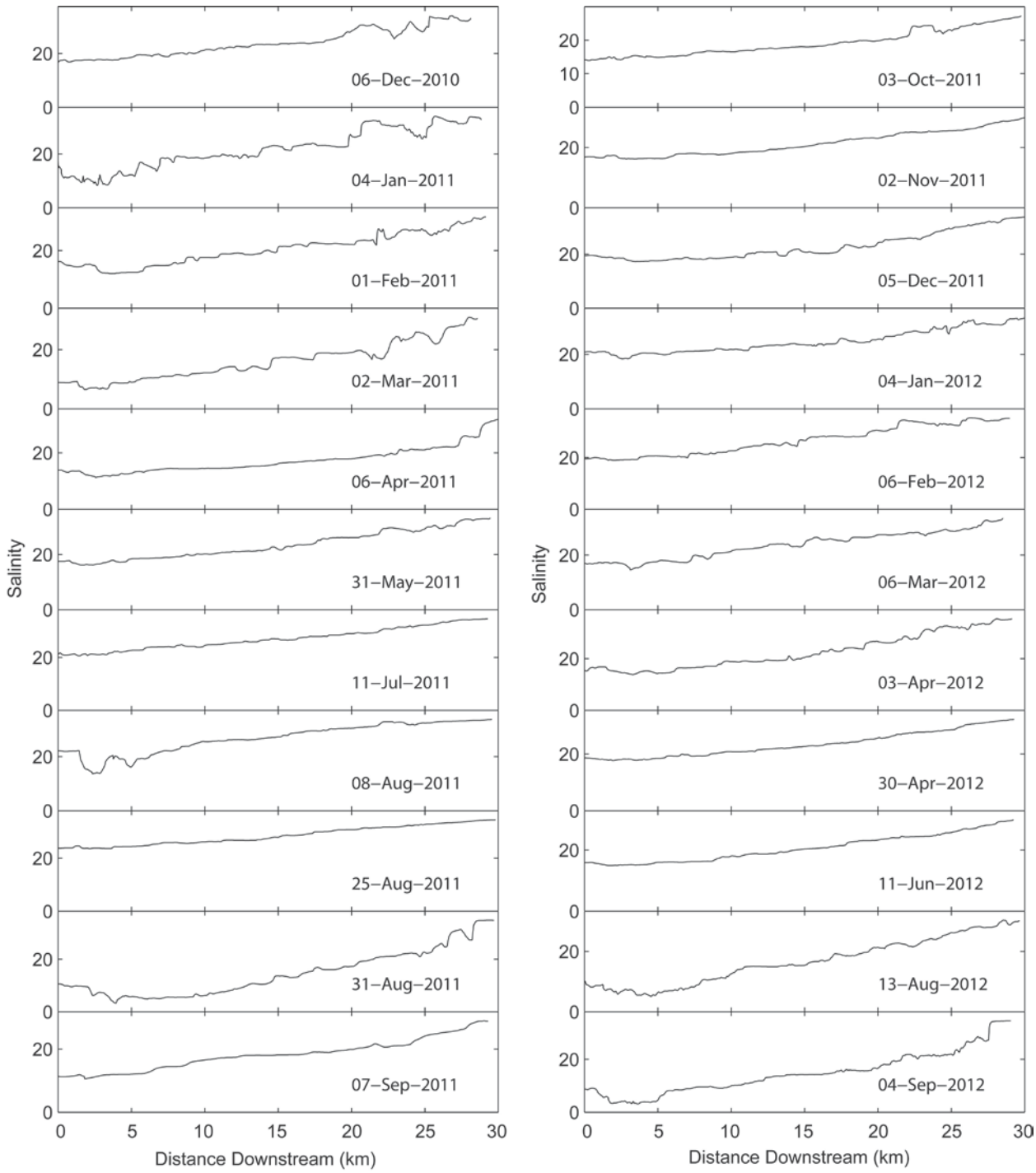

Figure 5-A-1. Dataflow traces for salinity (continued).

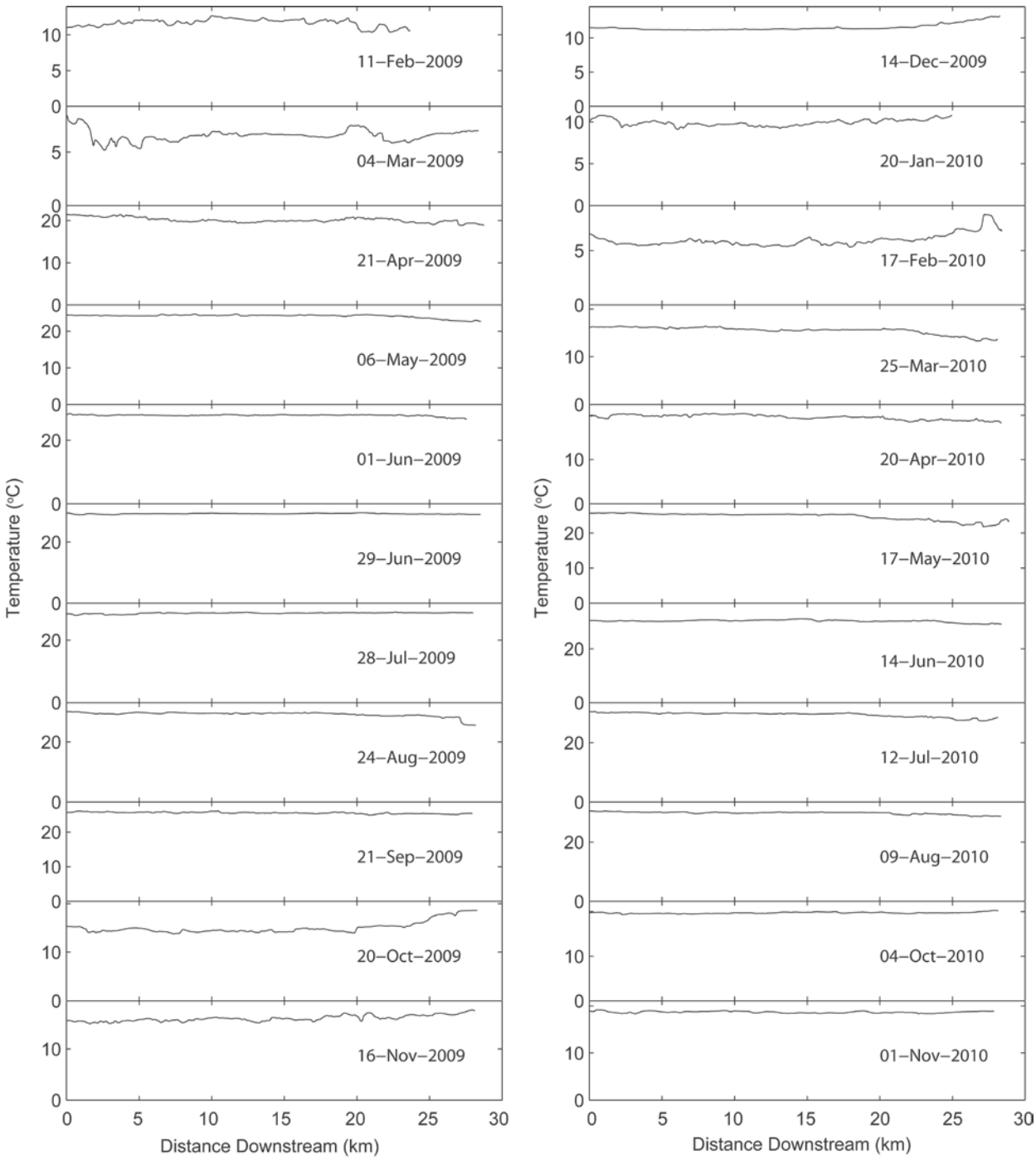

(continued)

Figure 5-A-2. Dataflow traces for temperature.

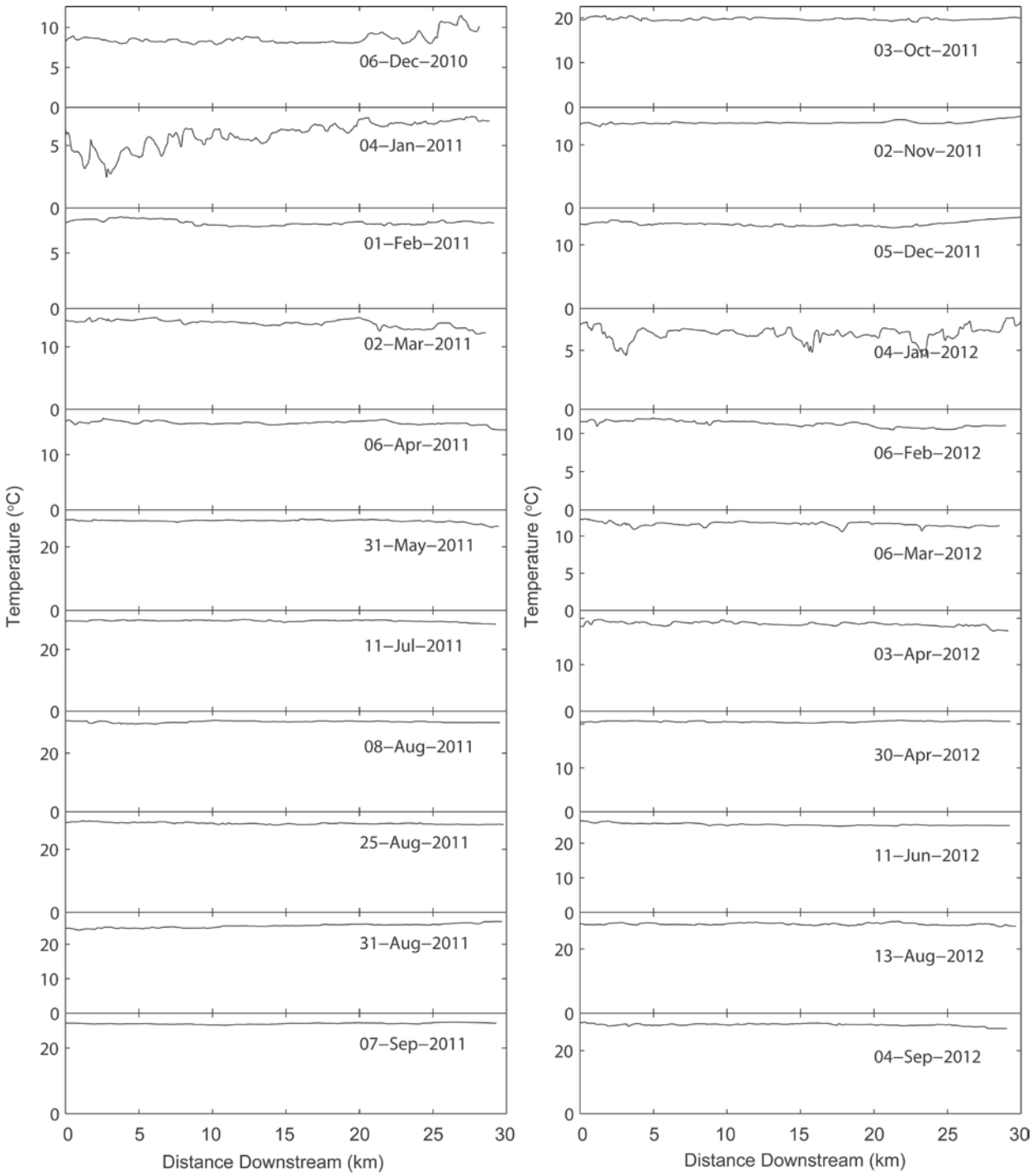

Figure 5-A-2. Dataflow traces for temperature (continued).

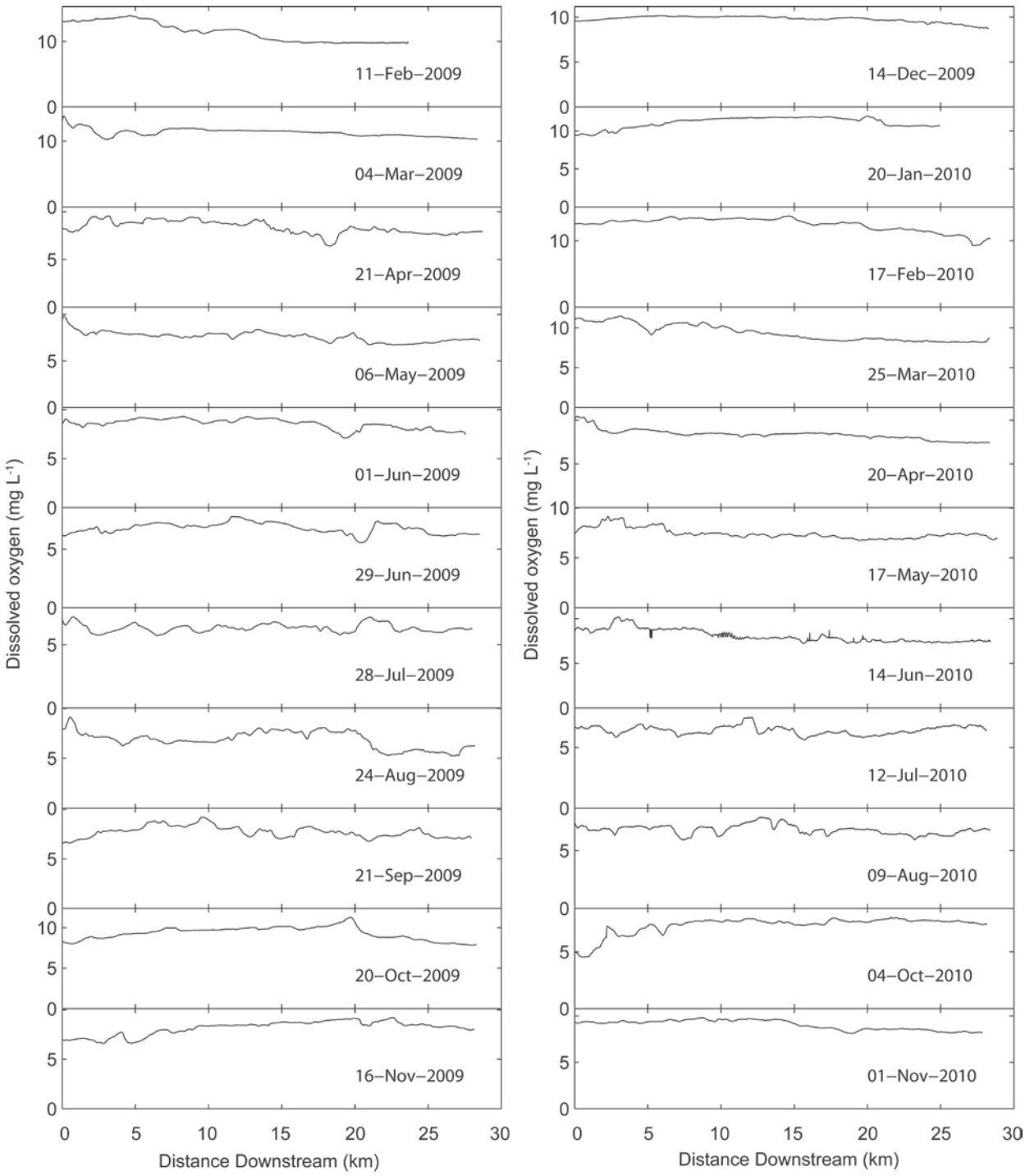

(continued)

Figure 5-A-3. Dataflow traces for DO.

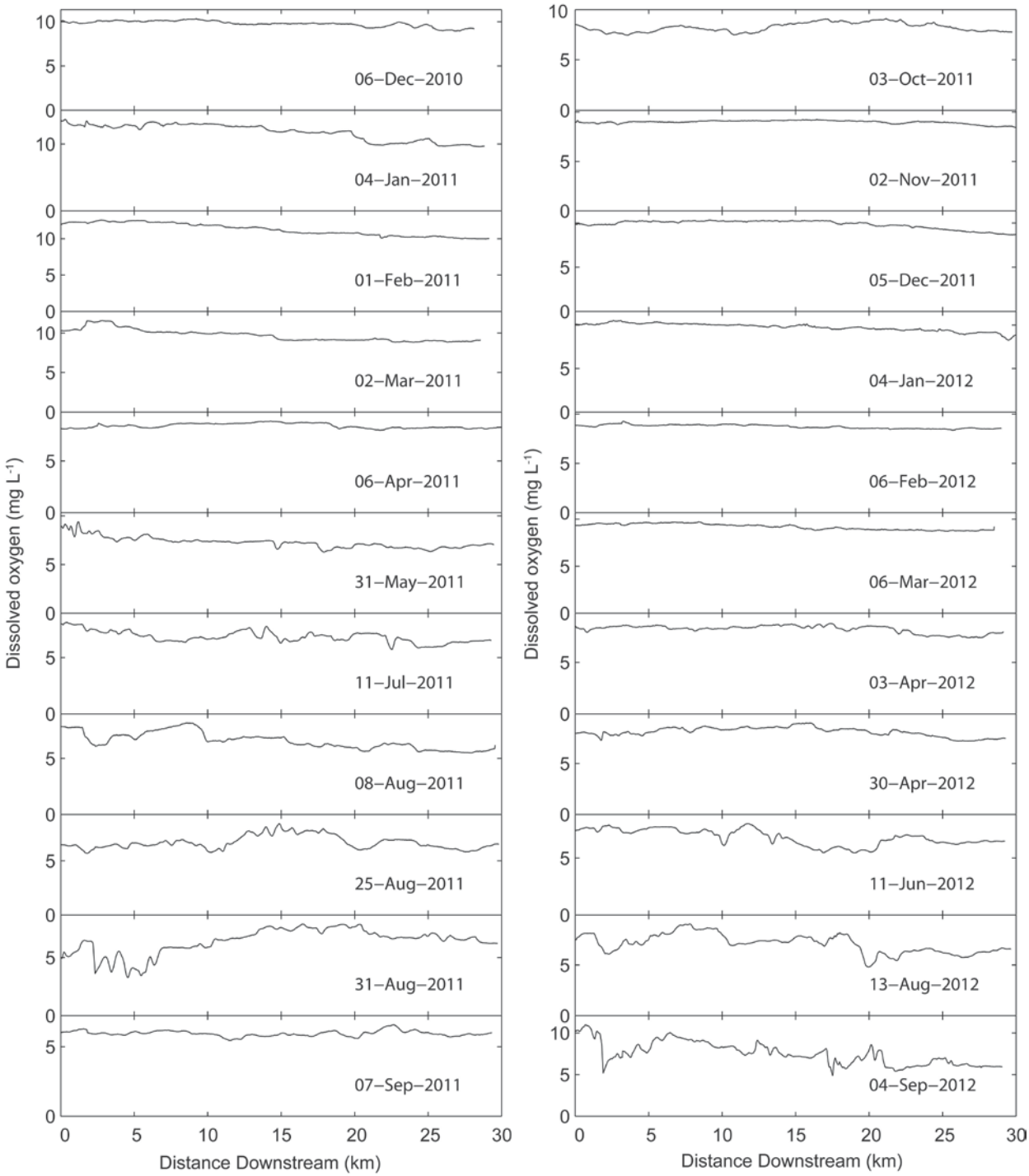

Figure 5-A-3. Dataflow traces for DO (continued).

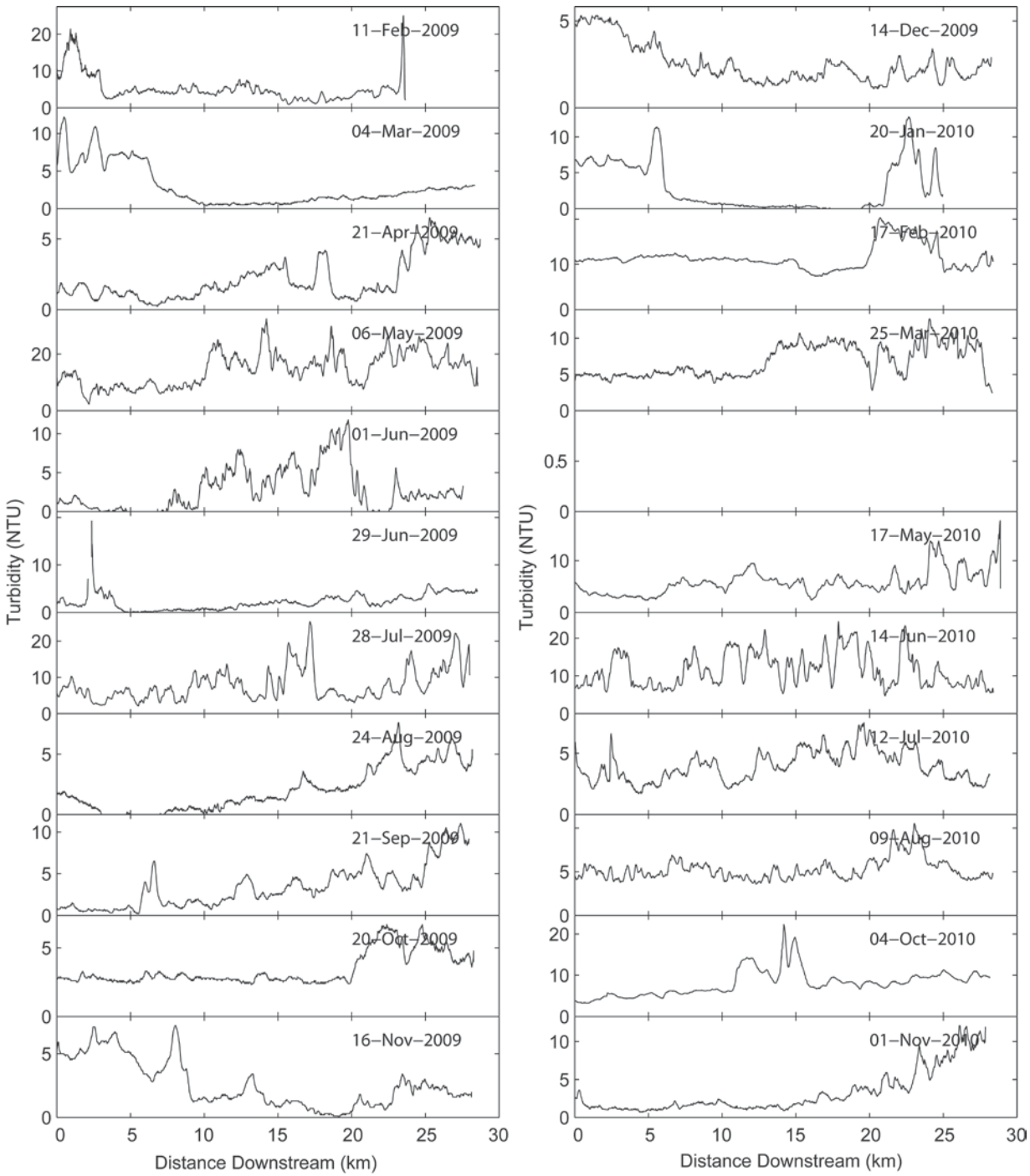

(continued)

Figure 5-A-4. Dataflow traces for turbidity.

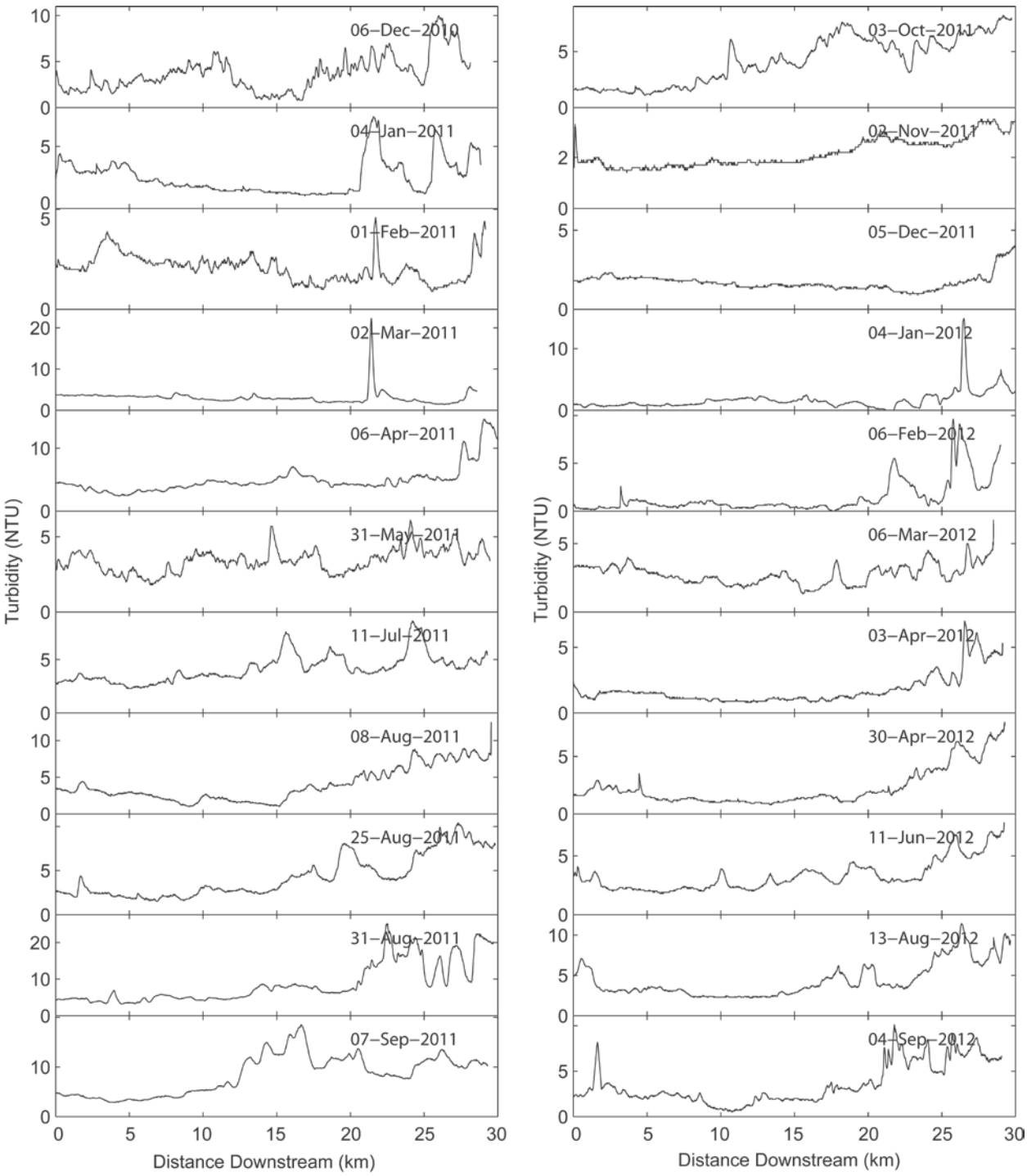

Figure 5-A-4. Dataflow traces for turbidity (continued).

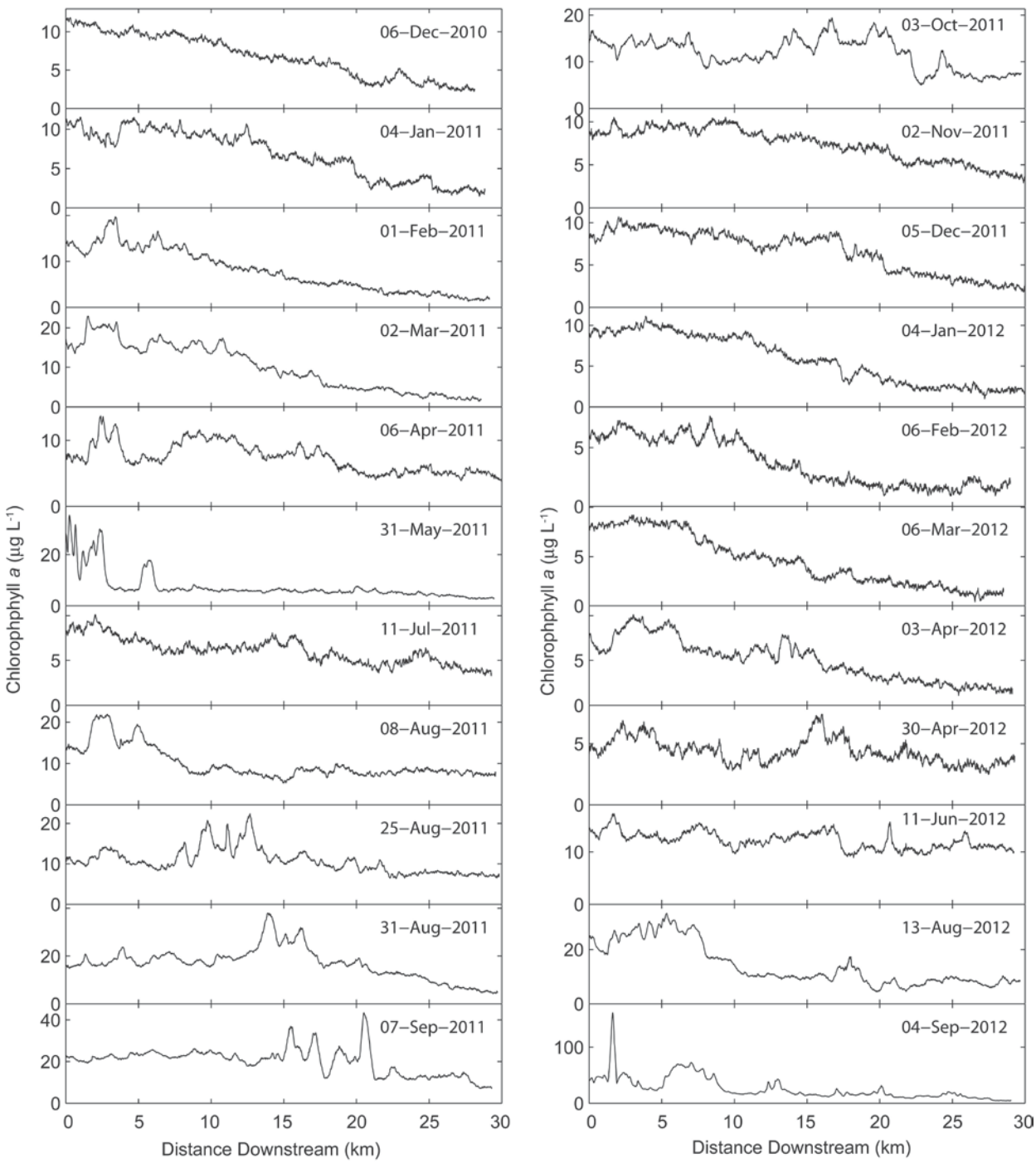

Figure 5-A-5. Dataflow traces for chl *a*.

Appendix 5-B

List of Scientific Publications

List of Scientific Publications

Papers

Altman, J.C., and H.W. Paerl. 2012. Composition of inorganic and organic nutrient sources influences phytoplankton community structure in the New River Estuary, North Carolina. Aquatic Ecology 42:269–282.

Hall, N.S., H.W. Paerl, B.L. Peierls, A.C. Whipple and K.L. Rossignol. 2012. Effects of climatic variability on phytoplankton biomass and community structure in the eutrophic, microtidal, New River Estuary, North Carolina, USA. Estuarine and Coastal Shelf Science. doi: http://dx.doi.org/10.1016/j.ecss.2012.10.004.

Kennish, M., and H.W. Paerl. 2010. Coastal Lagoons: Critical Habitats of Environmental Change. CRC Marine Science Series. CRC Press: Boca Raton, FL.

Paerl, H.W. 2009. Controlling eutrophication along the freshwater–marine continuum: Dual nutrient (N and P) reductions are essential. Estuaries and Coasts 32:593–601.

Paerl, H.W., and D. Justić. 2012. Estuarine phytoplankton. In Estuarine Ecology. Edited by J. Day, M. Kemp, A. Yanez and B. Crump. John Wiley: New York.

Paerl, H.W., and D. Justić. 2011. Primary producers: Phytoplankton ecology and trophic dynamics in coastal waters. Volume 6, pp. 23–42 in Treatise on Estuarine and Coastal Science. Edited by E. Wolanski, and D.S. McLusky. Academic Press: Waltham, MA.

Peierls, B.L., N.S. Hall and H.W. Paerl. 2012. Non-monotonic responses of phytoplankton biomass accumulation to hydrologic variability: A comparison of two coastal plain North Carolina estuaries. Estuaries and Coasts 35(6):1376–1392.

Whipple, A.C., J.V. Reynolds-Fleming, R. Neve, and R.A. Luettich Jr. 2012, in preparation. Spatial differences in sediment resuspension in the New River Estuary, North Carolina, USA. To be submitted to Estuarine Coastal and Shelf Science.

Thesis

Altman, J.C. 2011. *Impacts of Various Nitrogen Sources on Phytoplankton Community Structure in the New River Estuary*. M.Sc. Thesis, University of North Carolina at Chapel Hill, Chapel Hill, NC. 98 pages.

Presentations

Altman, J., and H. W. Paerl. 2011. Composition of Inorganic and Organic Nutrient Sources Influences Phytoplankton Community Structure in the New River Estuary, North Carolina. Presented at the Coastal and Estuarine Research Federation Conference, Daytona Beach, FL. November 6–10. (Aquatic/Estuarine Module)

Paerl, H.W. 2012. Controlling Nutrient Over-Enrichment Along the Freshwater to Marine Continuum Will Likely Require Both Nitrogen and Phosphorus Reductions: Lessons Learned from North Carolina Estuaries and Around the World. Presented at the North

Carolina Forum for Nutrient Over-Enrichment, sponsored by the North Carolina Department of Environment and Natural Resources, Durham, NC. May 23–24. (Aquatic/Estuarine Module)

Paerl, H.W. 2012. The Need for Dual Nutrient (N and P) Reductions to Stem Eutrophication Along the Freshwater-Estuarine Gradient. Invited seminar presented at McGill University, Montreal, Canada. January. (Aquatic/Estuarine Module).

Paerl, H.W. 2011. The Need for Dual Nutrient Removal Strategies for Protecting Water Quality North Carolina Estuarine Ecosystems. Presented to the North Carolina Wastewater Dischargers Association, Fayetteville, NC. August. (Aquatic/Estuarine Module)

Paerl, H.W. 2009. Application of Advanced Indicators to Distinguish Military from Other Human and Climatic Impacts on Estuarine Ecosystem Function. Presented at the Strategic Environmental Research and Development Program/Environmental Security Technology Certification Program Symposium, Washington, DC. December 3. (Aquatic/Estuarine Module)

Paerl, H.W., N.S. Hall, K.L. Rossignol, B.L. Peierls, I. Anderson, M. Brush, and J. Stanhope. 2011. The Role of Hydrologic Variability in Determining Microalgal Biomass and Community Structure in the New River Estuary, NC. Presented at the Strategic Environmental Research and Development Program/Environmental Security Technology Certification Program Partners in Environmental Technology Technical Symposium & Workshop, Washington, DC. November 29–December 1. (Aquatic/Estuarine Module)

Paerl, H.W., B.L. Peierls, N.S. Hall, K.L. Rossignol, and A.R. Joyner. 2011. Human and Climatic-Driven Ecological Change in Coastal North Carolina Shallow Water Systems: What's Manageable and What's Not? Presented at the Coastal and Estuarine Research Federation; Societies, Estuaries, and Coasts: Adapting to Change, Daytona Beach, FL. November 6–10. (Aquatic/Estuarine Module)

Paerl, H.W., I. Anderson, M. Brush, and M. Piehler. 2010. Application of Microalgal Indicators in the New River Estuary, NC: Quantifying Multiple Stresses to Water Quality. Presented at the Strategic Environmental Research and Development Program/Environmental Security Technology Certification Program Partners in Environmental Technology Technical Symposium & Workshop, Washington, DC, November 30–December 2. (Aquatic/Estuarine Module)

Peierls, B.L., N.S. Hall, and H.W. Paerl. 2011. Comparative Analysis of Climatic Forcing on Phytoplankton Community Dynamics in Two Neighboring, Mid-Atlantic Estuaries. Presented at the Coastal and Estuarine Research Federation Conference, Daytona Beach, FL. November 6–10. (Aquatic/Estuarine Module)

Whipple, A., J. Reynolds-Fleming, R. Neve, and R. Luettich. 2011. Spatial Changes in Sediment Resuspension in a Small Estuarine System. Presented at the Coastal and Estuarine Research Foundation Conference, Daytona Beach, FL. November 6–12. (Aquatic/Estuarine Module)

[This page intentionally left blank.]

Appendix 5-C

List of Students

- Julia Altman, M.Sc., Ecology, University of North Carolina at Chapel Hill, Chapel Hill, NC. 2011.
- Michael Clear, undergraduate independent study, University of North Carolina at Chapel Hill's Institute for the Environment, Chapel Hill, NC. Fall 2011.
- Timothy Otten, Ph.D., Environmental Sciences, Department of Environmental Sciences and Engineering, University of North Carolina at Chapel Hill, Chapel Hill, NC. 2012.
- Diana Rypkema, National Science Foundation's Research Experiences for Undergraduates student, Cornell University, Ithaca, NY. Summer 2010.

[This page intentionally left blank.]

Chapter 6

Land Cover and Shoreline Erosion

SERDP Project Number: RC-1413
Coastal Wetlands Module

Lead Researchers:
Dr. Carolyn Currin
NOAA NOS NCCOS CCFHR
Beaufort, NC
E-mail: Carolyn.currin@noaa.gov

Supporting Researchers:
Dr. Mark Fonseca
NOAA NOS NCCOS CCFHR
Beaufort, NC
E-mail: Fonseca.mark@gmail.com

Dr. James T. Morris
University of South Carolina
Columbia, SC
E-mail: James.morris@biol.sc.edu

June 27, 2013

Final

This report was prepared under contract to the U.S. Department of Defense (DoD) Strategic Environmental Research and Development Program (SERDP). The publication of this report does not indicate endorsement by DoD, nor should the contents be construed as reflecting the official policy or position of DoD. References herein to any specific commercial product, process, or service by trade name, trademark, manufacturer, or otherwise, do not necessarily constitute or imply its endorsement, recommendation, or favoring by DoD.

Table of Contents

List of Acronyms 6-vi
Abstract 6-1
Objectives of the Monitoring Activity 6-2
Background 6-2
Materials and Methods 6-3
General Description and Study Sites 6-3
Marsh Vegetation 6-5
Shoreline Habitat Type 6-8
Shoreline Location and Erosion Rate 6-9
Coastal Wetland Inventory 6-11
Snail Density and Distribution 6-11
Environmental Variables 6-11
Results and Discussion 6-12
Marsh Vegetation 6-12
Spartina alterniflora Density, Stem Height, and Biomass 6-15
Coastal Wetland Distribution 6-24
Shoreline Location and Erosion Rate 6-25
Environmental Variables 6-28
Assessment of Trends in the Data 6-31
Assessment of Monitoring Design 6-31
Assessment Seasonal and Annual Variability in the Data 6-32
Conclusions and Implications for Future Research 6-32
Key Scientific Findings—Fundamental Cause-and-Effect Relationships 6-33
Findings Supportive of Current Base Management Practices 6-33
Findings with Implications for Future Base Management 6-33
Findings with Implications for DCERP2 6-33
Literature Cited 6-34
Appendix 6-A: Supporting Data 6-A-1

List of Figures

6-1. Location of coastal wetlands monitoring sites on MCBCL. 6-5

6-2. An example of the relationship between monitoring sites, vegetation plots, and sample plots at two sites: (A) Pollocks Point and (B) Onslow Beach Backbarrier. 6-6

6-3. (A) A wheel-mounted receiver used to collect elevation points from the marsh surface at MHB. (B) A Trimble 5800 receiver mounted on a footed pole to obtain elevation points along the NRE shoreline at PPS. 6-9

6-4. Calculation of EPR from DEMs prepared for the Traps Bay (TBB) vegetation plot shoreline. 6-10

6-5. Mean values of the CVS cover category for marsh plants in the ICW vegetation plots. 6-13

6-6. Mean values of the CVS cover category for marsh plants in the ICW vegetation plots. 6-14

6-7. *Spartina alterniflora* live stem density in monitoring vegetation plots. 6-16

6-8. *Spartina alterniflora* mean stem height (in cm) in vegetation monitoring plots. 6-17

6-9. *Spartina alterniflora* estimated mean above-ground live biomass (g dw m-2) in vegetation monitoring plots. 6-17

6-10. Relationship between harvested *Spartina alterniflora* above-ground biomass and marsh surface elevation in 2010. 6-18

6-11. Above-ground biomass (g dw m^{-2}) of *Juncus roemerianus* from vegetation monitoring sites. 6-20

6-12. Density of the marsh snail (*Littoraria irrorata*) in vegetation plots from 2008 to 2012 at the monitoring sites adjacent to the ICW. 6-21

6-13. Density of the marsh snail (*Littoraria irrorata*) in vegetation plots from 2009 to 2012 at the monitoring sites adjacent to the NRE. 6-22

6-14. Appearance of the marsh snail (*Littoraria irrorata*) and potential impact on MCBCL marshes. 6-23

6-15. Distribution of dominant marsh species from fringing salt marshes along the NRE shoreline. 6-25

6-16. Aerial photographs of NRE shoreline sites, showing location of vegetation monitoring plots (yellow circles), SETs (yellow triangles), DEM of shoreline, calculated zero-line of shoreline in 2008 (turquoise line) and 2011 (white line), and shoreline as mapped from aerial photography in 1956 (orange line) and 1989 (yellow line). 6-27

6-17. Porewater salinity collected in 2010 from plots used for *Spartina alterniflora* harvest. 6-28

6-18. Relationship between summer MWL as recorded at MHB and *Spartina alterniflora* vegetation parameters at monitoring sites FC, OBB, and MHB. 6-30

6-19. Relationship between *Spartina alterniflora* above-ground biomass and summer precipitation at monitoring sites along the ICW. 6-31

List of Tables

6-1. Features of vegetation monitoring sites. FC, OBB, MHB, and MHL are located adjacent to the ICW. TBB, TBC, PPS, PPU, and FN are located in marshes adjacent to the NRE. 6-4

6-2. Imagery and shapefiles used to assemble a GIS coastal wetland inventory. 6-11

6-3. Marsh plant species recorded from permanent vegetation monitoring plots in 2008–2012 6-12

6-4. Results from change-analysis of marsh DEMs. 6-26

6-5. Comparison of independent long- and short-term estimates of shoreline erosion at NRE shoreline sites. 6-26

6-6. Mean water level (MWL) given as mean (standard deviation, maximum) for MHB (Mile Hammock Bay) and GM/WC (Gottschalk Marina/Wallace Creek) temporary tide gauge data (in meters mean sea level [MSL]). 6-29

List of Acronyms

°C	degrees Celsius
BF	*Borrichia frutescens*
CCFHR	Center for Coastal Fisheries and Habitat Research
cm	centimeter
CVS	Carolina Vegetation Survey
CW	Coastal Wetlands (Module)
DCERP1	first cycle of the Defense Coastal/Estuarine Research Program
DCERP2	second cycle of the Defense Coastal/Estuarine Research Program
DEM	Digital Elevation Model
DoD	U.S. Department of Defense
DS	*Distichlis spicata*
DSAS	Digital Shoreline Analysis System
EPR	end point rate
FC	Freeman Creek
FN	French Creek
g dw m^{-2}	grams dry weight per square meter
g m^{-2}	grams per square meter
GIS	geographic information system
GM/WC	Gottschalk Marina/Wallace Creek
GPS	global positioning system
ICW	Intracoastal Waterway
JR	*Juncus roemerianus*
LC	*Limonium carolinianum*
LCAC	landing craft air cushion
LiDAR	light detection and ranging
m^2	square meter
m^3	cubic meter
MCBCL	Marine Corps Base Camp Lejeune
MEM	Marsh Equilibrium Model
MHB	Mile Hammock Bay
MHL	Mile Hammock Bay – LCAC
MSL	mean sea level
MWL	mean water level
N/A	not applicable
NAVD 88	North American Vertical Datum of 1988
NOAA	National Oceanic and Atmospheric Administration

NRE	New River Estuary
NWI	National Wetland Inventory
OBB	Onslow Beach Backbarrier
PA	*Phragmites australis*
PP	Pollocks Point
PPS	Pollocks Point Shore
ppt	parts per thousand
PPU	Pollocks Point Upper
r^2	r-squared value
RTK-GPS	real-time kinematic global positioning system
RWE	relative wave energy
s	second
SA	*Spartina alterniflora*
SC	*Spartina cynosuroides*
SERDP	Strategic Environmental Research and Development Program
SET	surface elevation table
SLR	sea level rise
SP	*Spartina patens*
SV	*Salicornia virginica*
TBB	Traps Bay Bridge
TBC	Traps Bay Creek
TS	*Typha* spp.
WL	temporary tide gauges

[This page intentionally left blank.]

Abstract

Monitoring of coastal wetland vegetation on Marine Corps Base Camp Lejeune (MCBCL) was done to assess the spatial and temporal variability in marsh distribution and the dominant marsh plant species, *Spartina alterniflora* and *Juncus roemerianus*, and to provide baseline information in support of research efforts to predict the response of marshes at MCBCL to sea level rise, shoreline erosion and other potential sources of environmental change. Permanent monitoring sites were established at nine locations across a gradient in salinity, tide range, and proximity to the ocean inlets. At each site, annual surveys of marsh plant species cover, peak above-ground biomass of dominant marsh plant species, plot elevation, and density of the marsh snail (*Littoraria irrorata*) were conducted. In addition, remote sensing and field-based mapping were utilized to update a geographic information system–based inventory of MCBCL coastal wetlands, to map marsh plant species in fringing marshes, and to quantify shoreline erosion rates at vegetation monitoring sites. Finally, above-ground *Spartina* biomass was harvested across an elevation gradient at three sites in 2010 to support research and modeling efforts.

Site and elevation were significant factors affecting *Spartina* vegetation, as expected. Above-ground *Spartina* biomass exhibited a parabolic relationship with surface elevation. We found that peak *Spartina* biomass, of approximately 500–600 g dry wt m^{-2}, occurred at marsh surface elevations between 0.05 and 0.25 m North American Vertical Datum of 1988 (NAVD 88). At sites with nearly 1 m in tide range, *Spartina* occurred at surface elevations between −0.45 to 0.45 m NAVD 88. However, at sites near the New River Inlet, with its reduced tidal range, *Spartina* was only found at elevations between −0.15 and 0.35 m NAVD 88. *Juncus* biomass at NRE sites (600–1,500 g dry wt m^{-2}) was higher than that reported from elsewhere in North Carolina, but similar to estimates from Georgia.

Analysis of permanent vegetation plots revealed significant inter-annual variation in both *Spartina* and *Juncus* biomass. At nearly every site, biomass was reduced in 2012 as compared to other years. This reduction in plant biomass was negatively correlated with summer (June–August) water levels, and also with summer total precipitation. The density of *Littorina irrorata* also varied by site and year. The highest density of snails (120 snails m^{-2}) was recorded at Mile Hammock Bay in the summers of 2011 and 2012. However, increased snail density did not occur at every site exhibiting a decline in marsh biomass, and although a correlation between marsh dieback and high density of snails has been reported in other locations, snail grazing alone cannot account for the observed decline in marsh biomass.

Short-term shoreline erosion rates at marsh sites were similar to long-term rates determined from historic aerial photography. However, we also found that shoreline erosion resulted in an increase in marsh sediment volume, as eroded sediment appeared to be redistributed to the marsh surface.

The 1,090 ha (2,690 ac) of coastal wetlands on MCBCL provide important ecosystem services but are vulnerable to sea level rise and shoreline erosion, as illustrated by these monitoring results. These results provide the foundation for future research to develop a landscape-scale model of marsh response to sea level rise and to understand the factors affecting marsh primary production and carbon sequestration.

Keywords: above-ground biomass, coastal marshes, *Juncus*, shoreline erosion, shoreline habitat, *Spartina*, tidal amplitude, vegetation monitoring

Objectives of the Monitoring Activity

The Coastal Wetlands Module monitoring program has many related objectives. The first objective is to quantify spatial and inter-annual variability in the dominant marsh plant species biomass and distribution. A second objective is to provide baseline data to determine the ability of marshes within the New River Estuary (NRE) to perform a variety of ecosystem services and, in combination with research projects, to determine what factors affect marsh structure and function. The third objective is to provide baseline data, maps, and geographic information system data layers on shoreline location, habitat type, and erosion rate throughout the NRE. The fourth objective is to install and maintain benchmarks and water level sensors for the collection and distribution of accurate elevation and tidal data.

The Coastal Wetland Monitoring effort collected baseline information on estuarine shoreline habitats and marsh land cover to detect changes due to wave erosion, storm events, and sea level rise. Baseline monitoring data provided information to support research projects designed to forecast response of marshes to sea level rise (Research Project CW-1), develop effective shoreline stabilization plans (Research Project CW-2) and support development of adaptive management approaches for improving sustainability of coastal wetlands on Marine Corps Base Camp Lejeune. Monitoring data used in analyses to support research objectives of Research Projects CW-1 and CW-2 are reported in the *DCERP1 Final Research Report*. Shoreline mapping data was used in Research Project CW-2 to determine historic erosion rates and to analyze relationships between shoreline type, erosion rate, and environmental factors. In addition, this monitoring effort helped to determine whether impacts to marsh shoreline erosion from military activities (e.g., landing craft air cushion exercises, splash points) are significant, as reported in Chapter 7.

Background

Coastal wetlands provide a variety of ecosystem services, such as improving water quality by serving as nutrient transformers and trapping sediment (Harrison and Bloom, 1977; Jordan et al., 1983; Valiela and Teal, 1979), stabilizing estuarine shorelines via attenuation of wind wave and boat wake energy (Knutson, 1988; Leonard et al., 2002; Moller et al., 1999), providing critical habitat area for a diverse group of estuarine organisms and serving as nursery habitat for commercially important fishery species (Kneib, 1997), and stabilizing coastal barrier islands via sediment accretion (Roman et al., 1997). Threats to coastal wetlands include erosion from wind and boat waves and erosion from intense coastal storms, dredging, subsidence, and sea level rise (Dahl, 2011). Arecent assessment of coastal wetlands in the conterminous United States cited marsh conversion to open water as the primary cause for a net loss of wetlands (Dahl, 2011).

The ability of marshes to keep up with current and projected rates of sea level rise (SLR) depends on sediment availability, the rate of SLR, the density of marsh vegetation, the intensity and frequency of storms, and variables such as nutrient enrichment and salinity that affect the density and species distribution of marsh vegetation (Kirwan and Murray, 2007; Morris et al., 2002; Mudd et al., 2009). The vulnerability of coastal wetlands to SLR is a function of the local

tidal amplitude and marsh surface elevation relative to local mean and high water, and the relationship between marsh plant production and position in the tidal frame (Morris et al., 2002). As the rate of SLR increases, the equilibrium elevation of the marsh will decrease. As this elevation approaches the lower limit of a wetland's range of tolerance, the marsh will convert to open water upon any further increase in the rate of SLR. Crucial to predicting the future of salt marshes to the projected acceleration in SLR is understanding the relationship between surface elevation and plant biomass, and how this relationship may vary across estuarine gradients in salinity and tide range.

Materials and Methods

General Description and Study Sites

Marsh and shoreline habitats were monitored at several different spatial scales using both remote sensing and field-sampling methods. Monitoring parameters included (1) *Spartina alterniflora* and *Juncus roemerianus* stem density, mean height, and biomass data collected in replicate, permanent 1-m^2 plots from nine sites; (2) habitat type of New River Estuary (NRE) and Intracoastal Waterway (ICW) shorelines determined with ground-truthing and digitization of aerial photography; (3) shoreline edge erosion at vegetation monitoring sites adjacent to NRE shorelines; and (4) snail (*Littoraria irrorata*) density from permanent plots at nine sites. In addition, a large-scale analysis of the linkage between marsh distribution and surface elevation was conducted using available data on wetlands distribution and light detection and ranging (LiDAR) data, and an updated inventory of coastal marsh distribution on Marine Corps Base Camp Lejeune (MCBCL) was developed. Several of these monitoring efforts are incorporated into *DCERP1 Final Research Report*, as indicated below, and this *DCERP1 Final Monitoring Report* will emphasize results not previously reported.

Sites for monitoring marsh species composition, stem density, stem height, and snail density were established at Freeman Creek (FC), Onslow Beach Backbarrier (OBB), and Mile Hammock Bay (MHB) sites in 2008. Two sites were established in the Mile Hammock Bay area: one outside the boundaries of the assigned landing craft air cushion (LCAC) utilization area (MHB) and one within the designated LCAC area (MHL). Vegetation monitoring sites in the NRE were established in 2009 and include Traps Bay Bridge (TBB) and Traps Bay Creek (TBC), Pollocks Point Shore (PPS) and Pollocks Point Upper (PPU), and French Creek (FN). Sites were selected to encompass the gradient in tidal amplitude, salinity, and wave energy in accessible areas of MCBCL in which marshes occurred (**Figure 6-1**). Details of monitoring sites and vegetation plot dimensions are in **Table 6-1**.

Table 6-1. Features of vegetation monitoring sites. FC, OBB, MHB, and MHL are located adjacent to the ICW. TBB, TBC, PPS, PPU, and FN are located in marshes adjacent to the NRE.

Elevation range refers to range in sample plot elevations; study plot dimensions refer to vegetation monitoring plot which encompasses all sample plots.

Site	Abbreviation	Elevation Range	Number of Plots	Study Plot Size (m)	Years Sampled
Freeman Creek	FC	−0.23–0.26	25	40 × 100	2008–2012
Onslow Beach	OBB	0.08–0.55	25	40 × 80	2008–2012
Mile Hammock Bay	MHB	−0.04–0.22	25	40 × 100	2008–2012
Mile Hammock Bay—LCAC	MHL	0.05–0.30	25	50 × 100	2008–2010
Traps Bay Bridge	TBB	−0.10–0.15	15	50 × 20	2009–2012
Traps Bay Creek	TBC	−0.06–0.29	15	50 × 20	2009–2012
Pollocks Point Shore	PPS	0.05–0.25	15	50 × 20	2009–2012
Pollocks Point Upper	PPU	0.08–0.21	15	50 × 20	2009–2010
French Creek	FN	0.03–0.15	15	50 × 40	2009–2012

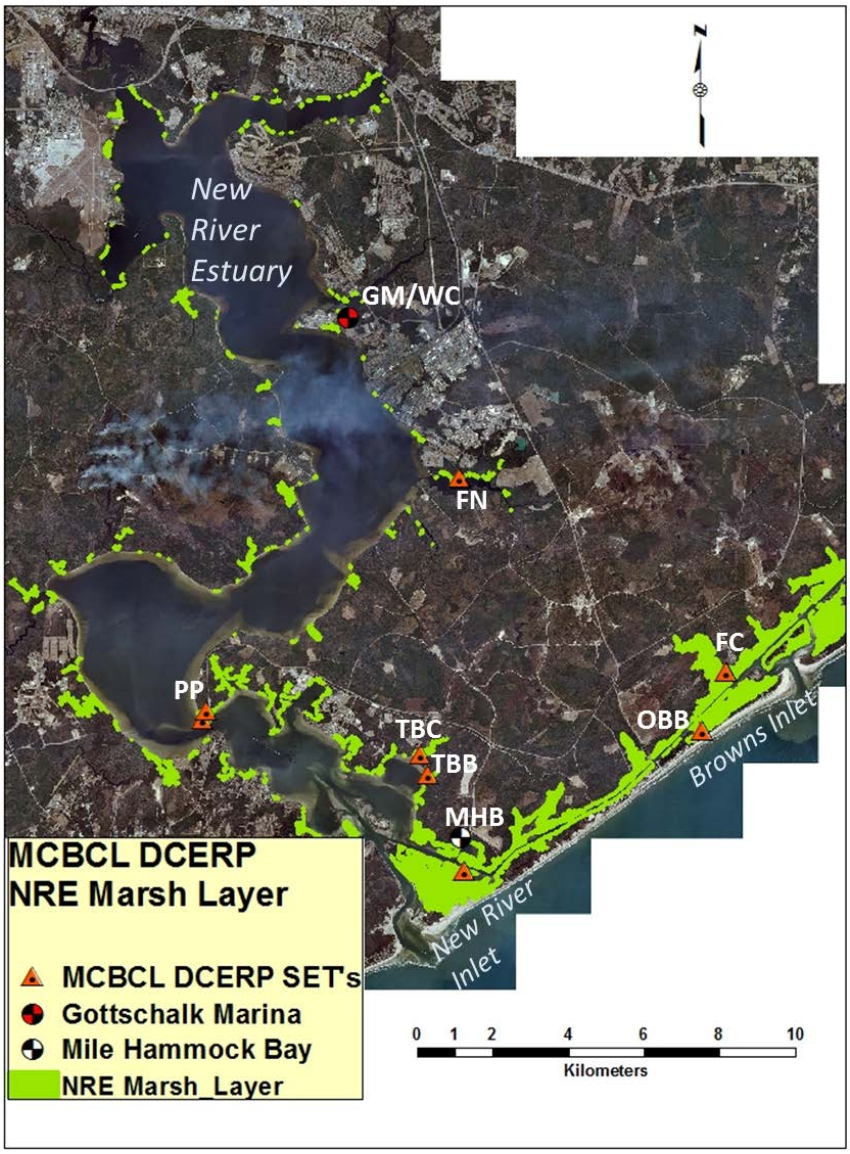

Figure 6-1. Location of coastal wetlands monitoring sites on MCBCL.

Map displays the distribution of coastal wetlands (salt and brackish marsh) on MCBCL. The location of surface elevation tables (SETs) and temporary tide gauges (MHB and GM/WC) are also indicated on the figure.

Marsh Vegetation

Vegetation monitoring sites encompass a surface elevation table (SET) at all sites except MHL. At each monitoring site, a vegetation plot was established with five shore-perpendicular transects located using stratified random sampling (Elzinga et al., 1998). Vegetation sampling was conducted on 1-m^2 sampling plots at regular intervals along each transect (Roman et al., 2001). At the larger monitoring sites adjacent to the ICW, sampling plots were established every 20–25 m, for a total of 25 plots per site (**Figure 6-2**). It should be noted that at Pollocks Point (PP), two monitoring sites were established at the shoreward and upper edges of the marsh, which are designated PPS (shore) and PPU (upper marsh, near woodland boundary), respectively, and are separated by 250 m (**Figure 6-2**). All other monitoring sites along NRE extend from the shore to

the upland or forest border. At the smaller monitoring sites in marshes located along the NRE, sampling plots were located every 10 m on shore-perpendicular transects for a total of 15 plots per site. All vegetation monitoring was conducted within a 4-week period, from mid-July to mid-August, to encompass the period of peak marsh biomass (Morris and Haskin, 1990).

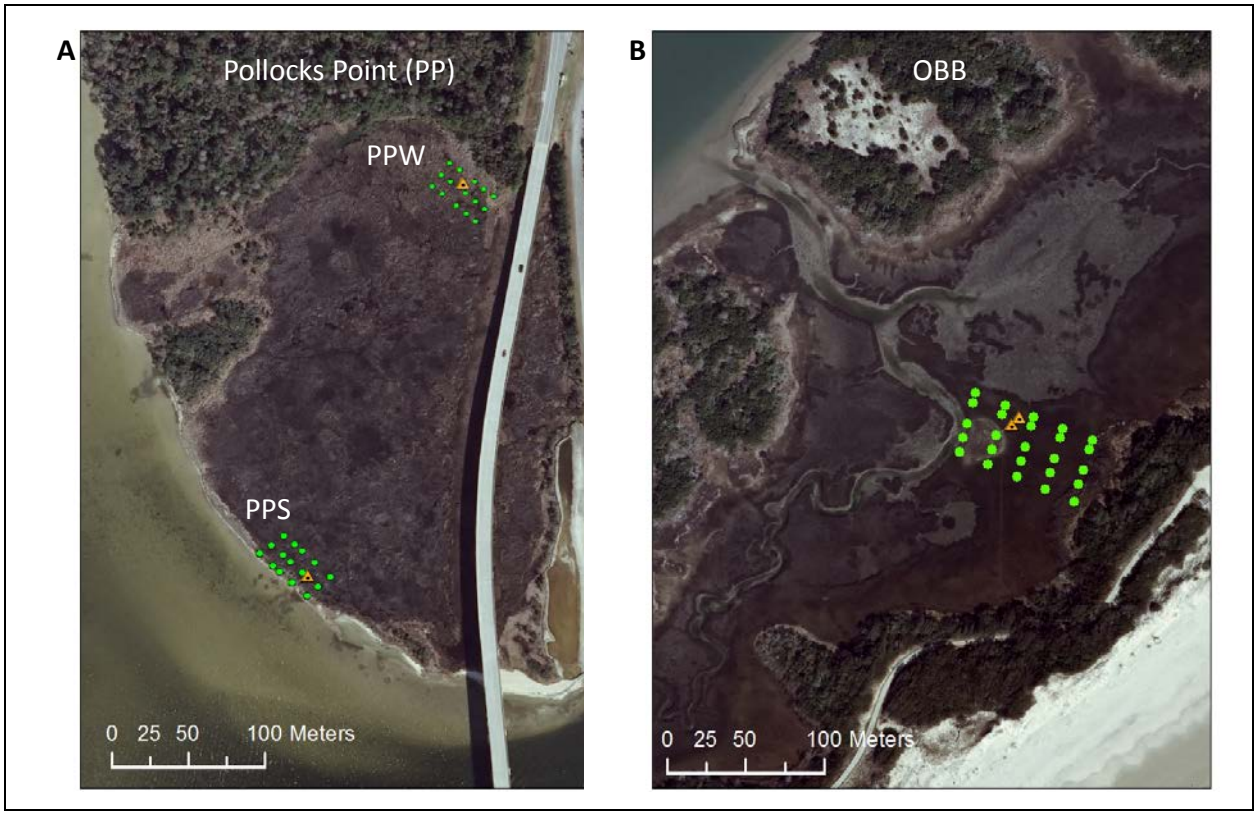

Figure 6-2. An example of the relationship between monitoring sites, vegetation plots, and sample plots at two sites: (A) Pollocks Point and (B) Onslow Beach Backbarrier.

Pollocks Point is located in the lower portion of the NRE (Highway 172 bridge can be seen in photo), and consists of two vegetation monitoring plots, as outlined with the green dots. Each green dot represents a 1-m^2 sample plot. There are 15 sample plots at each NRE site vegetation plot. Note: Each vegetation plot includes an SET, as indicated with an orange triangle. The Onslow Back Barrier vegetation site extends from a marsh creek edge to the upper marsh. There are 25 sample plots (indicated by green dots) and two SETs (indicated by orange triangles) within the vegetation monitoring plot. At this site, one of the SETs was fertilized as part of Research Project CW-1 activities.

At each sampling plot, researchers identified the plant species present and visually estimated the percent cover for each plant according to Carolina Vegetation Survey (CVS) categories (Peet et al., 1998). Live and dead stem densities for *Spartina alterniflora* were measured in 0.25-m^2 subplots, and 10 *Spartina* stem heights were recorded along a mid-plot transect. *Spartina alterniflora* stem height and stem density data were later used to estimate biomass (in grams dry weight per square meter). Sample plot biomass was calculated by first calculating stem weight for each of the measured stem heights, using a regression model that incorporated stem height and weight data from marshes in both North and South Carolina. The following regression was constructed from harvested *S. alterniflora* stem height and dry weight data:

$$y=-.0000142\ x^3+0.000903x^2+0.03467x \qquad \text{(Eq. 6-1)}$$

where *y* is dry weight (g) for a stem of height *x* cm. The relationship between stem height and dry weight has an r-squared (r^2) value of 0.91 and is similar to other published values (Morris and Haskin, 1990). The average weight of the 10 stems measured was multiplied by sample plot stem density to estimate peak above-ground biomass, referred to in this report as *Spartina* biomass.

NRE marshes consisted primarily of *Juncus roemerianus* and thus required a modified approach to biomass estimation. At these sites, *Juncus roemerianus* biomass was directly measured at nine plots per area (every other transect) by harvesting all of the standing above-ground biomass from a 0.0625 m^2 plot located adjacent to the sampling plot used for other parameters to avoid disturbance of the main sampling plot. In 2010, additional *Juncus* biomass samples were collected at FC and OBB to increase our sampling range along geographic, salinity, andelevation gradients. *Juncus* plants were harvested from three existing sampling plots at OBB, where *Juncus* occurs within the vegetation sampling area. At FC, *Juncus* was present along the upper periphery of the marsh, but none occurred within the vegetation monitoring plot. Therefore, three *Juncus* samples were collected from haphazardly located plots in a *Juncus*-dominated area of the upper marsh. (No *Juncus* samples were collected from ICW sites in 2009). In the laboratory, all harvested biomass was separated into live (green) *Juncus* leaves, dead (brown) *Juncus* leaves, and other species (Christian et al., 1990). Leaf length was recorded for all live *Juncus roemerianus* leaves. All fractions were washed to remove sediments and epiphytes, and then dried in the oven at 85°C overnight. We then measured the dry weight of each fraction to calculate the biomass in grams of dry weight per square meter. This sampling scheme was repeated in 2011 and 2012.

In August 2010, we obtained additional data on the relationship between above-ground *Spartina alterniflora* biomass and surface elevation from salt marshes on both sides of the ICW behind the Onslow Beach barrier island. These data helped to optimize the Morris Marsh Equilibrium Model (MEM; Morris et al. 2002), which forecasts the response of salt marshes to SLR. Above-ground *SA* biomass was harvested from existing vegetation monitoring sites at FC, OBB, and MHB. We attempted to harvest *Spartina* over a range of 10 elevation bins or intervals: −0.49 to −0.40; −0.39 to 0.30; −0.29 to −0.20; −0.19 to −0.10; −0.09 to 0.0; 0.01 to 0.10; 0.11 to 0.20; 0.21 to 0.30; 0.31 to 0.40; and 0.41 to 0.50 m North American Vertical Datum of 1988 (NAVD 88), with three replicates in each bin. Where possible, we located harvest plots within the existing vegetation plot (approximately 50 m × 100 m). However, sediment surface elevations within these plots generally did not vary more than 40 cm within a site, less than the total elevation range in which *Spartina* grows. Thus, we selected sample plots outside of the vegetation plot to obtain plants from all possible elevation bins. We used a restricted random sampling scheme to select the original plots, and, for elevations outside the original sample plots, we used randomized locations within a short transect (5–10 m) selected from within the target elevation interval. Some sites did not have *Spartina* growing across all the pre-determined elevation bins.

We harvested live *Spartina alterniflora* stems in small (0.25 m^2) plots by cutting the stems at the sediment interface with scissors. Prior to harvesting plants, we measured live and dead *Spartina* stem density and obtained five stem height measurements across the middle of each quadrat. We also obtained pore water salinity data from harvest plots using a filtered syringe and refractometer. Harvested plants were stored in plastic garbage bags and returned to the

University of South Carolina for processing. Cut stems were prepared by washing and removing all epiphytes and sediment, then drying at 85°C for at least 24 hours, until all material was dry. The dried material was then weighed.

In situ elevations were determined for each plot with a real-time kinematic global positioning system (RTK-GPS), using the SET mark as a reference. Although each plot belonged to an "elevation bin," as designated above, specific elevations were determined for the middle of each plot and recorded separately.

Statistical Analysis of Vegetation Monitoring Data

We examined inter-annual variability in *Spartina alterniflora* and *Juncus roemerianus* above-ground marsh structure by analyzing data from permanent plots with SAS Proc Mixed, which is designed for analysis of repeated measures. Permanent plots provide greater statistical power for detecting change over time (Bakker et al., 1996, Elzinga et al., 1998; Roman et al., 2001). Response variables included stem density, mean stem height, and peak above-ground biomass. Stem density and stem height were field measurements, while biomass is calculated from stem density and height data (see Materials and Methods section in this chapter). We examined the effect of surface elevation and year on each variable at each site. For analysis, sample plot surface elevations were binned into elevation intervals as in the harvest collection (see above). Where surface elevation was not significant, data were combined for further analysis. The relationship between snail density in permanent plots, year, and elevation was examined similarly.

Linear regression analysis was used to determine relationships between summer mean sea level and precipitation on *Spartina* and *Juncus* marsh stem density and stem height (Kirwan and Guntenspergen, 2012; Morris and Haskin, 1990). Analysis of variance was used to examine the relationship between plant biomass, snail density, and elevation.

Shoreline Habitat Type

Shoreline habitat type characterization of the main-stem NRE shoreline was completed in 2009, and a similar characterization of the ICW shoreline between Mile Hammock Bay and Browns Inlet was performed in April–June 2010. We initially used previously digitized 2004 aerial photography to classify shoreline habitat classified into one of five shoreline types (Swamp Forest, Marsh, Sediment Bank, Modified, and Miscellaneous). An initial ground-truthing effort demonstrated significant errors, and we subsequently completed ground-truthing of the entire NRE and ICW shorelines for habitat type classification using a small boat and survey-grade global positioning system (GPS) equipment. ArcGIS software was used to edit the data layer of shoreline habitat types that had been created using the 2004 aerial photography, based on real-time field observations. A Trimble Pro XH backpack GPS was used to collect points along the shoreline at modification structures such as dock corners. Ground-truthing also allowed us to refine the shoreline habitat type classifications further and include vegetation species, modification structure details, and relief (Sediment Bank and Modified types only). Results from this effort are incorporated into the *DCERP1 Final Research Report*, Chapter 8, and will be summarized briefly in this Monitoring Report.

Shoreline Location and Erosion Rate

We obtained short-term (2008–2011) estimates of shoreline erosion based on marsh Digital Elevation Models (DEMs) constructed for vegetation monitoring plots adjacent to the NRE shoreline. Marsh surface elevation at study sites was obtained using an RTK-GPS unit (Trimble 5800) and laser leveling (see Chapter 7 for marsh DEM methodology). Elevations obtained with both methods were used to create a DEM of the study sites using ArcGIS 9.2 In most instances, the marsh surface was sampled at 2-s intervals using an RTK rover mounted on a wheeled vehicle (bicycle) to obtain elevation points at roughly 1-m wide intervals (**Figure 6-3A and C**). Exceptions were in areas where either soft sediments, or density of vegetation, precluded use of the wheel-mounted receiver. In this case, elevation points were obtained with the receiver mounted on a footed pole **(Figure 6-3B**).

Figure 6-3. (A) A wheel-mounted receiver used to collect elevation points from the marsh surface at MHB. (B) A Trimble 5800 receiver mounted on a footed pole to obtain elevation points along the NRE shoreline at PPS.

Note narrow fringe of *Spartina* in front of *Juncus* marsh. (C) Density of elevation point collection using a wheeled receiver at OBB. At each site, SET marks were used as reference elevation points.

ArcGIS Data Management and Spatial Analyst Tools were used to create marsh DEMs and analyze elevation change. DEMs were created using the natural neighbor interpolation. DEM cell size used for analysis was set at 1 × 1 m and most closely represented real point placement. We

used DEMs prepared with marsh surface elevation data obtained in 2008 and 2011, and the Digital Shoreline Analysis System (DSAS) method (Thieler and Danforth, 1994), to determine the distance between the calculated 0-m elevation (zero-line) contour lines calculated from 2008 and 2011 DEMs. This analysis system uses a series of intersecting lines with extracted shoreline profiles and measures the rate of change using the shoreline collection dates (**Figure 6-4**). This estimate of shoreline change is called the end point rate (EPR), and the mean change is calculated as meters per year (Cowart et al., 2010). Erosion rates were calculated every 5 m over approximately 30 m of shoreline using DSAS, compared to the measures made every 50 m in the NRE and ICW estimates of shoreline erosion determined with aerial photography (see Chapter 8 in the *DCERP1 Final Research Report*). In addition, we calculated net volume change between the DEMs with ArcGIS v10.0 Spatial Analyst. At each site, a polygon was created to select the area adjacent to the water edge which was sampled in both time periods, and which extended from the −0.2-m to the +0.1-m contour intervals extracted from the DEM. Using the Cut/Fill tool in Spatial Analyst, an estimate of shoreline change was created as a function of volume.

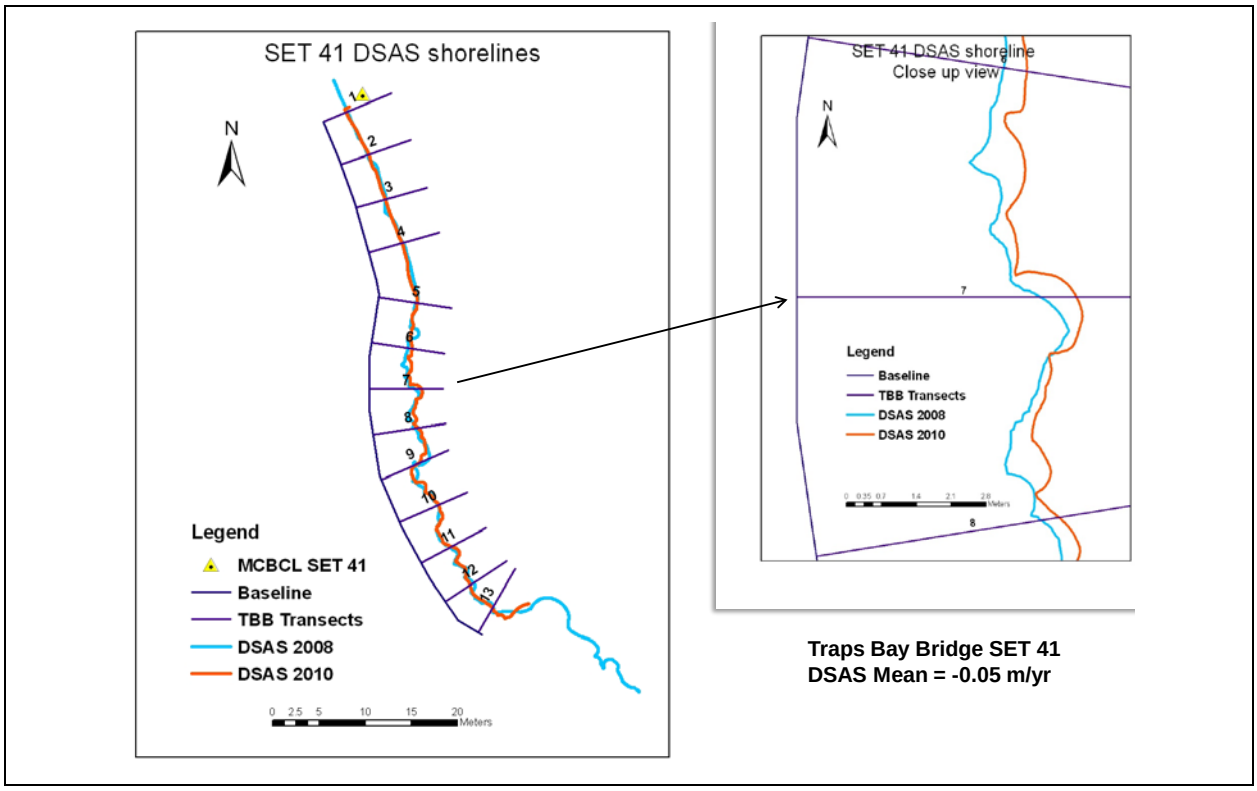

Figure 6-4. Calculation of EPR from DEMs prepared for the Traps Bay (TBB) vegetation plot shoreline.

The DSAS lines represent the 0-m NAVD 88 contour lines calculated from the 2008 (blue) and 2010 (orange) DEMs. The difference (horizontal distance) between the two shorelines was calculated at 5-m intervals along lines perpendicular to the shoreline using DSAS.

In 2010, we examined EPRs at intervals along the ICW shoreline near military splash points. A 60-m buffer was used to select shoreline adjacent to the splash points (splash point locations were obtained from a MCBCL shapefile), and shoreline change was calculated every 5 m from aerial photography obtained in 1956, 1989, and 2009. Results of and discussion about this are presented in the Chapter 8 of the *DCERP1 Final Research Report*.

We conducted an analysis of sediment bank relief and shoreline erosion rates to estimate the sediment input into the NRE via bank erosion. Results and discussion of these analyses are given in the Chapter 8 of the *DCERP1 Final Research Report*.

Coastal Wetland Inventory

Distribution of coastal wetlands on MCBCL was determined using existing wetland inventories, analysis of aerial imagery, and field observations. Sources of information and imagery are listed in **Table 6-2**. Existing wetland inventories were compared with recent imagery and results of shoreline mapping. We used our familiarity with MCBCL coastal wetlands to trim or expand polygons and used attribute information associated with the existing shapefiles to remove non-coastal wetlands from the inventory. The resulting shapefile combines these sources of wetland distribution into a single shapefile. To calculate wetland area, we assumed that fringing marshes mapped as part of the shoreline habitat type assessment had an average width of 5 m.

Table 6-2. Imagery and shapefiles used to assemble a GIS coastal wetland inventory.

Description	Source	Format	Year	Data Type and Description
NRE shoreline habitat type	NOAA CCFHR	Shapefile	2009	Marsh shorelines mapped in the field; dominant vegetation recorded
ICW shoreline habitat type	NOAA CCFHR	Shapefile	2010	Marsh shorelines mapped in the field; dominant vegetation recorded
MCBCL land cover area	MCBCL	Shapefile	2009	Extracted “marshland” cover type
NC-CREWS Onslow County	NC DCM	Shapefile	2003	Extracted “salt/brackish marsh” feature; file available at dcm2.enr.state.nc.us/wetlands/download.htm
Natural color digital orthophotography	MCBCL	Raster	2004	30-cm pixel size; used to verify coastal marsh feature classes

CCFHR = Center for Coastal Fisheries and Habitat Research; NOAA = National Oceanic and Atmospheric Administration

Snail Density and Distribution

The abundance of the marsh periwinkle snail *(Littoraria irrorata*) was obtained from each vegetation sample plot. In most plots, snail density was determined for the entire 1-m^2 area. However, when snail density exceeded 50 snails per 0.25 m^2, the snails were counted from only a 0.25-m^2 area. Snails were counted from both the sediment and plant surfaces.

Environmental Variables

Annual summer mean sea level was calculated for 2008−2012 by averaging the 6-minute water level data between June 1 to August 15 from the MHB and Gottschalk Marina/Wallace Creek (GM/WC) temporary tide gauge (WL) sensors (see Chapter 7, *Marsh Surface Elevation).* We note that in 2009, MHB WL data are missing between June 21 and July 9, due to an apparent boat collision with the sensor. This was a period of exceptionally high WL (Sweet et al., 2009); therefore, we compared our MHB WL data with the NOAA tide gauge in Beaufort, NC, from the period of 2008−2011. Based on the WL differences between these two stations during that

period, we have increased the 2009 summer WL mean upward by 1 cm to adjust for the missing 2 weeks of high WL data. Annual summer precipitation for the same time period was calculated similarly using precipitation data from the New River Air Station.

Results and Discussion

Marsh Vegetation

A total of nine plant species were recorded in marsh vegetation monitoring plots (**Table 6-3**). The low diversity of marsh plants is consistent with coastal wetlands in the southeast, and also reflects the small change in elevation over the monitoring plots (**Table 6-1**), as marsh diversity increases closer to the upland border (Bertness and Pennings, 2000). We note that the absence of a plant species from the vegetation monitoring plot does not necessarily mean the species is absent from the overall site. *Juncus*, for example, can be found near the upper edges of the marsh at FC, but not in areas within the vegetation plot. The use of permanent plots, however, does provide the opportunity to detect changes in plant species over time, particularly in marshes that are near transition zones. TBB, TBC, PPS, and PPU are located in the lower NRE and exhibit the highest plant diversity in the vegetation monitoring plots.

Table 6-3. Marsh plant species recorded from permanent vegetation monitoring plots in 2008–2012.

Species Name	FC	OBB	MHB	TBB	TBC	PPS	PPU	FN
Spartina alterniflora	●	●	●	●	●	●		
Salicornia virginica		●	●	●		●		
Distichlis spicata		●			●	●	●	
Limonium carolinianum		●	●	●	●			●
Juncus roemerianus		●		●	●	●	●	●
Borrichia frutescens		●				●		
Spartina patens				●				
Spartina cynosuroides					●		●	
Typha sp.							●	

Marsh Vegetation Percent Cover

We observed very little change over time in the distribution of marsh plants in the vegetation plots (**Figures 6-5** and **6-6**). As previously noted, the ICW marsh sites are dominated by *Spartina alterniflora*. The OBB plot contained the highest elevation sample plots (**Table 6-1**) and exhibited the greatest marsh plant species diversity. The percent cover data also indicate a higher density of *Spartina* at the MHB sites, and an increase in *Salicornia virginica* at MHB over time.

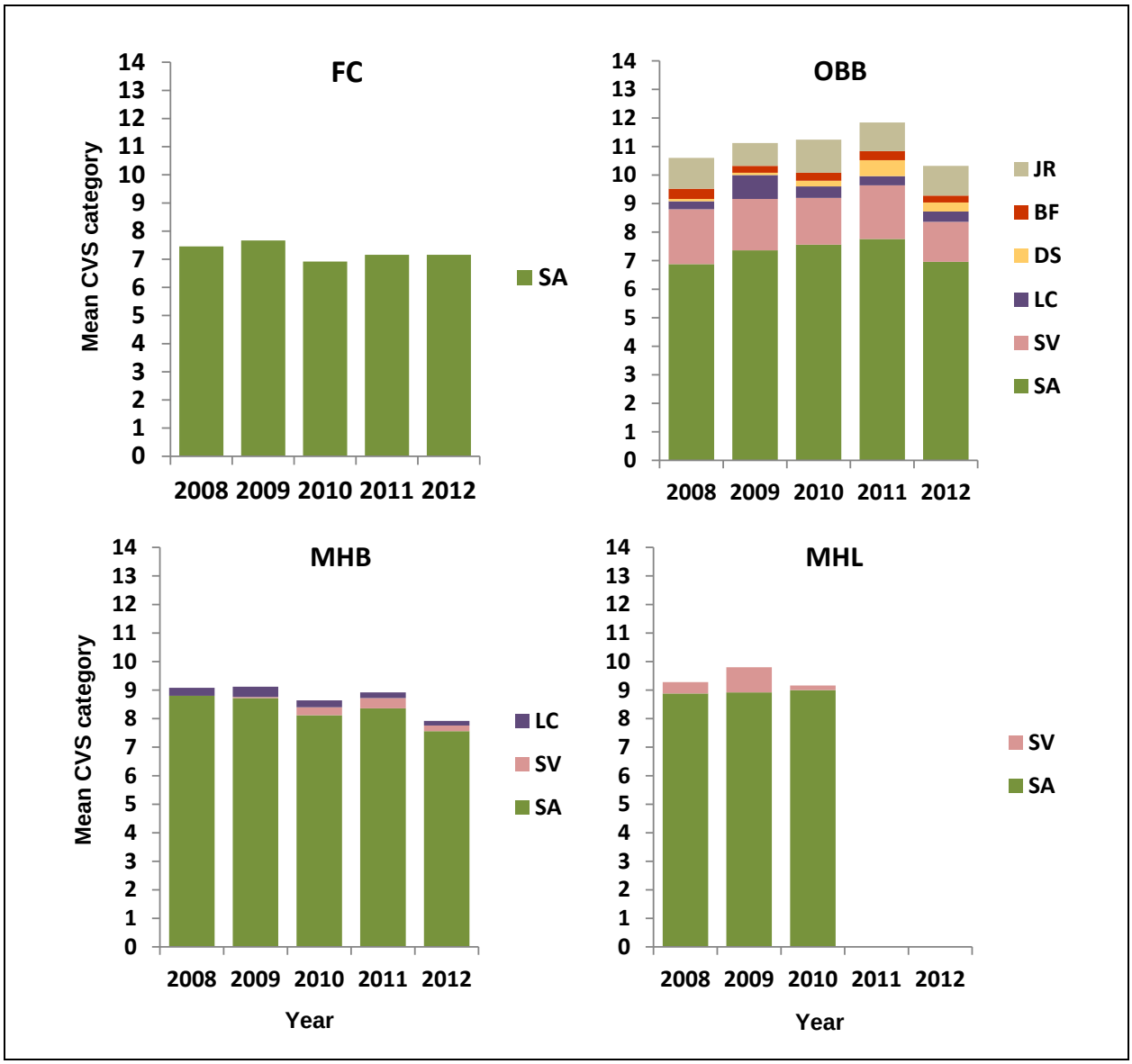

Figure 6-5. Mean values of the CVS cover category for marsh plants in the ICW vegetation plots.

CVS values range from 1–10 and increase with increasing percent cover. BF = *Borrichia frutescens*, DS = *Distichlis spicata*, JR = *Juncus roemerianus*, LC = *Limonium carolinianum*, SA = *Spartina alterniflora*, and SV = *Salicornia virginica*. See Peet et al. (1998) for cover class ranges.

In the NRE, the transition from *Spartina alterniflora*–dominated marshes in the lower estuary (TBB and TBC) to *Juncus roemerianus*–dominated marshes in the upper estuary (FN) is clearly seen in the CVS data (**Figure 6-6**). TBC is the only vegetation plot that included *S. cynosuroides*, and PPU is the only vegetation plot that included *S. patens*, although it was only recorded in 2009. The *S. cynosuroides* at PPU also decreased over time.

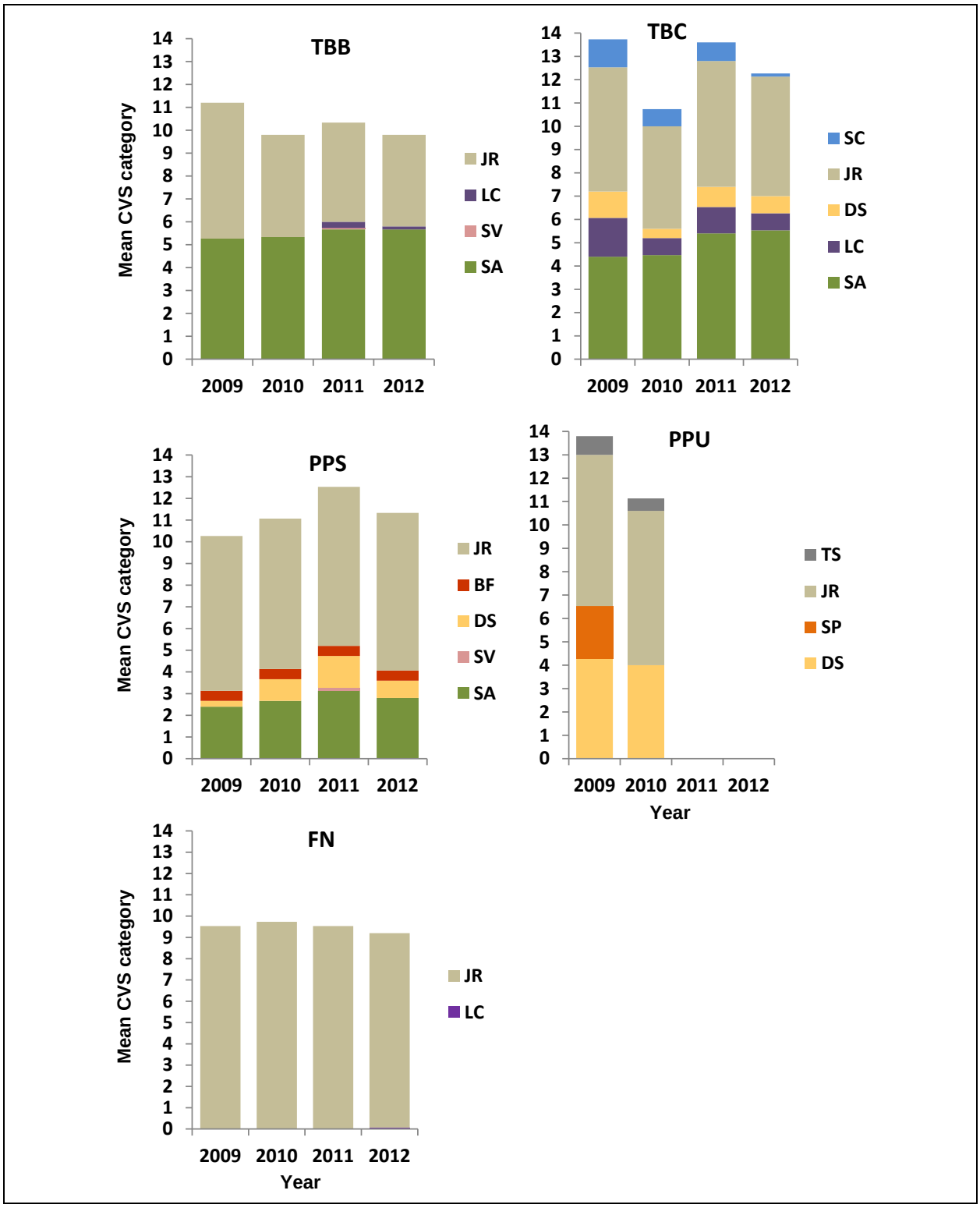

Figure 6-6. Mean values of the CVS cover category for marsh plants in the ICW vegetation plots.

CVS values range from 1–10 and increase with increasing percent cover. DS = *Distichlis spicata*, JR = *Juncus roemerianus*, LC = *Limonium carolinianum*, SA = *Spartina alterniflora*, SC = *Spartina cynosuroides*, SV = *Salicornia virginica*, and TS = *Typha* spp. (for cover class ranges, see Peet et al. [1998]).

Spartina alterniflora Density, Stem Height, and Biomass

Spartina alterniflora was found at six of the vegetation monitoring plots (**Table 6-3**). Results will be presented separately for ICW marshes (FC, OBB, MHB), which were sampled 2008–2012, and for NRE marshes (TBB, TBC, PPS), which were sampled 2009–2012. PPU was only sampled in 2009–2010 and was not included in statistical analyses. *Spartina alterniflora* occurred in 100% of the FC and MHB vegetation plots and was recorded in 92% of OBB plots. Overall, at ICW marshes, mean *Spartina* stem density in the vegetation plots was significantly different ($p<0.0001$) between sites, increasing from FC (104 stems m^{-2}), to OBB (391 stems m^{-2}) to MHB (749 m^{-2}). Mean stem height exhibited a different pattern, increasing from MHB (24 cm) to OBB (32 cm) to FC (68 cm). Above-ground biomass is calculated using both of these parameters, with the result that FC and MHB vegetation plot mean biomass do not differ significantly (407 and 365 g m^{-2}, respectively) and are both greater than OBB (253 g m^{-2}; $p=0.0005$). We note that these results are based on permanent plots designed to characterize the vegetation surrounding SETs and to detect inter-annual variability, and they were not randomly located over a large area to detect site differences. The difference in biomass between sites is in part due to different marsh surface elevations of the vegetation plots sampled at each site (**Table 6-1**).

Inter-annual variability and the effect of marsh surface elevation on marsh parameters were analyzed by site. There was a significant interaction between elevation and year on stem density and stem height at FC ($p=0.0268$, $p=<0.0001$) and a significant interaction between elevation and year on stem density only at MHB (**Appendix 6A, Table 6A-10**). At FC, overall stem density peaked in 2010, and was significantly higher than stem density in 2008–2009 and 2012 (**Figure 6-7, Appendix 6A, Table 6A-1**). However, mean stem height at FC was highest in 2009 (84.3 cm), but similar in other years, although stem height in 2012 was significantly lower than in 2011(**Appendix 6A, Table 6A-1**). Analysis by elevation bin revealed significant inter-annual variability in FC stem height and density at elevation bins −0.15, −0.05, and 0.25 m (**Appendix 6A, Table 6A-2**). The net result of these inter-annual trends in stem density and mean height is that peak biomass at FC differed by year and elevation bin, with an interaction between year and elevation (**Appendix 6A, Table 6A-10**). Biomass in 2012 was significantly less than in 2009–2011 at FC. Over the study period, biomass at FC was significantly higher in the 0.05 elevation bin, at 609 g m^{-2}, than in the −0.15, −0.05 or 0.25 elevation bins.

There was a significant year effect on stem density at OBB, and a significant year and elevation bin effect on stem height (**Appendix 6A, Table 6A-10)**. OBB *Spartina* stem density was significantly lower in 2008 and 2012 than in 2010–2011 ($p=0.0480$). Mean stem height, however, increased slightly throughout the study, from 29 cm to 34 cm at OBB (**Appendix 6A, Table 6A-1**). The annual increase in stem height was only significant, however, within the 0.15 elevation bin. These patterns translated to a non-significant change in *Spartina* biomass over the study period, with the lowest biomass recorded in 2008 and 2012 (**Figure 6-9**). *Spartina alterniflora* stem density at MHB varied both by elevation ($p=0.0017$) and year ($p<0.0001$), with a significant interaction ($p=0.0151$; **Appendix 6A, Table 6A-10**). Sample plots at MHB spanned only three elevation bins, from 0.05 to 0.25 m, and there were only five replicates of the 0.25 elevation bin, preventing analysis of inter-annual variation at this higher elevation at MHB. The overall trend was increasing stem density with elevation, with a mean of 434 stems m^{-2} at 0.05 m, 836 stems m^{-2} at 0.15 m, to 1,076 stems m^{-2} in the 0.25 m elevation plots. MHB stem

density was significantly reduced in 2012 as compared to all other years in both the 0.05 and 0.15 elevation bins at MHB, with highest stem density recorded in 2008 at 0.15 elevation bin and in 2010 in the 0.05 bin (**Figure 6-7**). *Spartina* mean stem height varied by elevation bin (p=<0.0001) but not year, with no interaction. Mean stem height was significantly greater in 0.05 elevation plots (34 cm) than at higher elevations, the reverse of the trend in stem density. The net result of these patterns for estimated peak above-ground biomass is that 2012 had significantly reduced biomass (p=0.00019; 263 g m^{-2}) compared to all other years, and biomass did not vary with elevation bin at MHB.

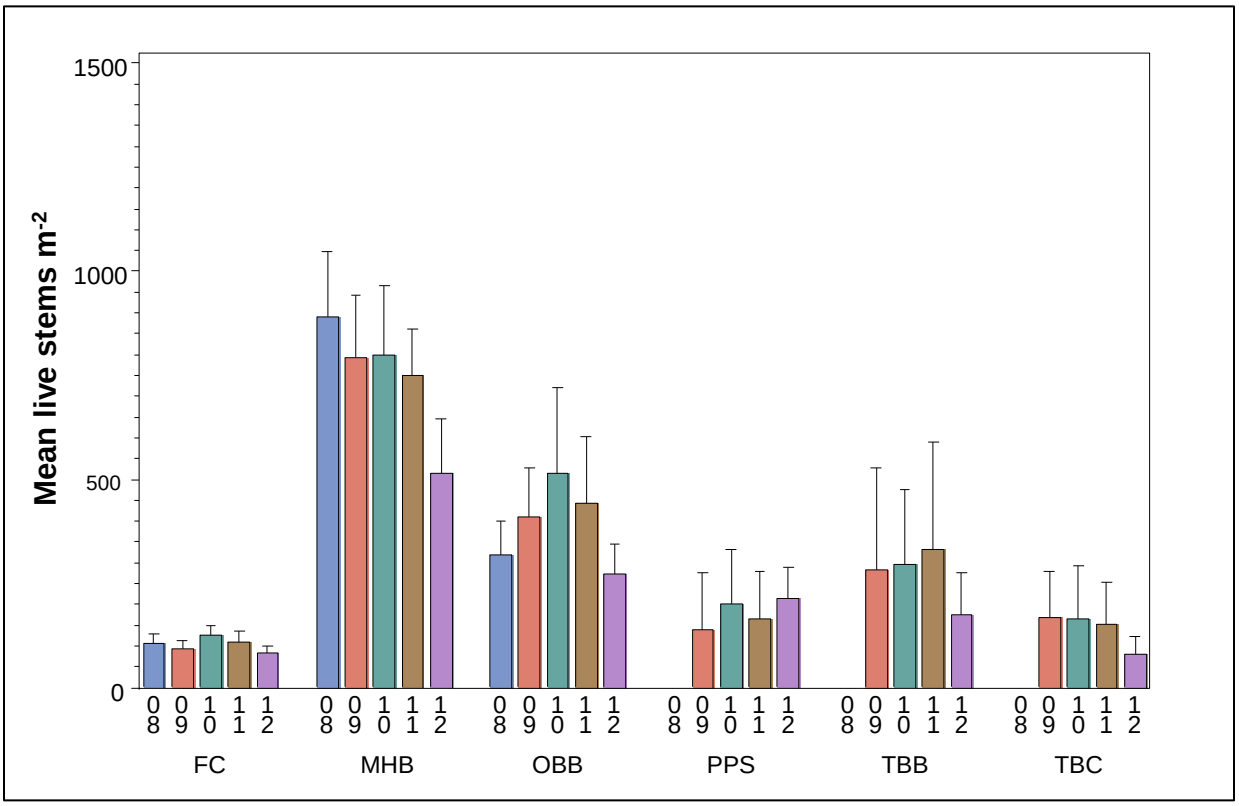

Figure 6-7. *Spartina alterniflora* live stem density in monitoring vegetation plots.

Error bars represent standard error. Sampling dates are 2008 through 2012. PPS, TBB, and TBC were not sampled in 2008.

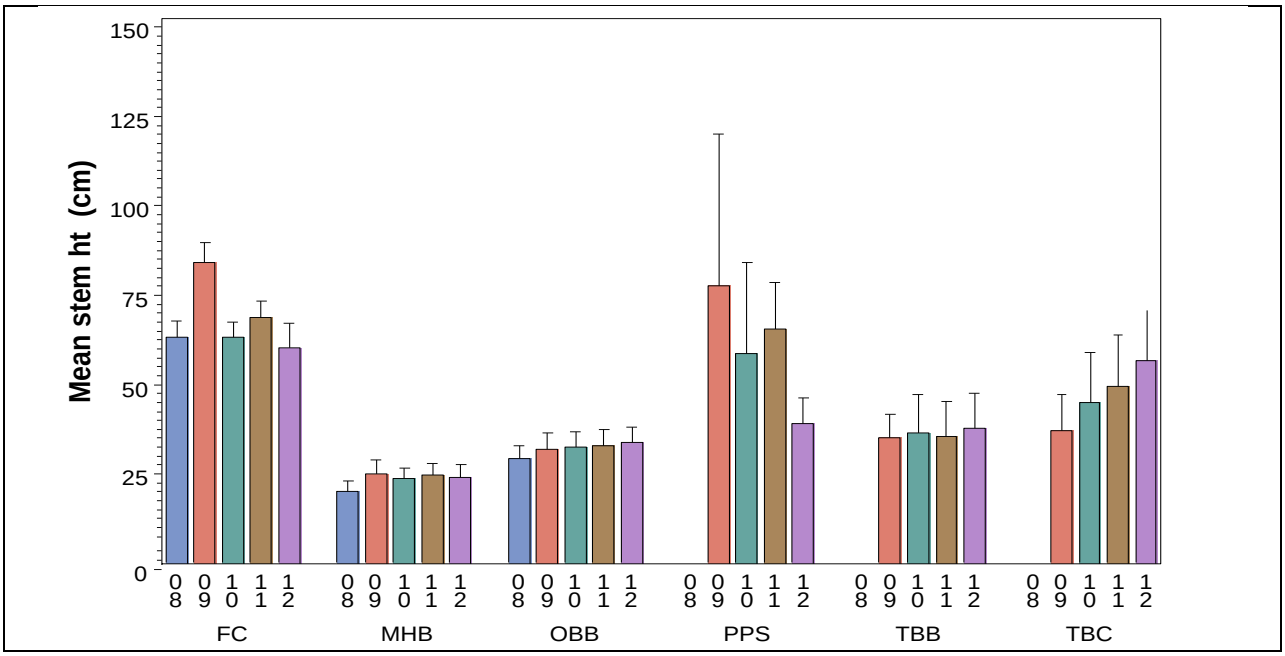

Figure 6-8. *Spartina alterniflora* mean stem height (in cm) in vegetation monitoring plots.

Error bars represent the 95% confidence interval. Sampling dates are 2008 through 2012. PPS, TBB, and TBC were not sampled in 2008.

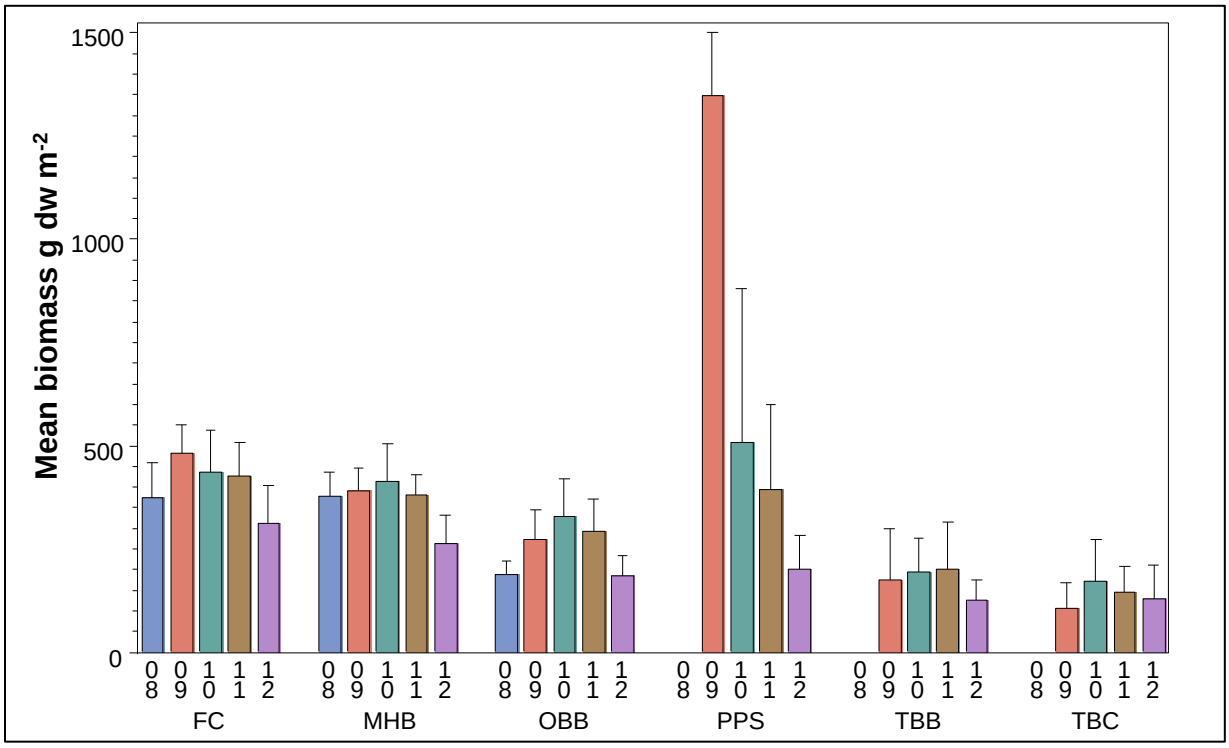

Figure 6-9. *Spartina alterniflora* estimated mean above-ground live biomass (g dw m-2) in vegetation monitoring plots.

Biomass estimates are for peak annual biomass and are calculated using stem density and mean stem height data. Error bars represent the 95% confidence interval. Sampling dates are 2008 through 2012. PPS, TBB, and TBC were not sampled in 2008.

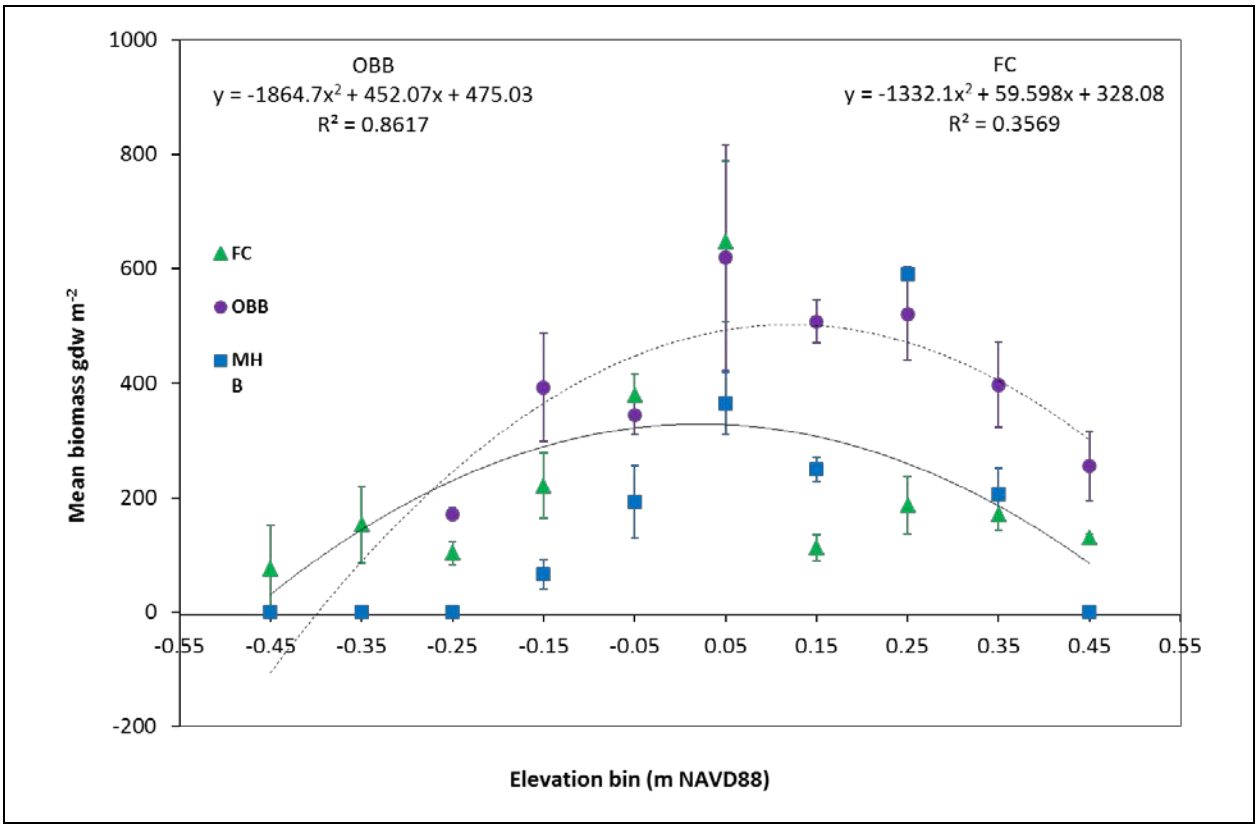

Figure 6-10. Relationship between harvested *Spartina alterniflora* above-ground biomass and marsh surface elevation in 2010.

Sites sampled in include Freeman Creek (FC), Mile Hammock Bay (MHB), and OBB (Onslow Backbarrier). Samples were obtained across the elevation range at which *Spartina* could be located at each site and encompass a wider range in elevation than occurs within the site vegetation monitoring plot. Error bars show standard error.

Peak above-ground *Spartina alterniflora* biomass was measured directly in 2010 at each of the ICW sites, in an effort that went outside the monitoring plot to obtain data from the entire elevation range at which *Spartina* occurred at each site. *Spartina* was found across a greater range of tidal elevations at FC and OBB than at MHB and in situ peak above-ground biomass was recorded at elevations between 0.05 and 0.25 m NAVD 88 (**Figure 6-10**). This is slightly lower than the elevation at which peak above-ground biomass was recorded from experimental mesocosms (Chapter 7, *DCERP Final Research Report*). In that study, above-ground biomass peaked at elevations between 0.20 and 0.40 m NAVD 88 in controls, whereas in fertilized treatments, peak biomass was found at 0.05 m NAVD 88, similar to the in situ results. It is important to determine the relationship between surface elevation and marsh biomass because this is one of the controls that determines "tipping point" at which marshes can sustain their surface elevation relative to SLR (Morris et al., 2005). The lower end of *Spartina* distribution in the intertidal is controlled by physical stress resulting from inundation; the upper end is controlled by competition from other marsh plants (Bertness and Pennings, 2000). By restricting porewater drainage, mesocosms may exacerbate some of the variables leading to physical stress, including porewater salinity, redox potential, and temperature, while eliminating the competition that restricts plant growth at the upper end. We did not find *Spartina* at any ICW sites above an

elevation of 0.45 m NAVD 88, although in mesocosms *Spartina* was able to grow at elevations between 0.50 and 0.90 m NAVD 88 (Chapter 7, *DCERP1 Final Research Report*)

Three NRE vegetation monitoring plots, which were sampled 2009–2012, included *Spartina alterniflora*, although in contrast to the ICW plots, *Spartina* was only recorded in 33% to 73% of NRE sample plots through the course of the study. This restricted distribution reduces the sampling size and statistical power of the analysis and may have contributed to the lack of significant difference in *Spartina* stem density at any of the NRE sites (**Appendix 6A, Table 6A-11**). However, we note that two of the NRE sites (TBB and TBC) had the lowest recorded *Spartina* stem densities in 2012, similar to the pattern observed at FC, MHB, and OBB **(Figure 6-7**). *Spartina* stem height was significantly lower in 2012 than in 2009 at PPS (p=0.0077), but did not vary significantly at TBB or TBC. All three NRE sites exhibited a decrease in mean *Spartina* biomass in 2012 as compared to all other years (**Figure 6-9**).

Juncus roemerianus was recorded at six of the vegetation monitoring plots (**Table 6-2**). *Juncus* was restricted to four sample plots at OBB, occurred in 60% of the sample plots at TBB and TBC, 93% at PPS, 73% at PPU, and dominated the vegetation community at FN, occurring in all sample plots. We supplemented *Juncus* collections from vegetation plots by collecting vegetation data from three plots in a *Juncus*-dominated area at FC in 2009–2012. This area was several hundreds of meters away from the FC vegetation plot, and was at a higher elevation (0.37–0.47 m NAVD 88). In the marshes bordering the NRE, *Juncus* above-ground live biomass varied significantly by site (p=0.0001) and year (p<0.0001), with no interaction. *Juncus* biomass was highest at FN (x=1324±72.8 g dw m^{-2}) and decreased downstream to TBB (535±102 g dw m^{-2}). There was no effect of elevation bin on *Juncus* biomass, perhaps in part due to the flat terrain in the vegetation plots, which varied less than 30 cm in the NRE sites. Although *Juncus* biomass was reduced in 2012 at all sites, the decrease was statistically significant only at TBB and TBC (**Figure 6-11**). Previous published reports of *Juncus* biomass in the area range from 688 g dw m^{-2} at the mouth of the Cape Fear River (Woerner and Hackney, 1997) to 843 g dw m^{-2} in Carteret County, NC (Williams and Murdoch, 1972). Christian et al. (1990) estimated an average annual *Juncus* above-ground production of 812 g dw m^{-2} along a salinity and hydroperiod gradient in Cedar Island, NC. Higher measures of live above-ground *Juncus* biomass (750 to 1,250 g dw m^{-2}) were made on Sapelo Island, GA and are consistent with the range we report from MCBCL (Gallagher et al., 1980).

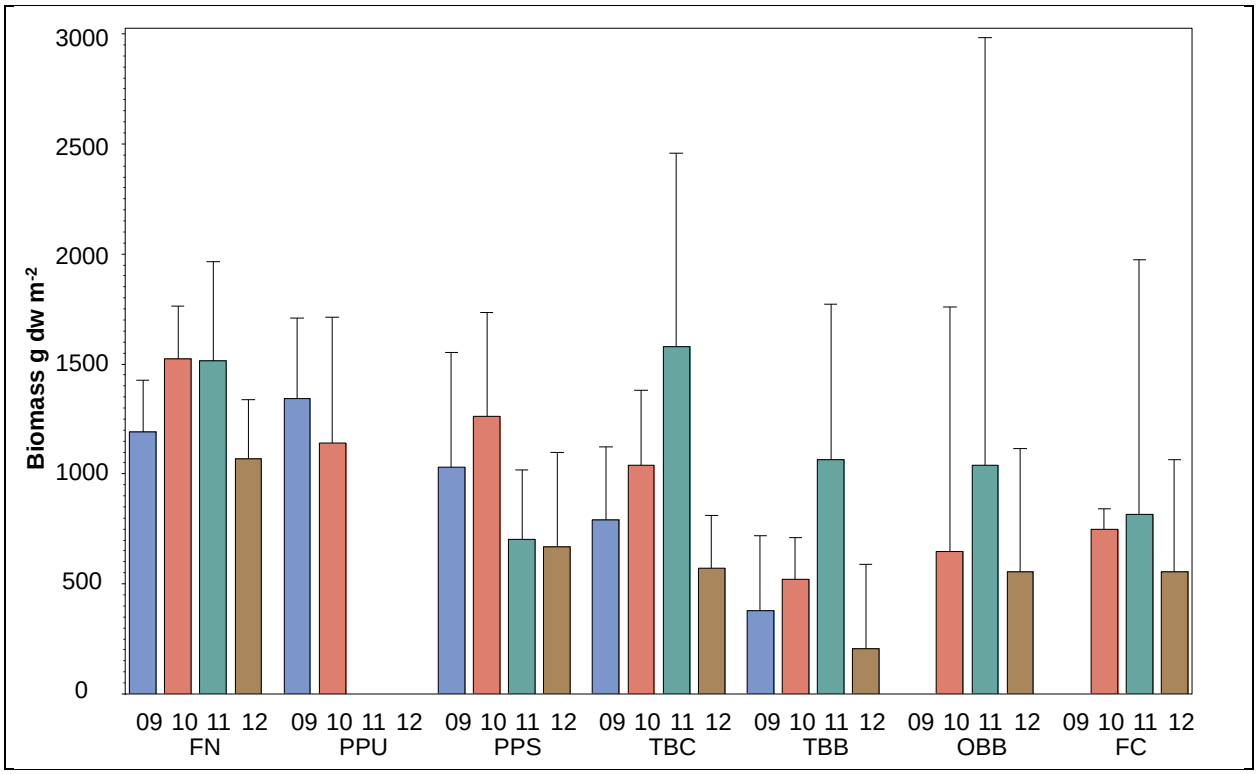

Figure 6-11. Above-ground biomass (g dw m^{-2}) of *Juncus roemerianus* from vegetation monitoring sites.

Bars represent the mean of sample plots containing *Juncus* for 2009, 2010, 2011, and 2012. Error bars represent the 95% confidence interval. Number of plots sampled for *Juncus* at each varies by site, from 10–15 plots at FN, PPU, PPS, TBC, and TBB to less than five plots at OBB and FC.

Snail Density and Distribution

The density of the marsh snail (*Littoraria irrorata*) varied significantly by site. Mean densities were less than 30 snails m^{-2} at each sampling time at all sites except MHB, where mean densities ranged from 73 to 127 snails m^{-2} (**Figure 6-12**). Snail density in 2011 and 2012 was significantly higher at MHB than in earlier years. Snails were rarely found at FN and PP sites, but were found in increasing numbers during the study period at TBB and TBC (**Figure 6-13**). In summer 2012, snails could be found at higher densities in areas surrounding the vegetation plots at both OBB and MHB (**Figure 6-14**).

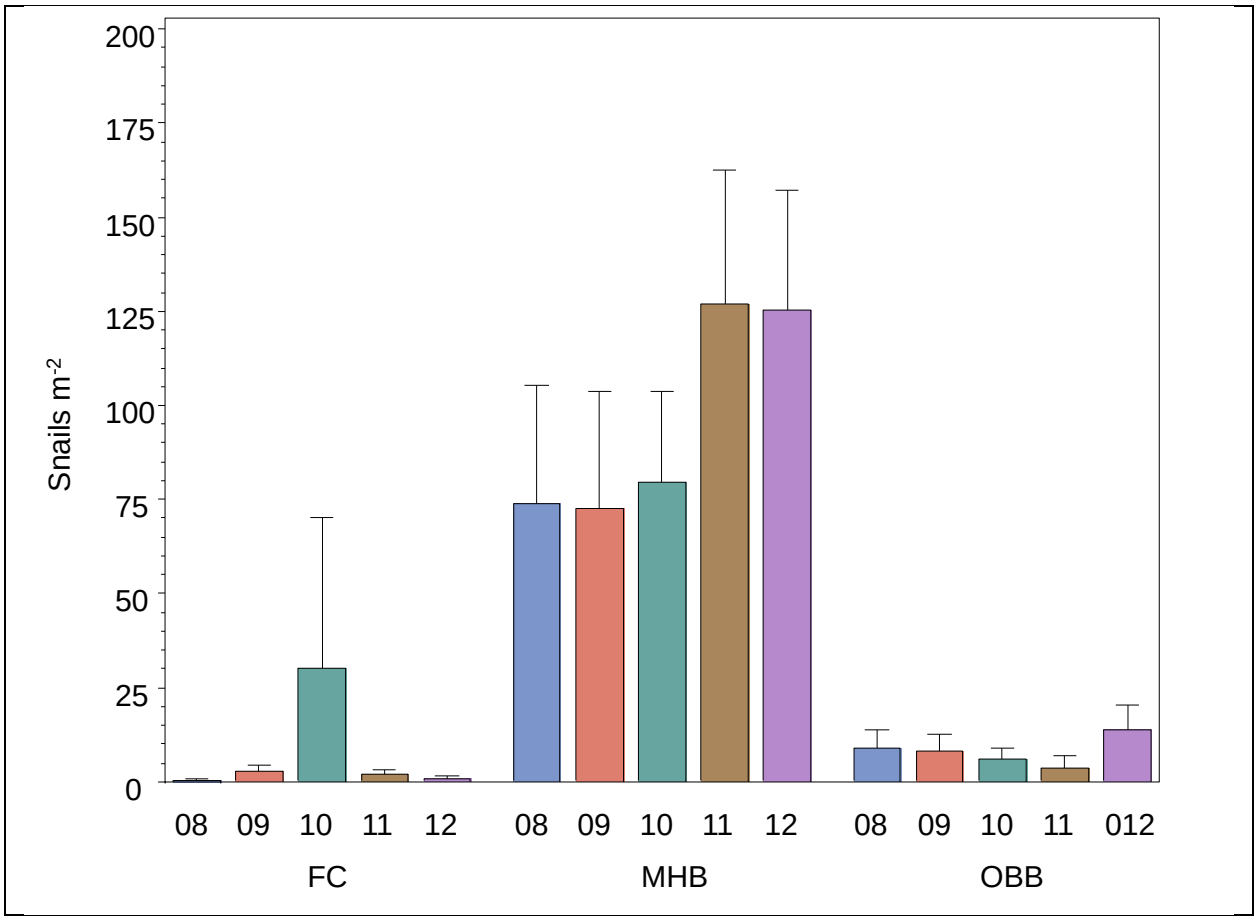

Figure 6-12. Density of the marsh snail (*Littoraria irrorata*) in vegetation plots from 2008 to 2012 at the monitoring sites adjacent to the ICW.

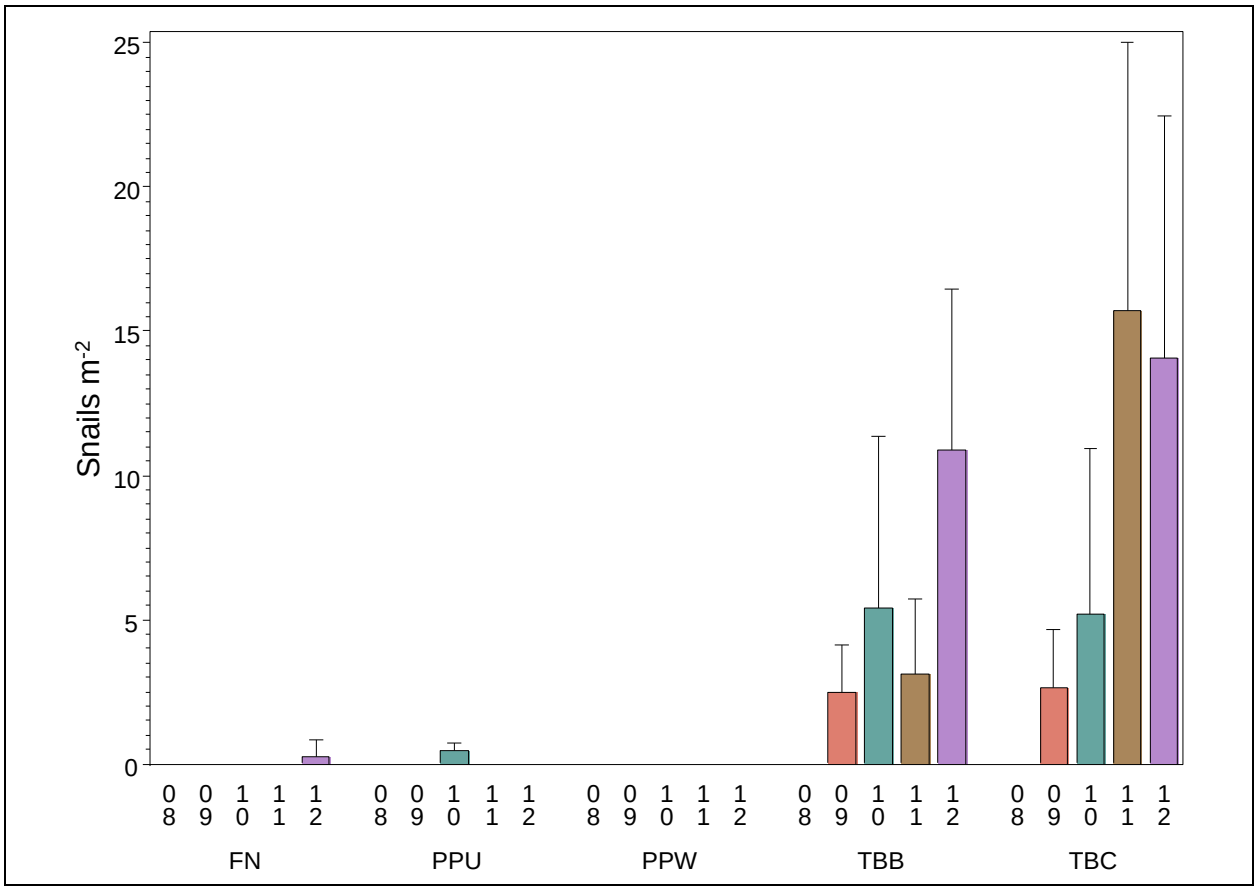

Figure 6-13. Density of the marsh snail (*Littoraria irrorata*) in vegetation plots from 2009 to 2012 at the monitoring sites adjacent to the NRE.

Over the last decade, a number of papers have demonstrated that the periwinkle snail can control *Spartina alterniflora* production (Silliman and Bertness, 2002; Silliman and Zieman, 2001; Silliman et al., 2005). Snail densities in experimental manipulations that resulted in significant reductions in marsh production ranged from 500 to 1,200 snails m^{-2}. These results were used to develop a hypothesis that a trophic cascade, originating with a decline in blue crabs due to overharvest leading to increased snail density, could decrease salt marsh production (Silliman and Bertness, 2002). More recently, high snail densities have been reported in several marsh die-off sites in the southeastern United States, and it was suggested that snails contribute to the expansion of marsh dieback during periods of drought (Silliman et al., 2005). Marshes characterized as "healthy" in that study had snail densities ranging from 1 to 558 snails m^{-2}, and marsh soil salinity ranged from 27 to 49 ppt in dieback areas (Silliman et al., 2005). However, these sites were located in more brackish portions of the estuary than the ICW marshes of this study, and reported estuarine salinity during drought periods (25-31 ppt) is less than the average salinity experienced by marshes adjacent to the ICW (**Figure 6-17**). In contrast, Kiehn and Morris (2009) found a positive relationship between stem density and snail density in a South Carolina marsh over a 40-month period and no evidence that snail grazing controlled marsh production. Snail density in this study was not manipulated and averaged 25–50 snails m^{-2} in what was characterized as "healthy marsh." An increase in snail density at several sites (MHB, OBB, TBB, and TBC) is correlated with a decrease in marsh biomass in 2012; however, other

sites, such as FC and PPS, also experienced a decrease in marsh biomass in 2012 and snails were virtually absent from those sites. The decline in *Spartina* at PPS and TBB is likely partly due to impacts from shore erosion (**Table 6-4**). Research results have clearly demonstrated the nitrogen limitation of *Spartina* at each of the ICW sites (Priest, 2012). The relative roles of snail grazing (top-down), nutrient availability (bottom-up), and environmental controls (mean sea level, precipitation) on marsh primary production is complex, and yet understanding these roles is crucial to the development of models forecasting marsh response to SLR and to developing adaptive management approaches.

The most dramatic change in salt marsh stem density and biomass over the study period was at MHB. In 2012, large portions of the marsh at both OBB and MHB exhibited visual signs of browning and decreased stem density (**Figure 6-14**), which was captured in the monitoring plot data.

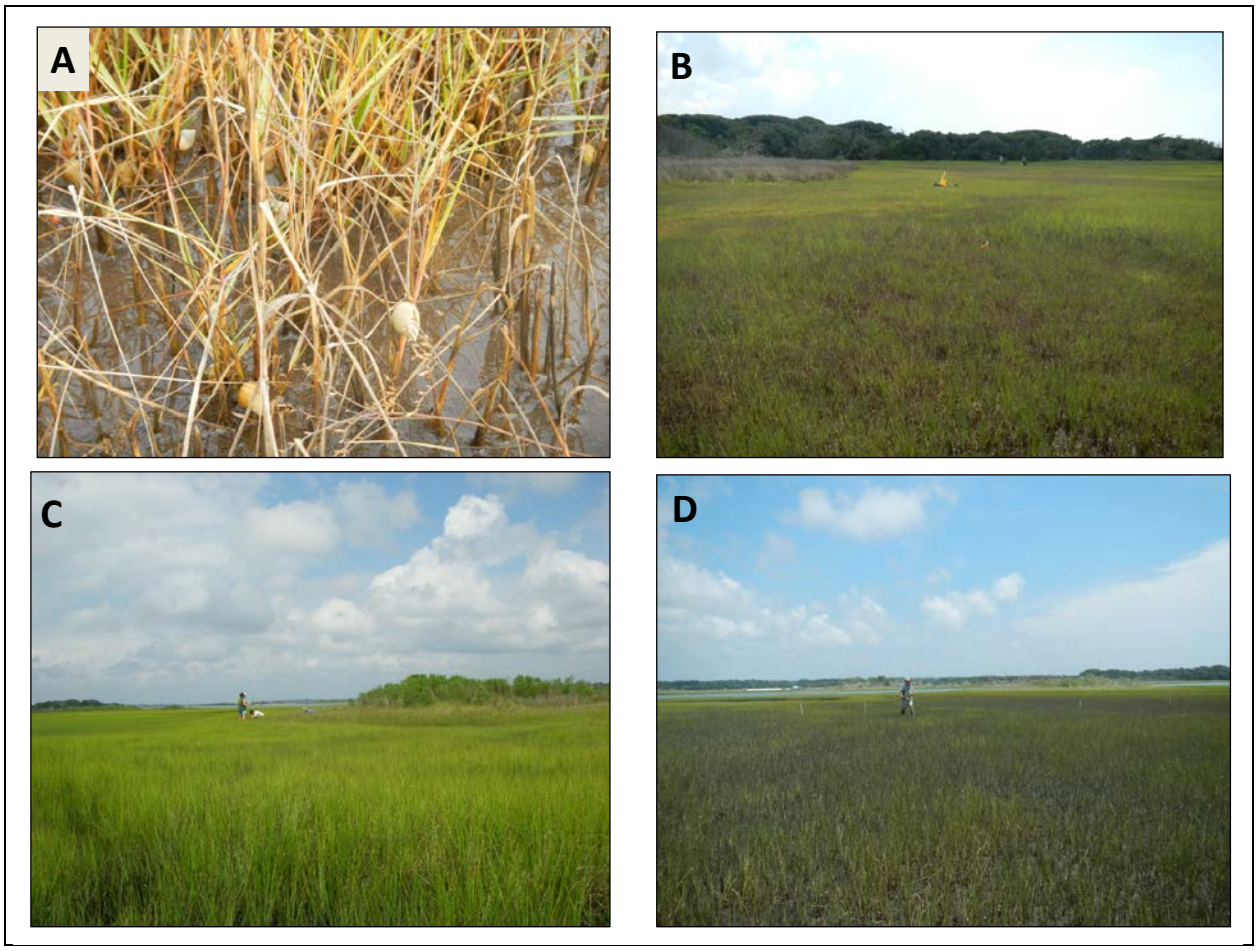

Figure 6-14. Appearance of the marsh snail (*Littoraria irrorata*) and potential impact on MCBCL marshes.

(A) High density of snails on marsh stems at OBB in 2012. (B) OBB Marsh vegetation plot in 2012, showing browned areas. (C) MHB Marsh vegetation plot in August 2010, showing healthy green marsh. (D) MHB Marsh vegetation plot in August 2012, showing browned areas of marsh. The view is in same direction as in panel C but from farther away.

Coastal Wetland Distribution

An inventory of MCBCL coastal wetlands, including salt and brackish marshes, was prepared using ArcGIS (**Figure 6-1**). The total area of coastal wetlands on MCBCL is approximately 1,090 ha (2,690 ac).

Shoreline Habitat Type and Mapping

Sediment banks are the most prevalent habitat type along the NRE shoreline, representing 53%, or 66 km, of the total shoreline. After sediment banks, Marsh (26.5%), Modified (24.3%), and Swamp Forest (7.3%) habitats compose the remainder of the NRE shoreline. Along the ICW, marsh is the Dominant Habitat Type (80%), followed by Sediment Bank (19%) and Modified (1%) shorelines. The distribution of coastal wetland dominant plant species from shoreline habitats is shown in **Figure 6-15**, which illustrates the transition from marine wetlands (*Spartina alterniflora*–dominated) to brackish marshes (*Juncus roemerianus, Spartina cynosuroides*) as one moves up-estuary. The map also documents the occurrence of *Phragmites australis*, an invasive marsh species along NRE shorelines, and the presence of freshwater marsh plants. These data provide baseline information to track potential changes in marsh distribution associated with climate change and/or SLR and can be used to guide wetland restoration efforts. Additional details on distribution and features of shoreline marsh habitats, their long-term erosion rates, and distribution relative to wave energy are available in the Chapter 8 of the *DCERP1 Final Research Report*.

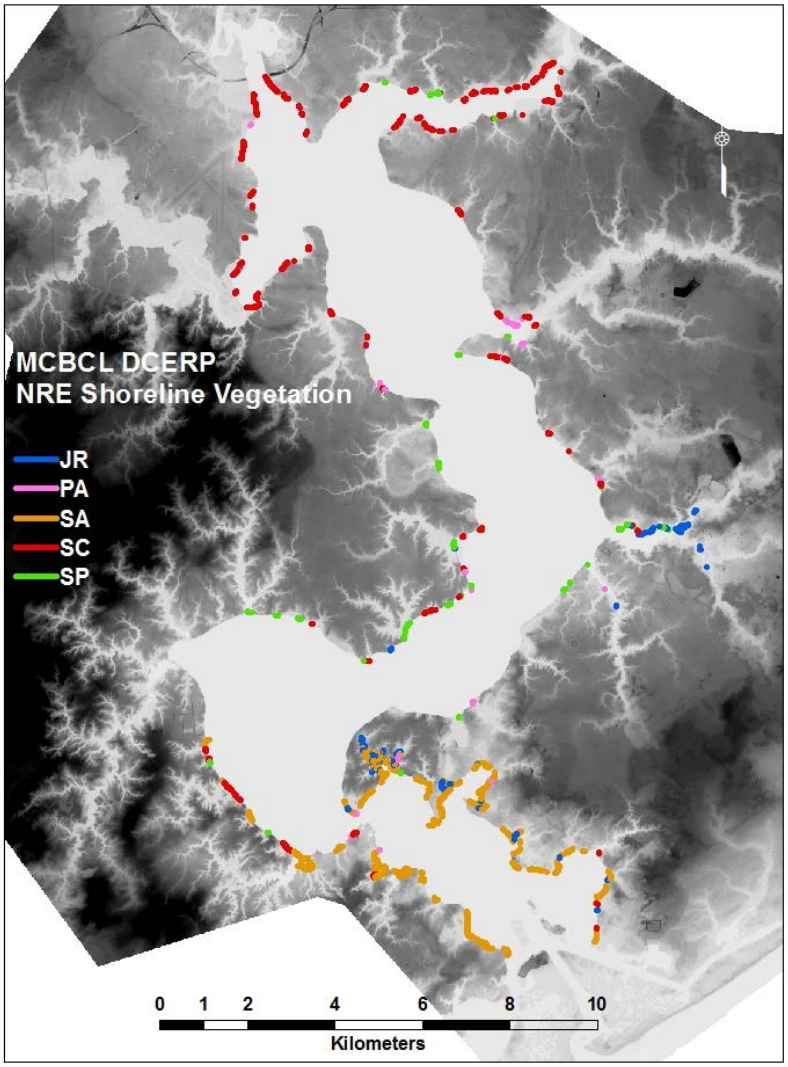

Figure 6-15. Distribution of dominant marsh species from fringing salt marshes along the NRE shoreline.

JR = *Juncus roemerianus*, PA = *Phragmites australis*, SA = *Spartina alterniflora*, SC = *Spartina cynosuroides*, and SP = *Spartina patens*. Marsh species determinations were made while ground-truthing shoreline habitat type from a small boat.

Shoreline Location and Erosion Rate

DEMs of three vegetation monitoring site shorelines on the NRE (PPS, TBC, and TBB) were used to calculate shoreline erosion rates and overall sediment volume change between 2008 and 2011 (**Figure 6-16a through d**). Calculated EPRs, or linear change in the zero-line contour, ranged from −0.08 m y^{-1} at PPS to 0.01 m y^{-1} at TBC (**Table 6-4**). All three sites showed a net gain in sediment volume between 2008 and 2011. The calculated average increase in marsh elevation for the shoreline sites ranged from 0.015 m at TBC to 0.063 m at PPS. There was an inverse relationship between calculated shoreline erosion (EPR) and mean surface elevation change. PPS had the most negative EPR and the highest mean increase in surface elevation, and TBC exhibited the highest EPR, showing net shoreline accretion, and the lowest mean increase

in surface elevation. These observations are consistent with a hypothesis that sediments eroded from the marsh edge are redistributed to the marsh surface, and contribute to observed increases in marsh surface elevation.

Comparison of these short-term (3-year) results with longer term measures of shoreline erosion obtained via digitization of shorelines from aerial photography reveal consistent patterns at the three sites sampled. As illustrated in **Figure 6-16**, the sections of shoreline sampled at both PPS and TBB have experienced long-term erosion, as determined by comparing the seaward location of the shoreline in 1956 and 1989 photography to the present day shoreline. TBC, which showed net shoreline accretion in our 3-year study, also showed net seaward movement of the shoreline from 1956 to 1989 to present day. **Table 6-5** also demonstrates that sites experiencing greater wave energy as calculated by WEMo (Malhotra and Fonseca, 2007) exhibited greater erosion rates than marsh shoreline sites in more protected areas. A complete analysis of NRE and ICW shoreline erosion rates, by habitat type and by RWE class, of NRE and ICW shorelines is provided in Research Project CW-2 (Chapter 8 in the *DCERP1 Final Research Report*).

Table 6-4. Results from change-analysis of marsh DEMs.

Initial and end date of data collection are given and the total DEM area used in calculations. Calculations include the EPR as calculated by DSAS, and total volume change as determined by the ArcGIS Spatial Analyst program.

Site	Initial Date	End Date	DEM Area (m^2)	EPR ($m\ yr^{-1}$)	Total Volume Change (m^3)	Mean Surface Elevation Change (m)
TBB	12/2008	4/2011	482.0	−0.05	12.55	0.026
TBB	12/2008	1/2011	394.0	0.01	5.99	0.015
PPS	12/2008	4/2011	116.0	−0.08	7.31	0.063

Table 6-5. Comparison of independent long- and short-term estimates of shoreline erosion at NRE shoreline sites.

Higher energy sites (RWE>100) indicated in bold text.

Site	SET	RWE (joules m^{-2})	SCR ($m\ y^{-1}$)		
			1956−2004	1989−2004	2008−2011
TBB	**41**	**122**	**–0.05**	**–0.18**	**–0.05**
TBC	42	1	0.13	0.36	N/A
PPS	**43**	**264**	**–0.11**	**–0.44**	**–0.06**
FNS	46	3	–0.01	0.08	N/A

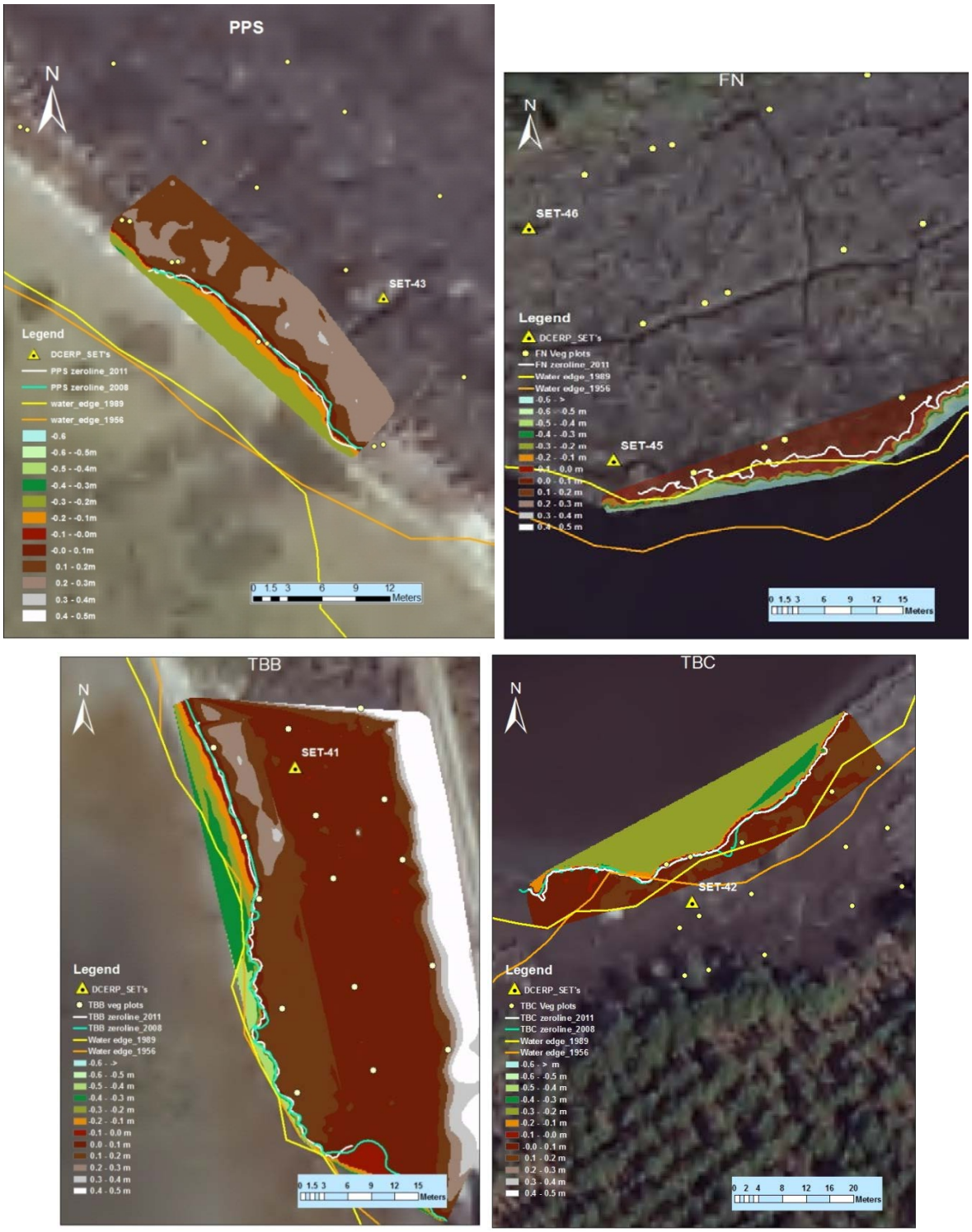

Figure 6-16. Aerial photographs of NRE shoreline sites, showing location of vegetation monitoring plots (yellow circles), SETs (yellow triangles), DEM of shoreline, calculated zero-line of shoreline in 2008 (turquoise line) and 2011 (white line), and shoreline as mapped from aerial photography in 1956 (orange line) and 1989 (yellow line).

Elevation of marsh along the shoreline was determined using a Trimble 5800 RTK-GPS receiver with the SET mark as a base station.

Environmental Variables

Porewater Salinity

Porewater salinity measured in 2010 from the *Spartina alterniflora* harvest plots ranged from 30 to 62 ppt. As expected in these regularly flooded sites, salinity was close to 35 ppt. The exception was at OBB where salinity exceeded 40 ppt at elevations greater than 0.25 m NAVD 88 (**Figure 6-17**).

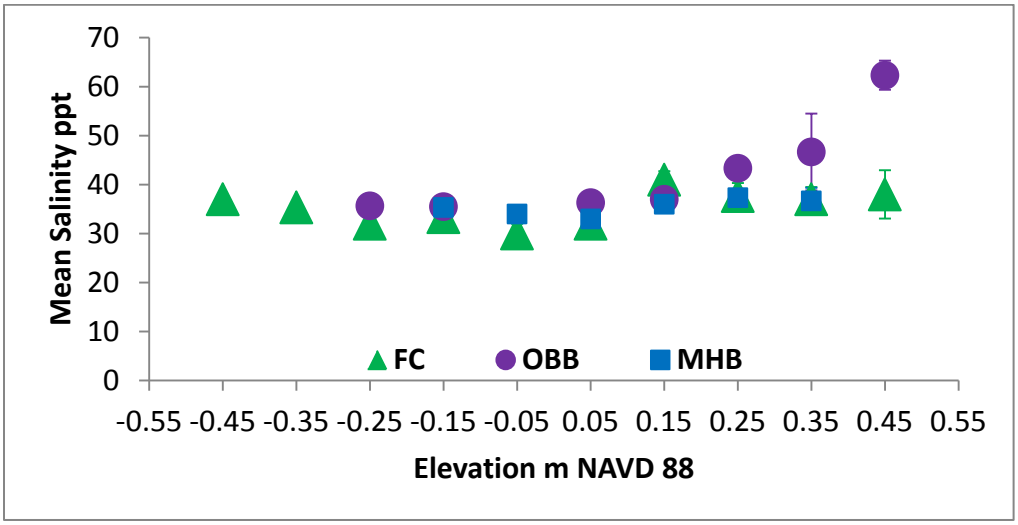

Figure 6-17. Porewater salinity collected in 2010 from plots used for *Spartina alterniflora* harvest.

Error bars show standard error.

Water Level and Precipitation

Mean values for WL and precipitation during the summer (June 1–August 15) are presented in **Table 6-6**. Although 2009 was noted for a summer time high water level event along the entire East Coast (Sweet et al., 2009), summer mean WL at both stations was higher during 2011 and 2012 than in 2009. However, the maximum WL at GM/WC during 2009 was higher than in any other year, and was the second highest at MHB. Summer precipitation varied by 12 cm between the 5 years, with the greatest summer precipitation occurring during 2012 (32 cm), and the least during 2009 (20 cm).

Table 6-6. Mean water level (MWL) given as mean (standard deviation, maximum) for MHB (Mile Hammock Bay) and GM/WC (Gottschalk Marina/Wallace Creek) temporary tide gauge data (in meters mean sea level [MSL]).

Precipitation data were obtained from New River Air Station. MHB 2009 WL data are adjusted for missing data. Summer period is defined as June 1–August 15 to correspond with marsh growing season and timing of peak biomass data collection.

Year	Summer MWL MHB (m MSL)	Summer MWL GM/WC (m MSL)	Summer Total Rainfall (cm)
2008	0.003 (0.252, 0.476)	0.029 (0.111, 0.344)	25
2009	0.038 (0.264, 0.612)	0.074 (0.144, 0.484)	20
2010	0.007 (0.260, 0.540)	0.017 (0.116, 0.355)	28
2011	0.068 (0.257, 0.513)	0.077 (0.109, 0.345)	23
2012	0.144 (0.262, 0.763)	0.129 (0.117, 0.466)	32

For the period 2008–2012, there was a slight negative relationship between summer mean sea level (MWL) and both *Spartina alterniflora* stem density and peak above-ground biomass as measured at FC, OBB, and MHB (**Figure 6-18**). However, these relationships were weak (r^2<0.20), and there was no relationship between summer MWL and *Spartina* mean stem height (**Figure 6-18**). We also observed a negative relationship between summer precipitation and *Spartina* peak above-ground biomass at the three ICW sites (**Figure 6-19**). These negative trends are driven by the decrease in *Spartina* biomass which occurred in 2012, which was observed at every monitoring site (**Figure 6-9**). This decline in biomass occurred in a year which had the highest summer MWL and highest summer precipitation during the study period (**Table 6-6**).

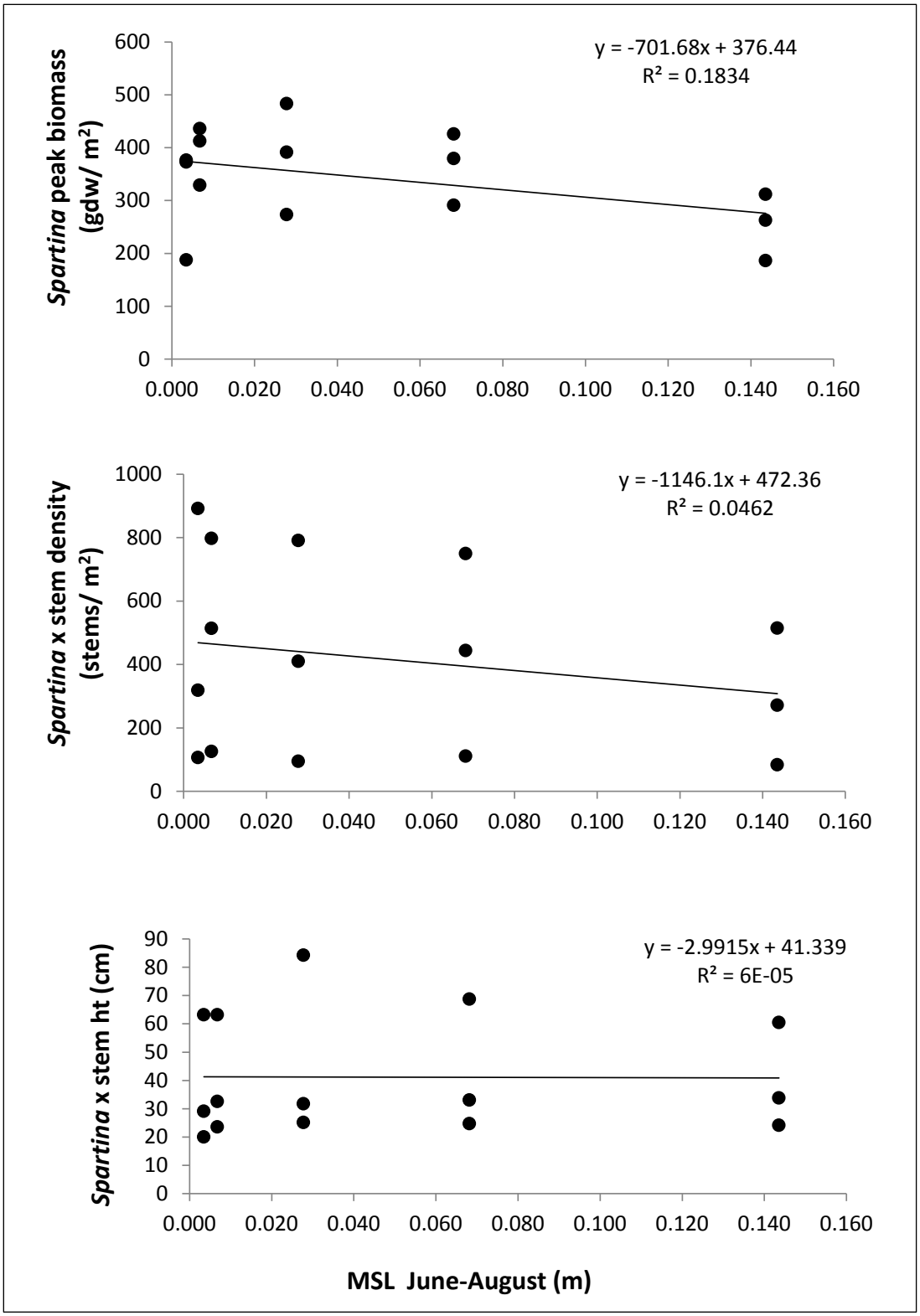

Figure 6-18. Relationship between summer MWL as recorded at MHB and *Spartina alterniflora* vegetation parameters at monitoring sites FC, OBB, and MHB.

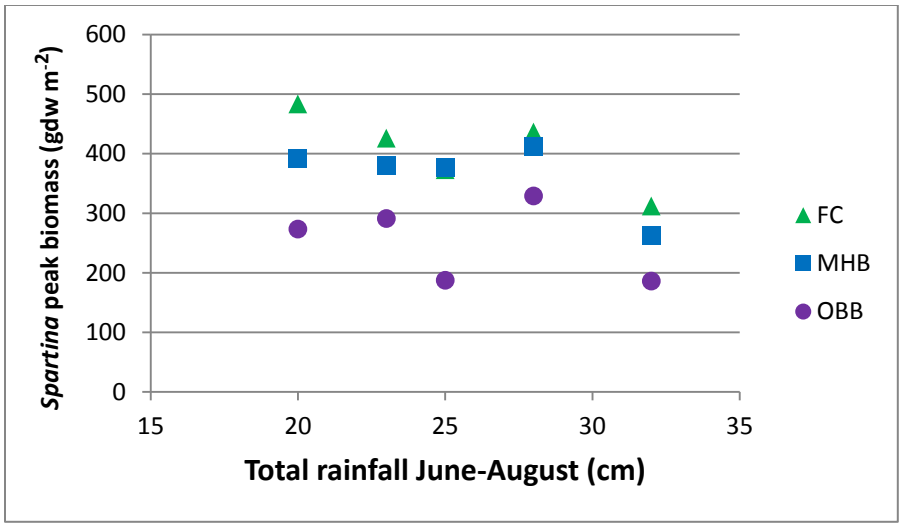

Figure 6-19. Relationship between *Spartina alterniflora* above-ground biomass and summer precipitation at monitoring sites along the ICW.

These results are in some contrast to other published reports of positive relationships between *Spartina alterniflora* production and summer MWL. A *Spartina* marsh in South Carolina exhibited a strong positive relationship between both summer rainfall and precipitation and annual production (Morris and Haskin, 1990). The South Carolina study was from a high marsh site (70 cm above MSL) with a canopy structure of shorter and denser plants (mean height less than 30 cm; greater than 1,000 stems m^{-2}). The SC study also made monthly measures of canopy structure, and so was able to estimate annual production, rather than the peak biomass measured in this study. Kirwan et al. (2012) compared the relationship between summer mean water level with *Spartina* peak above-ground biomass at seven marsh sites in Virginia over 7–10 years. Elevation at all these sites was generally higher (0.34–0.87 m NAVD 88) than surface elevation of most of the ICW sampling plots. Although there was significant inter-annual variability at the Virginia marsh sites, only two sites exhibited a significant relationship with summer MWL, which was positive at one site and negative at another (Kirwan et al., 2012). These authors suggest that a positive relationship between *Spartina* production and inundation is only found at sites in the mid-intertidal with significant slope (Kirwan et al., 2012).

Assessment of Trends in the Data

Assessment of Monitoring Design

The chief objective of the Coastal Wetlands Module, including research and monitoring activities, was to provide information to help resource managers improve the sustainability of coastal wetlands on MCBCL. Coastal Wetlands monitoring sites were chosen to encompass the wide range in salinity and geomorphological setting in which marshes occur on MCBCL. Along the ICW, marsh sites included a backbarrier island marsh (OBB), a marsh associated with a large tidal creek (FC), and marsh near the New River Inlet that was potentially impacted by military training exercises (MHB and MHL). We expected that patterns of marsh production might vary significantly by site, and if so, this would inform our ability to expand research results across the MCBCL landscape. Site variability was tested by performing univariate and multivariate analysis

of longitudinal data collected from permanent plots, using analysis designed for repeated measures of experimental units.

We did not know a priori that there was a two-fold increase in tidal range between Browns Inlet and the New River Inlet. However, water level monitoring documented the difference, and vegetation monitoring confirmed that this change in tidal amplitude altered the distribution of *Spartina alterniflora*. This important finding has implications for model predictions on the vulnerability of marshes to SLR, and was incorporated into Research Project CW-1 results and conclusions.

We emphasized fringing marshes in selecting monitoring sites in the NRE, and captured the change in dominant vegetation from *Spartina* to *Juncus*. The NRE monitoring sites also included sites experiencing significant erosion (PPS and TBB) and an accreting site (TBC). Monitoring of the NRE shoreline and determination of short and long-term erosion rates supported Research Project CW-2 objectives and helped to identify vulnerable shorelines. Marsh erosion rates were measured over different spatial and temporal scales, from base-wide to 30 m wide monitoring plots, and from a 60-year period at broad spatial scales to 2–3 year periods at smaller spatial scales, using EPR analysis and ArcGIS Spatial Analyst tools. This approach yielded consistent information across spatial and temporal scales, broadening and confirming Research Project CW-2 results. We extended the study of shoreline erosion into the ICW, provided crucial information for the development of a hypothesis on the role of maintenance dredging in limiting sediment supply to marshes adjacent to the ICW.

Assessment Seasonal and Annual Variability in the Data

Our monitoring program was designed to detect annual changes in marsh peak above-ground biomass and to collect data on biological and environmental parameters, which might be correlated with annual variability. We found significant annual variability in marsh above-ground biomass at most sites. This variability was inversely correlated with summer water level and precipitation. At three sites, an increase in grazer (marsh snail) density was also correlated with a decrease in marsh production. These results are consistent with predictions made by Research Project CW-1, in which the MEM forecast a decline in marsh biomass associated with SLR, particularly for marshes occupying elevations below the optimal for biomass production.

Conclusions and Implications for Future Research

Coastal wetlands monitoring, using existing sites, will provide the data needed to develop a landscape-scale model of marsh vulnerability to SLR. In addition, another 4–5 years of data collection will improve our ability to detect the response of marsh production to short-term (annual to seasonal) increases in sea level, in support of model predictions. Continued monitoring will also help to assess the potential impact of snail grazing on marsh production.

We will slightly alter our vegetation monitoring scheme to sample *Spartina* and *Juncus* above-ground biomass across the range of tidal elevations at which it occurs at each site. In particular, we will collect data to model the relationship between *Juncus* production and surface elevation across a salinity gradient, which has not existed previously.

Key Scientific Findings—Fundamental Cause-and-Effect Relationships

Both *Spartina alterniflora* and *Juncus roemerianus* above-ground biomass were reduced in 2012, compared to previous years. Summer 2012 was a period of higher mean water level and greater precipitation than preceding years. There is also a trend of an increase in snail density at several, but not all, of the sites exhibiting reduced marsh biomass. Results from an analysis of the in situ relationship between marsh surface elevation and biomass show that the optimal elevation for *Spartina* above-ground production is between 0.05 and 0.25 m NAVD 88. These results, in conjunction with research findings of Research Project CW-1, suggest that much of the MCBCL *Spartina* marshes are at or below the optimal elevation, and thus particularly vulnerable to accelerated SLR. The fact that higher water levels in 2012 resulted in a decrease in marsh production, despite greater precipitation and no increase in water column salinity, is consistent with conclusions of Research Project CW-1, where it was suggested that MCBCL marshes, particularly those west of the ICW, are situated well below the optimal elevation and are particularly vulnerable to SLR.

The intertidal distribution *of Spartina alterniflora* on MCBCL is determined, in main part, by salinity and the tidal amplitude of the site. *Spartina* grows at elevations between −0.45 to 0.45 m NAVD 88 in Freeman Creek, but is only found at elevations between −0.15 and 0.35 m at Mile Hammock Bay. Marshes in areas with a greater tidal range are more resilient to SLR, and changes in tidal amplitude, which may result from changes in inlet dynamics as a result of storms, SLR, or dredging, can have a profound impact on the vulnerability of marshes to SLR.

Findings Supportive of Current Base Management Practices

We found the effects of military training exercises to be limited in space and time. As reported in Chapter 8 of the *DCERP1 Final Research Report* for Research Project CW-2, we found only a few instances of increase erosion associated with splash points. The impact of LCAC passage over the MHB appears to be transient. However, we note that we have not been able to conduct a controlled experimental assessment of LCAC impacts.

Although MCBCL marshes are at risk both from accelerated SLR and erosion, current base management practices do not have a significant impact on marsh sustainability or resilience. It should be noted that although efforts to reduce suspended sediments and dissolved nitrogen result in improved water quality, they may also deprive marshes of the nutrients and sediments needed to thrive, particularly during a period of accelerated SLR.

Findings with Implications for Future Base Management

Findings are provided in Chapter 8 of the *DCERP1 Final Research Report*.

Findings with Implications for DCERP2

Erosion of the marsh edge represents a potential significant loss of carbon. Our monitoring effort documented the extent of marsh shoreline in both the mainstem NRE and the ICW, and calculated both long- and short-term erosion rates and sediment volume changes. These data, when combined with planned DCERP2 experiments on the lability of marsh carbon liberated via erosion, will allow the calculation of the contribution of this process to the NRE carbon budget.

Literature Cited

Bakker, J., H. Olff, J. Willems, and M. Zobel. 1996. Why do we need permanent plots in the study of long-term vegetation dynamics? *Journal of Vegetation Science 7*:147–156.

Bertness, M.D., and S.C. Pennings. 2000. Spatial variation in process and pattern in salt marsh plant communities in eastern North America. Pp. 39–57 in *Concepts and Controversies in Tidal Marsh Ecology*. Edited by M.P. Weinstein and D.A. Kreeger. New York, NY: Kluwer Academic Publishers.

Christian, R., W. Bryant Jr., and M. Brinson. 1990. *Juncus roemerianus* production and decomposition along gradients of salinity and hydroperiod. *Marine Ecology Progress Series 68*:137–145.

Cowart, L., J. Walsh and D.R. Corbett. 2010. Analyzing estuarine shoreline change: A case study of Cedar Island, North Carolina. *Journal of Coastal Research 26*(5):817–830.

Dahl, T.E. 2011. Status and trends of wetlands in the conterminous United States 2004-2009. U.S. Department of the Interior; Fish and Wildlife Service, Washington, D.C., 108 pp.

Elzinga, C.L., D. W. Salzer, and J.W. Willoughby. 1998. *Measuring and Monitoring Plant Populations*. Prepared for the Bureau of Land Management. Available at http://www.blm.gov/nstc/library/pdf/MeasAndMon.pdf.

Gallagher, J.L., R.J. Reimold, R.A. Linthurst, and W.J. Pfeiffer. 1980. Aerial production, mortality, and mineral accumulation-export dynamics in *Spartina alterniflora* and *Juncus roemerianus* plant stands in a Georgia salt marsh. *Ecology 61*(2):303–312.

Harrison, E.Z., and A.L. Bloom. 1977. Sedimentation rates on tidal salt marshes in Connecticut. *Journal of Sedimentary Research 47*(4):1484–1490.

Jordan, T.E., D.L. Correll, and D.F. Whigham. 1983. Nutrient flux in the Rhode River: tidal exchange of nutrients by brackish marshes. *Estuarine, Coastal and Shelf Science 17*:651–667.

Kiehn, W.M., and J.T. Morris. 2009. Relationships between *Spartina alterniflora* and *Littoraria irrorata* in a South Carolina salt marsh. *Wetlands 29*:818–825.

Kirwan, M.L., and A.B. Murray. 2007. A coupled geomorphic and ecological model of tidal marsh evolution. *Proceedings of the National Academy of Sciences USA 104*:6118–6122.

Kirwan, M.L., R.R. Christian, L.K. Blum and M.M. Brinson. 2012. On the relationship between sea level and *Spartina alterniflora* production. *Ecosystems 15*:140–147.

Kirwan, M.L., and G.R. Guntenspergen. 2012. Feedbacks between inundation, root production, and shoot growth in a rapidly submerging brackish marsh. *Journal of Ecology 100*:764–770.

Kneib, R.T. 1997. The role of tidal marshes in the ecology of estuarine nekton. *Oceanography and Marine Biology 35*:163–220.

Knutson, P.H. 1988. Role of coastal wetlands in energy dissipation and shore protection. Pp. 161–174 in *The ecology and management of wetlands. Volume 1 Ecology of wetlands.* Edited by D.D. Hook et al. Portland, OR: Timber Press.

Leonard, L.A., P.A. Wren, and R.L. Beavers. 2002. Flow dynamics and sedimentation in *Spartina alterniflora* and *Phragmites australis* marshes of the Chesapeake Bay. *Wetlands 22*:415–424.

Malhotra, A., and M.S. Fonseca. 2007. WEMo (Wave Exposure Model): Formulation, Procedures and Validation. Page 28. NOAA Technical Memorandum NOS NCCOS #65.

Moller, I., T. Spencer, J. R. French, D. J. Leggett and M. Dixon. 1999. Wave transformation over salt marshes: A field and numerical modelling study from north Norfolk, England. *Estuarine Coastal and Shelf Science 49*:411–426.

Morris, J.T., and B. Haskin. 1990. A 5-yr record of aerial primary production and stand characteristics of *Spartina alterniflora*. *Ecology 71*:2209–2217.

Morris, J.T., P.V. Sundareshwar, C.T. Nietch, B. Kjerfve, and D.R. Cahoon. 2002. Responses of coastal wetlands to rising sea level. *Ecology 83*:2869–2877.

Mudd, S.M., S.M. Howell, and J.T. Morris. 2009. Impact of dynamic feedbacks between sedimentation, sea-level rise, and biomass production on near-surface marsh stratigraphy and carbon accumulation. *Estuarine Coastal and Shelf Science 82*:377–389.

Peet, R.K., T.W. Wentworth, and P.S. White. 1998. A flexible, multipurpose method for recording vegetation composition and structure. *Castenea 63*:262–274.

Priest, B. 2012. *Effects of Elevation and Nutrient Availability on the Primary Production of Spartina alterniflora and the Stability of Southeastern Coastal Salt Marshes Relative to Sea Level Rise*. Master of Science thesis. University of South Carolina, Columbia, SC.

Roman, C.T., M.J. James-Pirri, and J.F. Heltsche. 2001. Monitoring salt marsh vegetation: A protocol for the long-term coastal ecosystem monitoring program at Cape Cod National Seashore. U.S. Geological Survey Patuxent Wildlife Research Center, Coastal Research Field Station, University of Rhode Island.

Roman, C.T., J.A. Peck, J.R. Allen, J.W. King, and P.G. Appleby. 1997. Accretion of a New England (USA) salt marsh in response to inlet migration, storms, and sea-level rise. *Estuarine Coastal and Shelf Science 45*:717–727.

Silliman, B.R., J. Van de Koppel, M.D. Bertness, L.E. Stanton, and I.A. Mendelssohn. 2005. Drought, snails, and large-scale die-off of southern U.S. salt marshes. *Science 310*:1803–1806.

Silliman, B.R., and M.D. Bertness. 2002. A trophic cascade regulates salt marsh primary production. In *Proceedings of the National Academy of Sciences USA 99*:10500–10505.

Silliman, B.R. and J.C. Zieman. 2001. Top-down control of *Spartina alterniflora* production by periwinkle grazing in a Virginia salt marsh. *Ecology 82*:2830–2845.

Sweet, W., C. Zervas, and S. Gill. 2009. *Elevated East Coast Sea Level Anomaly: June–July 2009*. NOAA Technical Report NOS CO-OPS 051. NOAA National Oceanic and Atmospheric Administration, Silver Spring, MD. Available at http://tidesandcurrents.noaa.gov/publications/EastCoastSeaLevelAnomaly_2009.pdf.

Thieler, E.R., and W.W. Danforth. 1994. Historical shoreline mapping (I): improving techniques and reducing positioning errors. *Journal of Coastal Research 10*(3):549–563.

Valiela, I., and J.M. Teal. 1979. The nitrogen budget for a salt marsh ecosystem. *Nature 280*:652–656.

Williams, R.B., and M.B. Murdoch. 1972. Compartmental analysis of the production of *Juncus roemerianus* in a North Carolina salt marsh. *Chesapeake Science 13*:69–79.

Woerner, L.S., and C.T. Hackney. 1997. Distribution of *Juncus roemerianus* in North Carolina tidal marshes: The importance of physical and biotic variables. *Wetlands 17*:284–291.

Appendix 6-A

Supporting Data

Table 6A-1. Summary statistics for *Spartina alterniflora* monitoring parameters.

Values shown are mean ± standard error. Missing data indicates a site was not monitored that year.

Parameter	Site	2008	2009	2010	2011	2012
Live stem density (stems m^{-2})	FC	107 ±10	95 ±8	126 ±11	111 ±13	84 ±8
	OBB	319 ±40	410 ±56	514 ±100	444 ±76	272 ±35
	MHB	892 ±75	791 ±73	798 ±81	750 ±54	515 ±63
	MHL	650 ±55	624 ±49	743 ±49	—	—
	TBB	—	284 ±110	297 ±80	331 ±117	175 ±46
	TBC	—	170 ±49	166 ±57	154 ±46	79 ±21
	PPS	—	140 ±49	202 ±47	166 ±40	214 ±27
Stem height (cm)	FC	63 ±2	84 ±3	63 ±2	69 ±2	60 ±3
	OBB	29 ±2	32 ±2	33 ±2	33 ±2	34 ±2
	MHB	20 ±1	25 ±2	24 ±2	25 ±2	24 ±2
	MHL	27 ±2	33 ±2	30 ±1	—	—
	TBB	—	35 ±3	37 ±5	35 ±4	38 ±4
	TBC	—	37 ±4	45 ±6	49 ±6	57 ±6
	PPS	—	78 ±15	59 ±9	65 ±5	39 ±3
Estimated live biomass (g dw m^{-2})	FC	373 ±42	483 ±33	436 ±49	426 ±41	312 ±44
	OBB	188 ±17	273 ±35	329 ±44	291 ±38	186 ±22
	MHB	376 ±29	392 ±26	413 ±45	379 ±25	263 ±34
	MHL	360 ±22	422 ±28	464±23	—	—
	TBB	—	174 ±55	195 ±37	201 ±51	127 ±22
	TBC	—	106 ±27	173 ±44	147 ±27	131 ±37
	PPS	—	1346 ±816	507 ±134	393 ±74	201 ±30

Table 6A-2. Summary statistics for *Spartina alterniflora* monitoring parameters at FC (Freeman Creek) by elevation bin and year.

Values shown are mean ± standard error.

Parameter	Elevation Bin (m)	2008	2009	2010	2011	2012
Stem density (stems m^{-2})	−0.15	77 ±13	67 ±6	93 ±13	60 ±6	52 ±9
	−0.05	76 ±10	74 ±17	124 ±9	73 ±11	79 ±15
	0.05	122 ±17	117 ±9	178 ±29	174 ±22	126 ±10
	0.25	155 ±19	152 ±10	148 ±10	190 ±4	116 ±10
Stem height (cm)	−0.15	64 ±4	94 ±3	64 ±3	68 ±4	52 ±5
	−0.05	58 ±8	84 ±5	59 ±6	72 ±7	54 ±6
	0.05	72 ±1	80 ±2	68 ±6	70 ±5	79 ±3
	0.25	57 ±2	67 ±1	60 ±2	66 ±2	64 ±3
Estimated live biomass (g dw m^{-2})	−0.15	394 ±77	510 ±56	377 ±66	299 ±43	177 ±35
	−0.05	259 ±80	434 ±135	455 ±66	376 ±74	261 ±42
	0.05	519 ±105	523 ±28	680 ±150	654 ±102	669 ±92
	0.25	300 ±54	425 ±40	308 ±37	518 ±37	293 ±21

Table 6A-3. Mean live stem density of *Spartina alterniflora* at MHB (Mile Hammock Bay) by elevation bin.

Values shown are mean ± standard error (stems m^{-2}).

Elevation Bin (m)	2008	2009	2010	2011	2012
0.05	457 ±88	329 ±47	634 ±104	444 ±82	307 ±80
0.15	1006 ±70	913 ±64	822 ±101	845 ±51	593 ±77
0.25	1456[a]	1360[a]	1344[a]	864[a]	356[a]

[a] Only one sample plot was measured at 0.25 elevation bin each year. No standard error.

Table 6A-4. Mean live stem height of *Spartina alterniflora* at MHB by elevation bin.

Values shown are mean ± standard error (cm).

Elevation Bin (m)	Stem Height
0.05	34 ±1
0.15	20 ±0
0.25	19 ±1

Table 6A-5. Mean live stem height of *Spartina alterniflora* at OBB (Onslow Beach Backbarrier) by elevation bin.

Values shown are mean ± standard error (cm).

Elevation Bin (m)	Stem Height
0.15	44 ±2
0.25	37 ±1
0.35	25 ±1
0.45	23 ±2

Table 6A-6. Summary statistics for *Juncus roemerianus* monitoring parameters.

Values shown are mean ± standard error. Missing data indicates a site was not monitored that year.

Parameter	Site	2009	2010	2011	2012
Leaf density (leaves m^{-2})	OBB	—	987 ±176	2037 ±163	896 ±24
	TBB	547 ±160	918 ±33	1482 ±329	371 ±199
	TBC	941 ±141	1197 ±145	1507 ±278	704 ±71
	PPS	1436 ±286	1621 ±267	1030 ±153	998 ±292
	PPU	1136 ±88	1095 ±192	—	—
	FN	1236 ±119	1451 ±93	1484 ±173	1305 ±152
Leaf height (cm)	OBB	—	51 ±11	46 ±12	50 ±10
	TBB	47 ±7	50 ±5	51 ±2	37 ±5
	TBC	61 ±4	65 ±5	65 ±3	47 ±6
	PPS	61 ±4	60 ±3	53 ±3	46 ±3
	PPU	82 ±4	68 ±5	—	—
	FN	80 ±4	76 ±3	73 ±3	64 ±3
Live biomass (g dw m^{-2})	OBB	—	648 ±259	1038 ±452	554 ±130
	TBB	380 ±132	524 ±68	1063 ±256	205 ±138
	TBC	789 ±129	1038 ±123	1578 ±316	573 ±86
	PPS	1031 ±220	1262 ±192	705 ±133	670 ±181
	PPU	1341 ±143	1139 ±235	—	—
	FN	1189 ±103	1522 ±105	1516 ±194	1069 ±117

Table 6A-7. Mean leaf density of *Juncus roemerianus* at OBB by elevation bin.

Values shown are mean ± standard error (leaves m^{-2}).

Elevation Bin (m)	Mean Leaf Density
0.45	1267 ±243
0.55	1387 ±400

Table 6A-8. Mean leaf height of *Juncus roemerianus* at TBB by elevation bin.

Values shown are mean ± standard error (cm).

Elevation Bin (m)	Mean Leaf Height
0.05	43 ±3
0.15	60 ±4

Table 6A-9. P-Value results from mixed model analysis of *Spartina alterniflora* and *Juncus roemerianus* biomass sampling are shown for each factor (site, year, elevation bin) and for interactions between these factors (i.e., site*year).

Parameters measured for *Spartina alterniflora* include live stem density, mean live stem height, and estimated live above-ground biomass. Parameters measured for *Juncus roemerianus* include live leaf density, mean green leaf height, and harvested live leaf biomass. *Spartina alterniflora* data from 2008–2012 include the sites FC, OBB, and MHB. Data from 2009–2012 also include TBB, TBC, and PPS. *Juncus roemerianus* data from 2009–2012 include the sites TBB, TBC, PPS, and FN. The 2010–2012 *Juncus roemerianus* data set also includes data from OBB. Values less than 0.05 were considered statistically significant.

Species	Parameter	Data Set	Site	Year	Elevation Bin	Site* Year	Site* Elevation Bin	Year* Elevation Bin	Site* Year* Elevation Bin
Spartina alterniflora	Live stem density	2008–2012	<.0001	<.0001	0.0046	<.0001	0.0176	0.0407	0.0175
		2009–2012	<.0001	<.0001	0.0156	0.0001	0.2343	0.1568	0.1181
	Stem height	2008–2012	<.0001	<.0001	<.0001	0.8495	0.1465	<.0001	0.8091
		2009–2012	<.0001	<.0001	<.0001	<.0001	<.0001	<.0001	0.0385
	Estimated biomass	2008–2012	0.0006	<.0001	0.0365	0.0416	0.0029	0.0053	0.8318
		2009–2012	0.0005	0.1105	0.4484	0.4328	0.5817	0.9872	0.9958
Juncus roemerianus	Leaf density	2009–2012	0.0139	0.3122	0.7598	0.585	0.4579	0.5531	0.9466
		2010–2012	0.0186	0.0045	0.886	0.7027	0.3293	0.8498	0.9864
	Leaf height	2009–2012	<.0001	<.0001	0.0205	0.9691	0.2282	0.6369	0.6262
		2010–2012	<.0001	0.0028	0.0006	0.9387	0.5255	0.9905	0.3593
	Live biomass	2009–2012	0.0015	0.1268	0.5328	0.707	0.5901	0.4233	0.971
		2010–2012	0.002	0.026	0.2997	0.6911	0.4534	0.4981	0.9985

Table 6A-10. P-Value results from mixed model analysis of *Spartina alterniflora* sampling are shown by site for the factors year and elevation bin and for interactions between year and elevation bin (year * elevation bin).

Parameters measured for *Spartina alterniflora* include live stem density, mean live stem height, and estimated live above-ground biomass. Values less than 0.05 were considered statistically significant.

Site	Parameter	Data Set	Year	Elevation Bin	Year* Elevation Bin
FC	Live stem density	2008–2012	0.0001	<.0001	0.0268
	Stem height	2008–2012	<.0001	0.0349	<.0001
	Estimated biomass	2008–2012	0.0394	0.0004	0.0214
OBB	Live stem density	2008–2012	0.048	0.2603	0.2636
	Stem height	2008–2012	0.0232	<.0001	0.3086
	Estimated biomass	2008–2012	0.0538	0.223	0.6466
MHB	Live stem density	2008–2012	<.0001	0.0017	0.0151
	Stem height	2008–2012	0.0601	<.0001	0.5898
	Estimated biomass	2008–2012	0.0019	0.3694	0.1526
TBB	Live stem density	2009–2012	0.3335	0.6115	0.9957
	Stem height	2009–2012	0.9617	0.2116	0.7126
	Estimated biomass	2009–2012	0.5741	0.4882	0.9792
TBC	Live stem density	2009–2012	0.8982	0.9608	0.7804
	Stem height	2009–2012	0.216	0.2243	0.7972
	Estimated biomass	2009–2012	0.0024	0.385	0.0002
PPS	Live stem density	2009–2012	0.4061	0.8083	0.9329
	Stem height	2009–2012	0.1029	0.7613	0.3772
	Estimated biomass	2009–2012	0.5263	0.9442	0.9862

Table 6A-11. P-Value results from mixed model analysis of *Juncus roemerianus* sampling are shown by site for the factors year and elevation bin, as well as for interactions between year and elevation bin (year * elevation bin).

Parameters measured for *Juncus roemerianus* include live leaf density, mean green leaf height, and harvested live leaf biomass. Values less than 0.05 were considered statistically significant.

Site	Parameter	Data Set	Year	Elevation Bin	Year* Elevation Bin
OBB	Leaf density	2010–2012	0.118	0.0245	0.9344
	Leaf height	2010–2012	0.1512	0.1584	0.4822
	Biomass	2010–2012	0.1247	0.1394	0.2102
TBB	Leaf density	2009–2012	0.0758	0.7536	0.6438
	Leaf height	2009–2012	0.449	0.0206	0.691
	Biomass	2009–2012	0.1281	0.7178	0.7576
TBC	Leaf density	2009–2012	0.5291	0.4828	0.9416
	Leaf height	2009–2012	0.1836	0.3042	0.7607
	Biomass	2009–2012	0.3597	0.5913	0.8868
PPS	Leaf density	2009–2012	0.5635	0.6678	0.3974
	Leaf height	2009–2012	0.0045	0.6285	0.23
	Biomass	2009–2012	0.282	0.9104	0.4937
FN	Leaf density	2009–2012	0.6949	0.844	0.3108
	Leaf height	2009–2012	0.0198	0.2916	0.7047
	Biomass	2009–2012	0.1004	0.765	0.3138

[This page intentionally left blank.]

Chapter 7

Marsh Surface Elevation

SERDP Project Number: RC-1413

Coastal Wetlands Module

Lead Researcher:
Dr. Carolyn A. Currin
NCCOS NOAA Center for Coastal Fisheries and Habitat Research
Beaufort, NC
E-mail: Carolyn.currin@noaa.gov

June 27, 2013

Final

This report was prepared under contract to the U.S. Department of Defense (DoD) Strategic Environmental Research and Development Program (SERDP). The publication of this report does not indicate endorsement by DoD, nor should the contents be construed as reflecting the official policy or position of DoD. References herein to any specific commercial product, process, or service by trade name, trademark, manufacturer, or otherwise, do not necessarily constitute or imply its endorsement, recommendation, or favoring by DoD.

Table of Contents

List of Acronyms 7-vi
Abstract 7-1
Objectives of the Monitoring Activity 7-2
Background 7-2
Materials and Methods 7-3
SETs and Marker Horizons 7-3
Marker Horizons 7-6
Height Modernization Program 7-6
Water Level/Tide Gauge 7-7
Inundation Calculations 7-8
Results and Discussion 7-9
Marsh Surface Elevation Change and Sediment Accretion Rates 7-9
Relationship Between Marsh Inundation, Surface Elevation, and Sediment Accretion 7-14
Water Level/Tide Gauge 7-16
Assessment of Trends in the Data 7-26
Assessment of Monitoring Design 7-26
Assessment Seasonal and Annual Variability in the Data 7-27
Conclusions and Implications for Future Research 7-28
Key Scientific Findings—Fundamental Cause-and-Effect Relationships 7-28
Findings Supportive of Current Base Management Practices 7-28
Findings with Implications for Future Base Management 7-28
Findings with Implications for DCERP2 7-29
Literature Cited 7-30

List of Figures

7-1. Location of coastal wetlands monitoring surface elevation table (SET) and water level (WL) stations on MCBCL. 7-4

7-2. SETs and MHs were used to measure marsh surface elevation change and sediment accretion rates in MCBCL marshes. 7-5

7-3. Sediment surface elevation (in meters [m]) measured at SETs for control (C) and fertilized (F) plots in ICW marshes. 7-11

7-4. Sediment surface elevation (in meters [m]) measured at SET plots in NRE marshes. 7-12

7-5. Sediment accretion, measured with feldspar MHs, versus marsh surface elevation change, measured with SETs, at each of the ICW marshes: (A) Freeman Creek, (B) Onslow Beach, and (C) Mile Hammock Bay. 7-14

7-6. Relationship between tidal inundation and sediment accretion during 2- to 5-month sample intervals at ICW and NRE marshes. 7-16

7-7. Hourly water level means at Mile Hammock Bay from April 2008 to September 2012. 7-17

7-8. Hourly temperature means at Mile Hammock Bay from April 2008 to September 2012. 7-18

7-9. Hourly salinity (ppt) means at Mile Hammock Bay from April 2008 to September 2012. 7-19

7-10. Hourly means of water level at Gottschalk Marina from May 2008 to September 2012. 7-20

7-11. Hourly temperature means at Gottschalk Marina from May 2008 to September 2012. 7-21

7-12. Hourly salinity (ppt) means at Gottschalk Marina from May 2008 to September 2012. 7-22

7-13. Monthly mean water level (WL) at Mile Hammock Bay (MHB) from April 2008 to September 2012 and Gottshalk Marina/Wallace Creek (GM/WC) from April 2008 to September 2012. 7-23

7-14. Comparison of water level as measured at Gottshalk Marina/Wallace Creek (GM/WC) by NOAA temporary tide gauge and at French Creek (FN) by pressure loggers in a monitoring well in September 2009 (A) and March 2010 (B). 7-24

7-15. Comparison of water level as measured at Mile Hammock Bay (MHB) by NOAA temporary tide gauge and at Freeman Creek (FC) by pressure loggers in a monitoring well in September 2009 (A) and March 2010 (B). 7-25

7-16. Comparison of water level as measured at Mile Hammock Bay (MHB) by NOAA temporary tide gauge and at Traps Bay (TB) by pressure loggers in a monitoring well in September 2009 (A) and March 2010 (B). 7-26

List of Tables

7-1. SET locations and starting elevations 7-7

7-2. Data intervals used in analysis of relationship between tidal inundation, surface elevation change, and sediment accretion. 7-9

7-3. Results of linear regression analysis of sediment surface elevation change (slope) as measured with SETs from 2008 to 2012. 7-10

7-4. Change in mean elevation (mm) as measured with SETs over each time interval. 7-10

7-5. Sediment accretion (mm) as measured with MHs over each time interval. 7-13

7-6. Results of regression analysis of relationship between marsh surface elevation change, as measured with SETs, and the length of time (h) that the SET was inundated. 7-15

7-7. Results from NOAA CO-OPS analysis of 6-minute water level data from tide gauge stations MHB (Mile Hammock Bay) and GC/WC (Gottshalk Marina/Wallace Creek)[a]. 7-22

List of Acronyms

A	sediment accretion
C	control
cm	centimeter
CO-OPS	Center for Operational Oceanographic Products and Services
DCERP1	first cycle of the Defense Coastal/Estuarine Research Program
DCERP1	second cycle of the Defense Coastal/Estuarine Research Program
DEM	Digital Elevation Model
DoD	U.S. Department of Defense
E	net surface elevation change
F	fertilized
FC	French Creek
FNS	French Creek Shoreline
FNU	French Creek Upper
GC/WC	Gottshalk Marina/Wallace Creek
GPS	global positioning system
Height Mod	Height Modernization (Program)
ICW	Intracoastal Waterway
M	meter
m y^{-1}	meters per year
m^2	square meter
MCBCL	Marine Corps Base Camp Lejeune
MEM	Marsh Equilibrium Model
MH	marker horizon
MHB	Mile Hammock Bay
mm, mm^{-1}	millimeter, per millimeter
mm/y, mm y^{-1}	millimeter per year
NAD 83	North American Datum of 1983
NAVD 88	North American Vertical Datum of 1988
NGS	National Geodetic Service
NRE	New River Estuary
NSRS	National Spatial Reference System
OBB	Onslow Beach Backbarrier
OPUS	Online Positioning User Service (program)
PC	primary control
PPS	Pollocks Point Shoreline
PPU	Pollocks Point Upper
ppt	parts per thousand

PVC	polyvinyl chloride
r^2	r-squared (value)
RTK-GPS	real-time kinematic global positioning system
SERDP	Strategic Environmental Research and Development Program
SET	surface elevation table
SLR	sea level rise
TBB	Traps Bay Bridge
TBC	Traps Bay Creek
USGS	U.S. Geological Survey
WC	Wallace Creek
WL	water level
YSI	Yellow Springs, Inc.

[This page intentionally left blank.]

Abstract

The overall objective of this monitoring activity was to facilitate Coastal Wetlands research and modeling to develop predictions of the response of Marine Corps Base Camp Lejeune (MCBCL) marshes to sea level rise (SLR). Present-day salt marshes have developed during a prolonged (thousands of years) period of SLR, and positive ecogeomorphic feedbacks between plant production, sediment accretion, and tidal inundation enable marshes to maintain the intertidal elevation required for their growth. Predictions of how marshes will fare under the projected accelerated SLR of the twenty-first century rely upon accurate knowledge of present-day marsh surface elevation, sediment accretion rates, contribution of subsurface processes to net elevation change, and tidal dynamics of the study area.

We used surface elevation tables (SETs) and marker horizons to measure net marsh surface elevation change and sediment accretion rates at nine salt marsh sites on MCBCL between 2008 and August 2012. Three of the sites were dominated by *Spartina alterniflora* and located adjacent to the Intracoastal Waterway (ICW), while the remaining sites were located in the New River Estuary and vegetation ranged from a *Spartina-Juncus* mix to *Juncus* dominated. Seven of the nine sites showed significant increases in marsh surface elevation during the study period, with significant slopes ranging from 9 mm y^{-1} at a low-elevation *Spartina* site to 2–3 mm y^{-1} at *Spartina* and *Juncus* sites higher in the intertidal. Sediment accretion measured with marker horizons at the same sites was 2–8 times greater than net surface elevation change, demonstrating the importance of subsurface processes, particularly compaction, on net marsh elevation change. Water level, temperature, and salinity were recorded at 6-minute intervals, consistent with the National Oceanic and Atmospheric Administration (NOAA) temporary tide gauge requirements, at two stations for the entire 2008–2012 study period. Additional water level data were recorded from three other sites for shorter periods of time, and utilized with the tide gauge data to determine the relationship between water level (inundation), sediment accretion and surface elevation change. Generally, there was a non-significant relationship between inundation and marsh elevation change and accretion rate over short-term, (2–4 month) intervals. Although over the long term, lower elevation sites experienced greater sediment accretion, short-term variability in suspended sediment concentration likely controlled sediment accretion and ultimately marsh elevation change).

Two temporary tide gauges, which were deployed to NOAA standards, provided data for the calculation of local tidal datums, and documented seasonal and annual variabilities in water level. Shorter term deployment of pressure sensors at study sites demonstrated that marshes near Browns Inlet experience twice the tidal amplitude as do marshes near the New River Inlet.

These results provided the foundation for developing and testing the Marsh Equilibrium Model, which provides predictions of marsh response to SLR. The identification of sediment accretion as the driving factor affecting marsh surface elevation change, and the documentation of large differences in tide range between the inlets at either end of Onslow Beach are important pieces of information, which will help guide future work to make landscape-scale predictions of marsh vulnerability to SLR, and develop adaptive management approaches to conserve marsh habitats.

Keywords: accretion, elevation, salt marsh, sediment, SET, tidal datum

Objectives of the Monitoring Activity

The overall objective of the monitoring activity in this section was to facilitate Research Projects CW-1 and CW-2 including Marsh Equilibrium Model (MEM) predictions of the response of coastal wetlands to SLR. The specific objectives of activities reported in this section were to install and maintain benchmarks and water level sensors for the collection and distribution of accurate marsh surface elevation and tidal data and to collect data on marsh sediment accretion rates. Together, the Coastal Wetlands Module's research and monitoring activities support efforts to develop a management plan to support the sustainability of marsh ecosystems and the estuarine shoreline.

Background

Monitoring changes in marsh surface elevation with the use of surface elevation tables (SETs; Cahoon et al., 2002a, 2002b) is an approach that has become widely employed by the academic research community and has supported efforts to understand the factors affecting marsh response to SLR, storm events and atmospheric carbon dioxide increase (Cahoon, 2007; Cahoon et al., 2006; Langley et al., 2009; Morris et al., 2002). In addition, numerous federal agencies with land management responsibilities (the U.S. Geological Survey [USGS], the National Park Service, the U.S. Fish and Wildlife Service, and the National Estuarine Research Reserve System) have incorporated SETs into monitoring efforts designed to detect ecosystem response to SLR and climate change (Cahoon et al., 2006; Roman et al., 2001).

The ability of salt marshes to accrete sediments is key to their ability to "keep up" with SLR. Present-day marshes have developed in conjunction with SLR rates of over the past 10,000 years by increasing surface elevation to maintain their position and by transgressing landward (Redfield, 1965). A number of factors combine to control surface elevation, including sediment supply and accretion rates, marsh above-ground and below-ground biomass production, decomposition rate, and subsurface subsidence (Cahoon et al., 2002a, 2002b; Kirwan et al., 2010; Morris et al., 2002; Mudd et al., 2010) Several studies have shown that, particularly in high marshes, organic matter accumulation is a dominant process in maintaining marsh elevation (Cahoon et al., 2004; Chmura and Hung, 2004; Nyman et al., 2006), whereas suspended sediment supply and tidal elevation are generally the key drivers in lower elevation marshes. To provide accurate predictions of the vulnerability of marshes to SLR in a particular landscape, it is necessary to know the distribution of the marsh within the tidal frame, and whether sediment accretion or organic matter accumulation is the dominant process affecting surface elevation change. The Marsh Equilibrium Model (MEM; Morris et al., 2002) combines the relationship between inundation time and sedimentation with the feedback response between vegetation, and inundation, which has been described as ecogeomorphic feedback (Kirwan et al., 2010), to predict the response of *Spartina* marshes to SLR. The monitoring data in this chapter provide both the baseline data needed to parameterize the MEM and to compare modeled predictions of marsh elevation change with observations (see Chapter 7 *DCERP1 Final Research Report*). In addition, this monitoring data, which includes *Juncus*-dominated marshes, provides the foundation for expanding MEM into a landscape model of Marine Corps Base Camp Lejeune (MCBCL) marsh sustainability.

Materials and Methods

SETs and Marker Horizons

SETs and feldspar marker horizons (MHs) were established at nine salt marsh sites in 2008 (see **Table 7-1 and Figure 7-1**). Deep-rod SETs were installed using 9 mm in diameter threaded stainless-steel rod to depths between 7 and 11 m, stabilized with concrete caps and polyvinyl chloride (PVC) collars, and identified with brass discs embedded in the concrete cap (**Figure 7-2B**; USGS's Web site). At each study site, one SET was designated as the primary control (PC) SET mark. Following and adapting National Geodetic Service (NGS) protocols and the Online Positioning User Service (OPUS) program, Orthometric Elevations (henceforth referred to as "elevation") and ellipsoid heights were established for the PC SET marks **(Figure 7-2A**). If more than one SET mark was located at a study site, all other SET mark elevations were derived by use of the OPUS program with real-time kinematic global positioning system (RTK-GPS) and checked using laser leveling. Although each static global positioning system (GPS) collection on a SET mark is independent, the root mean square (RMS) of any collection was less than 0.017 m. An NGS Height Modernization campaign, described below, will establish elevations of higher accuracies.

Each SET was read in four positions, with nine pins read at each position (**Figures 7-2C and D**). The sediment surface elevation change at each SET is obtained by measuring the distance (in mm) between the SET arm and the top of the pins. The height of the SET arm over the SET mark was determined with a laser level, and this value is used to calculate marsh surface elevation change relative to NAVD88. SET readings were taken every 1 to 3 months, following the method described in Cahoon et al. (2002a, 2002b). Pin heights were excluded from the mean sediment surface elevation calculation if the SET pin landed in a hole, on a shell, on a plant stem, or otherwise did not contact the actual sediment surface.

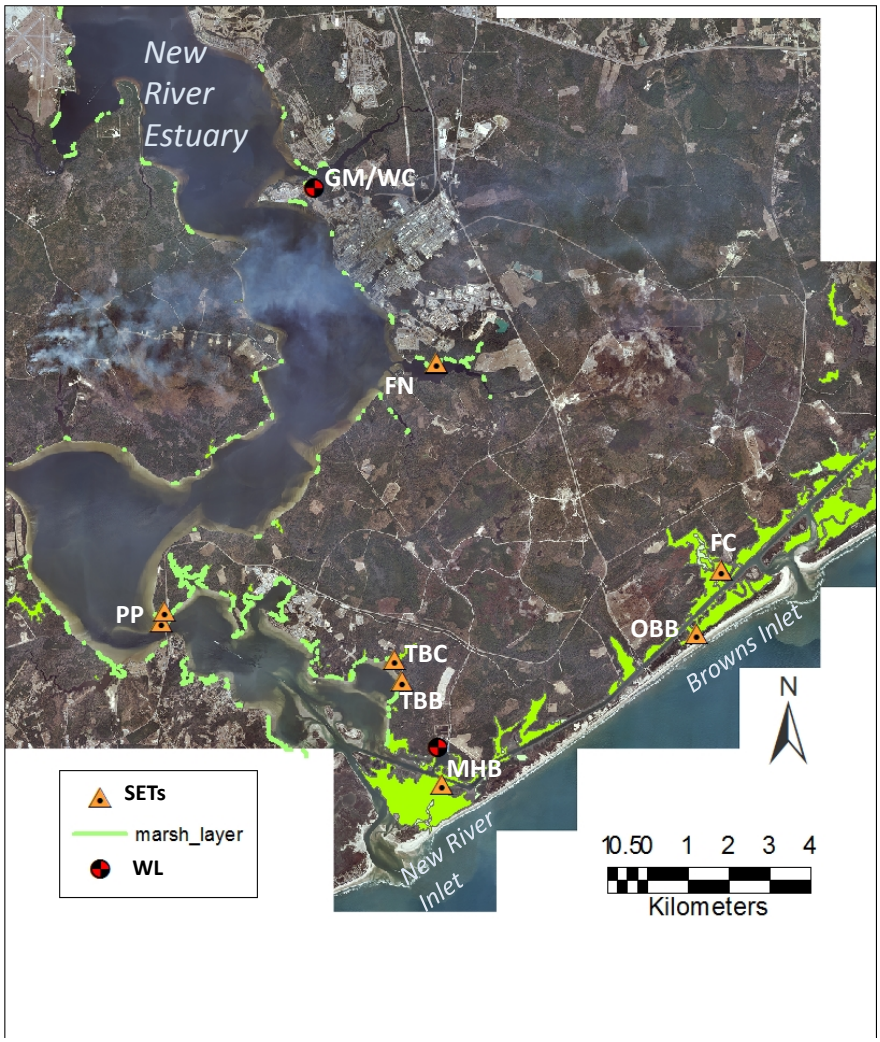

Figure 7-1. Location of coastal wetlands monitoring surface elevation table (SET) and water level (WL) stations on MCBCL.

Extent of coastal wetlands is illustrated with green layer.

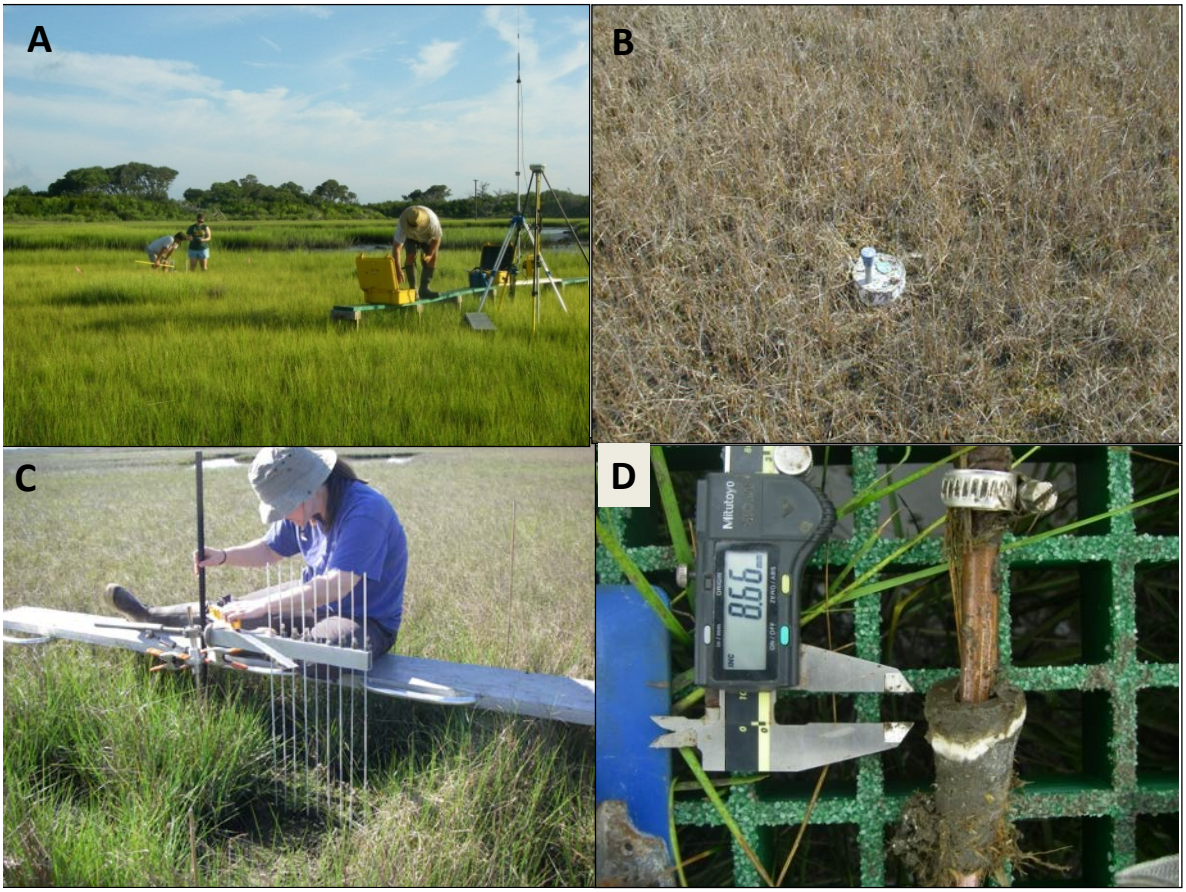

Figure 7-2. SETs and MHs were used to measure marsh surface elevation change and sediment accretion rates in MCBCL marshes.

(A) Acquiring SET mark position data using RTK-GPS at Onslow Beach Backbarrier. SETS are located to right of boardwalk, vegetation monitoring plot in background. (B) Concrete SET base with brass marker and SET rod with PVC cap in Mile Hammock Bay marsh. (C) Reading SET with nine pins positioned at sediment surface prior to measurement. (D) Cryocore used to measure depth of sediment over feldspar layer (MH) to determine sediment accretion rates.

The SETs at Freeman Creek, Onslow Beach Backbarrier (OBB), and Mile Hammock Bay (MHB) were established as paired experimental sites. Three SETs at Freeman Creek were fertilized with nitrogen and phosphorous from 2008–2010. Three SETs served as control plots with no fertilizer. At OBB and MHB, there was one fertilized SET and one control SET at each site. SETs in the New River Estuary (NRE; Traps Bay and Creek, Pollocks Point Shore and Upper, and French Creek Shore and Upper) received no fertilizer. Results from the fertilized SETs are presented and discussed in the Chapter 7 of the *DCERP1 Final Research Report* and will be presented briefly in this report.

The Freeman Creek SETs (SETs 31–36) are located approximately 60 m from the creek in a *Spartina alterniflora*–dominated marsh. The SETs at OBB are approximately 20 m from a tidal creek and approximately 100 m from the Intracoastal Waterway (ICW), in a *Spartina alterniflora* marsh. SETs at MHB are approximately 50 m south of the ICW, also in a *Spartina alterniflora*–dominated marsh. SETs at Traps Bay Bridge (SET 41) and Traps Bay Creek (SET 42) are located approximately 3-m landward of the shoreline. SETs at Pollocks Point are located within

10 m of the NRE shoreline (SET 43) and near the upland edge of the marsh at the woodland boundary (SET 44). SETs at French Creek are located within 5 m of the shoreline (SET 45) and near the woodland boundary (SET 46). All SETs are located within vegetation monitoring plots (see **Figure 6-2** in Chapter 6, *Land Cover and Shoreline Erosion*).

Marker Horizons

MH plots were installed in a demarcated plot near the SET locations by distributing a 2–4 mm layer of powdered feldspar clay over the marsh surface. Two to 6 months after installation, a cryocore was obtained by pouring liquid nitrogen into a funnel attached to copper tubing, which was pushed into the MH plot. This technique allowed the extraction of a small core of uncompacted sediment from the plot, and digital calipers were used to measure the thickness of the sediment accreted on top of the feldspar (**Figure 7-1D**). From 2008 to 2011, MH plots were 0.0625 m^2, and readings were taken every 2–3 months in a new quadrant of the plot. A new feldspar plot was installed after cores had been taken in all four quadrants, or if no feldspar was found. Beginning in November 2011, feldspar was installed in a new 0.01-m^2 plot at each reading. This approach minimized variability in readings over time that could be caused by compaction of sediment after its deposition to the marsh surface, as all readings represented approximately the same time interval since feldspar installation (3 months). At each reading, three cores were collected from each plot, and three depth readings were measured on each core, when possible. The average depth of sediment overlying the feldspar layer in the three cores was used to determine the mean sediment accretion rate for each site.

At FC, OBB, and MHB, there were three MH plots installed in fertilized areas of the marsh, and three in non-fertilized, control, areas from 2008 to November 2011. Because the fertilization ceased in 2010, we discontinued MHs in formerly fertilized areas. At all NRE sites there was one MH plot located near each SET. In November 2011, we increased the number of MH plots to three per SET location.

Height Modernization Program

In 2010, we initiated a Height Modernization (Height Mod) Program to improve position and vertical accuracies of the SET marks and Digital Elevation Models (DEMs) of intertidal wetlands on MCBCL (for details on National Oceanic and Atmospheric Administration's [NOAA's] Height Mod Program see http://www.ngs.noaa.gov/heightmod/Definition.shtml). This effort, conducted in collaboration with the North Carolina Geodetic Survey, will ultimately provide two Class C benchmarks, which can be submitted for inclusion in the National Spatial Reference System (NSRS, 2007[1]; which will be readily accessible to MCBCL personnel and contractors (unlike the SETs that are in marshes). In addition to improving measures of tidal wetlands elevations in support of research objectives, these benchmarks can be used to estimate crustal motion and subsidence, support surveys for construction projects, aid in emergency management planning, and support natural resource management and restoration efforts.

---

[1] NSRS 2007 is the re-adjustment of the North American Datum of 1983 (NAD 83) that was completed in 2007. NSRS 2007 adjusted 67,693 GPS control points in the NSRS to the nationwide Continuously Operating Reference Stations network. The NGS manages this consistent coordinate system that defines latitude, longitude, height, scale, gravity, and orientation throughout the United States.

Table 7-1. SET locations and starting elevations

Location	SET Number	Site Abbreviation	Treatment	Install Date	Surface Elevation (m NAVD 88)	First Read Date	Starting Sediment Elevation (m NAVD 88)	Number of Readings
Freeman Creek	31	FC	C	11/25/2007	−0.01	2/19/2008	−0.03	24
	32	FC	F	11/26/2007	0.00	2/19/2008	0.00	24
	33	FC	C	11/26/2007	0.06	2/19/2008	0.02	24
	34	FC	F	11/26/2007	0.02	2/19/2008	0.01	24
	35	FC	F	11/25/2007	0.06	2/19/2008	0.02	24
	36	FC	C	11/25/2007	0.11	2/19/2008	0.02	24
Onslow Beach	37	OBB	F	12/6/2007	0.30	2/19/2008	0.21	24
	38	OBB	C	12/6/2007	0.31	2/19/2008	0.26	24
Mile Hammock Bay	39	MHB	C	11/27/2007	0.18	2/19/2008	0.16	24
	40	MHB	F	11/27/2007	0.24	2/19/2008	0.16	24
Traps Bay Bridge	41	TBB	—	4/15/2008	0.13	5/16/2008	0.08	20
Traps Bay Creek	42	TBC	—	4/15/2008	0.14	5/16/2008	0.06	20
Pollocks Point Shoreline	43	PPS	—	4/15/2008	0.32	5/16/2008	0.17	20
Pollocks Point Upper	44	PPU	—	4/14/2008	0.27	5/16/08	0.18	20
French Creek Shoreline	45	FNS	—	4/15/2008	0.19	5/16/2008	0.13	20
French Creek Upper	46	FNU	—	4/15/2008	0.18	5/16/2008	0.13	20

Note: NAVD 88 = North American Vertical Datum of 1988; C = control; F = fertilized.

Water Level/Tide Gauge

NOAA's Beaufort Laboratory established water level stations at Mile Hammock Bay (Tactical Landing Zone Bluebird boat ramp) on February 21, 2008, and at Gottschalk Marina in Wallace Creek (GM/WC) on May 15, 2008, following protocols established in conjunction with the Center for Operational Oceanographic Products and Services (CO-OPS; NOAA, 2007a). At each station, a vented datasonde (Yellow Springs, Inc. [YSI] Model 600LS) was installed in a structure designed to allow vertical water movement and provide a stable platform. The datasonde was referenced to three physical reference points on the supporting structure and land-based reference marks. The datasondes recorded water level, temperature, and salinity every 6 minutes. Data were downloaded at least every 2 months, and datasondes were replaced every 3 to 6 months. The datasondes underwent calibration procedures prior to and after deployment to test for drift and data quality. Datasondes were checked for vertical movement prior to and after replacement using laser leveling techniques.

Water levels were corrected to North American Vertical Datum of 1988 (NAVD 88), using OPUS observations following protocols established by NOAA's NGS. Datasonde sensor NAVD 88 elevations were derived using the NGS OPUS, virtual reference station GPS, and RTK-GPS technology, and laser-leveling techniques modified from the *User's Guide for Installation of Bench Marks and Leveling Requirements for Water Level Stations* (NOAA, 1987), *NGS-58*

Guidelines for Establishing GPS–Derived Ellipsoid Heights (NOAA, 1997), and NOAA CO-OPS *User's Guide for GPS Observations* (NOAA, 2007b). Datasondes were referenced to at least three reference marks near the tide station. Data were provided to NOAA CO-OPS for quality assurance and quality control checks and data analysis of water level data to determine local tidal datum (NOAA, 2007a).

Water level data from tide gauges were used to calculate inundation at SET sites. The mean hourly water level was compared to the mean SET sediment surface elevation at each site to determine the total inundation for each SET reading interval. MHB SET inundation was calculated using data from the MHB tide gauge because of its close proximity to the site. Other sites did not have a nearby tide station, so we used water level data collected by Craig Tobias for Research Project CW-3 (**Table 7-2**). We also compared the water level data collected by Dr. Tobias at Freeman Creek, Traps Bay, and French Creek to the nearest YSI tide gauge for each site to determine if the YSI tide gauge water level data were representative of the water level measured at each site in the monitoring wells.

There were significant gaps in water level data collection at MHB due to instrument failure. Some of these gaps were due to collisions or disturbance of the datasonde by unknown parties. These time periods were: February 29, 2008–April 10, 2008; June 22, 2009–July 8, 2009; November 20, 2011–December 7, 2011. These intervals have been removed from the inundation analyses over SET reading intervals because they are incomplete. There were no significant gaps in the GM/WC data set.

Water level data were submitted to the NOAA CO-OPS in 2010. CO-OPS analysts used 12 months (January 1, 2009 to December 31, 2009) of 6-minute data from each tide station to calculate tidal datums using the modified-range ratio method, using the National Water Level Observation Network tide station 8656483 for tide control. CO-OPS also provided an analysis of the contribution of tidal harmonic constituents to the observed water levels.

Inundation Calculations

Water level data from MHB and GM/WC tide gauges and pressure sensors deployed by Dr. Tobias (Research Project CW-3) were used to determine the total hours of tidal inundation at each site between SET readings and MH intervals. We hypothesized that if tidal waters are the primary source of sediment to the marsh surface, and if suspended sediment concentration is consistent through time, then there should be a positive correlation between inundation and surface elevation change. However, sediment accretion can also be controlled by marsh biomass, which varies seasonally. We first identified SET and MH reading intervals for which local water level data were available, and then analyzed the relationship between the parameters using linear regression. Inundation hours were determined by calculating the number of hours in the interval in which water level exceeded the marsh surface at the SET site. The data utilized for this analysis are summarized in **Table 7-2**.

Table 7-2. Data intervals used in analysis of relationship between tidal inundation, surface elevation change, and sediment accretion.

Data sources include pressure sensors installed at French Creek and Traps Bay (TB) by Dr. Tobias as part of Research Project CW-3. These sensors were surveyed into SET marks (FC logger, TB logger).

Site	Data Source	Time Period
French Creek (FC)	FC logger	May 2009–April 2010
Onslow Beach Backbarrier (OBB)	FC logger	May 2009–April 2010
Mile Hammock Bay (MHB)	MHB tide station	February 2008–Aug 2012
Traps Bay Bridge (TBB) and Traps Bay Creek (TBC)	TB logger	January 2009–April 2010
Pollocks Point Shoreline (PPS) and Pollocks Point Upper (PPU)	WC tide station	May 2008–August 2012
French Creek Shoreline (FNS) and French Creek Upper (FNU)	WC tide station	May 2008–August 2012

Results and Discussion

Marsh Surface Elevation Change and Sediment Accretion Rates

The elevation of the marsh surface at SETs adjacent to the ICW (FC, OBB, and MHB) increased significantly over the study period (**Table 7-3**). Rates at unfertilized, control SETs ranged from 2.22 m y^{-1} at OBB to 9.31 mm^{-1} at FC, with the highest rates occurring at the lowest elevation SETS at FC (Figure 7-2). The effect of fertilization on SET readings is reported and discussed in Chapter 7 of the *DCERP1 Final Research Report*.

Significant increases in marsh surface elevation were found at only four of the SET sites adjacent to the NRE (**Table 7-3**). The sites which did not show a significant trend in surface elevation change included both a SET near the upper margin of the intertidal marsh (PPS), as well as a SET near the shoreline along French Creek. The highest increase in surface elevation in the NRE was at PPS, and this increase was also observed over a larger area with DEM change analysis, and occurred concurrently with erosion of the shoreline (Chapter 6, *DCERP1 Final Monitoring Report*). Sites Traps Bay Bridge (TBB) and Traps Bay Creek (TBC) are in the lower NRE near MHB **(Figure 7-1**), although at a slightly lower surface elevation than MHB, exhibited similar rates of surface elevation change. Overall, seven out of the nine SET locations exhibited a significant increase in surface elevation over the study period, and the rate of increase was equal to or higher than recent estimates of relative SLR for Wilmington (2.12 mm y^{-1}) and Beaufort (3.20 mm y^{-1}), the two closest NOAA tide gauges for which recent sea level trends have been assessed (Zervas, 2004).

Table 7-3. Results of linear regression analysis of sediment surface elevation change (slope) as measured with SETs from 2008 to 2012.

Site	Treatment	Slope (mm/y)	p value
FC	Control	9.31	<.0001
	Fertilized	12.4	<.0001
MHB	Control	3.03	<.0001
	Fertilized	6.46	<.0001
OBB	Control	2.22	<.0001
	Fertilized	6.57	<.0001
PPS	Control	5.58	<.0001
PPU	Control	−0.74	0.5724
FNU	Control	3.39	<.0001
FNS	Control	0.99	0.5198
TBB	Control	2.33	0.0043
TBC	Control	3.65	<.0001

Note: FC = French Creek; FNS = French Creek Shoreline; FNU = French Creek Upper; MHB = Mile Hammock Bay; OBB =Onslow Beach Backbarrier; PPS = Pollocks Point Shoreline; PPU = Pollocks Point Upper; TBB = Traps Bay Bridge; TBC = Traps Bay Creek.

Table 7-4. Change in mean elevation (mm) as measured with SETs over each time interval.

Site	February/ May[a] 2008–March 2009	March 2009–February 2010	February 2010–Feb 2011	February 2011–February 2012	February 2012–August 2012	Site Annual SET Mean (standard deviation)
FC	9.0	9.5	10.0	9.2	8.8	**9.3 (0.5)**
OBB	−2.6	0.6	3.2	3.8	−0.3	**0.9 (2.6)**
MHB	−1.9	8.3	−2.6	8.5	1.8	**2.8 (5.4)**
TBB	7.7	3.4	4.2	−6.8	1.5	**2.0 (5.4)**
TBC	8.2	0.8	3.6	3.1	1.4	**3.4 (2.9)**
PPS	10.6	11.7	2.1	1.9	−5.6	**4.1 (7.1)**
PPU	12.2	−8.1	3.8	4.2	−10.1	**0.4 (9.3)**
FNS	−6.5	8.4	−2.2	−23.7	34.5	**2.1 (21.5)**
FNU	−0.7	2.2	6.6	−3.2	7.7	**2.5 (4.7)**
Interval average	**4.0**	**4.1**	**3.2**	**−0.3**	**4.4**	

Note: FC = French Creek; FNS = French Creek Shoreline; FNU = French Creek Upper; MHB = Mile Hammock Bay; OBB = Onslow Beach Backbarrier; PPS = Pollocks Point Shoreline; PPU = Pollocks Point Upper; TBB = Traps Bay Bridge; TBC = Traps Bay Creek.

[a] The first interval for FC, OBB, and MHB was February 2008–March 2009. The first interval for all other sites was May 2008–March 2009.

We further examined spatial and temporal variability in surface elevation change by grouping the SET data into approximate annual intervals (**Table 7-4**). Note that the first and last intervals in

this series are for less than 12-month periods. The SET site with the highest surface elevation increase, FC, also exhibited the most consistent rate of elevation change (**Table 7-4**). However, it is important to note these data are the averages of three SETs, unlike other sites. FC and TBC were the only SET sites where the standard deviation of average elevation change over the five time intervals was less than the interval mean, reflecting the significant temporal variation in the process. Another feature is the large negative change in elevation at FNS over the 2011 interval, followed by a large increase in the 2012 interval, which resulted in little net change in elevation over the entire study period. A pattern of late winter/early spring decrease can be seen throughout the study at FNS (**Figure 7-4**). Overall, despite variability, the interval averages are remarkably consistent, approximately 4 mm per period, with the exception of 2011, which had several negative values in addition to FNS.

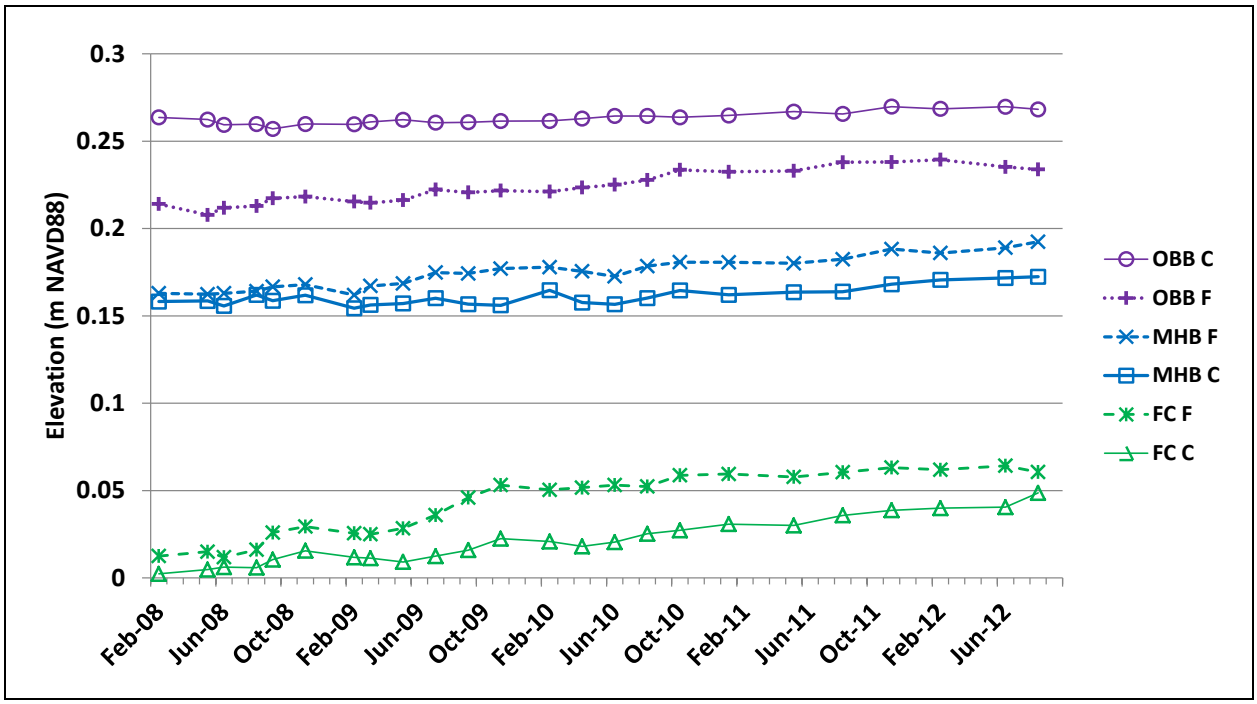

Figure 7-3. Sediment surface elevation (in meters [m]) measured at SETs for control (C) and fertilized (F) plots in ICW marshes.

Note: FC = French Creek; MHB = Mile Hammock Bay; OBB = Onslow Beach Backbarrier.
Initial site elevation surveyed relative to NAVD 88. Subsequent elevations calculated from the mean of 36 pins at each SET, except for FC F and FC F, where each point represents the average of 36 pins from each of three SETs.

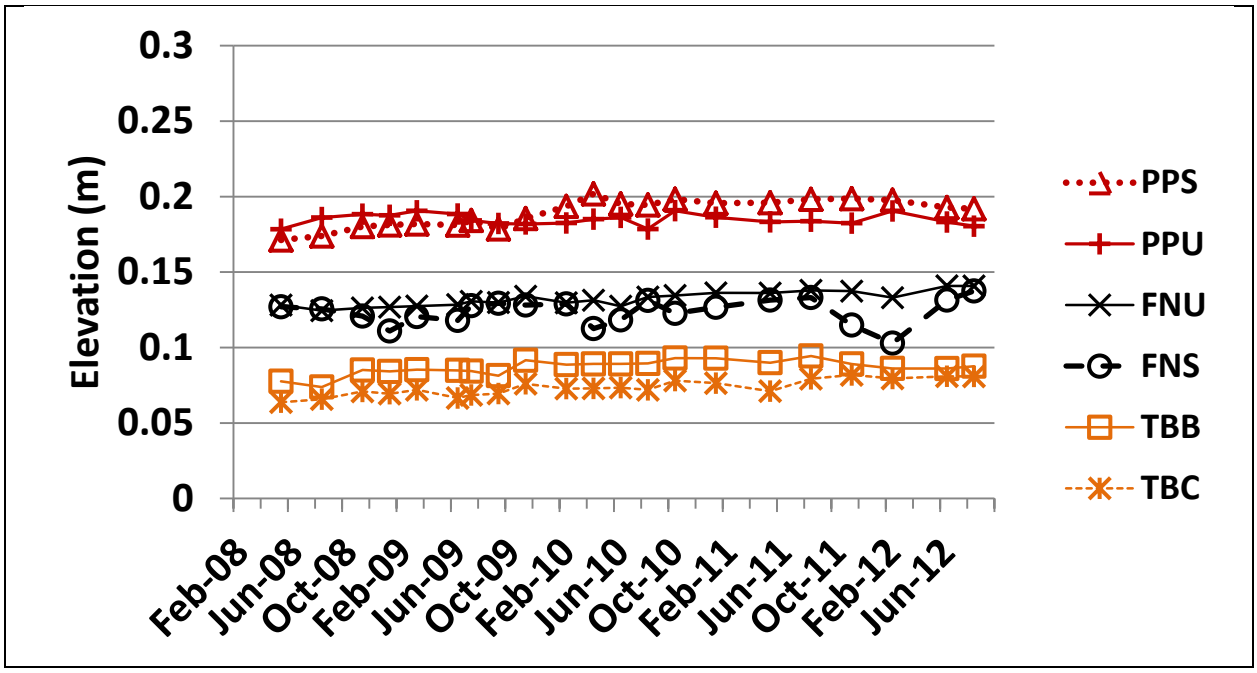

Figure 7-4. Sediment surface elevation (in meters [m]) measured at SET plots in NRE marshes.

Note: FNS = French Creek Shoreline; FNU = French Creek Upper; PPS = Pollocks Point Shoreline; PPU = Pollocks Point Upper; TBB = Traps Bay Bridge; TBC = Traps Bay Creek. Each point represents the mean of 36 pins read at one SET.

Sediment accretion rates, as measured by MH, were extremely variable and generally exceeded SET measures of net surface elevation change (**Table 7-5**; **Figure 7-5**) It is noted that erosion or loss of sediment is not readily measured with this technique, skewing the results toward the positive. As found with the SET measures of elevation change, the FC site exhibits the highest sediment accretion rate of any site. However, the PPS site also exhibited frequent instances of high sediment accretion (**Table 7-5**), and the lowest values overall were found at the *Juncus*-dominated sites at FN and PPU.

The contribution of sediment accretion (*A;* measured by MHs) to net surface elevation change (*E;* measured by SETs) provides an estimate of the role of subsurface processes to marsh surface elevation (Cahoon et al., 2002a, 200b). Subsurface processes include shallow subsidence, sediment compaction, and organic matter decomposition, which reduce marsh elevation, as well as accumulation of below-ground plant material and swelling, which would increase marsh elevation (Cahoon et al., 2002a, 2002b). Where $E<A$, it is an indication that sediment compaction, organic matter decomposition or soil shrinkage is occurring to reduce soil elevation. In instances where $E>A$, then it is likely that below-ground plant production is making a significant contribution to marsh elevation (Nyman et al., 2006). At each of the ICW sites in this study. $E<A$ in nearly every sample interval, often by a substantial margin (**Figure 7-5**). A similar pattern was found in the NRE marshes (**Tables 7-4 and 7-5**). Clearly, MCBCL marsh surface elevation change is driven by sediment accretion, and the processes of sediment compaction and perhaps below-ground decomposition are important contributors to net marsh surface elevation change.

Table 7-5. Sediment accretion (mm) as measured with MHs over each time interval.

Values represent the sum of mean sediment accretion measured during the sampling interval. Mean values are the average of interval sediment accretion, by site (MH mean), or the average of site-specific sediment accretion, by sampling interval (interval average).

Site	February/May[a] 2008–March 2009	March 2009–February 2010	February 2010–February 2011	February 2011–February 2012	February 2012–August 2012	MH mean
FC	22.99	24.84	19.04	21.47	18.95	**21.5**
OBB	6.93	12.71	8.27	10.46	7.56	**9.2**
MHB	11.91	14.49	8.92	7.25	8.72	**10.3**
TBB	23.03	16.72	10.76	3.08	8.85	**12.5**
TBC	11.19	19.40	9.08	14.07	4.25	**11.6**
PPS	18.31	25.06	23.68	11.66	—	**19.7**
PPU	11.00	17.64	1.95	1.96	0.78	**6.7**
FNS	6.10	5.86	10.30	1.08	9.65	**6.6**
FNU	11.13	15.66	7.27	1.86	1.84	**7.6**
Interval average	**13.6**	**16.9**	**11.0**	**8.1**	**7.6**	

Note: FC = French Creek; FNS = French Creek Shoreline; FNU = French Creek Upper; MHB = Mile Hammock Bay; OBB = Onslow Beach Backbarrier; PPS = Pollocks Point Shoreline; PPU = Pollocks Point Upper; TBB = Traps Bay Bridge; TBC = Traps Bay Creek.

[a] The first interval for FC, OBB, and MHB is February 2008–March 2009. The first interval for all other sites is May 2008–March 2009.

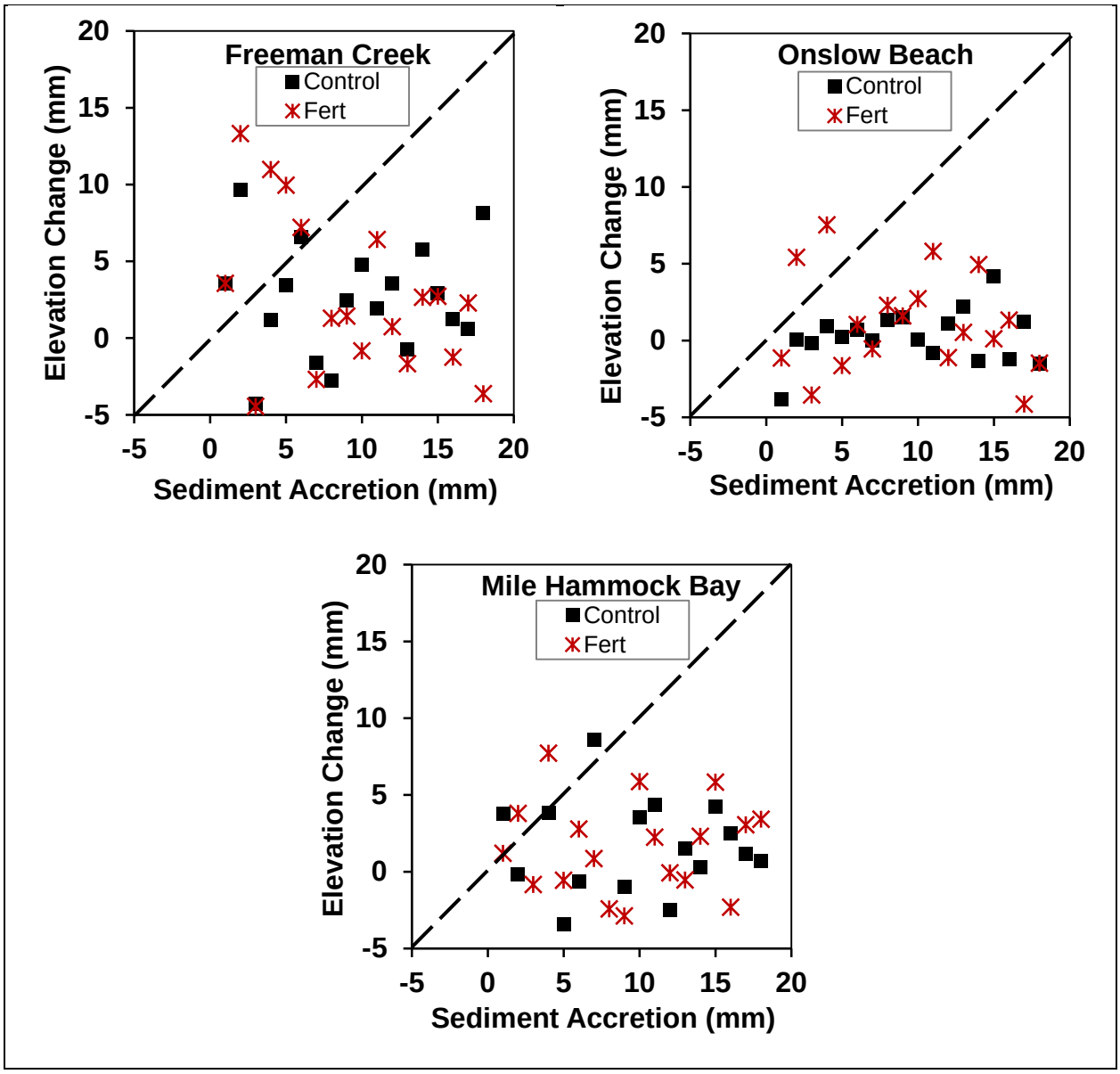

Figure 7-5. Sediment accretion, measured with feldspar MHs, versus marsh surface elevation change, measured with SETs, at each of the ICW marshes: (A) Freeman Creek, (B) Onslow Beach, and (C) Mile Hammock Bay.

Data points represent mean values of 1–4 month sampling intervals for each parameter. The dashed line represents a 1:1 ratio of sediment accretion to surface elevation change.

Relationship Between Marsh Inundation, Surface Elevation, and Sediment Accretion

There was not a significant relationship between time of inundation and either net elevation change or sediment accretion at any of the study sites (**Table 7-6**). In most cases, r-squared (r^2) values indicate that inundation explained little of the variability in elevation change, with values greater than 25% only recorded at FC, TBB, and TBC. These are also the sites with the lowest surface elevations (**Table 7-1**), and so are flooded more regularly than other sites. There was a similar low correlation between inundation and the MH data, as illustrated in **Figure 7-6**, with

overall r^2 values of less than 20% for combined data in the ICW and NRE. These results, together with the relatively high rates of sediment accretion (greater than 7 mm y^{-1}) recorded throughout MCBCL, suggest that suspended sediment concentration is highly variable and controls short-term (seasonal-monthly) surface elevation change.

Table 7-6. Results of regression analysis of relationship between marsh surface elevation change, as measured with SETs, and the length of time (h) that the SET was inundated.

Treatment includes fertilized and control. The number of sampling periods used in the analysis is given as "n." "Source" indicates the source of water level data for the site. Site elevation was determined using the average SET elevation during the sampling interval.

Site	Treatment	Pr>F	r^2	n	Source	Sample Interval
FC	Fertilized	0.8593	0.0123	5	FC pressure loggers	May 2009–April 2010
FC	Control	0.2754	0.3711	5	FC pressure loggers	May 2009–April 2010
OBB	Fertilized	0.9563	0.0012	5	FC pressure loggers	May 2009–April 2010
OBB	Control	0.8653	0.0112	5	FC pressure loggers	May 2009–April 2010
MHB	Control	0.2746	0.0789	17	MHB tide station	May 2008–August 2012 (with gaps)
MHB	Fertilized	0.0626	0.2124	17	MHB tide station	May 2008–August 2012 (with gaps)
TBB	Not applicable	0.0776	0.4953	7	TB pressure loggers	March 2009–April 2010
TBC	Not applicable	0.2535	0.2497	7	TB pressure loggers	March 2009–April 2010
PPS	Not applicable	0.0943	0.1559	19	GM/WC tide station	May 2008–August 2012
PPU	Not applicable	0.953	0.0002	19	GM/WC tide station	May 2008–August 2012
FNS	Not applicable	0.8065	0.0036	19	GM/WC tide station	May 2008–August 2012
FNU	Not applicable	0.141	0.123	19	GM/WC tide station	May 2008–August 2012

Note: FC = French Creek; FNS = French Creek Shoreline; FNU = French Creek Upper; GM/WC = Gottshalk Marina/Wallace Creek; MHB = Mile Hammock Bay; OBB = Onslow Beach Backbarrier; PPS = Pollocks Point Shoreline; PPU = Pollocks Point Upper; TB=Traps Bay; TBB = Traps Bay Bridge; TBC = Traps Bay Creek.

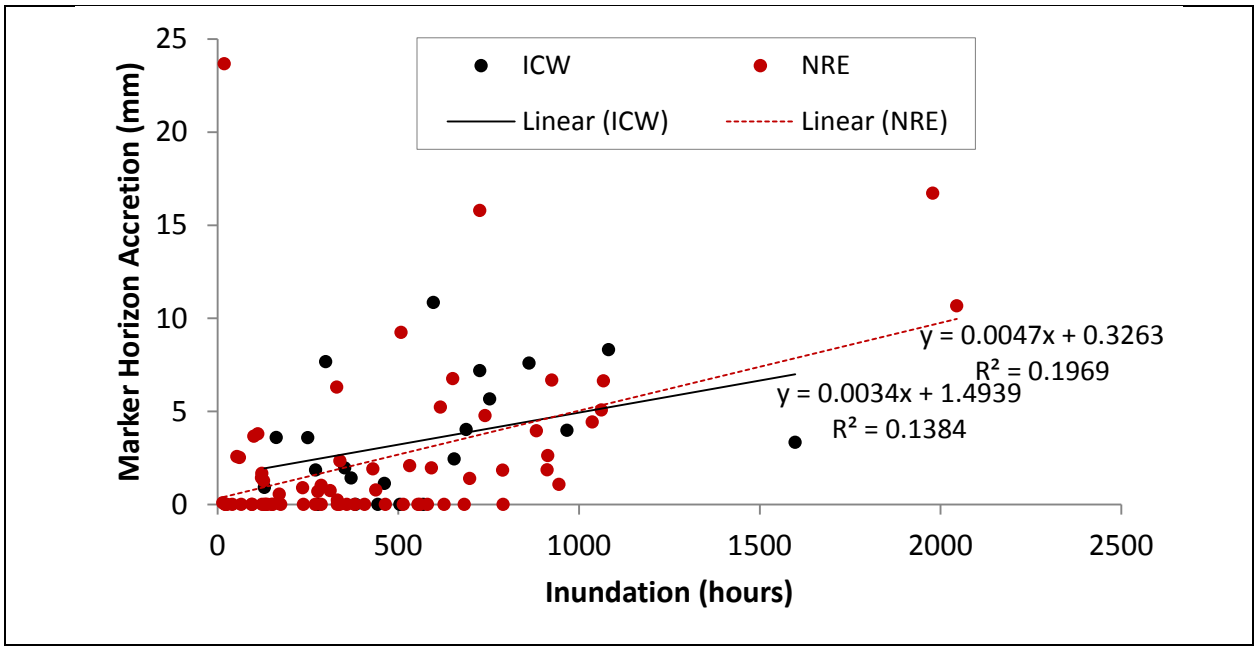

Figure 7-6. Relationship between tidal inundation and sediment accretion during 2- to 5-month sample intervals at ICW and NRE marshes.

Water Level/Tide Gauge

Water level, salinity, and temperature data from YSI datasondes deployed at MHB are shown in **Figures 7-7, 7-8,** and **7-9** and data from datasondes deployed at GM/WC are shown in **Figures 7- 10, 7-11,** and **7-12**. Noteworthy events recorded with these sensors include high water levels, often associated with tropical storms, occurring in late summer to early fall in 2008–2011. Subsequent drops in salinity are clearly seen in the GM/WC record (**Figure 7-12**). Water levels in 2012 are noteworthy for reaching a high water level earlier in the year (April), and sustaining high water level throughout the summer growing season (see also Chapter 6, *Land Cover and Shoreline Erosion*). Water level data from 2009 was used by NOAA CO-OPS to determine tidal datums for both sites. Results from this analysis are shown in **Table 7-7**, and provide the offset between mean sea level and NAVD 88 in the upper and lower NRE. This analysis also demonstrates the significant effect of meteorological events in the NRE, as harmonic constituents account for less than 75% of the variability in water level at both stations. Water level in the NRE also exhibits an average seasonal cycle, as mean water level in September is approximately 30 cm greater than in January at both stations (**Figure 7-13**). This pattern is consistent with that reported from NOAA tide stations in North Carolina (Zervas, 2004).

In addition to the temporary tide gauge stations, as part of Research Project CW-3, Onset sensors were deployed for shorter time periods at several sites (FC, near TBC, and FN). Seasonal comparisons of water level between these sites and the temporary tide gauges are shown in **Figures 7-14, 7-15,** and **7-16)**.

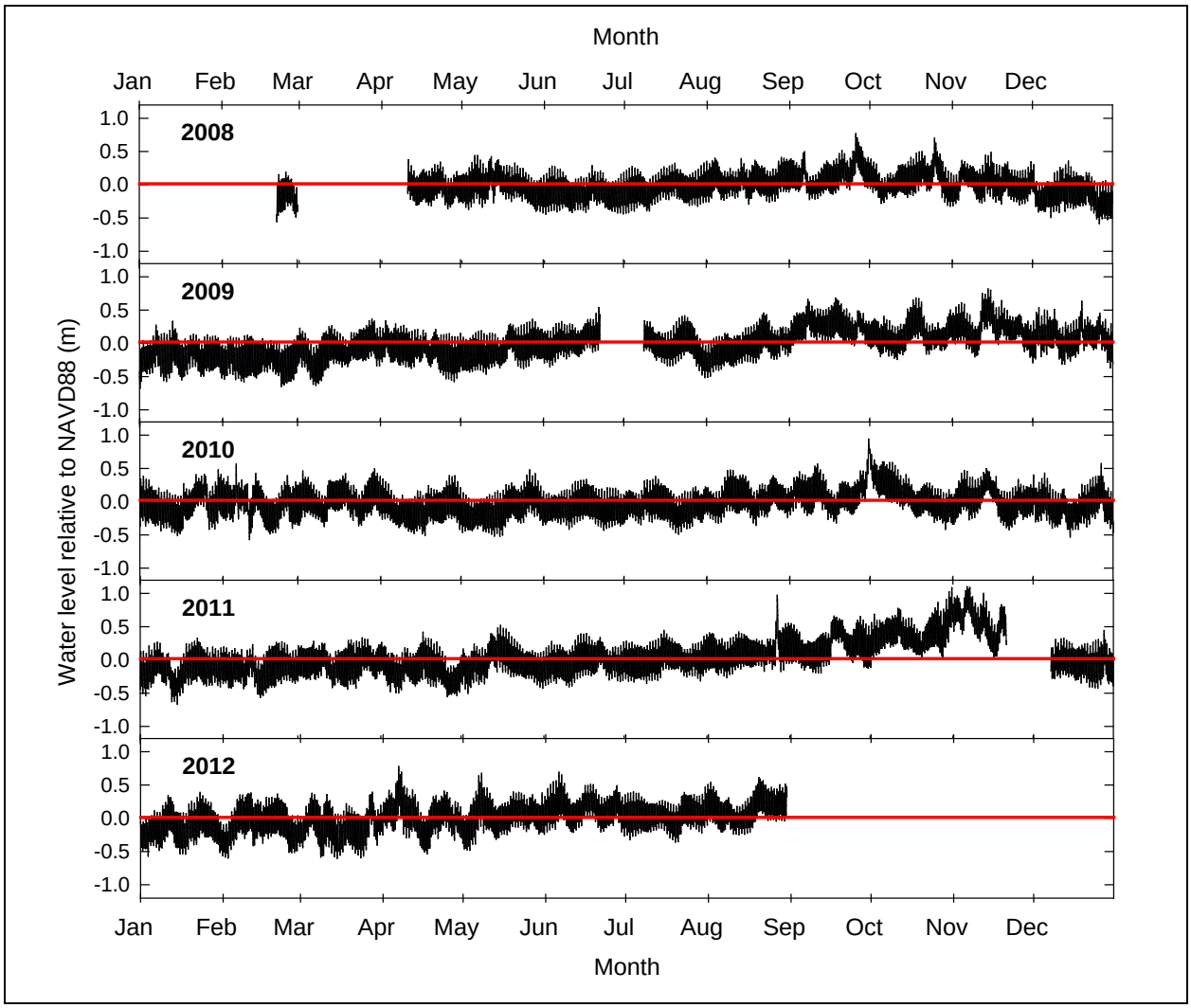

Figure 7-7. Hourly water level means at Mile Hammock Bay from April 2008 to September 2012.

Gaps in the record are due to logger failure (February 29 to April 10, 2008), disturbance by boat (June 22 to July 8, 2009), unknown disturbance displacing datasonde (November 20 to December 7, 2011).

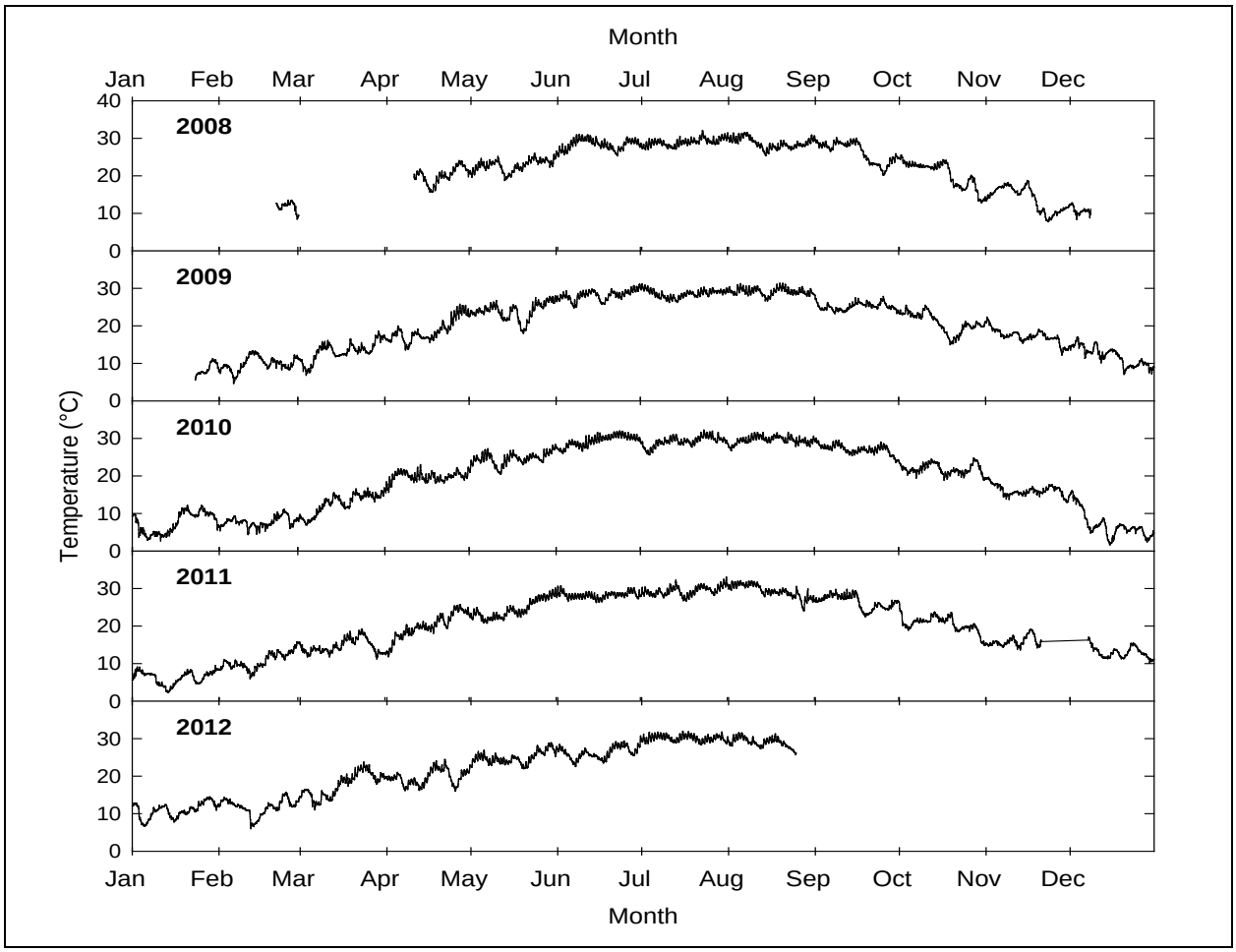

Figure 7-8. Hourly temperature means at Mile Hammock Bay from April 2008 to September 2012.

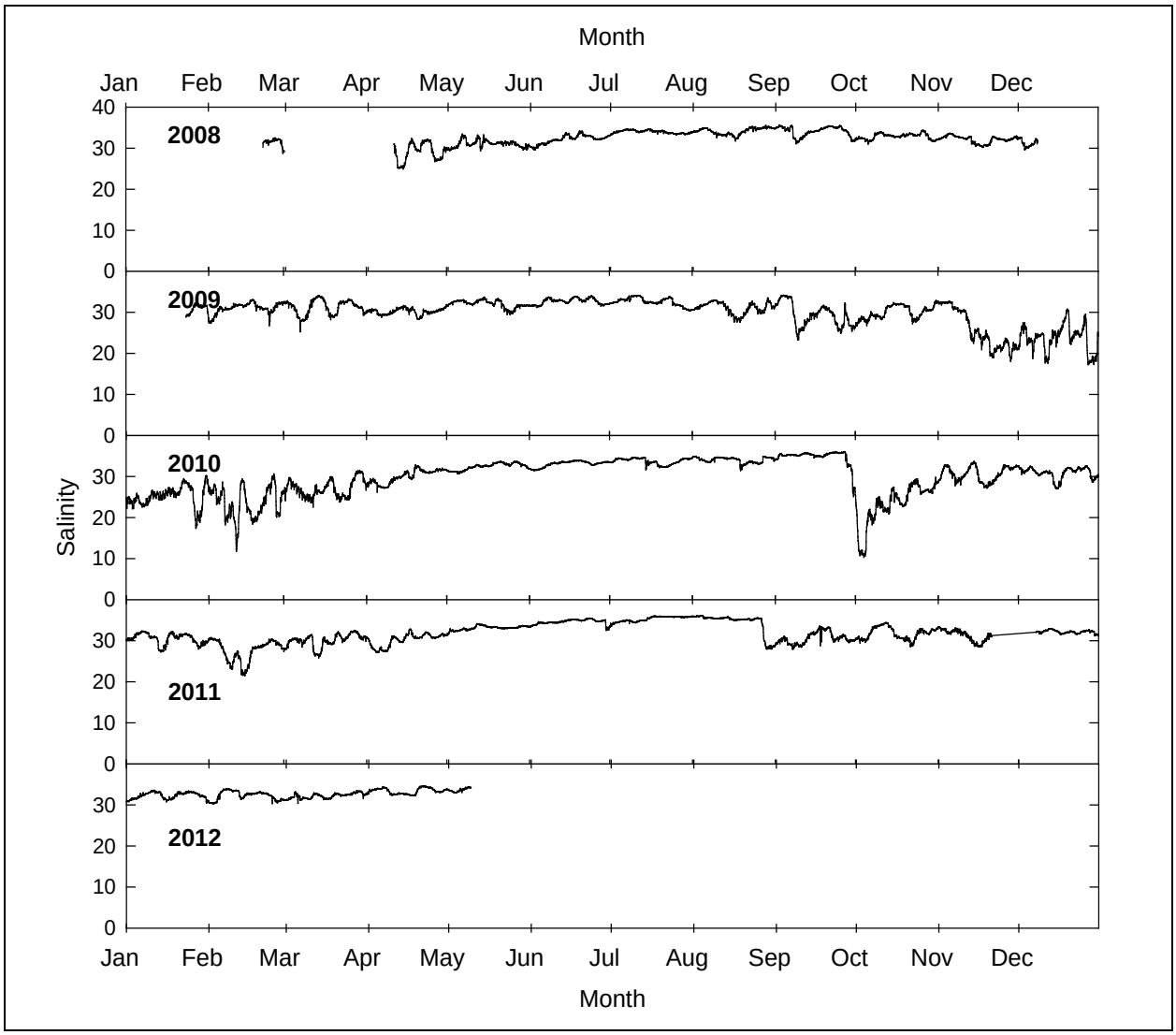

Figure 7-9. Hourly salinity (ppt) means at Mile Hammock Bay from April 2008 to September 2012.

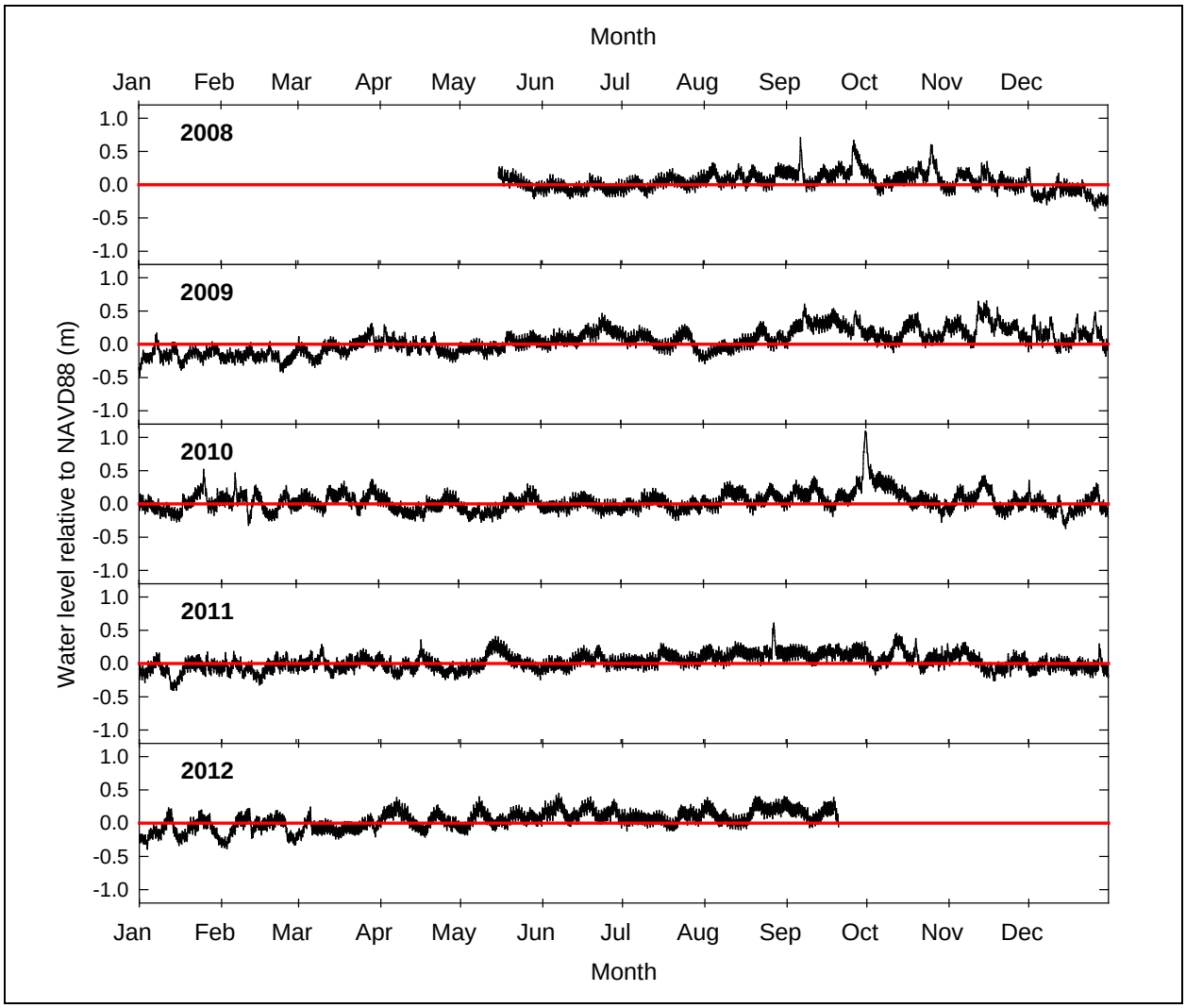

Figure 7-10. Hourly means of water level at Gottschalk Marina from May 2008 to September 2012.

Data were recorded at 6-minute intervals; the plot is of hourly means.

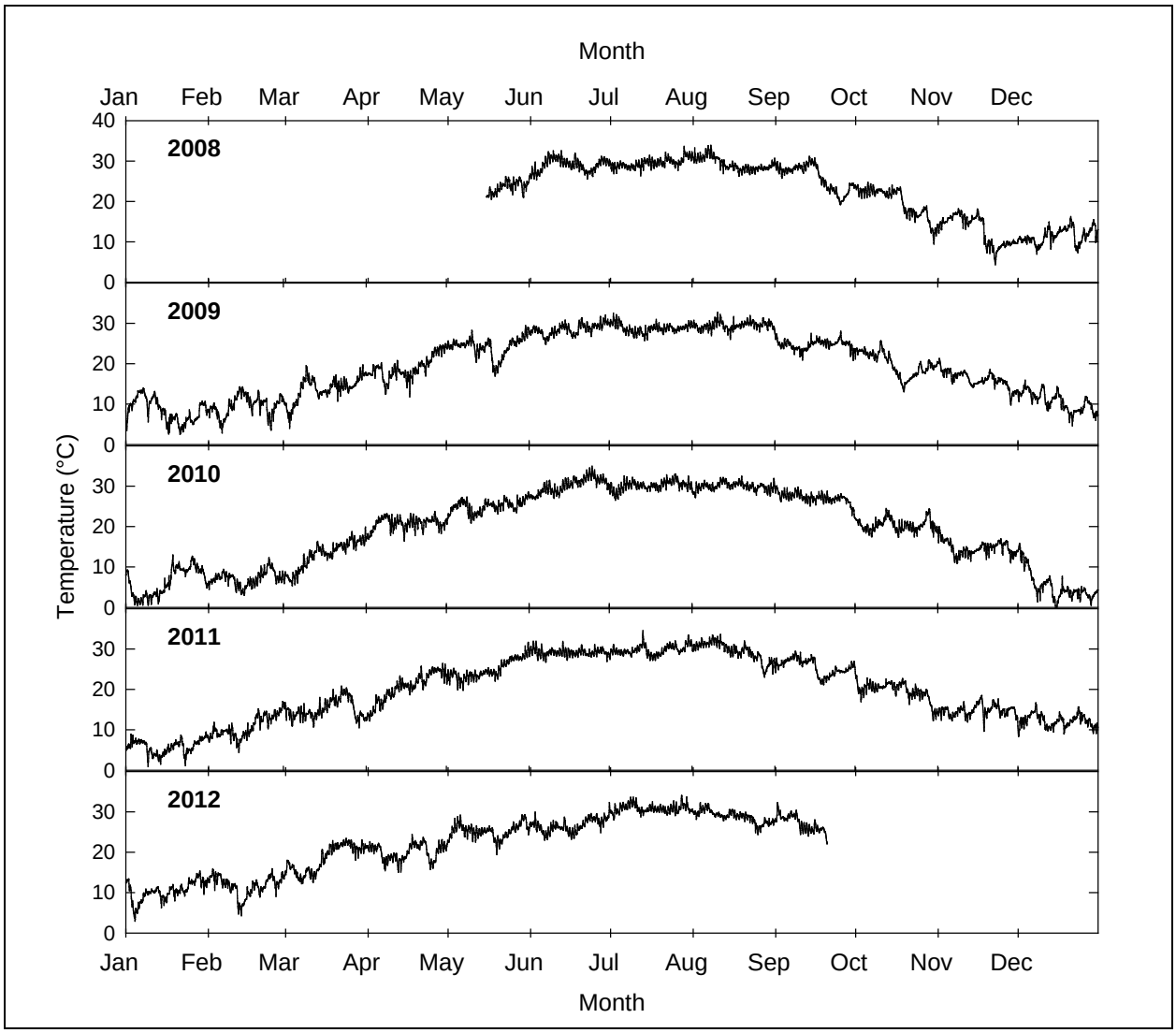

Figure 7-11. Hourly temperature means at Gottschalk Marina from May 2008 to September 2012.

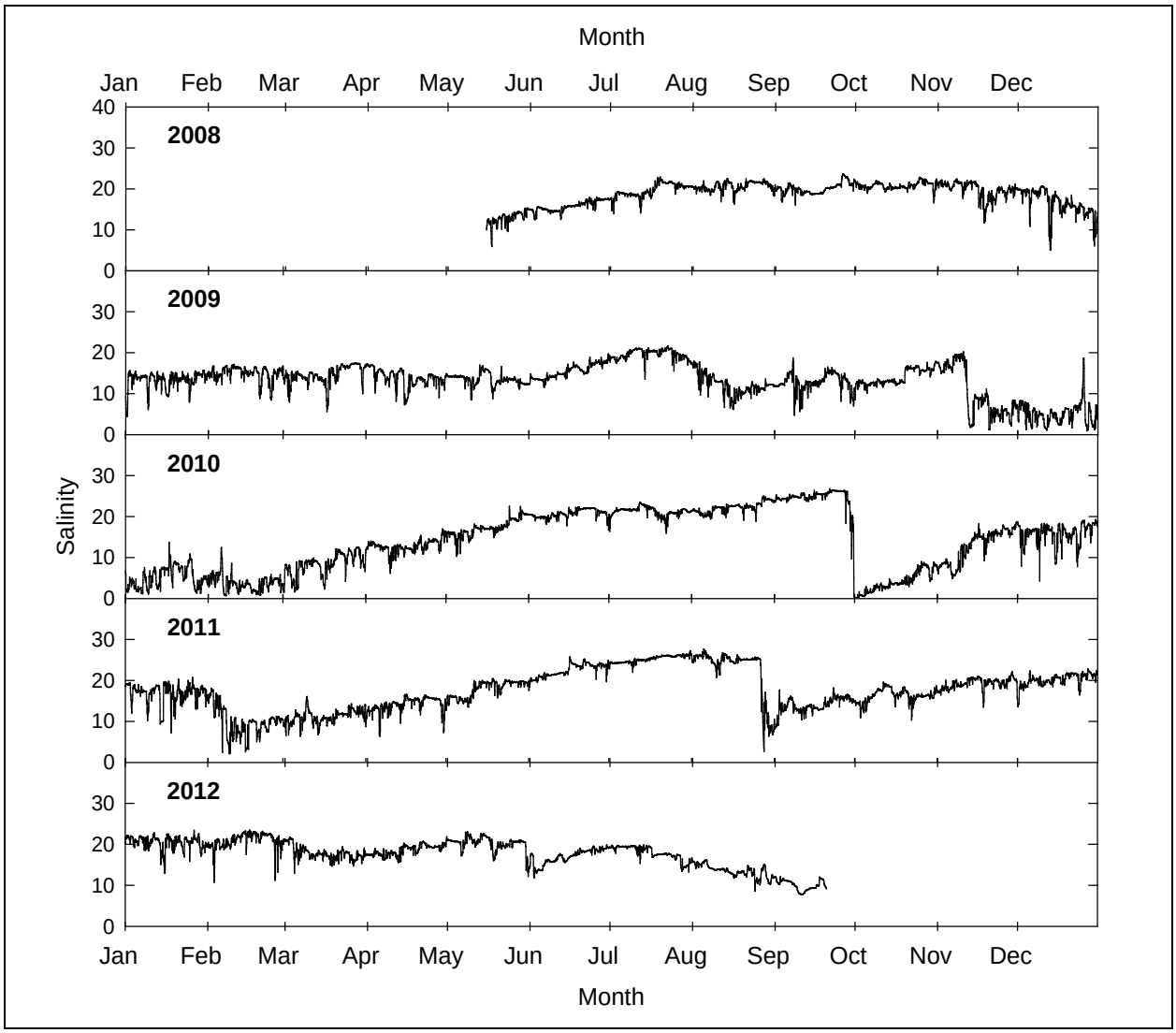

Figure 7-12. Hourly salinity (ppt) means at Gottschalk Marina from May 2008 to September 2012.

Table 7-7. Results from NOAA CO-OPS analysis of 6-minute water level data from tide gauge stations MHB (Mile Hammock Bay) and GC/WC (Gottshalk Marina/Wallace Creek)[a].

Station	Station Number	Latitude/ Longitude	Mean High Higher Water	Mean High Water	Mean Sea Level	Mean Low Lower Water	Great Diurnal Range	Mean Range of Tide	Harmonic Reduction of Variance
MHB	8657098	34.5538 77.3262	0.193	0.150	−0.073	−0.309	0.503	0.429	0.7194
GC/WC	8656648	34.5772 77.3627	0.089	0.066	−0.014	−0.123	0.213	0.167	0.6012

Note: GM/WC = Gottshalk Marina/Wallace Creek; MHB = Mile Hammock Bay.
[a] All datums are given in m NAVD 88.

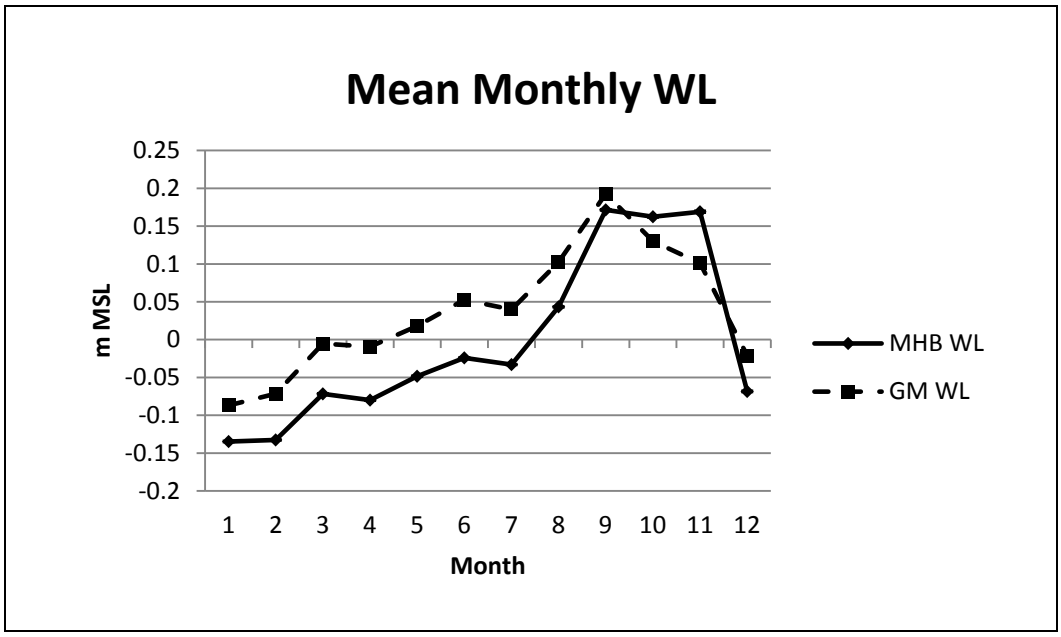

Figure 7-13. Monthly mean water level (WL) at Mile Hammock Bay (MHB) from April 2008 to September 2012 and Gottshalk Marina/Wallace Creek (GM/WC) from April 2008 to September 2012.

Comparisons of water level data between the temporary tide gauges at MHB and GM/WC with shorter term deployments of pressure sensors revealed important information on changes in tide range across study sites. We found good agreement between water level data collected at GM/WC and FN (**Figures 7-13**), supporting the use of the GM/WC data for marshes in the French Creek area. However, we found that the tide range at FC is nearly twice that.

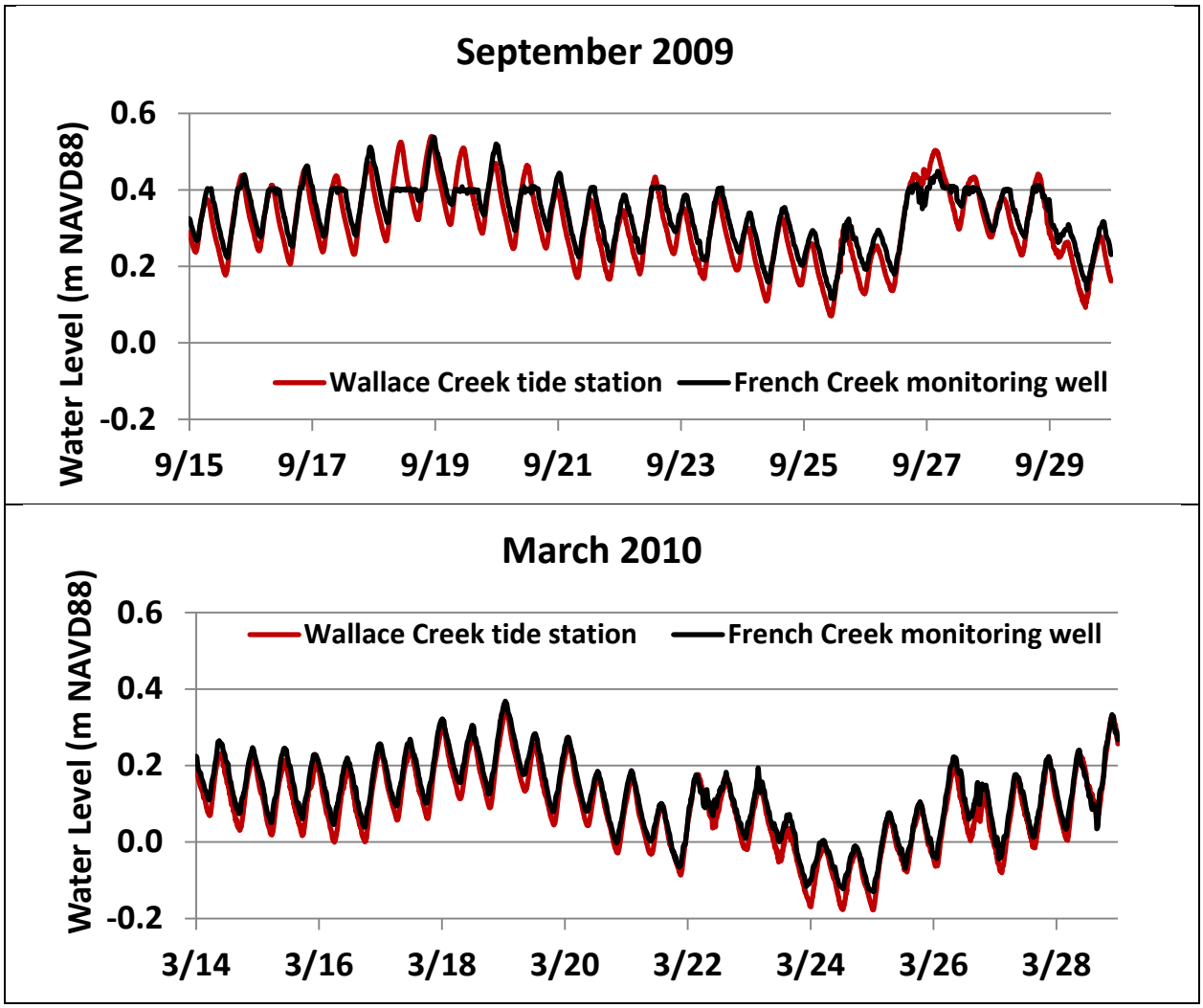

Figure 7-14. Comparison of water level as measured at Gottshalk Marina/Wallace Creek (GM/WC) by NOAA temporary tide gauge and at French Creek (FN) by pressure loggers in a monitoring well in September 2009 (A) and March 2010 (B).

GM/WC data were collected every 6 minutes, and FN data were collected every 15 minutes.

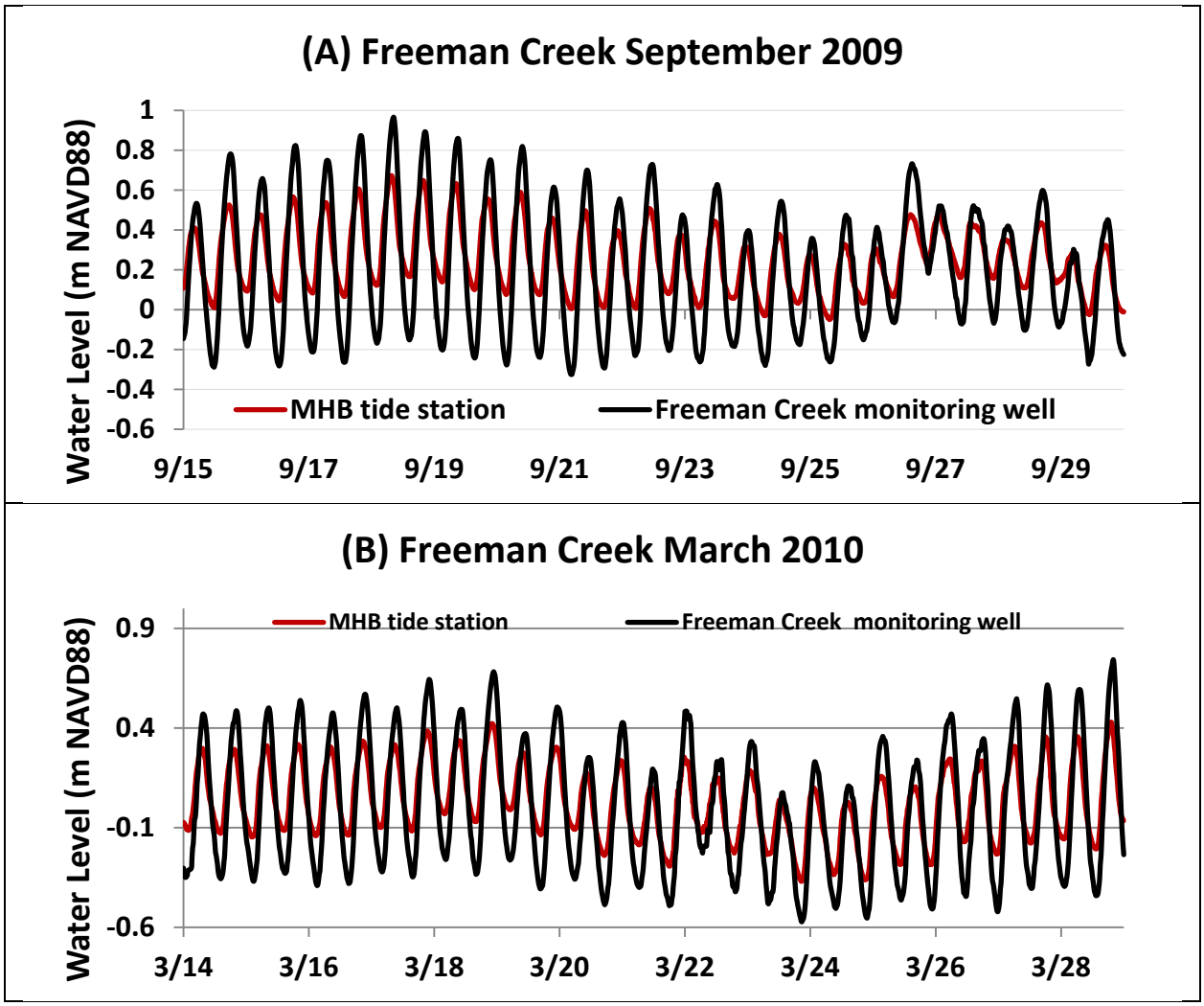

Figure 7-15. Comparison of water level as measured at Mile Hammock Bay (MHB) by NOAA temporary tide gauge and at Freeman Creek (FC) by pressure loggers in a monitoring well in September 2009 (A) and March 2010 (B).

MHB data were collected every 6 minutes, and FC data were collected every 15 minutes.

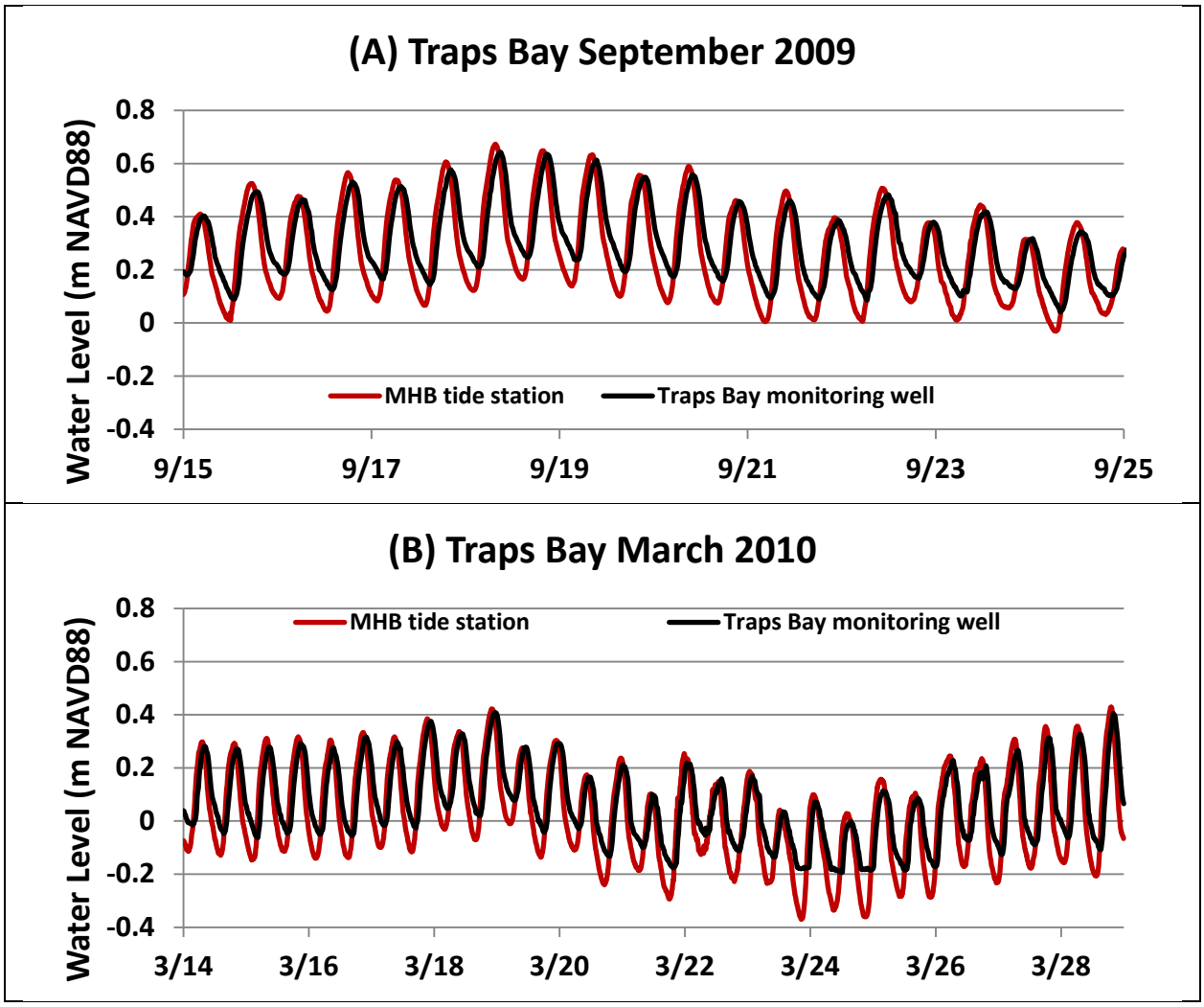

Figure 7-16. Comparison of water level as measured at Mile Hammock Bay (MHB) by NOAA temporary tide gauge and at Traps Bay (TB) by pressure loggers in a monitoring well in September 2009 (A) and March 2010 (B).

MHB data were collected every 6 minutes, and TB data were collected every 15 minutes.

Assessment of Trends in the Data

Assessment of Monitoring Design

Monitoring sites were selected to represent the variety of marsh geomorphological settings on MCBCL, from back-barrier marshes, to those adjacent to ocean inlets, to fringing marshes in the upper estuary. Across this varied landscape, we installed 16 SETs at nine stations to monitor surface elevation change and sediment accretion rates, in support of Research Project CW-1. The average initial surface elevation of control SETs at the ICW sites (FC, OBB, and MHB) ranged between −0.03 and 0.26 m relative to NAVD 88 (**Table 7-1**; see the Water Level section for the offsest between mean sea level and NAVD 88). As documented in Chapter 6 (*Land Cover and Shoreline Erosion*), *Spartina* vegetation occupied elevations between −0.45 m to 0.45 m in marshes adjacent to Browns Inlet and were restricted to a narrower range in the MHB area near

New River Inlet. Analysis of LIDAR imagery, reported in Chapter 7 of the *DCERP1 Final Research Report*, showed that marshes to the east of the ICW most frequently occurred at an elevation of 0.22 m NAVD 88, and those to the west most frequently occurred at an elevation of 0.08 m. Therefore, the surface elevation of SET stations is representative of the majority of the marsh in this area. Marsh occurs over a narrower elevation range in the NRE, and north of Pollocks Point is restricted to fringing marshes along the shoreline. NRE monitoring sites reflected the change in marsh vegetation found up-estuary, and exhibited different patterns of sediment accretion and erosion, depending on their setting in the landscape. Each of the monitoring sites had unique features in terms of tidal range, dominant vegetation, salinity, proximity to the shoreline, and/or surface elevation. However, we were unable to sample every type of marsh on MCBCL, and along the ICW we did not have SETs placed in high marsh, that is, areas dominated by high marsh species such as *Salicornia*, *Spartina patens or Juncus*. This may prove to be an important area to sample as future research expands to a landscape-scale examination of marsh response to SLR, and consequences for the C cycle. The SETs at PPU and FNU are both near the land-marsh boundary, and so provide some data for this habitat in the NRE.

The initial SET sampling frequency was quarterly; however this was increased to bimonthly during 2009 to improve our ability to compare MEM predictions to observations (Chapter 6, *DCERP1 Final Research Report*). Subsequently we returned to quarterly measures, and as the length of the record increases, the sampling frequency can remain at this level. We note that many SET monitoring programs measure annually or semi-annually, which is sufficient for a long-term (decades) monitoring program. All but two of the SET stations exhibit highly significant ($p<0.005$) slopes based on linear regression analysis, demonstrating the sufficient frequency with which data are collected. The placement of temporary NOAA tide gauge stations was limited in part by available surface infrastructure to support the datasondes. Marinas at Mile Hammock Bay and Wallace Creek provided the required structure and were selected as representative of the upper and lower NRE. Harmonic analysis of the water level data revealed significant differences in station tidal datums, including mean tide, and in the contribution of meteorological events to observed water level. The tide gauge data was supplemented by pressure sensors deployed in monitoring wells by CW-3, which provided crucial data which demonstrated the doubling in tidal amplitude between Browns Inlet and New River Inlet. Coupled with vegetation monitoring results and CW-1 research results, this finding has profound implications for predictions of marsh sustainability on MCBCL, as marshes occupying areas with reduced tidal range are reduced in distribution and are more vulnerable to SLR.

Assessment Seasonal and Annual Variability in the Data

The 5-year record of water level, temperature, and salinity at the temporary tide gauge stations revealed the expected seasonal change in temperature, and also detected a 30-cm seasonal effect on mean monthly water level. The data also illustrated the rapid decline in salinity associated with the passage of rainfall events, particularly in the upper NRE. This data also revealed substantially higher water levels in summer 2012 compared to prior summers, which was correlated with a decline in marsh biomass across the MCBCL. This finding is consistent with model results which predict a long-term decline in marsh biomass with SLR, but given the degree of annual variability in both biological and environmental parameters, it is premature to

assign a cause and effect relationship between the observed decrease in marsh biomass and increase in summer water level.

Despite the significant and fairly consistent trends in water level, regression analysis of SET, and MH data revealed little correlation with water level or station inundation over several-month time intervals. This short-term variability is most likely due to variability in suspended sediment concentration, and will be a focus of DCERP2 research efforts.

Conclusions and Implications for Future Research

Key Scientific Findings—Fundamental Cause-and-Effect Relationships

Differing inlet hydrodynamics result in a near two-fold increase in tide range between New River Inlet and Browns Inlet. As a result of this, marshes near Browns Inlet are distributed across a wider elevation range and, according to model predictions, are more resilient to SLR.

Marsh surface elevation increased throughout the study period at seven of nine monitoring sites. The study site at the lowest elevation, which is also adjacent to Browns Inlet, exhibited the highest surface elevation change, of 9 mm y^{-1}. Marshes at higher elevations, and those experiencing an attenuated tide range, had a net surface elevation change of 2 to 6 mm y^{-1}. Sediment accretion rates, as measured by marker horizons, were two to four times greater than the increase in marsh surface elevation change at every site. These observations support the conclusion that tidally transported sediment is the primary means by which MCBCL marshes maintain their elevation relative to SLR. However, the lack of a significant relationship between short-term (2–4 month) changes in surface elevation and tidal inundation suggest that suspended sediment concentration is highly variable and that accretion may be event-driven. In addition, the data suggest that compaction of sediments, and potentially decomposition of below-ground organic matter, are key processes controlling marsh surface elevation.

Findings Supportive of Current Base Management Practices

This monitoring effort did not directly address any current base management practices.

Findings with Implications for Future Base Management

The important role that tidal range and suspended sediment supply play in controlling the elevation of MCBCL marshes suggests that management practices that directly or indirectly affect inlet dynamics and the suspended sediment concentration of tidal waters may affect the health, productivity, and sustainability of MCBCL coastal wetlands. However, most of the relevant management practices are under the direct authority of other agencies, and may be implemented outside MCBCL boundaries. For example, efforts to maintain or realign the New River Inlet may alter both tide range and suspended sediment delivery to marshes in the lower NRE. Maintenance dredging of the ICW and NRE for navigation purposes also reduces sediment availability to marshes.

Given the apparent vulnerability of MCBCL coastal marshes to MCBCL managers may want to consider adaptive management practices to conserve salt marsh habitats. Possible actions include

marsh restoration, particularly along shorelines, thin-layer disposal of dredge material, and possibly fertilizing marshes in the lower NRE and Onslow Beach.

Findings with Implications for DCERP2

The major objectives of DCERP2 Coastal Wetlands research are to improve our understanding of the factors controlling salt marsh responses to SLR, provide predictive models for managers incorporating climate forcing factors, and develop and assess adaptive management strategies for sustaining coastal wetlands on MCBCL. DCERP1 results provided insight into important factors affecting the ability of MCBCL marshes to sustain marsh surface elevation and biomass under projected SLR, including (1) site variability in the relationship between elevation and marsh above-ground biomass, which improved predictions of marsh sustainability made by the MEM; (2) patterns in decadal and short-term marsh shoreline erosion rates along the NRE and the ICW; (3) differences in marsh surface elevation on opposite sides of the ICW based on ground-truthed and analyzed LIDAR data; and (4) significant variability in tide range between Browns Inlet at the north end of the barrier island (1.0 m) and New River Inlet at the south end (less than 0.5 m). These results led to hypotheses on the role of alterations in inlet dynamics and maintenance dredging in controlling the sediment supply sustaining salt marshes along the ICW. The results also highlighted the need for additional information on suspended sediment dynamics and marsh belowground production and decomposition to support predictive models and recommendations for adaptive management.

Another focus of DCERP2 is the carbon budget for MCBCL, and in particular to identify factors affecting carbon burial or sequestration. Marshes are known to have, per unit area, one of the highest burial rates for organic carbon of any ecosystem or habitat type, and this process is largely driven by the increase in surface elevation needed to keep pace with SLR. The baseline information on spatial and temporal variablity in marsh surface elevation change reported here will be crucial to DCERP2 experimental and modeling efforts to understand the marsh carbon cycle and predict impacts of SLR on marsh carbon sequestration.

Literature Cited

Cahoon, D. R. 2007. Factors affecting coastal wetland loss and restoration. Pp. 50–53 in *Synthesis of U.S. Geological Survey science for the Chesapeake Bay ecosystem and implications for environmental management*. Edited by S.W. Phillips. U.S. Geological Survey Circular 1316.

Cahoon, D.R., J.C. Lynch, P. Hensel, R. Boumans, B.C. Perez, B. Segura, and J.W. Day, Jr. 2002a. A device for high precision measurement of wetland sediment elevation: I. Recent improvements to the sedimentation-erosion table. *Journal of Sedimentary Research 72*(5):730–733.

Cahoon, D.R., J.C. Lynch, B.C. Perez, B. Segura, R. D. Holland, C. Stelly, G. Stephenson, and P. Hensel. 2002b. High-precision measurements of wetland sediment elevation: II. The rod surface elevation table. *Journal of Sedimentary Petrology 72*:734–739.

Cahoon, D.R., M.A. Ford, and P.G. Hensel. 2004. Ecogeomorphology of *Spartina patens*-dominated tidal marshes-soil organic matter accumulation, marsh elevation dynamics, and disturbance. *Coastal and Estuarine Studies 59*:247–266.

Cahoon, D.R., P.F. Hensel, T. Spencer, D.J. Reed, K.L. McKee, and N. Saintilan. 2006. Coastal wetland vulnerability to relative sea level rise: Wetland elevation trends and process controls. *Wetlands and Natural Resource Management: Ecological Studies 190*:271–292.

Chmura, G.L., and G. Hung. 2004. Controls on salt marsh accretion: a test in salt marshes of Eastern Canadian. *Estuaries 27*(1):70-81.

Kirwan, M.L., G.R. Guntenspergen, A. D'Alpaos, J.T. Morris, S.M. Mudd, and S. Temmerman. 2010. Limits on the adaptability of coastal marshes to rising sea level. *Geophysical Research Letters 37*:L23401.

Langley, J.A., K.L. McKee, D.R. Cahoon, J.A. Cherry, and J.P. Megonical. 2009. Elevated CO_2 stimulates marsh elevation gain, counterbalancing sea-level rise. *Proceedings of the National Academy of Sciences USA 106*:6182–6186.

Morris, J.T., P.V. Sundareshwar, C.T. Nietch, B. Kjerfve, and D.R. Cahoon. 2002. Responses of coastal wetlands to rising sea level. *Ecology 83*:2869–2877.

Mudd, S.M., A. D'Alpaos, and J.T. Morris. 2010. How does vegetation affect sedimentation on tidal marshes? Investigating particle capture and hydrodynamic controls on biologically mediated sedimentation: J*ournal of Geophysical Research 115*:F03029.

NOAA (National Oceanic and Atmospheric Administration). 1987. *User's Guide for Installation of Bench Marks and Leveling Requirements for Water Level Station.* U.S. Department of Commerce, National Oceanic and Atmospheric Administration, National Ocean Service, Office of Oceanography and Marine Assessment. October.

NOAA (National Oceanic and Atmospheric Administration). 1997. *Guidelines for Establishing GPS-Derived Ellipsoid Heights*. National Ocean Service, National Geodetic Survey, Silver Spring, MD. NOS NGS-58.

NOAA (National Oceanic and Atmospheric Administration). 2007a. *Guidelines for Determining Tidal Datums for Habitat Restoration and Monitoring Projects in North Carolina*. Draft Technical Report. U.S. Department of Commerce, National Oceanic and Atmospheric Administration, Center for Operational Oceanographic Products and Services. March.

NOAA (National Oceanic and Atmospheric Administration). 2007b. *User's Guide for GPS Observations*. Technical Report. U.S. Department of Commerce, National Oceanic and Atmospheric Administration, National Ocean Service, Center for Operational Oceanographic Products and Services. March.

Nyman, J.A., R.J. Walters, R.D. Delaune, and W.J. Patrick. 2006. Marsh vertical accretion via vegetative growth. *Estuarine Coastal Shelf Science 69*:370–380.

Redfield, A.C. 1965 Ontogeny of a salt marsh estuary. *Science 147*:50–55.

Roman, C.T., M.J. James-Pirri, and J.F. Heltsche. 2001. *Monitoring salt marsh vegetation: A protocol for the long-term coastal ecosystem monitoring program at Cape Cod National Seashore*. U.S. Geological Survey Patuxent Wildlife Research Center, Coastal Research Field Station, University of Rhode Island.

Zervas, C. 2004. *North Carolina Bathymetry/Topography Sea Level Rise Project: Determination of Sea Level Trends*. U.S. Department of Commerce, National Ocean Service, Center for Operational Oceanographic Products and Services. NOAA Technical Report NOS CO-OPS 041. Available at http://tidesandcurrents.noaa.gov/publications/techrpt41.pdf.

[This page intentionally left blank.]

Chapter 8

Onslow Bay Hydrodynamics

SERDP Project Number: RC-1413
Coastal Barrier Module

Lead Researchers:
Dr. Rick Luettich
UNC-CH Institute of Marine Sciences
Morehead City, NC 28557
E-mail: Rick_luettich@unc.edu

Dr. Janelle Reynolds-Fleming
Seahorse Coastal Consulting
Morehead City, NC
E-mail: janelle.fleming@gmail.com

June 27, 2013

Final

This report was prepared under contract to the U.S. Department of Defense (DoD) Strategic Environmental Research and Development Program (SERDP). The publication of this report does not indicate endorsement by DoD, nor should the contents be construed as reflecting the official policy or position of DoD. References herein to any specific commercial product, process, or service by trade name, trademark, manufacturer, or otherwise, do not necessarily constitute or imply its endorsement, recommendation, or favoring by DoD.

Table of Contents

List of Acronyms 8-v
Abstract 8-1
Objectives of the Monitoring Activity 8-1
    Oceanographic Data 8-1
    Acoustic Wave and Current Data 8-2
Background 8-2
Materials and Methods 8-3
    Monitoring Data 8-3
    Modeling Data 8-5
Results and Discussion 8-9
    Seasonal Trends—Winds and Waves 8-9
    Annual Trends—Currents, Waves, and Water Levels 8-10
    Extreme Event Trends—2008 Case Study 8-12
Assessment of Trends in the Data 8-18
    Assessment of Monitoring Design 8-18
    Assessment Seasonal and Annual Variability in the Data 8-18
    Recommendations for Future Monitoring 8-18
Conclusions and Implications for Future Research 8-18
    Key Scientific Findings—Fundamental Cause-and-Effect Relationships 8-18
    Findings Supportive of Current Base Management Practices 8-19
    Findings with Implications for Future Base Management 8-19
    Findings with Implications for DCERP2 8-19
Literature Cited 8-20
Appendix 8-A: List of Scientific Publications 8-A-1

List of Figures

8-1. (A) The eastern coast of North Carolina with data locations marked; (B) a close-up image of the Onslow Beach study site and Acoustic Wave and Current (AWAC) location. 8-3

8-2. (A) The trawl resistant Nortek AWAC frame and AWAC; (B) the NOAA NDBC wave buoys. 8-5

8-3. ADCIRC + SWAN unstructured finite element grid with high-resolution bathymetry and grid refinement. 8-8

8-4. Seasonal wind roses (in m s^{-1}) for (A) winter; (B) spring; (C) summer; and (D) autumn from NDBC Buoy 41036. 8-9

8-5. Seasonal wave roses (in m) for (A) winter; (B) spring; (C) summer; and (D) autumn from NDBC Buoy 41036. 8-10

8-6. Detided vertically averaged current roses (in m s^{-1}) from the AWAC location. 8-11

8-7. Annual time series of significant wave height at the AWAC location. 8-11

8-8. Annual time series water level at the AWAC location. 8-12

8-9. Model versus data comparison of water level at Onslow Beach. 8-14

8-10. Demeaned/detided water level at the AWAC location. 8-14

8-11. Model versus data comparisons of water level at the NOAA Beaufort station. 8-15

8-12. Demeaned/detided water level at Beaufort. 8-15

8-13. Model versus data comparison of water level at the NOAA Wrightsville station. 8-16

8-14. Demeaned/detided water level at Wrightsville Beach. 8-16

8-15. Significant wave heights at Onslow Beach: Model versus data comparison. 8-17

8-16. Alongshore distribution of extreme runup (thick lines) and mean runup (thinner lines; in m), calculated from model significant wave heights and wave period, from September 6, 2008 (- - - line) and September 26, 2008 (--- line) with alongshore distribution of average dune crest heights (in m) at seven sampling sites (-*-). 8-17

List of Acronyms

ADCIRC	Advanced Circulation (Model)
AST	acoustic surface tracking
AWAC	Acoustic Wave and Current (Profiler)
CORMP	Coastal Ocean Research Monitoring Program
cm	centimeter
DCERP1	first cycle of the Defense Coastal/Estuarine Research Program
DCERP2	second cycle of the Defense Coastal/Estuarine Research Program
DoD	U.S. Department of Defense
Hs	significant wave height
km	kilometer
km^2	square kilometer
m	meter
$m\ s^{-1}$	meters per second (a measure of velocity)
$m\ y^{-1}$	meters per year
MCBCL	Marine Corps Base Camp Lejeune
MHz	megahertz
NAM	North American Mesoscale(Model)
NDBC	National Data Buoy Center
NOAA	National Oceanic and Atmospheric Association
s	second
SERDP	Strategic Environmental Research and Development Program
SWAN	Simulating Waves Nearshore (Model)
WRF	Weather Research and Forecasting (Model)

[This page intentionally left blank.]

Abstract

Data from National Oceanic and Atmospheric Association–maintained wave buoys and water level gauges within Onslow Bay and the surrounding area as well as a purpose-deployed Nortek acoustic wave and current (AWAC) were used to understand the seasonal and inter-annual variability of the wind and wave climate of Onslow Bay. This information was then used to understand how the variation in seasonal and inter-annual climate would impact the morphology of the Onslow Beach, a fairly undeveloped barrier island within Marine Corps Base Camp Lejeune (MCBCL). These data were also used to validate a coupled hydrodynamic (Advanced Circulation [ADCIRC]) and waves (Simulating Waves Nearshore [SWAN]) model of the region that can be used in hindcast and forecast mode. In hindcast mode, the coupled models were used to determine the spatial distribution of water level and wave height during a tropical storm event and subsequent nor'easter. In forecast mode, the model can predict storm surge and wave heights based on encroaching tropical storms or other significant wind systems.

Seasonal analysis indicated that the wind and wave climate during the autumn and winter was geared more towards beach erosion, while the summer wind and wave climate worked towards beach accretion. The summer accretion tends to coincide with the MCBCL's most active training period for Onslow Beach. Inter-annual variability in water levels, waves, and currents indicate the necessity for continuous monitoring to determine beach morphologic response to changing conditions.

Keywords: ADCIRC, SWAN, hydrodynamic modeling, hydrodynamics, Onslow Beach, seasonal and inter-annual variability, wave modeling

Objectives of the Monitoring Activity

Monitoring the Onslow Bay hydrodynamics is a significant part of the overall objective of the Coastal Barrier Module's monitoring program to ensure sustainability of MCBCL activities into the future and to improve management capacity for MCBCL's coastal barrier system. The coastal barrier ecosystem is strongly influenced by meteorologically driven physical forcing, which has important short time scales of storm events (e.g., hurricane and nor'easters), seasonal signals of changing wind fields, and multi-annual time scales as sea level and frequency of intense storms both increase. This physical forcing transports sediments, driving changes in bathymetry, sub-aerial topography, shoreline position, and the presence, location, and extent of tidal flats on the inlet and backbarrier shores. Winds also mobilize sands on coastal barriers, and emergent vegetation acts to trap those wind-blown sands and thereby elevate the island land mass and render it more resilient to storm damage, overwash, and erosion of land area. The primary goal of the hydrodynamic monitoring was to collect a long in situ data set of water velocity, atmospheric information, and water hydrography to analyze for temporal and spatial trends that would aid the Coastal Barrier Module's morphology research projects.

Oceanographic Data

Oceanographic data are archived and currently collected as part of the Coastal Ocean Research Monitoring Program (CORMP). These data consist of water velocity, atmospheric information, and water hydrography on the continental shelf seaward of the New River Inlet. Analysis of

archived data was required to understand the basic physical characteristics of flow in this region, such as dominant tidal species and contribution of atmospheric forcing to variability in the flow field, and to calibrate hydrodynamic models. The currently available data was analyzed to support the overarching goal of understanding the physical processes as they relate to barrier island sustainability.

Acoustic Wave and Current Data

The collection of water velocity data concurrently with coastal barrier island sampling is crucial for understanding the processes behind the changes in coastal barrier island morphology. These data explain specifically what the conditions were during and between sampling intervals. Analyzing these data provide information about the basic physical characteristics of flow in the MCBCL region. These data were also used to verify the ADCIRC and SWAN hydrodynamic models of the region, which are based on data from the offshore buoys. Although the AWAC instrument was only deployed during the Defense Coastal/Estuarine Research Program, the offshore buoy monitoring stations will persist indefinitely. Consequently, our goal was to enhance the capability of using the offshore information on wave climate to predict hydrodynamic conditions at Onslow Beach.

Background

Onslow Beach, NC, is a 12-km long barrier island that covers an area of approximately 5 km^2 and sits halfway between Cape Lookout and Cape Fear on the coast of North Carolina (**Figure 8-1**). Onslow Beach is bordered by the New River Inlet to the southwest and Browns Inlet to the northeast. Prior to 1932, Onslow Beach was connected to the mainland by a marshy habitat containing narrow, sinuous channels. After 1932, its connection with the mainland was altered by the construction of the Intracoastal Waterway (ICW; Cleary and Riggs, 1999), which separated the island from the mainland by a 60-m channel.

Onslow Beach and the surrounding lands were purchased by the Department of the Navy in 1941 for use as an East Coast amphibious training facility and are now part of the Marine Corps Base Camp Lejeune (MCBCL). Although the barrier island and its shorelines are impacted by military training activities, the island is largely undeveloped and the military activities that do occur are regulated and documented in comparison to other anthropogenic impacts, such as shoreline stabilization techniques and renourishment projects on more developed neighboring barrier islands that would alter the natural state of the barrier island.

The northeastern segment of Onslow Beach is characterized by cuspate shoreline geometry with wide beaches, a recurved accretionary beach ridge, a nearly continuous high dune ridge, and shoreline accretion rates that average 2 m y^{-1} (Cleary and Hosier, 1987). In contrast, the southeastern segment is characterized by a narrow shoreface with abundant rock gravel on the beach, a single discontinuous scarped foredune ridge, presence of major washover terraces, and current erosion rates up to 6 m y^{-1} (Cleary, 1996).

A short data collection and numerical study was conducted in the region as part of the U.S. Navy and Marine Corps' Joint Task Force Exercise 97-3 in summer 1997. The study collected only 7 days' worth of data, which were used to validate a suite of nested models in the area (Allard et al., 2000). This DCERP monitoring activity increases the temporal resolution of data collected in this region and calibrates and validates a coupled hydrodynamic (Advanced Circulation

[ADCIRC]) and waves (Simulating Waves Nearshore [SWAN]) model, that was used to hindcast wave and current conditions during events and also to forecast wave and current conditions as storms approach.

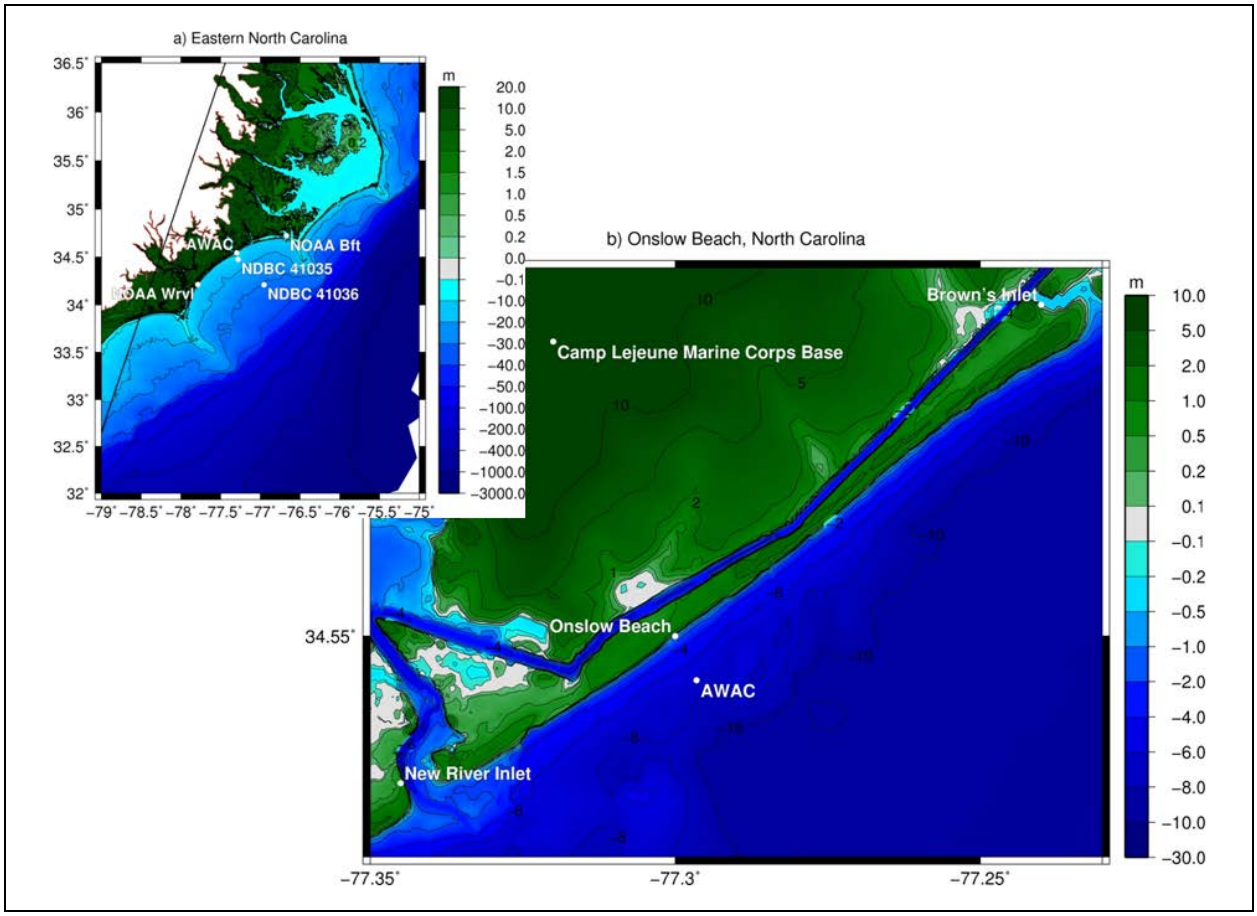

Figure 8-1. (A) The eastern coast of North Carolina with data locations marked; (B) a close-up image of the Onslow Beach study site and Acoustic Wave and Current (AWAC) location.

Materials and Methods

Monitoring Data

A 1-MHz Nortek Acoustic Wave and Current (AWAC) Profiler was deployed at 34°32'38.40" N, 77°17'47.40" W (**Figures 8-1 and 8-2**) in approximately 8 m of water and 500 m offshore from March 18, 2008, and presents a nearly continuous three year record at this location. The AWAC was programmed to collect water velocity in 0.5-m vertical bins throughout the water column every 6 minutes. The instrument was programmed in stand-alone mode with an external battery canister that supplied power with the raw data recorded internally. The AWAC measures wave height and period using the Nortek acoustic surface tracking (AST) feature, where a short acoustic pulse is transmitted vertically toward the water surface, and the time lag between the transmitted ping and its reflections is used to generate a time series of the surface elevation. Wave direction was calculated by combining AST with orbital velocity measurements in an

array near the surface. Upon retrieval, the raw data was downloaded to a PC, and then run through the Nortek QuickWave software for data quality checking and to calculate wave spectra using the maximum likelihood method. Because of the AST method of measurement, significant wave height (Hs) and mean wave period are calculated directly from the time series data. Peak and mean wave direction and period are derived from spectral analysis computed with the QuickWave software. Wave estimates for significant wave height have an accuracy of less than 1% of the measured value and a resolution of 1 cm. Wave estimates for direction have an accuracy of 2 degrees with a resolution of 0.1 degree.

Hourly wave records from within Onslow Bay are available from National Oceanic and Atmospheric Association's (NOAA's) National Data Buoy Center (NDBC). In particular, we downloaded and analyzed data from Buoys 41035 (34° 28' 34"N, 77° 16' 47"W; **Figures 8-1 and 8-2**) and 41036 (34° 12' 22"N, 76° 57' 6"W; **Figures 8-1 and 8-2**). NDBC Buoy 41035 is a 3-m discus buoy that has recorded wave properties, sea temperature, and meteorological conditions in half-hour increments since 2005. This buoy is located in 9.7 m of water and is approximately 8 km offshore. The quality checked data can be downloaded from http://www.ndbc.noaa.gov and used in analyzing software. NDBC Buoy 41036 is also a 3-m discus buoy that has recorded hourly wave properties and meteorological conditions since 2006. This buoy is located in 30 m of water approximately 25 km offshore. For both records, there are significant gaps in the data. In particular, NDBC Buoy 41035 was offline from October 2009 until April 2010, and then collected data from that point on until August 2011, when it was discontinued from service. NDBC Buoy 41036 was offline for almost all of 2010, came back online on November 29, 2010, and continues to collect data. We analyzed water level, significant wave height, and mean and peak wave period and direction.

Water level, barometric pressure, air and water temperature, and wind direction and speed were downloaded from the Wrightsville Beach, NC, NOAA tide gauge (34°12.8'N, 77°47.2W, Station 8658163; **Figure 8-1**) located on the offshore side of a pier and the Beaufort, NC, NOAA tide gauge (34°43.2' N, 76°40.2'W, Station 8656483; **Figure 8-1**) located at the Duke Marine Laboratory Dock inside the inlet. The Wrightsville Beach station was established in April 2004, and quality assured hourly data were downloaded directly from NOAA's Web site at http://tidesandcurrents.noaa.gov. The Beaufort tide gauge has been in its present installation since June 1990. All water level measurements have an estimated accuracy of ±0.02 m and a resolution of 0.001 m.

All data were downloaded and then converted for import into MATLAB. T-Tide is the tide-disseminating software package used to determine the important tidal frequencies from the time series current data (Pawlowicz et al., 2002). From there, standard time-series analysis tools employing power spectral analysis were used to partition the variance in the data according to frequencies with an emphasis on the low-frequency variability generally associated with atmospheric forcing. Seasonal time periods were designed and some of the data analyzed to determine seasonal trends and the likelihood of months filled with possible storm events. Additionally, the data are being used to validate hydrodynamic and wave models of the region.

(A)

(B)

Figure 8-2. (A) The trawl resistant Nortek AWAC frame and AWAC; (B) the NOAA NDBC wave buoys.

Modeling Data

Sea surface elevation and depth-averaged coastal currents are modeled using the fully non-linear, two-dimensional, barotropic hydrodynamic model ADCIRC-2DDI. ADCIRC, developed by Luettich et al. (1992) and Westerink et al. (1994), has a successful history of tidal and storm surge prediction in coastal waters and marginal seas (Bunya et al., 2010; Dietrich et al., 2010; Westerink et al., 2008). Water levels are obtained through solution of the Generalized Wave Continuity Equation as follows:

$$\frac{\partial^2 \zeta}{\partial t^2} + \tau_0 \frac{\partial \zeta}{\partial t} + \frac{\partial \widetilde{J_x}}{\partial x} + \frac{\partial \widetilde{J_y}}{\partial y} - UH \frac{\partial \tau_0}{\partial x} - VH \frac{\partial \tau_0}{\partial y} = 0$$

where

$$\tilde{J}_x = -Q_x \frac{\partial U}{\partial x} - Q_y \frac{\partial U}{\partial y} + f Q_y - \frac{g}{2}\frac{\partial \zeta^2}{\partial x} - gH \frac{\partial}{\partial x}\left[\frac{P_s}{g\rho_0} - \alpha\eta\right] + \frac{\tau_{sx,wind} + \tau_{sx,waves} - \tau_{bx}}{\rho_0} + (M_x - D_x) + U\frac{\partial \zeta}{\partial t} + \tau_0 Q_x - gH\frac{\partial \zeta}{\partial x}$$

$$\tilde{J}_y = -Q_x \frac{\partial V}{\partial x} - Q_y \frac{\partial V}{\partial y} + f Q_x - \frac{g}{2}\frac{\partial \zeta^2}{\partial y} - gH \frac{\partial}{\partial y}\left[\frac{P_s}{g\rho_0} - \alpha\eta\right] + \frac{\tau_{sy,wind} + \tau_{sy,waves} - \tau_{by}}{\rho_0} + \left(M_y - D_y\right) + V\frac{\partial \zeta}{\partial t} + \tau_0 Q_y - gH\frac{\partial \zeta}{\partial y}$$

The currents are obtained from the following the vertically integrated momentum equations:

$$\frac{\partial U}{\partial t} + U\frac{\partial U}{\partial x} + V\frac{\partial U}{\partial y} - fV = -g\frac{\partial}{\partial x}\left[\zeta + \frac{P_s}{g\rho_0} - \alpha\eta\right] + \frac{\tau_{sx,wind} + \tau_{sx,waves} - \tau_{bx}}{\rho_0} + \frac{M_x - D_x}{H}$$

$$\frac{\partial V}{\partial t} + U\frac{\partial V}{\partial x} + V\frac{\partial V}{\partial y} + fU = -g\frac{\partial}{\partial y}\left[\zeta + \frac{P_s}{g\rho_0} - \alpha\eta\right] + \frac{\tau_{sy,wind} + \tau_{sy,waves} - \tau_{by}}{\rho_0} + \frac{M_y - D_y}{H}$$

where $H=\zeta+h$ is the total water depth; ζ is the deviation of the water surface from the mean; h is the bathymetric depth; U and V are depth integrated currents in the x- and y- directions, respectively; $Q_x = UH$ and $Q_y = VH$ are fluxes per unit width in the x- and y- directions, respectively; f is the Coriolis parameter; g is the gravitational acceleration; P_s is the atmospheric pressure at the surface; ρ_0 is the reference density of water; η is the Newtonian equilibrium tidal potential and α is the effective earth elasticity factor; $\tau_{s,wind}$ and $\tau_{s,waves}$ are surface stresses due to winds and waves, respectively; τ_{bx} is the bottom stress; M represents lateral stress gradients; D represents momentum dispersion terms; and τ_0 is a numerical parameter that optimizes the phase propagation properties (Atkinson et al., 2004; Kolar et al., 1994). ADCIRC computes water levels ζ and currents U and V on an unstructured, triangular mesh by applying a linear Lagrange interpolation and solving for 3degrees of freedom at every mesh vertex.

ADCIRC has recently been coupled to the unstructured mesh version of the two dimensional multi-spectral SWAN Model (Booij et al., 1999; Dietrich et al., 2012). The SWAN Model is based on the wave action balance equation and can simulate wave refraction, shoaling, blocking, and reflection due to bathymetry, sea surface elevations, and currents. SWAN also has the capability of using sea surface elevations and currents as input for the calculation of the wave field. It should be noted that the SWAN Model cannot simulate wave diffraction and, therefore, results in regions where diffraction is significant (e.g., an obstacle) will not be accurate. This model has been widely used in the coastal engineering and science community (e.g., Chen et al., 2005; Gorman and Nielson, 1999; Lin et al., 2002).

SWAN predicts the evolution in geographical space ($\vec{x}$) and time (t) of the wave action density spectrum ($N[\vec{x}, t, \sigma, \theta]$), with the relative frequency (σ)the relative frequency and the relative direction (θ),as governed by the action balance equation as follows (Booij et al., 1999):

$$\frac{\partial N}{\partial t} + \nabla_x \cdot \left[\left(\vec{c}_g + \vec{U}\right) N\right] + \frac{\partial c_\theta N}{\partial \theta} + \frac{\partial c_\sigma N}{\partial \sigma} = \frac{S_{tot}}{\sigma}$$

The terms on the left side represent, respectively, the change of wave action in time, the propagation of wave action in $\vec{x}$ space (with $\nabla\vec{x}$ the gradient operator in geographic space, $\vec{c}_g$ the wave group velocity, and $\vec{U}$ the ambient current vector), depth- and current- induced refraction and approximate diffraction (with propagation velocity or turning rate c_θ), and the shifting of σdue to variations in mean current and depth (with propagation velocity or shifting rate c_σ). The source term, S_{tot}, represents wave growth by wind; action lost due to whitecapping, surf breaking, and bottom friction; and action exchanged between spectral components in deep and shallow water due to nonlinear effects. The associated SWAN parameterizations are given by Booij et al. (1999), with all subsequent modifications as present in version 40.72, including the phase-decoupled refraction-diffraction (Holthuijesen et al., 2003), although diffraction is not enabled in the present simulations.

The unstructured-mesh version of SWAN implements an analog to the four-direction Gauss-Seidel iteration technique employed in the structured version, and it maintains SWAN's unconditional stability (Zijlema, 2010). SWAN computes the wave action density spectrum $N(\vec{x}, t, \sigma, \theta)$ at the vertices of an unstructured triangular mesh, and it orders the mesh vertices so it can sweep through them and update the action density using information from neighboring vertices. It then sweeps through the mesh in opposite directions until the wave energy has propagated sufficiently through geographical space in all directions. It should be noted that, as a spectral model, SWAN does not attempt to represent physical processes at scales less than a wave length even in regions with fine-scale mesh resolution.

SWAN is driven by wind vectors, water levels and currents computed at the vertices by ADCIRC. Marine winds can be input to ADCIRC in a variety of formats, and these winds are adjusted directionally to account for surface roughness (Bunya et al., 2010). ADCIRC interpolates spatially and temporally to project these winds to the computational vertices, and then it passes them to SWAN. The water levels and ambient currents are computed in ADCIRC before being passed to SWAN where they are used to calculate all related wave processes (e.g., wave propagation, depth-induced breaking; Dietrich et al., 2011a).

ADCIRC and SWAN run in series on the same local mesh. The two models "leap frog" through time, each being forced with information from the other model. At the beginning of a coupling interval, ADCIRC can access the radiation stress gradients computed by SWAN at times corresponding to the beginning and end of the previous interval. ADCIRC uses that information to extrapolate the gradients at all of its time steps in the current interval. These extrapolated gradients are used to force the ADCIRC solution. Once the ADCIRC stage is finished, SWAN is run for one time step, to bring it to the same moment in time as ADCIRC. SWAN can access the wind speeds, water levels and currents computed at the mesh vertices by ADCIRC, at times corresponding to the beginning and end of the current interval. SWAN applies the mean of those values to force its solution on its time step. At the end of each of its time steps, SWAN computes the wave radiation stresses and their gradients and then passes those gradients as a forcing function to ADCIRC (see Dietrich et al., 2011b). Bathymetry data collected at the start of this project within the New River and along Onslow Beach was incorporated into the finite element grid of the area and refined for the modeling work (**Figure 8-3**). For this work, ADCIRC was run for 600 s with a Δt of 1 s and SWAN is run for 600 s with a Δt of 600 s.

For our work, a tidal spin-up was completed from July 20 through August 20, 2008 in order to ramp to a dynamic equilibrium prior to the start of wind and wave forcing. Thereafter, marine

winds from the National Centers for Environmental Prediction's North American Mesoscale (NAM) Model also called the Weather Research and Forecasting (WRF) Model (Skamarock et al., 2005) were incorporated into the model run. These model winds are a NOAA product that provides wind forecast fields up to 84 hours in the future that are data assimilated with offshore buoy data such as the NOAA NDBC buoys and are spaced at 12 km geographically and 3 hours temporally. The NAM winds are on a lambert conformal projection and are transformed and interpolated onto a regular latitude and longitude grid with one-eighth degree resolution outside of ADCIRC, and then read into ADCIRC and interpolated onto the irregular domain using standard techniques. A coupled ADCIRC and SWAN model run from August 28 through September 24, 2008 was completed. Model output was stored at half-hour intervals for subsequent analyses.

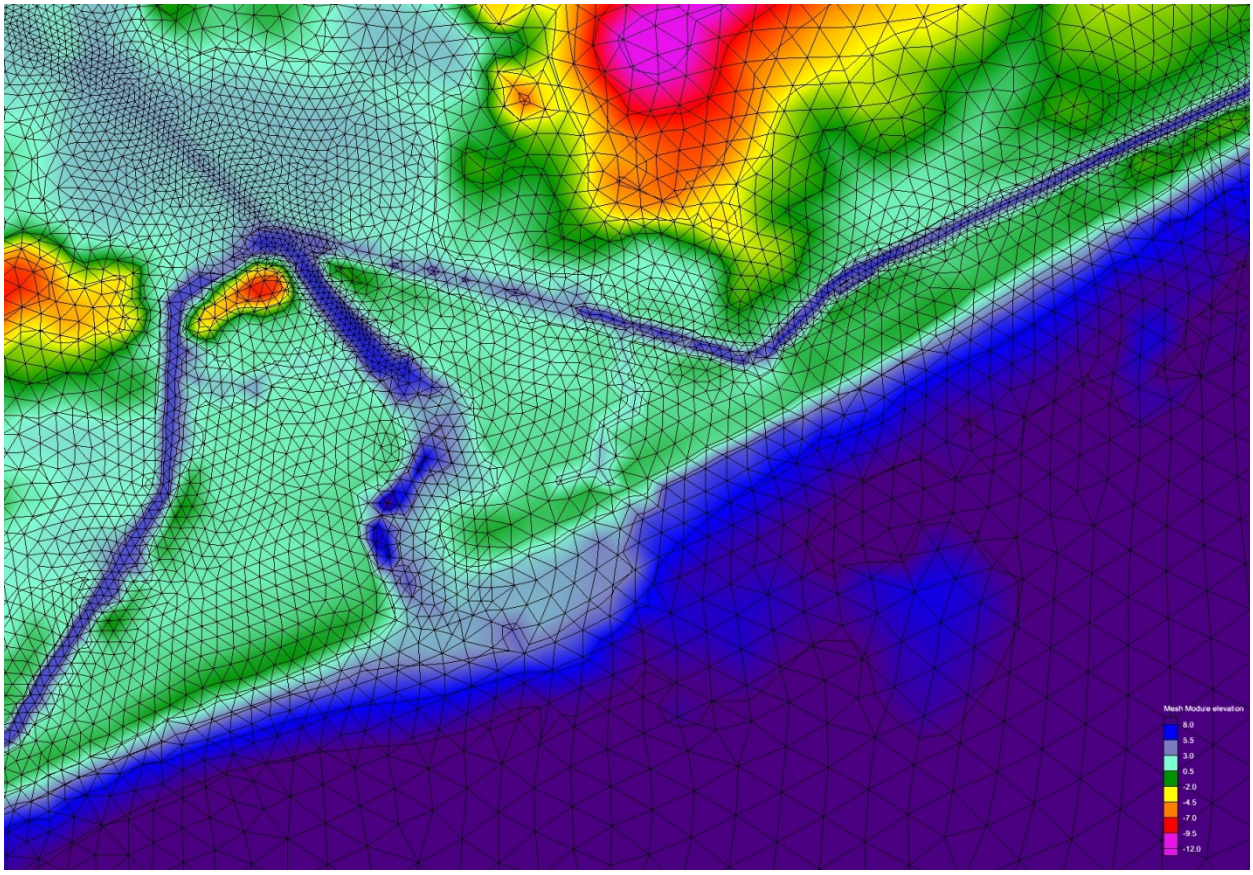

Figure 8-3. ADCIRC + SWAN unstructured finite element grid with high-resolution bathymetry and grid refinement.

Results and Discussion

Seasonal Trends—Winds and Waves

Data from the NDBC Buoys 41035 and 41036 showed similar trends; however, wind speeds and wave heights were generally stronger at the offshore buoy (i.e., 41036). Winds were typically from the northeast, northwest, and southwest during the winter (**Figure 8-4*),*** and waves were typically from the southeast (**Figure 8-5**) with significant wave height peaks ranging from 3.5 to 4 m. Winds turned bi-directional during the spring with the dominant directions of northeast and southwest (**Figure 8-4**). Waves are distributed from the southwest to the east-northeast with significant wave height peaks ranging from 5.5 to 6 m offshore (**Figure 8-5**). Southwest winds dominated the summer season with a large spread in wave directions from the east-northeast, southeast, and southwest (**Figure 8-4**) and significant wave height peaks ranging from 4 to 4.5 m (**Figure 8-5**). Northeast winds dominated the autumn season, and waves were primarily from the southeast with peaks ranging from 4 to 4.5 m (**Figures 8-4 and 8-5**). The significant wave height recorded from the AWAC showed similar seasonal frequency in terms of lower wave heights in the summer and higher wave heights in the winter and spring, excluding tropical events.

In summary, during winter, the strong winds and high waves have the effect of causing barrier island erosion. In spring, the barrier island should become redistributed with mid-range winds and mid-range waves. It appears to affect all parts of the island as the dominant wave directions are evenly distributed across the island. In summer, the barrier island should accrete due to the light winds and small waves. During autumn, there is a higher chance of barrier island erosion due to the strong wind and high waves, as well as the higher probability of storm events.

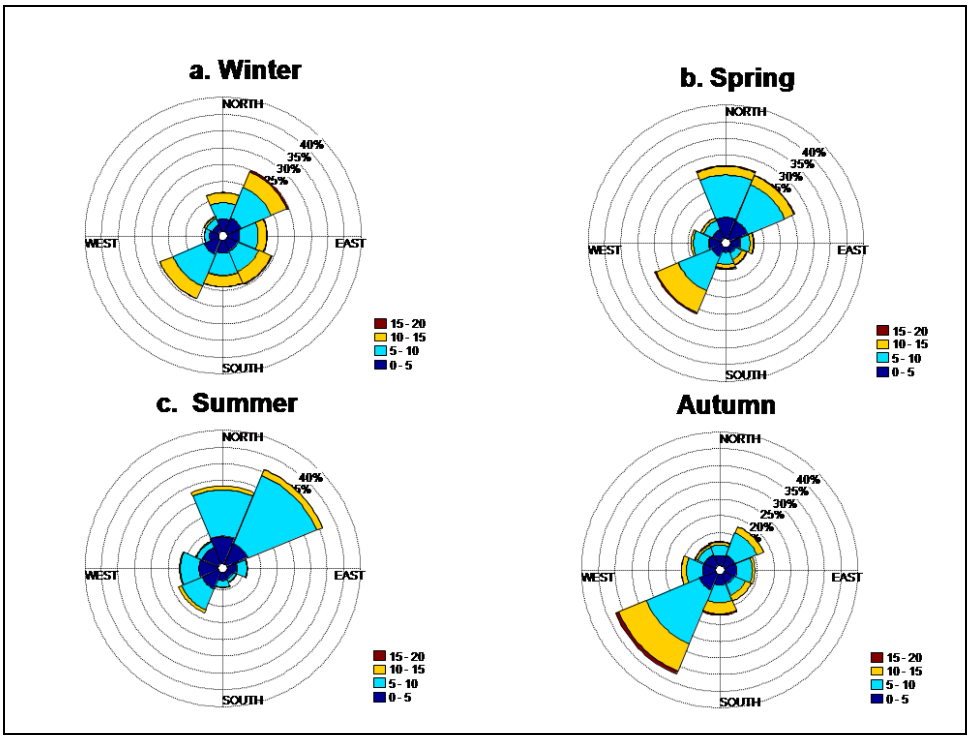

Figure 8-4. Seasonal wind roses (in m s^{-1}) for (A) winter; (B) spring; (C) summer; and (D) autumn from NDBC Buoy 41036.

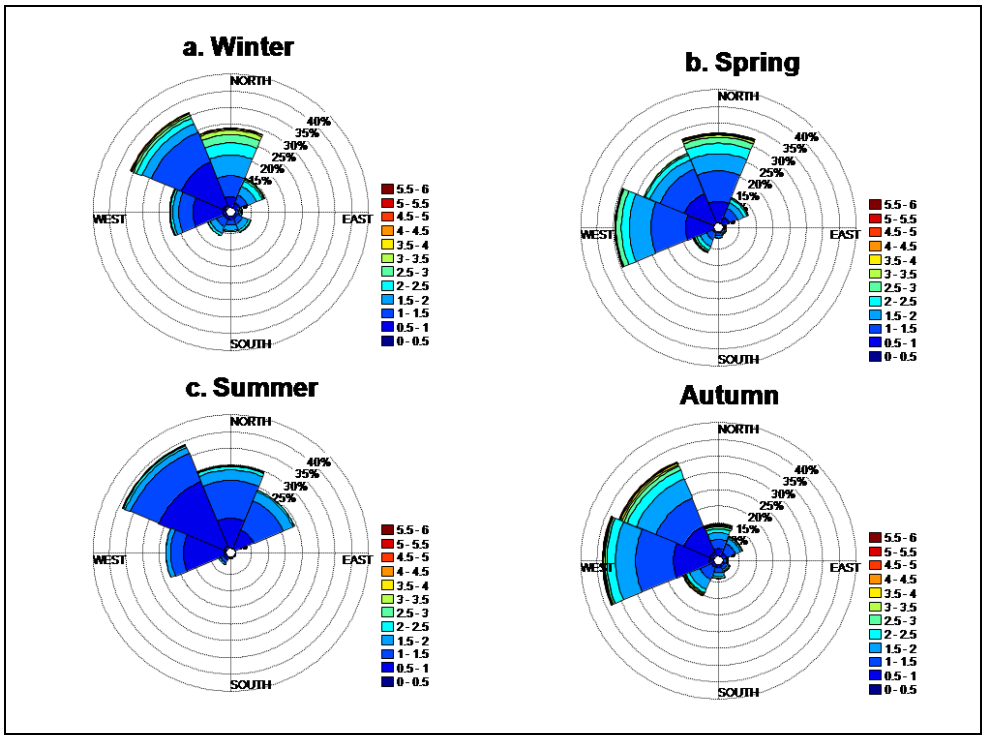

Figure 8-5. Seasonal wave roses (in m) for (A) winter; (B) spring; (C) summer; and (D) autumn from NDBC Buoy 41036.

Annual Trends—Currents, Waves, and Water Levels

The AWAC recorded water velocity throughout the water column at its location approximately 500 m from Onslow Beach. A higher percentage of stronger flow speeds were recorded in 2008 and 2010 than in 2009. As may be expected, there is a strong bilateral component to the flow that follows the along shore orientation of Onslow Beach (**Figure 8-6**). There is also an onshore presence to the flow. On an annual basis, approximately 30–40% of the total flow is towards Browns Inlet 20% towards NRE Inlet, and 10% offshore, leaving the other 30–40% onshore.

As may also be expected by the seasonal analysis, higher significant waves heights were recorded annually during the late summer/early fall when tropical storms are more likely to occur. Additionally, higher significant waves heights are recorded annually in the late fall/winter. The mean significant wave height varied yearly by as little as 0.05 m; however, the percentage of significant wave heights that exceeding the mean and 2 standard deviations varied by almost 2% (**Figure 8-7**).

Water levels, based on the AWAC location, also indicated annual variation (**Figure 8-8**). Water levels were significantly lower during 2008 than during 2009 and 2010 during the summer. The difference between years is approximately 20 cm. Annually, detided and demeaned water levels increase to a maximum during the late summer/early fall. Part of this may be due to the steric response of the oceans to thermal heating or a combination of this in conjunction with wind directional changes.

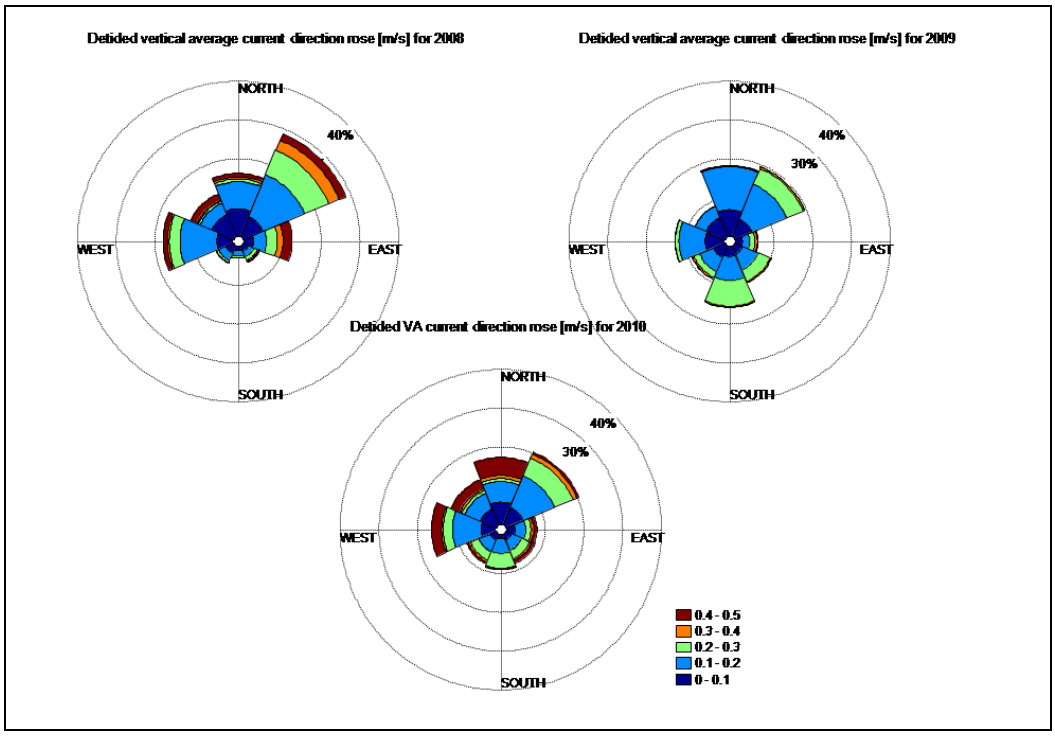

Figure 8-6. Detided vertically averaged current roses (in m s^{-1}) from the AWAC location.

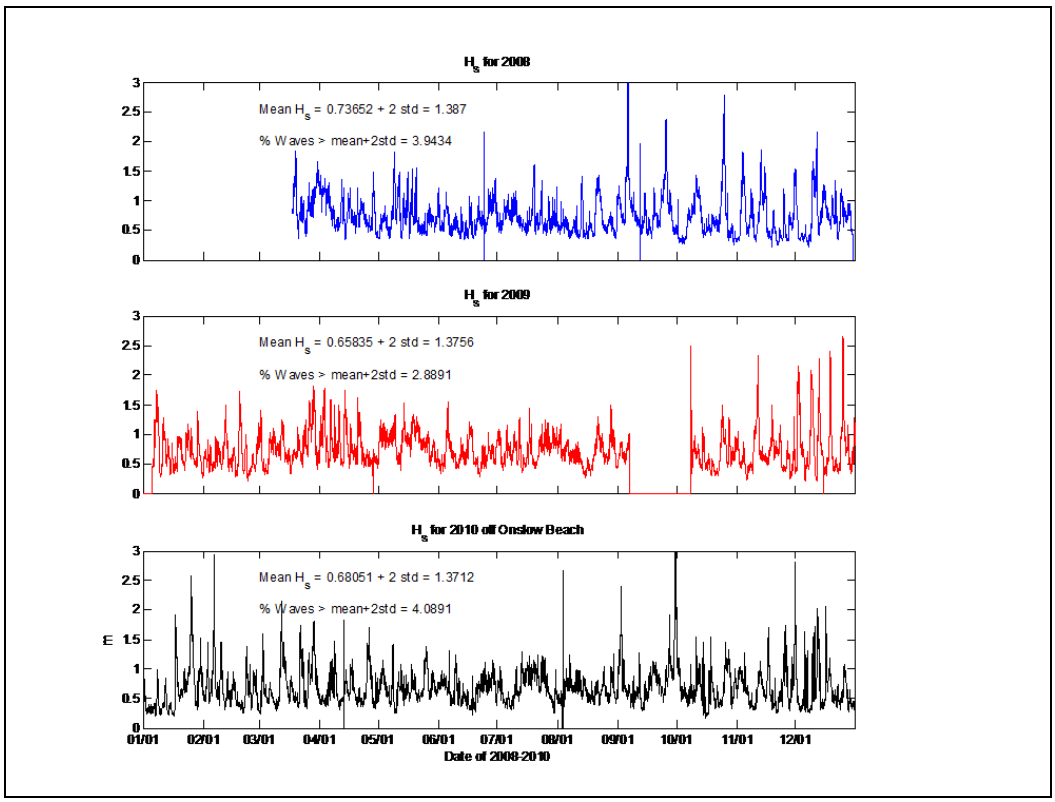

Figure 8-7. Annual time series of significant wave height at the AWAC location.

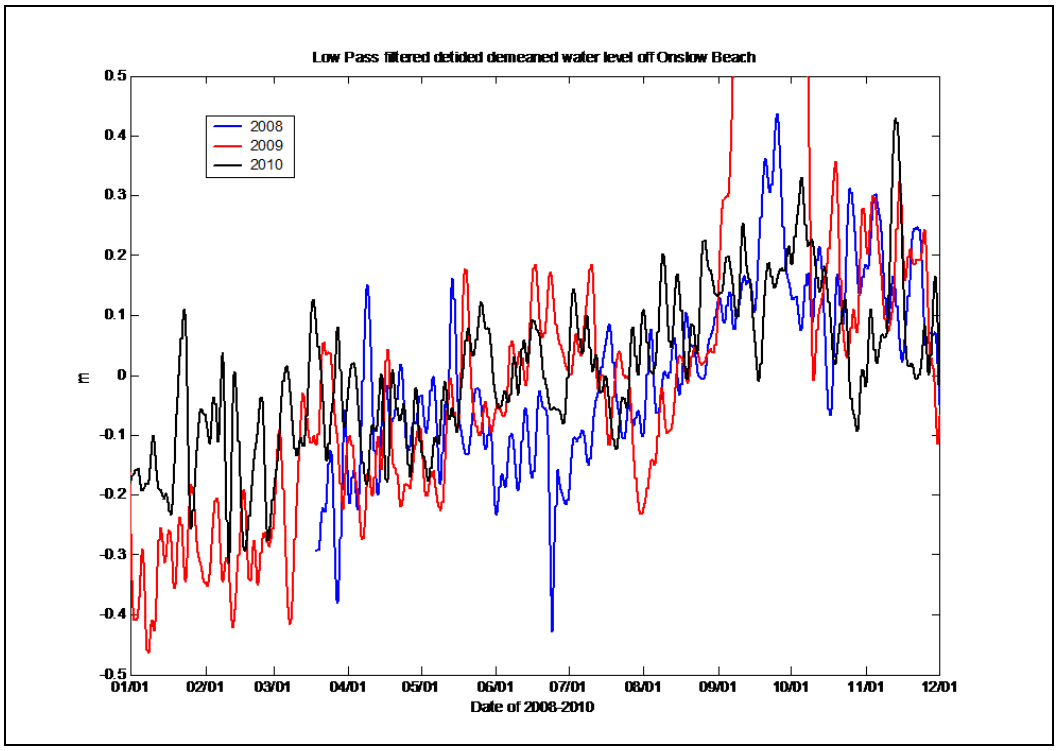

Figure 8-8. Annual time series water level at the AWAC location.

Extreme Event Trends—2008 Case Study

As described in the previous section, the ADCIRC+SWAN Model was run for a 2-month period in 2008, which covers the arrival of Tropical Storm Hanna and subsequent nor'easter. As with the NDBC buoy data, we also compared the model output to the collected AWAC data for model validation.

The ADCIRC+SWAN Model was run with tidal and atmospheric forcing as described in the previous section and ADCIRC output water levels every half hour for the period. Comparison of model water levels to recorded water levels compared favorably at the AWAC location (**Figure 8-9**) and indicated the expected semi-diurnal tidal signature over a spring/neap cycle with overall increases in water level at the end of the period due to the nor'easter. The model does a good job of capturing most of the storm surge due to storm events when the detided/demeaned water levels are compared (**Figure 8-10**). Comparisons between model output and NOAA water level gauges at Beaufort (**Figure 8-11** and **8-12**) and Wrightsville Beach (**Figure 8-13** and **8-14**) also compared favorably. Significant wave heights as computed from the SWAN portion of the model also compared remarkably well (**Figure 8-15**) leading the investigators to believe the ADCIRC+SWAN Model does a good job of estimating water levels and significant wave heights in the Onslow Beach region.

The model captured essential peaks in significant wave heights and water level in the Onslow Beach Region, and therefore the alongshore distribution of modeled significant wave heights, water level, and wave period was used to calculate the mean runup and the extreme runup, defined by the 2% exceedence value (Stockdon et al., 2006), during the Tropical Storm Hanna and nor'easter time frames. The mean runup and extreme runup (thick lines) for each period

where water levels were highest during Tropical Storm Hanna and the nor'easter was visualized and compared. A comparison of the extreme runup and the average dune heights (**Figure 8-16**) indicate that overwash was likely on the southwestern end of Onslow Beach where average dune crest heights are lower and not as likely on the northeastern end of Onslow Beach where average dune crest heights are higher. Extreme runup was also higher during the nor'easter than during Tropical Storm Hanna; however, mean runups were comparable between time periods. Compared with the dune heights, it seems plausible that the extreme runup during the peak of the nor'easter could have overwashed the beach approximately 4 km north of the New River Inlet.

The coupled ADCIRC+SWAN Models did a good job of simulating water level and wave characteristics and compare well with similar studies of the same area (Allard et al., 2000). Modeled ADCIRC water levels were strongly correlated with observation data with small RMS values and captured tides and storm surge events well. Modeled SWAN significant wave heights appeared to be underpredicted, but captured the peak events. This may be due the wind input to the model. As stated in the methods section, we used NAM Model winds, which are generally refined with NDBC buoy data, to drive the meteorology of the coupled models. These winds do a fine job for general meteorology, but are known to underpredict winds during strong events such as hurricanes (Forbes et al., 2010). As of now, it is not well known how the NAM Model winds compare with actual winds for a lesser storm like Tropical Storm Hanna. The winds, therefore, may not be strong enough to generate the right magnitude for significant wave heights.

The coupled ADCIRC+SWAN Model also showed interesting alongshore variability in combined water level along Onslow Beach. An average difference of 20 cm was modeled between the Tropical Storm Hanna peaks and the nor'easter peaks with a trend towards higher water levels on the southern portion of the island. Along the barrier island, there were peaks of 30 cm and minimums of 10 cm between the two time periods. Dune crest heights also increase dramatically from 2 m near New River Inlet to 8 m near Browns Inlet. Obviously, locations with higher dune heights will be less susceptible to the type of excess wave runup that we recorded here. Interestingly, when the combined water level is broken into its component parts, a nice picture develops of the controlling factors that differed between these two events. For Tropical Storm Hanna, wave heights are about twice as high as water levels, at least at the peak of the storm whereas during the nor'easter, wave heights were about one and a half times as high as water levels, but water levels were about 50 cm higher during the nor'easter than during Tropical Storm Hanna. Variability in the alongshore distribution of wave heights may be due to the fairly fixed offshore bathymetry (limestone ridges offshore, Dr. Jesse McNinch, personal communication) and the direction of the waves approaching the shore.

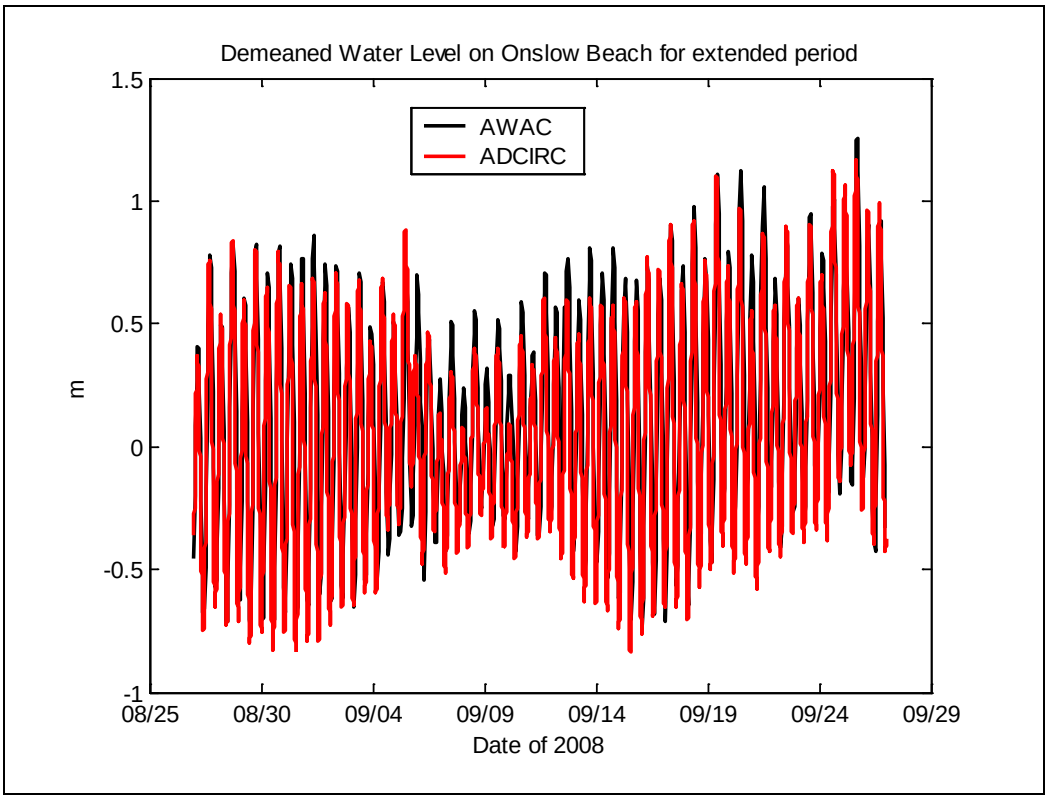

Figure 8-9. Model versus data comparison of water level at Onslow Beach.

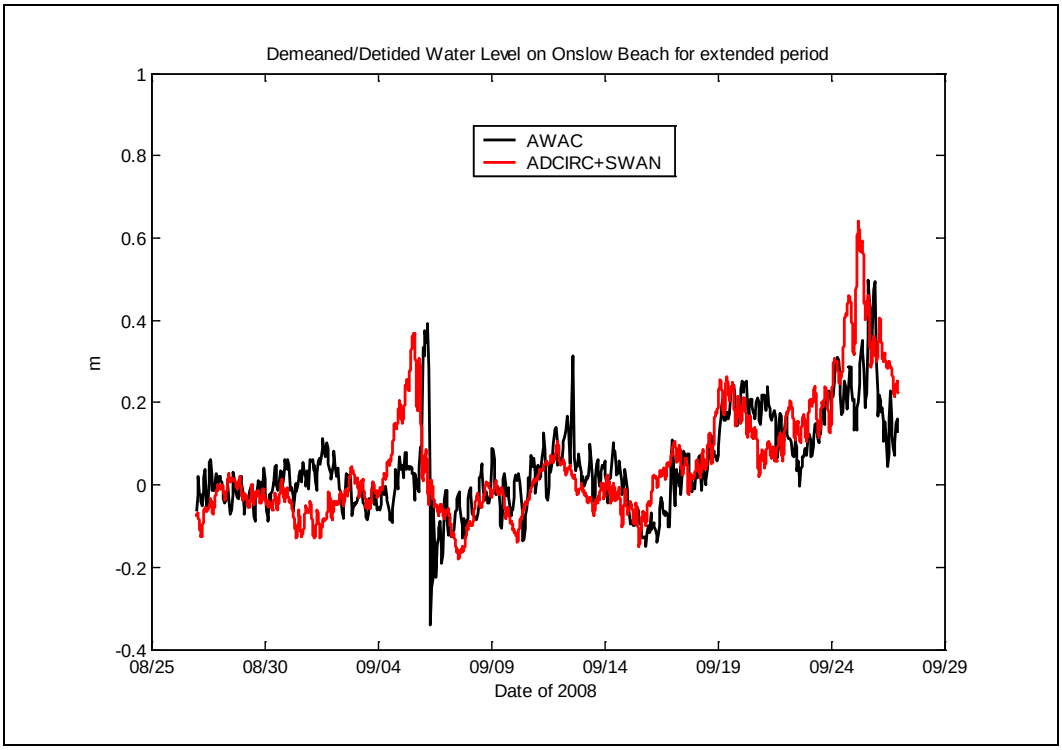

Figure 8-10. Demeaned/detided water level at the AWAC location.

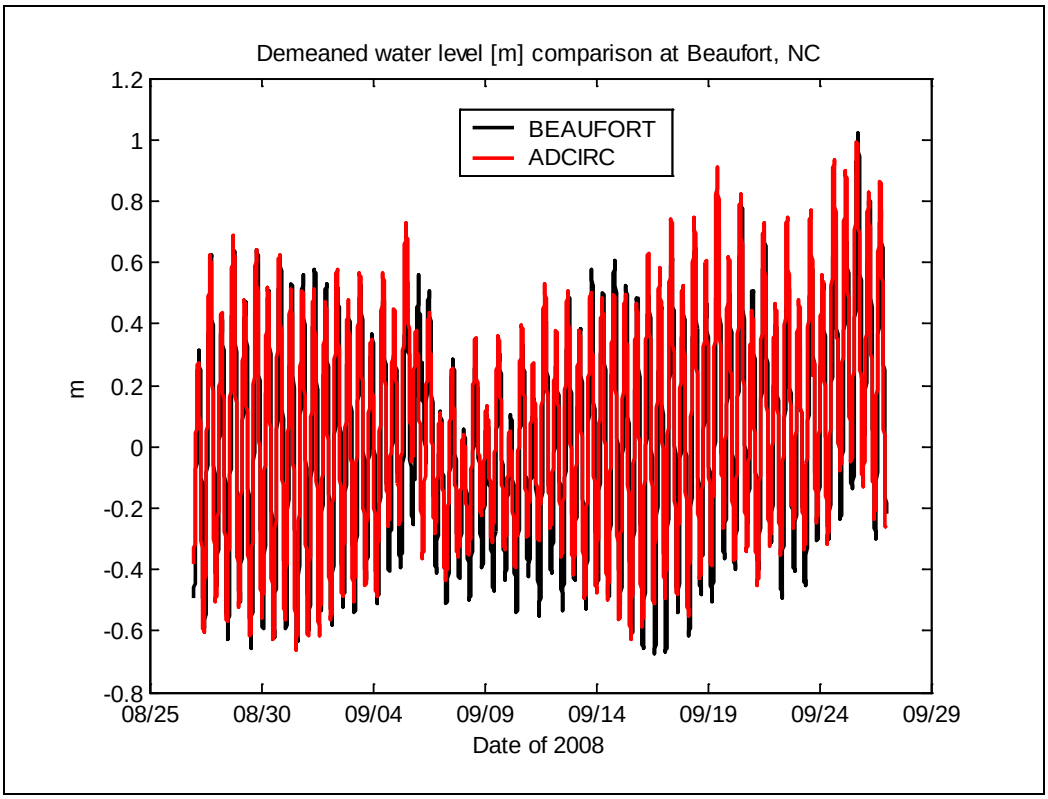

Figure 8-11. Model versus data comparisons of water level at the NOAA Beaufort station.

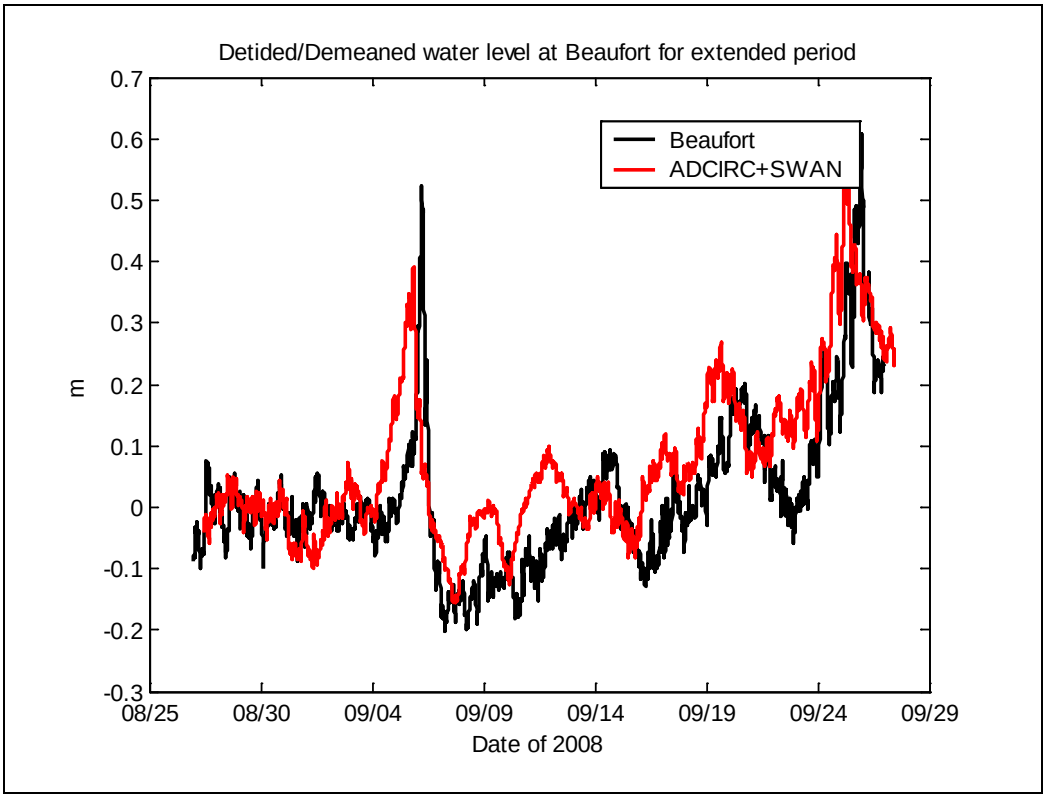

Figure 8-12. Demeaned/detided water level at Beaufort.

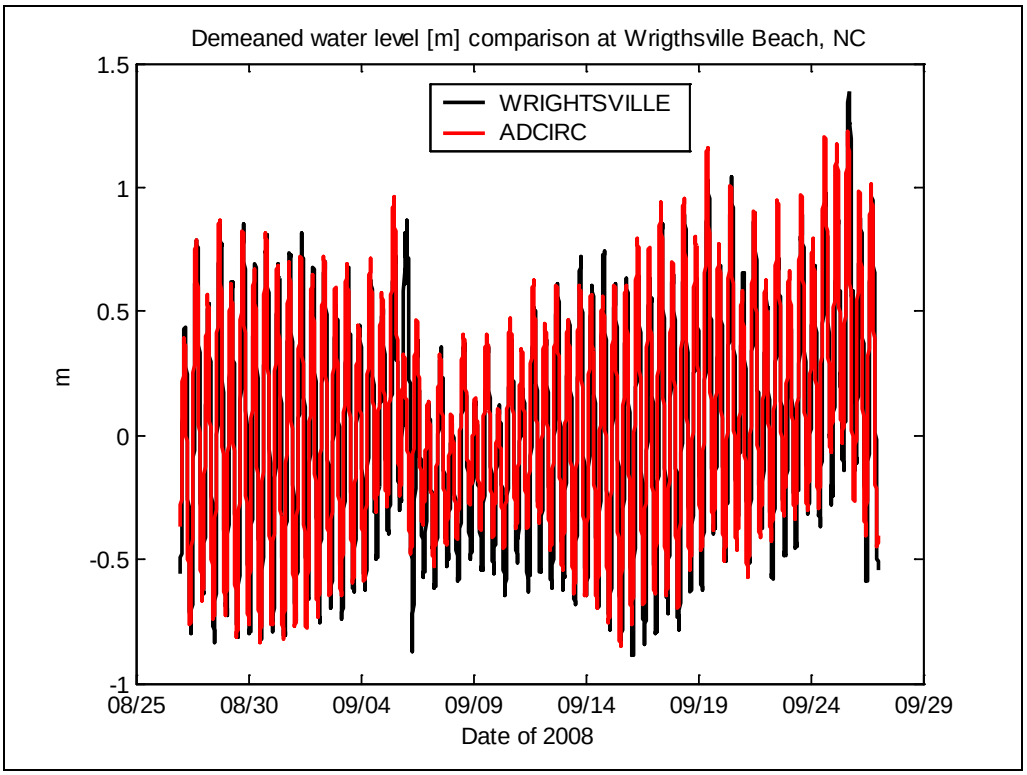

Figure 8-13. Model versus data comparison of water level at the NOAA Wrightsville station.

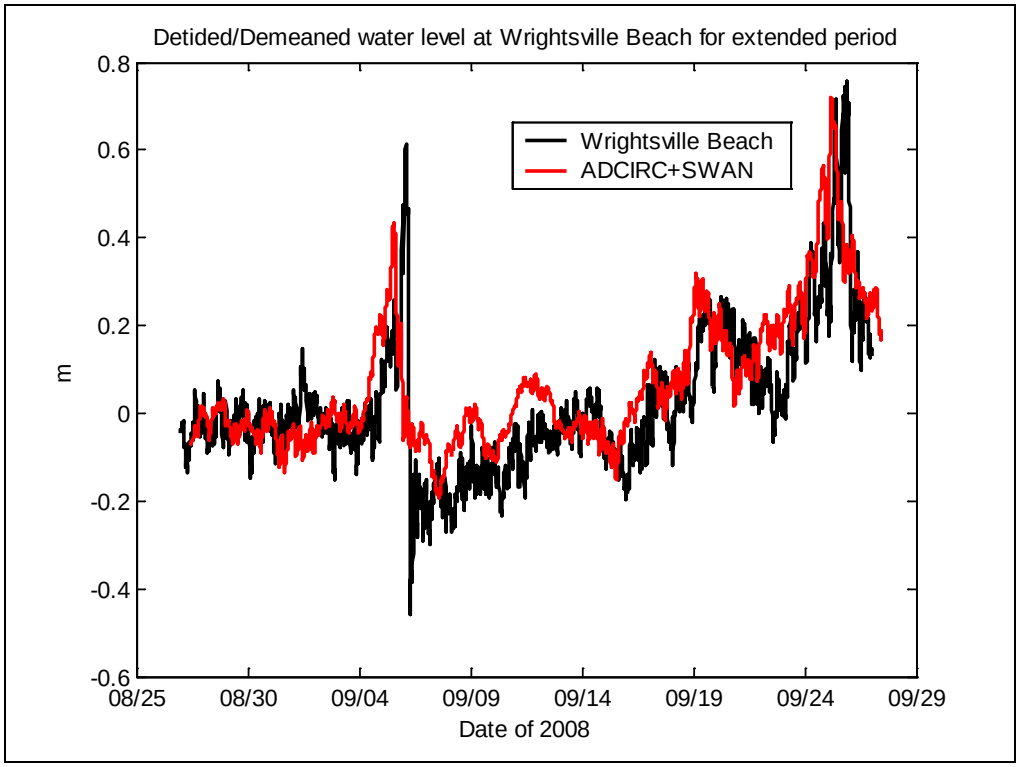

Figure 8-14. Demeaned/detided water level at Wrightsville Beach.

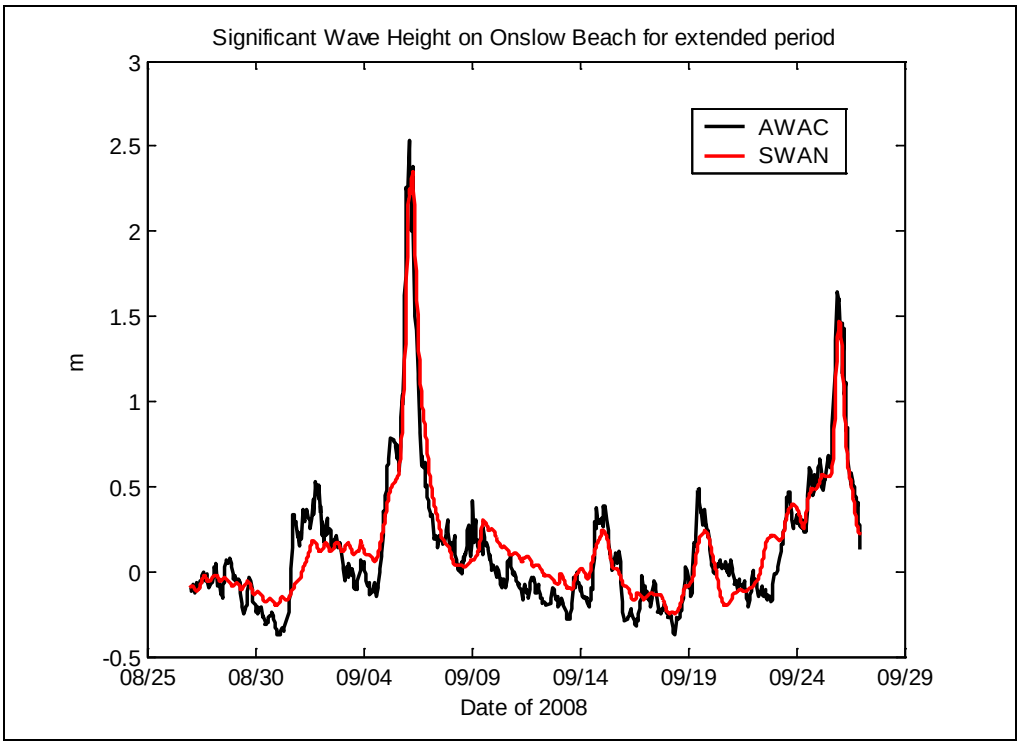

Figure 8-15. Significant wave heights at Onslow Beach: Model versus data comparison.

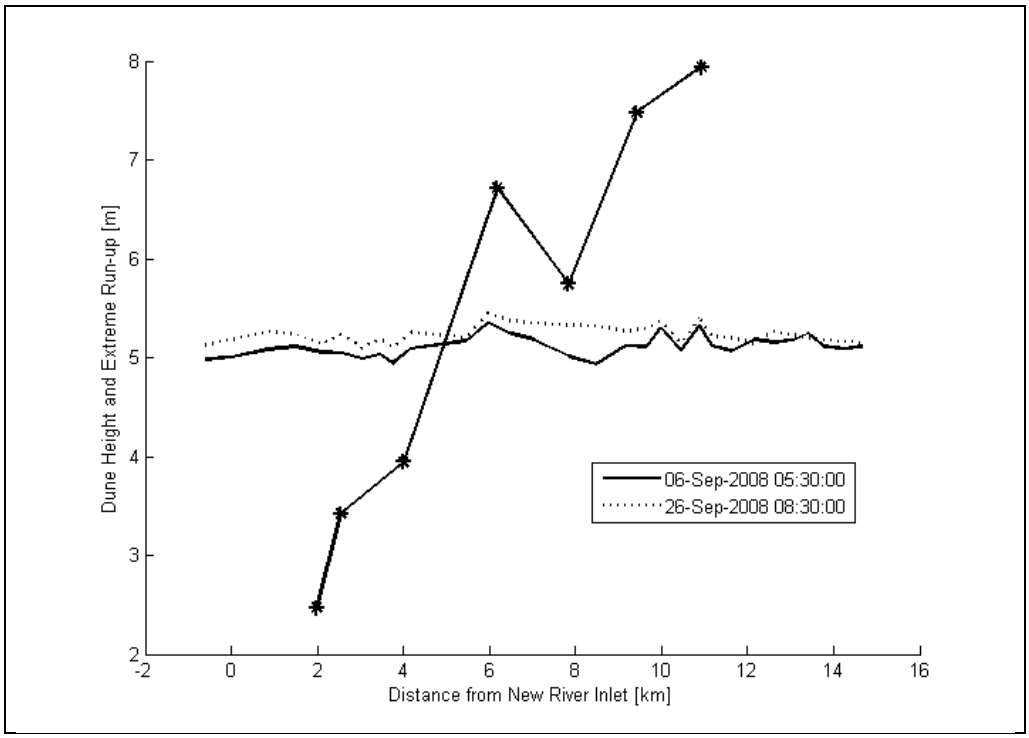

Figure 8-16. Alongshore distribution of extreme runup (thick lines) and mean runup (thinner lines; in m), calculated from model significant wave heights and wave period, from September 6, 2008 (- - - line) and September 26, 2008 (--- line) with alongshore distribution of average dune crest heights (in m) at seven sampling sites (-*-).

Assessment of Trends in the Data

Assessment of Monitoring Design

The monitoring design employed for this project is fairly standard in the physical oceanography community. Both the NDBC buoys are in good locations (5 and 25 miles) within Onslow Bay to give a good indication of the wave and wind field within the Bay. Their distances apart also provide an indication of wave transformation as the waves move from deeper offshore locations closer to the shore. The temporal resolution (30 minutes for NDBC Buoy 41035 and hourly for NDBC Buoy 41036) of the buoys is also excellent.

When all of the NDBC buoys are working, the data collected from these buoys provide excellent coverage, both temporally and spatially, of the wind and wave environments in Onslow Bay. Unfortunately, the NDBC buoys did not function for significant parts of the monitoring period. The data, when available, are an excellent tool for validating the ADCIRC+SWAN Model, which may ultimately be used in forecasting mode to predict the water level, depth averaged water velocities, and significant wave heights and direction at numerous locations along Onslow Beach.

The AWAC data are essential for model validation near the shoreline. As discussed in the previous section, NDBC Buoys 41035 and 41036 are excellent indicators of conditions inside Onslow Bay, proper, but they are fairly far from shore. Further model validation will increase the confidence with which the coupled ADCIRC/SWAN model can be used to predict the temporal and spatial variability in water level, significant wave height, and velocity along Onslow Beach and within the New River Estuary.

Assessment Seasonal and Annual Variability in the Data

The data presented in this report represent one of a few datasets with a semi-continuous time series. From these data, we were able to determine the seasonal and inter-annual differences in wind and wave climatology. We were also able to present rough predictions for periods of events that would be worth sub-sampling.

Recommendations for Future Monitoring

Quality wind, wave, and velocity data near Onslow Beach is essential if one is to understand fully the dynamics associated with barrier island morphology. The data from the wave buoys can be used for modeling purposes, however, we recommend the deployment of wave buoys and AWACs closer to shore.

Conclusions and Implications for Future Research

Key Scientific Findings—Fundamental Cause-and-Effect Relationships

- During the winter, 40% of the winds are in the northeast-southwest direction, 25% are in the north-northwest orientation, and strong winds are recorded 30% of the season. These winds lead to a south-southeast dominant wave direction with a 19% occurrence of high waves.

- During the spring, 65% of the winds are in the north-northeast-southwest direction, and strong wind speeds are recorded 15% of the season. The waves are dominated by east and south directions, with only 15% occurrence of high waves.
- During the summer, 55% of the winds are from the south-southwest direction, with a much lower percentage of high winds (6%). Wave directions are south-southeast dominant, with minimal occurrences of high waves.
- During the autumn, 42% of the winds are in the northeastern direction with the second highest occurrence of high winds (22%). Wave directions are dominated by the east-southeast direction with the second highest occurrence of high waves.
- During the winter, strong winds and high waves lead to barrier island erosion.
- During the spring, mid-range winds and waves lead to barrier island distribution that affects the whole island.
- During the summer, the light winds and small waves lead to barrier island accretion.
- During the autumn, the strong winds and high waves lead to barrier island erosion.
- Large storm events such as hurricanes and tropical storms can cause significant overwash and sediment re-working on the barrier island; however, sub-tropical and nor'easters can have similar effects.

Findings Supportive of Current Base Management Practices

- Although military training continues year round on the barrier island, the extensive training during the summer is best in terms of seasonal climate and barrier island fortitude.

Findings with Implications for Future Base Management

- It is important that scheduling of military training activities after a storm event coincide with calmer wind and wave periods as the barrier island is equilibrating after the event.

Findings with Implications for DCERP2

- Modeling data are only as good as the input and validation data. However, we will use the coupled ADCIRC+SWAN Model that was validated in DCERP1 to forecast a limited set of representative storms or storm scenarios that will input into a morphological model from the U.S. Army Corps of Engineers to compute response of the barrier as a part of a DCERP2 research project.

Literature Cited

Allard, R.A., Y.L Hsu, J.M. Smith, and K. Miles. 2000. *Validating a Coupled Suite of Wave, Tide, and Surf Models at Onslow Bay, North Carolina*. Final Report NRL/FR/73720-00-9699.Naval Research Laboratory, Stennis Space Center, MS. 29pages.

Atkinson, J.H., J.J. Westerink, and J.M. Hervouet. 2004. Similarities between the wave equation and the quasi-bubble solutions to the shallow water equations. *International Journal for Numerical Methods in Fluids 45*:689–714.

Booij, N., R.C. Ris, and L.H. Holthuijsen. 1999. A third-generation wave model for coastal regions, Part 1.Model description and validation. *Journal of Geophysical Research 104*(C4):7649–7666.

Bunya, S., J.C. Dietrich, J.J. Westerink, B.A. Ebersole, J.M. Smith, J.H. Atkinson, R. Jensen, D.T. Resio, R.A. Luettich, C. Dawson, V.J. Cardone, A.T. Cox, M.D. Powell, H.J. Westerink, and H.J. Roberts. 2010. A high-resolution coupled riverine flow, tide, wind, wind wave and storm surge model for Southern Louisiana and Mississippi: Part I—Model development and validation. *Monthly Weather Review 138*(2):345–377.

Chen, Q., H. Zhao, K. Hu, and S.L. Douglass. 2005. Prediction of wind waves in a shallow estuary. *Journal of Waterway, Port, Coastal and Ocean Engineering 131*(4):137–148. July/August.

Cleary, W.J.(Ed.). 1996. *Environmental Coastal Geology, Cape Lookout to Cape Fear, NC*. Carolina Geological Society.138 pages.

Cleary, W.J., and P.E. Hosier. 1987. Onslow Beach, NC: Morphology and Stratigraphy. Pp. 1745–1759 in *Proceedings Coastal Sediments '87*, New Orleans, LA.

Cleary, W.J., and S.R. Riggs. 1999. *Beach Erosion and Hurricane Protection Plan for Onslow Beach, Camp Lejeune: North Carolina: U.S. Marine Corps Comprehensive Geologic Characteristics Report*. 115 pages.

Dietrich, J.C., S. Tanaka, J.J. Westerink, C.N. Dawson, R.A. Luettich Jr., M. Zijlema, L.H. Holthuijsen, J.M. Smith, L.G. Westerink, and H.J. Westerink. 2012. Performance of the unstructured-mesh, SWAN+ADCIRC model in computing hurricane waves and surge. *Journal of Scientific Computing 52*(2):468–497.

Dietrich, J.C., M. Zijlema, J.J. Westerink, L.H. Holthuijsen, C.N. Dawson, R.A. Luettich Jr., R.E. Jensen, J.M. Smith, G.S. Stelling, and G.W. Stone. 2011a. Modeling hurricane waves and storm surge using integrally coupled, scalable computations. *Coastal Engineer 58*:45–65.

Dietrich, J.C., J.J. Westerink, A.B. Kennedy, J.M. Smith, R.E. Jensen, M. Zijlema, L.H. Holthuijsen, C. Dawson, R.A. Luettich Jr., M.D. Powell, V.J. Cardone, A.T. Cox, G.W. Stone, H. Pourtaheri, M.E. Hope, S. Tanaka, L.G. Westerink, H.J. Westerink, and Z. Cobell. 2011b. Hurricane Gustav (2008) waves and storm surge: Hindcast, synoptic analysis and validation in Southern Louisiana. *Monthly Weather Review 139*:2488–2522.

Dietrich, J.C., S. Bunya, J.J. Westerink, B.A. Ebersole, J.M. Smith, J.H. Atkinson, R. Jensen, D.T. Resio, R.A. Luettich, C. Dawson, V.J. Cardone, A.T. Cox, M.D. Powell, H.J. Westerink, and H.J. Roberts. 2010. A high-resolution coupled riverine flow, tide, wind,

wind wave and storm surge model for Southern Louisiana and Mississippi: Part II—Synoptic description and analysis of Hurricanes Katrina and Rita. *Monthly Weather Review 138*(2):378–404.

Forbes, C., R.A. Luettich Jr., C.A. Mattocks, and J.J. Westerink. 2010. A retrospective evaluation of the storm surge produced by hurricane Gustave (2008): Forecast and Hindcast Results. *Weather and Forecasting 25*:1577–1602.

Gorman, R.M., and C.G. Neilson. 1999. Modelling shallow water wave generation and transformation in an intertidal estuary. *Coastal Engineering 36*:187–217.

Holthuijsen, L.H., A. Herman, and N. Booij. 2003. Phase-decoupled refraction-diffraction for spectral wave models. *Coastal Engineering 49*:291–305.

Kolar, R.L., J.J. Westerink, M.E. Cantekin, and C.A. Blain. 1994. Aspects of nonlinear simulations using shallow water models based on the wave continuity equation. *Computers and Fluids 23*:523–538.

Lin, W., L.P. Sanford, and S.E. Suttles. 2002. Wave measurement and modeling in Chesapeake Bay. Continental Shelf Research 22:2673–2686.

Luettich, R.A., J.J. Westerink, and N.W. Scheffner. 1992. *ADCIRC: An Advanced Three-Dimensional Circulation Model for Shelves, Coasts, and Estuaries, Report 1: Theory and Methodology of ADCIRC-2DDI and ADCIRC-3DL*. Technical Report DRP-92-6.U.S. Army Corps of Engineers Waterways Experimental Station, Vicksburg, MS. 137 pages.

Pawlowicz, R., B. Beardsley, and S. Lentz. 2002. Classical tidal harmonic analysis including error estimates in MATLAB using T_TIDE. *Computers and Geosciences* (28):929–937.

Skamarock, W.C., J. B. Klemo, J. Dudhia, D. O. Gill, D. M. Barker, W. Wang, and J.G. Power. 2005. A Description of Advanced Research WRF Version 2. NCAR Technical Note. NCAR/TN-468 STR.

Stockdon, H.R., R.A. Holman, P.A. Howd, and A.H. Sallenger Jr. 2006. Empirical parameterization of setup, swash, and runup. *Coastal Engineering 53*:573–588.

Westerink, J.J., R.A. Luettich Jr., J.C. Feyen, J.H. Atkinson, C. Dawson, M.D. Powell, J.P. Dunion, H.J. Roberts, E.J. Kubatko, and H. Pourtaheri. 2008. A basin- to channel-scale unstructured grid hurricane storm surge model as implemented for Southern Louisiana. *Monthly Weather Review 136*:833–864.

Westerink, J.J., C.A. Blain, R.A. Luettich, and N.W. Scheffner. 1994. *ADCIRC: An Advanced Three-Dimensional Circulation Model for Shelves, Coasts, and Estuaries, Report 2: User's Manual for ADCIRC-2DDI*. Technical Report DRP-92.Department of the U.S. Army.

Zijlema, M. 2010. Computation of wind-wave spectra in coastal waters with SWAN on unstructured grids. *Coastal Engineering 57*:267–277.

[This page intentionally left blank.]

Appendix 8-A

List of Scientific Publications

List of Scientific Publications

Papers

Reynolds-Fleming, J.V., R.A. Luettich, and J.G. Fleming. 2012. Comparative hydrodynamics during events along a barrier island: Explanation for overwash. *Estuaries and Coasts*. doi: 10.1007/s12237-012-9578-8.

Reynolds-Fleming, J.V., and R.A. Luettich. 2012. Wave and wind climate of Onslow Bay. Submitted to *Continental Shelf Research*.

Presentations

Reynolds-Fleming, J., and R.A. Luettich. 2011. *Sequential Storm Effects on Barrier Island Morphology: Data and Modeling Analyses.* Presented at the Coastal and Estuarine Research Federation Biennial Meeting, Daytona Beach, FL. November 6–10.

Reynolds-Fleming, J., R.A. Luettich, A.B. Rodriguez, and S.R. Fegley. 2009. *Hydrodynamics and Barrier Island Morphology During Two Storm Events.* Presented at the Estuarine Research Federation Biennial Meeting, Portland, OR. November 1–5.

Fegley, S.R., C.H. Peterson, A.B. Rodriguez, J.V. Reynolds-Fleming, R.A. Luettich, B.M. Van Dusen, and C.M. Voss. 2010. *Perturbation in a Dynamic System: Variable Consequences of Coastal Storms on Habitat Structure and Faunal Composition in an Exposed Beach*. Presented at the 39th Benthic Ecology Meeting, Wilmington, NC. March 10–13.

Theuerkauf, E.J., A.B. Rodriguez, S.R. Fegley, and R. Luettich. 2012. *Barrier Island Response to an Elevated Sea-Level Anomaly: Onslow Beach, North Carolina, USA.* Presented at the American Geophysical Union's Fall Meeting, San Francisco, CA. December 3–7.

Theuerkauf, E.J., A.B. Rodriguez, S.R. Fegley, J.V. Fleming, J.E. McNinch, and H.M. Wadman. 2009. *Extreme Along-Beach Variations in Morphodynamics Attributed to Nearshore Bathymetry and Underlying Geology over the Short-Term, Onslow Beach, North Carolina*. Presented at American Geophysical Union's Fall Meeting, San Francisco, CA. December 14–18.

Chapter 9

Onslow Beach Morphology, Sediment Texture and Composition, and Aeolian Sand Transport

SERDP Project Number: RC-1413

Coastal Barrier Module

Lead Researchers:
Antonio B. Rodriguez and Stephen Fegley
University of North Carolina at Chapel Hill
Morehead City, NC
E-mails: abrodrig@email.unc.edu and srfegley@email.unc.edu

Supporting Researchers:
Patricia L. Rodriguez and Ethan J. Theuerkauf
University of North Carolina at Chapel Hill
Morehead City, NC
E-mails: prodrigu@email.unc.edu and ejtheu@email.unc.edu

June 27, 2013

Final

This report was prepared under contract to the U.S. Department of Defense (DoD) Strategic Environmental Research and Development Program (SERDP). The publication of this report does not indicate endorsement by DoD, nor should the contents be construed as reflecting the official policy or position of DoD. References herein to any specific commercial product, process, or service by trade name, trademark, manufacturer, or otherwise, do not necessarily constitute or imply its endorsement, recommendation, or favoring by DoD.

Table of Contents

List of Acronyms 9-v
Abstract 9-1
Objectives of the Monitoring Activity 9-2
    Barrier Morphology 9-2
    Sediment Texture and Composition 9-2
    Aeolian Sand Transport 9-3
Background 9-3
    Barrier Morphology 9-3
    Sediment Texture and Composition 9-4
    Aeolian Sand Transport 9-4
Materials and Methods 9-5
    Barrier Morphology 9-6
    Sediment Texture and Composition 9-9
    Aeolian Sand Transport 9-11
    Results and Discussion 9-15
    Sediment Texture and Composition 9-17
    Aeolian Sand Transport 9-21
Assessment of Trends in the Data 9-28
    Assessment of Monitoring Design 9-28
    Assessment Seasonal and Annual Variability in the Data 9-29
    Recommendations for Future Monitoring 9-29
Conclusions and Implications for Future Research 9-30
    Key Scientific Findings—Fundamental Cause-and-Effect Relationships 9-30
    Findings Supportive of Current Base Management Practices 9-30
    Findings with Implications for Future Base Management 9-31
Literature Cited 9-32
Appendix 9-A: Topographic Maps of the Focus Sites Illustrating the Changes in Morphology That Occurred over the Project Period 9-A-1
Appendix 9-B: List of Scientific Publications 9-B-1
Appendix 9-C: List of Students 9-C-1

List of Figures

9-1. Regional study area map of Onslow Beach, NC. 9-6

9-2. Regional study area map of Bear Island, NC. 9-6

9-3. Collecting terrestrial laser scanning data on Onslow Beach, NC. 9-7

9-4. Mean shoreline movement of the transects at FS 3 and FS 5 plotted through time. 9-9

9-5. Location of five beach zones sampled at each focus site. 9-9

9-6. Comparing the gravimetric method of deriving percent $CaCO_3$ (acid digestion) to counting carbonate grains in 11 samples. 9-11

9-7. Aeolian sediment sampling locations. 9-12

9-8. Daily mean wind vectors from offshore NOAA Buoy 41035 and 41036 during September 1, 2010 to September 29, 2011. 9-14

9-9. Along-beach variations in the rate of shoreline movement at Onslow Beach (left) and Bear Island (right), NC. 9-16

9-10. Oblique aerial photo of Onslow Beach, NC. 9-17

9-11. Mean grain size of sand along Onslow Beach and Bear Island, NC. 9-18

9-12. Percent gravel along Onslow Beach and Bear Island, NC. 9-18

9-13. Percent carbonate along Onslow Beach and Bear Island, NC. 9-19

9-14. Limestone particles as part of the total carbonate material (A) and variations in abundance (B) along Onslow Beach, NC. 9-20

9-15. Changes and sediment texture and beach elevation. 9-21

9-16. Aeolian-sediment captured in the traps and texture. 9-22

9-17. Saltmarsh cores. 9-24

9-18. Grain-size distribution of the top 1 cm of each core and the muddy sand beds at depth compared with the grain size distribution of the proximal and distal sand traps. 9-25

9-19. The percent of the backbarrier marsh that is composed of aeolian sand. 9-27

List of Tables

9-1. Pitfall-trap observation periods, percent of observation period when wind speed was greater than 6 m s^{-1}, and corresponding wind information included in the study 9-14

List of Acronyms

°C	degrees Celsius
µm	Micron
Φ	Phi
3-D	three dimensional
AGU	American Geophysical Union
$CaCO_3$	calcium carbonate
cm	Centimeter
CB	Coastal Barrier (Module)
cm/y	centimeter per year
DCERP	Defense Coastal/Estuarine Research Program
DEM	Digital Elevation Model
DoD	U.S. Department of Defense
FS	focus site
g	Gram
$g\ cm^{-3}$	grams per cubic centimeter
$g\ day^{-1}$	grams per day
GSU	Geological Society of America
HCl	hydrochloric acid
ID	Identification
km	Kilometer
LIDAR	light detection and ranging
LOI	loss on ignition
m	Meter
M	Mole
$m\ s^{-1}$	meters per second
m/y	meters per year
m^2	square meter
MARDIS	Monitoring and Research Data Information System
MCBCL	Marine Corps Base Camp Lejeune
MHW	mean high water
mL	Milliliter
mm	Millimeter
NAVD88	North American Vertical Datum of 1988
NCDCM	North Carolina Division of Coastal Management
NOAA	National Oceanic and Atmospheric Administration
PVC	polyvinyl chloride
R^2	R-squared value (coefficient of determination)

RTK-GPS	real-time kinematic global positioning system
SD	standard deviation
SEGSA	Southeastern Section of the Geological Society of America
SERDP	Strategic Environmental Research and Development Program
UTM	Universal Transverse Mercator

Abstract

Coastal geomorphology is principally defined by physical forcing (waves, currents, and wind), sediment supply (underlying lithology, cross- and along-shore sand sources and sinks), sea level change, and the framework geology (coastal plain slope, topography of the land before the coastline formed) of an area. In addition to those natural drivers, development and land use can also influence the shape and position of the shoreline, primarily through influencing sediment supply, sediment transport, and resistance to erosion. Marine Corps Base Camp Lejeune uses different areas of Onslow Beach for training and recreation. From the southwest to the northeast, the island is mainly used for off-road recreation vehicles (access to fishing spots near the inlet), military training (large wheel- and track-vehicles), recreation (foot traffic by sun bathers), and a buffer zone ("no-go zone" between the northeastern end of Onslow Beach and ordnance testing on Browns Island). The main goals of the monitoring were to determine if those different uses of Onslow Beach were impacting rates of shoreline movement along the island, to provide data to inform Research Project CB-1 and to provide data to support the biological monitoring effort. In addition, the contribution of wind-blown sand to the backbarrier marsh was examined over a 1-year period to examine the link between the barrier and wetlands.

Barrier morphology was constrained by collecting terrestrial laser scanning data (topographic data) semiannually at 15 focus sites spaced equally along the island. These data were processed into high-resolution (0.5-m grid spacing) Digital Elevation Models that were used to map shoreline changes. Around the same time as those topography data were being collected, the different beach zones (backshore, intertidal, and shallow subtidal zones) were sampled at seven of those focus sites for determining sediment grain size and composition. The samples were sieved to measure the greater than 2.0-mm fraction, run through a laser-diffraction instrument to measure the less than 2.0-mm fraction, and digested in acid to measure the percent carbonate. The contribution of wind-blown sand to the backbarrier was measured at two of those focus sites along the island continually throughout a year by pitfall traps and anemometers. A transect of cores across the backbarrier marsh were also collected to directly measure the amount of wind-blown sand in the marsh and how that changes with depth (time).

From the southwest to the northeast, Onslow Beach can be broken into an accreting area adjacent to the New River Inlet where the shoreline moved 30.9 to 4.3 m/y, an erosional southwestern area of the island where the shoreline moved −3.7 to −6 m/y, and a relatively stable northeastern part of the island where the shoreline moved 2.4 to −1.2 m/y. The spatial distribution of the three zones does not correspond with the various military-use zones indicating that military activities are not impacting erosion rates. Variations in the underlying geology and associated sediment availability on the inner continental shelf, however, explain why the southwestern (sediment starved) and northeastern (sediment rich) areas of the island are erosional and accretional, respectively. The area adjacent to the inlet is dynamic, and the accretion observed there is expected to be lost over the next few years. FS 7 (the most northern site) is heavily influenced by the disposal of dredged material every 2 years. The sediment texture sampled at the erosional southwestern area is distinct (coarser) than the sediment sampled at the accretionary northeastern area indicating limited sediment exchange between those two zones. The percent volume of the marsh that is aeolian sand, based on the upper 1 cm of marsh sediment, decreases by an order of magnitude only approximately 20 m from the edge. Near the edge, the backbarrier marsh

contains greater than 20% or less than 10% aeolian sand (by volume) where it is fronted by a washover fan (FS 1) or a high-elevation dune ridge (FS 6), respectively. Further into the marsh platform, the percent volume of aeolian sand is consistently low at both sites (less than 1%). Reported erosion rates should be used for beach management over the next few years (less than 5 years into the future). It is highly recommended that the monitoring of beach morphology be continued because the rate of sea level rise is increasing and because in many places, the dunes are narrow and the island is highly vulnerable to overwash. Once overwash occurs, it is likely that the shoreline-change rates measured here will no longer apply to that area of the beach. In addition, it is highly recommended that the monitoring of beach morphology be continued because the State of North Carolina is constantly changing coastal management rules and as a result, it is likely that a groin will be constructed on the southwest end of the New River Inlet. A coastal-engineering firm, hired by Topsail Island, predicts that the groin will cause increased erosion to the southwestern end of Onslow Beach.

Keywords: Barrier island, transgression, aeolian, dune, salt marsh, sea level rise, beach, overwash, beach erosion, geomorphology

Objectives of the Monitoring Activity

Barrier Morphology

The purpose of monitoring barrier morphology is to ensure sustainability of Base activities into the future and to improve management capacity for MCBCL's coastal barrier system. Morphologic changes in the coastal barrier indicate erosion, accretion, and vulnerability to extreme events and this information is needed to better manage the land mass in a form that sustains Base activities into the future. Base staff observed significant beach erosion over the few years leading up to the project, especially in the southwestern area of Onslow Beach. The primary goal of the barrier morphology monitoring effort was to quantify shoreline movements and variability along the length of the island and test whether training activities are impacting shoreline movements. In addition, the various barrier ecosystems are defined by their morphology making morphologic changes directly related to habitat availability. The morphology of Bear Island was also monitored to serve as a natural surrogate to the northeast end of Onslow Beach, which regularly receives dredging material. The northeast end of Onslow Beach has a similar morphology to Bear Island. Monitoring barrier morphology at Onslow Beach informs Research Project CB-2 and monitoring of benthic invertebrates and vegetation.

Sediment Texture and Composition

The objectives of monitoring sediment texture and composition are to inform Research Project CB-2 and to use these metrics as indicators of habitat quality (see benthic invertebrate and vegetation monitoring chapters). Sediment texture varies with the intensity of hydrodynamic processes, as the aerial extent of habitats change, and when dredge material is deposited on the barrier. Variations in sediment composition may help determine sediment-transport pathways, given the extreme variability in the framework geology along Onslow Beach. A rigorous accounting of the variations in mineralogy and sediment texture along Onslow beach will provide a benchmark that can be used to evaluate the compatibility of dredge spoil or nourishment material before distribution on the beach. The sediment texture and composition of

Bear Island was also monitored to compare with the northeast end of Onslow Beach, which has a similar morphology. In addition, we use these data to test the hypothesis that the Belgrade Formation (limestone) is not a significant active source of sand to Onslow Beach.

Aeolian Sand Transport

Sediment movement from the fore-dune to the backbarrier fringing salt marsh is being examined to test the hypothesis that aeolian-transported sand is an important inorganic sediment source that promotes backbarrier marsh accretion. Evaluating aeolian-sediment transport from the dune crest to the backbarrier shoreline improves integration of coastal barrier processes with marsh accretion. As the beach morphology changes, the aeolian sand transport pathways and flux will also change. Monitoring aeolian sand movement across the barrier over 1 year at two morphologically distinct areas of Onslow Beach, is a first step towards better understanding the connectivity between the beach and backbarrier marsh.

Background

Onslow Beach is a northeast–southwest trending barrier island located at Marine Corps Base Camp Lejeune (MCBCL) in southeastern North Carolina (**Figure 9-1**). It is a wave-dominated barrier with a mean wave height of 0.91 m and tidal range of 1.2 m based on National Oceanic and Atmospheric Administration's (NOAA's) tide gauge at Wrightsville Beach, NC (Station Identification [ID] 8658163, located 60 km southwest of Onslow Beach). This 12 km–long barrier fronts the salt marsh with sinuous tidal channels and is bounded by the New River Inlet to the southwest and Browns Inlet to the northeast. The Atlantic Intracoastal Waterway extends through the backbarrier marsh. The shoreline of Onslow Beach is sinusoidal with a central headland separating two embayments (Rodriguez et al., 2012). The morphology of the island also varies along its length. The northern arcuate section has a wide beach (approximately 80-m wide) with multiple well-developed dune ridges (7–9 m in height). Landward of the dune ridges a narrow (less than 100-m wide) maritime forest abuts the backbarrier salt marsh. This northeastern part of the island has a similar morphology as Bear Island, which is located northeast and adjacent to Browns Island (**Figure 9-2**). The central headland area of Onslow Beach has a narrow beach (approximately 20-m wide) with a single discontinuous dune ridge less than 4 m in height. Numerous washover fans extend less than 100 m across the dunes and the vegetation is dominated by shrub thickets, but dead standing and fallen trees are frequently observed. The beach widens significantly along the southern embayment from 20 m in the northeast to 80 m in the southwest. The discontinuous dunes are less than 2 m in height, and washover fans can be extensive (250-m wide) and extend across backbarrier marshes. The variable morphology of Onslow Beach reflects its central location within Onslow Bay because it defines the border between the high-elevation regressive islands with multiple beach ridges to the north and the low-elevation, narrow transgressive islands to the south (Cleary et al., 1996).

Barrier Morphology

The North Carolina Division of Coastal Management (NCDCM) measures shoreline movement across the state at decadal intervals from 1938 (Benton et al., 1993 and 2004). Shoreline monitoring by NCDCM is used to update set-back factors, which are based on the shoreline-movement rate, and includes Onslow Beach. The position of the shoreline is based on mapping

the wet-dry line of the beach using aerial photography. Erosion rates are determined by dividing the net shoreline movement by the time period covered by the aerial photographs. Erosion-rate maps are accessible from NCDCM's Web site at http://dcm2.enr.state.nc.us. These data show net erosion of Onslow Beach in the southwest and net accretion in the northeast.

Cleary and Riggs (1999) established a year-long beach monitoring program in 1997 to assess shoreline movements. The program included measuring elevations across 10 beach profiles, extending from the foredune to mean low water, along Onslow Beach. The profiles were occupied approximately every month to measure elevation changes. Similar to NCDCM's effort, those data show erosion in the southwest and accretion in the northeast during 1997.

Our monitoring effort is at a temporal scale (semiannual over 4 years) that is between Cleary and Riggs (1999) and NCDCM and is more spatially explicit than those previous studies. The technical objective is to identify variations in shoreline retreat along the barrier at a spatial scale that less than 1 km and quantify rates of shoreline movement and variability in shoreline movement.

Sediment Texture and Composition

From mapping the wet-dry line on aerial photos, previous studies (Cleary and Riggs, 1999; Riggs et al., 1995) and the NCDCM show Onslow Beach is eroding at rates up to 6 m/y in the south and is relatively stable in the north. Riggs et al. (1995) attribute much of this variability in erosion rates to variations in the underlying geology as mapped on the inner continental shelf and projected landward. Offshore, the Oligocene Belgrade Formation, which is a sandy limestone to calcite-cemented sandstone, forms a submarine headland along the southern part of Onslow Beach, whereas in the north, the younger Oligocene Silverdale Formation, which is primarily unconsolidated quartz sand, outcrops (Riggs and Cleary, 1998; Riggs et al., 1996 and 1998). It is thought that mechanical and bioerosion of these offshore units provide a continuous source of sand to Onslow Beach (Cleary and Riggs, 1999; Riggs et al., 1995 and 1998). Filardi (1999) concluded that the texture and mineralogy of the northeastern and southwestern ends of Onslow Beach are distinct and reflect the spatial distribution of the Belgrade and Silverdale formations on the inner continental shelf.

Aeolian Sand Transport

Under increasing sea level conditions, inorganic marsh sedimentation is commonly reported to be the limiting factor of a marsh's ability to maintain an appropriate marsh-surface elevation with respect to the tidal range (Allen, 1995; Hatton et al., 1983; Reed, 1990; Temmerman et al., 2004). In those cases, it is important to understand the sources of inorganic marsh sediment and how these sources may become modified and impact sediment flux in the future. Aeolian sediment transport may be a more continuous source of inorganic sediment from the barrier to the marsh than overwash, but has received little attention in coastal research. Aeolian sand is thought to be sequestered mostly at the marsh edge or dune ridge because vegetation efficiently captures saltating grains (Arens, 1996; Armon and McCann, 1979; de Groot et al., 2011; French and Spencer, 1993). However, Anderson and Walker (2006) show that grains can be transported up to 300-m landward from the foredune via modified suspension and grainfall. Even if the flux of aeolian sand to the backbarrier marsh is low, it could still be an important component to marsh

accretion because backbarrier marsh accretion rates are also commonly low (less than 1 cm/y; Bartholdy et al., 2004; Craft et al., 1993; DeLaune et al., 1986; Mattheus et al., 2010). The morphology, sediment texture, and vegetation cover of the beach, primary dunes, and dune field, along with the wind climate (e.g., speed, direction), are likely the principal controlling factors on the transport of aeolian sediment to the backbarrier marsh. There have been no past efforts at Onslow Beach looking at wind-transported sand to the backbarrier marsh.

Materials and Methods

The MCBCL created four spatially explicit use zones along Onslow Beach (**Figure 9-1**), and focus sites (FSs) were chosen to sample those different use areas and the different beach morphologies along the island. The southwestern part of the island is used primarily by off-road recreation vehicles. People drive to this end of the island mainly to access fishing spots near the inlet. The central part of the island is used for military training and the main disturbance is large vehicles and equipment creating ruts in the beach. An access road (unpaved) behind the dune line is maintained. Egress points connect the road to the beach and are situated at natural breaks in the dune line that were formed by storms. Northeast of the training zone is the recreational part of the beach where the main impact is from foot traffic. The northeastern end of the island serves as a buffer zone between Onslow Beach and adjacent Browns Island, which is an impact area that is used in ordnance testing and is restricted from foot and vehicular traffic. Bear Island is northeast of Browns Island and is a state park (**Figure 9-2**).

Barrier Morphology was examined at 15 sites along Onslow Beach and three sites along Bear Island (**Figures 9-1 and 9-2**). Seven of the 15 sites along Onslow Beach and the three sites along Bear Island (the whole-numbered sites) were also sampled for sediment texture and composition. All sampling occurred during the 2 hours before or after low tide and during the same 3–4 day period. Monitoring barrier morphology began in November 2007, and then took place every May and September until 2011. Monitoring sediment texture began in October 2007, and then took place every May and September until 2010. Aeolian transport across the barrier at FS1 and FS6 was monitored from November 2010 to November 2011.

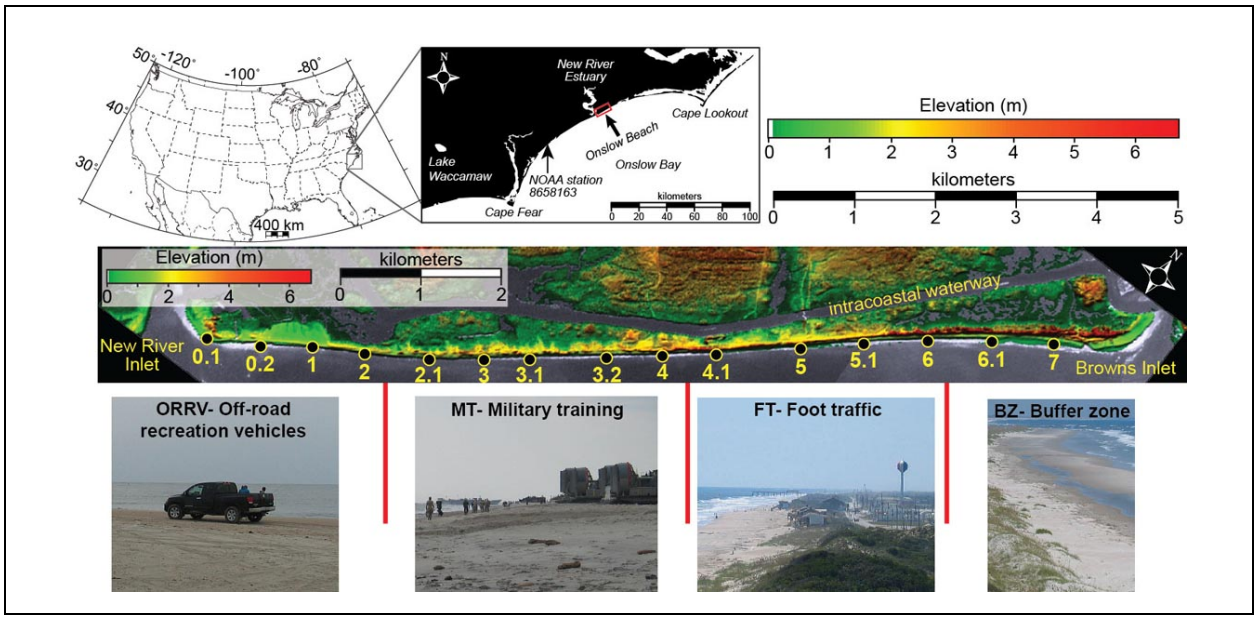

Figure 9-1. Regional study area map of Onslow Beach, NC.

Onslow Beach is located in the center of Onslow Bay. Sampling took place at 15 focus sites along the island and includes the various use zones and morphologies that exist there.

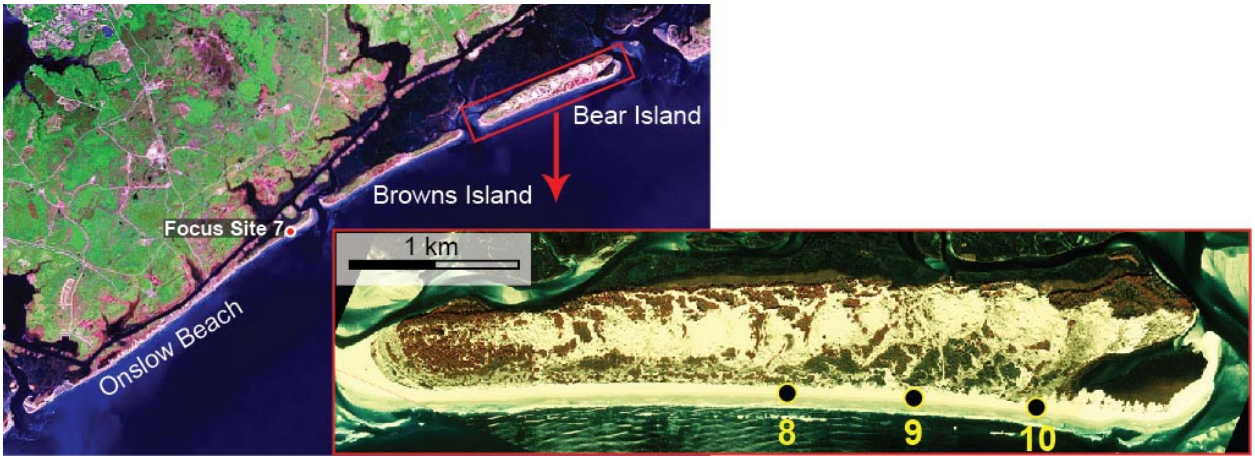

Figure 9-2. Regional study area map of Bear Island, NC.

Bear Island is located north of Onslow Beach. Sampling took place at three focus sites along the island, which is morphologically similar to the northeastern end of Onslow Beach.

Barrier Morphology

Data Collection

Topographic data were collected using a Riegl three-dimensional (3-D) LMSZ210ii terrestrial laser scanner. This scanner was mounted onto a truck and rotated 360 degrees while collecting approximately 2 million spatial (x, y, and z) data points from laser returns (**Figure 9-3**). Real-time kinematic global positioning system (RTK-GPS)–surveyed reflectors, positioned within the scan area, were used to georeference the data points to a global coordinate system (Universal Transverse Mercator [UTM]) (**Figure 9-3**). Two scan positions were occupied at each focus site,

resulting in approximately 200 m of coverage along the beach (approximately 4 million points per site per survey). Beach surveying was restricted to 2 hours before and after low tide to maximize sub-aerial beach coverage. Error in the 3-D topographic data is estimated to be ±3.0 cm, which includes a ±1.5-cm factory-estimated maximum instrument error and an average ±1.5-cm RTK-GPS error. The RTK-GPS error is reported from the instrument as horizontal and vertical errors and varies based on factors such as the number of satellites, the position of satellites, and cloud cover.

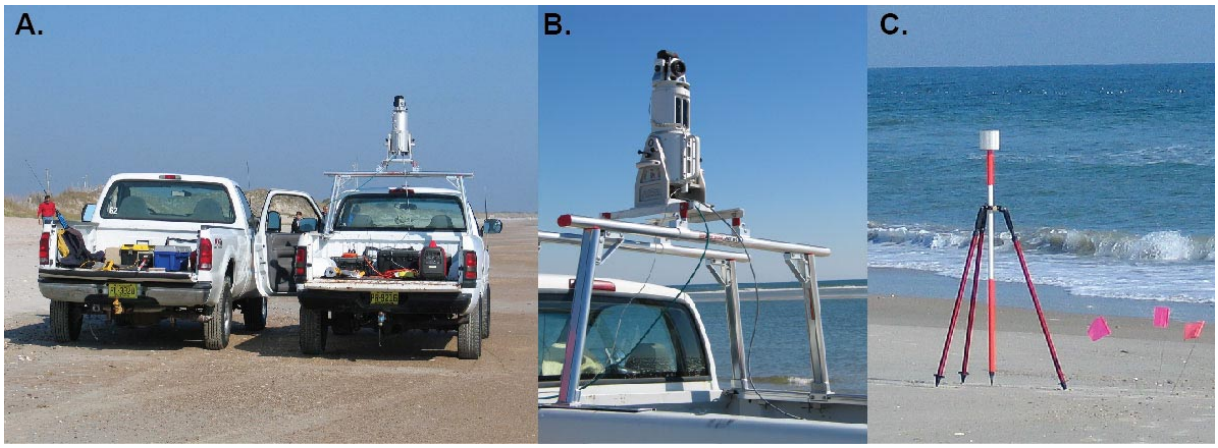

Figure 9-3. Collecting terrestrial laser scanning data on Onslow Beach, NC.

(A) We used a truck as a platform for collecting terrestrial laser scanning data. (B) The instrument rotates 360 degrees, collecting 2 million data points. (C) These points are converted into the UTM coordinate system and adjusted to North American Vertical Datum of 1988 by surveying retroreflectors with a Trimble global positioning system.

Data Processing

Ground points (x, y, and z data points) were isolated from the raw data using an algorithm included in the Terrasolid LTD software package and by manual editing. Surface-grid models were created from, approximately 125,000 ground points for sites with narrow cross-shore widths (e.g., F4) and approximately 500,000 ground points for sites with wide cross-shore widths (e.g., F7) using Delaunay triangulation. Woolard (1999) and Woolard and Colby (2002) suggest that Digital Elevation Models (DEMs) derived from airborne Light Detection and Ranging (LIDAR) most accurately represent coastal topography with a spatial resolution of 1–2 m. Given the high density of points derived from the laser scans at each site in this study, a 0.5-m grid spacing was used. This 0.5-m grid spacing is generally much larger than the spacing of the laser returns, thus each grid node is based on an average of several topographic measurements. Areas of the focus sites greater than 5 m^2 with no laser returns, which only occurs in the dunes, were not included in the surface model (i.e., the areas were defined with blanked grid nodes) because the limited data would not depict the ground surface accurately at the desired resolution. Surface-grid files were imported into Golden Software's Surfer 10.0, a surface and contour mapping program, to generate contour maps and DEMs.

The position of the laser scanner was not the same for each re-occupation of the focus sites due to changes in barrier morphology and unavoidable circumstances (e.g., beachgoers, MCBCL training activities). This caused the mapped area of a site to be slightly different for each survey.

To account for this, DEMs were cropped to reflect only areas of overlapping survey coverage; resulting in an along-beach extent of approximately 150 m for each focus site. The data points also extend further landward at sites with low-elevation dunes and overwash fans (e.g., FS 3), but these data are patchy landward of the foredune crest because of shadowing. Portions of the dune landward of the foredune crest were cropped out of the maps to normalize coverage across the beach between surveys. The seaward boundaries on the maps were cropped at zero meters North American Vertical Datum of 1988 (NAVD88) to normalize coverage across the beach caused by differences in tidal height (the laser does not penetrate the surface of the water) between surveys.

The shoreline was defined as the mean high water (MHW) line, which is 0.36-m NAVD88 at Onslow Beach (Weber et al., 2005). The MHW line was contoured from the DEMs and exported as a shapefile into ArcGIS. The shoreline position is the distance the shoreline is away from a known baseline, measured using the Digital Shoreline Analysis System (Thieler et al., 2009) along transects spaced 25-m apart at each site (i.e., the shoreline position was sampled in approximately six locations at each site). Shoreline change is measured as the difference between those distances for a given time step. The rate of shoreline movement is measured at each transect using linear regression (**Figure 9-4**). The coefficient of determination (R-squared value [R^2]) was also calculated and is an indicator of the applicability of using the reported rate of shoreline movement as a predictor. In addition, the R^2 value also indicates the degree to which the shoreline moved back and forth during the monitoring effort (**Figure 9-4**). For example, on one hand, at FS 5, the linear regression rate is low (less than 1 m/y), and the r^2 value is also low (less than 0.1), suggesting that the low rate of shoreline retreat is not accurate for making predictions at the yearly time scale because over the monitoring period, the shoreline experienced variable movement, including seaward and landward displacements (**Figure 9-4**). On the other hand, FS 3 has a high r^2 value (greater than 0.8), which suggests that the −4 m/y shoreline change rate is an accurate prediction of how that shoreline will move in the future (all else being equal; **Figure 9-4**). Measurements of the linear regression shoreline change rate and R^2 value at each of the six transects were averaged to derive one representative value for each site.

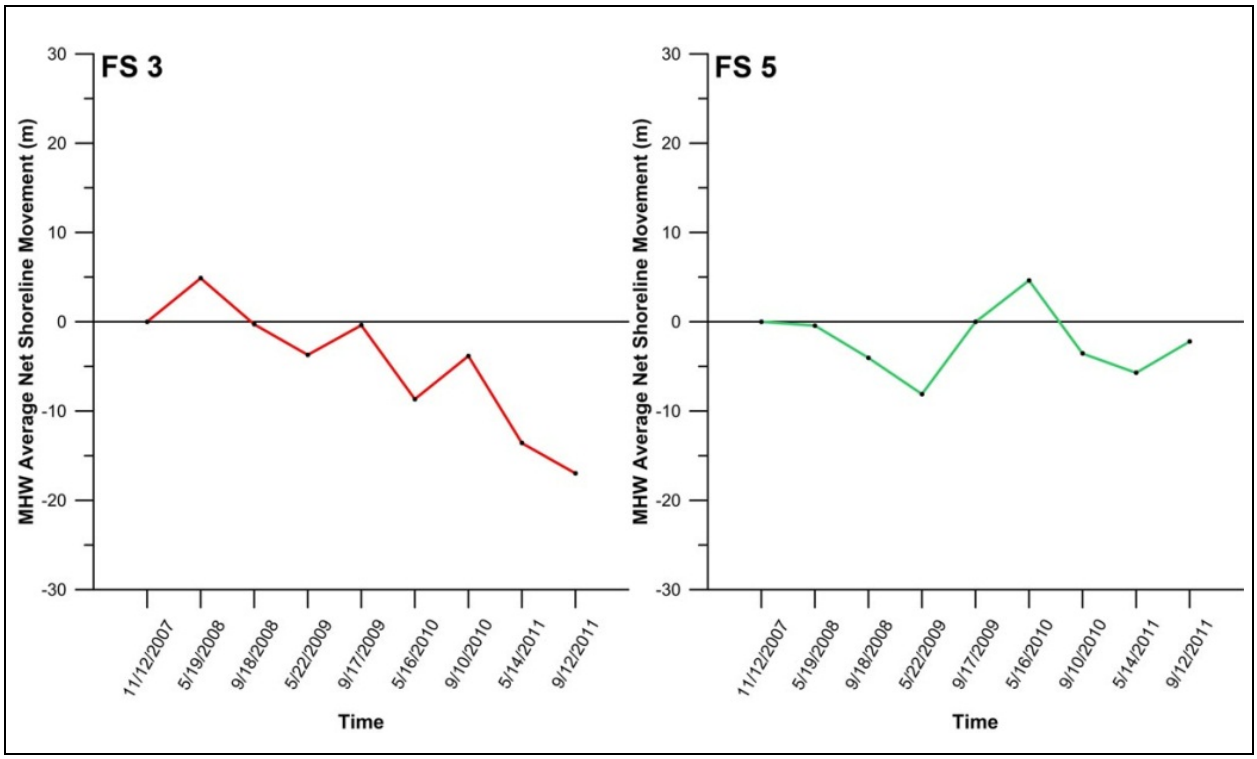

Figure 9-4. Mean shoreline movement of the transects at FS 3 and FS 5 plotted through time.

The zero line represents the shoreline position at the start of the monitoring. The shoreline movement rate is the calculated from the slope of the best fit line through the points. Overall, the MHW line at FS 3 moved landward through time and the high R^2 value indicates little variation in the trend. At FS 5, the MHW line moved landward and seaward and at the end of the monitoring is in almost the same location as it was in November 2007. This focus site has a low rate of shoreline movement and a low R^2 value, which indicates high variation in the trend.

Sediment Texture and Composition

Sample Collection

At each focus site we sampled along two transects approximately 30 m apart. The backshore, high intertidal, middle intertidal, low intertidal and subtidal zones were sampled along transects (**Figure 9-5**). At each of these five zones, 3- to 9.0-cm-long cores (4.60 cm in diameter) were collected randomly in a 2.0-m^2 area. The three cores were put into the same sample bag, homogenized, and then returned to the laboratory for analysis. Samples were collected over a 1-day period during the 2 hours before and after low tide.

Figure 9-5. Location of five beach zones sampled at each focus site.

Percent Gravel

Collected samples were dried in aluminum pans and passed through a sample splitter (Humboldt model H-3985) to obtain four unbiased samples. One quartered sample was selected at random, weighed (M1), and passed through a 2-mm mesh sieve. Gravel is defined as clasts greater than 2 mm. Most samples easily passed through the sieve dry. Agglomerates were gently broken up with a paint brush to pass all visible sand grains through the mesh. If the sample contained a significant proportion of clay, the sample was rinsed through the mesh using deionized water. Both fractions were retained and dried before weighing. Sieved material was retained to be sent through CILAS's laser particle size analyzer, gravel was weighed (M2), and percent gravel was calculated ([M2 ÷ M1] × 100). Gravel was bagged and retained for long-term storage.

Grain-Size Analysis of Less Than 2-mm Fraction

Dry sieved material less than 2 mm was mixed in a baggie, and a subsample was selected using a Chattaway's spatula and introduced into an ultrasound tank. The material was resealed within the baggie, shaken, and then another subsample was taken to enter into the well. This method was repeated until an obscuration between 10% and 15% was obtained. This parameter was determined as the amount of sample necessary for an accurate measurement. After running the sieved material through the CILAS, the particle size analyzer was cleaned, and the method was repeated a second time to ensure conformity among computations within the same bulk sample. Detailed information on the CILAS 1180 can be found on the company's Web site at http://www.cilas.com/index-us.htm and in the standard operating procedure located in the DCERP Monitoring and Research Data Information System (MARDIS).

Determination of Calcium Carbonate-Equivalent Content

Due to the large quantity of samples needing processing, we employed the gravimetric method because of its simplicity and an accepted error on the order of 5%. To obtain percent carbonate: one quartered, unsieved sample was selected at random (for details on sample splitting, see the percent gravel standard operating procedure). This sample was passed through a sample splitter repeatedly to obtain one-eighth of the original volume (approximately 20 g). The final split subsample was ground with a porcelain mortar and pestle. In an aluminum weigh pan, approximately 10.000 g of ground sample was weighed, and added to a 250-mL Erlenmeyer flask. The aluminum pan was then reweighed and total mass introduced to the flask (M1) was calculated ([mass of sample + pan] – [mass of pan + any retained sample in pan]). We added 20 mL of 1 M of hydrochloric acid (HCl) to each flask and allowed the sample to effervesce. We continued to add 20 mL of 1M of HCl at 2-hour intervals until there was no evidence of effervescence. Colorphast pH-indicator strips (pH 0−14) were dipped into each sample to ensure (pH 0−3) a continued acid solution and the reaction is complete.

We weighed Whatman 0.7-µm glass microfilter to 0.001g (M2) and placed the filter paper in a 250-mL filter funnel. The paper was moistened with deionized water, and the contents of a flask was filtered and rinsed until no solutes remained in the flask. The filter paper containing the acid-insoluble residue was placed inverted on an aluminum weigh pan and dried at 105°C for 24 hours. Once dry, the filter paper and acid-insoluble residue was allowed to equilibrate to room temperature and moisture conditions then weighed (M3). The percentage by mass of the calcium carbonate ($CaCO_3$)–equivalent in the ground subsample was determined: 100([M1−(M3−M2)] ÷ M1). We evaluated the accuracy of our laboratory methods by measuring percent $CaCO_3$ by counting carbonate grains under a microscope on 11 subsamples. Comparing these data to subsamples from the same sites analyzed for percent $CaCO_3$ using the gravimetric method, yield an R^2 value of 0.76 (**Figure 9-6**).

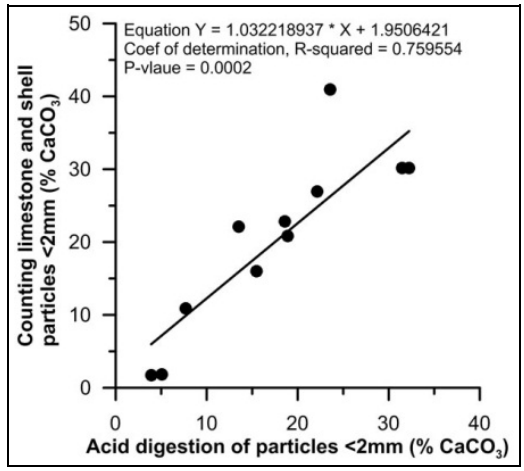

Figure 9-6. Comparing the gravimetric method of deriving percent $CaCO_3$ (acid digestion) to counting carbonate grains in 11 samples.

Linear regression shows a high R^2 value. This indicates that the gravimetric method for determining percent $CaCO_3$ is sound.

Aeolian Sand Transport

At the start of the monitoring in November 2010, DEMs were created for each site using an RTK-GPS and a Riegl LMS-Z210ii terrestrial laser scanner and the same methods outlined previously, except that the scanner was mounted onto a tripod instead of a truck. The DEMs served as base maps and helped with the positioning of sampling spots (**Figure 9-7**).

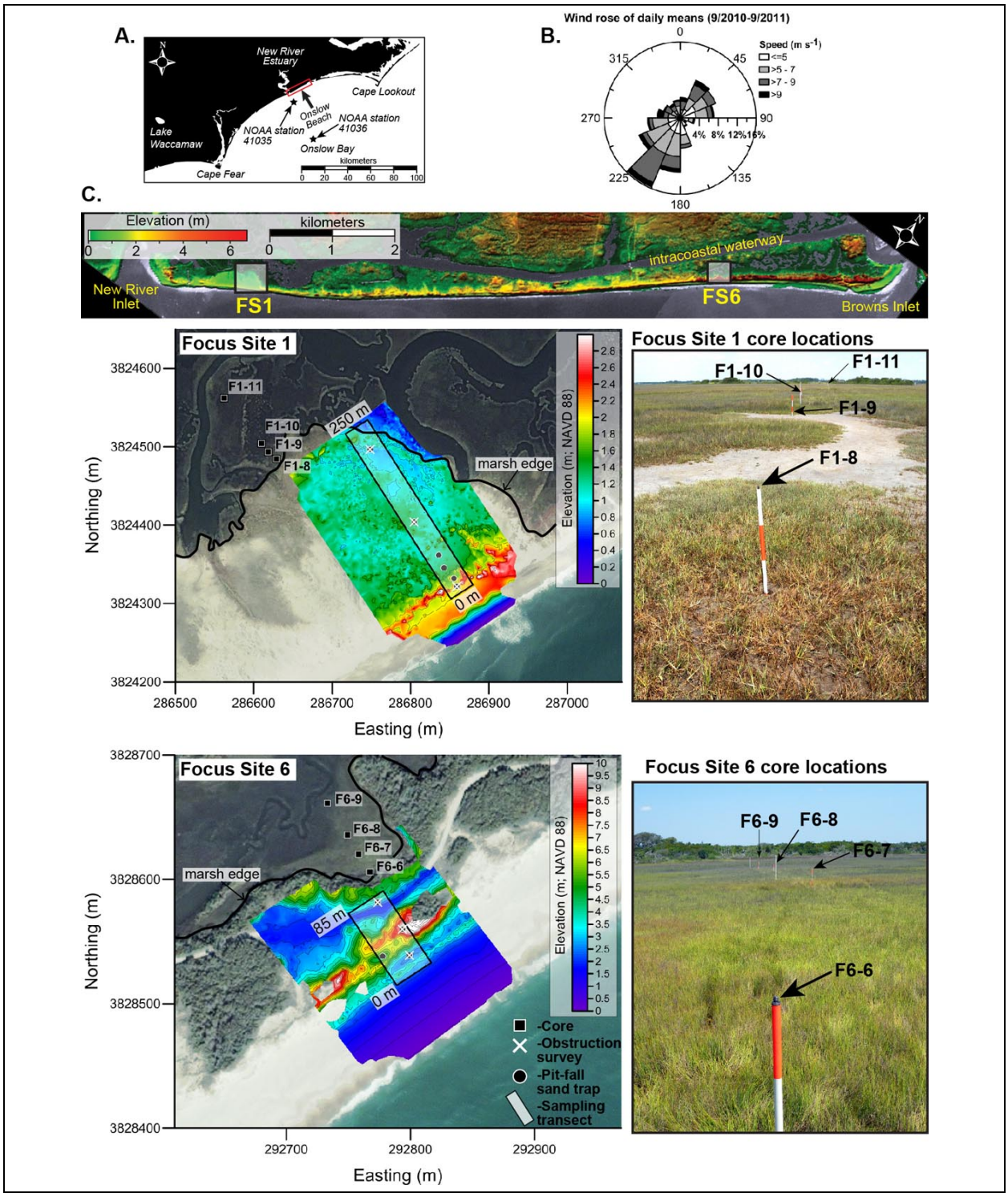

Figure 9-7. Aeolian sediment sampling locations.

(A) Location map of Onslow Beach. (B) Winds are predominantly out of the southwest. (C) Digital elevation data overlain on aerial photographs show the morphologic differences between the focus sites. Notice that the detailed maps for each of the sites are not scaled the same vertically or horizontally. Core locations are marked on the photographs by the orange and white rods and the northwest is towards the background. Obstruction surveys for vegetation density center around a pitfall and sand trap locations (for more information, see Chapter 12, Dune and Marsh Vegetation).

Wind Speed and Direction

Observations of wind speed and direction every 10 minutes were obtained from NOAA Buoys 41035 and 41036 located 7.5 km and 50.0 km directly offshore of Onslow Beach, respectively. NOAA discontinued servicing Buoy 41035 in August 2011, making it necessary to use the more distant Buoy 41036 for wind observations for the remainder of the year. The differences between the two buoy's daily mean wind speeds and directions are small. For example, during July 2011, the maximum and minimum differences in daily mean wind speed and direction between the two buoys was 0.13 m s^{-1} (1.76 degrees) and −0.11 m s^{-1} (−1.56 degrees), respectively.

Wind-Transported Sand

Wind-transported sand was monitored at each site from a series of pitfall sand traps distributed from the foredune to the edge of the backbarrier marsh (**Figure 9-7**). The traps were built from 3.8 cm in diameter × 61.0 cm–long polyvinyl chloride (PVC) pipe with a flexible pipe cap clamped on the bottom end and a 0.254-mm thick, shallow-cone-shaped collar glued to a 5-cm PVC coupler that slides onto the top end of the pipe. A 1.3-cm mesh plastic cloth is sandwiched between the PVC coupler and the pipe to exclude crabs from entering the trap (see supplementary data for a schematic and photograph). The pipe was buried with the brass collar flush to the ground to prevent excessive scouring around the pipe. No traps were installed in the marsh because the device is not effective at collecting wind-blown sediment underwater. The traps were emptied generally three times per month, and directly before and after some forecasted high wind events, which resulted in 40 observations throughout the year.

Sediment from the traps were bagged and returned to the laboratory for analyses, which included measuring mass and grain size. Grain-size analyses were carried out on subsamples using the same methodology described above. The amount of sediment collected in the pitfall sand traps, from the foredune to the marsh edge, should indicate whether aeolian sand is a viable source of sediment for backbarrier marshes. These data were collected continuously during the year and include periods when the wind was not exceeding the threshold velocity for sand movement or blowing from a direction conducive for the transport of sand landward across the barrier. Those periods when we assume the potential for moving sand across the barrier towards the salt marsh to be high (wind events) were isolated from the data set. Wind events are defined here as wind speeds greater than 6 m s^{-1} because that wind speed was shown at other beaches to have the potential for transporting sand 1.5–2.5 ϕ (0.35–0.18 mm), which is similar to the grain size at Onslow Beach (Delgado-Fernandez and Davidson-Arnott, 2011; Ridge et al., 2011). Wind data from the offshore buoy were high-pass filtered at 6 m s^{-1}, and those filtered data were binned based on the periods between sampling of the pitfall traps. Onslow Beach trends toward the northeast (N55°E) making winds blowing from 55–235 degrees, along and across the island from the ocean side, the most likely directions for delivering sand to the backbarrier marsh (**Figure 9-8**). Only those bins when the wind blew from within the 55- to 235-degree arc for greater than 50% of the time period were included in the study (**Figure 9-8 and Table 9-1**). This resulted in 14 pitfall trap observations over periods ranging from 1–19 days that include times when the mean weighted wind direction (weighted by wind speed) was 155.8–213.4 degrees, and the mean wind speed (using the filtered data set) was 7.02–9.97 m s^{-1} (**Table 9-1**).

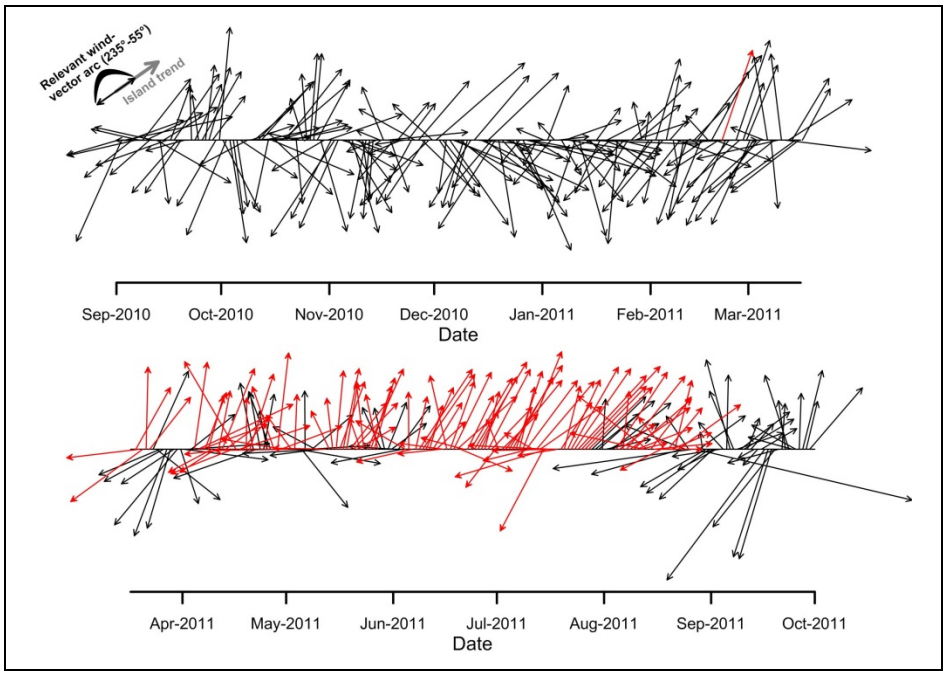

Figure 9-8. Daily mean wind vectors from offshore NOAA Buoy 41035 and 41036 during September 1, 2010 to September 29, 2011.

Table 9-1. Pitfall-trap observation periods, percent of observation period when wind speed was greater than 6 m s^{-1}, and corresponding wind information included in the study

Collection Date	Deployment Duration (Days)	Wind Speed >6 m s^{-1} (% deployment)	Observations Within Arc (%)[a, b]	Mean Weighted Direction (°)[a, b]	Mean Wind Speed (m s^{-1}) ±1 SD[a]
February 22	1	100	77.4	209.2	9.29 ±1.49
March 23	6	65.0	83.2	155.8	7.99 ±1.28
April 5	1	100	98.6	189.7	9.97 ±1.49
April 13	8	45.4	67.7	212.8	7.58 ±1.11
April 20	7	40.0	77.8	172.9	7.80 ±1.96
May 3	7	46.3	76.6	170.4	7.57 ±1.42
May 20	9	44.4	76.9	194.0	7.02 ±0.70
May 27	7	37.9	95.6	202.5	7.24 ±0.81
June 15	12	40.8	65.9	207.2	7.45 ±1.05
June 20	5	73.1	71.2	214.2	8.47 ±1.36
June 27	7	63.6	83.2	213.4	8.65 ±1.31
July 13	16	62.2	80.6	211.6	8.31 ±1.55
July 27	14	66.0	74.9	197.9	8.50 ±1.62
August 22	19	44.4	70.1	202.0	7.71 ±1.28

[a] Wind speeds below 6 m s^{-1} were filtered.

[b] The wind-direction arc of interest is 55–235 degrees.

Coring

Four vibracores were collected from the backbarrier marshes at each site. Core locations were distributed along a line from the barrier-marsh boundary to the middle of the marsh platform and surveyed using a Trimble RTK-GPS (**Figure 9-7**). The 7.6 cm in diameter cores sampled the entire marsh unit and underlying sediment and averaged 1.5 m in length. In the laboratory, we split the cores lengthwise prior to photographing, describing, and sampling them. Both core halves were used for sampling; we used a razor blade to cut through roots, and each sample was the width of the core barrel leaving no sediment behind. The entire top 1 cm of each core was sampled for grain-size analyses. One-half of the core (excluding core F1-9), beginning at 1 cm in depth, was sampled every 2 cm, from 0–25 cm, for grain-size analyses (applying the same methods previously described). Core F1-9 was sampled every 1 cm, from 0–25 cm, for grain-size analyses. The second half of all of the cores was sampled every 1 cm, from 0–25 cm, for to estimate organic matter content using the loss on ignition (LOI) method. Samples were exposed to 550°C for 4 hours (2% error), as outlined in Heiri et al. (2001).

Days included in the study are shown in red and summarized in **Table 9-1**. Up is north and minimum and maximum vector lengths represent 1.5 m s^{-1} and 19.5 m s^{-1}, respectively.

Results and Discussion

Barrier Morphology

Analyses of beach change include all of the semiannual monitoring data. Seasons are not analyzed separately because we found that "winter beaches" (the data collected in May) were not consistently in a more erosional state than "summer beaches" (the data collected in September). Rates of change are calculated using eight time steps for FS 1–FS 6, seven time steps for FS 6.1 and FS 7, and four time steps for FS 8–FS 10 (Bear Island sites). Changes observed over the entire 4-year effort are presented in **Appendix 9A**. The pattern of yearly changes in the MHW line along Onslow Beach from Site 2 to Site 6.1 shows an overall deceleration in the rate of landward movement (**Figure 9-9**), which is similar to the decadal rates of shoreline movement measured by NCDCM and reprocessed and presented in Rodriguez et al. (2012). Although the yearly and decadal patterns of shoreline change are similar, the rates are very different ranging between −6 m/y to 2 m/y for the yearly data set (**Figure 9-9**) and −1.25 m/y to 0.5 m/y for the decadal data set (Rodriguez et al., 2012). Some of this discrepancy could be due to the different methods used to measure the shoreline (aerial photography versus LIDAR) and/or the different time frames included (decadal versus yearly). Continuing the monitoring effort will help determine if this increase in erosion is persistent or just a temporary phenomenon.

The MHW line at FS 0.1–FS 1 moved seaward (accretion) in the yearly data set and landward in the decadal data set. Although FS 1 is located in a subtle embayment, which is likely trapping sediment, those three sites are heavily influenced by the New River Inlet. The high rates of accretion at FS 0.1 are likely temporary, and based on observations made after the monitoring effort ended; the area has already lost some of those gains. Beach areas adjacent to an inlet are typically the most dynamic parts of a barrier island because they respond to changes in the tidal inlet complex, which includes the inlet and the flood- and ebb-tidal deltas. Because changes in

the tidal inlet complex are difficult to predict, the shoreline change rates at FS 0.1–FS 1 should not be used as an indicator of future shoreline changes.

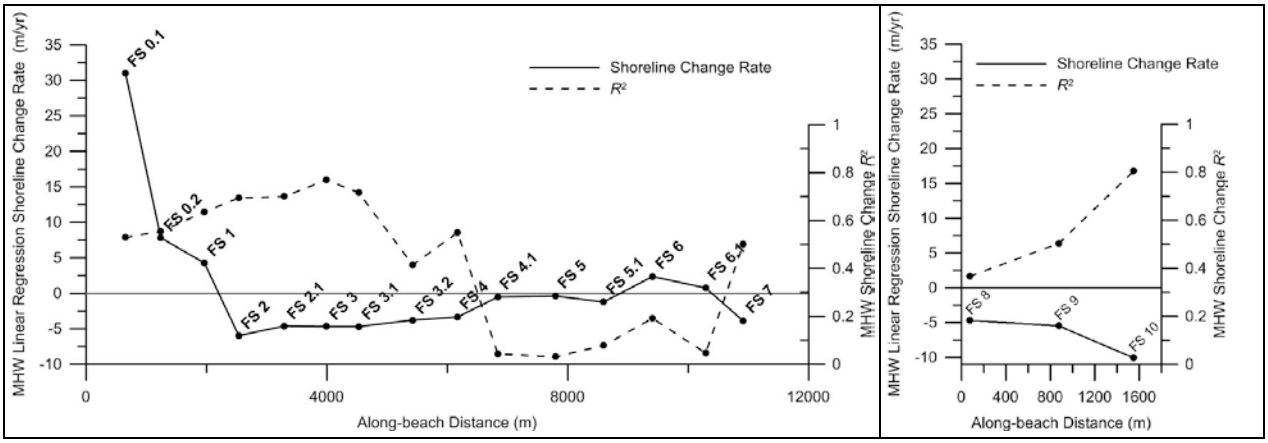

Figure 9-9. Along-beach variations in the rate of shoreline movement at Onslow Beach (left) and Bear Island (right), NC.

Along-beach distance is measured from the New River Inlet on Onslow Beach and from FS8 on Onslow Beach (for additional information, see **Figures 9-1 and 9-2**). Negative shoreline change rates represent erosion (landward movement of the shoreline) and low R^2 values indicate that the shoreline movement is not consistent through time (variable movements landward and seaward).

FS 7 shows a relatively large landward movement through time. The shoreline movement at FS 7 does not correspond with shoreline changes at the adjacent five sites to the southwest. This discrepancy is likely due to increased erosion in response to dredge-spoil disposal at FS 7 that occurred during March of 2008 and February 2010.

Overall, the MHW line at FS 0.1– FS 1 is moving seaward; at FS 2–FS 4, it is moving landward, and at FS 4.1–FS 7, it is relatively stable. The boundaries between these three morphologic-change zones are sharp; essentially less than the distance between two focus sites. With the exception of the border between the military training zone and the recreation zone (between FS 4 and FS 4.1), the morphologic-change zones do not correspond with the different military-use zones (**Figures 9-1 and 9-9**) indicating that the different military uses of the barrier is not causing the along-beach changes in shoreline movement rates. In addition, the border between the military training zone and the recreation zone was between FS 3.2 and FS 4 prior to when Riseley Pier was removed in March 2010, not at a boundary between morphologic-change zones as it is today. The irregular shape of the shoreline along the barrier, which is obvious in oblique aerial photographs (**Figure 9-10**), indicates that island evolution has been characterized by along-beach variations in shoreline movement over the long term (centennial to millennial time scales). The three morphologic change zones are produced by inlet influences (FS 0.1–FS 1) and variable underlying geology, which controls sediment supply to the island (FS 2–FS 4 and FS 4.1–FS 7). The central headland is produced by a submarine rock ridge that intersects Onslow Beach (**Figure 9-10**; Riggs et al., 1995). The rock ridge is composed of the Oligocene Silverdale Formation, a sandy, molluscan-mold limestone unit (Harris et al., 2000). The Quaternary sediment layer in this area is thin and patchy offshore of FS 2–FS 4, where more than 50% of the inner shelf is exposed limestone (Johnston, 1998) and Riggs et al. (1995) labeled this part of

Onslow Beach as being “sediment starved.” Offshore of FS 4.1–FS 7 there is a 0.5–2.5 m-thick layer of sand, which serves as a local sediment source for the northeastern part of the island.

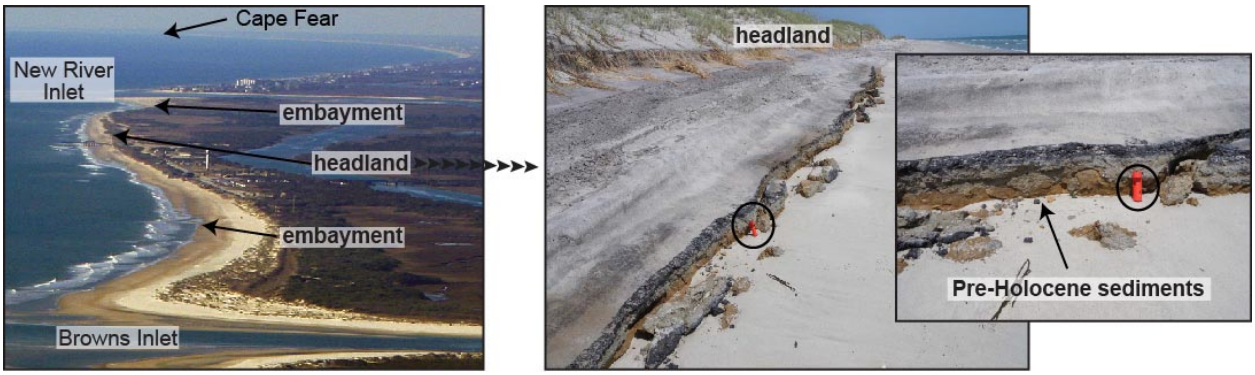

Figure 9-10. Oblique aerial photo of Onslow Beach, NC.

Oblique aerial photo looking towards the southwest shows the sinusoidal morphology of the island. At the headland, consolidated and oxidized gravelly sand is outcropping on the beachface. Offshore, the headland area is characterized by exposed rock ridges.

The purpose of collecting data at Bear Island, FS 8–FS 10, was to test whether the northern end of Onslow Beach, FS 6–FS 7, can be used as a control. Monitoring at Bear Island began September of 2009 and the analyses presented in **Figure 9-9** include four time periods. Although Bear Island is a state park, it is not without anthropogenic impacts. In spring 2009, FS 9 was nourished to mitigate erosion taking place in front of the bath-house. Results indicate that FS 6–FS 7 on Onslow Beach cannot be considered “control sites” in terms of barrier morphologic changes at Onslow Beach. There are three reasons for this. First, the shoreline changes in the southwestern end of the island (FS 2– FS 4) are consistently different than shoreline changes in the northeastern end (FS 4.1–FS 7). No one control site would apply to both of these morphologic change zones. Second, movement of the MHW line at FS 6–FS 7 is not similar to FS 8–FS 10 (different directions or magnitude). Third, both the northeastern end of Onslow Beach and Bear Island are responding to beach nourishment, which was not carried out in the same manner at both sites in terms of area nourished, volume of sand dispersed, and the way the nourishment material was graded.

Sediment Texture and Composition

Most of Onslow Beach sediment is siliciclastic sand ranging between 0.8 and 2.25 Φ (0.57–.21 mm; **Figure 9-11**). The grain-size data of the sand fraction, including sand-sized shell material, show that most of the samples fall within three distinct clusters, defined by mean grain size and Φ standard deviation (SD; **Figure 9-11**). Clusters 1 and 2 contain the coarser grained samples, including the ranges of 0.8–1.3 Φ and 1.3–1.6 Φ, respectively. Cluster 3 contains the finer grained samples between 1.8 and 2.5 Φ. Cluster 3 also contains samples that are better sorted (lower Φ SD) than Clusters 1 and 2. Most of the samples from FS 1, FS 2, FS 3, and FS 5 are contained in Clusters 1 and 2. Most of the samples from FS 4 and FS 6–FS 10 are contained in Cluster 3 (FS 8, FS 9, and FS 10, which are located on Bear Island).

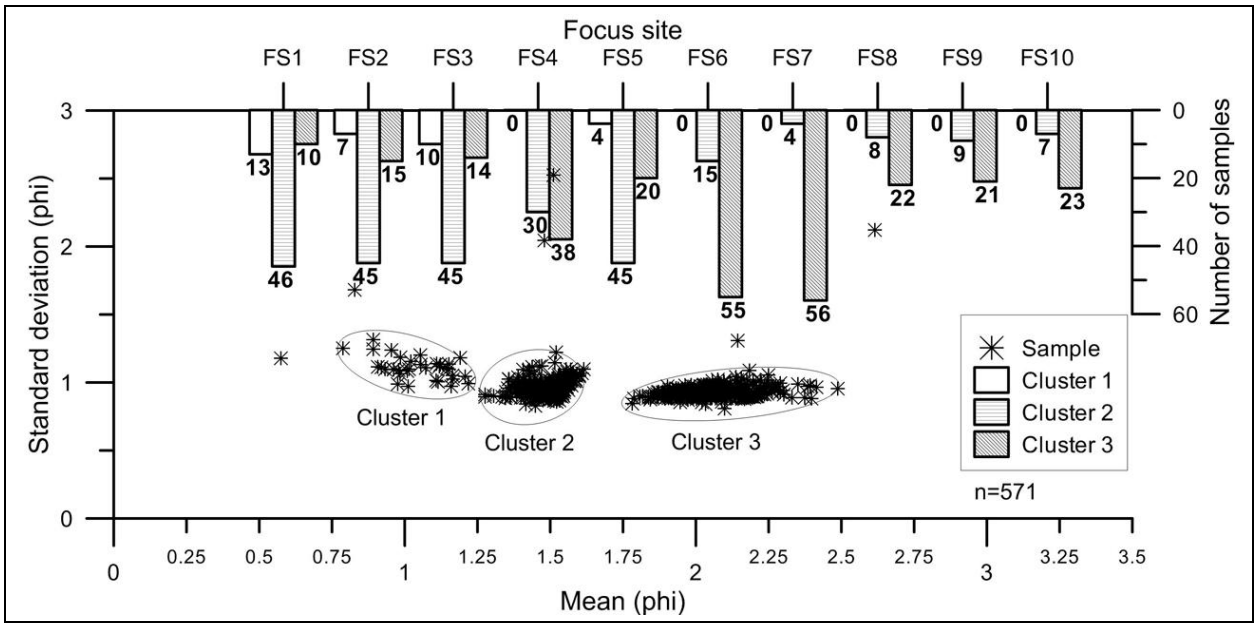

Figure 9-11. Mean grain size of sand along Onslow Beach and Bear Island, NC.

The gravel component of the samples (less than 2.0 mm) is shell material and well-rounded oblate silicate-mineral lithoclasts. Most of the samples contain less than 5% gravel (**Figure 9-12**). At each focus site, there is an overall increase in percent gravel from the backshore to the subtidal zones. FS 1, FS 2, FS 3, and FS 5 have more samples with higher percentages of gravel than FS 4 and FS 6–FS 10, and FS 3 contains more gravel than any of the other focus sites. The percent gravel and mean grain size of the sand fraction indicate that samples from FS 4 and FS 6 are finer grained than FS 1, FS 2, FS 3, and FS 5 (**Figures 9-11 and 9-12**). Cobble- (6.5–25.0 cm in diameter) and boulder-sized clasts (greater than 25 cm in diameter) are also present on Onslow Beach, but are most common in the backshore zone. Given that these particles have a low frequency of distribution (commonly less than 7–15 cobbles per 1 m^2 less than 1 boulder per 1 m^2) and a large size, they were not quantified. Cobbles are typically shells and well rounded, oblate lithoclasts (rocks). Boulders are grainstone and quartz sandstone clasts from the Oligocene Silverdale Formation that crops out on the inner shelf (Riggs et al., 1995).

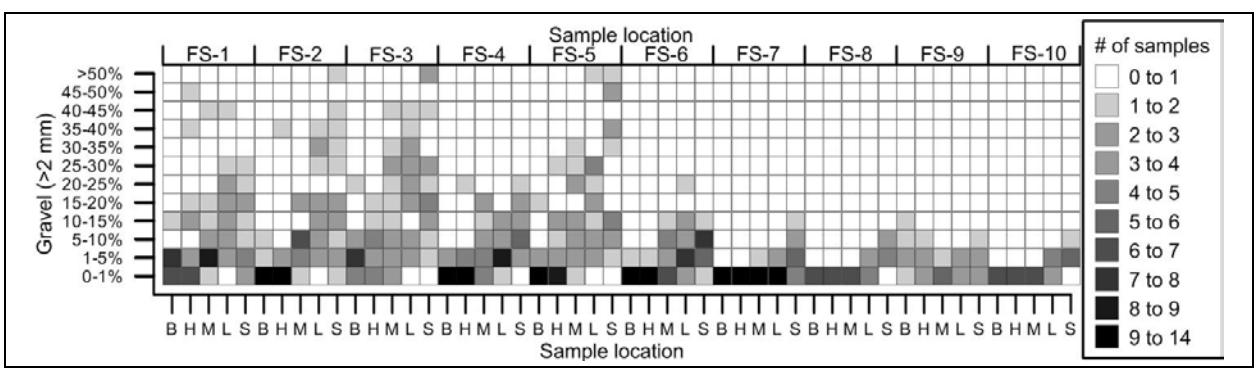

Figure 9-12. Percent gravel along Onslow Beach and Bear Island, NC.

B=backshore, H=high intertidal, M=middle intertidal, L=low intertidal, and S=subtidal. Notice that black cells represent a larger range of sample sizes (nine to 14 samples) than the other cells. Bear Island (FS 8–FS 10) was not sampled for as long of a period as Onslow Beach was.

The carbonate component of the samples consists of shell material. All of the samples contain greater than 2% carbonate. At each focus site, there is an overall increase in percent carbonate from the backshore to the subtidal zones (**Figure 9-13**). This parallels the trends in percent gravel, reflecting the shell material being included in the percent gravel measurement and the increased proximity towards mollusk habitat in the lower intertidal and subtidal zones. There is a systematic decrease in the number of samples with high percent carbonate along the beach from FS 1 to FS 6, although FS 5 diverges slightly from this trend. FS 6–FS 10 consistently have low percent gravel.

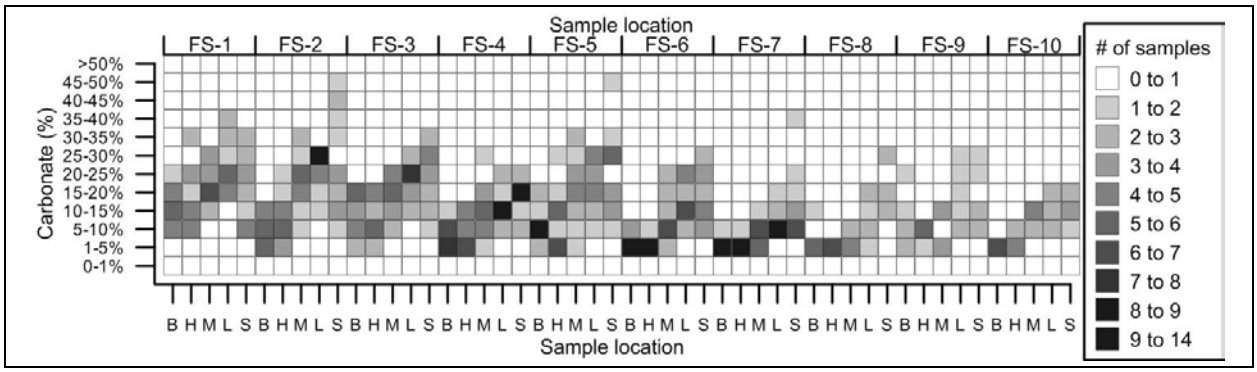

Figure 9-13. Percent carbonate along Onslow Beach and Bear Island, NC.

B=backshore, H=high intertidal, M=middle intertidal, L=low intertidal, and S=subtidal. Notice that black cells represent a larger range of sample sizes (nine to 14 samples) than the other cells. Bear Island (FS 8–FS 10) was not sampled for as long of a period as Onslow Beach was.

Sediments are distinct along Onslow beach. The southwestern end of the island (FS 1–FS 3) is composed of coarser sediment than the northeastern end of the island (FS 6 and FS 7), whereas the middle part of the island (FS 4 and FS 5) is a mixture. These differences were consistent throughout the monitoring effort and suggest that there is little exchange of sediment between the southern embayment and the northern embayment. Sand transported along the island by longshore currents is likely not moving across the headland.

Riggs et al. (1995) presents a conceptual model for sedimentation at Onslow Beach that identifies biological and physical weathering of exposed limestone rock on the inner shelf (Silverdale Formation) as an important source of sediment for the island. If that is the case, limestone particles should make up a large portion of the beach sediment and should increase in in abundance towards the southwest where those rock exposures cover more seafloor area. There is no direct relationship between the percent of limestone clasts and percent carbonate along the beach indicating that limestone material is not the primary source of carbonate grains on the island (**Figure 9-14A**). In addition, no systematic or abrupt increase in limestone particles exists towards the southwest (towards the New River Inlet; **Figure 9-14B**) where the limestone rock crops out near the shoreface. Limestone particles are present on the beach there, but principally as large cobble-sized particles.

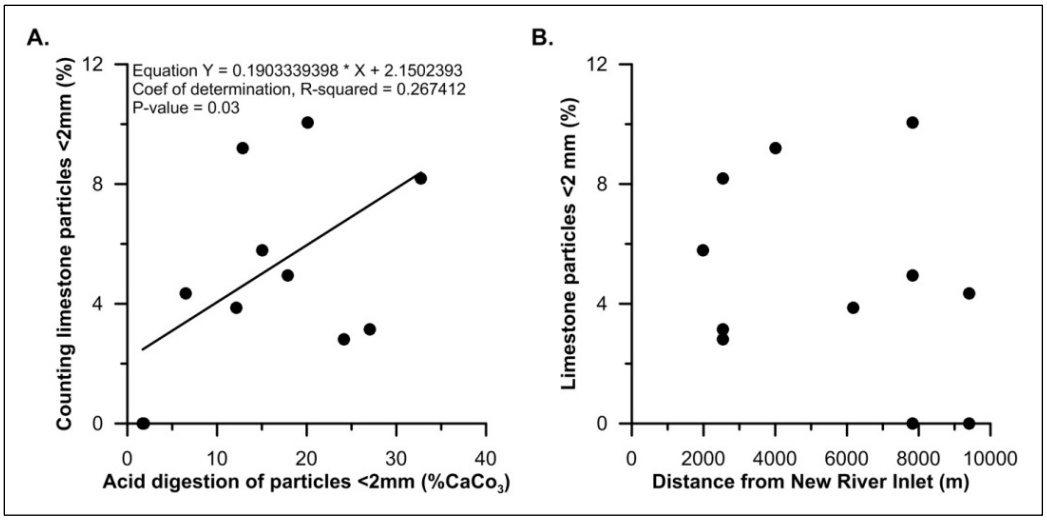

Figure 9-14. Limestone particles as part of the total carbonate material (A) and variations in abundance (B) along Onslow Beach, NC.

At each focus site, beach sediment texture coarsens in an offshore direction reflecting the increase in beach slope and associated wave energy impacting the beach in an offshore direction (**Figure 9-12**). The low-elevation intertidal and subtidal zones are influenced by waves for a longer duration throughout the year than the higher-elevation backshore and high intertidal zones. The finer grains at areas of a beach that experience high-energy conditions should erode away leaving the coarser particles behind.

The four time steps between November 2007 and September 2009 were examined to test if there was a systematic coarsening of the sediment associated with erosion. For example, a loss of elevation in the backshore might correspond with a coarsening of the sediment as the finer grains are preferentially transported away and the coarser grains are left behind. **Figure 9-15** shows that erosion is not consistently associated with a coarsening of the sediment. This finding is similar to the observed lack of correspondence between short-term erosion and increase in surface-sediment grain size at Sennen Cove, Cornwall, England (Masselink et al., 2007). Well-sorted medium-grained sand beds are common at depth and on the surface of Onslow Beach and if erosion extended into one of those units, there would be no coarse grains present to concentrate (Rodriguez et al., 2012). In addition, erosion of the dunes during high-energy events can supply well-sorted and finer grained sand to the beach replenishing any losses.

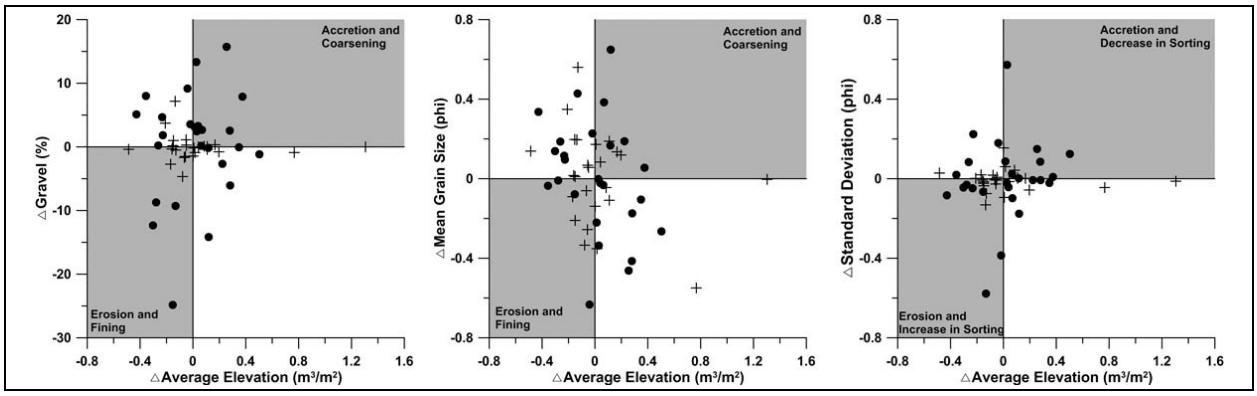

Figure 9-15. Changes and sediment texture and beach elevation.

Erosion of the backshore (cross) and high intertidal zone (circle) does not consistently correspond with a coarsening of the sediment or a decrease in sediment sorting. Elevation changes were measured at the same locations as the sediment samples using the laser scanner. Points that fall in the lower left grayed area represent erosion and sediment fining or increase in sorting, while points that fall in the upper right grayed area represent accretion and sediment coarsening or decrease in sorting.

Aeolian Sand Transport

Morphology and Vegetation

The sediment source for coastal dunes is the beach and beach width (fetch) is the dominant factor controlling sediment flux (Davidson-Arnott and Law, 1996). The beaches at both sites are about 55-m wide from the foredune toe to zero m NAVD88, which is close to mean sea level. Although the two beaches have similar widths, the beach at FS 1 is typically split into backshore and foreshore zones, and no prominent backshore exists at FS 6. Rodriguez et al. (2012) observed those same differences in beach morphology at the sites in 2009 and 2010, which suggests that those morphologies persist at least over yearly time scales.

The morphology and vegetation density of the dunes impact sediment flux to the backbarrier marsh because they modify wind speed, direction and turbulence, the trajectory of particles, and the volume of sediment eroding from the dune. The foredune ridge at FS 1 is discontinuous, approximately 20-m wide and has a maximum elevation of 3 m, which is also the maximum elevation of the entire site. The vegetation density of the foredune is high near the ground and vegetation density decreases and becomes patchy greater than 33 cm above the ground. A broad, 225-m wide washover fan separates the foredune ridge from the backbarrier marsh. The fan is generally flat with a mean elevation of 1.3 m and a high density of vegetation 0–33 cm above the ground. Vegetation 33–67 cm above the ground is patchy and those patches generally correspond with localized mounds of sand (less than 5 m^2), which are resolved in the DEM (**Figure 9-7**), and likely formed as a result of the vegetation trapping aeolian sand (Kuriyama et al., 2005; Lancaster and Baas, 1998). Vegetation is dense at the boundary between the washover fan and the backbarrier marsh where a continuous line of shrubs greater than 1 m in elevation exists. The backbarrier-marsh platform gently slopes towards the north from 0.2 m at the edge of the washover fan to 0.0 m at the first tidal channel and has an average elevation of 0.07 m (±0.05 SD).

The foredune ridge at the FS 6 is continuous, approximately 5-m wide, and has a maximum elevation of 4 m. The vegetation density of the foredune is very similar to that observed at FS 1. A linear, 8-m wide trough parallels the foredune along its landward edge. Elevations increase landward from 2.5 m in the trough to 11 m at the crest of the dune ridge, which is the highest elevation at the site. The high-elevation dune ridge is 40-m wide and densely vegetated by tall grasses. A beach-access trail at 2-m elevation separates the high-elevation dune ridge from a maritime forest composed of a dense canopy of trees and shrubs. The beach-access trail is not open to the public and is seldom used. The 20-m wide maritime forest colonized the salt-spray shadow in the lee of the high-elevation dune ridge and marks the transition to the backbarrier marsh environment. The backbarrier marsh platform is higher in elevation than at FS 1 and slopes towards the north from 0.43 m at the edge of the maritime forest to 0.03 m at the first tidal channel and has an average elevation of 0.29 m (±0.06 SD).

Sand Traps

Data from the pitfall traps were converted into mean sediment mass collected per day. The sediment trap is not sampling the total aeolian-sediment passing over it making any flux calculation problematic; however, each trap is the same, making comparisons of sediment captured (g day^{-1}) across the dunes a useful indicator of trends in sediment transport and flux. The mean sediment capture rate decreased across the dunes at both sites and was consistently low across the washover fan at FS 1 (**Figure 9-16**). At this site, the mean grain size of the sand captured in the traps increased across the boundary between the dunes and the washover fan (**Figure 9-16**). At FS 6, the mean grain size of the sand captured in the traps decreased slightly from 1.96 ϕ (0.26 mm) at the lee side of the foredune toe to 2.19 ϕ (0.22 mm) adjacent to the maritime forest. Smaller grains traveling larger distances from the foredune crest have been observed elsewhere (Anderson, 1988; Arens et al., 2002).

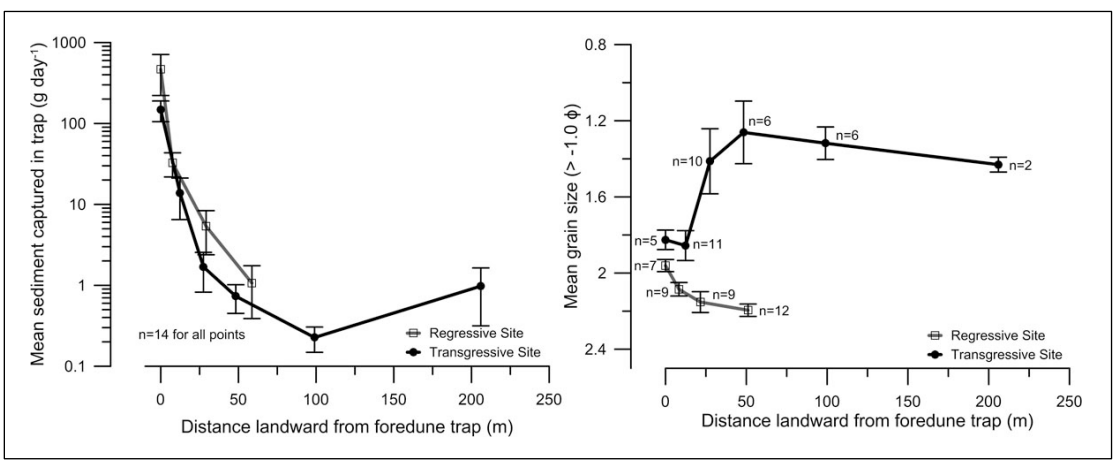

Figure 9-16. Aeolian-sediment captured in the traps and texture.

Mean sediment captured, ±1 SD, across the barrier (left) as based on 14 observations at each sampling location. The observations used for calculating the mean grain size, ±1 SD, of the sediment captured in the traps varies at each location (right). This is because during some periods not enough sediment was captured at a location to allow for reliable grain-size analysis. At FS 1 (Transgressive Site; Regressive Site is FS 6), approximately 200 m from the foredune, samples from consecutive periods were combined to yield enough material to determine grain size (for additional information, see **Figure 9-7**).

Vibracore Transects

If aeolian sediment reaches the backbarrier marsh, then vibracores collected from the edge of the washover fan and dunes should sample it. At both sites, the cores collected closest to the barrier sampled more sand than the cores collected on the marsh platform (**Figure 9-17**). At FS 1, all of the cores sampled a basal sandy mud unit with greater than 10% LOI. The two cores collected adjacent to the washover fan (FS 1-8 and FS 1-9) sampled a 9.5- to 12-cm-thick bed of surficial muddy sand overlying the sandy mud unit. The sand bed at the top of core FS 1-9 contains heavy minerals (e.g., magnetite, garnet). Further landward on the marsh platform, cores FS 1-10 and FS 1-11 also sampled a 4- to 6-cm-thick bed of muddy sand overlying the basal sandy mud. Unlike the cores collected close to the washover fan, the top 3–4 cm of FS 1-10 and FS 1-11 sampled a 5- to 6-cm-thick bed of sandy mud with a LOI greater than 20%, which is similar to the basal unit. The percent sand, as a portion of the total clastic sediment, in the upper 1 cm of the cores decreases from greater than 77% near the washover fan to 25% near the middle of the marsh platform.

Overall, the cores at FS 6 have less sand, higher LOI, and are 20 cm higher in elevation than the cores at FS 1 (**Figure 9-17**). Core FS 6-6, collected near the dunes, sampled a sandy mud to muddy sand unit with sand making up 36–60% of the clastic sediment component. The cores collected farther away from the barrier (i.e., FS 6-7, FS 6-8, and FS 6-9) sampled sandy mud with 2- to 4-cm-thick beds of sediment with higher concentrations of sand (greater than 40% of the clastic sediment) at various depths. The percent sand, as a portion of the total clastic sediment, in the upper 1 cm of the cores decreases from 60% near the dunes to approximately 25% on the marsh platform.

Contribution of Aeolian Sand to Marsh Accretion

The pitfall trap closest to the marsh at both sites collected sand consistently, indicating that wind does transport sand adjacent to the marsh, albeit at a mean rate that is three orders of magnitude less than the trap in the dunes (**Figure 9-16**). The marsh sediment at both sites contain some component of sand, which varies spatially and with depth, but was this sand sourced from the barrier and transported by wind, or was there another sand source or transport mechanism? The potential sources of sand to the backbarrier marsh include the tidal channels that exist close to the northernmost cores at both sites and the barrier island. The tidal channels are disregarded as being a significant source of sand to the marsh because a 50-cm-thick unit of organic-rich soft silty clay was examined along their banks in the field. Comparing the grain-size distribution curves of the 0- to 1-cm interval of the marsh cores provides some evidence for the source of marsh sand and the direction of sediment transport (**Figure 9-18**; McLaren and Bowels, 1986). With the exception of core FS 1-9, which was collected in a patch where no vegetation exists (**Figure 9-7**), at both sites the marsh surface sediment becomes coarser (increasing concentration of sand), the skewness of the surface sediment grain-size distribution curves becomes increasingly positive, and the sediment sorting (variance) becomes better (less variable) towards the washover fan or the dunes at FS 1 and FS 6, respectively. These trends indicate that the barrier island is likely the source of sand to the marsh and that the tidal channel is the likely source of fine-grained material (silt and clay) to the marsh (McLaren and Bowels, 1986). Overwash and wind are the mechanisms for delivering sand from the barrier to the backbarrier marsh at Onslow Beach.

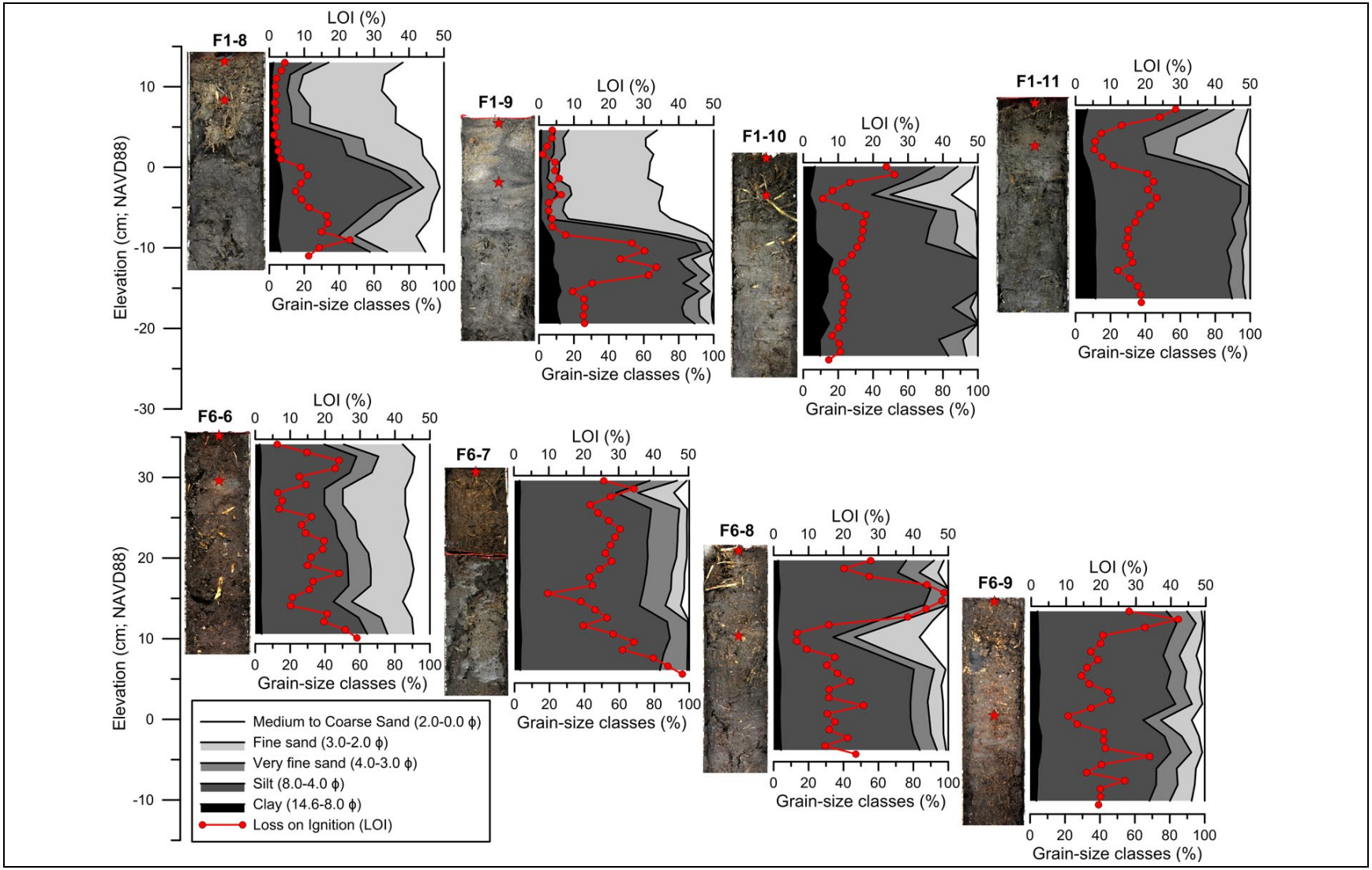

Figure 9-17. Saltmarsh cores.

Photographs of the cores collected across the backbarrier marshes at the Transgressive Site (top) and Regressive Site (bottom). Samples used for measuring grain size and LOI are plotted relative to NAVD88 at their midpoint depth, for example, a sample from 0–1 cm is plotted at 0.5 cm and adjusted for the elevation of the ground. The stars mark the locations of samples shown in **Figure 9-7** (for additional information, see **Figure 9-7**).

Backbarrier-Marsh Sand Source, FS 1. Historically, overwash has been a significant source of sand to the backbarrier marsh at this site. Hurricane Fran (in 1996) initially deposited the washover fan over backbarrier marsh there with a more recent landward expansion of the fan during Hurricane Floyd in 1999 (Foxgrover, 2009). Based on historical aerial photography, all of the cores for this study were collected northwest (landward) of the washover fan. Washover deposits are characterized by heavy-mineral laminae, are predominantly inversely graded and are composed of subhorizontal (landward dipping) planar stratification (Leatherman and Williams, 1977; Schwartz, 1982). None of the muddy-sand beds in the cores have those characteristics; however, it is possible that the sand bed sampled at the top of core FS 1-9, which contains heavy minerals, is part of the distal washover fan. In core FS 1-9, the distinct characteristic sedimentary structures and bedding, observed in many washover fans, may have been obscured by bioturbation after emplacement. Sediment texture should help distinguish whether water or wind was the transport medium. The storm surge and wave run up associated with Hurricane Irene (which impacted Onslow Beach during our study period), however, overwashed the dune at the Transgressive Site and distributed dune sediment 10–15 m across the washover fan with no textural modification to the sediment.

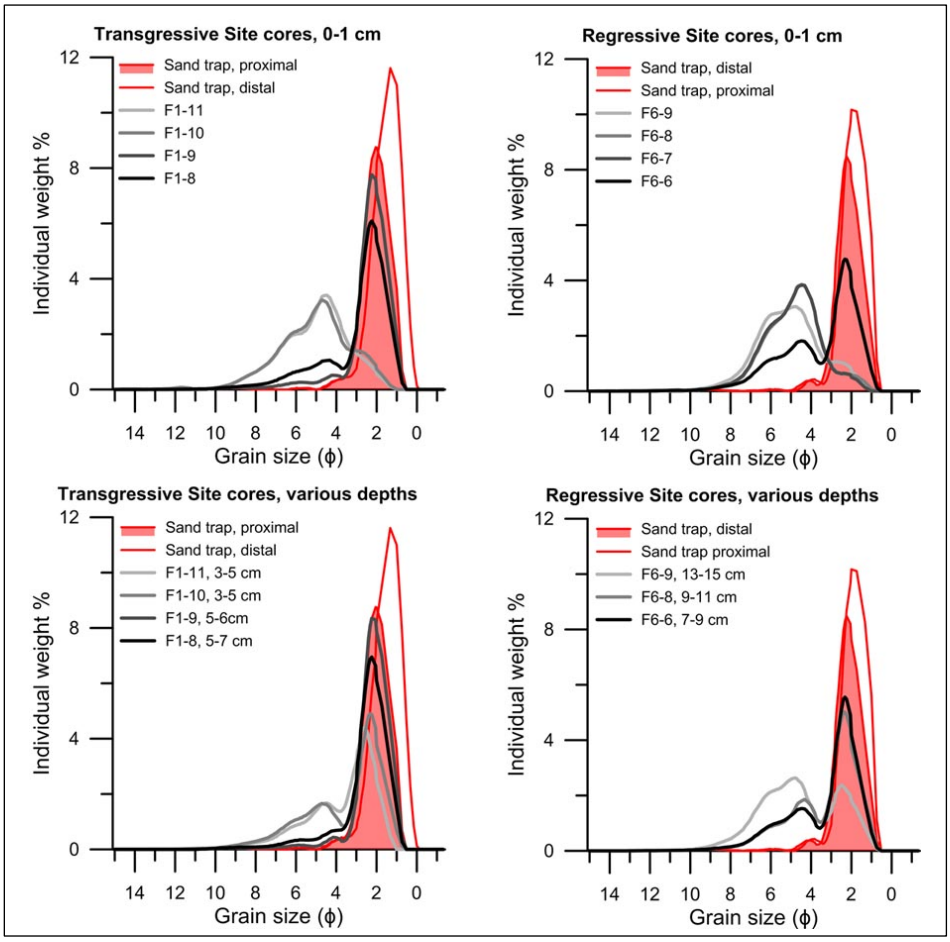

Figure 9-18. Grain-size distribution of the top 1 cm of each core and the muddy sand beds at depth compared with the grain size distribution of the proximal and distal sand traps.

FS 1 is the Transgressive Site and FS 6 is the Regressive Site. Notice that the grain-size distribution of the top 1 cm of cores FS 6-7 and FS 6-8 plot on top of each other.

The texture of the sand component of the muddy sand beds sampled in the backbarrier marsh should reflect the source material and transport mechanism. The sand component of the upper 1 cm of the marsh cores has a mean grain size of approximately 2.0 ϕ (0.25 mm), which is close to the mean grain size of sand collected in traps at the dune (proximal trap) and finer than the mean grain size of the sand collected in the traps on the washover fan close to the marsh (distal sand trap; **Figure 9-18**) and the other beach zones (**Figure 9-4**). The sand component of the discrete muddy-sand beds, sampled at depth in the marsh cores here, are also about 2.0 ϕ (0.25 mm), similar to the proximal trap near the dunes (**Figure 9-7**). Given that the dunes at this site were small prior to Hurricane Fran, it is unlikely that overwash associated with that storm could transport and deposit dune sand greater than 250 m landward into the marsh without some mixing and textural modification. Based on the similarity of the texture of the sand component of the sandy mud at the top of the cores, including the sand bed at the top of core F1-9 and the muddy sand beds at depth, the sand in the backbarrier marsh at FS 1 is sourced from the dune and transported via wind. The high density of vegetation bordering the backbarrier marsh (shrubs) and near the ground at the washover fan (grasses) presently prevents most dune sand from reaching the distal traps and the backbarrier marsh. Variations in vegetation density and type across the washover fan over time, principally controlled by storms, will strongly influence the flux of sediment to the backbarrier marsh. The discrete muddy sand layers sampled in the cores represent times of increased connectivity between the dunes and backbarrier marsh sediment, which was likely associated, in part, with a decrease in vegetation density.

Backbarrier-Marsh Sand Source, FS 6. Unlike FS 1, the high-elevation continuous dune line at FS 6 has prevented overwash from impacting the backbarrier marsh for at least the past 100 years (Foxgrover, 2009). The sand collected in the pitfall traps at this site is slightly finer near the marsh than near the foredune (**Figure 9-16**). The mean grain size of the sand component of the upper 1 cm of the marsh cores is 2.3 ϕ (0.20 mm). This is finer than the mean grain size of sand sampled from the other beach zones and in the foredune trap, but similar to the mean grain size of sand collected in the trap positioned closest to the marsh (**Figure 9-18**). The sand component of the muddy-sand beds sampled at depth also has a mean grain size that is similar to the sand collected in the most distal trap in the dunes (**Figure 9-18**). Across a morphologically similar coastal dune in the Netherlands, the mean grain size was also observed to decrease in a landward direction and this was attributed to small grains being lifted higher, falling more slowly, and traveling further landward than coarse grains (Arens et al., 2002). Based on the textural similarity of the sand sampled at the surface and at depth in the backbarrier marsh and the absence of overwash, we infer that the deposition of sand in the backbarrier marsh at this site is sourced from the dune and transported via wind.

Percent volume aeolian sand in the backbarrier marsh. To calculate the percent volume of backbarrier marsh surface composed of aeolian sand we assumed all sand within a sample was aeolian. We estimated the volume of sand by multiplying the mass of the sample after ignition by the percent of the post-ignited sample that was sand (based on grain-size analysis), and dividing that product by the density of the aeolian sand (measured in the laboratory to be 2.65 ±0.096 g cm^{-3}). The total volume of the sample was determined by the dimensions of the core tube. The top 1 cm of the backbarrier marsh inorganic sediment that is composed of aeolian sand at both sites decreases by an order of magnitude approximately 20 m from the marsh edge (**Figure 9-19**). The likely explanations for the sharp decrease in sand content of the marsh away from the barrier is the increased distance from the sediment source and the high vegetation

density of the marsh, which traps sand moving by saltation and traction and baffles the wind. In addition, the elevation of the marsh decreases away from the barrier and aeolian sediment movement close to the bed would be prevented during tidal inundation, the duration of which increases as intertidal elevations decrease.

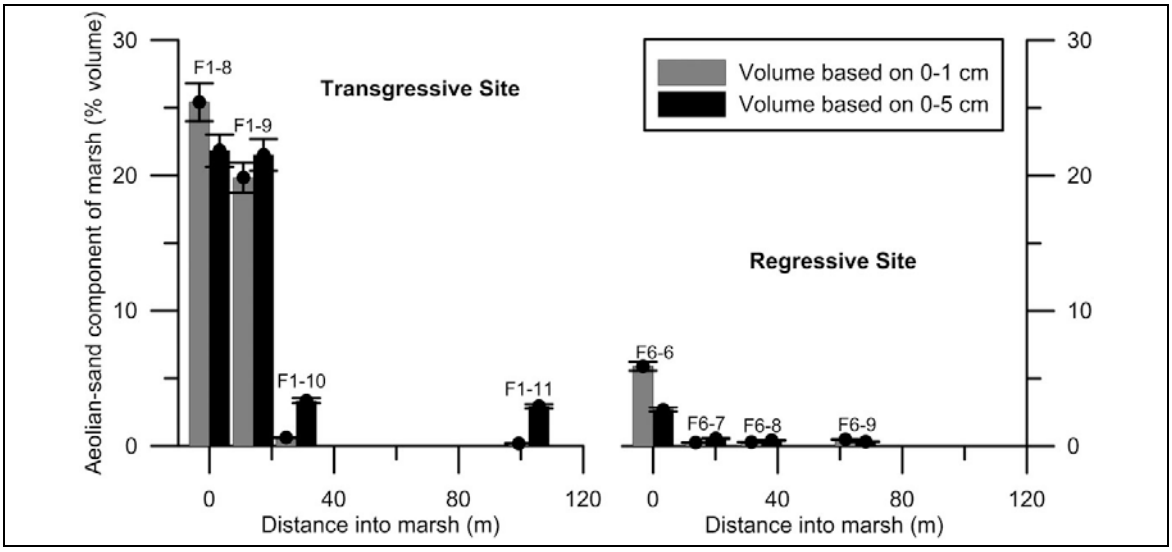

Figure 9-19. The percent of the backbarrier marsh that is composed of aeolian sand.

Calculations were made for the top 1 and 5 cm of each core (see **Figure 9-17** for additional information). Distance into the marsh is measured from the core collected closest to the barrier.

Many factors likely impacted sediment flux at our sites throughout the year, including changes in wind speed and direction, sediment moisture (Wiggs et al., 2004), seasonal vegetation cover (Lancaster and Baas, 1998), morphology of the foredune (Christiansen and Davidson-Arnott, 2004), and surface crusts (Belnap et al., 2001; O'Brien and McKenna Neuman, 2012). Sediment capture rates of the traps across the dunes at both sites and the washover fan at FS 1 were not constant through time, which is shown in **Figure 9-16** by the large SD around the mean. Similarly, near the backbarrier marsh the capture rates of the traps were also variable through time. The top 1 cm of cores FS 1-10 and FS 1-11 have 0.61 ±0.03% and 0.19 ±0.01% volume aeolian sand, respectively, which likely reflects the past 2–3 years of deposition. The top 5 cm of those same cores have approximately 3 ±0.18% aeolian sand by volume, which likely reflects the past 10–15 years of deposition. The difference in percent sand between the different sample sizes of cores FS 1-10 and FS 1-11 results from the 0–5 cm sample, including the top of a muddy-sand bed at approximately 3 cm down core (**Figure 9-17**).

Storms impact the flux of wind-blown sediment to the backbarrier marsh at FS 1, but over a timescale that is longer than the event itself. During overwash, a mixture of dune, beach and shoreface sediment is emplaced as a new washover fan or across an existing washover fan near the marsh. Subsequently, wind erodes the washover fan and transports sand, principally the dune-sand component of the fan, to the backbarrier marsh. In addition, storms decrease the vegetation density across a barrier through salinization of the water table and burial, which increases aeolian sediment transport to the backbarrier marsh until the vegetation can recover. Through time, the surface of the washover fan becomes "armored" with a coarse-grained sand and gravel layer, which was sampled in the surface sediment across the washover fan at FS 1

(**Figure 9-4**). As the armored surface develops across the washover fan and vegetation emerges, the flux of sand to the backbarrier marsh will decrease because of the decrease in source area (armoring and roots binding the sediment), flow, and transport.

Sand can also be delivered to the backbarrier marsh by suspended grainfall, which was found by Anderson and Walker (2006) to be capable of supplying a significant amount of sand greater than 300 m beyond the foredune in a coastal setting. At Onslow Beach, the foredune crest has a relatively low elevation making suspended grainfall an unlikely mechanism for delivering sand inland under current conditions. The lower sand content of the marsh at FS 6 is likely due to the higher elevation dunes fronting the marsh and creating a wind shadow, which has been colonized with maritime forest. A decrease in vegetation density of the high-elevation dunes at FS 6 should increase the contribution of sand to the backbarrier marsh via suspended grainfall. In addition, the flux of aeolian sand to the backbarrier marsh at this site is only dependent upon wind events: storm surge and associated overwash deposition is not a factor because of the continuous high dune ridge and muddy backbarrier tidal channels.

Assessment of Trends in the Data

Assessment of Monitoring Design

The number of stations and their spatial placement and the frequency of sampling are adequate to address all of the objectives.

Barrier Morphology

The three main use zones of Onslow Beach (off-road recreation vehicles, military training, and recreation or foot traffic) were each sampled with four to five 150-m wide (in an along-beach direction) focus sites. Spacing between sites is less than 600 m. That spacing is a much smaller distance than the variations in the underlying geology of Onslow Beach, which is at the 5,000-m scale (Riggs et al., 1995), and the width of the three main use zones, which is at the 3,000-m scale. **Figure 9-9** shows that the spatial placement of the sampling resolved areas of the beach influenced by the New River Inlet (FS 0.1–FS 1), the southern embayment with sediment-starved inner shelf (FS 2–FS 4) and northern embayment with sandy inner shelf (FS 4.1–FS 7). The timeframe we were interested in resolving morphologic changes over was yearly, making the semiannual sampling appropriate.

Sediment Texture and Composition

The three main use zones of Onslow Beach (off-road recreation vehicles, military training, and recreation or foot traffic) were each sampled with two 150-m wide (in an along-beach direction) focus sites. Although spacing between sites can be up to 2,000 m, the spacing is a much smaller distance than the variations in the underlying geology of Onslow Beach (Riggs et al., 1995). **Figures 9-11 and 9-12** show that the spatial placement of the sampling resolved distinct lithologies of the southern and northern embayments. The timeframe we were interested in resolving changes over was yearly, making the semiannual sampling appropriate.

Aeolian Sand Transport

The two sites chosen for monitoring aeolian transport at Onslow Beach represent morphologic end members. FS 6 has a high-elevation dune ridge and a wide beach, whereas FS 1 has a low-elevation dune ridge, a narrow beach, and a wide washover fan. Results from FS 1 are applicable to the southwestern portion of the island, and results from FS 6 are applicable to the northeastern portion of the island. Even though the morphology was different, both sites showed similar results, indicating that vegetation density drives cross-beach variations in aeolian transport. Sediment-capture rates of the traps across the dunes at both sites and the washover fan at FS 1 (the Transgressive Site) were not constant through time, which is shown in Figure 9-16 (left panel) by the large standard deviation around the mean. Similarly, near the backbarrier marsh, the capture rates of the traps were also variable through time. FS 1 is an old washover fan, and these results are likely not reflective of a new washover fan that has little vegetation, which will be studied in DCERP2.

Results from our 14 temporal observations (filtered for wind speed and direction) all indicate similar results. We would have expected that the standard deviation between the samplers would be much higher if our design was not appropriate. Therefore, we determined that both the spatial and temporal scales of our monitoring assessment are adequate to capture the range of vegetation densities that exist on the island. Additional analyses of our aeolian sand transport data are presented by Rodriguez et al. (2013).

Assessment Seasonal and Annual Variability in the Data

Trends in shoreline movement through time are presented in **Figure 9-9**. The R^2 valued indicates the applicability of using the shoreline movement rate for making predictions. A low R^2 indicates high variability in the position of the shoreline. Overall, no consistent change in beach sedimentology was observed through time. Beach surface sedimentology strongly reflects the lithology of the underlying sediment (Rodriguez et al., 2012). Aeolian transport of sand across the island primarily takes place in the spring and summer, when prevailing wind directions have a southerly component.

Recommendations for Future Monitoring

It is important to continue monitoring the morphology of Onslow Beach. The dunes from FS 2 to FS 5 are narrow and a large portion of this coastline is moving landward. The elevation of the dune line is an important factor in determining the potential for overwash during storms and tidal events (lower-elevation dunes higher potential of overwash). The dunes will eventually lower their elevations as waves begin to erode them, and in some places the dunes have already been lowered (e.g., FS 2). When overwash first occurs in an area, the connectivity between the beach and backbarrier increases abruptly, which changes the sediment budget and the shoreline movement rates. After overwash occurs, past rates of shoreline movement will likely not be relevant in that area for predicting future year-to-year shoreline changes. In addition, North Carolina is continually changing their coastal management rules. Recently, the legislation has opened the door to terminal groins and North Topsail has plans for installing one at the New River Inlet. It is important to continue monitoring to evaluate whether modifications adversely impact the southwestern end of Onslow Beach.

Conclusions and Implications for Future Research

Key Scientific Findings—Fundamental Cause-and-Effect Relationships

- Onslow Beach can be broken into three different zones, defined by distinct rates of shoreline movement from 2007 to 2011, including: (1) the accreting area adjacent to the New River Inlet (FS 0.1–FS 1), where the shoreline moved 30.9 to 4.3 m/y; (2) the erosional southwestern area of the island (FS 2–FS 4) where the shoreline moved −3.7 to −6.0 m/y; and (3) the relatively stable northeastern part of the island (FS 4.1–FS 6.1), where the shoreline moved 2.4 to −1.2 m/y.
- The spatial distribution of the three zones does not correspond with the various military-use zones indicating that military activities are not impacting erosion rates.
- Variations in the underlying geology and associated sediment availability on the inner continental shelf explain why the southwestern (sediment starved) and northeastern (sediment rich) areas of the island are erosional and accretional, respectively.
- The area adjacent to the inlet is dynamic, and the new area that formed over the past 4 years is expected to erode away during the next 4 years. FS 7 (the most northeastern site) is heavily influenced by disposal of dredged material, which is why that site eroded over the past 4 years.
- The sediment texture sampled at the erosional southwestern area (FS 1, FS 2, and FS 3) is distinct (coarser) than the sediment sampled at the accretionary northeastern area (FS 5 and FS 6), indicating limited sediment exchange between those two zones.
- Limestone exposures at the seafloor on the inner continental shelf are not an important source of sand to Onslow Beach.
- The percent volume of the marsh that is aeolian sand, based on the upper 1 cm of marsh sediment, decreases by an order of magnitude only approximately 20 m from the edge. Near the edge, the backbarrier marsh contains greater than 20% or less than 10% aeolian sand (by volume) where it is fronted by a washover fan (FS 1) or a high-elevation dune ridge (FS 6), respectively. Further into the marsh platform, the percent volume of aeolian sand is consistently low at both sites (less than 1%).

Findings Supportive of Current Base Management Practices

- Maintaining the current practice of keeping vehicles and people off the dunes, especially in the military training zone where the shoreline is moving landward rapidly, will temper shoreline recession rates.
- The low erosion rates measured at the northeastern part of the barrier supports the placement of recreational infrastructure there, as opposed to at the southwestern part of the barrier, where erosion rates are higher.

Findings with Implications for Future Base Management

- Sand emplaced at the northeastern end of the island will not be transported naturally along shore past the headland (FS 5) and mitigate erosion in the southwest part of the island.
- Additional investment in beach infrastructure (permanent structures) should be limited so that losses from storm impacts are minimized.

Literature Cited

Allen, J.R.L. 1995. Salt-marsh growth and fluctuating sea level: Implications of a simulation model for Flandrian coastal stratigraphy and peat-based sea-level curves. *Sedimentary Geology 100*:21–45.

Anderson, J.L., and I.J. Walker. 2006. Airflow and sand transport variations within a backshore–parabolic dune plain complex: NE Graham Island, British Columbia, Canada. *Geomorphology 77*:17–34.

Anderson, R.S. 1988. The pattern of grainfall deposition in the lee of aeolian dunes. *Sedimentology 35*:175–188.

Arens, S.M. 1996. Patterns of sand transport on vegetated foredunes. *Geomorphology* 17:339–350.

Arens, S.M., J.H. van Boxel, and J.O.Z. Abuodha. 2002. Changes in grain size of sand in transport over a foredune. *Earth Surface Processes and Landforms 27*:1163–1175.

Armon, J.W., and S.B. McCann. 1979. Morphology and landward sediment transfer in a transgressive barrier island system, southern Gulf of St. Lawrence, Canada. *Marine Geology 31*:333–344.

Bartholdy, J., C. Christiansen, H. Kunzendorf. 2004. Long-term variations in backbarrier salt marsh deposition on the Skallingen peninsula—the Danish Wadden Sea. *Marine Geology 203*:1–21.

Belnap, J., J. Kaltenecker, R. Rosentreter, J. Williams, S. Leonard, and D. Eldridge. 2001. *Biological Soil Crusts: Ecology and Management*. Technical Reference 1730-2. U.S. Department of the Interior, Bureau of Land Management, U.S. Geological Survey, Forest and Rangeland Ecosystem Science Center, Denver, CO. Edited by P. Peterson. Available at http://nature.nps.gov/geology/soils/biological%20soil%20crusts.pdf.

Benton, S.B., C.J. Bellis, J.M. Knisel, M.F. Overton, and J.S. Fisher. 2004. *1998 Long-Term Average Annual Erosion Rate Update: Methods Report (March 18)*. North Carolina Division of Coastal Management, North Carolina Coastal Resources Commission. 23 pages.

Benton, S.B., C.J. Bellis, M.F. Overton, M.F. Fisher, and J.L. Hench. 1993. *Long-Term Average Annual Rates of Shoreline Change: Methods Report 1992 Update*. North Carolina Department of Environmental and Health Natural Resources, Division of Coastal Management, Raleigh, NC. 16 pages.

Christiansen, M.B., and R. Davidson-Arnott. 2004. Rates of landward sand transport over the foredune at Skallingen, Denmark and the role of dune ramps. *Danish Journal of Geography 104*:31–43.

Cleary, W.J., and S.R. Riggs. 1999. Beach erosion and hurricane protection plan for Onslow Beach, *Camp Lejeune, North Carolina: Management Plan*. U.S. Marine Corps. Report 1277.

Cleary, W.J. and O.H. Pilkey. 1996. Environmental coastal geology: Cape Lookout to Cape Fear, North Carolina regional overview. *Environmental Coastal Geology: Cape Lookout to Cape Fear, NC*. Edited by W.J. Cleary. *Carolina Geological Society Fieldtrip Guidebook*:87–128.

Craft, C.B., E.D. Seneca, and S.W. Broome. 1993. Vertical accretion in microtidal regularly and irregularly flooded estuarine marshes. *Estuarine, Coastal and Shelf Science 37*:371–386.

Davidson-Arnott, R.G.D., and M.N. Law. 1996. Measurement and prediction of long-term sediment supply to coastal foredunes. *Journal of Coastal Research 12*:654–663.

de Groot, A.V., R.M. Veeneklaas, and J.P. Bakker. 2011. Sand in the salt marsh: Contribution of high-energy conditions to salt-marsh accretion. *Marine Geology 282*:240–254.

DeLaune, R.D., C.J. Smith, and W.H. Patrick. 1986. Sedimentation patterns in a Gulf Coast backbarrier marsh: Response to increasing submergence. *Earth Surface Processes and Landforms 11*:485–490.

Delgado-Fernandez, I., and R. Davidson-Arnott. 2011. Meso-scale aeolian sediment input to coastal dunes: The nature of aeolian transport events. *Geomorphology 126*:217–232.

Filardi, M.P. 1999. *Influence of Underlying Geology on Beach Erosion: Onslow Beach, North Carolina*. M.S. Thesis. East Carolina University, Greenville, NC. 186 pages.

Foxgrover, A.C. 2009. *Quantifying the Overwash Component of Barrier Island Morphodynamics: Onslow Beach, NC*. Page 145 in Master's Thesis. The College of William and Mary, Williamsburg, VA.

French, J.R., and T. Spencer. 1993. Dynamics of sedimentation in a tide-dominated backbarrier salt marsh, Norfolk, UK. *Marine Geology 110*:315–331.

Harris, W.B., S. Mendrick, and P.D. Fullagar. 2000. Correlation of onshore-offshore Oligocene through lower Miocene strata using $^{87}Sr/^{86}Sr$ isotopic ratios, north flank of Cape Fear Arch, North Carolina, USA. *Sedimentary Geology 134*:49–63.

Hatton, R.S., R.D. DeLaune, and W.H.J. Patrick. 1983. Sedimentation, accretion, and subsidence in marshes of Barataria Basin, Louisiana. *Limnology and Oceanography 28*:494–502.

Heiri, O., A.F. Lotter, and G. Lemcke. 2001. Loss on ignition as a method for estimating organic and carbonate content in sediments: Reproducibility and comparability of results. *Journal of Paleolimnology 25*:101–110.

Johnston, M.K. 1998. *The Inherited Geologic Framework of the New River Submarine Headland Complex, North Carolina, and Its Influence on Modern Sedimentation*. M.S. Thesis. University of North Carolina at Wilmington, Wilmington, NC. 83 pages.

Kuriyama, Y., N. Mochizuki, and T. Nakashima. 2005. Influence of vegetation on aeolian sand transport rate from a backshore to a foredune at Hasaki, Japan. *Sedimentology 52*:1123–1132.

Lancaster, N., and A. Baas. 1998. Influence of vegetation cover on sand transport by wind: Field studies at Owens Lake, California. *Earth Surface Processes and Landforms 23*:69–82.

Leatherman, S.P., and A.T. Williams. 1977. Lateral textural grading in overwash sediments. *Earth Surface Processes 2*:333–341.

Masselink, G., N. Auger, P. Russell, and T. O'Hare. 2007. Short-term morphological change and sediment dynamics in the intertidal zone of a macrotidal beach. *Sedimentology 54*:39–53.

Mattheus, C.R., A.B. Rodriguez, B.A. McKee, and C. Currin. 2010. Impact of land-use change and hard structures on the evolution of fringing marsh shorelines. *Estuarine, Coastal and Shelf Science 88*:365–376.

McLaren, P., and D. Bowles. 1986. The effects of sediment transport on grain-size distributions. *Journal of Sedimentary Petrology 55*:457–470.

O'Brien, P., and C. McKenna Neuman. 2012. A wind tunnel study of particle kinematics during crust rupture and erosion. *Geomorphology 173–174*:149–160.

Reed, D.J. 1990. The impact of sea-level rise on coastal salt marshes. *Progress in Physical Geography 14*:24–40.

Ridge, J.T., A.B. Rodriguez, S.R. Fegley, R. Browne, and D. Hood. 2011. A new "pressure sensitive" method of measuring aeolian sediment transport using a Gauged Sediment Trap (GaST). *Geomorphology 134*:426–430.

Riggs, S.R., and W.J. Cleary. 1998. *Textural Analysis of the* Silverdale Formation *on the Inner Continental Shelf, Onslow Bay, NC: Top Priority Cross-Shelf Corridor for the Shallow Water Training Range*. U.S. Marine Corps Base Camp Lejeune. 30 pages.

Riggs, S.R., W.G. Ambrose, J.W. Cook, S.W. Snyder and S.W. Snyder. 1998. Sediment production on sediment-starved continental margins: The interrelationship between hardbottoms, sedimentological and benthic community processes, and storm dynamics. *Journal of Sedimentary Research 68*:155–168.

Riggs, S.R., S.W. Snyder, A.C. Hine, and D.L. Mearns. 1996. Hardbottom morphology and relationship to the geologic framework: Mid-Atlantic continental shelf. *Journal of Sedimentary Research 66*:830–846.

Riggs, S.R., W.J. Cleary, and S.W. Snyder. 1995. Influence of inherited geologic framework on barrier shoreface morphology and dynamics. *Marine Geology 126*:213–234.

Rodriguez, A.B., S.R. Fegley, J.T. Ridge, B.M. VanDusen, and N. Anderson. 2013. Contribution of aeolian sand to backbarrier marsh sedimentation. *Estuarine, Coastal, and Shelf Science 117*:248–259.

Rodriguez, A.B., P.L. Rodriguez, and S.R. Fegley. 2012. One-year along-beach variation in the maximum depth of erosion resulting from irregular shoreline morphology. *Marine Geology 291–294*:12–23.

Schwartz, R.K. 1982. Bedform and stratification characteristics of some modern small-scale washover sand bodies. *Sedimentology 29*:835–849.

Temmerman, S., G. Govers, S. Wartel, and P. Meire. 2004. Modelling estuarine variations in tidal marsh sedimentation: response to changing sea level and suspended sediment concentrations. *Marine Geology 212*:1–19.

Thieler, E.R., E.A. Himmelstoss, J.L. Zichichi, and A. Ergul. 2009. *Digital Shoreline Analysis System (DSAS) Version 4.0—An ArcGIS Extension for Calculating Shoreline Change*. U.S. Geological Survey Open-File Report 2008-1278.

Weber, K.M., J.H. List, and K.L.M. Morgan. 2005. *An Operational Mean High Water Datum for Determination of Shoreline Position from Topographic LiDAR Data*. U.S. Geological Survey Open-File Report 2005-1027.

Wiggs, G.F.S., A.J. Baird, and R.J. Atherton. 2004. The dynamic effects of moisture on the entrainment and transport of sand by wind. *Geomorphology 59*:13–30.

Woolard, J.W. 1999. Volumetric change of coastal dunes using airborne LiDAR, Cape Hatteras National Seashore, North Carolina. M.S. Thesis. East Carolina University, Greenville, NC. 109 pages.

Woolard, J.W., and J.D. Colby. 2002. Spatial characterization, resolution, and volumetric change of coastal dunes using airborne LiDAR: Cape Hatteras, North Carolina. *Geomorphology 48*:269–287.

[This page intentionally left blank.]

Appendix 9-A

Topographic Maps of the Focus Sites Illustrating the Changes in Morphology That Occurred over the Project Period

Focus Site 0.1. The MHW line is shown as a solid red line in the first (November 2007; top) and last (September 2011; bottom) topographic maps. The MHW of November 2007 is overlain on the September 2011 map as a dashed red line. Units are in meters and both maps are at the same scale. Notice the change in orientation and position of the shoreline.

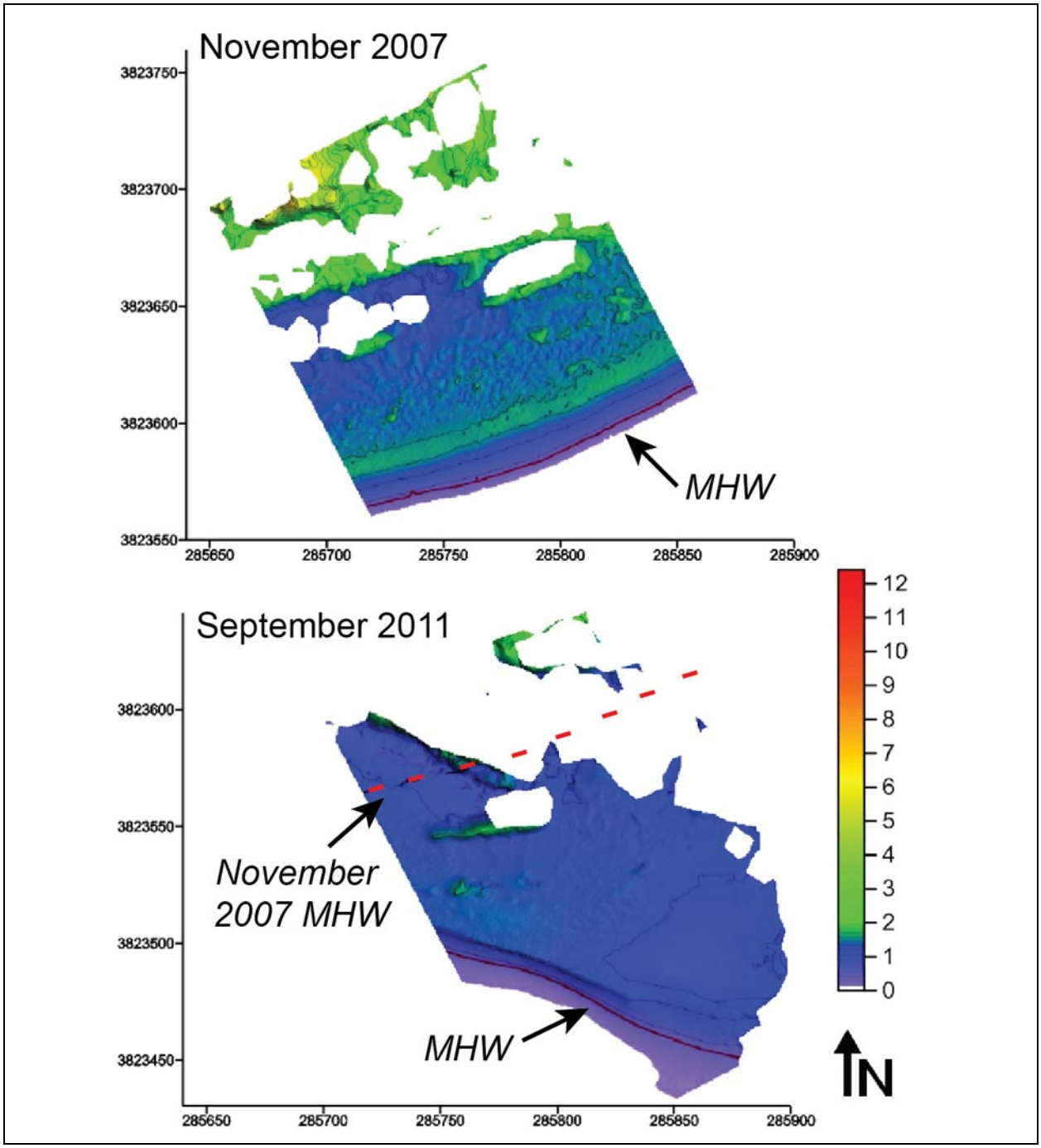

Focus Site 0.2. The MHW line is shown as a solid red line in the first (November 2007; top) and last (September 2011; bottom) topographic maps. The MHW of November 2007 is overlain on the September 2011 map as a dashed black line. Units are in meters and both maps are at the same scale.

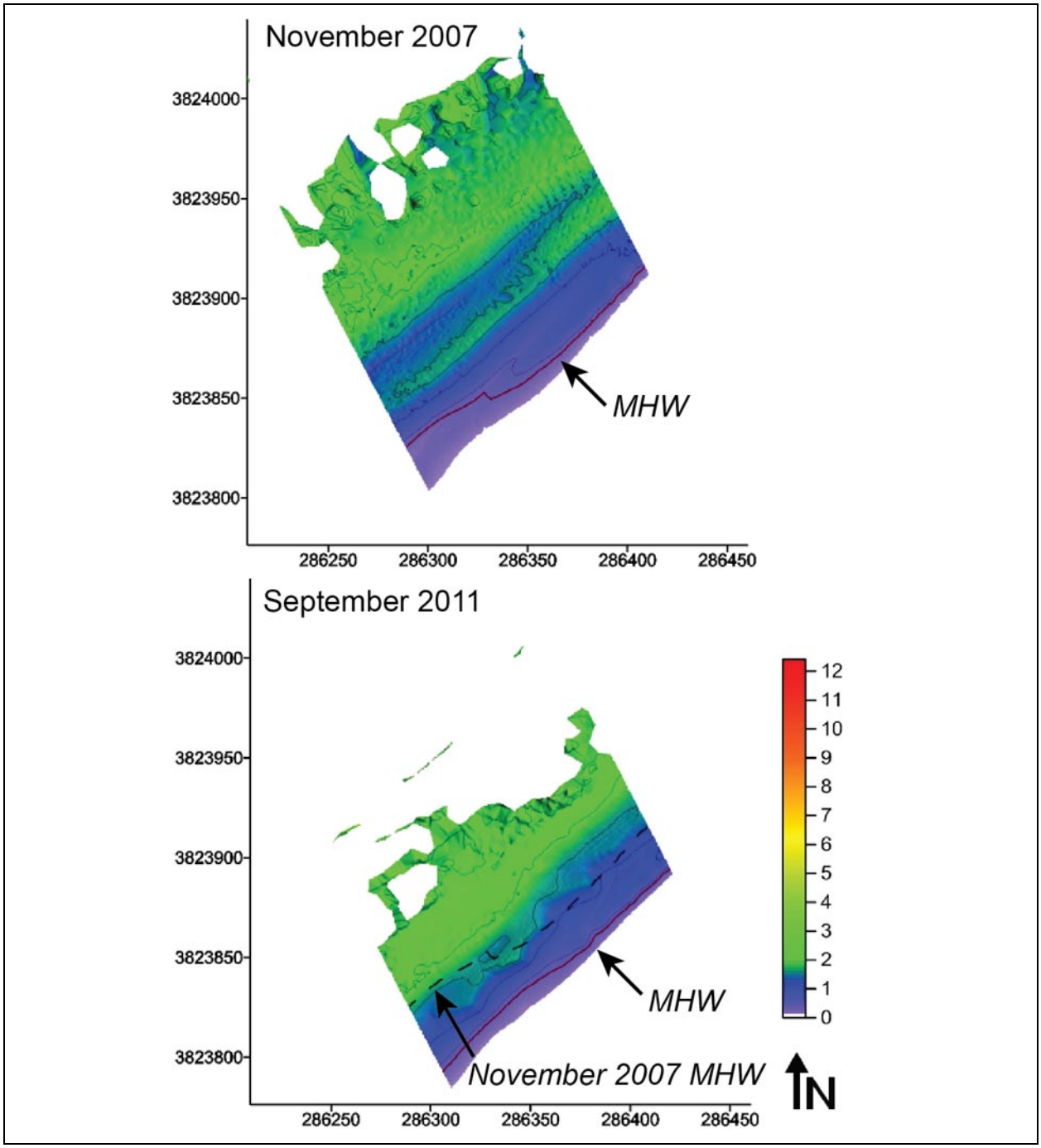

Focus Site 1. The MHW line is shown as a solid red line in the first (November 2007; top) and last (September 2011; middle) topographic maps. The MHW of November 2007 is overlain on the September 2011 map as a dashed black line. The bottom map shows the difference in elevation between the two previously mentioned maps, with blue areas representing accretion (positive elevation change), red areas representing erosion (negative elevation change), and the white areas representing no change. Units are in meters, and all maps are at the same scale.

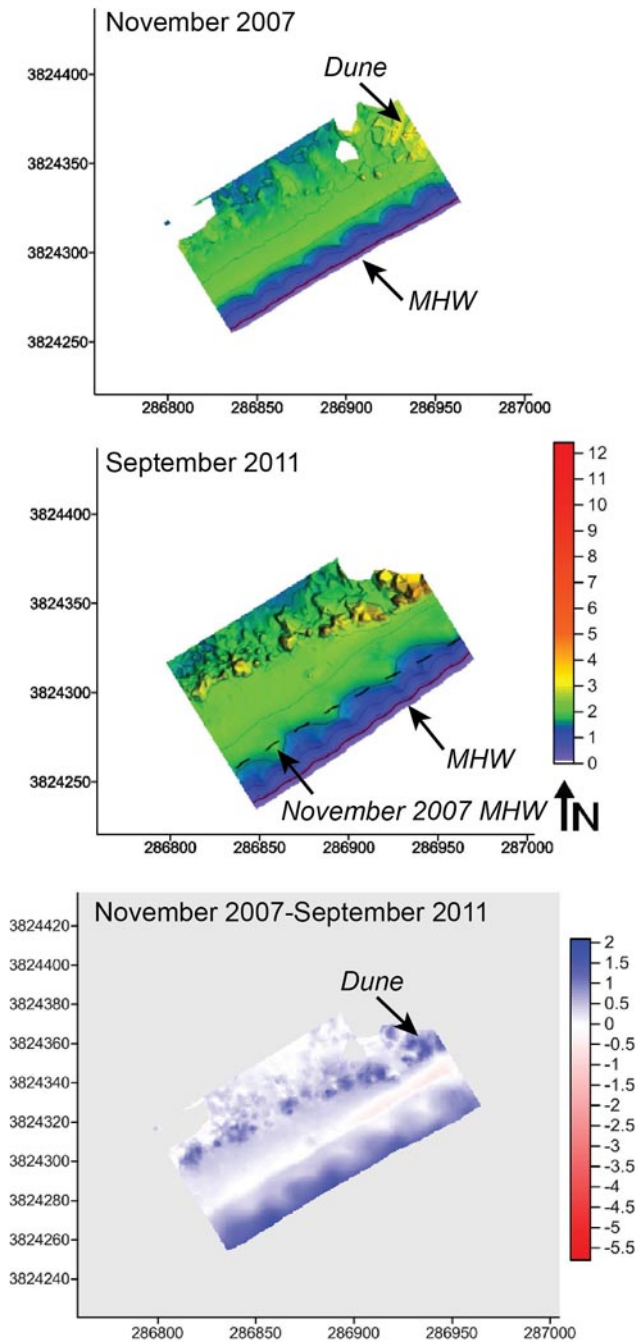

Focus Site 2. The MHW line is shown as a solid red line in the first (November 2007; top) and last (September 2011; middle) topographic maps. The MHW of November 2007 is overlain on the September 2011 map as a dashed red line. The bottom map shows the difference in elevation between the two previously mentioned maps, with blue areas representing accretion (positive elevation change), red areas representing erosion (negative elevation change), and the white areas representing no change. Units are in meters, and all maps are at the same scale.

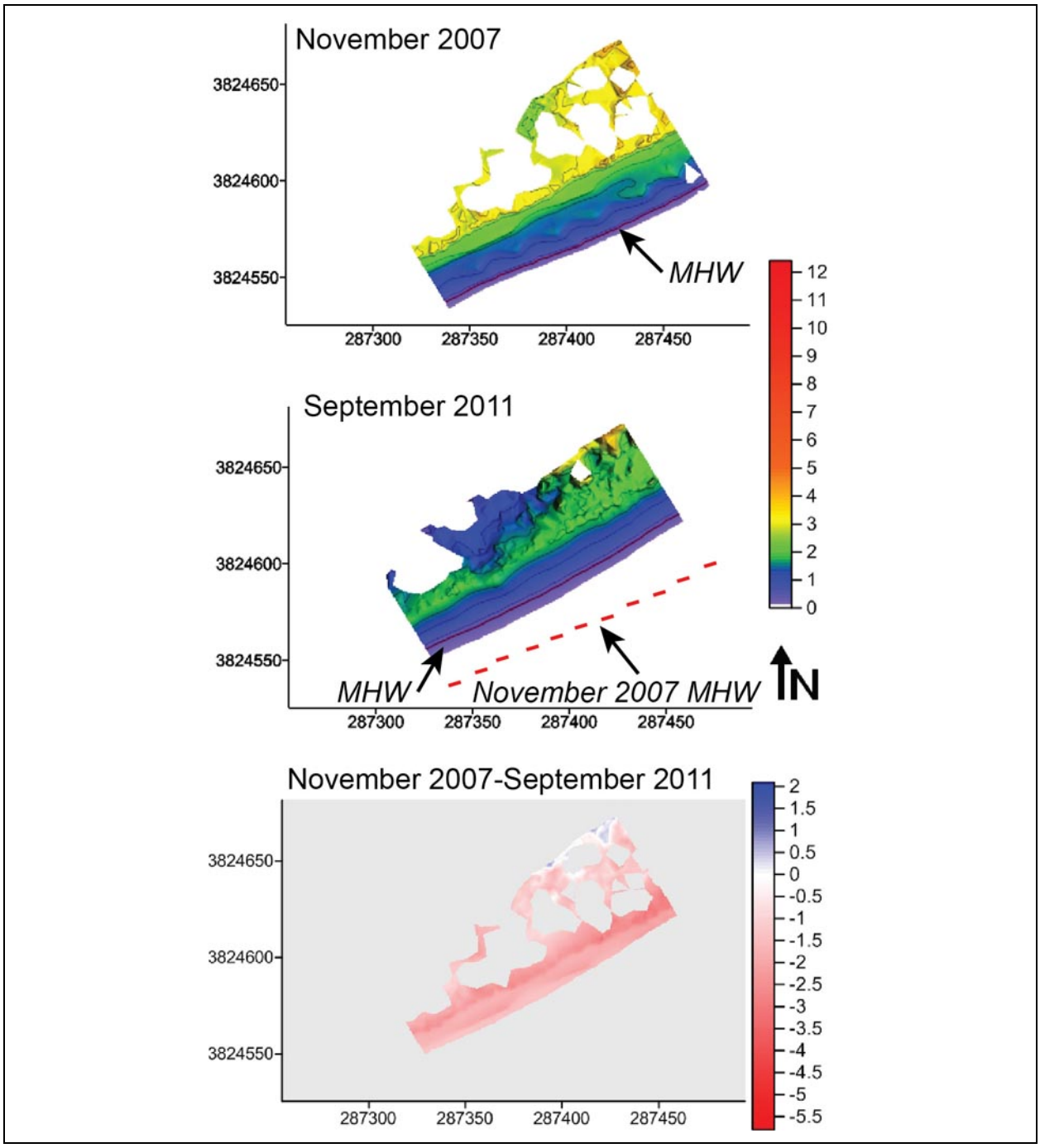

Focus Site 2.1. The MHW line is shown as a solid red line in the first (November 2007; top) and last (September 2011; middle) topographic maps. The MHW of November 2007 is overlain on the September 2011 map as a dashed red line. The bottom map shows the difference in elevation between the two previously mentioned maps, with blue areas representing accretion (positive elevation change), red areas representing erosion (negative elevation change), and the white areas representing no change. Units are in meters, and all maps are at the same scale.

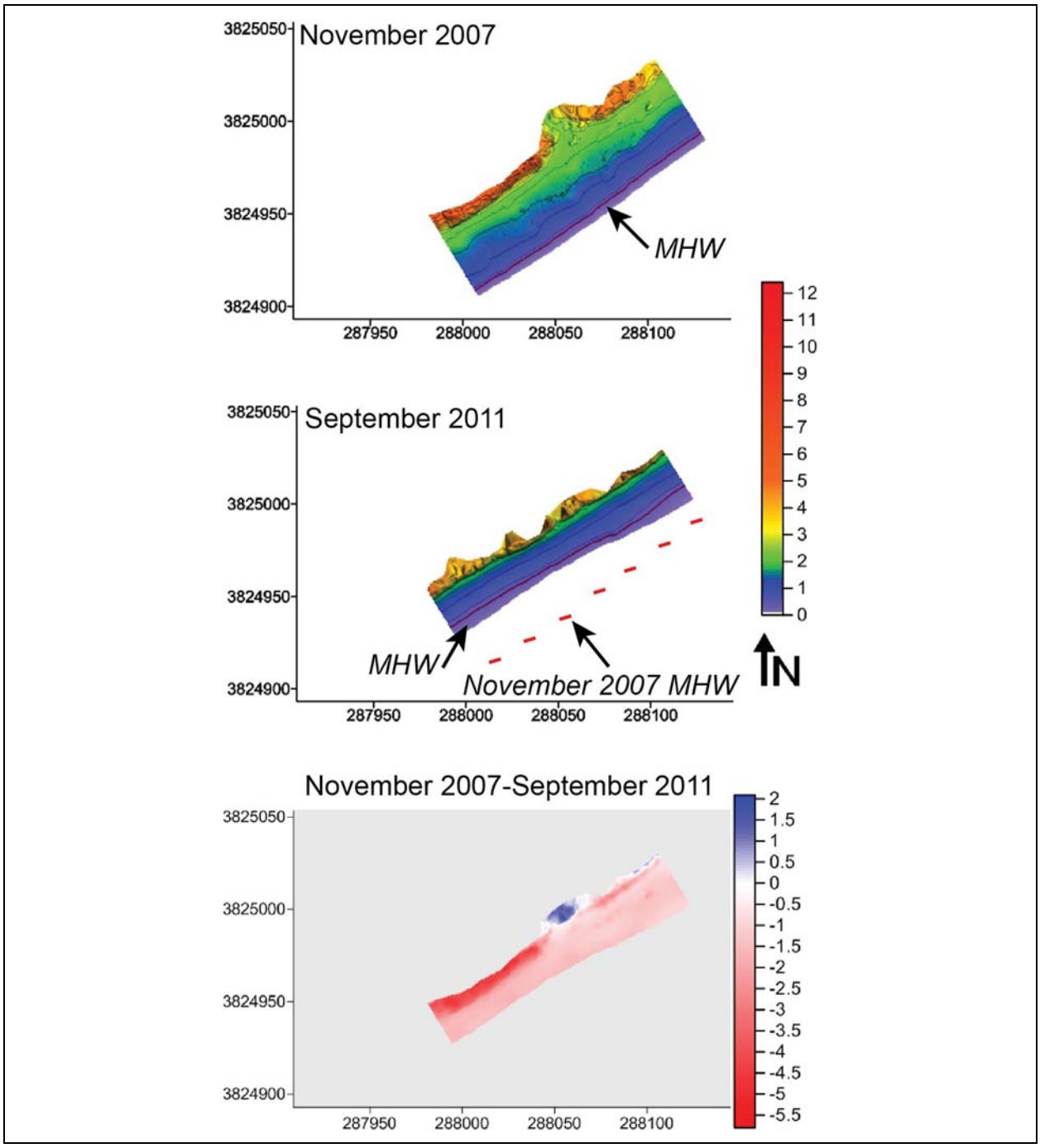

Focus Site 3. The MHW line is shown as a solid red line in the first (November 2007; top) and last (September 2011; middle) topographic maps. The MHW of November 2007 is overlain on the September 2011 map as a dashed red line. The bottom map shows the difference in elevation between the two previously mentioned maps, with blue areas representing accretion (positive elevation change), red areas representing erosion (negative elevation change), and the white areas representing no change. Units are in meters, and all maps are at the same scale.

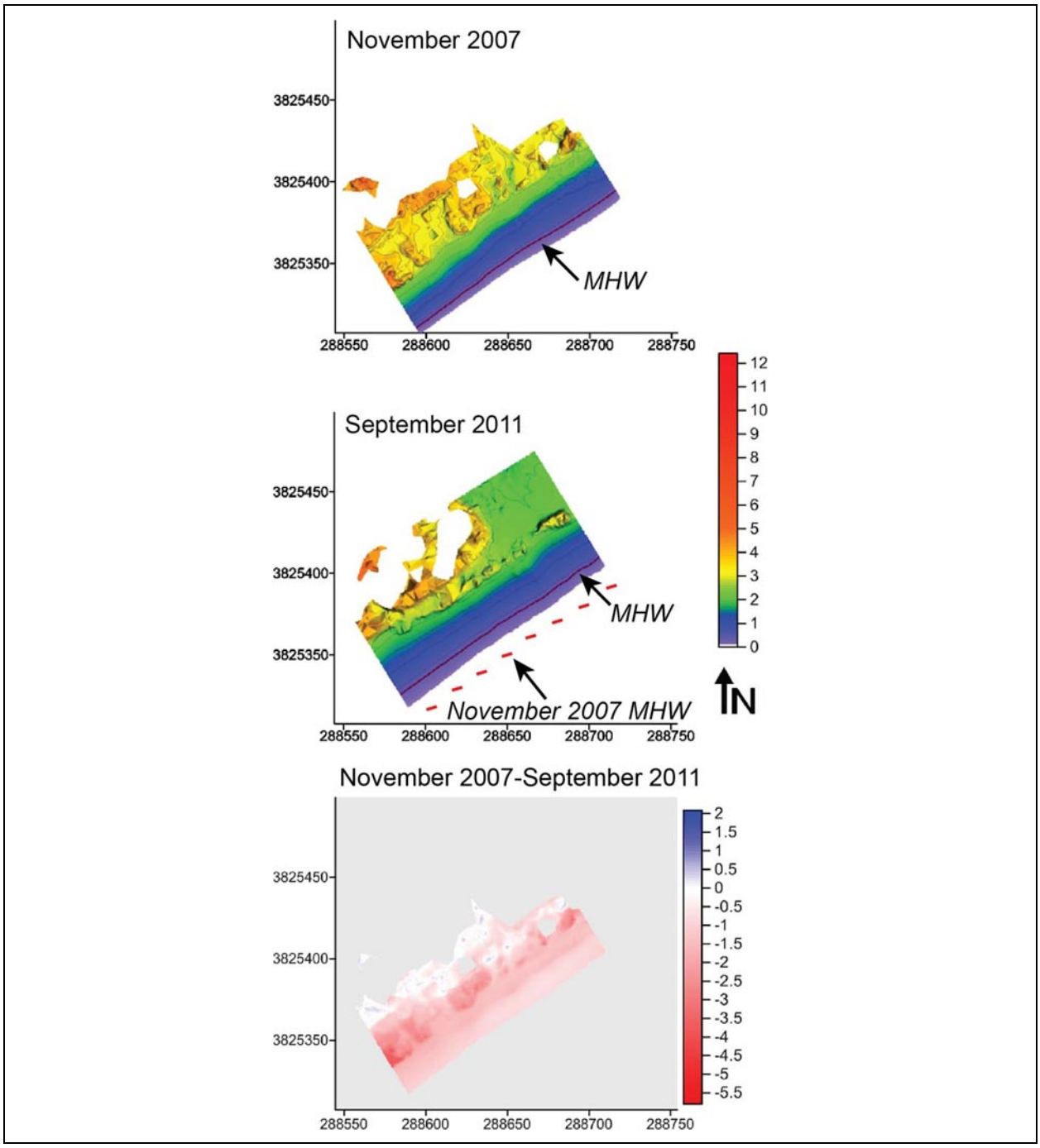

Focus Site 3.1. The MHW line is shown as a solid red line in the first (November 2007; top) and last (September 2011; middle) topographic maps. The MHW of November 2007 is overlain on the September 2011 map as a dashed red line. The bottom map shows the difference in elevation between the two previously mentioned maps, with blue areas representing accretion (positive elevation change), red areas representing erosion (negative elevation change), and the white areas representing no change. Units are in meters, and all maps are at the same scale.

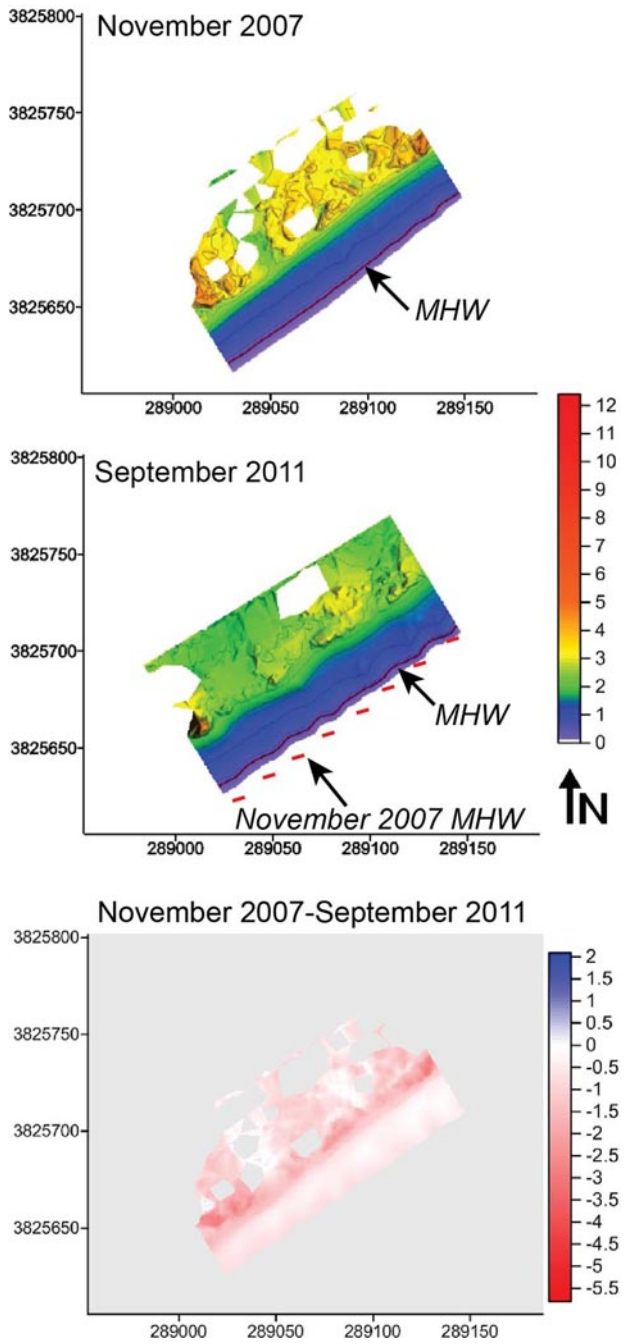

Focus Site 3.2. The MHW line is shown as a solid red line in the first (November 2007; top) and last (September 2011; middle) topographic maps. The MHW of November 2007 is overlain on the September 2011 map as a dashed red line. The bottom map shows the difference in elevation between the two previously mentioned maps, with blue areas representing accretion (positive elevation change), red areas representing erosion (negative elevation change), and the white areas representing no change. Units are in meters, and all maps are at the same scale.

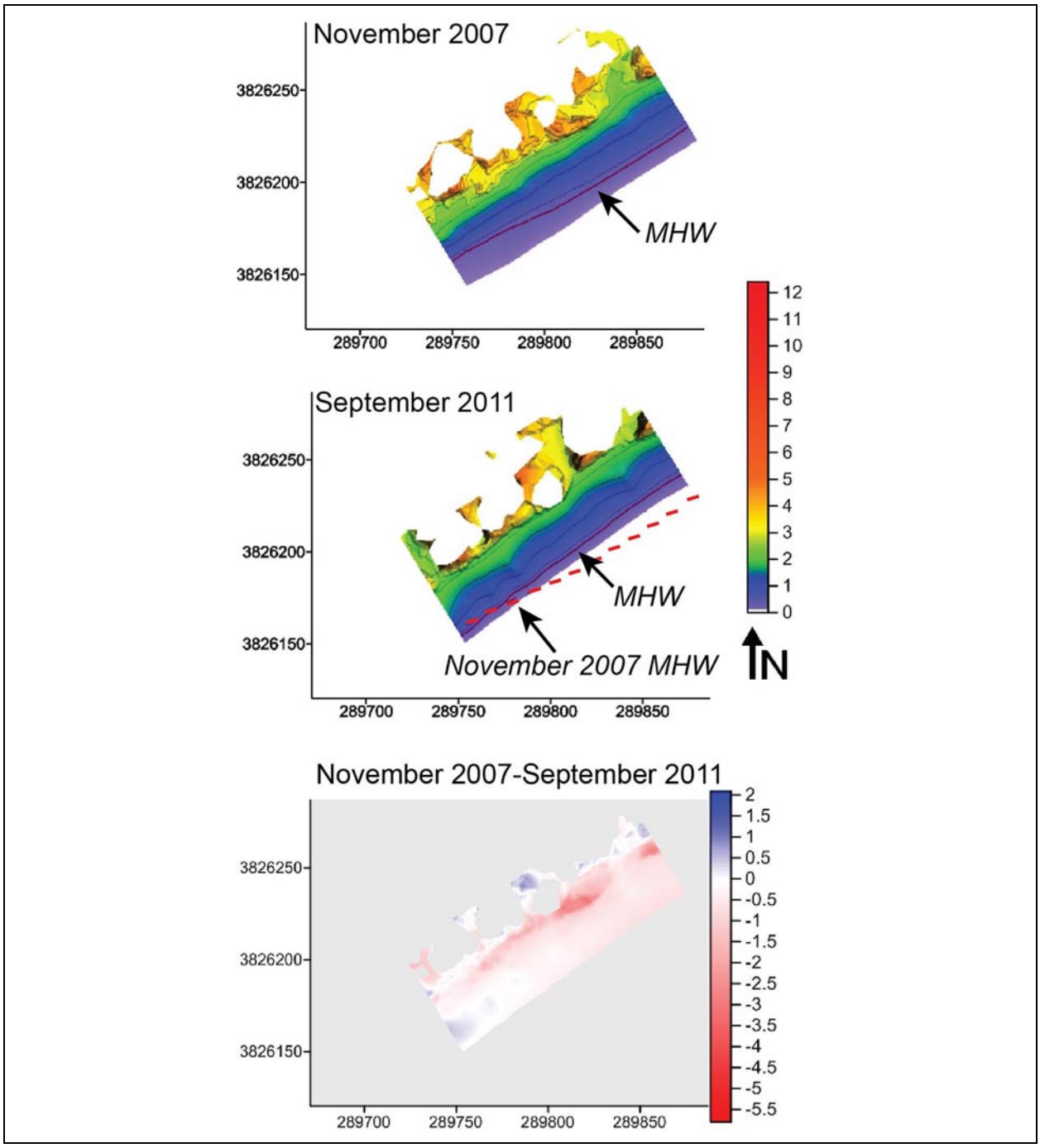

Focus Site 4. The MHW line is shown as a solid red line in the first (November 2007; top) and last (September 2011; middle) topographic maps. The MHW of November 2007 is overlain on the September 2011 map as a dashed red line. The bottom map shows the difference in elevation between the two previously mentioned maps, with blue areas representing accretion (positive elevation change), red areas representing erosion (negative elevation change), and the white areas representing no change. Units are in meters, and all maps are at the same scale.

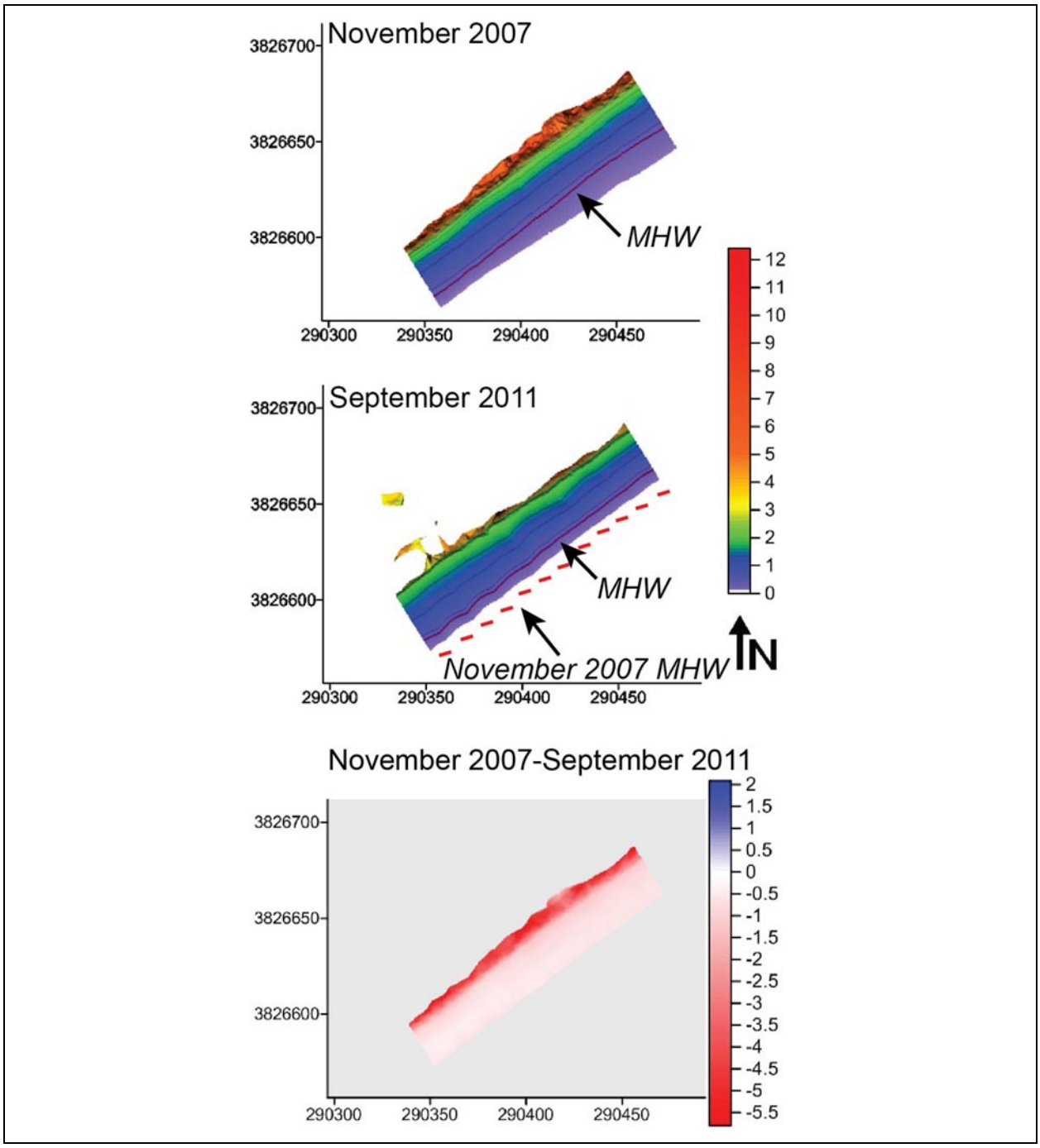

Focus Site 4.1. The MHW line is shown as a solid red line in the first (November 2007; top) and last (September 2011; middle) topographic maps. The MHW of November 2007 is overlain on the September 2011 map as a dashed red line. The bottom map shows the difference in elevation between the two previously mentioned maps, with blue areas representing accretion (positive elevation change), red areas representing erosion (negative elevation change), and the white areas representing no change. Units are in meters, and all maps are at the same scale.

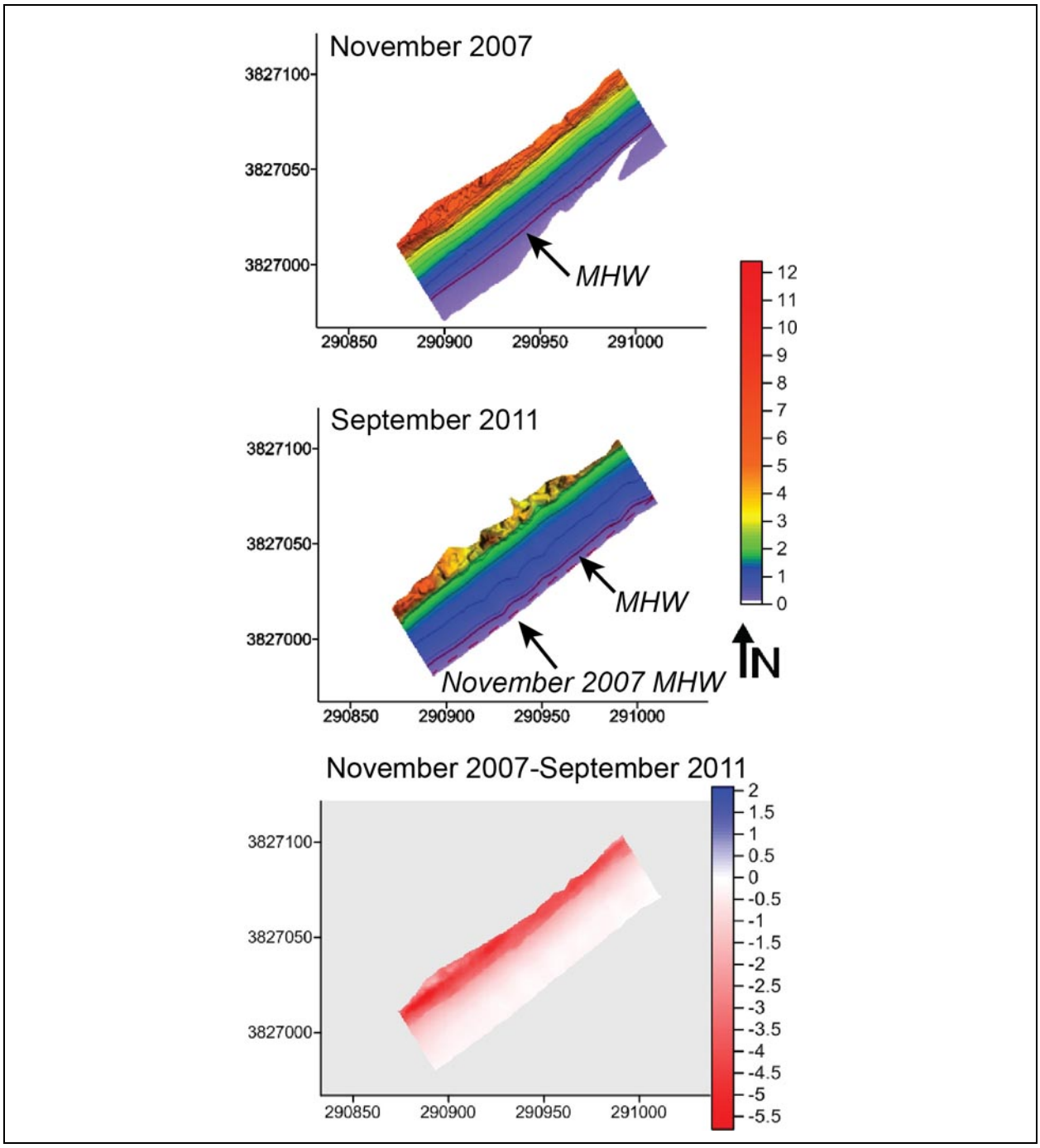

Focus Site 5. The MHW line is shown as a solid red line in the first (November 2007; top) and last (September 2011; middle) topographic maps. The MHW of November 2007 is overlain on the September 2011 map as a dashed red line. The bottom map shows the difference in elevation between the two previously mentioned maps, with blue areas representing accretion (positive elevation change), red areas representing erosion (negative elevation change), and the white areas representing no change. Units are in meters, and all maps are at the same scale.

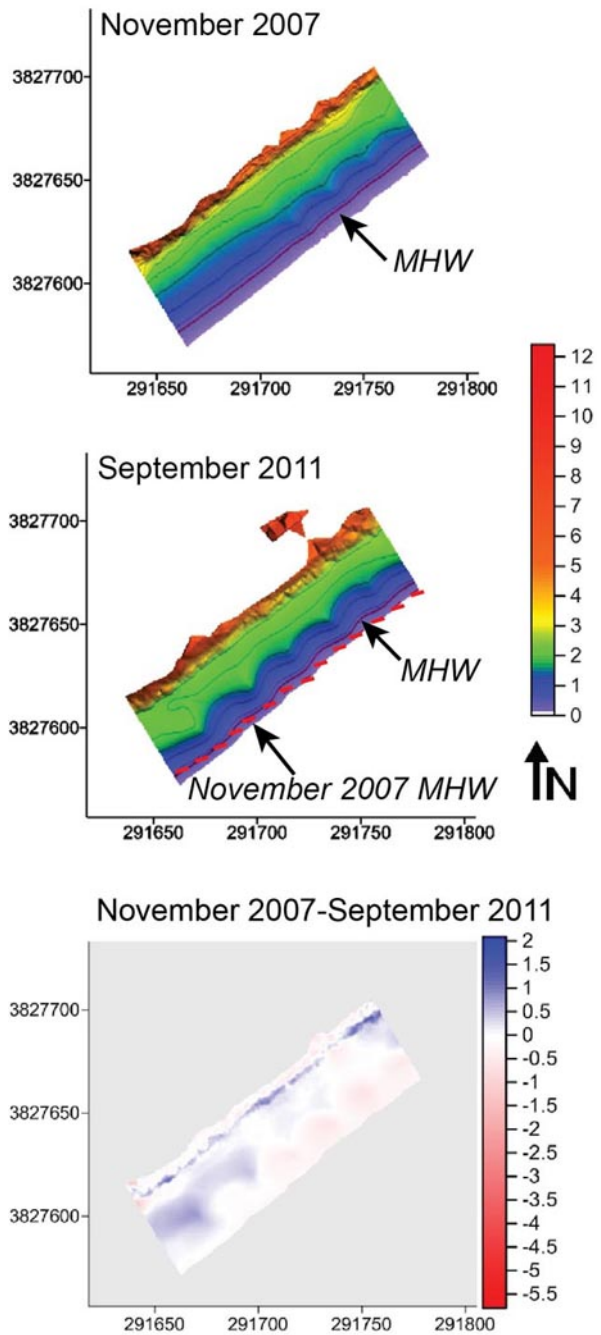

Focus Site 5.1. The MHW line is shown as a solid red line in the first (November 2007; top) and last (September 2011; middle) topographic maps. The MHW of November 2007 is overlain on the September 2011 map as a dashed red line. The bottom map shows the difference in elevation between the two previously mentioned maps, with blue areas representing accretion (positive elevation change), red areas representing erosion (negative elevation change), and the white areas representing no change. Units are in meters, and all maps are at the same scale.

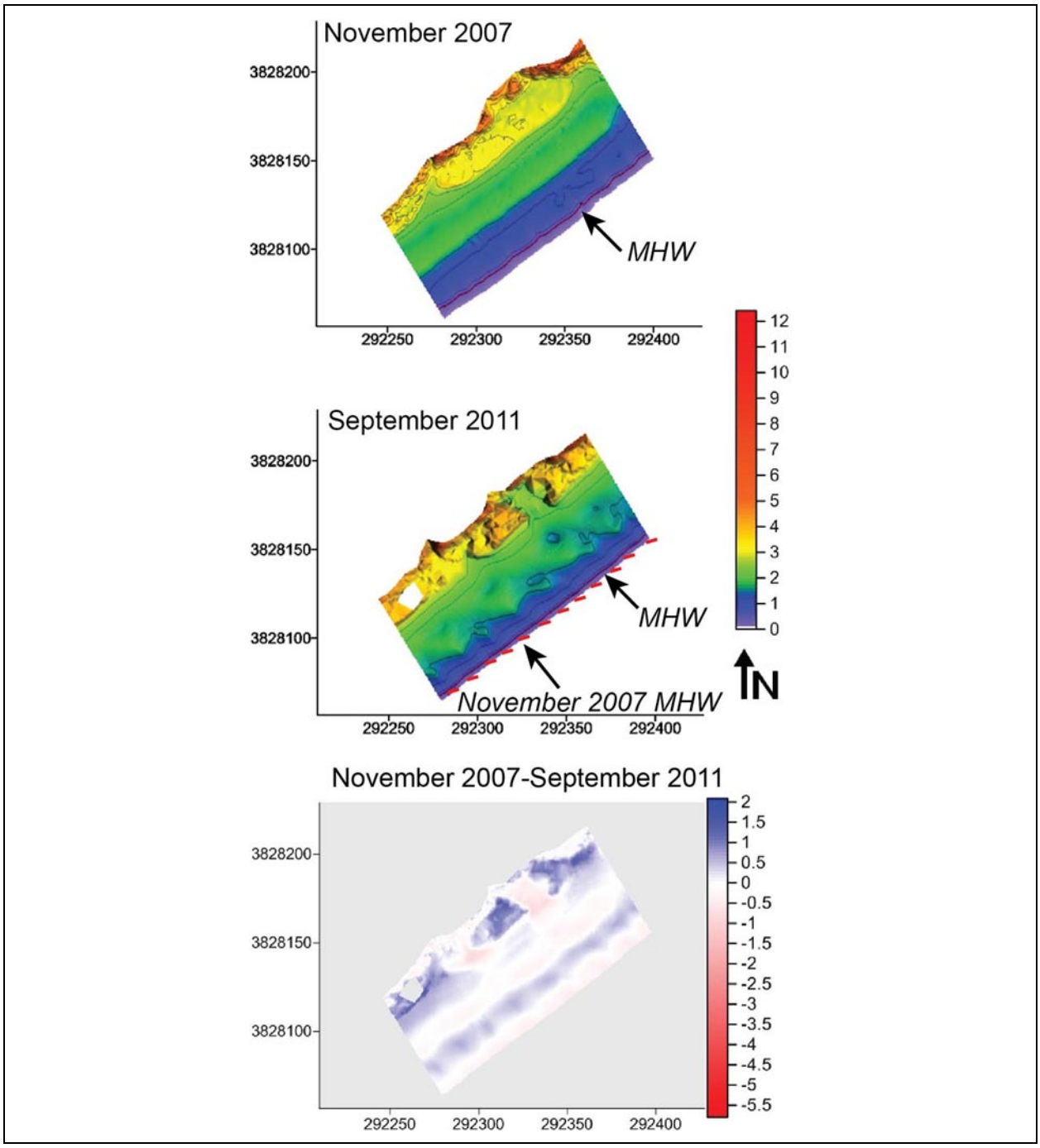

Focus Site 6. The MHW line is shown as a solid red line in the first (November 2007; top) and last (September 2011; middle) topographic maps. The MHW of November 2007 is overlain on the September 2011 map as a dashed red line. The bottom map shows the difference in elevation between the two previously mentioned maps, with blue areas representing accretion (positive elevation change), red areas representing erosion (negative elevation change), and the white areas representing no change. Units are in meters, and all maps are at the same scale.

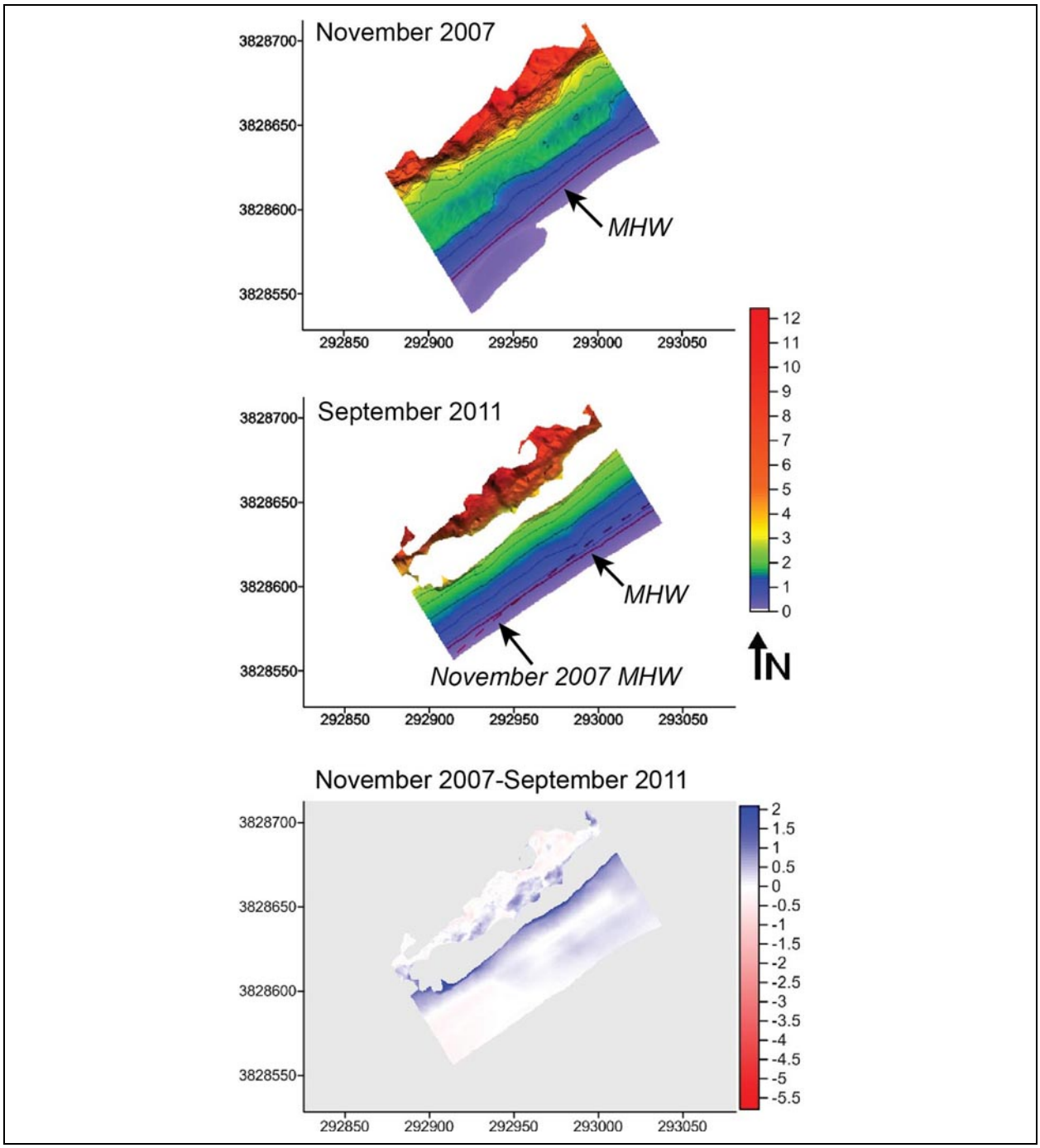

Focus Site 6.1. The MHW line is shown as a solid red line in the first (May 2008; top) and last (September 2011; middle) topographic maps. The MHW of May 2008 is overlain on the September 2011 map as a dashed black line. The bottom map shows the difference in elevation between the two previously mentioned maps, with blue areas representing accretion (positive elevation change), red areas representing erosion (negative elevation change), and the white areas representing no change. Units are in meters, and all maps are at the same scale.

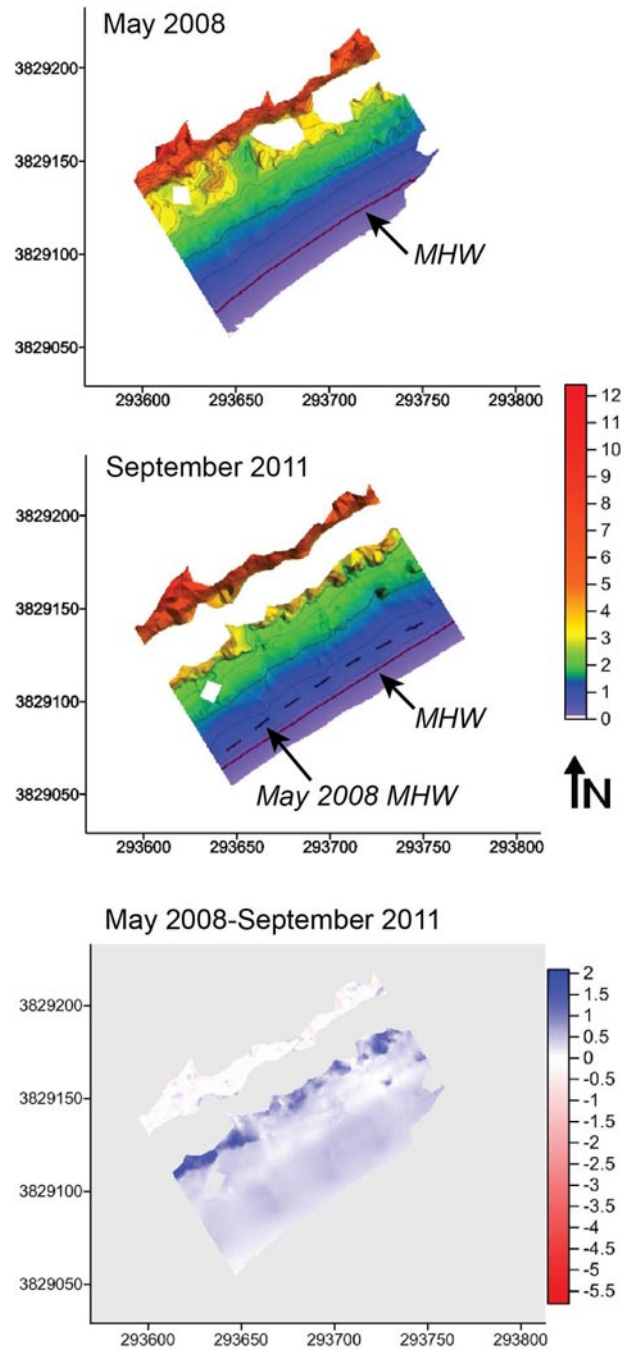

Focus Site 7. The MHW line is shown as a solid red line in the first (May 2008; top) and last (September 2011; middle) topographic maps. The MHW of May 2008 is overlain on the September 2011 map as a dashed red line. The bottom map shows the difference in elevation between the two previously mentioned maps, with blue areas representing accretion (positive elevation change), red areas representing erosion (negative elevation change), and the white areas representing no change. Units are in meters, and all maps are at the same scale.

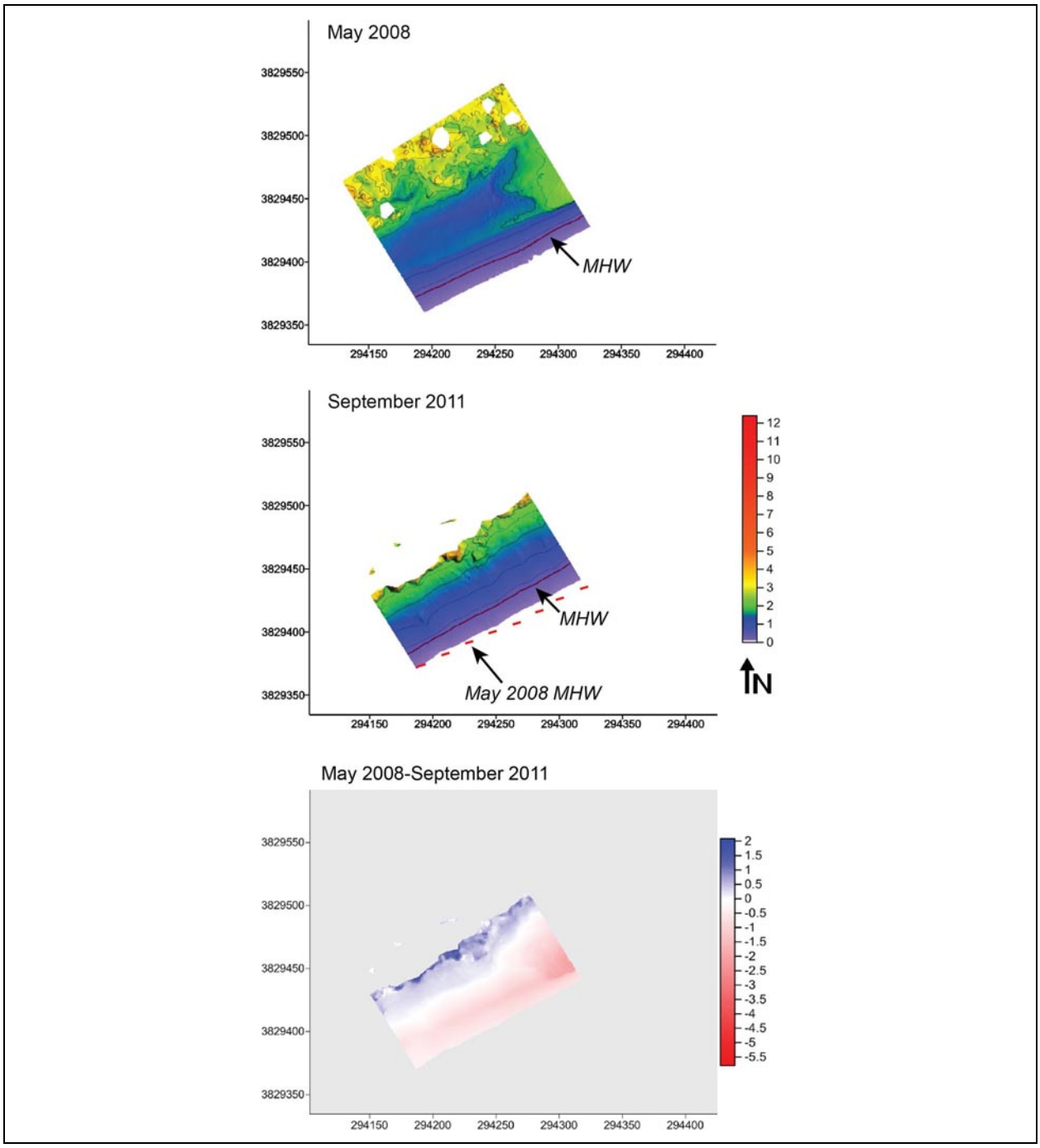

Focus Site 8. The MHW line is shown as a solid red line in the first (September 2009; upper left) and last (September 2011; lower left) topographic maps. The MHW of September 2009 is overlain on the September 2011 map as a dashed red line. The upper-right map shows the difference in elevation between the two maps to the left, with blue areas representing accretion (positive elevation change), red areas representing erosion (negative elevation change), and the white areas representing no change. Units are in meters, and all maps are at the same scale.

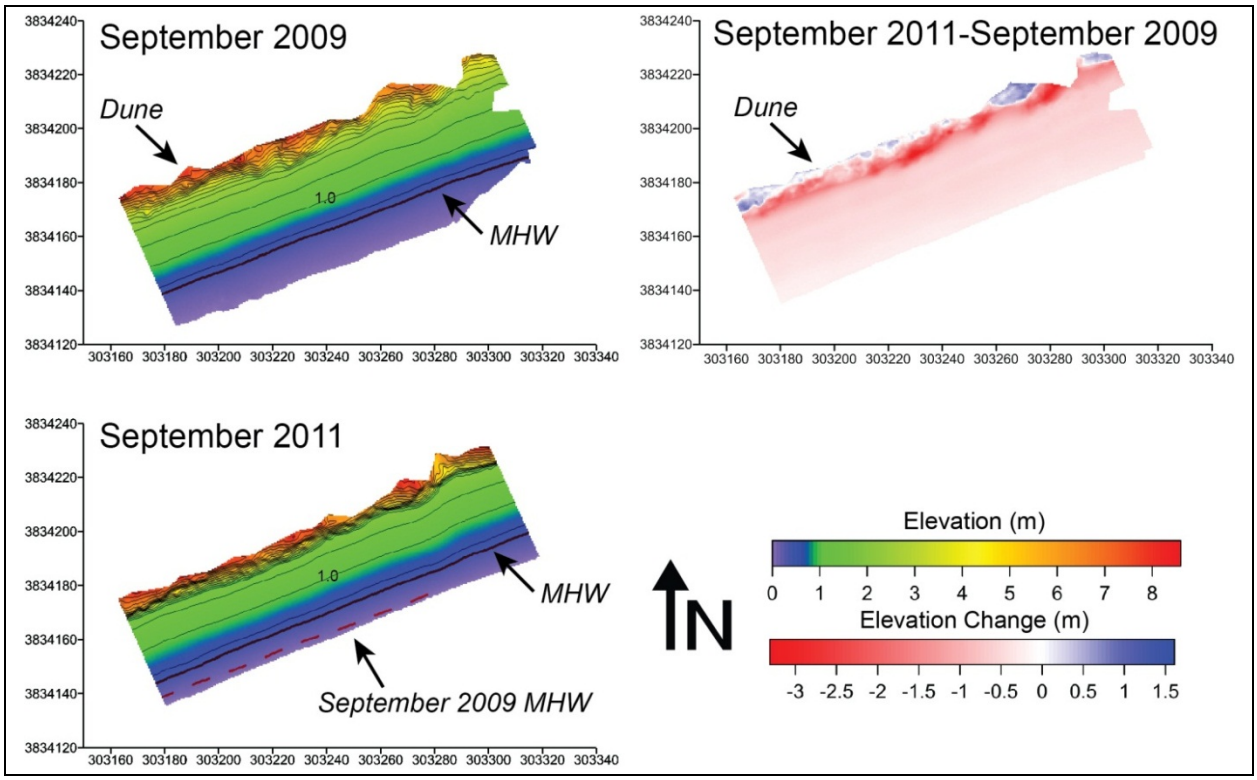

Focus Site 9. The MHW line is shown as a solid red line in the first (September 2009; upper left) and last (September 2011; lower left) topographic maps. The MHW of September 2009 is overlain on the September 2011 map as a dashed red line. The upper-right map shows the difference in elevation between the two maps to the left, with blue areas representing accretion (positive elevation change), red areas representing erosion (negative elevation change), and the white areas representing no change. Units are in meters, and all maps are at the same scale.

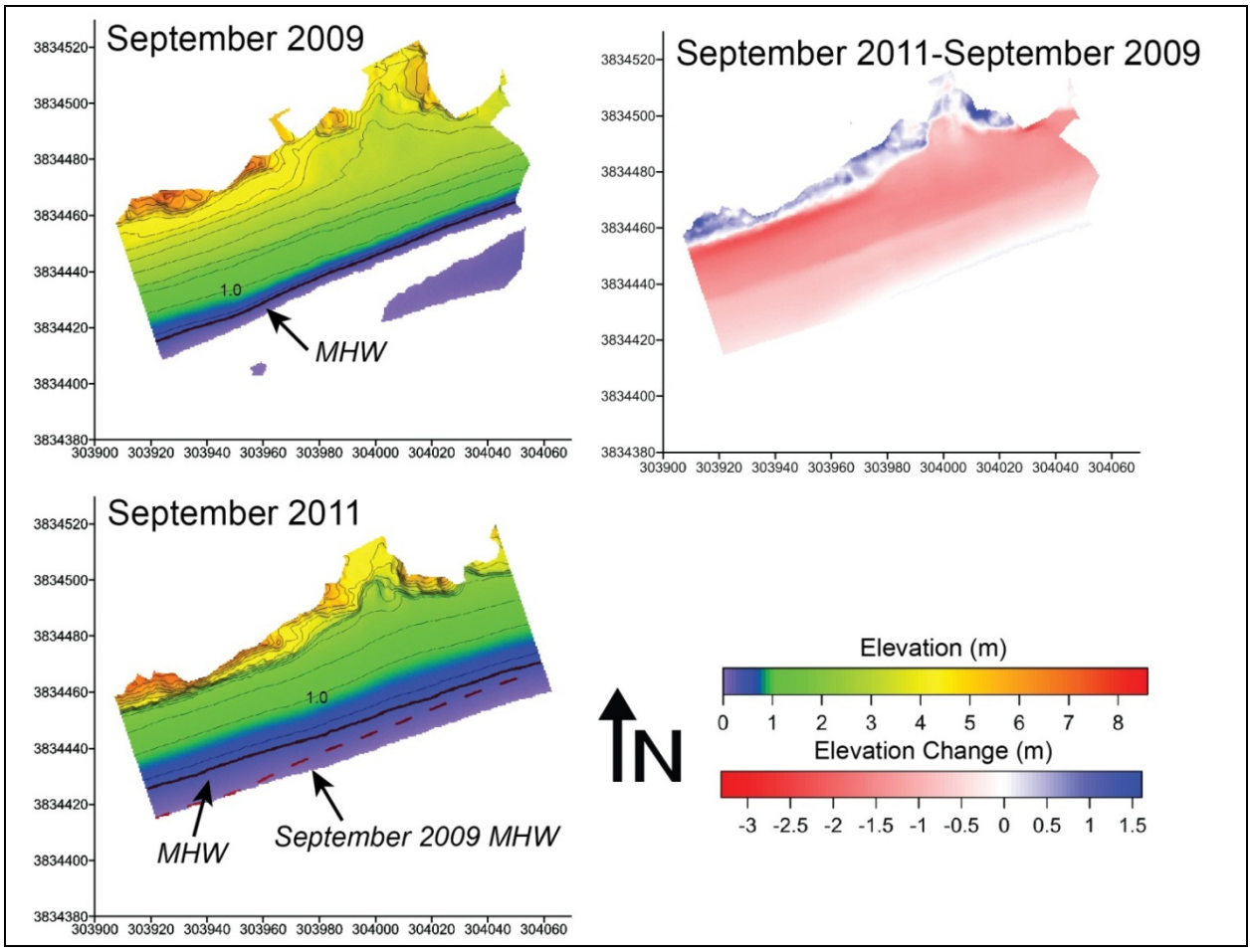

Focus Site 10. The MHW line is shown as a solid red line in the first (September 2009; upper left) and last (September 2011; lower left) topographic maps. The MHW of September 2009 is overlain on the September 2011 map as a dashed red line. The upper-right map shows the difference in elevation between the two maps to the left, with blue areas representing accretion (positive elevation change), red areas representing erosion (negative elevation change) and the white areas representing no change. Units are in meters and all maps are at the same scale.

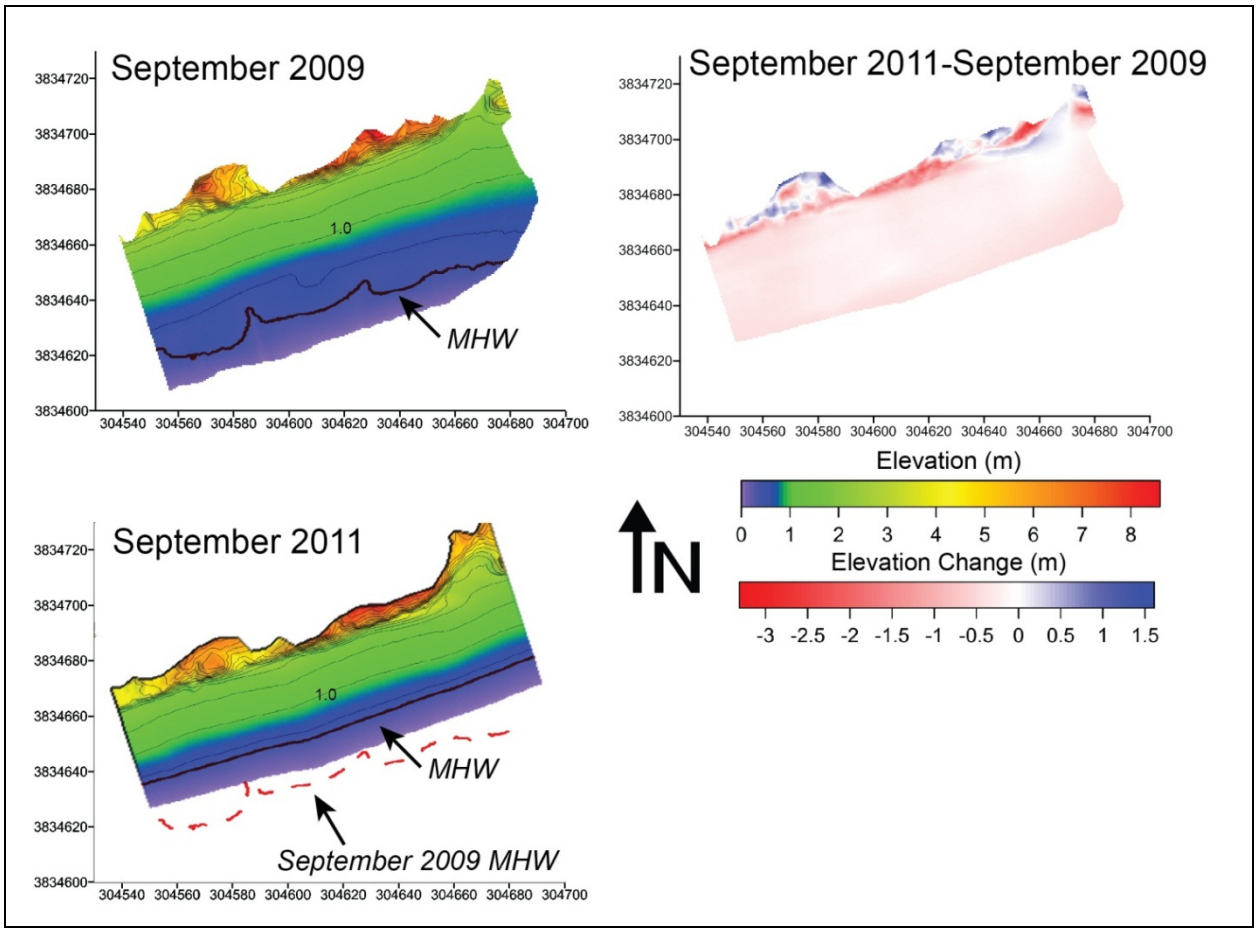

[This page intentionally left blank.]

Appendix 9-B

List of Scientific Publications

List of Scientific Publications

Papers

Rodriguez, A.B., J.T. Ridge, S.R. Fegley, and N. Anderson. 2012. Contribution of aeolian sand to backbarrier marsh sedimentation. *Estuarine Coastal and Shelf Science*. In revision.

Theuerkauf, E.J., and A.B. Rodriguez. 2012. Evaluating proxies of subaerial beach volume change across various short time scales and morphodynamics. *Geomorphology*. In revision.

Theuerkauf, E.J., and A.B. Rodriguez. Discussion of the article titled of transect location and variations in along-beach morphology on measuring volume change. In *Journal of Coastal Research 28*(3):707–718. *Journal of Coastal Research*. In press.

Theuerkauf, E.J., and A.B. Rodriguez. 2012. Impacts of transect location and variations in along-beach morphology on measuring volume change. *Journal of Coastal Research 28*(3):707–718.

Rodriguez, A.B., P.L. Rodriguez, and S.R. Fegley. 2012. One-year along-beach variation in the maximum depth of erosion resulting from irregular shoreline morphology. *Marine Geology 291*:12–23.

Ridge, J.T., A.B. Rodriguez, S.R. Fegley, R. Browne, and D. Hood. 2011. A new "pressure" sensitive method of measuring aeolian sediment transport using a Gauged Sediment Trap (GaST). *Geomorphology 134*:426–430.

Mattheus, C.R., and A.B. Rodriguez. 2011. Controls on late Quaternary incised-valley dimension along passive margins evaluated using empirical data. *Sedimentology 58*:1113–1137.

Rodriguez, A.B. 2009. *Onslow Beach Sediment Texture and Mineralogy*. Technical Report. 393 pages.

Theses

Theuerkauf, E.J. 2012. Evaluating Proxies of Subaerial Beach Volume Change Using Terrestrial LIDAR Data from Onslow Beach, NC, USA. Master's thesis, Department of Marine Sciences, University of North Carolina at Chapel Hill, Chapel Hill, NC.

Yu, W. 2012. Impacts of Storms and Sea-Level Rise on Coastal Evolution Between Two Capes: Onslow Bay, NC, USA. Master's thesis, Department of Marine Sciences, University of North Carolina at Chapel Hill, Chapel Hill, NC.

Presentations

Theuerkauf, E.J., A.B. Rodriguez, S.R. Fegley, and R. Luettich. 2012. *Barrier Island Response to an Elevated Sea-Level Anomaly: Onslow Beach, North Carolina, USA*. Presented at

the American Geophysical Union's (AGU's) Fall Meeting, San Francisco, CA. December 3–7.

Theuerkauf, E.J., and A.B. Rodriguez. 2012. *Erosion or Error: Are Beach Profiles and the Mean High Water Shoreline Appropriate Proxies for Measuring Subaerial Volume Change?* Presented at the Geological Society of America's (GSA's) Annual Meeting, Charlotte, NC. November 4–7. Volume 44, issue 7.

Rodriguez, A.B., S.R. Fegley, J.T. Ridge, B. VanDusen, and N. Anderson. 2012. *What Is the Aeolian Component of Backbarrier Marsh Sedimentation?* Presented at GSA's Annual Meeting, Charlotte, NC. November 4–7. Volume 44, issue 7

Theuerkauf, E.J., W. Yu, and A.B. Rodriguez. 2011. *The Influence of Framework Geology on the Evolution of Onslow Beach, NC, at Multiple Time Scales*. Presented at the Southeastern Section of the Geological Society of America's (SEGSA's) 60th Annual Meeting, Wilmington, NC. March 23–25. Volume 43, issue 1.

Ridge, J.T., A.B. Rodriguez, and S.R. Fegley. 2011. *Shifting Sands: Quantifying Landscape Effects on the Contribution of Aeolian Sand to Back-Barrier Accretion*. Presented at SEGSA's 60th Annual Meeting, Wilmington, NC. March 23–25. Volume 43, issue 1

Theuerkauf, E.J., and A.B. Rodriguez. 2010. *Quantifying Differences in Beach Volume Change Between 2-D and 3-D Survey Methods*. Presented at AGU's Fall Meeting, San Francisco, CA. December 13–17.

Yu, W., D. Hood, R. Browne, and A.B. Rodriguez. 2010. *Variations in Barrier-Island Evolution at Millennial and Decadal Time Scales Related to Underlying Geology, Onslow Beach, NC, USA*. Presented at AGU's Fall Meeting, San Francisco, CA. December 13–17.

Rodriguez, A.B., S.R. Fegley, and P.L. Rodriguez. 2010. *A Novel Method for Quantifying the Maximum Depth of Beach Erosion over a 1-Year Period at Onslow Beach, North Carolina Resolves Along- and Across-Beach Variability*, Presented at AGU's Fall Meeting, San Francisco, CA. December 13–17.

Fegley, S.R., C.H. Peterson, A.B. Rodriguez, J.V. Reynolds-Fleming, R.A. Luettich, B.M. VanDusen, and C.M. Voss. 2010. *Perturbation in a Dynamic System: Variable Consequences of Coastal Storms on Habitat Structure and Faunal Composition in an Exposed Beach*. Presented at the 39th Benthic Ecology Meeting, Wilmington, NC. March 10–13.

Theuerkauf, E.J., A.B. Rodriguez, S.R. Fegley, J.V. Fleming, J.E. McNinch, and H.M. Wadman. 2009. *Extreme Along-Beach Variations in Morphodynamics Attributed to Nearshore Bathymetry and Underlying Geology over the Short-Term, Onslow Beach, North Carolina*. Presented at AGU's Fall Meeting, San Francisco, CA. December 14–18.

Reynolds-Fleming, J., R. Luettich, and A.B. Rodriguez. 2009. *Sequential Storm Effects on Barrier Island Morphology*. Presented at the Coastal Estuarine Research Federation's 20th Biennial Conference, Portland, OR. November 1–5.

Foxgrover, A.C., J. McNinch, H. Wadman, and A.B. Rodriguez. 2008. *Quantifying Barrier-Island Overwash Through Sedimentological, Geophysical, and Geospatial Analyses: Onslow Beach, NC*. Presented at AGU's Fall Meeting, San Francisco, CA. December 15–19.

Wadman, H., J. McNinch, A.C. Foxgrover, and A.B. Rodriguez. 2008. *Spatial Variation of Shoreline Change Along an Important Marine Corps Amphibious Training Ground, Onslow Beach, NC; Part 1: Nearshore Geology and Morphology*. Presented at the Joint Meeting of the Geological Society of America, Soil Science Society of America, American Society of Agronomy, Crop Science Society of America, Gulf Coast Association of Geological Societies with the Gulf Coast Section of the Society for Sedimentary Geology, Houston, TX. October 5–9. Volume 40, issue 6.

Rodriguez, A.B., S.R. Fegley, C.R. Mattheus, E.A. Timmons, J. McNinch, and H. Wadman. 2008. *Spatial Variation of Shoreline Change Along An Important Marine Corps Amphibious Training Ground, Onslow Beach, North Carolina; Part 2: Beach Morphology*. Presented at the Joint Meeting of the Geological Society of America, Soil Science Society of America, American Society of Agronomy, Crop Science Society of America, Gulf Coast Association of Geological Societies with the Gulf Coast Section of the Society for Sedimentary Geology, Houston, TX. October 5–9. Volume 40, issue 6.

Appendix 9-C

List of Students

- Ethan Theuerkauf, M.S., University of North Carolina at Chapel Hill, Chapel Hill, NC. Graduated May 2012.
- Winnie Yu, M.S., University of North Carolina at Chapel Hill, Chapel Hill, NC. Graduated December 2012.

[This page intentionally left blank.]

Chapter 10

Shorebirds and Seabirds Monitoring Activity

SERDP Project Number: RC-1413

Coastal Barrier Module

Lead Researchers:
Drs. Sarah Karpanty and Jim Fraser
Virginia Tech
Blacksburg, VA
E-mails: karpanty@vt.edu and fraser@vt.edu

October 30, 2011

Final

This report was prepared under contract to the U.S. Department of Defense (DoD) Strategic Environmental Research and Development Program (SERDP). The publication of this report does not indicate endorsement by DoD, nor should the contents be construed as reflecting the official policy or position of DoD. References herein to any specific commercial product, process, or service by trade name, trademark, manufacturer, or otherwise, do not necessarily constitute or imply its endorsement, recommendation, or favoring by DoD.

Table of Contents

List of Acronyms 10-vi
Objectives 10-1
Background 10-1
Methods 10-1
MCBCL Historic and Present-day Shorebird Monitoring Procedures 10-1
DCERP Shorebird Monitoring Procedures 2008–2009 10-2
Results and Discussion 10-5
Exploratory Analyses of Historical Data Collected by MCBCL on Shorebirds 10-5
Comparison of Findings from MCBCL and DCERP Concurrent Surveys 10-22
Recommendations for Future Monitoring at MCBCL 10-24
Literature Cited 10-25

List of Figures

10-1. Study area at Onslow Beach on MCBCL, North Carolina, 2008–2009. 10-3

10-2. Seasonal counts of Wilson's plover at MCBCL, NC, from 2001 to 2006, from MCBCL's reformatted database. 10-7

10-3. Seasonal counts of least tern at MCBCL, NC, from 2001 to 2006, from MCBCL's reformatted database. 10-8

10-4. Seasonal counts of piping plover at MCBCL, NC, from 2001 to 2007, from MCBCL's reformatted database. 10-13

10-5. Seasonal counts of American oystercatcher at MCBCL, NC, from 2002 to 2006, from MCBCL's reformatted database. 10-17

10-6. Beach-front surveys were conducted by both the VA Tech (on foot) and MCBCL (by vehicle, stopping every mile) crews on March 18, 2009, in the Wildlife Area (Beach Zone 3 in other charts). 10-20

10-7. Beach-front surveys were conducted by both the VA Tech (on foot) and MCBCL (by vehicle, stopping every mile) crews on April 9, 2009, in the Wildlife Area (Beach Zone 3 in other charts). 10-20

10-8. Beach-front surveys were conducted by both the VA Tech (on foot) and MCBCL (by vehicle, stopping every mile) crews on April 17, 2009, in Developed Recreation Area (Beach Zone 1 in other charts). 10-21

10-9. Beach-front surveys were conducted by both the VA Tech (on foot) and MCBCL (by vehicle, stopping every mile) crews on June 5, 2009, during the breeding season in the Wildlife Area (Beach Zone 3 in other charts). 10-21

10-10. Beach-front surveys were conducted by both the VA Tech (on foot) and MCBCL (by vehicle, stopping every mile) crews on July 9, 2009, in all three beach zones, (A) Developed Recreation Area, (B) Military Amphibious Training Zone, and (C) Wildlife Area. 10-23

List of Tables

10-1. Shorebird and tern species included in this study's summary analyses, along with each species' federal and state listing status, the U.S. Shorebird Conservation Plan's prioritization designation, and temporal occurrence on Onslow Beach at MCBCL, North Carolina, 2008–2009. 10-3

10-2. Wilson's plover survey data extracted from the reformatted database for Onslow Beach, MCBCL from 2001–2006. 10-6

10-3. Number of occurrences of Wilson's plover observations at each mile marker on Onslow Beach, MCBCL, NC, from 2001 to 2006, as extracted from the reformatted database. 10-7

10-4. Wilson's plover nesting data from MCBCL, NC from 2001 and 2004. 10-8

10-5. Least tern survey data extracted from the reformatted database for Onslow Beach, MCBCL (from 2001 to 2006). 10-9

10-6. Number of occurrences of least tern observations at each mile marker on Onslow Beach, MCBCL, NC, from 2001 to 2006, as extracted from the reformatted database. 10-11

10-7. Least tern nesting information from Camp Lejeune, NC, 2001 and 2004 only 10-12

10-8. Piping plover survey data extracted from the reformatted database for Onslow Beach, MCBCL, from 2001 to 2006. 10-14

10-9. Number of occurrences of piping plover observations at each mile marker on Onslow Beach, MCBCL, NC, from 2001 to 2007 as summarized from reformatted database. 10-17

10-10. American oystercatcher survey data extracted from the reformatted database for Onslow Beach, MCBCL, from 2001 to 2006. 10-18

10-11. Number of occurrences of American oystercatcher observations at each mile marker on Onslow Beach, MCBCL, NC, from 2002 to 2006. 10-19

10-12. American oystercatcher nesting data from MCBCL, NC, only 2001 and 2004. 10-19

List of Acronyms

°C	degrees Celsius
°F	Degrees Fahrenheit
DCERP	Defense Coastal/Estuarine Research Program
DCERP1	first cycle of the Defense Coastal/Estuarine Research Program
DoD	U.S. Department of Defense
GPS	global position system
m	meter
MCBCL	Marine Corps Base Camp Lejeune
N/A	not applicable
NPS	National Park Service
SERDP	Strategic Environmental Research and Development Program
VA Tech	Virginia Polytechnic Institute and State University

Objectives

Our overarching objective was to determine if a simplified, more efficient monitoring protocol for shorebirds could be implemented by Marine Corps Base Camp Lejeune (MCBCL). To accomplish this goal, we completed three related objectives.

1. To reorganize MCBCL's existing historical database of shorebird monitoring into a spatially explicit, searchable database for analyses related to this project and future analyses.
2. To conduct exploratory analyses of relevant historical data collected by MCBCL on shorebirds.
3. To compare the results of surveys conducted using MCBCL's monitoring protocol with Virginia Tech's survey protocol to assist in making recommendations on future monitoring efforts, while simultaneously conducting research on Wilson's plover (*Charadrius wilsonia*) reproduction and survival (see *DCERP1 Final Research Report* for details on Wilson's plover research).

Keywords: Historical data, monitoring, protocol comparisons, shorebird, surveys

Background

In the context of the Defense Coastal/Estuarine Research Program's (DCERP's) Coastal Barrier Module, the purpose of monitoring shorebirds was to use the responses (e.g., abundance by habitat type) of these mid-trophic level vertebrates as indicators to the ecosystem impacts of anthropogenic and random forces in Marine Corps Base Camp Lejeune's (MCBCL's) coastal barrier system. Shorebirds are predicted to respond to alterations in both benthic prey and the balance of predators, and so monitoring these taxa in the long-term will serve as an indicator of overall barrier island ecosystem integrity.

In the context of key MCBCL management objectives, the research and monitoring of shorebirds by the Coastal Barrier Module group was intended to provide information to improve the ability of MCBCL to support all required military training activities while complying with the Endangered Species Act and other wildlife requirements, such as the Migratory Bird Treaty Act.

Methods

MCBCL Historic and Present-day Shorebird Monitoring Procedures

Because the distribution and nest-site selection of avian species cannot be predicted down to an exact location between years, MCBCL monitors the barrier island ocean beaches from the New River Inlet to the impact zone in the north. Habitats monitored by MCBCL include ocean beach, overwash areas, and inter-tidal areas adjacent to inlets. This historic and ongoing shorebird monitoring performed by MCBCL involves driving the entire ocean beach and inlet shore and counting using binoculars all shorebirds by species for each mile segment of shore. Prior to the start of this DCERP monitoring activity, data were collected on shorebirds from 2001–2006. Although the goal is to conduct a survey of all of Onslow Beach every 7 to 10 days, our post-hoc

review of the data suggests that the surveys sometimes do not obtain complete spatial coverage at that frequency.

At the onset of the project, we worked closely with MCBCL to access its existing shorebird database, and any paper files that were not yet in its database. The database we received contained most of the data from 2001–2006 and was arranged such that a row of data described all birds, locations, and behaviors recorded on a survey day; in other words a row corresponded to all the data from a given day. We entered all paper files from this time period that were not yet present in the database.

As formatted, it was not possible to query by species or location on Onslow Beach without extensive manipulation of the data. We decided to reformat the database, with permission and cooperation from MCBCL, to make it spatially explicit and searchable by species and beach section. Records were rearranged so that each row now corresponds to the records for a given species on a given survey date, by beach mile. This reorganization now easily allows MCBCL to search and analyze data by both species and beach mile, which will be useful in assessing future management or training actions in different regions of Onslow Beach. This reformatted database was provided to MCBCL in August 2008.

DCERP Shorebird Monitoring Procedures 2008–2009

We conducted shorebird surveys along established transects on the beach and in the marsh (**Figure 10-1**) at least 1 time per 7 to 10 days in 2008 and 2009. We walked along the beach and boated or kayaked through the marsh to conduct surveys during the morning hours of 0630–1030. We counted all focal shorebird and tern species (**Table 10-1**) seen and heard within approximately 100 m of our location on the transect (ocular and auditory estimations) beachfront and marshside, and recorded our geographic coordinates at the time of identification using a global position system (GPS; Garmin 76, Garmin International, Olathe, KS). We recorded environmental variables at the beginning of each survey, which included temperature (in °C), wind speed (knots) and cardinal direction, tidal stage (low, low-rising, mid-rising, high, high-falling, mid-falling), time of first high and low tides, and an ocular estimate of cloud cover (%).

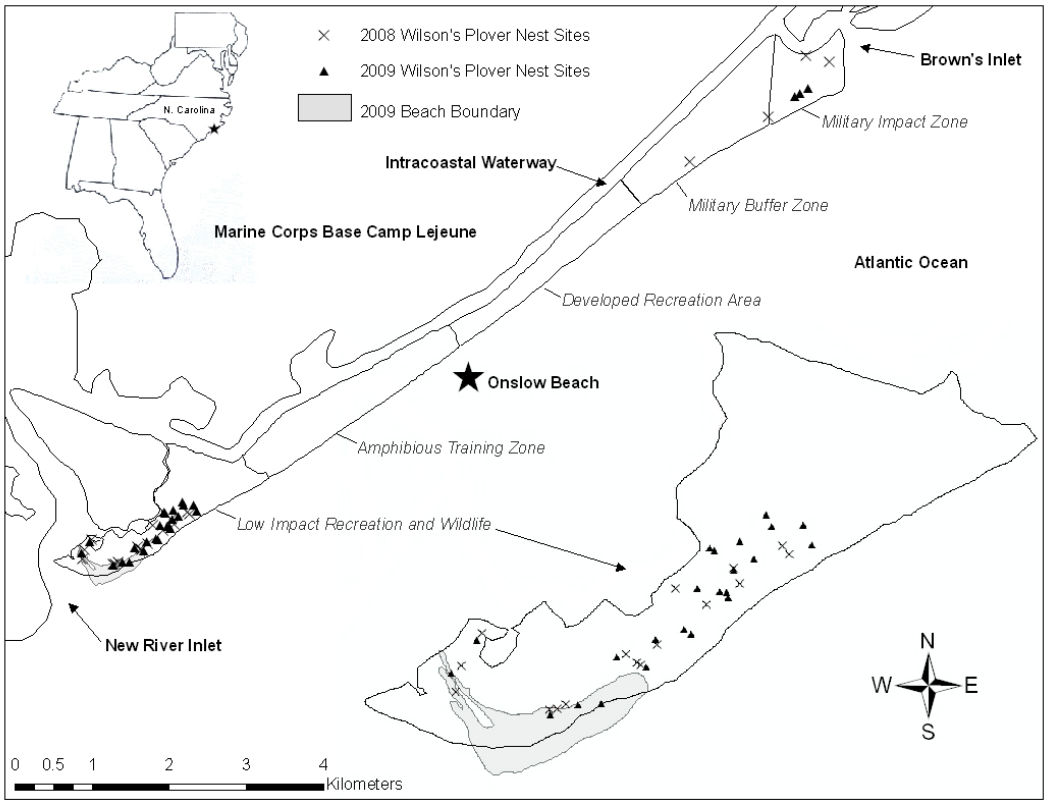

Figure 10-1. Study area at Onslow Beach on MCBCL, North Carolina, 2008–2009.

The low impact recreation and wildlife area is enlarged to clearly depict Wilson's Plover (*Charadrius wilsonia*) nest site locations, and changes in the beach boundary between years.

Table 10-1. Shorebird and tern species included in this study's summary analyses, along with each species' federal and state listing status, the U.S. Shorebird Conservation Plan's prioritization designation, and temporal occurrence on Onslow Beach at MCBCL, North Carolina, 2008–2009.

Common Name	Scientific Name	Federal Status	State Status	U.S. Shorebird Conservation Plan Status	Temporal Occurrence
American oystercatcher	*Haematopus palliates*	None	Special concern	Species of high concern (4)	Breeding resident
Black-bellied plover[a]	*Pluvialis squatarola*	None	None	Species of moderate concern (3)	Wintering, migratory
Killdeer	*Charadrius vociferus*	None	None	Species of moderate concern (3)	Breeding resident
Piping plover	*Charadrius melodus*	Threatened	Endangered	Highly imperiled (5)	Breeding
Semipalmated plover	*Charadrius semipalmatus*	None	None	Species of low concern (2)	Wintering, migratory
Wilson's plover	*Charadrius wilsonia*	None	Special concern	Species of high concern (4)	Breeding

(continued)

Table 10-1. Shorebird and tern species included in this study's summary analyses, along with each species' federal and state listing status, the U.S. Shorebird Conservation Plan's prioritization designation, and temporal occurrence on Onslow Beach at MCBCL, North Carolina, 2008–2009. (continued)

Common Name	Scientific Name	Federal Status	State Status	U.S. Shorebird Conservation Plan Status	Temporal Occurrence
Red knot	*Calidris canutus*	Candidate species	None	Species of high concern (4)	Resident, migratory
Sanderling[a]	*Calidris alba*	None	None	Species of high concern (4)	Wintering, migratory
Willet	*Catoptrophorus semipalmatus*	None	None	Species of moderate concern (3)	Breeding resident
Common tern	*Sterna hirundo*	None	Special concern	Not applicable	Breeding
Gull-billed tern	*Sterna nilotica*	None	Threatened	Not applicable	Breeding
Forster's tern	*Sterna forsteri*	None	None	Not applicable	Wintering
Least tern	*Sterna antillarum*	None along the Atlantic Coast	Special concern	Not applicable	Breeding
Royal tern	*Sterna maxima*	None	None	Not applicable	Breeding resident
Sandwich tern	*Sterna sandvicensis*	None	None	Not applicable	Breeding

[a] Potentially non-breeding birds observed during breeding season.

Although we temporally standardized our surveying efforts, tidal stages fluctuated daily and throughout each breeding season and thus, accounted for tidal variation. We alternated the starting point on all transects for each survey to minimize detection bias potentially influenced by tidal state. We did not conduct surveys when ocular estimates of cloud cover were ≥95%, precipitation (e.g., rain, fog, storms) was persistent for ≥3 hours, and/or winds ≥17 knots during the designated morning survey period (i.e., 0630–1030).

We minimized double counting birds through careful observation that included noting the direction birds or flocks flew, and counting only birds observed on the leading portion of the transect. In cases of large aggregations of birds (e.g., colonial nesting terns, birds resting and foraging on sandbars) observed in the same micro-habitat, we tallied individuals by species within boundaries of physical landmarks (e.g., fence posts or signs, dunes, vegetation, pylons, buoys, landmark on an adjacent visible island) and summed the total of each species for the given geographical location.

We conducted five concurrent monitoring surveys in 2009 with MCBCL to determine if MCBCL survey techniques resulted in missing key species or significant numbers of individuals by focusing almost completely on ocean beaches. Although we had hoped for a higher number of concurrent surveys, it was not possible because MCBCL did not conductshorebird surveys during the time that we were conducting our work on Onslow Beach, and instead used our data.

Results and Discussion

Exploratory Analyses of Historical Data Collected by MCBCL on Shorebirds

We used the reformatted historical database to conduct exploratory analyses of data on a subset of shorebirds and terns that use Onslow Beach, MCBCL. We explored data for Wilson's plover (*Charadrius wilsonia*), least terns (*Sterna antillarum*), piping plover (*Charadrius melodus*), and American oystercatcher (*Haematopus palliates*) because all use Onslow Beach for breeding and migration, and all are either species of special concern in North Carolina, or federally threatened (piping plover). For more information on the status and ecology of these shorebirds, please see the *DCERP1 Final Research Report*.

We report Wilson's plover survey data from 2001–2006 overall (**Table 10-2** and **Figure 10-2**), abundance by beach mile (**Table 10-3**), and nesting frequency (**Table 10-4**). In all cases, the overall abundance and nest estimates reported in the historical database are much lower than our estimates of Wilson's plover abundance and nesting effort from 2008–2009 (20, 26 pairs nesting, respectively). Wilson's plovers are a very secretive bird during the nesting season, and the best way to estimate their numbers and find nests is to walk on foot on the beach front and through the inter-dune sandflats. Rarely were we able to detect Wilson's plovers from our vehicles.

Table 10-2. Wilson's plover survey data extracted from the reformatted database for Onslow Beach, MCBCL from 2001–2006.

ID	Date	Season	Number Observed	Time	General Weather	Tide Stage	Tide Movement	Approximate Temperature (°F)	Wind Speed	Wind Direction	Habitat Located_WP	Behavior_WP	Location_WPa	Location_WPb	Location_WPc
13	December 26, 2001	Non-breeding	4	9:15	Sunny	Mid	Falling	45	0			Other	215	218	213
33	April 12, 2002	Breeding	6	11:30	Partly cloudy	Mid	Falling	64	7	Northeast		Foraging	218	Inlet	
34	April 19, 2002	Breeding	3	13:55	Partly cloudy	High	Falling	87	8	Southwest		Standing	212	213	
38	May 29, 2002	Breeding	5	12:20	Rain/cloudy	High	Falling	77	13	East-northeast		Foraging	Inlet		
39	June 4, 2002	Breeding	1	7:50	Partly cloudy	Low	Falling	72	5	East-northeast		Foraging		Inlet	
41	June 11, 2002	Breeding	1	9:00	Sunny	High	Falling	68	2	West northwest		Other		Inlet	
45	July 12, 2002	Breeding	3	13:26	Overcast	Mid	Falling	81	0			Resting	213		
48	August 16, 2002	Breeding	1	8:30	Partly cloudy	Low	Rising	85	0			Foraging		215	
52	September 25, 2002	Non-breeding	3	10:52	Overcast	High	Falling	75	0			Resting		Inlet	
53	October 4, 2002	Non-breeding	4	9:55	Overcast	Mid	Falling	85	0			Foraging	214	213	
54	October 12, 2002	Non-breeding	2	2:15	Overcast	High	Falling	72	9	Northwest		Resting		212	
55	October ,22, 2002	Non-breeding	3	1:48	Overcast	Mid	Falling	0	0			Foraging		212	
56	October 30, 2002	Non-breeding	5	11:15	Overcast	Low	Rising	0	0			Resting	213	Inlet	212
59	November 29, 2002	Non-breeding	5	10:45	Sunny	Mid	Rising		0			Foraging		212	
73	March 21, 2003	Breeding	4	1:40	Partly cloudy	Low	Falling	74	12	West-southwest		Foraging		Inlet	
75	March 31, 2003	Breeding	2	8:37	Sunny	Mid	Falling	42	18	Northeast		Together in dunes		212	
81	June 2, 2003	Breeding	1		Sunny		Falling	0				Foraging		213	
102	March 22, 2004	Breeding	1	2:55	Sunny			51	0			Foraging		212	
112	August 6, 2004	Breeding	5	6:36	Overcast	Low	Rising	72	0		Sand Beach	Foraging		212	
113	September 8, 2004	Non-breeding	4	9:34	Rain	Low	Falling	81	0			Foraging			
115	November 4, 2004	Non-breeding	9	7:37	Overcast	Low	Rising	66	14	Southeast	Sand Beach	Foraging	217	213	
116	December 3, 2004	Non-breeding	25	11:57	Sunny	High	Falling	55	10	Northwest	Sand Beach	Other		212	
120	March 2, 2005	Breeding	1	7:30	Sunny	Mid	Rising	37.8	7	Northwest	Sand Beach	Foraging		217	
163	June 5, 2006	Breeding	2	9:55	Overcast	Low	Rising	75	0			Foraging		218	
165	June 19, 2006	Breeding	1	6:40	Sunny	Mid	Falling	70	0			Foraging		212	
169	July 21, 2006	Breeding	5	7:30	Partly cloudy	High	Falling	76	10	Southwest		Foraging	Inlet	212	
173	July 28, 2006	Breeding	2	7:30	Sunny	Mid	Rising	87	10	Southwest		Roosting		212	
			108												

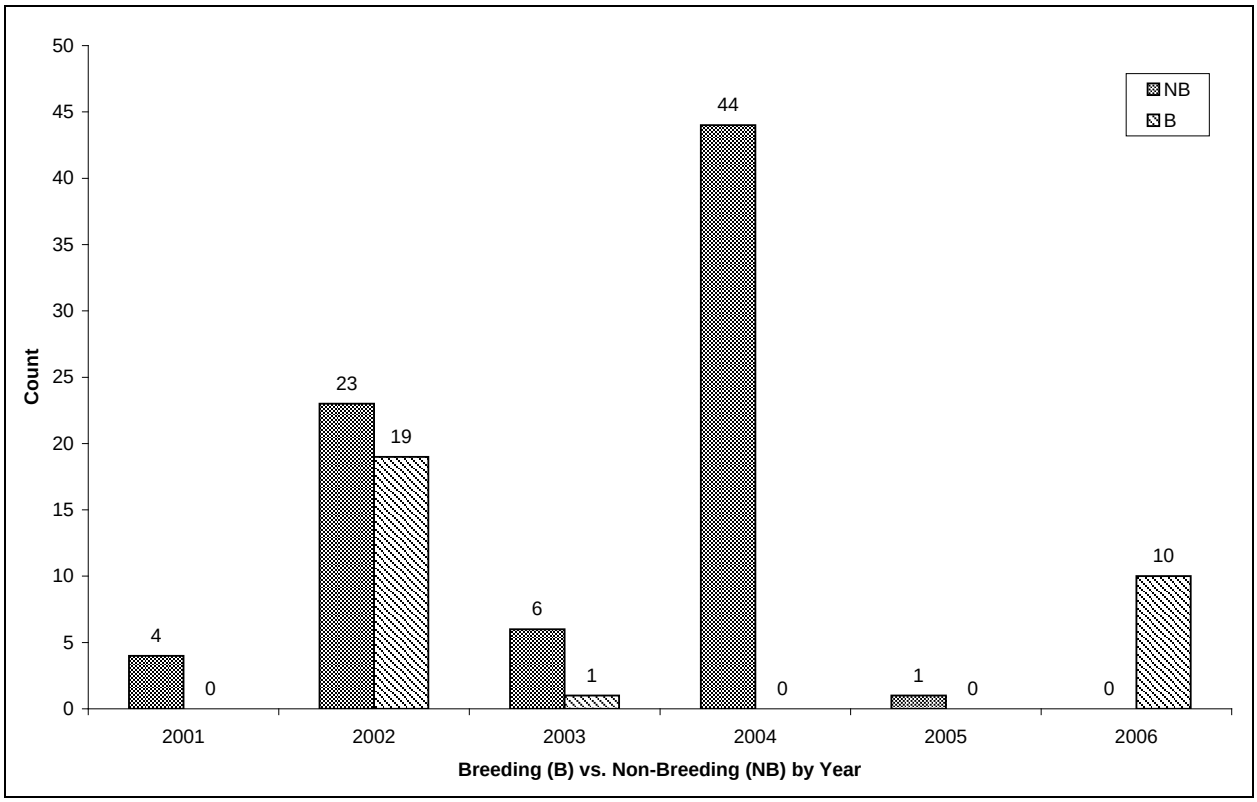

Figure 10-2. Seasonal counts of Wilson's plover at MCBCL, NC, from 2001 to 2006, from MCBCL's reformatted database.

Note: Effort may be inconsistent across years, and effort is not accounted for in this figure. NB (solid gray bar) is non-breeding season, and B (hatched bar) is breeding season.

Table 10-3. Number of occurrences of Wilson's plover observations at each mile marker on Onslow Beach, MCBCL, NC, from 2001 to 2006, as extracted from the reformatted database.

Note: Effort may be inconsistent across years, and effort is not accounted for in this table.

Year	Number Observed	MM212	MM213	MM214	MM215	MM216	MM217	MM218	Inlet
2001	4	0	1	0	1	0	0	1	0
2002	42	5	4	1	1	0	0	1	**6**
2003	7	1	1	0	0	0	0	0	1
2004	44	**3**	1	0	0	0	1	0	0
2005	1	0	0	0	0	0	1	0	0
2006	10	**3**	0	0	0	0	0	1	1
Total	**108**	**12**	**7**	**1**	**2**	**0**	**2**	**3**	**8**

Table 10-4. Wilson's plover nesting data from MCBCL, NC from 2001 and 2004.

Site Name	Date	Year	Name	Season	Number of Birds	Number of Breeding Pairs	Habitat	Land Side	Land Type	Comments
Onslow Beach	June 13	2001	Wilson's plovers	Breeding	6	3	Sand beach		Barrier island	NC-ON-025-04 Overwash
Onslow Beach	June 2	2004	Wilson's plovers	Breeding	15	7		Ocean, inlet	Barrier island	One single bird

We report least tern survey data from 2001–2006 overall (**Figure 10-3** and **Table 10-5**), abundance by beach mile (**Table 10-6**), and nesting frequency (**Table 10-7**). Similar to above, the estimates of least tern abundance in the historical database were much lower than the estimates that we obtained from our surveys. For example, we found approximately 30–40 least terns per survey along the ocean front in the wildlife area alone, compared to the fairly low seasonal counts. Least terns can be difficult to detect from a vehicle, and we found that we used both visual and acoustic signals to locate these birds.

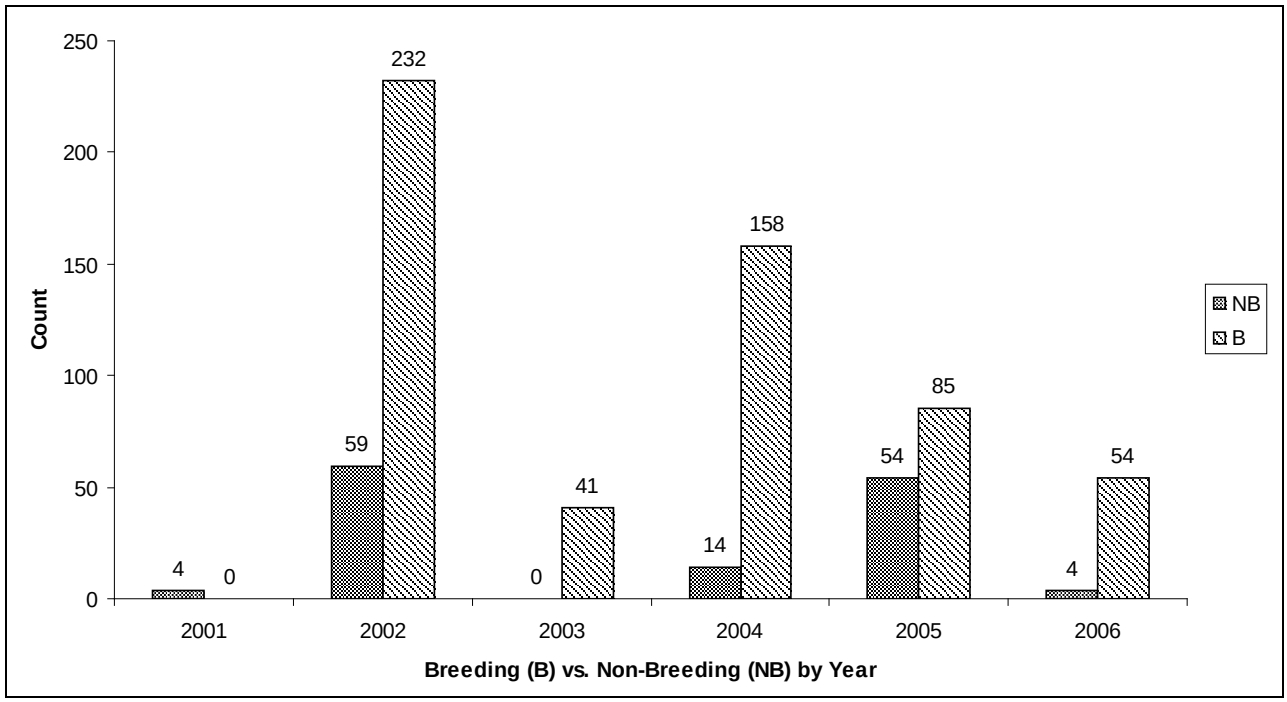

Figure 10-3. Seasonal counts of least tern at MCBCL, NC, from 2001 to 2006, from MCBCL's reformatted database.

Note: Effort may be inconsistent across years, and effort is not accounted for in this figure. NB (solid gray bar) is non-breeding season, and B (hatched bar) is breeding season.

Table 10-5. Least tern survey data extracted from the reformatted database for Onslow Beach, MCBCL (from 2001 to 2006).

ID	Date	Season	Number Observed	Time	General Weather	Tide Stage	Tide Movement	Approximate Temperature (°F)	Wind Speed	Wind Direction	Least Tern	Habitat Located_ LT	Behavior_ LT	Location_ LTa	Location_ LTb	Location_ Lc
13	December 26, 2001	Non-breeding	4	9:15	Sunny	Mid	Falling	45	0		True		Resting	215		
33	April 12, 2002	Breeding	3	11:30	Partly cloudy	Mid	Falling	64	7	Northeast	True		Flying	Inlet		
34	April 19, 2002	Breeding	5	13:55	Partly cloudy	High	Falling	87	8	Southwest	True		Resting	218		
37	May 22, 2002	Breeding	4	9:00	Partly cloudy	Low	Falling	57	13	North	True		Foraging/ flying	218	Inlet	214
38	May 29, 2002	Breeding	18	12:20	Rain/cloudy	High	Falling	77	13	East-northeast	True		Courtship/ flying	217	218	Inlet
39	June 4, 2002	Breeding	25	7:50	partly cloudy	Low	Falling	72	5	East-northeast	True		Courtship/ foraging/ grooming/ flying	Washover flat	Inlet	Mudflat
41	June 11, 2002	Breeding	14	9:00	Sunny	High	Falling	68	2	West-Northwest	True		Nesting/ foraging	217	218	Inlet (mudflat)
42	June 21, 2002	Breeding	3	9:15	Partly cloudy	High	Falling	75	0	N/A	True		Flying	218	Inlet	
43	June 26, 2002	Breeding	12	11:00	Overcast	High	Falling	78	0	N/A	True		Resting	217	218	Inlet
44	July 2, 2002	Breeding	23	14:15	Sunny	High	Falling	92	0		True		Foraging	214	216	217
45	July 12, 2002	Breeding	60	13:26	Overcast	Mid	Falling	81	0		True		Flying	218	217	Inlet
46	July 25, 2002	Breeding	65	9:50	Partly cloudy	High	Falling	85	0		True		Foraging	218	217	215
47	August 7, 2002	Non-breeding	9	13:00	Sunny	Low	Rising	0	0		True		Resting	218	217	
48	August 16, 2002	Non-breeding	46	8:30	Partly cloudy	Low	Rising	85	0		True		Resting	213	217	214
50	September 6, 2002	Non-breeding	4	9:05	Sunny	High	Falling	80	0		True		Flying/ foraging	217	218	
78	May 2 2003	Breeding	3	9:00	Partly cloudy	High	Falling	66	10	Northwest	True		Resting	218		
80	May 22, 2003	Breeding	6	8:29	Partly cloudy	Low	Falling	77	8	Southeast	True		Foraging/ resting	213	217	
81	June 2, 2003	Breeding	8		Sunny		Falling	0			True		Foraging	216	218	
82	June 13, 2003	Breeding	13	8:44	Overcast	High	Falling	79	12	Northwest	True		Nesting	218	217	
83	June 26, 2003	Breeding	4	8:35	Sunny	Mid	Falling	86	9	West-southwest	True		Foraging			
84	July 7, 2003	Breeding	2	9:00	Sunny	Low	Rising	0	0		True		Flying	217		

(continued)

Table 10-5. Least tern survey data extracted from the reformatted database for Onslow Beach, MCBCL (from 2001 to 2006). (continued)

ID	Date	Season	Number Observed	Time	General Weather	Tide Stage	Tide Movement	Approximate Temperature (°F)	Wind Speed	Wind Direction	Least Tern	Habitat Located_ LT	Behavior_ LT	Location_ LTa	Location_ LTb	Location_ Lc
85	July 16,2003	Breeding	5		Sunny	High	Rising	0	0		True		Foraging	218		
108	May 19, 2004	Breeding	12	8:25	Partly cloudy	High	Falling	81	13	Southwest	True		Foraging	217	213	Inlet
109	June 16, 2004	Breeding	9	8:25	Sunny	Mid	Falling	78	0		True	Sand beach	Foraging	Inlet	217	218
110	July 2, 2004	Breeding	95	8:00	Partly cloudy	High	Falling	81	5	South	True	Sand beach	Foraging	214	213	Inlet
111	July 8, 2004	Breeding	42	6:34	Sunny	Low	Falling	85	7	West	True	Sand beach	Other	Inlet	217	219
112	August 6, 2004	Non-breeding	5	6:36	Overcast	Low	Rising	72	0		True		Flying	218		
114	October 6, 2004	Non-breeding	7	8:00	Sunny	Low	Falling	59	4	Northeast	True	Sand beach	Flying	215		
115	November 4, 2004	Non-breeding	2	7:37	Overcast	Low	Rising	66	14	Southeast	True	Sand beach	Flying	216		
124	May 5, 2005	Breeding	6	12:00	Overcast	Low	Rising	63			True	Dry sand above high tide line	Flying	216	218	Inlet
126	June 1, 2005	Breeding	5	9:32	Overcast	Low	Falling	68	2		True		Flying	217		
129	July 13, 2005	Breeding	60	7:58	Partly cloudy	Low	Rising	89	2	Southwest	True	Dry sand above high tide line	Flying	214	213	212
130	July 27, 2005	Breeding	14		Sunny	Low	Rising	92			True	Sand beach	Roosting	215	217	218
131	August 10, 2005	Non-breeding	31	7:40	Partly cloudy	Low	Rising	78	0		True	Sand beach	Foraging	215	216	217
132	August 20, 2005	Non-breeding	1	8:24	Partly cloudy	High	Falling	74	0		True	Sand beach	Flying	217		
133	August 26, 2005	Non-breeding	6	6:40	Sunny	Mid	Rising	69	5	Northeast	True	Sand spit	Roosting	218		
143	November 29, 2005	Non-breeding	16	9:30	Overcast	Mid	Falling	66	20	South	True		Roosting	212		
161	May 23, 2006	Breeding	18	9:03	Sunny	Mid	Falling	70	0		True		Nesting	218		
162	June 2, 2006	Breeding	8	9:45	Partly cloudy	Mid	Rising	80	0		True		Foraging	217	218	
163	June 5, 2006	Breeding	4	9:55	Overcast	Low	Rising	75	0		True		Nesting	217	218	
164	June 13, 2006	Breeding	7	7:40	Overcast	Mid	Rising	71	10	Northeast	True		Flying	218		

(continued)

Table 10-5. Least tern survey data extracted from the reformatted database for Onslow Beach, MCBCL (from 2001 to 2006). (continued)

ID	Date	Season	Number Observed	Time	General Weather	Tide Stage	Tide Movement	Approximate Temperature (°F)	Wind Speed	Wind Direction	Least Tern	Habitat Located_ LT	Behavior_ LT	Location_ LTa	Location_ LTb	Location_ Lc
165	June 19, 2006	Breeding	6	6:40	Sunny	Mid	Falling	70	0		True		Roosting	218		
166	June 28, 2006	Breeding	3	11:45	Sunny	High	Falling	80	0		True		Roosting	212	218	
169	July 21, 2006	Breeding	4	7:30	Partly cloudy	High	Falling	76	10	Southwest	True		Flying	217	Inlet	
173	July 28, 2006	Breeding	4	7:30	Sunny	Mid	Rising	87	10	Southwest	True		Roosting	218		
181	August 10, 2006	Non-breeding	1	7:00	Sunny	High		79	0		True		Flying	217		
190	December 1, 2006	Non-breeding	3	8:00	Rain	Low	Rising	75	0		True	Sand beach	Foraging	218		
188			3					0	0		True	Sand beach	Foraging	218		
			708													

Table 10-6. Number of occurrences of least tern observations at each mile marker on Onslow Beach, MCBCL, NC, from 2001 to 2006, as extracted from the reformatted database.

Year	Number Observed	212	213	214	215	216	217	218	219	Inlet	Washover Flat
2001	4	0	0	0	1	0	0	0	N/A	0	N/A
2002	291	0	1	3	1	1	**9**	**10**	N/A	9	1
2003	41	0	1	0	0	1	3	4	N/A	0	N/A
2004	172	0	2	1	1	1	3	2	1	4	N/A
2005	139	2	1	1	2	2	4	3	N/A	1	N/A
2006	58	1	0	0	0	0	4	**8**	N/A	1	N/A
Total	**705**	**3**	**5**	**5**	**5**	**5**	**23**	**27**	**1**	**15**	**1**

Table 10-7. Least tern nesting information from Camp Lejeune, NC, 2001 and 2004 only.

Note: Effort may be inconsistent across years, and effort is not accounted for in this table.

Site Name	Species	Date	Number of Nests	Cover	Height	Colony Substrate	Current Disturbance	Potential Disturbance	Colony Habitat	Nest Stage	Nest Substrate	Census Technique
Onslow Beach Overwash	Least tern	May 15, 2001	**5**	0%	Bare	Natural	Flooding	Flooding/ predation	Beach/bare-sand	Incubation	Sand/shell	Visual total estimate
Onslow Beach Lifeguard Tower	Least tern	June 13, 2001	4	0%	Bare	Natural	Vehicles/ recreation	Predation/ pets/ vehicles/ recreation	Beach/bare-sand	Incubation	Sand/shell	Total ground count
New River Inlet, Northside	Least tern	June 2, 2004	2	0%	Bare	Natural	Predation/ pets/ vehicles/ recreation	Predation/ pets/ vehicles/ recreation	Beach/bare-sand	Chicks out of nest	Sand/shell	Visual total estimate

We report piping plover survey data from 2001–2006 overall (**Figure 10-4** and **Table 10-8**), and by beach mile (**Table 10-9**). In contrast to the other species, we found that the estimates from MCBCL of piping plovers were very similar to those in our later surveys. We understand that all Base staff are very well-trained to search for and identify piping plovers, given their federally threatened status, and our experience with them and these data would suggest that they are finding and counting fairly well the piping plovers that use the Base.

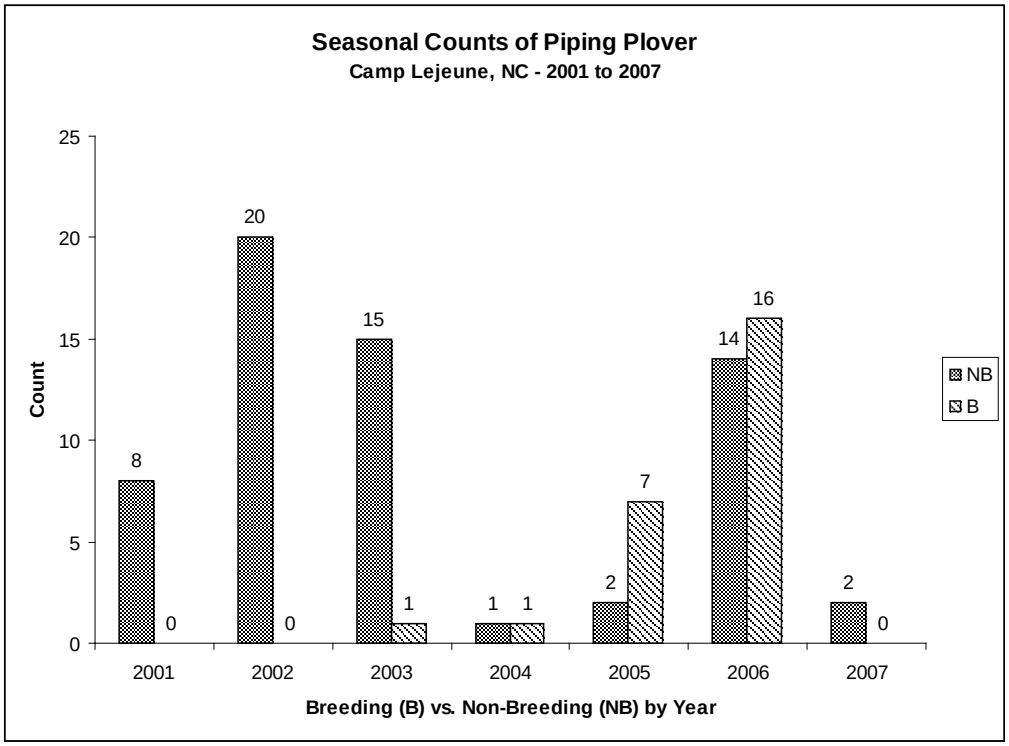

Figure 10-4. Seasonal counts of piping plover at MCBCL, NC, from 2001 to 2007, from MCBCL's reformatted database.

Note: Effort may be inconsistent across years, and effort is not accounted for in this figure. NB (solid gray bar) is non-breeding season, and B (hatched bar) is breeding season.

Table 10-8. Piping plover survey data extracted from the reformatted database for Onslow Beach, MCBCL, from 2001 to 2006.

ID	Date	Season	Number Observed	Time	General Weather	Tide Stage	Tide Movement	Approximate Temperature (°F)	Wind Speed	Wind Direction	Piping Plover	Habitat Located_ PP	Behavior_ PP	Location_ PPa	Location_ PPb	Location_ PPc
7	November 21, 2001	Non-breeding	1	8:30	Clear	Low	Rising	0	0	Northeast	True	Sand beach	Foraging	212		
12	December 20, 2001	Non-breeding	6	11:30	Sunny	High	Falling		0		True	Dry sand above high tide line	Resting	213		
14	December 28, 2001	Non-breeding	1	8:45	Sunny	Mid	Falling	55	16	Southwest	True	Sand beach	Foraging	212		
24	February 21, 2002	Non-breeding	3	14:10	Sunny	High	Falling	61	0		True	Sand beach	Foraging	212		
27	March 13, 2002	Non-breeding	3	13:00	Partly cloudy	Mid	Falling	67	0		True	Sand beach	Foraging	212		
28	March 15, 2002	Non-breeding	3	11:20	Sunny	Mid	Falling	68	8	South	True	Sand beach	Foraging	212		
31	April 2, 2002	Non-breeding	3	12:52	Sunny	High	Falling	75	0		True	Sand beach	Foraging	Inlet	212	
32	April 10, 2002	Non-breeding	2	12:30	Overcast	Low	Falling	67	7	West	True	Sand beach	Foraging	215		
47	August 7, 2002	Breeding	0	13:00	Sunny	Low	Rising	0	0		True	Sand beach	Foraging	Inlet	215	
50	September 6, 2002	Non-breeding	1	9:05	Sunny	High	Falling	80	0		True	Sand beach	Resting	213		
57	November 8, 2002	Non-breeding	3	12:00	Sunny	High	Falling	50	0		True	Sand beach	Foraging	212		
58	November 19, 2002	Non-breeding	2	9:55	Sunny	Mid	Falling	50	0		True	Sand beach	Foraging	212		
5	February 25, 2003	Non-breeding	2	8:30	Sunny	High	Falling	0	10	Southwest	True	Sand beach	Foraging	212		
72	March 18, 2003	Non-breeding	1	10:30	Partly cloudy	Low	Falling	63	10	North	True	Dry sand above high tide line	Foraging	218		
73	March 21, 2003	Non-breeding	4	1:40	Partly cloudy	Low	Falling	74	12	West-southwest	True		Foraging	216		
74	March 25, 2003	Non-breeding	1	10:30	Sunny	Low	Rising	69	0		True		Foraging	216		

(continued)

Table 10-8. Piping plover survey data extracted from the reformatted database for Onslow Beach, MCBCL, from 2001 to 2006. (continued)

ID	Date	Season	Number Observed	Time	General Weather	Tide Stage	Tide Movement	Approximate Temperature (°F)	Wind Speed	Wind Direction	Piping Plover	Habitat Located_ PP	Behavior_ PP	Location_ PPa	Location_ PPb	Location_ PPc
75	March 31 , 2003	Non-breeding	1	8:37	Sunny	Mid	Falling	42	18	Northeast	True		Foraging	213		
76	April 14, 2003	Non-breeding	2	9:00	Sunny	Mid	Falling	51	0		True	Dry sand above high tide line	Foraging	213		
77	April 23, 2003	Non-breeding	0	10:30	Sunny	Mid	Falling	0	0	East	True	Dry sand above high tide line	Foraging	213		
83	June 26, 2003	Breeding	1	8:35	Sunny	Mid	Falling	86	9	West-southwest	True	Dry sand above high tide line	Foraging	218		
88	September 11, 2003	Non-breeding	4	2:00	Overcast	Low	Falling	75	5	Northeast	True		Foraging	216		
102	March 22, 2004	Non-breeding	1	2:55	Sunny			51	0		True		Foraging	213		
112	August 6, 2004	Breeding	1	6:36	Overcast	Low	Rising	72	0		True	Sand beach	Foraging	212		
124	May 5, 2005	Breeding	2	12:00	Overcast	Low	Rising	63			True	Sand beach	Foraging	213	212	
127	May 10, 2005	Breeding	2	13:23				0	0		True	Sand beach	Foraging	212		
125	May 14, 2005	Breeding	1	6:50	Rain	Low	Falling	70	15	Northeast	True	Sand beach	Foraging			
126	June 1, 2005	Breeding	1	9:32	Overcast	Low	Falling	68	2		True	Sand beach	Foraging	212		
175	July 24, 2005	Breeding	1	6:30				0	0		True			212		
135	October 11, 2005	Non-breeding	1	10:45	Sunny	Low	Falling	75	5	Northeast	True		Foraging	214		
136	October 13, 2005	Non-breeding	1	9:06	Overcast	Low	Rising	62	5	North	True		Foraging	213		
156	March 22, 2006	Non-breeding	10	12:40	Sunny	Mid	Falling	50	0		True		Foraging	213		
157	March 31, 2006	Non-breeding	4	11:40	Sunny	Mid	Falling	70	11	Southeast	True		Foraging	212		
170	June 7, 2006	Breeding	1	6:40				0	0		True			218		

(continued)

Table 10-8. Piping plover survey data extracted from the reformatted database for Onslow Beach, MCBCL, from 2001 to 2006. (continued)

ID	Date	Season	Number Observed	Time	General Weather	Tide Stage	Tide Movement	Approximate Temperature (°F)	Wind Speed	Wind Direction	Piping Plover	Habitat Located_ PP	Behavior_ PP	Location_ PPa	Location_ PPb	Location_ PPc
171	July 18, 2006	Breeding	1	8:25				0	0		True					
172	July 19, 2006	Breeding	1	8:25				0	0		True					
169	July 21, 2006	Breeding	1	7:30	Partly cloudy	High	Falling	76	10	Southwest	True		Foraging	212		
174	July 23, 2006	Breeding	1	6:30				0	0		True			212		
179	July 24, 2006	Breeding	1	6:31				0	0		True			212		
176	July 25,2006	Breeding	1	6:32				0	0		True			212		
177	July 26, 2006	Breeding	1	6:33				0	0		True			212		
178	July 27, 2006	Breeding	1	6:34				0	0		True			212		
173	July 28, 2006	Breeding	1	7:30	Sunny	Mid	Rising	87	10	Southwest	True		Foraging	212		
182	August 3, 2006	Breeding	3	9:00				0	0		True		Foraging	212		
183	August 4, 2006	Breeding	3	9:00				0	0		True		Foraging	212		
198	March 21, 2007	Non-breeding	2	1:25	Sunny	Mid	Falling	70	0		True	Sand beach	Foraging	213		
			87													

Table 10-9. Number of occurrences of piping plover observations at each mile marker on Onslow Beach, MCBCL, NC, from 2001 to 2007 as summarized from reformatted database.

Note: Effort may be inconsistent across years, and effort is not accounted for in this table.

Year	Number Observed	212	213	214	215	216	217	218	Inlet
2001	8	2	1	0	0	0	0	0	0
2002	20	**6**	1	0	2	0	0	0	2
2003	16	1	3	0	0	3	0	2	0
2004	2	1	1	0	0	0	0	0	0
2005	9	**4**	2	1	0	0	0	0	0
2006	30	**10**	1	0	0	0	0	1	0
2007	2	0	1	0	0	0	0	0	0
	87	**24**	**10**	**1**	**2**	**3**	**0**	**3**	**2**

Finally, we report American oystercatcher data from 2001–2006 overall (**Figure 10-5** and **Table 10-10**), by beach mile (**Table 10-11**), and by nesting frequency (**Table 10-12**). We found that MCBCL's counts from the earlier years (e.g., 2002–2003) were fairly similar to our counts in 2008–2009 of approximately 4.5 American oystercatchers per breeding season survey (see *DCERP1 Final Research Report*). However, counts from 2004–2006 were much lower than we would expect, given our counts and lack of significant habitat changes during that time period.

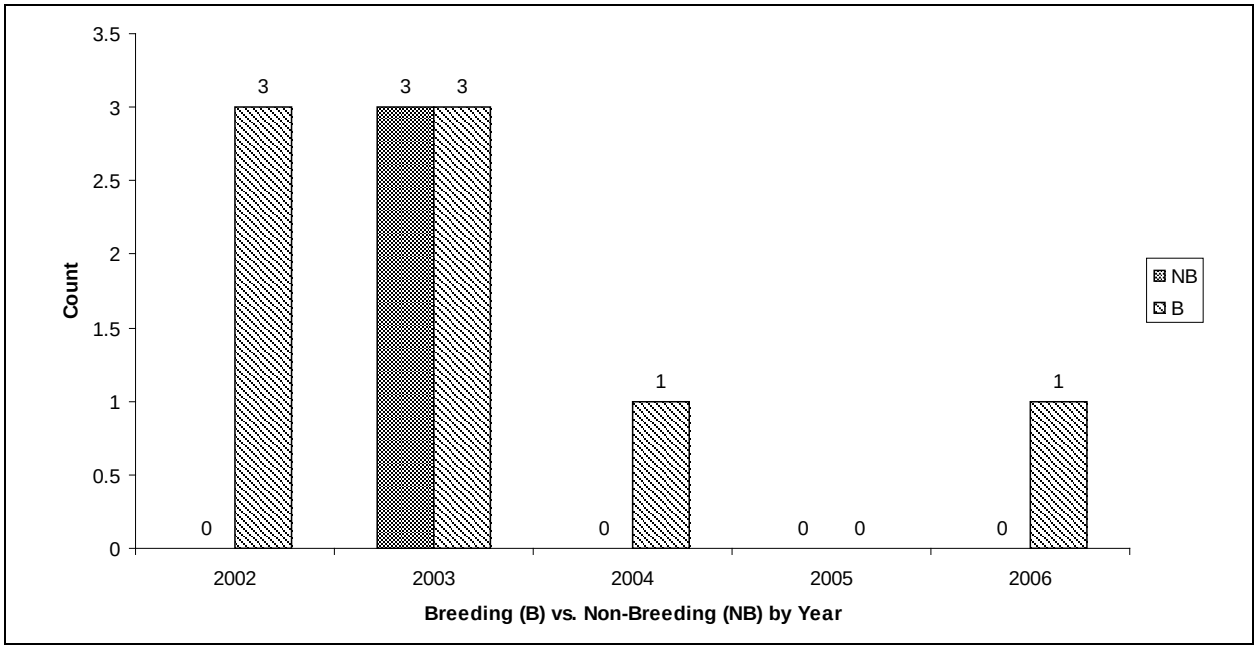

Figure 10-5. Seasonal counts of American oystercatcher at MCBCL, NC, from 2002 to 2006, from MCBCL's reformatted database.

Note: Effort may be inconsistent across years, and effort is not accounted for in this figure. NB (solid gray bar) is non-breeding season, and B (hatched bar) is breeding season.

Table 10-10. American oystercatcher survey data extracted from the reformatted database for Onslow Beach, MCBCL, from 2001 to 2006.

ID	Date	Season	Number Observed	Time	General Weather	Tide Stage	Tide Movement	Approximate Temperature (°F)	Wind Speed	Wind Direction	Habitat Located_AO	Behavior_ AO	Location_ AOa	Location_ AOb	Location_ AOc
39	June 4, 2002	Breeding	1	7:50	Partly cloudy	Low	Falling	72	5	East-northeast		Foraging	Inlet		
47	August 7, 2002	Breeding	2	13:00	Sunny	Low	Rising	0	0			Resting	Inlet		
71	March 10, 2003	Non-breeding	2	12:05	Sunny	High	Falling	55	12	North		Resting	Inlet		
73	March 21, 2003	Non-breeding	1	1:40	Partly cloudy	Low	Falling	74	12	West-southwest		Resting	Inlet		
77	April 23, 2003	Breeding	2	10:30	Sunny	Mid	Falling	0	0	East	Dry sand above high tide line	Resting	218		
79	May 12, 2003	Breeding	1	8:15	Sunny	Low	Falling	81	20	West		Resting	213		
112	August 6, 2004	Breeding	1	6:36	Overcast	Low	Rising	72	0			Flying	212		
169	July 21, 2006	Breeding	1	7:30	Partly cloudy	High	Falling	76	10	Southwest		Foraging	218		
			11												

Table 10-11. Number of occurrences of American oystercatcher observations at each mile marker on Onslow Beach, MCBCL, NC, from 2002 to 2006.

Note as described in text that effort may be inconsistent across years, and effort is not accounted for in this table.

Year	Number Observed	212	213	214	215	216	217	218	Inlet
2002	3	0	0	0	0	0	0	0	**2**
2003	6	0	1	0	0	0	0	1	**2**
2004	1	1	0	0	0	0	0	0	0
2005	0	0	0	0	0	0	0	0	0
2006	1	0	0	0	0	0	0	1	0
	11	1	1	0	0	0	0	**2**	**4**

Table 10-12. American oystercatcher nesting data from MCBCL, NC, only 2001 and 2004.

Site Name	Date	Name	Season	Number of Birds	Number of Breeding Pairs	Habitat	Land Side	Land Type	Comments
Onslow Beach	June 13, 2001	AMOY	Breeding	2	1	Sand beach		Barrier island	NC-ON-025-04 Overwash

We are unable to perform more formal trends analysis because the frequency and spatial extent of the data varies significantly across years, making cross-year comparisons that attempt to control for date or location impossible. Although we present the data in **Figures 10-6** through **10-9** by year, differences across years should not be viewed as trends because efforts were very inconsistent across years and seasons. This should not be taken as a criticism of the Base, but rather just a statement of reality. We suggest that the best use of the historical data may be for determining the presence or absence of certain key species, by general location on Onslow Beach (e.g., Developed Recreation Area, Military Training Zone, protected Wildlife Area). We do not recommend using the data to estimate abundance or relative abundance for use in cross-year comparisons.

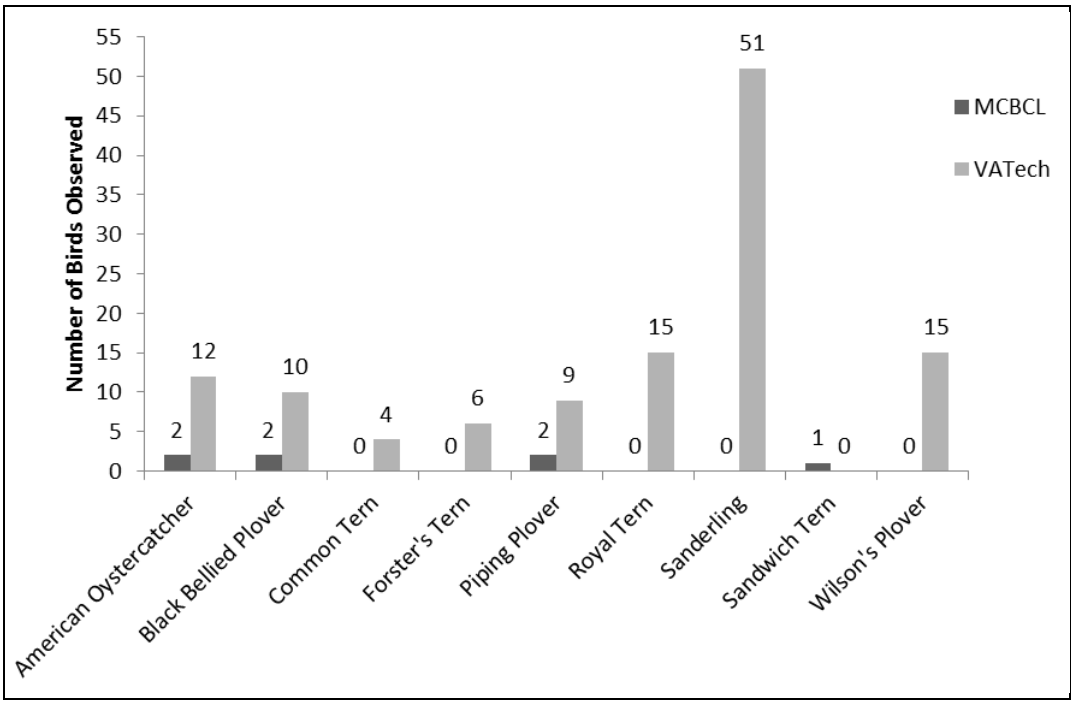

Figure 10-6. Beach-front surveys were conducted by both the VA Tech (on foot) and MCBCL (by vehicle, stopping every mile) crews on March 18, 2009, in the Wildlife Area (Beach Zone 3 in other charts).

During this time period, both wintering birds and early migrants may be present at Onslow Beach.

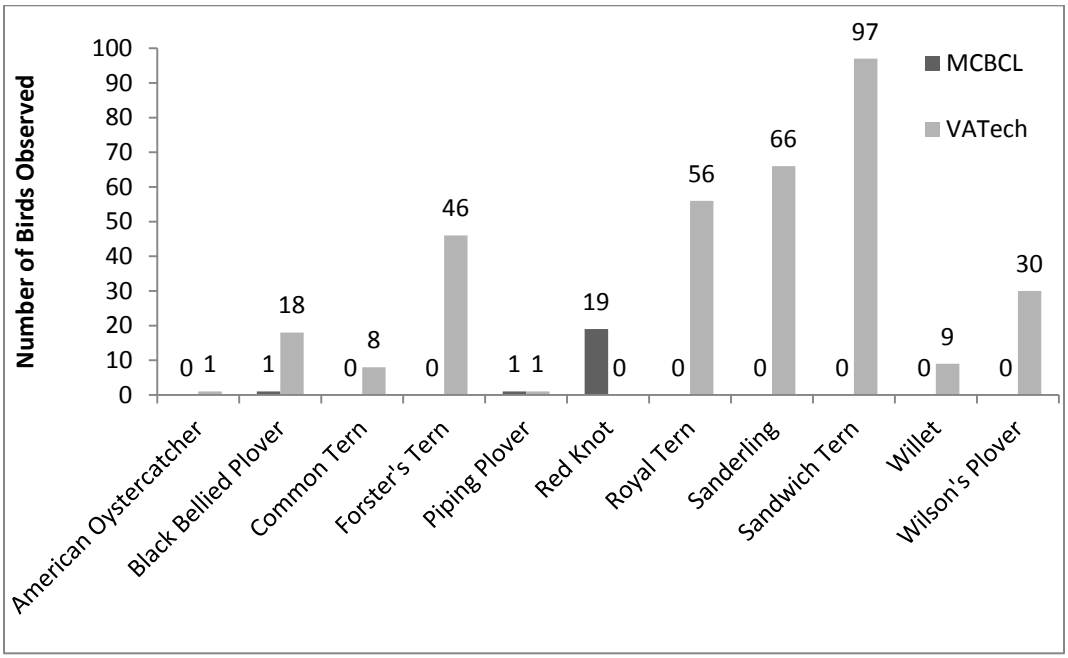

Figure 10-7. Beach-front surveys were conducted by both the VA Tech (on foot) and MCBCL (by vehicle, stopping every mile) crews on April 9, 2009, in the Wildlife Area (Beach Zone 3 in other charts).

During this time period, both migrants and early breeding birds may be present at Onslow Beach.

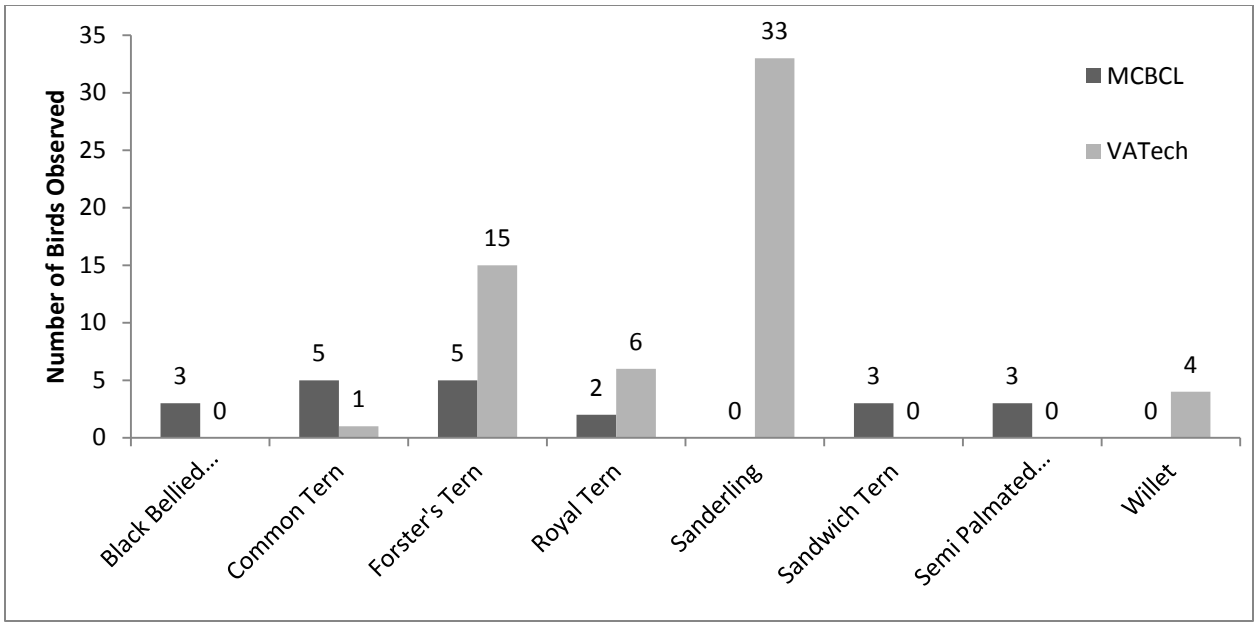

Figure 10-8. Beach-front surveys were conducted by both the VA Tech (on foot) and MCBCL (by vehicle, stopping every mile) crews on April 17, 2009, in Developed Recreation Area (Beach Zone 1 in other charts).

Although the VA Tech crew surveyed all of Onslow Beach on this day, MCBCL did not complete surveys of the whole beach. During this time period, both migrants and early breeding birds may be present at Onslow Beach.

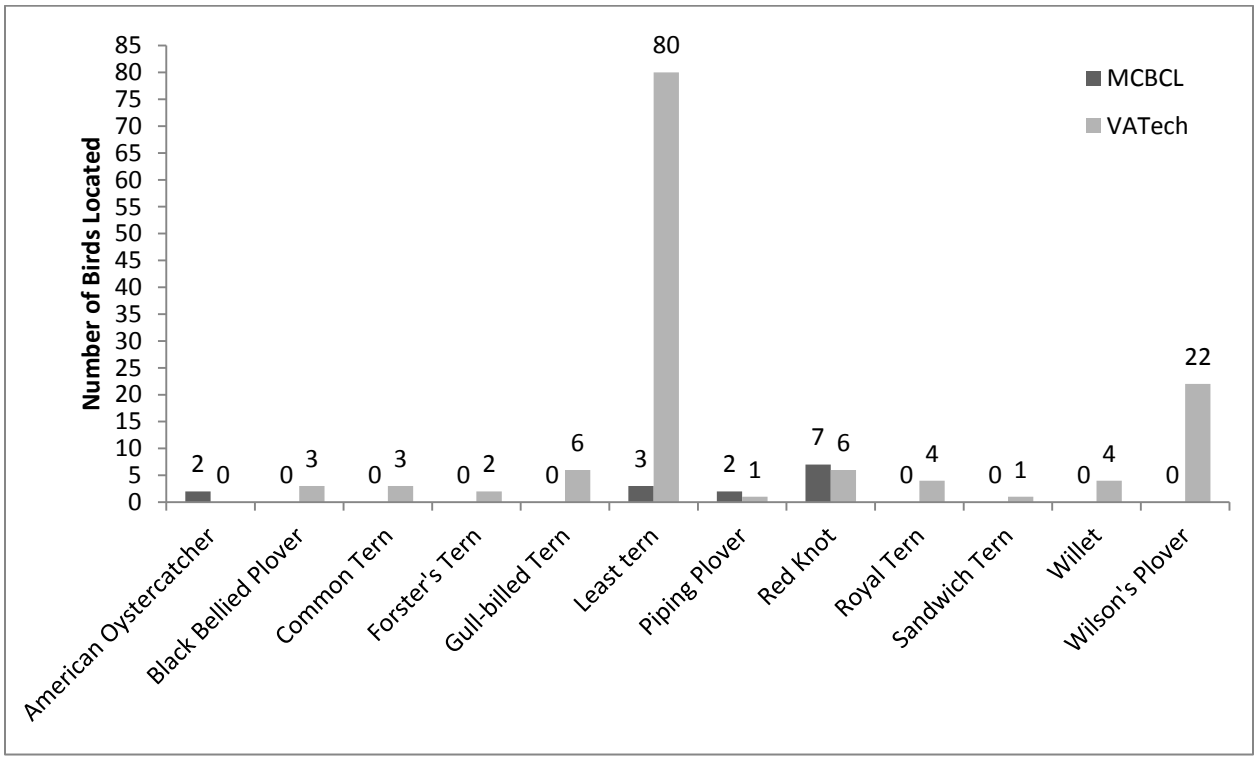

Figure 10-9. Beach-front surveys were conducted by both the VA Tech (on foot) and MCBCL (by vehicle, stopping every mile) crews on June 5, 2009, during the breeding season in the Wildlife Area (Beach Zone 3 in other charts).

Comparison of Findings from MCBCL and DCERP Concurrent Surveys

We were able to conduct surveys concurrently with MCBCL on five dates in 2009. On only one date was MCBCL staff able to conduct the survey of all of Onslow Beach on the same day that we did the survey. As previously stated, this was fewer than expected because the Base leveraged our presence and our shorebird surveys to reallocate staff time to other much needed efforts in all of 2008 and much of 2009 during the breeding season. In both 2008 and 2009, our team worked with MCBCL Environmental Management Division to provide our shorebird data to it for the Division's needs, and to the State of North Carolina. In the surveys that were conducted concurrently, we compared how the different techniques affected numbers of species detected, and abundance of those species detected.

On concurrent surveys that were conducted on March 18, 2009 only in the Wildlife Area (**Figure 10-6**), during late winter/early migration for shorebirds at Onslow Beach, we detected five more species, and a higher abundance of all species, on foot than MCBCL detected in their vehicular surveys.

During concurrent surveys conducted on April 9, 2009, in only the Wildlife Area only (**Figure 10-7**), during late migration/early breeding season, we detected eight additional species than were detected by MCBCL. However, MCBCL detected 19 red knots (*Calidris canutus;* a candidate species for federal listing under the Endangered Species Act), but we did not detect any red knots. Approximately equal numbers of piping plovers were detected by both teams in that survey, but there was a major difference in Wilson's plover detections. We counted 30 Wilson's plovers, but MCBCL did not detect any.

On surveys jointly conducted again during late migration/early breeding season on April 17, 2009, in the Developed Recreation Area only (**Figure 10-8** [i.e., MCBCL was not able to survey the entire beach that day]), each team had a very different record of species detection. MCBCL detected two species not detected by DCERP researchers, and DCERP researchers detected three species not detected by MCBCL.

During the breeding season, we conducted two joint surveys. First, on June 5, 2009 (**Figure 10-9**), we found that again MCBCL was quite efficient at detecting Piping Plovers, even using vehicles as the mode for surveys as both teams recorded similar numbers of that threatened species. However, as noted earlier, DCERP researchers detected many more of the secretive Wilson's plovers by walking surveys along the beachfront (22 Wilson's plovers detected) than were detected by MCBCL (0 Wilson's plovers detected). Similar to earlier surveys, there were 8 species of birds detected by DCERP researchers that were not detected by MCBCL. The MCBCL team did detect an American Oystercatcher while the DCERP team did not detect any oystercatchers on that survey.

Finally, on July 9, 2009 (**Figure 10-10**), during the breeding season, the two teams were able to concurrently survey all of Onslow Beach on the same day. The trends between the two survey techniques on this date were consistent with other dates: walking the ocean front beach by foot consistently results in both a higher number and abundance of species detected.

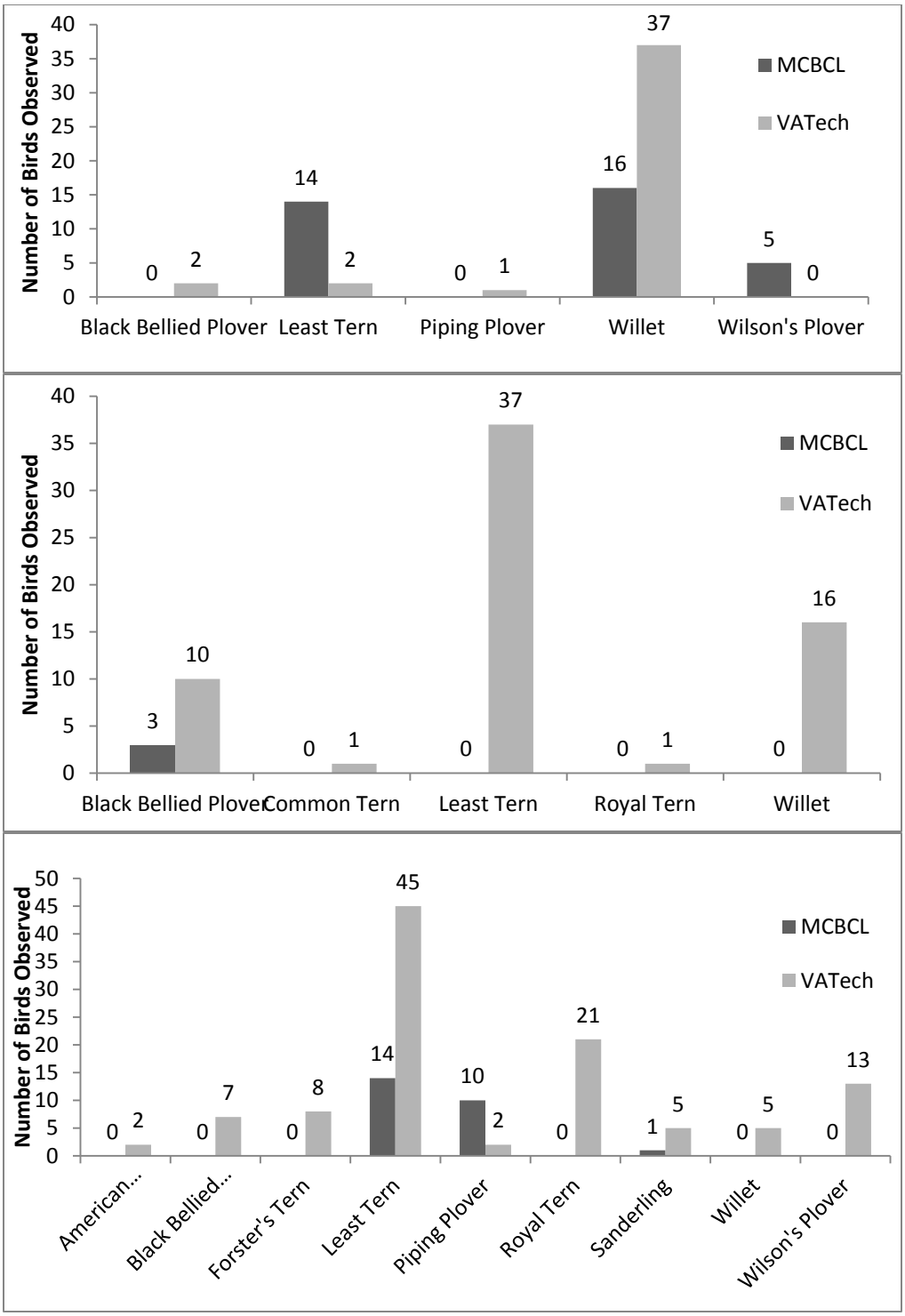

Figure 10-10. Beach-front surveys were conducted by both the VA Tech (on foot) and MCBCL (by vehicle, stopping every mile) crews on July 9, 2009, in all three beach zones, (A) Developed Recreation Area, (B) Military Amphibious Training Zone, and (C) Wildlife Area.

Recommendations for Future Monitoring at MCBCL

Our overarching goal was to explore the historical and present-day monitoring data to assess how MCBCL may best use its limited resources to meet their needs to monitor shorebirds and terns on Onslow Beach. Recommendations will change depending on (1) how the state and federal statuses of certain species changes, and (2) how MCBCL's use of various regions of Onslow Beach changes.

Our first recommendation is to recognize the limitations and strengths of the historical MCBCL data. The strength of this data is that for a significant period of time, MCBCL has been making an effort to survey shorebirds along the length of Onslow Beach. The possible weaknesses of the data stem from the reality that surveys are (1) performed by vehicle, which limits the use of auditory cues to detect birds and the ability to visually detect secretive birds; and (2) conducted often at an irregular frequency, and often not of the entire island on the same day. These factors lead us to recommend that the historical data be primarily used to identify the absence or presence of species by general beach zone, but not for abundance or relative abundance by beach zone.

Given that personnel resources are always limited, we recommend that the Base consider systematic surveys each year for those species that are listed as Candidate, Threatened, or Endangered by the federal government, and similarly as Special Concern, Threatened, or Endangered by the State of North Carolina. By "targeted" surveys, we mean surveys that are not necessarily conducted every 7 to 10 days, but rather stratified by key seasons, for example winter, spring migration, breeding, and fall migration yet repeated at the same frequency and intensity across years. At present, the key species that we recommend for MCBCL to target include piping plovers (federally threatened), gull-billed terns (*Sterna nilotica*; endangered in North Carolina; not detected in our surveys, but may be present), red knot (candidate species for federal listing), and the following breeding species of special concern in North Carolina: American oystercatchers, Wilson's plovers, least terns, common terns (*Sterna hirundo*), and black skimmers (*Rynchops niger*).

The spatial extent of surveying will depend upon the targeted species and season. For example, red knots may be best surveyed by simply driving the length of Onslow Beach as is currently performed several times in April and May of each year. However, surveys for Wilson's plovers would best be performed by foot, should encompass both beach front and inter-dune sandflat, and might be just confined to the Wildlife Area, given limited resources, as our research data suggest that this species is primarily found in that zone of Onslow Beach. Each species will have slightly different spatial and temporal recommendations, which must also accommodate MCBCL resource and logistic constraints.

We recommend MCBCL consider the following two general approaches. First, the Base might choose to conduct migratory and breeding bird surveys each year in a manner consistent with North Carolina's annual red knot surveys, and with their breeding coastal bird surveys (which are actually conducted only once every 3 years at present; NCWRC, 2005). Second, the Base might adopt transect-based survey procedures used by the National Park Service (NPS) in the southeastern region, transects are stratified by different habitat types or disturbance regimes and sampled by season (Byrne et al., 2009). Using the NPS protocol might lead the Base to more heavily sample the Wildlife Area, with its higher diversity and abundances of shorebirds, compared to the other zones.

Literature Cited

Byrne, M.W., J.C. DeVivo, J.M. Maxfield, C.J. Wright, and E. Thompson. 2009. *Methods for Monitoring Migratory and Wintering Shorebirds in Southeast Coast Network Parks*. Natural Resource Report NPS/SECN/NRR—2009/107. National Park Service, Fort Collins, CO.

NCWRC (North Carolina Wildlife Resources Commission). 2005. North Carolina Wildlife Action Plan. Raleigh, NC.

[This page intentionally left blank.]

Chapter 11

Onslow Beach Benthic Invertebrates, Surf Fish, and Sea Turtles

SERDP Project Number: RC-1413

Coastal Barrier Module

Lead Researchers:
Stephen R. Fegley and Charles H. Peterson
University of North Carolina at Chapel Hill's Institute of Marine Sciences
Morehead City, NC
E-mails: sfegley@email.unc.edu and cpeters@email.unc.edu

Supporting Researchers:
Beth M. VanDusen and Antonio B. Rodriguez
University of North Carolina at Chapel Hill's Institute of Marine Sciences
Morehead City, NC

June 27, 2013

Final

This report was prepared under contract to the U.S. Department of Defense (DoD) Strategic Environmental Research and Development Program (SERDP). The publication of this report does not indicate endorsement by DoD, nor should the contents be construed as reflecting the official policy or position of DoD. References herein to any specific commercial product, process, or service by trade name, trademark, manufacturer, or otherwise, do not necessarily constitute or imply its endorsement, recommendation, or favoring by DoD.

Table of Contents

List of Acronyms 11-vii
Abstract 11-1
Objectives of the Monitoring Activity 11-2
Beach and Shallow Subtidal Invertebrate Infauna 11-2
Surf Fish 11-2
Sea Turtle Nesting 11-2
Background 11-2
Beach and Shallow Subtidal Invertebrate Infauna 11-3
Surf Fish 11-3
Sea Turtle Nesting 11-4
Materials and Methods 11-4
Beach Infauna 11-4
Surf Fish 11-7
Sea Turtle Nesting Activity 11-7
Shorebird Abundances on Onslow Beach 11-7
Results and Discussion 11-8
Benthic Invertebrates: Effects of Anthropogenic Activities and Natural Processes 11-8
Surf Fish 11-25
Sea Turtle Nesting 11-30
Assessment of Trends in the Data 11-37
Assessment of Monitoring Design 11-37
Assessment of Seasonal and Annual Variabilities in the Data 11-38
Recommendations for Future Monitoring 11-38
Conclusions and Implications for Future Research 11-39
Key Scientific Findings—Fundamental Cause-and-Effect Relationships 11-39
Findings Supportive of Current Base Management Practices 11-39
Findings with Implications for Future MCBCL Management 11-39
Findings with Implications for DCERP2 11-40
Literature Cited 11-41
Appendix 11-A: List of Scientific Publications 11-A-1
Appendix 11-B: List of Students 11-B-1

List of Figures

11-1. Locations of Onslow Beach, the focus sites used in this study, and the anthropogenic areas. 11-5

11-2. The location of Bear Island, NC, relative to Onslow Beach and specific locations of Focus Sites 8–10. 11-6

11-3. The location of beach zones sampled at each focus site for infauna and ghost crabs. 11-6

11-4. Mean (±1 standard error [SE]) across-shore width (m) of the backbeach and forebeach at each of the sites receiving different anthropogenic activity through nine successive samplings. 11-12

11-5. Mean (+1 standard error [SE]) density of shorebirds in each of 3 years partitioned into 1-mile North Carolina Wildlife Resource Commission Zones along the length of Onslow Beach. 11-13

11-6. Mean (±1 standard error [SE]) abundances of active ghost crab burrows per linear meter in the dunes and beach at each of three sites extending from the west to the east from the New River Inlet. 11-16

11-7. Mean (±1 SE) densities (left panels) and abundances (right panels) of active ghost crab burrows in the dunes and beach at each of three sites, each of which receives different anthropogenic activity, prior to and after several consecutive storms in 2008 (top panels) and Hurricane Irene (lower panels). 11-19

11-8. Mean (±1 SE) width of the backbeach and forebeach at each of three sites prior to, after, and several weeks after storms. 11-20

11-9. Aerial view and beach-level photographs of the 2008 disposal of dredge material on Onslow Beach. 11-21

11-10. Mean (±1 SE) biomass of *Donax* per unit area at control and spoil-impacted sites prior to, during, and after at increasing intervals from the 2011 disposal of dredge material on Onslow Beach. 11-23

11-11. Multivariable dimensional scaling indicating the similarity in densities of the most abundant benthic invertebrates in samples taken from September 2009 through September 2011 at Onslow Beach (Focus Sites 1–7) and Bear Island (Focus Sites 8–10). 11-24

11-12. Mean (±(+1 SE) density (left panel) and abundance (right panel) of active ghost crab burrows at focus sites along Onslow and Bear Islands. 11-25

11-13. Mean (+1 SE) number of species per seine haul. 11-28

11-14. Mean (+1 SE) number of nekton individuals per seine haul in September 2010. 11-29

11-15. Accumulated turtle events (false crawl and nest sums in the top panel and nests false crawls in the bottom panel) occurring at 160-m intervals along the length of Onslow Beach (1982, 1985, 1987–88, 1990–1994, and 1997–2011). 11-31

11-16. Alongshore patterns of accumulated turtle events (nests, false crawls, and the difference between nests and false crawls) occurring at 160-m intervals along the length of Onslow Beach (1982, 1985, 1987–88, 1990–94, and 1997–2011). 11-32

11-17. Mean Emergence Success Rates (ESR) and Adjusted Emergence Success Rates (ESRA) of Onslow Beach sea turtle nests, from 1982-2011. 11-33

11-18. Trends in Emergence Success Rates (ESR) for natural and relocated sea turtle nests on Onslow Beach. 11-33

11-19. Annual mean nest success (ESRA) for Bald Head, Bear, and Onslow islands. 11-34

11-20. The nMDS plot of the frequency of island-specific annual adjusted emergence success rate (ESRA). 11-35

11-21. Location and frequency of sea turtle nest inundation on Onslow Beach, 2007–2010. 11-36

11-22. Sea turtle nest inundation relative to distance from high water line. 11-37

List of Tables

11-1. Results of repeated-observation multivariate analysis of variance (MANOVA) analyses testing the effects of type of anthropogenic activity, the intensity of each activity, and the interaction of activity and intensity across sampling events (time in the table) on infauna abundance or biomass. 11-9

11-2. Results of Tukey's comparisons following separate ANOVA analyses conducted after significant multivariate analysis of variance (MANOVA) examining whether, within each sampling event, there were differences in infaunal density (m^{-2}), *Donax* and *Emerita* biomass (m^{-2}), infaunal abundance (linear m^{-1} of beach), and *Donax* and *Emerita* biomass (linear m^{-1} of beach) depending on anthropogenic activities, the intensity of those activities, or the interaction of these two factors. 11-10

11-3. Results of separate MANOVA analyses examining whether ghost crab burrow density (per m^2) or ghost crab burrow abundance (active burrows per linear meter of beach) differed depending on type of anthropogenic activity, the intensity of the activity, or the interaction of activity and intensity across sampling events (time in the table). 11-14

11-4. Results of Tukey's comparisons for separate ANOVA analyses conducted after significant MANOVA examining whether, within each sampling event, there were differences in active ghost crab burrows per m^2 and per linear meter of beach depending on anthropogenic activities, the intensity of those activities, or the interaction of the two factors. 11-14

11-5. Results of separate MANOVA analyses examining whether ghost crab burrow density (per m^2) or ghost crab burrow abundance (active burrows per linear meter of beach) differed depending upon the effects of storms. 11-17

11-6. Results of Tukey's comparisons for separate ANOVA analyses conducted after significant MANOVA examining whether, relative to the occurrence of coastal storms, there were differences in active ghost crab burrows per square meter and per linear meter of beach and dune field from areas that experience different anthropogenic activities. 11-18

11-7. Results of separate MANOVA analyses examining whether the density of beach infaunal abundances (individuals m^{-2}) or summed biomasses of *Donax* and *Emerita* (g m^{-2}) differed relative to dredge spoil disposals on the beach at an impacted and nearby (approximately 2 km away) control site in each of 2 years. 11-22

11-8. Relative abundances (%) of surf nekton captured in seine samples. 11-26

11-9. Relative frequencies (%) of surf nekton captured in seine samples. 11-27

11-10. Results of two separate MANOVA analyses examining whether species richness (species per seine haul) or total abundance (individuals per seine haul) differed depending on type of anthropogenic activity, the intensity of each activity, the interaction of activity by intensity, or years (time in the table). 11-28

11-11. Relative abundances (percentage of all individuals within an island) and relative frequencies (percentage of all seine hauls within an island) of surf nekton from Onslow Beach and Bear Island in September of 2009, 2010, and 2011 (pooled across years). 11-30

List of Acronyms

°C	degrees Celsius
ANOVA	analysis of variance
BEST	Biological Environmental Stepwise Procedure
BFR	buffer (area or zone)
CB	Coastal Barrier (Module)
cm	centimeter
DCERP1	first cycle of the Defense Coastal/Estuarine Research Program
DCERP2	second cycle of the Defense Coastal/Estuarine Research Program
DoD	U.S. Department of Defense
EMD	Environmental Management Division
ESR	emergence success rate
ESRA	adjusted emergence success rate
g	gram
$g\ m^{-2}$	grams per square meter
HSD	Tukey's Honestly Significant Differenced (test)
km	kilometer
L	liter
m, m^{-1}	meter, per meter
m^2, m^{-2}	square meter, per square meter
MANOVA	multivariate analysis of variance
mm	millimeter
mm/y	millimeters per year
MT	military training
nMDS	non-metric multidimensional scaling
NOAA	National Oceanic and Atmospheric Administration
ORRV	off-road recreational vehicle
PERMANOVA	permutational multivariate analysis of variance
REC	recreation (area)
SE	standard error
SERDP	Strategic Environmental Research and Development Program

[This page intentionally left blank.]

Abstract

Barrier islands and their ecological communities regularly experience substantial wind, wave, and current energies. For the organisms constituting the ecological communities, surviving this regime requires specific adaptations to high levels of spatial and temporal variability in environmental conditions. Adaptation to high environmental stresses has left many barrier island species susceptible to higher mortality when anthropogenic stressors are imposed on them. When humans work, live, and recreate on barrier islands they inevitably add stress to these communities. Preserving natural habitats requires us to understand how and when our activities cause harm to inform management attempts to mediate these undesirable effects.

Currently, Marine Corps Base Camp Lejeune (MCBCL) natural resources management focuses on preventing conditions that increase mortality of ground-nesting shorebirds, nesting sea turtles, and the fish that attract recreational attention. We determined the effects of several types of persistent human activities (off-road recreational vehicle use, military training, and sunbathing) occurring at Onslow Beach on the primary food source for shorebirds and surf fish (intertidal invertebrates), ghost crabs (an indicator species in the system), surf fish, and sea turtle nesting. Our basic design recognized that the various anthropogenic activities occur in spatially discrete areas on the island. We quantified in these areas the abundances of our target species. Intertidal invertebrates were sampled by coring, ghost crabs by assessing active burrows, and surf fish by seining. Sea turtle nesting data were gathered along the entire island by MCBCL personnel as part of its existing management program. We also studied the effects of two short-term perturbations on these species: storms and dredge disposal operations.

Although we found many significant differences among seasons, years, and locations in the abundances of intertidal invertebrates, none of these differences were consistently associated with the spatial pattern of human activity on Onslow Beach. Environmental factors, such as grain size and beach slope, explained intertidal invertebrate patterns more frequently. In contrast, ghost crab abundances showed a clear and consistent depression in the beach section where military training occurs that could not be explained by any of the environmental factors we measured. The surf fish, like the intertidal invertebrates, did not show any pattern that could be related to human activities. Storms had little effect on intertidal invertebrates and only modest effects on ghost crab distribution. Dredge disposal did have some negative effects that could be enhanced if the volume of dredge material disposed on the beach increases. Based on the emergence success rates of sea turtle hatchlings from nests and the proportions of nests surviving to hatching, the existing sea turtle management program effectively mediates the potential negative impacts of anthropogenic activities occurring on Onslow Beach, including military training.

Current restrictions and procedures regulating both recreational and military activities on Onslow Beach constrain habitat degradation. The sole negative impact that could be related to an anthropogenic activity, military training on ghost crabs, should be examined further to better understand the process leading to this relationship. However, we detected no cascading effects of the impact to ghost crabs to other species or habitats of management interest.

Keywords: Barrier island, dredge disposal, exposed beach, ghost crabs, sea turtle nesting, shorebird foraging, storms, surf fish

Objectives of the Monitoring Activity

Beach and Shallow Subtidal Invertebrate Infauna

Sandy-beach macroinvertebrates (infauna) along the ocean beaches represent the universal food supply for all demersal surf fish and shorebirds. Studies conducted elsewhere have demonstrated that this prey resource can be impacted by natural physical–sedimentological forcing mechanisms and by anthropogenic activities (i.e., physical disturbance by vehicles and, more importantly, by massive sediment deposition and potential changes in sediment character during and after potential beach nourishment). Monitoring infaunal abundances provides a means to test whether recent Base activities on the beach (both recreational and training) influence this food resource utilized by birds and fish that are of management and recreational interest. Some of this information was utilized in determining shorebird productivity in Research Project CB-3 (see the *DCERP1 Final Research Report* for more information). In addition, ghost crab (*Ocypode quadrata*) abundances were followed because they are recognized globally as an important indicator species for negative anthropogenic activities on beach habitats and because the species plays complex but critical roles in sea turtle nest and hatchling success.

Surf Fish

The main objective of monitoring surf fish once each year was to quantify the habitat value of Onslow Beach as nursery and foraging grounds for recreationally and commercially important surf fish, notably pompano (*Trachinotus* sp.), Gulf kingfish (*Menticirrhus littoralis*), red drum (*Sciaenops ocellatus*), spot (*Leiostomus xanthurus*), and flounder (*Paralichthys* sp.). These demersal surf fish prey upon benthic macroinvertebrates and, along with shorebirds, contribute to inducing seasonal changes in abundance of the benthos and patterns of abundance relative to natural and human disturbances. These species of surf fish can also be affected by the sedimentological character of the intertidal and subtidal portions of the beach which means that Base activities that influence nearshore morphology and granulometry could impact surf fish.

Sea Turtle Nesting

Sea turtles (primarily loggerhead turtles [*Caretta caretta*]) use Onslow Beach for nesting annually. Because all sea turtles are protected by the Endangered Species Act, MCBCL maintains an active nest management program. We used MCBCL monitoring data to provide insight into how sea turtle nesting site choice and hatching success vary with natural conditions and Base activities. We also used these data to assess the relative success of the MCBCL management practices with respect to comparable nest management programs conducted in North Carolina. Finally, we used the data we collected from beach morphology to provide insight into how sea turtle nesting site choice and hatchling success are influenced by transgression and regression of Onslow Beach.

Background

Exposed beaches, from the subtidal to the dunes, regularly receive sufficient mechanical energy from waves, winds, and currents to alter the shape and granulometry of the habitat. Organisms using and exploiting this habitat must possess adaptations that enable them to maintain

themselves in this dynamic matrix. Recognition of this condition in the past led ecologists and environmental managers to assume human activities had little or no effect on the beach biological communities. In the last decade many studies have demonstrated that this assumption is untenable.

The entire ecology of coastal barriers is organized directly and indirectly by the physical dynamics of meteorologically driven ocean forcing and the resulting sediment transport (Godfrey and Godfrey, 1976; Wells and Peterson, 1986). Physical processes operating in the nearshore, including wind, waves, and currents, vary in magnitude on time scales from hours (e.g., coastal storms) and months (e.g., seasonal weather patterns) to years and decades (e.g., climate change). Sea level rise is the background stage on which the physical processes are operating. The rate of rise is currently is greater than 3 mm/y at the National Oceanic and Atmospheric Administration (NOAA) tide gauge in Beaufort, NC, located 65 km northeast of the study area, but this rate is predicted to accelerate because of global warming (NCCRC, 2010). Variations in the underlying geology and bathymetry of coastal areas, as well as the structure and topography of the subaerial beach, influence how shorelines will respond (i.e., accrete, erode, change in sediment type) to different physical forcings (McNinch, 2004; Rodriguez et al., 2004).

Beach and Shallow Subtidal Invertebrate Infauna

The intertidal portion of the shoreface enjoys high production of characteristic invertebrates, such as coquina clams and mole crabs, because of high fluxes of suspended diatoms from oscillating wave action on shore. The high densities of these invertebrates qualify the intertidal beach as a key habitat, one that supplies food for abundant and valuable surf fishes, crabs, and shorebirds, including piping plover (*Charadrius melodus;* federally threatened), red knot (*Calidris canutus;* candidate species for listing), and many other state and federal bird species of concern (Brown and McLachlan, 1990; Fraser et al., 2005; Karpanty et al., 2006). The sediment mobility and changes in its size distribution and mineralogical composition help determine the abundance and composition of the benthic invertebrates on the ocean beach and on sand flats on the inlet and backbarrier shores. These benthic invertebrates provide the prey on which the entire surf fish and shorebird community depends: this is the trophic base that dictates habitat quality for species of importance that are managed by humans.

Superimposed upon this background of natural physical, geological, and biological processes that interact to determine the state, health, and persistence of the barrier island ecosystem are human interventions. Such human interventions on Onslow Beach include recreational off-road driving, amphibious training, dune restoration of topography and vegetation, inlet dredging, unintentional augmentation of predatory vertebrates such as raccoons, and potentially beach nourishment or application of alternative protections against shoreline erosion.

Surf Fish

No quantitative sampling of the surf zone fishes has been conducted in the waters of Onslow Beach although recreational sampling (i.e., fishing) of large-sized individuals has long been practiced and is one of the primary recreational activities on the island. The surf zone of exposed beaches is suspected to play an important role as a nursery for many species as the physical turbulence in this area reduces the effectiveness of avian and fish piscivores (Romer, 1990;

Wilber et al., 2003). The distribution of surf zone fish has been shown to be affected by wave energy (Clark, 1997), the presence of muddy sediments (Mont'Alverne et al., 2012), and beach nourishment operations (Wilber et al., 2003). This raises the possibility that the different types of anthropogenic activities on Onslow Beach and the different physical conditions of the nearshore geology and hydrodynamic energy could produce site-specific patterns of variable surf zone quality for fish habitat along the island.

Sea Turtle Nesting

Worldwide, sea turtles have experienced substantial and alarming declines in abundance over decades and centuries (Bjorndal et al., 2010; Magnuson et al., 1990), establishing them as an important target of ocean wildlife conservation. Threatened species of sea turtles lay eggs on the high beach during late spring and through the summer. The eggs require approximately 60 days to develop and hatch. The nesting success is strongly influenced by physical processes: storms can wash away nests or drown developing sea turtles in the nests. Predation on sea turtle eggs and hatchlings by invertebrate, avian, and mammalian predators forms a top-down control on success of the species that can be more important than the bottom-up physical forcing (Bolten et al., 2011; Peterson et al., 2012). Humans also affect sea turtle eggs and hatchlings directly (egg consumption) and indirectly (lighting beachfronts and driving on the beach) in ways that lead to lower survival (Garcia et al., 2003; Wolcott and Wolcott, 1984).

On Onslow Beach the Threatened and Endangered component of the Environmental Management Division conducts an intensive program to reduce or eliminate the majority of mortality sources to sea turtle eggs and hatchlings. During nesting season when adult, gravid females visit Onslow Beach (May 1 through October 1) the entire beach is surveyed every morning as early as possible to detect the presence of any turtle nests laid the night before. All of the nests they find have anti-predator cages placed over them to inhibit entry by mammalian predators and curious humans. Nests laid in locations on shore low enough to be at risk of erosion or flooding and any nests found in the active military training zone are moved to more protected locations on Onslow Beach before emplacing the turtle cage. The landscape around nests approaching their hatching date is managed to reduce light distractions (by putting light-blocking screens landward of the nest) if necessary and by smoothing the beach surface seaward to avoid having hatchlings fall into depressions created by anthropogenic activities. After hatchlings emerge the nest is excavated, generally within 2–3 days, to determine the nest emergence success rate (ESR) by determining the proportion of unhatched eggs or unemerged hatchlings remaining in the nest out of the total eggs that were present.

Materials and Methods

Beach Infauna

Sampling Design

Macroinvertebrates and ghost crab burrows were sampled at several focus sites over 4½ years. Anthropogenic activities are compartmentalized on Onslow Beach into four, contiguous areas (**Figure 11-1**). The westernmost quarter of the island is frequently available for driving on the beach with off-road recreational vehicles (ORRVs). Heading east from the ORRV area, the next quarter of the island is used for military training (MT) and, when MT activities have not closed

the beach, to ORRV traffic. Abutting the MT area, the next eastern quarter of the island is used for swimming and sunbathing recreation (REC). Finally, the easternmost quarter of the island is restricted from almost all human activity because the eastern tip of Onslow Beach is in an impact area, which is separated from the REC area by a precautionary buffer (BFR) zone.

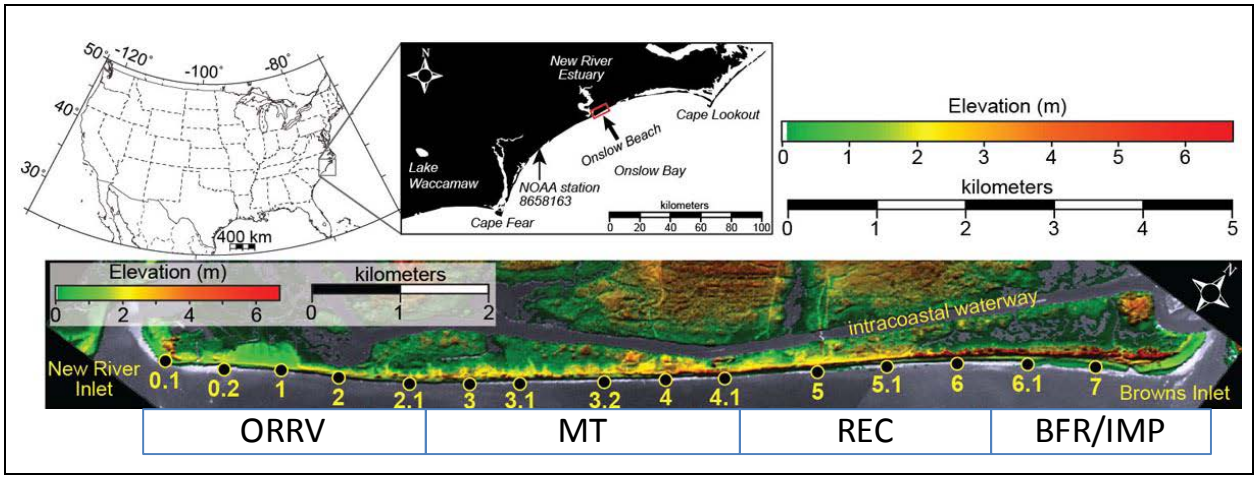

Figure 11-1. Locations of Onslow Beach, the focus sites used in this study, and the anthropogenic areas.

To test the effects of anthropogenic activities on benthic invertebrate abundances, six primary focus sites were established on Onslow Island: two in the ORRV area (Focus Sites 1 and 2), two in the MT area (Focus Sites 3 and 4), and two in the REC area (Focus Sites 5 and 6). One additional focus site was established in the BFR area (Focus Site 7). Based on our own observations and discussions with Base personnel, one of the focus sites within each area (except BFR) was located in a specific site that frequently received higher intensities of the respective anthropogenic activity, and the other was placed in a specific site experiencing lower intensities of the respective activity. Each of these focus sites was sampled in the late summer/early fall and mid-spring of every year starting in October 2007 and ending in September 2011. The BFR focus site was established in May 2008 and sampled seasonally thereafter to test the effects of periodic disposal of dredge material on the beach infaunal abundances. Several additional focus sites, intermediate in location between the primary focus sites, were sampled less regularly. To capture the effects of strong storms on beach invertebrates, we visited one focus site each in the ORRV, MT, and REC areas when a tropical storm approached MCBCL and sampled immediately prior to the onset of the storm and as soon as possible after the storm ended.

Beginning in September 2009, three additional focus sites were established on Bear Island to compare faunal abundances between a barrier island with multiple anthropogenic activities (Onslow Beach) to one with limited human activity (Bear Island; **Figure 11-2**).

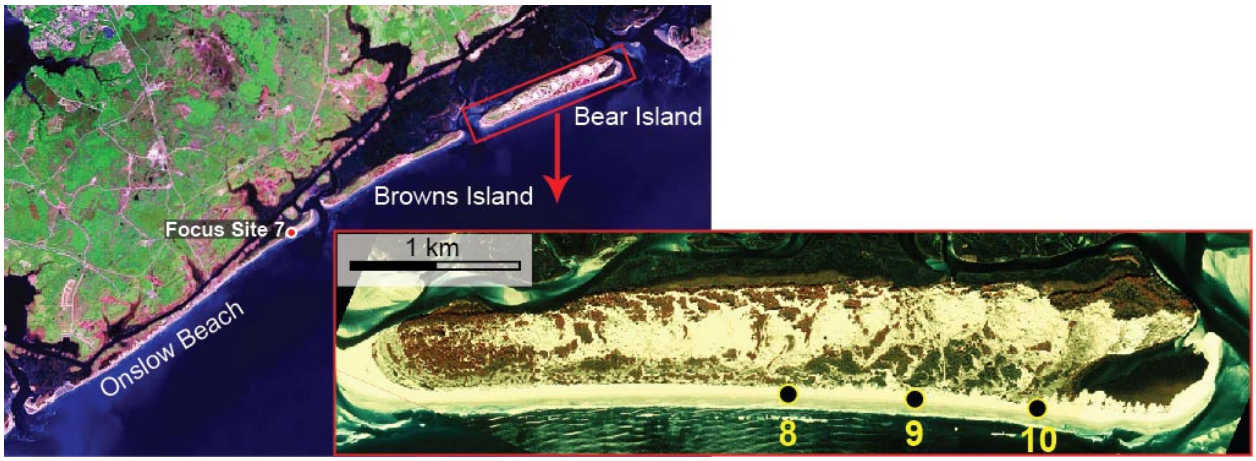

Figure 11-2. The location of Bear Island, NC, relative to Onslow Beach and specific locations of Focus Sites 8–10.

Sampling and Enumerating Procedures

Each time we sampled a focus site the infaunal macroinvertebrates within the beach were quantified from each of three elevation zones: (1) from the top of the intertidal wetted sediments down to the top of the intertidal saturated sediments (middle intertidal); (2) from the top of the intertidal saturated sediments down through the swash zone (low intertidal); and (3) into the shallow subtidal to 1-m deep (**Figure 11-3**). We used a procedure similar to that used in previous studies quantifying beach infauna from North Carolina (Peterson et al., 2000 and 2006); within each elevation zone the contents of three, separate, haphazardly located, vertical cores (corer opening surface area=0.0078 m^2) taken to a depth of 15 cm were placed into a single, 1-mm mesh sieve and washed in the field. The material remaining on the sieve constituted a single sample and was placed with a label into a 1-L plastic bag that was sealed and placed on ice in a cooler. Four replicate samples were collected within each of the three elevation zones from each of two transects (located 30–40 m apart) within each focus site.

Figure 11-3. The location of beach zones sampled at each focus site for infauna and ghost crabs.

In the laboratory, all samples were kept in a 4.5°C walk-in cold room until they were processed (within hours to, at most, 3 days of when they were taken in the field). Processing consisted of placing the contents of each sample bag into a white, plastic tray (35 cm × 45 cm × 9 cm), adding some freshwater, and picking out all fauna while systematically progressing through the material. Each organism was identified, the number of individuals of each species counted, and the length of all coquina clams (*Donax variabilis*) and mole crabs (*Emerita talpoida*) measured

to the nearest 0.1 mm using vernier calipers. The volume of the remaining sedimentary material (shell hash, sand, and gravel all greater than 1 mm in diameter) was measured in a 2-L graduated cylinder.

At the same time that benthic cores were taken in the field at each focus site we estimated the abundance of ghost crabs by quantifying the number of active ghost crab burrows using a procedure modified from Wolcott (1978). For each transect at each focus site, a pair of observers, walking in tandem, counted all of the active burrows (as indicated by the presence of ephemeral traces of crab activity in the sand around the burrow opening) in (2–4) replicate 4-m wide, across-shore swaths per transect per focus site originating at the mid intertidal and continuing to the furthest inland extent of ghost crab habitat. The observers also categorized the diameter of each active burrow as small (less than 2.5 cm), medium (2.5–5 cm), or large (greater than 5 cm).

Surf Fish

Monitoring sites for surf fish occurred at the same 10 focus sites (seven on Onslow Beach and three on Bear Island) used to estimate beach infauna and ghost crab abundances. The seine used is 1.83-m high and 12.2-m wide with a uniform 0.1-cm mesh and a centrally located 1.83-m deep bag. At each focus site, replicate (n=2) beach seine hauls were performed at low tide under calm sea conditions in September. The contemporaneous, replicate seine hauls were positioned with 50-m separation between them as subsamples for each site. Each seine was hauled along the shore, perpendicular to the beach, a distance of 35–40 m with the shoreward end of the seine positioned within the swash zone. At the end of the haul the seine was pulled onto the intertidal of the beach and all nekton captured in the seine were identified to species, enumerated, and released back into the surf.

Sea Turtle Nesting Activity

Sea turtle nesting attempts, successes, and failures are determined (by MCBCL Environmental Management Division [EMD] personnel) daily during sea turtle nesting season by early morning drives along the entirety of the ocean and inlet beaches of Onslow Beach using observations of tracks and digging disturbances. Both untouched and relocated nests are marked, which allows nests to be inventoried after hatchlings emerge in order to calculate the percentage of eggs successfully hatched.

Shorebird Abundances on Onslow Beach

We also used data collected by EMD on the seasonal and alongshore abundances of shorebirds on Onslow Beach. At approximately 2-week intervals throughout Year 2 or more, observers drive the length of the island in a truck and record the bird species, the number of individuals of each, and the approximate location of each sighting relative to island length.

Results and Discussion

Benthic Invertebrates: Effects of Anthropogenic Activities and Natural Processes

Responses to Persistent Disturbances: Infauna

General Characterization of the Infaunal Assemblage

Our sampling of the intertidal and shallow subtidal exposed beach collected 24 different species of invertebrate infauna. Four species dominated numerically (96.6% of all individuals), occurred frequently (in 33% to more than 50% of all samples), and were collected at every sample site on every occasion. These dominant species included coquina clams (*Donax variabilis* and *D. fossor*), mole crabs (*Emerita talpoida*), digger amphipods (at least three species in the family Haustoridae), and beach palp worms (*Scolelepis squamata*). As the species with the largest individual sizes in the infauna, coquina clams and mole crabs constituted the greatest biomass in virtually all samples with any organisms. All of these abundant species are known prey for shorebirds and surf fish. We assess the effects of anthropogenic and natural factors on prey by examining separately the total number of all individuals and, separately, the sum of coquina clam and mole crab biomass. Each of these response variables are further standardized, by density (individuals or biomass m^{-2}) or abundance (individuals or biomass per linear meter of beach; the latter is a 1-m wide transect extending perpendicular to the water line across the width of the available habitat). Density measures provide insight into the biological responses of organisms to environmental factors: abundance measures better represent the amount of prey available to the next trophic level at a given beach at a given time.

Effects of Persistent Anthropogenic Activities

Initial examination of the data showed large annual and seasonal differences in the abundances of infauna. To increase our ability to detect differences associated with anthropogenic activities we removed annual and seasonal variation by calculating z-values (with respect to each sampling period) for each observation. In all cases, Box-Cox power transformations were required subsequently to remove heteroscedasticy within the data as determined by non-significant O'Brien tests. For both the density of all individuals and per unit area biomass, the sampling time × activity × intensity interactions were significant indicating that activity × intensity effects were present for at least some sampling times (**Table 11-1**). To examine within the specific sampling times, we conducted separate two-way analyses of variance (ANOVAs) using activity type and intensity level as main effects for each sampling time for each response variable (**Table 11-2**). Because we conducted multiple independent tests we used a Bonferroni corrected P value ($P<0.0055$) for recognizing significant differences and to avoid Type I errors.

Table 11-1. Results of repeated-observation multivariate analysis of variance (MANOVA) analyses testing the effects of type of anthropogenic activity, the intensity of each activity, and the interaction of activity and intensity across sampling events (time in the table) on infauna abundance or biomass.

Separate tests were conducted for each variable on both a per unit area or per linear meter basis. Biomass is the sum of *Donax* and *Emerita* (g) biomasses. Seasonal differences were removed from the response variables before testing for anthropogenic effects. Values in the table represent the probabilities associated with the respective F values of the indicated source of variation. Significant differences (P<0.05) are indicated in boldface and gray boxes.

Source	Density (m^{-2})		Abundance (linear m^{-1})	
	Number of Individual	Biomass	Number of Individual	Biomass
	Between Subjects			
Activity	0.18	0.06	0.99	0.07
Intensity	0.87	0.16	**<0.0001**	0.96
Activity × intensity	0.22	**0.002**	0.48	**<0.0001**
	Within Subjects			
Time	0.06	**<0.0001**	0.87	**0.026**
Time × activity	**<0.0001**	**<0.0001**	**<0.0001**	**<0.0001**
Time × intensity	**0.011**	0.15	**<0.0001**	**<0.0001**
Time × activity × intensity	**0.002**	**<0.0001**	**<0.0001**	**<0.0001**

Significant differences in density of individuals was observed several times in the spring (May) sampling in each year; no significant differences among anthropogenic activity zones and the intensity of the activity were found in the late summer/early fall samples except in 2011 (**Table 11-2**). The September 2011 sampling occurred approximately 3 weeks after Hurricane Irene had substantially changed the granulometry and morphology of the beaches potentially altering or erasing many of the effects that anthropogenic activities may have had on the infauna during the preceding summer. Among the four spring samplings the pattern of differences in infaunal density varied among years with no single site, activity, or intensity consistently showing higher or lower infaunal densities. For biomass per unit area, in six out of the nine sampling times no significant differences could be detected and in the three times when differences were observed (September 2009, May 2011, and September 2011) no consistent pattern among activities and intensities emerge (**Table 11-2**). Considered together, no evidence is seen of persistent, direct effects of existing Onslow Beach anthropogenic activities on beach infauna density or biomass.

Table 11-2. Results of Tukey's comparisons following separate ANOVA analyses conducted after significant multivariate analysis of variance (MANOVA) examining whether, within each sampling event, there were differences in infaunal density (m^{-2}), *Donax* and *Emerita* biomass (m^{-2}), infaunal abundance (linear m^{-1} of beach), and *Donax* and *Emerita* biomass (linear m^{-1} of beach) depending on anthropogenic activities, the intensity of those activities, or the interaction of these two factors.

Only results for Bonferroni-corrected significant differences (P<0.0055) are provided. In each case the activities, intensities, or combinations are ranked from highest to lowest (A to D) respective to their associated mean values. Means followed by the same letters are not significantly different. Ellipses indicate no significant differences. Low = lower intensity; high = higher intensity; MT = military training area; ORRV = off-road recreational vehicle area; REC = recreation area.

Metric	Factor	October 7	May 8	September 8	May 9	September 9	May 10	September 10	May 11	September 11
Density (m^{-2})	MT	...	...	...	...	...	A	...	B	...
	ORRV						A		A	
	REC						B		A	
	High	...	...	...	B	...	...	...	...	...
	Low				A					
	MT—high	...	B C	...	...	...	...	...	...	C D
	MT—low		A B C							B C D
	ORRV—high		A B							A
	ORRV—low		C							A B
	REC—high		C							B C
	REC—low		A							D
Biomass (m^{-2})	MT	...	...	...	...	A	...	...	B	...
	ORRV					B			A	
	REC					C			A	
	High	...	...	...	...	...	...	...	...	...
	Low									
	MT—high	...	...	...	...	...	...	...	...	C D
	MT—low									B C D
	ORRV—high									A
	ORRV—low									A B
	REC—high									B C
	REC—low									D

(continued)

Table 11-2. (continued)

Metric	Factor	October 7	May 8	September 8	May 9	September 9	May 10	September 10	May 11	September 11
Abundance (linear m^{-1})	MT	A					A B			B
	ORRV	B	...	...	...	...	A	...	...	A
	REC	C					B			B
	High	A	...	...	...	...	B	B	...	...
	Low	B					A	A		
	MT—high	...	B	...	B	A B	...	...	C	...
	MT—low		B		A	B C			C	
	ORRV—high		B		B	D			C	
	ORRV—low		B		B	C D			B	
	REC—high		B		B	A			B C	
	REC—low		A		A	C			A	
Biomass (linear m^{-1})	MT	...	...	...	...	A	...	...	C	...
	ORRV					B			B	
	REC					B			A	
	High	...	...	...	...	...	...	...	...	...
	Low									
	MT—high	...	...	...	A	...	B C	B	...	B C
	MT—low				A B		B	A B		B
	ORRV—high				A		B C	A B		A
	ORRV—low				C		C	A B		A
	REC—high				B C		B C	A		B
	REC—low				A B		A	B		C

As with infaunal densities, multivariate analysis of variance (MANOVA) indicated that both infaunal abundances and biomasses per linear meter of beach varied among sampling times (**Table 11-1**). Examination of activity and intensity effects within times revealed substantially more differences than the analyses of per unit area data indicated. Infaunal abundances per linear meter of beach were non-significant on one sampling occasion only (**Table 11-2**). Inspection of the spring samplings indicates that infaunal abundances were higher generally in the REC area, especially the low intensity REC area, than elsewhere. In our spring samplings, the relative abundances of coquina clams were consistently higher than most other species and greater than they are in the late summer samplings, a pattern that has been observed on other North Carolina beaches (Peterson et al., 2002 and 2006). Within a season, coquina clams show their greatest abundances wherever beach sediments were finer. Analysis of granulometry from all of the sites showed that the low-intensity REC area (Focus Site 6) consisted of finer sediments (see Chapter 9, **Figure 9-11**). Consequently, this spring pattern is most likely a result of the coincidence of preferred sediment type in the low-intensity REC area for one of the dominant infaunal species. Biomass per linear meter was not significantly different among sites from October 2007 through September 2008 and highly variable among sites in subsequent samplings. Again, no clear effect of type or intensity of anthropogenic activity on infauna emerges.

Consideration of the widths of the beach at the different areas during the samplings can provide further insight of the variable abundances. Two areas, ORRV-low and REC-low, varied more in forebeach width among all samplings than the other four areas (**Figure 11-4**). Because both are low-intensity representatives of the dominant anthropogenic activities that occur in those areas, the variation in beach width likely result from physical forcing by waves and currents. These two specific areas also usually have the widest forebeaches among all areas sampled. Infaunal abundance is a function of the density of the infauna and the spatial extent of the habitat so variable, large changes in beach width will certainly produce large changes in abundance if no compensatory change in infaunal density occurs. We demonstrated that density and per unit area biomass did not differ generally among areas so the higher frequency of differences detected in abundance and biomass per linear meter arise primarily from changes in habitat size.

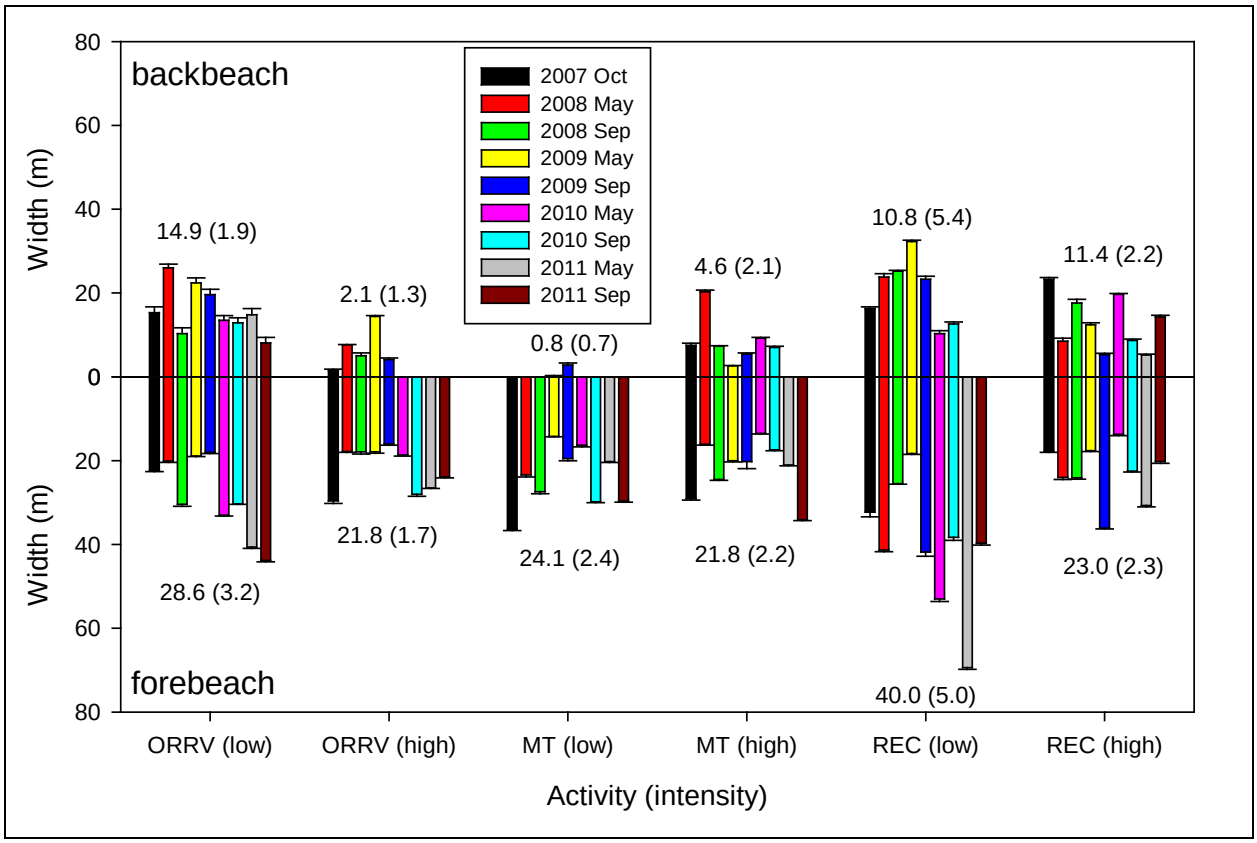

Figure 11-4. Mean (±1 standard error [SE]) across-shore width (m) of the backbeach and forebeach at each of the sites receiving different anthropogenic activity through nine successive samplings.

Numbers above and below the bars represent the mean (±1 SE) width of the respective forebeach or backbeach averaged across all samplings. Note that the ***y***-axis always increases positively from the origin.

Infaunal distribution among areas and beach geology did have a significant influence on the distribution of shorebirds. In both the spring (April–June) and late summer/early fall, the alongshore distribution of shorebirds enumerated by the Base truck survey followed a consistent pattern with higher abundances towards both inlets and depressed abundances in the middle of the island (**Figure 11-5**). BEST analysis (a procedure that matches patterns between multivariate environmental data sets and multivariate biological data sets to estimate how they may relate to

each other) found that in the spring 21.4% of the annual variance in shorebird abundance and distribution was related to variance in the abundance of coquina clams, the width of the forebeach, and the slope of the forebeach. In the fall, 40.4% of shorebird abundances and distribution was related to the density of all infauna, the percent gravel present in the intertidal, and the width of the forebeach.

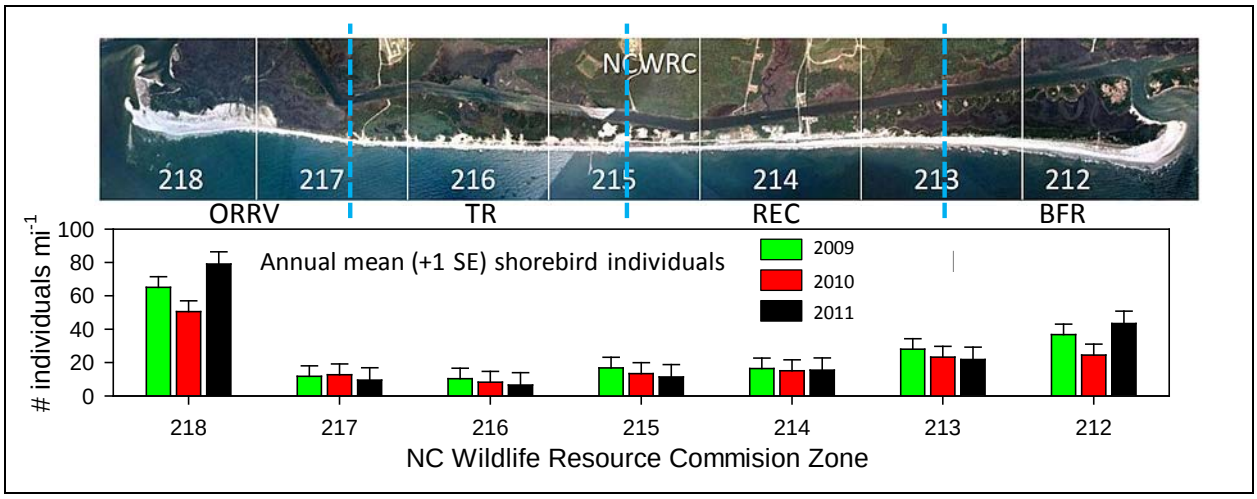

Figure 11-5. Mean (+1 standard error [SE]) density of shorebirds in each of 3 years partitioned into 1-mile North Carolina Wildlife Resource Commission Zones along the length of Onslow Beach.

For orientation, the blue dashed lines in the map above indicate the borders between the anthropogenic areas used in this study in relation to the North Carolina Wildlife Resources Commission.

Responses to Persistent Disturbances: Ghost Crabs

The densities (m^{-2}) and abundances (per linear meter of beach) of active ghost crab burrows seaward of the primary dunes both differed with respect to activity and intensity across sampling times (**Table 11-3**). Perusal of the within-sampling tests comparing activity type and intensity show some differences in the precise pattern among sampling times but, overall, densities and abundances are higher in the REC area, lowest in the MT area, and usually lower where the intensity of each anthropogenic activity is higher (**Table 11-4**).

Table 11-3. Results of separate MANOVA analyses examining whether ghost crab burrow density (per m^2) or ghost crab burrow abundance (active burrows per linear meter of beach) differed depending on type of anthropogenic activity, the intensity of the activity, or the interaction of activity and intensity across sampling events (time in the table).

Annual differences were removed before testing for anthropogenic effects.
Significant differences (P<0.05) are indicated in boldface.

Source	Density (m^{-2})	Abundance (linear m^{-1})
	Between Subjects	
Activity	**<0.0001**	**<0.0001**
Intensity	**0.0088**	**<0.0001**
Activity × intensity	**<0.0001**	**0.001**
	Within Subjects	
Time	0.15	**<0.0001**
Time × activity	**<0.0001**	**<0.0001**
Time × intensity	0.33	0.84
Time × activity × intensity	**0.0002**	**0.0042**

Table 11-4. Results of Tukey's comparisons for separate ANOVA analyses conducted after significant MANOVA examining whether, within each sampling event, there were differences in active ghost crab burrows per m^2 and per linear meter of beach depending on anthropogenic activities, the intensity of those activities, or the interaction of the two factors.

Only results for Bonferroni-corrected significant differences (P<0.0055) are provided. In each case the activities, intensities, or combinations are ranked from highest to lowest (A–D) respective to their associated mean values of ghost crab burrows. Means with the same letters are not significantly different. Ellipses indicate no significant differences. Low = lower intensity; high = higher intensity; MT = military training area; ORRV = off-road recreational vehicle area; REC = recreation area.

Metric	Factor	October 7	May 8	September 8	May 9	September 9	May 10	September 10	May 11	September 11
Active burrows (m^{-2})	MT						C	C		B
	ORRV	...	...	...		...	B	B	...	B
	REC						A	A		A
	High	...	...	...	B	...	...	...	...	...
	Low				A					
	MT—high	B C	C	B		B			B	
	MT—low	A B	A	B		B			A B	
	ORRV—high	B	B C	A	...	A	...	...	A	...
	ORRV—low	C	B C	B		B			A B	
	REC—high	A B	A B	B		B			A B	
	REC—low	A	A B	A B		A B			A	

(continued)

Table 11-4. (continued)

Metric	Factor	October 7	May 8	September 8	May 9	September 9	May 10	September 10	May 11	September 11
Active burrows (linear m^{-1})	MT	...	B	C	...	C	B	B	B	B
	ORRV		B	B		B	C	B	A	B
	REC		A	A		A	A	A	B	A
	High	...	B	B	...	B	B	...	B	B
	Low		A	A		A	A		A	A
	MT—high	C D	...	...	...	...	...	...	...	...
	MT—low	B C								
	ORRV—high	C								
	ORRV—low	D								
	REC—high	A B								
	REC—low	A								

This pattern is most apparent in the results of the abundances of active ghost crab burrows. For infauna, inclusion of beach width and estimation of total abundance complicated the pattern of results; the opposite occurs for ghost crab burrows because the preferred zone of ghost crabs on the beach is the backbeach, which is absent at many areas of Onslow Beach, narrower than the forebeach, and, when present, less variable (**Figure 11-4**). Numerous studies, conducted on beaches around the globe, have found a negative relationship between intensity of anthropogenic activities and the abundances of ghost crabs (Schlacher et al., 2011). On Onslow Beach, the depression in active ghost crab burrows and sightings of active ghost crabs are consistently lowest, across all nine of our seasonal samplings, in the MT area. We increased the spatial precision of our sampling for ghost crab burrows in September 2009 and found that low ghost crab abundances occurred throughout the MT area on the beach and in the dune and dune fields landward of the beach in that area (**Figure 11-6**).

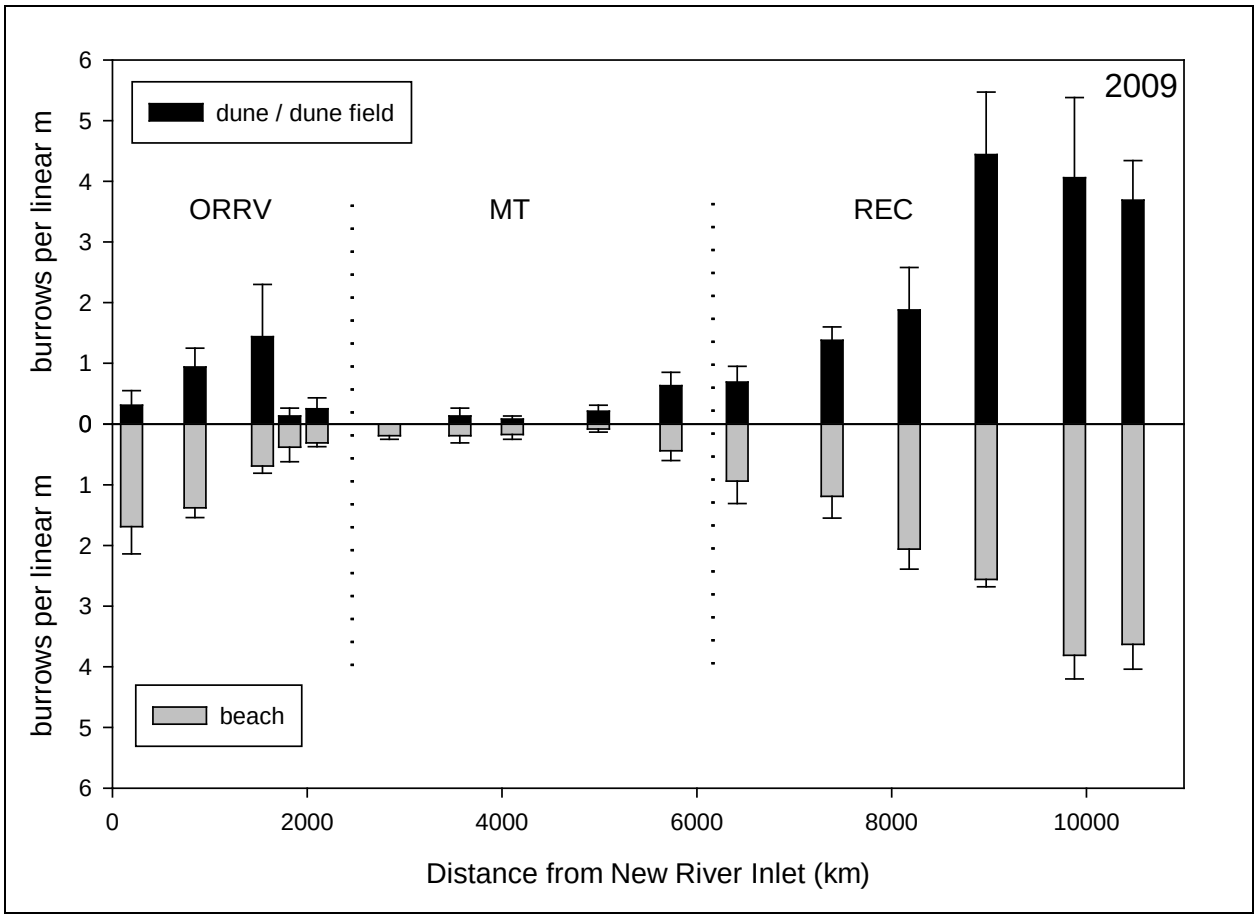

Figure 11-6. Mean (±1 standard error [SE]) abundances of active ghost crab burrows per linear meter in the dunes and beach at each of three sites extending from the west to the east from the New River Inlet.

Note that the *y*-axis always increases positively from the origin.

Responses to Occasional Disturbances: Storms

Tropical Storm Hanna and the Nor'easter (2008)

Infauna. MANOVA repeated measures analysis indicated significant differences among mean infaunal densities (individuals m^{-2}) across areas ($F_{2,69}$=10.8, P<0.0001), but not for time (before Tropical Storm Hanna, after Hanna, and after the nor'easter; $F_{2,68}$=1.86, P=0.163) or the interaction of area x time ($F_{4, 136}$=0.53, P=0.710). A Tukey's test demonstrated that before and after both storms infaunal densities were not different between the ORRV (mean ±1 standard error [SE]: 5.6 ±0.9 individual m^{-2}) and MT (mean ±1 SE: 3.8 ±0.5 individual m^{-2}) areas, but were significantly lower at the REC area (mean ±1 SE: 2.2 ±0.2 individual m^{-2}). Neither of the 2008 storms that were large enough to affect beach morphology had a detectable effect on the density of beach infauna.

Using the same analyses for the per linear meter of beach measure indicated significant differences in both area ($F_{2,21}$=44.5, P<0.0001)and time ($F_{2,20}$=10.9, P=0.0006) for prey abundance, but not the interaction of area × time ($F_{4,40}$=0.59, P=0.675). Planned comparisons

found that the area effect arose because infaunal abundances were always higher in the MT area and the time effect resulted from the highest infaunal abundances occurring after both storms had affected the beach.

Ghost crabs. The interaction of time (prior to, immediately after, and several weeks after a storm) × activity (anthropogenic area) × location (shoreward of the dunes versus landward of the beach) was significant for both densities and abundances of active ghost crab burrows in response to the consecutive storms of 2008, Tropical Storm Hanna, and the nor'easter (**Table 11-5**). Examination of comparisons of means (**Table 11-6**) and the magnitudes of mean densities and abundances across the storms (**Figure 11-7**) reveal complex patterns of ghost crab abundances and distributions. During the 2008 storms active ghost crab burrow density increased both on the beach and in the dune field in the REC area, increased on the beach while decreasing in the dune field in the ORRV area, and did not change in either the beach or the dunes in the MT area. The absence of large increases in abundances over time and the narrowing of the backbeach (**Figure 11-8**) both suggest that increased beach densities resulted in part from loss of beach habitat at the ORRV and REC areas. However, immediately after Tropical Storm Hanna there was a significant increase in ghost crab abundances on the beach that may have been a function of crabs concentrating in areas that received drift material from the storms because ghost crabs are attracted to potential sources of carrion (Wolcott, 1978).

Table 11-5. Results of separate MANOVA analyses examining whether ghost crab burrow density (per m^2) or ghost crab burrow abundance (active burrows per linear meter of beach) differed depending upon the effects of storms.

Significant differences (P<0.05) are indicated in boldface.

Source	2008 Storms		2011 Irene	
	Density (m^{-2})	Abundance (linear m^{-1})	Density (m^{-2})	Abundance (linear m^{-1})
	Between Subjects			
Activity	**<0.0001**	**<0.0001**	**<0.0001**	**<0.0001**
Location	**0.009**	**<0.0001**	**0.0300**	0.150
Activity × location	**0.027**	**<0.0001**	**0.0034**	0.096
	Within Subjects			
Time	**0.014**	0.055	0.070	0.054
Time × activity	**0.004**	0.106	0.222	0.121
Time × location	0.078	**<0.0001**	0.094	0.183
Time × activity × location	**0.007**	**0.022**	**0.024**	**0.038**

Table 11-6. Results of Tukey's comparisons for separate ANOVA analyses conducted after significant MANOVA examining whether, relative to the occurrence of coastal storms, there were differences in active ghost crab burrows per square meter and per linear meter of beach and dune field from areas that experience different anthropogenic activities.

Only results for Bonferroni-corrected significant differences (P<0.017) are provided. In each case, the activities, intensities, or combinations are ranked from highest to lowest (A–D) respective to their associated mean values of ghost crab burrows. Means with the same letters are not significantly different. Ellipses indicate no significant differences. Beach = mid intertidal through backbeach; dune = dune and dune field; MT = military training area; ORRV = off-road recreational vehicle area; REC = recreation area.

Metric	Factor	Pre-Hanna	Post-Hanna	Post-Nor'easter	Pre-Irene	Post-Irene	Post-Irene +3 weeks
Active burrows (m^{-2})	MT	B	B				B
	ORRV	A	B	...	...	...	B
	REC	A	A				A
	Beach	...	...	...	...	...	...
	Dune						
	MT—beach	...	...	D	B	C	...
	MT—dune			D	B	B C	
	ORRV—beach			B C	B	B C	
	ORRV—dune			C D	B	C	
	REC—beach			A B	B	A B	
	REC—dune			A	A	A	
Active burrows (linear m^{-1})	MT	...	...	...	B	C	...
	ORRV				A	B	
	REC				A	A	
	Beach	...	...	...	...	...	...
	Dune						
	MT—beach	D	C	B	...	...	C
	MT—dune	C	C	B			C
	ORRV—beach	C D	B C	A			B
	ORRV—dune	A	A	A			A
	REC—beach	C	A B	A			A B
	REC—dune	B	A B	A			A B

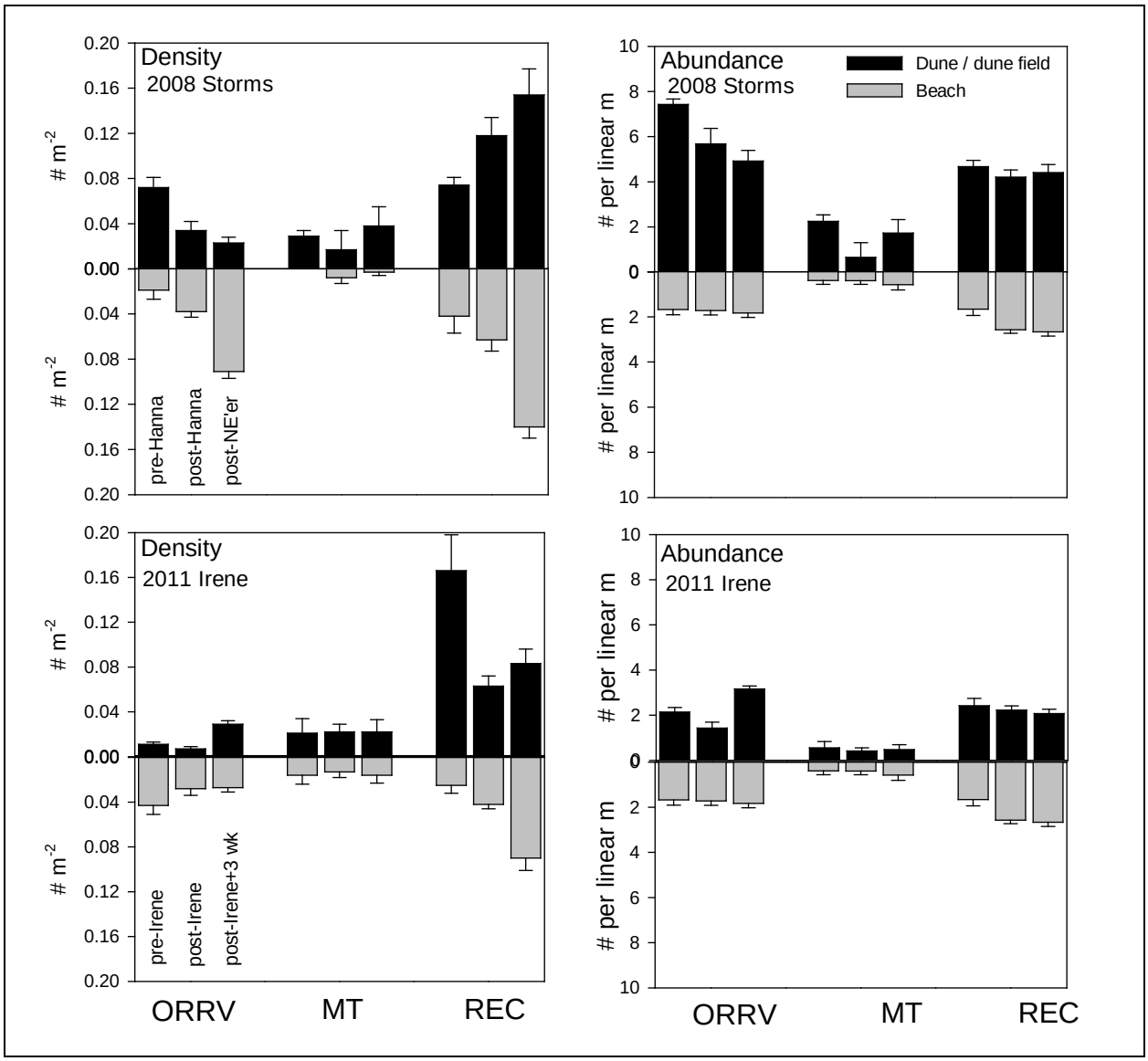

Figure 11-7. Mean (±1 SE) densities (left panels) and abundances (right panels) of active ghost crab burrows in the dunes and beach at each of three sites, each of which receives different anthropogenic activity, prior to and after several consecutive storms in 2008 (top panels) and Hurricane Irene (lower panels).

For each of the areas the respective (ORRV, MT, and REC) means proceed from prior to the storm to after the storm(s). Note that the *y*-axes always increase positively from the origin.

Hurricane Irene (2011)

Infauna. Hurricane Irene affected infauna differently than did the storms observed in 2008. MANOVA found no differences in infaunal density among sites ($F_{2,69}$=1.64, P=0.20) nor was the interaction of site × time significant ($F_{4, 136}$=1.22, P=0.30), but infaunal densities were lower ($F_{2,68}$=17.8, P<0.0001) immediately after Hurricane Irene at all sites. Infaunal densities recovered to pre-storm densities within 3 weeks at each site.

Ghost Crabs. Overall, ghost crabs maintained higher densities and abundances in the REC area, especially in the dunes, after Hurricane Irene (**Table 11-6**). There is some evidence of ghost crabs moving from the dune field and concentrating in the beach after Hurricane Irene and, in the ORRV area, for ghost crabs migrating from the beach into the dune field, but in general there are fewer changes in density and overall abundance associated with this hurricane than were seen around the 2008 storms (**Figure 11-7**). Our ability to interpret this difference between years is confounded by the later seasonal occurrence of Tropical Storm Hanna and the nor'easter as compared to Hurricane Irene. Ghost crabs become less active as temperatures cool and remain in closed burrows. As our method for determining ghost crab abundances relies on detecting active burrow opening, part of the decreases in 2008 may have resulted from seasonal changes in behavior by the crabs.

Both infauna and ghost crabs experienced changes in the overall size of their habitat as a consequence of these storms. In both 2008 and 2011, the forebeach increased in width as the storms deposited subtidal sand and dune sediments onto the beaches (**Figure 11-8**). The behavior of the backbeach, which would affect the ghost crabs most and not the intertidal infauna, differed from the forebeach. In general it either stayed the same (after Tropical Storm Hanna) or decreased in width (after the nor'easter and after Hurricane Irene; **Figure 11-8**). The absence of negative effects to the intertidal infauna suggests the physical energy associated with storm waves do not induce high mortalities and the net result of the storms were an increase in the size of habitat for these organisms. Ghost crabs did lose some habitat (backbeach), but responded by shifting distributions to the dunefield or by increasing their concentration in the remaining habitat. All of these beach invertebrates were largely unaffected by the storms.

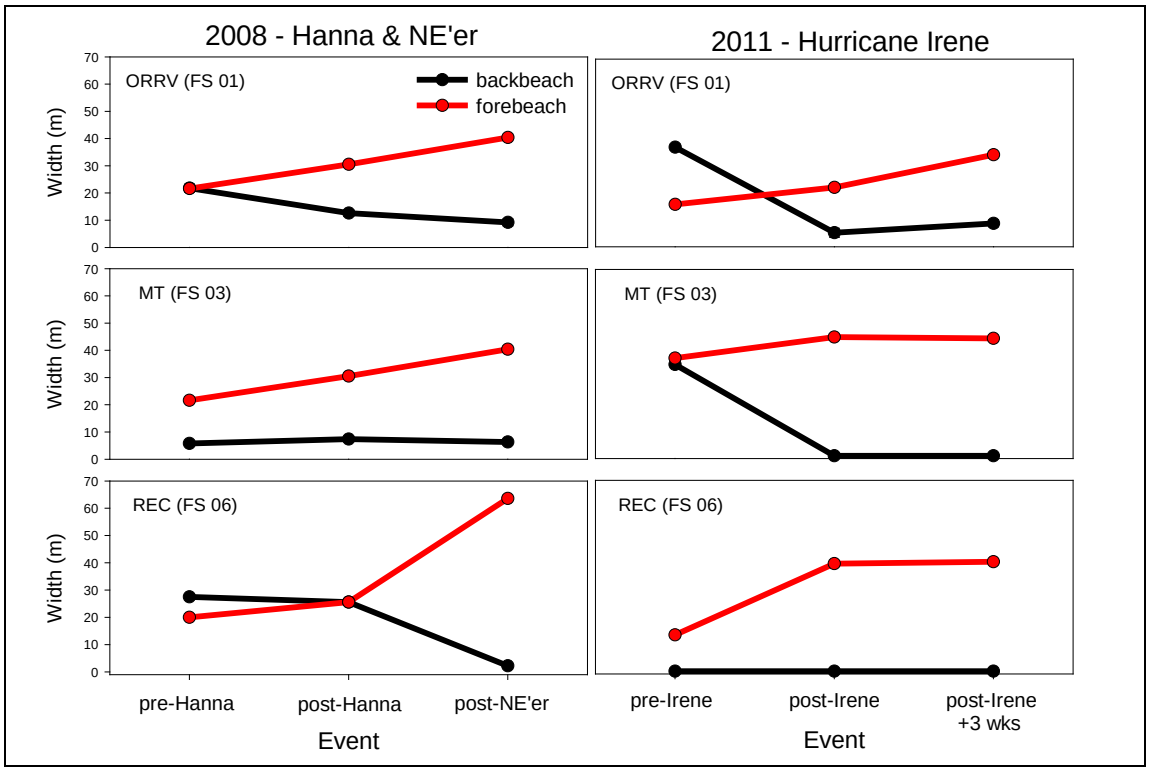

Figure 11-8. Mean (±1 SE) width of the backbeach and forebeach at each of three sites prior to, after, and several weeks after storms.

Responses to Occasional Disturbances: Dredge Material Disposal

Infauna

In 2008, when dredge disposal operations ended in early March all of the dredge material was mounded on the backbeach and upper intertidal in a 1-m+ high platform. We had not been notified that this event was going to occur, so we have no prior samples from the impacted and control sites. Our samples were collected from the impacted and control sites 1 week, 2 months, and 6 months after disposal concluded. Both the density of infauna and the biomass of *Donax* and *Emerita* showed significant differences across these sampling times but neither showed a significant interaction of site × sampling time (**Table 11-7**). In other words, there is no evidence that placing the dredge spoil on the upper beach had any effect on the infauna. Depositing dredge material on exposed beaches has been documented to have substantial negative effects on beach infauna elsewhere (Peterson et al., 2006). The lack of an effect from the 2008 dredge disposal on Onslow beach infauna is likely a consequence of three conditions. First, disposal occurred in February when infaunal abundances, except for coquina clams (*Donax*) are near seasonal lows. Second, the volume of dredge material deposited was relatively low compared to the amount placed on beaches where negative effects have been documented. Third, the dredge material was deposited primarily on the backbeach, landward of the intertidal and subtidal where the infauna live (**Figure 11-9**). Over the subsequent months the dredge material slowly eroded away, dissipating many adverse effects associated with rapid deposition of sediment into the intertidal. The scarp did act as a barrier to sea turtles attempting to build nests away from the water. Late in the summer, a sea turtle breached the scarp and laid a nest in the dredge material mound. This nest was subsequently lost as the spoil mound continued to erode away with surf reaching the nest before the turtles could hatch. This observation led us to recommend to MCBCL to request that future dredge material disposals be bulldozed to produce a typical beach profiles.

Figure 11-9. Aerial view and beach-level photographs of the 2008 disposal of dredge material on Onslow Beach.

The aerial view demonstrates how the intertidal was displaced seaward by disposal activities. The beach-level photograph shows how the disposal material was left mounded in the backbeach. The high-water mark is at the base of the disposal mound scarp.

In 2010, we received notice of a planned disposal event, in the same location as was used in 2008, prior to the project beginning. We sampled a nearby control site and the impact site one week prior to, during, one week after, one month after, two months after, and six months after

commencement of disposal operations. The volume of material deposited during this disposal event was greater than the 2008 disposal but less than that used in typical beach nourishments. The disposal material was bulldozed this time to prevent mounding. The results were similar to those from 2008 in that there were significant differences among sampling times and no significant interactions of site x sampling time for both infauna density and biomass (**Table 11-7**). However, a significant difference between sites in the sum of *Donax* and *Emerita* biomass did occur. This led us to analyze *Donax* and *Emerita* biomasses separately using MANOVA for repeated measures. Neither the main factors (site and sampling time) nor the interaction of the main factors were significant for *Emerita* density or biomass. However, a significant ($F_{5, 42}$=4.50, P=0.002) interaction of site × sampling time did occur for *Donax* biomass (the *Donax* density result was similar but with a P=0.008). Subsequent ANOVA's for each sampling time along with Tukey comparisons of significant interaction results found that *Donax* biomass was significantly reduced at the dredge impact site during the disposal event and one week after completion of disposal operations (Bonferroni corrected P=0.0083; **Figure 11-10**).

Table 11-7. Results of separate MANOVA analyses examining whether the density of beach infaunal abundances (individuals m^{-2}) or summed biomasses of *Donax* and *Emerita* (g m^{-2}) differed relative to dredge spoil disposals on the beach at an impacted and nearby (approximately 2 km away) control site in each of 2 years.

In 2008, the two sites were sampled within 1 week, 2 months, and 6 months after disposal was completed. In 2010, the two sites were sampled 2 weeks before, during, 1 week after, 1 month after, 2 months after, and 6 months after the disposal operation was conducted. Significant differences (P<0.05) are indicated in boldface.

Source	2008		2010	
	Number of Individual	Biomass	Number of Individual	Biomass
	Between Subjects			
Site (impact versus control)	0.09	0.17	0.48	**<0.0001**
	Within Subjects			
Sampling time	**0.0012**	**<0.0001**	**<0.0001**	**0.006**
Sampling time × site	0.52	0.46	0.12	0.20

Although *Donax* densities and biomass did recover at the impact site within 2 months of the end of the disposal activity there is special concern associated with the observed negative effect of dredge disposal on *Donax*. These clams serve as a critical energy resource for threatened red knots (*Calidris canutus*) during their annual vernal migration to breeding grounds (Cohen et al., 2010). Although the volume of material was not large (relative to typical beach nourishment events) and the area impacted was relatively small (less than 2 km) compared to the length of Onslow Beach, it still took between 1 and 4 weeks for the local population of *Donax* to recover. Larger volume disposals of dredge material could lead to longer intervals of recovery or even prevent recovery of the important *Donax* prey resource.

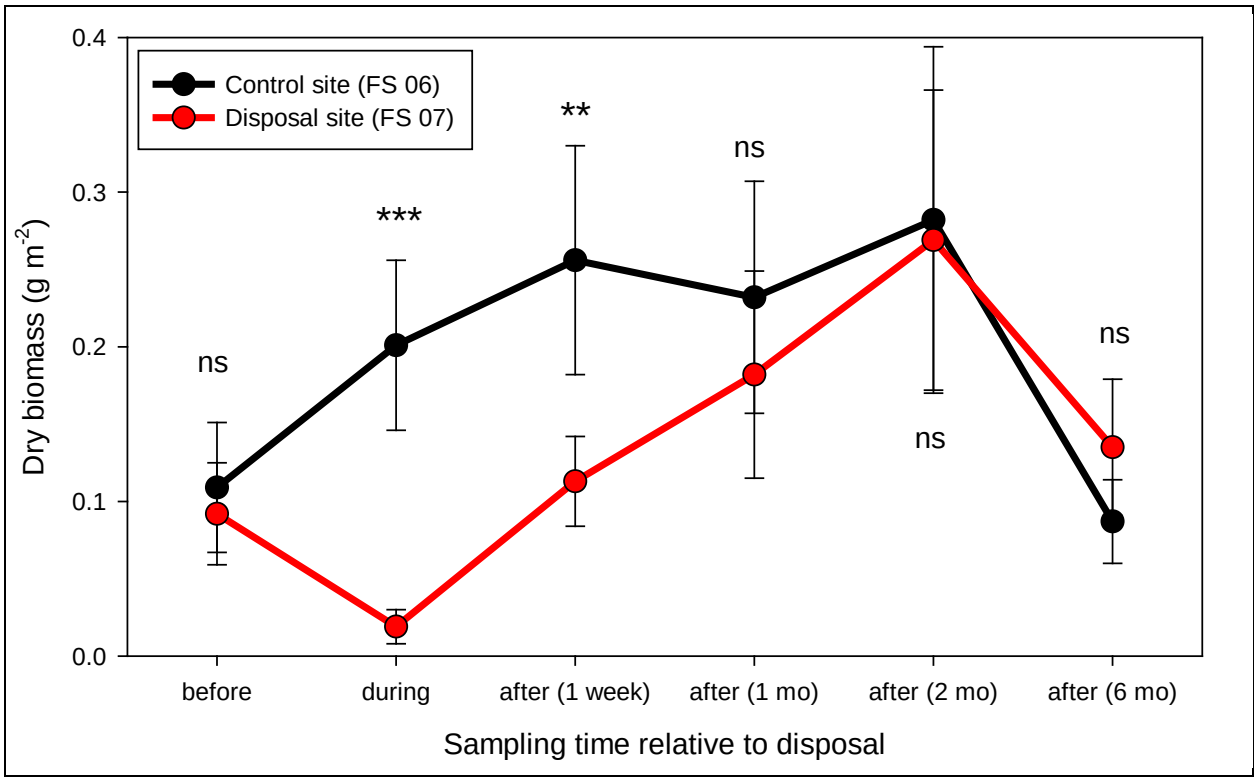

Figure 11-10. Mean (±1 SE) biomass of *Donax* per unit area at control and spoil-impacted sites prior to, during, and after at increasing intervals from the 2011 disposal of dredge material on Onslow Beach.

Sampling after both disposal events did find that the proportion of coarse sediments (greater than 1 mm) found in our infaunal samples was significantly higher at the control site ($F_{1,46}$=82.6, P<0.0001) indicating that the dredge material placed on the beach was low in coarse sediments. Coarse sediments represent poorer habitat for *Donax* (Manning et al., 2012), so the decrease in *Donax* at the disposal site did not result from addition of coarse material to the intertidal. *Donax* have been shown to experience substantial mortality from burial due to rapid deposition of sediments on beaches (Peterson et al., 2000).

Between Island Comparison: Onslow Beach Versus Bear Island

Infauna

Multivariate procedures (non-metric multidimensional scaling [nMDS]) to assess similarity (variables used in the multivariate construction of similarities included densities of *Donax*, *Emerita*, haustorids, and *Scolelepis* plus the sizes of *Donax* and *Emerita* individuals) in faunal assemblages from different sampling sites followed by permutational multivariate analysis of variance (PERMANOVA) to determine whether patterns among the sites are significant, showed no overall difference between Onslow Beach and Bear Island (**Figure 11-11**, top panel) over the five successive periods (September 2009 through September 2011) when both islands were sampled. There was a significant difference (P=0.001) among focus sites (**Figure 11-11**, bottom panel); Focus Sites 6 through 10 were different from Focus Sites 1 through 5 as indicated by PERMANOVA. Focus Sites 6 and 7 occur on Onslow Island in the REC-low and BFR areas,

respectively, and are both located on the northeastern end of the island that morphologically is most similar to Bear Island.

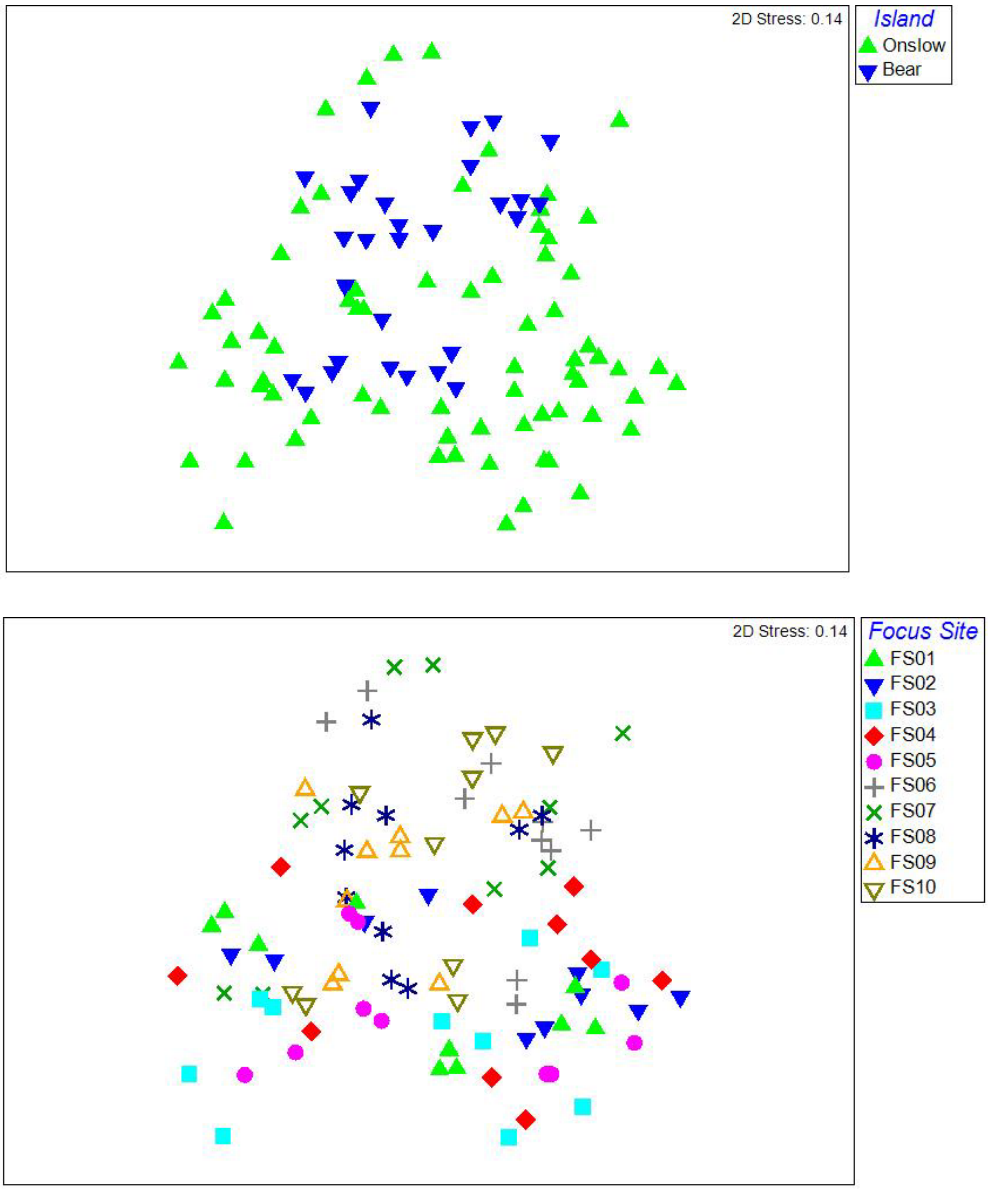

Figure 11-11. Multivariable dimensional scaling indicating the similarity in densities of the most abundant benthic invertebrates in samples taken from September 2009 through September 2011 at Onslow Beach (Focus Sites 1–7) and Bear Island (Focus Sites 8–10).

The top panel shows the pattern of similarities among the two islands and reveals no distinction relative to each other. The bottom panel demonstrates the same pattern, but for individual focus sites, and indicates that even at this level of resolution, no distinct pattern emerges.

Ghost Crabs

No significant differences were found in the density of active ghost crab burrows between islands in either the beach or dunes (P=0.153 and 0.253, respectively; **Figure 11-12**). The

densities of active ghost crab burrows were lowest in locations on the westernmost portion of Onslow Island and the easternmost of Bear Island. The former appears to be a function of limited dune habitat, the latter due to human activities in the bathhouse and camping areas.

Similarly, no significant differences were found in the abundance of active ghost crab burrows (number per transect) between islands in either the beach or dunes (P=0.153 and 0.253, respectively; **Figure 11-12**). Those locations on either island that had high burrow densities and greater amounts of habitat (Focus Sites 6 and 7 on Onslow Beach and Focus Site 8 on Bear Island) had significantly (P<0.001) more burrows per transect than all other sites.

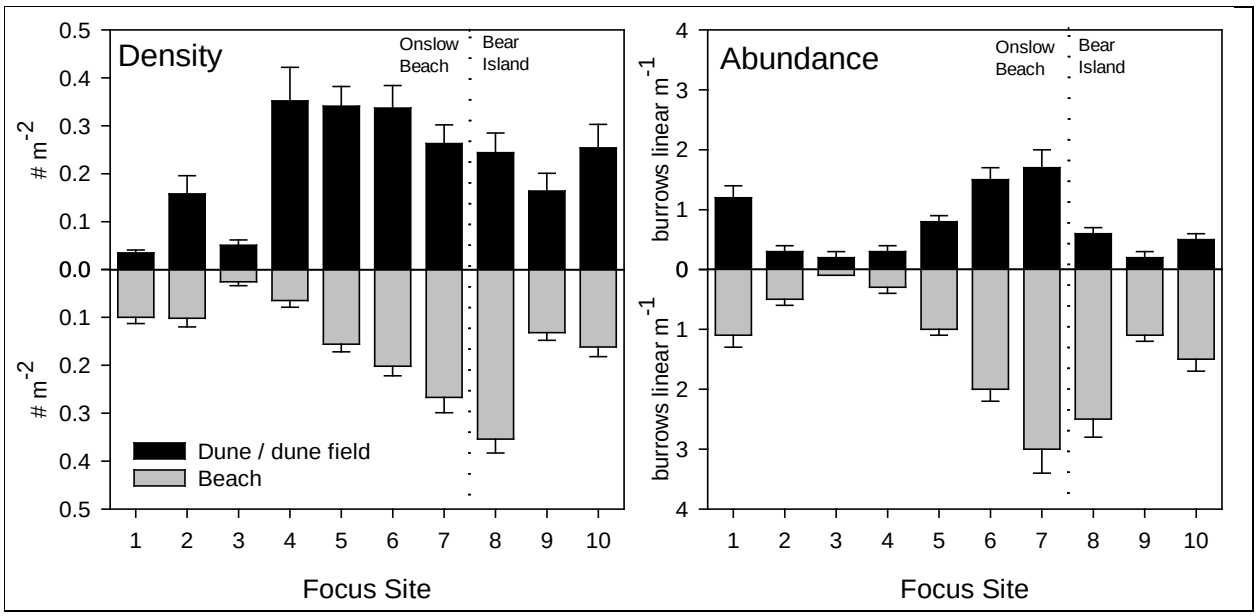

Figure 11-12. Mean (±(+1 SE) density (left panel) and abundance (right panel) of active ghost crab burrows at focus sites along Onslow and Bear Islands.

Means are averaged over five, contemporaneous, successive May/September samplings starting in September 2009. Note that the ***y***-axes always increase positively from the origin.

Surf Fish

Effects of Anthropogenic Activities and Natural Processes (Persistent Disturbances Only)

Of the 22 different species (and 4,471 individuals) of surf nekton captured in late summer seine samples two species, Atlantic silversides (*Menidia beryllina*) and bay anchovy (*Anchoa* sp.), comprised more than 85% of all individuals captured (**Table 11-8**). These two species, along with gulf kingfish (*Menticirrhus* spp.) and pompano (*Trachinotus carolinensis*), occurred in 45–67% of all tows taken over the 5 years, and all four of these species were found at each of the six primary focus sites (**Table 11-9**). The majority (greater than 90%) of individuals of all species were juveniles except for the two species of portunid crabs we captured (*Callinectes sapidus* and *Ovalipes ocellatus*).

Table 11-8. Relative abundances (%) of surf nekton captured in seine samples.

The data are pooled over five successive years (2007-2011) of late summer sampling and partitioned by the relative intensities (low vs. high) of different anthropogenic activities.

Species	ORRV		MT		REC		Σ
	Low	High	Low	High	Low	High	
Anchoa hepsetus	0.72	2.08	0.63	13.26	0.27	3.89	20.8
Arenaeus cribrarius	0	0	0	0	0.02	0.02	0.04
Callinectes sapidus	0	0	0	0	0.04	0.02	0.07
Caranx crysos	0	0	0.11	0.22	0.13	0.69	1.16
Chloroscombrus chrysurus	0	0.04	0.36	2.44	0.11	0	2.95
Elops saurus	0	0.04	0	0	0	0	0.04
Gymnura ***sp.***	0	0	0	0.02	0	0	0.02
Lagodon rhomboides	0	0.13	0.04	0.07	0.02	0	0.27
Leiostomus xanthurus	0	0	0.04	0	0	0	0.04
Menidia beryllina	28.65	4.63	4.79	13.4	13.22	0.45	65.1
Menticirrhus spp.	0.13	0.11	1.61	0.47	0.09	0.96	3.38
Monacanthus hispidus	0.04	0	0	0.18	0.02	0.07	0.31
Mugil curema	0.2	0.16	0.11	0.13	0	0.22	0.83
Ovalipes ocellatus	0	0	0	0.04	0.04	0.96	1.05
Opisthonema oglinum	0	0	0	0	0	0.02	0.02
Pogonias cromis	0.02	0	0	0.04	0	0	0.07
Pomatomus saltatrix	0.11	0.04	0.04	0.09	0.07	0.09	0.45
Scomberomorus maculatus	0	0.02	0	0.02	0.02	0	0.07
Selene vomer	0	0	0	0	0	0.02	0.02
Sphoeroides maculatus	0.02	0.02	0	0	0	0	0.04
Syngnathus sp.	0	0	0	0.04	0	0.02	0.07
Trachinotus spp.	0.25	0.51	0.25	1.12	0.67	0.31	3.11
Σ	30.15	7.81	7.98	31.56	14.74	7.76	100

Table 11-9. Relative frequencies (%) of surf nekton captured in seine samples.

The data are pooled over five successive years (2007–2011) of late summer sampling and partitioned by the relative intensities (low versus. high) of different anthropogenic activities.

Species	ORRV		MT		REC		Σ
	Low	High	Low	High	Low	High	
Anchoa hepsetus	40	40	60	30	60	40	45
Arenaeus cribrarius	0	0	0	0	10	10	3.3
Callinectes sapidus	0	0	0	0	10	10	3.3
Caranx crysos	0	0	20	30	30	30	18.3
Chloroscombrus chrysurus	0	20	50	10	0	20	16.7
Elops saurus	0	10	0	0	0	0	1.7
Gymnura ***sp.***	0	0	10	0	0	0	1.7
Lagodon rhomboides	0	20	30	20	0	10	13.3
Leiostomus xanthurus	0	0	0	10	0	0	1.7
Menidia beryllina	70	50	100	60	40	80	66.7
Menticirrhus spp.	30	40	60	70	60	20	46.7
Monacanthus hispidus	10	0	30	0	20	10	11.7
Mugil curema	30	10	20	30	20	0	18.3
Ovalipes ocellatus	0	0	10	0	20	20	8.3
Opisthonema oglinum	0	0	0	0	10	0	1.7
Pogonias cromis	10	0	10	0	0	0	3.3
Pomatomus saltatrix	40	10	30	20	10	20	21.7
Scomberomorus maculatus	0	10	10	0	0	10	5
Selene vomer	0	0	0	0	10	0	1.7
Sphoeroides maculatus	10	10	0	0	0	0	3.3
Syngnathus sp.	0	0	20	0	10	0	5
Trachinotus spp.	40	50	60	50	50	40	48.3

The results of repeated-observation MANOVA tests indicate that there were no significant differences in species richness or total abundance associated with type of anthropogenic activity or the intensity of each activity (**Table 11-10**). There were significant effects associated with time. For species richness, a Tukey's unplanned comparison on annual mean species per seine haul indicated that in 3 out of the 5 years, the number of species was 2–2.5 times higher (**Figure 11-13**). For total nekton abundance, a significant three-way interaction indicated that the activity × intensity interaction differed among years. Consequently, we examined the nekton abundance within each of the 5 years separately with independent ANOVA'S and Bonferroni corrected the P-values. In this instance the only significant result (P=0.0055) occurred in the activity × intensity interaction in 2010 (**Figure 11-14**). Nekton were most abundant at the high-intensity ORRV site and the low-intensity MT site. Main effects in every year and all interactions in years other than 2010 were non-significant. Overall, there were no consistent, site-specific or anthropogenic activity effects on surf nekton. Replication was low (n=2 seine hauls) per location per year limiting our ability to detect anything but large differences. With the exception of pompano (*Trachinotus carolinensis*), surf nekton are mobile and show little site fidelity (Ross

and Lancaster, 2002), making it likely that only long-term, large-scale, negative press disturbances would affect surf nekton.

Table 11-10. Results of two separate MANOVA analyses examining whether species richness (species per seine haul) or total abundance (individuals per seine haul) differed depending on type of anthropogenic activity, the intensity of each activity, the interaction of activity by intensity, or years (time in the table).

Significant differences (P<0.05) are indicated in boldface.

Source	Species Haul^{-1}	Individuals Haul^{-1}
	Between Subjects	
Activity	0.07	0.17
Intensity	0.14	0.13
Activity × intensity	0.43	0.33
	Within Subjects	
Time	**0.04**	**0.01**
Time × activity	0.32	0.06
Time × intensity	0.80	0.19
Time × activity× intensity	0.81	**0.02**

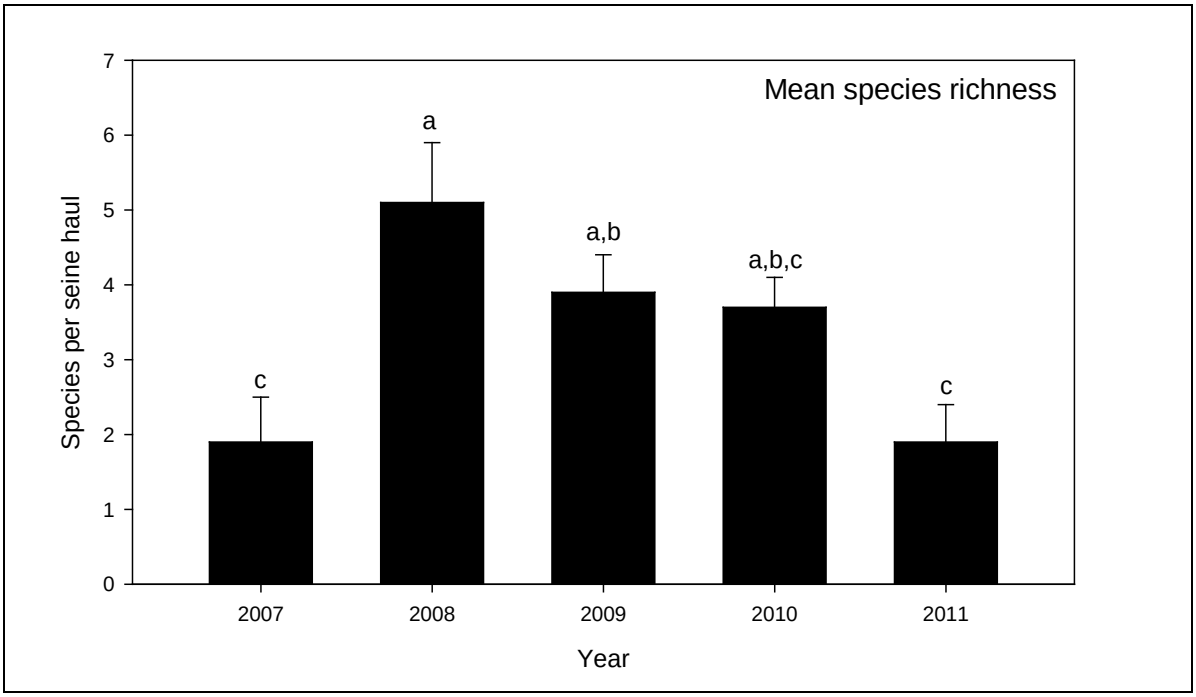

Figure 11-13. Mean (+1 SE) number of species per seine haul.

Years with the same letters over the error bar are not significantly different (P>0.05).

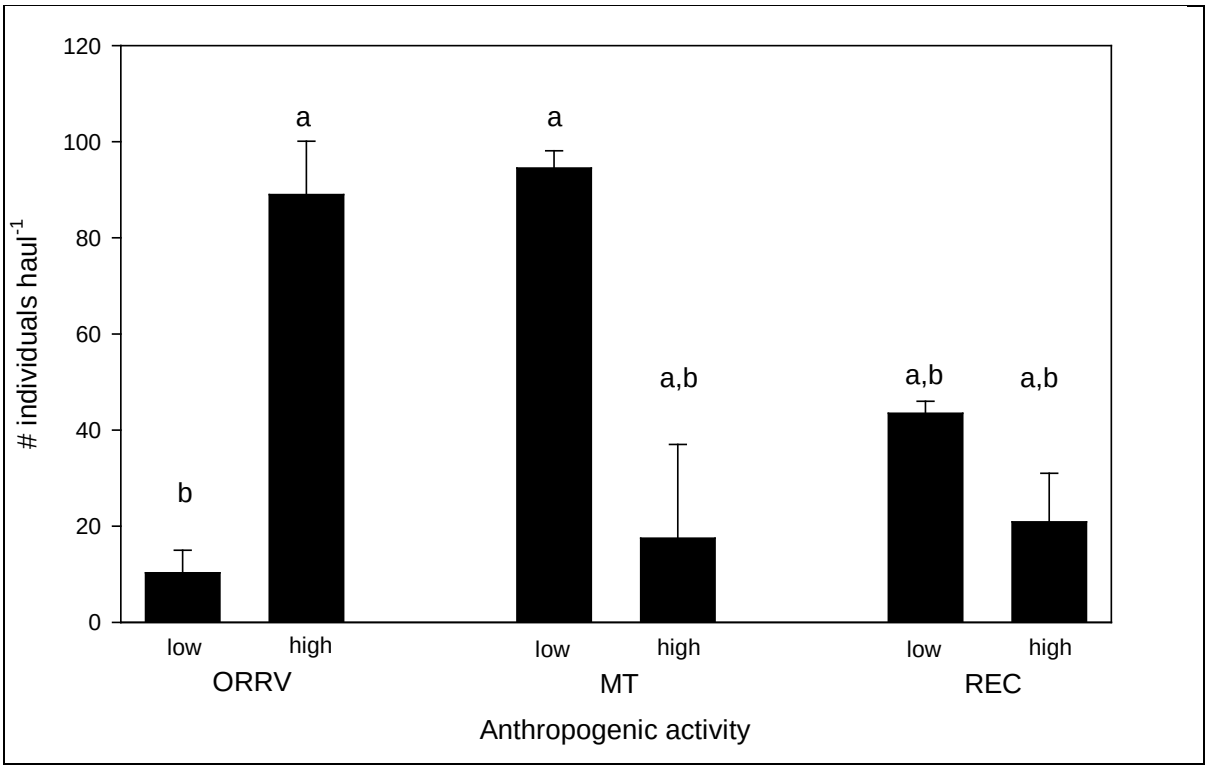

Figure 11-14. Mean (+1 SE) number of nekton individuals per seine haul in September 2010.

Means with the same letters over the error bar are not significantly different (P>0.05).

Between Island Comparison: Onslow Beach Versus Bear Island

Seine hauls from both islands revealed that the Atlantic silverside (*Menidia beryllina*) was both the most abundant species and the most frequently captured on both islands in every year (**Table 11-11**). The most notable difference between the nekton captured on Onslow Island versus that collected on Bear Island is the almost complete absence of bay anchovies (*Anchoa hepsetus*) and mullet (*Mugil* spp.) in Bear Island hauls (**Table 11-11**). Multivariate analysis (PERMANOVA) of the surf nekton community from both islands in all three years in which both islands were sampled found a significant (P=0.01) island × year interaction. This difference arose largely because silversides were relatively less abundant in Onslow Beach samples and kingfish (*Menticirrhus* spp.) were relatively more abundant in Bear Island samples for some years.

Table 11-11. Relative abundances (percentage of all individuals within an island) and relative frequencies (percentage of all seine hauls within an island) of surf nekton from Onslow Beach and Bear Island in September of 2009, 2010, and 2011 (pooled across years).

Total number of individuals: Onslow Beach=4,007 and Bear Island=3,362.
Total number of hauls: Onslow Beach=42 and Bear Island=18.

Species	Onslow Beach		Bear Island	
	Percentage of Individual	Percentage of Hauls	Percentage of Individual	Percentage of Hauls
Anchoa hepsetus	19.67	47.50	0.09	5.56
Arenaeus cribrarius	0.05	5.00	0.00	0.00
Callinectes sapidus	0.05	2.50	0.03	5.56
Caranx crysos	0.10	5.00	0.03	5.56
Chloroscombrus chrysurus	1.75	12.50	3.06	11.11
Dorosoma petenense	0.65	5.00	0.00	0.00
Eucinostomus gula	0.00	0.00	0.09	11.11
Lagodon rhomboids	0.17	7.50	0.42	33.33
Leiostomus xanthurus	0.05	2.50	0.00	0.00
Menidia beryllina	71.60	82.50	92.56	61.11
Menticirrhus spp.	2.62	42.50	2.08	44.44
Monacanthus hispidus	0.02	2.50	0.00	0.00
Mugil curema	0.62	17.50	0.06	5.56
Opisthonema oglinum	1.30	15.00	0.98	5.56
Pogonias cromis	0.05	2.50	0.00	0.00
Pomatomus saltatrix	0.22	20.00	0.06	11.11
Scomberomorus maculatus	0.05	5.00	0.15	11.11
Syngnathus sp.	0.02	2.50	0.00	0.00
Trachinotus spp.	1.00	47.50	0.39	27.78

Sea Turtle Nesting

Anthropogenic Influences on Sea Turtle Nesting

Along-Island Spatial Patterns

There is a distinct pattern in the absolute and relative frequencies of sea turtle false crawls and nests along the length of the island over the 30 years for which data are available (**Figure 11-15**).

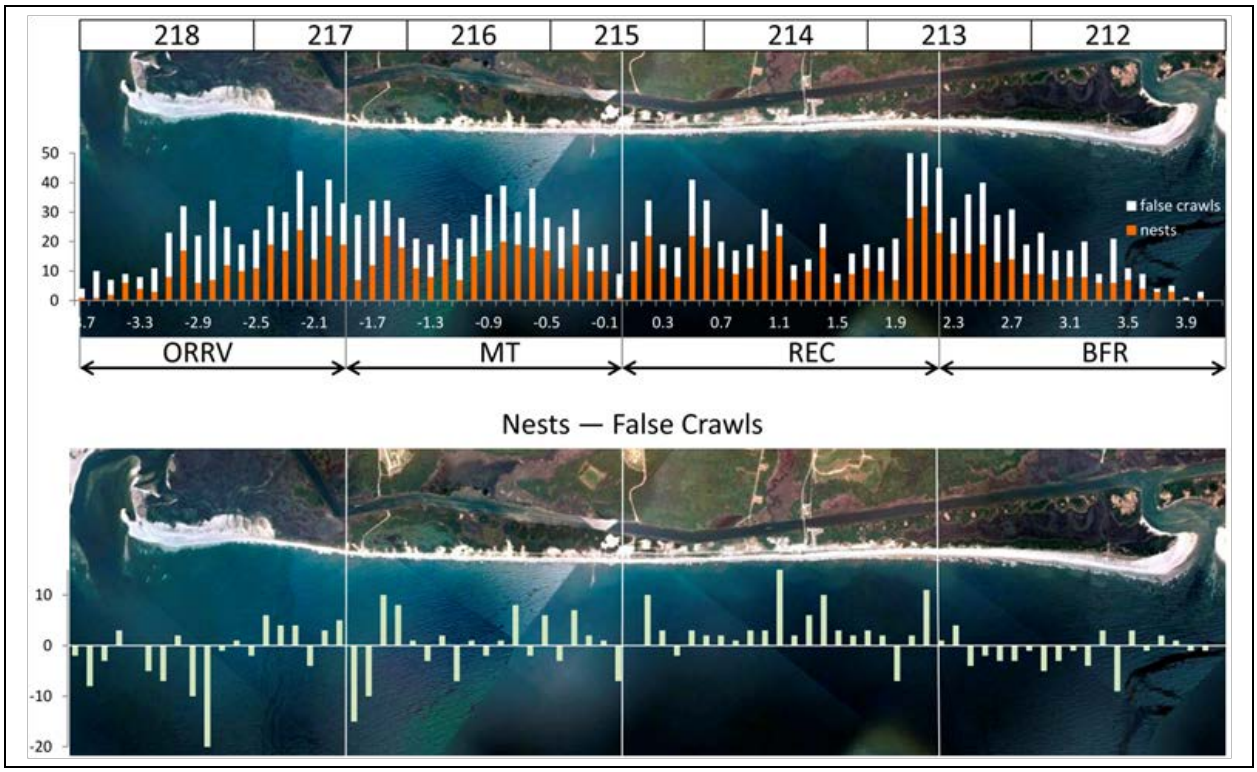

Figure 11-15. Accumulated turtle events (false crawl and nest sums in the top panel and nests false crawls in the bottom panel) occurring at 160-m intervals along the length of Onslow Beach (1982, 1985, 1987–88, 1990–1994, and 1997–2011).

The top panel shows the total events at a given location (white bar: false crawls; orange bar: nests). The bottom panel shows the difference in the number of events (nests false crawls) at a given location with any excess number of nests indicated above the line and an excess number of false crawls indicated below the line. In the top panel, the demarcations indicate the North Carolina Wildlife Resources Commission zones occurring on the island (numbers on the top of the figure) and the MCBCL anthropogenic areas (at the bottom of the figure). *Anthropogenic areas*: Off-road recreational vehicles (ORRV) → military training (MT) → recreational (REC) → buffer/impact area (BFR).

We used separate runs tests on the frequency of nests, frequency of false crawls, and the difference in frequencies of nests and false crawls for every 160-m interval (0.10 miles) to determine whether observed alongshore patterns were significantly different from random. For each response variable the runs tests were highly significant indicating that one or more runs (contiguous intervals along the island having high or low numbers of events relative to the median) are present (nests, P=0.00004; false crawls, P=0.000005; nests false crawls, P=0.0158). Separate one-way ANOVA's conducted for each variable found no significant differences in the mean number of nests ($F_{3,75}$=2.23, P=0.091) or mean number of false crawls ($F_{3,75}$=2.08, P=0.11) among anthropogenic zones indicating that the patterns detected by the runs test do not correspond to the spatial limits of each anthropogenic activity on the island. Inspection of the runs reveals that the numbers of false crawls decrease strongly towards the inlets and modestly in the middle of the island, starting around the former location of Riseley Pier and extending through most of the REC area (**Figure 11-16**). Nests show a similar pattern but begin to increase somewhat further from New River Inlet and show more variability in the REC area. A one-way ANOVA testing the mean differences in nest and false crawl frequencies among the anthropogenic areas was significant ($F_{3,75}$=4.14, P=0.009). A subsequent Tukey's test indicated

that the mean difference observed in the REC area was significantly greater than those observed in the ORRV and BFR areas. The MT area was intermediate. So, although relatively fewer crawls occur in the REC area, crawl events are more likely to result in nests in that part of the island. The relatively high proportion of successful crawls in the recreational area suggests that the MCBCL's efforts to limit light pollution and disturbance by humans in that area are successful. The lower proportion of nests to false crawls in the buffer area may result from the substantially greater width of the beach throughout that part of the island.

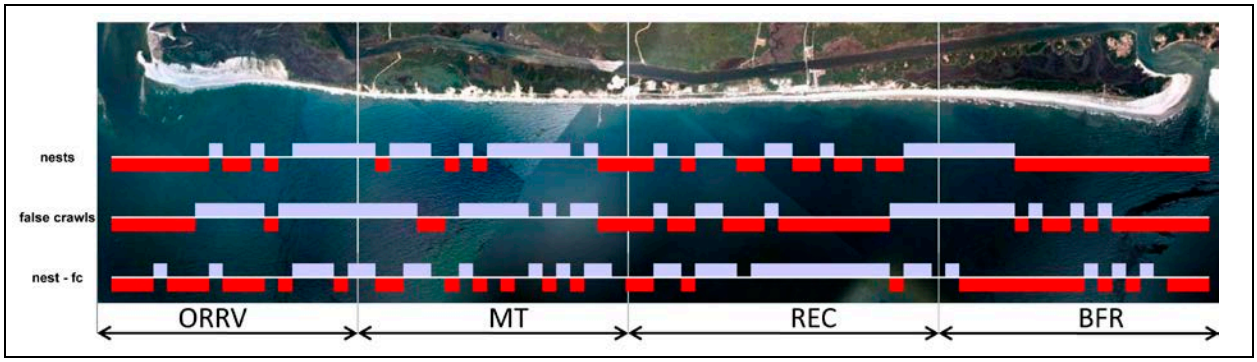

Figure 11-16. Alongshore patterns of accumulated turtle events (nests, false crawls, and the difference between nests and false crawls) occurring at 160-m intervals along the length of Onslow Beach (1982, 1985, 1987–88, 1990–94, and 1997–2011).

Thick blue lines above the center line for each measure indicate that accumulated events exceeded the overall median, and thick red lines below the center line indicate that accumulated events were below the overall median. The absence of a thick line means the value for each measure at that location equaled the median.

Nest Hatching Success Through Time

We calculated the ESR ([the number of eggs hatched − the number of dead hatchlings in the nest − the number of live hatchlings in the nest] ÷ [the number of eggs hatched + the number of unhatched eggs] × 100%) and adjusted emergence success rate (ESRA). For the ESRA, we omitted subtracting the number of live hatchlings found in the nest from the formula to better reflect EMD's management practice. Because all Onslow Beach turtle nests are inventoried (except those in the N1-BT3 impact area, which covers the northeast tip of the island) and all live hatchlings are released at the time of the inventory, they should not be subtracted from the number of hatchlings that emerge. Although ESR and ESRA means have fluctuated between approximately 40% and 90% over the past three decades (**Figure 11-17**), an analysis of medians detected no overall trends through time (regression analyses: P=0.69 and 0.71 for arcsine transformed ESR and ESRA medians, respectively).

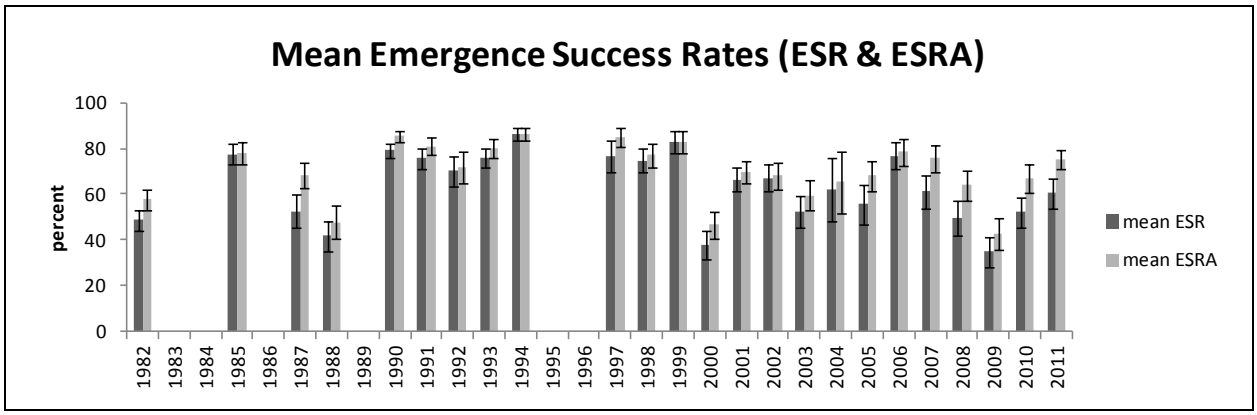

Figure 11-17. Mean Emergence Success Rates (ESR) and Adjusted Emergence Success Rates (ESRA) of Onslow Beach sea turtle nests, from 1982-2011.

No available nest inventory data for 1983-84, 1986, 1989, and 1995-96.
All nests affected/destroyed by hurricanes and tropical storms were excluded from analysis.

However, when nest ESRs are assessed based on management intervention level (i.e., relocation versus *in situ* "natural" incubation), natural nests show a declining ESR, and the ESR of relocated nests has not changed over time (**Figure 11-18**). This pattern suggests that the decrease in average ESR for natural nests is not a consequence of factors relating to sea turtle biology (e.g., reduced fertility of eggs or embryo vitality) or to general environmental conditions (e.g., beach temperature, elevated ground water levels) that could alter nest hatching success. At least part of the difference in ESR trend between natural and relocated nests results from the ability of EMD managers to consistently select superior locations for placing the nests.

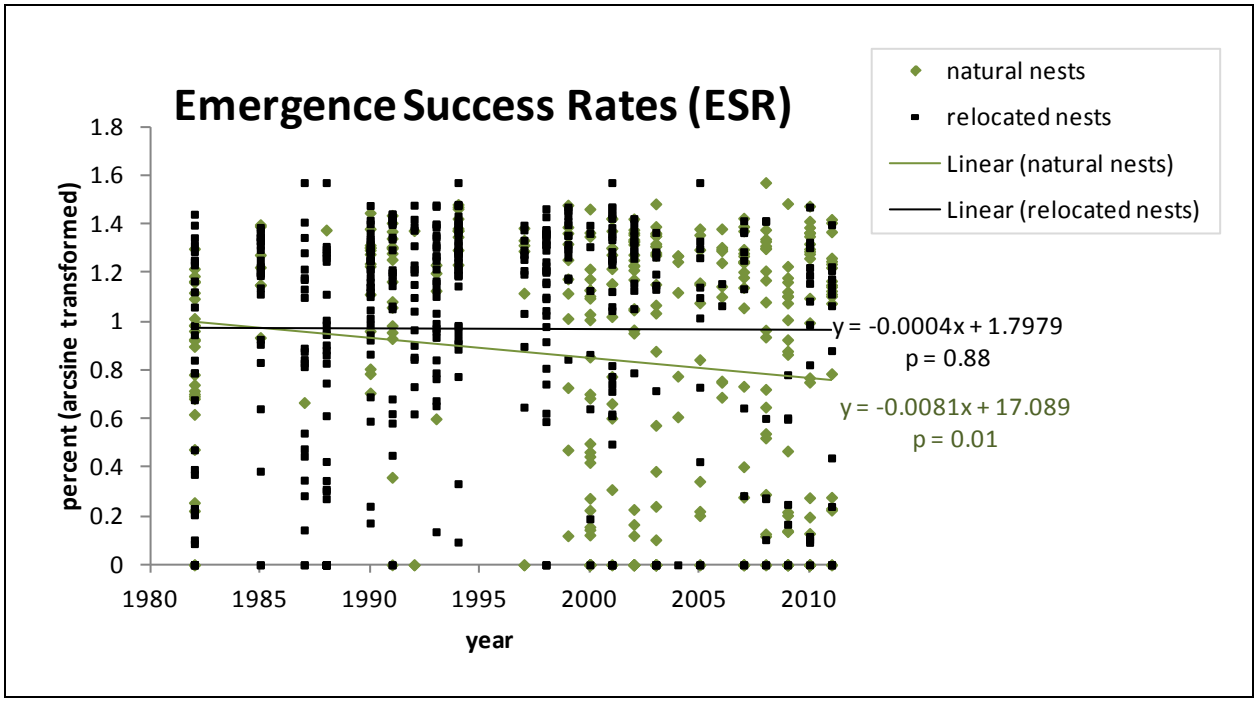

Figure 11-18. Trends in Emergence Success Rates (ESR) for natural and relocated sea turtle nests on Onslow Beach.

Nests affected/destroyed by hurricanes and tropical storms excluded from analysis.

Comparing Nest Management Success

We also compared sea turtle nest hatching success from Onslow Beach to comparable data from two other locations, Bear Island (1984–2008) and Bald Head Island (1980–1988 and 1990–2009). Bald Head Island is moderately developed, but a significant portion of the land is closed to development and managed as a nature preserve. Because of differences among the data sets, we had to restrict our statistical analysis to nests laid between June 1 and July 31 in each year for each location and to years in which data were available from all three islands (18 out of 30 years; **Figure 11-19**). A one-way ANOVA comparing annual average ESRA for each island indicated an overall significant difference among islands (P=0.0007). Tukey's Honestly Significant Differenced (HSD) post-hoc pair-wise comparisons revealed that mean annual ESRA on Onslow Island was significantly higher than on Bald Head Island (75.8% versus 69.5%, respectively). The mean annual ESRA for Bear Island was intermediate between these two (73.1%) and not significantly different from either.

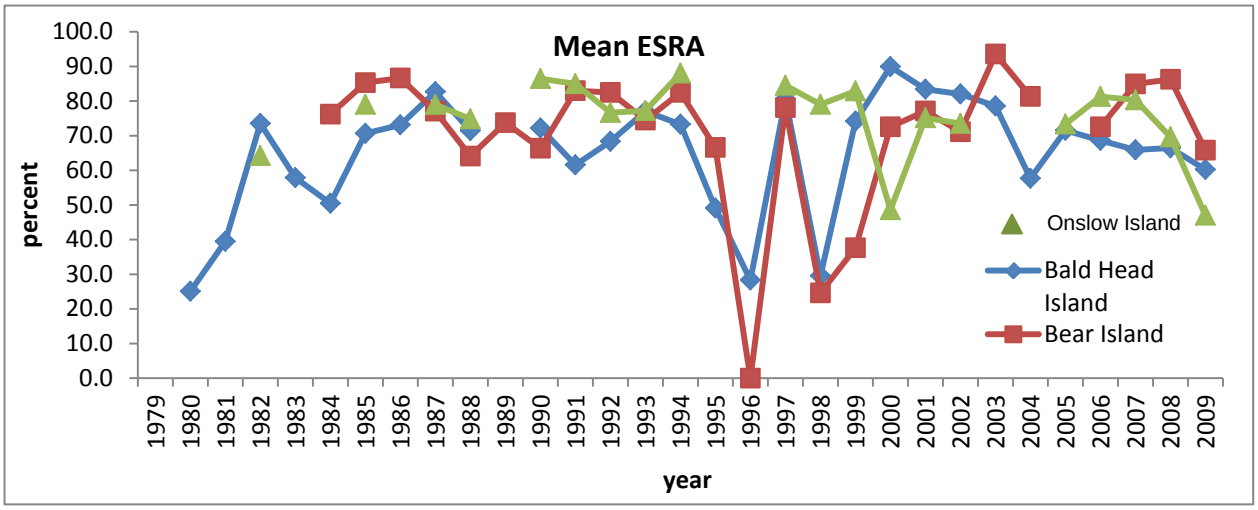

Figure 11-19. Annual mean nest success (ESRA) for Bald Head, Bear, and Onslow islands.

All available data were used (the years when five or fewer nests were all that hatched are excluded to avoid biasing the percentages with results from very small sample sizes). Statistical analyses were restricted to years in which data were available from all three islands.

To further explore these differences, for each island and for each year, we determined the proportion of nests that fell within 10% histogram bins (i.e., proportion of nests with ESRA within 0–10%, 10–20%, 20–30%, …, 90–100%). PERMANOVA indicated that all three islands were significantly different (P=0.0001) from each other. The nMDS plot indicates that Bear Island similarities were dispersed differently from Bald Head and Onslow Islands (**Figure 11-20**). A test of the dispersion of Bear Island similarities was significant, suggesting that annual ESRA is more variable there than on the other islands. Examination of the fate of nests and notes recorded in the data suggests that the differences between Onslow Beach and the other islands arise because of greater predation on Bald Head and Bear Islands (only in some years in the latter case), resulting in more partial and complete nest losses than occurred on Onslow Island. Turtle nests are caged generally on both Bald Head and Bear Islands, and nest predator control by trapping occurs. However, Bald Head Island houses substantial numbers of red fox (*Vulpes*

vulpes), which are notorious turtle nest predators, and raccoon (*Procyon lotor*) predation on Bear Island is periodically intense.

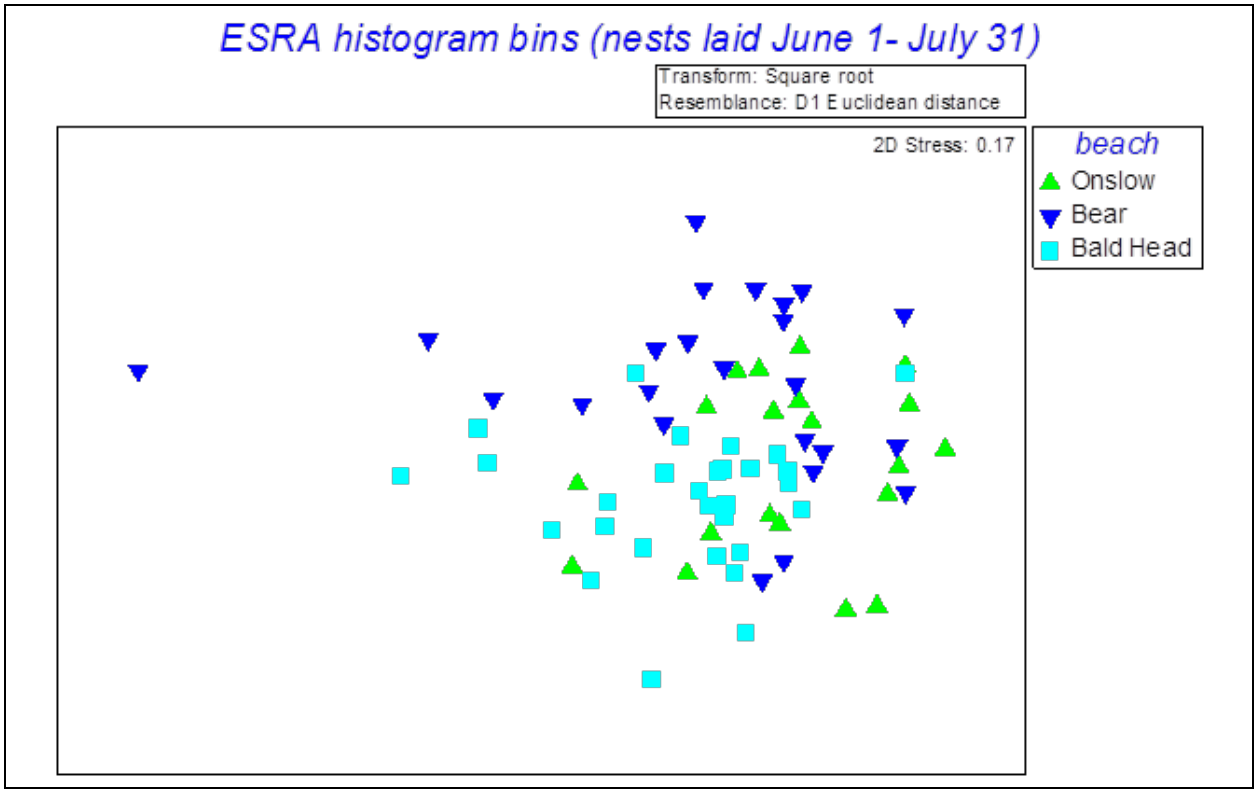

Figure 11-20. The nMDS plot of the frequency of island-specific annual adjusted emergence success rate (ESRA).

Turtle Nests and Barrier Island Transgression and Regression

We assessed spatial patterns of nest inundation for 2007–2010 (the only years with available spatial and inundation data). Along-beach inundation patterns vary from year to year (**Figure 11-21**), demonstrating that nest inundation can occur on different parts of the beach in different years. For a given nest, we expected the likelihood of nest inundation to increase with decreasing distance to the high water line (recorded by MCBCL EMD personnel when nests were first laid). We found distance to high water line to be a reasonable predictor of inundation risk for 2007–2009, but surprisingly, there was no relationship between distance to high water line and nest inundation in 2010 (**Figures 11-21 and 11-22**). In 2009, a protracted interval of elevated sea level occurred along the U.S. East Coast, including North Carolina, (Sweet et al., 2009) that resulted in morphological changes to the backbeach and dune faces on Onslow Beach in several locations that persisted into 2010. The morphological changes to the shorefront may have reduced the ability of female sea turtles to select appropriate nesting sites.

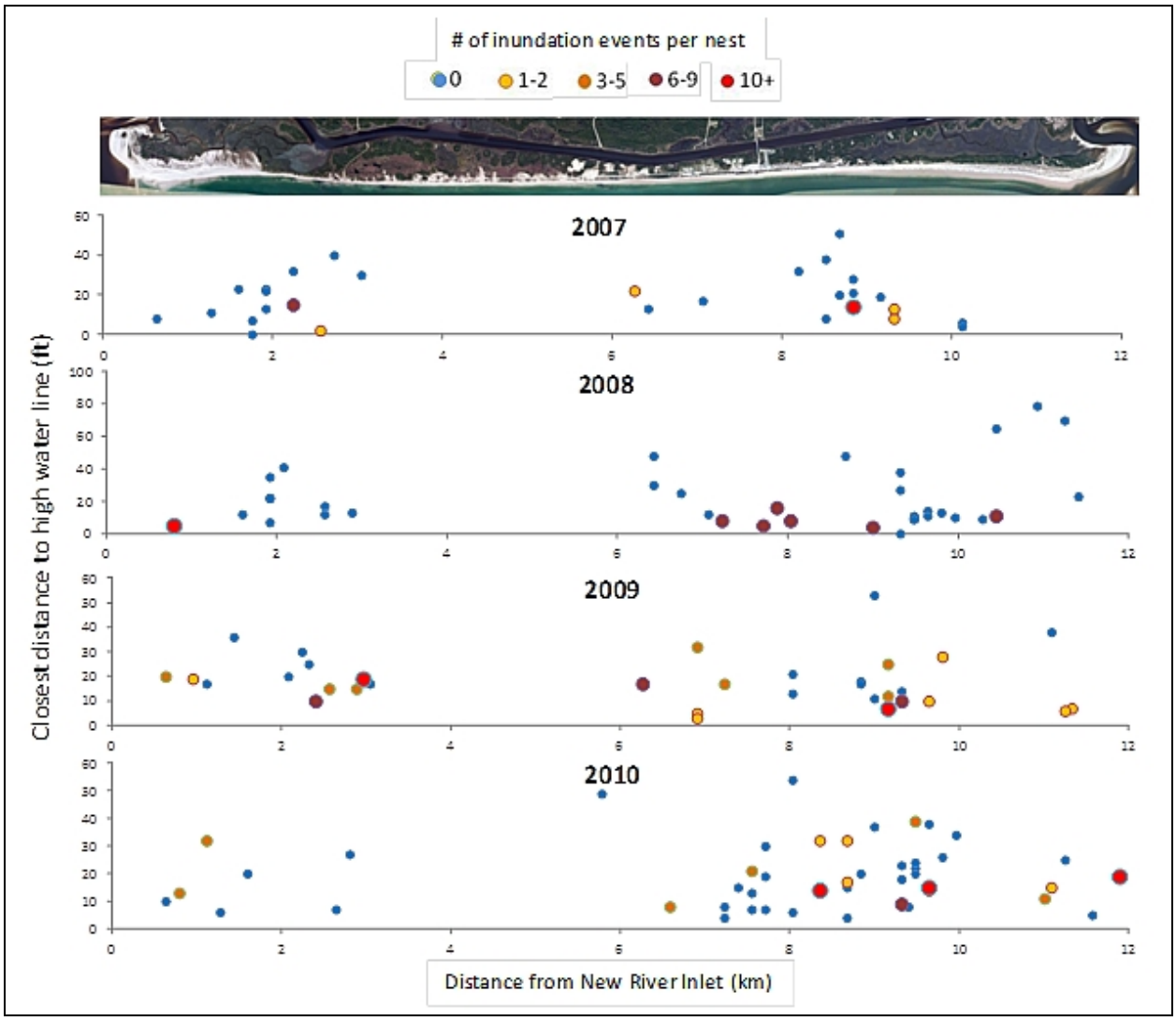

Figure 11-21. Location and frequency of sea turtle nest inundation on Onslow Beach, 2007–2010.

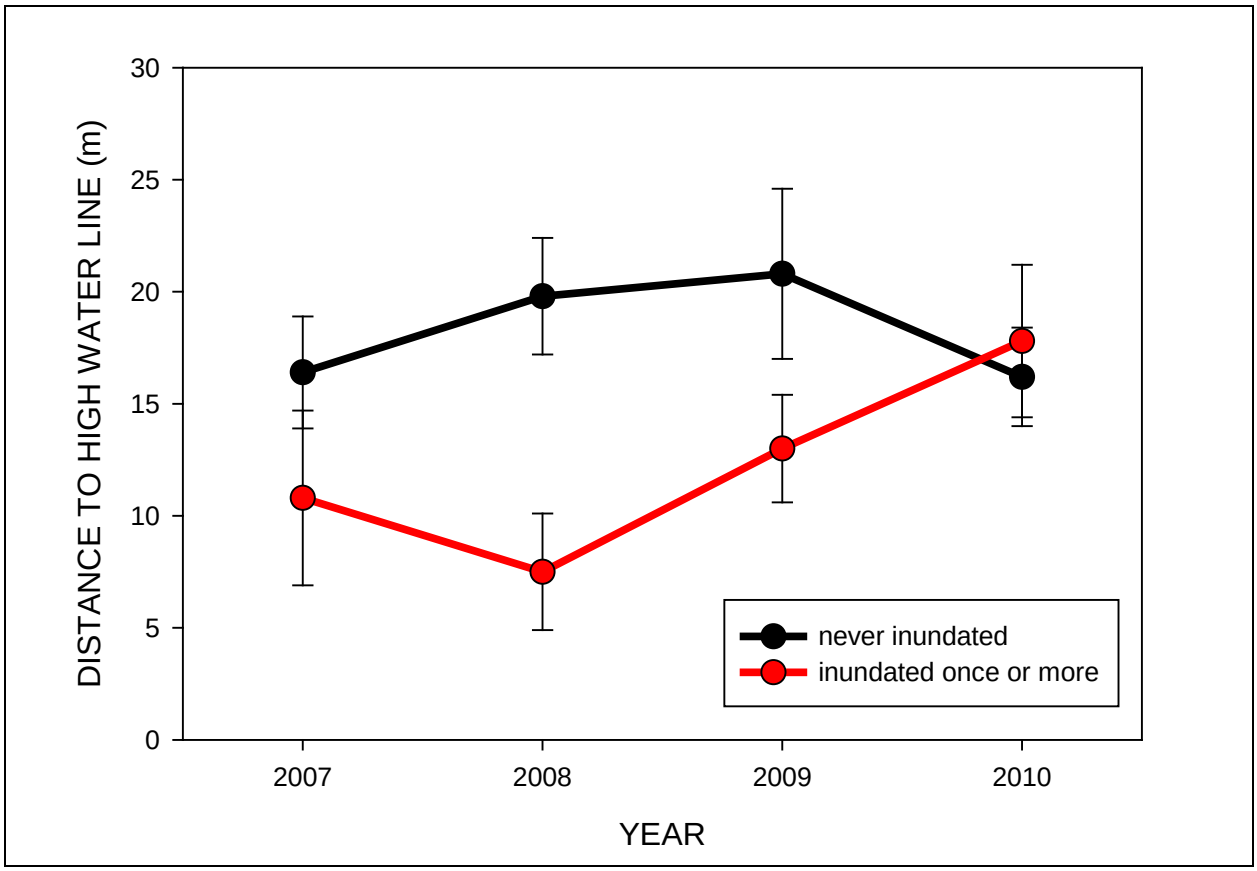

Figure 11-22. Sea turtle nest inundation relative to distance from high water line.

The mean (±1 SE) distance to the high water line of all nests that were never inundated, and all nests that were inundated at least one time, by year.

Assessment of Trends in the Data

Assessment of Monitoring Design

Our goals were to determine whether human activities, persisting over several years or from short-term, large-scale physical alterations of the environment, affected organisms living in the beach habitat that are of direct or indirect management interest. All of the organisms utilizing the beach move alongshore or across shore on relatively short time scales (days to weeks at the longest), requiring the spatial extent of the monitoring design to extend along the entire island, which it did. The compartmentalization of types of human activities on Onslow Beach required the monitoring design to have replicate sampling areas within each compartment, which it did. The target organisms show substantial annual variability which required a temporal extent of the monitoring design to encompass replicate samplings within years for several successive years, which it did. Subsequent analyses of our infaunal and ghost crab burrow data detected significant differences among the combinations of space and time indicating that our overall level of replication was sufficient to provide discrimination of differences within the very noisy beach ecosystem. Estimated statistical power where we failed to detect differences ranged from 50–70% supporting our contention that no large changes in faunal abundances were missed. Finally, because the faunal sampling design was congruent and contemporaneous with sampling of beach

morphology and granulometry we were able to quantify the degree to which these important physical features explained variation in the abundances and distribution of the fauna.

Surf fish sampling was adequate only for questions associated with juvenile fish inhabiting the shallow portion of the surf zone. Although we detected some differences among locations and times, estimated statistical power is very low when we do not find differences. Furthermore, many individual species of interest, such as pompano, were captured too infrequently to allow targeted analyses on those species. When we were sampling in the field, we suspected that our methodology was inadequate to capture larger, faster swimming fish species. Furthermore, we were depth limited during our sampling by the height of the individuals hauling the seines. More efficient, complete, and adequate sampling of surf zone nekton would require much larger (greater than 100-m long) nets deployed and retrieved from boats launching from the beach. The costs of this methodology exceeded our budget.

EMD censuses turtle nests efficiently in their rigorous management program. In 4 years of observation of EMD's effort, we have found evidence of only two nests missed out of the greater than 200 nests found, which is an error rate of less than 1%.

Assessment of Seasonal and Annual Variabilities in the Data

Both seasonal and annual variabilities in densities and abundances existed for the invertebrate and fish species we followed. Other than some instances in which seasonal population biology of specific species induced seasonal differences, this variability was not consistent nor did it, in most cases, relate to Base activities. There were no increasing or decreasing trends in the populations we followed over 4 years. The temporal patterns of fauna we observed on Onslow Beach were not different from those we observed at our control site, Bear Island.

Recommendations for Future Monitoring

MCBCL should continue to monitor sea turtle nests and conduct the alongshore bird surveys. Both of these data sets proved useful to us for testing whether newly collected data cohered to the spatial and temporal patterns of sea turtle nests or bird use of the beach. They also are the only data sets that have been collected long enough to provide a sense of whether subtle, but important, changes are occurring in these species of management interest. We recommend that increased rigor be added to the bird surveys by increasing the consistency of when the surveys are conducted and in maintaining spatial information on the birds in their database. Our ability to relate the information we gathered on prey abundance and beach geology to the historical data set was severely limited on some occasions by gaps in the bird survey, thereby decreasing the value of the entire monitoring effort. The Base may consider adding surveys of ghost crab abundance. This species plays multiple roles as both predators and prey in the barrier island trophic web that includes ground nesting bird eggs and fledglings and sea turtle hatchlings. They are also widely known as the most sensitive indicator of human activity in the beach environment. The persistent and significant depression of ghost crab abundances in the military training zone could not be related to any environmental features we measured.

Conclusions and Implications for Future Research

Key Scientific Findings—Fundamental Cause-and-Effect Relationships

All of the faunal species we followed exhibited substantial year-to-year variation in abundance, but their life cycles enable them to have substantial resilience to environmental and anthropogenic stressors as long as habitat loss does not occur. Ghost crabs demonstrated consistent, depressed abundances in the MT area of the island; a pattern that could not be attributed to a spatially explicit distribution of environmental factors (such as no habitat or unsuitable sediment type) and thereby raising the possibility that some aspect of military training affects ghost crab abundances there. We also confirmed by observation and experimental test that individual or small emergences of sea turtle hatchlings increase the risk of ghost crabs predating them (detailed in Peterson et al., 2012).

Findings Supportive of Current Base Management Practices

Direct Effects of Anthropogenic Activities

Existing military training practices are constrained to levels of environmental disturbance that are well within the ecosystem's range of resilience, with the exception of one species: ghost crabs. Currently military traffic over/through dunes and dune fields are restricted to well-defined corridors. There is no evidence that beach erosion, sediment character, sediment compaction, intertidal benthos densities, or surf fish abundances are influenced in the long-term (months to years) by training activities. Likewise, ORRV activity and pedestrian disturbances are well constrained. The only significant effects appear to be related to changing the distribution of shorebirds. However, as several kilometers of beach are still available for bird foraging and resting this displacement does not appear to have any negative effects.

Sea Turtle Nesting

The Base should continue existing practices for finding nests, preventing depredation, and conducting well-timed inventories to enhance hatchling ESRs by freeing trapped but live hatchlings. These practices have produced a nest management program that is demonstrably as good if not superior to analogous programs on nearby islands.

Findings with Implications for Future MCBCL Management

Direct Effects of Anthropogenic Activities

The use of the northern end of Onslow Beach for disposal of dredge material needs to be monitored and constrained. Failure to construct a typical beach profile after the material has been added will adversely affect turtle nesting in a region of the island that normally is ideal for nesting turtles and their hatchlings. Also, the relatively small volume disposals that have occurred had short-term, negative effects on an important shorebird prey resource. Larger volume disposals can be expected to cause longer lasting, more substantial decreases in shorebird prey abundance. Finally, the sediments deposited by the two disposals we observed were, for the most part, a good match with the existing beach sediments without large proportions of either very fine or very coarse material. Disposal of very fine or very coarse dredge material on

beaches has been demonstrated to have substantial, long-lasting negative effects on the infaunal prey and surf fish feeding on other North Carolina beaches, so the Base should continue to encourage disposal of only medium sands to Onslow Beach.

The absence of the backbeach in the training and ORRV zones could lead to greater intensities of pedestrian and vehicular traffic onto and through the dunes and in the habitats behind the dunes. These areas have been shown to be highly sensitive to human and vehicular traffic in numerous studies and human encroachment on dune habitats needs to be monitored.

Sea Turtle Nesting

MCBCL should expect changes in the near future on nest-site selection by the turtles. A greater proportion of sea turtle nests could be at higher risk in the coming years because of beach landscape changes such as reduced or absent backbeach (leading to inundation of misplaced seaward nests) and scarped dunes (which may slough). The decision rules used by turtles for specific nest-site selection and by resource managers in assessing future risk of inundation and identifying safe sites for relocation may be less effective in the altered landscape of Onslow Beach than they have been in the past. Future monitoring of sea turtle nests should record additional variables, including the following: (1) precise measurements of elevation and location on the beach; (2) proximity of local landscape features (e.g., vegetation, dune or scarp features, sediment type); and (3) beach width and slope. This information would improve the ability of EMD personnel to predict the likely fate of nests in backbeach areas subject to erosion and dune collapse.

Findings with Implications for DCERP2

Island transgression on the southern third of the island in response to sea level rise will have the greatest effects (assuming no large changes in human activities occur) on shorebirds and nesting sea turtles by changing island morphology. In some cases the changes may have positive effects on fauna: creation of washover fans will provide new habitat for foraging for a broad suite of bird species and, for a fewer number of species, nesting. In other cases the changes could reduce faunal use: loss of backbeach and primary dunes could induce changes in distribution or behavior (ghost crabs and nesting sea turtles, respectively) resulting in increased mortalities. Changes to the landscape could also affect travel corridors for hatchling birds and for nest and hatchling predators producing complex, and currently unpredictable consequences. Finally, the quality of habitat for birds, sea turtles, and their predators will depend upon the type and rate of ecological succession by flora in these altered habitats. Continued success in management of habitat for threatened and endangered species on the southern end of the island will depend upon understanding how both flora and fauna respond to the novel environmental conditions imposed by island rollover.

Literature Cited

Bolten, A.B., L.B. Crowder, M.G. Dodd, S.L. MacPherson, J.A. Musik, B.A. Schroeder, B.E. Witherington, K.J. Long, and M.L. Snover. 2011. Quantifying multiple threats to endangered species: an example from loggerhead sea turtles. *Frontiers in Ecology and Environment 9*:295-301.

Brown, A.C., and A. McLachlan. 1990. *Ecology of Sandy Shores*. Elsevier Press: Amsterdam, The Netherlands.

Bjorndal, K.A., B.W. Bowen, M. Chaloupka, L.B. Crowder, S.S. Heppell, C.M. Jones, M.E. Lutcavage, A.R. Solow, and B.E. Witherington. 2010. *Assessment of Sea-Turtle Status and Trends, Integrating Demography and Abundance*. National Academies Press: Washington, DC.

Clark, B.M. 1997. Variation in surf zone fish community structure across a wave-exposure gradient. *Estuarine, Coastal and Shelf Science 44*:659–674.

Cohen, J.B., S.M. Karpanty, J.D. Fraser, and B.R. Truitt. 2010. The effect of benthic prey abundance and size on red knot (*Calidris canutus*) distribution at an alternative migratory stopover site on the U.S. Atlantic Coast. *Journal of Ornithology 51*:355–364.

Fraser, J.D., S.H. Keane, and P.A. Buckley. 2005. Prenesting use of intertidal habitats by piping plovers on South Monomoy Island. *Journal of Wildlife Management 69*(4):1731–1736.

Garcia, A., G. Ceballos, and R. Adaya. 2003. Intensive beach management as an improved sea turtle conservation strategy in Mexico. *Biological Conservation 111*:253–261.

Godfrey, P.J., and M.M. Godfrey. 1976. *Barrier Island Ecology of Cape Lookout National Seashore and Vicinity, North Carolina*. *National Park Service Scientific Monograph Series 9*.

Karpanty, S.M, J.D. Fraser, J. Berkson, L.J. Niles, A. Dey, and E.P. Smith. 2006. Horseshoe crab eggs determine red knot distribution in Delaware Bay habitats. *Journal of Wildlife Management 70*(6):1704–1710.

Magnuson, J.J., K.A. Bjorndal, W.D. DuPaul, G.L. Graham, D.W. Owens, C.H. Peterson, P.C.H. Pritchard, J.I. Richardson, G.E. Saul, and C.W. West. 1990. Decline of the sea turtles: Causes and prevention. National Academies Press: Washington, DC.

Manning, L.M., C.H. Peterson, and S.R. Fegley. 2012. Degradation of surf fish foraging habitat driven by persistent sedimentological modifications caused by beach nourishment. *Bulletin of Marine Science*. In press. doi: http://dx.doi.org/10.5343/bms.2012.1005.

McNinch, J.E. 2004. Geologic control in the nearshore: shore-oblique sandbars and shoreline erosion hotspots, Mid-Atlantic Bight, USA. *Marine Geology 211*:121–141.

Mont'Alverne, R., L.E. MA. Moraes, F.L. Rodrigues, and J.P. Vieira. 2012. Do mud deposition events on sandy beaches affect surf zone ichthyofauna? A southern Brazilian case study. *Estuarine, Coastal and Shelf Science 102–103*:116–125.

NCCRC (North Carolina Coastal Resources Commission). 2010. North Carolina sea-level rise assessment report. Raleigh, NC.

Peterson, C.H., M.J. Bishop, G.A. Johnson, L.M. D'Anna, and L.M. Manning. 2006. Exploiting beach filling as an unaffordable experiment: benthic intertidal impacts propagating upwards to shorebirds. *Journal of Experimental Marine Biology and Ecology 338*:205–221.

Peterson, C.H., D.H.M. Hickerson, and G.G. Johnson. 2000. Short-term consequences of nourishment and bulldozing on the dominant large invertebrates of a sandy beach. *Journal of Coastal Research 16*:368–378.

Peterson, C.H., S.R. Fegley, C.M. Voss, S.R. Marschhauser, and B.M. VanDusen. 2012. Conservation implications of density-dependent predation by ghost crabs on hatchling sea turtles running the gauntlet to the sea. *Marine Biology* http://doi 10.1007/s00227-012-2118-z.

Rodriguez, A.B., J.B. Anderson, F.P. Siringan, and M. Taviani. 2004. Holocene evolution of the east Texas coast and inner continental shelf: Along-strike variability in coastal retreat rates. Journal of Sedimentary Research 74:406–422.Romer, G.S.1990. Surf zone fish community and species response to a wave energy gradient. *Journal of Fish Biology 36*:279–287.

Ross, S.W., and J.E. Lancaster. 2002. Movements and site fidelity of two juvenile fish species using surf zone nursery habitats along the southeastern North Carolina coast. *Environmental Biology of Fishes 63*:161–172.

Schlacher, T.A., R. de Jager, and T. Nielsen. 2011. Vegetation and ghost crabs in coastal dunes as indicators of putative stressors from tourism. *Ecological Indicators 11*:284–294.

Sweet, W., C. Zervas, and S. Gill. 2009. *Elevated East Coast Sea Levels Anomaly: June–July 2009*. NOAA Technical Report NOS CO-OPS 051. 30 pages. National Oceanic and Atmospheric Administration, National Ocean Service, Center for Operational Oceanographic Products and Services. Available at http://tidesandcurrents.noaa.gov/publications/EastCoastSeaLevelAnomaly_2009.pdf.

Wells, J.T., and C.H. Peterson. 1986. *Restless Ribbons of Sand: Atlantic and Gulf Coastal Barriers*. U.S. Fish and Wildlife Service, National Wetlands Research Center, Slidell, LA. 24 pages.

Wilber, D.H., D.G. Clarke, G.L. Ray, and M. Burlas. 2003. Response of surf zone fish to beach nourishment operations on the northern coast of New Jersey, USA. *Marine Ecology Progress Series 250*:231–246.

Wolcott, T.G. 1978. Ecological role of ghost crabs, *Ocypode quadrata* (Fabricius) on an ocean beach: Scavengers or predators? *Journal of Experimental Marine Biology and Ecology 31*:67–82.

Wolcott, T.G., and D.L. Wolcott. 1984. Impact of off-road vehicles on macroinvertebrates of a mid-Atlantic beach. *Biological Conservation 29*:217–240.

[This page intentionally left blank.]

Appendix 11-A

List of Scientific Publications

List of Scientific Publications

Papers

Manning, L.M., C.H. Peterson, and S.R. Fegley. 2012. Degradation of surf fish foraging habitat driven by persistent sedimentological modifications caused by beach nourishment. *Bulletin of Marine Science*. In press. doi: http://dx.doi.org/10.5343/bms.2012.1005.

VanDusen, B.M, Fegley, S.R, and C.H. Peterson. 2012. Prey distribution, physical habitat features, and guild traits interact to produce contrasting shorebird assemblages among foraging patches. *PLOS One 7*(12):e52694. doi:10.1371/journal.pone.0052694

Peterson, C.H., S.R. Fegley, C.M. Voss, S.R. Marschhause and B.M. VanDusen. 2012. Conservation implications of density-dependent predation by ghost crabs on hatchling sea turtles running the gauntlet to the sea. *Marine Biology*. doi 10.1007/s00227-012-2118-z.

Theses

Marschhauser, S.R. 2010. *Ghost Crab (*Ocypode quadrata*) Abundance and Depredation on Loggerhead Sea Turtle (*Caretta caretta*) Hatchlings on Onslow Beach, North Carolina*. M.S. Thesis, College of Natural Resources, North Carolina State University, Raleigh, NC.

VanDusen, B.M. 2010. *Habitat Complexity and Patch Choice: Spatiotemporal Distribution of Foraging Shorebirds on Intertidal Sand Flats*. M.S. Thesis, University of North Carolina at Chapel Hill, Chapel Hill, NC.

Presentations

2012. *Employing Experimental and Monitoring Research to Preserve Both Ecological Habitats and Human Uses on Barrier Islands*. Presented at Methodist University, Department of Biology, Fayetteville, NC.

2010. *Perturbation in a Dynamic System: Variable Consequences of Coastal Storms on Habitat Structure and Faunal Composition in an Exposed Beach*. Presented at the Benthic Ecology Meeting, Wilmington, NC.

Appendix 11-B

List of Students

- Sara Marschhauser, M.S., Fish and Wildlife Studies, North Carolina State University, Raleigh, NC. March 2010.
- Beth M. VanDusen., M.S., Ecology (Curriculum for the Environment and Ecology), University of North Carolina at Chapel Hill, Chapel Hill, NC. May 2010.

[This page intentionally left blank.]

Chapter 12

Onslow Beach Dune, Shrub, and Marsh Plants

SERDP Project Number: RC-1413

Coastal Barrier Module

Lead Researchers:
Dr. Stephen R. Fegley
Dr. Charles H. Peterson
University of North Carolina at Chapel Hill Institute of Marine Sciences
Morehead City, NC
E-mails: sfegley@email.unc.edu and cpeters@email.unc.edu

Supporting Researcher:
Beth M. VanDusen
University of North Carolina at Chapel Hill Institute of Marine Sciences
Morehead City, NC
E-mail: vandusen@unc.edu

June 27, 2013

Final

This report was prepared under contract to the U.S. Department of Defense (DoD) Strategic Environmental Research and Development Program (SERDP). The publication of this report does not indicate endorsement by DoD, nor should the contents be construed as reflecting the official policy or position of DoD. References herein to any specific commercial product, process, or service by trade name, trademark, manufacturer, or otherwise, do not necessarily constitute or imply its endorsement, recommendation, or favoring by DoD.

Table of Contents

List of Acronyms 12-v
Abstract 12-1
Objectives of the Monitoring Activity 12-2
Species Composition and Relative Abundance 12-2
Vertical Structure of Island Vegetation 12-2
Effects of Dune Erosion and Overwash Events on Island Vegetation 12-2
Background 12-2
Species Composition and Relative Abundance 12-2
Vertical Structure of Island Vegetation 12-3
Effects of Dune Erosion and Overwash Events on Island Vegetation 12-3
Materials and Methods 12-3
Species Composition and Relative Abundance 12-3
Vertical Structure of Island Vegetation 12-5
Effects of Dune Erosion and Overwash Events on Island Vegetation 12-6
Results and Discussion 12-6
Species Composition and Relative Abundance 12-6
Vertical Structure 12-8
Effects of Dune Erosion and Overwash 12-9
Assessment of Trends in the Data 12-13
Assessment of Monitoring Design 12-13
Assessment of Seasonal and Annual Variability in the Data 12-14
Recommendations for Future Monitoring 12-14
Conclusions and Implications for Future Research 12-14
Key Scientific Findings—Fundamental Cause-and-Effect Relationships 12-14
Findings Supportive of Current Base Management Practices 12-14
Findings with Implications for Future Base Management 12-14
Findings with Implications for DCERP2 12-15
Literature Cited 12-16
Appendix 12-A: List of Scientific Publications 12-A-1

List of Figures

12-1. Onslow Beach vegetation transects and plots. 12-4

12-2. A non-metric multidimensional scale (nMDS) plot illustrating the patterns of similarities among vegetation plots across all anthropogenic areas and intensities. 12-7

12-3. Bubble plots overlaying the nMDS plot in 12-2 indicating relative abundance of each individual species. 12-7

12-4. Vertical density of vegetation in the 1 m closest to the substrate partitioned into contiguous 33-cm intervals. 12-9

12-5. Dune erosion on Onslow Beach after Hurricane Irene. 12-10

12-6. Vegetation shoreward of the high-intensity ORRV transect (FS 2) before (on left) and after (on right) Hurricane Irene. 12-11

12-7. Changes in percent cover of floral species in vegetation plots experiencing storm overwash due to Hurricane Irene. 12-12

12-8. An nMDS plot illustrating the effects of hurricane overwash on the patterns of similarities among vegetation plots at the high-impact ORRV area..... 12-13

List of Tables

12-1. Percent cover categories used to assess relative abundance of plant species in long-term vegetation plots. 12-5

List of Acronyms

cm	centimeter
CVS	Carolina Vegetation Survey
DCERP2	second cycle of the Defense Coastal/Estuarine Research Program
DoD	U.S. Department of Defense
FS	focus site
GPS	global positioning system
ICW	Intracoastal Waterway
m	meter
m^2	square meter
MCBCL	Marine Corps Base Camp Lejeune
MT	military training
nMDS	non-metric multidimensional scaling
ORRV	off-road recreational vehicle
PERMANOVA	permutational multivariate analysis of variance
PVC	polyvinyl chloride
REC	recreational use
SERDP	Strategic Environmental Research and Development Program

[This page intentionally left blank.]

Abstract

Although only a limited number of vascular plant species can survive in the harsh environmental conditions omnipresent on barrier islands, the ecological communities these plant species produce play vital roles in stabilizing dunes, providing nesting areas for shorebirds, and creating habitat for numerous bird and mammalian species. Barrier island vegetation communities have been shown globally to be sensitive to added stressors, especially human and vehicular trespass. Maintaining the important ecosystem services arising from barrier island vegetation requires an ability to observe and quantify changes in the floral communities to anticipate, and hopefully mediate, habitat loss or alteration produced by anthropogenic activities and storm events.

Unperturbed ecological succession on barrier islands occurs over long time scales, years to decades. Consequently, creating and following site-specific baseline plots is the most effective means for documenting both short-term impacts and slower, more subtle changes to floral structure. We established an array of 5-m × 20-m permanent sample plots along and across Onslow Island in which we identified all species of plants and recorded the relative abundances of each. The alongshore siting of the plots encompasses transgressive, stable, and regressive parts of Onslow Beach. Across the island at each of these sites the plots begin at the primary dunes fronting the beach and extend to the back barrier and where salt marsh habitat occurs, into the salt marsh. The intervening plots are spaced to capture all of the within-island variation in plant communities. We also have quantified the above ground extent of vegetation across the island on the southwestern and northeastern ends by using a profile board technique.

As has been found in studies conducted in other barrier islands, on Onslow Island distinctive plant communities occur in linear, alongshore bands extending from the beach to the back barrier except where human development or training activities have disrupted this pattern. Behind the back beach on the exposed side of the island there is an elevated dune community, followed landward by a dune field/slack community, and then, depending on local elevation, either maritime shrub/scrub, maritime forest, or freshwater communities. On the back barrier these latter communities abut onto salt marsh or the Intracoastal Waterway. At the northeastern, regressive end of the island the aerial portions of the well-developed, high plant communities disconnect sediment transport from the beach to the back barrier. At the southwestern, transgressive end of the island the plant communities alter the direction and retard across island sediment transport but do not prevent it from occurring.

Storm-induced changes to the vegetation have also been documented. The dune communities at half of our sites along the island have been completely or partially removed due to dune erosion associated with a high sea level anomaly event and, subsequently, effects of Hurricane Irene. At two of our sites, the dune field community was also lost or decimated by these high water events. These events have begun the process of translocating the barrier islands landforms and habitats landward as part of island rollover.

Keywords: Barrier island vegetation, dune erosion, plant burial, washover fan

Objectives of the Monitoring Activity

Species Composition and Relative Abundance

The objective of vegetation monitoring is to provide the means to document the short- and long-term changes in the various plant communities as they respond to natural forcing events, such as storms and sea level rise, and anthropogenic stresses, including military training and recreational use. This information will be used to develop a management plan that preserves the natural vegetation, and the important ecosystem services they provide, while sustaining Base training and recreation activities.

Vertical Structure of Island Vegetation

No quantitative information has been gathered on vertical structure of vegetation associated with the different floral communities on Onslow Island. Recent studies of Onslow Beach's back-barrier salt marshes has indicated they may be susceptible to drowning by rising sea level if the rates of sedimentation and organic matter accumulation do not exceed sea level rise. One potential source of sediment for salt marshes associated with barrier islands is sand present on the exposed beaches and washover fans. One pathway for this sand to move to the marshes is aeolian transport, which is mediated by vegetation presence and structure. Gathering information on the spatial characteristics of vegetation height is necessary to quantify how it affects sand movement as well as vertebrate use of the habitats.

Effects of Dune Erosion and Overwash Events on Island Vegetation

Dune erosion and overwash both have the ability to remove or alter the floral communities that stabilize dunes and form important habitats across the barrier island. These processes are most frequent where island transgression occurs. To decide whether management intervention is required specific information on the frequency, alongshore and across-shore spatial extent, and the degree of restructuring of floral communities in response to these specific events must be quantified. Dune erosion and overwash generally occur as discrete events but most floral responses to these events reveal themselves over intervals of years or more. The focus of this effort is to document dune and overwash short-term effects and to establish plots that enable tracking long-term floral community responses to those events into the future.

Background

Species Composition and Relative Abundance

The first intensive surveys of Onslow Beach floral communities were conducted in the mid to late 1980s (Alexander et al., 1989; Williams, 1991). By sampling from across-shore transects Alexander et al. (1989) identified a total of 170 species and Williams (1991) found an additional 21 species for a total of 191 species occurring on Onslow Beach. Using a combination of physical attributes (i.e., principally sediment composition, tidal regime, elevation, and exposure to salt spray) and lists of dominant species, both studies defined several vegetation units. They observed the following: (1) open grassland, (2) closed grassland, (3) brackish marsh, (4) irregularly flooded marsh, (5) tidal marsh, (6) shrub thicket, (7) maritime forest, and

(8) urban and disturbed units. Alexander et al. (1989) also included a woodland unit confined to just some of the dredge spoil islands located near the Intracoastal Waterway (ICW). Using a combination of orthophotography and ground-truthing, a vegetation habitat map was produced in spring 2003 (Versar, Inc., 2003) that summarized the spatial findings of the earlier studies (**Figure 12-1**, second panel from the top).

None of the vegetation units described by these studies were novel; all have been observed on southeastern U.S. barrier islands in other studies (Au, 1974; Erhenfeld, 1990).

Vertical Structure of Island Vegetation

Above-ground vegetation influences many aspects of the barrier island environment. The density, height, and spatial structure of vegetation influences the following: (1) across-island transport of sand by decreasing the effectiveness of aeolian transport and reducing the ability of wind to erode sediment (Arens, 1996a and b; de Groot et al., 2011); (2) spatial variation in airflow patterns resulting in dune blowouts and spatial patterns of sediment accumulation (Walker et al., 2006); (3) the distribution of fauna, including ground-nesting birds and their predators by alternately providing cover or travel corridors (Nudds, 1977; Ray, 2011); and (4) the formation of specific forms of dune fields (Hesp et al., 2010).

Effects of Dune Erosion and Overwash Events on Island Vegetation

Low-lying coastal barriers, such as those of Marine Corps Base Camp Lejeune (MCBCL), experience frequent overwash during storms. This process reinitiates the succession of dune and shrub-zone plant communities, provides new habitat for bird nesting and foraging, and extends and revitalizes salt marshes when overwash progresses across the island to the sound shoreline. Rare beach plants are sensitive to storm impacts, although the abundance of some species, such as the seabeach amaranth (*Amaranthus pumilus*), may be enhanced by natural environmental perturbations. The dune and shrub plants of the coastal barrier suffer physiological stress from wind-borne salt spray, yet receive limited nutrients from that same source and atmospheric deposition (Au, 1974). The inlets of coastal barriers are especially dynamic, and storm overwash at inlets plays an important role in maintaining flat and sparsely vegetated areas suitable for nesting and foraging by piping plovers, other shorebirds, terns, and gulls (Fraser et al., 2005).

Materials and Methods

Species Composition and Relative Abundance

Landward of seven primary focus sites (FS 1–7; **Figure 12-1**) on Onslow Island, transects were established beginning at the foredunes and extending to the ICW (except where MCBCL restrictions prevented us from entering behind the dunes). Each of these transects consisted of multiple 5-m × 20-m plots (with the long axis of each plot oriented parallel to the long axis of the island) that were sampled using procedures adapted from the Carolina Vegetation Survey (CVS) methodology (Peet et al., 1998). Once the southwest corner of each plot was staked the plot border was delineated with measurement tape. Then two observers systematically scanned the interior of the plot to identify all floral species present. When the species list was complete for the plot the relative abundance (percent cover) of each species was estimated and recorded into

one of 10 categories (**Table 12-1**). Before moving to the next plot the southwest corner of each plot had a 3.25-cm diameter × 2 m–long polyvinyl chloride (PVC) pole hammered 0.5 m vertically into the ground and the global positioning system (GPS) location of each pole was recorded. Separate plots on a given transect were spaced a minimum of 30 m from each other unless an obvious change in vegetation composition or a distinctive morphological feature likely to influence the floral community dictated a shorter between-plot distance.

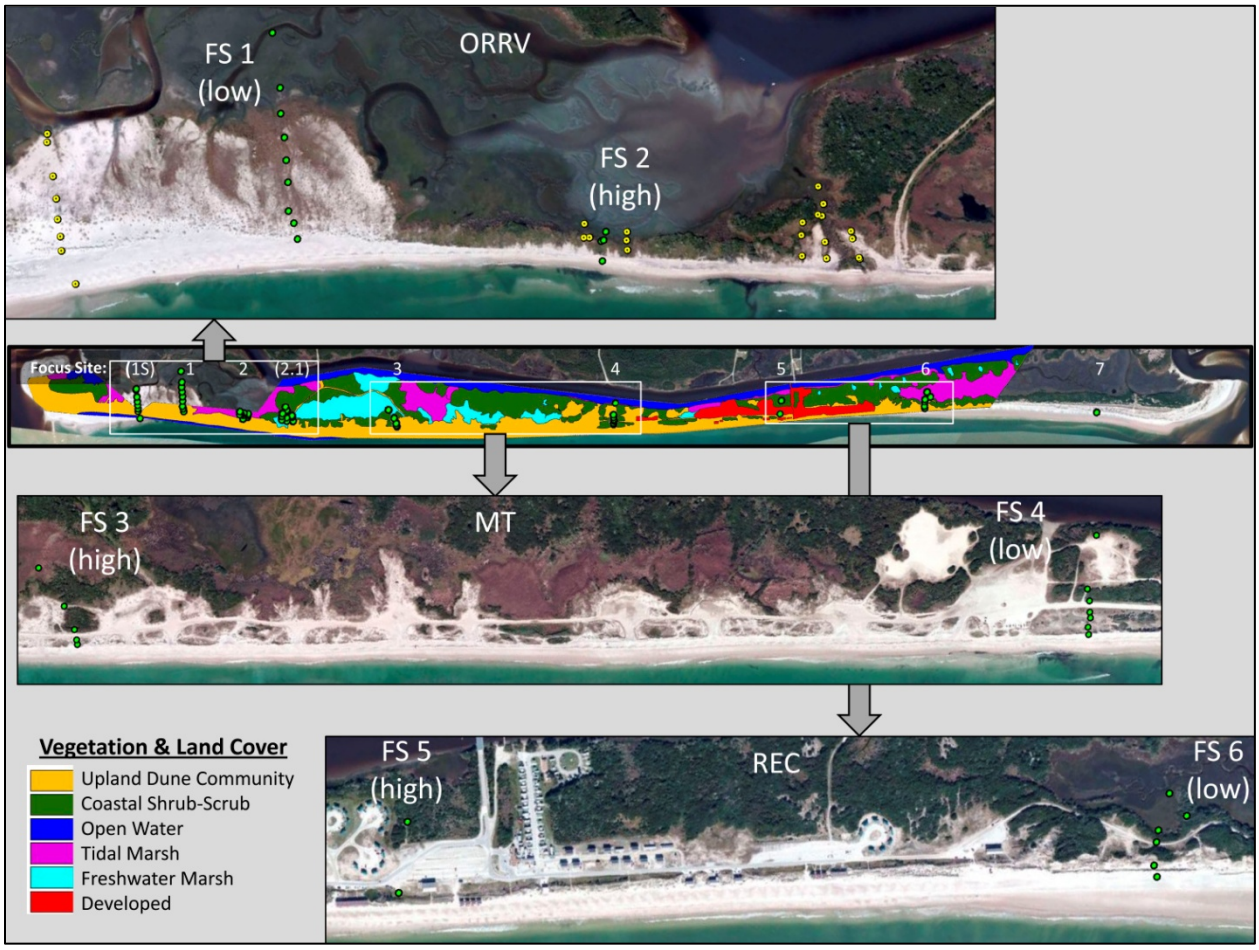

Figure 12-1. Onslow Beach vegetation transects and plots.

On enlargements, green circles denote locations of original vegetation plots; yellow circles indicate plots that were added after Hurricane Irene. Anthropogenic use codes: ORRV = off-road recreational vehicles; MT = military training; REC = recreation/swimming beach; "high" indicates higher use; "low" indicates lower use. Vegetation and land cover delineations in the second panel from the top are from Versar, Inc., 2003.

Table 12-1. Percent cover categories used to assess relative abundance of plant species in long-term vegetation plots.

Category	Percent Cover
1	trace
2	0–1%
3	1–2%
4	2–5%
5	5–10%
6	10–25%
7	25–50%
8	50–75%
9	75–95%
*	95–100%

Plots were established and surveyed initially in summer and fall 2009. In early fall 2011, additional plots were established in a new overwash created by Hurricane Irene (near FS 2.1), and additional transects of plots were established near existing vegetation plots at FS 1 and FS 2 (**Figure 12-1**, yellow circles in the top panel).

Vertical Structure of Island Vegetation

We quantified the vertical density of above-ground vegetation across the island on two transects that constrain the range of vertical structure present on the island. One transect was located parallel to the long-term vegetation plots in the low-intensity off-road recreational vehicle (ORRV) area where the dominant community consists of dune and dune field species and the highest landform structures are discontinuous protodunes less than 1-m high. The second transect was parallel to the long-term vegetation plots in the low-intensity recreation/swimming beach (REC) area, which has a mix of floral communities, including dune field and maritime forest and overlies a continuous, high (greater than 6 m) dune ridge.

We modified a profile board technique (Dudley et al., 1998; Haukos et al., 1998; Nudds, 1977) to quantify plant vertical structure. Our profile board consisted of three 20 cm–wide × 33.3 cm–high sections, painted flat black, stacked vertically above each other and separated by orange borders for visibility. In the field, a digital camera was placed approximately 0.5 m above a haphazardly selected primary central point and a picture was taken of the profile board (and intervening vegetation) after it was placed vertically a distance 10 m away. This was repeated for each cardinal and subcardinal direction around a central point. We then expanded the area covered around each primary point to encompass a total of 1,950 m^2 by selecting four more photograph centers, placed approximately 21 m from the primary point location along each subcardinal direction and repeating the entire procedure conducted at the central point. In the laboratory, we used Adobe Photoshop to determine the percentage of pixels that were flat black (no vegetation) in each 33-cm interval from the ground surface. We used these spatially explicit point estimates of vegetation density to derive contour maps of vegetation density at successive 33-cm intervals above the ground by kriging.

Effects of Dune Erosion and Overwash Events on Island Vegetation

In October 2011, 6 weeks after Hurricane Irene passed through the area, all plots were revisited, and those that were overwashed or eroded by the storm were resurveyed, using the same modified CVS procedure we employed when the plots were established.

Results and Discussion

Species Composition and Relative Abundance

Composition of Characteristic Communities

Non-dimensional multivariate scaling revealed that species assemblages sampled within our long-term plots sort into four distinct assemblages (**Figure 12-2**). The majority of the plots contain dune and open or closed grassland species. Assemblages nearer the beach at each site were dominated by sea oats (*Uniola paniculata*). *Uniola* decreased in abundance inland as saltmeadow cordgrass (*Spartina patens*) increased in percent cover of dune field assemblages (**Figure 12-3**). The maritime shrub/forest habitat was the most diverse, with several predominant species, including wax myrtle (*Morella cerifera*), Virginia creeper (*Parthenocissus quinquefolia*), saw greenbrier (*Smilax bona-nox*), broomsedge bluestem (*Andropogon virginicus*), seaside goldenrod (*Solidago sempervirens*), and live oak (*Quercus virginiana*) co-occurring in relatively high abundances. Both of the marsh communities were dominated by a single species of grass. Salt marsh assemblages were dominated by smooth cordgrass (*Spartina alterniflora*), and the lone freshwater marsh was dominated by common reed (*Phragmites communis*).

At all of the sites, except the high-intensity recreation area, the habitat types previously described occurred in zones paralleling the beach with dunes, dune field, maritime shrub/scrub, and salt marsh following in sequence from the beach to the backside of the barrier island. Extensive development of buildings, roads, parking lots, and picnic areas and the introduction of non-native plants has disrupted this general across-island pattern of vegetation in the high-intensity recreation area.

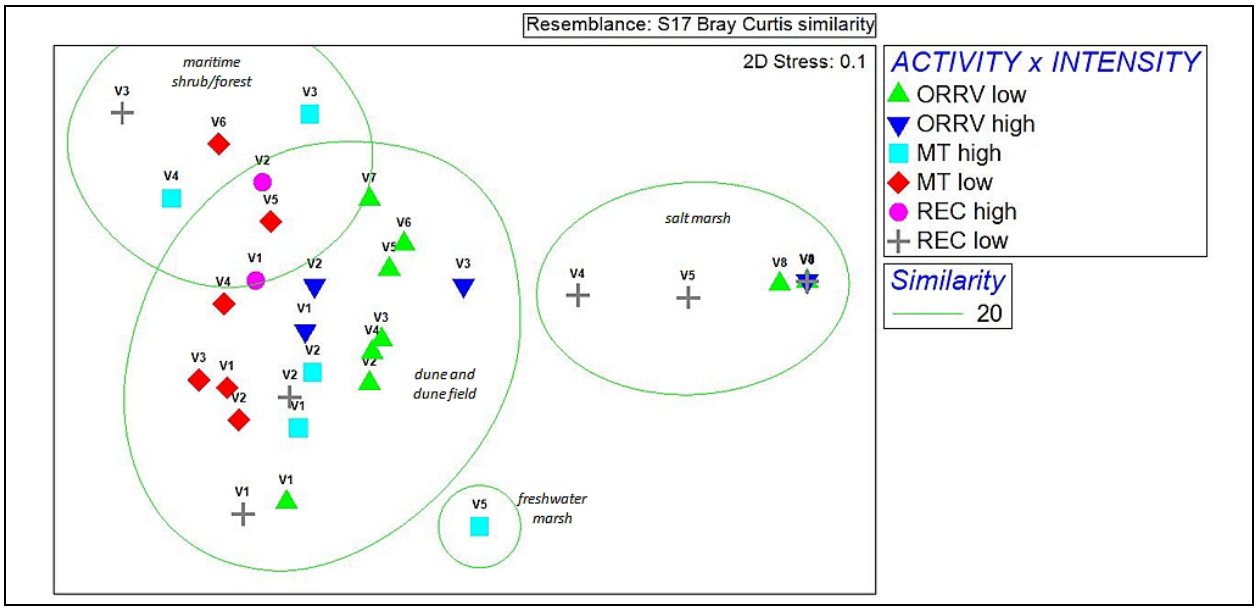

Figure 12-2. A non-metric multidimensional scale (nMDS) plot illustrating the patterns of similarities among vegetation plots across all anthropogenic areas and intensities.

Labels for plots closest to the beach have lower numbers. The habitat type as determined by dominant floral species is indicated by each cluster.

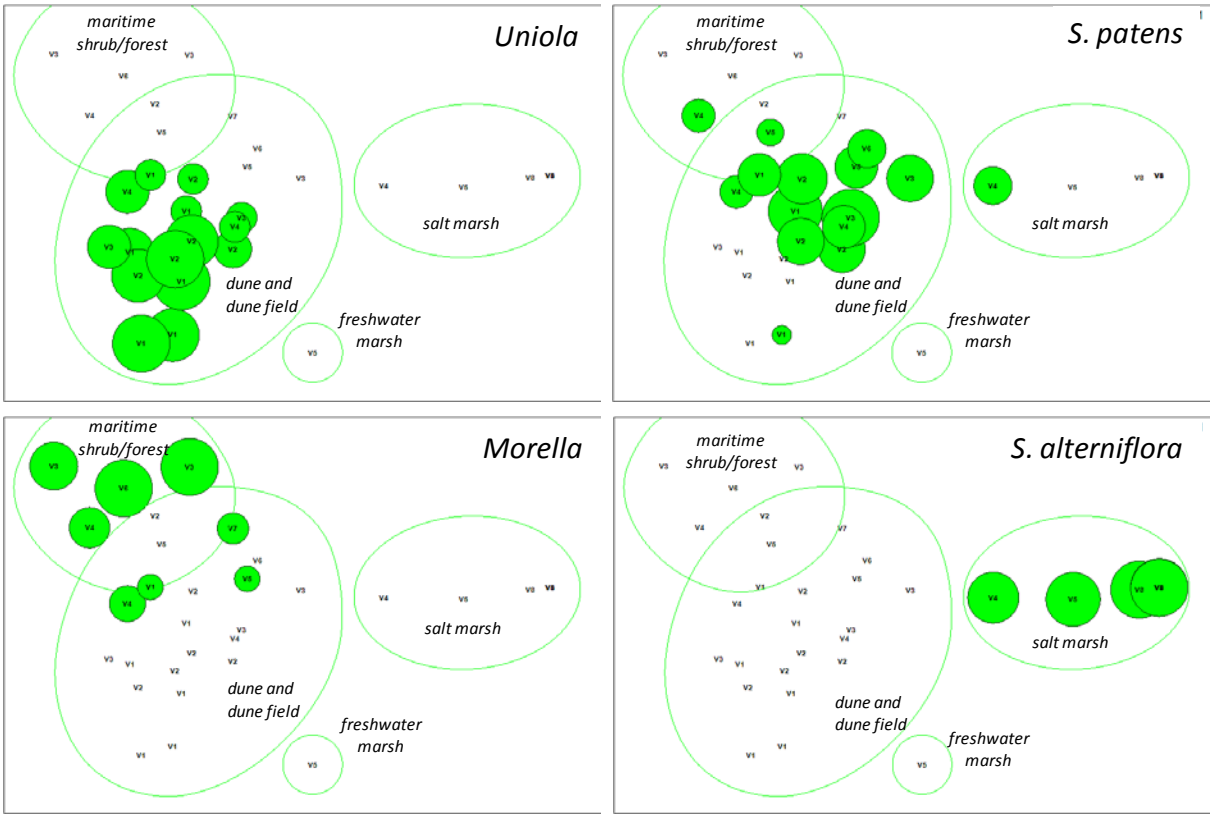

Figure 12-3. Bubble plots overlaying the nMDS plot in Figure 12-2 indicating relative abundance of each individual species.

The larger the bubble, the greater the percent cover of that species in the designated plot.

The four assemblages revealed by the non-metric multidimensional scale (nMDS) ordination correspond to the primary vegetation units described by Alexander et al. (1989) and Williams (1991). The dominant species characterizing each community and the linear structure of the respective communities correspond to patterns observed elsewhere on barrier islands along the East Coast (Ehrenfeld, 1990).

Comparison of the distribution and spatial extent of these communities currently to those documented by Alexander et al. (1989) in the mid-1980s indicates that relatively little change has occurred over the past two decades except where storm-induced washover fans have been created on the southwestern end of the island. There is some indication that the irregularly flooded marshes have become less diverse as *Phragmites australis* has almost formed a monoculture and the other species found in this habitat in the 1980s (*Typha* spp., *Cladium jamaicense*, and *Spartina cynosuroides*) have all but disappeared. This does not indicate that land-use changes have altered the habitat as *Phragmites* has been well documented to be an aggressive competitor (Holdredge and Bertness, 2011).

Vertical Structure

Vertical structure of the vegetation differed substantially between the southwestern and northeastern ends of the island. At the southwestern end (low-intensity ORRV area), vegetation density of the foredune is high near the ground, but it decreases and becomes patchy greater than 33 cm above the ground (**Figure 12-4A**). Across the washover fan, vegetation density is also high near the ground (0–33 cm), and patches of increased vegetation density 33–67 cm above the ground usually correspond with localized mounds of sand (less than 5 m^2). Vegetation is dense at the boundary between the washover fan and the backbarrier marsh, where an almost continuous line of shrubs greater than 1 m in height exists (**Figure 12-4A**). Although the vegetation density of the foredune at the northeastern end of the island (low-intensity REC area) is very similar to the foredune vegetation at the southwestern end, the high-elevation dune ridge behind the foredune is densely vegetated by tall grasses, even at 1 m above the ground (**Figure 12-4B**). In addition, the low-intensity REC area includes a dense maritime forest, which colonized the salt-spray shadow in the lee of the high-elevation dune ridge and marks the transition to the backbarrier marsh environment (**Figure 12-4B**).

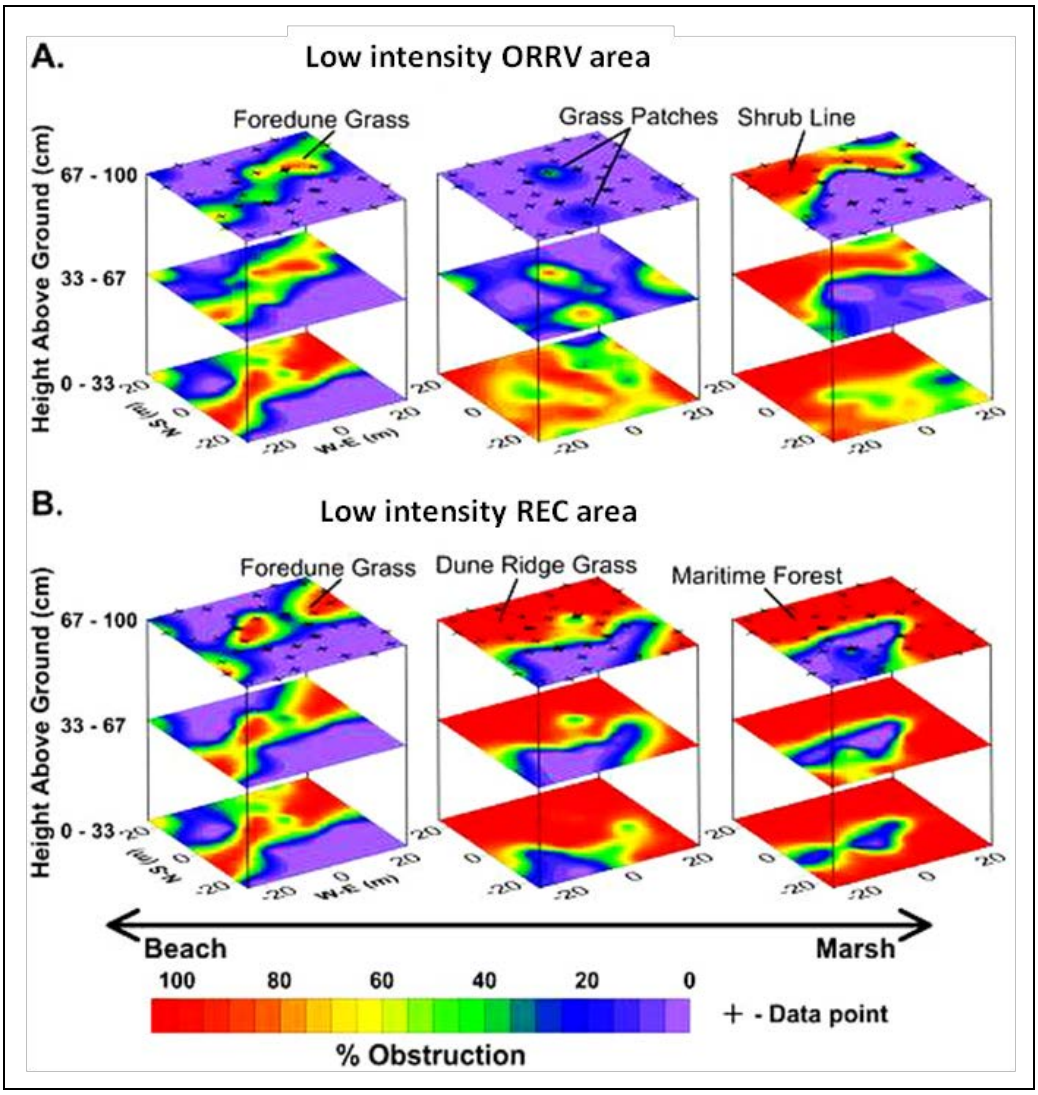

Figure 12-4. Vertical density of vegetation in the 1 m closest to the substrate partitioned into contiguous 33-cm intervals.

These differences in vertical structure of the vegetation within and between the two locations had substantial effects on the movement of sand across the barrier island and into the salt marsh (see Chapter 9 for details of the sediment results). At the northeastern end of the island the combination of tall vegetation and high landform prevented significant wind-driven sand transport to the marsh from the beach. In the southwestern end of the island modest aeolian sand transport from the beach into the dune field-slack region occurred but the high ridge of shrubs at the dune field salt marsh interface inhibit almost all sediment movement into the marsh.

Effects of Dune Erosion and Overwash

Dune Erosion

Rapid erosion due to elevated water levels and waves produced scarping on the seaward face of the dunes along several km of the southern half of the island extending from the middle of the

REC zone, through the entire military training (MT) zone, and into the ORRV zone as far as our high-intensity ORRV site (**Figure 12-5**). When dune scarping occurred, the roots of the dominant dune grasses (primarily *Uniola* on Onslow Beach) were exposed, leading subsequently to a die-back of the grasses on the crest of the dune. The unstable geometry of the scarped dunes and the loss of a contiguous grass mat on the dune crest led to slumping of the upper portions of the dune, in some cases causing the dune crest to retreat into established dune field assemblages that included shrubs. In some instances this retreat extended landward so far that dune field shrubs fell into the beach. Two of our most seaward permanent plots that were situated on dune crests at the high-intensity ORRV (FS 2) and low-intensity MT (FS 4) transects were completely lost as the dunes retreated landward. In both cases, the spatial locations those plots occupied previously are now in the upper intertidal of the beach.

Figure 12-5. Dune erosion on Onslow Beach after Hurricane Irene.

The bottom panel shows a scarped dune with extensive exposure of grass roots. The top panel shows a primary dune that has continued to retreat under the influence of erosion of the dune toe combined with slumping of the upper portion near the dune crest. In this case, the shoreward movement has led to dune field shrubs (*Morella* pictured in the top panel) collapsing onto the beach.

Overwash

All of the permanent vegetation plots at the high-intensity ORRV transect (FS 2) were overwashed during Hurricane Irene. As previously mentioned, the most seaward plot on the dune

face (Veg Plot 1) disappeared. All of the remaining plots were affected by the resulting washover fan and were buried by sediments to varying degrees (**Figure 12-6**). The two plots behind the former dune (Veg Plots 2 and 3) experienced reduced species richness, decreased total and species-specific percent cover, and different relative abundances of the remaining species. The monospecific plot closest to the salt marsh (Veg Plot 4) still had *Spartina alterniflora* present after being overwashed but this species experienced a 92.1% loss in percent cover (**Figure 12-7**).

Figure 12-6. Vegetation shoreward of the high-intensity ORRV transect (FS 2) before (on left) and after (on right) Hurricane Irene.

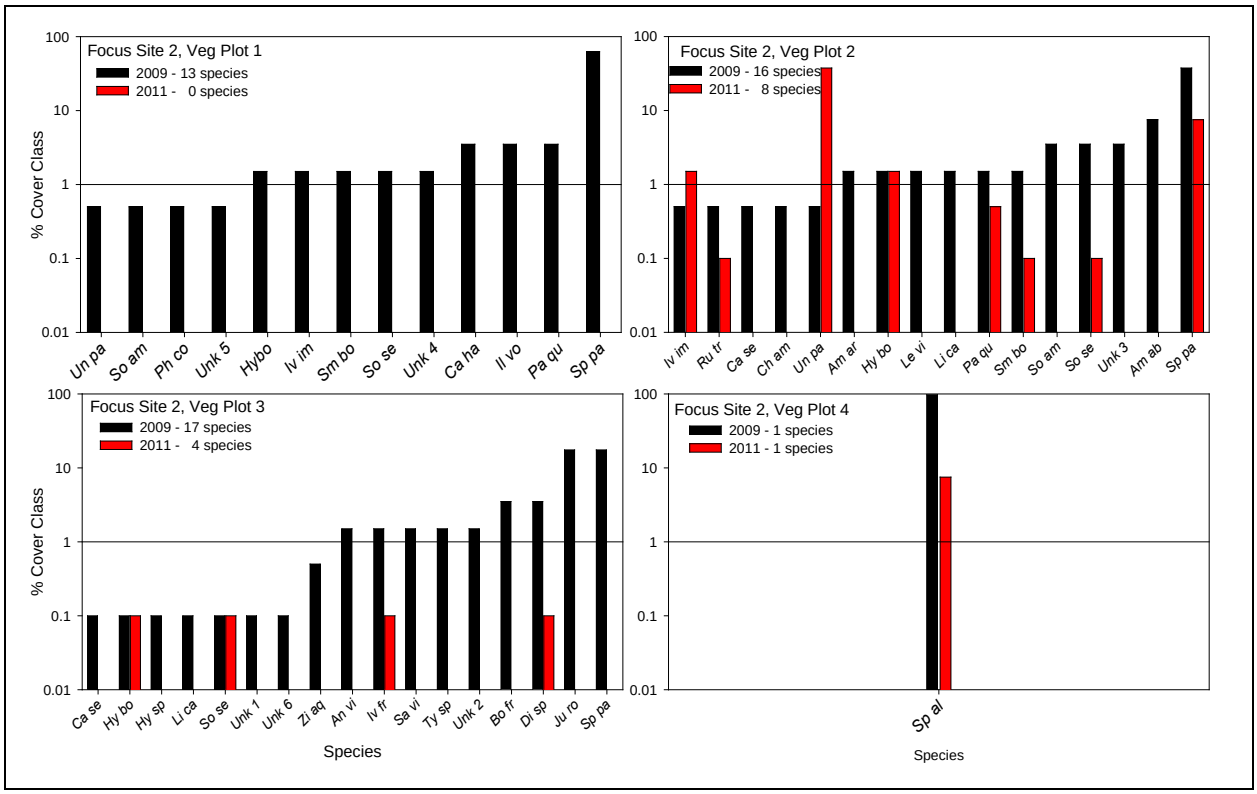

Figure 12-7. Changes in percent cover of floral species in vegetation plots experiencing storm overwash due to Hurricane Irene.

The higher the plot number, the further the plot is from the dune. Note that the *y*-axis is a $\log_{10}$ scale. The species codes are as follows: Am ab = *Ampelopsis arborea;* Am ar = *Ambrosia artemesiifolia;* An vi = *Andropogon virginicus;* Bo fr = *Borrichia frutescens;* Ca ha = *Cakile harperi;* Ca se = *Calystegia sepium;* Ch am = *Chenopodium ambrosioides;* Di sp = *Distichlis spicata;* Hy bo = *Hydrocotyle bonariensis;* Hy sp = *Hypericum* sp.; Il vo = *Ilex vomitorium;* Iv fr = *Iva frutescens;* Iv im = *Iva imbricate;* Ju ro = *Juncus roemerianus;* Le vi = *Lepidium virginicum;* Li ca = *Limonium carolinianum;* Pa qu = *Parthenocissus quinquefolia;* Ph co = *Phragmites communis;* Ru tr = *Rubus trivialis;* Sa vi = *Salicornia virginica;* Sm bo = *Smilax bona-nox;* So am = *Solanum americanum;* So se = *Solidago sempervirens;* Sp al = *Spartina alterniflora;* Sp pa = *Spartina patens;* Ty sp = *Typha* sp.; Un pa = *Uniola paniculata;* Unk 1 = Unk. sp. 1 (*Aster*); Unk 2 = Unk. sp. 2 (composite shrub); Unk 3 = Unk. sp. 3 (grass 1); Unk 4 = Unk. sp. 4 (large *Solidago*); Unk 5 = Unk. sp. 5 (lge serrate leaf); Unk 6 = Unk. sp. 6 (small infl); Zi aq = *Zizania aquatica*

An nMDS ordination plot further demonstrates the magnitude of change in community assemblages induced by overwash and sediment deposition (**Figure 12-8**). Although many species in the plot landward of the former dune (Veg Plot 2) persisted, a clear change in relative abundances is apparent. The plot in the dune slack in middle of the island (Veg Plot 3) changed dramatically. Seventy-six percent of the species found in 2009 were no longer present in 2011 after the overwash event and the relative abundances of the remaining species were reduced. Overall, permutational multivariate analysis of variance (PERMANOVA) indicated that the community composition of the plots were significantly different ($P<0.0001$) in 2011 from what they were in 2009. This change was not due to a loss of annual species; of all the species recorded in 2009 only four are annuals (two species, *Lepidium* and *Solanum*, have both annual or perennial forms). Furthermore, dune slack plots in locations that did not experience overwash did not show any patent, large declines in either species numbers or percent cover. Cover by overwash sediment clearly induced the severe changes to plant community structure and

composition at this location. By the time of our sampling in 2011 (6 weeks after Hurricane Irene), two of three burial-tolerant species (sensu Stallins, 2002), *Hydrocotyle* and *Solidago*, had shown signs of some recovery, but *Spartina patens* had not.

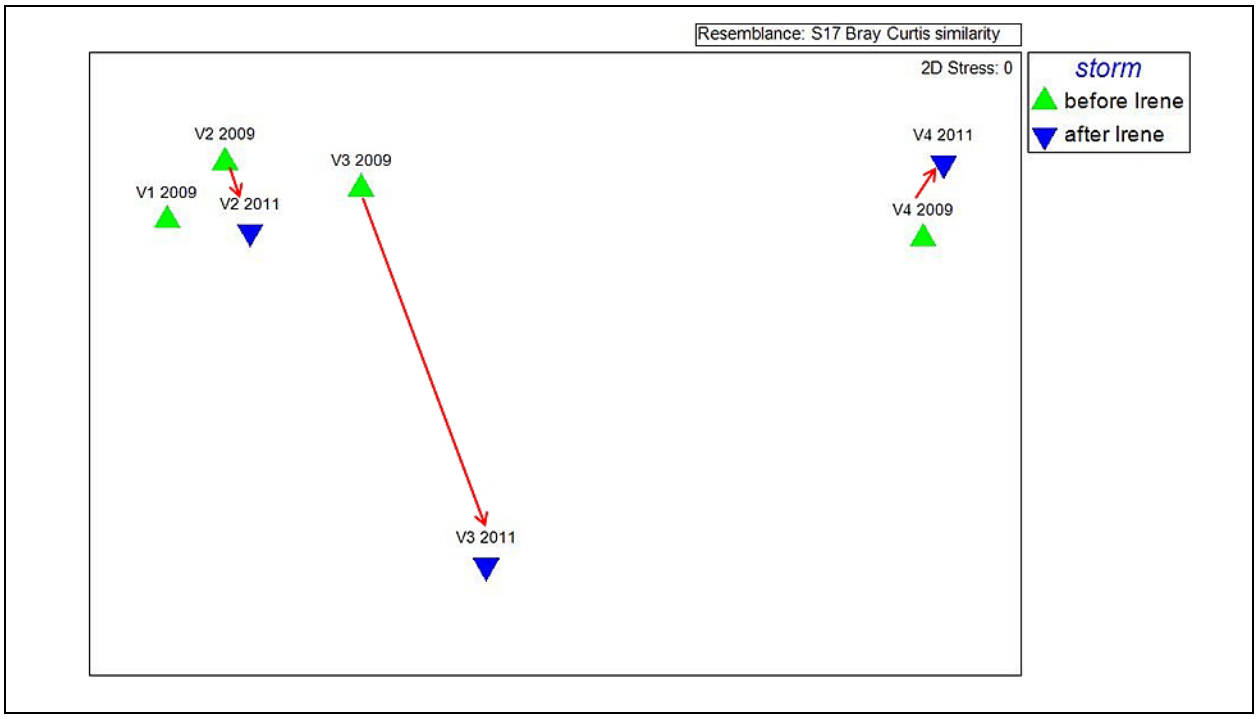

Figure 12-8. An nMDS plot illustrating the effects of hurricane overwash on the patterns of similarities among vegetation plots at the high-impact ORRV area.

Red arrows indicate the direction and amount of change in community composition within plots between 2009 and after Hurricane Irene in 2011. Labels for plots closest to the beach have lower numbers. In 2009, Vegetation Plot 1 (V1) was on the primary dune, which was completely eroded away by the storm in 2011. Vegetation Plot 4 (V4) is in the *Spartina alterniflora* marsh behind the island.

Under rising sea level conditions, the frequency of overwash events is likely to increase and, because storms are predicted to be stronger, the resulting washover fans may increase in size. To document the short-term (several weeks) and long-term (a few years) effects of the island rollover process on vegetation, we established new, long-term plots in several new locations on the southwestern end of the island that will be followed during DCERP2.

Assessment of Trends in the Data

Assessment of Monitoring Design

Inspection of the placement of our long-term plots shows that they encompass all of the habitat types that had been described by previous investigators. Transects of the plots extend through each of the anthropogenic areas defined in the present study. Analysis of the community composition captured by our long term plots demonstrated that we had representative plots in all habitat types that had been identified in studies conducted on Onslow Beach in previous years. In addition, when an event occurred that affected vegetation in some locations and not others (Hurricane Irene), we were able to quantify the extent of vegetation changes both within and

along the island and detect significant changes in composition. We see no reason to suspect that this baseline vegetation information will not be able to detect other natural and anthropogenic changes in the future.

Assessment of Seasonal and Annual Variability in the Data

Except where we documented storm effects, no annual variability was observed during the past 3 years. There were seasonal floristic patterns (e.g., flowering, senescence of annual species), but none that demand management attention at this time.

Recommendations for Future Monitoring

The primary objective for this monitoring activity was to establish permanent plots in which detailed information on floral species composition and cover were recorded. These plots need only be sampled in the future as conditions warrant. Such conditions would include storm-related events, such as overwash and erosion, and changes in existing vehicle, pedestrian, and building practices. Because of the generally slow pace of ecological succession for barrier island communities, a complete survey of these plots needs only be conducted every 5 to 10 years.

Conclusions and Implications for Future Research

Key Scientific Findings—Fundamental Cause-and-Effect Relationships

Over the past decade, no major changes in the extent of the barrier island floral communities has occurred except where washover fans have been produced and where dunes have been eroded. In both the northeastern and southwestern ends of the island, the height of vegetation is severely limiting or completely blocking aeolian sediment transport across the island.

Findings Supportive of Current Base Management Practices

Comparing the patterns of distribution of the barrier island vegetation community types to those recorded in studies conducted within the past two decades indicates very little change except where island transgression is occurring. What changes that are seen in the past two decades are fewer and smaller than those documented by Alexander et al. (1989) occurring during the interval from 1940 to 1980. Current MCBCL management practices of restricting both recreational and military traffic to well-defined corridors has prevented habitat loss to one of the most well-documented threats to barrier island habitats, vehicular traffic.

Findings with Implications for Future Base Management

Recent storms and sea level anomalies have altered the structure of the beach and dunes on the southwestern end of the island, including the area where military training occurs. Should the frequency and intensity of military training increase, encroachment on the near-beach floral communities could increase.

Findings with Implications for DCERP2

Sea level rise will produce further erosion of dunes and create more washover fans. The information we have gathered to date will enable us to quantify this encroachment on existing habitats and follow the rates of primary or secondary succession that occur. A key component of DCERP2 research on this topic will focus on determining how initial variables, such as washover fan sediment depth, which species are buried, and proximity to persisting, emergent vegetation stands affects: (1) short-term (less than 2 years) utilization of the habitat by foraging and nesting birds, (2) the trajectory of ecological succession, and (3) the localized capture of sediment within the island.

Literature Cited

Alexander, R.E., W.J. Cleary, P.E. Hosier, L.A. Williams, J.S. Fisher, M.F. Overton, and J.J. Swain, Jr. 1989. *Onslow Beach Coastal Management Study. Final Report*. University of North Carolina Sea Grant College Program. 107 pages.

Arens, S.M. 1996a. Rates of aeolian transport on a beach in a temperate humid climate. *Geomorphology* 17:3–18.

Arens, S.M. 1996b. Patterns of sand transport on vegetated foredunes. *Geomorphology* 17:339–350.

Au, S. 1974. Vegetation and ecological processes on Shackleford Bank, North Carolina. *National Park Service Scientific Monograph Series 6.*

de Groot, A.V., R.M. Veeneklaas, and J.P. Bakker. 2011. Sand in the salt marsh: Contribution of high-energy conditions to salt-marsh accretion. *Marine Geology 282*:240–254.

Dudley, S.J., C.D. Bonham, S.R. Abt, and J.C. Fischenich. 1998. Comparison of methods for measuring woody riparian vegetation density. *Journal of Arid Environments 38*:77–86.

Ehrenfeld, J.G. 1990. Dynamics and processes of barrier island vegetation. *Reviews in Aquatic Sciences 2*:437–480.

Fraser, J.D., S.E. Keane, and P.A. Buckley. 2005. Prenesting use of intertidal habitats by piping plovers on South Monomoy Island, Massachusetts. *Journal of Wildlife Management 69*:1731–1736.

Haukos, D.A., H.Z. Sun, D.B. Wester, and L.M. Smith. 1998. Sample size, power, and analytical considerations for vertical structure data from profile boards in wetland vegetation. *Wetlands 18*:203–215.

Hesp, P., M. Martinez, G.M. da Silva, N. Rodríguez-Revelo, E. Gutierrez, A. Humanes, D. Laínez, I. Montaño, V. Palacios, A. Quesada, L. Storero, G.G. Trilla, and C. Trochine. 2010. Transgressive dunefield landforms and vegetation associations, Doña Juana, Veracruz, Mexico. *Earth Surface Processes and Landforms 36*:285–295.

Holdredge, C. and M.D. Bertness. 2011. Litter legacy increases the competitive advantage of invasive *Phragmites australis* in New England wetlands. *Biological Invasions* 13:423–433.

Nudds, T.D. 1977. Quantifying the vegetative structure of wildlife cover. *Wildlife Society Bulletin* 5:113–117.

Peet, R.K., T.R. Wentworth, and P.S. White. 1998. A flexible, multipurpose method for recording vegetation composition and structure. *Castanea 63*:262–274.

Ray, K. 2011. *Factors Affecting Wilson's Plover (Charadius wilsonia) Demography and Habitat Use at Onslow Beach, Marine Corps Base Camp Lejeune, North Carolina*. M.S. Thesis. Virginia Polytechnic Institute and State University, Blacksburg, VA.

Stallins, J.A. 2002. Dune plant species diversity and function in two barrier island biogeomorphic systems. *Plant Ecology 165*:183–196.

Versar, Inc. 2003. Onslow Beach Vegetation: GIS Layers and Species List. Unpublished products delivered to U.S. Marine Corps Base Camp Lejeune.

Walker, I.J., P.A. Hesp, R.G. Davidson-Arnott, and J. Ollerhead. 2006. Topographic steering of alongshore airflow over a vegetated foredune: Greenwich Dunes, Prince Edward Island, Canada. *Journal of Coastal Research 22*:1278–1291.

Williams, L.A. 1991. *A Vegetational Study of Onslow Beach, Onslow County, North Carolina*. M.S. Thesis: University of North Carolina at Wilmington, Wilmington, NC. 82 pages.

[This page intentionally left blank.]

Appendix 12-A

List of Scientific Publications

List of Scientific Publications

Paper

Rodriguez, A.B., S.R. Fegley, J.T. Ridge, B.M. VanDusen, and N. Anderson. In press. Contribution of aeolian sand to backbarrier marsh sedimentation. *Estuarine, Coastal and Shelf Science*. doi: http://dx.doi.org/10.1016/j.ecss.2012.12.001.

Thesis

None

Presentation

Rodriguez, A.B., S.R. Fegley, J.T. Ridge, B. VanDusen, and N. Anderson. 2012. *What Is the Aeolian Component of Backbarrier Marsh Sedimentation?* Presented at the Geological Society of America's Annual Meeting, Charlotte, NC. November 4–7. Available at https://gsa.confex.com/gsa/2012AM/webprogrampreliminary/Paper210965.html.

Chapter 13

Monitoring Change in Plant Species Composition, Diversity and Distribution at MCBCL

SERDP Project Number: RC-1413

Terrestrial Module

Lead Researcher:
Dr. Norman L. Christensen
Duke University
Durham, NC 27708
E-mail: normc@duke.edu

Supporting Researcher:
Dr. Stephen R. Mitchell
Duke University
Durham, NC 27708
E-mail: stephen.mitchell@duke.edu

June 27, 2013

Final

This report was prepared under contract to the U.S. Department of Defense (DoD) Strategic Environmental Research and Development Program (SERDP). The publication of this report does not indicate endorsement by DoD, nor should the contents be construed as reflecting the official policy or position of DoD. References herein to any specific commercial product, process, or service by trade name, trademark, manufacturer, or otherwise, do not necessarily constitute or imply its endorsement, recommendation, or favoring by DoD.

Table of Contents

List of Acronyms 13-v
Abstract 13-1
Objectives of the Research Project 13-2
Background 13-3
Materials and Methods 13-5
MCBCL Pine Forest Plant Diversity and Composition 13-5
Soil Sampling 13-7
Statistical Analyses 13-8
Results and Discussion 13-8
Overall Patterns of Terrestrial Plant Species Composition and Diversity on MCBCL 13-8
Patterns of Terrestrial Plant Species Composition and Diversity in Pine-Dominated Ecosystems 13-14
Changes in Species Composition and Diversity in Longleaf Pine Stands from 1991 to 2010 13-21
Conclusions and Implications for Future Research 13-23
Literature Cited 13-25
Appendix 13-A: List of species encountered in 133 permanent MCBCL vegetation monitoring plots 13-A-1
Appendix 13-B: NMS Axes 1 and 2 scores for 133 permanent MCBCL vegetation monitoring plots 13-B-1
Appendix 13-C: Summary of MCBCL monitoring plot site and soil characteristics 13-C-1
Appendix 13-D: Matrix of correlation coefficients for soil variables measured in permanent MCBCL vegetation monitoring plots 13-D-1
Appendix 13-E: NMS Axes 1 and 2 scores for 93 pine-dominated permanent MCBCL vegetation monitoring plots 13-E-1
Appendix 13-F: Correlation coefficients (r) and coefficients of determination (r^2) for plant species with NMS Axes 1 and 2 scores for 85 pine-dominated permanent MCBCL vegetation monitoring plots. 13-F-1
Appendix 13-G: List of Scientific Publications 13-H-1
Appendix 13-H: List of Students 13-I-1

List of Figures

13-1. The distribution of 137 georeferenced 0.1-ha sample plots in terrestrial ecosystems of MCBCL. 13-6

13-2. Diagram of a CVS permanent sample plot. 13-7

13-3. MCBCL terrestrial vegetation monitoring plots arrayed on NMS Axes 1 and 2. 13-9

13-4. NMS ordination of 93 pine-dominated stands at MCBCL (see Appendix 13-E for actual stand scores). 13-15

13-5. Comparison of soil BD and species richness for 93 pine-dominated stands (r 0.49, p<0.0001). 13-17

13-6. NMS ordination of 21 mature longleaf pine stands sampled in both 1991 and 2010, using the CVS sampling protocol. 13-23

List of Tables

13-1. Average basal area, species richness, soil pH, CEC, SOM content, extracP, and BD for monitoring plots representing different MCBCL vegetation cover types 13-11

13-2. Indicator species for each MCBCL vegetation cover type 13-12

13-3. Correlations Between Soil or Stand Vegetation Characteristics and NMS Ordination Axes 13-16

13-4. Correlations between species' abundances and NMS axes for 93 pine-dominated plots 13-18

13-5. Estimated fuel loads (Mg C/ha) in 1- (0–0.6 cm), 10- (0.6–2.5 cm), 100- (2.5–7.6 cm), and 1,000 (greater than 7.6 cm)-hour moisture lag classes 13-21

13-6. Mean species richness among 21 permanent plots sampled in 1991 and 2009 13-21

13-7. Species richness (number of species per 0.1 ha) for each of the 21 mature longleaf pine plots sampled in 1991 and 2010 13-22

List of Acronyms

°C	degrees Celsius
µg/g	micrograms per gram
Al	aluminum
ANOVA	analysis of variance
B	boron
BA	basal area
BD	bulk density
Ca	calcium
CEC	cation exchange capacity
cm	centimeter
Cu	copper
CVS	Carolina Vegetation Survey
dbh	diameter at breast height (1.5 m)
DoD	U.S. Department of Defense
Fe	iron
g/cm^3	gram per cubic centimeter
ha	hectare
ISA	indicator species analysis
K	kotassium
km	kilometer
m	meter
m^2	square meter
m^2/ha	square meter per hectare
MCBCL	Marine Corps Base Camp Lejeune
Mg	magnesium
mg C/ha	milligrams of carbon per hectare
mm	millimeter
Mn	manganese
Na	sodium
NMS	non-metric multidimensional scaling
NOAA	National Oceanic and Atmospheric Administration
P	phosphorus
PCA	principal components analysis
PO_4–P	orthophosphate
r	correlation coefficient

r^2	coefficient of determination (r-squared value)
RCH	species richness
RCW	red cockaded woodpecker
S	sulfur
SD	standard deviation
SERDP	Strategic Environmental Research and Development Program
SOM	soil organic matter
sp.	species (singular)
spp.	species (plural)
Zn	zinc

Abstract

The terrestrial ecosystems of Marine Corps Base Camp Lejeune (MCBCL) have experienced considerable change over the past two centuries. Land use, agriculture, and forest management have greatly altered forest ecosystems. In particular, many areas that were once dominated by open longleaf pine (*Pinus palustris*) savanna now support closed canopy stands of loblolly pine (*Pinus taeda*) with a dense understory and midstory of broadleaved shrubs and trees. The absence of fire on these landscapes has exacerbated this trend. Change continues in these ecosystems. Training activities and associated construction and road development locally alter soils and vegetation, and they have the potential to change drainage patterns and to fragment habitats at larger spatial scales. Over the past two decades, MCBCL managers have applied prescribed fire at approximately 3-year return intervals to restore longleaf pine and certain wetlands habitats and to reduce wildfire risk. In recent years, longleaf pine restoration at MCBCL has focused on the use of understory and midstory thinning (using HydroAx equipment) to produce savanna-like conditions and allow restoration of historical fire regimes using prescribed burning. Terrestrial ecosystems are also being influenced by invasive non-native species, episodic disturbances such as hurricanes, and changes in climate. The primary objective of the Terrestrial Module monitoring activities was the development of a uniform, geographically explicit database for plant species and composition in 133 georeferenced 0.1 ha permanent sample plots to serve as the basis for assessing regional and site -specific changes in plant communities (and associated parameters, such as fuel conditions). Vegetation sampling was performed during the 2009 and 2010 growing seasons and followed protocols established by the Carolina Vegetation Survey (CVS). Among the permanent plots were 21 longleaf pine stands that were also sampled by the CVS in 1991. Initial analysis of this database provides a detailed model of the linkages between plant species composition and diversity, MCBCL environmental gradients, and patterns of diversity. More than 600 individual plant taxa were sampled, with species richness (number of species per 0.1 ha) ranging from eight in pocosin wetlands to 119 in a longleaf pine savanna. Over the entire MCBCL, non-metric multidimensional scaling (NMS) ordination revealed that vegetation composition and diversity vary continuously in response to the gradient of factors such as salt spray from near coastal to inland sites. Among inland sites, vegetation varies in response to soil organic matter, bulk density, cation exchange capacity, and the local conditions that affect drainage (e.g., depression wetlands). Among the 93 pine-dominated permanent plots, NMS Axis 1 scores were high correlated with a variety of soil factors, most especially bulk density and organic matter. Axis 2 was correlated with indicators of disturbance such as the density of small (less than 20 cm diameter at breast height) stems and abundance of ruderal species. Species richness in pine-dominated stands was highly and positively correlated with soil bulk density, and negatively correlated with disturbance indicators (NMS Axis 2). Variations in surface fuels were correlated with the history of fire management in different pine stands. Specifically, fine fuels were considerably less abundant in longleaf pine stands receiving regular prescribed burns compared to long-unburned longleaf, loblolly, or pocosin pine stands. During the period from 1991 to 2009, species richness increased in 19 of the 21 longleaf pine stands previously sampled by the CVS. Based on NMS analyses, compositional change in these plots was consistent with the restoration goals of MCBCL management. These analyses provide MCBCL natural resources managers with a focused set of species and site indicators to facilitate future monitoring by MCBCL that is efficient and relevant to assessing important changes in terrestrial ecosystem health.

Keywords: Forest management practices, fuels, indicator species, loblolly pine, longleaf pine, ordination, plant species composition and richness, pocosin, prescribed burning, red cockaded woodpecker, soils.

Objectives of the Research Project

The overall goal of the Terrestrial Module monitoring activity was to provide a uniform, geographically explicit database for plant species composition and abundance to serve as the basis for assessing regional and site-specific changes in plant communities (and associated parameters, such as fuel conditions). In addition, this activity is designed to provide Marine Corps Base Camp Lejeune (MCBCL) natural resources managers with a focused set of species and site indicators to facilitate future monitoring by MCBCL that is efficient and relevant to assessing important changes in terrestrial ecosystem health. Specific objectives include the following:

1. Establish permanent, georeferenced 0.1-ha sample plots at 133 locations representative of the diversity of terrestrial ecosystems across MCBCL. Sample plots will include 21 plots in mature longleaf pine stands previously sampled by the Carolina Vegetation Survey (CVS) in 1991.
2. Sample each permanent plot for plant species composition and diversity using protocols established by the CVS (Peet et al., 1998).
3. Estimate forest canopy cover in each plot using fisheye lens canopy photographs.
4. Sample and analyze soils from each of the permanent plots for a range of soil factors, including bulk density, organic matter content, cation exchange capacity, pH, and concentrations of a variety of nutrients.
5. Evaluate amounts of surface fuels in each plot using fuel load estimation protocols for the National Fire Danger Rating System model (Andrews and Bradshaw, 1997).
6. Analyze data using ordinations and correlation analysis to provide a detailed model of the linkages among species composition and diversity, soil characteristics, fuels, and past disturbance across MCBCL.
7. Compare changes in species composition in plots sampled in 1991 with data gathered in 2009 as a demonstration of the utility of repeated sampling of permanent plots.
8. Identify key species indicators of environmental and disturbance gradients using indicator species analysis and correlation analysis.

Because plant species are high-fidelity indicators of variation in the physical environmental template (e.g., soils, hydrology, site fertility) and the effects of human activities that may affect that template, a network of permanent vegetation plots provides a useful barometer of habitat condition. Furthermore, data on species composition are critical to the assessment of potential changes in the abundance of species of interest, including threatened and endangered species and invasive, non-native species. Spatial and temporal variations in species composition and diversity not only provide important indices of ecosystem health, but they are also often diagnostic of specific environmental effects, such as soil compaction or altered fire regimes. Therefore, monitoring of plant communities is essential to understanding possible local- and

landscape-level changes in habitat for species, such as the red cockaded woodpecker. The foundation data set provided here for such a monitoring program involved more exhaustive sampling and included more variables (e.g., species and site measurements) than can practically be used in an operational monitoring program. Therefore, an important objective of our effort was to identify indicator species and relatively easily measured site conditions to focus future monitoring by MCBCL staff.

Background

The terrestrial vegetation of North Carolina's lower coastal plain is known for its diversity across a wide range of spatial scales. Marine Corps Base Camp Lejeune (MCBCL) lands capture much of that variation. At the landscape scale, geomorphic variations such as relict dune and estuarine deposits and subtle changes (±1 m) in elevation of the soil surface relative to the shallow water table produce remarkable variations in ecosystem structure, composition and processes. Within a few kilometers of the coast, vegetation composition is heavily influenced by salt aerosol and maritime climatic gradients. In pre-settlement times, inland vegetation varied along a continuum from shrub bog (pocosin) wetlands on deep peat soils to pine-dominated flatwoods with an understory of shrubs on poorly drained mineral soils and longleaf pine savannas on well-drained sands (Christensen, 2000). There was nearly complete turnover of plant species composition from one end of this gradient to the other. Some of these ecosystems display remarkable species richness and high levels of species endemism at very local scales. For example, longleaf pine savannas may support more than 60 vascular plant species per square meter and more than 120 species per hectare (Walker and Peet, 1983).

Ecosystem composition and structure was also heavily influenced by variations in pre-settlement fire regimes along this gradient. Pocosins typically experience intense, crown-killing fires at return intervals of more than 40 years, whereas longleaf pine savannas are maintained by light surface fires at intervals of 1–5 years (Christensen 1981, 1992, and 2000; Bailey et al., 2007). The relative amount and distribution of pocosin, flatwood, and savanna ecosystems on pre-settlement landscapes was heavily influenced by the frequency and behavior of fire. Repeated, low severity fires can maintain savanna on very moist soils with relatively high amounts of organic matter. Indeed, it is just these situations that support the highest plant species richness at small (square meter) spatial scales. It is also these sites that support a number of unique endemic species, including several insectivorous plant species. On all but very well-drained sites, the absence of fire for periods longer than 5–6 years results in the invasion of shrubs and a variety of understory trees. This invasion also changes the amounts and distribution of fuels such that subsequent fires are likely to be severe enough to kill and even consume canopy trees.

Post-settlement land use and disturbance have influenced the mosaic of terrestrial ecosystems on lower coastal plain landscapes such as on MCBCL. Except for the wettest and driest sites, forests on much of this landscape were cleared for agriculture during the eighteenth and nineteenth centuries (Crowley, 1996). Longleaf pine savannas that were not cut were heavily managed for naval stores (Early, 2004). Much of this farmland was abandoned in the years following the Civil War and Reconstruction up to World War II; post abandonment succession generally produced an even-aged overstory of loblolly pine with an understory dominated by shrubs and understory trees on all but the driest sites (Christensen, 2000). Fire was not only excluded from these forests, but the successional changes promoted understory vegetation and fuels that are

comparatively difficult to burn (Nowacki and Abrams, 2008). In the period of 1940–1960, large tracts of such land were acquired by timber companies who managed them to maintain loblolly pine dominance.

Across the Southeast, this history of land use led to the transformation of more than 95% of the land once dominated by longleaf pine savanna to loblolly pine dominated flatwoods. Even where longleaf pine remained, fire suppression often led to the invasion of woody understory plants and the loss of endemic plant and animal species. In many places longleaf pine ecosystems are represented by relatively small and often isolated stands.

Altered fire regimes and habitat loss and fragmentation have contributed to the significant number of plant and animal species found in communities dominated by longleaf pine that are currently listed as threatened or endangered under the Endangered Species Act. The red cockaded woodpecker (RCW) is probably most notable among these listed species. These listings, along with general concerns about the loss of longleaf pine habitat, have been the impetus for restoration of loblolly pine flatwoods to longleaf pine savannas. Indeed, maintenance and restoration of longleaf pine habitat and, hopefully, associated populations of RCWs have been prominent objectives of forest management over much of the MCBCL landscape.

Over the past several decades, MCBCL natural resources managers have undertaken steps to maintain natural ecosystems such as depression wetlands, mature hardwoods and longleaf pine savannas wherever they exist on MCBCL. Such steps have, where appropriate, included the use of prescribed fire. Fire prescriptions in longleaf pine savannas most commonly involve low intensity surface fires ignited during the dormant season (winter and early spring) at 3-year intervals. This time interval is partly a matter of management constraints (i.e., insufficient resources and personnel to burn more frequently) and research indicating that this return time is appropriate for conservation of plant diversity (Walker and Peet, 1983) and maintenance of RCW populations (Hutto et al., 2008).

Much of MCBCL once dominated by longleaf pine savannas is today occupied by closed stands of loblolly pine with dense hardwood understories. Managers have undertaken a number of steps to restore these ecosystems. In some parts of MCBCL, restoration has taken the form of clear-cutting, followed by planting of longleaf pine and eventual re-establishment of an appropriate prescribed fire program. Restoration of mature longleaf pine habitat by this approach will, of course, require many decades. As an alternative strategy to accelerate habitat restoration, MCBCL staff have implemented mechanical thinning treatments (using HydroAx equipment) to remove understory and midstory hardwoods (generally stems less than 20 cm diameter at breast height [dbh]) and open savanna-like stand structures and understory composition and fuels that are more typical of longleaf pine ecosystems. Such management is currently being applied to hundreds of MCBCL acres each year. Variations on this management theme include different seasons (growing and dormant) of mechanical control of the woody understory. Restoration of low-severity, high-frequency fire regimes is a key objective. Therefore, all thinned areas receive a late winter or early spring prescribed fire in the year following treatment.

Anthropogenic disturbance regimes are superimposed on natural regimes that occur across the MCBCL (Demarais et al., 1999). The urbanized area and military training areas are a mix of heavily disturbed areas with little natural vegetation. Terrestrial training ranges in particular tend

to be cleared areas whose vegetative cover differs significantly from the historical. The military mission also depends on the conservation of natural ecosystems and their key ecological processes. Such ecosystems often are important for training in their own right because they provide training realism. The ecosystems also provide resilience at landscape scales and critical ecosystem services to the military and its ability to sustainably use these landscapes (Demarais et al., 1999).

In addition to the effects of prescribed burning and restoration management, MCBCL terrestrial ecosystems are also changing as a consequence of external drivers such as episodic storm events, invasive non-native species, and climate change. Forest management, including prescribed burning and restoration treatments, will have to account for the underlying shifts in ecosystem processes and biodiversity that will as a consequence of these global phenomena. To detect such changes, a system of regularly sampled monitoring plots is essential.

The goal of the Terrestrial Module monitoring activity was to provide a uniform, geographically explicit database for plant species composition and abundance that will serve as the basis for assessing regional and site-specific changes in plant communities (and associated parameters, such as fuel conditions). This activity is also intended to provide MCBCL natural resources managers with a focused set of species and site indicators to facilitate future monitoring by MCBCL that is efficient and relevant to assessing important changes in terrestrial ecosystem health. Because plant species, individually and in groups (e.g., communities, guilds) are high-fidelity indicators of variation in the physical environmental template (e.g., soils, hydrology, site fertility) and the effects of human activities that may affect that template (for a discussion about these relationships, see Christensen, 2000), a network of permanent vegetation plots provides a useful barometer of habitat condition. Furthermore, data on species composition are critical to the assessment of potential changes in the abundance of species of interest, including threatened and endangered species and invasive, non-native species. Spatial and temporal variations in species composition and diversity not only provide important indices of ecosystem health, but they are also often diagnostic of specific environmental effects, such as soil compaction or altered fire regimes. Finally, as the ecosystems' primary producers, the community of plants in any location is the ultimate source of carbon energy and defines the structure of habitat for a diverse array of consuming and decomposing organisms. Therefore, monitoring of plant communities is key to understanding possible local- and landscape-level changes in habitat for species, such as the RCW. The foundation data set for such a monitoring program will involve more exhaustive sampling and will include more variables (e.g., species, site measurements) than can practically be used in an operational monitoring program. Therefore, an important objective of this effort will be to identify a set of indicator species and relatively easily measured site conditions and develop sampling and analytical protocols that will provide a practical and efficient monitoring tool that can be used by MCBCL staff.

Materials and Methods

MCBCL Pine Forest Plant Diversity and Composition

A total of 133 permanent vegetation monitoring plots were established in terrestrial ecosystems across MCBCL (**Figure 13-1**). Site location and field sampling were initiated in early 2009 and continued through the growing seasons of 2009 and 2010. Each site was located, permanently marked with heavy steel posts, and subsequently sampled for fuel load, woody and herbaceous

vegetation and soil characteristics. The Carolina Vegetation Survey (CVS) protocol (Peet et al., 1998) was used at all sites. Individual plots were located within the sample stands to avoid obvious vegetation transitions and represent relatively uniform environmental conditions. Within a 20-m × 50-m (0.1-ha) plot, all living and dead stems (greater than 1-cm dbh) were tallied by species and dbh. For the herbaceous layer, the plot was further subdivided into ten 10-m × 10-m plots. Four of these plots were termed as "intensive," and the other six plots were referred to as "residual." Each intensive plot was sampled for herbaceous species (recorded as percent cover) with five nested plots that increased in sizes of 0.01 m^2, 0.09 m^2, 1.0 m^2, 9.0 m^2, and 100.0 m^2 in two corners of the intensive plot (see **Figure 13-2**). After intensive plots were sampled, the residual plots were surveyed to identify all species not found in any of the four intensive plots. We measured species diversity in terms of richness, the total number of species present in a sample. Species composition refers to identities and relative abundances of the community of species.

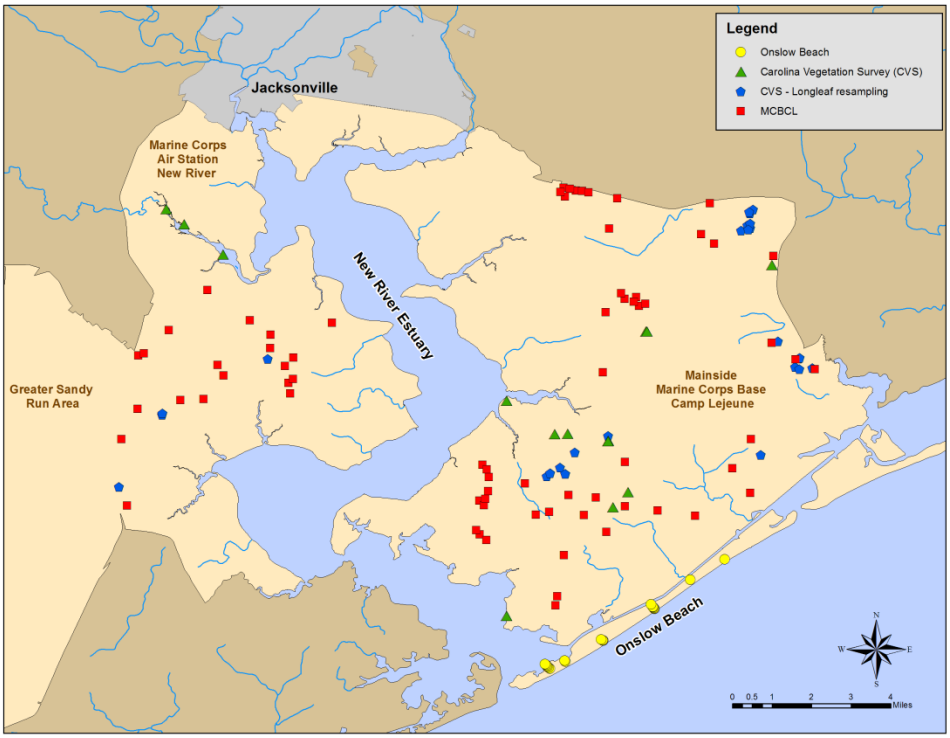

Figure 13-1. The distribution of 133 georeferenced 0.1-ha sample plots in terrestrial ecosystems of MCBCL.

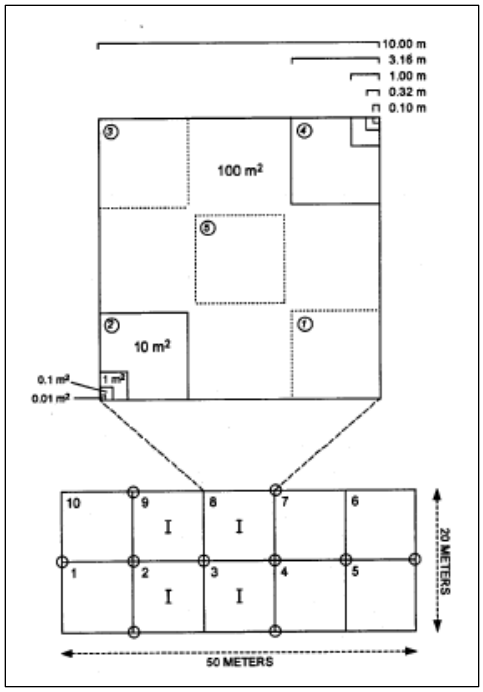

Figure 13-2. Diagram of a CVS permanent sample plot.

Intensive plots (Cells 2, 3, 8, and 9) are indicated by an "I."

In 89 of the pine-dominated plots (e.g., plots subject to prescribed burning), fuels such as logs and woody debris were assessed by size class using line intercept transects across the plot (Harmon and Sexton, 1996). Finally, fuel condition was assessed in each plot using standard U.S. Department of Agriculture Forest Service protocols for fuel load estimation for the National Fire Danger Rating System model (Andrews and Bradshaw, 1997).

In 80 permanent sample plots pine-dominated forests, forest canopy cover was assessed by analyzing hemispherical canopy photos at each site. Five photos were taken at 10-m intervals along the centerline of each 0.1-ha plot using a Nikon 8-mm fisheye lens and Nikon D-50 digital camera. Photos were analyzed for percent canopy cover using MATLAB's Image Processing Toolbox (Korhonen and Heikkinen, 2008). Canopy photos were not taken at the Onslow Beach site.

Soil Sampling

Soil samples were collected from each permanent plot, with the exception of the Onslow Beach sites. Using a 5-cm in diameter piston corer, a uniform sample of the top 0–10 cm of mineral soil (soil beneath layers of litter and duff) was collected at each of four points located 10 m from the center point of each experimental plot. Each soil sample was subsequently analyzed by Brookside Laboratories (New Knoxville, OH). Soil pH is measured using a glass electrode in a 1:1 slurry of soil and distilled water (McLean, 1982). Percent soil organic matter (SOM) was determined by weight loss after ignition at 360°C. Aluminum (Al), boron (B), calcium (Ca), copper (Cu), iron (Fe), phosphorus (P), potassium (K), magnesium (Mg), manganese (Mn), sodium (Na), sulfur (S), and zinc (Zn) were extracted according to Mehlich (1984). P concentrations in the Mehlich extractant were measured colorimetrically; concentrations of other

elements were determined by plasma emission spectroscopy. Cation exchange capacity (CEC) was measured by summation of all cations as milliequivalents 100 grams of soil (Ross, 1995). Several of these soil features have been shown to have a high correlation with the distribution of many coastal plain plant species (Christensen, 2000; Christensen et al., 1988; Peet, 2006; Walker and Peet, 1983). These analyses were considerably more detailed than originally proposed to provide a more complete set of baseline data and to permit direct comparison with other CVS samples on MCBCL and surrounding lands.

Statistical Analyses

Data for monitoring and experimental plots were analyzed using standard statistical tools for product-moment correlation and analysis of variance (ANOVA) provided in the data analysis and graphics system R (Venables and Smith, 2011). Non-metric multidimensional scaling (NMS) ordination (Kruskal and Wish, 1978) was used to analyze trends in species composition in monitoring and experimental plots. Each NMS axis represents a component of variation in the multivariate data set that is similar to a principal components analysis (PCA). However, NMS ordination is much better suited for use with non-normal species composition data than PCA. Plots with similar scores for a particular NMS axis are more similar to one another with respect to the trends in species composition represented by that axis than stands with less similar scores. Our NMS analyses used the Sørenson dissimilarity metric for 1,000 iterations to derive two-dimensional ordination axes, which represent the main axes of compositional variation. We ran PC-ORD software with random starting configurations for 100 runs with real data with a maximum of 1,000 iterations per run and a stability criterion of 0.00001. Indicator species analysis (ISA, Dufrêne and Legendre, 1997), and correlation and regression tree analyses (McCune and Grace, 2002) were used to identify those species and site measures that are most highly correlated to variations in species composition represented in the NMS ordination (McCune and Grace, 2002).

Results and Discussion

Overall Patterns of Terrestrial Plant Species Composition and Diversity on MCBCL

More than 600 individual plant taxa were encountered among the 133 plots with an average species richness of 41.6 species per 0.1 ha. A complete list of plant taxa is provided in **Appendix 13-A** (Nomenclature follows Weakley 2011). The range of species richness among plots was large, with as few as nine species per 0.1 ha in a pocosin stand, to as many as 119 species per 0.1 ha in a longleaf pine stand.

Ordination data from all 133 sample plots reveals general trends in understory species composition across MCBCL (**Figure 13-3**). NMS scores for each sample plot are listed in **Appendix 13-B**. The ordination of Axis 1 is clearly related to the gradient from near coastal to inland sites. Plots located on the Onslow Island dunes have the highest Axis 1 scores, followed by back dunes and maritime scrub forest. All inland plots have NMS Axis 1 scores of 1 or less. NMS Axis 2 corresponds to the gradient from well-drained longleaf pine stands (low axis scores) to hardwoods and depression wetlands (high Axis 2 scores).

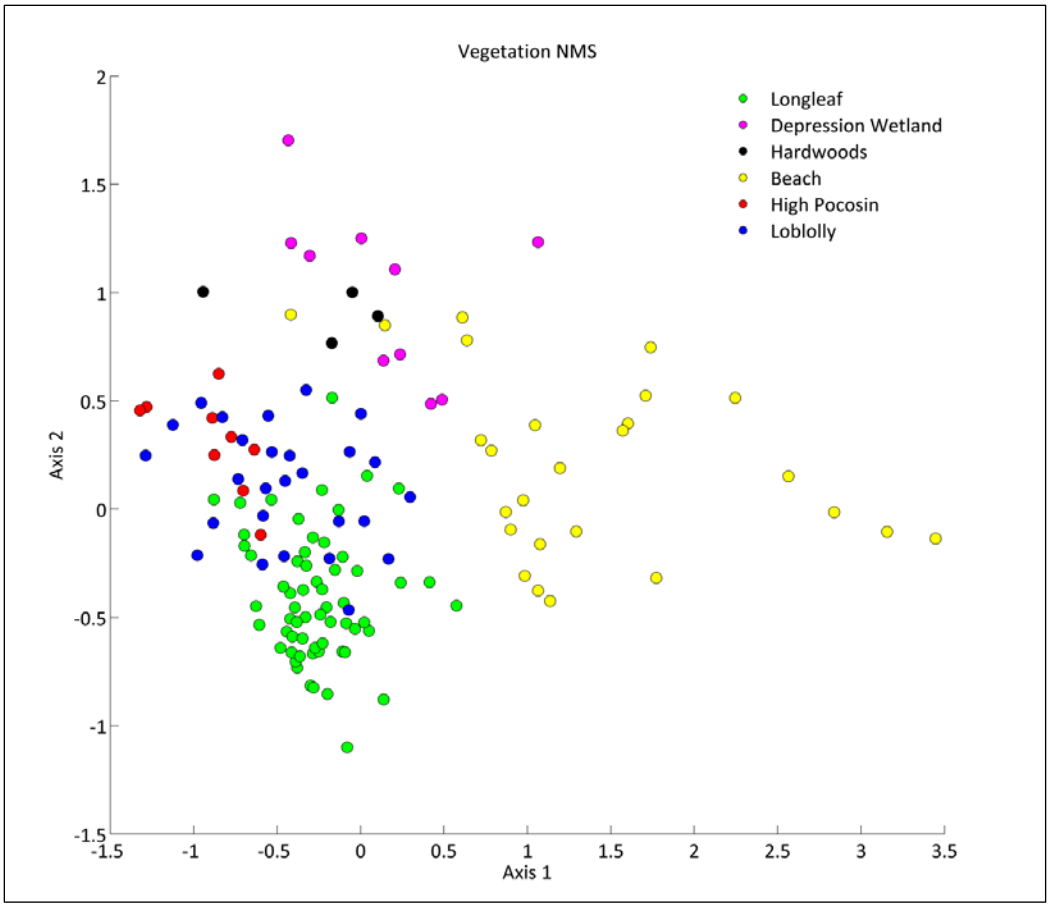

Figure 13-3. MCBCL terrestrial vegetation monitoring plots arrayed on NMS Axes 1 and 2.

Distances among points reflect relative differences in plant species composition.

The distribution of monitoring plots among different vegetation cover types is shown in **Table 13-1**, along with data for stand basal area, species richness and important soil characteristics. Because of their aerial extent and their conservation importance, longleaf pine forests are especially well represented in this data set (note the high plant species richness in these stands, particularly compared to pocosins).

For each permanent plot (except those on Onslow Beach) average values (± standard deviation [SD]) for each of the soil variables are listed in **Appendix 13-C**, and the correlation matrix for all soil variables is displayed as **Appendix 13-D**. Soil bulk density (BD), for example, was highly correlated with SOM ($r=0.87$, $p<0.00001$) and CEC ($r=0.64$, $p<0.00001$). Soil BD is thus a relatively good proxy for a variety of soil characteristics, and it can be easily measured.

Within the depression wetlands, hardwood, and longleaf pine cover types, stands with the highest pH (greater than 5.0) had the highest NMS Axis 2 scores. Soils in these stands also had the highest CECs and extractable phosphorus concentrations. These high pH sites occur on soils weathered from calcareous parent rocks, whereas soils at most other sites are weathered from unconsolidated coastal plain sediments or organic peats.

ISA identified species that are particularly abundant and concentrated in each vegetation cover type (**Table 13-2**). The high number of indicator species in the longleaf, depression wetlands, coastal dune and hardwood cover types is a reflection of the unique features of their respective environments and the relative absence of disturbance. Although pocosins have few indicator species, the number is high relative to their generally low species richness. The fact that only a single species, black gum (*Nyssa sylvatica*), had a significant indicator value for loblolly pine stands is probably reflective of the history of disturbance in these forests and the wide range of conditions over which they occur.

Table 13-1. Average basal area (BA), species richness (RCH), soil pH, cation exchange capacity (CEC), soil organic matter (SOM) content, extractable phosphorus (P), and bulk density (BD) for monitoring plots representing different MCBCL vegetation cover types

Description	N	BA (m^2/ha)	RCH (#/0.1 ha)	pH	CEC (milliequivalents/ 100 g)	Organic Matter %	P (µg/g)	BD (g/cm^3)
Longleaf pine mature	56	27.7 (7–110.9)	57.9 (22–119)	4.25 (3.89–5.68)	4.1 (1.6–10.1)	3.6 (1.2–12.7)	10.2 (3.2–185.7)	1.19 (0.63–1.45)
Loblolly pine	23	12.3 (1.0–39.7)	33.4 (16–55)	4.24 (3.85–4.83)	6.2 (2.8–14.4)	10.5 (1.6–31.6)	7.0 (2.7–14.2)	0.87 (0.42–1.18)
Pocosin	13	17.5 (7.6–26.3)	17.6 (9–35)	3.85 (3.63–3.98)	8.6 (5.2–11.3)	48.6 (11.3–85.5)	5.9 (3.2–13.0)	0.43 (0.18–0.70)
Hardwood	4	4.7 (1.4–10.0)	35.5 (23–66)	5.35 (4.45–6.85)	67.1 (8.5–143.9)	29.8 (3.0–58.4)	76.8 (4.6–246)	0.80 (0.38–1.25)
Depression wetlands	10	1.23 (0–10.1)	28.8 (16–42)	4.28 (3.5–5.41)	15.5 (4.9–76.5)	27.0 (19.3–80.2)	11.8 (0.5–66)	0.72 (0.22–1.20)
Barrier island	26	N/A	84	N/A	N/A	N/A	N/A	N/A

Ranges for each value are shown in parentheses. Soils were not sampled or analyzed for barrier island sites.

Table 13-2. Indicator species for each MCBCL vegetation cover type

Cover Type	Species	Indicator Value	p Value
Longleaf pine	*Carphephorus bellidifolius*	32.3	0.013
	Carphephorus odoratissimus	49.1	0.0016
	Dicanthelium angustifolium	17.3	0.0382
	Dichanthelium portoricense ssp. patulum	21.2	0.0378
	Euphorbia ipecacuanhae	19.2	0.039
	Ionactix linariifolia	40.4	0.0044
	Iris verna	43.7	0.0038
	Lespedeza virginica	15.4	0.046
	Morella pumila	32.7	0.0108
	Pityopsus graminifolia	30.7	0.0276
	Quercus incana	30.8	0.0192
	Quercus laevis	46.3	0.0068
	Sericocarpus tortifolius	34.2	0.0108
	Solidago odora var. odora	21.2	0.049
	Stylosanthes biflora	21.2	0.0338
	Symphyotrichum walteri	26.9	0.025
	Tephrosia hispidula	23.1	0.0326
	Toxicodendron pubescens	25	0.0276
	Tragia urens	32.7	0.012
	Vaccinium stamineum	25	0.0278
Depression wetlands	*Andropogon glaucopsis*	31.5	0.0396
	Aristida virgata	19.7	0.0472
	Centella erecta	28.7	0.0092
	Dicanthelium	50.8	0.0124
	Drosera capillaris	30	0.002
	Drosera intermedia	30	0.002
	Eriocaulon sp.	60	0.0002
	Eupatorium sp.	35.1	0.0062
	Eupatorium capillifolium	61.7	0.0018
	Eupatorium mohrii	19.5	0.0436
	Euthamia caroliniana	34.4	0.0114
	Ilex myrtifolia	40	0.003
	Juncus sp.	55	0.001
	Lachnanthes caroliniana	60	0.0002
	Ludwigia sp.	40	0.0018
	Nymphaea odorata	40	0.0016
	Nymphoides aquatica	30	0.0014
	Nyssa biflora	60	0.0004
	Panicum longleaf.	80	0.0002
	Panicum haematomum	40	0.003
	Pluchea baccharis	69.1	0.0004
	Polygala cymosa	40	0.0048

(continued)

Table 13-2. Indicator species for each MCBCL vegetation cover type (continued)

Cover Type	Species	Indicator Value	p Value
Depression wetlands (continued)	*Rhexia aristosa*	40	0.0026
	Rhynchospora	58.2	0.002
	Scleria	60	0.0002
	Xyris caroliniana	60	0.0004
Coastal dunes	*AmpeloP. serotinais arborea*	25.6	0.0194
	Cakile harperi	34.6	0.0074
	Distichlis spicata	30.8	0.0076
	Euphorbia polygonifolia	30.8	0.011
	Fimbristylis spadicea	19.2	0.0434
	Hydrocotyle bonariensis	72	0.0002
	Ilex vomitorium	30.8	0.0068
	Iva imbricata	50	0.0018
	Juniperus virginia	19.2	0.0492
	Oenothera humifusa	46.2	0.0006
	Opuntia compressa	19.2	0.0362
	Rubus trivialis	19.2	0.0128
	Solidago sempervirens	25.3	0.0302
Pocosin	*Cyrilla racemiflora*	24.6	0.028
	Gordonia lasianthus	51	0.0028
	Magnolia virginiana	45	0.0098
	Rhynchospora plumosa	27	0.0224
	Zenobia pulverulenta	23.1	0.0032
	Smilax laurifolia	46.6	0.0218
Loblolly	*Nyssa sylvatica*	43.4	0.0062
Hardwoods	*Aesculus pavia*	44.4	0.0008
	Baccharis halimifolia	41.9	0.0092
	Calicarpa americana	49	0.0004
	Carex sp.	23.8	0.012
	Cirsium	24.3	0.014
	Galium hispidulum	45.5	0.0008
	Ilex opaca	39.8	0.022
	Juniperus virginia var solicicola	75	0.0002
	Kosteletzkya virginica	29.2	0.0014
	Liriodendron tulipifera	21.6	0.0328
	Marshallia graminifolia	21.7	0.0286
	Parthenocisus quinquefolia	35.2	0.0072
	Quercus falcata	23.8	0.0368
	Rubus sp.	21.5	0.0408
	Smilax rotundifolia	71.9	0.0002
	Symphyotrichum	21	0.0278
	Symplocos tinctoria	24.6	0.0172
	Toxicodendron radicans	74.6	0.0002

The indicator value is a measure of the strength of the species association. The p value indicates the likelihood that the association is random.

Patterns of Terrestrial Plant Species Composition and Diversity in Pine-Dominated Ecosystems

The vast majority of the forested MCBCL landscape supports ecosystems dominated by longleaf, loblolly, or pond pine. It is presumed that longleaf pine stands were far more common in pre-settlement times, and that the current dominance of loblolly pine is a consequence of combined effects of land abandonment from agriculture, silvicultural practices, and the suppression of fire. Pond pine is generally most common on organic soils, but there too disturbance and silviculture have favored increased prevalence of loblolly pine. Because they represent such a large proportion of the landscape and are the central targets of management to maintain and/or restore key biodiversity elements, pine-dominated stands are particularly well-represented in our monitoring data set (93 out of 133 plots), and they are analyzed separately here.

Among the pine-dominated plots, 357 plant taxa were encountered. Plot scores for NMS Axes 1 and 2 are plotted in **Figure 13-4**. A correlation matrix comparing NMS stand scores with key vegetation and soil variables is presented in **Table 13-3**. NMS Axis 1 corresponds to the gradient from longleaf pine stands on well-drained sands to pocosins on wet peat soils. As expected, Axis 1 is very strongly correlated with SOM (r=0.727) and negatively correlated with soil BD (r=−0.761). NMS Axis 2 corresponds to a gradient mature longleaf pine stands with negative scores to loblolly pine and immature (less than 20 years old) and disturbed longleaf stands with NMS Axis 2 scores greater than 0.5. NMS Axis 2 scores are negatively correlated with species richness (r=−0.444) and stand basal area (r=−0.367); they are positively correlated with the density of stems less than 20 cm (r=0.444), SOM (r=0.348) and CEC (r=0.416). The higher amounts of SOM in the loblolly and disturbed longleaf stands are largely a consequence of the absence of fire over significant periods of time.

Percent canopy cover was significantly positively correlated with both NMS Axes 1 and 2 (r=0.40 and r=0.43, respectively). This reflects the open, savanna-like conditions characteristic of mature longleaf stands and increased canopy cover associated with moister plots (Axis 1) and greater cover of shrubs and midstory plants in disturbed plots (Axis 2).

Correlations between species richness and other factors are noteworthy. Species richness is negatively correlated with the density of small stems (r=−0.361) and positively correlated with basal area (r=0.483), and density of large stems (r=0.293). The correlation between species richness and soil BD (r=0.489) is also notable (**Figure 13-5**). There is, however, considerable variation in species richness for stands with soil BD greater than 1. These differences appear to be related to stand maturity. Basal area averages 31.6 m^2/ha for stands with species richness ≥50/0.1 ha and BD ≥1, but only 19.4 m^2/ha for stands with species richness less than 50 and BD less than 1.

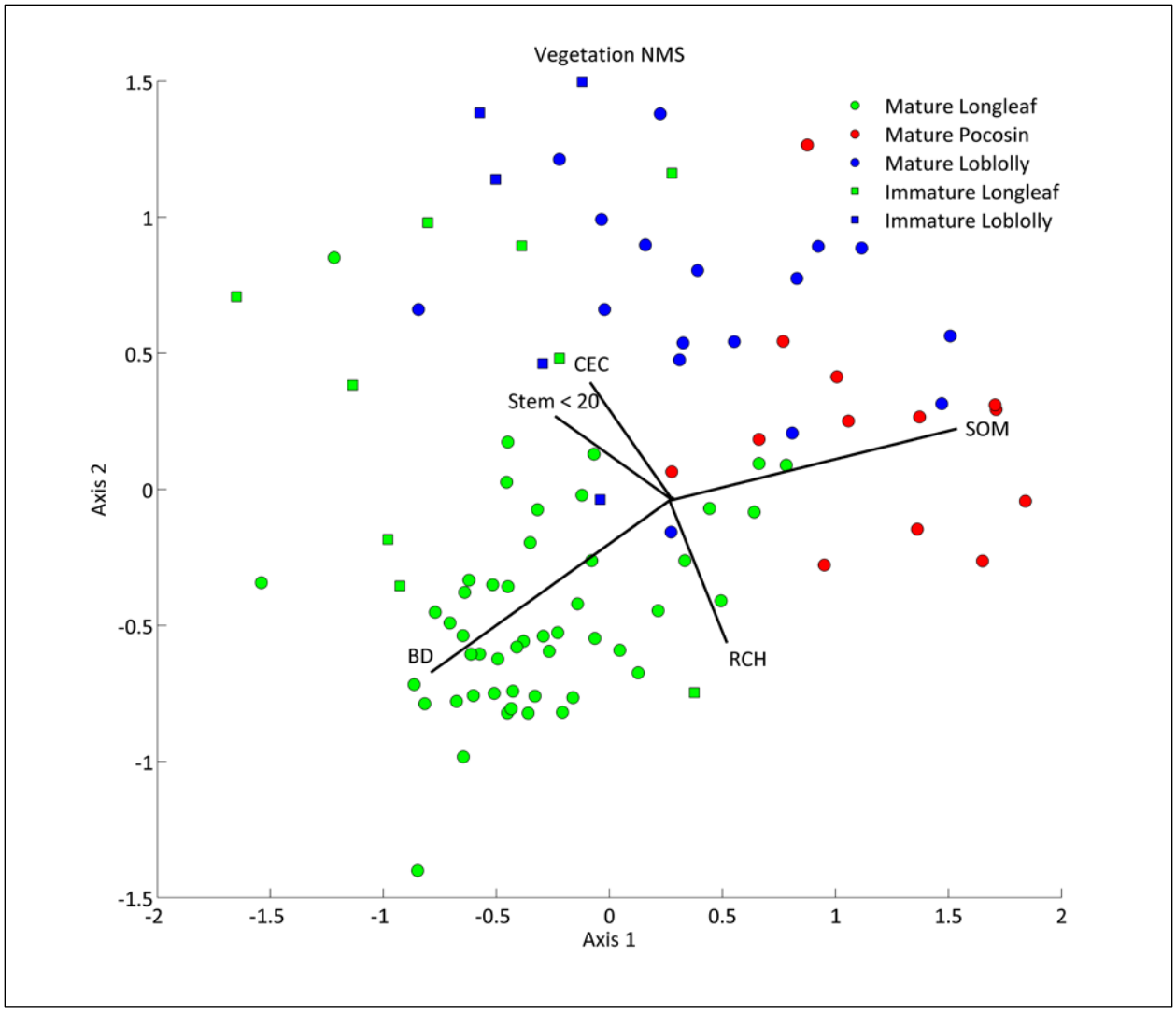

Figure 13-4. NMS ordination of 93 pine-dominated stands at MCBCL (see Appendix 13-E for actual stand scores).

The distance between individual plots in ordination space is a measure of dissimilarity in species composition. The black line vectors relate to the relationships between specific soil or stand characteristics and NMS axes. The vector length reflects the strength of the correlation (see **Table 13-3**) and vector direction indicates the trajectory in which the characteristic increases in the ordination space.

Table 13-3. Correlations Between Soil or Stand Vegetation Characteristics and NMS Ordination Axes

	RCH	Stem <20	Stem >20	BA	BD	pH	CEC	SOM	P	NMS Axis 1	NMS Axis 2
RCH	1	−0.3612	0.2938	0.4836	0.4891	−0.1321	−0.2137	−0.4398	−0.1005	−0.2949	−0.4443
Stem <20	−0.3612	1	−0.1339	−0.0833	−0.3779	−0.1377	0.2325	0.2855	−0.0210	0.3393	0.4442
Stem >20	0.2938	−0.13395	1	0.4272	0.1450	−0.2009	−0.0107	−0.0072	−0.0359	−0.0360	−0.3113
BA	0.4836	−0.08334	0.4272	1	0.2037	−0.2942	−0.0484	−0.0689	−0.0585	−0.0926	−0.3674
BD	0.4891	−0.3779	0.1450	0.2037	1	0.3663	−0.6460	−0.8745	0.0775	−0.7616	−0.5294
pH	−0.1321	−0.1377	−0.2009	−0.2942	0.3663	1	−0.4228	−0.4427	0.4768	−0.4417	−0.1196
CEC	−0.2137	0.2325	−0.0107	−0.0484	−0.6460	−0.4228	1	0.5506	−0.0364	0.4253	0.4164
SOM	−0.4398	0.2855	−0.0072	−0.0689	−0.8745	−0.4427	0.5506	1	−0.0648	0.7273	0.3481
P	−0.1005	−0.0210	−0.0359	−0.0588	0.0775	0.4768	−0.0364	−0.0648	1	−0.1945	−0.0069
NMS Axis 1	−0.2949	0.3393	−0.0360	−0.0926	−0.7616	−0.4417	0.4253	0.7273	−0.1945	1	0.2699
NMS Axis 2	−0.4443	0.4442	−0.3113	−0.3674	−0.5294	−0.1196	0.4164	0.3481	−0.0069	0.2699	1

Yellow indicates $p<0.05$, green indicates $p<0.01$, blue indicates $p<0.001$, and red indicates $p<0.0001$.

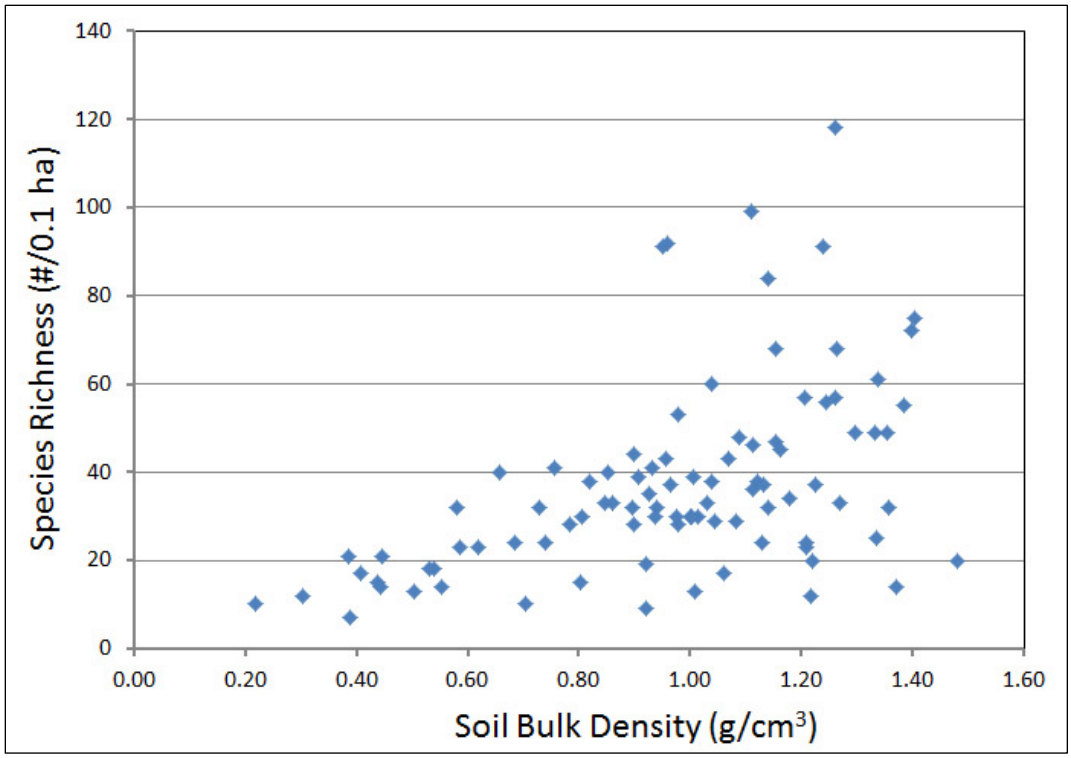

Figure 13-5. Comparison of soil bulk density and species richness for 93 pine-dominated stands (r 0.49, p<0.0001).

The NMS ordination reveals that, with regard to plant species composition, pine-dominated stands do not fall into distinct groups. Instead, species composition varies continuously along gradients related to variation in soil properties (i.e., BD, SOM, and CEC) and patterns of disturbance. Thus, correlation analysis of species' abundances with the NMS axes is a more suitable technique than ISA to identify those species that are representative of different portions of these gradients (McCune and Grace, 2002). Significant species correlations with NMS axes are presented in **Table 13-4** (for a tally of r and r-squared [r^2] values for all species with NMS Axes 1 and 2, see **Appendix 13-F**).

Species with significant positive correlations with NMS Axis 1 include *Acer rubrum, Gordonia lasianthus, Lyonia lucida, Persea palustris and Zenobia pulverulenta*, which are especially common in pocosin ecosystems. Species with significant negative correlations with NMS Axis 1 include *Aristida stricta, Cnidoscolus stimulosus, Pinus palustris, Pityopsis graminifolia and Seriocarpus tortifolium,* along with several oak species (*Quercus* longleaf) that are characteristic of sandy soils.

Such correlation analyses support the assertion that NMS Axis 2 represents a complex disturbance gradient extending from relatively undisturbed plots with low Axis 2 scores to highly disturbed stands with high Axis 2 scores. Nearly all stands dominated by loblolly pine are distributed on the high end of NMS Axis 2. Most of the species with strong positive correlations with NMS Axis 2 are commonly found in disturbed locations. Among these are weedy herbs such as *Dicanthelium sp., Eupatorium capillifolium, Panicum virgatum,* and *Solidago odora* and

several vine species such as *Gelsemium sempervirens, Parthenocissus quinquefolia, Rubus spp., Smilax spp.,* and *Vitis rotundifolia.* Increased abundance of these species is a reliable indicator of disturbance, and special attention should be paid to them in future monitoring. A diverse list of species has significant negative correlations with NMS Axis 2. They include *Aristida stricta, Carphephorus bellidus, Euphorbia ipecacuanhae, Ionactis linariifolia, Iris verna, Pinus palustris,* and several *Vaccinium* species. The large number of species with negative NMS Axis 2 correlations is consistent with the negative correlation ($r=-0.44$, $p<0.0001$) between NMS Axis 2 scores and species richness.

Stands with high (greater than zero) NMS Axis 2 scores are not characterized by a single disturbance type. Some of these stands are in early stages of succession following cutting and others are immature longleaf pine plantations. Loblolly pine plots with dense woody understories from which fire has been excluded for decades are also included among these stands. Some of these stands have very recently received midstory and understory thinning using HydroAx equipment.

In summary, species composition in MCBCL pine stands is highly correlated with a complex site and soil moisture gradient from comparatively wet, organic soils with low bulk densities to well-drained sandy soils with high bulk densities. Plant species richness also increases along this same gradient. Additional variation in species composition (represented in NMS Axis 2) is related to the effects of disturbance. Disturbances include cutting and replanting over the past several decades. Exclusion of fire is also considered a disturbance in this context.

Table 13-4. Correlations between species' abundances and NMS axes for 93 pine-dominated plots

Species with Significant Positive Correlations with NMS Axis 1	r
Acer rubrum	0.36
Desmodium spp.	0.31
Gordonia lasianthus	0.40
Ilex coriacea	0.39
Lyonia lucida	0.71
Nyssa sylvatica	0.24
Persea palustris	0.41
Pinus taeda	0.22
Rhyncospora plumosa	0.24
Smilax laurifolia	0.21
Zenobia pulverulenta	0.28

(continued)

Table 13-4. Correlations between species' abundances and NMS axes for 93 pine-dominated plots (continued)

Species with Significant Negative Correlations with NMS Axis 1	r
Aristida stricta	−0.39
Cnidoscolus stimulosus	−0.34
Diospyros virginiana	−0.25
Morella pumila	−0.22
Pinus palustris	−0.35
Pityopsis graminifolia	−0.3
Quercus hemispherica	−0.22
Quercus laevis	−0.28
Quercus marilandica	−0.24
Rhus copalina	−0.24
Sassafras albida	−0.23
Seriocarpus tortifolius	−0.35
Toxicodendron radicans	−0.22
Tragia urens	−0.21
Vaccinium tenellum	−0.32

Species with Significant Positive Correlations with NMS Axis 2	r
Acer rubrum	0.29
Carex spp.	0.25
Dicanthelium spp.	0.3
Eupatorium capillifolium	0.29
Gelsemium sempervirens	0.28
Liquidambar styraciflua	0.25
Nyssa sylvatica	0.24
Osmunda cinnamomea	0.26
Panicum virgatum	0.26
Parthenocissus quinquefolia	0.22
Rubus spp.	0.24
Smilax bona nox	0.28
Smilax glabra	0.23
Smilax laurifolia	0.27
Solidago odora	0.21
Vitis rotundifolia	0.22

(continued)

Table 13-4. Correlations between species' abundances and NMS axes for 93 pine-dominated plots (continued)

Species with Significant Negative Correlations with NMS Axis 2	r
Aristida stricta	−0.68
Asclepias pedicullata	−0.21
Carphephorus bellidifolius	−0.38
Carphephorus odoratus	−0.35
Cnidoscolus stimulosus	−0.33
Desmodium tenuifolium	−0.22
Dicanthelium ovale	−0.28
Euphorbia ipecacuanhae	−0.32
Gaylusacia dumosa	−0.42
Gentiana autumnalis	−0.21
Gymnopodium brevifolius	−0.21
Hieraceum gronovii	−0.23
Ilex glabra	−0.26
Ionactis linariifolia	−0.33
Iris verna	−0.34
Lespediza virginica	−0.25
Liatris pilosa	−0.27
Lyonia mariana	−0.285
Morella pumila	−0.3
Pinus palustris	−0.64
Pterocaulon pycnostachyum	−0.21
Quercus geminate	−0.3
Quercus hemispherica	−0.31
Quercus laevis	−0.35
Scleria nitida	−0.22
Seriocarpus tortifolius	−0.37
Stylosanthes biflora	−0.24
Symphotrichium dumosum	−0.22
Symphotrichium walteri	−0.28
Tragia urens	−0.29
Vaccinium crassifolium	−0.3
Vaccinium stamineum	−0.33
Vaccinium tenellum	−0.36
Xyris caroliniana	−0.28

Only significant correlations are listed (for $r \geq 0.21$, $p<0.05$; for $r \geq 0.25$, $p<0.01$; for $r \geq 0.33$, $p<0.001$; for $r \geq 0.40$, $p<0.0001$).

Table 13-5. Estimated fuel loads (Mg C/ha) in 1- (0–0.6 cm), 10- (0.6–2.5 cm), 100- (2.5–7.6 cm), and 1,000 (greater than 7.6 cm)-hour moisture lag classes

Vegetation Type	1 hour (0–0.6 cm)	10 hours (0.6–2.5 cm)	100 hours (2.4–7.6 cm)	1,000 hours (>7.6 cm)	Total Fine Fuels
Longleaf pine	0.161	0.072	0.004	15.103	0.237
	(0.105)	(0.079)	(0.004)	(30.908)	(0.168)
Loblolly pine—mature	0.265	0.419	0.007	19.708	0.691
	(0.156)	(0.610)	(0.004)	(42.038)	(0.747)
Loblolly pine—disturbed	0.355	0.385	0.011	17.614	0.751
	(0.316)	(0.344)	(0.013)	(40.569)	(0.612)
Pocosin	0.341	0.821	0.005	3.208	1.167
	(0.181)	(0.497)	(0.004)	(9.623)	(0.605)

Total fine fuels are the sum of 1-, 10-, and 100-hour fuels. Standard deviations are indicated in parentheses.

Changes in Species Composition and Diversity in Longleaf Pine Stands from 1991 to 2010

Twenty-one mature longleaf pine plots were deliberately selected for sampling because they had been previously sampled in 1991 by the CVS. This provided the opportunity for the direct evaluation of change in these stands over an 18-year period. This time period is significant because during this time, MCBCL managers implemented a 3-year rotation prescribed burning program in these stands. The 1991 and 2009 data were combined and analyzed in a single NMS ordination that included all 93 pine-dominated plots. The PC-ORD software allows resampled plots to be joined as an arrow representing a time vector in the ordination space.

At all spatial scales, from 1 m^2 to 0.1 ha, species richness increased among these 21 plots (**Table 13-6**). The increase in species richness at smaller spatial scales is a favorable indicator of successful restoration in longleaf pine stands. It is very likely a consequence of regular prescribed burning. The increase in richness was remarkably consistent across these 21 sample plots; the number of species per 0.1 ha increased in 19 plots, and it remained unchanged in the other two plots (**Table 13-7**).

Table 13-6. Mean species richness among 21 permanent plots sampled in 1991 and 2009

Area	Number of Species in 1991	Number of Species in 2009	p Value
0.1 ha	52	58	<0.0001
400 m^2	46	51	<0.0001
100 m^2	31	36	<0.0001
10 m^2	18	21	<0.0001
1 m^2	10	11	<0.04

The p value indicates the probability that differences between sample dates are random.

Table 13-7. Species richness (number of species per 0.1 ha) for each of the 21 mature longleaf pine plots sampled in 1991 and 2010

Plot Number	Species Richness in 1991	Species Richness in 2010	Change
116-1-53	44	50	6
116-1-54	42	47	5
116-1-58	74	76	2
116-2-54	46	46	0
116-2-58	59	69	10
116-2-59	80	94	14
116-3-51	34	34	0
116-3-52	59	79	20
116-3-55	99	101	2
116-4-53	48	52	4
116-4-54	32	34	2
116-4-56	54	57	3
116-4-57	46	50	4
116-4-58	54	62	8
116-4-59	67	69	2
116-5-54	49	58	9
116-5-55	61	72	11
116-5-58	30	33	3
116-5-59	74	86	12
116-5-60	53	57	4
116-6-52	69	71	2

NMS scores for the 21 resampled plots are indicated in **Figure 13-6.** Most (17 out of 21) of the 1991 samples are clustered in the lower left quadrant of the NMS ordination (i.e., low Axis 1 and 2 scores). This corresponds to the distribution of mature longleaf pine stands in the ordination of 2009–2010 data from all 93 pine-dominated plots (cf. **Figure 13-4**). Variation direction and magnitude of change in NMS scores between 1991 and 2009 was random. However, four stands (indicated by red arrows in **Figure 13-6**) had significantly higher NMS Axis 2 scores in 1991, corresponding to disturbed or immature stands in the ordination of 2009–2010 data from all 93 pine-dominated plots. NMS scores in 2009 for these same four plots moved significantly toward the lower left quadrant (i.e., toward species composition indicative of mature stands) of the ordination. As with changes in species richness, these changes in species composition are consistent with long-term management goals for restoration and maintenance of longleaf pine ecosystems at MCBCL.

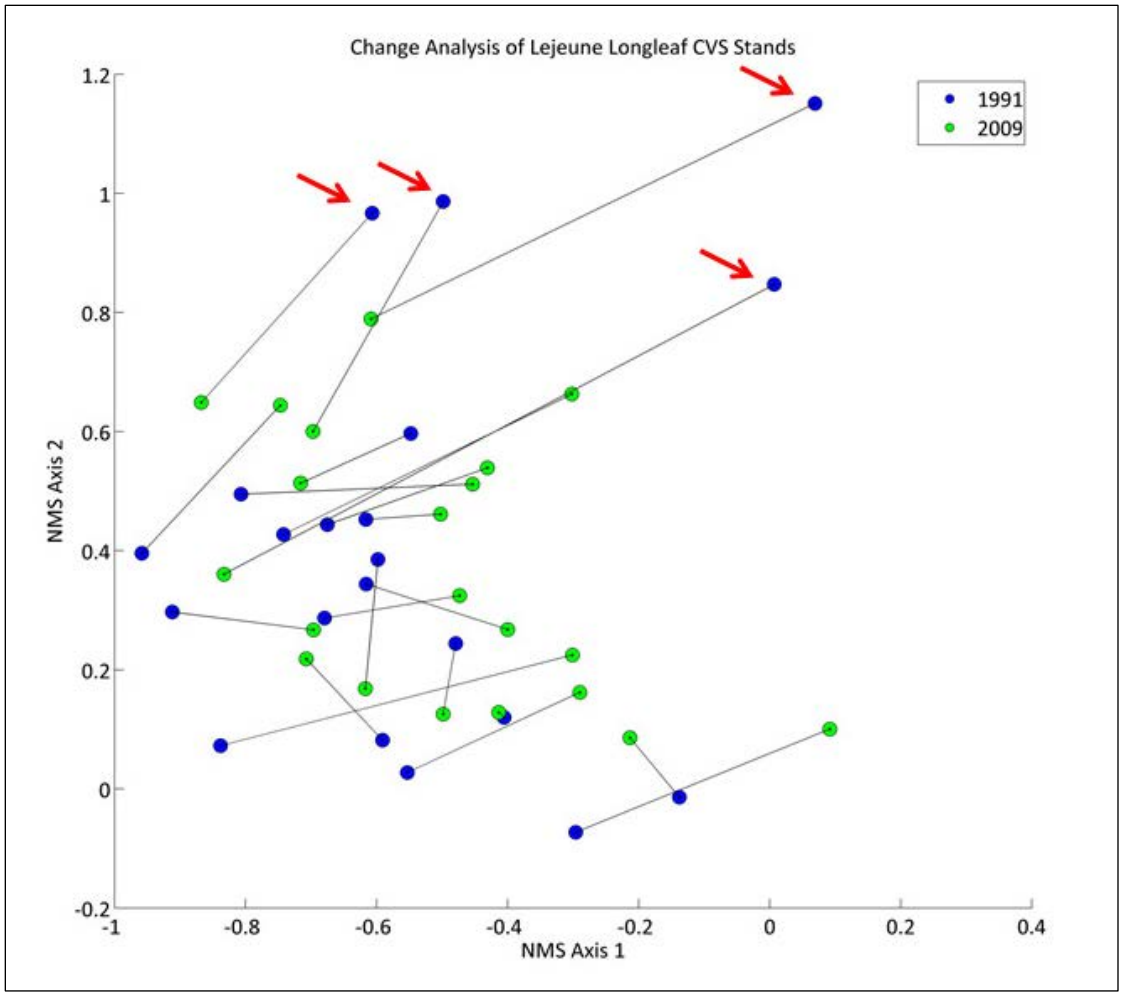

Figure 13-6. NMS ordination of 21 mature longleaf pine stands sampled in both 1991 and 2010, using the CVS sampling protocol.

Each arrow represents a single plot; the tail end is the 1991 sample and the arrow point is the 2010 sample.

Conclusions and Implications for Future Research

The primary goal for the terrestrial monitoring program was to establish a system of permanent, benchmarked plots (133 total) that can be sampled at 5–10 year intervals to assess future changes in species composition and diversity. Analysis of the initial data from these sites provides important insights into the factors influencing plant species composition and diversity across MCBCL. These insights are presented as follows:

1. More than 600 individual plant taxa were encountered among the 133 plots with an average species richness of 41.6 species per 0.1 ha. The range of species richness among plots was large, with as few as nine species per 0.1 ha in a pocosin stand to as many as 119 species per 0.1 ha in a longleaf pine stand.
2. MCBCL terrestrial vegetation composition and diversity vary in response to two major environmental gradients. Near coastal ecosystems (with 1 km of the coast) vary from

dune to maritime scrub and are heavily influenced by the effects of salt spray. Inland, terrestrial forests vary along a gradient from well-drained soils dominated by longleaf pine to broadleaved hardwoods and depression wetlands. Loblolly pine forests composition and diversity is generally intermediate to longleaf pine forests and broadleaved hardwoods. Species richness was notably lower in pocosin sites than in any other forest type.

3. ISA identified species that are particularly abundant and concentrated in each vegetation cover type, with the exception of loblolly pine stands which had only one significant indicator species (i.e., *Nyssa sylvatica*). This is indicative of the disturbance history of these forests and the wide range of conditions over which they occur.
4. In pine-dominated plots, 357 taxa were encountered. Species richness was highest in longleaf pine stands (40–119 species per 0.1 ha) and lowest in pocosins (8–20 species per 0.1 ha).
5. Based on NMS ordination, species composition varies in pine-dominated stands in relation to soil and disturbance gradients. Longleaf pine stands occur on soils with high BD and low organic matter, and pocosins dominate where BD is low and organic matter is high.
6. Loblolly pine stands segregated from longleaf and pocosin stands along Axis 2 and are indicative of past land-use history and the past exclusion of fire.
7. Plant species richness is markedly lower in disturbed loblolly pine stands than in longleaf pine stands with similar soil conditions.
8. Correlation of species abundances with NMS axes identifies indicator species of the MCBCL soil gradient and indicators of forest disturbance.
9. In 21 longleaf pine plots sampled in both 1991 and 2009, species richness uniformly increased at spatial scales ranging from 1 m^2 to 0.1 ha.
10. Stands that, based on species composition, appeared to have been disturbed in 1991 had species compositions in 2009 more indicative of undisturbed conditions.

These early results have a number of implications for MCBCL as follows:

- Future sampling of this network of permanent plots will provide important information on vegetation change in response to anthropogenic and non-anthropogenic drivers. Analysis of 21 plots sampled in both 1991 and 2009 support the value of such longitudinal studies.
- ISA and correlations with NMS axes provide the basis for identifying a subset of species upon which future sampling can be focused. This will greatly simplify sampling and diminish sampling costs.
- Changes observed in the 21 resampled plots support the assertion that current management practices (e.g., the prescribed burning program, are meeting management objectives).

Literature Cited

Andrews, P.L., and L.S. Bradshaw. 1997. *FIRES: Fire Information Retrieval and Evaluation System—A Program for Fire Danger Rating Analysis*. General Technical Report INT-GTR-367. U.S. Department of Agriculture, Forest Service, Intermountain Research Station. Available at http://www.fs.fed.us/rm/pubs_int/int_gtr367.pdf.

Bailey, A.D., R. Mickler, and C. Frost. 2007. Presettlement fire regime and vegetation mapping in Southeastern Coastal Plain forest ecosystems. Longleaf. 275–286 in The Fire Environment—Innovations, Management, and Policy. Conference Proceedings RMRS-P-46CD. Edited by B.W. Butler, and W. Cook. Destin, FL. March 26–30. U.S. Department of Agriculture, Forest Service, Rocky Mountain Research Station, Fort Collins, CO. Available at http://www.treesearch.fs.fed.us/pubs/contents/28545.

Christensen, N.L. 2000. Vegetation of the Coastal Plain of the southeastern United States. Longleaf. 397–448 in *Vegetation of North America* (2nd edition). Edited by M. Barbour and W.D. Billings. Cambridge University Press: Cambridge, United Kingdom.

Christensen, N.L. 1992. Variable fire regimes on complex landscapes: Ecological consequences, policy implications, and management strategies. Longleaf. ix–xiii in *Fire in the Environment*. General Technical Report SE-69. Edited by T. Waldrop. U.S. Department of Agriculture, Forest Service.

Christensen, N.L. 1981. Fire regimes in southeastern ecosystems. Longleaf. 112–136 in *Fire Regimes and Ecosystem Properties*. General Technical Report WO-26. Edited by H.A. Mooney, T.M. Bonnicksen, N.L. Christensen, J.E. Lotan, and W.A. Reiners. U.S. Department of Agriculture, Forest Service. 594 pages.

Christensen, N.L., R.B. Wilbur, and J.S. McLean. 1988. Soil-vegetation correlations in pocosins of Croatan National Forest, North Carolina. U.S. Fish and Wildlife Service Biological Report 88 (28), 98 Longleaf.

Crowley, A.E. 1996. *This Land, This South: An Environmental History*. University of Kentucky Press: Lexington, KY.

Demarais, S., D.J. Tazik, P.J. Guertin, and E.J. Jorgensen. 1999. Disturbance associated with military exercises. Chapter 15 in *Ecosystems of Disturbed Ground*. Edited by L.R. Walker. Elsevier: Amsterdam, NL.

Dufrêne, M., and P. Legendre. 1997. Species assemblages and indicator species: The need for a flexible assymetrical aLongleafroach. *Ecological Mongographs 67*:345–366.

Early, L.S. 2004. *Looking for Longleaf*. University of North Carolina Press: Chapel Hill, NC.

Harmon, M.E., Sexton, J., 1996. Guidelines for Measurements of Woody Detritus in Forest Ecosystems (US LTER Publication No. 20). US LTER Network Office, University of Washington, Seattle, WA, USA.

Hutto, R.L., C.J. Conway, V.A. Saab, and J.R. Walters. 2008. What constitutes a natural fire regime? Insight from the ecology and distribution of coniferous forest birds in North America. *Fire Ecology 4*:115–132.

Kruskal, J.B., and M. Wish. 1978. *Multidimensional Scaling*. Sage Publications: Beverly Hills, CA.

Korhonen, L., and J. Heikkinen. 2008. Automated analysis of in situ canopy images for the estimation of forest canopy cover. *Forest Science 55*:323–334.

McCune, B., and J.B. Grace. 2002. *Analysis of Ecological Communities*. MjM Software Design, Gleneden Beach, OR. Available at http://tocs.ulb.tu-darmstadt.de/106964135.pdf.

McLean, E.O. 1982. Soil pH and lime requirement. Longleaf. 199–223 in Methods of Soil Analysis, Part 2. Chemical and Microbiological Properties (2nd edition). Agronomy Monograph 9 (part 2) in the series. Edited by A.L. Page, R.H. Miller, and D.R. Keeney. ASA and SSSA, Madison, WI.

Mehlich, A. 1984. Mehlich-3 soil test extractant: A modification of Mehlich-2 extractant. *Communications in Soil Science and Plant Analysis 15*:1409–1416.

Nowacki, G.J., and M.D. Abrams. 2008. The demise of fire and the "mesophication" of forests in the eastern United States. *Bioscience 58*:124–138.

Peet, R.K. 2006. Ecological classification of longleaf pine woodlands. Longleaf. 51–94 *Longleaf Pine Ecosystems: Ecology, Management, and Restoration.* Edited by S. Jose, E. Jokela, and D. Miller. Springer: New York, NY.

Peet, R.K., T.R. Wentworth, and P.S. White. 1998. A flexible, multipurpose method for recording vegetation composition and structure. *Castanea 63*:262–274.

Ross, D. 1995. Recommended soil tests for determining exchange capacity. Longleaf. 62–69 in *Recommended Soil Testing Procedures for the Northeastern United States*. Northeastern Regional Bulletin #493. Edited by J.T. Sims and A. Wolf. University of Delaware, Agricultural Experiment Station, Newark, DE.

Venables, W.N., and D.M. Smith. 2011. *An Introduction to R. Notes on R: A Programming Environment for Data Analysis and Graphics, Version 2.15.2*. Available at http://cran.r-project.org/doc/manuals/R-intro.pdf.

Walker, J., and R.K. Peet. 1983**.** Composition and species diversity of pine-wire grass savannas of the Green Swamp, North Carolina. *Vegetatio 55*:163–179.

Weakley, A.S. 2011. Flora of the Southern and Mid-Atlantic States. University of North Carolina Herbarium, North Carolina Botanical Garden, University of North Carolina at Chapel

Hill, Chapel Hill, NC. Working Draft of 15 May 2011. Available at http://www.herbarium.unc.edu/FloraArchives/WeakleyFlora_2011-May-nav.pdf.

[This page intentionally left blank.]

Appendix 13-A

List of Species Encountered in 133 MCBCL Permanent Vegetation Monitoring Plots

List of Species Encountered in 133 MCBCL Permanent Vegetation Monitoring Plots

Species codes refer to acronyms used in field notes and in various computer analyses.

	Species Name	Species Code
1.	*Andropogon ternarius, A. elliottii, Schizachyrium scoparium, A. virginicus*	ANDCOM
2.	*Acer rubrum*	ACERUB
3.	*Agalinis fasciculate*	AGAFAS
4.	*Agalinis setacea*	AGASET
5.	*Aletris farinose*	ALEFAR
6.	*Amelanchier Canadensis*	AMECAN
7.	*Amorpha herbacea*	AMOHER
8.	*Andropogon capillipes*	ANDCAP
9.	*Andropogon glaucopsis*	ANDGLA
10.	*Andropogon glomeratus var. glomeratus*	ANDGLO
11.	*Andropogon glomeratus var. hirsutior*	ANDGLOH
12.	*Andropogon mohrii*	ANDMOH
13.	*Antennaria plantaginifolia*	ANTPLA
14.	*Aristida stricta*	ARISTR
15.	*Aristida virgate*	ARIVIR
16.	*Aronia arbutifolia*	AROARB
17.	*Aronia melanocarpa*	AROMEL
18.	*Arundinaria tecta*	ARUTEC
19.	*Asclepias*	ASCSLONGLEAF
20.	*Asclepias amplexicaulis*	ASCAMP
21.	*Asclepias humistrata*	ASCHUM
22.	*Asclepias pedicellata*	ASCPED
23.	*Asteraceae*	ASTSLONGLEAF
24.	*Baccharis halimifolia*	BACHAL
25.	*Bacopa*	BACOPA
26.	*Baptisia tinctoria*	BAP. TAEDAIN
27.	*Bigelowia nudata var. nudata*	BIGNUD
28.	*Callicarpa Americana*	CALAME
29.	*Carex*	CARSLONGLEAF
30.	*Carex reniformis*	CARREN
31.	*Carex striata var. brevis*	CARSTR
32.	*Carphephorus paniculatus*	CARSLONGLEAF
33.	*Carphephorus paniculatus + odor*	CARTOM
34.	*Carphephorus tomentosus*	CAROLONGLEAF
35.	*Carya glabra*	CARGLA
36.	*Carya pallida*	CARPAL

	Species Name	Species Code
37.	*Centella erecta*	CENERE
38.	*Cercis Canadensis*	CERCAN
39.	*Chamaecrista [nictitans + fasciculata]*	CHANPF
40.	*Chamaecyparis thyoides*	CHATHY
41.	*Chasmanthium*	CHAMAN
42.	*Chasmanthium laxum*	CHALAX
43.	*Chrysopsis gossypina*	CHRGOS
44.	*Chrysopsis mariana*	CHRMAR
45.	*Cirsium*	CIRSIU
46.	*Cirsium horridulum*	CIRHOR
47.	*Cirsium lecontei*	CIRLEC
48.	*Cirsium repandum*	CIRREP
49.	*Cirsium virginianum*	CIRVIR
50.	*Cirsium vulgare*	CIRVUL
51.	*Cleistes [bifaria + divaricata]*	CLEBPD
52.	*Clethra alnifolia*	CLEALN
53.	*Cnidoscolus stimulosus*	CNISTI
54.	*Comptonia*	COMP. TAEDAON
55.	*Coreopsis falcate*	CORFAL
56.	*Coreopsis linifolia*	CORLIN
57.	*Coreopsis UK**	CORUK
58.	*Coreopsis verticillata*	CORVER
59.	*Crataegus aprica*	CRAAPR
60.	*Crocanthemum carolinianum*	CROCAR
61.	*Crotalaria purshii*	CROPUR
62.	*Ctenium aromaticum*	CTEARO
63.	*Cuscuta*	CUSCUT
64.	*Cyperus retrorsus*	CYPRET
65.	*Cyrilla racemiflora*	CYRRAC
66.	*Desmodium*	DESSLONGLEAF
67.	*Desmodium ciliare*	DESCIL
68.	*Desmodium glabellum*	DESGLA
69.	*Desmodium lineatum*	DESLIN
70.	*Desmodium marilandicum*	DESMAR
71.	*Desmodium obtusum*	DESOBT
72.	*Desmodium paniculatum*	DESPAN
73.	*Desmodium perplexum*	DESPER
74.	*Desmodium tenuifolium*	DESTEN
75.	*Dichanthelium*	DICSLONGLEAF

	Species Name	Species Code
76.	*Dichanthelium [longiligulatum + ensifolium]*	DICLPE
77.	*Dichanthelium strigosum*	DICSLS
78.	*Dichanthelium aciculare*	DICACI
79.	*Dichanthelium angustifolium*	DICANG
80.	*Dichanthelium arenicoloides*	DICARE
81.	*Dichanthelium chamaelonche ssp. chamaelonche*	DICCHA
82.	*Dichanthelium commutatum*	DICCOM
83.	*Dichanthelium commutatum var. ashei*	DICCOM
84.	*Dichanthelium consanguineum*	DICCON
85.	*Dichanthelium dichotomum*	DICDIC
86.	*Dichanthelium dichotomum var. dichotomum*	DICDID
87.	*Dichanthelium ensifolium*	DICENS
88.	*Dichanthelium mattamuskeetense*	DICMAT
89.	*Dichanthelium ovale*	DICOVA
90.	*Dichanthelium ovale var. addisonii*	DICOVA
91.	*Dichanthelium ovale var. ovale*	DICOPO
92.	*Dichanthelium portoricense*	DICPOR
93.	*Dichanthelium portoricense ssp. Patulum*	DICP. SEROTINAP
94.	*Dichanthelium portoricense ssp. Portoricense*	DICP. SEROTINAO
95.	*Dichanthelium portoricense X*	DICP. SEROTINAX
96.	*Dichanthelium scoparium*	DICSCO
97.	*Dichanthelium species 2*	DICSP2
98.	*Dichanthelium sphaerocarpon*	DICSPH
99.	*Dichanthelium strigosum*	DICSTR
100.	*Dichanthelium strigosum var. glabrescens*	DICSPG
101.	*Dichanthelium strigosum var. leucoblepharis*	DICSPL
102.	*Dichanthelium strigosum var. strigosum*	DICSP. SEROTINA
103.	*Dichanthelium tenue*	DICTEN
104.	*Dichanthelium villosissimum var. villosissimum*	DICVIL
105.	*Diodia virginiana*	DIOVIR
106.	*Dionaea*	DIONAE
107.	*Dionaea muscipula*	DIOMUS
108.	*Dioscorea*	DIOSCO
109.	*Diospyros virginiana*	DIOVIR
110.	*Drosera [brevifolia + capillaris]*	DROBPC
111.	*Drosera brevifolia*	DROBRE
112.	*Elephantopus nudatus*	ELEPHA
113.	*Eragrostis refracta*	ERAREF
114.	*Eragrostis spectabilis*	ERASPE

	Species Name	Species Code
115.	*Erigeron strigosus var. strigosus*	ERISTR
116.	*Erigeron vernus*	ERIVER
117.	*Eubotrys racemosa*	EUBRAC
118.	*Eupatorium*	EUPSPP
119.	*Eupatorium [mohrii + recurvans]*	EUPMPR
120.	*Eupatorium album*	EUPALB
121.	*Eupatorium capillifolium*	EUPCAP
122.	*Eupatorium hyssopifolium*	EUPHYS
123.	*Eupatorium leucolepis*	EUPLEU
124.	*Eupatorium linearifolium*	EUPLIN
125.	*Eupatorium mohrii*	EUPMOH
126.	*Eupatorium pilosum*	EULONGLEAFIL
127.	*Eupatorium rotundifolium*	EUPROT
128.	*Euphorbia curtisii*	EUPCUR
129.	*Euphorbia ipecacuanhae*	EUPIPE
130.	*Eurybia compacta*	EURCOM
131.	*Eurybia paludosa*	EURPAL
132.	*Euthamia caroliniana*	EUTCAR
133.	*Fimbristylis annua*	FIMANN
134.	*Galactia [regularis + volubilis var. volubilis]*	GALRVV
135.	*Galactia erecta*	GALERE
136.	*Galactia regularis*	GALREG
137.	*Galactia volubilis var. volubilis*	GALVPV
138.	*Gaylussacia dumosa*	GAYDUM
139.	*Gaylussacia frondosa*	GAYFR
140.	*Gaylussacia tomentosa*	GAYTOM
141.	*Gelsemium sempervirens*	GELSEM
142.	*Gentiana autumnalis*	GENAUT
143.	*Gleditsia triacanthos*	GLETRI
144.	*Gnaphalium*	GNAPHA
145.	*Gordonia lasianthus*	GORLAS
146.	*Gymnopogon brevifolius*	GYMBRE
147.	*Helianthus angustifolius*	HELANG
148.	*Helianthus atrorubens*	HELATR
149.	*Helianthus heterophyllus*	HELHET
150.	*Hexastylis*	HEXAST
151.	*Hieracium gronovii*	HIEGRO
152.	*Hieracium marianum*	HIEMAR
153.	*Hydrocotyle bonariensis*	HYDBON

	Species Name	Species Code
154.	*Hypericum cistifolium*	HYPCIS
155.	*Hypericum crux-andreae*	HYPCRU
156.	*Hypericum hypericoides*	HYPHYP
157.	*Hypericum setosum*	HYP. SEROTINAET
158.	*Hypericum tenuifolium*	HYP. TAEDAEN
159.	*Hypoxis hirsute*	HYPHIR
160.	*Hypoxis juncea*	HYPJUN
161.	*Ilex coriacea*	ILECOR
162.	*Ilex glabra*	ILEGLA
163.	*Ilex opaca var. opaca*	ILEOPA
164.	*Ilex vomitoria*	ILEVOM
165.	*Ionactis linariifolia*	IONLIN
166.	*Ipomoea*	IPOMOE
167.	*Iris verna var. verna*	IRIVER
168.	*Juncus*	JUNSLONGLEAF
169.	*Juncus acuminatus*	JUNACU
170.	*Juncus biflorus*	JUNBIF
171.	*Juncus Canadensis*	JUNCAN
172.	*Juncus dichotomus*	JUNDIC
173.	*Juncus scirpoides*	JUNSCI
174.	*Kalmia Carolina*	KALCAR
175.	*Lachnocaulon anceP. Serotina*	LACANC
176.	*Lactuca Canadensis*	LACCAN
177.	*Lechea [pulchella var. ramosissima + torreyi var. congesta]*	LECPRT
178.	*Lechea minor*	LECMIN
179.	*Lechea pulchella var. ramosissima*	LECLONGLEAFR
180.	*Lechea tenuifolia*	LECTEN
181.	*Lespedeza angustifolia*	LESANG
182.	*Lespedeza capitata*	LESCAP
183.	*Lespedeza hirta*	LESHIR
184.	*Lespedeza hirta var. curtissii*	LESHPC
185.	*Lespedeza hirta var. hirta*	LESHPH
186.	*Lespedeza virginica*	LESVIR
187.	*Leucothoe axillaris*	LECAXI
188.	*Liatris [pilosa + virgata]*	LIALONGLEAFV
189.	*Liatris spicata*	LIASPI
190.	*Liatris spicata var. resinosa*	LIASPI
191.	*Linum floridanum*	LINFLO
192.	*Liquidambar styraciflua*	LIQSTY

	Species Name	Species Code
193.	*Liriodendron tulipifera*	LIRTUL
194.	*Lobelia nuttallii*	LOBNUT
195.	*Ludwigia virgata*	LUDVIR
196.	*Lycopodiella alopecuroides*	LYCALO
197.	*Lycopodium*	LYCOPO
198.	*Lyonia ligustrina*	LYOLIG
199.	*Lyonia ligustrina var. foliosiflora*	LYOLIG
200.	*Lyonia lucida*	LYOLUC
201.	*Lyonia mariana*	LYOMAR
202.	*Lysimachia loomisii*	LYSLOO
203.	*Magnolia virginiana*	MAGVIR
204.	*Marshallia graminifolia*	MARGRA
205.	*Mikania scandens*	MIKSCA
206.	*Mitchella repens*	MITREP
207.	*Morella caroliniensis*	MORCAR
208.	*Morella cerifera*	MORCER
209.	*Morella pumila*	MORPUM
210.	*Muhlenbergia expansa*	MUHEXP
211.	*Nyssa sylvatica*	NYSSYL
212.	*Orbexilum pedunculatum var. psoralioides*	ORBPED
213.	*Osmunda cinnamomea var. cinnamomea*	OSMCIN
214.	*Osmunda regalis*	OSMREG
215.	*Osmunda regalis var. spectabilis*	OSMRP. SEROTINA
216.	*Oxypolis denticulata*	OXYDEN
217.	*Panicum amarum*	PANAMA
218.	*Panicum anceps*	PANANC
219.	*Panicum anceps var. rhizomatum*	PANAPR
220.	*Panicum virgatum*	PANVIR
221.	*Parthenium*	PARSLONGLEAF
222.	*Parthenocissus quinquefolia*	PARQUI
223.	*Paspalum praecox var. praecox*	PASPRA
224.	*Paspalum setaceum var. stramineum*	PASSET
225.	*Persea palustris*	PERPAL
226.	*Picea*	PICSLONGLEAF
227.	*Pinus palustris*	PINPAL
228.	*Pinus serotina*	PINSER
229.	*Pinus taeda*	PINTAE
230.	*Pityopsis graminifolia*	PITGRA
231.	*Platanthera*	PLATAN

	Species Name	Species Code
232.	*Platanthera ciliaris*	PLACIL
233.	*Pleea tenuifolia*	PLETEN
234.	*Pluchea baccharis*	PLUBAC
235.	*Polygala [brevifolia + hookeri + cruciata]*	POLBHC
236.	*Polygala brevifolia*	POLBRE
237.	*Polygala cruciata*	POLCRU
238.	*Polygala incarnata*	POLINC
239.	*Polygala lutea*	POLLUT
240.	*Potentilla*	POTSLONGLEAF
241.	*Prenanthes*	PRESLONGLEAF
242.	*Prunus serotina*	PRUSER
243.	*Pteridium aquilinum var. pseudocaudatum*	P. TAEDAEAQU
244.	*Pterocaulon pycnostachyum*	P. TAEDAEPYC
245.	*Pycnanthemum flexuosum*	PYCFLE
246.	*Pyxidanthera barbulata*	PYXBAR
247.	*Quercus*	QUESLONGLEAF
248.	*Quercus falcata*	QUEFAL
249.	*Quercus geminata*	QUEGEM
250.	*Quercus hemisphaerica*	QUEHEM
251.	*Quercus incana*	QUEINC
252.	*Quercus incana X marilandica*	QUEIXM
253.	*Quercus laevis*	QUELAE
254.	*Quercus laevis X marilandica*	QUELXM
255.	*Quercus margaretta*	QUEMAR
256.	*Quercus marilandica*	QUEMVM
257.	*Quercus marilandica var. marilandica*	QUEMPM
258.	*Quercus michauxii*	QUEMIC
259.	*Quercus nigra*	QUENIG
260.	*Quercus stellata*	QUESTE
261.	*Quercus virginiana*	QUEVIR
262.	*Quercus xashei*	QUEXASH
263.	*Quercus xcaduca*	QUEXCA
264.	*Quercus xincomita*	QUEXIN
265.	*Rhexia [nashii + mariana var. mariana]*	RHENMM
266.	*Rhexia alifanus*	RHEALI
267.	*Rhexia lutea*	RHELUT
268.	*Rhexia mariana*	RHEMAR
269.	*Rhexia nashii*	RHENAS
270.	*Rhexia petiolata*	RHEPET

	Species Name	Species Code
271.	*Rhizophora*	RHIZOP
272.	*Rhododendron atlanticum*	RHOATL
273.	*Rhus copallinum*	RHUCOP
274.	*Rhynchosia tomentosa*	RHYTOM
275.	*Rhynchospora*	RHYSLONGLEAF
276.	*Rhynchospora baldwinii*	RHYBAL
277.	*Rhynchospora divergens*	RHYDIV
278.	*Rhynchospora fascicularis var. distans*	RHYFVD
279.	*Rhynchospora fascicularis var. fascicularis*	RHYFVF
280.	*Rhynchospora grayi*	RHYGRA
281.	*Rhynchospora harveyi*	RHYHAR
282.	*Rhynchospora plumosa*	RHYPLU
283.	*Robinia nana*	ROBSLONGLEAF
284.	*Rubus*	RUBSLONGLEAF
285.	*Sabatia difformis*	SABDIF
286.	*Saccharum*	SACCHA
287.	*Salix caroliniana*	SALCAR
288.	*Sarracenia flava*	SARFLA
289.	*Sarracenia rubra x flava*	SARRXF
290.	*Sassafras albidum*	SASALB
291.	*Schizachyrium scoparium*	SCHSCO
292.	*Scleria [ciliata var. ciliata + elliottii]*	SCLCCE
293.	*Scleria [ciliata var. glabra + pauciflora var. pauciflora]*	SCLCGP
294.	*Scleria [nitida + triglomerata]*	SCLNP. TAEDA
295.	*Scleria ciliata*	SCLCIL
296.	*Scleria ciliata var. ciliata*	SCLCVC
297.	*Scleria ciliata var. glabra*	SCLCVG
298.	*Scleria nitida*	SCLNIT
299.	*Scleria oligantha*	SCLOLI
300.	*Scleria pauciflora var. pauciflora*	SCLPVP
301.	*Scleria triglomerata*	SCLTRI
302.	*Sericocarpus asteroides*	SERAST
303.	*Sericocarpus linifolius*	SERLIN
304.	*Sericocarpus tortifolius*	SERTOR
305.	*Seymeria cassioides*	SEYCAS
306.	*Silphium compositum*	SILCOM
307.	*Sisyrinchium capillare*	SISCAP
308.	*Smilax bona-nox*	SMIBON
309.	*Smilax glauca*	SMIGLA

	Species Name	Species Code
310.	*Smilax laurifolia*	SMILAU
311.	*Smilax rotundifolia*	SMIROT
312.	*Solidago arguta*	SOLARU
313.	*Solidago odora*	SOLODO
314.	*Solidago odora var. odora*	SOLOVO
315.	*Solidago pulchra*	SOLPUL
316.	*Solidago stricta*	SOLSTR
317.	*Sophronanthe pilosa*	SOLONGLEAFIL
318.	*Sorbus americana*	SORAME
319.	*Spiranthes*	SPISLONGLEAF
320.	*Spiranthes eatonii*	SPIEAT
321.	*Spiranthes lacera var. gracilis*	SPILVG
322.	*Spiranthes praecox*	SPIPRA
323.	*Sporobolus pinetorum*	SPOPIN
324.	*Stylosanthes biflora*	STYBIF
325.	*Symphyotrichum concolor*	SYMCON
326.	*Symphyotrichum concolor var. concolor*	SYMCVC
327.	*Symphyotrichum dumosum var. dumosum*	SYMDVD
328.	*Symphyotrichum tenuifolium*	SYMTEN
329.	*Symphyotrichum walteri*	SYMWAL
330.	*Symplocos tinctoria*	SYMTIN
331.	*Tephrosia florida*	TEPFLO
332.	*Tephrosia hispidula*	TEPHIS
333.	*Toxicodendron pubescens*	TOXPUB
334.	*Toxicodendron radicans*	TOXRAD
335.	*Toxicodendron radicans var. radicans*	TOXRVR
336.	*Tragia urens*	TRAURE
337.	*Uvularia puberula*	UVUPUB
338.	*Vaccinium arboreum*	VACARB
339.	*Vaccinium corymbosum*	VACCOR
340.	*Vaccinium crassifolium*	VACCRA
341.	*Vaccinium formosum*	VACFOR
342.	*Vaccinium fuscatum*	VACFUS
343.	*Vaccinium stamineum*	VASTA
344.	*Vaccinium tenellum*	VACTEN
345.	*Viola primulifolia*	VIOPRI
346.	*Viola seP. taedaemloba*	VIOSEP
347.	*Vitis rotundifolia*	VITROT
348.	*Vitis rotundifolia var. rotundifolia*	VITRVR

	Species Name	Species Code
349.	*Woodwardia areolata*	WOOARE
350.	*Woodwardia virginica*	WOOVIR
351.	*Xyris ambigua*	XYRAMB
352.	*Xyris caroliniana*	XYRCAR
353.	*Zigadenus glaberrimus*	ZIGGLA
354.	*Zenobia pulverulenta*	ZENPUL

[This page intentionally left blank.]

Appendix 13-B

NMS Axes 1 and 2 Scores for 133 Permanent MCBCL Vegetation Monitoring Plots

MCBCL Vegetation Monitoring Plots

Number	Plot Name	Dominant Pine	NMS Axis 1	NMS Axis 2
1.	6x-1-53	LONGLEAF	0.61419	−0.4719
2.	6x-1-54	LONGLEAF	0.74759	−0.47243
3.	6x-1-58	LONGLEAF	0.90756	0.17752
4.	6x-2-54	LONGLEAF	0.86571	−0.41059
5.	6x-2-58	LONGLEAF	0.69034	−0.21325
6.	6x-2-59	LONGLEAF	0.1569	0.14158
7.	6x-3-51	LONGLEAF	0.82855	−0.37238
8.	6x-3-53	LONGLEAF	0.49165	0.33787
9.	6x-4-53	LONGLEAF	0.62017	−0.27774
10.	6x-4-54	LONGLEAF	1.12505	−0.41213
11.	6x-4-56	LONGLEAF	0.42528	−0.3012
12.	6x-4-57	LONGLEAF	0.67587	−0.45495
13.	6x-4-58	LONGLEAF	0.81135	−0.33025
14.	6x-4-59	LONGLEAF	0.80338	−0.22602
15.	6x-5-54	LONGLEAF	0.72381	−0.10248
16.	6x-5-55	LONGLEAF	0.87677	−0.36766
17.	6x-5-58	LONGLEAF	1.14166	−0.19049
18.	6x-5-59	LONGLEAF	0.27532	−0.02883
19.	6x-5-60	LONGLEAF	0.49802	−0.22684
20.	6x-8-1	LONGLEAF	0.59131	−0.25772
21.	6x-8-2	LONGLEAF	0.10175	−0.35128
22.	6x-8-3	LONGLEAF	0.89967	−0.06008
23.	6x-8-4	LONGLEAF	0.32478	−0.48416
24.	6x-8-5	LONGLEAF	1.02055	−0.2142
25.	CR1	LONGLEAF	0.30001	0.45959
26.	CT1	LONGLEAF	1.14257	−0.08891
27.	CT2	LONGLEAF	0.85287	−0.13465
28.	CT4	LONGLEAF	0.9508	0.05422
29.	DC2	LONGLEAF	0.89926	0.01509
30.	FGE-C	P. TAEDA	−1.52872	−0.68128
31.	FGW-C	P. TAEDA	−1.53495	−0.62361
32.	FGE-G	P. TAEDA	−0.62774	−0.17138
33.	FGW-G	P. TAEDA	−1.02088	−0.34787
34.	FGE-D	P. TAEDA	−1.09509	−0.06874
35.	FGW-D	P. TAEDA	−0.23701	−0.10289
36.	GT1	LONGLEAF	0.63212	−0.18651
37.	GT2	LONGLEAF	0.87831	−0.1331

Number	Plot Name	Dominant Pine	NMS Axis 1	NMS Axis 2
38.	GT3	LONGLEAF	0.76711	−0.00474
39.	GT4	LONGLEAF	0.7568	0.09355
40.	GT6	LONGLEAF	0.90209	−0.26664
41.	HA-C	P. TAEDA	−1.11971	0.29928
42.	HA-G	P. TAEDA	−0.51165	0.22852
43.	HA-D	P. TAEDA	−0.56809	0.32073
44.	IEN-C	P. TAEDA	−1.28177	−0.49336
45.	IES-C	P. SEROTINA	−1.54982	−0.31862
46.	IEN-G	P. TAEDA	−0.95642	0.04131
47.	IES-G	P. SEROTINA	−1.40092	0.20367
48.	IEN-D	P. TAEDA	−1.37066	0.70397
49.	IES-D	P. SEROTINA	−1.3678	−0.55005
50.	MC-C	P. TAEDA	−0.79124	−0.16841
51.	MF-G	P. TAEDA	−1.27222	0.25251
52.	MF-D	P. TAEDA	−0.76833	0.15511
53.	NE2	LONGLEAF	0.65591	−0.02674
54.	NE4	LONGLEAF	0.46299	0.00071
55.	PN17	LONGLEAF	1.00596	0.3882
56.	PN18	LONGLEAF	0.83674	0.98564
57.	PN19	P. SEROTINA	−0.08364	−0.38343
58.	PN23	LONGLEAF	1.05941	0.21936
59.	PN33	LONGLEAF	−0.61837	1.03024
60.	PN34	LONGLEAF	0.33835	0.21189
61.	PN39	LONGLEAF	0.36928	0.27189
62.	PN47	P. TAEDA	0.00458	1.55609
63.	PN51	LONGLEAF	0.31335	1.33316
64.	PN60	LONGLEAF	−0.28137	−0.34093
65.	PN62	P. TAEDA	−0.1462	1.2726
66.	PN65	LONGLEAF	0.09856	−0.07279
67.	PN66	P. TAEDA	−0.65647	1.43361
68.	PN69	LONGLEAF	0.36497	0.61174
69.	RBE-C	P. TAEDA	−0.37976	1.19608
70.	RBW-C	P. TAEDA	−0.17899	1.53099
71.	RBE-G	P. TAEDA	−0.98429	1.05857
72.	RBW-G	P. TAEDA	−0.75715	0.53483
73.	RBE-D	P. TAEDA	−0.27122	0.65807
74.	RBW-D	P. TAEDA	−0.64428	0.71765
75.	SC1	LONGLEAF	−0.69305	−0.28208
76.	SC2	LONGLEAF	0.31149	−0.64961

Number	Plot Name	Dominant Pine	NMS Axis 1	NMS Axis 2
77.	VL2	LONGLEAF	−0.00372	0.15791
78.	VL3	LONGLEAF	−0.60865	−0.31306
79.	VL4	LONGLEAF	−0.11169	−0.28379
80.	VL5	LONGLEAF	−0.45343	−0.52996
81.	VL6	LONGLEAF	0.11906	−1.54827
82.	POC11	P. SEROTINA	−1.46645	−1.01023
83.	POC12	P. SEROTINA	−1.20074	−1.09799
84.	POC9	P. SEROTINA	−1.05872	−0.81341
85.	POC10	P. SEROTINA	−0.63862	−0.73411

Appendix 13-C

Summary of MCBCL Monitoring Plot Site and Soil Characteristics

For MCBCL vegetation monitoring plots (excluding Onslow Beach plots), averaged values for species richness (number per 0.1 ha), stems less than 20 cm (number per ha), stems greater than 20 cm (number per ha), basal area (m^2/ha), cation exchange capacity (CEC, milliequivalents/100 g of soil), bulk density (BD, g/cm^3), pH, soil organic matter (SOM %), and extractable sulfur (S), orthophosphate (PO_4–P), calcium (Ca), magnesium (Mg), potassium (K), and aluminum (Al) in each of the experimental treatment plots. Extractable element concentrations are expressed in µg/g; "N/A" indicates missing data.

Plot Name	Species Richness	Stems <15 cm	Basal Area	CEC	BD	pH	SOM %	P	Ca	Mg	K	Al
1. 6x-01-0053	48	50	10.69	3.78	1.33	4.15	2.15	2.25	140.00	31.00	18.50	110.50
2. 6x-01-0054	46	20	30.34	5.01	1.16	4.28	3.28	1.00	221.75	32.50	24.75	119.75
3. 6x-01-0058	75	160	42.28	2.91	1.40	4.00	1.01	1.00	98.25	18.00	9.00	292.50
4. 6x-02-0054	45	120	56.81	5.22	1.16	4.40	3.97	2.25	228.00	42.25	36.00	186.00
5. 6x-02-0058	68	90	51.94	5.11	1.16	4.18	3.75	3.25	183.50	33.50	54.75	306.50
6. 6x-02-0059	91	50	28.03	3.66	1.24	4.18	2.90	1.50	126.00	23.00	20.75	391.25
7. 6x-03-0051	34	190	72.82	4.85	1.18	4.13	3.67	1.25	183.75	30.75	22.00	101.00
8. 6x-03-0053	118	160	33.05	2.68	1.26	4.18	2.43	1.50	100.50	16.00	20.00	798.00
9. 6x-04-0053	49	130	19.56	4.27	1.30	3.95	3.09	1.00	109.50	40.00	25.75	117.75
10. 6x-04-0054	32	130	11.59	4.23	1.14	4.80	4.46	2.50	254.50	34.00	26.75	89.25
11. 6x-04-0056	57	20	10.59	5.84	1.26	3.80	3.50	1.25	162.50	43.25	22.00	145.50
12. 6x-04-0057	49	130	45.43	2.89	1.36	4.10	1.90	1.00	101.25	20.75	14.75	52.50
13. 6x-04-0058	61	280	42.12	2.33	1.34	4.20	1.75	1.00	88.75	15.00	11.75	578.75
14. 6x-04-0059	68	110	27.10	6.06	1.26	4.30	3.16	2.75	286.75	31.00	31.75	172.75
15. 6x-05-0054	55	250	30.15	3.85	1.39	4.00	2.84	1.00	105.25	35.00	20.75	122.00
16. 6x-05-0055	72	140	26.24	2.55	1.40	4.38	1.45	1.25	121.75	19.50	16.00	401.50
17. 6x-05-0058	32	30	37.99	3.21	1.36	4.08	1.73	4.00	128.50	16.25	13.75	80.50
18. 6x-05-0059	84	190	41.45	3.01	1.14	3.88	4.01	2.75	77.25	21.00	20.25	713.00
19. 6x-05-0060	56	260	41.58	3.20	1.25	4.08	2.36	5.25	111.50	21.50	18.25	233.25
20. 6x-08-0001	91	110	110.88	8.30	0.95	3.85	10.64	2.50	267.50	50.00	37.75	277.75
21. 6x-08-0002	92	50	18.95	9.50	0.96	3.83	10.28	1.50	276.25	65.75	36.50	424.75
22. 6x-08-0003	57	30	20.81	5.40	1.21	4.20	3.52	1.25	218.50	28.25	26.00	149.25

Plot Name	Species Richness	Stems <15 cm	Basal Area	CEC	BD	pH	SOM %	P	Ca	Mg	K	Al
23. 6x-08-0004	60	70	6.38	11.12	1.04	3.73	10.51	1.25	302.50	83.50	56.25	149.75
24. 6x-08-0005	46	160	77.93	5.86	1.11	4.10	3.54	4.25	230.75	45.50	23.50	135.50
25. CR1	37	760	8.11	3.29	1.23	4.68	2.24	6.00	170.00	39.75	13.50	87.00
26. CT1	23	90	9.95	2.07	1.21	4.85	2.10	5.25	116.50	23.75	14.00	76.00
27. CR2	20	250	13.99	N/A	N/A	N/A	N/A	N/A	N/A	N/A	N/A	N/A
28. CT4	38	490	11.19	3.06	1.04	4.60	4.49	4.25	160.25	28.00	12.50	102.25
29. DC2	28	0	12.52	4.17	0.90	4.33	18.35	4.00	159.25	35.75	20.00	89.00
30. FGE-C	10	2,880	26.28	9.57	0.22	3.78	67.83	3.25	216.75	96.00	46.50	231.25
31. FGW-C	7	2,430	25.60	9.88	0.39	3.78	51.44	3.00	251.00	84.75	46.75	208.50
32. FGE-G	18	2,060	19.69	6.89	0.54	3.98	34.27	3.00	243.25	52.75	24.00	198.50
33. FGW-G	17	2,060	19.69	7.36	0.41	4.00	37.39	3.75	235.75	60.25	31.25	400.75
34. FGE-D	18	2,060	19.69	7.19	0.53	3.78	41.19	6.25	196.75	47.50	46.50	574.50
35. FGW-D	30	2,060	19.69	9.47	0.81	4.08	11.91	4.25	351.25	63.25	37.00	118.25
36. GT1	48	280	12.72	3.83	1.09	4.73	2.75	9.00	233.50	36.25	22.50	131.75
37. GT2	38	50	20.28	3.04	1.12	4.63	2.21	7.50	149.75	31.25	21.00	126.25
38. GT4	39	590	8.38	4.46	1.01	4.80	3.74	6.50	272.75	36.75	19.25	167.00
39. GT5	53	110	13.69	7.13	0.98	4.45	7.19	4.25	347.75	59.75	20.50	220.00
40. GT6	30	40	10.96	4.56	1.02	4.50	8.17	4.25	180.50	44.00	28.00	230.25
41. HAC	24	1,580	18.11	6.21	0.69	4.10	13.83	5.50	186.25	56.00	34.50	527.00
42. HAG	35	360	8.48	6.57	0.93	4.45	6.07	4.25	301.25	39.00	25.75	658.50
43. HAD	41	360	8.48	8.60	0.76	4.18	13.37	6.75	390.75	54.75	30.00	640.50
44. IEN-C	14	5,470	7.66	6.68	0.55	3.88	30.33	10.25	172.50	48.25	41.00	868.25
45. IES-C	12	100	19.78	7.93	0.30	3.73	68.12	3.75	93.75	103.00	77.25	167.75
46. IEN-G	21	0	17.66	11.29	0.45	3.85	43.43	6.50	336.75	80.75	48.50	496.00
47. IES-G	13	350	13.59	10.74	0.50	3.93	33.82	5.00	346.75	69.75	43.25	418.75
48. IEN-D	23	1,880	10.23	7.42	0.59	3.85	33.67	6.25	170.50	71.75	41.00	786.00
49. IES-D	15	590	18.51	7.65	0.44	3.85	53.26	6.00	193.25	72.00	29.50	379.25

Plot Name	Species Richness	Stems <15 cm	Basal Area	CEC	BD	pH	SOM %	P	Ca	Mg	K	Al
50. MFC	24	4,940	21.36	5.71	0.74	3.93	14.38	12.25	172.25	42.00	31.75	866.50
51. MFG	21	240	16.50	5.54	0.39	3.90	30.22	10.25	170.00	40.50	30.25	841.75
52. MFD	32	60	23.64	6.98	0.58	3.95	25.49	9.00	193.75	59.25	43.00	626.75
53. NE2	43	230	10.93	4.52	1.07	4.23	3.29	4.75	177.75	33.25	20.25	159.25
54. NE4	41	160	11.74	3.57	0.93	4.25	5.52	4.50	129.75	35.25	20.50	351.25
55. PN17	25	340	3.17	3.42	1.22	4.43	1.41	2.50	170.25	24.50	8.25	70.75
56. PN17	14	800	1.82	4.11	1.34	4.68	1.03	2.50	265.75	22.25	11.00	62.25
57. PN18	32	1,080	4.35	3.86	1.37	4.55	0.91	5.00	226.75	21.75	11.25	60.25
58. PN23	28	870	0.07	8.16	0.98	4.85	4.96	148.50	741.00	48.25	24.00	473.25
59. PN33	30	4,330	39.71	5.75	0.98	4.18	8.98	8.50	229.00	42.00	17.75	504.25
60. PN34	29	270	4.33	4.37	0.97	4.43	5.95	6.75	186.75	40.00	27.75	498.50
61. PN39	30	1,540	8.96	4.20	1.00	4.68	5.10	5.75	215.75	49.00	29.25	352.25
62. PN47	37	630	0.42	4.29	1.13	4.65	2.86	5.25	207.00	57.75	72.25	501.25
63. PN51	33	1,290	8.34	N/A	N/A	N/A	N/A	N/A	N/A	N/A	N/A	N/A
64. PN60	30	100	10.59	4.67	1.00	4.10	5.15	6.00	153.75	41.00	24.00	391.00
65. PN62	39	4,020	7.18	7.59	0.91	4.30	7.91	6.00	309.00	50.25	25.25	579.75
66. PN65	38	280	12.70	10.64	0.82	4.08	9.56	8.75	450.50	57.50	16.75	322.00
67. PN66	19	1,390	1.19	5.17	0.92	4.28	5.26	9.25	231.50	39.25	23.00	220.00
68. PN69	36	290	15.32	3.26	1.11	4.40	4.36	4.50	130.50	33.50	18.25	206.50
69. RBE-C	15	3,660	23.89	8.09	0.80	4.45	16.05	7.00	401.00	56.75	37.75	692.00
70. RBW-C	13	3,340	26.08	4.97	1.01	4.43	5.69	7.50	229.25	47.00	36.00	852.00
71. RBE-G	33	110	13.31	9.64	0.85	4.03	7.95	10.50	369.50	64.50	33.00	545.00
72. RBW-G	32	30	19.07	8.03	0.90	4.23	6.52	7.25	359.00	56.75	30.50	393.75
73. RBE-D	29	910	18.37	4.54	1.05	4.60	5.18	6.50	242.00	40.25	28.50	382.75
74. RBW-D	40	2,920	22.05	10.04	0.66	4.23	17.92	8.25	458.75	83.50	66.50	361.50
75. SC1	29	1,010	9.20	4.82	1.08	4.15	5.96	5.50	171.75	43.00	17.00	232.25
76. SC2	24	1,120	12.86	3.95	1.21	4.30	2.51	3.75	160.75	31.50	16.75	131.00

Plot Name	Species Richness	Stems <15 cm	Basal Area	CEC	BD	pH	SOM %	P	Ca	Mg	K	Al
77. VL2	40	0	13.54	5.26	0.85	4.05	8.05	3.50	176.50	44.25	20.25	254.75
78. VL3	44	50	12.85	4.77	0.90	3.98	9.39	4.75	120.00	53.00	17.00	256.50
79. VL4	43	880	12.64	1.63	0.96	4.10	5.34	3.38	9.13	30.25	12.00	462.75
80. VL5	33	3,530	12.89	3.92	0.86	4.08	6.91	5.50	122.50	36.00	27.25	339.25
81. VL6	30	50	8.77	5.38	0.94	4.05	4.91	6.25	174.75	47.25	27.00	137.25
82. POC11	9	N/A	N/A	3.78	0.71	4.95	21.69	3.50	138.00	98.00	23.75	127.75
83. POC12	10	N/A	N/A	4.38	0.44	4.55	41.41	3.50	167.25	74.25	23.25	174.50
84. POC9	14	N/A	N/A	6.70	0.78	4.58	8.01	9.25	410.50	56.00	30.75	604.25
85. POC10	28	N/A	N/A	3.79	0.92	4.70	5.12	3.50	175.75	48.50	17.75	170.00

[This page intentionally left blank.]

Appendix 13-D

Matrix of Correlation Coefficients for All Soil Variables Measured in Permanent MCBCL Vegetation Monitoring Plots

Matrix of correlation coefficients for all soil variables measured in permanent vegetation monitoring plots on MCBCL.

	BD	CEC	SOM	P	Ca	Mg	K	Na	B	Fe	Mn	Cu	Zn	Al
BD	1.000	−0.646	−0.874	−0.066	−0.273	−0.796	−0.563	−0.601	−0.297	−0.015	0.215	−0.117	−0.082	−0.377
CEC	−0.646	1.000	0.552	0.163	0.705	0.760	0.635	0.534	0.244	0.020	−0.053	0.160	0.330	0.240
SOM	−0.874	0.552	1.000	−0.026	0.072	0.738	0.559	0.599	−0.012	−0.108	−0.242	0.088	0.042	0.192
P	−0.066	0.163	−0.026	1.000	0.586	0.054	0.002	−0.033	0.151	0.150	0.092	0.029	0.034	0.151
Ca	−0.273	0.705	0.072	0.586	1.000	0.394	0.290	0.192	0.281	0.064	0.222	0.021	0.173	0.164
Mg	−0.796	0.760	0.738	0.054	0.394	1.000	0.700	0.674	0.224	−0.104	−0.154	0.121	0.244	0.126
K	−0.563	0.635	0.559	0.002	0.290	0.700	1.000	0.667	0.217	0.047	−0.052	0.120	0.243	0.284
Na	−0.601	0.534	0.599	−0.033	0.192	0.674	0.667	1.000	0.073	0.073	−0.161	0.083	0.103	0.287
B	−0.297	0.244	−0.012	0.151	0.281	0.224	0.217	0.073	1.000	0.349	−0.113	0.145	0.087	0.460
Fe	−0.015	0.020	−0.108	0.150	0.064	−0.104	0.047	0.073	0.349	1.000	−0.205	0.221	0.081	0.740
Mn	0.215	−0.053	−0.242	0.092	0.222	−0.154	−0.052	−0.161	−0.113	−0.205	1.000	−0.056	−0.041	−0.275
Cu	−0.117	0.160	0.088	0.029	0.021	0.121	0.120	0.083	0.145	0.221	−0.056	1.000	0.819	0.219
Zn	−0.082	0.330	0.042	0.034	0.173	0.244	0.243	0.103	0.087	0.081	−0.041	0.819	1.000	0.081
Al	−0.377	0.240	0.192	0.151	0.164	0.126	0.284	0.287	0.460	0.740	−0.275	0.219	0.081	1.000

Appendix 13-E

NMS Axes 1 and 2 Scores for 93 Pine-Dominated Permanent MCBCL Vegetation Monitoring Plots

NMS Axes 1 and 2 scores for 93 pine-dominated permanent MCBCL vegetation monitoring plots.

Number	Plot Name	NMS Axis 1	NMS Axis 2
1	6x-1-53	−0.7635	−0.1719
2	6x-1-54	-0.829	−0.0096
3	6x-1-58	−0.9216	0.2617
4	6x-2-54	−0.9427	0.0773
5	6x-2-58	−0.6549	0.1275
6	6x-2-59	−0.0616	0.1128
7	6x-3-51	−0.9033	−0.0106
8	6x-3-53	−0.4507	−0.1933
9	6x-3-55	−0.4326	-0.019
10	6x-4-53	−0.6183	0.0413
11	6x-4-54	−1.1649	0.1944
12	6x-4-56	−0.5438	−0.1791
13	6x-4-57	−0.8382	−0.1493
14	6x-4-58	−0.8564	0.0957
15	6x-4-59	−0.7552	0.2047
16	6x-5-54	−0.701	0.1297
17	6x-5-55	−0.9139	0.0628
18	6x-5-58	−1.0562	0.4224
19	6x-5-59	−0.2703	−0.025
20	6x-5-60	−0.578	−0.0157
21	6x-8-1	−0.6484	0.0035
22	6x-8-2	−0.313	−0.3664
23	6x-8-3	−0.7579	0.3753
24	6x-8-4	−0.562	−0.3756
25	6x-8-5	−0.992	0.2948
26	6x-R-73	−1.6163	0.2233
27	CR1	−0.0247	0.4732
28	CR2	−0.9347	1.2708
29	CT1	−1.0057	0.5058
30	CT2	−0.7949	0.2757
31	CT4	−0.7272	0.5261
32	DC2	−0.7368	0.4428
33	FGCOEAST	0.9538	−1.4485
34	FGCOWEST	0.9668	−1.4387
35	FGGREAST	0.4289	−0.536
36	FGGRWEST	0.6561	−0.8703

Number	Plot Name	NMS Axis 1	NMS Axis 2
37	FGWHEAST	0.7859	−0.7547
38	FGWHWEST	0.1705	−0.2312
39	GT1	−0.5135	0.2641
40	GT2	−0.805	0.3137
41	GT3	−0.6047	0.4354
42	GT4	−0.5583	0.4325
43	GT6	−0.9003	0.1604
44	HACO	1.0427	−0.4462
45	HAGR	0.5716	−0.087
46	HAWH	0.6326	−0.0772
47	IECONORT	0.7958	−1.1533
48	IECOSOUT	1.1287	−1.1539
49	IEGRNORT	0.8063	−0.4866
50	IEGRSOUT	1.2578	−0.6702
51	IEWHNORT	1.5099	−0.2904
52	IEWHSOUT	0.8772	−1.2227
53	MFCO	0.5167	−0.6556
54	MFGR	1.1877	−0.4876
55	MFWH	0.7169	−0.2876
56	NE2	−0.527	0.3297
57	NE4	−0.3211	0.2471
58	PN11	−0.1854	−0.6176
59	PN16	−0.008	1.7898
60	PN17	−0.5702	0.8231
61	PN18	−0.1063	1.198
62	PN19	−0.0404	−0.3175
63	PN23	−0.6918	0.6956
64	PN31	0.272	1.0562
65	PN33	1.1818	0.2187
66	PN35	0.3001	0.46
67	PN39	−0.1616	0.4338
68	PN47	1.0223	1.0923
69	PN51	0.5705	1.1149
70	PN57	0.3528	0.3963
71	PN60	0.1096	−0.4473
72	PN62	0.8349	0.8885
73	PN64	0.6578	0.7179
74	PN65	−0.0564	0.0225
75	PN66	1.3169	0.7308

Number	Plot Name	NMS Axis 1	NMS Axis 2
76	PN69	−0.537	−0.6426
77	POC10	0.124	−0.9842
78	POC11	0.6968	−1.706
79	POC12	0.4206	−1.6201
80	POC9	0.4134	−1.3082
81	RBCOEAST	1.0259	0.6876
82	RBCOWEST	0.8987	0.4363
83	RBGREAST	1.3534	0.3599
84	RBGRWEST	0.8941	−0.0219
85	RBWHEAST	0.5951	0.2847
86	RBWHWEST	0.8923	0.2117
87	SC1	0.3984	−0.678
88	SC2	−0.2017	0.2883
89	VL2	0.0952	0.1108
90	VL3	0.3522	−0.5739
91	VL4	−0.098	−0.4029
92	VL5	0.1793	−0.6329
93	VL6	0.2922	1.4442

Appendix 13-F

Correlation Coefficients (r) and Coefficients of Determination (r^2) for Plant Species with NMS Axes 1 and 2 Scores for 85 Pine-Dominated Permanent MCBCL Vegetation Monitoring Plots

Correlation coefficients (r) and coefficients of determination (r^2) for plant species with NMS Axes 1 and 2 scores for 85 pine-dominated permanent MCBCL vegetation monitoring plots.

Species codes correspond to the species names listed in Appendix 13-A.

Species Code	NMS Axis 1 r	NMS Axis 1 r^2	NMS Axis 2 r	NMS Axis 2 r^2
ANDCOM	0.266	0.071	0.198	0.039
ACERUB	−0.45	0.203	−0.111	0.012
AGAFAS	0.024	0.001	0.022	0
ANDCAP	0.152	0.023	−0.011	0
ANDGLA	−0.075	0.006	−0.24	0.058
ANDGLO	0.104	0.011	−0.163	0.027
ARISTR	0.708	0.501	−0.258	0.067
AROARB	−0.124	0.015	−0.127	0.016
ARUTEC	−0.09	0.008	−0.142	0.02
ASCAMP	0.123	0.015	−0.038	0.001
ASCPED	0.182	0.033	−0.091	0.008
ASTSLONGLEAF	0.086	0.007	0.045	0.002
BACHAL	−0.119	0.014	0.033	0.001
CARSLONGLEAF	−0.161	0.026	−0.044	0.002
CARBEL	0.119	0.014	−0.09	0.008
CAROLONGLEAF	0.462	0.214	−0.214	0.046
CARTOM	−0.044	0.002	0.285	0.081
CHANPF	0.085	0.007	−0.013	0
CHAMAN	0.076	0.006	−0.199	0.04
CHRGOS	0.174	0.03	−0.087	0.008
CIRREP	0.203	0.041	−0.074	0.005
CIRVUL	0.21	0.044	0.036	0.001
CLEBPD	0.155	0.024	−0.113	0.013
CLEALN	0.041	0.002	−0.131	0.017
CNISTI	0.421	0.178	−0.08	0.006
CORLIN	0.048	0.002	−0.149	0.022
CORUK	−0.074	0.005	0.301	0.091
CROPUR	0.157	0.025	−0.095	0.009
CTEARO	0.055	0.003	−0.128	0.016
CYRRAC	0.015	0	−0.105	0.011
DESSLONGLEAF	0.017	0	0.27	0.073
DESCIL	0.141	0.02	−0.079	0.006
DESLIN	0.084	0.007	0.085	0.007
DESMAR	0.08	0.006	0.105	0.011

Species Code	NMS Axis 1 r	NMS Axis 1 r^2	NMS Axis 2 r	NMS Axis 2 r^2
DESPAN	0.193	0.037	−0.139	0.019
DESTEN	0.186	0.035	−0.174	0.03
DICSPP	−0.137	0.019	0.351	0.123
DICANG	0.225	0.051	−0.175	0.03
DICCOM	−0.044	0.002	0.234	0.055
DICENS	0.187	0.035	0.127	0.016
DICMAT	0.045	0.002	0.033	0.001
DICOVA	0.117	0.014	−0.036	0.001
DICPOR	0.015	0	0.145	0.021
DICPSP	0.21	0.044	−0.189	0.036
DICTEN	0.13	0.017	−0.073	0.005
DICVIL	0.194	0.038	−0.094	0.009
DIOMUS	−0.038	0.001	−0.266	0.071
DIOVIR	0.166	0.028	0.245	0.06
ELEPHA	−0.025	0.001	0.166	0.028
ERIVER	0.047	0.002	−0.138	0.019
EUBRAC	0.124	0.015	−0.093	0.009
EUPSPP	0.095	0.009	0.039	0.002
EUPALB	0.194	0.038	−0.121	0.015
EUPCAP	−0.098	0.01	0.373	0.139
EUPLEU	0.089	0.008	0.111	0.012
EUPPIL	0.049	0.002	−0.183	0.034
EUPROT	−0.012	0	−0.16	0.025
EUPIPE	0.326	0.107	−0.129	0.017
EURPAL	0.077	0.006	−0.148	0.022
EUTCAR	0	0	−0.113	0.013
GALRVV	0.277	0.077	−0.063	0.004
GALERE	0.174	0.03	−0.095	0.009
GALVPV	0.134	0.018	0.043	0.002
GAYDUM	0.423	0.179	−0.188	0.035
GAYFR	0.156	0.024	−0.086	0.007
GELSEM	−0.097	0.009	0.3	0.09
GENAUT	0.16	0.025	−0.139	0.019
GORLAS	−0.179	0.032	−0.142	0.02
GYMBRE	0.161	0.026	−0.178	0.032
HELANG	0.164	0.027	−0.149	0.022
HELHET	0.062	0.004	−0.137	0.019
HIEGRO	0.197	0.039	−0.158	0.025
HIEMAR	0.167	0.028	−0.074	0.005

Species Code	NMS Axis 1 r	NMS Axis 1 r^2	NMS Axis 2 r	NMS Axis 2 r^2
HYPCRU	0.052	0.003	−0.114	0.013
HYPHYP	0.041	0.002	0.194	0.038
HYPTEN	−0.014	0	0.309	0.096
ILECOR	−0.192	0.037	−0.035	0.001
ILEGLA	0.058	0.003	−0.127	0.016
ILEOPA	−0.13	0.017	−0.006	0
IONLIN	0.323	0.104	−0.152	0.023
IPOMOE	0.122	0.015	−0.084	0.007
IRIVER	0.42	0.176	−0.166	0.028
JUNSCI	0.035	0.001	0.104	0.011
KALCAR	0.05	0.002	−0.121	0.015
LACANC	0.086	0.007	−0.148	0.022
LECMIN	0.158	0.025	−0.047	0.002
LESANG	0.126	0.016	0.038	0.001
LESCAP	−0.024	0.001	0.283	0.08
LESHIR	0.139	0.019	−0.006	0
LESHPC	0.135	0.018	−0.082	0.007
LESVIR	0.215	0.046	−0.181	0.033
LIAPPV	0.394	0.155	0.052	0.003
LIQSTY	−0.182	0.033	0.147	0.022
LOBNUT	0.104	0.011	−0.129	0.017
LUDVIR	0.132	0.017	−0.17	0.029
LYCALO	0.047	0.002	−0.138	0.019
LYOLIG	0.05	0.003	−0.139	0.019
LYOLUC	−0.592	0.35	−0.268	0.072
LYOMAR	0.184	0.034	−0.031	0.001
MAGVIR	0.078	0.006	−0.172	0.029
MORCAR	0.1	0.01	−0.176	0.031
MORCER	0.192	0.037	0.071	0.005
MORPUM	0.266	0.071	−0.186	0.034
MUHEXP	0.068	0.005	−0.057	0.003
NYSSYL	−0.165	0.027	0.046	0.002
OSMCIN	−0.3	0.09	−0.215	0.046
OSMREG	−0.136	0.018	0.015	0
PANVIR	−0.091	0.008	0.287	0.082
PARQUI	−0.132	0.017	0.19	0.036
PERPAL	−0.379	0.144	−0.248	0.061
PINPAL	0.573	0.329	−0.304	0.093
PINSER	0.114	0.013	−0.196	0.038

Species Code	NMS Axis 1 r	NMS Axis 1 r^2	NMS Axis 2 r	NMS Axis 2 r^2
PINTAE	−0.285	0.081	−0.042	0.002
PITGRA	0.311	0.097	0.072	0.005
PLATAN	0.11	0.012	−0.159	0.025
POLINC	0.079	0.006	−0.1	0.01
POLLUT	0.088	0.008	0.215	0.046
PRUSER	0.162	0.026	−0.116	0.013
PTQU	0.046	0.002	−0.329	0.109
PTEPYC	0.211	0.045	−0.085	0.007
PYXBAR	0.086	0.007	−0.132	0.017
QUESPP	−0.049	0.002	0.229	0.052
QUEFAL	0.142	0.02	−0.085	0.007
QUEGEM	0.187	0.035	−0.101	0.01
QUEHEM	0.253	0.064	−0.05	0.002
QUEINC	0.299	0.089	−0.143	0.02
QUELAE	0.318	0.101	−0.06	0.004
QUEMAR	0.21	0.044	0.082	0.007
QUEMVM	0.105	0.011	0.038	0.001
QUEMPM	0.187	0.035	−0.069	0.005
QUENIG	0.107	0.011	0.008	0
QUESTE	0.142	0.02	−0.065	0.004
QUEVIR	0.049	0.002	0.096	0.009
QUEXASH	0.206	0.042	−0.042	0.002
RHEALI	0.039	0.002	0.052	0.003
RHELUT	0.041	0.002	−0.098	0.01
RHEMAR	−0.07	0.005	0.254	0.064
RHEPET	−0.01	0	−0.122	0.015
RHOATL	0.098	0.01	−0.12	0.014
RHUCOP	0.131	0.017	0.224	0.05
RHYSPP	−0.026	0.001	−0.058	0.003
RHYPLU	0.151	0.023	−0.082	0.007
ROBSPP	0.139	0.019	0.091	0.008
RUBSPP	0.005	0	0.299	0.089
SACCHA	0.082	0.007	−0.159	0.025
SASALB	0.215	0.046	0.069	0.005
SCLCCE	0.163	0.026	−0.089	0.008
SCLCVG	0.147	0.021	−0.089	0.008
SCLNIT	0.261	0.068	−0.059	0.003
SERAST	0.169	0.029	−0.133	0.018
SERLIN	0.068	0.005	−0.139	0.019

Species Code	NMS Axis 1 r	NMS Axis 1 r^2	NMS Axis 2 r	NMS Axis 2 r^2
SERTOR	0.453	0.205	0.019	0
SILCOM	0.139	0.019	−0.039	0.001
SISCAP	0.101	0.01	−0.158	0.025
SMIBON	−0.034	0.001	0.38	0.144
SMIGLA	−0.032	0.001	0.265	0.07
SMILAU	−0.214	0.046	0.05	0.002
SMIROT	−0.09	0.008	0.106	0.011
SOLARU	0.132	0.017	−0.049	0.002
SOLODO	−0.049	0.002	0.302	0.091
SOLOVO	0.331	0.11	−0.181	0.033
SOLPUL	0.066	0.004	−0.153	0.023
SOLSTR	0.054	0.003	−0.157	0.025
SORAME	−0.037	0.001	−0.022	0
SPILVG	0.227	0.051	−0.153	0.023
SPOPIN	0.054	0.003	−0.112	0.012
STYBIF	0.256	0.065	−0.111	0.012
SYMDVD	0.166	0.028	−0.162	0.026
SYMWAL	0.253	0.064	−0.189	0.036
SYMTIN	0.008	0	−0.006	0
TEPFLO	0.173	0.03	−0.056	0.003
TEPHIS	0.26	0.068	−0.146	0.021
TOXPUB	0.221	0.049	−0.031	0.001
TOXRAD	−0.085	0.007	0.231	0.054
TRAURE	0.315	0.099	−0.124	0.015
VACARB	0.174	0.03	−0.072	0.005
VACCRA	0.227	0.052	−0.132	0.018
VACFOR	−0.117	0.014	0.21	0.044
VACFUS	0.046	0.002	0.01	0
VASTA	0.311	0.097	−0.144	0.021
VACTEN	0.458	0.21	−0.012	0
VIOPRI	0.007	0	−0.088	0.008
VITROT	−0.058	0.003	0.327	0.107
WOOVIR	0.041	0.002	−0.083	0.007
XYRAMB	0.106	0.011	−0.169	0.028
XYRCAR	0.166	0.028	−0.06	0.004

Appendix 13-G

List of Scientific Publications

List of Scientific Publications

Published Papers

Smart, L., J.J. Swenson, N.L. Christensen, and J.O. Sexton. 2012. Three-dimensional characterization of pine forest type and red-cockaded woodpecker habitat by small-footprint, discrete-return LIDAR. *Forest Ecology and Management 281*:100–110.

Papers in Preparation

Mitchell, S.R., N.L. Christensen, J.W. Walters, S.A. Cohen, M. Bertone, and K. Palmquist. Soil properties drive differences in taxonomic groups among pine forests of the Atlantic coastal plain. To be submitted to *Ecological Applications*.

Mitchell, S.R., N. Christensen, and J.R. Walters. Responses to forest restoration among three trophic levels. To be submitted to *Conservation Biology*.

Mitchell, S.R., and N.L. Christensen. Dormant and growing season understory thinning to restore herbaceous plant communities typical of longleaf pine ecosystems. To be submitted to *Forest Ecology and Management*.

Mitchell, S.R., and N.L. Christensen. Vegetation variation among disturbed and managed pine stands on the lower coastal plain of North Carolina. To be submitted to *Plant Ecology*.

Christensen, N.L., and S. Mitchell. Vegetation variation on the lower Coastal Plain of North Carolina: the role of environment and disturbance. To be submitted to *Forest Ecology and Management*.

Appendix 13-H

List of Students

- Lindsey Smart, M.E.M., Nicholas School of the Environment, Duke University, Durham, NC. Three-Dimensional Characterization of Pine Forest Type and Red-Cockaded Woodpecker Habitat by Small-Footprint, Discrete Return Radar. Master's project Graduated May 2009.
- Kyle Palmquist, Ph.D. candidate, Department of Biology, University of North Carolina at Chapel Hill, Chapel Hill, NC. Species Turnover and Compositional Shifts of the Longleaf Pine Ecosystem After 18 Years.[doctoral thesis] Research Assistant, May–August 2010; expected graduation: May 2013.

[This page intentionally left blank.]

Chapter 14

Assessment of Land-Use and Land-Cover Change: Multi-temporal Vegetation Change Detection at Marine Corps Base Camp Lejeune

SERDP Project Number: RC-1413

Terrestrial Module

Lead Researcher:
Peter Harrell
Duke University Nicholas School of the Environment
Levine Science Research Center
Durham, NC 27708
E-mail: pharrel@duke.edu

June 27, 2013

Final

This report was prepared under contract to the U.S. Department of Defense (DoD) Strategic Environmental Research and Development Program (SERDP). The publication of this report does not indicate endorsement by DoD, nor should the contents be construed as reflecting the official policy or position of DoD. Reference herein to any specific commercial product, process, or service by trade name, trademark, manufacturer, or otherwise, does not necessarily constitute or imply its endorsement, recommendation, or favoring by DoD.

Table of Contents

List of Acronyms 14-v
Abstract 14-1
Objectives of the Monitoring Project 14-2
Background 14-2
Materials and Methods 14-5
    Step 1: Acquisition of Landsat TM imagery 14-5
    Step 2: Landsat Image Pre-Processing 14-7
    Step 3: Land-Cover Change Detection—Creating CVA Change Pairs 14-8
    Step 4: Land-Cover Change Detection—Multi-Temporal Change Codes 14-10
    Methods Summary 14-11
Results and Discussion 14-12
    Greenness Change Trends at MCBCL 14-12
    Permanent Change Estimates and Spatial Patterns 14-19
    Transient Change at MCBCL 14-25
    Management Implications 14-26
Assessment of Trends in the Data 14-27
Conclusions/Recommendations for Future Monitoring 14-28
Literature Cited 14-30

List of Tables

14-1. Thematic Mapper images used in the greenness change detection..... 14-7

14-2. Greenness gain and loss for MCBCL using Category 2 as a threshold..... 14-12

14-3. Greenness gain and loss for MCBCL using Category 3 as a threshold..... 14-13

14-4. Regression results of years since 1984 against % change at MCBCL. 14-15

14-5. Regression results of years since 1984 against % of change at MCBCL using change code corrected values..... 14-18

14-6. Greenness loss change occurring before and during the GTF initiative as a percentage of the land area of MCBCL. 14-26

List of Figures

14-1. Reference location of MCBCL showing satellite Path/Row boundaries and the White Oak watershed with a 2-km buffer..... 14-3

14-2. Greenness loss for MCBCL using Category 3 as a threshold..... 14-14

14-3. Greenness gain for MCBCL using Category 3 as a threshold..... 14-14

14-4. Percent loss at MCBCL for locations with change code classes showing loss in only one time interval. 14-16

14-5. % Gain at MCBCL for locations with change code classes showing gain in only one time frame. 14-17

14-6. Graphics of years since 1984 against: (A) % loss at MCBCL; (B) % gain at MCBCL..... 14-18

14-7. Change period greenness loss at MCBCL from 1984–2009 using the Threshold 3 data..... 14-20

14-8. MARSOC Rifle Range, MCBCL. 14-21

14-9. 1984–2009 change period greenness gain at MCBCL using the Threshold 3 data..... 14-22

14-10. Greenness gain data for GSRA, using the change code Threshold 2 data..... 14-24

14-11. A close-up view of several permanent re-growth areas in the GSRA. 14-25

14-12. Greenness loss (1984–2009 change pair, Threshold 3 data) as a percentage of MCBCL compartment area..... 14-27

List of Acronyms

CVA	Change Vector Analysis
DCERP	Defense Coastal/Estuarine Research Program
DoD	U.S. Department of Defense
GIS	geographic information systems
GSRA	Greater Sandy Run Area
GTF	Grow the Force (initiative)
ha	hectare
km	kilometer
m	meter
m^2	square meter
MARSOC	Marine Special Operations Command
MCBCL	Marine Corps Base Camp Lejeune
MMU	minimum mapping unit
PCA	Principal Components Analysis
r^2	r-squared values
SD	standard deviation
SDSS	Spatial Decision-Support System
SEMP	SERDP Ecosystem Management Project
SERDP	Strategic Environmental Research and Development Program
TM	Thematic Mapper (satellite imagery)
USGS	U.S. Geological Survey

[This page intentionally left blank.]

Abstract

An assessment of land-use and land-cover change was conducted to provide a comprehensive estimate of ecosystem change at regular intervals for Marine Corps Base Camp Lejeune (MCBCL) as part of the Strategic Environmental Research and Development Program's (SERDP's) Defense Coastal/Estuarine Research Program (DCERP). The objective was to monitor impacts on the vegetation resulting from human activities to aid in implementation of a long-term ecosystem-based management approach. Landsat Thematic Mapper imagery from 1984 to 2011 was used to measure vegetation greenness changes.

Images anniversary dates were spatially and atmospherically corrected. A simplified change vector analysis method was used to create change pairs and a combined multi-temporal change code. Two thresholds were established to define change/no change levels. One threshold included medium to severe intensity greenness change, and the second included only more severe change. This provided a method to bracket all change estimates.

- Based on the 1984–2009 individual change period, between 7.23–10.64% of MCBCL experienced permanent vegetation loss. Based on a conservative set of codes from the change code data, this is a range of 5.41–7.72%.
- Between 2.57% and 3.87% of the greenness loss occurred between 2005 and 2009, a period of rapid development from the Grow the Force initiative.
- Approximately 1.7% of additional greenness loss occurred from 2009 to 2011. The 2009 to 2011 change period is likely an underestimate due to problems with the 2011 image.
- Between 13.31% and 25.36% of MCBCL experienced significant greenness loss at some point between 1984 and 2009. Most of this is transient and experienced regrowth following the loss; 7.23% to 10.64% of this is permanent.
- Based on the 1984–2009 individual change period, between 3.96–10.29% of MCBCL experienced permanent vegetation gain. Based on a conservative set of codes from the change code data, this is a range of 2.75–6.79%.
- Although the Greater Sandy Run Area (GSRA) is only 33% of the area of MCBCL, it accounts for 65–75% of the permanent greenness gain. The re-growth in the GSRA follows clear-cutting performed by the paper company, which owned this area before it was acquired by MCBCL. These areas are large blocks of forest re-growth, whereas the re-growth occurring in the main unit of the MCBCL are small areas, much of which is landscaping following construction.

In addition to these quantitative results, the geographic information systems (GIS) data layers produced are spatially explicit and can be used to address any number of spatially related questions that will help the MCBCL in understanding the impact and consequences of past, present, and future management and development decisions. The data layers can address the amount of change that has occurred in any area of interest, from political management units to watershed boundaries. This information can be used as inputs to models, directly as an aid to managerial decisions through maps, tables, and GIS analysis or incorporated into a Spatial

Decision-Support System for end users to simplify the process of balancing need with ecosystem health to maintain an ecosystem-based management approach.

Keywords: Remote sensing, change detection, tassled cap, greenness change, land-cover change, change vector analysis, Marine Corps Base Camp Lejeune

Objectives of the Monitoring Project

An assessment of land-use and land-cover change was conducted to provide a comprehensive estimate of ecosystem change at regular intervals for Marine Corps Base Camp Lejeune (MCBCL) as part of the Strategic Environmental Research and Development Program's (SERDP's) Defense Coastal/Estuarine Research Program (DCERP). This was completed for the time period from 1984 to 2011. The objective was to monitor impacts on the vegetation by MCBCL activities such as construction and training exercises. This was quantified using Landsat Thematic Mapper (TM) satellite imagery to measure vegetation greenness changes, both gains and losses. Geographic information systems (GIS) data layers of the individual change intervals and the combined multi-temporal sequence are the products from this monitoring project. These data sets can be used to determine the consequences of past activities and management decisions, and provide information to help improve management choices in the future. To accomplish this, these data sets can be directly incorporated into models from the other DCERP modules to help understand ecosystem processes such as water quality. The change data sets can also be used by managers directly or within Spatial Decision-Support System (SDSS) tools to aid the application of this information to new management plans. This monitoring objective relates directly to the SERDP statement of need to develop a long-term research and monitoring program to better understand the interactions between ecologically and economically important ecosystems and military activity necessary to maintain the mission of MCBCL.

Background

The U.S. Department of Defense (DoD) intends to develop an ecosystem-based management approach for its training and testing facilities to optimize its mission objectives and the conservation of natural resources. This is a response to the increasing pressures on these facilities from development/urbanization on lands adjacent to the facility ("urban encroachment"), degradation of facility natural resources from development and training within the facility, and requirements to comply with environmental regulations. Because military installations often become refuges for rare ecological communities, an ecosystem-based management approach will help ease conflicts that may arise among the needs of the ecosystem, the environmental regulations designed to protect them, and the military objectives of the installation.

To implement sustainable management practices, SERDP has funded two research projects. An initial study was completed at Fort Benning, GA, to study the fall line/sand hill environment in a military setting. DCERP is a second research program conducted at MCBCL to study coastal and estuarine ecosystems in a military training environment. MCBCL was selected as the study site because it encompasses a large variety of natural environments in a coastal setting (**Figure 14-1**). This provides an effective training area for the U.S. Marines, but these natural environments are often fragile and/or rare and support rare and endangered species and habitats. These include well-known examples such as sea turtles and their beach nesting habitat, and the red-cockaded

woodpecker and its habitat in the pine savannas. As such, MCBCL is an ideal example of the problems facing these facilities.

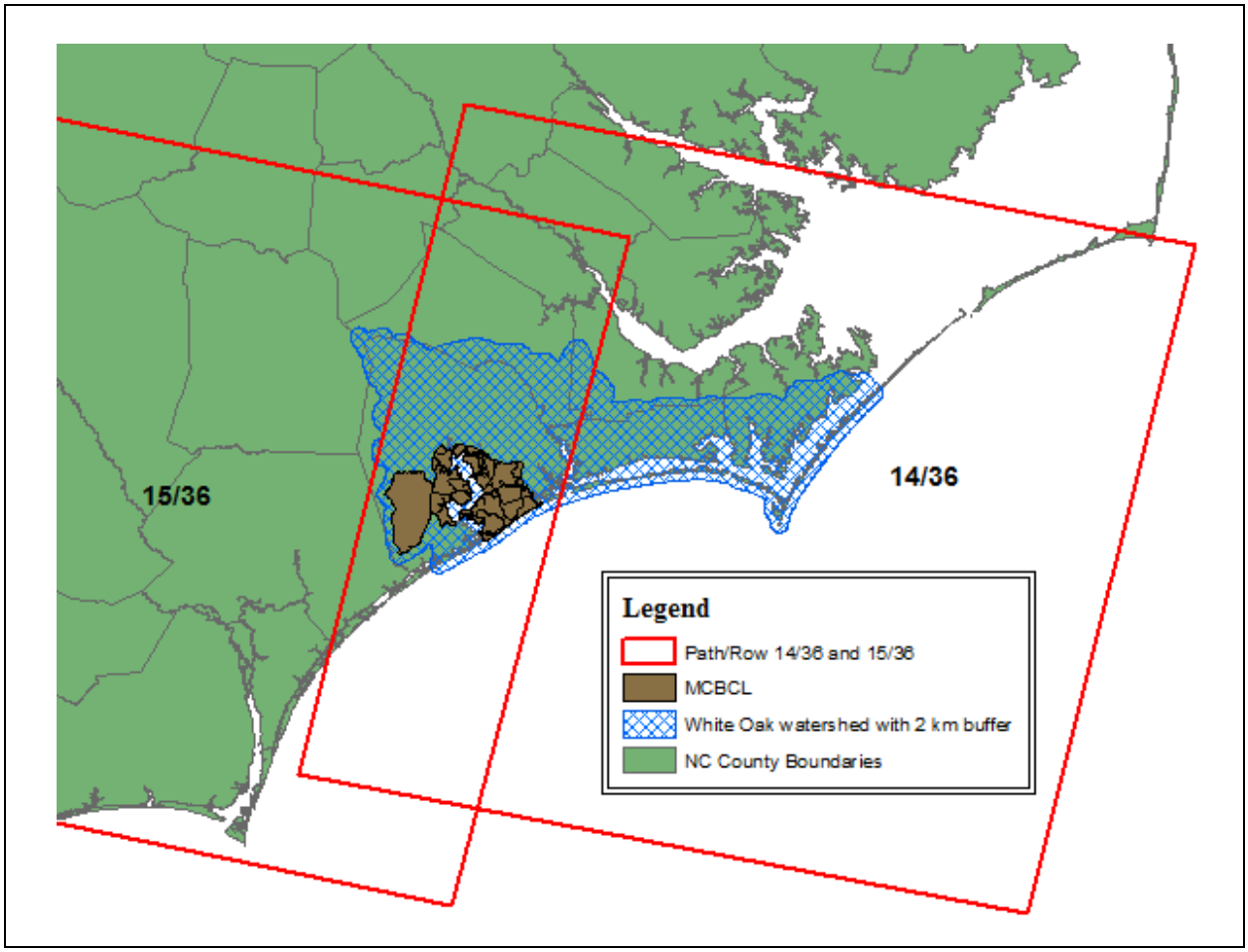

Figure 14-1. Reference location of MCBCL showing satellite Path/Row boundaries and the White Oak watershed with a 2-km buffer.

In support of this goal, a multi-temporal vegetation change detection analysis was developed as a part of the DCERP Terrestrial Module Monitoring Program. The greenness change detection assesses the impacts on the vegetation of MCBCL resulting from disturbance over time. The time sequence includes seven Landsat TM 5 images beginning in 1984 and continuing to 2011. The change detection will identify both natural and anthropogenic disturbances, but specifically focuses on military impacts resulting from infrastructure development and training activities. Change in vegetation represents both loss and grain of greenness—removal or re-growth. Further, removal can be complete, as in a clear-cut, or partial, as in reduction of greenness from training impacts.

There are many techniques for land-cover change detection (Coppin and Bauer, 1996; Coppin et al., 2004; Hayes and Sader, 2001; Yuan, et al., 1998). Change detection is often used to quantify changes in a vegetated surface, but there is no consensus as the “best” method because results depend upon the type of changes, location, and imagery used.

One effective method of vegetation change detection is Change Vector Analysis (CVA; Allen and Kupfer, 2000; Lambin and Strahler, 1994, Johnson and Kasischke, 1998; Kuzera et al., 2005; Lorena et al., 2002; Lunetta et al., 2004). CVA tracks change using a multi-dimensional space, measuring the change from initial condition to final condition as a vector direction and magnitude. The input axes for the CVA can be the original reflective bands or a derived transformation of these bands. Lambin and Strahler (1994) used a Principal Component Analysis (PCA) to create the axes used in the CVA. A better transformation, however, is the tasseled cap defined by Kauth and Thomas (1976) and updated for use with Landsat TM data by Crist and Cicone (1984a and b). Tasseled cap has been used as the input to CVA by many change studies (Allen and Kupfer, 2000; Johnson and Kasischke, 1998; Kuzera et al., 2005; Lorena et al., 2002; Lunetta et al., 2004). Using the tasseled cap has several advantages, as follows:

1. The tasseled cap reduces the data volume. The original imagery has six bands of correlated data, whereas with the transformation, you can reduce the data volume to three tasseled cap axes, all independent, that typically account for greater than 95% of the information in the original six bands (Crist and Kauth, 1986).
2. Interpretation of the tasseled cap image is more intuitive than the original reflective bands. The original reflective bands represent only a relative brightness level, whereas Crist and Cicone (1984a and b) experimentally derived the first three tasseled cap axes to represent real physical properties of the surface (brightness, greenness, and wetness).
3. The tasseled cap is an invariant transformation—the same axes are used for every image. This makes different images more comparable between scenes and over time, unlike PCA, which is highly scene dependent.

It is important to note the tasseled cap transformation does not alter the original information in the six bands of reflective data. It simply reorganizes the data for better interpretation.

CVA can then be performed on two image dates using the tasseled cap brightness, greenness, and wetness axis to identify all change (Johnson and Kasischke, 1998). Every spatial location (pixel) in the two images can now be mapped in this three-dimensional space, once at Time 1, and again at Time 2. If the pixel did not change between dates, the initial and final location in this three-dimensional space would be identical, or in practical terms, below a threshold. If there is change, the initial and final location would differ by more than the threshold value, and the change is then defined by a vector in tasseled cap space, with a given direction and magnitude.

Given that we are interested specifically in greenness gain and loss, we do not need the full dimensionality of the CVA. The first two axes of brightness and greenness can be used, simplifying the CVA to a two-dimensional space. Johnson and Kasischke (1998) suggest that vegetation reduction or removal is likely represented as a loss of greenness and gain in brightness. Conversely, we expect vegetation re-growth to be a loss of brightness and gain in greenness. This relationship is also described by Lunetta et al. (2004), who found a consistent inverse relationship between greenness and brightness and used the brightness and greenness axes to characterize change. We found brightness-greenness axes to perform well with pilot studies on greenness change for a scene, including Durham, NC (path/row 16/35), and for portions of the Tar-Pamlico watershed (path/row 15/35), also in North Carolina.

The basic method examines change between two image dates, but the CVA approach can also be used for multiple change periods in a long-term, multiple interval change study (Johnson and Kasischke, 1998). Each individual change period can be combined, using various methods to provide a temporal trajectory of change in a change code. At each spatial location, a pixel or other minimum mapping unit (MMU), the change is recorded for each interval. When recorded for all intervals, we then have a history of the change occurring at that location over time.

The greatest difficulty with this approach to greenness change is agriculture. Agriculture causes considerable confusion in the greenness change data as the status of an agricultural field is frequently different from year to year—different crops planted at different times of year or left fallow. This greenness change is generally not of interest because, although the land-cover condition changes, the land use remains the same. Lunetta et al. (2002) found a similar problem, with errors of commission for the agricultural class being much higher than other land-cover types. MCBCL has essentially no agriculture to cause this problem, making this approach particularly effective at MCBCL.

A general limitation, however, is that this process provides dynamic information, that a change has occurred, but does not inherently identify the state of the vegetation at the beginning or end dates (Johnson and Kasischke, 1998). In an over-simplified example, we may know an area lost 10 units of greenness from Time 1 to Time 2, but this could represent loss from a forest to a shrubby meadow, or a shrubby meadow to bare soil; both could give a similar greenness loss magnitude. Thus, it cannot identify qualitative differences.

One additional change detection study should be noted, as it was performed in the area directly adjacent to MCBCL. This study by Lozar et al. (2003) for the U.S. Army Corps of Engineers used Landsat satellite imagery to examine urbanization/encroachment in areas surrounding MCBCL. This change detection examined increases in urban areas in a decadal time frame for the 1970s, 1980s, and 1990s and provided this as GIS data layers. The documented change provided MCBCL with the information to plan and manage for this encroachment problem. Although its methodology differed, and the study did not include MCBCL itself, this is a useful example of a previous change detection study examining the potential conflicts that can arise between military facilities or activities and other interests.

Materials and Methods

There are four main steps in the methods for developing the vegetation change detection monitoring products. These steps are as follows: (1) selecting the Landsat TM satellite imagery, (2) pre-processing the Landsat TM images, (3) developing the individual change detection pairs, and (4) combining the individual change pairs into a multi-temporal change code. All work was conducted using ERDAS IMAGINE 9.3 and ESRI ArcGIS 10.

Step 1: Acquisition of Landsat TM imagery

A series of Landsat TM images was selected to provide both an historical and current perspective on vegetation change at MCBCL. The interval between image dates affects what change can be detected. The base reference year was 1984, which was the first year when the TM satellite was fully operational. Our goal was then to establish a two-year interval between image dates starting

in 2005 and continuing until 2011, the end of DCERP Phase II. Intervals of 1–2 years are necessary to detect all vegetation change, even if transient, in an area of rapid re-growth. This was shown by Lunetta et al. (2004) in a study using the North Carolina Piedmont/Coastal Plain. This two-year interval allows us to track vegetation change concurrent with the DCERP study. However, a two-year interval for historical images prior to 2005 would be impractical. Instead, we selected two additional images as equally spaced between 1984 and 2005 as possible to provide an historical perspective.

Ideal image intervals are complicated by a few important factors. The primary problem is with cloud cover. Images must be cloud free for the area of MCBCL. This eliminates many images. Also, Landsat TM 5 was launched on March 1, 1984. Prior to this, TM images were not available. Older imagery from the Landsat program had reduced spatial and spectral resolution that would not be comparable to the TM data, so no images prior to this date are used. To avoid adding seasonal variability to the change detection, images must be anniversary dates, within a reasonable time window. What anniversary date is optimal (spring, summer, fall) continues to be argued (Coppin and Bauer, 1996). It is likely that this depends on the type of change being studied, the location and the vegetation type. However, in practical terms, this is often less a question of what would be best than it is a matter of when you are most likely to get acceptable quality cloud-free images for the entire time period of interest, in this case, from 1984–2011. For this study, the yearly anniversary interval was from approximately the last week of April through the end of May and, if necessary, the first week of June. We found this time range the most likely to provide cloud-free images. Also, this is a time period by which trees are fully leafed out, but before high-temperature and high-humidity summer conditions create cloudy days and hazy atmospheric conditions that impact the change detection.

Given these restrictions of time and condition, acceptable images are not always available for a specific year. One advantage is that MCBCL is located in the overlap between two TM scenes—path/row 14/36 and 15/36 (**Figure 14-1**). This doubles the chances of finding acceptable images. One scene is imaged every 16 days, giving approximately four possible images of MCBCL per scene within the late April to the first week of June time frame. With two scenes, we often had eight images to choose from in a year. Even so, finding a cloud-free image every other year from 2005 onward was a challenge. We ended up with acceptable images for MCBCL from late spring in 1984, 1990, 1998, 2005, 2007 and 2009 (**Table 14-1**). The path/row boundaries vary somewhat from image to image. As such, the 1984 image from May 16, path/row 14/36 (**Table 14-1**) did not include a small area on the North West corner of Greater Sandy Run Area (GSRA), despite the "official" scene boundaries shown in **Figure 14-1**. We filled this in from the June 8, 1984, image shown in **Table 14-1** in parentheses. An image from 2011 was also included in the change detection, but was from June 19, outside the desired anniversary time window. This image had significantly more haze in the atmosphere than the other images. Also, tree leaves reflect light differently throughout the season (Coppin and Bauer, 1996), so the later June 2011 image may have a different greenness quality than it would have in May. This created problems with including this image in the change detection data. However, because this was the last year of the DCERP1 and considerable construction had occurred since the 2009 image, we used the 2011 image to produce an additional set of data specifically to cover the 2009 to 2011 period. Together, this set of images allows us to examine change over a 27-year time period at MCBCL. All images were downloaded from the U.S. Geological Survey (USGS)

Table 14-1. Thematic Mapper images used in the greenness change detection.

Additional scenes in parentheses were used for the 1984–2007 change pair to create a mosaic to cover the entire White Oak watershed. Note that May 16, 1984, path/row 14/36 was missing a small portion of the northwestern corner of the GSRA. This was filled in by the TM scene from June 8, 1984.

Date	Path/Row
May 16, 1984 (June 8, 1984)	14/36 (15/36)
May 8, 1990	15/36
May 14, 1998	15/36
May 26, 2005	14/36
April 30, 2007 (April 21, 2007)	14/36 (15/36)
April 26, 2009	15/36
June 19, 2011	15/36

Step 2: Landsat Image Pre-Processing

Images must be spatially georeferenced and radiometrically normalized before being used for change detection. The more images involved in a time sequence the more critical this becomes. Spatially, it is important that the pixels from one image to the next be georeferenced—overlap exactly—or spurious change will be identified. Horizontal accuracy of half a pixel or better is required (Lunetta, 1998). In this case, with pixels of 30 m, an error of less than 15 m was necessary. Dai and Khoram (1998) suggest that even half a pixel is insufficient and that a spatial registration of less than one-fifth of a pixel is necessary for change detection error of less than 10%. It is rarely practical, however, to achieve one-fifth of a pixel accuracy level. Objects one-fifth the size of a pixel generally are not very clear in an image and the reference data used as the "true" position also has error. In addition, USGS has different levels of processing for delivered products and, unfortunately, the processing completed by USGS amongst the seven images varied. This resulted in different horizontal accuracy amongst the images when initially acquired. For this work all images were compared to detailed North Carolina Department of Transportation road and airport vector data. Those images with a horizontal accuracy worse than 15 m were manually georeferenced so all seven images aligned. Georeferencing results were between 5.6-m and 8.3-m root mean square error, significantly better than the 15-m minimum error.

Change detection also requires consistency in the radiometric values of each image to be spectrally comparable (Coppin et al., 2004; Lunetta, 1998). Limiting imagery to anniversary dates diminishes spectral variability, as previously discussed. However, further normalization is necessary. This was done through two procedures. The first is described by Markham and Barker (1986) and updated by Chander et al. (2007), converting the image to "at-satellite" reflectance. The second procedure adjusts for atmospheric conditions and produces "at-surface" reflectance, a form of "absolute" radiometric normalization. We used a Dark Object Subtraction method to perform the atmospheric correction as described by Chavez (1996). This method was evaluated

in comparison to other methods by Song et al. (2001) and Mahiny and Turner (2007) and found to be an effective method that improved data analysis for change detection. The end result was images that were effectively normalized and comparable.

The 2011 image was an exception. The atmospheric correction for the 2011 image indicated a large haze correction was necessary; large enough that atmospheric correction was not adequate to make the 2011 image entirely comparable to the remaining images. As previously mentioned, the quality of the green vegetation is also likely to be different from the images earlier in the season. With certain caveats, however, the 2011 image can still provide useful information. Overall, the 1984–2011 pair does not effectively estimate total greenness change over the entire MCBCL. However, individual greenness change sites will still be indicated, just with a less accurate area estimate. As such, it is useful to identify new construction or new regrowth locations that occurred after the 2009 image and can be cautiously used in the multi-temporal combination of images to examine the change trajectories.

Step 3: Land-Cover Change Detection—Creating CVA Change Pairs

Following the pre-processing, the tasseled cap transformation was applied to all seven images. The tasseled cap reduces data volume and makes interpretation of the spectral information more intuitive, as discussed in the background. DCERP began in 2007, so the 1984–2007 image pair was the first set acquired and was used to establish the thresholds of what level of change was significant (specified later in the methods). We chose to use the entire White Oak watershed with a 2-km buffer as the unit for threshold determination (**Figure 14-1**). The 2-km buffer was necessary as a small portion of the GSRA is outside of the White Oak watershed, but covered by the 2-km buffer. Using the full White Oak watershed was done with two reasons in mind. First, we hoped to complete the change detection at each time interval for the entire White Oak watershed and compare change on MCBCL to change in the adjacent watershed. This proved impossible due to cloud cover—we could not put together complete cloud free coverage of the entire watershed. Second, we were concerned that MCBCL alone was too small a sample on which to base the thresholds of change or no change, but the full scene may not be representative of MCBCL. The watershed boundary provides an ecologically meaningful unit and a good compromise. To cover the entire White Oak area for 1984 and 2007, both scenes 14/36 and 15/36 (**Figure 14-1**) were necessary. In one scene, the primary scene used for MCBCL is listed first; the second scene used to include the remainder of the White Oak water shed is listed second and in parentheses. Once the thresholds for 1984–2007 were established, the 1984 and 2007 image composites were clipped to the MCBCL boundary. All other change pairs were simply sub-set to MCBCL. Water was then masked out of each change pair so the condition of waterbodies did not affect the results.

Change was then mapped using images in temporal pairs. The first two tasseled cap axes (brightness and greenness) were retained for us in the change detection. We created the following six change pairs for analysis with CVA from the seven images:

- 1984–1990
- 1984–1998
- 1984–2005

- 1984–2007
- 1984–2009
- 1984–2011.

The initial condition was always 1984. This benefits the change detection in two ways. First and most importantly, this eliminates a source of variability—our initial condition reference is always the same for every change pair. Normalization can never make the images completely calibrated, so change pairs of 1984–1990, 1990–1998, and so on would have additional error. Second, this results in a longer time window for consecutive change pair—6 years for 1984–1990 up to 27 years for 1984–2011. A longer time window emphasizes long-term or persistent change, so the increasing time period in each change pair emphasizes persistent change. The disadvantage is that in the 1984–2011 pair, for example, you would not know when, within the 27-year time frame, a change occurred. But, this information is in the other change pairs and is identified when the six change pairs are combined into a temporal change code (described later in the Methods section).

To calculate change, the brightness and greenness axes are subtracted for any given pair of images to provide a difference image:

- Brightness Time 2 = brightness; Time 1 = brightness difference
- Greenness Time 2 = greenness; Time 1 = greenness difference.

Both greenness and brightness information is necessary to identify greenness change to eliminate a number of false greenness changes that resulted if the greenness difference alone was used as described in the background. Using these difference images, Johnson and Kasischke (1998) and Lunetta et al. (2004) found a consistent inverse relationship of an increase in brightness with a decrease in greenness. We confirmed this with the pilot studies performed in the Durham, NC, area and in the Tar-Pamlico watershed. Vegetation losses are then those pixels with a gain in brightness (difference is positive) and a loss in greenness (difference is negative), whereas vegetation gains are those pixels with a loss in brightness and a gain in greenness.

Thresholds were then established to separate insignificant differences from important changes. With the variability inherent in a natural surface and the passage of time, very few pixels will be identical in the two images of a change pair. This is one difficulty in applying image differencing techniques. Fung and LeDrew (1987) and Hayes and Sader (2001) tested quantitative methods for developing thresholds, but given the small area involved here, we chose to use known change sites to determine the change threshold. Because image normalization was effective and the distribution of values for the greenness axis in all images was very similar, the 1984–2007 image pair was used to define the thresholds, and these were applied to all other change pairs.

We manually altered threshold values and compared resulting estimates of change area and location to known locations of greenness change at MCBCL and the surrounding White Oak watershed. Based on this, we established the following five categories using the mean and standard deviation of the greenness difference between the 2007 and 1984 data rather than a single cutoff:

- 0 = No change

- 1 = Minimal change (> 0 to ≤ mean – standard deviation [SD])
- 2 = Moderate change (> mean − SD to ≤ mean)
- 3 = Major change (mean to ≤ mean + SD)
- 4 = Extreme change (> mean + SD)

We again examined these different breaks in conjunction with known greenness change sites. The mean was determined as an effective value on which to base the categories. This was again confirmed with the North Carolina pilot studies. Category 1 was discarded as insignificant and set to 0. Categories 2, 3, and 4 were kept to examine the impact the different thresholds had on the change results. Every pixel then has a possible value of 0, 2, 3, or 4. When applying this data, we can then compare the estimate of change using Categories 2–4 (more area) versus only Categories 3–4 (less area, more conservative). This gives upper and lower bounds to the estimates.

The resulting change data identifies the location, size, and intensity of greenness change. However, there are many very small change sites identified. Many of these small areas represent real change, but at a scale that is not very useful. Others are registration and normalization errors or resolution issues at land-cover edges. To simplify the change data, a MMU of 5 pixels (4,500 m^2 [1.1 acres]) was applied. Change patches less than 5 pixels in size were removed, using an eight-direction model to determine connectedness. This eliminated the majority of the separate patches, but maintained the great majority of the total change area. For example, using the 1984–2007 change pair for Categories 2, 3, and 4, the 5-pixel MMU resulted in 79% fewer individual change patches, but retained 95% of the change area for the greenness loss data.

The final products from this procedure were gain and loss of greenness GIS data layers for each of the six change periods. Thus, there are six greenness gain GIS data layers and six greenness loss GIS data sets. Each identifies change locations, size, and if that change was Category 2, 3, or 4.

Step 4: Land-Cover Change Detection—Multi-Temporal Change Codes

We then used the six separate change periods to create combined multi-temporal change data sets, for greenness gain and greenness loss. This was done by creating a change code. A given change period from Step 3, such as 1984–1990, has pixels with values of “0” (no change) and “2,” “3,” or “4” (one of the significant change categories). This was converted to a simple binary condition of “0” (no change) or “1” (change) for every pixel. Because we have six individual change pairs, we need a six-digit change code to maintain an unambiguous binary code before we can combine all the change periods into one. Expanding the 0, 1 binary condition out to six digits, every pixel in the 1984–1990 change pair will now have a value of either 0 (no change) or 000001 (change). 1984–1998 will have values of 0, 000010, and so on as follows:

- 1984–1990: 0, 000001 (no change, change)
- 1984–1998: 0, 000010
- 1984–2005: 0, 000100
- 1984–2007: 0, 001000

- 1984–2009: 0, 010000
- 1984–2011: 0, 100000.

Codes are literally then added together to produce a range of pixel values from 000000, no change found at that location in any time period, to 111111, a change recorded at that location in all change periods. As with the individual change period data, we wanted to be able to bracket the change estimates from the multi-temporal change code. To accomplish this, we created two versions of this six-digit change code, one using Categories 2–4 to define change, and the second using only Categories 3–4. The six-digit change code includes the 2011 image. As noted, this image is problematic, so we also created a set of five-digit change codes without the 2011 image, ending instead with the 2009 image.

This change code process results in eight GIS data layers; four greenness gain change codes (composed of two thresholds [2, 3, 4 versus 3, 4] and with or without the 2011 image), and four greenness loss change codes (composed of two thresholds [2, 3, 4 versus 3,4] and with or without the 2011 image).

Methods Summary

These products, the individual change pairs and the multi-temporal change codes are applied to produce spatially explicit and quantitative estimates of greenness change at MCBCL. When possible, both are used to arrive at an estimate of change. Although related, each product provides an estimate of change using a different process. This allows corroboration of the estimate. The two products work well for this purpose. We can arrive at an estimate of change from the 1984–2009 change pair, for example. We then also estimate change during this period using the change code products which uses all the images in sequence. If both the multi-temporal change code and the individual change pair provides a consistent estimate of the change (each also with an upper and lower estimate), our certainty of this estimate is greatly improved. It is important to note that there are different ways to measure change and even what constitutes change. These results are estimates, not absolutes, but they are consistent and accurate relative to the change as defined in this study and provide a useful landscape metric to monitor land-use change at MCBCL.

There are two primary error sources in this data. The largest source of error in this data is georeferencing—spatially aligning each individual image. Despite efforts to reference each image, it is not possible for them to perfectly overlap. This results in edge errors of false change. The second is the normalization of one image to the next, making sure that a given value in one image means the same in another. This was the primary problem with the 2011 image. This type of error results in the difference between images being larger or smaller than the true difference. Both of these types of errors are minimized by use of the MMU and connectedness rules applied in the data processing and further reduced in importance by the use of bracketing the change estimates with two threshold values and calculating estimates using both data products. Errors that remain are a small percentage of the total and tend to be edge effects on patches and a few linear change errors along roads.

Results and Discussion

These methods result in two sets of data products—GIS data layers related to the six individual change pairs and GIS data layers related to the combination of these individual change pairs into multi-temporal change codes. These GIS data sets are both quantitative and spatially explicit, allowing us to determine what type, how much and where change occurred. This provides a history of the vegetation patterns at MCBCL since 1984.

Greenness change is a loss or gain from one time period to the next. At MCBCL, consistent greenness loss at a location over time is indicative of development and training activities. Vegetation loss typically results in habitat loss and fragmentation. Gain is indicative of re-growth following a disturbance. These changes can be permanent or transient. A permanent change is one that persists over the time periods of the study; the change is observed in one image and remains a change in following images. This is driven by development and consistently used training areas. Transient change is a gain or loss that does not persist; it is typically observed in one image, but does not continue to be indicated as a change in later images. Transient change is driven by natural annual variability in growth and human impacts, typically training areas that are used for a time then abandoned and allowed to regrow. We are able to track transient change with the change code products, but the emphasis of this work is anthropogenic permanent change at MCBCL.

Greenness Change Trends at MCBCL

Tables 14-2 and **14-3** show the greenness gain and loss results from the individual change pairs for all the land area of MCBCL, presented as area in hectares and percentages. **Table 14-2** uses Threshold 2 data (and thus includes all change of Categories 2, 3, and 4) and **Table 14-3** uses Threshold 3 data (and uses change Categories 3 and 4 only). As described in the Methods section, the 1984–2011 change pair is inconsistent with the other pairs and is not an effective measure of total change area and so is not used here.

Table 14-2. Greenness gain and loss for MCBCL using Category 2 as a threshold.

Change code corrected values are in parentheses.

Change Period	Loss (Ha) Intensity 2–4	% MCBCL	Gain (Ha) Intensity 2–4	% MCBCL
1984–1990	3422.43	6.78	15315.66	30.34
1984–1998	4842.18	9.59	8506.08	16.85
1984–2005	6773.67	13.42	10027.80	19.87 (14.76)
1984–2007	14398.74	28.52 (12.12)	4376.07	8.67
1984–2009	5372.82	10.64	5192.28	10.29

In 1984, a certain amount of land at MCBCL was already developed for structures, roads, and training areas. Over time, through to 2009, more and more area of the Base was developed for infrastructure and training. Development is generally a permanent or at least persistent change for the time scales used here. Development also results in vegetation removal or reduction. As such, we would expect the amount of greenness loss to be greater in each successive change pair relative to the 1984 condition. Conversely, we would expect the area of green gain to decrease as

some of the vegetation regrowth is again disturbed and converted to developed areas. Some transient change is recorded in this data if the temporary change occurred close in time to the end date image, but, with 6 years or more between images in the change pairs, permanent development is the primary factor and the longer the time window, the more this is true.

In **Table 14-2**, we do see this pattern to some extent, but with a great deal of variability in both the greenness loss and gain data, particularly with the 2005 and 2007 end dates, which indicate large, temporary increases in change. The change is responding to more than permanently developed areas, which are not appearing and disappearing. This data uses Categories 2, 3 and 4, and Category 2 in particular (moderate change), includes a great deal of natural year to year variability probably due to growing conditions.

In **Table 14-3**, we eliminate Category 2 as change, and only look at change Categories 3 and 4. The change in greenness necessary to register as significant is considerably higher for this threshold. Natural variability has less impact on this type of change, though tornadoes or hurricanes can certainly cause this type of vegetation reduction. Nevertheless, the change results should be more closely linked to persistent change resulting from development and we do in fact see much more consistent patterns. Greenness loss increases from 2.87% of MCBCL in the 1984–1990 time frame to 7.23% by 2009 and gain decreases from 7.72% of MCBCL showing regrowth in the 1984–1990 time frame to 3.96% in 2009.

Table 14-3. Greenness gain and loss for MCBCL using Category 3 as a threshold.

Change code corrected values are in parentheses.

Change Period	Loss (Ha) Intensity 3-4	% MCBCL	Gain (Ha) Intensity 3-4	% MCBCL
1984–1990	1447.92	2.87	3895.29	7.72
1984–1998	2279.97	4.52	2911.32	5.77
1984–2005	2351.97	4.66	4204.44	8.33 (5.92)
1984–2007	6264.54	12.41 (6.08)	1781.73	3.53
1984–2009	3647.52	7.23	2000.34	3.96

There are still two major departures from this trend, however, still the 2005 and 2007 image dates. In the 1984–2007 period, there is 12.41% of MCBCL showing a loss of greenness, much higher than 2005 or 2009. In the 1984–2005 period, greenness gain is higher than would be expected from the trend in the remaining time periods, higher even than the initial 1984–1990 pair. The data in **Table 14-3** is shown graphically in **Figure 14-2** (loss) and **Figure 14-3** (gain). The outliers for greenness loss in 1984–2007 and gain in 1984–2005 are clear in these figures.

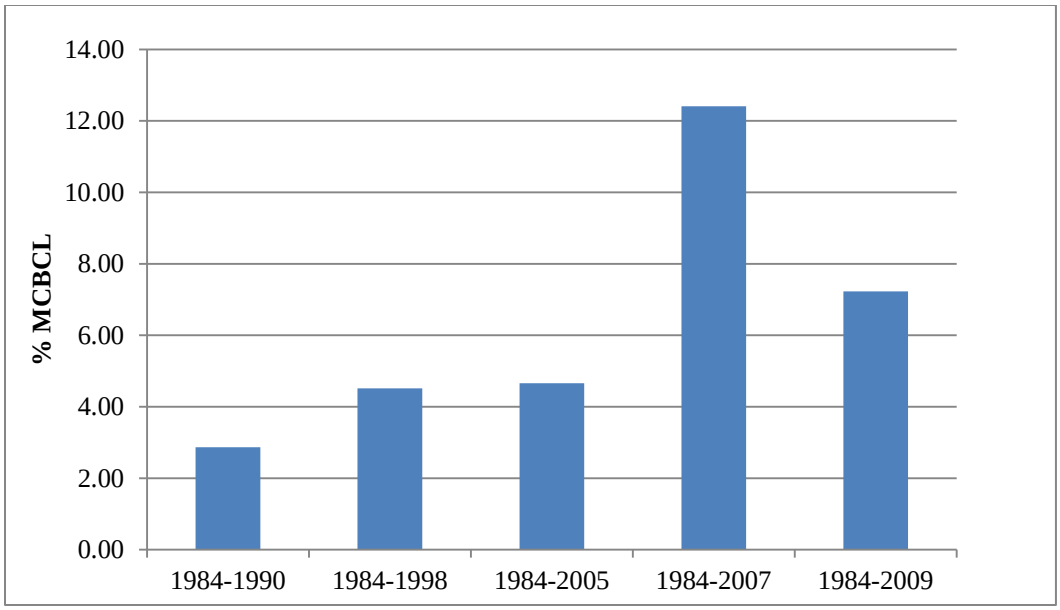

Figure 14-2. Greenness loss for MCBCL using Category 3 as a threshold.

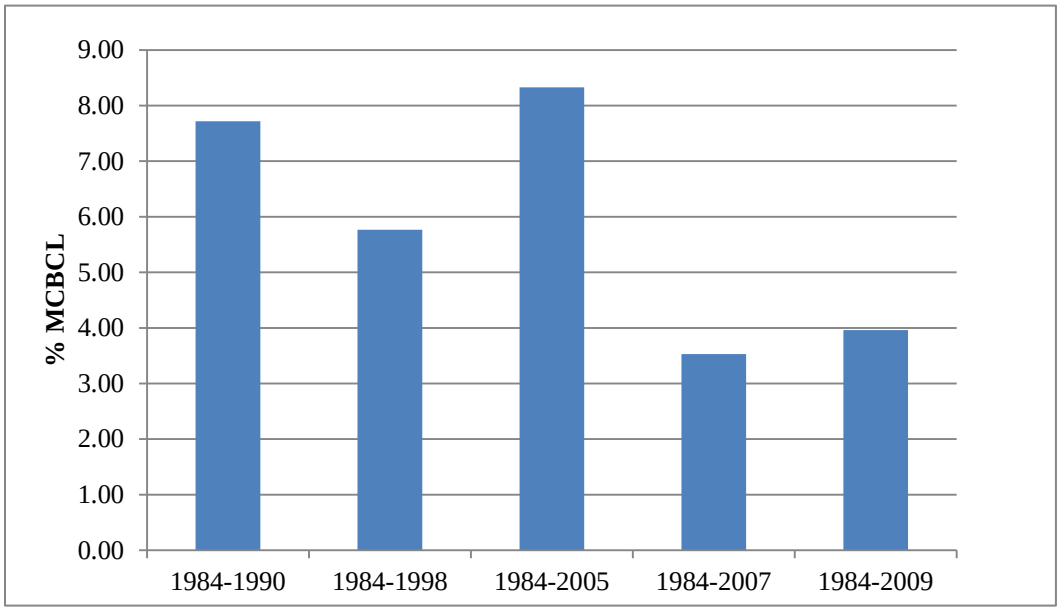

Figure 14-3. Greenness gain for MCBCL using Category 3 as a threshold.

To quantify the significance of the trend, we created very simple regressions of the data shown in **Table 14-3** and **Figures 14-2** and **14-3** with number of years since 1984 used to predict % change (**Table 14-4)**. This shows very low adjusted r-squared (r^2) values and no significance for this trend of increasing loss area and decreasing gain area over time, but this is largely due to the one outlier in both the loss and gain data, which is greatly driving the fitted regression line. Other factors than developed area are playing a bigger role for the 1984–2007 loss data and the 1984–2005 gain data than in the rest of the change pairs.

Table 14-4. Regression results of years since 1984 against % change at MCBCL.

Data used are from Tables 14-2 and 14-3.

Change	Adjusted r^2	Probability
Gain, Threshold 3	0.13	0.2980
Loss, Threshold 3	0.30	0.1963

We can be more specific about the timing of these two outliers. The extreme greenness loss we see at these specific locations in the 1984–2007 pair is only present in the 2007 image—it is not present in the 2005 image or any other images prior to this. It also does not exist in the 2009 image, so the greenness loss did not persist beyond 2007. Similarly, the high levels of greenness gain at these specific locations that we see in the 1984–2005 pair is only present in the 2005 image, not in any others before or after. These events are showing high levels of change only in these specific images; no change at these same locations is found in images before or after. Given this specificity, we can use the change code data products to quantify how much greenness loss is unique to only the 2007 image and how much gain is unique to the 2005 image.

The change code records when a change occurred relative to our image dates for every pixel location at MCBCL. To identify how much greenness loss is unique to only 2007, we look for a greenness loss change code of 01000 (see methods, Step 4 for a description of the codes). A pixel with a change code of 01000 indicates a greenness loss occurred at that pixel after the 2005 image and is present in the 2007 image and no others. Summing all pixels with a value of 01000 gives the area and percentage of MCBCL that had a loss only in the 2007 image. This relates directly to the very high greenness loss for the 1984–2007 change period in **Table 14-3**. We can use this value to correct the 12.41% of greenness loss for the 1984–2007 change period. To identify how much greenness gain is unique to only 2005, we look for a greenness gain change code of 00100. This relates directly to the high greenness gain values for the 1984–2005 change period in **Table 14-3**. This can be used to correct the 8.33% of greenness gain for the 1984–2005 change period.

However, we need to know if we are justified in making this correction. Every image will have some amount of area that shows change that is unique to that specific image and no other—are these gains and losses in 2005 and 2007 truly unusual compared to the other images? This type of change unique to one image is transient change that occurred just before the image was captured. This may result from error, natural variability or anthropogenic change, typically a temporary loss of greenness that is captured in the image before it greens back up again by the time the next image is taken. We examined all these unique change codes to be certain that the 2007 image is an outlier from the rest and has much more greenness loss, and the 2005 image is an outlier with more greenness gain. These unique changes are pixels with change codes 00001 (change only in 1990), 00010 (change only in 1998), 00100 (change only in 2005), 01000 (change only in 2007), and 10000 (change in 2009). We compared these to see if the loss outlier code 01000 and the gain outlier code 00100 that corresponded to the unexpected values in **Table 14-3** were significantly higher than the others.

In **Figures 14-4 and 14-5**, we can see these codes were at least double the values of the other time periods. In **Figure 14-4**, we see that some major impact after the 2005 and before the 2007

image caused considerable greenness loss, 6.33%, unique only to the 2007 image. These locations on the Base did not record a greenness loss before or after this. This is much larger loss unique to one time period than any other time frame in the change analysis. Codes for the images of 1990, 1998, and 2005 are all 1.41% of the greenness loss or less. The 2009 change (code 10000) is somewhat higher, but this is due to it being the final image in the change code. Not all of this 2.20% is unique. We do not have an effective 2011 image that would likely show a portion of this 2009 loss is actually persistent development that continues as a loss into the next time period.

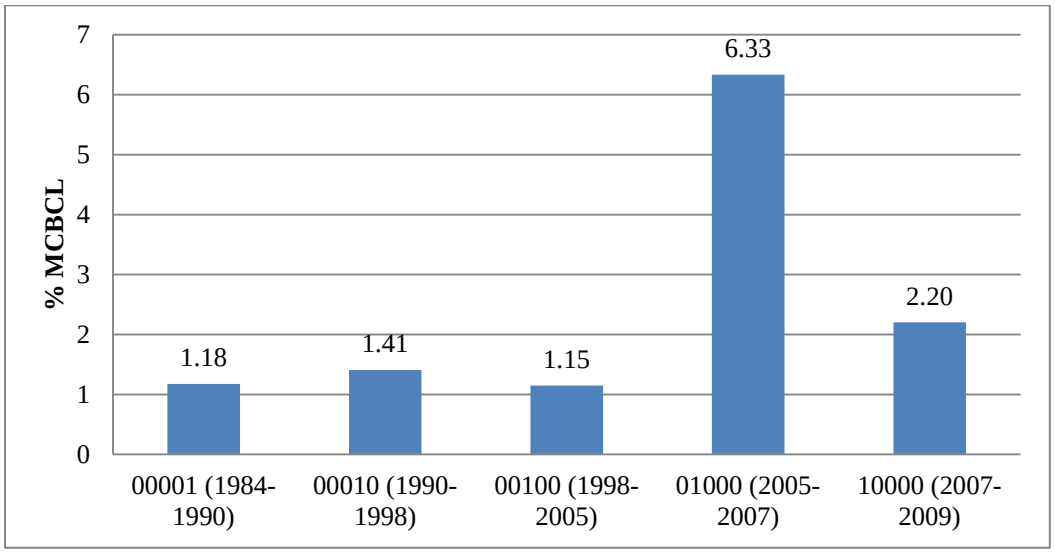

Figure 14-4. Percent loss at MCBCL for locations with change code classes showing loss in only one time interval.

These results are using a threshold of 3, major greenness loss only.

This loss anomaly in the 2007 image is a likely result of drought and heat stress. According to National Oceanic and Atmospheric Administration records from approximately late 2005 to winter 2007, the Southeast experienced abnormally high temperatures and severe drought, particularly in 2007, which, by some measures, was the worst drought on record in North Carolina. Based on the change results, this was severe enough to cause a major reduction in vegetation greenness, and the 6.33% shown in **Figure 14-4** is a direct measure of its impact. We overlaid the land-cover types for MCBCL with the locations of greenness loss change code 01000. The great majority of this "loss" is in vegetated areas of the MCBCL, largely pocosin types that remained unchanged in terms of land-cover type before and after 2007. These areas likely suffered reduced productivity and leaf area during the severe 2007 weather, but recovered by the time the 2009 image was captured.

Figure 14-5 shows the results of the greenness gains unique to a specific image. We see two values of gain higher than the remainder. The data from the 1984–2005 change period that we believe relates to the gain outlier shown in **Table 14-3** is the highest value at 2.41%, several times as large as any other time period except for the 1984–1990 period with 1.96%. The 1984–1990 period had considerable area that was clear-cut prior to 1984 with vegetation regrowth by 1990, resulting in the 1.96% of greenness gain. The great majority of this vegetation regrowth

was occurring in the GSRA, which was owned by a paper company until 1992. Much of this regrowing clear-cut area was then cleared again for military use prior to the 1998 image, so this gain unique to 1984–1990 is a real identifiable event and will be discussed in more detail later. This leaves the anomalous gain that occurred in the 2005 image. We are not certain of the cause of this gain, but it is much greater than gains in 1998, 2007 or 2009. There is no indication of land use as the cause. Regrowth after cuts made prior to 1998 and regrowth prior to 2005 could cause a spike in greenness gain just as it did with the 1990 data, but there is no record of clear-cuts in the greenness loss data for 1998 or MCBCL records to support this. The gain is not present in obvious clear-cut patches, but scattered as small areas throughout the MCBCL. It is not as large a deviation as the 2007 loss anomaly and there are 6 years in this time frame between images rather than the 2 years between 2005 and 2007 which results in more uncertainty. Perhaps the conditions immediately leading up to the image in 2005 resulted in an excellent period of growth and this resulted in a significantly higher greenness value for vegetated areas of the MCBCL. However, we cannot be certain. Good growing periods are not documented so obviously as disasters like severe drought. We do know the amount of gain for this specific time was unusually high and this relates to the greenness gain outlier in **Table 14-3** for 2005.

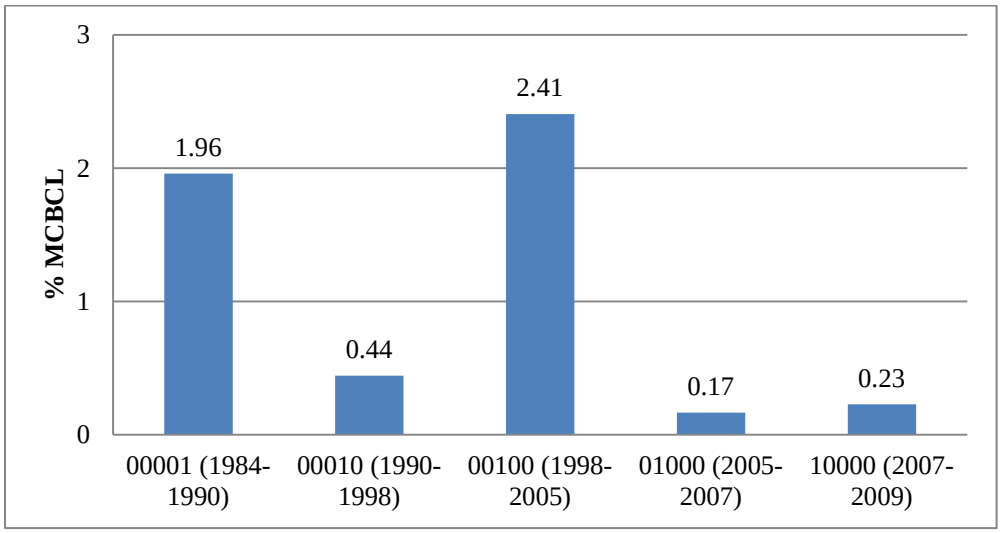

Figure 14-5. % Gain at MCBCL for locations with change code classes showing gain in only one time frame.

These results are using a threshold of 3, major greenness gain only.

Based on the results presented in **Figures 14-4** and **14-5**, we believe these percentages from greenness loss change code 01000 and greenness gain change code 00100 can be used as corrections to the outliers in **Table 14-3**. For greenness loss, the 01000 change code correction value is 6.33%. For greenness gain, the 00100 change code correction value is 2.41%. The corrected values for the 1984–2007 loss period and 1984–2005 gain period are shown in parentheses in **Table 14-3**. They are lower by the corresponding change code correction value. **Table 14-5** shows the regression results using the corrected values.

Table 14-5. Regression results of years since 1984 against % of change at MCBCL using change code corrected values.

Data used are from Tables 14-2 and 14-3.

Change	Adjusted r^2	Probability
Gain, Threshold 3	0.74	0.0381
Loss, Threshold 3	0.79	0.0268

Compared to **Table 14-4**, adjusted r^2 values are much higher, and both significant at 0.05 probability level. For gain, the r^2 value went from 0.13 to 0.74 with the correction. For loss, the r^2 value went from 0.30 to 0.79. **Figure 14-6** shows the regression results from **Table 14-5** graphically. Results are solid and the line fit is not driven by a single outlier.

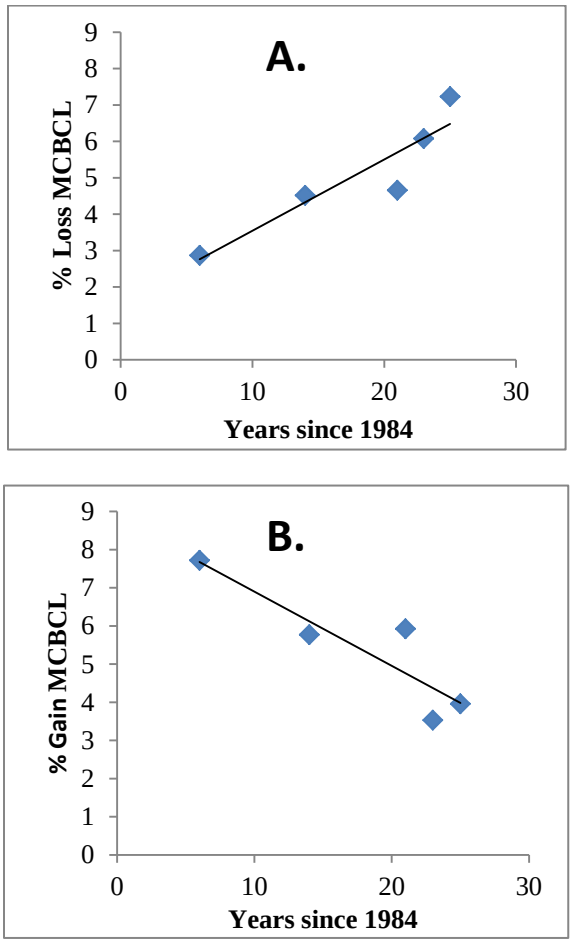

Figure 14-6. Graphics of years since 1984 against: (A) % loss at MCBCL; (B) % gain at MCBCL.

Results based on a threshold of 3. Data are from Table 14-3. Line fit represents regression results shown in Table 14-4.

Permanent Change Estimates and Spatial Patterns

The previous results show the overall quantitative trends of greenness gain and loss at MCBCL. But, one of the real strengths of these data sets is that they can be used to address spatial patterns. As stated, the primary goal is identifying permanent anthropogenic change. We can examine the spatial patterns in the change pair data from **Table 14-3**, and also estimate permanent change using the change code.

As mentioned previously, the 1984–2009 change period is one estimate of permanent change. With the long time period of 25 years between the start and end dates, we have confidence that most of the recorded change has persisted for many years and greenness loss of the 1984–2009 change period is then due primarily to development of new infrastructure and continuously used training facilities and permanent within the time frame of this study. We can use data with a threshold of 2 (more liberal) and with a threshold of 3 (more conservative) to bracket this estimate. From **Table 14-2**, we have an estimate of 10.64% of MCBCL that has lost greenness between 1984 and 2009. Using the Threshold 3 data (**Table 14-3**), our estimate is 7.23%. Again, using Category 2 does include some natural change, but also less severe but persistent anthropogenic loss. These may be training areas consistently used, but not completely cleared of vegetation. The data using only major change (with Category 3 as the threshold) eliminate much of the non-anthropogenic loss from the estimate, and we can have more certainty of this value. This results in a range of 7.23–10.64%, and represents permanent loss of vegetation, locations that are now buildings, parking lots, roads, and consistently used training areas. **Figure 14-7** shows the distribution of greenness loss across MCBCL for the 1984–2009 change period, using Threshold 3. Distinct patches of cleared areas are obvious, a result of vegetation removal for training activities, structures, and linear features from road construction.

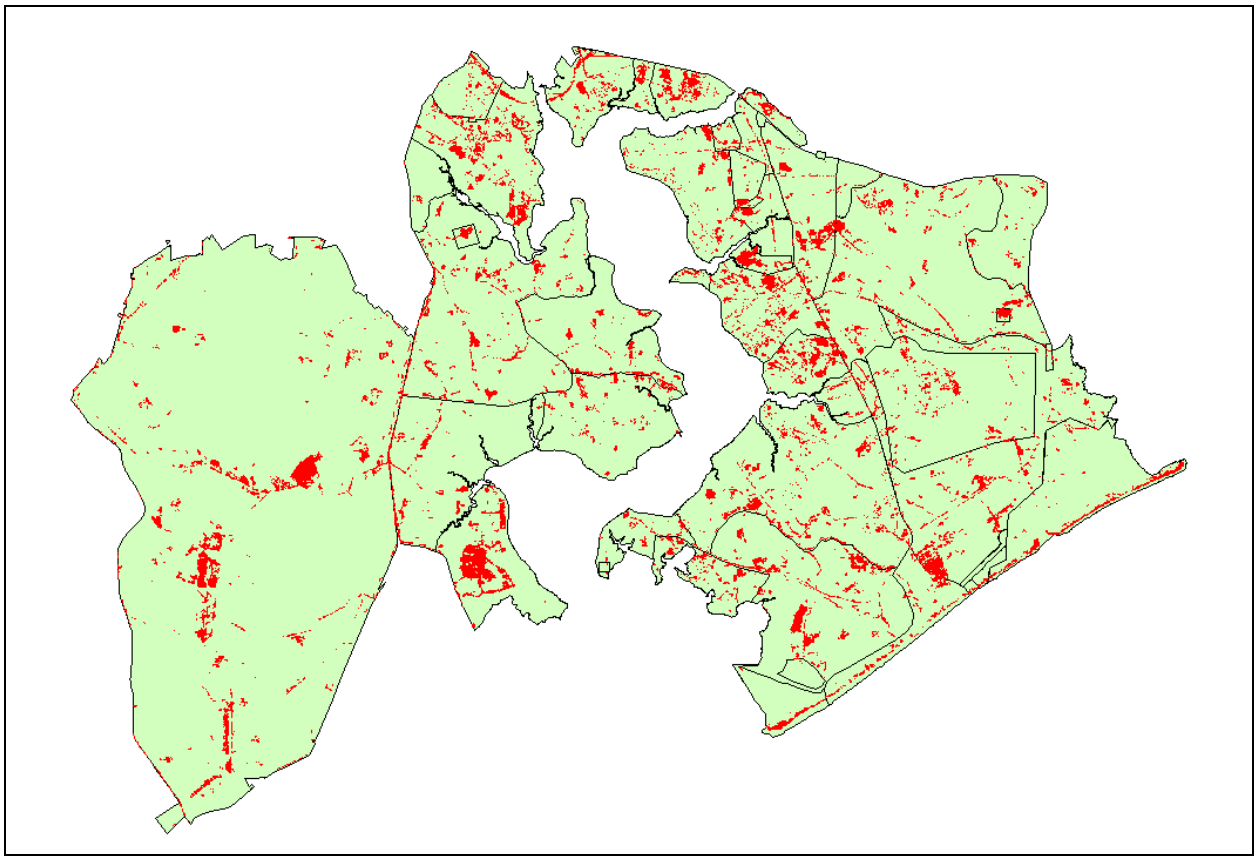

Figure 14-7. Change period greenness loss at MCBCL from 1984–2009 using the Threshold 3 data.

This is the spatial representation of the data shown in Table 14-3.

Figure 14-8 shows this greenness loss in more detail for one specific loss patch, the development of the Marine Special Operations Command (MARSOC). The locator map shows the location within the greater MCBCL area. **Figure 14-8**A shows the greenness loss identified from the 1984–2009 change period in red overlaid on the 1984 image. In 1984, this area is forested, as indicated by the dark green color within the patch. **Figure 14-8B** shows this same greenness loss patch overlaid on the 2009 image, where we see the forest has been removed, resulting in an area of high brightness and low greenness. Small pockets of vegetation that have remained can be seen as small green "islands" in the 2009 image.

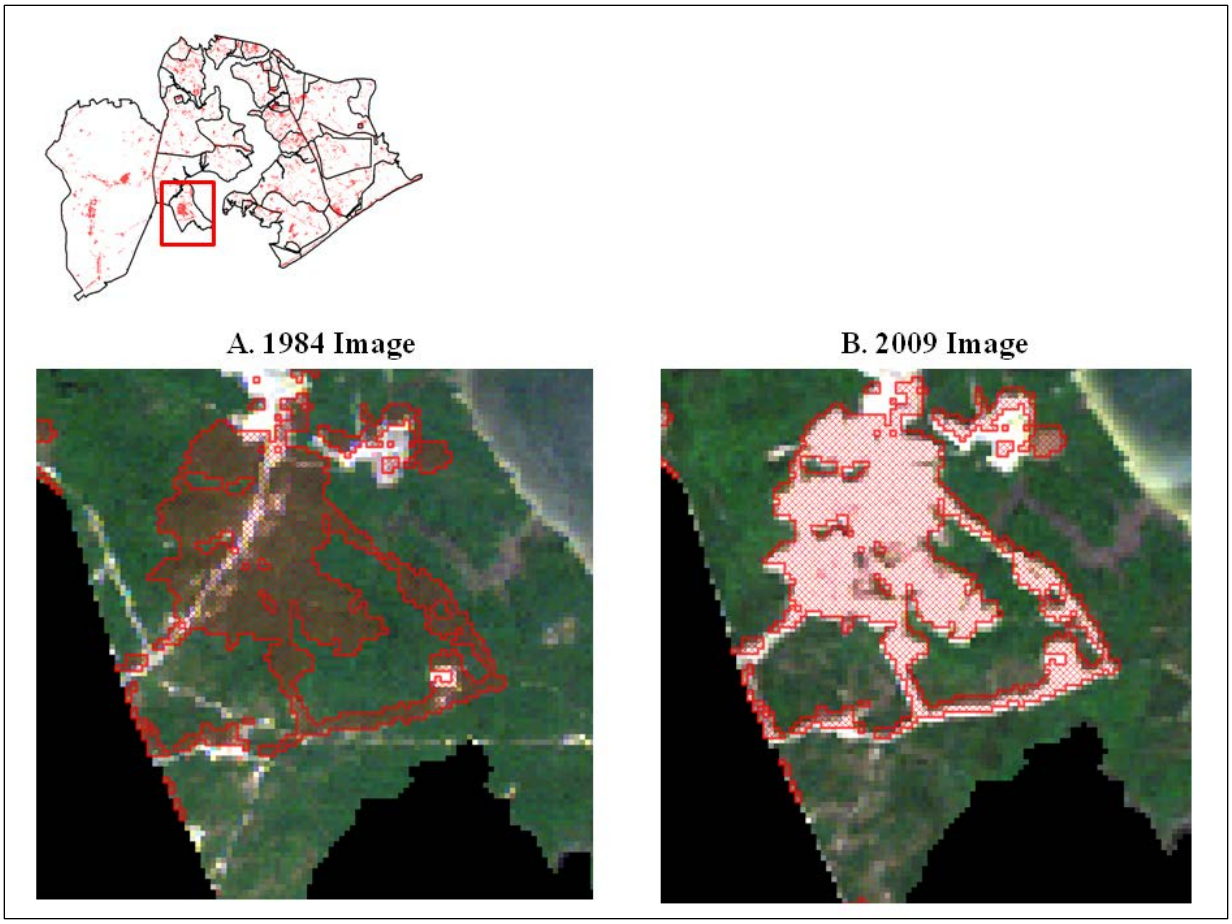

Figure 14-8. MARSOC Rifle Range, MCBCL.

Greenness loss patch from 1984–2009 change period depicted over the (A) 1984 and (B) 2009 Landsat TM images.

We can also derive and estimate of permanent greenness loss from the change code data. As described previously, the change code data specifies when a change occurred within the framework of the images dates we have available. To develop the correction factor for the 2007 greenness loss and the 2005 greenness gain anomalies, we used change codes that identified change that occurred only in one image. Here, we had to define what set of change codes would represent permanent change. We decided to define a conservative estimate of permanent loss as areas that once lost vegetation, remained a loss in all subsequent images. This would be codes 10000 (first greenness loss observed in 2007–2009), 11000 (first greenness loss in 2005–2007 and persisted to 2009), 11100 (first greenness loss in 1998–2005 and persisted to 2009), 11110 (first greenness loss in 1990–1998 and persisted to 2009), and 11111 (first greenness loss in 1984–1990 and persisted to 2009). A code of 11111 is a location that recorded loss at that location in the first change period and in all images afterwards. As discussed in the methods, this is always relative to the 1984 condition. This set of permanent codes has a high certainty of being accurate as they show a consistent pattern over time. However, with five periods between our 6 images, there are many other codes. Our definition of permanent codes is a conservative one as it does not include codes such as 11011 or 11101. These probably are permanent, but what about codes such as 10001 or 01010? These we have less confidence in as they are not a consistent pattern over time, going back and forth between change and no change. They are

likely transient change areas, used for some time period, then not used for periods of time, or natural variability in growth. These types of codes would also contain the error in the change data. We based our decision to use this set of codes for permanent change on the distribution of area in each individual code. The permanent codes have larger amounts of area than the other codes, a result we expect if in fact they represent permanent change. By comparison, a code such as 01010 represents very little area at MCBCL. Even codes such as 11011 have much less area on the Base than the codes we define here as permanent.

We can again bracket our estimate by using the change codes with the Thresholds 3 and 2 data. Using this set of codes, the permanent loss estimate from the change code data is a range of 5.41–7.72% of MCBCL, good agreement with the 7.23–10.64% permanent loss estimate from the 1984–2009 change period, particularly as the change code is more conservative. At the scale of the full area of MCBCL, the spatial representation of permanent loss based on the change code data would be difficult to distinguish from **Figure 14-7**, the data based on the 1984–2009 change period.

We can examine greenness gain in the same way. We begin again with the change pair estimates. As with loss, the longest time period gives the best estimate of long-term greenness gain using the individual change periods. Using the 1984–2009 change period and bracketing the estimate we see a greenness gain of 3.96–10.29%, as shown in **Tables 14-2** and **14-3**. **Figure 14-9** represents the greenness gain for 1984–2009 using the Threshold 3 data.

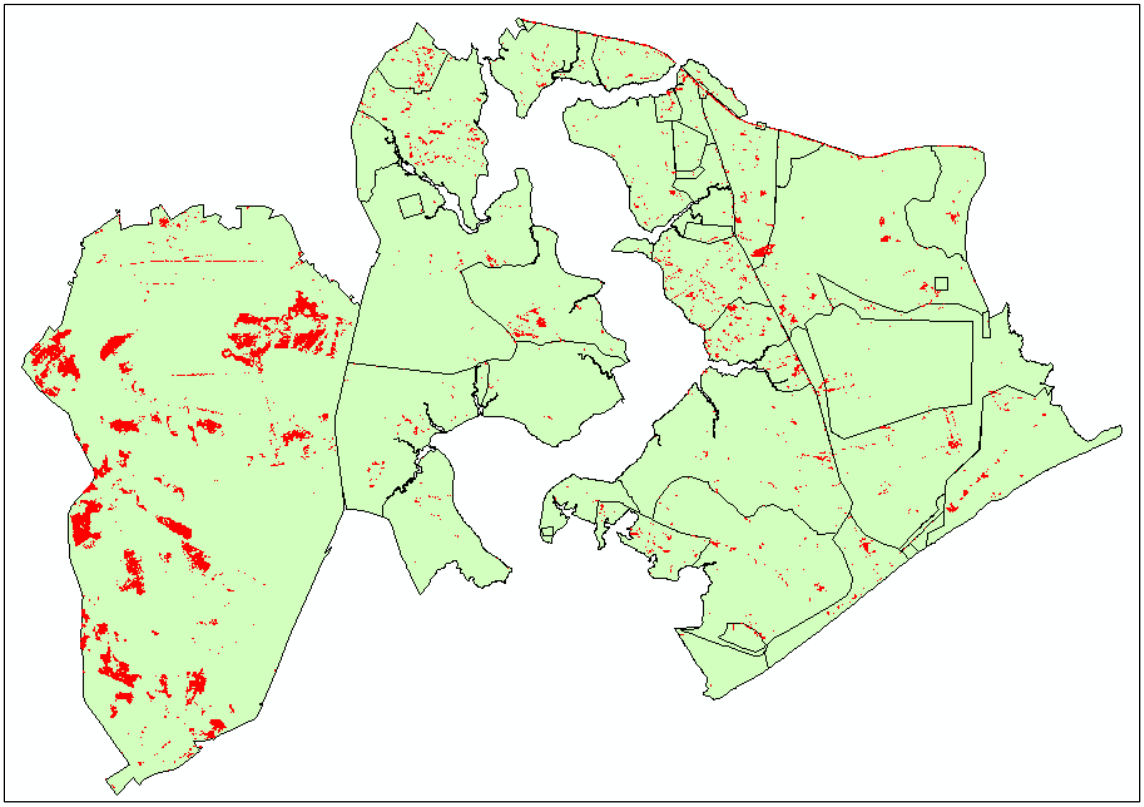

Figure 14-9. 1984–2009 change period greenness gain at MCBCL using the Threshold 3 data.

This is the spatial representation of the data shown in Table 14-3.

We can compare this to an estimate of permanent gain based on the change code data. Using the same definition of permanent codes—10000, 11000, 11100, 11110, and 11111—and again bracketing the estimate with Threshold 3 and 2, this gives a range of greenness gain of 2.75–6.97%, compared to the 1984–2009 change period estimate of 3.96–10.29%. As with the greenness loss data, the greenness gain estimates from the change code are lower than those from the 1984–2009 change pair. Again, this is expected as we have defined a very conservative set of codes to represent permanent change.

Comparing **Figures 14-7** and **14-9** shows the distribution of greenness gain and loss is quite different. Greenness loss in **Figure 14-7** is distributed throughout MCBCL, both the main unit and GSRA. Greenness gain (**Figure 14-9**), however, is much more common in the GSRA than the main unit of MCBCL. There are very few significant patches of greenness gain in the main unit, and those tend to be small in area. The GSRA, however, shows many large patches of vegetation re-growth. The GSRA is 33% of the area of MCBCL, but represents 65–75% of the permanent greenness gain, again bracketing using Thresholds 2 and 3, respectively.

This is a result of the different histories of these two portions of MCBCL. According to MCBCL's Web site (http://www.lejeune.marines.mil/UnitHome.aspx), MCBCL has been the home of the U.S. Marines since September 1941, but the GSRA was acquired from the International Paper Company in 1992. In the original unit of MCBCL, the small areas of re-vegetation looks to be a result of training areas that are no longer used and landscaping in areas after construction is complete. Re-growth in these developed areas is lawns, shrubs, and others, not forested areas. In the GSRA, however, there are large areas of forest re-growth.

Figure 14-10 shows the distribution of greenness gain for the GSRA, using the change code data at the Threshold 2 level (we used Threshold 2 data for the change codes, the more liberal estimate, because the codes are already more conservative than the 1984–2009 change pair). The change code is used rather than the 1984–2009 change period because this allows us to determine when the gain was first recorded; the patches are color coded based on what image date the greenness gain was first identified. As shown in **Figure 14-10**, nearly all these areas of permanent growth patches were clear-cut prior to the 1984 image and were showing significant re-growth by the 1990 image (dark red). Comparatively, little of the greenness gain area was still barren in the 1990 or later images, although there is a significant area in bright red that showed re-growth between 1990 and 1998 in **Figure 14-10** near the northwest border. This means that although the paper company owned the land until 1992, nearly all the clear-cuts were performed just prior to the 1984 image.

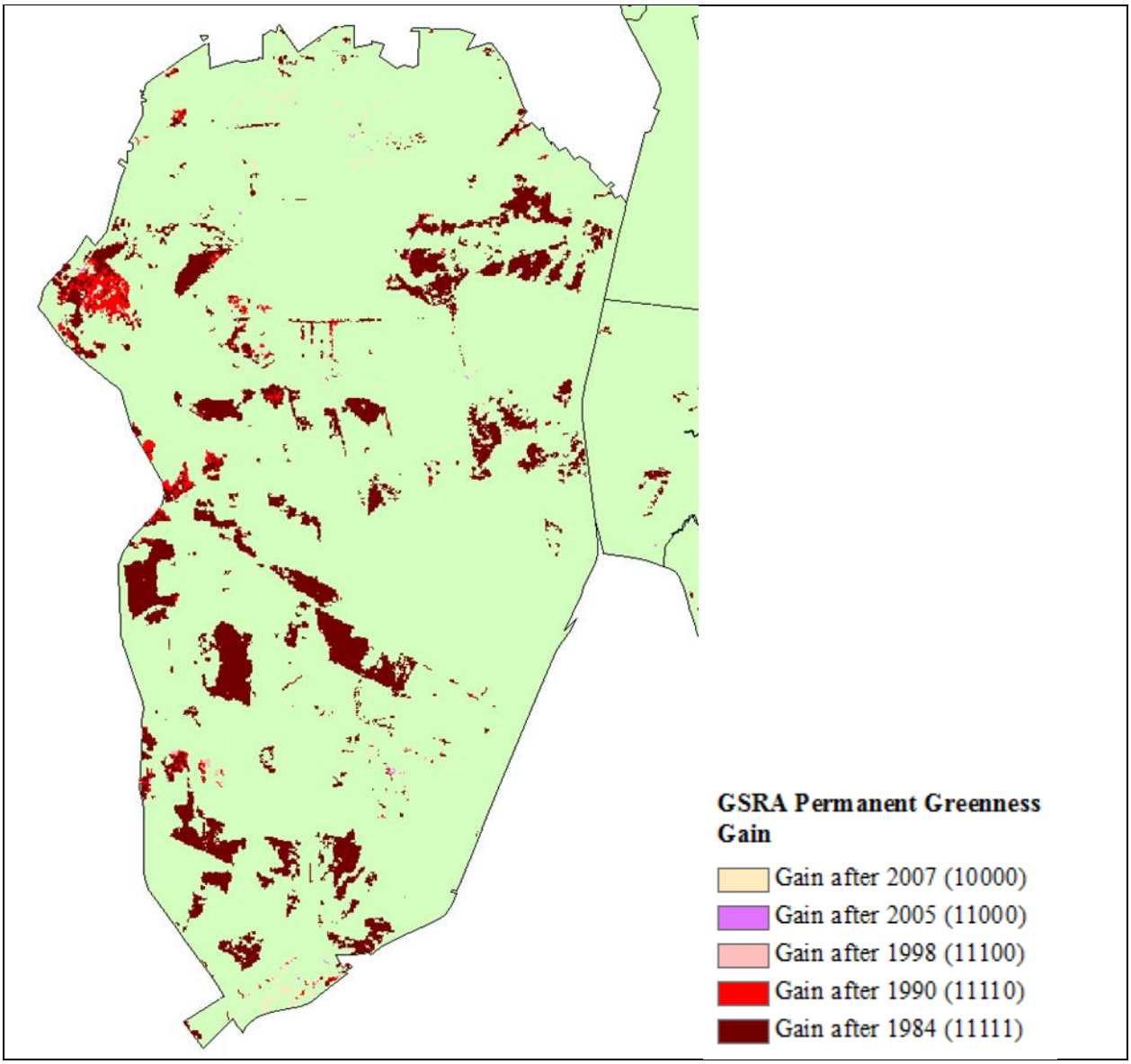

Figure 14-10. Greenness gain data for GSRA, using the change code Threshold 2 data.

Greenness gain is color coded according to the time period when the gain first was recorded.

We can see this more clearly in the close up of several of these patches in the GSRA, shown in **Figure 14-11**. Frame A uses the same data as shown **Figure 14-10**, zoomed-in to the area shown in the locator map. The backdrop is the 1984 Landsat image. Frame B shows areas that represent only code 11111 (barren in 1984, green by 1990, and remained vegetated through 2009) with red outlines so the image is visible within each patch. The backdrop is again the 1984 image. We can see these patches are barren in the 1984 image, with a light brown, relatively bright color, and low greenness. Frame C shows these same patches with the 2009 image as a backdrop. In 2009, these patches are now dark green, representing pine forest. It is this type of change that makes up the majority of permanent greenness gain in the GSRA. Also note in Frame C an area of greenness loss, showing as a bright vertical strip in the image, which is visible in **Figure 14-7** as a greenness loss patch.

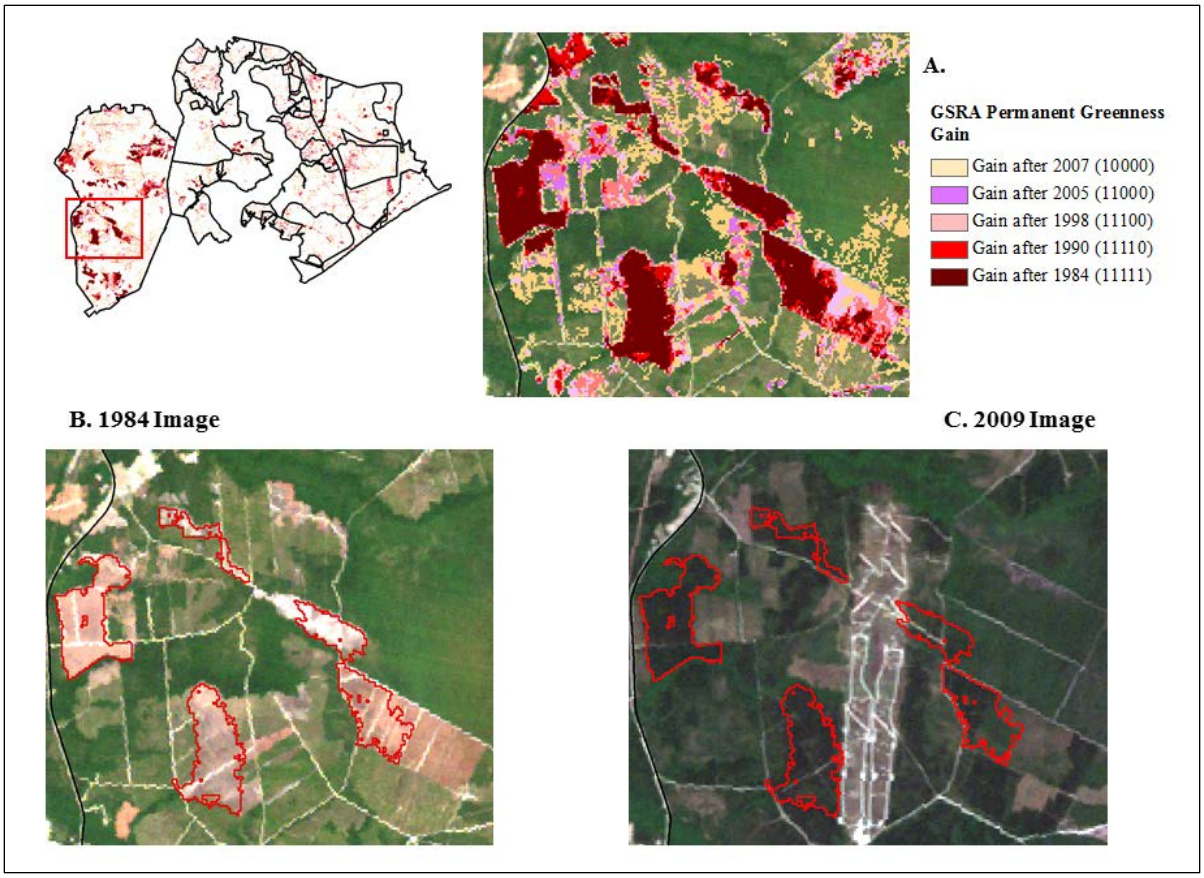

Figure 14-11. A close-up view of several permanent re-growth areas in the GSRA.

Frame A shows the change code gain data also shown in Figure 14-10. Frame B shows gain locations for change code 11111 only overlaid on the 1984 image. Frame C shows gain locations for change code 11111 only overlaid on the 2009 image.

Transient Change at MCBCL

We have specified permanent greenness change at MCBCL since 1984 as a range of approximately 5–10% greenness loss and another 3–10% of permanent greenness gain. This does not mean that 80% of MCBCL is undisturbed. It is important to emphasize that we can only measure change relative to the 1984 image. This is the earliest Landsat TM data available. However, development occurring prior to 1984 includes considerable land area at MCBCL. All these infrastructure developments and training impacts are not considered here, unless further change occurred at these sites after 1984. Also, much of the Base between 1984 and 2009 experienced impacts to the vegetation, but that vegetation loss was not permanent. These transient loss areas are important as well, because, as mentioned earlier, areas of the Base that re-vegetated after an impact do not necessarily represent the same ecosystem type or provide the same ecosystem services. We can monitor these transient losses effectively for the 2005–2009 period because the images are only 2 years apart. The 1984–2005 period, with 6–8 year time periods, will be much less effective at recording all transient change before it can green up again. However, using the change code for 1984 through 2009 (corrected for the 2007 drought impact in the same manner as described for **Tables 14-2** and **14-3**), between 13.32–25.36% of MCBCL (bracketed by Threshold 3 and 2, respectively) experienced greenness loss at some point in this

time period. This is a large area of the Base, particularly if we were able to combine this with the amount of area already developed by 1984.

Management Implications

An important management issue at MCBCL is the Grow the Force (GTF) initiative. MCBCL began a number of construction projects to house and train additional marines, families and support staff beginning after the 2005 image date. This resulted in a period of rapid development evident as greenness loss in the 2007, 2009, and 2011 images. Using the change period and change code data, we examined this greenness loss pattern, shown in **Table 14-6**, using Threshold 3 data for all estimates for consistency. In the 21 years prior to the GTF initiative (1984–2005), we found a greenness loss more than 4.66% of the land area of MCBCL, a rate of 0.22% per year. In the 4 years from the 2005 image to the 2009 image, a period when the GTF initiative was occurring, we have an estimate of greenness loss of 2.57% (0.64% per year) from the change pairs and 3.87% (0.96% per year) from the change code data. This is much greater rate of change than the average observed in the previous 21 years. The 3.87% estimate derived from the change code data can be further specified. From 2005 to 2007, there was a greenness loss of 1.67% and from 2007 to 2009, this was 2.2%. 2009 to 2011 was also a period of rapid development as part of the GTF initiative. We have not used data from the 2011 image to this point. As described in the Materials and Methods section of this chapter, this image was problematic. The spectral differences in this image relative to the others resulted in underestimates for greenness loss and overestimates for gain. However, even an underestimate of greenness loss shows the impacts of the GTF initiative and identifies locations of loss between 2009 and 2011. New greenness loss occurring after 2009 and before 2011 covers 1.7% of MCBCL based on this data. This is a rate of 0.85% per year, very much in line with the rates shown in **Table 14-6** for 2005–2007 (0.84%) and 2007–2009 (1.10%). We believe it is likely the actual 2009–2011 greenness loss is probably closer to 2.2% during the 2007–2009 period. Nevertheless, the change data are clearly identifying a rapid period of development resulting in vegetation loss, at a rate at least three times the long-term average seen prior to the GTF initiative.

Table 14-6. Greenness loss change occurring before and during the GTF initiative as a percentage of the land area of MCBCL.

Data presented use Threshold 3.

Time Period	% Loss	Source	%/year
1984–2005	4.66	Change pair data	0.22%/year
2005–2009	2.57	Change pair data	0.64%/year
2005–2009	3.87	Change codes 11000 + 10000	0.96%/year
2005–2007	1.67	Change code 11000	0.84%/year
2007–2009	2.2	Change code 10000	1.10%/year
2009–2011	1.7	Change code 100000	0.85%/year

The GIS data layers representing greenness change can be applied to any spatial question where knowing the amount of change in an area would be beneficial. We used the data to examine what management areas at MCBCL have had the most permanent greenness loss since 1984. Using

the data shown in **Table 14-3** and **Figure 14-7** (1984–2009 change period using Threshold 3), we sampled the change in each named compartment. The result, showing greenness loss as a percentage of compartment area, is shown in **Figure 14-12**. Not surprisingly, more developed areas such as Hadnot Point, French Creek, and Tarawa Terrace show high percentages of permanent greenness loss.

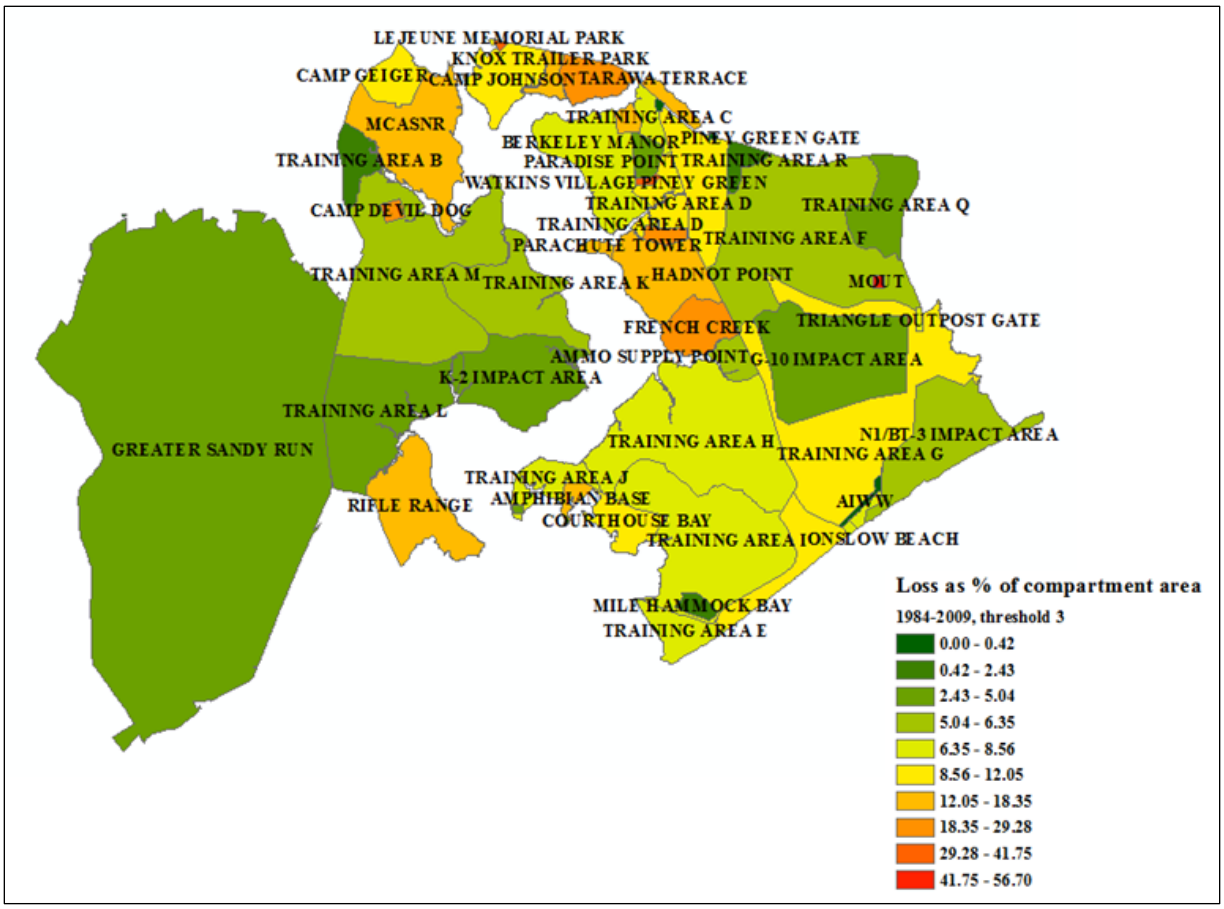

Figure 14-12. Greenness loss (1984–2009 change pair, Threshold 3 data) as a percentage of MCBCL compartment area.

This process used political boundaries, but any spatial unit could be used. Vegetation loss and gain will likely affect runoff amount and water quality, for example. The data can be used to identify the amount of greenness change in any defined watershed on the Base, or within any given buffer distance of a steam or sensitive wetland area and linked to field monitoring data to look for patterns. The GIS skills necessary to do this type of application are relatively simple once the change data sets are available. The data can be used directly by a GIS analyst or integrated as part of a model or SDSS utility for stakeholders or Base management personnel.

Assessment of Trends in the Data

Landsat TM images are the raw monitoring data used for this study. We selected a series of Landsat TM images to provide both an historical and current perspective on vegetation change at MCBCL. The interval between image dates affects what change can be detected. The reference

year is 1984, which is the first year when the TM satellite was fully operational. Our goal was then to establish a 2-year interval between image dates starting in 2005 and continuing until 2011. Intervals of 1–2 years are necessary to detect all vegetation change, even if transient, in an area of rapid re-growth. This was shown by Lunetta et al. (2003) in a study using the North Carolina Piedmont/Coastal Plain. This 2-year interval allows us to track vegetation change concurrent with the DCERP. However, a 2-year interval for historical images prior to 2005 would be impractical. Instead, we selected two additional images as equally spaced between 1984 and 2005 as possible to provide an historical perspective. The final set of image dates is 1984, 1990, 1998, 2005, 2007, 2009, and 2011.

Conclusions/Recommendations for Future Monitoring

The primary goal of this project was to identify changes in the vegetation patterns over time at MCBCL, particularly those resulting from MCBCL activities—infrastructure development and training impacts. The following is a summary of the primary quantitative results:

- Based on the 1984–2009 individual change period, between 7.23–10.64% of MCBCL experienced permanent vegetation loss (**Tables 14-2** and **14-3**). Based on a conservative set of codes from the change code data, this is a range of 5.41–7.72%.
- Between 2.57% and 3.87% of the greenness loss occurred between 2005 and 2009, a period of rapid development from the GTF initiative (**Table 14-6**)
- Approximately 1.7% of additional greenness loss occurred from 2009 to 2011 (**Table 14-6**). The 2009 to 2011 change period is likely an underestimate due to problems with the 2011 image.
- Between 13.31% and 25.36% of MCBCL experienced significant greenness loss at some point between 1984 and 2009. Most of this is transient and experienced regrowth following the loss; 7.23% to 10.64% of this is permanent.
- Based on the 1984–2009 individual change period, between 3.96–10.29% of MCBCL experienced permanent vegetation gain (**Tables 14-2** and **14-3**). Based on a conservative set of codes from the change code data, this is a range of 2.75–6.79%.
- Although the GSRA is only 33% of the area of MCBCL, it accounts for 65–75% of the permanent greenness gain. The re-growth in the GSRA follows clear-cutting performed by the paper company, which owned this area before it was acquired by MCBCL. These areas are large blocks of forest re-growth. The re-growth occurring in the main unit of the Base are small areas, much of which is landscaping following construction.

In addition to these quantitative results, the GIS data layers produced are spatially explicit and can be used to address any number of spatially related questions that will help the Base in understanding the impact and consequences of past, present, and future management and development decisions. The data layers can address the amount of change that has occurred in any area of interest, from political management units to watershed boundaries. This information can be used as inputs to models, directly as an aid to managerial decisions through maps, tables and GIS analysis, or incorporated into the SDSS for end users to simplify the process of balancing need with ecosystem health to maintain an ecosystem-based management approach.

Continuation of vegetation change detection at a 2-year interval, imagery permitting, will allow the Base to monitor both transient and permanent changes. With the change data, the impacts resulting from management decisions are apparent, allowing for more informed decisions concerning future management and development choices.

Literature Cited

Allen, T.R., and J.A. Kupfer. 2000. Application of spherical statistics to Change Vector Analysis of Landsat data: Southern Appalachian spruce-fir forests. *Remote Sensing of the Environment 74*:482–493.

Chander, G., B.L. Markham, and J.A. Barsi. 2007. Revised Landsat 5 Thematic Mapper radiometric calibration. IEEE *Geoscience and Remote Sensing Letters 4*(3):490–494.

Chavez, Jr., P.S. 1996. Image-based atmospheric corrections—Revisited and improved. *Photogrammetric Engineering & Remote Sensing 62*(9):1025–1036.

Coppin, P., I. Jonckheere, K. Nackaerts, B. Muys, and E. Lambin. 2004. Digital change detection methods in ecosystem monitoring: A review. *International Journal of Remote Sensing, 25*(9):1565–1596.

Coppin, P.R., and M.E. Bauer. 1996. Change detection in forest ecosystems with remote sensing digital imagery. *Remote Sensing Reviews 13*:207–234.

Crist, E.P., and R.C. Cicone. 1984a. Application of the tasseled cap concept to simulated Thematic Mapper data. *Photogrammetric Engineering and Remote Sensing 50*(3):343–352.

Crist, E.P., and R.C. Cicone. 1984b. A physically based transformation of Thematic Mapper data—the TM tassled cap. *IEEE Transactions on Geoscience and Remote Sensing*. *GE-22*(3):246–263.

Crist, E.P., and R.J. Kauth. 1986. The tasseled cap de-mystified. *Photogrammetric Engineering and Remote Sensing 52*(1):81–86.

Dai, X.L., and S. Khorram. 1998. The effects of image misregistration on the accuracy of remotely sensed change detection. *IEEE Transactions on Geoscience and Remote Sensing 36*(5):1566–1577.

DCERP (Defense Coastal/Estuarine Research Program). 2007. *DCERP Fact Sheet SI-1413*. Available at https://dcerp.rti.org/Portals/0/final%20SI_FS_1413.pdf.

Fung, T., and E. LeDrew. 1987. Application of Principal Components Analysis to change detection. *Photogrammetric Engineering & Remote Sensing 53*:1649–1658.

Hayes, D.J., and S.A. Sader. 2001. Comparison of change-detection techniques for monitoring tropical forest clearing and vegetation regrowth in a time series. *Photogrammetric Engineering & Remote Sensing* 67(9):1067–1075.

Johnson, R.D., and E.S. Kasischke. 1998. Change Vector Analysis: A technique for the multispectral monitoring of land cover and condition. *International Journal of Remote Sensing* 19(3):411–426.

Kauth, R.J., and G.S. Thomas. 1976. The tasseled cap—A graphic description of the spectral-temporal development of agricultural crops as seen by Landsat. Pp. 4B-41–4B-51 in *Proceedings of the Symposium on Machine Processing of Remotely Sensed Data*, Purdue University of West Lafayette, IN.

Kuzera, K., J, Rogan, and J.R. Eastman. 2005. Monitoring vegetation regeneration and deforestation using Change Vector Analysis: Mt. St. Helens Study area. ASPRS 2005 Annual Conference, Baltimore, MD. March 7–11.

Lambin, E.F., and A.H. Strahler. 1994. Change Vector Analysis in multi-temporal space: A tool to detect and categorize land-cover change processes using high temporal-resolution satellite data. *Remote Sensing of the Environment 48*:231–244.

Lorena, R.B., J.R. dos Santos, Y.E. Shimabukuro, I.F. Brown, and H.J.H. Kux. 2002. A Change Vector Analysis technique to monitor land use/land cover in SW Brazilian Amazon: Acre state. In *Proceedings of Integrated Remote Sensing at the Global, Regional, and Local Scale: ISPRS Commission I Mid-Term Symposium*, in conjunction with Pecora 15/Land Satellite Information IV Conference, Denver, CO. November 10–15.

Lozar, R.C., C.R. Ehlshlaeger, and J. Cox. 2003. *A Geographic Information Systems (GIS) and Imagery Approach to Historical Urban Growth Trends Around Military Installations*. U.S. Army Corps of Engineers ERDC/CERL TR-03-9. May. Available at http://www.cecer.army.mil/techreports/Lozar_GISImagery/Lozar_GISImagery_TR.pdf.

Lunetta, R.S. 1998. Applications, project formulation, and analytical approach. Chapter 1, pp. 1–19 in *Remote Sensing Change Detection—Environmental Monitoring, Methods, and Applications*. Edited by R.S. Lunetta and C.D. Elvidge. Ann Arbor Press: Ann Arbor, MI.

Lunetta, R.S., D.M. Johnson, J.G. Lyon, and J. Crotwell. 2004. Impacts of imagery temporal frequency on land-cover change detection monitoring. *Remote Sensing of the Environment 89*:444–454.

Lunetta, R.S., J. Ediriwickrema, J. Iiames, D.M. Johnson, J.G. Lyon, A. McKerrow, and A. Pilant. 2003. A quantitative assessment of a combined spectral and GIS rule-based land-cover classification in the Neuse River basin of North Carolina. *Photogrammetric Engineering and Remote Sensing 69*(3):299–310.

Lunetta, R.S., J. Ediriwickrema, D.M. Johnson, J.G. Lyon, and A. McKerrow. 2002. Impacts of vegetation dynamics on the identification of land-cover change in a biologically complex community in North Carolina, USA. *Remote Sensing of Environment 82*(2–3):258–270.

Mahiny, A., and B.J. Turner. 2007. A comparison of four common atmospheric correction methods. *Photogrammetric Engineering & Remote Sensing 73*(4):361–368.

Markham, B.L., and J.L. Barker. 1986. Landsat MSS and TM post-calibration dynamic ranges, exoatmospheric reflectances and at-satellite temperatures. *EOSAT Technical Notes*. August.

Song, C., C.E. Woodcock, K.C. Seto, M.P. Lenney, and S.A. Macomber. 2001. Classification and change detection using Landsat TM Data: When and how to correct atmospheric effects? *Remote Sensing Environment 75*:230–244.

Yuan, D., C.D. Elvidge, and R.S. Lunetta. 1998. Survey of multispectral methods for land cover change analysis. Chapter 2, pp. 21–39 in *Remote Sensing Change Detection—Environmental Monitoring Methods and Applications*. Edited by R.S. Lunetta and C.D. Elvidge. Ann Arbor Press; Ann Arbor, MI.

Chapter 15

Local and Regional Air Quality Monitoring

SERDP Project Number: RC-1413

Atmospheric Module

Lead Researcher:
Dr. Karsten Baumann
Atmospheric Research & Analysis, Inc.
1000 Perimeter Park Drive (Suite G), Morrisville, NC 27560
E-mail: kbaumann@atmospheric-research.com

June 27, 2013

Final

This report was prepared under contract to the U.S. Department of Defense (DoD) Strategic Environmental Research and Development Program (SERDP). The publication of this report does not indicate endorsement by DoD, nor should the contents be construed as reflecting the official policy or position of DoD. References herein to any specific commercial product, process, or service by trade name, trademark, manufacturer, or otherwise, do not necessarily constitute or imply its endorsement, recommendation, or favoring by DoD.

Table of Contents

List of Acronyms 15-vii
Abstract 15-1
Objectives of the Monitoring Activity 15-2
Background 15-2
Materials and Methods 15-6
Results and Discussion 15-11
    Temperature 15-13
    Humidity and Precipitation 15-17
    Winds and Air Mass Transport 15-21
    Solar Radiation 15-23
    Criteria Pollutants 15-25
Assessment of Trends in the Data 15-47
    Assessment of Monitoring Design 15-47
    Assessment Seasonal and Annual Variability in the Data 15-48
    Recommendations for Future Monitoring 15-50
Conclusions and Implications for Future Research 15-50
    Key Scientific Findings—Fundamental Cause-and-Effect Relationships 15-50
    Findings Supportive of Current and Future Base Management Practices 15-52
Literature Cited 15-52
Appendix 15-A: List of Scientific Publications 15-A-1
Appendix 15-B: List of Students 15-B-1

List of Figures

15-1. Conceptual model for the Atmospheric Module. 15-3

15-2. On-Base location of the four comprehensive monitoring sites (red circles); MCA monitoring meteorological parameters are co-located with Marine Corps Air Station New River (NRA; photosynthetically active radiation [PAR], O_3, $PM_{2.5}$, and PM_{10}). 15-7

15-3. Off-Base monitoring and research stations for the Atmospheric Module. 15-8

15-4. Sub-regional temperature rankings across the continental United States for 2011 period April–September (left panel) and June alone (right panel). 15-14

15-5. Monthly mean temperatures from sites in study domain compared to the 30-year normals of the Southern Coastal Plain (SCP) ending in 2008 (N30*). 15-16

15-6. Seasonally averaged diurnal profiles for air temperature from October 2010 to September 2011. 15-17

15-7. Seasonally averaged diurnal profiles for relative humidity in 2010–2011. 15-17

15-8. Seasonally averaged diurnal profiles of hourly summed rainfall in 2010–2011. 15-18

15-9. Sub-regional precipitation rankings across the continental United States for 2011 period April–September (left panel), and August alone (right panel). 15-19

15-10. Monthly total rainfall amounts from sites in the study domain compared to the 30-year normals (N30*) of the Southern Coastal Plain (SCP). 15-20

15-11. Seasonally averaged diurnal profiles of horizontal wind speed in 2010–2011. 15-22

15-12. Seasonally averaged wind frequency distribution wind roses for 2010–2011. 15-22

15-13. Seasonally averaged wind speed roses for 2010–2011. 15-22

15-14. Seasonally averaged diurnal profiles of solar radiation in 2010–2011. 15-23

15-15. Linear regression of hourly PAR measured inland (*y*–axis) versus simultaneous measurements at the RIP beach site (*x*–axis) during the third quarter of 2011. 15-24

15-16. Seasonally averaged SO_2 wind roses for 2010–2011. 15-25

15-17. Seasonally averaged diurnal profiles of SO_2 for 2010–2011. 15-26

15-18. Seasonally averaged diurnal profiles of O_3 for 2010–2011. 15-27

15-19. Seasonally averaged O_3 wind roses for 2010–2011. 15-27

15-20. Regional comparison of O_3 DVs to meet the primary NAAQS (top panel) and fraction of time with hourly O_3 greater than or equal to 60 ppb during each season (bottom panel) spanning 2002 to 2011. 15-29

15-21. Comparison of daily (top) and annual (bottom) $PM_{2.5}$ DVs from four MCBCL sites with corresponding DVs from six off-Base sites across the study region. 15-31

15-22. Seasonally averaged $PM_{2.5}$ wind roses for 2010–2011. 15-33

15-23. Seasonally averaged PM_c wind roses for 2010–2011. 15-33

15-24. Wind roses of seasonally averaged $PM_{2.5}$:PM_c ratios for 2010–2011. 15-33

15-25. Seasonally averaged diurnal profiles for $PM_{2.5}$ in 2010–2011. 15-35

15-26. Seasonally averaged diurnal profiles for PM_c in 2010–2011. 15-35

15-27. Seasonally averaged diurnal profiles of $PM_{2.5}$:PM_c ratio in 2010–2011. 15-35

15-28. Progression map of the SR-8 wildfire in March 2011. 15-37

15-29. Hourly wind vectors, $PM_{2.5}$, and PM_c, and O_3 at different study sites, and acres burned at SR-8 by wildfire in March 2011. 15-38

15-30. Location and progression map of the Pains Bay wildfire in Dare County of eastern North Carolina from May and June 2011. 15-39

15-31. Daily maximum and minimum vertical temperature difference between 40 m (SRT) and the ground (SRG), wind vectors, $PM_{2.5}$ and PM_c concentrations and ratio at different study sites in May and June 2011. 15-40

15-32. Maps of smoke drifting from the Juniper Road Fire from June 24 to 27, 2011. 15-42

15-33. Hourly wind vectors, temperature, relative humidity, O_3, $PM_{2.5}$ and PM_c concentrations and ratio at different study sites from June 21 to 27, 2011. 15-43

15-34. Daily maximum and minimum vertical temperature difference between 40 m (SRT) and the ground (SRG), wind vectors, $PM_{2.5}$ and PM_c concentrations and ratio at different study sites from June 17 through July 31, 2011..... 15-45

15-35. State- and Base-wide total acres burned and number of days exceeding 35 $\mu g\ m^{-3}$ daily $PM_{2.5}$ concentration averages at different study sites between 2008 and 2011..... 15-46

List of Tables

15-1. Locations and parameters monitored at on-Base (shaded yellow) and off-Base sites. 15-9

15-2. Percentage levels of monthly data coverage (on hourly basis) in 2010 and 2011 for meteorological parameters monitored on-Base (shaded yellow) and off-Base..... 15-12

15-3. Percentage levels of monthly data coverage (on hourly basis) in 2010 and 2011 for EPA criteria pollutants monitored on-Base (shaded yellow) and off-Base. 15-13

15-4. Monthly mean air temperatures with 30-Year normals (*italicized*) in degrees Celsius (°C) for period from October 2010 to September 2011 and all study sites are on-Base (shaded yellow) and off-Base. 15-15

15-5. Monthly total rainfall amounts with 30-year normals (*italicized*) in millimeters for period from October 2010 to September 2011 and all study sites on-Base (shaded yellow) and off-Base..... 15-20

15-6. Given periods' total rainfall amounts (in millimeters) from MCBCL sites relative to 30-year normals regionally averaged over the Southern Coastal Plain (SCP; N30*). 15-21

15-7. Monthly daily maximum 8-hour averages of PAR in watts per square meter at three on-Base sites. 15-24

15-8. Monthly means (average daily maximum of 8 hours for O_3) of pollutant concentrations from sites on-Base (shaded yellow) and off-Base in period October 1, 2010, to September 30, 2011. 15-26

15-9. Significant wildfires affecting the study domain in 2011. 15-36

15-10. Annual coverage of daily average $PM_{2.5}$ data for different study sites 15-47

15-11. State- and Base-wide total acres burned and average daily $PM_{2.5}$ level of each site's exceedance days. 15-47

List of Acronyms

°C	degrees Celsius
°F	degrees Fahrenheit
$\mu g/m^3$	micrograms per cubic meter
µm	micrometer
ac	acre
Al	aluminum
ARA	Atmospheric Research & Analysis, Inc.
AUR	Aurora (Site)
AVG	average
BL	boundary layer (atmospheric)
BP	barometric pressure
CASAC	Clean Air Scientific Advisory Committee
CFR	*Code of Federal Regulations*
CHN	Castle Hayne (Site)
CIG	Ceiling
CO	carbon monoxide
DCERP	Defense Coastal/Estuarine Research Program
DLL	Dillard–Goldsboro (Site)
DoD	U.S. Department of Defense
dv	Deciview
DV	design value (to determine compliance with National Ambient Air Quality Standards)
EPA	U.S. Environmental Protection Agency
Fe	iron
FM	fuel moisture
FT	fuel temperature
GSRA	Greater Sandy Run Area
H_2SO_4	sulfuric acid
HYSPLIT	HYbrid Single-Particle Lagrangian Integrated Trajectory (Program)
Hz	hertz
ISO	International Organization for Standardization
JVL	Jacksonville (Site)
KBDI	Keetch-Byram Drought Index
km	kilometer
KVL	Kenansville (Site)
LCC	Lenoir Community College (Site)

Lpm	liters per minute
m^{-1}	per meter
MCA	Marine Corps Air Station New River (Site)
MCASNR	Marine Corps Air Station New River
MCBCL	Marine Corps Base Camp Lejeune
MET	meteorological parameters
Mg	magnesium
mm	millimeter
MW	MesoWest
NAAQS	National Ambient Air Quality Standards
NC DENR	North Carolina Department of Environment and Natural Resources
NH_3	ammonia
$(NH_4)_2SO_4$	ammonium nitrate
Ni	nickel
nm	nanometer
NOAA	National Oceanic and Atmospheric Administration
NO_x	nitrogen oxides
NRA	Marine Corps Air Station New River (Site)
NWS	National Weather Service
MARDIS	Monitoring and Research Data Information System
MCBCL	Marine Corps Base Camp Lejeune
MW	MesoWest data repository run by the University of Utah's Department of Meteorology
O_3	ozone
OA	organic aerosol
PAR	photosynthetically active radiation in 400–700 nm range
Pb	lead
PB	prescribed burning
PCP	precipitation
PCS	Potash Corporation of Saskatchewan
pDR	*personal* DataRAM nephelometer (for real-time particulate matter mass measurement)
PM	particulate matter
$PM_{2.5}$	fine PM with an aerodynamic diameter of less than or equal to 2.5 µm
PM_{10}	particulate matter with an aerodynamic diameter of less than or equal to 10 µm
PM_c	coarse PM with size between 2.5 and 10 µm (also PM_{10-25})
ppb	parts per billion (molecules mixing ratio in ambient air)
ppbv	parts per billion by volume

ppm-hours	parts per million-hours
RH	relative humidity
RIP	Riseley Pier
SERDP	Strategic Environmental Research and Development Program
SO_2	sulfur dioxide
SOA	secondary organic aerosol
SR	solar radiation (in the 200–1,100 nm range)
SRG	GSRA Ground (Site)
SRT	GSRA Tower (Site)
SUM06	sum of hours with ambient ozone (O_3) concentration exceeding 60 ppb
T-diff	vertical temperature difference
TMP	temperature
VIS	visibility
VOC	volatile organic compound
WAS	Washington, NC (Site)
WD	wind direction
WIA	Wilmington International Airport (Site)
WIL	Wilmington (Site)
WS	wind speed
Zn	zinc

[This page intentionally left blank.]

Abstract

The objective of our monitoring activities was to characterize the role of air quality in the natural ecosystem of Marine Corps Base Camp Lejeune (MCBCL) by capturing meteorological and climatological processes and their occurrence in different spatial and temporal scales in support of various research projects within the Defense Coastal/Estuarine Research Program (DCERP). To track and compare meteorological and air pollution trends observed on Base in the context of more regional trends, we expanded the network of existing monitoring sites and developed procedures for merging data from the two major regional networks (MesoWest and the North Carolina Department of Environment and Natural Resources) into a common and consistent time base for hourly averages of all acquired parameters. Three new on-Base sites began acquiring data in March 2008 that consisted of various meteorological parameters (i.e., ozone [O_3], $PM_{2.5}$ [fine particulate matter [PM], and PM_{10}). In October 2010, two more PM measurement sites were added to increase spatial resolution in tracking on- and off-Base pollution sources. The reporting of merged quality controlled data from all five on-Base sites and a total of nine off-Base sites started in July 2008 and continued until September 2011. Statistical data summary reports were provided to the RTI DCERP Team each month. These reports included diurnal profiles and wind rose plots; hourly resolved data were submitted to MARDIS, the program's central data access platform. Our study domain experienced general drought conditions during the 3.5-year study period except for a few locations and events with extreme rainfall amounts from individual tropical storms or hurricanes. Annual average rainfall amounts consistently decreased along the inland gradient across the study domain. Several significant wildfires burned in the North Carolina coastal area during March, June, and July 2011. Despite several direct impacts of wildfire smoke plumes, O_3 levels that are harmful to human health continued to decrease at similar rates across all sites. However, the declining trend in seasonal levels that are harmful to vegetation had reversed and increased since 2009, mainly due to the unusual warm and dry weather conditions in early spring, favoring photochemical O_3 production. $PM_{2.5}$ levels for short-term and especially long-term exposure thresholds have decreased steadily during the past 10 years, and the regional trend of increasing $PM_{2.5}$ levels with increasing distance from the coast outside MCBCL boundaries has remained true in 2011. This trend correlated with decreasing amounts of rainfall away from the coast and held again for the most recent 2011 period, indicating rainfall of effectively removing $PM_{2.5}$ from the atmosphere. Our monitoring approach afforded the measurement of coarse PM (PM_c) from the PM_{10}–$PM_{2.5}$ difference. High-resolution data of simultaneously measured $PM_{2.5}$ and PM_c provide powerful diagnostics into potential sources and source impact processes causing local air pollution. For periods with smoke-laden air masses blowing into the MCBCL area, both $PM_{2.5}$ and PM_c levels were elevated. However, the PM_c elevation relative to background was smaller than for $PM_{2.5}$, indicating that the wildfire smoke plumes contained substantially more $PM_{2.5}$ than PM_c. The $PM_{2.5}$:PM_c ratio in those plumes was even more enhanced under warmer conditions in late spring and summer, pointing to new particle formation from emitted reactive precursor gases and semi-volatile aerosol species.

Keywords: Atmospheric boundary layer, air quality, coarse PM, fine PM, impact, meteorology, ozone, smoke, trend, wildfire

Objectives of the Monitoring Activity

The objective of the Atmospheric Module's monitoring activities is to characterize the role of air quality in MCBCL's ecosystem by capturing meteorological and climatological processes and their occurrence in different spatial and temporal scales in support of various research projects that consider and depend upon certain biosphere–atmosphere interactions. Atmospheric processes, conditions and constituents influence the terrestrial, aquatic/estuarine, coastal wetlands, and coastal barrier island ecosystems in different specific ways over time and space.

Long-term collection and evaluation of spatially and temporally resolved meteorological data allow for the establishment of a detailed climatology for the MCBCL area, including the capture of extreme events that affect hydrological processes in the estuarine and the terrestrial ecosystems (e.g., benthic response to upwelling during storm conditions, vegetation diversity change in response to increasing temperatures). Furthermore, the collection of meteorological data in combination with real-time measurements of O_3, $PM_{2.5}$ and PM_c will help identify atmospheric stressors and potential critical levels during certain episodes (e.g., heat stress accompanied by high O_3 and $PM_{2.5}$), causing measurable impact on certain vegetation species.

Characterization of the air quality's role requires a good understanding of atmospheric dynamics and composition, including the identification of air pollutants, their sources, their distribution and dispersion mechanisms in the atmospheric boundary layer above the ecosystem, and their deposition processes following wet and dry deposition pathways. The use of existing state government–operated air quality monitoring stations' data in support of the data generated by the newly established on-Base stations will enhance our understanding of air quality in MCBCL's airshed. These criteria air pollutants are regulated by the U.S. Environmental Protection Agency via specific National Ambient Air Quality Standards and are mandated by the Clean Air Act for the protection of human health and welfare. Hourly meteorological data are available through the MesoWest (MW) network and through the National Weather Service, whose sites in most cases are associated with local airports.

Background

The input of nutrients and potential pollutants via atmospheric deposition interacts with most key terrestrial and aquatic ecological processes occurring at Marine Corps Base Camp Lejeune (MCBCL), as illustrated in **Figure 15-1** and as reported for similar ecosystems (Lawrence et al., 2000; Van Der Salm et al., 1999). Atmospheric deposition is a direct source of inputs onto the open-water surfaces of the aquatic ecosystem and onto the vegetation surfaces of the terrestrial ecosystem, with the frequency, level, and composition of these inputs posing an important influence on flora diversity. For example, changes in the dominant forms of a given nutrient (e.g., nitrogen) over time will lead to shifts in the dominant flora within the aquatic ecosystem (Paerl et al., 2002) and shorter term vegetation effects from ozone (O_3) exposure have been observed and accounted for by concentration-weighted cumulative exposures to O_3 on an hourly basis (U.S. EPA, 2006).

In addition to direct sources of atmospheric input, the aquatic ecosystem is impacted by atmospheric deposition after it is filtered and altered by passage through the terrestrial ecosystem. This impact occurs during all time scales, ranging from rapid inputs following large rainfall events (runoff) to slow, but critical, changes in baseflow from the superficial aquifer

(Hunsaker et al., 1994; Osgood and Zieman, 1998). It may not always be immediately evident which impact is playing the dominant role in forcing change within the aquatic ecosystem. Similarly, terrestrial ecosystem impacts that will become evident from the satellite-supported seasonal evaluations might be due to exposure to a complex combination of long-term climatological stress (e.g., temperature, drought) and shorter term air pollutant stress (oxidants and metals). Heavy metals in particulate matter with diameters less than or equal to 2.5 µm ($PM_{2.5}$) have been associated with forest decline partly due to their correlated deposition pattern, and in vitro studies have found that iron (Fe), aluminum (Al), nickel (Ni), zinc (Zn), magnesium (Mg), and lead (Pb) played the most important roles in tree injury and decline (U.S. EPA, 2004).

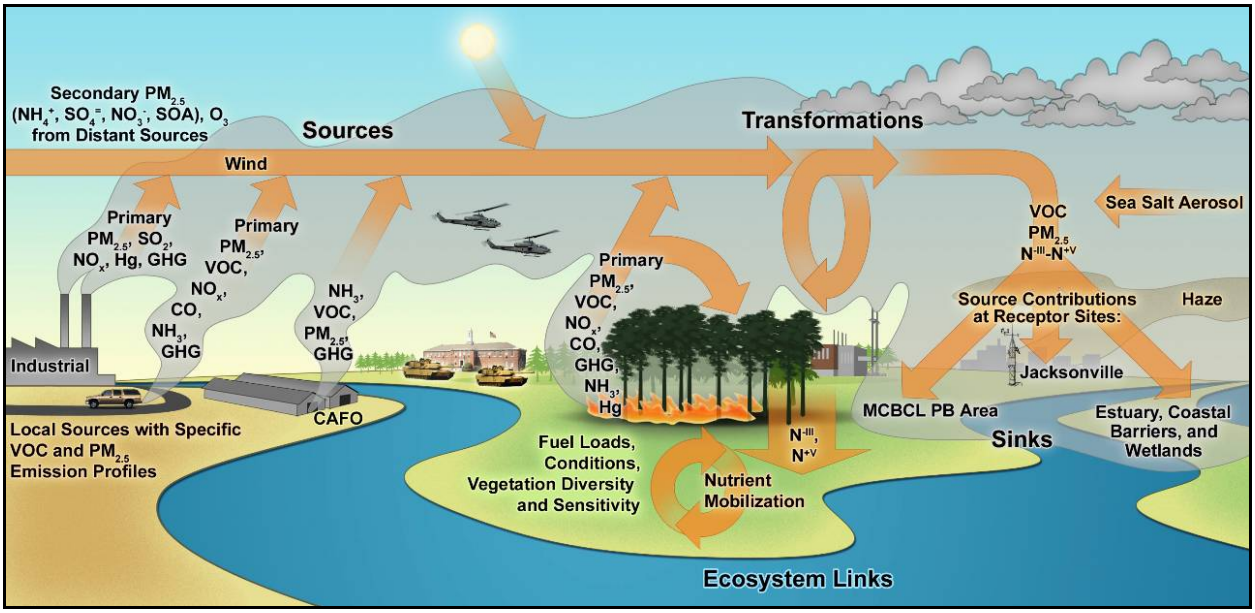

Figure 15-1. Conceptual model for the Atmospheric Module.

Fire is a natural part of this landscape, and natural fire regimes (e.g., frequency, intensity, season) vary across this soil–hydrology–vegetation gradient, from frequent surface fires in longleaf pine savannas to relatively infrequent and intense crown fires in pocosin (Kodama and Van Lear, 1980). However, prescribed burning (PB) was used by Native Americans for improving access, hunting, and farming and was adopted by the early European settlers for these purposes. By the 1980s, PB had become the dominant land management tool in the southeastern United States. Since that time, MCBCL managers have implemented this technique to reduce wildfire risk, manage range and forest ecosystems, and provide and maintain terrain for training and testing. PB is highly recommended by the Endangered Species Act to re-create the natural fire regimes needed to maintain the health of native forest ecosystems and, thus, to protect the habitat of threatened and endangered species. Despite its essential ecosystem benefits, PB is a major source of $PM_{2.5}$ and other air pollutants because of its incomplete and largely uncontrolled combustion process, which involves flaming and smoldering phases with different effective fuel consumption, unknown ecological sensitivities toward burning conducted in growing versus dormant seasons (Johnston, 1998), and unclear ecological benefits on larger spatial and temporal scales (MacLean et al., 1983; Raison et al., 1985). Certain fuel and fire meteorological parameters influence the emissions from the different combustion phases, which in turn participate in transport processes within the atmospheric boundary layer (BL), causing air quality impacts on local and regional scales (Friedli et al., 2007; Lee et al., 2005).

Dry deposition of atmospheric constituents, either nutrients or pollutants, is directly dependent upon their ambient concentration near the ground. These concentrations are influenced by different anthropogenic and biogenic sources, meteorological conditions driving their atmospheric dispersion and transformation, and sinks (see **Figure 15-1**). Among the six criteria air pollutants regulated for the protection of human health and welfare under 40 *Code of Federal Regulations* (CFR) of the Clean Air Act, O_3 and $PM_{2.5}$ are the most difficult to control because they (or parts of $PM_{2.5}$) are products of complex atmospheric formation processes involving heterogeneous photochemical reactions of certain precursors (Seinfeld and Pandis, 1998; U.S. EPA, 1996 and 1997). In 1997, the U.S. Environmental Protection Agency (EPA) and the Clean Air Scientific Advisory Committee (CASAC) recommended a cumulative seasonal standard for O_3 in the form of SUM06 (the sum of hours with ambient O_3 concentration exceeding 60 ppb). Many plant species are more sensitive to O_3 exposure than are humans, therefore requiring a type of protection that is different in time scale and level. These considerations led to EPA's promulgation of a stronger primary O_3 standard (75 ppb instead of 80 ppb) in the Final Rule from March 2008 (U.S. EPA, 2008a and b).

In a review of the Final Rule for the O_3 National Ambient Air Quality Standards (NAAQS) from April 7, 2008 (EPA-CASAC-08-009, Letter to the EPA Administrator), cumulative O_3 indices have been recommended by EPA and CASAC to be considered in the promulgation of a secondary (seasonal) standard for the protection of public welfare based on Heck and Cowling (1997) and other publications. Based on this review, EPA recently proposed a new cumulative, seasonal standard expressed as an annual index of the sum of weighted hourly concentrations, cumulated over 12 hours per day (from 8 a.m. to 8 p.m.) during the consecutive 3-month period within the O_3 season, with the maximum index value set at a level within the range of 7–15 ppm-hours (U.S. EPA, 2010). EPA furthermore proposed a reduction of the 8-hour primary standard, which was set at 75 ppb in the 2008 Final Rule, to a level between 60 ppb and 70 ppb, providing increased protection for children and other at-risk populations against an array of O_3-related adverse health effects. A recent study, however, revealed that O_3 produced during long-range transport from Asia across the Pacific Ocean increases the O_3 background levels over North America and may hinder compliance with the lower standard in times of booming Asian economies (Cooper et al., 2010).

In fall 2010, the EPA Administrator asked the CASAC to further interpret the underlying epidemiological and clinical studies to ensure that EPA's decision is grounded in the best science. In August 2012, the EPA Office for Air Quality Planning and Standards provided a first draft Policy Assessment and updates to the first draft Risk and Exposure Assessments for Health and Welfare, discussing the adequacy of the primary and secondary O_3 standards. In the Policy Assessment (U.S. EPA, 2012b), the EPA staff reached the preliminary conclusion that "the body of information now available supports consideration of revising the current 8-hour secondary O_3 standard, so as to afford greater and more appropriate public welfare protection by selecting a different form, averaging time and level than that of the primary standard, and that it does not support retention of the current secondary O_3 standard." EPA had immediately requested public comments about their elaborations and conclusions. The public comments period has closed at the end of October 2012, and the comments are currently being evaluated.

Ammonia (NH_3) and volatile organic compounds (VOCs) are of particular importance because of their precursor role in these processes yielding secondary organic and inorganic aerosols (secondary organic aerosol [SOA] and ammonium nitrate $[NH_4]_2SO_4$), respectively. Other Clean

Air Act–regulated criteria pollutants are sulfur dioxide (SO_2), nitrogen oxides (NO_x), carbon monoxide (CO), and Pb. Increased nitrogen oxide and NH_3 emissions add to the formation of $PM_{2.5}$ and alter patterns in atmospheric deposition through changes in the amount, composition, and distance of transport.

In a Policy Assessment released in April 2011 (U.S. EPA, 2011), EPA staff concluded that "the currently available information clearly calls into question the adequacy of the current suite of annual and 24-hour $PM_{2.5}$ standards" meant to protect public health against short- and long-term exposures to fine PM ($PM_{2.5}$). Consideration should be given to revise the suite of standards providing increased public health protection. The annual standard provides adequate protection from both long and short-term $PM_{2.5}$ exposures, with the 24-hour standard providing supplemental protection for days with high peak concentrations. However, the current annual $PM_{2.5}$ standard level of 15 μg m^{-3} should be preferably lowered to a range of 12 to 11 μg m^{-3}. For this range, EPA considered retaining the current 24-hour $PM_{2.5}$ standard level at 35 μg m^{-3}. However, if the annual standard level was 13 μg m^{-3}, EPA recommended lowering the 24-hour $PM_{2.5}$ standard level down to 30 μg m^{-3}.

After an extensive review process, in June 2012, EPA proposed to revise the annual standard by lowering the level to within a range of 12 to 13 μg m^{-3} and to retain the 24-hour standard (U.S. EPA, 2012a). In the same announcement, EPA proposed to retain the current 24-hour PM_{10} standard to continue providing protection against effects associated with short-term exposure to thoracic coarse particles (i.e., $PM_{10–2.5}$ or PM_c). EPA also proposed to revise the suite of secondary particulate matter (PM) standards by adding a distinct standard for $PM_{2.5}$ to address PM–related visibility impairment and to retain the current standards generally to address non-visibility welfare effects. The proposed distinct secondary standard would be defined in terms of a $PM_{2.5}$ visibility index, which would use speciated $PM_{2.5}$ mass concentrations and relative humidity data to calculate $PM_{2.5}$ light extinction, translated to the deciview (dv) scale, similar to the Regional Haze Program; a 24-hour averaging time; a 90th percentile form averaged over 3 years; and a level set at one of two options: either 30 dv or 28 dv.

In assessing the adequacy of the current suite of secondary PM standards (which are identical to the primary $PM_{2.5}$ and PM_{10} standards) meant to protect against PM related effects other than visibility impairment, EPA staff considered PM related effects on climate, ecological effects, and effects on materials. EPA came to the conclusion that the currently available information supports retaining control of both fine and coarse particles to address PM–related effects on ecosystems and materials damage and soiling, but that there is *insufficient information to assess the adequacy of protection afforded by the current standards*, and that there is *insufficient information at this time to base a NAAQS on climate impacts associated with current ambient concentrations of PM or its constituents*.

Biomass burning has raised considerable concern because it is a significant source to regional and global PM into the atmosphere. Much of the concern comes about the largely unknown interplay between initially emitted (primary) PM and new (secondary) PM formed from precursors during the atmospheric transport and dispersion of the fire emissions. The evolution of fire emissions into the atmosphere due to gas-particle partitioning and photo-oxidation can substantially alter the composition of gas and particle constituents. As emissions are diluted downwind of a fire source, semi-volatile particulate organic compounds may evaporate, reducing the organic aerosol (OA) concentrations relative to conserved species such as CO (Lipsky and

Robinson, 2006). This can be a major source of organic vapors, which can contribute to the formation of O_3 and SOA, and increase the OA concentration within a plume. Indeed, SOA formation in the transport of PB emissions had the greatest influence on $PM_{2.5}$ concentrations during a severe air quality event in Atlanta, GA (Lee et al., 2008). The atmospheric processes leading to SOA formation are complex and the role that biomass burning emissions play in these processes was discussed in the accompanying Research Project Air-1 Research Report Chapter 15, *Optimization of Prescribed Burning by Considering Mechanical Thinning as a Viable Land Management Option*.

Materials and Methods

The monitoring activities support the Atmospheric Module's research projects in describing and improving our understanding of critical pollutant transport and advection processes that are part of complex land–sea breeze circulation patterns, and their effects on the atmospheric abundance and composition of a variety of air pollutants on local and regional scales. **Figures 15-2** and **15-3** illustrate the location of the relevant monitoring stations on and off the Base, respectively. This improved understanding can be gained through the analysis of existing data and the integrated analysis of essential newly acquired monitoring data. Through comprehensive analysis of all monitored data, linking observations with local and regional air pollutant emissions data, including specific military training activities and land management procedures, the relative importance and potential of certain emissions sources exerting stress on certain parts of MCBCL's ecosystem will be indicated.

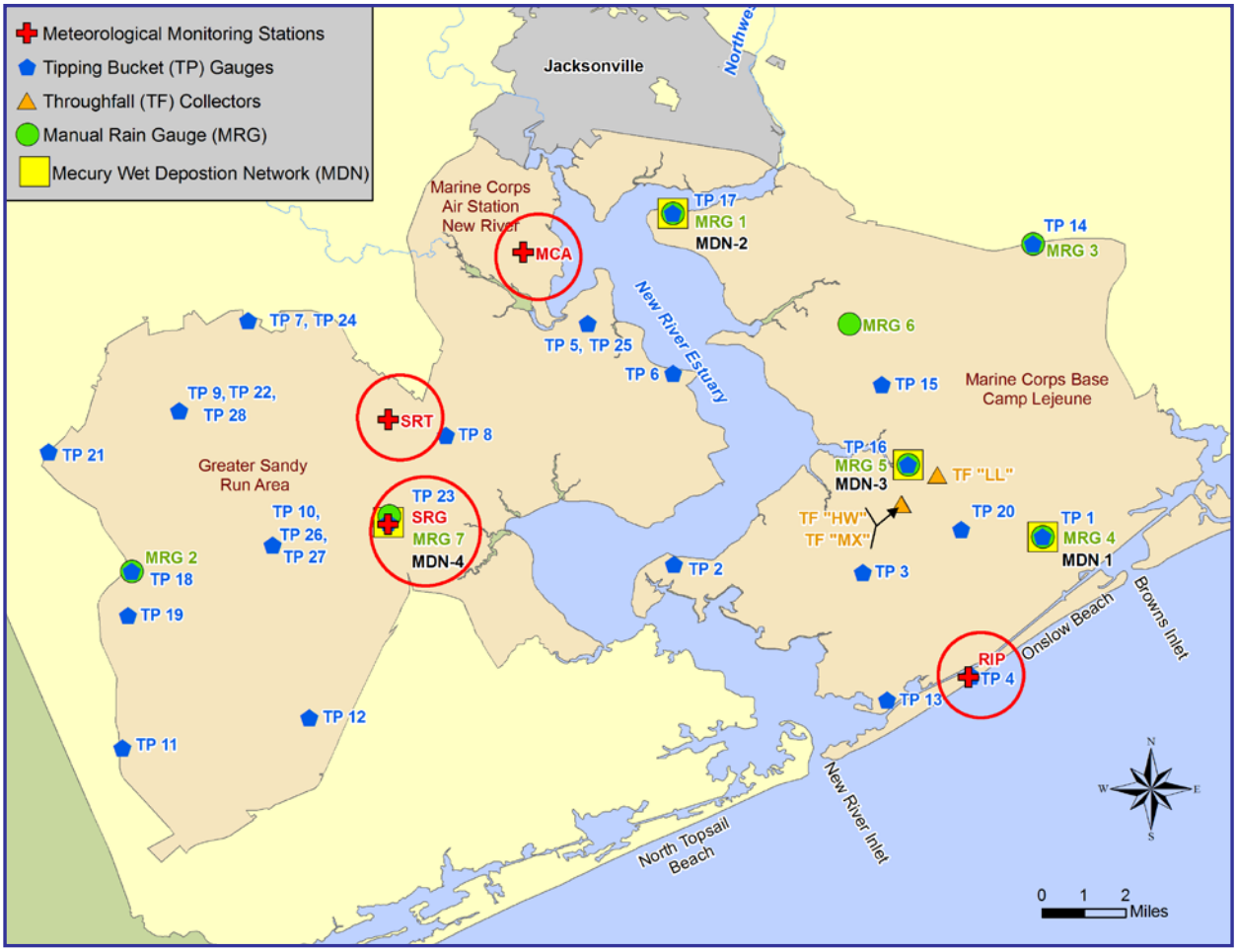

Figure 15-2. On-Base location of the four comprehensive monitoring sites (red circles); MCA monitoring meteorological parameters are co-located with Marine Corps Air Station New River (NRA; photosynthetically active radiation [PAR], O_3, $PM_{2.5}$, and PM_{10}).

Table 15-1 references the depicted monitoring locations and lists all individual meteorological and air quality parameters measured at each location. Except for the Riseley Pier (RIP) and Greater Sandy Run Area (GSRA) Tower (SRT) sites, meteorological data are being reported through the MW's Web site (http://mesowest.utah.edu/index.html) run by the University of Utah's Department of Meteorology. The data represent different averaging intervals and different reporting frequencies.

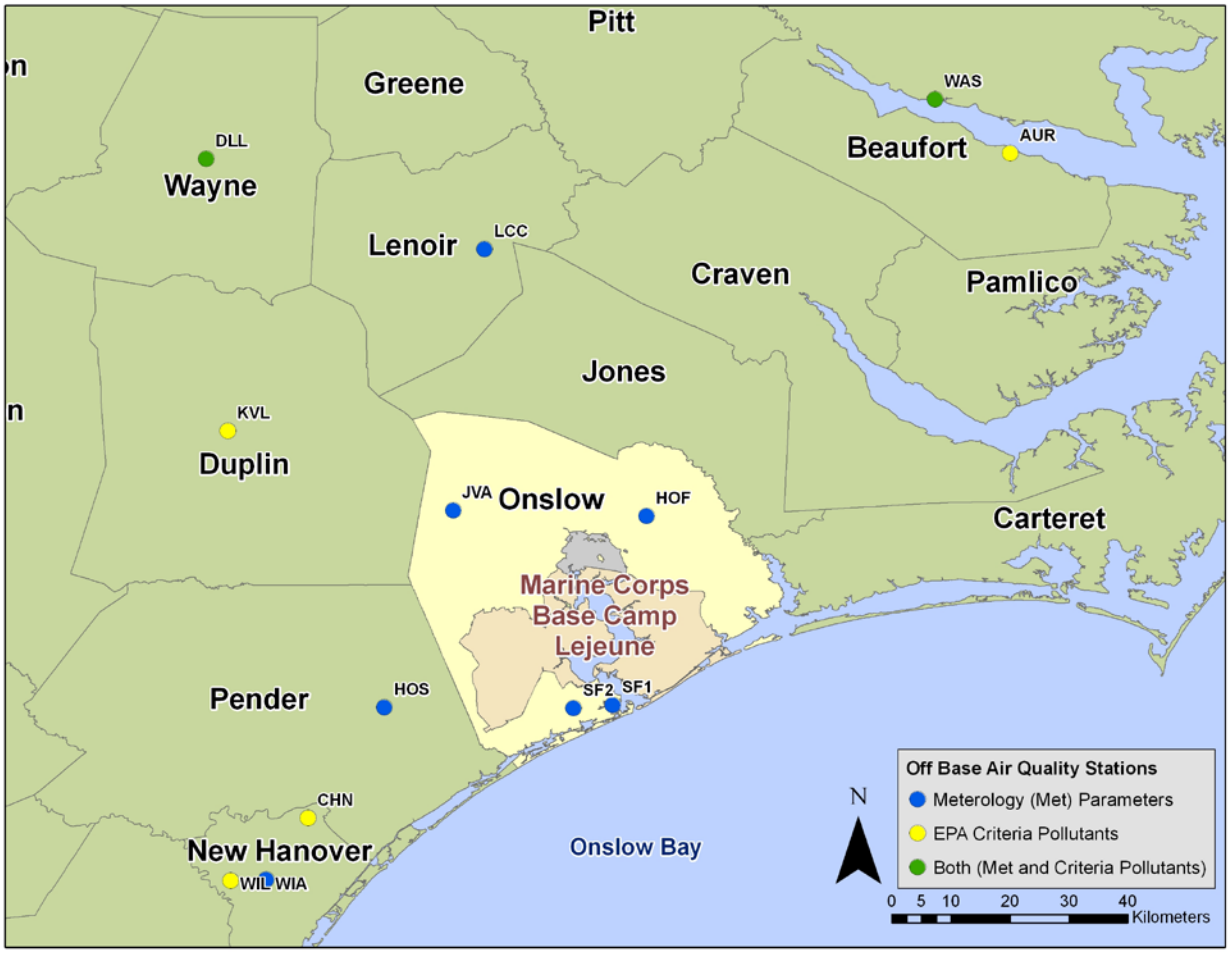

Figure 15-3. Off-Base monitoring and research stations for the Atmospheric Module.

This program supports three photosynthetically active radiation (PAR) sensors (Li-Cor quantum sensor LI-190SL measuring PAR in the spectral range of 400–700 nm), four nephelometers for continuous $PM_{2.5}$ and PM_{10} measurements, respectively. From the beginning in June 2008, PAR sensors have been installed and operated at Marine Corps Air Station New River (NRA) and RIP sites, as well as on top of a 40-m tower (SR-7 near Landing Zone Snipe) approximately 3 km north of the GSRA Ground (SRG) site. The SRT site had been equipped with additional barometric pressure (BP), temperature (TMP), relative humidity (RH), wind speed (WS), and wind direction (WD) sensors (contributed to Defense Coastal/Estuarine Research Program [DCERP] by Atmospheric Research & Analysis, Inc. [ARA]), allowing for monitoring of more regional conditions due to the measurements' height above ground. In March 2009, the National Oceanic and Atmospheric Administration's (NOAA's) National Weather Service (NWS) office in Morehead City, NC, provided a physical connection to its data logger at the RIP site, allowing acquisition of their meteorological raw data (reporting every 5 seconds). Since then, BP, TMP, RH, WS, WD, and precipitation (PCP; via a tipping bucket) data are being continuously ingested into the ARA data logger and subjected to ARA–specific routine quality assurance, quality control, and data-reduction procedures. In October and November 2010, instruments for continuous measurement of $PM_{2.5}$ and PM_{10} (coarse PM, whereas coarse PM (PM_c) is obtained from the mathematical difference between PM_{10} and $PM_{2.5}$) were implemented and put in operation at the NRA and SRG sites, complementing the PM measurements made at RIP and

SRT from the beginning of DCERP. All the supporting sensor signals are acquired via independent data loggers at a sampling rate of 1 Hz, reduced to 5-minute averages, quality assured, and reported as hourly averages. The continuous, hourly database serves to establish a detailed climatology for the different ecosystems on MCBCL.

Table 15-1. Locations and parameters monitored at on-Base (shaded yellow) and off-Base sites.

Network Name	Network ID	DCERP Name	DCERP ID	Latitude (North)	Longitude (East)	Elevation (m)	Parameters
Beaufort County	370130006	Aurora	AUR[c]	35.3778	−76.7669	1.5	SO_2
New Hanover County, Castle Hayne	371290002	Castle Hayne	CHN	34.3642	−77.8386	12.0	O_3, $PM_{2.5}$
Wayne County Dillard	371910005	Goldsboro	DLL	35.3692	−77.9939	33.0	WS, WD, $PM_{2.5}$
Hofmann Forest	HFMN7	Hofmann Forest	HOF	34.82500	−77.3219	12.8	BP, FT, PCP, RH, SR, TMP, WD, WS
Back Island	BKIN7	Holly Shelter	HOS	34.53280	−77.7219	6.1	BP, FT, FM, PCP, RH, SR, TMP, WD, WS
Jacksonville Airport	KOAJ	Jacksonville Airport	JVA	34.8333	−77.6166	29.0	BP, RH, TMP, VIS, WD, WS
Lenoir Community College	371070004	Kinston	LCC	35.2315	−77.5688	15.0	PCP, RH, SR, TMP, WD, WS, O_3
Jacksonville	KNCA	MCASNR	MCA	34.7058	−77.4408	7.0	BP, CIG, RH, TMP, VIS, WD, WS
N. a.	ARA	MCASNR	NRA[a]	34.7226	−77.4510	7.0	PAR, O_3, $PM_{2.5}$, PM_{10}
Riseley Pier	KRIS (ARA)	RIP	RIP[a]	34.5542	−77.2965	1.0	PAR, RH, TMP, WD, WS, O_3, $PM_{2.5}$, PM_{10}
Sneads Ferry	C7779	Sneads Ferry	SF1[b]	34.5364	−77.3734	10.0	BP, RH, TEMP, WD, WS
Sandy Run	CLJN7	GSRA Ground	SRG	34.6119	−77.4875	45.7	FT, FM, PCP, RH, SR, TMP, WD, WS, $PM_{2.5}$, PM_{10}
N. a.	ARA	GSRA Tower	SRT[a]	34.6479	−77.4874	85.0	BP, PAR, RH, TMP, WD, WS, O_3, $PM_{2.5}$, PM_{10}

(continued)

Table 15-1. Locations and parameters monitored at on-Base (shaded yellow) and off-Base sites. (continued)

Network Name	Network ID	DCERP Name	DCERP ID	Latitude (North)	Longitude (East)	Elevation (m)	Parameters
Washington	C4175	Washington	WAS	35.4596	−76.8813	2.1	BP, PCP, RH, TMP, WD, WS
New Hanover County	371290006	Wilmington	WIL	34.2684	−77.9565	6.0	SO_2
Wilmington International Airport	KILM	Wilmington	WIA	34.2706	−77.9025	10.1	BP, CIG, PCP, RH, TMP, VIS, WD, WS

BP = barometric pressure; CIG = ceiling; FM = fuel moisture; FT = fuel temperature; GSRA = Greater Sandy Run Area; MCASNR = Marine Corps Air Station New River; PAR = photosynthetically active radiation; PCP = precipitation; RH = relative humidity; SR = solar radiation; TMP = temperature; VIS = visibility; WD = wind direction; WS= wind speed

[a] Stations supported by DCERP.

[b] Nearby station, SF2, is used as a backup to SF1 (see **Figure 15-2**).

[c] The site was moved to Bayview Ferry (370130151, 35.428/-76.740) and started reporting on January 28, 2011.

$PM_{2.5}$ and PM_{10} mass concentrations were measured using an integrating nephelometer, the active-flow, *personal* DataRAM (*p*DR; Model MIE *p*DR-1200), and a newer replacement model, *p*DR-1500 (Thermo Fisher Scientific, Franklin, MA) that continuously measures the amount of light (at a wavelength of 880 nm) scattered by particles (scattering coefficient range 1.5×10^{-6} to 0.6 m^{-1}) drawn though an optical chamber at a specific flow rate. The amount of light scattered is converted to particle concentration readings using a well-established light scattering theory (Kerker, 1969). The two different sized fractions of 2.5 µm and 10 µm are achieved by drawing the sample air through two cyclones with different aerodynamic separation characteristics. In early 2010, diffusion driers were added to the sample inlet line configurations so that all nephelometers sense dry sample air. For this reporting period, the drying agent's capacity was never exhausted, making the following empirical correction obsolete, and hence reducing the overall measurement uncertainty. Before, when the drying agent's capacity to absorb water vapor from the sample air was exhausted, the nephelometer's in situ particle mass measurement was elevated relative to PM collected on filter material and an empirical correction had to be applied according to Chakrabarti et al. (2004). The *p*DR operates with a 37-mm Teflon membrane filter downstream from the optical chamber, allowing for confirmation of the continuous data by determining the gravimetric mass of PM collected on the filter membrane during a discrete sampling interval and comparing with the average scattering signal readings for this interval. At flow rates of 1.2 to 1.5 Lpm, filter loading from 1 week of sampling corresponds roughly with a 24-hour Federal Reference Method sample. Filters are collected in the field and shipped to ARA (Morrisville, NC), where they are processed in an International Organization for Standardization (ISO) Class 6 clean room (less than 10^6 particles per cubic meter) that allows accurate and precise mass measurement at 35 ±1% RH and 21 ±0.1°C.

O_3 was measured at three DCERP–operated sites on MCBCL (NRA, SRT, and RIP; **Table 15-1**), and $PM_{2.5}$ and PM_{10} were measured at four sites (RIP, SRT, NRA, and SRG). Because measurements at NRA and SRG were added in October and November 2010, the last report only covered the first three quarters of 2010; therefore, this report now includes the fourth quarter of 2010 with PM data from NRA and SRG. In contrast to the North Carolina Department of

Environment and Natural Resources' (NC DENR's) Division of Air Quality's regulatory network, which operates from April to October, O_3 at these DCERP–operated sites is monitored year round. O_3 was measured following an EPA–approved reference method using a pressure- and temperature-compensated commercial ultraviolet absorption instrument (Model TEI 49C, Thermo Fisher Scientific, Franklin, MA), following Lambert-Beer's law for the known absorption coefficient of O_3 at 254 nm. The signal is generated by the difference of frequently alternating measure and reference (zero) cycles (i.e., full transfer of O_3 through versus complete removal of O_3 from the flow's optical path). The linearity and precision of the analyzer were checked before and after the regulatory O_3 season (April through October). Precision-check mixing ratios of 0, 60, 100, 200, 300, and 400 ppbv are provided by a primary standard calibrator with active feedback control (Model TEI 49C-PS). Each precision check results in a six-point linear regression. Assuming normal distribution of the regressions' intercepts, the O_3 analyzer's detection limits are typically 0.5 ppb to 1 ppb, and the slopes of the linear regressions yield ±3% to ±7% precision. The accuracy is estimated to be the same.

The NC DENR's Division of Air Quality's data from surrounding counties (**Table 15-1** and **Figure 15-2**) were used in support of the routine evaluation of the O_3 and PM data collected on the Base.[1] It is important to note that NC DENR discontinued $PM_{2.5}$ and PM_{10} measurements in the Jacksonville (JVL) site, effective January 1, 2008. Nevertheless, data from this station played an important role in the analysis and evaluation of historical data preceding the field component of Research Project Air-1. Sampling frequencies vary with the parameter (e.g., SO_2 and O_3 data are reported hourly; daily average $PM_{2.5}$ and PM_{10} mass are reported every third or sixth day, respectively, with $PM_{2.5}$ speciation data from Kinston, NC, available every sixth day); however, the data collected provide a reliable, long-term temporal scale for Base analyses. Although the comprehensive analysis of the criteria pollutant measurements on the Base in the context of regional air quality is the subject of Research Project Air-1, the purpose of this monitoring task was to collect and merge the NC DENR's Division of Air Quality data with our Base data and provide joint statistical summaries on a monthly basis. The statistical summaries include graphical displays of wind rose plots, average diurnal behaviors, and frequency distributions of most prominent measurement parameters. Each of the monthly summaries for this reporting period (October 2010 to September 2011) has been uploaded to DCERP's Collaborative Web site.

Results and Discussion

The high level of completeness in data coverage achieved for most of 2010 continued into 2011. **Tables 15-2 and 15-3** provide an overview of the meteorological and air pollutant data completeness achieved during the fourth quarter of 2010 and the first three quarters of 2011. Note that data from only the first 9 months of 2011 are being presented in this report and that annual quarters are assumed equal to the four seasons of the year (i.e., winter [first quarter = January, February, March], spring [second quarter = April, May, June], summer [third quarter = July, August, September], and fall [fourth quarter = October, November, December); the latter is represented here by October, November, and December 2010).

[1] The NC DENR's air quality data were obtained from "real-time" repositories (see http://airnowtech.org) used for reporting daily meteorological and Air Quality Index information to the public. As such, NC DENR has not had an opportunity to fully verify and validate these data through its established quality assurance procedures to publish and certify them as official, accurate, and complete data.

Because EPA mandates that states monitor O_3 only between April and October, CHN and LCC sites report 0% coverage in the off-season months. Near 100% coverage was achieved across the network especially during the peak O_3 months July and August. Combined problems with Internet connection (via satellite), electrical power outages, and restricted access due to military training caused the lower coverage at SRT and RIP towards the end of the reporting period. Instead of PM_{10}, **Table 15-3** shows the more meaningful PM_c (i.e., the coarse fraction of PM_{10} from the measured $PM_{10}-PM_{2.5}$ difference). Coarse particles originate mainly from surface abrasion induced by natural processes (e.g., wind-blown dust) and anthropogenic processes (e.g., transportation, construction, metal fabrication). In the case of MCBCL, military training involving the movement of troops and weaponry are a primary source for PM_c. Also, in contrast to fine particles ($PM_{2.5}$), coarse particles deposit faster to the ground and, therefore, are confined closer to their primary sources. Fine particles settle more slowly and are also produced from secondary processes in the atmosphere involving gas-to-particle conversion and nucleation.

Table 15-2. Percentage levels of monthly data coverage (on hourly basis) in 2010 and 2011 for meteorological parameters monitored on-Base (shaded yellow) and off-Base.

Site ID[a]	Par.[b]	2010			2011 Percentage of Hourly Coverage								
		Oct	Nov	Dec	Jan	Feb	Mar	Apr	May	Jun	Jul	Aug	Sep
MCA	MET	96	100	97	99	99	93	99	99	100	100	96	100
NRA[c]	PAR	97	99	100	100	100	100	100	90	100	100	85	0
RIP[c]	PAR	83	86	65	100	100	100	100	97	98	100	86	75
	MET	40	50	60	80	99	59	24	26	27	0	0	0
SRG	MET	100	98	100	100	100	96	97	100	100	100	100	100
SRT[c]	MET	100	100	100	97	100	75	78	97	100	91	38	30
	PAR	100	100	100	97	100	75	78	97	100	91	38	30
DLL	MET	100	100	100	100	100	100	100	100	100	100	78	95
HOF	MET	100	98	100	100	98	93	87	90	98	100	99	92
HOS	MET	100	98	100	99	100	96	98	100	100	100	100	100
JVA	MET	100	100	96	98	99	94	99	100	100	100	93	100
LCC	MET	100	95	100	100	100	100	93	74	98	100	80	98
SF1	MET	91	98	99	99	98	90	100	99	100	100	100	100
WAS	MET	91	92	94	80	90	44	94	86	89	87	69	84
WIA	MET	100	100	97	99	100	93	98	100	100	99	100	100

[a] Site ID: See **Table 15-1** for definitions and **Figures 15-1** and **15-2** for mapped locations.

[b] Parameters: MET = meteorological parameters; PAR = photosynthetically active radiation.

[c] Stations operated by DCERP.

Table 15-3. Percentage levels of monthly data coverage (on hourly basis) in 2010 and 2011 for EPA criteria pollutants monitored on-Base (shaded yellow) and off-Base.

Site ID[a]	Par.[b]	2010			2011 Percentage of Hourly Coverage								
		Oct	Nov	Dec	Jan	Feb	Mar	Apr	May	Jun	Jul	Aug	Sep
NRA[c]	O_3	97	99	100	87	100	53	83	90	100	100	85	0
	$PM_{2.5}$	97	99	100	97	88	53	100	90	100	100	66	0
	PM_c	97	99	100	97	88	53	100	90	100	100	66	0
RIP[c]	O_3	84	85	50	82	89	92	100	97	100	100	85	75
	$PM_{2.5}$	78	76	37	82	100	97	98	80	100	88	85	27
	PM_c	78	76	37	82	100	97	98	80	100	88	85	27
SRG[c]	$PM_{2.5}$	0	62	37	89	81	40	97	100	100	100	82	0
	PM_c	0	62	37	89	81	40	97	100	100	100	82	0
SRT[c]	O_3	100	65	100	97	100	75	78	97	100	77	0	29
	$PM_{2.5}$	100	100	100	97	100	69	78	97	97	91	38	30
	PM_c	100	100	100	97	100	69	78	97	97	91	38	30
AUR	SO_2	100	100	93	10	100	100	100	100	100	100	79	95
CHN	O_3	99	2	0	0	0	2	100	100	100	100	87	100
	$PM_{2.5}$	100	100	100	100	100	100	100	100	95	87	86	100
DLL	$PM_{2.5}$	100	100	100	100	100	95	100	100	97	95	75	95
LCC	O_3	100	5	0	0	0	75	100	100	100	100	84	100
WIL	SO_2	100	100	100	96	100	100	100	100	100	100	83	94

[a] Site ID: See **Table 15-1** for definitions and **Figures 15-1** and **15-2** for mapped locations.
[b] Parameters: O_3 = ozone; $PM_{2.5}$ = fine particulate matter (PM); PM_c = coarse PM; SO_2 = sulfur dioxide.
[c] Stations or equipment operated by DCERP.

Monthly statistical summaries based on merged hourly averages, as well as monthly diurnal averages and wind rose plots for the main parameters (BP, TMP, RH, PAR, solar radiation [SR], and WS), were compiled from all sites and presented to the DCERP Team via the Collaborative Web site. The following sections will present the results for main meteorological parameters and air pollutants from the five on-Base sites in the context of more regional features, characterizing the study domain's climatology. All parameters are presented and discussed based on monthly, quarterly, and annual averages and by means of diurnal profiles and wind rose plots.

Temperature

Figure 15-4 indicates much above normal temperatures recorded in many areas of the east and southeast between April and September (from www.ncdc.noaa.gov/temp-and-precip/maps.php) compared only with June. For the second consecutive year, the summer began with exceptionally warm temperatures across the southeastern United States. June mean temperatures reached 2.2–3.3°C (4–6°F) above normal across most of the region, with several locations in the Southeast experiencing their warmest June on record, including Columbus, GA, and Cape Hatteras, NC. Tallahassee Regional Airport in Florida recorded an all-time maximum temperature of 40.6°C (105°F) on the 15th of the month, breaking the old record of 40°C (104°F) last set in 1933. In Columbia, SC, and Savannah, GA, maximum temperatures reached 90°F (32.2°C) or higher on

all 30 days of the month, breaking earlier records of 27 days set back in 1911 and 1952, indicating also noteworthy persistence of warm temperatures. This June weather pattern was a continuation of an upper-level high pressure ridge over the southern to eastern United States and an upper low pressure trough over the Northwest, with the storm track mostly keeping to the northern states. Occasional weather systems moved across the middle of the country toward the east, dragging weak fronts into the Southeast and keeping the weather hot and dry.

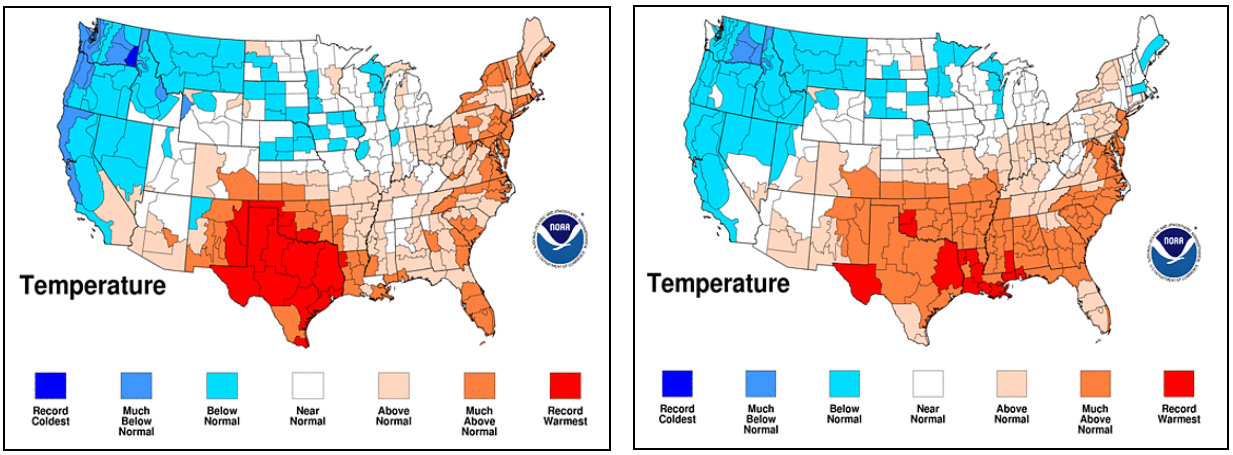

Figure 15-4. Sub-regional temperature rankings across the continental United States for 2011 period April–September (left panel) and June alone (right panel).

Source: National Climatic Data Center; National Environmental Satellite, Data, and Information Service; NOAA.

The upper-level high pressure ridge persisted over the southern to eastern United States through most of the summer, causing July to be excessively hot across the eastern two-thirds of the United States and causing the third quarter averages to be consistently above normal at all our study sites. For the month, 78 all-time high maximum temperature records were broken along with 209 all-time high minimum temperature records, providing little relief from the extreme daytime heat. The heat wave brought at least 38°C (100°F) temperatures to Raleigh, NC, every day from July 20 to 24, breaking a new record for the most consecutive days the area has recorded triple digit temperatures. Cape Hatteras, NC, tied its warmest month ever in a record extending back to 1898. Additionally, several locations recorded one of their top 3 warmest July's on record, including Raleigh (warmest on record), Asheville, and Greensboro (all in North Carolina), and Columbia, SC. For the second consecutive year, the end of August marked one of the warmest meteorological summers (June–August) on record at several locations across the Southeast. Locations that experienced their warmest summer on record in 2011 included Augusta, Athens, Columbus, and Savannah (all in Georgia); Charleston and Columbia (both in South Carolina, and Cape Hatteras (North Carolina).

Table 15-4 summarizes monthly average temperatures among the stations on and off Base, in comparison with each location's long-term normal. Both individual locations' averages and regional averages indicate consistently above normal conditions during the warm spring and summer months and below normal during colder fall and winter months (i.e., November, December, and January). June marked the highest above normal across the locations on and off Base, which was in line with conditions across the entire southeast region. **Table 15-4** is organized by the sites' latitudes, presenting the values from the northern most site (Washington, WAS) at the top and the ones from the southernmost site (Wilmington International Airport,

WIA) at the bottom. The average from all of the sites' monthly means is listed below the WIA entries. For some of the sites, 30-year normals were available from the State Climate Office of North Carolina's Web site at http://www.nc-climate.ncsu.edu. This office also provides regionally averaged temperature and rainfall data for the Southern Coastal Plain, encompassing our study area. From those values, 30-year normals were calculated and added to the table as N30* (30-year period ending in 2008) and N30# (30-year period ending in 1978).

Table 15-4. Monthly mean air temperatures with 30-Year normals (*italicized*) in degrees Celsius (°C) for period from October 2010 to September 2011 and all study sites are on-Base (shaded yellow) and off-Base.

Site ID	2010			2011 Monthly and Annual Mean Temperatures *with 30-year normals* in °C									
	Oct	Nov	Dec	Jan	Feb	Mar	Apr	May	Jun	Jul	Aug	Sep	Avg
WAS	18.3	11.4	2.1	2.9	8.9	9.9	18.0	20.8	26.1	27.4	27.1	23.3	**16.3**
	17.3	*12.4*	*7.7*	*5.7*	*6.9*	*11.1*	*15.7*	*20.1*	*24.2*	*26.3*	*25.6*	*23.1*	*16.3*
LCC	16.1	9.4	1.3	2.9	8.3	9.9	16.1	18.8	25.0	26.4	25.2	21.9	**15.1**
	16.0	*11.4*	*6.8*	*5.2*	*6.6*	*10.8*	*15.4*	*19.9*	*24.0*	*26.1*	*25.1*	*22.1*	*15.8*
HOF	17.9	11.6	2.5	3.9	9.7	11.5	18.2	21.1	26.1	27.3	26.6	23.1	**16.6**
	17.6	*13.3*	*8.9*	*7.6*	*9.0*	*12.4*	*16.6*	*20.7*	*24.4*	*26.7*	*26.1*	*23.3*	*17.2*
JVA	18.2	12.6	2.9	4.7	9.7	12.9	19.1	20.9	25.3	26.7	25.2	23.1	**16.8**
MCA	17.9	11.6	2.5	3.9	9.7	11.5	18.2	21.1	26.1	27.3	26.6	23.1	**16.6**
	17.6	*12.9*	*8.7*	*7.1*	*8.4*	*12.2*	*16.4*	*20.7*	*24.6*	*26.8*	*26.0*	*23.4*	*17.1*
SRG	17.6	11.2	2.5	4.0	9.7	11.8	18.1	20.9	25.8	27.0	26.3	23.0	**16.5**
SRT	18.2	12.6	2.9	4.7	9.7	12.9	19.1	20.9	25.3	26.7	25.2	23.1	**16.8**
RIP	19.3	13.4	3.5	3.4	8.9	12.2	16.8	21.0	24.9	-	-	-	**13.7**
SF1	18.6	12.7	3.2	4.5	9.3	11.8	17.9	21.7	26.2	27.5	27.1	24.0	**17.1**
HOS	16.2	9.5	1.3	2.8	8.9	10.8	17.0	19.8	25.7	27.8	26.5	23.2	**15.8**
WIA	18.7	12.4	3.4	4.6	10.1	12.1	18.6	21.6	26.8	27.5	26.9	23.6	**17.2**
	18.2	*13.6*	*9.4*	*7.8*	*9.2*	*12.8*	*17.1*	*21.2*	*25.0*	*27.3*	*26.5*	*23.9*	*17.7*
AVG	**17.9**	**11.9**	**3.1**	**3.8**	**9.4**	**11.6**	**17.9**	**20.8**	**25.8**	**27.2**	**26.3**	**23.2**	**16.6**
*N30**	*16.9*	*12.4*	*7.9*	*6.4*	*8.1*	*11.8*	*16.3*	*20.4*	*24.6*	*26.7*	*25.8*	*22.7*	*16.7*
N30#	*17.0*	*11.6*	*7.5*	*6.8*	*7.8*	*11.4*	*16.3*	*20.6*	*24.1*	*26.0*	*25.6*	*22.6*	*16.4*

N30* = 30-year normals regionally averaged over the Southern Coastal Plain (SCP) with period ending in 2008.
N30# = Same as N30*, but with the period ending in 1978.

The annual average from the measured monthly means (here only January–September) is 16.6°C and 0.1 degree lower than Southern Coastal Plain's 30-year normal. This is largely due to the extreme low temperatures experienced in December 2010 and January 2011. Their 2-month average temperature ranked among the top five coldest in many locations across the Southeast since 1937. The cold temperatures and wide-spread snowfall were linked to a strong west-to-east flow in the jet stream circulation over the contiguous United States. Deep, low-pressure systems developed in this flow, resulting in intense winter storms across the nation and outbreaks of cold Canadian air, especially east of the Rockies. The local area received even some snowfall during that time, with the snow cover promoting more efficient nocturnal cooling and the formation of

strong surface inversions. Comparing the two consecutive 30-year normals N30* and N30#, reveals that the region experienced a warming trend for all months except for January and May.

The site-specific deviations from the normal are easier to see in **Figure 15-5**, indicating that all temperatures deviated high especially in June, July, and August, and only on-Base locations recorded above normal in April. Although the ground station (SRG) is only 3 km south from the tower (SRT), a comparison of the data reveals that SRT experienced higher temperatures especially during March and April. It is important to note that although the October, November and December data were acquired in 2010, these data were plotted to the right of the January–September 2011 period for visual purposes.

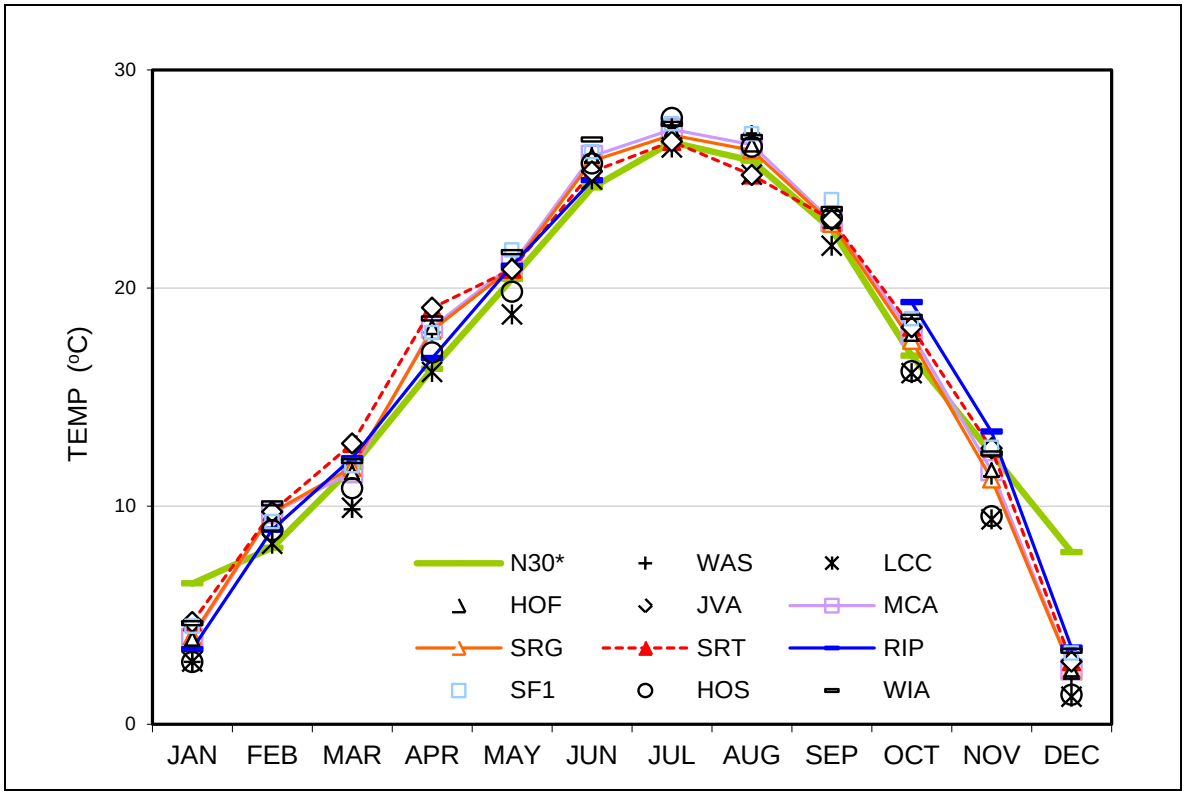

Figure 15-5. Monthly mean temperatures from sites in study domain compared to the 30-year normals of the Southern Coastal Plain (SCP) ending in 2008 (N30*).

Figure 15-6 presents quarterly average diurnal profiles of ambient air temperatures measured at four sites on Base (i.e., RIP, SRG, SRT, and MCA). The fact that RIP is on average the warmest site during the fall transition (fourth quarter) can be attributed to its proximity to the Atlantic Ocean. The effect of the ocean's heat capacity seems most pronounced during fall nights and early mornings. Average temperatures at SRT (40 m above ground) being consistently above those from nearby SRG during transition seasons in the fourth and second quarters are due to nocturnal stratification effects, keeping the air aloft warmer due to radiative cooling near the ground forming temperature inversions at night.

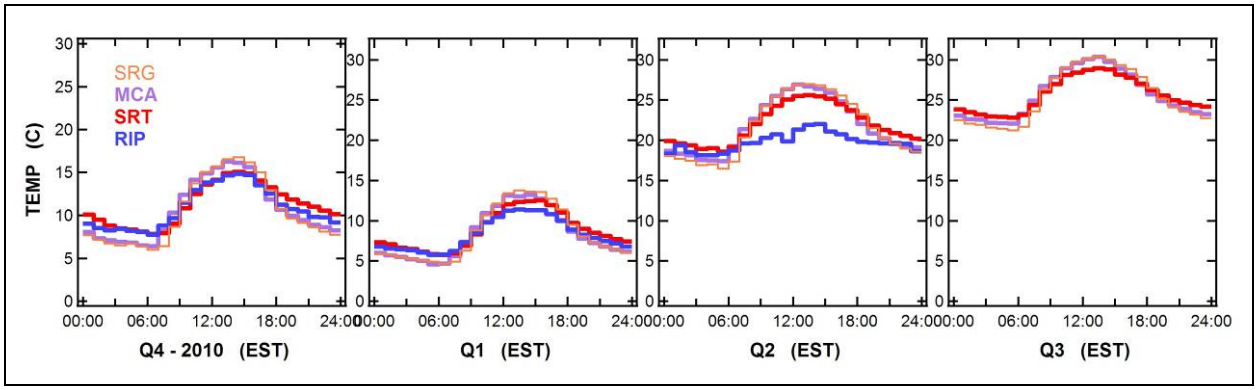

Figure 15-6. Seasonally averaged diurnal profiles for air temperature from October 2010 to September 2011.

Humidity and Precipitation

The nocturnal temperature inversions cause significant horizontal stratification, leaving air layers aloft (40 m above ground) consistently drier and yielding a significant vertical gradient (**Figure 15-7**). During mid-afternoon these gradients become smallest due to vertical mixing of the air in the lower atmospheric BL. The proximity to the ocean causes RIP to show the least amount of drying during midday hours relative to the other sites further inland. In 2010, conditions were significantly drier than normal except for August, when hurricane Irene made landfall near Cape Lookout, NC, as a Category 1 hurricane on August 27, marking the first hurricane landfall in the United States since hurricane Ike in September 2008. Hurricane Irene made a second landfall in New Jersey on August 28, and yet another landfall as a tropical storm along Long Island, NY, later that same day. Hurricane Irene brought torrential rainfall and flooding to the Eastern Seaboard between August 27 and 29, contributing to New Jersey, New York, Vermont, and New Hampshire having their wettest August on record. It also explains the large contributions to the total diurnal rainfall amounts in the third quarter of 2011 as shown in **Figure 15-8**.

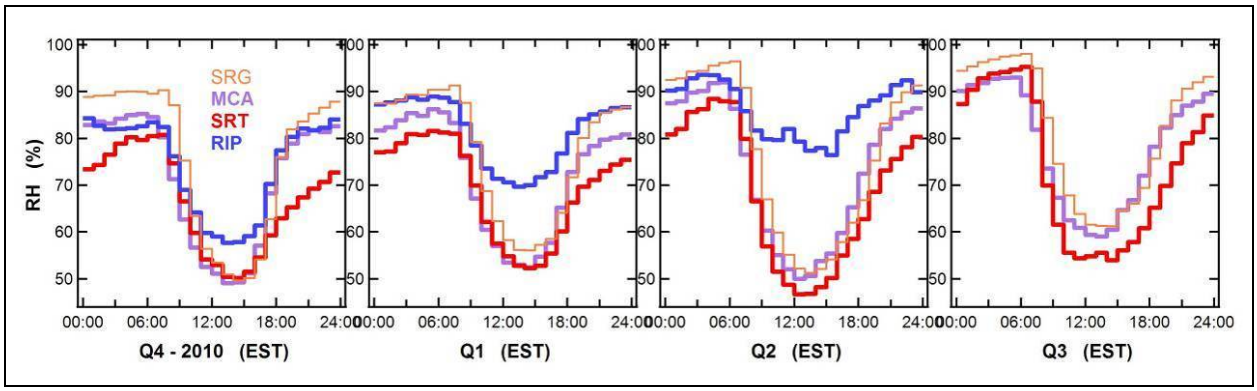

Figure 15-7. Seasonally averaged diurnal profiles for relative humidity in 2010–2011.

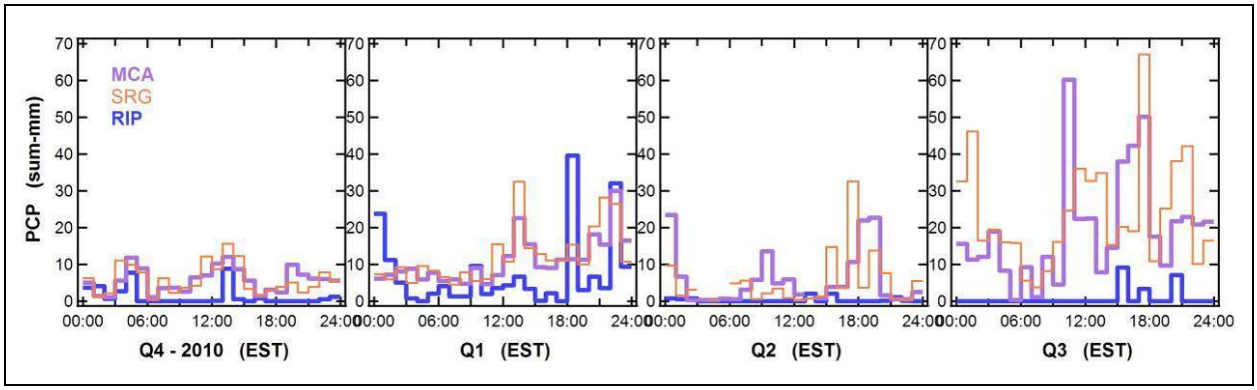

Figure 15-8. Seasonally averaged diurnal profiles of hourly summed rainfall in 2010–2011.

The combination of heavy rain and high wind resulted in numerous downed trees, power lines, and extensive property damage across eastern sections of North Carolina and Virginia. Large sections of North Carolina Highway 12 were severely damaged, cutting off access to several villages and beaches along the Outer Banks. Prior to making landfall in North Carolina, Hurricane Irene pounded Puerto Rico with heavy rain and hurricane-force winds, dropping 471 mm of rain in San Juan, Puerto Rico, which set a new all-time monthly record. Hurricane Irene also dropped between 203 and 381 mm of rain across eastern sections of North Carolina and Virginia on August 27 and 28.

Before Hurricane Irene hit, precipitation in August had been generally below normal across the Southeast. The driest locations across the Southeast remained across most of Georgia, eastern Alabama, and the Florida Panhandle. Tallahassee, FL, recorded 51 mm of rain for the month, making it both the driest August as well as the driest meteorological summer in a record extending back to 1892. Although Hurricane Irene helped alleviate severe and extreme drought across eastern North Carolina, dryness continued across much of Georgia, contributing to several wildfires. According to the Georgia State Climate Office, more than 2,230 acres burned across the state in August, which was double the long-term average for the month.

Figure 15-9 compares the nation-wide precipitation rankings from August with those from the 6-month period April–September, illustrating the continued drought in many areas of the Southeast and South, especially in Texas. An analysis of Texas statewide tree-ring records dating back to 1550 indicates that the summer 2011 drought in Texas is matched by only one summer (1789) in the 429-year tree-ring record, indicating that the summer 2011 drought appears to be unusual even in the context of the multi-century tree-ring record. Similar to Georgia, these extreme drought conditions caused large wildfires. Thus, the Texas Forestry Service reported 20,155 fires since the beginning of Wildfire Season on November 15, 2010 burning more than 3.5 million acres. In a later section, we will demonstrate the utility of our monitoring data to identify and characterize the air quality impacts from distant wildfires.

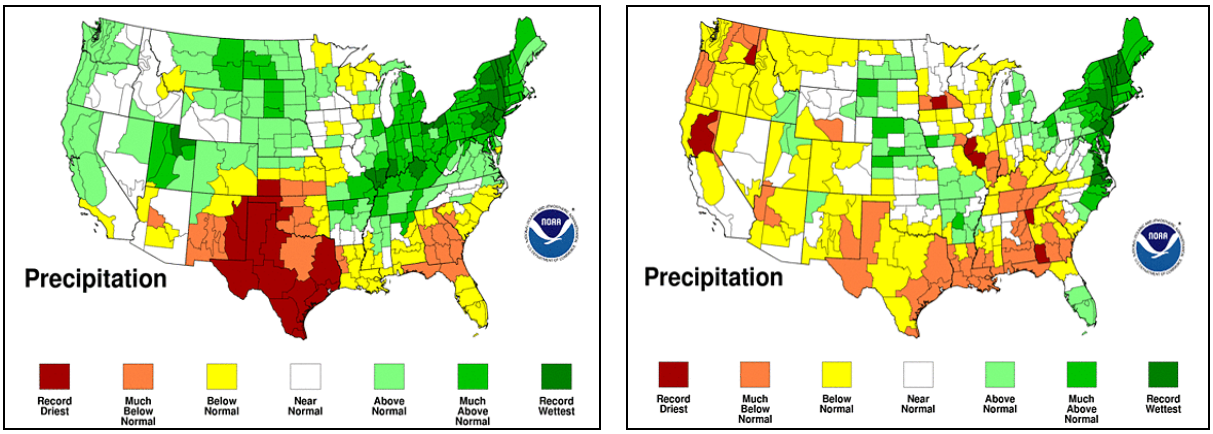

Figure 15-9. Sub-regional precipitation rankings across the continental United States for 2011 period April–September (left panel), and August alone (right panel).

Source: National Climatic Data Center; National Environmental Satellite, Data, and Information Service; NOAA.

The spatial and temporal distribution of rainfall on the Base is investigated extensively as part of Research Project Air-2 led by Dr. Wayne Robarge (chapter 16 of the Final Research Report). **Table 15-5** looks beyond the MCBCL borders and compares October 2010 thru September 2011 rainfall data from five sites in the greater study domain off-Base with data from the three on-Base sites (i.e., MCA, SRG, and RIP). **Figure 15-10** depicts these monthly totals from all eight sites relative to each other, to their average, and to the regional Southern Coastal Plain's 30-year Normals similar to the temperature. The Table also lists individual sites' 30-year Normals for each month and as an annual sum (although October, November, and December being from 2010 and not 2011). Monthly totals from the eight sites are averaged and compared with two consecutive, regionally representative 30-year normals at the bottom of **Table 15-5** and in **Figure 15-10**. The sites are listed again according to their latitudes with the northern most site at the top and southern most site at the bottom, which also somewhat reflects the sites' decreasing distance from the ocean. The on-Base sites' coastal gradient MCA-SRG-RIP is highlighted yellow in **Table 15-5**. The study domain's monthly average rainfall amounts were consistently below normal during most of the period except August, which received record rainfall region-wide thanks to Hurricane Irene as previously discussed. However, comparing the average of all measured monthly totals with the 30-year normals for the region Southern Coastal Plain, the study domain still suffered a drought, receiving on average 1 mm less rain per month than the normal in 2010–2011. **Figure 15-9** clearly shows that this was mainly due to at or below normal rainfall during all months except August.

Table 15-5. Monthly total rainfall amounts with 30-year normals (*italicized*) in millimeters for period from October 2010 to September 2011 and all study sites on-Base (shaded yellow) and off-Base.

Site ID	2010 Totals			2011 Monthly Totals with 30-yr Normals in mm									Annual Sum
	Oct	Nov	Dec	Jan	Feb	Mar	Apr	May	Jun	Jul	Aug	Sep	
LCC	30	2	66	43	56	104	74	9	40	115	47	92	**678**
	89	*71*	*90*	*113*	*87*	*108*	*87*	*104*	*118*	*149*	*143*	*138*	*1298*
HOF	27	23	95	80	95	95	56	26	53	130	304	81	**1064**
	93	*94*	*93*	*129*	*98*	*116*	*79*	*102*	*123*	*171*	*173*	*164*	*1435*
JVA			19	17	25	38	31	10	30	182	230	78	**661**
MCA	33	30	74	65	102	89	49	58	36	91	272	98	**997**
	84	*85*	*94*	*114*	*91*	*102*	*78*	*98*	*124*	*180*	*164*	*159*	*1373*
SRG	17	34	90	78	105	107	62	9	51	105	385	75	**1118**
RIP		13	18	35	55	85	5	2				20	233
HOS	22	25	82	55	108	91	54	27	29	95	307	142	**1037**
WIA	45	16	99	60	109	83	26	42	62	69	324	182	**1117**
	82	*83*	*96*	*115*	*93*	*107*	*75*	*112*	*136*	*194*	*186*	*172*	*1450*
AVG	**29**	**20**	**68**	**54**	**82**	**86**	**45**	**23**	**43**	**112**	**267**	**96**	**926**
*N30**	*89*	*80*	*82*	*101*	*89*	*106*	*80*	*96*	*122*	*155*	*154*	*151*	*1305*
N30#	*76*	*76*	*84*	*92*	*93*	*104*	*79*	*103*	*137*	*170*	*151*	*121*	*1286*

N30* = 30-year period ending in 2008; N30# = 30-year period ending in 1978.

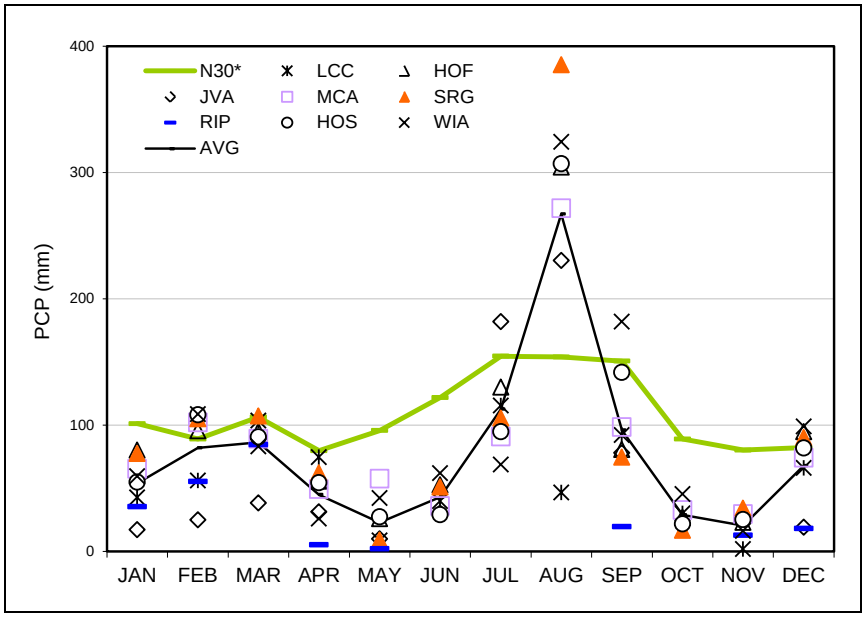

Figure 15-10. Monthly total rainfall amounts from sites in the study domain compared to the 30-year normals (N30*) of the Southern Coastal Plain (SCP).

Looking back on the entire study period, **Table 15-6**, compares rainfall totals from previous years with the most recent 2011 period among the same sites. Although WIA, HOS, and SRG are parallel to the North Carolina coastline (approximately 10–15 km off of the East Coast), sites

SRG, MCA, JVA, and LCC line up with increasing distance to the coast. The latter two sites are farthest from the coast at ca. 40 and 100 km, respectively, and both are excluded in the coastal average (AVG) used to compare with the 30-year normal (N30*). Although rainfall amounts in the second half of 2008 were significantly below normal, the following 2 years averaged above normal with 2011 again falling behind. For all periods, though, average rainfall amounts consistently decreased along the inland gradient. However, more complex patterns in nutrient deposition were observed in the highly resolved spatial sampling of rainfall amounts and composition across MCBCL as part of Research Project Air-2 (see *DCERP1 Final Research Report*).

Table 15-6. Given periods' total rainfall amounts (in millimeters) from MCBCL sites relative to 30-year normals regionally averaged over the Southern Coastal Plain (SCP; N30*).

Period	*N30**	AVG	WIA	HOS	SRG	MCA	HOF	JVA	LCC
Jul–Dec 2008	*711*	621	690	572	699	510	634	306	484
Jan–Dec 2009	*1,305*	1,544	1,564	1,709	1,682	1,343	1,423	1,096	***862***
Jan–Dec 2010	*1,305*	1,415	1,596	1,382	1,464	1,191	1,443	***721***	901
Jan–Sep 2011	*1,053*	924	957	908	977	860	920	642	580

Note: Values in bold italics indicate incomplete records.

Winds and Air Mass Transport

Figures 15-11, 15-12, and 15-13 characterize wind and air flow patterns observed on the Base. Except for SRT, winds are measured between 5 m and 10 m above ground. Being close to the coast, all on-Base sensors exhibit the influence from land–sea breeze circulation and associated BL dynamics. The differential heating between the land area and the adjacent ocean water leads to lifted isobaric surfaces over the land, which, in turn, leads to divergence in the upper portion of the BL, creating low pressure and high wind speeds at the surface. The surface winds peak around the time of maximum differential temperature (mid to late afternoon), which seems best confirmed by the winds measured at MCA, during the warmer half of the year (second and third quarters). As SR and hence differential heating decreases from summer to winter, the pressure minimum and associated wind speed maximum appears slightly earlier in the day. At sunset, the well-mixed BL collapses and the nocturnal inversion starts to build, causing increased effects from surface friction and hence slowing of the winds. Due to their distinct locations, RIP and SRT sites experience the least amount of nocturnal slowing compared to the other sites. Relative to the winds at SRG, the SRT profile indicates possible occasional influence from nocturnal jet streams with stronger winds above the shallow ground inversion. The decrease in wind speed gradient after sunrise is indicative of BL transitioning from stable shallow to turbulent (neutral) deep, entraining air masses from the "reservoir" layer aloft in the process. Although daytime peaks in wind speed consistently increase, moving from the cold winter to the warmer spring season (first and second quarters in **Figure 15-10**), the reverse trend appears transitioning to summer (third quarter), indicating the slowing effect of a convectively well-mixed BL that is deepest in summer over land, but not over the ocean. The sonic anemometer operated by the NWS at RIP became inoperative in early March 2011 and was not restored before the end of this study.

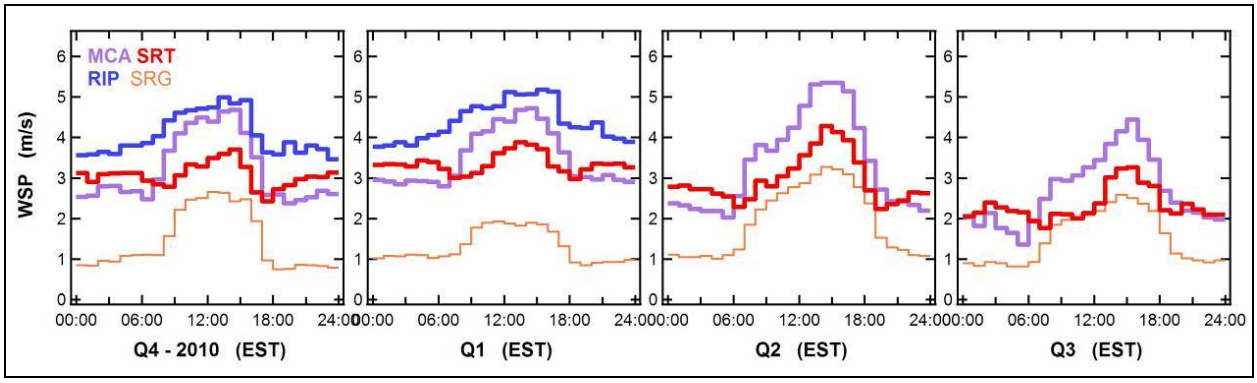

Figure 15-11. Seasonally averaged diurnal profiles of horizontal wind speed in 2010–2011.

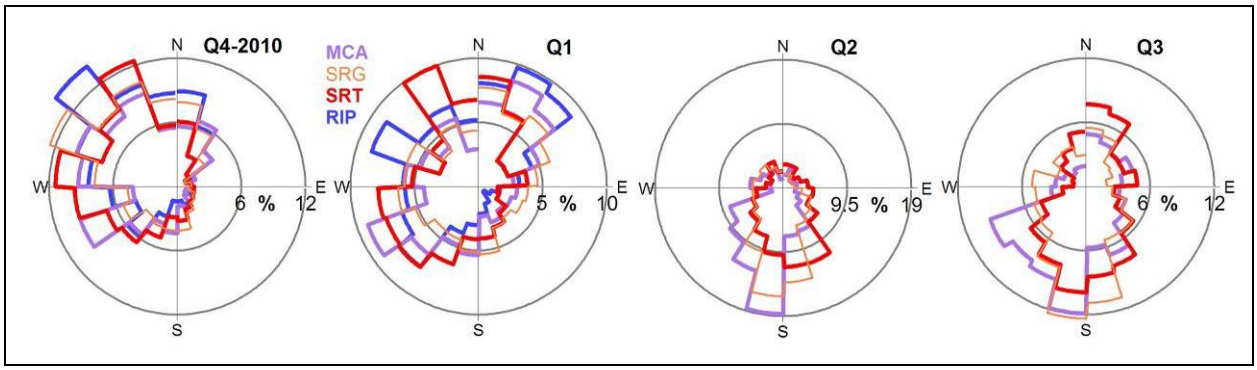

Figure 15-12. Seasonally averaged wind frequency distribution wind roses for 2010–2011.

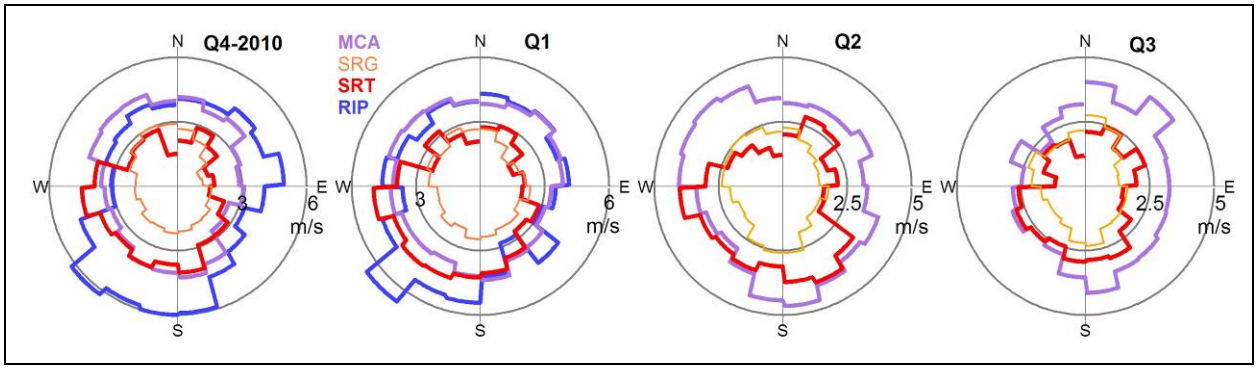

Figure 15-13. Seasonally averaged wind speed roses for 2010–2011.

Figures 15-12 and **15-13** show wind rose compass plots representing the distribution of wind direction and associated wind speed averages for each of the four on-Base sites during the different quarters. Wind rose plots assume that the sites are positioned in the center of the compass and receive air masses from the outlined directions with the indicated frequency (**Figure 15-12**) and speed (**Figure 15-13**) of all occurrences reported in percentage and m/s, respectively. Hourly wind directions were determined from wind vector calculations based on 5-minute averages, and wind speed was averaged arithmetically over each occurring wind sector; because 20 sectors are used, each sector spanned 18 degrees. Assuming that SRT is the least influenced by terrain effects and most representative of more regional synoptic conditions, the Base appears to be under mostly westerly flow in fall (fourth quarter), shifting to more northerly

in winter (first quarter), southerly flow in spring (second quarter) and split between south-westerly and north-easterly flow during summer (third quarter) when absolute temperatures are highest and surface heating effects drive the land–sea breeze circulation. The wind rose plots show that winds from the most frequent directions are typically not the strongest; the strongest winds blow from southerly and southwesterly directions year round. Similar patterns were found in previous years.

Solar Radiation

Across MCBCL lands, measurements of PAR (400–700 nm) were made continuously at NRA, SRT, and RIP, and global SR (200–1,100 nm) was measured at SRG. The PAR sensors achieved near 100% coverage for the entire reporting period, except the one at SRT. Data acquisition at this site suffered from a combination of circumstances including access (restricted due to military training), damage due to severe weather, and maintenance, which was difficult to provide due to limited access and operator availability. During the last few months of the study, we had to hire and train a new local operator twice. Beginning in May 2010, the PAR sensor manufacturer (Li-Cor) used the DCERP sites as a test platform for the development of new, more robust sensors that could perform reliably in extremely corrosive environments. The RIP site benefitted from the new sensor design as its PAR data coverage achieved near 100% up until Hurricane Irene hit the study domain late August, affecting all sites.

Figure 15-14 and Table 15-7 show that in spring and summer 2011, statistically significant higher midday PAR levels were reported at RIP compared to SRT and NRA further inland. Based on daily maximum 8-hour averages (calculated similar to O_3) listed in **Table 15-7**, a consistent sea-land gradient occurs with RIP values remaining highest above SRT and NRA registering the lowest values. For two pairs of sites at different distances from the coast (i.e., SRT and NRA), coinciding hourly averages of PAR are compared for the third quarter summer season (**Figure 15-15**). Very similar to 2010, the inland tower site (SRT) reaches 87.4 ±0.6% of the PAR measured at the beach site (RIP), whereas the farther inland ground site (NRA) reaches only 80.8 ±0.5%. Although third quarter measurements in 2010 yielded very similar results, the relative difference between SRT and NRA data was reversed previously (i.e., in 2008 and 2009, PAR seemed to have been attenuated more at SRT than at NRA relative to RIP). Although the difference in PAR between the inland and the beach is significant, the difference observed between the two inland sites is much smaller, although local differences in atmospheric PM loadings likely influence individual PAR readings.

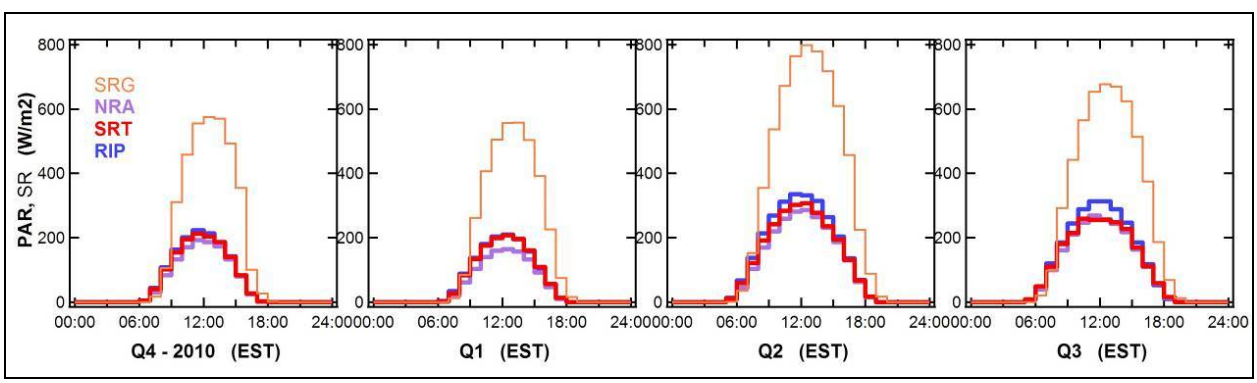

Figure 15-14. Seasonally averaged diurnal profiles of solar radiation in 2010–2011.

Table 15-7. Monthly daily maximum 8-hour averages of PAR in watts per square meter at three on-Base sites.

Site ID	2010			2011 Monthly Average Daily Max 8h								
	Oct	Nov	Dec	Jan	Feb	Mar	Apr	May	Jun	Jul	Aug	Sep
NRA	244	200	163	169	223	239	299	303	302	304	283	—
SRT	274	218	179	176	235	284	319	329	337	340	291	252
RIP	270	217	172	181	236	285	338	363	354	358	348	309

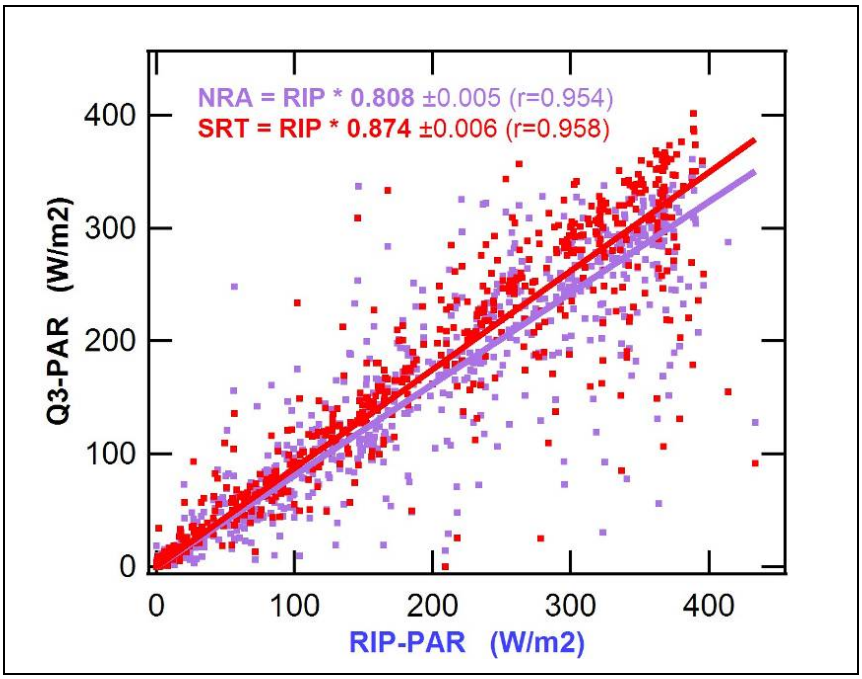

Figure 15-15. Linear regression of hourly PAR measured inland (*y*–axis) versus simultaneous measurements at the RIP beach site (*x*–axis) during the third quarter of 2011.

The observed land-sea difference is not solely due to meteorological differences. The difference is also influenced by the mix of particles in the ambient aerosol and their ability to affect both the direct and diffuse component of the flux of SR passing through the atmosphere. Relative to SRT, the NRA site in 2011 (similar to 2010) exhibits a greater influence from fine particles reducing the direct PAR, which is discussed later in this report. Foliar interception by canopy elements occurs for both up- and down-welling radiation. Therefore, the effect of $PM_{2.5}$ on atmospheric turbidity influences canopy processes both by radiation attenuation and by changing the efficiency of radiation interception in the canopy through conversion of direct to diffuse radiation. However, diffuse radiation is more uniformly distributed throughout the canopy and may increase canopy photosynthetic productivity by distributing radiation to lower leaves. The enrichment in PAR present in diffuse radiation may offset a portion of the effect of an increased atmospheric albedo due to atmospheric particles. In a recent Integrated Science Assessment, EPA concluded that further research is needed to determine the effects of PM alteration of radiative flux on the growth of vegetation in the United States (U.S. EPA, 2009). Differences in air pollutants, including $PM_{2.5}$, are discussed in the following sections of this report.

Criteria Pollutants

Table 15-8 shows the data averages corresponding to the information presented in **Table 15-3**, but is organized by measured parameter for better comparison among sites. Assuming complete data coverage and considering the typical O_3 diurnal profile with daytime maximum and nighttime minimum (see **Figure 15-18**), the mean between the month's upper 67th percentile and maximum closely resembles the concentration of the average 8-hour daytime period for that month. A more accurate evaluation was performed for the regional comparison presented later. Data in **Table 15-8** indicate that the maximum 8-hour values are lowest in winter, which is expected from a photochemical-produced species such as O_3. However, the highest values do not appear exclusively in the typically hottest summer months July and August; but equally high O_3 levels were registered region-wide also in May and June, corresponding with the unusually dry and hot conditions previously described. The values are also similar across the network, pointing to the regional character of O_3 being produced during atmospheric transport. Similar to previous years, RIP averaged the lowest $PM_{2.5}$ concentrations within the study domain, most of the time, whereas SRT reported averages at significantly higher levels than elsewhere, especially in June and July. This is also the period when SRT reported the highest levels of PM_c. The reasons for this are detailed below.

Sulfur Dioxide

The Aurora (AUR) site at the northern edge of the study domain shows systematically lower SO_2 values, whereas Wilmington (WIL) in the south experiences generally higher SO_2 levels predominately from the west-northwest direction, the direction in which the three-unit 575 MW coal-fired Sutton plant is located. This plant is scheduled to be taken offline in 2014. Air quality impacts from this plant are apparent in the SO_2 wind rose plots and diurnal profiles shown in **Figures 15-16 and 15-17**, respectively. Thermally buoyant SO_2 emissions released into the atmosphere via tall stacks typical for coal fired power plants, become mixed down to the ground when vertical mixing sets in with sunrise and subsequent heating of the ground during the morning hours. Thus, the average diurnal profile from both AUR and WIL sites show this distinct feature. As stated in the footnote to **Table 15-3**, the AUR site was moved to the north side of Pamlico River, approximately 6 km north-northeast from Potash Corporation of Saskatchewan (PCS; latitude = 35.34; longitude = −76.78) to Bayview Ferry (latitude = 35.428; longitude = −76.740) and started reporting from that new location on January 28, 2011. Emissions from PCS impact the site regularly from the southwest, as seen in the SO_2 wind rose plots.

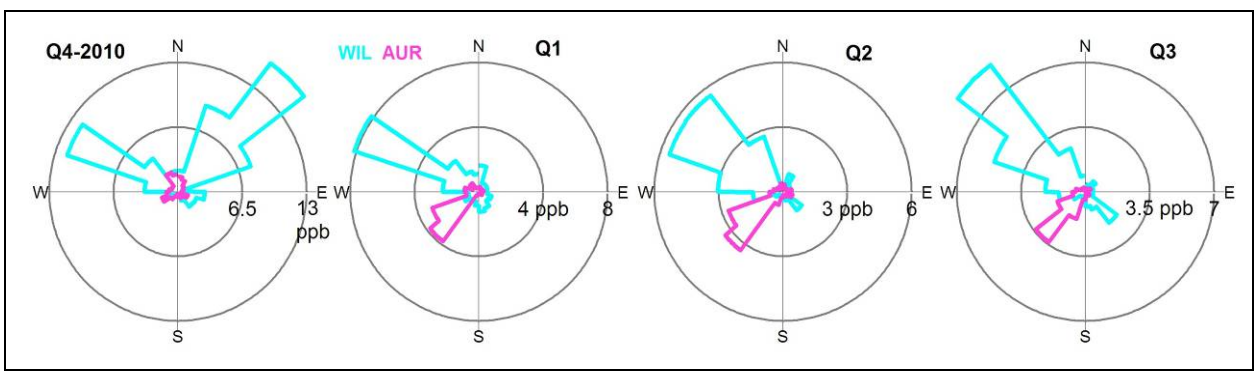

Figure 15-16. Seasonally averaged SO_2 wind roses for 2010–2011.

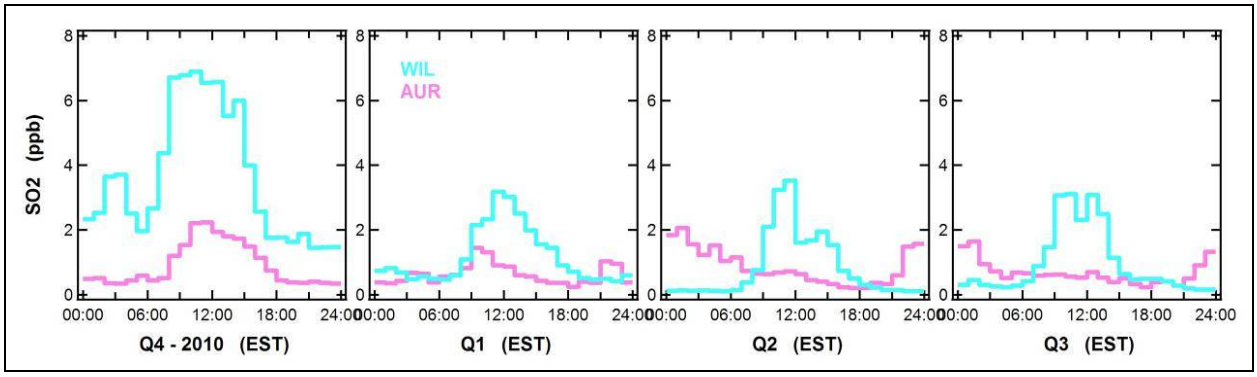

Figure 15-17. Seasonally averaged diurnal profiles of SO_2 for 2010–2011.

Table 15-8. Monthly means (average daily maximum of 8 hours for O_3) of pollutant concentrations from sites on-Base (shaded yellow) and off-Base in period October 1, 2010, to September 30, 2011.

O_3 and SO_2 are in ppb; PM is in µg m^{-3}.

		Q4-2010			Q1			Q2			Q3		
Site ID	**Par.**	**Oct**	**Nov**	**Dec**	**Jan**	**Feb**	**Mar**	**Apr**	**May**	**Jun**	**Jul**	**Aug**	**Sep**
NRA	O3	59	47	37	42	52	53	55	67	68	61	57	—
SRT	O3	61	49	40	46	53	61	59	64	65	56	—	43
RIP	O3	62	44	39	38	50	58	59	65	65	63	65	54
CHN	O3	57	—	—	—	—	—	55	58	62	60	65	52
LCC	O3	58	—	—	—	—	58	57	63	68	68	64	53
AUR	SO2	0.7	1.0	1.0	0.7	0.8	0.5	0.8	0.8	0.9	1.2	0.5	0.2
WIL	SO2	2.2	4.9	3.8	1.8	0.8	0.9	1.0	0.6	1.0	0.8	1.3	0.8
DLL	PM2.5	9.2	8.6	10.0	11.0	9.7	8.5	8.6	11.1	17.8	17.6	12.7	8.4
CHN	PM2.5	8.3	5.9	7.0	7.8	7.2	8.5	7.9	9.1	15.0	16.5	12.1	6.7
NRA	PM2.5	8.8	8.5	8.9	8.0	7.4	10.5	9.6	12.1	43.5	29.4	15.2	—
SRG	PM2.5	—	5.2	7.2	8.2	7.2	17.5	9.5	11.6	34.0	31.1	12.7	—
SRT	PM2.5	14.7	5.7	8.1	9.8	6.5	13.5	9.7	17.5	55.2	66.8	19.6	5.9
RIP	PM2.5	6.8	4.4	5.1	4.4	3.9	3.1	5.6	6.6	15.6	11.2	10.3	7.1
NRA	PMc	2.8	3.0	2.4	1.6	2.7	2.2	2.7	2.7	3.7	3.8	2.7	—
SRG	PMc	—	1.8	3.4	2.0	1.5	2.4	2.0	1.8	3.6	4.5	3.9	—
SRT	PMc	8.7	2.8	2.7	2.2	3.9	2.3	2.9	4.8	9.9	11.8	7.9	1.7
RIP	PMc	1.5	1.0	0.9	1.6	1.4	0.9	0.7	1.0	2.1	1.8	1.6	2.1

O_3 = ozone; $PM_{2.5}$ = fine particulate matter; PM_c = coarse PM fraction; ppb = parts per billion; SO_2 = sulfur dioxide; µg/m^3 = micrograms per cubic meter

Ozone

Figure 15-18 shows the diurnal profiles of air pollutant concentrations for O_3 from the different monitoring sites. All sites show daytime maxima and nighttime minima, with the minima at NRA being consistently lower than at the more rural MCBCL sites, which likely results from primary emissions titrating O_3 away at night. The NRA site is close to an on-Base airfield and

busy roadways outside the northern border of the Base, therefore experiencing more urban conditions similar to the off-Base CHN and LCC sites. Nighttime levels remain high at the more rural sites, indicating the BL effect of nocturnal stratification and land–sea breeze circulation (previously discussed) enables regional redistribution of O_3 conserved in the reservoir layer aloft and away from primary surface emissions. Hence, the SRT and RIP profiles have generally lower diurnal amplitudes, which are smallest in winter, when photochemical production is minimal.

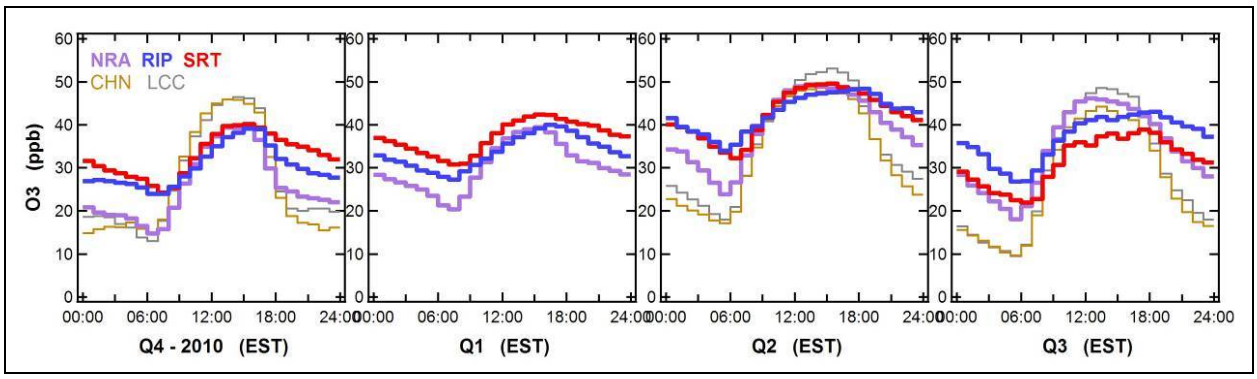

Figure 15-18. Seasonally averaged diurnal profiles of O_3 for 2010–2011.

Seasonal O_3 wind roses plotted in **Figure 15-19** indicate that in fall (fourth quarter), the RIP beach site received the highest average O_3 concentrations from southern directions, pointing to effects from preferential photochemical production of O_3 under maritime conditions and transport to the site with the sea breeze. Note that due to the lack of wind measurements at RIP since late March 2011, RIP traces are missing in the second and third quarters wind roses. It is also important to consider that data coverage at SRT was poor in August and September (**Table 15-3**), making the SRT rose in the third quarter less representative of regional conditions. Considering that continental background levels of O_3 may vary between 30 and 35 ppb, the low levels observed region-wide under northerly and westerly flow in summer, fall and winter, indicate that O_3 losses from chemical reactions (titration by primary pollutants) and surface deposition outweighed O_3 production in those continental air masses. Assuming the SRT Tower site reflects more regional conditions in fall, winter and spring (excluding summer due to poor data coverage) highest O_3 levels seem to be transported into the study domain from mostly easterly and northeasterly directions, similar to previous years.

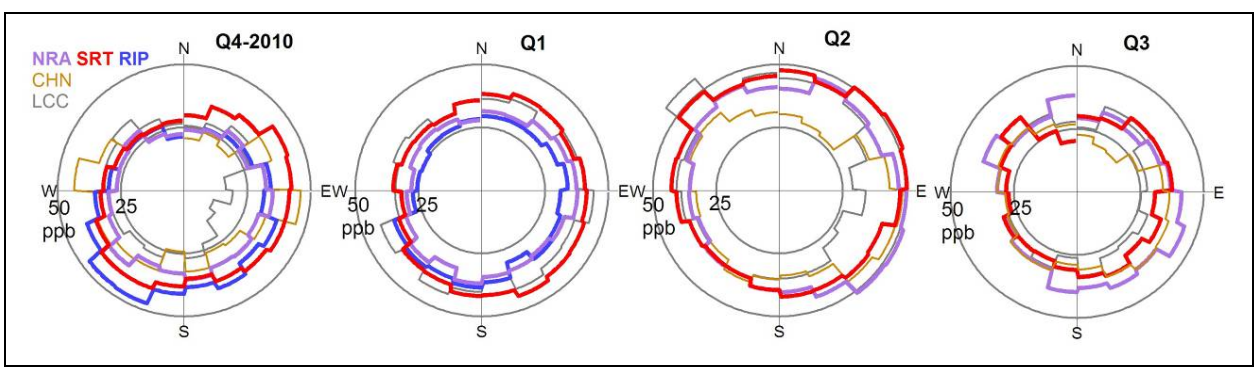

Figure 15-19. Seasonally averaged O_3 wind roses for 2010–2011.

Comparing the two urban sites, CHN consistently receives highest O_3 from easterly directions, being in line with the on-Base observations, whereas LCC receives highest O_3 from northerly directions, shifting to westerly in fall. Average O_3 levels for those directions are even higher than the corresponding SRT levels, suggesting that LCC, being the farthest site north in our study domain, is spatially decoupled and part of a different airshed. This systematic difference was also apparent in previous years.

Although the local on-Base measurements did not meet (and were not intended to meet) regulatory requirements, the metrics employed by EPA were applied here as a basis for regional comparison of air quality. The EPA set two types of NAAQS for ground-level O_3: (1) a primary standard to protect public health, including the health of sensitive human populations such as asthmatics, children, and the elderly; and (2) a secondary standard to protect public welfare, including protection against visibility impairment and damage to animals, crops, vegetation, and buildings. Effective May 27, 2008, the 3-year average of the fourth-highest daily maximum 8-hour average O_3 concentration measured at each monitoring site within an area over each year must not exceed 75 ppb to be in attainment. This value was proposed to be set between 60 ppb and 70 ppb in January 2010 and is part of the 5-year review of the updated science, which is scheduled to be completed in 2013. The measured 3-year average is called a design value (DV). The DVs were calculated for the sites in our study domain and are presented in **Figure 15-20**.

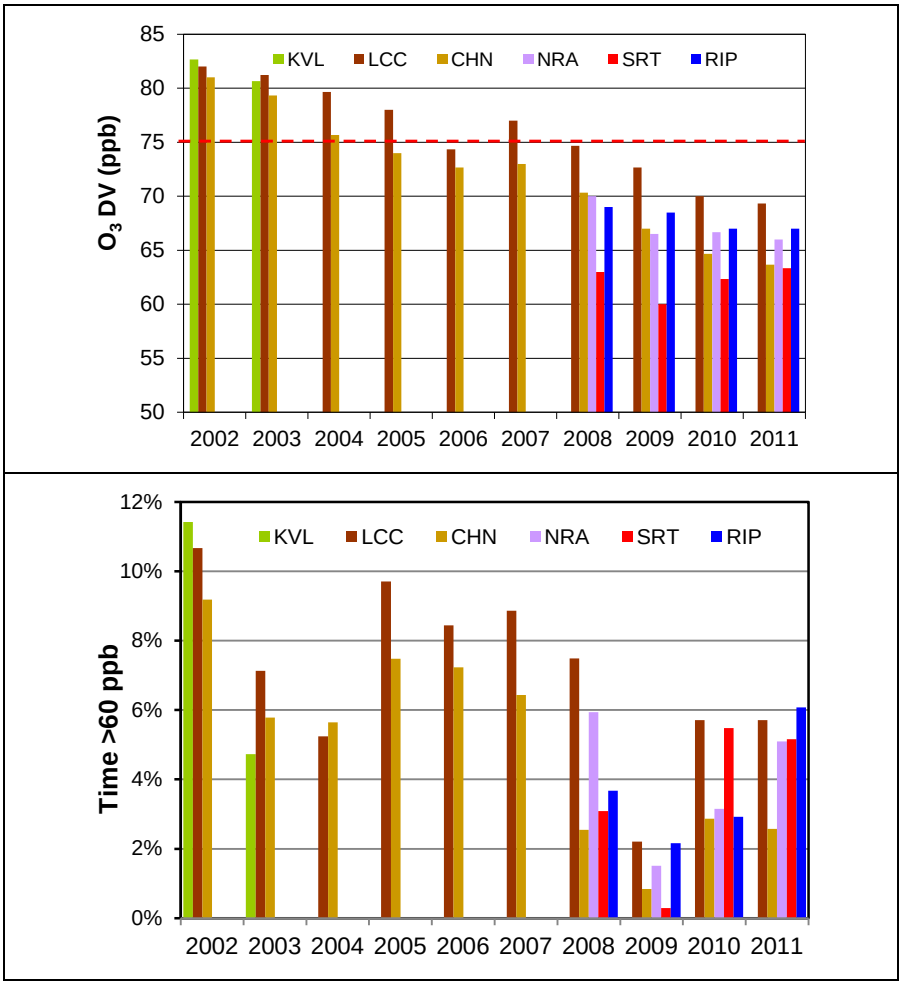

Figure 15-20. Regional comparison of O_3 DVs to meet the primary NAAQS (top panel) and fraction of time with hourly O_3 greater than or equal to 60 ppb during each season (bottom panel) spanning 2002 to 2011.

KVL = Kenansville; LCC = Lenoir Community College; CHN = Castle Hayne; NRA = Marine Corps Air Station New River; SRT = GSRA Tower site; and RIP = Riseley Pier.

Following the methods from previous reports, the SUM06 concept was used as surrogate of a long-term standard protecting sensitive vegetation from harmful exposure to O_3 during the growing season. This concept was also applied to the 2011 data and the number of hours with O_3 greater than or equal to 60 ppb was determined for each site. The seasonal fraction of O_3 exposure to levels greater than or equal to 60 ppb is shown in **Figure 15-18** for comparison with the short-term exposure conditions. It should be noted that (1) 2008 data from NRA, SRT, and RIP are missing the first 3 months of the O_3 season, and (2) the NRA, SRT, and RIP values shown as DVs in the left panel of the Figure are truly comparable only for 2010 and 2011 due to the 3-year averaging requirement. Thus a decreasing trend in short-term O_3 exposure levels is observed along the sea-to-land gradient only locally (i.e., DVs decrease with increasing distance from the ocean [RIP is higher than NRA], and both short-term and seasonal O_3 levels at the farthest inland LCC site remained consistently highest).

Over the past 10 years, the short-term O_3 exposure levels declined steadily across the region (except for 2007), which was in line with the nationwide trend (see EPA's Web site at

http://www.epa.gov/airtrends/ozone.html). Thus, EPA reports that above average temperatures and below average humidity across most of the United States in 2007 contributed to increased ozone formation, while below average temperatures and above average humidity across much of the United States in the summer of 2009 contributed to decreased O_3 formation. EPA's statistical model accounts for these effects by adjusting the seasonal average O_3 trend downward in 2007 and upward in 2009, yielding a steady downward trend, which is attributed mainly to reductions in O_3 precursor emissions NO_x and methane.

The seasonal exposure levels show a less consistent declining trend, with reversal to an increasing trend in 2009 (season showing the lowest O_3 levels region-wide), mainly due to the higher levels in spring over-compensating the declining summer levels. Differences in temporal trends between the short- and long-term levels are largely due to the smoothing effect in the calculation of the short-term DV (maximum 8-hour averaged over the past 3 years). However, the threshold level at which continuous long-term exposure causes permanent damage to certain vegetation or even the entire ecosystem of the study domain is currently unknown.

Fine and Coarse Particulate Matter

It is important to note that because the last 3 months of 2011 are excluded in the presented analysis, any expressed quantity referred to as "annual" covers the period from January through September 2011. Similar to O_3, **Figure 15-21** compares the short-term (24-hour) and long-term (annual) $PM_{2.5}$ DV calculated for DCERP sites SRT and RIP with corresponding values from six state regulatory network sites within the study domain (i.e., DLL, LCC, KVL, JVL, CHN, WIL; see **Figure 15-3** for locations). To attain the annual standard, the 3-year average of the weighted annual mean $PM_{2.5}$ mass concentration must not exceed 15 $\mu g\ m^{-3}$. The daily standard is attained as long as the 3-year average of the 98th percentile of daily (24-hour) mass concentrations is below 35 $\mu g\ m^{-3}$.

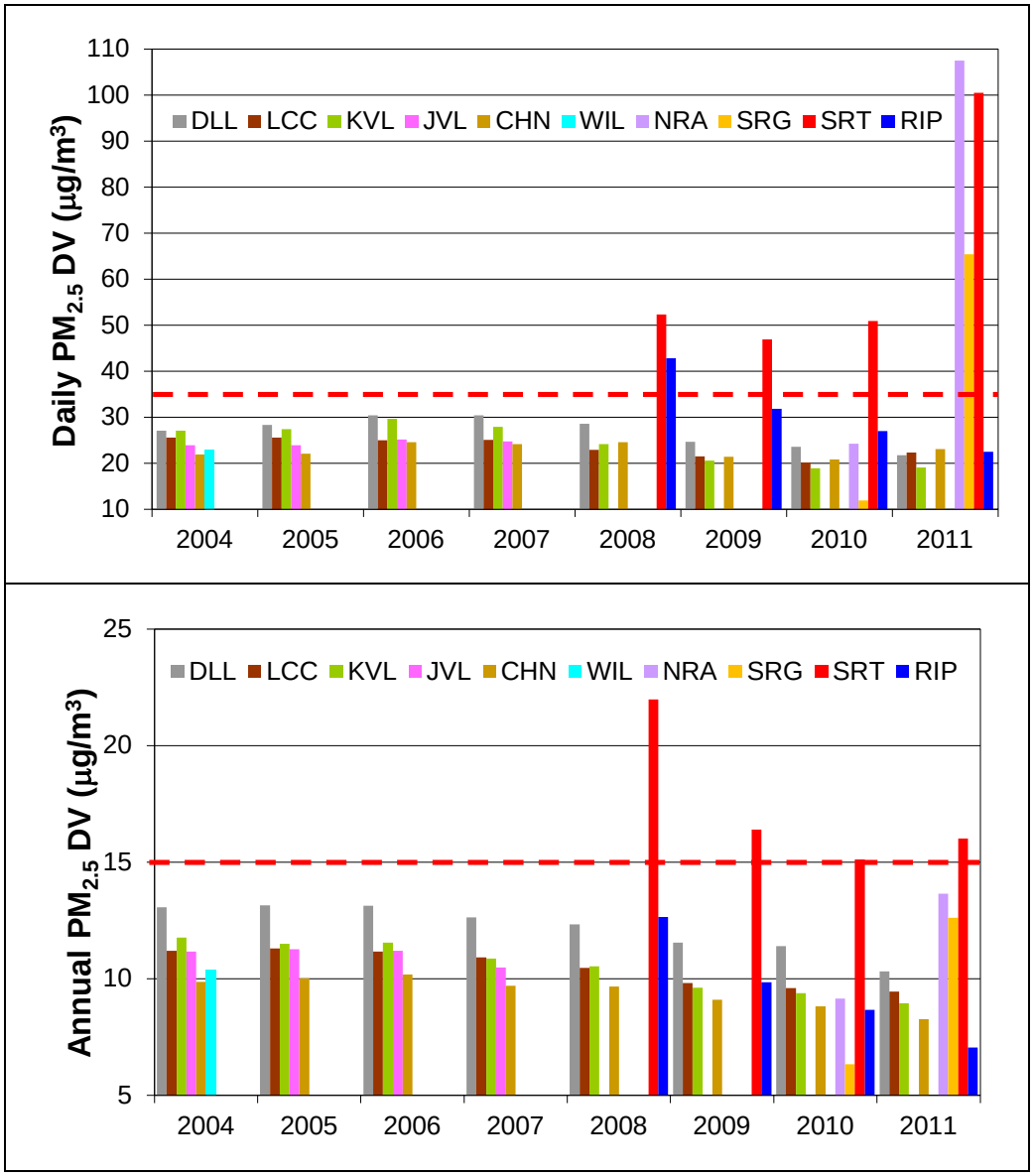

Figure 15-21. Comparison of daily (top) and annual (bottom) $PM_{2.5}$ DVs from four MCBCL sites with corresponding DVs from six off-Base sites across the study region.

Off Base: DLL = Dillard–Goldsboro; LCC = Lenoir Community College; KVL = Kenansville; JVL = Jacksonville; CHN = Castle Hayne; WIL = Wilmington. On Base: NRA = New River Air Station; SRG = GSRA Ground site; SRT = GSRA Tower; RIP = Riseley Pier.

Similar to O_3, but less pronounced, $PM_{2.5}$ levels for both short-term and especially long-term exposure thresholds have decreased steadily during the past 10 years across the study region. Based on data from CHN and DLL, the regional trend of increasing $PM_{2.5}$ levels with increasing distance from the coast outside MCBCL boundaries has remained true in 2011. This trend was previously shown to correlate with decreasing amounts of rainfall away from the coast and holds again for this most recent January–September 2011 period (see **Table 15-6),** because rainfall is the most effective sink for atmospheric $PM_{2.5}$.

Because both the daily and the annual DV are based on 3-year averages, only 2010 and 2011 values from SRT and RIP on Base can now truly be compared in the regional context. The annual DV at the RIP beach site follows the regional trend in that it presents the lowest annual level compared to CHN and DLL farther inland, while it experiences similar levels on the daily basis, due to brief occurrences of elevated $PM_{2.5}$ concentrations at the beach as shown later. Because these excursions to high $PM_{2.5}$ levels are much more enhanced and occur much more frequent at SRT (due to its vicinity to active military training activities but also due to wildfire plume encounters that were particularly frequent in 2011 as shown below), it is not surprising that both daily and annual DVs from SRT stand out. $PM_{2.5}$ levels at SRG and NRA, the two on-Base sites that had been added in third quarter of 2010, appear distinctly different. Although NRA levels are close to the ones observed at SRT, both the daily and annual DV levels at SRG, which is only 3 km south from SRT are significantly lower, suggesting that (1) SRT must be influenced by very local $PM_{2.5}$ sources immediately below the tower, and (2) certain conditions of atmospheric stratification must exist that allow the top of the 40-m tower to be exposed to layers with accumulated $PM_{2.5}$, which do not extend down to the ground. This phenomenon is discussed later in connection with the different wildfire occurrences on and off the Base.

The $PM_{2.5}$ concentration wind roses in **Figure 15-22** corroborate the unique character of the high pollution levels encountered at SRT in the spring (second quarter) and summer (third quarter) because their traces are not matched by the traces from any other site during those two periods. The only feature seeming regionally consistent is that the lowest concentrations of $PM_{2.5}$ at SRT match the levels that the other sites encounter from similar directions (e.g., north and east during winter [first quarter], northeast and southeast during spring [second quarter], and any easterly component winds during summer [third quarter]). At all sites but especially the ones on-Base, the $PM_{2.5}$ measurements indicate a regional character that is distinctly less homogeneous than that for O_3, pointing to a greater influence from primary emissions sources on local scales. Such local influences are enhanced whenever vertical mixing near the surface is limited due to stratification, allowing pollutants to accumulate inside a shallow BL instead of being diluted under convectively well-mixed conditions. As discussed below, the high $PM_{2.5}$ levels observed on Base from southwesterly directions were all associated with nearby wildfires. Note, that wind sensors at RIP were down during the second and third quarters of 2011.

Since PM_{10} was measured simultaneously at the research sites on Base, similar wind rose plots were created for PM_c from the difference between PM_{10} and $PM_{2.5}$ as well as for the $PM_{2.5}$:PM_c ratio, which are depicted in **Figures 15-23 and 15-24**, respectively, for comparison with $PM_{2.5}$. A large $PM_{2.5}/PM_c$ ratio indicates: (1) depletion of PM_c due to gravitational settling and surface deposition, (2) influence from combustion sources, and (3) formation of new particles from nucleation and heterogeneous gas-particle conversion processes that are typical for SOA. In contrast, a low ratio would point to a potential influence from windblown dust and marine (sea-salt) aerosol.

Aromatic hydrocarbons, biogenic terpenes (especially isoprene), and other reactive VOCs are primary species involved in SOA formation, which was discussed extensively in conjunction with the PB emissions results presented in the *DCERP1 Final Research Report*. One of the conclusions was that PB emissions have not enough potential to form significant amounts of SOA within the local impact zone of the typical wildland urban interface during the first 5 hours after emission.

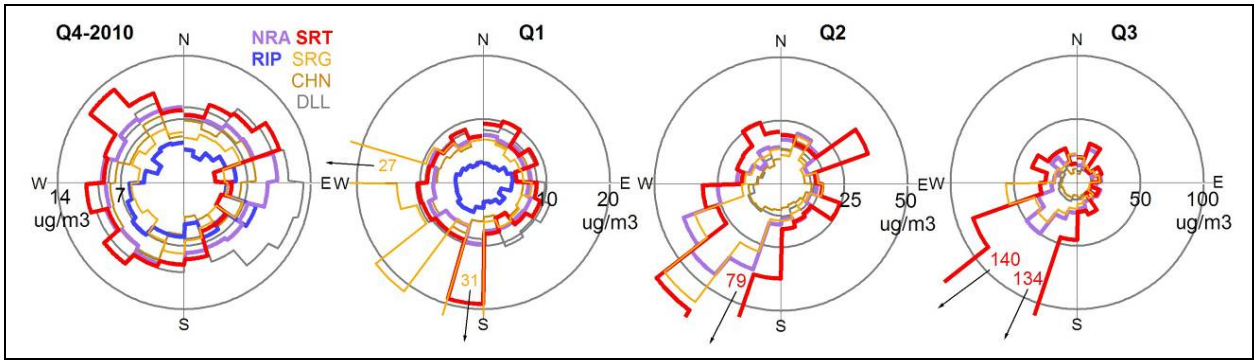

Figure 15-22. Seasonally averaged $PM_{2.5}$ wind roses for 2010–2011.

Off-Base: DLL = Dillard–Goldsboro; CHN = Castle Hayne. On-Base: NRA = New River Air Station; SRG = GSRA Ground site; SRT = GSRA Tower; RIP = Riseley Pier.

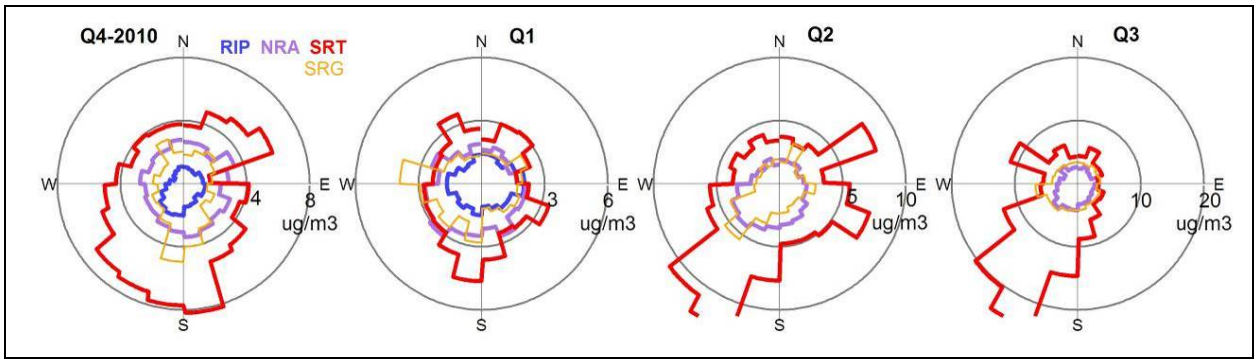

Figure 15-23. Seasonally averaged PM_c wind roses for 2010–2011.

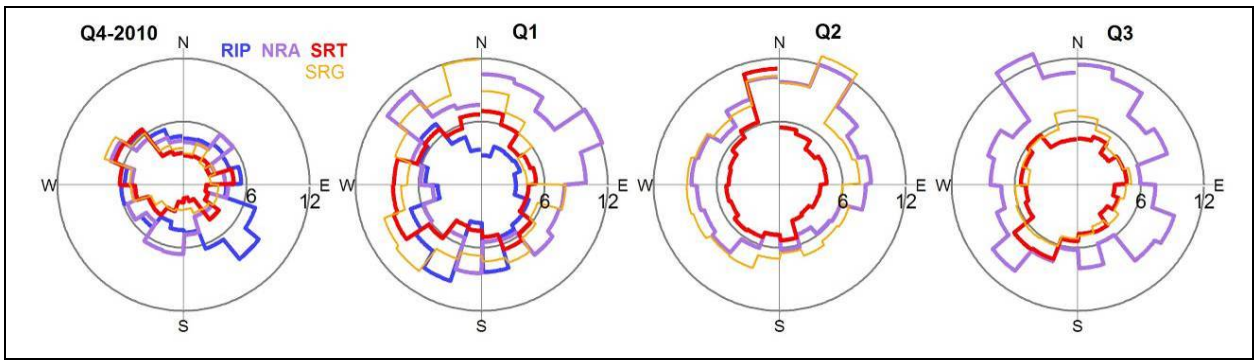

Figure 15-24. Wind roses of seasonally averaged $PM_{2.5}$:PM_c ratios for 2010–2011.

One of the more important conditions enhancing PM_c in our study domain stems from the proximity of MCBCL to the ocean, providing an environment conducive to sulfate formation via oxidation of SO_2 to sulfate in sea-salt containing cloud droplets and deliquesced sea-salt aerosols. This process can result in a substantial fraction of non-sea-salt sulfate to be present on large sea salt particles, especially under conditions where the rate of photochemical sulfuric acid H_2SO_4) production is low and the amount of sea-salt aerosol surface area is high. In coastal areas, freshly formed sea-salt aerosol also absorbs secondary semi-volatile organic oxidation products into its surface organic layer, which consequently allows for the partitioning of the secondary organics to the sea-salt aerosol brine core, adding another layer of complexity.

Another PM_c enhancing factor is the reaction of nitric acid with sea-salt aerosol to form coarse mode sodium nitrate particles. Under clean marine conditions, the sea-salt displacement reaction can be expected to yield a complete conversion of nitrate from the fine to the coarse aerosol mode, thereby potentially increasing the PM_c mass. The $PM_{2.5}$:PM_c ratios at NRA are highest in most seasons especially for air mass transport from northerly and easterly directions, where the major traffic corridors are located for thousands of daily commuters.

For periods with smoke-laden air masses blowing into the Base area from southwest, PM_c was also elevated. However, the level of elevation relative to other directions was smaller than for $PM_{2.5}$, indicating that the wildfire smoke emissions contained substantially more $PM_{2.5}$ than PM_c. Smoke plume encounters at SRT in winter (first quarter) yielded an average $PM_{2.5}$:PM_c ratio noticeably lower than the maritime background, pointing to the previously mentioned PM_c enhancing processes in the confluence of smoke plume and maritime air mass during colder months. Smoke plume encounters at SRT in spring (second quarter) and summer (third quarter), however, suggest these PM_c enhancing processes being overwhelmed by large $PM_{2.5}$ fire emissions (especially during the hot flaming phase of fuel combustion) and new particle formation processes driven by emitted reactive precursor gases and semi-volatile aerosol species, causing a consistently higher $PM_{2.5}$:PM_c ratio in smoke plumes that are carried by the sea breeze in warmer months.

Average diurnal profiles of $PM_{2.5}$, PM_c, and $PM_{2.5}$:PM_c ratio as shown in **Figures 15-25, 15-26, and 15-27** are distinctly different among the different sites. The monthly averages in above **Table 15-8** indicated SRT levels being generally highest, and the diurnal profiles now show why: nighttime levels consistently exceed those from all other locations by a significant margin, while they approach those from all other sites during midday and afternoon. This behavior reflects the before mentioned scenario of injecting buoyant fire smoke plumes into atmospheric surface layers that evolve dynamically over the course of the day. At night, the smoke cools to ambient conditions in a stratified layer slightly elevated above ground, in which it advects horizontally without much dilution due to lack of turbulence. Such layers are being sampled by the SRT tower sensors but are missed by the sensors on the ground, unless some mixing down occurs, which can be more regional due to low level jet occurrences, or more locally confined due to heat capacity effects. For example, NRA is more open and surrounded by concrete structures and paved areas (e.g., airport runways, roads), and SRG is more sheltered inside a forested area. Local differences in surface albedo, associated BL mixing and proximity to $PM_{2.5}$ sources (mainly airport and road traffic) explain the observed differences in evening and nighttime $PM_{2.5}$ levels at NRA exceeding those at SRG. Surface inversion effects appear to also play a role in urban environments, explaining the diurnal features observed at CHN and DLL sites: These sites were either upwind of the wildfires (CHN) or sheltered from the advecting plumes due to nocturnal temperature inversion at the ground (DLL), so that the nocturnal increases in $PM_{2.5}$ concentration are due to emissions from local pollutant sources such as traffic, industries and domestic heating, being trapped and accumulated in shallow surface layers. The high PM_c levels at SRT are associated with the wildfire plume encounters, as discussed the following section titled “Assessment of Trends in the Data”. It is interesting to note that average $PM_{2.5}$:PM_c ratios in these plumes are between 4 and 6, corresponding to an average PM_c level of 17–25% of $PM_{2.5}$, or 14–20% of PM_{10}, respectively.

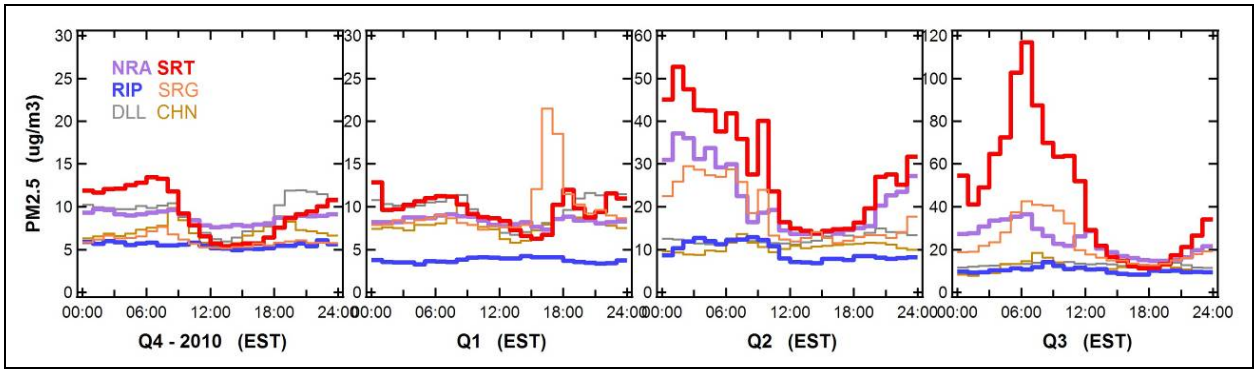

Figure 15-25. Seasonally averaged diurnal profiles for $PM_{2.5}$ in 2010–2011.

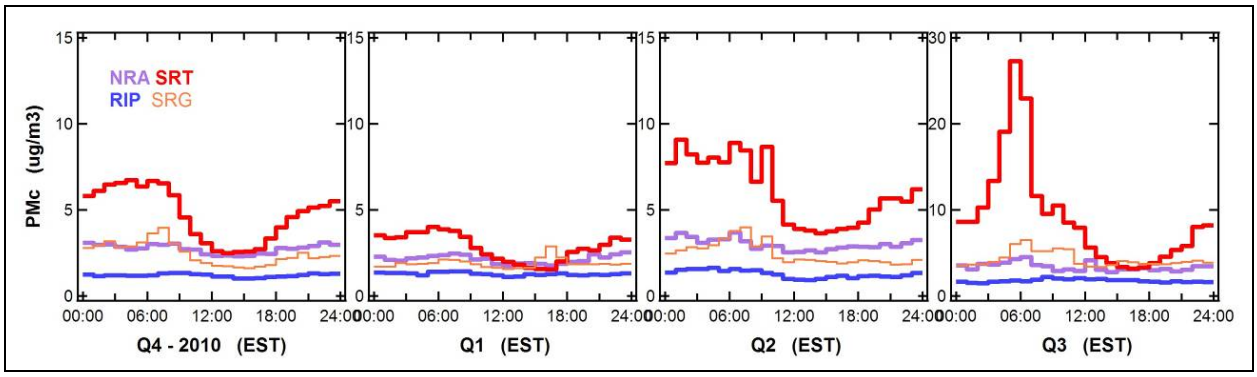

Figure 15-26. Seasonally averaged diurnal profiles for PM_c in 2010–2011.

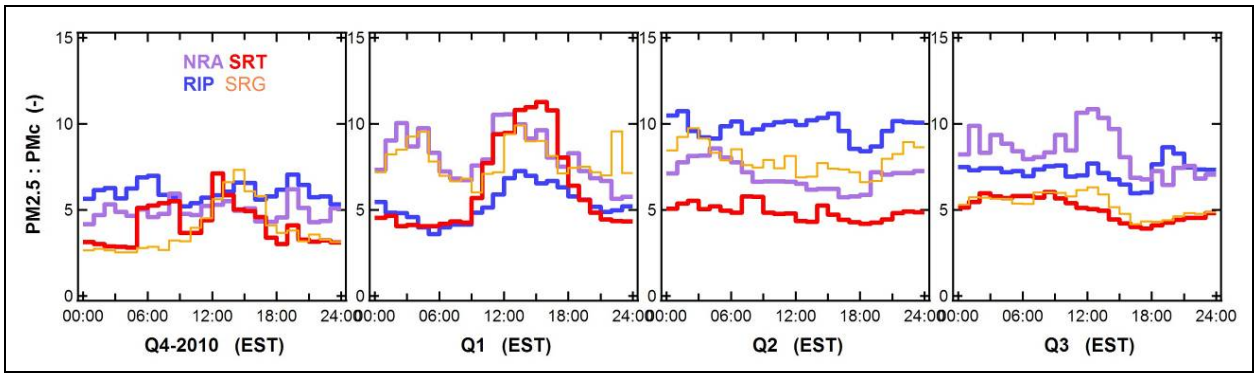

Figure 15-27. Seasonally averaged diurnal profiles of $PM_{2.5}$:PM_c ratio in 2010–2011.

Several wildfires occurred in North Carolina during 2011 that had significant impacts on the PM measurements in our study domain. The most important fires are summarized in **Table 15-9** and discussed in more detail in the following sections. Most fires were started by lightning strikes hitting dry grounds in May and June, months with significantly below normal rainfall (see above). The biggest fire started in that fashion early May in the Alligator River National Wildlife Refuge, about 160 km northeast from MCBCL. Although the main flaming phase occurred between May 5–8, the fire smoldered and intermittently flamed until early July, burning a total of 45,300 acres. During heavy thunderstorms on June 19 and 20, lightning sparked the Juniper Road and Simmons Road fires, respectively, with the former impacting our study area much more severely due to size and proximity. Intermittent lightning strikes re-ignited these fires until

the end of July, and they smoldered until mid to late August. A large wildfire occurred also on Base (SR-8), just south from our SRG site, which is discussed first.

Table 15-9. Significant wildfires affecting the study domain in 2011.

Name	County	Location Relative to MCBCL	Cause	Flaming	Smolder	Area (ac)
SR-8	Onslow	On Base, S from SRG and SRT	Military training	Mar 19–25	Early May	12,500
Pains Bay	Dare	160 km NE in Alligator River NWR	Lightning	May 5–8	Early Jul	45,300
Juniper Rd	Pender/ Onslow	Holly Shelter Game Land to SW	Lightning	Jun 19–Jul 29*	Late Aug	31,140
Simmons Rd	Bladen/ Cumberland	110 km WNW, S from Fayetteville	Lightning	Jun 20–Jul 31*	Mid-Aug	5,400

Impact from Wild Fire SR-8 on Base

The SR-8 fire was accidentally started by tracers being fired during military training in the SR-8 training area south from SRG. Tracers are bullets with a small pyrotechnic charge that burns and causes a bright glow when fired in order to quality assure target aiming. **Figure 15-28** shows a map outlining the total burned area relative to the locations of SRG and SRT. The differently colored areas indicate the progression of this fire between March 19 and 25, although exact hourly burn rates are not known. We assume a moderate rate of 50 acres per hour until early afternoon of May 24, accelerating then to more than 300 acres and up to 400 acres per hour by late afternoon of May 25, when the fire was contained, entering a strict smoldering phase. This fire behavior is reflected in the bottom panel of **Figure 15-29**, which also shows hourly concentrations of O_3, $PM_{2.5}$ and PM_c, and wind vector flags for the main study sites on 6 days between March 21 and 26. Clear skies and sunshine characterized the first four days of this period with weather conditions becoming increasingly cloudy on March 25 and again on March 26. Nevertheless, daytime maximum O_3 levels decreased region wide during the sunny period, suggesting that the SR-8 fire emissions did not cause an increase in regional O_3 that time of year (relatively cool with temperatures swinging between 5°C and 30°C), instead rather a decrease.

Figure 15-29 shows the effect of meteorological conditions on the smoke dispersion, affecting the nearby sites SRG and SRT at different times and different levels of $PM_{2.5}$ and PM_c. The first spike right before midnight on March 22 is relatively brief and short-lived at SRG and SRT under stagnant conditions. The second broad spike lasts through the following afternoon with $PM_{2.5}$ and PM_c peak levels occurring at all three on-Base sites (SRG, SRT, NRA) within one hour of each other. Naturally, corresponding to the increasing distance to the fire source, the peak levels declined due to the dispersion of the plume, from the nearest site (SRG) to SRT to the farthest NRA site from 880 to 320 to 100 $\mu g/m^3$ for $PM_{2.5}$, and 88 to 28 to 7 $\mu g/m^3$ for PM_c. Thus, the PM_c to $PM_{2.5}$ ratio also declined with increasing distance from 1:10 to 1:11 to 1:14, indicating more rapid atmospheric removal of PM_c due to gravimetric settling and surface deposition. Unfortunately, PM measurements ceased at SRG and SRT after the 24th so that no comparisons can be made to the peaks observed at the distant urban cites DLL (Goldsboro) and CHN (Wilmington) close to midnight on the 25th and 14 hours later, respectively. Wind

directions at both locations indicate a high likelihood of smoke from the SR-8 fire causing these spikes. The smoke never drifted towards the beach, leaving the RIP site unaffected.

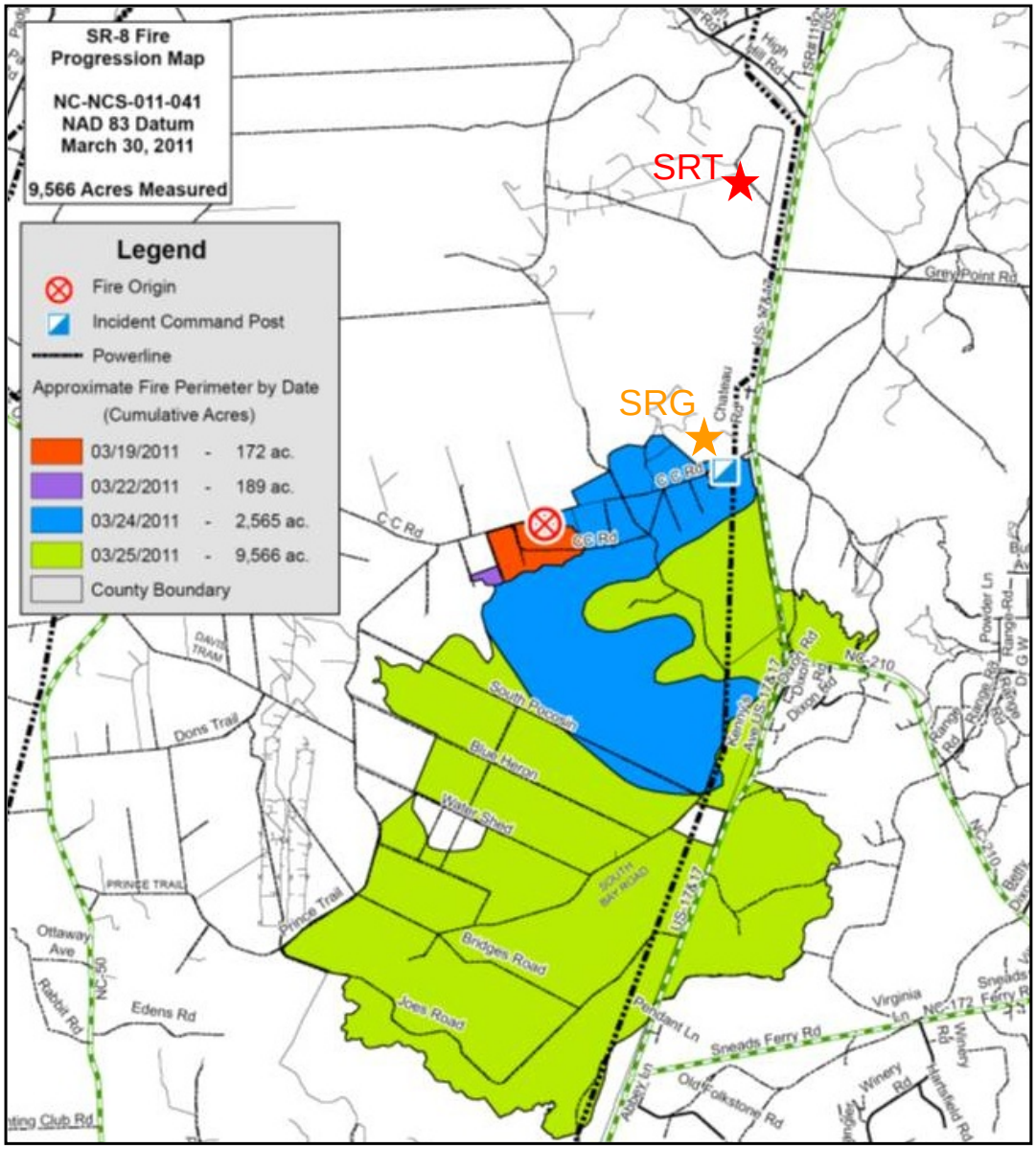

Figure 15-28. Progression map of the SR-8 wildfire in March 2011.

The March 23rd daily average $PM_{2.5}$ levels at SRG, SRT and NRA are 119, 51 and 24 μg/m^3, respectively, ranking 3rd, 22nd, and 34th highest daily average at each site in 2011. Apparently, many more pollution days occurred in 2011, which were mainly part of other wildfire impacts described next.

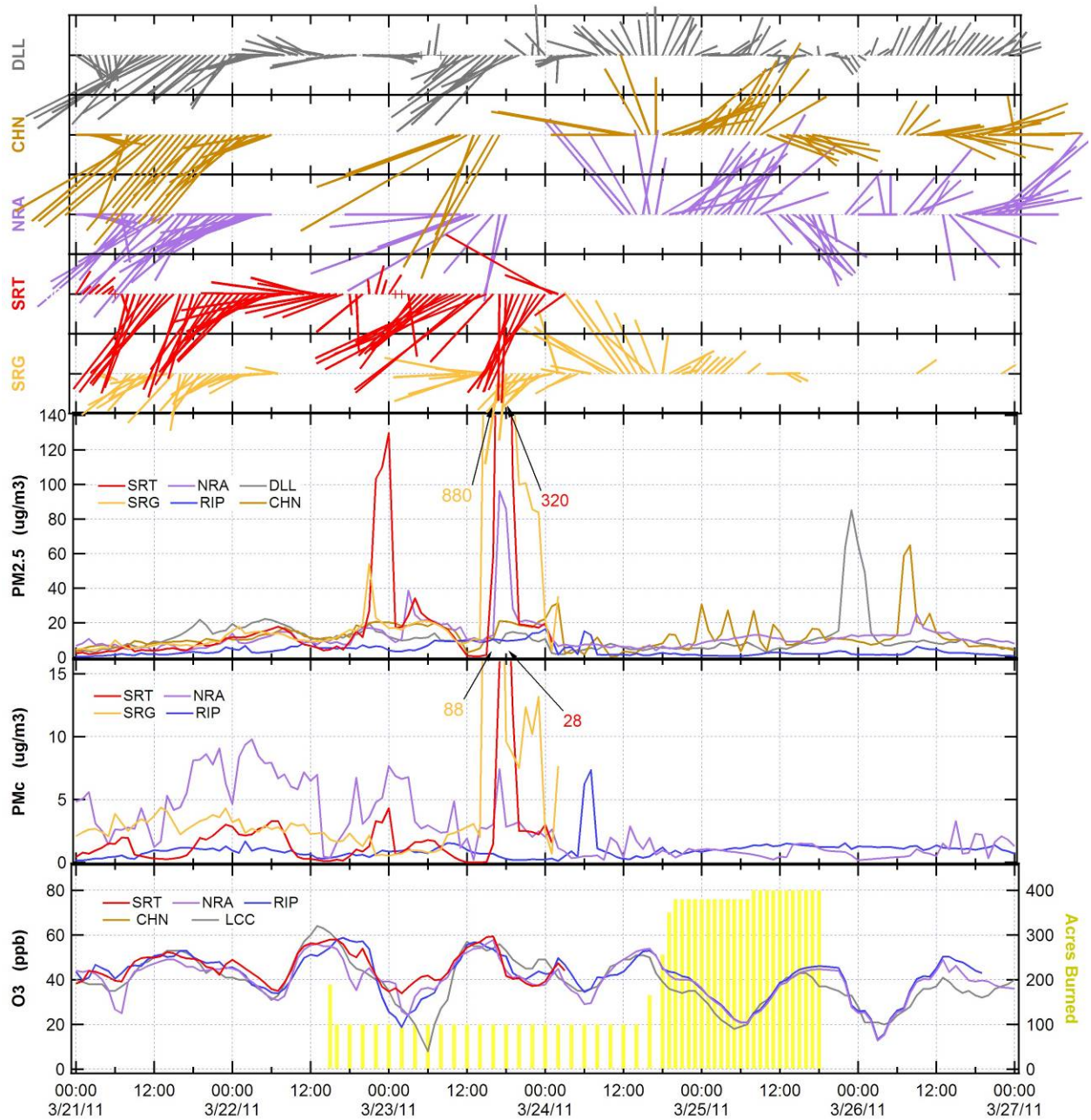

Figure 15-29. Hourly wind vectors, $PM_{2.5}$, and PM_c, and O_3 at different study sites, and acres burned at SR-8 by wildfire in March 2011.

Impact from More Distant Wild Fires Off Base

The Pains Bay Fire. The Pains Bay fire was reported on the afternoon of Thursday, May 5, 2011. It was most likely caused by lightning strikes in the wetlands between Pains and Parched Corn Bays on the south side of U.S. Highway 264 just south of Stumpy Point and in the southeast corner of the Alligator River National Wildlife Refuge in Dare County, NC. Low relative humidity, extremely dry and dense fuels, and gusty winds caused the fire to rapidly spread north, jumping across U.S. Highway 264 and into the U.S. Air Force practice range. By

Saturday evening, May 7, the fire had grown to more than 15,000 acres and had become a multi-jurisdictional fire, managed jointly by the U.S. Fish and Wildlife Service and the N.C. Forest Service, which has fire suppression responsibility for the U.S. Department of Defense's Dare County Range.

The progression map in **Figure 15-30** shows spread of the fire via active flaming until early June, when the fire reached its final size of 45,300 acres. On May 8 and June 4, the largest areas burned, with 12,312 acres (dark blue) and 12,234 acres (dark orange), respectively. **Figure 15-30** also shows a forecasted air quality alert map released by NC DENR on June 15 for the June 18–19 weekend, by which time the fire had been largely contained and had entered a state of relatively minor residual smoldering.

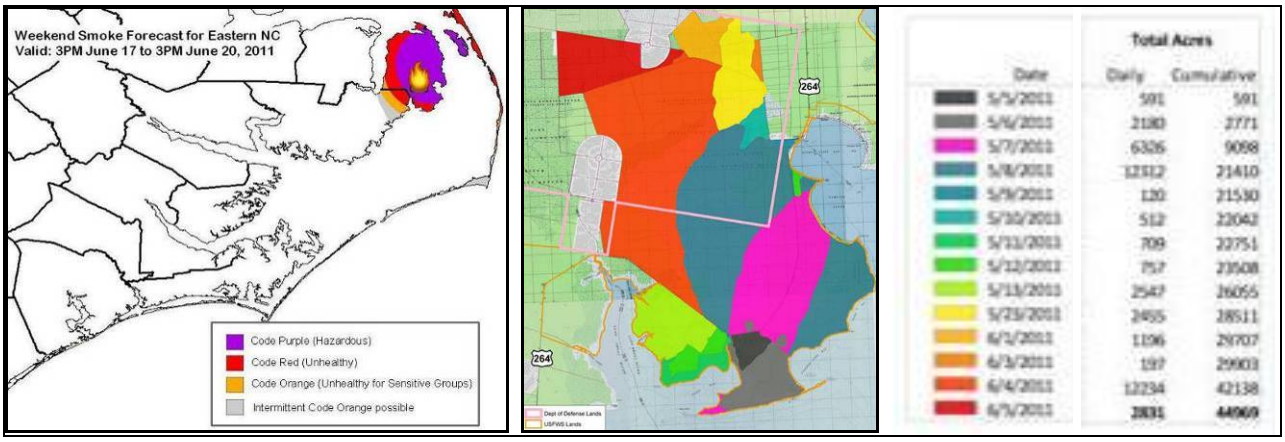

Figure 15-30. Location and progression map of the Pains Bay wildfire in Dare County of eastern North Carolina from May and June 2011.

Figure 15-31 shows the daily average $PM_{2.5}$ concentrations observed at the four on-Base sites RIP, SRG, SRT, and NRA and two off-Base sites, CHN near Wilmington to the southwest and DLL at Goldsboro to the northwest. The Pains Bay fire was due east from DLL and northeast from all other $PM_{2.5}$ measurement locations. Because highly resolved PM_{10} was measured only at the on-Base study sites, PM_c concentration and $PM_{2.5}$:PM_c ratio are depicted only for those locations. In combination with the wind vectors, the vertical temperature difference (T-diff) derived from the SRG ground data subtracted from those 40 m above at SRT, gives some idea of the dynamic condition of the atmospheric BL. The vertical lines represent each day's nighttime maximum and daytime minimum temperature difference, indicating the strength of the nocturnal inversion decoupling stratified layers from the ground, and the subsequent change to daytime labile conditions reversing the temperature gradient conducive to vertical mixing and dissolution of the previously stable layers.

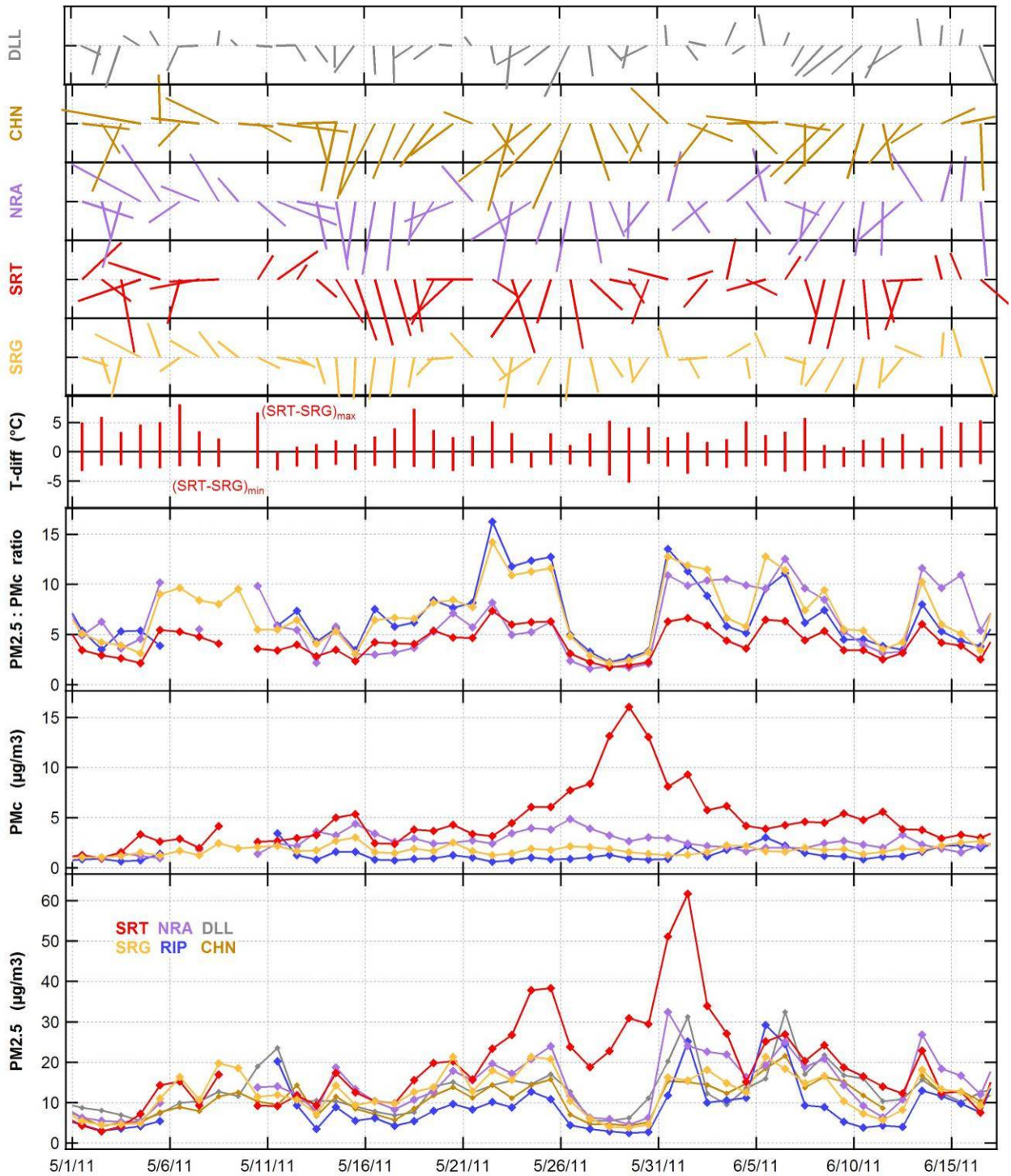

Figure 15-31. Daily maximum and minimum vertical temperature difference between 40 m (SRT) and the ground (SRG), wind vectors, $PM_{2.5}$ and PM_c concentrations and ratio at different study sites in May and June 2011.

The period between May 11 and 18 was characterized by strong winds and relatively small changes in daily minimum and maximum temperature gradients and little fire activity (see the

progression map). Therefore, both $PM_{2.5}$ and PM_c concentrations were relatively low across all sites with $PM_{2.5}$:PM_c ratios between 4 and 6. When the fire picked up under strong southerly winds on May 24 and again on June 1 under relatively calm easterly flow conditions, all sites seem to be impacted accordingly (i.e., average $PM_{2.5}$ increased more prominently and wide-spread on June 1 and 2 than on May 24 and 25). However, the $PM_{2.5}$:PM_c ratios were similar, pointing to the fire as the same source responsible for these domain-wide increases, although impacts were more direct during the later period, when even the northern most DLL site found itself downwind from the fire, receiving smoke from due easterly directions.

The period between the fire impacts is characterized by strong southerly winds with low pollution levels and consistently low $PM_{2.5}$:PM_c ratios region-wide, suggesting regional dilution in $PM_{2.5}$ and similar local processes (windblown dust from the ground) causing consistent levels of PM_c. SRT is exceptional due to its elevated location on the tower 40 m above the ground, capturing different plumes from residual smoldering in different portions of the area that burned during the SR-8 fire in late March. Base foresters provided anecdotal evidence of isolated residual smoldering. Due to the proximity of these smoldering sources, the SRT PM sensors were sensitive to slight changes in wind direction, which was the case during May 28–30. The fact that May 30 was Memorial Day adds complexity to the matter because traffic amounts are known to substantially increase over this holiday weekend, which explains the change in $PM_{2.5}$/PM_c ratio from approximately 6 to 11 at NRA, which is near heavily used traffic roads.

The Juniper and Simmons Road Fires. The Juniper Road fire was started by lightning in Pender County on the afternoon of June 19, 2011. The starting location was at 34.544 °N latitude and −77.673 °E longitude inside the Holly Shelter Game Land between Juniper Road and County Line Road, 8 miles north of Topsail. The fire quickly spread north and east into Onslow County a few days later. The final size of 31,140 acres was reached by July 29, 2011 but the fire smoldered, forcing suppression operations to continue until finally contained and extinguished by the end of August. Most of the fuel burned during the first 1–2 weeks but intermittent lightning and wind re-ignited the fire several times, so that it was a constant source for smoke but at variable strength. Only one day after this fire had started, the North Carolina Forest Service responded to a lightning caused another wildfire in the Live Oak community in Bladen County along Simmons Road. Strong and erratic winds caused that fire to cross containment lines on June 21, destroying three homes and eleven outbuildings. The fire spread to several Carolina bays containing dense vegetation and organic soil. The Simmons Road fire burned much less fuel and reached its final size of only about 5,400 acres within the first two weeks but smoldered until August 12, when it received between 1.5 inches and 3.5 inches of rain across the entire burn area.

Figure 15-32 shows smoke drift maps created by the North Carolina Division of Forest Resources and the U.S. Fish and Wildlife Service based on the HYbrid Single-Particle Lagrangian Integrated Trajectory (HYSPLIT) program with new interactive internet platform created by Draxler and Rolph (2012). These maps are posted at the Incident Information System Web site http://www.inciweb.org/incident/maps/2218/10 and focus on the period from June 24 to 27, with the Juniper Road fire being the most active and strongest source for smoke in the region.

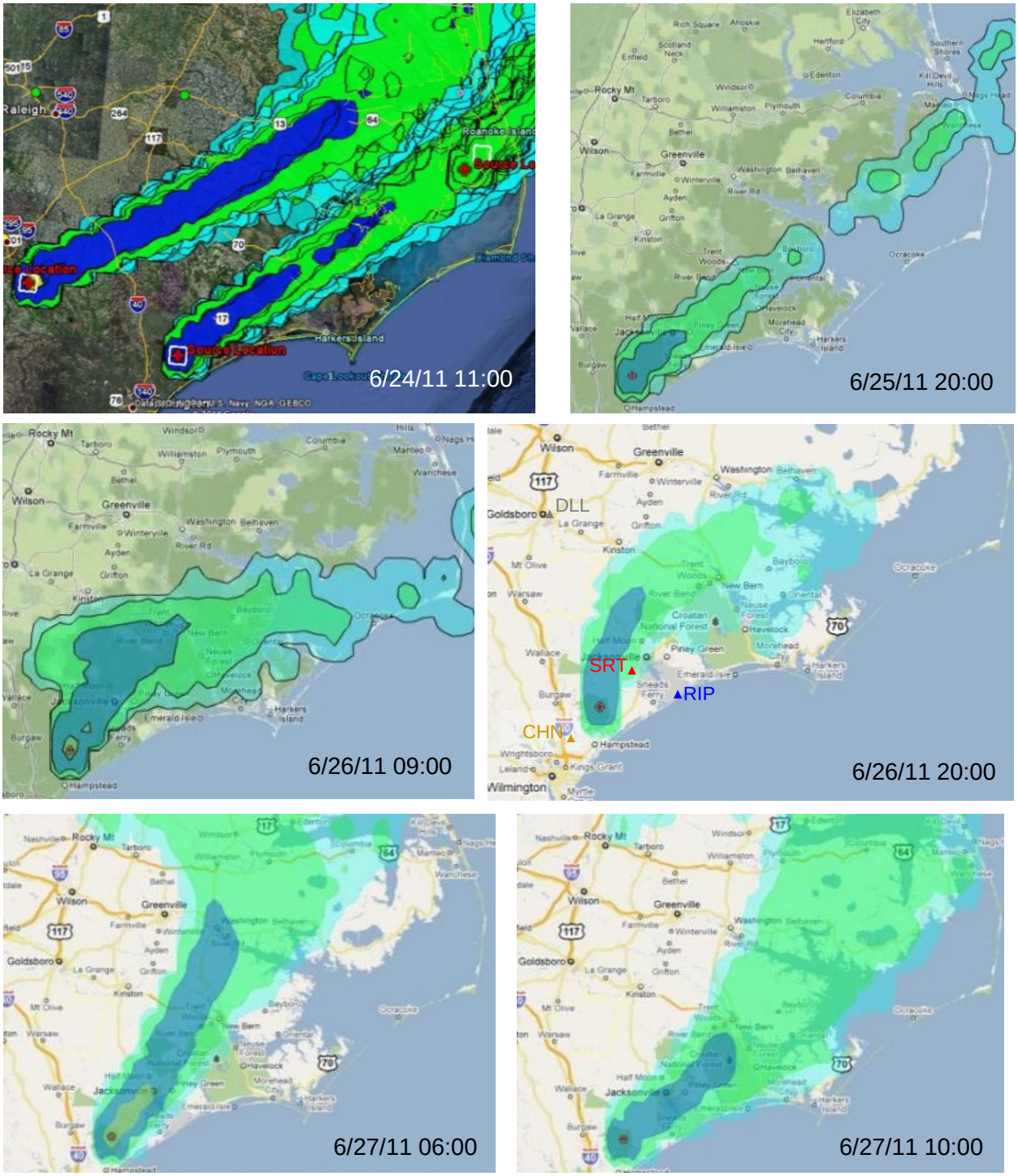

Figure 15-32. Maps of smoke drifting from the Juniper Road Fire from June 24 to 27, 2011.

Center right panel shows study sites for comparison with **Figure 15-30**.

Figure 15-33 shows hourly data from the ground measurements at our study sites between June 21 and 27, for comparison with the smoke drift maps in the above figure. Weather conditions changed from initially cloudy to progressively sunny with winds blowing consistently from southerly directions and SRT naturally experiencing systematically stronger winds due to its elevation. Vertical temperature difference (SRT minus SRG) indicates strong convective

mixing for the large red area, neutral to weakly labile are thin red areas, and strongly stratified stable conditions are in blue. The latter occurred early mornings only on June 22 and 26.

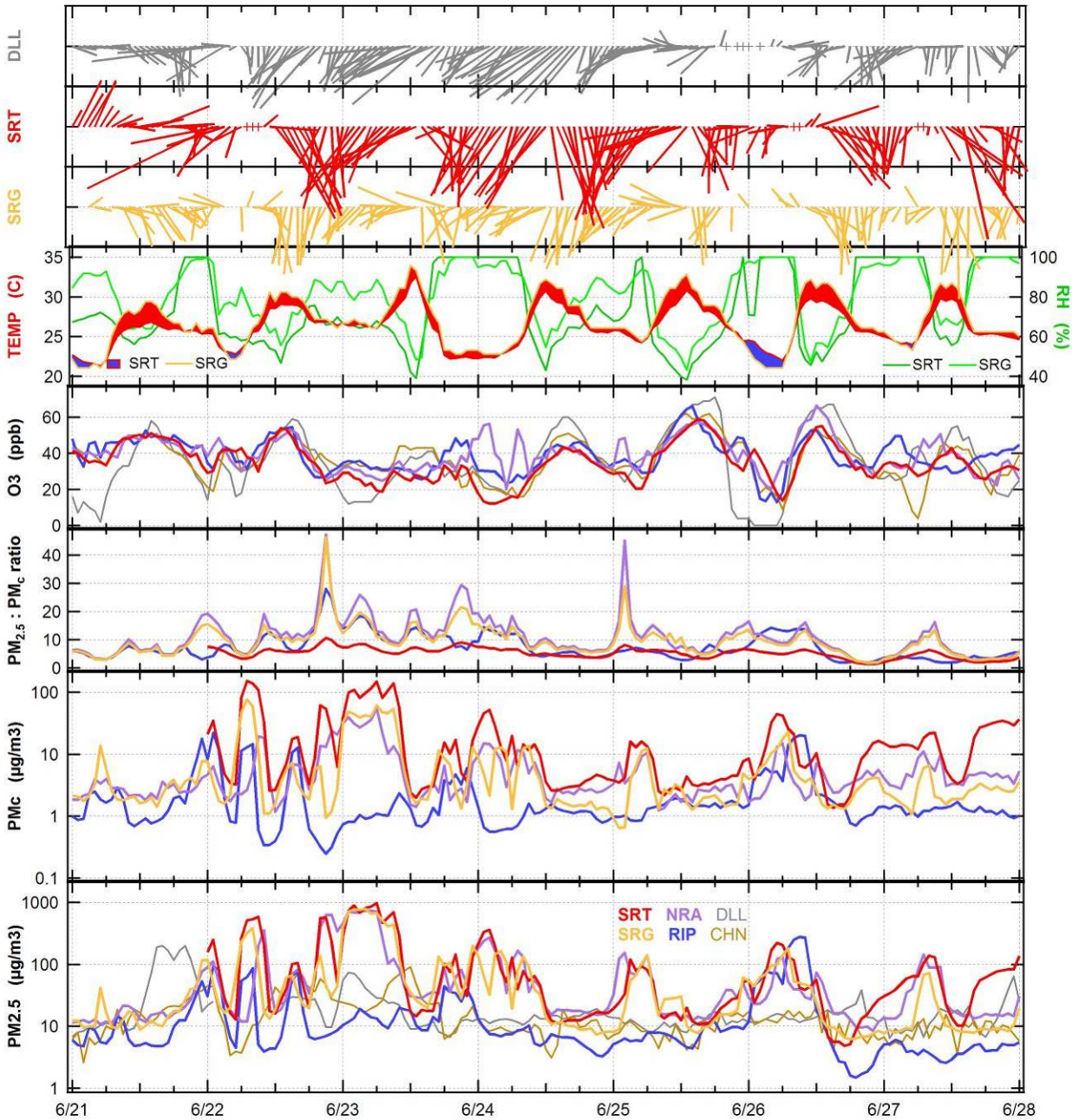

Figure 15-33. Hourly wind vectors, temperature, relative humidity, O_3, $PM_{2.5}$ and PM_c concentrations and ratio at different study sites from June 21 to 27, 2011.

Also depicted are hourly concentrations of O_3, as well as $PM_{2.5}$ and PM_c, which are presented on logarithmic scales due to their large daily excursions. The PM excursions occurred mostly during the early morning hours when atmospheric BL conditions were stably stratified or near neutral (blue or thin red in TEMP panel). As previously mentioned, the stably stratified periods occurred on June 22 and 26 under low winds and calm conditions, and caused large excursions in $PM_{2.5}$

and PM_c at all on-Base sites but not at CHN, which sat upwind from the main fire, and also not at DLL, which was not impacted by the eastward drifting smoke on June 26 and did not report any data between 0200 and 1300 on June 22. DLL was, however, impacted by the smoke during the afternoon of June 21, when it received air masses from the southeast with hourly $PM_{2.5}$ concentrations of up to 200 μg m^{-3}, averaging 143 μg m^{-3} between 1400 and 2300, and 61 μg m^{-3} for the 24-hour day.

As suggested by the smoke drift maps, the on-Base sites reported largest PM impact when hit directly by the plume under neutral BL conditions and strong southwesterly winds in the morning hours of June 23, 24, and 25. On each day, convective mixing would become effective by mid-afternoons, diluting the local PM levels down to regional background (explaining the diurnal averages presented earlier). The RIP beach site was largely unaffected by the smoke plume during this period, except for June 22 and 26 (i.e., the periods where strong nocturnal temperature inversions helped accumulate high PM levels in elevated layers above ground that eventually became mixed down to the ground during sunny morning hours under relatively calm conditions). Such conditions are difficult to forecast and to model, explaining why the smoke drift maps did not capture the beach impact correctly: The maps predicted impacting the beach on June 27 rather than on June 26.

PM_c showed the same diurnal pattern like $PM_{2.5}$, however, the $PM_{2.5}$:PM_c ratio at SRT was different from the other sites. Although the ratios were similar across all study sites during well mixed afternoon conditions, indicating the plume being homogeneously well-mixed over the entire Base area, during most severe plume impacts at nights and early mornings, however, the $PM_{2.5}$/PM_c ratio up at the SRT remained low, and it increased at the ground sites. Especially under due southerly flow at the beginning of the plume hits and before the wind would shift to southwesterly directions, the ground sites report brief excursions to very large $PM_{2.5}$/PM_c ratios, seemingly caused by drops in PM_c rather than spikes in $PM_{2.5}$, possibly pointing to certain heterogeneity of the meandering smoke plume with emissions from a hot flaming front of the fire passing the sites. As the sea breeze developed during the mornings and more uniformly carried the smoke plume inland, the ground sites registered more uniform $PM_{2.5}$:PM_c ratios at approximately 10, which increased to approximately 20 by afternoons and evenings. Such an increase can be caused by new particles forming in the confluence of reactive gases and semi-volatile species from the fire with maritime air masses in the sea breeze, according to the previously mentioned processes.

For comparison with **Figure 15-31**, daily PM concentrations and $PM_{2.5}$:PM_c ratios, daily minimum and maximum vertical temperature gradients (SRT–SRG) and wind vectors are presented in **Figure 15-34** for the period from June 17 through July 31, 2011. During the main smoke period from June 22–30, the daily $PM_{2.5}$:PM_c ratios were similar to the Pains Bay fire, approximately 5 up at the SRT tower and between 5 and 10 at the ground except for on June 22 and 29, when the NRA site reported between 17 and 19. The RIP beach site was also impacted on June 23, 26, and 29, and saw its daily ratios jump up to 10, 11, and 12, respectively. On July 4, fireworks were held at WPT Hill Field ca. 4 km southwest from the NRA site, which contributed to the observed increase in daily $PM_{2.5}$ and PM_c concentrations there, at a ratio of approximately 12.

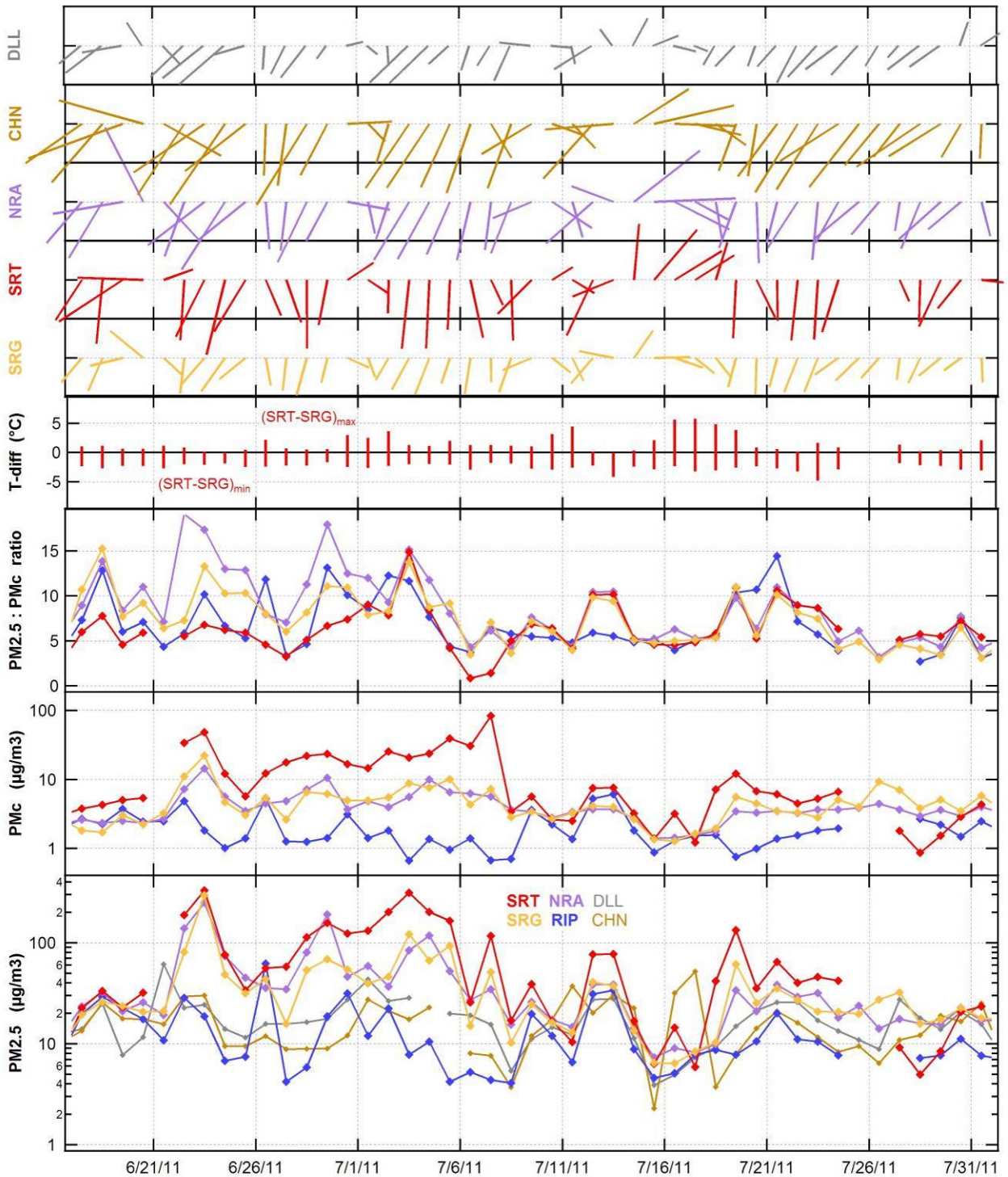

Figure 15-34. Daily maximum and minimum vertical temperature difference between 40 m (SRT) and the ground (SRG), wind vectors, $PM_{2.5}$ and PM_c concentrations and ratio at different study sites from June 17 through July 31, 2011.

Starting in the afternoon of the July 7, a low-pressure system moved through the region causing wide-spread rainfall late morning of July 8 with MCA (near NRA), SRG, and CHN sites

reporting 37, 2, and 4 mm, respectively. The regional rainfall caused the $PM_{2.5}$ and PM_c concentrations to uniformly drop and settle at a $PM_{2.5}$:PM_c ratio between 4 and 6. However, the rain was not enough to extinguish the wildfires, so that during the subsequent drying period and shift to easterly flow, the CHN site became impacted by smoke several times (on July 11, 13, 16, and 17), causing elevated daily $PM_{2.5}$ levels between 30 and 52 µg m^{-3}. It is important to note that the daily average $PM_{2.5}$ mass concentration is important for the determination of compliance with the NAAQS, in that the 3-year average of the 98th percentile of this measure (usually the third highest value of the year) is below 35 µg m^{-3}.

To illustrate the relationship between fire activity and the associated risk for $PM_{2.5}$ pollution, **Figure 15-35** compares the number of days when this threshold of 35 µg m-3 had been exceeded at each study site with the annual total acres burned (both via PB and wildfires) statewide and on Base. In contrast to the Federal Reference Method filter based data that went into the determination of the NAAQS DVs presented earlier, here the daily $PM_{2.5}$ averages were determined from the high-resolution data collected at the state's monitoring sites CHN and DLL. This is the proper basis for comparison with the daily $PM_{2.5}$ averages from our on-Base study sites, which were determined similarly from high resolution (hourly) data. It is important to note that 2008 and 2011 comprise only partial years because our study's monitoring began in late March of 2008 and ended in early October 2011.

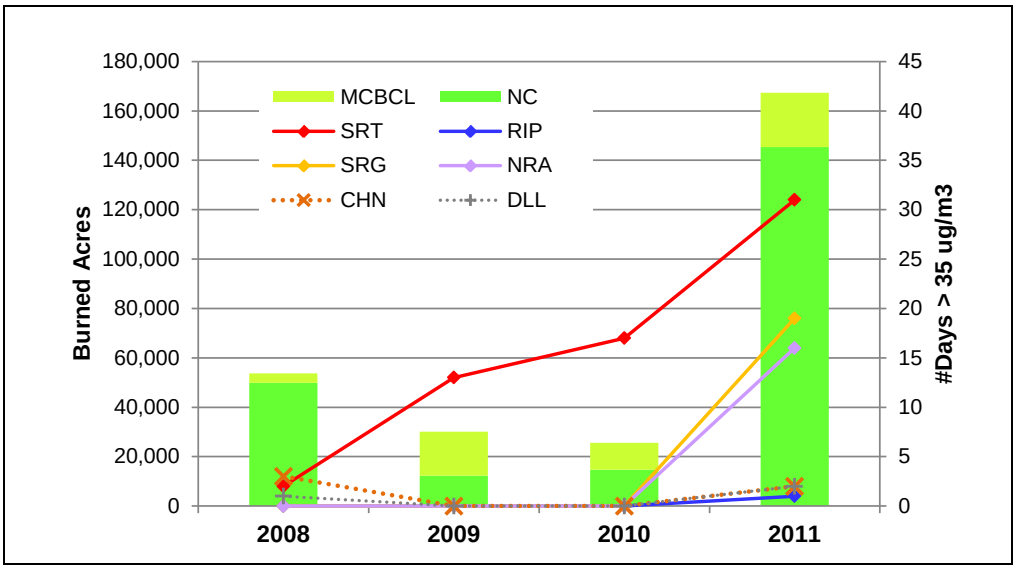

Figure 15-35. State- and Base-wide total acres burned and number of days exceeding 35 µg m^{-3} daily $PM_{2.5}$ concentration averages at different study sites between 2008 and 2011.

The relative completeness in data coverage at each site is summarized in **Table 15-10**. Because $PM_{2.5}$ measurements at NRA and SRG were added to the project in late 2010, their annual completeness is very low relative to the other sites with only 25% and 9%, respectively. Despite the low coverage, none of the late days in 2010 registered daily $PM_{2.5}$ values above 35 µg m^{-3}. This is very different for the RIP beach site and SRT tower site, where at relatively high data coverage in 2010, actually 0 and 17 days with average $PM_{2.5}$ greater equal to 35 µg m^{-3} were registered, respectively. As previously mentioned, RIP experienced generally the lowest $PM_{2.5}$ pollution and registered only one day in 2011 (June 26) with 62 µg m^{-3}. CHN and DLL did also

not register any exceedance days in all of 2009 and 2010, and only three and one in 2008, and two each in 2011, respectively.

Table 15-10. Annual coverage of daily average $PM_{2.5}$ data for different study sites.

YEAR	SRT	SRG	NRA	RIP	CHN	DLL
2008	60%			66%	96%	95%
2009	92%			93%	99%	99%
2010	95%	9%	25%	80%	98%	100%
2011	80%	78%	78%	86%	98%	97%

To further illustrate the air pollution risk associated with unwanted regional wildfires, **Table 15-11** summarizes the fire data presented in the figure and compares them with the average daily $PM_{2.5}$ concentrations for all registered exceedance days. The bottom column focuses on the wildfire active period between March and July of 2011, during which almost 56% and 78% of all 2011 state- and Base-wide fires occurred, respectively. During that period, each site reported the listed value as its third highest daily average $PM_{2.5}$ concentration, pointing to the increased risk of exceeding the NAAQS under future potential increase of wildfire occurrences in the state.

Table 15-11. State- and Base-wide total acres burned and average daily $PM_{2.5}$ level of each site's exceedance days.

Bottom numbers (italic) are third highest daily $PM_{2.5}$ in period.

Year	NC (ac)	MCBCL (ac)	SRT µg/m^3	SRG µg/m^3	NRA µg/m^3	RIP µg/m^3	CHN µg/m^3	DLL µg/m^3
2008	49,929	3,735	38.2	—	—	—	53.7	73.4
2009	12,328	17,729	52.2	—	—	—	—	—
2010	14,703	10,862	64.5	—	—	—	—	—
2011	145,387	21,962	101.4	74.3	82.7	62.2	44.4	52.3
Mar-Jul	*81,840*	*17,093*	*201.5*	*119.0*	*138.8*	*31.4*	*31.7*	*32.4*

Assessment of Trends in the Data

Assessment of Monitoring Design

The spatial distribution and temporal resolution of additional meteorological and air pollution measurements made at MCBCL complemented well the existing network of measurement sites to adequately capture both short- and long-term variations and to compare regional trends. The SRT tower site delivered very interesting and important data, revealing effects of atmospheric turbulence and mixing that help explain the shape of concentration profiles and conditions observed on the ground. The increase in the spatial resolution of PM measurements across MCBCL by adding two sites in October 2010 (NRA near the northern border and SRG 3 km south from SRT) helped significantly improve the characterization of the general PM burden over MCBCL, and particularly the different levels of impact from distant versus near-by wildfires.

Assessment Seasonal and Annual Variability in the Data

The spatial distribution and temporal resolution of O_3 measurements made at MCBCL were adequate to capture both short- and long-term variations and to compare to regional trends. MCBCL lands received the highest average O_3 concentration from a southeasterly direction, pointing to effects from photochemical production of O_3 in maritime air masses transported by sea breezes. The LCC site farthest to the north appeared to be decoupled from this air shed in that it received its highest O_3 from northeasterly direction in spring only. Especially April and June 2011 were unusually dry, sunny and warm, providing conditions conducive for in situ photochemical O_3 formation. Our PAR measurements suggest increased radiation levels with increasing distance from the Atlantic Ocean, potentially enhancing the yield of O_3-forming photochemical reactions. Lastly, spring was also characterized by higher winds than during any other season, especially at the sites further inland (including LCC), so that stratospheric intrusion of high O_3 concentrations possibly contributed to the increased O_3 levels arriving from the northeast. At the coastal sites, however, removal of O_3 via chemical reactions and surface deposition overwhelmed O_3 production in continental air masses, making the sea breeze carry relatively higher O_3 concentrations to those sites. Over the past 10 years, O_3 concentrations declined steadily across the region, in line with the nation-wide trend attributed primarily to reductions in O_3 precursor emissions (NO_x and methane). However, the declining trend in seasonal levels harmful to vegetation reversed in 2009 and increased since then, mainly due to the unusual warm and dry weather conditions in early spring being conducive for photochemical O_3 production. These conditions resulted in monthly levels exceeding those from summer, which followed the declining trend from previous summers. Thus, the high spring values more than compensated the downward trending summer O_3 levels, and yielded an overall O_3 increase for the biologically relevant growing season.

$PM_{2.5}$ levels for both short-term and especially long-term exposure thresholds have decreased steadily during the past 10 years across the study region (except for the smoke impacted sites). Based on data from off-Base sites CHN to the southwest and DLL to the north, the regional trend of increasing $PM_{2.5}$ levels with increasing distance from the coast outside MCBCL boundaries has remained true in 2011. This trend was previously shown to correlate with decreasing amounts of rainfall away from the coast and held again for this most recent January–September 2011 period, because rainfall is the most effective sink for atmospheric $PM_{2.5}$. This increase in $PM_{2.5}$ with increasing distance from the ocean stands in contrast to O_3, indicating that secondary (atmospheric) particle formation in maritime air masses played only a minor role in the local burden of $PM_{2.5}$. At all sites but especially the ones on-Base, the $PM_{2.5}$ measurements revealed a regional character that was distinctly less homogeneous than that for O_3, pointing to a greater influence from primary emissions sources on local scales. Such local influences were enhanced whenever vertical mixing near the surface was limited due to stratification, allowing pollutants to accumulate inside a shallow BL instead of being diluted under convectively well-mixed conditions.

In addition to the meteorological features enhancing $PM_{2.5}$ levels locally, several wildfires occurred near the North Carolina coast during 2011 that had significant impacts on the PM measurements in our study domain, standing in stark contrast to previous years. The most important fires were one on Base at SR-8 directly south from two of our sites (SRG and SRT tower ca. 3 km away) in March, and two off-Base fires at Pains Bay in the Alligator River National Wildlife Refuge, about 160 km northeast from MCBCL and at Juniper Road in the

neighboring Holly Shelter Game Land to the southwest in June. Comparing regional PM concentration levels based on the daily and annual standards, the RIP beach site followed the regional trend in that it reported the lowest annual $PM_{2.5}$ level of all study sites, while it experienced similar levels on the daily basis, due to brief occurrences of elevated $PM_{2.5}$ concentrations when occasionally impacted by smoke from the wildfires. Due to its elevated location, SRT experienced these wildfire plume encounters at much higher frequency and intensity than any other site, causing outstanding exceedances of both daily and annual standards. $PM_{2.5}$ levels at SRG and NRA, the two on-Base sites that had been added in the third quarter of 2010, appeared distinctly different: Although NRA levels were close to the ones observed at SRT, both the daily and annual levels at SRG which is only 3 km south from SRT were significantly lower, suggesting that: (1) SRT must be influenced by very local $PM_{2.5}$ sources immediately below the tower, and (2) certain conditions of atmospheric stratification must exist that allow the top of the 40-m tower to be exposed to accumulated $PM_{2.5}$ from the lofted fire smoke, which was somewhat decoupled from the ground.

For periods with smoke laden air masses blowing into the Base area from southwest, PM_c (the PM_c fraction from $PM_{10}-PM_{2.5}$ difference) was also elevated. However, the level of elevation relative to other directions was smaller than for $PM_{2.5}$, indicating that the wildfire smoke emissions contained substantially more $PM_{2.5}$ than PM_c. Smoke plume encounters at the SRT site in winter (first quarter) yielded an average $PM_{2.5}$:PM_c ratio noticeably lower than the maritime background, pointing to certain PM_c enhancing processes in the confluence of smoke plume and maritime air mass during colder months. Smoke plume encounters at SRT in spring (second quarter) and summer (third quarter), however, suggest these PM_c enhancing processes being overwhelmed by large $PM_{2.5}$ fire emissions (especially during the hot flaming phase of fuel combustion) and new particle formation processes driven by emitted reactive precursor gases and semi-volatile aerosol species, causing a consistently higher $PM_{2.5}$:PM_c ratio in smoke plumes that are carried by the sea breeze in warmer months. The high PM_c levels at SRT associated with the wildfire plume encounters, yield average $PM_{2.5}$:PM_c ratios between 4 and 6, corresponding to an average PM_c level of 17–25% of $PM_{2.5}$, or 14–20% of PM_{10}, respectively; in less polluted air, this ratio ranged between 2 and 3 (33–50% of $PM_{2.5}$ or 25–33% of PM_{10}).

The urban sites CHN to the southwest and DLL to the far north were either upwind of the wildfires (CHN) or sheltered from the advecting plumes due to nocturnal temperature inversion at the ground (DLL), so that the nocturnal increases in $PM_{2.5}$ concentration were due to emissions from local pollutant sources such as traffic, industries and domestic heating, being trapped and accumulated in shallow surface layers. This behavior is consistent with the observations in previous years, and presents a systematic difference to the more rural sites on Base (with NRA near the MCNRAS being the exception). Especially in evenings of colder months, $PM_{2.5}$ levels farther inland consistently exceeded those at the coast, likely due to residential heating and wood burning in urban areas. The MCBCL PM measurements point to a greater local influence from primary emission sources, of which PB and the movement and operation of heavy military equipment are the most important. The local, more highly resolved PM monitoring on MCBCL (aside from SRT) fit the regional trend of increasing $PM_{2.5}$ with increasing distance from the ocean.

The spatial and temporal distribution of rainfall, reported more than 30 years to the NWS's repository from hardened rainfall monitors located on and around MCBCL, revealed drought conditions during the 3.5-year study period except for a few locations and periods with extreme

rainfall amounts, helping to push annual totals above 30-year normals. Thus, although rainfall amounts in the second half of 2008 were significantly below normal, the following 2 years averaged slightly above normal (thanks to Tropical Storm Danny and Hurricane Ida in August and November 2009, respectively, and Tropical Storm Nicole in September 2010) with 2011 again falling behind. For all periods, though, total rainfall amounts regionally across the entire study domain consistently decreased with increasing distance from the coast. However, more complex patterns in nutrient deposition were observed in the highly resolved spatial sampling of rainfall amounts and composition across MCBCL as part of *DCERP1 Final Research Report* (Chapter 16, *Nitrogen Deposition to Terrestrial and Aquatic Ecosystems*).

Recommendations for Future Monitoring

In an environment of increased risk for wildfires, the Base is expected to be impacted by heavy smoke with increasing deposition of especially PM_c onto potentially sensitive vegetation and waterbodies. To keep track of occurrence frequency and intensity of such deposition events, continuation of a small monitoring network of similar size is recommended. Additional monitoring of size resolved PM chemical composition would enhance the ability to develop effective remediation strategies if symptoms of ecosystem stress or even damage were discovered down the road.

Conclusions and Implications for Future Research

Our monitoring activity started in April 2008 and continued through October 2011. Based on recommendations from the TAC, spatial resolution was enhanced of both $PM_{2.5}$ and PM_c measurements across the Base, to primarily assess the impact and spatial extent of certain on-Base sources such as PB and military training activities. The purpose of the expansion was to delineate PM transport onto the Base from external sources and to distinguish impacts from external sources. The 2011 study period afforded us with an opportunity to test our monitoring capacity on the basis of large wildfires occurring at different distances and directions away from the Base. Our network was adequate to capture the effects of these external pollution sources on the main pollutants and potential ecosystem stressors of concern: O_3, $PM_{2.5}$ and PM_c. The following summarizes our key findings.

Key Scientific Findings—Fundamental Cause-and-Effect Relationships

Despite several direct impacts of wildfire smoke plumes in March, June and July, O_3 levels that are harmful to human health continued to decreased at similar rates across all sites in the study area. However, the declining trend in seasonal levels that are harmful to vegetation has reversed and increased again since 2009, mainly due to the unusual warm and dry weather conditions in early spring being conducive for photochemical O_3 production. These conditions resulted in monthly levels exceeding those from summer, which followed the declining trend from previous summers. Thus, the high spring values more than compensated the downward trending summer O_3 levels (thanks to reduced anthropogenic emissions in precursors), and yielded an overall O_3 increase for the biologically relevant growing season. Smoke impacts from the more distant fires caused a noticeable but short-term increase in O_3 locally, whereas smoke from the near-by fires caused a temporary small decrease in local O_3 levels, indicating chemical loss mechanisms being more effective in those relatively fresh plumes than O_3 forming reactions.

$PM_{2.5}$ levels for both short-term and especially long-term exposure thresholds have decreased steadily during the past 10 years. Based on data from off-Base sites to the southwest and to the north, the regional trend of increasing $PM_{2.5}$ levels with increasing distance from the coast outside MCBCL boundaries has remained true in 2011. This trend correlated with decreasing amounts of rainfall away from the coast and held again for this most recent January–September 2011 period, because rainfall effectively removes $PM_{2.5}$ from the atmosphere.

Our monitoring approach afforded the measurement of PM_c from the PM_{10}-$PM_{2.5}$ difference. High resolution data of simultaneously measured $PM_{2.5}$ and PM_c provides powerful diagnostics into potential sources and source impact processes causing local air pollution. For example, a large $PM_{2.5}/PM_c$ ratio indicates: (1) depletion of PM_c due to gravitational settling and surface deposition, (2) influence from combustion sources, and (3) formation of new particles from nucleation and heterogeneous gas-particle conversion processes that are typical for SOA. In contrast, a low ratio would point to a potential influence from windblown dust and marine (sea-salt) aerosol.

One of the more important conditions enhancing PM_c in our study domain stems from the proximity of MCBCL to the Atlantic Ocean, providing an environment conducive to sulfate formation via oxidation of SO_2 to sulfate in sea-salt containing cloud droplets and deliquesced sea-salt aerosols. This process can result in a substantial fraction of non-sea-salt sulfate to be present on large sea salt particles. Another PM_c enhancing factor is the reaction of nitric acid with sea-salt aerosol to form coarse mode sodium nitrate particles. Under clean marine conditions, the sea-salt displacement reaction can be expected to yield a complete conversion of nitrate from the fine to the coarse aerosol mode, thereby potentially increasing the PM_c mass.

Aromatic hydrocarbons, biogenic terpenes (especially isoprene), and other reactive VOC are primary species involved in SOA formation, which was discussed extensively in conjunction with the PB emissions results presented in the Air-1 Research Report (Chapter 15: *Optimization of Prescribed Burning by Considering Mechanical Thinning as a Viable Land Management Option*). One of the conclusions was that PB emissions have not enough potential to form significant amounts of SOA within the local impact zone of the typical wildland urban interface during the first 5 hours after emission.

The $PM_{2.5}$:PM_c ratio at NRA (the on-Base site farthest away from the coast) was highest in most seasons especially for air mass transport from northerly and northeasterly directions, where the major traffic corridors are located for thousands of daily commuters. For periods with smoke laden air masses blowing into the Base area from southwest, both $PM_{2.5}$ and PM_c levels were elevated. However, the PM_c elevation relative to other directions was smaller than for $PM_{2.5}$, indicating that the wildfire smoke emissions contained substantially more $PM_{2.5}$ than PM_c. Smoke plume encounters at SRT in winter and early spring yielded an average $PM_{2.5}$:PM_c ratio noticeably lower than the maritime background, pointing to the previously mentioned PM_c enhancing processes in the confluence of smoke plume and maritime air mass during colder months. Smoke plume encounters at SRT in late spring and summer however, suggest these PM_c enhancing processes being overwhelmed by large $PM_{2.5}$ fire emissions (especially during the hot flaming phase of fuel combustion) and new particle formation processes driven by emitted reactive precursor gases and semi-volatile aerosol species, causing a consistently higher $PM_{2.5}$:PM_c ratio in smoke plumes that are carried by the sea breeze in warmer months.

Findings Supportive of Current and Future Base Management Practices

In their routine PB planning, on-Base forest managers consult the NWS fire weather forecasts and pay particular attention to ventilation rate and the Keetch-Byram Drought Index (KBDI). The (KBDI) indicates dryness of soil and duff layers towards the potential of causing unwanted wildfires. In addition to focusing on ventilation rate, the transport wind direction should be considered in the current planning with land breeze being preferred over the sea breeze. This would mean to possibly ignite PB fires earlier in the mornings.

The bulk of the managed area receives PB during the dormant season(i.e., mainly between December and March). Based on the previously mentioned findings, it appears critically important to avoid summer time wildfires due to their potential in causing significant increases in local and regional O_3 and $PM_{2.5}$ concentration levels. Therefore, the removal of unwanted fuel and the prevention of fuel accumulation in areas prone for wildfire and uncontrolled spread should be emphasized.

Literature Cited

Chakrabarti, B., P.M. Fine, R. Delfino, and C. Sioutas. 2004. Performance evaluation of the active-flow *personal* DataRAM $PM_{2.5}$ mass monitor (Thermo pDR-1200) designed for continuous personal exposure measurements. *Atmospheric Environment 38*:3329–3340.

Cooper, O.R., D.D. Parrish, A. Stohl, M. Trainer, P. Nédélec, V. Thouret, J.P. Cammas, S.J. Oltmans, B.J. Johnson, D. Tarasick, T. Leblanc, I.S. McDermid, D. Jaffe, R. Gao, J. Stith, T. Ryerson, K. Aikin, T. Campos, A. Weinheimer, and M.A. Avery. 2010. Increasing springtime ozone mixing ratios in the free troposphere over western North America. *Nature 463*:344–348.

Draxler, R.R., and G.D. Rolph. 2012. HYSPLIT (HYbrid Single-Particle Lagrangian Integrated Trajectory) Model. Access via http://ready.arl.noaa.gov/HYSPLIT.php. NOAA Air Resources Laboratory, Silver Spring, MD.

Friedli, H.R., L.F. Radke, N.J. Payne, D.J. McRae, T.J. Lynham, and T.W. Blake. 2007. Mercury in vegetation and organic soil at an upland boreal forest site in Prince Albert National Park, Saskatchewan, Canada. *Journal of Geophysical Research 112*(G1):G01004.

Heck, W., and E. Cowling. 1997. The need for a long-term cumulative secondary ozone standard: An ecological perspective. *Environmental Management*:23–33.

Hunsaker, C.T., C.T. Garten, and P.J. Mulholland. 1994. Modeling nitrogen cycling in forested watersheds of Chesapeake Bay. Pp. in *Proceedings of the Water Environment Federation 67th Annual Conference & Exposition 4*:481–491, Chicago, IL. October 15–19.

Johnston, M.K. 1998. The inherited geologic framework of the New River submarine headland complex, North Carolina, and its influence on modern sedimentation. M.S. Thesis: University of North Carolina at Wilmington, Wilmington, NC.

Kerker, M. 1969. *The Scattering of Light*. Academic Press: New York.

Kodama, H.E., and D.H. Van Lear. 1980. Prescribed burning and nutrient cycling relationships in young loblolly pine plantations. *Journal of Applied Forestry 4*(3):118–121.

Lawrence, G.B., K.A. Vogt, D.J. Vogt, J.P. Tilley, P.M. Wargo, and M. Tyrrell. 2000. Atmospheric deposition effects on surface waters, soils, and forest productivity. *Ecological Studies 139*:275–330.

Lee, S., H. Kim, B. Yan, C. Cobb, C. Hennigan, S. Nichols, M. Chamber, E. Edgerton, J. Jansen, Y. Hu, M. Zheng, R. Weber, and A. Russell. 2008. Diagnosis of aged prescribed burning plumes impacting an urban area. *Environmental Science and Technology 42*:1438–1444.

Lee, S., K. Baumann, J.J. Schauer, R.J. Sheesley, L.P. Naeher, S. Meinardi, D.R. Blake, E.S. Edgerton, A.G. Russel, and M. Clements. 2005. Gaseous and particulate emissions from prescribed burning in Georgia. *Environmental Science and Technology 39*:9049–9056.

Lipsky, E.M., and A.L. Robinson. 2006. Effects of dilution on fine particle mass and partitioning of semi-volatile organics in diesel exhaust and wood smoke. *Environmental Science and Technology 40*:155–162.

MacLean, D.A., S.J. Woodley, M.G. Weber, and R.W. Wein. 1983. Fire and nutrient cycling. *SCOPE 18*:111–132.

Osgood, D.T., and J.C. Zieman. 1998. The influence of subsurface hydrology on nutrient supply and smooth cordgrass (*Spartina alterniflora*) production in a developing barrier island marsh. *Estuaries 21*(4B):767–783.

Paerl, H., R.L. Dennis, and D.L. Whitall. 2002. Atmospheric deposition of nitrogen: Implications for nutrient over-enrichment of coastal waters. *Estuaries 25*(4):677–693.

Raison, R.J., P.K. Khanna, and P.V. Woods. 1985. Transfer of elements to the atmosphere during low intensity prescribed fires in three Australian subalpine eucalypt forests. *Canadian Journal of Forest Research 15*(4):657–664.

Seinfeld, J.H., and S.N. Pandis. 1998. *Atmospheric Chemistry and Physics: From Air Pollution to Climate Change*. John Wiley & Sons: New York.

U.S. EPA (Environmental Protection Agency). 2012a. *National Ambient Air Quality Standards for Particulate Matter: Proposed Rule*. 40 CFR Parts 50, 51, 52, 53, and 58. EPA–HQ–OAR–2007–0492; FRL–9682–9. *Federal Register 77*(126). June 29.

U.S. EPA(Environmental Protection Agency). 2012b. *Policy Assessment for the Review of the Ozone National Ambient Air Quality Standards*. First External Review Draft. EPA–452/P–12–002. Office of Air Quality Planning and Standards, Research Triangle Park, NC. August.

U.S. EPA (Environmental Protection Agency). 2011. *Policy Assessment for the Review of the Particulate Matter National Ambient Air Quality Standards*. EPA 452/R-11-003. Office of Air Quality Planning and Standards, Research Triangle Park, NC. April.

U.S. EPA (Environmental Protection Agency). 2010. *Availability of Additional Information Related to the Review of the National Ambient Air Quality Standards for Ozone*. 40 *CFR* Parts 50 and 58. *Federal Register 75*(11).

U.S. EPA (Environmental Protection Agency). 2009. *Integrated Science Assessment for Particulate Matter*. FRL–9090–9. Docket ID No. EPA–HQ–ORD–2007–0517. *Federal Register 74*(239).

U.S. EPA (Environmental Protection Agency). 2008a. *National Primary and Secondary Ambient Air Quality Standards*. 40 *CFR* Part 50. *Federal Register 73*(60).

U.S. EPA (Environmental Protection Agency). 2008b. *Ambient Air Quality Surveillance*. 40 *CFR* Part 58. *Federal Register 73*(60).

U.S. EPA (Environmental Protection Agency). 2006. *Air Quality Criteria for Ozone and Related Photochemical Oxidants*, Vol. 1. EPA 600/R-05/004aF. National Center for Environmental Assessment, Office of Research and Development, Research Triangle Park, NC.

U.S. EPA (Environmental Protection Agency). 2004. *Air Quality Criteria for Particulate Matter*, Vol. 1. EPA/600/P-99-002aF. Office of Research and Development, National Center for Environmental Assessment, Research Triangle Park, NC. October.

U.S. EPA (Environmental Protection Agency). 1997. *National Ambient Air Quality Standards for Particulate Matter: Final Rule*. *Federal Register 62*(138).

U.S. EPA (Environmental Protection Agency). 1996. *The Review of the National Ambient Air Quality Standards for Ozone: Policy Assessment of Scientific and Technical Information, Staff Paper*. EPA-452/R-96-007. Office of Air Quality Planning and Standards, Research Triangle Park, NC. June.

Van Der Salm, C., W. De Vries, M. Olsson, and K. Raulund-Rasmussen. 1999. Modeling impacts of atmospheric deposition, nutrient cycling and soil weathering on the sustainability of nine forest ecosystems. *Water, Air, and Soil Pollution 109*(1–4):101–135.

Appendix 15-A

List of Scientific Publications

List of Scientific Publications

Papers

Baumann, K., J.J. Schauer, D.R. Blake, S.R. Mitchell, N.L. Christensen, J.M. Fort, and E.S. Edgerton. 2013. *Effects of Mechanical Thinning on Fuel Consumption and Emissions from Prescribed Burning in Coastal NC*. In preparation. *Atmospheric Environment*.

Presentations

Balachandran, S., K. Baumann, J. Pachon, J. Mulholland, and A. Russell. 2012. *Verification of Fire Weather Forecasts Using $PM_{2.5}$ Sensitivity Analysis*. Presented at the 31st Annual Conference of the American Association for Aerosol Research, Minneapolis, MN. October 8–12.

Baumann, K., J.J. Schauer, D.R. Blake, S.R. Mitchell, N.L. Christensen, J.M. Fort, and E.S. Edgerton. 2012. *In situ Measurements of Gas and Fine Particle Species Emissions from Prescribed Burning of Differently Treated Fuels in the Southeastern United States*. Presented at the Air Quality Measurement Methods and Technology Conference of the Air & Waste Management Association, Durham, NC. April 24–26.

Baumann, K., J.J. Schauer, D.R. Blake, S.R. Mitchell, J.M. Fort, and E.S. Edgerton. 2011. *Gas and Fine Particle Species Emissions from Prescribed Burning in Managed Forests of the Southeastern United States*. Presented at the 10th Annual Community Multiscale Air Quality Conference, Friday Center in Chapel Hill, NC. October 24–26.

Baumann, K., B.K. Gullett, J. Aurrell, D.R. Blake, A.L. Robinson, J.M. Fort, and E.S. Edgerton. 2011. *Chemical Character of Prescribed Burning Emissions at the Ground and Above the Canopy of Managed Forests in the Southeastern United States*. Presented at the 30th Annual Conference of the American Association for Aerosol Research, Orlando, FL. October 3–7.

Baumann, K., J.J. Schauer, D.R. Blake, S.R. Mitchell, W.P. Robarge, J.M. Fort, and E.S. Edgerton. 2011. *Primary and Secondary PM Emissions from Prescribed Burning of Differently Treated Fuels in Managed Forests*. Presented at the 43rd Annual Air Pollution Workshop and International Symposium, Fort McMurray, Alberta, Canada. May 23–26.

Baumann, K., J.M. Fort, J.J. Schauer, D.R. Blake, S.R. Mitchell, W.P. Robarge, B.E. Hartsell, and E.S. Edgerton. 2010. *Gaseous and Particulate Emissions from Prescribed Burning of Differently Treated Fuels in Managed Forests of Marine Corps Base Camp Lejeune*. Presented at the 15th Strategic Environmental Research and Development Program (SERDP) and Environmental Security Technology Certification Program Partners in Environmental Technology Symposium, Washington DC. November 30–December 2.

Baumann, K., J.M. Fort, J.J. Schauer, D.R. Blake, B.E. Hartsell, and E.S. Edgerton. 2010. *Gaseous and Particulate Species Emissions from Different Forest Management*

Strategies Employing Prescribed Burning. Presented at the 29th Annual Conference of the American Association for Aerosol Research, Portland, OR. October 25–29.

Baumann, K., S.R. Mitchell, W.P. Robarge, J.M. Fort, J.J. Schauer, D.R. Blake, B.E. Hartsell, and E.S. Edgerton. 2010. *Gaseous and Particulate Emissions from Prescribed Burning in Pine Dominated Forest Ecosystems of the Southeastern United States*. Presented at the 103rd Annual Conference and Exhibition of the Air and Waste Association, Calgary, Alberta, Canada. June 22–25.

[This page intentionally left blank.]

Appendix 15-B

List of Students

- None.

[This page intentionally left blank.]